

THE BIOMEDICAL ENGINEERING HANDBOOK

FOURTH EDITION

Molecular,
Cellular, and
Tissue Engineering

THE BIOMEDICAL ENGINEERING HANDBOOK

FOURTH EDITION

Molecular, Cellular, and Tissue Engineering

Edited by

Joseph D. Bronzino

Founder and President

Biomedical Engineering Alliance and Consortium (BEACON)

Hartford, Connecticut, U.S.A.

Donald R. Peterson

Professor of Engineering

Dean of the College of Science, Technology, Engineering, Mathematics, and Nursing

Texas A&M University – Texarkana

Texarkana, Texas, U.S.A.



CRC Press

Taylor & Francis Group

Boca Raton London New York

CRC Press is an imprint of the
Taylor & Francis Group, an **informa** business

MATLAB® is a trademark of The MathWorks, Inc. and is used with permission. The MathWorks does not warrant the accuracy of the text or exercises in this book. This book's use or discussion of MATLAB® software or related products does not constitute endorsement or sponsorship by The MathWorks of a particular pedagogical approach or particular use of the MATLAB® software.

CRC Press
Taylor & Francis Group
6000 Broken Sound Parkway NW, Suite 300
Boca Raton, FL 33487-2742

© 2015 by Taylor & Francis Group, LLC
CRC Press is an imprint of Taylor & Francis Group, an Informa business

No claim to original U.S. Government works
Version Date: 20150213

International Standard Book Number-13: 978-1-4398-2531-0 (eBook - PDF)

This book contains information obtained from authentic and highly regarded sources. Reasonable efforts have been made to publish reliable data and information, but the author and publisher cannot assume responsibility for the validity of all materials or the consequences of their use. The authors and publishers have attempted to trace the copyright holders of all material reproduced in this publication and apologize to copyright holders if permission to publish in this form has not been obtained. If any copyright material has not been acknowledged please write and let us know so we may rectify in any future reprint.

Except as permitted under U.S. Copyright Law, no part of this book may be reprinted, reproduced, transmitted, or utilized in any form by any electronic, mechanical, or other means, now known or hereafter invented, including photocopying, microfilming, and recording, or in any information storage or retrieval system, without written permission from the publishers.

For permission to photocopy or use material electronically from this work, please access www.copyright.com (<http://www.copyright.com/>) or contact the Copyright Clearance Center, Inc. (CCC), 222 Rosewood Drive, Danvers, MA 01923, 978-750-8400. CCC is a not-for-profit organization that provides licenses and registration for a variety of users. For organizations that have been granted a photocopy license by the CCC, a separate system of payment has been arranged.

Trademark Notice: Product or corporate names may be trademarks or registered trademarks, and are used only for identification and explanation without intent to infringe.

Visit the Taylor & Francis Web site at
<http://www.taylorandfrancis.com>

and the CRC Press Web site at
<http://www.crcpress.com>

Contents

Preface.....	xiii
Editors.....	xix
Contributors	xxi

SECTION I Molecular Biology

Michael M. Domach

1 Historical Perspective and Basics of Molecular Biology.....	1-1
<i>Nathan R. Domagalski and Michael M. Domach</i>	
2 Biomolecular Interactions.....	2-1
<i>Gordon Rule</i>	
3 Recent Advances in DNA Separations: Plasmid Purification, Rapid Electrophoresis, and Affinity-Based Recovery.....	3-1
<i>James W. Schneider and Jeffrey M. Savard</i>	
4 Systems and Technology Involving Bacteria	4-1
<i>Nicole Bleckwenn and William Bentley</i>	
5 Expression in Mammalian Cells.....	5-1
<i>Tina Sauerwald and Michael Betenbaugh</i>	
6 DNA Vaccines Production and Engineering.....	6-1
<i>Michael M. Domach, Jonathan W. Meade, and Mohammad A. Ataai</i>	

SECTION II Transport Phenomena and Biomimetic Systems

Robert J. Fisher and Robert A. Peattie

7 Biomimetic Systems: Concepts, Design, and Emulation	7-1
<i>Robert J. Fisher</i>	
8 Transport/Reaction Processes in Biology and Medicine	8-1
<i>E.N. Lightfoot</i>	
9 Microvascular Heat Transfer	9-1
<i>James W. Baish</i>	

10	Fluid Dynamics for Bio Systems: Fundamentals and Model Analysis	10-1
	<i>Robert A. Peattie and Robert J. Fisher</i>	
11	Animal Surrogate Systems	11-1
	<i>Michael L. Shuler, Sarina G. Harris, Xinran Li, and Mandy B. Esch</i>	
12	Arterial Wall Mass Transport: The Possible Role of Blood Phase Resistance in the Localization of Arterial Disease	12-1
	<i>John M. Tarbell and Yuchen Qiu</i>	
13	Transport Phenomena and the Microenvironment	13-1
	<i>Robert J. Fisher and Robert A. Peattie</i>	
14	Transport and Drug Delivery through the Blood–Brain Barrier and Cerebrospinal Fluid	14-1
	<i>Bingmei M. Fu</i>	
15	Interstitial Transport in the Brain: Principles for Local Drug Delivery....	15-1
	<i>W. Mark Saltzman</i>	
16	Surfactant Transport and Fluid–Structure Interactions during Pulmonary Airway Reopening	16-1
	<i>David Martin, Anne-Marie Jacob, and Donald P. Gaver III</i>	

SECTION III Physiological Modeling, Simulation, and Control

Joseph L. Palladino

17	Modeling Strategies and Cardiovascular Dynamics.....	17-1
	<i>Joseph L. Palladino, Gary M. Drzewiecki, and Abraham Noordergraaf</i>	
18	Compartmental Models of Physiological Systems	18-1
	<i>Claudio Cobelli, Giovanni Sparacino, Maria Pia Saccomani, Gianna Maria Toffolo, and Andrea Caumo</i>	
19	Cardiovascular Models and Control	19-1
	<i>Madhusudan Natarajan, Fernando Casas, and W.D. Timmons</i>	
20	Respiratory Models and Control	20-1
	<i>Chi-Sang Poon</i>	
21	Biomimetic Approaches to Physiological Control	21-1
	<i>James J. Abbas and Amit Abraham</i>	
22	Methods and Tools for Identification of Physiologic Systems.....	22-1
	<i>Vasilis Z. Marmarelis</i>	
23	Modeling Vascular Vibrations: Autoregulation and Vascular Sounds	23-1
	<i>Gary M. Drzewiecki, John K-J. Li, and Abraham Noordergraaf</i>	
24	External Control of Movements	24-1
	<i>Dejan B. Popović and Mirjana B. Popović</i>	

- 25 The Fast Eye Movement Control System25-1
John Denis Enderle
- 26 A Comparative Approach to Analysis and Modeling of
Cardiovascular Function26-1
John K-J. Li, Ying Zhu, and Abraham Noordergraaf
- 27 A Biomedical and Biophysical Approach to the Science in
Cardiopulmonary Resuscitation 27-1
*Gerrit J. Noordergraaf, Igor W.F. Paulussen, Alyssa Venema, Gert Jan Scheffer, and
Abraham Noordergraaf*
- 28 Kinematic Modeling of Left Ventricular Diastolic Function28-1
Leonid Shmuylovich, Charles S. Chung, and Sándor J. Kovács

SECTION IV Stem Cell Engineering: An Introduction

David V. Schaffer

- 29 Engineering the Pluripotent Stem Cell Niche for Directed Mesoderm
Differentiation29-1
Céline L. Bauwens, Kelly A. Purpura, and Peter W. Zandstra
- 30 Cell Mechanobiology in Regenerative Medicine: Lessons from Cancer30-1
Badriprasad Ananthanarayanan and Sanjay Kumar
- 31 Systems-Engineering Principles in Signal Transduction and Cell-Fate
Choice 31-1
Karin J. Jensen, Anjun K. Bose, and Kevin A. Janes
- 32 Biomaterial Scaffolds for Human Embryonic Stem Cell Culture and
Differentiation32-1
Stephanie Willerth and David V. Schaffer
- 33 Stem Cells and Regenerative Medicine in the Nervous System.....33-1
Shelly Sakiyama-Elbert
- 34 Stem Cells and Regenerative Medicine for Treating Damaged
Myocardium34-1
Rohini Gupta, Kunal Mehtani, Kimberly R. Kam, and Kevin E. Healy
- 35 Stem Cells and Hematopoiesis 35-1
Krista M. Fridley and Krishnendu Roy
- 36 Synthetic Biomaterials and Stem Cells for Connective Tissue
Engineering36-1
Ameya Phadke and Shyni Varghese
- 37 Derivation and Expansion of Human Pluripotent Stem Cells..... 37-1
Sean P. Palecek
- 38 Bioreactors for Stem Cell Expansion and Differentiation38-1
*Carlos A.V. Rodrigues, Tiago G. Fernandes, Maria Margarida Diogo, Cláudia Lobato
da Silva, and Joaquim M.S. Cabral*

SECTION V Tissue Engineering

John P. Fisher and Antonios G. Mikos

39	Strategic Directions.....	39-1
	<i>Peter C. Johnson</i>	
40	Silks	40-1
	<i>Monica A. Serban and David L. Kaplan</i>	
41	Calcium Phosphates	41-1
	<i>Kemal Sariibrahimoglu, Joop G.C. Wolke, Sander C.G. Leeuwenburgh, and John A. Jansen</i>	
42	Engineered Protein Biomaterials.....	42-1
	<i>Andreina Parisi-Amon and Sarah C. Heilshorn</i>	
43	Synthetic Biomaterials	43-1
	<i>Joshua S. Katz and Jason A. Burdick</i>	
44	Growth Factors and Morphogens: Signals for Tissue Engineering.....	44-1
	<i>A. Hari Reddi</i>	
45	Signal Expression in Engineered Tissues	45-1
	<i>Martha O. Wang and John P. Fisher</i>	
46	Pluripotent Stem Cells	46-1
	<i>Todd C. McDevitt and Melissa A. Kinney</i>	
47	Hematopoietic Stem Cells.....	47-1
	<i>Ian M. Kaplan, Sebastien Morisot, and Curt I. Civin</i>	
48	Mesenchymal Stem Cells.....	48-1
	<i>Pamela C. Yelick and Weibo Zhang</i>	
49	Nanobiomaterials for Tissue Engineering.....	49-1
	<i>Pramod K. Avti, Sunny C. Patel, Pushpinder Uppal, Grace O'Malley, Joseph Garlow, and Balaji Sitharaman</i>	
50	Biomimetic Approaches in Tissue Engineering.....	50-1
	<i>Indong Jun, Min Sup Kim, Ji-Hye Lee, Young Min Shin, and Heungsoo Shin</i>	
51	Molecular Biology Techniques.....	51-1
	<i>X.G. Chen, Y.L. Fang, and W.T. Godbey</i>	
52	Biomaterial Mechanics.....	52-1
	<i>Kimberly M. Stroka, Leann L. Norman, and Helim Aranda-Espinoza</i>	
53	Mechanical Conditioning	53-1
	<i>Elaine L. Lee and Horst A. von Recum</i>	
54	Micropatterned Biomaterials for Cell and Tissue Engineering.....	54-1
	<i>Murugan Ramalingam and Ali Khademhosseini</i>	
55	Drug Delivery.....	55-1
	<i>Prinda Wanakule and Krishnendu Roy</i>	

56	Gene Therapy	56-1
	<i>C. Holladay, M. Kulkarni, W. Minor, and Abhay Pandit</i>	
57	Nanotechnology-Based Cell Engineering Strategies for Tissue Engineering and Regenerative Medicine Applications	57-1
	<i>Joaquim Miguel Oliveira, João Filipe Mano, and Rui Luís Reis</i>	
58	Cell Encapsulation	58-1
	<i>Stephanie J. Bryant</i>	
59	Coculture Systems for Mesenchymal Stem Cells	59-1
	<i>Song P. Seto and Johnna S. Temenoff</i>	
60	Tissue Engineering Bioreactors	60-1
	<i>Sarindr Bhumiratana, Elisa Cimetta, Nina Tandon, Warren Grayson, Milica Radisic, and Gordana Vunjak-Novakovic</i>	
61	Shear Forces.....	61-1
	<i>Jose F. Alvarez-Barreto, Samuel B. VanGordon, Brandon W. Engebretson, and Vasillios I. Sikavitsas</i>	
62	Vascularization of Engineered Tissues.....	62-1
	<i>Monica L. Moya and Eric M. Brey</i>	
63	Biomedical Imaging of Engineered Tissues	63-1
	<i>Nicholas E. Simpson and Athanassios Sambanis</i>	
64	Multiscale Modeling of <i>In Vitro</i> Tissue Cultivation	64-1
	<i>Kyriacos Zygourakis</i>	
65	Bone Engineering.....	65-1
	<i>Lucas A. Kinard, Antonios G. Mikos, and F. Kurtis Kasper</i>	
66	Dental and Craniofacial Bioengineering.....	66-1
	<i>Hemin Nie and Jeremy J. Mao</i>	
67	Tendon and Ligament Engineering	67-1
	<i>Nicholas Sears, Tyler Touchet, Hugh Benhardt, and Elizabeth Cosgriff-Hernández</i>	
68	Cartilage Tissue Engineering	68-1
	<i>Emily E. Coates and John P. Fisher</i>	
69	TMJ Engineering.....	69-1
	<i>Michael S. Detamore</i>	
70	Interface Tissue Engineering.....	70-1
	<i>Helen H. Lu, Nora Khanarian, Kristen Moffat, and Siddarth Subramony</i>	
71	The Bioengineering of Dental Tissues.....	71-1
	<i>Rena N. D'Souza, Katherine R. Regan, Kerstin M. Galler, and Songtao Shi</i>	
72	Tissue Engineering of the Urogenital System	72-1
	<i>In Kap Ko, Anthony Atala, and James J. Yoo</i>	

- 73 Vascular Tissue Engineering 73-1
Laura J. Suggs
- 74 Neural Engineering..... 74-1
Yen-Chih Lin and Kacey G. Marra
- 75 Tumor Engineering: Applications for Cancer Biology and
Drug Development 75-1
Joseph A. Ludwig and Emily Burdett

SECTION VI Artificial Organs

Donald R. Peterson

- 76 Artificial Heart and Circulatory Assist Devices 76-1
Gerson Rosenberg
- 77 Cardiac Valve Prostheses 77-1
Sivakkumar Arjunon, Neelakantan Saikrishnan, and Ajit P. Yoganathan
- 78 Artificial Lungs 78-1
Keith E. Cook, Timothy M. Maul, and William J. Federspiel
- 79 Blood Substitutes..... 79-1
Amy G. Tsai, Pedro Cabrales, and Marcos Intaglietta
- 80 Liver Support Systems 80-1
Matthew S. Chang and Robert S. Brown, Jr.
- 81 Peritoneal Dialysis Equipment..... 81-1
Carlo Crepaldi, Carla Estremadoyro, Francesca Katiana Martino, Maria Pia Rodighiero, and Claudio Ronco
- 82 Artificial Skin and Dermal Equivalents 82-1
Dennis P. Orgill, Raul Cortes, and Ioannis V. Yannas

SECTION VII Drug Design, Delivery Systems, and Devices

Yong Wang

- 83 Physiological Barriers to Drug Transport 83-1
Fan Yuan
- 84 Nucleic Acid Aptamers in Drug Delivery..... 84-1
Mark R. Battig, Jing Zhou, and Yong Wang
- 85 Dendrimers for Drug Delivery 85-1
Giridhar Thiagarajan and Hamidreza Ghandehari
- 86 Noninvasive Targeted Protein and Peptide Drug Delivery 86-1
Pradeep K. Karla, Durga K. Paturi, Nanda K. Mandava, Animikh Ray, Sulabh Patel, Ranjana Mitra, and Ashim K. Mitra
- 87 Environment-Responsive Hydrogels for Drug Delivery 87-1
Byung Kook Lee, Jong-Ryoul Kim, Kinam Park, and Yong Woo Cho

88 Biodegradable PLGA Scaffolds for Growth Factor Delivery **88-1**
Yusef Khan and Cato Laurencin

SECTION VIII Personalized Medicine

Gualberto Rúaño

89 Physiogenomic Contours: The Application of Systems Biology for
 Engineering Personalized Healthcare **89-1**
Andreas Windemuth, Richard L. Seip, and Gualberto Rúaño

90 The Evolution of Massively Parallel Sequencing Technologies:
 Facilitating Advances in Personalized Medicine **90-1**
Ian Toma, Georges St. Laurent III, Samuel Darko, and Timothy A. McCaffrey

91 Computational Methods and Molecular Diagnostics in Personalized
 Medicine **91-1**
Roland Valdes, Jr. and Mark W. Linder

92 Need for Point-of-Care Testing Devices for Cardiac Troponin in
 Patients with Acute Coronary Syndromes **92-1**
Alan H.B. Wu and Amy E. Herr

SECTION IX Ethics

93 An Introduction to Bioethics and Ethical Theory for Biomedical
 Engineers **93-1**
D. John Doyle

Index..... **Index-1**

Preface

During the past eight years since the publication of the third edition—a three-volume set—of *The Biomedical Engineering Handbook*, the field of biomedical engineering has continued to evolve and expand. As a result, the fourth edition has been significantly modified to reflect state-of-the-field knowledge and applications in this important discipline and has been enlarged to a four-volume set:

- Volume I: *Biomedical Engineering Fundamentals*
- Volume II: *Medical Devices and Human Engineering*
- Volume III: *Biomedical Signals, Imaging, and Informatics*
- Volume IV: *Molecular, Cellular, and Tissue Engineering*

More specifically, this fourth edition has been considerably updated and contains completely new sections, including

- Stem Cell Engineering
- Drug Design, Delivery Systems, and Devices
- Personalized Medicine

as well as a number of substantially updated sections, including

- Tissue Engineering (which has been completely restructured)
- Transport Phenomena and Biomimetic Systems
- Artificial Organs
- Medical Imaging
- Infrared Imaging
- Medical Informatics

In addition, Volume IV contains a chapter on ethics because of its ever-increasing role in the biomedical engineering arts.

Nearly all the sections that have appeared in the first three editions have been significantly revised. Therefore, this fourth edition presents an excellent summary of the status of knowledge and activities of biomedical engineers in the first decades of the twenty-first century. As such, it can serve as an excellent reference for individuals interested not only in a review of fundamental physiology but also in quickly being brought up to speed in certain areas of biomedical engineering research. It can serve as an excellent textbook for students in areas where traditional textbooks have not yet been developed and as an excellent review of the major areas of activity in each biomedical engineering sub-discipline, such as biomechanics, biomaterials, bioinstrumentation, medical imaging, and so on. Finally, it can serve as the “bible” for practicing biomedical engineering professionals by covering such topics as historical perspective of medical technology, the role of professional societies, the ethical issues associated with medical technology, and the FDA process.

Biomedical engineering is now an important and vital interdisciplinary field. Biomedical engineers are involved in virtually all aspects of developing new medical technology. They are involved in the design, development, and utilization of materials, devices (such as pacemakers, lithotripsy, etc.), and techniques (such as signal processing, artificial intelligence, etc.) for clinical research and use, and they serve as members of the healthcare delivery team (clinical engineering, medical informatics, rehabilitation engineering, etc.) seeking new solutions for the difficult healthcare problems confronting our society. To meet the needs of this diverse body of biomedical engineers, this handbook provides a central core of knowledge in those fields encompassed by the discipline. However, before presenting this detailed information, it is important to provide a sense of the evolution of the modern healthcare system and identify the diverse activities biomedical engineers perform to assist in the diagnosis and treatment of patients.

Evolution of the Modern Healthcare System

Before 1900, medicine had little to offer average citizens, since its resources consisted mainly of physicians, their education, and their “little black bag.” In general, physicians seemed to be in short supply, but the shortage had rather different causes than the current crisis in the availability of healthcare professionals. Although the costs of obtaining medical training were relatively low, the demand for doctors’ services also was very small, since many of the services provided by physicians also could be obtained from experienced amateurs in the community. The home was typically the site for treatment and recuperation, and relatives and neighbors constituted an able and willing nursing staff. Babies were delivered by midwives, and those illnesses not cured by home remedies were left to run their natural, albeit frequently fatal, course. The contrast with contemporary healthcare practices in which specialized physicians and nurses located within hospitals provide critical diagnostic and treatment services is dramatic.

The changes that have occurred within medical science originated in the rapid developments that took place in the applied sciences (i.e., chemistry, physics, engineering, microbiology, physiology, pharmacology, etc.) at the turn of the twentieth century. This process of development was characterized by intense interdisciplinary cross-fertilization, which provided an environment in which medical research was able to take giant strides in developing techniques for the diagnosis and treatment of diseases. For example, in 1903, Willem Einthoven, a Dutch physiologist, devised the first electrocardiograph to measure the electrical activity of the heart. In applying discoveries in the physical sciences to the analysis of the biological process, he initiated a new age in both cardiovascular medicine and electrical measurement techniques.

New discoveries in medical sciences followed one another like intermediates in a chain reaction. However, the most significant innovation for clinical medicine was the development of x-rays. These “new kinds of rays,” as W. K. Roentgen described them in 1895, opened the “inner man” to medical inspection. Initially, x-rays were used to diagnose bone fractures and dislocations, and in the process, x-ray machines became commonplace in most urban hospitals. Separate departments of radiology were established, and their influence spread to other departments throughout the hospital. By the 1930s, x-ray visualization of practically all organ systems of the body had been made possible through the use of barium salts and a wide variety of radiopaque materials.

X-ray technology gave physicians a powerful tool that, for the first time, permitted accurate diagnosis of a wide variety of diseases and injuries. Moreover, since x-ray machines were too cumbersome and expensive for local doctors and clinics, they had to be placed in healthcare centers or hospitals. Once there, x-ray technology essentially triggered the transformation of the hospital from a passive receptacle for the sick to an active curative institution for all members of society.

For economic reasons, the centralization of healthcare services became essential because of many other important technological innovations appearing on the medical scene. However, hospitals remained institutions to dread, and it was not until the introduction of sulfanilamide in the mid-1930s and penicillin in the early 1940s that the main danger of hospitalization, that is, cross-infection among

patients, was significantly reduced. With these new drugs in their arsenals, surgeons were able to perform their operations without prohibitive morbidity and mortality due to infection. Furthermore, even though the different blood groups and their incompatibility were discovered in 1900 and sodium citrate was used in 1913 to prevent clotting, full development of blood banks was not practical until the 1930s, when technology provided adequate refrigeration. Until that time, “fresh” donors were bled and the blood transfused while it was still warm.

Once these surgical suites were established, the employment of specifically designed pieces of medical technology assisted in further advancing the development of complex surgical procedures. For example, the Drinker respirator was introduced in 1927 and the first heart–lung bypass in 1939. By the 1940s, medical procedures heavily dependent on medical technology, such as cardiac catheterization and angiography (the use of a cannula threaded through an arm vein and into the heart with the injection of radiopaque dye) for the x-ray visualization of congenital and acquired heart disease (mainly valve disorders due to rheumatic fever) became possible, and a new era of cardiac and vascular surgery was established.

In the decades following World War II, technological advances were spurred on by efforts to develop superior weapon systems and to establish habitats in space and on the ocean floor. As a by-product of these efforts, the development of medical devices accelerated and the medical profession benefited greatly from this rapid surge of technological finds. Consider the following examples:

1. Advances in solid-state electronics made it possible to map the subtle behavior of the fundamental unit of the central nervous system—the neuron—as well as to monitor the various physiological parameters, such as the electrocardiogram, of patients in intensive care units.
2. New prosthetic devices became a goal of engineers involved in providing the disabled with tools to improve their quality of life.
3. Nuclear medicine—an outgrowth of the atomic age—emerged as a powerful and effective approach in detecting and treating specific physiological abnormalities.
4. Diagnostic ultrasound based on sonar technology became so widely accepted that ultrasonic studies are now part of the routine diagnostic workup in many medical specialties.
5. “Spare parts” surgery also became commonplace. Technologists were encouraged to provide cardiac assist devices, such as artificial heart valves and artificial blood vessels, and the artificial heart program was launched to develop a replacement for a defective or diseased human heart.
6. Advances in materials have made the development of disposable medical devices, such as needles and thermometers, a reality.
7. Advancements in molecular engineering have allowed for the discovery of countless pharmacological agents and to the design of their delivery, including implantable delivery systems.
8. Computers similar to those developed to control the flight plans of the Apollo capsule were used to store, process, and cross-check medical records, to monitor patient status in intensive care units, and to provide sophisticated statistical diagnoses of potential diseases correlated with specific sets of patient symptoms.
9. Development of the first computer-based medical instrument, the computerized axial tomography scanner, revolutionized clinical approaches to noninvasive diagnostic imaging procedures, which now include magnetic resonance imaging and positron emission tomography as well.
10. A wide variety of new cardiovascular technologies including implantable defibrillators and chemically treated stents were developed.
11. Neuronal pacing systems were used to detect and prevent epileptic seizures.
12. Artificial organs and tissue have been created.
13. The completion of the genome project has stimulated the search for new biological markers and personalized medicine.
14. The further understanding of cellular and biomolecular processes has led to the engineering of stem cells into therapeutically valuable lineages and to the regeneration of organs and tissue structures.

15. Developments in nanotechnology have yielded nanomaterials for use in tissue engineering and facilitated the creation and study of nanoparticles and molecular machine systems that will assist in the detection and treatment of disease and injury.

The impact of these discoveries and many others has been profound. The healthcare system of today consists of technologically sophisticated clinical staff operating primarily in modern hospitals designed to accommodate the new medical technology. This evolutionary process continues, with advances in the physical sciences such as materials and nanotechnology and in the life sciences such as molecular biology, genomics, stem cell biology, and artificial and regenerated tissue and organs. These advances have altered and will continue to alter the very nature of the healthcare delivery system itself.

Biomedical Engineering: A Definition

Bioengineering is usually defined as a basic research-oriented activity closely related to biotechnology and genetic engineering, that is, the modification of animal or plant cells or parts of cells to improve plants or animals or to develop new microorganisms for beneficial ends. In the food industry, for example, this has meant the improvement of strains of yeast for fermentation. In agriculture, bioengineers may be concerned with the improvement of crop yields by treatment of plants with organisms to reduce frost damage. It is clear that future bioengineers will have a tremendous impact on the quality of human life. The potential of this specialty is difficult to imagine. Consider the following activities of bioengineers:

- Development of improved species of plants and animals for food production
- Invention of new medical diagnostic tests for diseases
- Production of synthetic vaccines from clone cells
- Bioenvironmental engineering to protect human, animal, and plant life from toxicants and pollutants
- Study of protein–surface interactions
- Modeling of the growth kinetics of yeast and hybridoma cells
- Research in immobilized enzyme technology
- Development of therapeutic proteins and monoclonal antibodies

Biomedical engineers, on the other hand, apply electrical, mechanical, chemical, optical, and other engineering principles to understand, modify, or control biological (i.e., human and animal) systems as well as design and manufacture products that can monitor physiological functions and assist in the diagnosis and treatment of patients. When biomedical engineers work in a hospital or clinic, they are more aptly called clinical engineers.

Activities of Biomedical Engineers

The breadth of activity of biomedical engineers is now significant. The field has moved from being concerned primarily with the development of medical instruments in the 1950s and 1960s to include a more wide-ranging set of activities. As illustrated below, the field of biomedical engineering now includes many new career areas (see Figure P.1), each of which is presented in this handbook. These areas include

- Application of engineering system analysis (physiological modeling, simulation, and control) to biological problems
- Detection, measurement, and monitoring of physiological signals (i.e., biosensors and biomedical instrumentation)
- Diagnostic interpretation via signal-processing techniques of bioelectric data
- Therapeutic and rehabilitation procedures and devices (rehabilitation engineering)
- Devices for replacement or augmentation of bodily functions (artificial organs)

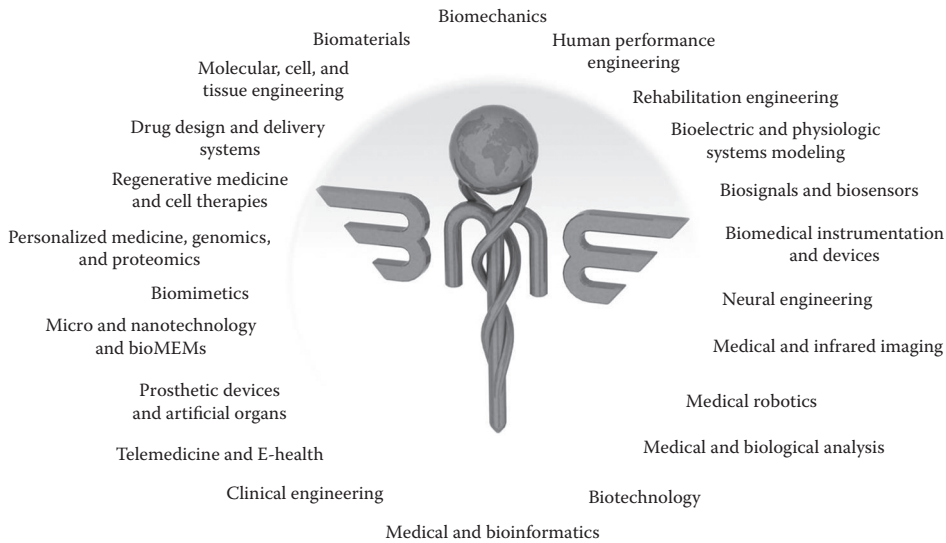


FIGURE P.1 The world of biomedical engineering.

- Computer analysis of patient-related data and clinical decision making (i.e., medical informatics and artificial intelligence)
- Medical imaging, that is, the graphic display of anatomic detail or physiological function
- The creation of new biological products (e.g., biotechnology and tissue engineering)
- The development of new materials to be used within the body (biomaterials)

Typical pursuits of biomedical engineers, therefore, include

- Research in new materials for implanted artificial organs
- Development of new diagnostic instruments for blood analysis
- Computer modeling of the function of the human heart
- Writing software for analysis of medical research data
- Analysis of medical device hazards for safety and efficacy
- Development of new diagnostic imaging systems
- Design of telemetry systems for patient monitoring
- Design of biomedical sensors for measurement of human physiological systems variables
- Development of expert systems for diagnosis of disease
- Design of closed-loop control systems for drug administration
- Modeling of the physiological systems of the human body
- Design of instrumentation for sports medicine
- Development of new dental materials
- Design of communication aids for the handicapped
- Study of pulmonary fluid dynamics
- Study of the biomechanics of the human body
- Development of material to be used as a replacement for human skin

Biomedical engineering, then, is an interdisciplinary branch of engineering that ranges from theoretical, nonexperimental undertakings to state-of-the-art applications. It can encompass research, development, implementation, and operation. Accordingly, like medical practice itself, it is unlikely that any single person can acquire expertise that encompasses the entire field. Yet, because of the

interdisciplinary nature of this activity, there is considerable interplay and overlapping of interest and effort between them. For example, biomedical engineers engaged in the development of biosensors may interact with those interested in prosthetic devices to develop a means to detect and use the same bioelectric signal to power a prosthetic device. Those engaged in automating clinical chemistry laboratories may collaborate with those developing expert systems to assist clinicians in making decisions based on specific laboratory data. The possibilities are endless.

Perhaps, a greater potential benefit occurring from the use of biomedical engineering is identification of the problems and needs of our present healthcare system that can be solved using existing engineering technology and systems methodology. Consequently, the field of biomedical engineering offers hope in the continuing battle to provide high-quality care at a reasonable cost. If properly directed toward solving problems related to preventive medical approaches, ambulatory care services, and the like, biomedical engineers can provide the tools and techniques to make our healthcare system more effective and efficient and, in the process, improve the quality of life for all.

Joseph D. Bronzino
Donald R. Peterson
Editors-in-Chief

MATLAB® and Simulink® are registered trademarks of The MathWorks, Inc. For product information, please contact:

The MathWorks, Inc.
3 Apple Hill Drive
Natick, MA 01760-2098 USA
Tel: 508 647 7000
Fax: 508-647-7001
E-mail: info@mathworks.com
Web: www.mathworks.com

Editors

Joseph D. Bronzino is currently the president of the Biomedical Engineering Alliance and Consortium (BEACON; www.beaconalliance.org), which is a nonprofit organization dedicated to the promotion of collaborative research, translation, and partnership among academic, medical, and industry people in the field of biomedical engineering to develop new medical technologies and devices. To accomplish this goal, Dr. Bronzino and BEACON facilitate collaborative research, industrial partnering, and the development of emerging companies. Dr. Bronzino earned a BSEE from Worcester Polytechnic Institute, Worcester, Massachusetts, in 1959, an MSEE from the Naval Postgraduate School, Monterey, California, in 1961, and a PhD in electrical engineering from Worcester Polytechnic Institute in 1968. He was recently the Vernon Roosa Professor of Applied Science and endowed chair at Trinity College, Hartford, Connecticut.

Dr. Bronzino is the author of over 200 journal articles and 15 books, including *Technology for Patient Care* (C.V. Mosby, 1977), *Computer Applications for Patient Care* (Addison-Wesley, 1982), *Biomedical Engineering: Basic Concepts and Instrumentation* (PWS Publishing Co., 1986), *Expert Systems: Basic Concepts* (Research Foundation of State University of New York, 1989), *Medical Technology and Society: An Interdisciplinary Perspective* (MIT Press and McGraw-Hill, 1990), *Management of Medical Technology* (Butterworth/Heinemann, 1992), *The Biomedical Engineering Handbook* (CRC Press, 1st Edition, 1995; 2nd Edition, 2000; 3rd Edition, 2006), *Introduction to Biomedical Engineering* (Academic Press, 1st Edition, 1999; 2nd Edition, 2005; 3rd Edition, 2011), *Biomechanics: Principles and Applications* (CRC Press, 2002), *Biomaterials: Principles and Applications* (CRC Press, 2002), *Tissue Engineering* (CRC Press, 2002), and *Biomedical Imaging* (CRC Press, 2002).

Dr. Bronzino is a fellow of IEEE and the American Institute of Medical and Biological Engineering (AIMBE), an honorary member of the Italian Society of Experimental Biology, past chairman of the Biomedical Engineering Division of the American Society for Engineering Education (ASEE), a charter member of the Connecticut Academy of Science and Engineering (CASE), a charter member of the American College of Clinical Engineering (ACCE), a member of the Association for the Advancement of Medical Instrumentation (AAMI), past president of the IEEE-Engineering in Medicine and Biology Society (EMBS), past chairman of the IEEE Health Care Engineering Policy Committee (HCEPC), and past chairman of the IEEE Technical Policy Council in Washington, DC. He is a member of Eta Kappa Nu, Sigma Xi, and Tau Beta Pi. He is also a recipient of the IEEE Millennium Medal for “his contributions to biomedical engineering research and education” and the Goddard Award from WPI for Outstanding Professional Achievement in 2005. He is presently editor-in-chief of the Academic Press/Elsevier BME Book Series.

Donald R. Peterson is a professor of engineering and the dean of the College of Science, Technology, Engineering, Mathematics, and Nursing at Texas A&M University in Texarkana, Texas, and holds a joint appointment in the Department of Biomedical Engineering (BME) at Texas A&M University in College Station, Texas. He was recently an associate professor of medicine and the director of the

Biodynamics Laboratory in the School of Medicine at the University of Connecticut (UConn) and served as chair of the BME Program in the School of Engineering at UConn as well as the director of the BME Graduate and Undergraduate Programs. Dr. Peterson earned a BS in aerospace engineering and a BS in biomechanical engineering from Worcester Polytechnic Institute, in Worcester, Massachusetts, in 1992, an MS in mechanical engineering from the UConn, in Storrs, Connecticut, in 1995, and a PhD in biomedical engineering from UConn in 1999. He has 17 years of experience in BME education and has offered graduate-level and undergraduate-level courses in the areas of biomechanics, biodynamics, biofluid mechanics, BME communication, BME senior design, and ergonomics, and has taught subjects such as gross anatomy, occupational biomechanics, and occupational exposure and response in the School of Medicine. Dr. Peterson was also recently the co-executive director of the Biomedical Engineering Alliance and Consortium (BEACON), which is a nonprofit organization dedicated to the promotion of collaborative research, translation, and partnership among academic, medical, and industry people in the field of biomedical engineering to develop new medical technologies and devices.

Dr. Peterson has over 21 years of experience in devices and systems and in engineering and medical research, and his work on human–device interaction has led to applications on the design and development of several medical devices and tools. Other recent translations of his research include the development of devices such as robotic assist devices and prosthetics, long-duration biosensor monitoring systems, surgical and dental instruments, patient care medical devices, spacesuits and space tools for NASA, powered and non-powered hand tools, musical instruments, sports equipment, computer input devices, and so on. Other overlapping research initiatives focus on the development of computational models and simulations of biofluid dynamics and biomechanical performance, cell mechanics and cellular responses to fluid shear stress, human exposure and response to vibration, and the acoustics of hearing protection and communication. He has also been involved clinically with the Occupational and Environmental Medicine group at the UConn Health Center, where his work has been directed toward the objective engineering analysis of the anatomic and physiological processes involved in the onset of musculoskeletal and neuromuscular diseases, including strategies of disease mitigation.

Dr. Peterson's scholarly activities include over 50 published journal articles, 2 textbook chapters, 2 textbook sections, and 12 textbooks, including his new appointment as co-editor-in-chief for *The Biomedical Engineering Handbook* by CRC Press.

Contributors

James J. Abbas

School of Biological and Health Systems
Engineering
Arizona State University
Tempe, Arizona

Amit Abraham

School for Engineering of Matter, Transport
and Energy
Arizona State University
Tempe, Arizona

Jose F. Alvarez-Barreto

Human Tissue Engineering Laboratory
Ciencia y Tecnologia para la Salud
Instituto de Estudios Avanzados
Caracas, Venezuela

Badriprasad Ananthanarayanan

Department of Bioengineering
University of California, Berkeley
Berkeley, California

Helim Aranda-Espinoza

Fischell Department of Bioengineering
University of Maryland
College Park, Maryland

Sivakkumar Arjunon

Wallace H. Coulter Department of Biomedical
Engineering
Georgia Institute of Technology
and
Emory University
Atlanta, Georgia

Mohammad A. Ataai

University of Pittsburgh
Pittsburgh, Pennsylvania

Anthony Atala

Wake Forest Institute for Regenerative
Medicine
Wake Forest University School of
Medicine
Winston-Salem, North Carolina

Pramod K. Avti

Department of Biomedical Engineering
Stony Brook University
Stony Brook, New York

James W. Baish

Department of Biomedical Engineering
Bucknell University
Lewisburg, Pennsylvania

Mark R. Battig

Department of Chemical, Materials and
Biomolecular Engineering
University of Connecticut
Storrs, Connecticut

Céline L. Bauwens

Department of Chemical Engineering and
Applied Chemistry
University of Toronto
Toronto, Canada

Hugh Benhardt

Department of Biomedical
Engineering
Texas A&M University
College Station, Texas

William Bentley

Biotechnology Institute
University of Maryland
Baltimore, Maryland

Michael Betenbaugh

Johns Hopkins University
Baltimore, Maryland

Sarindr Bhumiratana

Department of Biomedical
Engineering
Columbia University
New York, New York

Nicole Bleckwenn

Biotechnology Institute
University of Maryland
Baltimore, Maryland

Anjun K. Bose

Department of Biomedical Engineering
University of Virginia
Charlottesville, Virginia

Eric M. Brey

Pritzker Institute of Biomedical Science and
Engineering
Department of Biomedical Engineering
Illinois Institute of Technology
and
Research Service
Edward Hines Jr. Veterans Hospital
Chicago, Illinois

Robert S. Brown, Jr.

New York Presbyterian Hospital
Columbia University
New York, New York

Stephanie J. Bryant

Department of Chemical and Biological
Engineering
University of Colorado
Boulder, Colorado

Emily Burdett

Department of Bioengineering
BioScience Research Collaborative
Houston, Texas

Jason A. Burdick

Department of Bioengineering
University of Pennsylvania
Philadelphia, Pennsylvania

Joaquim M.S. Cabral

Institute for Biotechnology and
Bioengineering
and
Centre for Biological and Chemical
Engineering
Instituto Superior Tecnico
Lisbon, Portugal

Pedro Cabrales

Department of Bioengineering
University of California, San Diego
La Jolla, California

Fernando Casas

Advanced Product Development
HeartWare, Inc.
Miami Lakes, Florida

Andrea Caumo

San Raffaele Scientific Institute
Milan, Italy

Matthew S. Chang

New York Presbyterian Hospital
Columbia University
New York, New York

X.G. Chen

Department of Chemical and Biomolecular
Engineering
Tulane University
New Orleans, Louisiana

Yong Woo Cho

Division of Materials Science and Chemical
Engineering
Hanyang University
Seoul, South Korea

Charles S. Chung

Cardiovascular Biophysics Laboratory
Washington University
St. Louis, Missouri

Elisa Cimetta

Department of Biomedical Engineering
Columbia University
New York, New York

Curt I. Civin

Center for Stem Cell Biology and Regenerative
Medicine
University of Maryland School of Medicine
Baltimore, Maryland

Emily E. Coates

Fischell Department of Bioengineering
University of Maryland
College Park, Maryland

Claudio Cobelli

University of Padua
Padua, Italy

Keith E. Cook

Department of Surgery and Biomedical
Engineering
University of Michigan
Ann Arbor, Michigan

Raul Cortes

Brigham and Women's Hospital
Boston, Massachusetts

Elizabeth Cosgriff-Hernández

Department of Biomedical Engineering
Texas A&M University
College Station, Texas

Carlo Crepaldi

Nephrology Department
St. Bortolo Hospital
Vicenza, Italy

Rena N. D'Souza

Department of Biomedical Sciences
Texas A&M Health Science Center—Baylor
College of Dentistry
Dallas, Texas

Samuel Darko

National Institutes of Health
National Institutes for Allergies and Infectious
Diseases
Vaccine Research Center
Bethesda, Maryland

Cláudia Lobato da Silva

Institute for Biotechnology and
Bioengineering
and
Centre for Biological and Chemical
Engineering
Instituto Superior Tecnico
Lisbon, Portugal

Michael S. Detamore

Department of Chemical and Petroleum
Engineering
University of Kansas
Lawrence, Kansas

Maria Margarida Diogo

Institute for Biotechnology and Bioengineering
and
Centre for Biological and Chemical
Engineering
Instituto Superior Tecnico
Lisbon, Portugal

Michael M. Domach

Carnegie Mellon
Pittsburgh, Pennsylvania

Nathan R. Domagalski

Bristol-Myers Squibb
New Brunswick, New Jersey

D. John Doyle

Department of General Anesthesiology
Cleveland Clinic
Case Western Reserve University
Cleveland, Ohio

Gary M. Drzewiecki

Department of Biomedical Engineering
Rutgers University
New Brunswick, New Jersey

John Denis Enderle

University of Connecticut
Storrs, Connecticut

Brandon W. Engebretson

Department of Bioengineering
University of Oklahoma
Norman, Oklahoma

Mandy B. Esch

Department of Biomedical Engineering and
School of Chemical and Biomolecular
Engineering
Cornell University
Ithaca, New York

Carla Estremadoyro

Nephrology Department
St. Bortolo Hospital
Vicenza, Italy

Y.L. Fang

Department of Chemical and Biomolecular
Engineering
Tulane University
New Orleans, Louisiana

William J. Federspiel

Department of Biomedical Engineering
Departments of Critical Care Medicine and
Chemical Engineering
McGowan Institute of Regenerative Medicine
University of Pittsburgh
Pittsburgh, Pennsylvania

Tiago G. Fernandes

Institute for Biotechnology and
Bioengineering
and
Centre for Biological and Chemical
Engineering
Instituto Superior Tecnico
Lisbon, Portugal

John P. Fisher

Fischell Department of Bioengineering
University of Maryland
College Park, Maryland

Robert J. Fisher

SABRE Institute and Department of Chemical
Engineering
Massachusetts Institute of Technology
Cambridge, Massachusetts

Krista M. Fridley

Department of Biomedical Engineering
University of Texas, Austin
Austin, Texas

Bingmei M. Fu

Department of Biomedical Engineering
City College of the City University of New York
New York, New York

Kerstin M. Galler

Department of Restorative Dentistry and
Periodontology
University of Regensburg
Regensburg, Germany

Joseph Garlow

Department of Biomedical Engineering
Stony Brook University
Stony Brook, New York

Donald P. Gaver III

Department of Biomedical Engineering
Tulane University
New Orleans, Louisiana

Hamidreza Ghandehari

Departments of Pharmaceutics and
Pharmaceutical Chemistry, and
Bioengineering
University of Utah
Salt Lake City, Utah

W.T. Godbey

Department of Chemical and Biomolecular
Engineering
Tulane University
New Orleans, Louisiana

Warren Grayson

Department of Biomedical Engineering
Johns Hopkins University
Baltimore, Maryland

Rohini Gupta

Department of Bioengineering
University of California, Berkeley
Berkeley, California

Sarina G. Harris

Department of Biomedical Engineering and
School of Chemical and Biomolecular
Engineering
Cornell University
Ithaca, New York

Kevin E. Healy

Department of Bioengineering
and
Department of Materials Science and
Engineering
University of California, Berkeley
Berkeley, California

Sarah C. Heilshorn

Department of Materials Science and
Engineering
Stanford University
Stanford, California

Amy E. Herr

Bioengineering
University of California, Berkeley
Berkeley, California

C. Holladay

Network of Excellence for Functional
Biomaterials
National University of Ireland
Galway, Ireland

Marcos Intaglietta

Department of Bioengineering
University of California, San Diego
San Diego, California

Anne-Marie Jacob

Department of Biomedical Engineering
Tulane University
New Orleans, Louisiana

Kevin A. Janes

Department of Biomedical Engineering
University of Virginia
Charlottesville, Virginia

John A. Jansen

Department of Biomaterials
Radboud University Nijmegen
Medical Center
Nijmegen, The Netherlands

Karin J. Jensen

Department of Biomedical Engineering
University of Virginia
Charlottesville, Virginia

Peter C. Johnson

Research and Development
Avery-Dennison Medical Solutions
Chicago, Illinois

and

Scintellix, LLC
Raleigh, North Carolina

Indong Jun

Department of Bioengineering
Hanyang University
Seoul, Korea

Kimberly R. Kam

Department of Materials Science and
Engineering
University of California, Berkeley
Berkeley, California

David L. Kaplan

Department of Biomedical Engineering
Tufts University
Medford, Massachusetts

Ian M. Kaplan

Program in Cellular and Molecular
Medicine
Johns Hopkins School of Medicine
and
Center for Stem Cell Biology and Regenerative
Medicine
University of Maryland School of Medicine
Baltimore, Maryland

Pradeep K. Karla

Department of Pharmaceutical Sciences
School of Pharmacy
Howard University
Washington, DC

F. Kurtis Kasper

Department of Bioengineering
Rice University
Houston, Texas

Joshua S. Katz

Dow Chemical Company
Spring House, Pennsylvania

Ali Khademhosseini

WPI Advanced Institute for Materials Research
Tohoku University
Sendai, Japan

and

Department of Medicine
Brigham and Women's Hospital
Harvard Medical School
and
Harvard-MIT Division of Health Sciences and
Technology
Massachusetts Institute of Technology
Cambridge, Massachusetts

Yusef Khan

University of Connecticut Health Center
Farmington, Connecticut

Nora Khanarian

Columbia University
New York, New York

Jong-Ryoul Kim

Division of Materials Science and Chemical
Engineering
Hanyang University
Seoul, Korea

Min Sup Kim

Department of Bioengineering
Hanyang University
Seoul, Korea

Lucas A. Kinard

Department of Bioengineering
Rice University
Houston, Texas

Melissa A. Kinney

Georgia Institute of Technology
Atlanta, Georgia

In Kap Ko

Wake Forest Institute for Regenerative
Medicine
Wake Forest University School of Medicine
Winston-Salem, North Carolina

Sándor J. Kovács

Cardiovascular Biophysics Laboratory
Washington University
St. Louis, Missouri

M. Kulkarni

Network of Excellence for Functional
Biomaterials
National University of Ireland
Galway, Ireland

Sanjay Kumar

Department of Bioengineering
University of California, Berkeley
Berkeley, California

Cato Laurencin

University of Connecticut Health Center
Farmington, Connecticut

Georges St. Laurent III

Immunovirology – Biogenesis Group
University of Antioquia
Medellin, Colombia

Byung Kook Lee

Division of Materials Science and Chemical
Engineering
Hanyang University
Seoul, Korea

Elaine L. Lee

Department of Biomedical Engineering
Case Western Reserve University
Cleveland, Ohio

Ji-Hye Lee

Department of Bioengineering
Hanyang University
Seoul, Korea

Sander C.G. Leeuwenburgh

Department of Biomaterials
Radboud University Nijmegen
Medical Center
Nijmegen, The Netherlands

John K-J. Li

Department of Biomedical Engineering
Rutgers University
Piscataway, New Jersey

Xinran Li

Department of Biomedical Engineering
School of Chemical and Biomolecular
Engineering
Cornell University
Ithaca, New York

E.N. Lightfoot

Department of Chemical and Biological
Engineering
University of Wisconsin
Madison, Wisconsin

Yen-Chih Lin

Department of Plastic Surgery
University of Pittsburgh
Pittsburgh, Pennsylvania

Mark W. Linder

School of Medicine
University of Louisville
and
PGXL Laboratories, LLC
Louisville, Kentucky

Helen H. Lu

Department of Biomedical Engineering
Columbia University
New York, New York

Joseph A. Ludwig

Department of Sarcoma Medical Oncology
MD Anderson Cancer Center
University of Texas
Houston, Texas

Nanda K. Mandava

Division of Pharmaceutical Sciences
School of Pharmacy
University of Missouri, Kansas City
Kansas City, Missouri

João Filipe Mano

3B's Research Group—Biomaterials,
Biodegradables, and Biomimetics
University of Minho
and
ICVS/3B's
PT Government Associated Laboratory
Guimaraes, Portugal

Jeremy J. Mao

Tissue Engineering and Regenerative Medicine
Laboratory
Center for Craniofacial Regeneration
Columbia University Medical Center
New York, New York

Vasilis Z. Marmarelis

Department of Biomedical Engineering
Viterbi School of Engineering
University of Southern California
Los Angeles, California

Kacey G. Marra

Departments of Plastic Surgery and
Bioengineering
University of Pittsburgh
Pittsburgh, Pennsylvania

David Martin

Department of Biomedical Engineering
Tulane University
New Orleans, Louisiana

Francesca Katiana Martino

Nephrology Department
St. Bortolo Hospital
Vicenza, Italy

Timothy M. Maul

Department of Cardiothoracic Surgery
Children's Hospital of Pittsburgh
University of Pittsburgh Medical Center
Pittsburgh, Pennsylvania

Timothy A. McCaffrey

Department of Medicine
George Washington University
Medical Center
Washington, DC

Todd C. McDevitt

Georgia Institute of Technology
Atlanta, Georgia

Jonathan W. Meade

Carnegie Mellon
Pittsburgh, Pennsylvania

Kunal Mehtani

Division of Internal Medicine
Kaiser Permanente
San Francisco, California

Antonios G. Mikos

Department of Bioengineering
Rice University
Houston, Texas

W. Minor

Network of Excellence for Functional
Biomaterials
National University of Ireland
Galway, Ireland

Ashim K. Mitra

Division of Pharmaceutical Sciences
School of Pharmacy
University of Missouri, Kansas City
Kansas City, Missouri

Ranjana Mitra

Division of Pharmaceutical Sciences
School of Pharmacy
University of Missouri, Kansas City
Kansas City, Missouri

Kristen Moffat

Columbia University
New York, New York

Sebastien Morisot

Center for Stem Cell Biology and Regenerative
Medicine
University of Maryland School of
Medicine
Baltimore, Maryland

Monica L. Moya

Department of Biomedical
Engineering
University of California, Irvine
Irvine, California

Madhusudan Natarajan

Quantitative Biotherapeutics Modeling Group
Shire Pharmaceuticals
Cambridge, Massachusetts

Hemin Nie

Tissue Engineering and Regenerative
Medicine Laboratory
Center for Craniofacial Regeneration
Columbia University Medical Center
New York, New York

Abraham Noordergraaf

Cardiovascular Studies Unit
University of Pennsylvania
Philadelphia, Pennsylvania

Gerrit J. Noordergraaf

Department of Anesthesia and
Resuscitation
St. Elisabeth Hospital
Tilburg, The Netherlands

Leann L. Norman

Fischell Department of Bioengineering
University of Maryland
College Park, Maryland

Joaquim Miguel Oliveira

3B's Research Group—Biomaterials,
Biodegradables, and Biomimetics
University of Minho
and
ICVS/3B's
PT Government Associated
Laboratory
Guimaraes, Portugal

Grace O'Malley

Department of Biomedical Engineering
Stony Brook University
Stony Brook, New York

Dennis P. Orgill

Brigham and Women's Hospital
Boston, Massachusetts

Sean P. Palecek

Department of Chemical and Biological
Engineering
University of Wisconsin, Madison
and
WiCell Research Institute
Madison, Wisconsin

Joseph L. Palladino

Department of Engineering
Trinity College
Hartford, Connecticut

Abhay Pandit

Network of Excellence Functional
Biomaterials
National University of Ireland
Galway, Ireland

Andreina Parisi-Amon

Department of Bioengineering
Stanford University
Stanford, California

Kinam Park

Departments of Biomedical Engineering
and Pharmaceutics
Purdue University
West Lafayette, Indiana

Sulabh Patel

Division of Pharmaceutical Sciences
School of Pharmacy
University of Missouri, Kansas City
Kansas City, Missouri

Sunny C. Patel

Department of Biomedical
Engineering
Stony Brook University
Stony Brook, New York

Durga K. Paturi

Division of Pharmaceutical Sciences
School of Pharmacy
University of Missouri, Kansas City
Kansas City, Missouri

Igor W.F. Paulussen

Department of Anesthesia and
Resuscitation
St. Elisabeth Hospital
Tilburg, The Netherlands
and

Philips Research, BioSensing Systems
High Tech Campus
Eindhoven, The Netherlands

Robert A. Peattie

Department of Biomedical Engineering
Tufts University
Medford, Massachusetts

Ameya Phadke

Department of Bioengineering
University of California, San Diego
La Jolla, California

Chi-Sang Poon

Institute for Medical Engineering and Science
Massachusetts Institute of Technology
Cambridge, Massachusetts

Dejan B. Popović

University of Belgrade
Belgrade, Serbia

Mirjana B. Popović

University of Belgrade
Belgrade, Serbia

Kelly A. Purpura

Department of Chemical Engineering and
Applied Chemistry
University of Toronto
Toronto, Canada

Yuchen Qiu

Cordis Corporation
Bridgewater, New Jersey

Milica Radisic

Department of Chemical Engineering and
Applied Chemistry
University of Toronto
Toronto, Ontario, Canada

Murugan Ramalingam

WPI Advanced Institute for Materials Research
Tohoku University
Sendai, Japan

Animikh Ray

Division of Pharmaceutical Sciences
School of Pharmacy
University of Missouri, Kansas City
Kansas City, Missouri

A. Hari Reddi

University of California, Davis
Davis, California

Katherine R. Regan

Department of Biomedical Sciences
Texas A&M Health Science Center—
Baylor College of Dentistry
Dallas, Texas

Rui Luís Reis

3B's Research Group—Biomaterials,
Biodegradables, and Biomimetics
University of Minho
and
ICVS/3B's
PT Government Associated Laboratory
Guimaraes, Portugal

Maria Pia Rodighiero

Nephrology Department
St. Bortolo Hospital
Vicenza, Italy

Carlos A.V. Rodrigues

Institute for Biotechnology and Bioengineering
and
Centre for Biological and Chemical Engineering
Instituto Superior Tecnico
Lisbon, Portugal

Claudio Ronco

Nephrology Department
St. Bortolo Hospital
Vicenza, Italy

Gerson Rosenberg

Pennsylvania State University
State College, Pennsylvania

Krishnendu Roy

Department of Biomedical Engineering
University of Texas, Austin
Austin, Texas

Gualberto Ruaño

Genomas, Inc.
and
Genetics Research Center
Hartford Hospital
Hartford, Connecticut

Gordon Rule

Department of Biological Sciences
Carnegie Mellon University
Pittsburgh, Pennsylvania

Maria Pia Saccomani

University of Padua
Padua, Italy

Neelakantan Saikrishnan

Wallace H. Coulter Department of
Biomedical Engineering
Georgia Institute of Technology
and
Emory University
Atlanta, Georgia

Shelly Sakiyama-Elbert

Department of Biomedical Engineering
Washington University in St. Louis
St. Louis, Missouri

W. Mark Saltzman

Department of Biomedical Engineering
Yale University
New Haven, Connecticut

Athanassios Sambanis

School of Chemical and Biomolecular
Engineering
Georgia Institute of Technology
Atlanta, Georgia

Kemal Sariibrahimoglu

Department of Biomaterials
Radboud University Nijmegen Medical
Center
Nijmegen, The Netherlands

Tina Sauerwald

Johns Hopkins University
Baltimore, Maryland

Jeffrey M. Savard

Merck & Co.
Kenilworth, New Jersey

David V. Schaffer

Department of Chemical Engineering
and
Department of Bioengineering
and
Helen Wills Neuroscience Institute
University of California, Berkeley
Berkeley, California

Gert Jan Scheffer

Department of Anesthesiology
University Medical Center Nijmegen
St Radboud
Nijmegen, The Netherlands

James W. Schneider

Carnegie Mellon University
Pittsburgh, Pennsylvania

Nicholas Sears

Department of Biomedical Engineering
Texas A&M University
College Station, Texas

Richard L. Seip

Genomas, Inc.
Hartford, Connecticut

Monica A. Serban

Department of Biomedical Engineering
Tufts University
Medford, Massachusetts

Song P. Seto

Department of Biomedical Engineering
Georgia Institute of Technology
and
Emory University
Atlanta, Georgia

Songtao Shi

Center for Craniofacial Biology
University of Southern California School of
Dentistry
Los Angeles, California

Heungsoo Shin

Department of Bioengineering
Hanyang University
Seoul, Korea

Young Min Shin

Department of Bioengineering
Hanyang University
Seoul, South Korea

Leonid Shmuylovich

Cardiovascular Biophysics Laboratory
Washington University
St. Louis, Missouri

Michael L. Shuler

Department of Biomedical Engineering and
School of Chemical and Biomolecular
Engineering
Cornell University
Ithaca, New York

Vasillios I. Sikavitsas

Department of Bioengineering
University of Oklahoma
Norman, Oklahoma

Nicholas E. Simpson

Department of Medicine
University of Florida
Gainesville, Florida

Balaji Sitharaman

Department of Biomedical Engineering
Stony Brook University
Stony Brook, New York

Giovanni Sparacino

University of Padua
Padua, Italy

Kimberly M. Stroka

Fischell Department of Bioengineering
University of Maryland
College Park, Maryland

Siddarth Subramony

Columbia University
New York, New York

Laura J. Suggs

Department of Biomedical Engineering
University of Texas, Austin
Austin, Texas

Nina Tandon

Department of Biomedical Engineering
Columbia University
New York, New York

John M. Tarbell

Department of Biomedical Engineering
The City College of the City University of
New York
New York, New York

Johnna S. Temenoff

Department of Biomedical Engineering
Georgia Institute of Technology
and
Emory University
Atlanta, Georgia

Giridhar Thiagarajan

Bard Access Systems
Salt Lake City, Utah

W.D. Timmons

CGK Consultants, LLC
Hilliard, Ohio

Gianna Maria Toffolo

Department of Information Engineering
University of Padua
Padua, Italy

Ian Toma

Department of Medicine
George Washington University Medical Center
Washington, DC

Tyler Touchet

Department of Biomedical Engineering
Texas A&M University
College Station, Texas

Amy G. Tsai

Department of Bioengineering
University of California, San Diego
La Jolla, California

Pushpinder Uppal

Department of Biomedical Engineering
Stony Brook University
Stony Brook, New York

Roland Valdes, Jr.

University of Louisville School of Medicine
and
PGXL Laboratories LLC
Louisville, Kentucky

Samuel B. VanGordon

Department of Bioengineering
University of Oklahoma
Norman, Oklahoma

Shyni Varghese

Department of Bioengineering
University of California, San Diego
La Jolla, California

Alyssa Venema

Department of Surgery
St. Elisabeth Hospital
Tilburg, The Netherlands

Horst A. von Recum

Department of Biomedical Engineering
Case Western Reserve University
Cleveland, Ohio

Gordana Vunjak-Novakovic

Department of Biomedical
Engineering
Columbia University
New York, New York

Prinda Wanakule

Department of Biomedical Engineering
University of Texas, Austin
Austin, Texas

Martha O. Wang

Fischell Department of
Bioengineering
University of Maryland
College Park, Maryland

Yong Wang

Department of Chemical, Materials and
Biomolecular Engineering
University of Connecticut
Storrs, Connecticut

Stephanie Willerth

Department of Mechanical
Engineering
and
Division of Medical Sciences
University of Victoria
Victoria, British Columbia, Canada
and

International Collaboration On Repair
Discoveries (ICORD)
University of British Columbia
Vancouver, British Columbia, Canada

Andreas Windemuth

Genomas, Inc.
and
Genetics Research Center
Hartford Hospital
Hartford, Connecticut

Joop G.C. Wolke

Department of Biomaterials
Radboud University Nijmegen Medical
Center
Nijmegen, The Netherlands

Alan H.B. Wu

Department of Laboratory Medicine
University of California, San Francisco
San Francisco, California

Ioannis V. Yannas

Massachusetts Institute of Technology
Cambridge, Massachusetts

Pamela C. Yelick

Tufts University School of Dental Medicine
Boston, Massachusetts

Ajit P. Yoganathan

Wallace H. Coulter Department of Biomedical
Engineering
Georgia Institute of Technology
and
Emory University
Atlanta, Georgia

James J. Yoo

Wake Forest Institute for Regenerative Medicine
Wake Forest University School of
Medicine
Winston-Salem, North Carolina

Fan Yuan

Department of Biomedical Engineering
Duke University
Durham, North Carolina

Peter W. Zandstra

Department of Chemical Engineering and
Applied Chemistry
University of Toronto
and
McEwen Centre for Regenerative
Medicine
University Health Network
and
Heart and Stroke Richard Lewar Centre of
Excellence
Toronto, Canada

Weibo Zhang

Tufts University School of Dental
Medicine
Boston, Massachusetts

Jing Zhou

Department of Chemical, Materials and
Biomolecular Engineering
University of Connecticut
Storrs, Connecticut

Ying Zhu

Adow Innovation
Robbinsville, New Jersey

Kyriacos Zygorakis

Department of Chemical and Biomolecular
Engineering
Rice University
Houston, Texas



Molecular Biology

Michael M. Domach
Carnegie Mellon University

1 Historical Perspective and Basics of Molecular Biology <i>Nathan R. Domagalski and Michael M. Domach</i>	1-1
Introduction • Molecular Biology: A Historical Perspective • Central Dogma of Modern Molecular Biology • Molecular Biology Leads to a Refined Classification of Cells • Mutations • Nucleic Acid Processing Mechanisms and Inspired Technologies with Medical and Other Impacts • Probing Gene Expression • Internet Resources • References and Recommended Further Reading • Backgrounds on Some Molecular Biology Pioneers • Databases and Other Supplementary Materials on Molecular Biology	
2 Biomolecular Interactions <i>Gordon Rule</i>	2-1
Overview of Molecular Forces • Ligand Binding • Isothermal Titration Calorimetry • Surface Plasmon Resonance • Nuclear Magnetic Resonance Spectroscopy • X-Ray Diffraction Methods • Computational Methods • Emerging Techniques: Single Molecules • References	
3 Recent Advances in DNA Separations: Plasmid Purification, Rapid Electrophoresis, and Affinity-Based Recovery <i>James W. Schneider and Jeffrey M. Savard</i>	3-1
Introduction • Advances in Plasmid DNA Purification • Advances in Electrophoretic DNA Separations • Advances in Affinity-Based DNA and RNA Recovery • Conclusions • References	
4 Systems and Technology Involving Bacteria <i>Nicole Bleckwenn and William Bentley</i>	4-1
Introduction • Elements for Expression • A Cell-to-Cell Communications Operon • Marker Proteins • Growth of Bacterial Cultures • Regulons • Engineering the System • Emerging Technologies and Issues • Final Remarks • References	
5 Expression in Mammalian Cells <i>Tina Sauerwald and Michael Betenbaugh</i>	5-1
Introduction • Vector Design • Inducible Systems • Cell Lines • Transfection Methods • Transient versus Stable Transfection • Selectable Markers • Single Cell Cloning Methods • References	
6 DNA Vaccines Production and Engineering <i>Michael M. Domach, Jonathan W. Meade, and Mohammad A. Ataai</i>	6-1
Introduction • DNA Vaccine Plasmid Design • Issues in Plasmid Design • DNA Vaccine Production at a Large Scale • Prospects for Improvement • Final Remarks • References	

Preface

Molecular biology is the one answer to the question, “How can the understanding of cell and whole organism behavior be made to be more deterministic and mechanistic?” Isolating the working parts of cells and then deciphering how they interact and connect to make a functional whole is the impetus. Behind the action of all the molecular “hardware” lies the information encoded in DNA, which provides the instructions for a building, maintaining, and adapting a sustainable system. Once prevalent mainly in the confines of basic science laboratories, molecular biology ideas and methodologies now span applications that range from inspiring new clinical trials to solving crimes.

This section of this edition of the Handbook is double that of the last edition. Chapter 1 provides some historical background and basic working knowledge. It has been updated to include a glossary of current terms, useful websites, the importance of measuring plasmid copy number in some applications, and getting the most from kits. Because molecular biology is by definition molecule-centric, and intermolecular interactions result in whether gene expression and other important events occur or not, Chapter 2 is a new contribution that provides an up-to-date look at interactions and the means used to explore and quantify their nature. Because DNA encodes the information for molecular biology to occur, Chapter 3 is a new contribution that covers DNA isolation and sequencing. Chapters 4 and 5 present applications in microbial and animal cell systems. Additions in cultivation techniques and long pathway engineering can be found in Chapter 4. RNA silencing methods and examples have been added to update Chapter 5. Chapter 6 is a new contribution that illustrates one medical impact of molecular biology. The basics and challenges of DNA vaccines are described. Additionally, a survey of ongoing clinical trials is presented in web-linked form.

1

Historical Perspective and Basics of Molecular Biology

1.1	Introduction	1-1
1.2	Molecular Biology: A Historical Perspective	1-2
1.3	Central Dogma of Modern Molecular Biology.....	1-3
	DNA Base Composition, Connectivity, and Structure • Base Sequence, Information, and Genes • Codon Information to a Protein • DNA Replication • mRNA Dynamics • Variations and Refinements of the Central Dogma	
1.4	Molecular Biology Leads to a Refined Classification of Cells	1-9
1.5	Mutations	1-10
1.6	Nucleic Acid Processing Mechanisms and Inspired Technologies with Medical and Other Impacts.....	1-11
	Nucleic Acid Modification Enzymes • Copying DNA in the Laboratory • Basic Bacterial Transformation Techniques • Measuring Plasmid Copy Number • Deliberate Mutagenesis • Getting the Most from Kits • Transfecting Eukaryotic Cells	
1.7	Probing Gene Expression	1-21
	DNA Microarrays Profile Many Gene Expression Events	
1.8	Internet Resources	1-23
	References and Recommended Further Reading.....	1-24
	Backgrounds on Some Molecular Biology Pioneers.....	1-25
	Databases and Other Supplementary Materials on Molecular Biology	1-25

Nathan R.
Domagalski
Bristol-Myers Squibb

Michael M. Domach
Carnegie Mellon University

1.1 Introduction

This chapter provides first a historical perspective on the origins of molecular biology. A historical perspective is important because the emergence of molecular biology has radically altered how living systems are viewed by scientists and biomedical engineers. It is thus useful for a biomedical engineer to be acquainted with the evolution of the discipline in order to fully appreciate the technological and social impact of molecular biology. For example, a mechanistic basis for the origin of many diseases can now be established, which paves the way for developing new treatments. It is also possible now to manipulate living systems for technological purposes, such as developing bacteria that can produce the therapeutic, human insulin. Acquiring the capability to manipulate the genetic potential of organisms and ultimately humans also raises new and important ethical issues. After summarizing the major historical developments, the “central dogma of molecular biology” will be presented and the salient

mechanistic details will be provided. Thereafter, some practical aspects of transforming cells, introducing mutations, and working with kits will be covered. This chapter concludes with Internet resources that can provide quick definitions of terms, documentaries of prominent molecular biologists and their accomplishments, as well as other useful resources that include links to primer design, kits, methods forums, and genotype abbreviations.

1.2 Molecular Biology: A Historical Perspective

Nineteenth-century biologists and their predecessors emphasized the collection and inventorying of life on Earth. The physical or other similarities between organisms led to classification schemes. As new organisms were discovered or new ideas emerged, schemes were often debated and then reorganized. Thus, unlike physics or chemistry, unifying rules and descriptions that had a mechanistic basis and could account for behavior were scant in biology.

Toward the end of the nineteenth century, scientists began to gaze within cells, and as a result, some striking observations were made that began to demystify biological systems. In 1897, Buchner found that cell-free extracts (i.e., the molecules found within yeast cells) executed chemical reactions. His finding was significant because a debate had been underway for decades. The question driving the debate was “What exactly is the role of cells, such as yeast, in practical processes such as wine making?” Hypotheses were abundant. The German chemist Jutus von Liebig, for example, proposed in 1839 that yeast emit certain vibrations that can reorganize molecules, which accounts for the yeast-mediated conversion of sugar to alcohol. In 1876, William Kuhne coined the term “enzyme” to imply that something contained within yeast is associated with processes, such as converting sugar to alcohol. Bucher’s experiments were powerful because the results showed that cells are not required for chemical reactions to occur. Rather, it seemed plausible that the “rules” of chemistry apply to living systems as opposed to “vibrations” or other phenomena unique to living systems being operative. Many now credit the Bucher brothers with launching the modern field of biochemistry. In 1894, Emil Fisher developed a theoretical model for how enzymes function. Later in 1926, *Charles Sumner* provided some useful closure and a method for characterizing cells at the molecular level. He and his colleagues showed that enzymes are proteins and crystallization is one means that can be used to isolate specific enzymes from cells.

The omnipresence of deoxyribonucleic acid (DNA) within cells piqued curiosity. Miescher discovered the DNA molecule in 1869, which was 3 years after Mendel published his experiments on heredity in plants. Mendel’s work incorporated the notion that a “gene” is a conserved and transmittable unit of trait information. However, science had to wait until 1943 for the link to be made between the manifestation of traits and the presence of DNA within a cell. Oswald Theodore Avery (1877–1955) and his coworkers showed that by simply adding the DNA from a virulent form of the bacterium *Pneumococcus* to a suspension of nonvirulent *Pneumococcus*, the nonvirulent bacterium acquired the traits of the virulent form. With this link established, the nature of the DNA molecule became a subject of intense interest. In 1951, Pauling and Corey proposed that the DNA molecule forms an α -helix structure, and experimental evidence was reported by Watson and Crick in 1953.

By the 1950s, knowledge had accumulated to the extent that it was known that (1) enzymes catalyze reactions, (2) cellular reactions are understandable in terms of organic chemistry fundamentals, (3) the DNA molecule possesses the information for traits, and (4) the DNA molecule has an intriguing spatial organization that may “somehow” confer information storage and expression capabilities. Additionally, it had been established that all DNA molecules contain four bases: adenine (A), thymine (T), guanine (G), and cytosine (C). However, how information is actually stored in DNA and used were still mysteries. Interestingly, basic questions on how life “works” were unresolved while at the same time, Yuri Alexeyevich Gagarin’s (1961) and John Glenn’s (1962) pioneering orbits of Earth extended the reach of human life to space.

Molecular biology had now supplanted descriptive biology, and inspired further research. Through the 1950s to the mid-1960s, many workers from varied disciplines solved many key problems in molecular biology. In 1958, François Jacob and Jacques Monod predicted the existence of a molecule that is

a working copy of the genetic information contained in DNA (messenger ribonucleic acid (mRNA)), and the information is conveyed from where DNA is stored (the cell's nucleus) to where proteins are produced (the ribosomes). In 1966, Marshall Nirenberg and colleagues cracked the genetic code. They showed that sequences of three of the four bases (e.g., AAT, GCT) that compose DNA specifies each of the 20 different amino acids used by a cell to produce proteins. In 1971, this accumulated knowledge enabled Stanley Cohen and Herbert Boyer to insert into a bacterial cell the DNA that encodes an amphibian protein, and, in turn, compel the bacterium to produce a protein from a vastly different organism. The prospect of using bacteria and simple raw materials (e.g., glucose) to produce human-associated and other proteins with therapeutic or commercial value led to the formation of the company Genentech in 1976. More recently, the DNA from humans and other sources has been successfully sequenced, which should lead to further commercial and medical impacts, as well as ethical challenges. Molecular biology is now organized around the “central dogma,” which is summarized next.

1.3 Central Dogma of Modern Molecular Biology

The central dogma of molecular biology/molecular genetics in its original form proposes that information encoded by DNA is first transcribed to a working copy. The working copy is mRNA. The information contained by a given mRNA is then translated to produce a particular protein. The collection of proteins/enzymes a cell possesses at any point in time, in turn, has a strong bearing on a cell's behavior and capabilities.

The central dogma has been proven to be largely correct. Salient aspects of how the central dogma is manifested at the molecular level are described below. Thereafter, an important deviant from the central dogma and additional refinements are presented.

1.3.1 DNA Base Composition, Connectivity, and Structure

Because DNA contains information, it follows that the composition of DNA must play a role in the information that the molecule encodes. DNA is composed of four different mononucleotide building blocks. As shown in [Figure 1.1](#), a mononucleotide molecule has three “parts” (1) a five-carbon ribose sugar, (2) an organic nitrogen-containing base, and (3) one (i.e., “mono”) phosphate group (PO_4). The ribose sugar can possess one or two hydroxyl groups ($-\text{OH}$); the “deoxy” form, which is present in DNA, has one hydroxyl. Five bases are commonly found within cells: adenine (A), guanine (G), cytosine (C), uracil (U), and thymine (T). A, G, C, and T are the four bases that appear in the nucleotides that comprise the DNA molecule, and thus the base present distinguishes one building block from another. A, G, C, and U appear in RNA molecules. Thus, DNA and RNA molecules differ by the number of hydroxyl constituents possessed by the ribose, and whether thymine (DNA) or uracil (RNA) is the base present.

The number of bound phosphates can vary in a nucleotide. When phosphate is absent, the molecule is referred to as a *nucleoside* or a *deoxynucleoside*, depending on the hydroxylation state of the sugar. Up to three phosphate groups can be present. When one or more phosphates are present, the compound is commonly referred to by the base present, how many phosphates are present, and whether the deoxy form of the sugar is used. For example, when the base adenine is present and there are two phosphates, the corresponding deoxyribonucleotide and ribonucleotide are typically referred to by the abbreviations, dADP and ADP. The former and latter abbreviations indicate “deoxy-adenine diphosphate” and “adenine diphosphate,” respectively. Overall, the deoxy monophosphates, dAMP, dTMP, dGMP, and dCMP, are the constituents of the DNA molecule.

The mononucleotides in DNA are connected by phosphodiester bonds as shown in [Figure 1.2a](#). This polymeric chain is commonly called single-stranded DNA (abbreviated as ssDNA). Based on the numerical labeling of the carbon atoms in ribose, links exist between the third and fifth carbons of successive riboses; hence, “3'-5' bridges or links” are said to exist. Also, based on this numbering scheme, practitioners note that a strand has either a “free 3' or 5' hydroxyl end.”

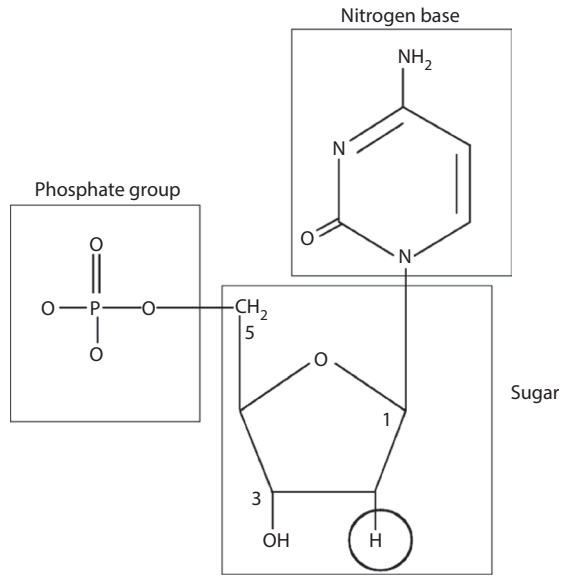


FIGURE 1.1 The mononucleotide deoxycytidine 5'-phosphoric acid. A less formal or more likely used name and abbreviation are deoxycytosine monophosphate and dCMP, respectively. Replacing the circled hydrogen with a hydroxyl group (OH) would produce cytosine monophosphate (CMP). The 3' and 5' carbons are marked as well as the 1' carbon, which is the starting point of the labeling system in the five-carbon sugar (pentose) ring.

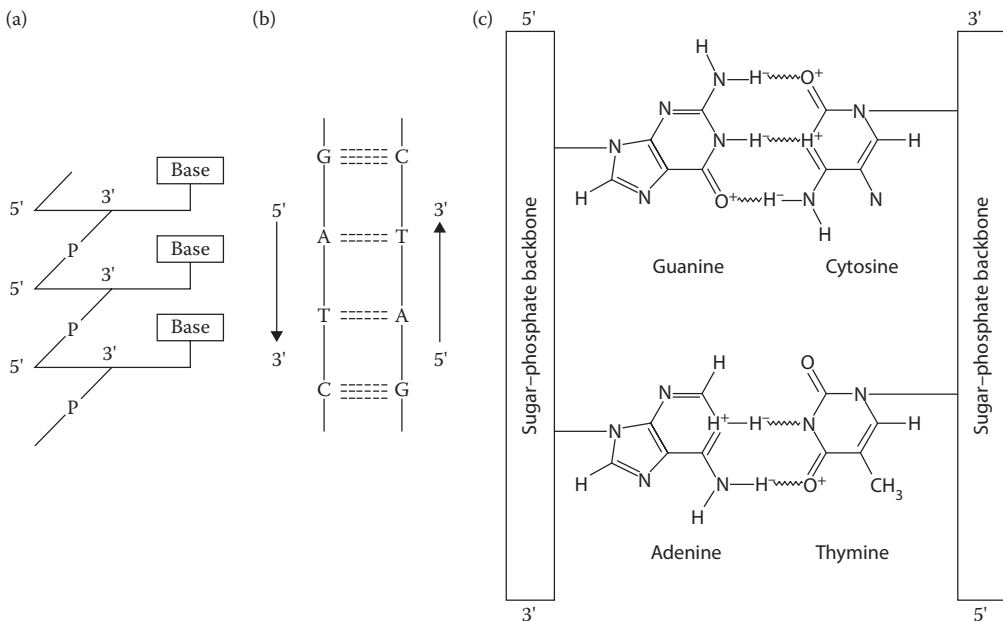


FIGURE 1.2 Connections and pairing of strands in the DNA duplex. (a) A connected strand has a direction where the example shown has a “free” 3' end. (b) In the cell, two strands run in an “antiparallel direction” allowing the G–C and A–T residues to base-pair, thereby holding the duplex together. (c) The illustration demonstrates that hydrogen bonding, shown as zig-zag lines, dictates which bases are complementary to one another. Three hydrogen bonds form between guanine and cytosine. Similarly, two hydrogen bonds form between adenine and thymine (or uracil in RNA).

When discussing the nucleotide composition or sequence present in DNA from a particular source, experts often drop naming formalities and simply use the bases' names or abbreviations, because the base distinguishes the building blocks. For example, the "G + C percent content" of the DNA from one organism is often compared to the content in the DNA from another organism in order to highlight a difference between the two organisms. The sequence in which the nucleotide building blocks appear in a section of a DNA molecule is also abbreviated. For example, GCCATCC refers to the order in which the guanine-, cytosine-, adenine-, and thymine-containing mononucleotides appear in a section of DNA.

Within a cell, the DNA molecule actually consists of two hydrogen-bonded antiparallel strands as depicted in Figure 1.2b. The strands are "antiparallel" because the end of one strand has a free 3' OH while the adjacent end of the companion strand has a free 5' OH. Thus, one strand is said to run in the 3' → 5' direction, while the other has the opposite 5' → 3' "polarity." This allows the A, G, C, and T bases on the two strands to interact via hydrogen bonding, as illustrated in Figure 1.2c. An A on one strand can interact with a T residue on the other strand via two hydrogen bonds. Likewise, G and C residues on adjacent strands interact, but the interaction is stronger because three hydrogen bonds can be formed in a G–C association. The interaction between bases on different strands is referred to as base-pairing, and a complex of two strands is known as a duplex or doubled-stranded DNA (abbreviated as dsDNA). Although individually rather weak when compared to ionic or covalent bonds, the cumulative effect of numerous hydrogen bonds results in a rather strong and stable molecular interaction. Finally, the two strands of DNA have to be complementary in that every position an A (or G) appears, the other strand must have a T (or C) present. The base-paired, duplex assumes an α -helical structure.

The DNA molecule represents only a small fraction of the total weight of a cell. However, each DNA molecule itself is quite large in terms of molecular weight. The DNA molecule found in the bacterium *Escherichia coli*, for example, contains about 4.2 million base pairs, which represents a molecular weight on the order of 2.8 billion daltons.

1.3.2 Base Sequence, Information, and Genes

Some details on the molecular species that actually decipher and then use the information in DNA for producing a functional protein will be described after summarizing how information storage is accomplished at the "base sequence information level." A sequence of three bases encodes for an amino acid in a protein. That is, when the information encoded by a strand of DNA is read in a fixed direction, the "word" formed from three letters (e.g., ATT) denotes that a particular amino acid should be added to a lengthening protein chain. There are a total of 20 amino acids; hence, at the minimum, 20 code words are required. Words consisting of different three-letter combinations of A, G, C, and T can yield $4^3 = 64$ unique "code words," which exceed the 20 required for all the amino acids; hence, there are 44 extra "words." The extra words result in synonyms for amino acids; hence, the code is degenerate. Other extra "words" provide signals for where a protein's code starts and stops. A sequence of three bases that encode for a particular amino acid is called a codon or triplet. Table 1.1 summarizes the genetic code. The set of all codons that encode the amino acid sequence of a protein is called a structural gene.

1.3.3 Codon Information to a Protein

As shown in Figure 1.3, the information encoded by a gene on one DNA strand is first translated by the enzyme, RNA polymerase (RNAPol). The copy of the gene RNAPol has helped to produce what is called mRNA. The raw materials for mRNA synthesis are ATP, CTP, GTP, and UTP. The analogous mRNA copy is complementary to the original DNA; hence, wherever G, C, A, and T appear in the DNA-encoded gene, C, G, U, and A appear in the mRNA.

Thinking mechanistically, if mRNA synthesis is blocked, then a protein cannot be produced. Therefore, one logical place to exercise control over gene expression is at the level of mRNA synthesis.

TABLE 1.1 The Genetic Code

		Second Position				
		U	C	A	G	
First position (5' end)	U	Phenylalanine	Serine	Tyrosine	Cysteine	U
		Phenylalanine	Serine	Tyrosine	Cysteine	C
		Leucine	Serine	STOP	STOP	A
		Leucine	Serine	STOP	Tryptophan	G
	C	Leucine	Proline	Histidine	Arginine	U
		Leucine	Proline	Histidine	Arginine	C
		Leucine	Proline	Glutamine	Arginine	A
		Leucine	Proline	Glutamine	Arginine	G
	A	Isoleucine	Threonine	Asparagine	Serine	U
		Isoleucine	Threonine	Asparagine	Serine	C
		Isoleucine	Threonine	Lysine	Arginine	A
		Methionine ^a	Threonine	Lysine	Arginine	G
	G	Valine	Alanine	Aspartic acid	Glycine	U
		Valine	Alanine	Aspartic acid	Glycine	C
		Valine	Alanine	Glutamic acid	Glycine	A
		Valine	Alanine	Glutamic acid	Glycine	G

^a Also START.

One example of gene regulation is illustrated in [Figure 1.3](#). As shown, a binding site upstream from the gene, known as an operator region, is often used to control whether mRNA is produced or not. A protein called a repressor normally binds to a repressor region that lies within the operator region. When the repressor is bound, RNApol's access to the gene is blocked. The repressor normally possesses another binding site. The second site can bind a ligand that serves as a signal for indicating that the protein the gene codes for is now needed. Such a ligand is termed an inducer. When the inducer binds, the repressor's three-dimensional structure is altered such that its ability to bind to the operator site is significantly reduced. Consequently, the tendency for the repressor to dissociate from the promoter site increases. The result of repressor dissociation is that RNApol can now access the gene and commence mRNA synthesis. It is important to note that there are many variations in how binding is used to regulate gene expression that differ from the scenario in [Figure 1.3](#). For example, in addition to providing RNApol access to a gene, binding between RNApol and other molecular "signals" occur that actually increase the avidity of RNApol–DNA binding.

Ribosomes, which are large protein–nucleic acid complexes, bind to the newly produced mRNA usually before synthesis of the entire strand is even complete. In fact, multiple ribosomes will bind to the same mRNA molecule, thereby creating a polyribosome. Ribosomes mediate the sequential addition of amino acids, where each amino acid is prescribed by the complementary codon information now contained in the mRNA. What occurs is that all 20 amino acids have been "prepped" by being enzymatically esterified to an amino acid-specific transfer RNA (tRNA). Each tRNA possesses a binding site that binds to one amino acid's codon(s) on the mRNA; the binding site on the tRNA is called an anticodon. The enzymes that mediate the attachment of a particular amino acid to its tRNA are very specific for both the amino acid and its tRNA. Any sloppiness could result in a tRNA being "charged" with the wrong amino acid. The consequence of an error is that the wrong amino acid would be added to a protein even though the correct anticodon–codon binding event occurred.

The growing strand of amino acids is joined together by an amide linkage known as a peptide bond. Without knowing structural or functional information, this strand may be simply referred to as a polypeptide. However, when the polypeptide is organized into an active conformation, it is finally called a protein.

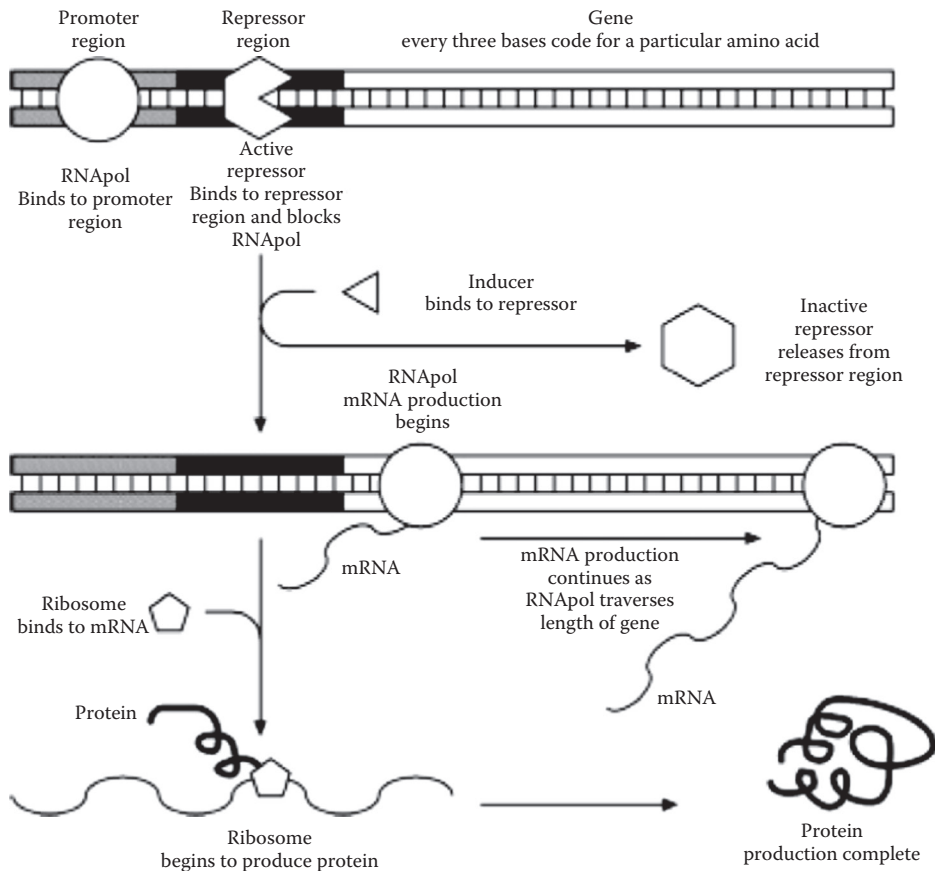


FIGURE 1.3 Simplified schematic demonstrating one example of gene regulation. RNAPol binds to the promoter region forward of a gene. However, an active repressor may bind to the repressor region and block the RNAPol from translating the gene into a molecule of mRNA. Binding of an inducer molecule to the repressor leads to inactivation and causes the repressor to release from the DNA. RNAPol is now free to produce mRNA from the gene. Ribosomes next bind to the mRNA, sequentially adding amino acids in a growing chain that becomes a protein.

Although this description of the central dogma is operative in many microorganisms, there are other significant intermediate steps that are required by higher organisms. One such step is RNA splicing. As shown in [Figure 1.4](#), a typical gene in, for example, a human cell is composed of numerous coding (exons) and noncoding (introns) stretches of DNA sequences. While bacterial proteins are predominantly encoded by a continuous, uninterrupted DNA sequence, most higher cells, such as those that compose humans, must have the translated introns removed to produce a molecule of mRNA. After the entire gene is translated into a large RNA molecule known as a primary transcript, a complex of RNA modification enzymes deletes the introns and splices the exons into a true mRNA molecule. The splicing process is known as ligation. Subsequently, the mRNA is processed by the mechanisms described previously.

1.3.4 DNA Replication

While the base composition of DNA explains much, a lingering issue is how DNA replication occurs and results in the faithful transmission of genetic information when a parent cell divides and forms two cells. DNA replication has been proven to be a semiconservative replication process. When a cell undergoes asexual division to form two cells, each daughter cell must obtain identical amounts of DNA, and

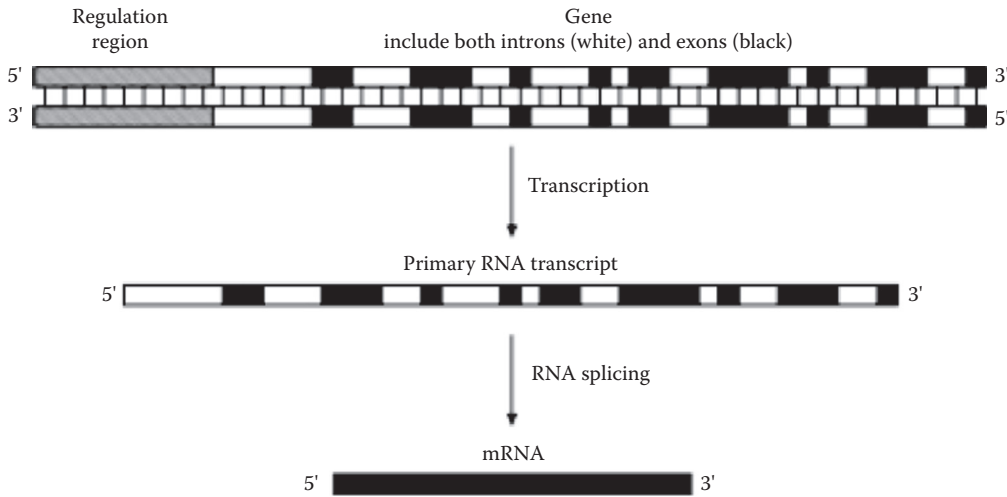


FIGURE 1.4 RNA splicing. Genes found in humans include coding sequences (introns) and noncoding sequences (exons). After both transcription and RNA splicing, an mRNA molecule is created.

each copy should contain all the information that the parent possessed. It has been established that each strand in a parental duplex serves as a template for its reproduction. Enzymes called DNA polymerases replicate each strand. The result is that the resulting two duplexes that are derived from the parental duplex each possess one of the original strands from the parental DNA.

1.3.5 mRNA Dynamics

For the central dogma to work, the control of gene expression should depend on whether or not mRNA synthesis occurs. Implicit in this requirement is mRNA must have a short lifetime in cells. If the lifetime of mRNA was on the order of cell lifetime or more, then “ON–OFF” controls of mRNA synthesis would have little effect because working copies of mRNA from many genes would be ample and omnipresent. It has been found that in bacterial cells, for example, the lifetime of mRNA is on the order of minutes. From the engineering standpoint, an interesting control system and dynamics is thus manifested by many cells. “ON–OFF” controls dictate whether new mRNA is produced or not, and the transduced output from repressor–promoter binding (mRNA) has a short lifetime, which leads to “sharp” ON–OFF dynamics for the production of specific, gene-encoded proteins.

1.3.6 Variations and Refinements of the Central Dogma

Some viruses do not directly follow the DNA → mRNA → protein path. Retroviruses, for example, are composed of RNA and consequently replicate by a pathway of RNA → DNA → mRNA → protein. After a retrovirus infects a cell, the viral RNA cargo is converted to DNA via the enzyme, reverse transcriptase. The viral DNA then integrates into the host cell’s DNA. Expression of the viral genes by the host’s transcriptional and translational machinery build the components for new viruses. Self-assembly of the components then occurs. Retroviruses are not biological curiosities; they are the agents of diseases, such as human T-cell leukemia and acquired immune deficiency syndrome (AIDS).

Another variant is found on the border of living versus self-assembling/propagating systems. We note this case because of its medical importance. Prions are altered proteins that lead to diseases, such as Creutzfeldt–Jakob disease in humans, chronic wasting disease in deer and elk, and bovine spongiform

encephalopathy in cattle. It is now thought that a prion is a protein that has been altered to be significantly more resistant to natural degradation mechanisms as well as the heat treatment that occurs during sterilization or the preparation of food. When a prion encounters a natural form of its precursor protein, a binding interaction is thought to occur that converts the normal protein into a likewise degradation-resistant form. Subsequent binding events result in a chain reaction that propagates the accumulation of prions. The accumulation of prions can interfere with normal neurological function leading to the aforementioned diseases. Prions are currently under intense investigation. Future research will reveal if the “protein-only hypothesis” is a sufficient explanation, or if an expanded or alternate mechanistic model is required to explain prion formation and propagation.

It is now also known that controls beyond ON–OFF mRNA synthesis also play a role in whether the information in a gene is expressed within cells. These other controls do not necessarily negate the utility of the central dogma as a model. Rather, from the control engineering standpoint, these additional mechanisms represent different interesting means of “fine tuning” and adding additional levels of control over gene expression. At the protein level, where enzymes are gene products, some enzymes possess binding sites to which reaction products or other metabolites can bind. When binding occurs, the rate of the enzyme-catalyzed reaction is either accelerated or decreased leading to feedback and feed-forward control of the pace at which some expressed gene products function.

The prior description of mRNA regulation (see [Figure 1.3](#)) has many steps. Thus, it is not surprising to find that other processes can also influence the rate and extent to which the information in a gene can be manifested as an active functional protein. Such translational-level controls can entail competition for ribosomes by the numerous mRNAs from different genes. Alternately, the base interactions that occur in a duplex DNA molecule that lead to the α -helix can also result in structural organization in mRNA. For example, the bases within an mRNA strand can self-complement, thereby leading to the formation of hairpin loops. Such “secondary structures” that result from a primary structure (the base sequence) can influence how fast and successfully the ribosomal-mediated translation process occurs.

Lastly, the control architecture of cellular gene expression is not limited to the previously described case of one promoter–one signal–one structural gene. Different genes can be expressed from a particular set of environmental “signals” when shared control elements and/or molecular components are used. This aggregated response from genes and control loci distributed throughout the genome is often referred to as a “regulon” arrangement. One example entails the “stress response of cells.” Here, nutrient deprivation or another “signal” unleashes the expression of various genes that collectively enhance the survival chances for a cell. Sometimes these “circuits” utilize different transcriptional molecular components, which thereby provides for subsystem isolation and specialization. Alternately, even microbes are capable of intercellular communication, a trait more typically attributed to different cells in a complex biosystem, such as a human. Examples of such distributed and specialized control circuits will be provided in the Chapter 2.

1.4 Molecular Biology Leads to a Refined Classification of Cells

The science of classification is called taxonomy and the organization of life by ancestor–descendent (evolutionary) relationships is called phylogeny. The characterization and comparison of key intracellular molecules has altered prior classification and relationship schemes.

The components of the ribosomes found in cells are the basis for modern taxonomy. A ribosome is composed of different parts that enable mRNA binding and amino acid addition. The parts are called subunits. Different subunits are characterized and distinguished by centrifugation. Based on such physical sorting, the subunits are assigned *S*-values, where “*S*” stands for a Svedberg unit. The larger the value of *S*, the more readily a subunit is driven to the bottom of a centrifuge tube. The sedimentation unit’s namesake, Theodor Svedberg (1884–1971), studied the behavior of macromolecules and small particles; for his pioneering work, he received a Noble Prize in 1926.

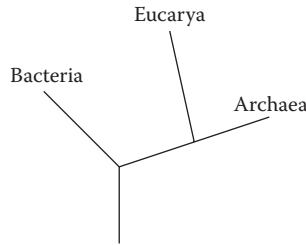


FIGURE 1.5 Family tree of three cell types originating and then diverging from one ancestor.

One key part of a ribosome is the 16S ribosomal RNA (rRNA) component, which is found in the 30S subunit along with proteins. Many seemingly different cells are actually similar based on their constituent 16S rRNA. Not only is the *S*-value the same, the genes that encode for the 16S RNAs in seemingly different cells exhibit similar base sequences. When the degree of base overlap in a coding sequence is extensive, the DNAs from different sources are said to exhibit high homology. Other cells, however, have been found to possess significantly different components that make up the intact ribosome. The *S*-value can also vary somewhat. For example, in mammalian cells, the rRNA that fulfills the 16S rRNA function in bacterial cells settles somewhat faster at 18S on the Svedberg scale. More notably, the genes that encode 18S mammalian and 16S bacterial rRNA exhibit low homology. Thus, cells are grouped together based on the homology of their 16S rRNA-encoding genes.

The current classification of cell types and how they are believed to have evolved from one ancestor are shown in Figure 1.5. The three types are bacteria, archaea, and eukarya. *Bacteria* are unicellular organisms capable of reproduction. Bacteria vary in size and shape; a typical length scale is 1 μm (10^{-6}m). *Archaea* resemble bacteria in many ways. They are about the same size and they can metabolize an array of raw materials. One notable difference is that archaea are often found in extreme environments, such as hot springs and acidic waters. Such environments may resemble those present in the early days of Earth; hence, archaea are believed to be remnants of the early Earth. The ability of archaea to function well in extreme environments has also intensified some people's curiosity about the possibility of life beyond Earth. Others regard archaea proteins and other molecular constituents as potentially useful catalysts and medicinal compounds due to their stability or environmental coping properties (see polymerase chain reaction, which is discussed later). *Eukarya* include the cells that compose the human body. One distinguishing characteristic is that unlike bacteria or archaea, eukarya have compartments within them. The compartments are called organelles. One important organelle is the nucleus, which houses the DNA molecule.

1.5 Mutations

What traits an organism presents is called the phenotype, and the traits are linked to the instructions encoded in the DNA. The raw instructions are, in turn, called the genotype. An alteration in an organism's genetic code is termed a mutation.

Mutations can occur that involve large sections of DNA. Some common examples are described below:

- Translocations involve the interchange of large segments of DNA between two different chromosomes. Gene expression can change when the gene is located at the translocation breakpoint, or if the gene is reattached such that its expression is controlled by a new promoter region that responds to a different inducer.

- Inversions occur when a region of DNA flips its orientation with respect to the rest of the chromosome. An inversion can have the same consequences as a translocation.
- Sometimes large regions of a chromosome are deleted, which can lead to a loss of important genes.
- Sometimes chromosomes can lose track of where they are supposed to go during cell division. One of the daughter cells will end up with more or less than its share of DNA. This is called a chromosome nondisjunction. When a new cell gets less or more than its share of DNA, it may have problems with gene dosage. Fewer or more copies of a gene can affect the amount of gene-encoded protein present in a cell.

More modest alterations occur at the single base level and are called point mutations. Common examples and consequences are summarized below:

- A nonsense mutation creates a stop codon where none previously existed. The resulting protein is thus shortened, which can eliminate functionality.
- A missense mutation changes the amino acid “recipe.” If an AGU is changed to an AGA, the protein will have an arginine where a serine was meant to go. This amino acid substitution might alter the shape or properties of the protein. The sickle-cell mutation is an example of a missense mutation occurring on a structural gene. Hemoglobin has two subunits. One subunit is normal in people with sickle-cell disease. The other subunit has the amino acid valine at position 6 in the protein chain instead of glutamic acid.
- A silent mutation has no effect on protein sequence. Changing one base results in a redundant codon for a particular amino acid.
- Within a gene, small deletions or insertions of a number of bases not divisible by three will result in a frame shift. Consider the coding sequence:

AGA UCG ACG UUA AGC → arginine–serine–threonine–leucine–serine

Inserting a C–G base pair between bases 6 and 7 would generate the following altered code and amino acid errors following the insertion:

AGA UCG CAC GUU AAG C → arginine–serine–histidine–valine–lysine

A frame shift could also introduce a stop codon, which would yield an incomplete protein.

Mutations can also alter gene expression. For example, a mutated promoter region may lose the ability to bind a repressor. Consequently, gene expression always occurs. Such a cell is often called a constitutive mutant and the gene product is constitutively expressed. Alterations in the sequence that encodes for the repressor protein could also result in constitutive expression in that the altered repressor protein can no longer bind to the promoter region and block mRNA synthesis.

1.6 Nucleic Acid Processing Mechanisms and Inspired Technologies with Medical and Other Impacts

The experiment performed by Avery and colleagues revealed the function of DNA via a natural process whereby a bacterium imported raw DNA, and after incorporating the DNA into its genetic material, cellular properties were consequently altered. Today, DNA is routinely inserted into many types of cells for the purpose of altering what cells do or produce. Cell transformation (bacterial) or transfection (mammalian) relies on exploiting the many natural DNA uptake, modification, and repair processes that cells use. This section first reviews the types of enzymes that can alter DNA, and then provides an example of their use in technological processes.

1.6.1 Nucleic Acid Modification Enzymes

To remain viable and sustain reproduction, cells have to replicate DNA, destroy unwanted RNA, repair broken DNA strands, eliminate any foreign DNA inserted by viruses, and execute other maintenance and defense functions. Three important enzymes have been found to enable these functions within cells: nucleases, ligases, and polymerases.

Nucleases are enzymes that cut both DNA and RNA. These enzymes may be further classified as cutting both DNA and RNA, DNA-only (DNases), or RNA-only (RNases). Additionally, enzymes that cut strands of nucleic acids starting at the ends are known as exonucleases. Those enzymes that instead cut only at internal sites are called endonucleases. Exonucleases have a variety of uses, such as removing unwanted DNA or RNA. Although some nucleases will cleave nucleic acids indiscriminately, restriction enzymes are high-specificity endonucleases that only cut double-stranded DNA wherever a particular internal base sequence occurs. Sequence specificity is certainly the greatest strength of this type of nuclease. For example, the restriction enzyme *EcoR* I only cuts when the sequence 5'-GAATTC-3' occurs. When DNA is exposed to this particular restriction enzyme, double-stranded fragments with sticky ends are formed as shown in Figure 1.6. The ends are called “sticky” because each free single strand end has the ability to base pair with any complementary base sequence. A given organism tends to have only a few restriction enzymes, and those few enzymes are generally unique to the organism. However, the wide diversity of organisms that exist in nature has resulted in the discovery of a large number of different restriction enzymes.

Just as strands of nucleic acids may be cut, they can also be repaired. In fact, the ligase’s functionality can simply be thought of as the reverse of that of a restriction enzyme. A critical difference, however, is that the ligase is not site specific. DNA ligase is an enzyme that seals breaks in the sugar–phosphate backbone that can occur within one strand of a duplex. DNA ligase is thus used to repair broken DNA.

Lastly, DNA polymerase catalyzes the synthesis of duplex DNA from a single strand of DNA when a primer is used to initiate the process. The primer is simply a short strand of complementary nucleic acids. DNA replicates in nature using RNA primers. Once the polymerase has elongated the strand to some extent, organisms possess a special repair mechanism that removes the RNA primer and replaces

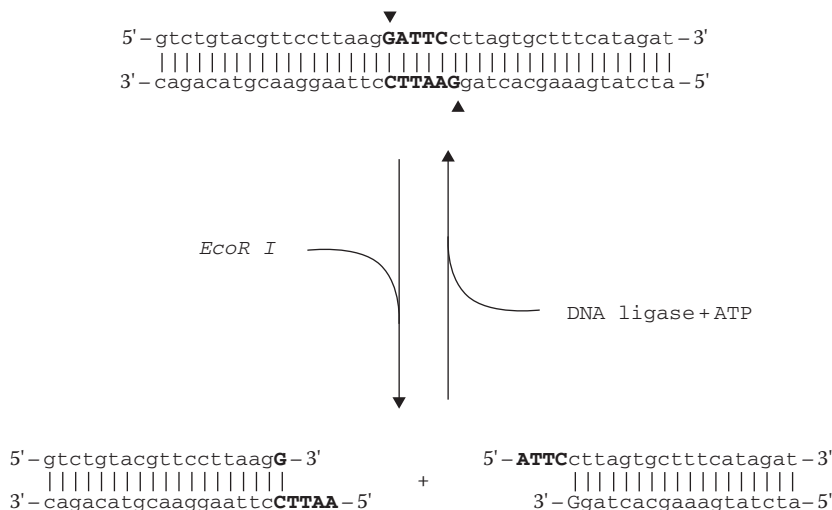


FIGURE 1.6 Cutting and joining DNA. *EcoR* I is an example of a restriction endonuclease that cleaves dsDNA at a specific, internal recognition sequence (shown here as 5'-GAATTC-3'). By contrast, a nonspecific DNA ligase can join the two complementary DNA molecules by repairing the sugar–phosphate backbone.



FIGURE 1.7 DNA polymerase. PCR is a routine procedure for amplifying DNA. Primers first anneal to a complementary sequence on the target ssDNA molecule. Next, DNA polymerase synthesizes the remainder of the complementary sequence from the four deoxyribonucleotide triphosphates.

it with DNA. In contrast, DNA replication in the laboratory is usually accomplished by using oligonucleotides (DNA primers). How the primer-based synthesis of duplex DNA works is shown in Figure 1.7.

Perhaps one of the most important properties of a polymerase is its fidelity. The possibility always exists that a noncomplementary nucleotide can be inadvertently added to an elongating strand. A polymerase’s fidelity is defined as the frequency at which wrong nucleotide addition errors occur. Because of the potentially life-threatening mutations such errors may cause, organisms have an enzymatic proof-reading mechanism. Although the details may differ slightly between organisms, in general, if an incorrect nucleotide is added, the proof-reading enzymes pause the polymerase, remove the troubled nucleotide, and then allow the polymerase to continue the elongation process.

1.6.2 Copying DNA in the Laboratory

Many aspects of how cells replicate their DNA can now be reproduced in the laboratory without using intact cells. When a subset of biomolecular components is used in, for example, a beaker to execute a cellular reaction, the reproduced natural process is said to be conducted *in vitro* (e.g., “*in vitro* DNA replication”).

Conducting primer-based, DNA polymerase-catalyzed reactions *in vitro* is the basis for both gene amplification and crime scene investigation technologies. One application is the synthesis of a large quantity of a particular protein. Using *in vitro* DNA replication, the sequence that encodes the gene for this desirable protein may be amplified. Obtaining more DNA would enable the insertion of the gene into a bacterium. Given the relative ease with which bacteria can be cultivated and processed on a large scale, the exogenous protein may be then produced in a quantity that far exceeds that of the parent organism. Another use of the technology of gene amplification involves producing both normal and mutated protein products. Such altered proteins can provide insights on the gene’s properties and the effect of the mutations of protein’s three-dimensional structure and biological activity.

The laboratory process of amplifying DNA is known as polymerase chain reaction (PCR). To demonstrate how this process works, consider the amplification of a gene encoded within a fragment of dsDNA as shown in Figure 1.8. The process begins outside the laboratory by designing a pair of DNA

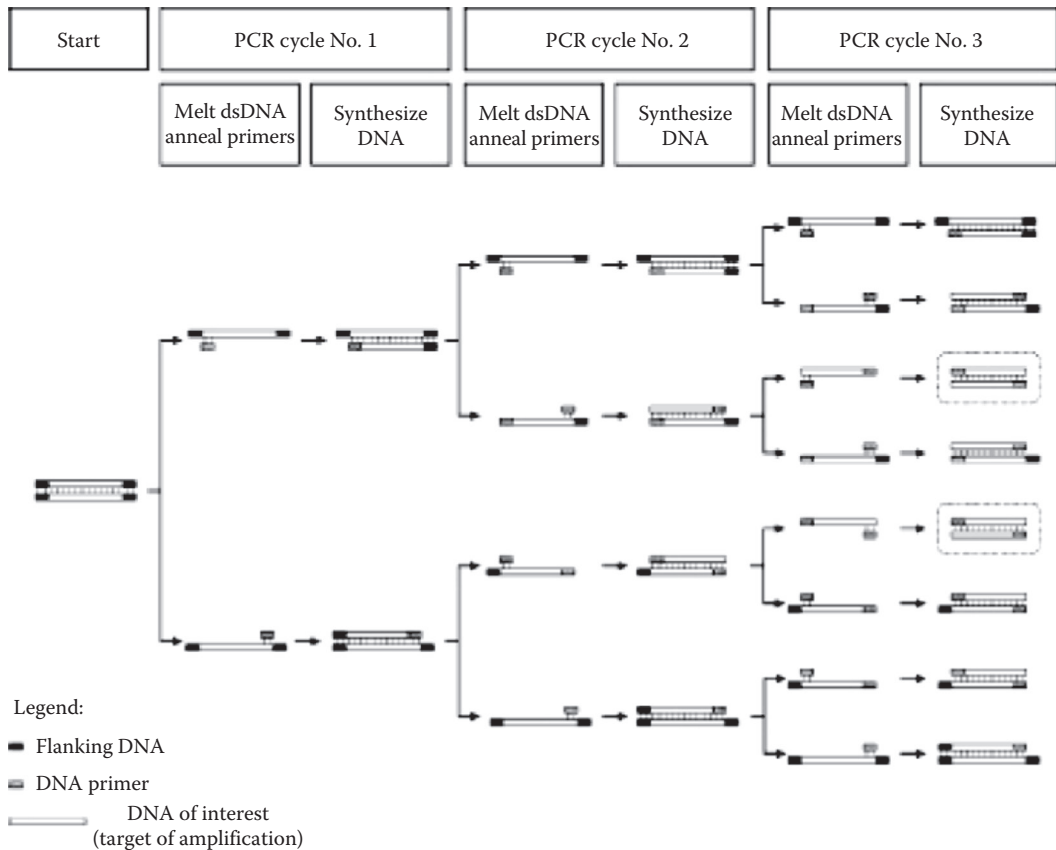


FIGURE 1.8 Amplification of DNA by PCR. A fragment of DNA may be amplified by means of the PCR. The starting fragment of double-stranded DNA (dsDNA) consists of the sequence of interest as well as flanking sequences. At the beginning of each cycle, the temperature rises and dsDNA is melted into single-stranded DNA (ssDNA). After reducing the temperature, DNA primers anneal to the sequence of interest. The temperature is elevated to the ideal conditions for the DNA polymerase and complementary strands are synthesized. The cycle is repeated until the sequence of interest has been amplified in great numbers. Any dsDNA, which includes the flanking sequence, will soon become only a very small percentage of the population. After 20 or more cycles, the dsDNA sequence of interest (circled in PCR cycle No. 3) will be the dominant product.

primers. With a design in hand, the primers may then be synthesized using a gene machine, which adds the bases A, T, G, and T in a user-specified order. As a side note, most investigators typically do not synthesize their own primers. Rather, they submit a design over the Internet to a commercial supplier who produces and purifies the primers. Resources for primer design can be found at the end of this chapter.

Next, a buffered mixture is prepared with the dsDNA fragment (which is often called the template), the primers, the four deoxyribonucleotide triphosphates (dNTPs), and DNA polymerase. The mixture is loaded into a thermal cycler, which is a device that precisely controls temperature according to a specified temporal program. A cycle of PCR starts by heating the mixture so that the individual strands of the dsDNA fragment separate into two single strands of DNA (ssDNA). This “melting” of the dsDNA is the result of the thermal energy exceeding the strength of the G–C and A–T associations. The mixture is cooled and the complementary primer binds to each ssDNA molecule. The temperature is then elevated to the ideal conditions for the DNA polymerase to function and new DNA is synthesized, starting from the primer and elongating to the end of template. This marks the end of a cycle and each dsDNA

molecule has been doubled into two new dsDNA molecules. Since PCR is normally carried out for at least 20 cycles, the product is a million-fold increase over the original starting material.

As mentioned previously, the fidelity of the polymerase determines the frequency at which incorrect nucleotides will be added to the growing strand of DNA. Although *Taq* DNA polymerase is widely used for PCR, it lacks a proof-reading mechanism and will introduce errors after several cycles of amplification. Any application requiring very low error rates, such as molecular cloning, analysis of rare mutations, or amplification of very small quantities of template DNA, should use high fidelity polymerases. The increase in fidelity is due to the presence of proof-reading activity. Several DNA polymerases, including *Pfu* and Deep Vent, are commercially available that will greatly minimize incorrect incorporation of nucleotides. As the name “Deep Vent” suggests, these enzymes are found in archaea, which illustrates one technologically important use of molecules found in the organisms that dwell in extreme environments.

PCR and restriction enzymes have many practical uses outside of life science or biotechnology laboratories. DNA from blood, hair follicle, or other samples from evidence gathered in a murder investigation can be cut with restriction enzymes to produce a fragment profile that has a high probability of belonging only to one person. Such a fingerprint enables victim identification, or whether the accused is linked to the blood trail. If the sample from the crime scene is small, PCR can be first used to increase the amount of DNA prior to treatment with restriction enzymes. Interestingly, the early uses of “DNA” fingerprinting in the criminal justice system were in appeal cases to exonerate some inmates on “death row” as opposed to strengthening criminal prosecutions.

1.6.3 Basic Bacterial Transformation Techniques

When bacterial cells are manipulated to internalize and use the instructions encoded by a piece of foreign DNA, the process is known as bacterial transformation. Using bacteria to produce a protein based on human genetic instructions has many advantages. A historical example is provided by the protein insulin. Before gaining the means to produce human proteins in microbes, insulin was obtained from animals that produce a similar protein. Insulin from pigs and cows differ from the human molecule by one and three amino acids, respectively. Although the animal-derived insulin substitute works, the differences between the human and animal insulin molecules can result in immune system activation. One adverse consequence is that a higher dose of the animal-derived insulin is required to offset the effort the immune system exerts on removing the “foreign” molecule from the body. Now that transformation technology is readily available, microbes can be used to express the actual human gene directly rather than searching for a surrogate protein from another species. Additional benefits are bacteria such as *E. coli* reproduce quickly and require only basic, inexpensive raw materials, such as glucose and salts. Hence, the production costs associated with therapeutic production can be managed. Many practitioners use the term “metabolic engineering” to refer to the directed alteration and management of cellular synthetic machinery for the purpose of producing a target molecule.

The first step in any transformation is selection of an appropriate host. That is, one must decide which microorganism will express the exogenous DNA. The choice can play an important role in subsequent steps, including the overall success of transformation, the relative ease of purifying the protein product, and even as basic a concept as whether the microorganism is even capable of producing an active form of the given protein. Sometimes this choice is an obvious one and on other occasions, it can pose a considerable challenge.

For the purpose of our example, let us choose the Gram-negative* microorganism *E. coli*, which is a well-known bacteria that is routinely used by many investigators. Although *E. coli* can be toxic to

* Gram negative and Gram positive refer to whether a stain is lost or retained by microbes after application and destaining procedures, respectively. The difference in stainability relates to the cell wall structure, which, in turn, provides a means for contrasting different types of bacteria.

humans due to the lipopolysaccharide constituents of its cell wall, numerous strains have been isolated that cannot propagate in the human body and are generally regarded as safe. Having been studied for many years, *E. coli* also offers a great opportunity to utilize a number of proven technologies.

Once a host is chosen, codon optimization is often considered. While the genetic code is universal, organisms differ in which degenerate codon that they tend to use. Thus, if high expression of a heterologous gene is desired, then apart from using a strong promoter, optimizing the codon sequence is often done through resynthesizing the structural gene. The optimized gene is then, for example, spliced into a plasmid vector using restriction enzymes and a ligase.

DNA is generally inserted into a microorganism by one of two methods. The exogenous DNA can be carried on a plasmid or integrated into the host's chromosome. In either case, the key is that the foreign DNA utilizes a means of replication as it is transferred from a parent to progeny during cell division.

A plasmid is a closed-circular piece of dsDNA that persists apart from the cell's chromosome. In nature, plasmids carry only a small amount of information, such as the genes needed for a cell to survive a particular environment. When this environmental pressure is removed, the plasmid is no longer needed and the cells tend to lose the plasmid after several generations. Laboratories often use plasmids that carry a gene-encoding factor that confers resistance to a particular antibiotic. Therefore, if a cell carries the plasmid, it can grow in the presence of the antibiotic. Likewise, the plasmid may be lost from the cells if the antibiotic is removed. Such survivability is an important tool that is routinely exploited when screening for successful transformants.

By contrast, integration means that the foreign DNA is inserted within the cell's chromosome, and thus becomes a permanent part of the genome. Such integration can add a new gene to an organism's repertoire. Alternately, integration of foreign DNA into a genome can be done to inactivate a gene normally present, which is called a "knock out." Here, inactivation occurs because the gene product is not functional because the inserted DNA sequence interrupts the functional coding.

The use of a plasmid to introduce a new functionality can be illustrated by using the human insulin gene as an example, where the goals are (1) to insert the foreign insulin-encoding DNA into a plasmid, and (2) then insert the altered plasmid into *E. coli*. Let us also presume that the chosen plasmid includes a gene for survival in the presence of the antibiotic ampicillin. Such a survival gene will provide a means for screening for and isolating a successful transformant when manipulated cells are grown in ampicillin-containing growth medium.

As shown in [Figure 1.8](#), the first step is to amplify the source of human insulin DNA, where codon optimization has been done beforehand. Using PCR and an appropriate primer design, the DNA encoding for insulin is amplified and flanked with restriction sites of our choosing. These restriction sites are a consequence of the primer design. After purifying the PCR product, the amplified DNA is treated with restriction enzymes, which create sticky ends. The plasmid is also exposed to the same restriction enzymes. To foster the binding of the complementary sequences, the treated insulin-encoding DNA and the plasmid are mixed. Finally, a DNA ligase repairs the sugar-phosphate backbone, yielding a plasmid that now possesses the human insulin gene.

The new plasmid, carrying the genes for human insulin as well as ampicillin resistance, can now be inserted into *E. coli*. There are several common insertion techniques, each with their strengths and weaknesses. These techniques, in order of relative ease, are heat shock, electroporation, and protoplast fusion. Furthermore, a cell that has been treated to optimize a given means of DNA uptake is described as competent.

Although many commercial suppliers offer competent *E. coli* for heat shock, it is fairly easy to create such cells in the laboratory. Under appropriate conditions, the bacteria is cultured, harvested, washed, and finally frozen. In general, bacteria grown in batch cultures will experience a peak ability to uptake foreign DNA. This peak may be correlated to cell concentration or a particular time point during the growth and nutrient exhaustion process. Banks exist that can provide many types of competent cells. In other cases, for a given organism, ample empirical evidence has recorded when such peaks in

competence occur. Other investigators that seek to produce their own competent cells exploit the information published on peaks.

Frozen competent cells are first thawed and then mixed with a plasmid. After incubating the mixture on ice for some time, it is quickly exposed to an elevated temperature, which creates small pores in the cell surface. The plasmid enters the cell through these pores. Thereafter, the pores are quickly closed by exposure to cold. The cells are then allowed to relax for about an hour to permanently reseal the pores. Finally, the cells are spread onto media and incubated overnight. In our example, the plasmid provides resistance to the antibiotic ampicillin. When ampicillin is added to the growth medium, only cells that carry the plasmid can survive, which, in turn, provides a useful first step in screening for successful transformants.

Another method of plasmid insertion into the cell is electroporation. Using competent cells specially prepared for electroporation, a device called an electroporator exposes the cells to a high-strength electric field. Much like heat shock, electroporation creates pores in the cells' surface for DNA to enter. From this point, the methodology is just like that used when heat shock is employed; the cells are allowed to relax, grow on antibiotic-containing media overnight, and then screened for surviving transformants.

Electroporation routinely provides more successful transformants than heat shock. This can be very important when working with bacteria that are difficult to transform. Fortunately, *E. coli* is quite easy to transform and electroporation is generally not required. Some Gram-positive bacteria like *Bacillus subtilis*, a cousin of the agent of the disease anthrax, are easier to transform via electroporation.

Protoplast fusion is the last method to be addressed. It is an old technique that is rarely used today because it is quite demanding. However, protoplast fusion can be useful when other methods have failed. Although the details differ from one bacterium to another, the central concept is that the cell wall is chemically and/or enzymatically removed. The resulting protoplasts, which are spherical cells that lack a cell wall, are then mixed with plasmid and a chemical, such as polyethylene glycol (PEG). The PEG causes the protoplasts to fuse with one another, often trapping DNA within the newly formed protoplasts in the process. The transformed protoplasts are carefully cultured under osmotically controlled conditions to both regenerate their cell walls and bear the new plasmid. Antibiotic resistance conferred by the plasmid again facilitates the screening process.

By using antibiotic selection, some of the successfully transformed cells can be isolated. In many cases, this is the end of the process; namely, *E. coli* has acquired the instructions for producing a new protein, such as insulin. In other cases, *E. coli* is simply used to amplify the DNA further via growing a quantity of plasmid-containing cells. After processing the amplified DNA isolated from *E. coli*, the DNA may be used for transforming another type of cell. Chromosomal integration is a possible end point for plasmid-based strategies as well. Such integration, if it does not knock out an essential gene, is advantageous because the new DNA is permanently imbedded in the genome as opposed to be associated with a peripheral plasmid.

The use of recombinant DNA technology has yielded a number of microbial-produced therapeutics. The transformed bacteria are grown in specialized vessels called bioreactors or fermenters. The growth vessel and solution of raw materials and nutrients (growth medium) are first sterilized. Thereafter, a starter culture of transformed cells is added. As the cells grow, they are supplied with oxygen and nutrients to foster their growth and to manage their metabolism such that the recombinant gene product is produced at a high level. A partial listing of products of medical importance is provided in Table 1.2.

The experimental techniques used to accomplish integration are varied. An example protocol follows where it is desired to knock out pyruvate kinase (Pyk) activity in *E. coli*.

Pyk activity can be abolished by using double cross-over recombination. There are two genes, *pykA* (AMP-activated) and *pykF* (FBP-activated), where PykF is the dominant activity. Clone 300 bp of sequences upstream and downstream of the *pyk* gene into the pSK265-based vector in *B. subtilis*. The result should be that these sequences surround the antibiotic resistance gene used in pSK265.

TABLE 1.2 Examples of Products Produced from Transformed Microbes

Product	Medical Use
Insulin	Diabetes management
Factor VIII	Treatment for hemophilia A
Factor IX	Treatment for hemophilia B
Human growth hormone	Treatment of dwarfism
Erythropoietin	Treatment of anemia
Tissue plasminogen activator	Blot clot dissolution
Interferon	Augment immune system function

Propagate and then isolate the recombinant plasmid from *B. subtilis*, plasmid DNA, and then introduce into *E. coli* by electroporation. *E. coli* transformants are then isolated and checked by PCR analysis for the replacement of the chromosomal *pyk* gene by the resistance gene surrounded by small regions of the *pyk* gene. As an alternative, a 300–400 bp internal region of the *pyk* gene can be amplified by PCR and cloned into the pSK265-based vector. The recombinant plasmid is then isolated from transformed *B. subtilis*, and used to transform *E. coli*. Antibiotic-resistant *E. coli* colonies are then isolated and should represent integration of the recombinant plasmid into the chromosomal *pyk* gene of *E. coli*. This can be confirmed by PCR analysis of chromosomal DNA from wild-type *E. coli* and strains in which the plasmid has inserted into the gene.

In the above, the pSK265 plasmid replicates in both *E. coli* and a quite different bacterium, *B. subtilis*. Such plasmids are often referred to as shuttle plasmids. They offer the ability to amplify DNA through propagation in one cell type, and then alter the genotype of another type of organism.

1.6.4 Measuring Plasmid Copy Number

When bacteria are transformed with plasmids, it is useful to determine the average number of plasmids per cell, which is referred to as a plasmid's "copy number." Indeed, many reported works leave out this information where instead it is directly or implicitly assumed that a value for copy number cited elsewhere is good enough and not subject to much change. This notion is driven by the assumption that plasmid copy number is tightly controlled. While negative control systems are in place that regulate plasmid copy number, what nutrients the bacteria are grown on can affect the copy number as well as the cellular growth rate. Copy number can be further affected by alterations to the host strain in the process of metabolic engineering. Finally, many modern plasmids have loosened negative controls, as described in Chapter 6 on producing vaccines.

A simple case that illustrates the need to measure copy number is as follows. An investigator hypothesizes that a particular set of host cell mutations will improve the synthesis of a recombinant protein. The wild-type and mutant are transformed with the same plasmid that contains the gene for the recombinant protein. When the protein production of the mutant and wild-type are compared, it is found that the mutant made 50% more recombinant protein per gram of cell mass. The explanation could simply be that the copy number increased from 100 to 150 in the mutant, thereby elevating the gene dosage. In this case, the mutations somehow helped the cell to maintain a higher copy number, and the mutations may have not been beneficial for synthesizing the target protein. Another scenario is despite the copy number decreasing to 50, more protein was produced. This scenario is quite different, and if true, the meaning of the mutations has deepened in that yield increased despite reduced gene dosage. In all, without copy number measurements, one does not have sufficient information to account for the apparent successful outcome as well as prove or disprove the hypothesis.

Kits are available for isolating and purifying plasmid DNA such as the QIAGEN Plasmid Plus Midi Kit. Knowing the mass of plasmid DNA isolated per mass of cells assayed along with the molecular

weight of the plasmid enables one to estimate the copy number. Such kits often work well, but protein or other contamination in the plasmid isolate can affect the outcome because the determination of mass of the plasmid isolated is based on optical absorbance measurements. To enable one to discern whether the level of contamination is unacceptable, a kit usually stipulates that the ratio of the absorbance at 260 and 280 nm should be around some target such as 1.8. If the target is hit, then the isolate has acceptable DNA purity. Here, however, variability in cell lysis outcome can still occur, which may obscure comparisons across replicates or host cell mutations. Thus, measurements are made in comparison to an internal control such as the genomic DNA garnered from cell lysis.

The traditional method of polyacrylamide gel electrophoresis (PAGE) is robust and provides a reasonable “seeing is believing” estimate. Chromosomal DNA migrates much differently than plasmid DNA, and PAGE clearly shows under what cases plasmid copy number changes relative to genomic DNA. Following labeling, quantification requires densitometry or some other spot size/opaqueness determining technique.

Quantification can be improved upon if PCR is used. The simplest implementation is to amplify a plasmid-encoded gene and a single-copy chromosomal gene from the same starting cell lysate. Thus, four primers must be designed; a forward and reverse for each gene. A good set of primers will have melting temperatures that are within 1°C of each other. Being close in melting temperature is good because the probability is enhanced that each gene will be amplified similarly and about twofold during each temperature cycle. While in the exponential phase of amplification, the signal from a fluorescent dye that emits when bound to duplex DNA will attain some preset value that represents a value significantly above the background. The number of cycles needed to attain the threshold is denoted the C_T value. The more the number of copies of the gene initially, the smaller the C_T will be. The ratio of plasmid DNA to chromosomal DNA is $2^{C_{T,g}-C_{T,p}}$, where $C_{T,g}$ and $C_{T,p}$ refer to the threshold cycles for the genomic and plasmid gene, respectively. Different sample dilutions are usually performed and analyzed to validate the protocol.

One advantage of the technique is it is internally referenced. That is, variations in cell lysis efficiency will not have an effect because what is measured is the amount of plasmid DNA relative to a genomic gene in a given sample. However, differences in the efficiency of copying can have an effect.

1.6.5 Deliberate Mutagenesis

It is often advantageous to deliberately introduce a point mutation into a sequence of DNA. For example, it may be desirable to up- or down-regulate a promoter in order to increase or decrease, respectively, gene expression. Alternately, changing the coding sequence for an enzyme may alter its stability, activity, and/or selectivity in a desirable manner. In molecular biology, what used to be thesis projects can now be accomplished with kits, and site-directed mutagenesis is no exception.

The QuikChange® Site-Directed Mutagenesis Kit vended by Stratagene (La Jolla, California) provides an example. A link to the manual is provided at the end of this chapter. It offers the ability to work with duplex DNA and the procedure requires a reasonably short number of four steps. First, a plasmid bearing the DNA sequence of interest is isolated or obtained. Second, the plasmid is thermally denatured and a mutagenic primer synthesized beforehand is allowed to hybridize with the sequence surrounding the desired mutation point. The mutagenic primer contains the mutated codon. In this temperature cycling process, nonstrand-displacing, high-fidelity *PfuTurbo* DNA polymerase extends the primers. The result is that nicked circular strands of DNA are produced. Here, envision the original duplex, closed circle plasmid now has a mutated strand of DNA associated with each original closed circle. However, the mutant strands yet require ligation to be fully closed circular strands of DNA. In the third step, the original plasmid template is digested away with *Dpn* I. Fourth and last, cells are transformed with the mutant plasmid, and the host's enzyme repertoire includes a ligase that seals the nick in the mutant plasmid.

Included in the kit is a control plasmid, which allows one to assess the efficacy of the protocol and reagents in the user's hands. The pWhitescript™ 4.5-kb control plasmid has a stop codon (TAA) instead of

a glutamine codon (CAA) in the β -galactosidase gene. Cells transformed with the control plasmid appear white on LB-ampicillin agar plates that contain isopropyl β -D-1-thiogalactopyranoside (IPTG) and X-gal, because β -galactosidase activity has been extinguished. The control primers create a point mutation on the pWhitescript 4.5-kb control plasmid that restores the glutamine codon. Therefore, following transformation, colonies can be screened for the β -galactosidase activity. If blue colonies appear on the aforementioned type of agar plate, then one has successfully used the kit to introduce a point mutation.

1.6.6 Getting the Most from Kits

Just as genomic and other databases are now heavily relied upon, kits are integral to how molecular biology work is conducted now. Kits greatly accelerate research throughput, simplify the organization of chemical inventories, and provide some economy where excess reagent inventories are minimized. Additionally, kits provide some degree of standardization that enables more precise communication between investigators and of research results. However, like calculators, kits can sometimes present downsides. These downsides arise from a combination of two sources: (i) the investigator and (ii) not all kits are created equal.

When one is first taught arithmetic with a calculator versus doing basic operations on paper or in their head, they can get stuck when the calculator dies or misbehaves. Alternately, they will be less likely to detect an obviously wrong answer that was generated by a key stroke error. Likewise, when one personally develops and trouble shoots a method, they acquire a deep knowledge about how each factor works and a sense of when good results are being generated or not. Also, the old-fashioned do-it-yourself approach can result in customization for a particular application albeit with a lot of effort. In contrast, it can be easy to simply try a kit and blindly accept the results. The inclusion of reference or control factors with a kit can greatly reduce the generation of replicated yet questionable results; hence, such kits are recommended especially when an investigator is venturing into new territory.

Concerning not all kits are created equal, there are two dimensions. First, some kits are really better than others. Second, a class of kits may be excellent in a general sense, but some differences in their components and design may render them more robust for a particular application. For example, cyclic AMP can be measured using an enzyme-linked immunosorbent assay (ELISA) strategy. While all use the excellent ELISA platform, they can differ in the effect exerted by putative interferents in the sample. Thus, for a particular sample, one kit may work considerably better than another.

Overall, kit manufacturers typically provide updated information on confounding factors and troubleshooting tips. Also, as in the mutagenesis kit described above, reference and control materials are commonly supplied. In all though, while it is hard to imagine working without the diverse array of useful kits, hang ups can still occur despite best efforts and following the instructions to the letter. Consequently, there are numerous forums on the Internet where questions and problems can be posed, and others respond by weighing in with their experience and opinions. Some examples are provided at the end of this chapter.

1.6.7 Transfecting Eukaryotic Cells

It is also possible to transfect eukaryotic cells. The steps and strategies can resemble that used to transform bacterial cells. For example, plasmids can be used to transfect yeast cells. However, additional challenges can arise due to the compartmental nature of eukaryotic cells. In this case, the foreign DNA to be inserted has to cross the cell wall and/or membrane and travel through several physical compartments before the nuclear DNA is encountered. Then, recombination with nuclear DNA must successfully occur before enzymes that destroy DNA have a chance to diminish the outcome.

It is desirable to perfect eukaryotic transfection for a number of reasons. Some proteins with therapeutic value have sugar residues attached to them. Such proteins are known as glycosylated proteins. As is the case for insulin production, it would be beneficial to use cell culture-based processes to produce specific glycosylated proteins with therapeutic potential. However, glycosylated proteins are not

produced by bacteria, whereas many eukaryotic cells have the synthetic capability to glycosylate proteins. Thus, a means to efficiently transfect eukaryotic cells such that genetic instructions are provided to produce specific proteins at a high level while controlling the glycosylation pattern of the protein of interest is under active investigation. The progress and challenges associated with transfecting eukaryotic cells are discussed in Chapter 5.

Another motivation for perfecting eukaryotic cell transformation is driven by many diseases that are now known to have specific genetic determinants. For example, as noted earlier, sickle-cell anemia is the result of a missense mutation. Therefore, some envision that the genes within humans can be repaired or replaced to eliminate disease-driving mutations. Gene therapy is the practice of transfecting cells within the human body for the purpose of remedying genetic-based diseases and pathologies. Researchers are either attempting to harness the infecting properties of viruses or they are developing particle-based DNA delivery systems.

To understand further the technology and medical impacts of transfecting eukaryotic cells, an interesting example of fusing tissue engineering with molecular biology technology to demonstrate a means for treating human disease was reported by Stephen et al. (2001). Tissue engineers typically seek to replace diseased tissue with a functional replacement that integrates with the host. In this example, the somewhat altered goal was to implant cells that integrate with host tissue, and because of the engineered genetic “programming,” substances are produced by the implanted cells that alter the course of a disease, such as ovarian cancer.

Mullerian inhibiting substance (MIS) was the substance of interest. MIS is a glycosylated protein that normally fosters regression of the ducts in the human embryo. MIS has also been found to promote the regression of ovarian tumor cells; hence, some researchers view MIS as a potentially useful chemotherapeutic. However, purifying MIS and then targeting delivery to a particular location within the body are not easy tasks.

The alternative investigated was to implant genetically modified, MIS-producing cells proximal to the therapeutic’s tissue target. Stephen et al. (2001) explored this strategy in mice with compromised immune systems. The transfected MIS-producing cells that were implanted into the mice were Chinese hamster ovary (CHO) cells. CHO cells are commonly used in studies that require transfected cells because much is known on how to successfully transfect them. Because the immune systems of normal mice would normally attack CHO cells, mice with suppressed immune systems were used to demonstrate the concept.

Transfected CHO cells were first seeded and grown on polyglycolic acid (PGA) scaffolds. After implant preparation, the effect of different size implants was investigated. A correspondence was found between implant size and MIS blood level. Thereafter, human tumor tissue was implanted into different mice, and the subsequent tumor mass that developed in MIS-producing and untreated mice was measured. The results were encouraging; tumor proliferation was statistically less significant in MIS-producing mice.

Overall, molecular biology has generated an array of diverse and more effective therapeutics, which biomedical and biochemical engineers now help to produce and develop administration technologies. Many new applications await to be developed that can vanquish animal and human diseases in novel ways.

1.7 Probing Gene Expression

As reviewed above, we now know how many mechanisms of gene expression operate. Moreover, we have made major progress on being able to manipulate the genetic inventory of cells as well as which genes are expressed. Consequently, interest has turned to fathoming how the collection of all gene expression events relate to each other and corresponds to particular disease conditions or behavioral traits. For example, some genes may be involved in interactive circuits where gene products interact with each other or expression occurs when a common set of external stimuli is present. Additionally, some genes may

have alterations that lead to diseases or the loss of circuit function. Elucidating the operating gene circuits is important for yielding more predictable outcomes for metabolic and tissue engineering. For example, modifying a gene or inserting a new gene may either have a positive effect or there may be no effect because an alteration to one component in a circuit is overridden by the imbedded control mechanisms.

An obvious method for probing gene expression profiles and interrelationships is to analyze for the product(s) of each gene's expression. When a given gene encodes for an enzyme, then the protein isolated from a cell can be analyzed to determine what enzyme activities are present. This traditional method has significantly contributed to our current knowledge. However, it is labor intensive, and clues on when genes with unknown function are expressed and thus suggestions on their potential function cannot be obtained. A global view of how gene expression networks function is also difficult to construct with the single measurement approach.

1.7.1 DNA Microarrays Profile Many Gene Expression Events

Recall that when a gene is expressed, mRNA is first produced. This working copy of mRNA is then translated to yield a protein. If one could obtain a "snapshot" of all the mRNAs that are present in a cell as well as their relative abundance, then one would possess a profile of what genes are currently expressed and to what extent. The latter assumes that particular mRNA's abundance is proportional to the extent a particular gene is expressed. Additionally, if a baseline profile is established for a particular environmental situation, then one can determine which genes are "up-regulated" or "down-regulated" when environmental conditions are changed.

The apparatus for obtaining the mRNA profile described above is commonly referred to as a DNA microarray, biochip, or gene array. Different segments of a cell's DNA are first attached to a surface, such as a glass slide. A slide can contain thousands of different "spots," where a different DNA sequence is present at each spot location, or multiples are used to permit replication. The cells subjected to analysis under a particular biological or environmental state contain many different mRNAs of varying abundances. DNA copies of the mRNAs are made using the activity of the enzyme, reverse transcriptase, which is viral in origin; the enzyme's activity reverses the central dogma in that mRNA \rightarrow DNA occurs. When the mRNA-derived DNA copies (complementary DNAs, cDNAs) are introduced to a gene chip, a given cDNA will bind to surface-bound segment via base-pairing when a significant base-pairing opportunity is present. The cDNAs are also labeled with a fluorescent dye. Wherever a binding event occurs on the gene array, a fluorescent spot will appear. Nonfluorescent spots indicate that no match existed between the surface-bound DNA and mRNA-derived, copy DNA. One interpretation is that the gene encoded by the surface-bound segment was not expressed under the particular conditions used to propagate the cells.

There are many experimental designs used. Often, two treatments are applied to a DNA array. In this case, the cDNAs are obtained from cells grown under two different conditions. The cDNAs obtained from cells growing in two different conditions are also labeled with different fluorescent dyes. For example, a bacterium such as *E. coli* can be grown on two different carbon sources. When grown on one carbon source, the cDNAs are labeled red. When grown on a different carbon source, the cDNAs of the mRNAs are labeled green. When the red- and green-labeled cDNAs are applied to DNA arrays, there are four "spot" coloration results: (1) bright spots absent, (2) red spots, (3) green spots, and (4) spots that vary in yellow coloration. The first case indicates that some particular genes are not expressed when either carbon source is used. The second and third cases indicate that different groups of genes are expressed depending on the carbon source metabolized. The fourth case suggests that some genes are coexpressed. The procedure just outlined is used for expression analysis because it is the level of mRNA that is analyzed, although indirectly due to the use of the mRNA \rightarrow fluorescent DNA copying step. To enable quantification, the fluorescent intensities are measured with a scanner. Lasers are used to excite the fluorescence and the image is digitized. Digitization allows for the calculation of intensity ratios.

Another useful application is genome typing. As before, DNA fragments are first spotted on a glass slide or another surface. However, instead of determining mRNA levels, genomic DNA fragments from a cell are directly used after they have been tagged with a fluorescent dye. One use of genome typing is to determine if an organism possesses a gene similar to different, yet more completely characterized organism. A gene inventory can be built for the less characterized organism because a binding event suggests that the less characterized organism possesses a gene found in the well-characterized organism.

The website managed by the National Center for Biotechnology Information (NCBI) is one archive for genomic and expression data. The link to this source and another archive are provided in the reference list.

Ongoing work aims to improve the “chip” technology further. For example, depending on how the DNA is processed prior to binding to the surface, different false-positive and false-negative results can occur. Thus, it is important to understand the details of DNA binding reactions in order to minimize confounding results. Another active research direction is to improve how data from such large-scale screening experiments is processed such that relationships between genes and environmental conditions are clearly extracted. One basic challenge is represented by the size of the dataset; hundreds or thousands of signals cannot be interpreted by the unaided human mind; hence, computer-aided statistical methods are used. Thresholding techniques are often used to include or exclude particular signals from a gene chip and if done incorrectly, false positives and false negatives can result. Finally, the analysis of time series data is of high interest. Such data can reveal the temporal sequence of how gene circuits operate. Again, large datasets are used, which presents challenges, and tools used in other fields for model identification from data with potential inherent uncertainty are being explored for use in this context.

1.8 Internet Resources

Earlier it was noted that PCR primers are usually designed and then submitted to synthesizers using resources on the Internet. The Internet also archives other data and resources that are relevant to molecular biology. Listed below are prominent databases used today as well as other useful resources.

Primer design and acquisition

- A good website for ordering purposes and the simplex method used to maximize weighted variables
<http://www.idtdna.com/Scitools/Applications/Primerquest/Default.aspx>
- A useful online worksheet
<http://frodo.wi.mit.edu/primer3/>

Kits

- QuikChange® Site-Directed Mutagenesis Kit vended by Stratagene (La Jolla, California)
<http://www.tufts.edu/~mcourt01/Documents/Stratagene%20Quikchange%20mutagenesis.pdf>
- Online queries and discussions of protocols and kits
<http://www.protocol-online.org/>
<http://molecularbiology.forums.biotechniques.com/index.php>
<http://biowww.net/browse-13.html>

Gene expression and DNA arrays

- National Center for Biotechnology Information
<http://www.ncbi.nlm.nih.gov/guide/genes-expression/>
<http://www.wip.ncbi.nlm.nih.gov/geo/>
- Stanford Microarray Database
<http://genome-www5.stanford.edu/>

E. coli information and decoding genetic abbreviations

- *E. coli* stats
http://redpoll.pharmacy.ualberta.ca/CCDB/cgi-bin/STAT_NEW.cgi
- *E. coli* genotypes (very useful)
http://openwetware.org/wiki/E._coli_genotypes#JM101
- Dam and Dcm methylases of *E. coli*
http://www.neb.com/nebecomm/tech_reference/restriction_enzymes/dam_dcm_methylases_of_ecoli.asp

Nucleic acid sequences

- National Center for Biotechnology Information
<http://www.ncbi.nlm.nih.gov/>
- European Bioinformatics Institute
<http://www.ebi.ac.uk/>
- Center for Information Biology and DNA Data Bank of Japan
<http://www.cib.nig.ac.jp/>
<http://www.ddbj.nig.ac.jp/>

Nucleic acid structure

- Nucleic Acid Database
<http://ndbserver.rutgers.edu/>

Protein sequences

- Swiss-Prot and TrEMBL
<http://us.expasy.org/sprot/>

Protein structures

- RCSB Protein Data Bank
<http://www.rcsb.org/pdb/>
- Swiss-3DImage
<http://us.expasy.org/sw3d/>

Protein families and domains

- Prosite
<http://us.expasy.org/prosite/>

References and Recommended Further Reading

- Alberts, B., Bray, D., Lewis, J., Raff, M., Roberts, K., and Watson, J.D. *Molecular Biology of the Cell*. Garland Publishing, New York, 1994.
- Dieffenbach, C.W. and Dveksler, G.S., eds. *PCR Primer: A Laboratory Manual*. Cold Spring Harbor Laboratory Press, Cold Spring Harbor, New York, 2003.
- McPherson, M.J. and Møller, S.G. *PCR*. BIOS Scientific Publishers Limited, Oxford, 2001.
- Stephen, A.E., Masiakos, P.T., Segev, D.L., Vacanti, J.P., Donahoe, P.K., and MacLaughlin, D.T. Tissue-engineered cells producing complex recombinant proteins inhibit ovarian cancer *in vivo*. *Proc. Natl Acad. Sci. USA*, 98, 3214–3219, 2001.

Backgrounds on Some Molecular Biology Pioneers

The Oswald T. Avery Collection from the National Library of Medicine <http://profiles.nlm.nih.gov/CC/>

Herbert Boyer http://www.accessexcellence.com/AB/BC/Herbert_Boyer.html

Jacques Monod, François Jacob, and André Lwoff <http://www.nobel.se/medicine/laureates/1965/>

James Sumner <http://www.nobel.se/chemistry/laureates/1946/>

Theodor Svedberg <http://www.nobel.se/chemistry/laureates/1926/svedberg-bio.html>

Databases and Other Supplementary Materials on Molecular Biology

The American Society for Microbiology <http://www.asm.org/>

A page on *Archaea* sponsored by the American Society for Microbiology <http://www.microbe.org/microbes/archaea.asp>

The Comparative RNA Web (CRW) Site: An online database of comparative sequence and structure information for ribosomal, intron, and other RNAs. Jamie J. Cannone, Sankar Subramanian, Murray N. Schnare, James R. Collett, Lisa M. D'Souza, Yushi Du, Brian Feng, Nan Lin, Lakshmi V. Madabusi, Kirsten M. Müller, Nupur Pande, Zhidi Shang, Nan Yu, and Robin R. Gutell. *BMC Bioinformatics*, 2002; 3:2. Copyright © 2002, Cannone et al.; licensee BioMed Central Ltd. Verbatim copying and redistribution of this article are permitted in any medium for any purpose, provided this notice is preserved along with the article's original URL. <http://www.pubmedcentral.nih.gov/articlerender.fcgi?artid=65690&rendertype=abstract>

Genentech Corporate Website <http://www.gene.com/gene/index.jsp>

General Glossary of Molecular Life Science Terms and Concepts from National Human Genome Research Institute (The glossaries also talk to you). <http://www.genome.gov/10002096>

Human Genome Project Information: DNA Forensics http://www.ornl.gov/TechResources/Human_Genome/elsi/forensics.html

Report and Recommendations of the Panel to Assess the NIH Investment in Research on Gene Therapy <http://www.nih.gov/news/panelrep.html>

Science Magazine Guide to On-Line Life Science Glossaries (The glossaries also talk to you). <http://www.sciencemag.org/feature/plus/sfg/education/glossaries.shtml>

2

Biomolecular Interactions

2.1	Overview of Molecular Forces.....	2-2
	van der Waals Interactions • Electrostatic Interactions • Hydrogen Bonds • Hydrophobic Effects • Configurational Entropy	
2.2	Ligand Binding.....	2-4
2.3	Isothermal Titration Calorimetry.....	2-5
2.4	Surface Plasmon Resonance.....	2-6
2.5	Nuclear Magnetic Resonance Spectroscopy.....	2-7
	Fundamental Principles • Environmental Effects on Resonance Frequencies • Multidimensional NMR • Measurement of Binding Affinity and Rate Constants Using NMR	
2.6	X-Ray Diffraction Methods.....	2-14
	Accuracy of X-Ray-Derived Structures • Limitations of X-Ray-Derived Structures	
2.7	Computational Methods.....	2-17
	Representation of Interaction Energy • Molecular Mechanics • Prediction of Ligand Binding Energy • Docking	
2.8	Emerging Techniques: Single Molecules.....	2-21
	References.....	2-21

Gordon Rule

Carnegie Mellon University

One of the most important aspects of biological systems is the interaction between molecules. The complexity of these interactions range from the binding of small molecules to proteins, such as in enzyme–drug interactions, to complex protein–protein and protein–nucleic acid interactions, as in the ribosome. There are numerous levels to the characterization of these interactions, at the structural level, at the thermodynamic level, and at the kinetic level. Characterization at the structural level is usually accomplished using x-ray crystallographic methods. Although x-ray methods are well established as a routine method of determining structures, nuclear magnetic resonance (NMR) spectroscopy offers a viable alternative, with some limitations (see Section 2.5). Although the structure of a biomolecular complex provides a rich source of information, it is far from a complete description of the complex. First of all, the structure is usually only one pose, or at best a number of snapshots of the conformational space available to the molecule. The dynamic properties of these complexes can be addressed by a number of techniques, such as fluorescence (Weiss, 2000), NMR relaxation studies (Mittermaier and Kay, 2006; Kay, 2005), or computational approaches (Klepeis et al., 2009), which are beyond the scope of this chapter. This chapter focuses mainly on (i) methods that experimentally measure the strength of biomolecular interactions, (ii) how characterizing the thermodynamic signature of the interaction can provide additional information on the nature of the interactions, and (iii) how the measurement of kinetic rate constants using surface plasmon resonance or NMR can provide useful information to develop a more complete characterization of the interaction. Although binding and kinetic rate constants can also be measured using more traditional fluorescence (Eftink, 1997) and stop-flow methods (see Fersht, 1998), they are not discussed here. An additional topic that is discussed is the use of x-ray crystallographic

information in conjunction with computational approaches to characterize biomolecular interactions. The major limitations of x-ray derived structures are discussed, followed by a brief overview of computational methods to discover and quantify protein–small molecule interactions.

2.1 Overview of Molecular Forces

The forces that affect the association of biological molecules are the same, regardless of the complexity of the interaction. These forces are briefly summarized below.

2.1.1 van der Waals Interactions

van der Waals interactions were first described by Johannes van der Waals to explain the nonideal nature of gases due to intermolecular attraction. The attractive force between two uncharged molecules can be due to either the interaction between permanent dipoles or the interaction between induced dipoles (London dispersion forces). The latter effect arises from fluctuations in the electron density on each atom, leading to transient attractive forces. A useful analytical representation of van der Waals potential energy between two particles is the Lennard–Jones potential:

The first term in Equation 2.1 is a repulsive term, the second attractive, r_{\min} is the distance that minimizes the energy, and ϵ is the energy at r_{\min} . Note that this interaction falls off quickly, at a rate of $1/r^6$ (see Figure 2.1). Although van der Waals interactions are weak, on the order of 1–2 kJ/mol-Å², the large and intimate contact area found in most biological interactions generates significant interaction energy (see Figure 2.2). From a thermodynamics perspective, van der Waals interactions largely contribute to the enthalpy change in complex formation.

2.1.2 Electrostatic Interactions

Electrostatic interactions can play a dominant role in biochemical interactions. The force between two charged particles is given in Equation 2.2. This interaction falls off more slowly as a function of distance

$$V(r) = \epsilon \left[\left(\frac{r_{\min}}{r} \right)^{12} - 2 \left(\frac{r_{\min}}{r} \right)^6 \right] \quad (2.1)$$

(see Figure 2.1) and it also depends on the dielectric constant (D) of the solvent. Water has a high dielectric constant (80), attenuating electrostatic interactions. The nonpolar interior of proteins and membranes have low dielectric constants (~ 4), enhancing electrostatic interactions. Since desolvation of the

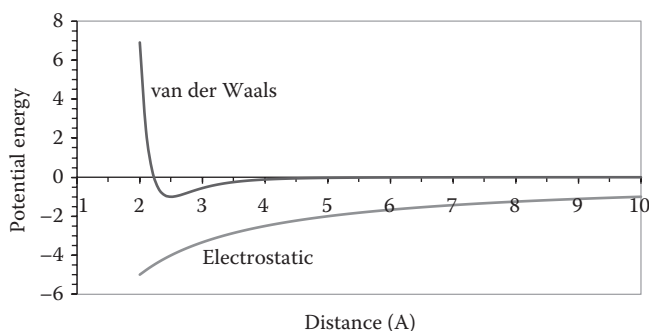


FIGURE 2.1 Distance dependence of molecular forces. Comparison of the distance dependence of van der Waals interactions (blue) and electrostatic interactions between unlike charges (purple).

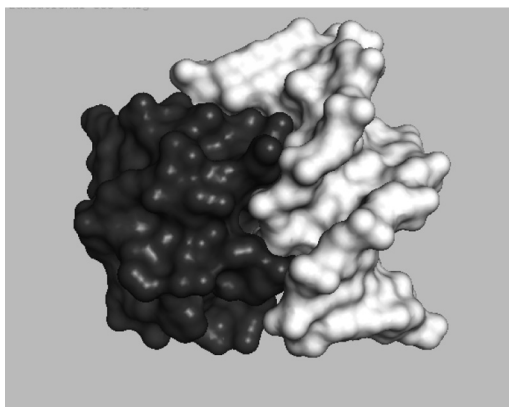


FIGURE 2.2 van der Waals interactions. Surface complementarily optimizes van der Waals interactions. Lambda cro protein (dark gray) fits tightly into the major groove of DNA (white). PDB file 3cro, figure generated using Pymol. (DeLano, W.L. 2002. *The PyMOL Molecular Graphics System*. DeLano Scientific, San Carlos, CA, USA. <http://www.pymol.org>.)

molecular interface often occurs during the formation of complexes, electrostatic interactions generally make a significant contribution to binding energies. It is also important to consider that the ionization of most biochemical functional groups occurs in a pH range of 3–9, making electrostatic interactions sensitive to pH. Electrostatic interactions contribute directly to the enthalpy of biomolecular interactions, but an entropic contribution can also occur due to an increase in the entropy of counterions that are displaced during the formation of the complex.

$$V(r) = \frac{1}{D} \frac{q_1 q_2}{r} \quad (2.2)$$

2.1.3 Hydrogen Bonds

Hydrogen bonds are formed between an electronegative hydrogen bond donor and an electropositive hydrogen bond acceptor (see Figure 2.3). This interaction is largely electrostatic, but has some degree of covalent character (~10%). Hydrogen bonds provide an interaction mechanism that is directional in space, thus enhancing the specificity of interactions. Although the intrinsic energy of a hydrogen bond is substantial, on the order of 20 kJ/mol, most biochemical interactions that involve hydrogen bonds are exchange reactions; a hydrogen bond to water is broken and then reformed in the complex, leading to only a modest gain of energy, on the order of 1–5 kJ/mol.

2.1.4 Hydrophobic Effects

Hydrophobic effects are important in the interaction of nonpolar compounds with water and provide the thermodynamic energy for phase separation of oil and water, the self-assembly of membranes, the folding of proteins, and the binding of nonpolar ligands to proteins. The common feature of all

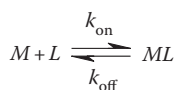


FIGURE 2.3 Hydrogen bonds. Hydrogen bonds (blue) form between electronegative acceptor groups (O) and electropositive donor groups (NH).

these phenomena is the exposure of nonpolar groups, which causes the ordering of water molecules in ice-like clathrates around the nonpolar group. Sequestering of the nonpolar group in a nonpolar environment releases this water, causing a favorable increase in the entropy of the system. The role of hydrophobic effects in biomolecular interactions can often be identified by heat capacity changes, which are negative when nonpolar surface areas become buried in the interaction (Livingstone et al., 1991; Loladze et al., 2001).

2.1.5 Configurational Entropy

Configurational entropy commonly destabilizes biochemical interactions. The entropy associated with different configuration states of a system is given by Boltzmann's equation: $S = R \ln W$, where W is the number of conformations. In general, the number of states is large for unbound systems, leading to an unfavorable decrease in entropy upon binding as conformational states of the interacting molecules are frozen out (Mills et al., 2009). However, some proteins maintain high entropy states after binding of ligands (Kay et al., 1996).



2.2 Ligand Binding

Biomolecular association can be characterized by the kinetic scheme shown on the right; the macromolecule (M) binds the ligand (L) to form the protein–ligand complex (ML). The macromolecule is usually a protein or enzyme and ligands are usually small molecules, such as drugs; however, the same analysis can be applied to any interacting molecules. The dissociation constant, K_D , is the equilibrium constant for the reverse reaction and it is equal to $[M][L]/[ML]$, or equivalently to the ratio of the kinetic rate constants: $k_{\text{off}}/k_{\text{on}}$. For simple noncooperative systems, the free energy of binding can be obtained directly from the K_D . Note that many proteins can often bind more than one ligand of the same type, for example, the oxygen transport protein hemoglobin binds four oxygen molecules, or multiple different ligands.

In simple systems, the association rate constant, k_{on} , is the rate at which molecules collide in solution, and diffusion limits this value to $\sim 10^8 \text{ M}^{-1}\text{s}^{-1}$. Note that the observed on-rate also depends on the ligand concentration: $k_{\text{on}}^{\text{obs}} = k_{\text{on}}[L]$, with units of s^{-1} . The kinetic off-rate, k_{off} , is sensitive to the strength of the interaction in the ML complex; the off-rate decreases as the strength of the interaction increases. Typical values for the off-rate vary from 10^{-2} to 10^6 s^{-1} , corresponding to K_D values of 10^{-10} to 10^{-2} M . One of the strongest interactions that can be found in biological systems is the interaction between the protein avidin and the small molecule biotin; the K_D for this interaction is $\sim 10^{-15} \text{ M}$, corresponding to a phenomenally slow off-rate of 1 event every 115 days.

Although knowledge of the K_D for a protein–ligand pair allows prediction of the amount bound at any given $[L]$, information on the kinetic rate constants provides additional information regarding the binding mechanism. In particular, if the kinetic on-rate is smaller than the diffusion limit, it is likely that a conformational change is required for binding (Fersht, 1998).

$$Y = \frac{[ML]}{[M] + [ML]} = \frac{[L]}{K_D + [L]} \quad (2.3)$$

Noncooperative systems have the property that the binding of multiple ligands to the same protein are independent; the binding of one ligand has no effect on the affinity of subsequent ligands. In this case, the fraction of protein with ligand bound, or the fractional saturation (Y), can be defined as in

Equation 2.3. Note that the ligand concentration that half-saturates the protein is equal to the dissociation constant, making the K_D a useful characteristic of the system.

Cooperative systems occur if the binding of one ligand affects the binding of subsequent ligands. A system can either show positive cooperativity, where the binding of one ligand enhances the binding of others, or negative cooperativity, where the binding of one ligand reduces the affinity of subsequent ligands. The nature and degree of cooperativity can be obtained from experimental measurements of Y versus $[L]$ using a Hill plot. The slope of a plot of $\log(Y/(1 - Y))$ versus $\log[L]$ as the x-axis is crossed gives the Hill coefficient. This coefficient is one for noncooperative systems, less than one for negatively cooperative systems, and greater than one for positively cooperative systems.

2.3 Isothermal Titration Calorimetry

This technique measures the amount of heat released or absorbed due to the formation of biomolecular complexes (Leavitt & Freire, 2001). Since most biomolecular interactions result in a change of enthalpy, this technique can be used to characterize a large number of interactions without the necessity to modify the protein to introduce a detectable spectroscopic signal. In addition to characterizing protein–ligand interactions in detail, titration calorimetry can be used to screen compound libraries to identify potential drug candidates (Ward & Holdgate, 2001).

The instrument titrates a known amount of one solution (e.g., ligand) into a solution of protein (see Figure 2.4). Modern instruments typically require only 50 μM of protein in a volume of ~ 1.5 mL. The amount of electrical energy required to maintain the sample cell at the same temperature as the reference cell is used to determine the heat change that occurred due to binding. Typically, the heat evolved from a series of ligand titrations is measured (see Figure 2.5). The resultant data can be fit to theoretical binding equations (e.g., Equation 2.3). Under ideal conditions, it is possible to obtain the enthalpy, entropy, and free energy ($=RT\ln(1/K_D)$) of binding, along with the number of binding sites, and the cooperativity of binding.

An additional feature of this technique is that it is very easy to obtain the heat capacity change during binding, $C_p = dH/dT$, by simply measuring the enthalpy at different temperatures. Studies with model proteins have shown that the change in heat capacity is negative ($\Delta C_p = -0.32$ cal mol/deg-Å²) when

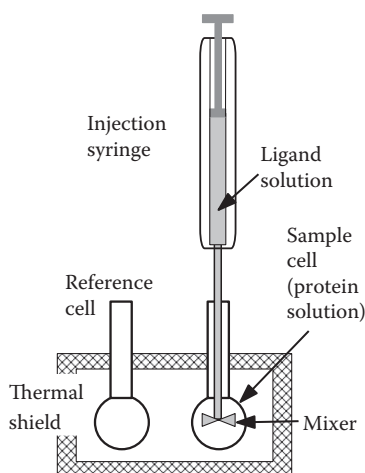


FIGURE 2.4 An ITC instrument. The sample cell contains the protein solution. The ligand is injected into the sample cell and mixed with the protein solution by mechanical stirring. The electrical current required to maintain the same temperature in the sample cell as in the reference cell is used to calculate the amount of heat released by the formation of the protein–ligand complex.

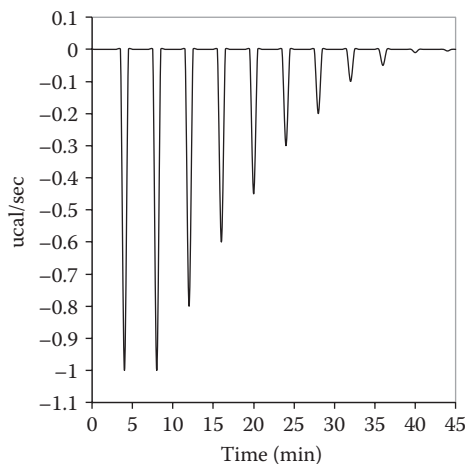


FIGURE 2.5 Titration calorimetry data. Equal amounts of ligand are injected every 4 min and the heat evolved per second is measured. The first two injections indicate that essentially all of the injected ligand is bound to the protein. Subsequent injections evolve less heat since the protein is becoming saturated with the ligand; the last titration does not produce any heat since the protein is saturated with the ligand.

nonpolar surfaces become buried and positive when polar surfaces become buried ($\Delta C_p = +0.14$ cal mol/deg-Å²) (Loladze et al., 2001). Consequently, considerable information on the energetic contributions of interfacial groups can be obtained from this measurement.

When the binding affinity is too tight (low K_D), it is only possible to obtain a reliable measure of the enthalpy because all of the added ligand binds to the protein, regardless of the degree of saturation. In this case, the titration peaks are the same for all titrations until the protein becomes saturated, at which point no additional heat is produced. The dissociation constant for the reaction can be obtained if another, weakly binding ligand is available. In this case, the presence of the weakly binding ligand during the titration of the tightly bound ligand lowers the apparent affinity of the strongly binding ligand such that the amount of heat evolved varies as a function of ligand (Sigurskjold, 2000).

A particularly useful application of titration calorimetry has been to evaluate the thermodynamic signature of antiretroviral compounds that inhibit HIV protease (Velazques-Campoy et al., 2001). In this study, it was found that a series of compounds with similar binding free energies had distinctly different enthalpic and entropic contribution to the binding, ranging from entropically driven (ΔH° for binding is positive) to an equal balance between enthalpic and entropic terms. The latter class of drugs, with a more balanced thermodynamic profile, appear to be more adaptable to mutations in the HIV protease.

2.4 Surface Plasmon Resonance

This technique can be used to measure the binding affinity as well as obtain information on kinetic on- and off-rates (Nguyen et al., 2007). The principal advantage of this technique is that it indirectly measures an increase in mass as a ligand binds to its target on an immobilized surface. Consequently, it is not necessary to modify the protein (or ligand) in any way to perform the measurement. The technique is sufficiently sensitive that it is possible to screen libraries of compounds in parallel using microfluidic sample cells. The fundamental operating principle of the instrument is illustrated in Figure 2.6. The base of the sample cell consists of a glass plate that is coated with gold. The sample cell is illuminated from underneath and the light is completely reflected at the glass-water (buffer) interface due to the difference

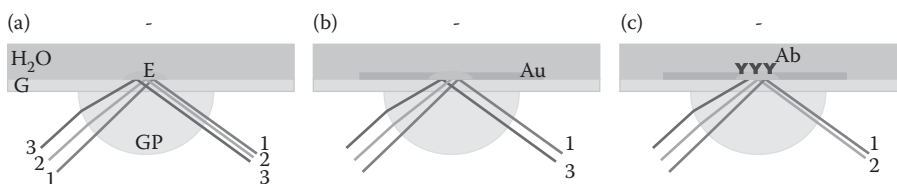


FIGURE 2.6 SPR instrumentation. Panel (a) illustrates only the optical path. Light beams 1, 2, and 3 are refracted by the circular glass (GP) prism and show total internal reflection at the glass (G)–water interface, generating an electrical field (E, yellow) that extends several hundred angstroms into the aqueous compartment. Note that the three light beams strike the glass plate at different angles due to the curvature of the prism. Although three light beams are shown, in practice, a continuous spread of light is used. In an SPR sample cell (b), a thin layer of gold (Au) is coated on the glass slide. Coupling between the light and the electrons will excite plasmon waves in the metal, leading to absorption of the light. The strength of the coupling depends on the angle of incidence and the refractive index of the aqueous compartment. In this example, light beam 2 is absorbed by the gold film. Panel (c) shows the effect of increasing the mass at the gold surface by the attachment of antibody molecules (Ab). The change in refractive index alters the incidence angle that stimulates plasmon waves. In this example, light beam 3 is now selectively absorbed by the gold after the attachment of antibodies. The binding of ligand to the antibody (not illustrated) would lead to a further change in the angle of incidence that stimulates plasmon waves in the gold. The change in the incidence angle required to stimulate plasmon waves is measured by the instrument.

in the refractive index of the buffer versus the glass. Although the light is reflected at the interface, an electrical field is generated that extends into the buffer; thus, the optical properties of the interface are sensitive to binding events at the surface, provided they cause a change in the refractive index. Although the changes in the refractive index are small, they can be easily detected by taking advantage of the fact that light can excite electrons in metal films, forming plasmon waves, and this excitation leads to the absorption of light instead of reflection. The amount of excitation depends on the angle of incidence and the refractive index of the buffer solution. Consequently, as the refractive index changes due to binding to the interface, the angle of incidence that stimulates plasmon waves also changes. The change in angle is reported by the instrument in arbitrary units (response units, RU).

Typically, one of the binding partners (e.g., protein and antibody) is immobilized on a surface within the sample cell and ligand is flowed over the immobilized protein. Owing to the small size of the sample cells, very little (μg) protein is required for immobilization. By varying the ligand concentration, it is possible to determine the dissociation constant, K_D , from the measured RU at equilibrium. The initial rate of the RU change after addition of the ligand can be used to estimate the kinetic on-rate, using the relationship that the observed $k_{\text{on}}^{\text{obs}}$ is equal to the on-rate times the free ligand concentration: $k_{\text{on}}^{\text{obs}} = k_{\text{on}}[L]$. The off-rate can be obtained by measuring the signal after washing the surface with solution without ligand. Under these conditions, there is no rebinding of the ligand and the off-rate can be obtained directly from the decay of the signal (see Figure 2.7). The on- and off-rates that are obtained with surface plasmon resonance (SPR) are generally similar to those measured in solution. However, immobilization of the protein on the surface can alter the binding kinetics due to steric factors as well as mass transport issues (Schuck & Zhao, 2010).

2.5 Nuclear Magnetic Resonance Spectroscopy

NMR has a number of potential applications in the area of biomolecular interactions. Changes in the positions of resonance lines from the protein can be used to detect protein–ligand interactions as well as provide an estimate of the dissociation constant. Under favorable conditions, it is also possible to obtain the kinetic on- and off-rates from the spectra. Lastly, NMR can be used to determine the structure of the protein–ligand complex in solution at atomic resolution (see Figure 2.8). Although it is usually more

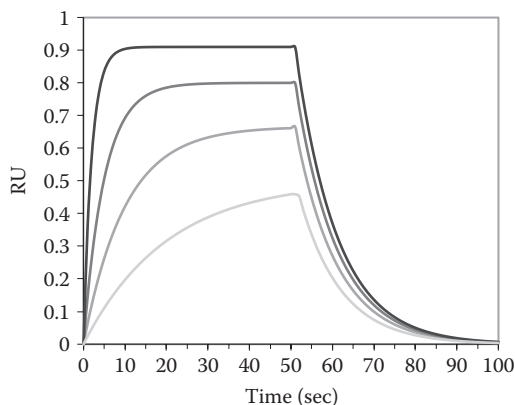


FIGURE 2.7 SPR data. Increasing amounts of ligand (cyan, blue, magenta, red) were introduced at time = 0 to a plate containing protein. As the ligand absorbs to the plate, the response increases. At $t = 50$, the ligand was removed. The height of the response after equilibrium reached is proportional to the fractional saturation, Y . The rate of signal build-up at different ligand concentrations can be used to estimate the on-rate. The decay of the signal after ligand is removed provides the off-rate.

efficient to determine structures by x-ray crystallography, it may be difficult to obtain suitable crystals of protein–ligand complexes, or the x-ray derived structure may have been distorted by crystal packing, making NMR a viable alternative to x-ray diffraction for structure determination. One of the major limitations of NMR spectroscopy is the size of the complex that can be studied. This limitation depends somewhat on the desired application, and current limits are given in [Table 2.1](#).

Certain applications listed in [Table 2.1](#) require NMR assignments. The assignment process involves determining the chemical shift of each NMR active atom in the protein and typically requires samples that are labeled with ^{15}N and ^{13}C . Fortunately, advances in heterologous protein production in *Escherichia coli* have made it relatively straightforward to obtain sufficient quantities of labeled material for most applications. Although the assignment process in such complex molecules appears complicated at first glance, robust methods for assignment have been developed to obtain these assignments (Ikura et al., 1990) and automated computer programs that can automatically assign spectra and determine structures are available (Altieri & Byrd, 2004; Guntert, 2009).

Although relatively concentrated protein solutions are required for most NMR experiments (e.g., 0.5–1 mM in a sample volume of 0.4 mL), the same expression systems used for isotopic labeling typically provide sufficient protein for routine studies, such as a detailed characterization of the structure,

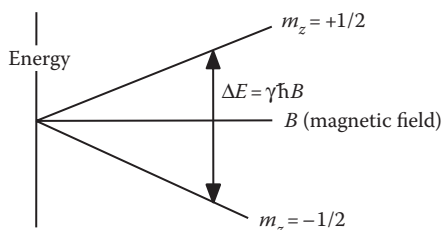


FIGURE 2.8 Effect of magnetic field on transition energies. The energies of the ground and excited state decrease and increase as the static field increases, respectively, making the overall transition energy, ΔE , linearly proportional to the field.

TABLE 2.1 Size Limitation for NMR Applications

Technique	Size Limit (Upper)
High-resolution structure determination ^a	25 kDa
Low-resolution structure determination ^a	50–80 kDa
Detection of ligand binding	100–200 kDa
Measurement of binding kinetics	100–200 kDa
Mapping ligand-binding sites ^a	50–80 kDa

^a Requires assignment of NMR resonances to individual atoms.

thermodynamics, and kinetics of protein–ligand interactions. In many cases, large amounts of material can be generated for screening chemical libraries for potential lead compounds using NMR.

2.5.1 Fundamental Principles

NMR is a form of spectroscopy that detects transitions of nuclear spin states. Like any other form of spectroscopy, the sample is irradiated with light (radiowaves in this case) and the absorption as a function of frequency (instead of wavelength) is measured. The major difference between NMR and other forms of spectroscopy is that a static magnetic field has to be present to generate an energy difference between the two nuclear spin states. The energy of each state is $E_{Mz} = \mu_M B = \gamma \hbar m_z B$, where μ_M is the nuclear magnetic dipole, B is the field at the nucleus, γ is the gyromagnetic ratio, and m_z is the quantum number for the z -component of the angular momentum. The gyromagnetic ratio (γ) represents the strength of the interaction between the applied field and the nuclear spin. It depends on the type of nuclei, for example, hydrogen atoms show one of the highest values of γ (26,750 rad/G-s), while the γ for ^{13}C is 6728, and for ^{15}N γ is -2712 . For spin one-half nuclei, $m_z = \pm 1/2$ and the energy difference between the two states is $\Delta E = \gamma \hbar B$, which is equivalent to a resonance (absorption) frequency of $\omega = \gamma B$. Note that both the absorption energy and the sensitivity increase as the gyromagnetic ratio and the magnetic field strength increase, hence the desire to perform NMR experiments that detect resonance signals from hydrogen atoms at the highest available field.

In order to standardize absorption frequencies to account for different magnetic field strengths in different laboratories, a chemical shift scale has been developed to remove the dependence on the external magnetic field strength. This is accomplished by dividing the observed frequency of a resonance, ν , by the frequency of a reference compound, ν_o (Equation 2.4). The units of chemical shift are in ppm, or parts per million.

$$\delta = \frac{\nu - \nu_o}{\nu_o} \times 10^6 \quad (2.4)$$

2.5.2 Environmental Effects on Resonance Frequencies

The actual absorption frequency of a spin is dependent on the magnetic field at the nucleus. This field can be altered by a number of factors, resulting in an absorption frequency that depends on the *environment* of the spin.

The electronegativity of nearby atoms will change the absorption frequency because electrons that surround a nucleus reduce the effective magnetic field at the nucleus. As the number of electron withdrawing groups increases, the electron density at the atom decreases, leading to a higher field at the nucleus and a higher absorption frequency (see [Figure 2.9](#)). The resonance frequency can also be affected by the presence of local fields that are generated by delocalized electrons on aromatic compounds (e.g., Tyr, Trp, Phe, nucleotide bases) in response to the external magnetic field. The local field can either increase or decrease the total field at the observed spin, depending on its location relative to the aromatic group. The field is increased at the edge of rings and decreased above or below rings.

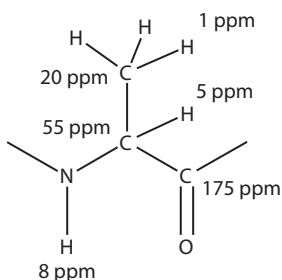


FIGURE 2.9 Typical chemical shifts of an Ala residue in a protein. Note that the amide proton has the highest proton shift (8 ppm) since it is directly attached to the electronegative nitrogen. The proton shifts of the H. proton (5 ppm) and the methyl protons (1 ppm) decrease systematically due to their increased distance from the electronegative atoms. The carbon shifts follow the same trend, with the carbonyl showing the highest chemical shift, followed by the alpha and then the beta carbon. Note that the three methyl protons will have the same chemical shift because they are equivalent.

The extreme sensitivity of the chemical shift to its environment, coupled with the relative narrow linewidths of NMR transitions, often generates resolved resonance lines from chemically similar groups with a protein, allowing one to probe systems at the atomic level with NMR. In contrast, the large line-width associated with electronic (e.g., UV-Vis) and vibrational transitions (e.g., IR) generally lead to severely overlapping lines for such groups.

If ligand binding alters the environment of even a single nuclear spin in a protein, it is generally possible to detect the binding event by observing a change in the position of the resonance line that arises from that spin. For example, a protein that contains four alanine residues will often show four distinct resonance lines from the alanine methyl protons, one line for each alanine in the protein (see Figure 2.10). If the ligand binds close to one of the alanine residues, it is likely that the resonance peak from that alanine will show an altered chemical shift. Note that the detection of binding does not require the assignment of a resonance line to a particular atom; it is just that the chemical shift is altered due to binding. However, the assignment of resonance lines to individual atoms is necessary if it is desirable to either map the ligand-binding site, or to determine the structure of the protein-ligand complex.

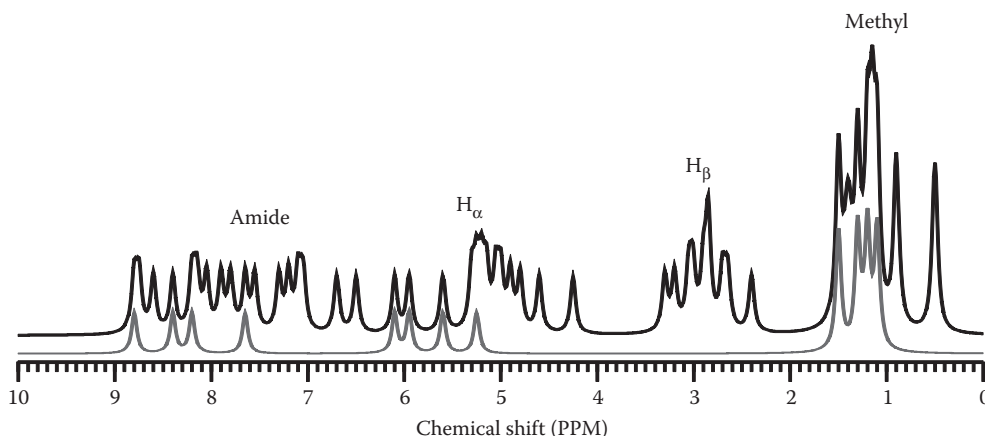


FIGURE 2.10 Proton NMR spectrum of a small 15-amino-acid protein. The upper (black) spectrum shows the complete spectrum, the lower (red) spectrum shows the contribution to the overall spectrum of the resonances that arise from the four Ala residues in the protein. Although many protons give rise to resolved resonance lines, many resonances overlap to some extent, even in this relatively small protein.

2.5.3 Multidimensional NMR

The spectra shown in [Figure 2.10](#) is an NMR spectrum of a small protein: as the protein size increases, the number of lines and the width of the lines increase, leading to severely overlapped resonance lines in larger proteins. Multidimensional NMR provides a method to reduce the spectral overlap by spreading the spectral lines over two (or more) dimensions. The generation of multidimensional NMR spectra requires coupling of some form between the spins and the frequencies of the coupled spins define the location of the peak in the spectra. The two forms of coupling are dipolar or scalar (also referred to as J) coupling. Dipolar coupling involves an interaction between the local magnetic field induced by one spin on another nearby spin. This form of coupling depends on the distance and is the basis for structure determination by NMR spectroscopy. Generally, proton–proton dipolar couplings are measured and the two coupled protons need to be within 5–6 Å to produce measurable coupling. Protein structures are constructed from NMR spectra by measuring a large number of short interproton distances.

The second form of coupling, scalar coupling, occurs via bonding electrons and is generally only detectable if the spins are separated by three or fewer bonds. One-bond scalar couplings, for example, $\text{H-}^{15}\text{N}$ or $\text{H-}^{13}\text{C}$, are much stronger than multiple-bond couplings and provide a sensitive method of generating two-dimensional proton–nitrogen or proton–carbon coupled spectra. Spectra of these types are either HSQC (heteronuclear single quantum coherence) or HMQC (heteronuclear multiple quantum coherence) (Rule & Hitchens, 2005; Mandal & Majumdar, 2004), depending on the details of data acquisition. Two-dimensional proton–nitrogen and proton–carbon (methyl region) spectra of the small protein are shown in [Figure 2.11](#). Note that the amide and methyl peaks in these two-dimensional spectra are now completely resolved; consequently, information can be obtained from each amide and methyl group in this protein.

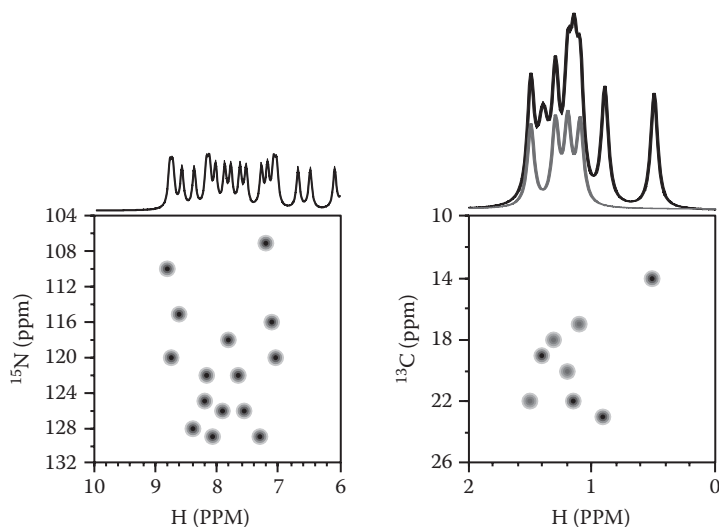


FIGURE 2.11 Two-dimensional NMR spectra. Two-dimensional proton–nitrogen (left) and proton–carbon spectra (right) of the same protein shown in [Figure 2.10](#). Each dot is a peak whose position is defined by the chemical shift of the coupled spins. For example, the uppermost peak in the right spectrum is an Ile delta methyl group with a proton shift of 0.5 ppm and a carbon shift of 14 ppm. The one-dimensional proton spectrum is shown on the top of each Two-dimensional spectrum. The three rightmost peaks above the proton–nitrogen spectrum correspond to alpha protons; consequently, they do not appear in the proton–nitrogen Two-dimensional spectra because those protons are coupled to carbon atoms instead of nitrogen. The methyl resonances from the four Ala residues are indicated in red.

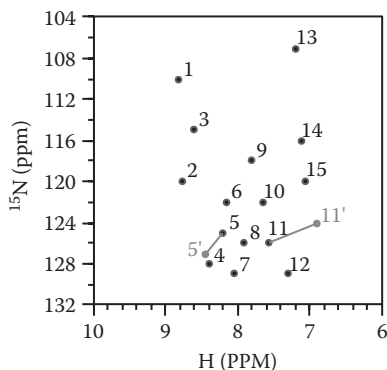


FIGURE 2.12 Effect of ligand binding on the two-dimensional proton–nitrogen spectrum. The numbers adjacent to the peaks indicate the residue assignment for that peak. The magenta peaks indicate resonance peaks that moved due to ligand binding; in this case, from residues 5 and 11. This suggests that the ligand binds close to residues 5 and 11 in the tertiary structure of the protein.

The binding of a ligand to the protein will alter the environment of the nuclear spins, leading to chemical shift changes of the spins. Ligand-induced changes to the mainchain atoms are usually detected in proton–nitrogen two-dimensional spectra. Figure 2.12 shows an overlay of proton–nitrogen spectra acquired with and without ligand. Peaks that changed their position in the spectra are colored magenta. Note that each peak is labeled with the corresponding residue number of the amide group that gave rise to the peak, that is, this spectrum has been assigned. The resonance peaks corresponding to residues 5 and 11 show significant changes in chemical shift due to ligand binding. In general, the closer the amide group is to the ligand-binding site, the larger the chemical shift. Consequently, this spectrum suggests that the ligand binds in the vicinity of residues 5 and 11 in the tertiary structure, providing some structural information on the protein–ligand interaction. Ligand-induced changes in the proton–nitrogen spectra have proven useful for screening chemical libraries (Hajduk et al., 1999) as well as identifying drug-binding sites (Medek et al., 2000).

Ligand-induced environmental changes of the mainchain NH atoms can be small in the case of some protein–ligand pairs, making it difficult to detect ligand binding using proton–nitrogen spectra. In this case, observation of the methyl groups often shows chemical shift changes due to ligand binding. The assignment of methyl groups can be more difficult than amides, especially for larger proteins. However, even in the absence of assignments, the observation of significant changes of methyl proton and carbon shift from the protein in the presence of a ligand is indicative of an interaction between the two molecules and is therefore useful for chemical library screening (Hajduk et al., 2000).

2.5.4 Measurement of Binding Affinity and Rate Constants Using NMR

When ligand binding causes a change in the chemical shift of a resonance line, it is usually possible to determine the binding affinity from these changes. Under certain circumstances, the kinetic on- and off-rates for binding can also be determined. Whether this can be accomplished depends on the relationship between the kinetic rate constants, k_{on} and k_{off} , and the size of the ligand-induced change in resonance frequency $\Delta\nu_{12} = \nu_1 - \nu_2$. In this analysis, it is useful to define an average exchange rate, $k_{\text{ex}} = (k_{\text{on}} + k_{\text{off}})/2$. There are four general possibilities:

1. If the exchange rate is smaller than the frequency difference between the two states, $k_{\text{ex}} \ll \Delta\nu_{12}$, then the system is said to be in slow exchange. In this case, the equilibrium binding constant and the individual rate constants can be measured. Under conditions of slow exchange, the spin spends a sufficiently long time in one environment to record its resonance frequency. Consequently, two

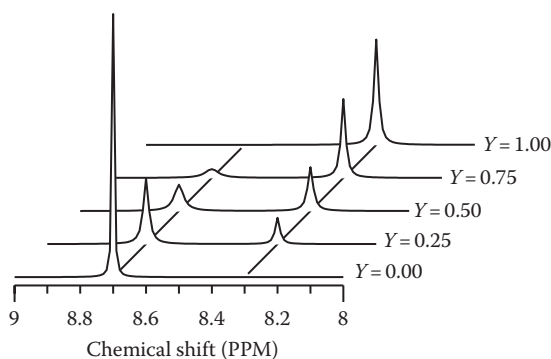


FIGURE 2.13 Slow exchange kinetics. The chemical shift of a resonance line is 8.7 ppm in the absence of ligand. Ligand binding changes the environment of the spin, moving its resonance frequency to 8.3 ppm. As the ligand is added, the intensity (integrated area) of the peak corresponding to the free state decreases while the intensity of the peak associated with the bound state increases. The relative areas of the peaks gives the fractional saturation: $Y = I_B / (I_B + I_F)$. In this example, the linewidth of the resonance from the free state increases as the ligand is added; the increase in linewidth is proportional to the kinetic on-rate. The plots are displaced to the right as Y increases to clearly illustrate the change in peak intensity; the positions of the resonance lines are not changing, only their intensities.

- resonance lines will be observed, one from each environment (e.g., in the absence or presence of ligand). The intensity of each line is proportional to the population of the system in that state, providing a direct measurement of the dissociation constant from the line intensities (see Figure 2.13).
- The exchange process can also affect the linewidth, and this effect can be used to obtain the individual rate constants. In the absence of exchange, the linewidth of an NMR resonance line, $\Delta\nu$, is proportional to the decay rate (R_2) of the excited state: $\Delta\nu = R_2 / \pi$. The decay rate of excited nuclear spins is largely defined by the overall molecular weight of the complex; spins in larger proteins have larger R_2 values. When exchange occurs, the decay of the excited state is enhanced by the exchange process; the spin now has two processes by which to leave the excited state: the normal relaxation process (R_2) or by exchanging to another environment due to ligand binding. Therefore, the increase in linewidth due to the presence of the ligand directly gives the exchange rate: $\pi\Delta\nu = R_2 + k$; k_{on} is obtained from the resonance lines in the unbound state and k_{off} is obtained from the increase in linewidth of the resonances in the bound state.
 - If the exchange rate is much higher than the frequency difference between the two states, $k_{\text{ex}} \gg \Delta\nu_{12}$, then the system is said to be in fast exchange. In this case, the environment of the spin is changing between the bound and unbound states too rapidly to measure its frequency in either state and the observed chemical is simply the weighted average of the chemical shift in the bound (b) and ligand-free (f) state: $\delta_{\text{obs}} = f_b\delta_b + f_f\delta_f$ (see Figure 2.14). This provides a particularly easy way to measure the fraction saturated at any ligand concentration: $Y = (\delta_{\text{obs}} - \delta_f) / (\delta_b - \delta_f)$, from which a dissociation constant, K_D , can be readily obtained. The observed linewidth is the weighed average of the ligand-bound and free states and contains no information on the rate constants for chemical exchange.
 - If the exchange rate is similar to the frequency difference between the two states, $k_{\text{ex}} \approx \Delta\nu_{12}$, then a complex lineshape is observed that depends on the individual rate constants, the ligand concentration, and the chemical shifts of the ligand-bound and free states. Closed form equations exist that describe this lineshape (McConnell, 1958); consequently, it is possible to directly fit the lineshape to obtain the kinetic on-, and off-rate, and indirectly the K_D . In practice, a series of spectra is collected at different fractional saturation levels and these spectra are fit to obtain global estimates of the kinetic rate constants (see Hitchens et al., 2006).

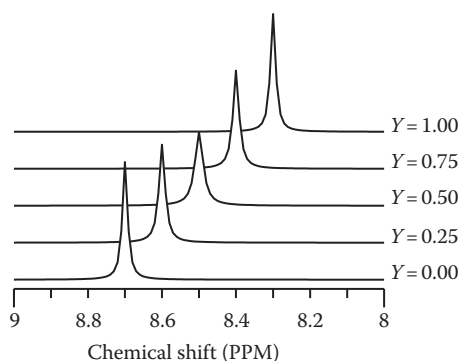


FIGURE 2.14 Fast exchange kinetics. An average chemical shift is observed, beginning with the unliganded state at 8.7 ppm. As the ligand is added, the observed chemical shift changes in proportion to the amount of bound ligand, reaching the chemical shift for the bound state, 8.3 ppm, when the protein is fully saturated. Some line broadening may be observed at intermediate points in the titration, as illustrated here, if the exchange rate is approaching the intermediate state.

2.6 X-Ray Diffraction Methods

Structure determination using x-ray diffraction methods provides an atomic-level description of the protein–ligand complex. In general, protein–ligand structures that are determined by diffraction methods are more precise than those determined by NMR methods. Such structures, determined by either method, are typically used as the starting point for computational methods for rational drug design or compound library screening for the discovery of lead compounds. The overall process of structure determination by x-ray diffraction is well described in many biophysics texts and therefore only briefly outlined here (Figure 2.15). The focus in this section will be a description of the potential pitfalls in the use of x-ray-derived structures in the analysis of protein–ligand interactions. The reader is referred to several excellent reviews on errors in x-ray-derived structures for more details (Davis et al., 2003; Brown & Ramaswamy, 2007; Wlodawer et al., 2008).

$$R = \frac{\sum_{\text{hkl}} || F_{\text{obs}}(h,k,l) | - | F_{\text{CALC}}(h,k,l) ||}{\sum_{\text{hkl}} | F_{\text{obs}}(h,k,l) |} \quad (2.5)$$

2.6.1 Accuracy of X-Ray-Derived Structures

The final result of structure determination is a coordinate, or protein database (pdb) file, that describes the model that was built from the scattering data/electron density map. This file contains the Cartesian coordinates for the protein, any bound ligands, numerous water molecules, as well as any other atoms/molecules whose positions are relatively fixed in the crystal. The accuracy of this model can be assessed using a number of parameters, including (i) a comparison of the R-factor to the free R-factor, (ii) the temperature (or B) factor, and (iii) the number of Ramachandran outliers. Although these factors can be combined to form a single quality index (Brown and Ramaswamy, 2007), it is useful to discuss the individual parameters since these parameters can often be directly obtained from the downloaded coordinate file.

The R-factor is a measure of how well the measured scattering, F_{obs} , agrees with the scattering that is calculated from the model, F_{CALC} (see Equation 2.5). Acceptable R-factors depend on the resolution

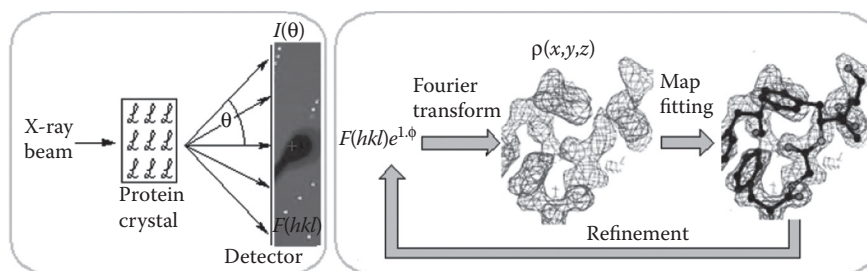


FIGURE 2.15 Structure determination by x-ray diffraction. The process consists of two major steps, data acquisition (left) and model building (right). The protein of interest is crystallized either with bound ligand, or preexisting crystals are soaked with ligand. The intensities, I , of x-rays that are scattered from the electrons in the crystal are detected for different scattering angles, θ . Higher-resolution structures require data at high scattering angles. Owing to the periodicity of the crystal lattice, the scattering angles that give measurable scattering are discrete, as shown by the localized yellow dots on the detector image. The final data set consists of structure factors, F , indexed by their position on the detector plate, $|F(h,k,l)|^2 = I(\theta)$. In the second phase, the electron density in space, $\rho(x,y,z)$, is obtained by Fourier transformation of the structure factors. The phase of the structure factor, ϕ , cannot be obtained from the diffraction data directly. The phase is obtained either by using several heavy atom derivative crystals, or by measuring the scattering of selenium–methionine substituted crystals at multiple wavelengths, or by calculation from a similar structure. The latter technique is referred to as molecular replacement. Since the phases are more important in the generation of the electron density map, model bias from similar structure used in molecular replacement can easily occur. After the calculation of the electron density map, atoms are placed into the density, a process called map fitting. This initial model is used to recalculate the phases and multiple cycles of model adjustment, and map calculations are typically required during refinement of the structure. Maintenance of good molecular geometry and van der Waals interactions during this process is aided by molecular mechanics calculations. Toward the end of the model-building process, water molecules are added to regions of unoccupied electron density near appropriate hydrogen bond donors and acceptors. Thermal disorder factors, or B-factors, are also refined at this time.

of the structure (see Kleywegt and Jones, 2002), with smaller R-factors expected for higher-resolution structures; typical R-factors for a 2 Å structure are about 20%. Overfitting of the model to the experimental data will lead to low R-factors; consequently, the free-R, which is obtained by refining the structure with the omission of a subset of the data and then determining the agreement between the omitted data and the model is a better estimate of how well the structural model fits the data. Typically, the value of R-free should be ~5% higher than the R-factor; larger discrepancies between the two values strongly suggest errors in the structural model.

The temperature (or B) factor is related to the intrinsic disorder of an atom (Δx), as indicated by the spread of its associated electron density, by the following equation: $B = 8\pi^2(\Delta x)^2$ and it is reported for each atom in the structure. B-factors that are $<20 \text{ \AA}^2$ indicate well-ordered regions of a protein with a well-defined electron density. In contrast, B-factors that approach 100 \AA^2 indicate very weak electron density, making it difficult to determine the position of an atom with any certainty.

Lastly, the number of Ramachandran outliers is often reported in the coordinate data file, or they can be calculated by submission of the coordinate file to a web-based server (Davis et al., 2007). Outliers are residues whose peptide phi and psi values fall in energetically unfavorable regions of the Ramachandran plot, suggesting that there is an error in the conformation in at least that region of the protein. Typically, the number of outliers should be $<5\%$.

2.6.2 Limitations of X-Ray-Derived Structures

Assuming that an x-ray-derived structure is accurate, there are a number of limitations to its use. First, it is virtually impossible to distinguish oxygen atoms from nitrogen atoms since they differ by only one

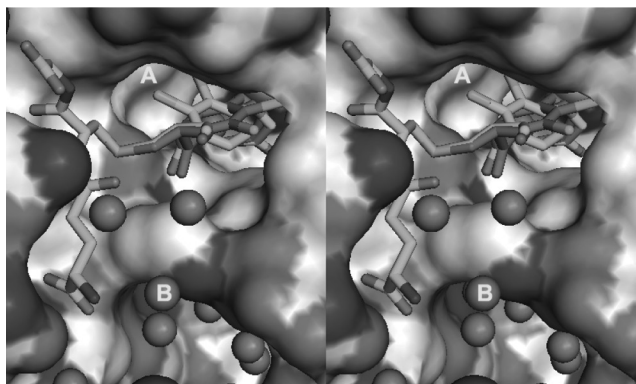


FIGURE 2.16 Crossed-stereo view of an enzyme–inhibitor complex. The x-ray-derived structure of a human class alpha glutathione transferase, complexed with the glutathione–ethacrynic acid complex is shown. The solvent accessible surface of the protein in the vicinity of the ligand-binding site is shown and the bound inhibitor is rendered as sticks. The dichlorobenzyl group of the inhibitor (region A) is found in two orientations, one colored magenta and the other colored cyan (chlorine is colored green in both). The binding site contains a number of ordered water molecules (red spheres), some of which (e.g., B) mediate hydrogen-bonded contacts from the ligand to the protein. Figure produced using Pymol (DeLano, 2002) using the PDB file 1gse.pdb (Cameron et al., 1995).

electron. Although this is not an issue for mainchain atoms, it is an issue for amide sidechains from glutamine and asparagine. Second, especially in higher-resolution structures, multiple positions may be given for the same atom (see Figure 2.16). The relative occupancy of each position is given in the pdb file (see Figure 2.17) and usually differs, with one conformation more heavily weighted than the other. Regardless of the relative occupancies, each alternate position should be regarded as a possible structural variant for computational studies. Lastly, the resolution of the structure affects the precision of the atomic coordinates, as well as other properties of the structural model. Figure 2.18 shows electron density maps for a structure that were computed using either data at 3 Å or 1.6 Å resolution. The map computed using higher-resolution data allows a more precise localization of the atomic positions of the polypeptide chain. Since the amount of data that is used in model fitting increases as the resolution of the structure decreases, higher-resolution models tend to have a more accurate placement of water molecules in the final model, a more reliable refinement of B-factors, and an accurate determination of occupancies for alternate atomic positions.

Atom name	Residue name	x, y, z Coordinates			Occupancy	B-factor	
HETATM 1844	CL1 AEA1 A 224	90.794	28.603	14.325	0.60	31.70	1GSE2072
HETATM 1844	CL1 AEA1 A 224	89.998	25.102	17.081	0.40	35.48	1GSE2073

FIGURE 2.17 Multiple atomic positions. Two lines from the pdb file 1gse.pdb are shown, representing two alternate positions of the same chlorine atom that is part of the ligand (see Figure 2.16). The relative occupancies are highlighted and indicate that the first position is found in 60% of the molecules in the unit cell and the second is found in 40% of the molecules. There is no information regarding whether the two different conformations interchange within the binding site. Both positions show similar B-factors, indicating a similar level of precision in defining the location of the atom in each position.

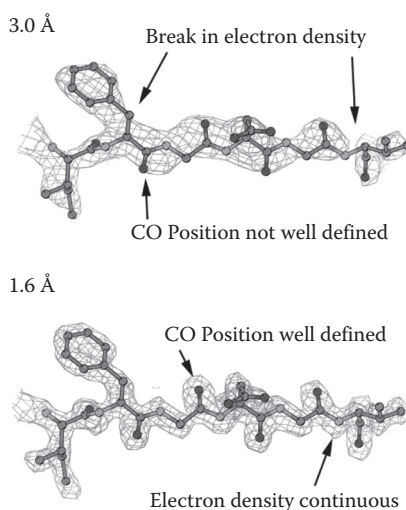


FIGURE 2.18 Effect of resolution on the electron density map. The same data set was used to calculate either a 1.6 Å or a 3.0 Å map. The 1.6 Å map was calculated with ~6 times the amount of data used for the 3 Å map.

2.7 Computational Methods

Computational methods play an important role in many aspects of protein–ligand interactions, including the refinement of both x-ray and NMR structures, the prediction of binding enthalpies and entropies from known structures, dissection of the energetics of the biomolecular interaction at the functional group level (see Chong et al., 1999), and high-throughput docking to screen chemical libraries.

2.7.1 Representation of Interaction Energy

The most accurate energetic representation of molecular interactions is obtained from quantum mechanical (QM) calculations. However, these calculations are currently too time consuming to have much practical use in typical biomolecular interactions. Instead, empirical force fields are used to represent the energetics of biomolecular interactions (Gilson & Zhou, 2007). These force fields consist of a number of terms that are summed to represent the energy of the system, including bond lengths (Equation 2.6a), bond angles (Equation 2.6b), dihedral (torsional) angles (Equation 2.6c), planarity of conjugated systems (e.g., aromatic, peptide bond) (Equation 2.6d), van der Waals interactions (Equation 2.6e), and electrostatics (Equation 2.6f). During refinement of experimentally determined structures, an additional pseudoenergetic term (Equation 2.6g) is added that represents the agreement between data calculated from the model (Calc) and the observed experimental data (Obs). The relative contribution of experimental data to other terms is varied by the adjustment of w . The goal in structure refinement is to find a structural model whose energy is at a minimum, which implies good agreement with both experimental constraints and intrinsic structural features.

$$\sum_{i=1}^{N_{\text{bond}}} k_i^{\text{bond}} (d - d_o)^2 \quad (2.6a)$$

$$\sum_{i=1}^{N_{\text{angle}}} k_i^{\text{angle}} (\theta - \theta_o)^2 \quad (2.6b)$$

$$\sum_{i=1}^{N_{\text{dihedral}}} k_{\phi_i} (\cos(n\phi - \phi_o))^2 \quad (2.6c)$$

$$\sum_{i=1}^{N_{\text{imp}}} k_i^{\text{imp}} (\omega - \omega_o)^2 \quad (2.6d)$$

$$\sum_i^N \sum_{j \neq i}^N \left[\frac{A_{ij}}{r_{ij}^{12}} - \frac{B_{ij}}{r_{ij}^6} \right] \quad (2.6e)$$

$$\sum_i^N \sum_{j \neq i}^N \left[\frac{q_i q_j}{D r_{ij}} \right] \quad (2.6f)$$

$$w \sum |\text{Obs} - \text{Calc}| \quad (2.6g)$$

Note that each of these terms in Equations 2.6a through 2.6e has an energetic weight or parameter, for example, k_i , which must be determined for each type of interaction in the molecule. For example, the weight k_i^{bond} for a C–C bond is different than that for a C–N or C–O bond. Although considerable effort has been expended to develop weighting factors that produce energies that agree reasonably well with experimental data, the weights should be regarded as empirical estimations of the true energetics of the interaction. In addition, one should keep in mind that these parameters are only well established for common functional groups, such as those found in proteins, and it may be necessary to use fundamental QM methods to obtain parameters for many of the uncommon functional groups that are found on small ligands such as drugs. Lastly, one should also keep in mind that all of these parameters are static during a calculation, and thus do not take into account induced polarity during the formation of the biomolecular complex.

A particularly difficult term to model is the electrostatic term (Equation 2.6f) due to both the long range of the interaction and the wide range of possible dielectric constants, which can vary from 80 in bulk solvent to 4 in nonpolar environments. Because of the difficulties in calculating the electrostatic contribution to the overall energy, this term is usually ignored during structure refinement. This is acceptable since the pseudoenergy term from the experimental observations makes a large contribution to the overall energy. However, for calculations of binding energies, it is essential to retain the electrostatic term. The electrostatic component can be solved accurately using Poisson–Boltzmann methods or more approximately using generalized Born models (see Gilson & Zhou, 2007). In both cases, the system is hydrated with water molecules, accounting for the effect of solvent polarity on the dielectric constant.

2.7.2 Molecular Mechanics

The above energetic terms allow one to minimize the energy of the system by adjustment of the atomic positions until there is no further change in the energy. In cases where the energy surface is rough, with numerous local minima, this approach is unlikely to find the true global energy minimum. One approach to circumvent this problem is molecular mechanics. In this case, the atoms in the system are given a random velocity (kinetic energy) that is reflective of the temperature of the system and allowed

to move under the influence of a force that is classically derived from the interaction energies: $F = -\nabla U$, where U is the sum of the terms in Equation 2.6. By controlling the temperature of the system, it is possible to impart on the structure sufficient kinetic energy to allow it to transition over barriers and sample numerous energy minima in search of the global minima. This method has proven particularly robust in the refinement of experimentally determined structures because the motion of atoms in the system is also driven by the pseudoenergy from the experimental constraints, allowing relatively inaccurate energy terms to be used, or the omission of certain terms altogether, such as electrostatics. Molecular mechanics are also required for accurate calculations of binding energies, as described in the next section.

2.7.3 Prediction of Ligand Binding Energy

Given a known structure of a protein–ligand complex, it is useful to be able to compute the free energy change due to binding. Of particular utility is the prediction of how a change in the chemical structure of the ligand affects its binding; this allows one to test how the modification of a drug will affect binding without the need for chemical synthesis. The same approach can be used to calculate the effect of a protein mutation on the binding of a ligand.

Determining the absolute free energy of a system requires calculation of both its enthalpy and entropy. The enthalpy can be obtained directly from the potential functions. The entropy can only be obtained by determining the number of different conformational states of the system. The number of states can be obtained by the analysis of molecular dynamics simulations of fully solvated systems. Owing to the need to perform extensive molecular dynamics simulations to obtain the entropy, accurate calculations of the free energy require a considerable amount of computation time.

The calculated free energies of different states are used to determine binding free energies by the use of thermodynamic cycles (see Figure 2.19). In the case of estimating the overall net binding energy, the ligand is slowly annihilated from the binding site and resurrected in the solvent by selectively turning off and on force field terms (Deng & Roux, 2009). The energy changes that occur during this process sum to give the overall energy change due to binding. This approach has been used to predict the

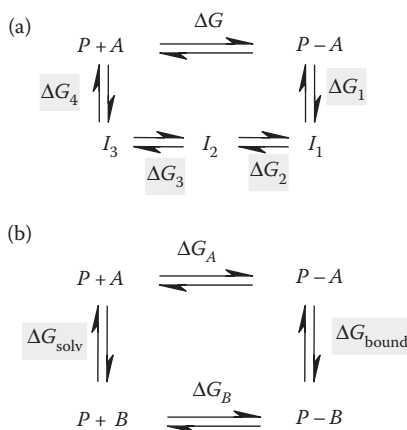


FIGURE 2.19 Thermodynamic cycles. The top cycle (a) is used to determine the overall binding energy by first starting with the hydrated complex and undergoing a series of transformations that essentially remove the ligand from the binding pocket and cause it to appear in the solvent. The highlighted calculated free energy changes between the intermediate states (I_1 , I_2 , I_3) sum to the overall free energy of binding, ΔG . The lower cycle (b) is used to calculate relative free energies of binding between two ligands. The calculated energy difference (highlighted) between free and bound ligands for each ligand is used to obtain $\Delta\Delta G = \Delta G_B - \Delta G_A$.

absolute binding affinities of nonpolar ligands to a cavity mutation in T4 lysozyme and the binding of inhibitors to FKBP12. Remarkably, many of the calculated values are within a few 1/10ths of a kcal/mol of the measured values, and most are within a kcal/mol (Deng and Roux, 2009). A similar approach is used to compare the binding of two related ligands. The starting point for this process is a high-resolution structure of one ligand bound to the protein. The original ligand is transformed to the other ligand by a continuous structural change (e.g., conversion of a methyl group to a hydrogen) and the free energy of both ligand–protein complexes and solvated ligands are determined. The difference in the free energy of binding of each ligand is obtained from the differences of the two calculated free energies (see [Figure 2.19](#)). This approach has been used to compute the relative free energy of binding of HIV protease inhibitors (Reddy et al., 1991) and histone deacetylase inhibitors (Park & Lee, 2004) with reasonable accuracy, generally within a kcal/mol.

2.7.4 Docking

In the identification of lead compounds in drug discovery, it is necessary to investigate which members of a large chemical library bind to the target protein. These lead candidates can then be further modified to optimize their binding and other pharmacological properties. Computational methods to accomplish this screening are usually referred to as docking. Reviews of the various computational programs that perform docking, as well as information on their proficiencies, are described by Kellenberger et al. (2004), Sousa et al. (2006), and Brooijmans & Kuntz (2003).

In docking programs, the orientation of the ligand is systematically changed and the interaction energy of each orientation of the ligand with the protein is evaluated using computational methods. Typically, only a subarea of the protein surface is investigated; the putative binding area can be identified using information from crystallographic or NMR studies on one, or a small number, of protein–ligand complexes. The necessity to test multiple configurations of the ligand was recognized early on in the field; thus, most docking programs automatically generate a manifold of ligand configurations using information on the number of rotatable bonds in the ligand. The importance of testing different conformations of the protein-binding site has also been recognized theoretically and demonstrated experimentally (Murray et al., 1999; Erickson et al., 2004). However, the computational power to generate a respectable ensemble of protein structures is currently not within reach; however, some investigators have begun to incorporate a limited collection of alternate protein conformers in docking protocol (Osterberg et al., 2002; Alberts et al., 2005; Alonso et al., 2006; Totrov & Abagyan, 2008).

To rank how well different candidates bind to the protein target, it is necessary to determine the energy of the interaction. In order to allow for rapid screening, it is necessary to approximate the energetics of the protein–ligand interaction by only considering a subset of the energetic terms given in Equation 2.6, such as van der Waals and electrostatics, or by defining a completely empirical scoring function. The systems are not solvated and the absence of water in these calculations is a considerable deficiency as water molecules are often seen bridging ligands and their binding partners (see [Figure 2.16](#)). Entropic considerations are the most difficult to estimate. The contribution of the hydrophobic effect to entropy changes are approximated from the change in surface area that occur during binding. Entropic changes in the protein or the ligand that may occur during binding are clearly ignored.

Given the inability to allow protein flexibility, and the rather inaccurate evaluation of binding energies, the expectation is that docking should be of limited utility in screening compound libraries. Surprisingly, the success rate is higher than one might expect and most docking programs are able to identify a number of their targets in test studies. The performance of the different programs is somewhat idiosyncratic; different programs perform differently with different test sets. The ability of docking programs to predict the binding affinity is somewhat poorer than the full-scale calculations discussed above (Section 2.7.3c) and the results are also dependent on the test set. A study by Wang et al. (2004) showed that most programs gave correlation coefficients between measured and calculated

binding affinities of <0.5 for HIV protease inhibitors, but performed somewhat better with trypsin ligands, giving a correlation coefficient as high as 0.78 for some programs. In summary, the current docking programs are able to identify potential candidates from compound libraries, thus increasing the efficiency of library screening by experimental methods. Fully automated docking systems are currently under development, which will further increase the throughput of this method in drug discovery (Irwin et al., 2009).

2.8 Emerging Techniques: Single Molecules

Most studies of biomolecular interactions currently investigate the behavior of large ensembles of molecules; a typical 0.2 mm protein crystal harbors about 10^{13} protein molecules and the final structure is an average over all molecules. Experimentally determined binding (or kinetic rate) constants, whether they are measured by NMR, calorimetry, or surface plasmon resonance, are also an average over the entire ensemble of molecules. If the protein exists in a single conformation, then the average of the measured parameter is a valid characteristic of the protein's binding properties. Conversely, if the protein exists in two or more different conformational states, then the average value of any property can be meaningless. Numerous studies have indicated that many proteins sample multiple conformational states and these states have different properties (see Min et al., 2005). Clearly, it is not yet possible to directly observe a single molecule with current diffraction or NMR spectroscopic measurements. However, single-molecule methods can provide an opportunity to characterize the distribution of states of a protein to determine the extent to which ensemble measurements of structure, binding, and kinetics can be used to characterize biomolecular interactions. These methods include fluorescence (Blank et al., 2009), as well as atomic force techniques (Alegre-Cebollada et al., 2010). In many cases, these techniques can also provide information on the strength of the interaction at the single-molecule level. Although it may not be possible to apply single-molecule techniques in every instance, they should be considered when characterizing biomolecular interactions.

References

- Alberts, I.L., Todorov, N.P., and Dean, P.M. 2005. Receptor flexibility in de novo ligand design and docking. *J. Med. Chem.*, **48**, 6585–6596.
- Alegre-Cebollada, J., Perez-Jimenez, R., Kosuri, P., and Fernandez, J.M. 2010. Single-molecule force spectroscopy approach to enzyme catalysis. *J. Biol. Chem.*, **285**, 18961–18966.
- Alonso, H., Bliznyuk, A.A., and Gready, J.E. 2006. Combining Docking and molecular dynamic simulations in drug design. *Med. Res. Rev.*, **26**, 531–568.
- Altieri, A.S. and Byrd, R.A. 2004. Automation of NMR structure determination of proteins. *Curr. Opin. Struct. Biol.*, **14**, 547–553.
- Blank, K., De Cremer, G., and Hofkens, J. 2009. Fluorescence-based analysis of enzymes at the single-molecule level. *Biotechnol. J.*, **4**, 465–479.
- Brooijmans, N. and Kuntz, I.D. 2003. Molecular recognition and docking algorithms. *Annu. Rev. Biophys. Biomol. Struct.*, **32**, 335–373.
- Brown, E.N. and Ramaswamy, S. 2007. Quality of protein crystal structures. *Acta Crystallogr. Sect. D*, **D63**, 941–950.
- Cameron, A.D., Sinning, I., L'Hermite, G., Olin, B., Board, P.G., Mannervik, B., and Jones, T.A. 1995. Structural analysis of human alpha-class glutathione transferase A1-1 in the apo-form and in complexes with ethacrynic acid and its glutathione conjugate. *Structure*, **3**, 717–727.
- Chong, L.T., Duan, Y., Wang, L., Massova, I., and Kollman, P.A. 1999. Molecular dynamics and free-energy calculations applied to affinity maturation in antibody 48G7. *Proc. Natl. Acad. Sci.*, **96**, 14330–14335.
- Davis, A.M., Teague, S.J., and Kleywegt, G.J. 2003. Application and limitations of x-ray crystallographic data in structure-based ligand and drug design. *Angew. Chem.*, **42**, 2718–2736.

- Davis, I.W., Leaver-Fay, A., Chen, V.B., Block, J.N., Kapral, G.J., Wang, X., Murray, L.W., Arendall, W.B., Snoeyink, J., Richardson, J.S., Richardson, D.C. 2007. MolProbity: All-atom contacts and structure validation for proteins and nucleic acids. *Nucleic Acids Res.*, **35**, 375–383.
- DeLano, W.L. 2002. *The PyMOL Molecular Graphics System*. DeLano Scientific, Palo Alto, CA, USA. <http://www.pymol.org>.
- Deng, Y., and Roux, B. 2009. Computations of standard binding free energies with molecular dynamics simulations. *J. Phys. Chem.*, **113**, 2234–2246.
- Eftink, M.R. 1997. Fluorescence methods for studying equilibrium macromolecule-ligand interactions. *Methods Enzymol.*, **278**, 221–257.
- Erickson, J.A., Jalaie, M., Robertson, D.H., Lewis, R.A., and Vieth, M. 2004. Lessons in molecular recognition: The effects of ligand and protein flexibility on molecular docking accuracy. *J. Med. Chem.*, **47**, 45–55.
- Fersht, A. 1998. *Structure and Mechanism in Protein Science: A Guide to Enzyme Catalysis and Protein Folding*. W.H. Freeman, New York, NY.
- Gilson, M.K. and Zhou, H.-X. 2007. Calculation of protein-ligand binding affinities *Annu. Rev. Biophys. Biomol. Struct.*, **36**, 21–42.
- Guntert, P. 2009. Automated structure determination from NMR spectra. *Eur. Biophysics J.*, **38**, 129–143.
- Hajduk, P.J., Augeri, D.J., Mack, J., Mendoza, R., Yang, J., Betz, S.F., and Fesik, S.W. 2000. NMR-Based Screening of Proteins Containing ¹³C-Labeled Methyl Groups. *J. Am. Chem. Soc.*, **122**, 7898–7904.
- Hajduk, P.J., Gerfin, T., Boehlen, J.M., Häberli, M., Marek, D., and Fesik, S.W. 1999. High-throughput nuclear magnetic resonance-based screening. *J. Med. Chem.*, **42**, 2315–2317.
- Hitchens, T.K., Zhan, Y., Richardson, L.V., Richardson, J.P., and Rule, G.S. 2006. Sequence-specific interactions in the RNA-binding domain of *Escherichia coli* transcription termination factor Rho. *J. Biol. Chem.*, **281**, 33697–33703.
- Ikura, M., Kay, L.E., and Bax A. 1990. A novel approach for sequential assignment of ¹H, ¹³C, and ¹⁵N spectra of proteins: heteronuclear triple-resonance three-dimensional NMR spectroscopy. Application to calmodulin. *Biochemistry*, **29**, 4659–4667.
- Irwin, J.J., Shoichet, B.K., Mysinger, M.M., Huang, N., Colizzi, F., Wassam, P., and Cao, Y. 2009. Automated docking screens: A feasibility study. *J. Med. Chem.*, **52**, 5712–5720.
- Kay, L.E., Muhandiram, D.R., Farrow, N.A., Aubin, Y., Forman-Kay, J.D. 1996. Correlation between dynamics and high affinity binding in an SH2 domain interaction. *Biochemistry*, **35**, 361–368.
- Kay, N.E. 2005. NMR studies of protein structure and dynamics. *J. Magn. Reson.*, **173**, 193–207.
- Livingstone, J.R., Spolar, R.S., and Record, M.T. Jr. 1991. Contribution to the thermodynamics of protein folding from the reduction in water-accessible nonpolar surface area. *Biochemistry*, **30**, 4237–4244.
- Kellenberger, E., Rodrigo, J., Muller, P., and Rognan, D. 2004. Comparative evaluation of eight docking tools for docking and virtual screening accuracy. *Proteins Structure Function Bioinformatics*, **57**, 225–242.
- Klepeis, J.L., Lindorff-Larsen, K., Dror, R.O., and Shaw, D.E. 2009. Long-timescale molecular dynamics simulations of protein structure and function. *Curr. Opin. Struct. Biol.*, **19**, 120–127.
- Kleywegt, G.J. and Jones, T.A. 2002. Homo crystallographicus—Quo Vadis? *Structure*, **10**, 466–472.
- Leavitt, S. and Freire, E. 2001. Direct measurement of protein binding energetics by isothermal titration calorimetry. *Curr. Opin. Struct. Biol.*, **11**, 560–566.
- Loladze, V.V., Ermolenko, D.N., and Makhatadze, G.I. 2001. Heat capacity changes upon burial of polar and nonpolar groups in proteins. *Protein Sci.*, **10**, 1343–1352.
- Mandal, P.K. and Majumdar, A. 2004. A comprehensive discussion of HSQC and HMQC pulse sequences. *Concepts Magn. Reson.*, **20A**, 1–23.
- McConnell, H.M. 1958. Reaction rates by nuclear magnetic resonance. *J. Chem. Phys.*, **28**, 430–431.
- Medek, A., Hajduk, P.J., Mack, J., and Fesik, S.W. 2000. The use of differential chemical shifts for determining the binding site location and orientation of protein-bound ligands. *J. Am. Chem. Soc.*, **122**, 1241–1242.

- Mills, J.L., Liu, G., Skerra, A., and Szyperski, T. 2009. NMR structure and dynamics of the engineered fluorescein-binding lipocalin FluA reveal rigidification of beta-barrel and variable loops upon enthalpy-driven ligand binding. *Biochemistry*, **48**, 7411–7419.
- Min, W., English, B.P., Luo, G., Cherayil, B.J., Kou, S.C., and Xie, X.S. 2005. Fluctuating enzymes: Lessons from single-molecule studies. *Acc. Chem. Res.* **38**, 923–931.
- Mittermaier, A. and Kay, L.E. 2006. New tools provide new insights in NMR studies of protein dynamics. *Science*, **312**, 224–228.
- Murray, C.W., Baxter, C.A., and Frenkel, A.D. 1999. The sensitivity of the results of molecular docking to induced fit effects: Application to thrombin, thermolysin and neuraminidase. *J. Comput. Aid. Mol. Des.*, **13**, 547–562.
- Nguyen, B., Taniou, F.A., and Wilson W.D. 2007. Biosensor-surface plasmon resonance: Quantitative analysis of small molecule–nucleic acid interactions. *Methods*, **42**, 160–161.
- Osterberg, F., Morris, G.M., Sanner, M.F., Olson, A.J. and Goodsell, D.S. 2002. Automated docking to multiple target structures: Incorporation of protein mobility and structural water heterogeneity in autodock. *Proteins Structure Function Bioinformatics*, **46**:34–40.
- Park, H. and Lee, S. 2004. Homology modeling, force field design, and free energy simulation studies to optimize the activities of histone deacetylase inhibitors. *J. Comput. Aid. Mol. Des.*, **18**, 375–388.
- Reddy, M.R., Viswanadhan, V.N., and Weinstein, J.N. 1991. Relative differences in the binding free energies of human immunodeficiency virus 1 protease inhibitors: A thermodynamic cycle-perturbation approach. *Proc. Natl. Acad. Sci.*, **88**, 10287–10291.
- Rule, G.S. and Hitchens, T.K. 2005. *Fundamentals of Protein NMR Spectroscopy*. Springer, the Netherlands.
- Schuck, P. and Zhao, H. 2010. The role of mass transport limitation and surface heterogeneity in the biophysical characterization of macromolecular binding processes by SPR biosensing. *Methods Mol. Biol.*, **627**, 15–54.
- Sigurskjold, B.W. 2000. Exact analysis of competition ligand binding by displacement isothermal titration calorimetry. *Anal. Biochem.*, **277**, 260–266.
- Sousa, S.F., Fernandes, P.A., and Ramos, M.J. 2006. Protein–Ligand docking: Current status and future challenges. *Proteins Structure Function Bioinformatics*, **65**, 15–26.
- Totrov, M. and Abagyan, R. 2008. Flexible ligand docking to multiple receptor conformations: A practical alternative. *Curr. Opin. Struct. Biol.*, **18**, 178–184.
- Velazques-Campoy, A., Kiso, Y., and Freire, E. 2001. The binding energetics of first- and second-generation HIV-1 protease inhibitors: Implications for drug design. *Arch. Biochem. Biophys.*, **390**, 169–175.
- Wang, R., Lu, Y., Fang, X., and Wang, S. 2004. An extensive test of 14 scoring functions using the PDBbind refined set of 800 protein-ligand complexes. *J. Chem. Inf. Comput. Sci.*, **44**, 2114–2125.
- Ward, W.H. and Holdgate, G.A. 2001. Isothermal titration calorimetry in drug discovery. *Prog. Med. Chem.*, **38**, 309–376.
- Weiss, S. 2000. Measuring conformational dynamics of biomolecules by single molecule fluorescence spectroscopy. *Nat. Struct. Biol.*, **7**, 724–729.
- Wlodawer, A., Minor, W., Dauter, Z., and Jaskolski, M. 2008. Protein crystallography for non-crystallographers, or how to get the best (but not more) from published macromolecular structures. *FEBS J.*, **275**, 1–21.

4

Systems and Technology Involving Bacteria

Nicole Bleckwenn
*University of Maryland
Biotechnology Institute*

William Bentley
*University of Maryland
Biotechnology Institute*

4.1	Introduction	4-1
4.2	Elements for Expression	4-1
4.3	A Cell-to-Cell Communications Operon	4-3
4.4	Marker Proteins	4-4
4.5	Growth of Bacterial Cultures.....	4-4
4.6	Regulons.....	4-7
4.7	Engineering the System	4-9
4.8	Emerging Technologies and Issues	4-10
4.9	Final Remarks.....	4-12
	References.....	4-12

4.1 Introduction

Bacteria are unicellular, relatively simple, and can double in very short times. These attributes can be exploited for technological advantage. They are useful for the expression of large quantities of products, such as proteins and enzymes, as well as small molecules that are not efficiently synthesized in the laboratory via bio-organic chemistry. Since bacteria lack the posttranslational machinery endogenous to eukaryotic cells (e.g., glycosylation; see Chapter 1), they are unable to process very complex proteins. However, a number of proteins with therapeutic value, such as insulin can be readily produced using bacteria. We will describe the molecular basis, from a systems viewpoint, for the many technological achievements already realized using bacteria, as well as those that are likely to see continued research and development.

4.2 Elements for Expression

To utilize bacterial culture as a production system for recombinant products, the cells must be “genetically engineered” to contain the genes for the products that are desired and the proper control elements that will allow expression of those products under the chosen conditions. Chapter 1 described some basic background information on the genetic elements and their function. As previously stated, *plasmid vectors* are generally the method-of-choice for inserting a gene of interest into the bacterial cells. The plasmid DNA is altered to contain the gene for the protein of interest with upstream cognate control sequences. This plasmid is then inserted or “transformed” into “competent” bacteria. The most common methods to transform these cells are either through electrical or chemical means. These processes make the cells competent, which in a sense, open pores in the bacterial membranes big enough to allow entry of plasmid DNA. Because plasmids are naturally occurring among the *Eubacteria*, they are readily accepted by the cells. However, since plasmids are redistributed among the daughter cells upon cell division, there is a

finite probability that the transformed cells are capable of losing or transferring plasmids. Some plasmids are thought to be randomly distributed to the daughter cells and in these cases, mother cells with few plasmids will generate daughter cells with no plasmids at a relatively high frequency. For example, if a dividing cell has just one plasmid, then one of the daughter cells will be born without a plasmid. Once that cell divides, it begins a process where its own progeny overtake cells with plasmids. Typically, cells that have more plasmids redirect more of the cellular machinery to functions encoded by the plasmid, and the cells grow more slowly. A schematic of this process is shown in Figure 4.1.

The loss of the recombinant plasmid must thus be prevented. This can be accomplished by inserting genetic stability elements, such as genes that encode antibiotic resistance, into the same plasmid as the gene of interest, and then provide antibiotics in the growth medium. In Chapter 1, the selection marker was used to identify positive clones. Here, the same marker can serve to maintain a productive bioreactor. If the culture is grown under conditions of selection for a marker, such as in the presence of an antibiotic, only those cells retaining the plasmid with the resistance gene product will grow and proliferate in the culture. Another technique to minimize this problem is to use an inducible promoter so that resources are directed to protein production only after the culture has grown sufficiently. When product expression is *inducible*, the cells are less stressed because they are not producing product. Hence, they will be less likely to lose their plasmids, as reallocated resources are only needed for plasmid DNA replication. Also important for the expression of our gene of interest is the plasmid *copy number*, or the number of plasmid copies per cell or per chromosome. Generally, the higher the copy number, the more product is made, but there can be a trade-off in that high copy number cells may become overburdened and not grow properly.

In addition to maintaining the gene of interest on the plasmid, one needs to incorporate genetic switches that “turn on” or “turn off” expression. *Operons* are the natural molecular switches used by prokaryotic organisms to control expression of genes (see Figure 4.3). These natural segments can be “cut” and “pasted” into plasmids using restriction enzymes and ligases (biomolecular scissors and glue, respectively) to control expression of specific gene sequences that are desired, leading to the expression of recombinant products. The reconstruction of “controllable” promoters upstream (5′) of a gene of

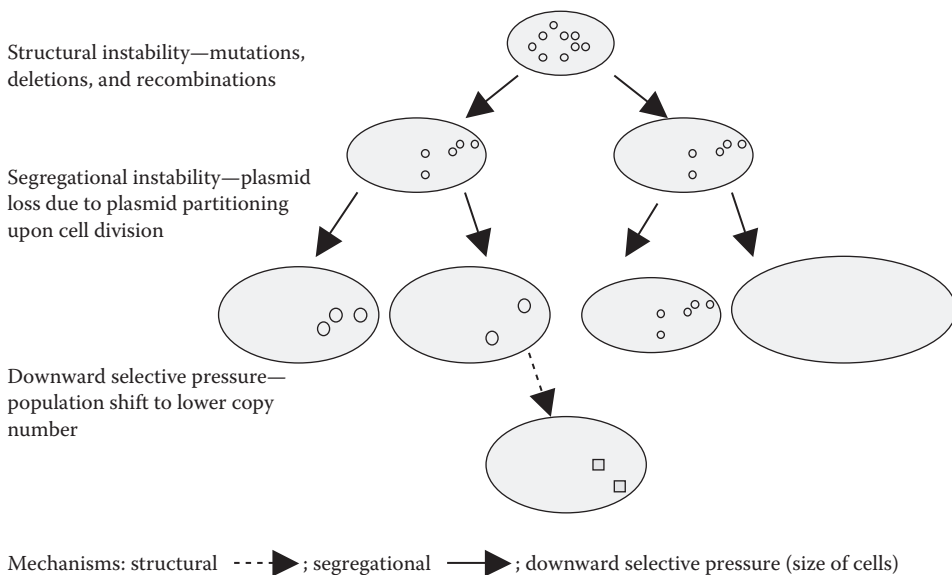


FIGURE 4.1 Mechanisms for plasmid loss (instability). Structural instability can lead to plasmid defects; segregational instability is caused by uneven distribution of plasmids to daughter cells; downward selective pressure is the combination of segregational and structural instability and the observation that plasmid-free cells grow (and divide) more quickly (denoted by large cells).

interest creates an *inducible expression system*. The best understood operon is the lactose or *lac* operon (see <http://web.mit.edu/esgbio/www/pge/lac.html>). It consists of genes for the repressor protein, promoter, operator, and three enzyme genes, *lacZ*, *lacY*, and *lacA*, which code for β -galactosidase, lactose permease, and galactoside transacetylase, respectively. Incidentally, genes are italicized and lowercase when written; proteins are capitalized and not italicized (e.g., *LacZ* for β -galactosidase). Lactose, as the inducer, binds the repressor preventing binding of the repressor to the operator, allowing transcription by RNA polymerase.

In the prior chapter, it was noted that sometimes more than inducer or repressor binding to an operator can be involved with turning genes on or off. *Catabolite repression* is one classic example that occurs at the *lac* promoter site. In the absence of the preferred carbon source, such as glucose, the intracellular cyclic AMP (cAMP) level rises. The rise reflects a deficiency in the usual molecular source of energy used to drive biosynthetic reactions, ATP. The cAMP complexes with CAP (“catabolite gene activator protein” or also called “cAMP Repressor Protein,” CRP) to bind to the promoter, which further enhances RNA polymerase binding, and amplifies transcription and translation of the three enzymes. This can be a problem in industrial fermentations where glucose is used as the principal carbon source: when glucose is present there is little production of the desired protein.

Industrial utilization of the *lac* operon has been tailored, therefore, for controlled expression of proteins. Part of the *lac* promoter sequence (–10 region), which provides for *lac* induction is included; but the –35 region is taken from the tryptophan operon because it is not subject to catabolite repression. The combination, *tac*, is reportedly 10 times stronger than the native *lac* sequence. A gratuitous (nonmetabolized) inducer, IPTG (isopropyl- β -D-thiogalactopyranoside), has been shown to act as an effective inducer for this hybrid system.

4.3 A Cell-to-Cell Communications Operon

Many operons have been studied that take queues from the environment or other parts of the cell and modulate protein expression at the level of transcription. Some of these are simple sugars, such as lactose for the *lac* operon, but other operons involve different small molecules in their control architectures. Another example has to do with all our cell warfare: survival of microbes that live in a symbiotic relationship with squid [1,2]. It turns out that the nocturnal Hawaiian bobtail squid emits light downwards through its mantle cavity and, by matching the intensity of the moon- and starlight above, the squid becomes invisible to other predators below. The adult squid is ~2 cm long and some very interesting photos are found in Fuqua and Greenberg [1]. How does this squid make light? There is a *Vibrio fischeri* light organ close to the ink sac within the mantle cavity of the animal. This light organ contains ~ 10^{11} *V. fischeri* cells per milliliter, and these *Vibrio* actually make the light by the expressing light-emitting genes denoted *lux* (as per the Latin saying “*fiat lux*: let there be light”). So, in the absence of the *Vibrio*, the squid (and the *Vibrio*) would be swallowed up by large fish.

The *lux* genes are transcribed in an operon that responds to another small molecule, 3-oxo-C6-HSL (which is an acylated homoserine lactone [HSL]), one of a family of HSLs that stimulate gene expression in many different bacteria. The interesting part of this phenomenon is that as the cells accumulate (like in the mantle cavity of the bobtail squid), they secrete HSLs that act as autoinducers (AI), which in turn, accumulate in concentration. As the autoinducer concentration reaches a critical point, the bacteria all respond in a multicellular coordinated fashion: they emit light! To accomplish this, the HSLs bind to cognate transcriptional activators, which then stimulate expression of the *lux* genes. The *lux* gene products use ATP and luciferin to produce small quantities of light. This process was given the name “quorum sensing” by Greenberg, who recognized that a certain number of bacteria (or, more appropriately, a certain concentration of its secreted autoinducer), was needed for a formal “vote.”

The *lux* genes proved interesting from the perspective of the operon structure and the need to elucidate mechanisms by which bacteria respond to queues from their microenvironment. They are also interesting because they serve as *markers* of gene expression. That is, because the protein products of

lux genes are easily seen (quantified), they are used as reporters of gene transcription. LacZ, from the *lac* operon, is another often used marker of gene expression. To delineate the function of gene sequences that putatively serve as promoters, operators, initiation sites, and so on, marker genes are often included downstream of the DNA regulatory sequence in question. Then, expression of the marker is quantitatively compared, reflecting the strength of the promoter region under study.

4.4 Marker Proteins

Marker proteins have been used as vital tool in the study of bacterial systems and have also been used to evaluate the production of recombinant products from them. These markers make use of nature's diversity for specific purposes. Marker proteins are easily detected and measured. Markers allow us to assess what's happening in cells at the protein level. They also provide a measure of localized gene expression. They are inserted in series or in parallel in plasmid expression vectors to monitor the level of expression from the system and promoter. Common markers include β -galactosidase, green fluorescent protein (GFP), and dsRed. The use of protein markers accelerated during the late 1990s due, in large part, to the exquisite attributes of green fluorescent protein (reviewed in March et al. [3]). GFP requires no cofactors (such as ATP for *lux* genes) and no substrates (such as X-gal for *lacZ*). GFP can be readily visualized from within cells and tissues because it absorbs light in the UV/blue/violet range and emits it back at a longer wavelength, green. This is the basic premise of fluorescence. In the case of GFP, a simple photodiode detector can be used to quantify the level of its fluorescence [4].

Green fluorescent protein has been used to study gene regulation. It has been used to evaluate localization of proteins within cells. It has been used to visualize phagocytosis, where big cells (such as white blood cells in humans) devour little cells, such as microbes, swimming around in our blood stream. GFP has also been used to mark product protein synthesis in a host of organisms, from bacteria to insect larvae. Some interesting photos are available at www.chesapeakeperl.com, a company that makes proteins in caterpillars.

In the bacterial systems world, GFP has also been used to indicate both high and low oxygen tension in bioreactors. That is, the bacteria are transformed into mini cell-based sensors. In the case of high oxygen, DNA and protein damage can result due to the elicitation of oxygen radicals and reactive oxygen species (ROS), such as hydrogen peroxide. By inserting the *gfp* gene downstream of an ROS-sensitive promoter, cells that become exposed to ROS synthesize GFP. This is readily detected by a GFP-specific optical probe that can be inserted into the fermentor. In this way, one can use the fluorescence measurement as an indicator of the cell's physiology.

It is common in industrial fermentations to use hardwired analytical instrumentation to monitor reactor conditions, such as temperature, pH, and oxygen. But, it is only in the most recent years, that bioprocess engineers have begun to examine the responses of the cells as indicators of their own micro-environments. Thus, one might typically equip a bioreactor with one (or several) oxygen probes, but this indicates the oxygen level in the liquid at the precise location of the probe. The cells, however, are constantly circulating in and out of spatially restricted areas like those near baffles, or areas of high shear rate like near the impellers. They might also pass by a feed tube, or the oxygenating air sparging ring (see Figure 4.2). By measuring their physiological response to oxygen, we learn more about the actual environment they experience. Hence, we can develop more sophisticated process control schemes, tank and impeller designs, and even tailor host cells and protein expression vectors, that are designed to meet the physiological demands of the cells when they produce products.

4.5 Growth of Bacterial Cultures

One of the advantages of using bacteria to make products is their rapid doubling time. Bacteria reproduce by binary fission: one becomes two, two become four, and so on. The time over which the cells undergo a generation is also known as the doubling time. The number of cells, growing under binary

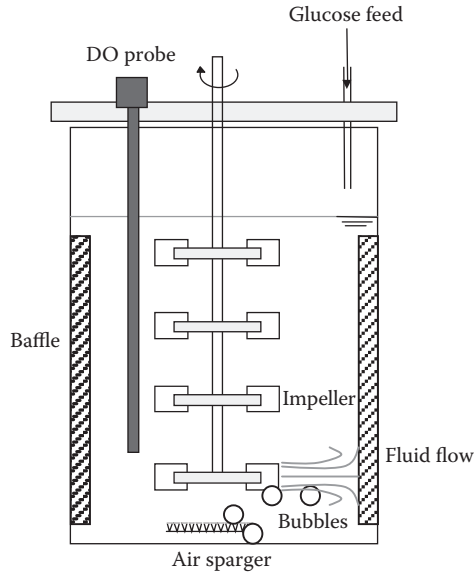


FIGURE 4.2 Schematic of a bioreactor. Oxygen is introduced to the reactor at the air sparger. Bubbles are sheared at the impellers and entrained in the liquid, which impinges on the vessel walls and then is forced to circulate vertically. A well-mixed reactor has few “dead” or “stagnant” regions where circulation is minimal.

fission, continually increases in an exponential manner. Thus, if a cell is making a protein and the cell grows exponentially, one can get copious quantities of protein in a short time.

Bacterial cultures are typically grown in liquid medium. Once inoculation occurs, the cells’ growth can generally be described by a set of growth phases (see Figure 4.3). These begin with the lag phase, where the cells are adapting to the new environment and the cell number does not increase significantly. The next phase, called exponential or logarithmic growth phase, occurs when the cells are dividing rapidly and the cell mass and cell number are increasing exponentially. Here, the doubling time (τ_D), or time it takes the cell mass to double, is about 20 min for rapidly growing *Escherichia coli*. The growth

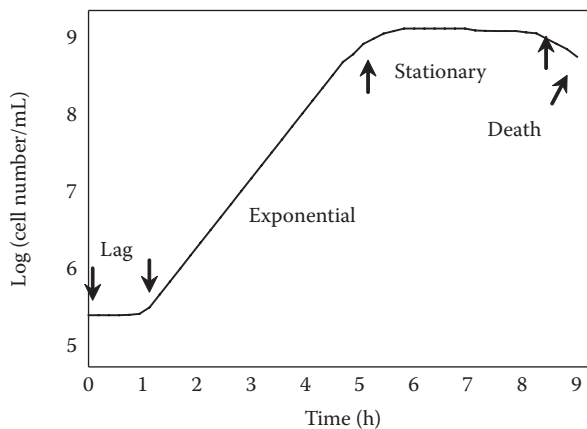


FIGURE 4.3 Phases of bacterial cell growth. After inoculation, cells adapt to their new environment during the *lag phase*, grow rapidly by regular binary fission during the *exponential phase*, stop growing from nutrient limitation during the *stationary phase*, then eventually die (*death phase*).

rate of exponentially growing cultures can be determined mathematically using the equation $\ln(X/X_0) = \mu(t-t_0)$ where X and X_0 are the cell concentrations at time t and time t_0 , and μ is the *specific growth rate* in units of inverse time. The growth rate can also be determined graphically by plotting the logarithm (natural log scale) of the cell number data during this phase against time, the slope of the straight line will be the growth rate. The third phase of growth in a bacterial cell culture is the *stationary phase* where either nutrients become limiting or waste products become inhibiting. Here, the net growth rate becomes zero as the growth and death rates equal each other. Secondary metabolism may occur during this time, where nongrowth associated products and building blocks for survival in the changing environment are produced. When the cells finally succumb to the nutrient depleted conditions, they enter the *death phase*, where the cell number and optical density (measured as light absorbance in the visible region) actually decline.

The environment for growth of bacterial cultures must be carefully controlled to minimize the lag and stationary phases. This can be accomplished by increasing the inoculum size to increase the initial cell number and reduce the amount of time it takes for doubling of the culture to become apparent. If a low inoculum size is used, an extended “apparent” lag phase may just be due to the small number of cells which may be doubling, but do not register as a significant increase by the methods used to measure cell number. One can also ensure that the cells used in the inoculum are themselves growing exponentially. Then they will adapt more quickly to their new environment. The stationary phase can also be delayed, to maintain a longer exponential growth phase, by ensuring the culture environment through precise control of culture parameters, such as dissolved oxygen, pH, and temperature and also through appropriate medium exchange, which will provide all the necessary nutrients and remove any harmful waste products which may inhibit growth of the cells.

In industry, fed-batch cultivation is often used to propagate bacterial cells. This mode of operation entails feeding concentrated growth medium to a batch reactor vessel. As the cells accumulate due to growth, the rate at which medium is fed increases with time in order to keep up with the growing total mass of cells. When the aim is to sustain a constant specific growth rate (μ), the operational equations for time-dependent feed rate (F), volume (V), and cell mass concentration (X) are

$$F(t) = [(\mu V_0 X_0) / (S_f Y)] \exp(\mu t) \quad (4.1)$$

$$V(t) = V_0 + [(V_0 X_0) / (S_f Y)] [\exp(\mu t) - 1] \quad (4.2)$$

$$X = X_0 \exp(\mu t) / [1 + (X_0 / Y S_f) (\exp(\mu t) - 1)] \quad (4.3)$$

In the above equations, V_0 , X_0 , S_f , and Y refer to initial batch volume prior to feeding, initial cell mass concentration prior to feeding (e.g., g/L), concentration of limiting nutrient in the feed (e.g., 100 g/L glucose), and cell mass yield (e.g., 0.4 g cells/g glucose), respectively.

Fed-batch operation offers numerous advantages. First, the process can achieve 30–50 vol% of cells at the end, which represents high volumetric productivity (mass product/volume time) and thus good economic utilization of capital and labor resources. One cannot attain such a high final concentration of cells by simply initiating a batch growth process with a high glucose concentration. While bacteria are hardy and versatile, most have relatively high water activity requirements. Here, the activity of a component in a mixture refers to the product of the component's mole fraction and activity coefficient. *E. coli* has a water activity threshold of about 0.96 meaning if the value is lower, growth will be lessened or nil. Concentrated glucose solutions that also contain salts and other nutrients often present a prohibitively low value of water activity. Thus, one can envision fed-batch processing as slowly providing a lot of glucose over time, while the glucose concentration in the medium is generally in the mg/L to g/L range. A second advantage is maintaining a specific growth rate less than, for example, 0.3 h^{-1} lowers acetate

production, which can become inhibitory as it accumulates. Also, acetate production is an inefficient use of carbon resources.

When growing bacteria to produce recombinant proteins, one of the most critical aspects is *oxygen transfer*. Indeed, oxygen supply can become a major limitation toward the end of fed-batch fermentations when the cell mass concentration is large. Typically this is a problem because the solubility of oxygen in water (or growth media) is very low. Cells utilize what is dissolved in the liquid and bacterial cells (which grow rapidly) use this oxygen at a very high rate. Hence, it is vital to deliver oxygen to the liquid phase at a rate that at least matches the bacterial consumption rate. The transport of oxygen is proportional to the *driving force* for mass transfer (concentration difference between the level of O_2 in the water at saturation and current O_2 level). The proportionality constant, the volumetric oxygen transfer coefficient from the gas-to-liquid interface, is denoted $k_1 a$. This constant contains both a liquid film intrinsic rate constant, k_1 (e.g., h^{-1}), and an interfacial area per unit volume, a (e.g., $cm^2/cm^3 = cm^{-1}$), over which the transport from the gas-to-liquid phases occurs. Aeration is most commonly achieved by sparging the liquid medium through tubing and other distribution devices having small orifices. Bubbles are generated in the liquid medium providing surface area for mass transfer surface. The impeller is typically located just above the sparger, this is the main distributor of oxygen because it shreds bubbles into tiny droplets of high surface-area-to-volume ratio, a parameter that needs to be maximized for effective transfer. Hence, bubble creation, sizing, and distribution are all key to oxygen mass transfer in any given bioreactor.

Importantly, as the scale of a fermentation process increases (from lab to production), the height-to-diameter ratio of the bioreactor is often kept constant in the range of 1:2–1:3, and this means that the surface-area-to-volume ratio of the entire reactor dramatically decreases at higher volumes. It then becomes even more important to understand the physical reactor system and the methods used to attain high levels of dissolved oxygen, as well as the interplay between the physical reactor and the cell physiology. Oxygen is important because bacterial metabolism is exquisitely controlled, as noted with respect to ROS. At times cell responses can so dramatically influence physiology, that the cells become completely nonproductive from a product standpoint. That is, depending on the insult, a cell response can influence many cellular activities.

The *heat-shock response*, for example, is a well-characterized physiological response in that many molecules have been identified that are either *upregulated* or *downregulated* due to the specific environmental insult (a rapidly increased temperature). The players that are changed include *proteases* (enzymes that digest proteins), *chaperones* (proteins that help fold proteins), transcription factors, as well as components of cell synthesis machinery [5]. In general, the cells rearrange or adapt their physiology for enhanced survival in the new condition. One of the key upregulated elements is the *heat-shock transcription factor*, *sigma* 32 (σ^{32}). As noted previously (e.g., bacterial autoinducers, HSLs), transcription is modulated by small molecule *effectors* that bind to cognate transcription factors, such as repressors and activators. One of the other vital components of bacterial transcription is the *sigma factor*, a protein that helps the polymerase bind to the specific initiation sites in order to carry out transcription. *E. coli* have seven sigma factors, each responsible for a specific regulatory domain. The sigma factor is thus a part of the transcriptional polymerase *holoenzyme*. Under normal conditions, bacteria use sigma factor 70 (σ^{70}) to target transcription of normal *housekeeping genes*. Under heat shock, σ^{32} overrides σ^{70} , and serves to amplify transcription of heat-shock genes. The protein products of these genes are collectively known as *heat-shock proteins* (*hsps*), and are coordinately regulated by (σ^{32}). When cells overexpress recombinant protein, a “stress” response results, similar but not identical to the heat-shock response. When genes are coordinately regulated, they constitute a *regulon*, which will be described in more detail in Section 4.6.

4.6 Regulons

The regulon consists of genes that are not necessarily located near each other in the genome nor do they necessarily have the same promoter/operator elements. The heat-shock response regulon is a primary

example whereby, in response to a sudden stress, such as a rise in temperature, the regulon initiates production of certain proteins at a higher (or lower) level than normal. Another regulon is associated with HSL-mediated quorum sensing: a series of proteins are up or downregulated in direct response to a particular quorum. Understanding regulons, and how they interact, is an emerging area of *systems biology*. For example, a sigma factor associated with nutrient limitation, σ^S , is known to influence levels of proteins that also play a role in the heat-shock response.

An effective way to characterize operons, regulons, and their role within the stoichiometry of bacterial metabolism is to refer to the interactions as *genetic circuits*. For example, in *Salmonella*, Bassler and coworkers [6] recently discovered that the uptake mechanism of the quorum sensing autoinducer was itself regulated by AI-2. Thus, the cells make autoinducer AI-2 in one biosynthesis pathway and they use this autoinducer to regulate its own uptake from the extracellular media by modulating transcription of the uptake genes. This constitutes a small genetic circuit. Interestingly, glucose (which plays a huge role in physiology) seems to play a direct role in quorum sensing. That is, CRP directly binds to the promoter region of *lsr* genes and modulates their transcription. Previous researchers had already shown that the bacterial autoinducer AI-2 regulates genes in other bacteria. Thus, it has become apparent that quorum circuitry and glucose circuitry intersect, and these intersections are not confined to *E. coli*, but rather are conserved among many bacteria.

Understanding the underpinning regulation of gene transcription in bacteria is important if we are to exploit their tremendous biosynthetic potential. Understanding the mapping of regulation onto metabolic pathways is important for generating microbial and eukaryotic systems that produce products. Manipulating metabolic flow using recombinant DNA techniques, as pointed out in Chapter 1, is now commonly referred to as *metabolic engineering* [7]. By altering existing pathways and augmenting cells with nonnative enzymatic capabilities, metabolic engineers have created microbes that make new products, including even plastics.

In bioreactors, cells damaged by high doses of oxygen that form radicals, peroxide, and so on, upregulate stress-related proteins that, in turn, have been exquisitely tailored and designed to deal with the high oxygen. Among the proteins that deal with oxygen transfer are peroxide scavengers, such as *superoxide dismutase* (SOD) and oxygen carriers, such as bacterial *hemoglobin*. In a metabolic engineering application, Stark and coworkers [8] transformed *E. coli* with hemoglobin from *Vitreoscilla* and after cultivating them at high cell density in an environment not noted for good oxygen transfer, they found increased product production. By metabolically engineering the cells, they transformed the oxygen genetic circuit into a positive regulatory element for increasing protein production when the cells were grown deprived of oxygen.

As noted above, some physiological and metabolic elements are tightly coordinated. This is not always the case. In fact, it is more likely that any two given elements are only loosely linked, even when they are directly connected by biochemical pathways. In this way, Nature's regulatory and control mechanisms can fine-tune systems to meet widely varied conditions that are typically experienced by the cells. Glycolysis, for example, is only loosely tied to the *tricarboxylic acid cycle* (TCA cycle), even though they are directly linked biochemically (see <http://web.mit.edu/esgbio/www/glycolysis/dir.html>). In glycolysis, glucose is brought into the cell and *catabolized* into three carbon sugars, such as *pyruvate*. Pyruvate is then converted into acetyl-CoA, which is brought into the TCA cycle. This circular pathway yields many compounds including CO₂, ATP, and chemical reducing potential in the form of NADH. The NADH is recycled to NAD⁺, with concomitant generation of ATP, during *respiration (oxidative phosphorylation)*. Glucose uptake can actually exceed the electron transfer capacity of respiration, particularly if cells are grown in a rich growth medium containing high amounts of glucose. A result is the overflow of semi-oxidized sugars, such as acetate [9]. Metabolic engineering efforts to direct control of glycolysis and respiration have led to reduced acetate and higher product yields.

The desire to understand rates of material flow through metabolic pathways has received the attention of many researchers seeking to quantitatively describe cell physiology. *Metabolic Flux Analysis* [10,11], *Metabolic Control Analysis* [12], and several other mathematical techniques have been successfully

applied to bacterial systems for the external manipulation of metabolic activities, including synthesis of nonnative compounds of commercial interest.

4.7 Engineering the System

As might be inferred from above, altering pathways for specific purposes requires first, a preliminary understanding of the interconnectedness of the pathway in question with other pathways. Then, one needs to understand the regulation of the flux through the pathway. Neither of these is trivial. Databases, such as KEGG (<http://www.genome.ad.jp/kegg/>), EcoCyc (<http://ecocyc.org/>), and NRCAM (<http://www.nrcam.uchc.edu/>) can help. Ultimately, one needs molecular tools to appropriately engineer the system.

Suppose material A moves down a path where it will be converted into either B or C, the specific direction decided by access to one of two enzymes (e_1 or e_2) (see Figure 4.4). In chemical reaction engineering, it is common to explain reaction kinetics by referring to reactants and products as “A,” “B,” or “C,” and so on. In the biochemical pathway for autoinducer AI-2 synthesis, “A,” “B,” and “C,” might represent S-adenosylmethionine (SAM), S-adenosylhomocysteine (SAH), and S-ribosylhomocysteine (SRH), respectively. By incorporating the gene for enzyme, e_1 , on a plasmid and by transforming the plasmid into the host bacteria, one can increase the level of enzyme, e_1 , with the hope that it will increase the flux of material through that enzymatic pathway. This is, by far, the most common route for metabolically engineering the system. Another tack is to mutate the gene for e_2 (using one or more of the techniques from the last chapter) so that it is either of diminished activity or completely ablated. Under this scenario, the flux must proceed along enzyme, e_1 . Again, this technique works extremely well, particularly for systems where there are few target enzymes or proteins that need to be mutated. Many examples have been developed for altering small molecule synthesis, such as decreased acetate production from *E. coli*. Another excellent example, that has to do with macromolecule synthesis, is the mutation of proteases that degrade recombinant proteins [13], so that overexpression of proteins is met with a less severe cell response (at least one devoid of product degrading proteases!). In general, however, this seemingly simple manipulation is met with unexpected cell responses. Such *pleiotropy* is common and is beginning to be elucidated, in large part because of the emerging experimental techniques that are used to understand cell physiology at the systems level (e.g., DNA microarrays from Chapter 1).

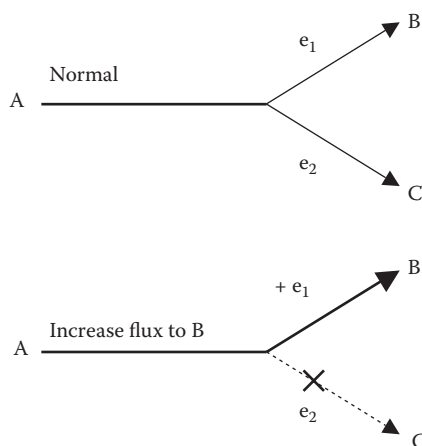


FIGURE 4.4 Pathway engineered to increase yield of compound “B.” Normally (upper panel), flux of A proceeds through both enzymes e_1 and e_2 , to produce B and C, respectively. By augmenting cells with additional e_1 , or by deleting or downregulating e_2 , one can increase yield of B (lower panel).

4.8 Emerging Technologies and Issues

Bacteria have demonstrated great utility for producing many protein products and some small molecules. An emerging technology builds upon the success with proteins. Now, workers are imbedding long synthetic pathways into bacteria in order to produce therapeutics as well as other small molecules that range from fuels to common industrial chemicals. To create a new synthetic pathway in *E. coli* or another microbe, components are obtained from the genomes of diverse biological sources. The strategy is to use the additional enzymatic components as a means for withdrawing metabolites that are naturally present within *E. coli* and then transform them to the desired product. It is envisioned that a cheap and renewable carbon source such as glucose can be to provide energy and carbon for the novel synthesis.

The prospects for using long and foreign pathways in common hosts such as *E. coli* initially had it skeptics. It was argued that cellular regulation could stymie the achievement of economical yields. Also, the presence of nonnative molecules within *E. coli* could lead to insurmountable toxicity effects. Examples are emerging that indicate that such potential problems and others can be solved.

A first problem that is easily dealt with is codon bias. All organisms use the same genetic code, but there is also redundancy in the code. Consequently, each organism tends to recognize a codon alternative preferentially over another. Because *E. coli* codon preferences are well known, modern DNA synthesis methods allow one to readily change the codons used by a source to the “dialect” used by *E. coli*. From there, the challenges become greater. A long synthetic pathway will by definition necessitate the insertion of numerous new genes into a production strain. Chromosomal integration and polycistronic plasmids can be used for this purpose.

Having achieved foreign gene expression, the prospect of toxicity from a pathway intermediate or final product can become the next obstacle. If the final product is toxic but rapidly excreted, then the problem can be managed albeit product dilution occurs, which can raise isolation costs. Toxicity from an intermediate in a heterologous pathway represents both good and bad news. If toxicity is observed, the good news is the pathway’s functionality upstream of the intermediate is high. The bad news is toxicity may impair the host’s ability to grow and also curtail the production of the glucose-derived precursors needed for product synthesis. Thus, yield and kinetics can both suffer at this stage.

The Keasling group adopted an effective approach for dealing with toxicity that arose in the synthesis of the antimalarial drug, Artemisinin, by *E. coli* [14]. Gene-expression profiling and metabolite analyses indicated that the toxic culprit was 3-hydroxy-3-methyl-glutaryl-coenzyme A (HMG-CoA). Rebalancing the metabolic fluxes thus necessitated modulating HMG-CoA reductase activity in order to consume the accumulating HMG-CoA. The group also explored another strategy. For many years, the notion of metabolic channeling has existed, which refers to the physical association of enzymes that are related by a reaction path. If channeling occurs, then pathway intermediates are transformed before they have a chance to diffuse away from their enzymatic-production centers and then interfere with other reactions or processes ongoing in the cell. Thus, the Keasling group hypothesized that the intracellular production of a poly-ligand structure could physically tether some of the enzymes involved in the new pathway thereby forcing metabolite channeling to occur. They found that compared to an untethered control, some mitigation of toxicity occurred. Overall, imbedded nonnative pathways based on heterologous genes will likely not be subject to feedback controls. The lack of feedback controls can be advantageous for diverting ample metabolic resources toward product synthesis. The down side, however, is if enzymatic capacities are not balanced, toxic intermediates may accumulate.

When the aim is to use bacteria to produce small molecules at high yield, another issue that can arise is cofactor balancing. Cofactors participate in enzymatic reactions, and they fulfill numerous functions such as activating reactants and serving as intermediaries in redox reactions. Cycling of two forms occurs and the intracellular abundance of cofactors is low. To illustrate the issue, the following discussion will consider redox carriers.

Bacteria use two redox carriers: nicotinamide adenine dinucleotide (NADH) and nicotinamide adenine dinucleotide phosphate (NADPH). The abbreviations in the parentheses denote the carriers when they are in the reduced form. When these molecules are in their oxidized forms (NAD⁺, NADP⁺), they abstract electrons from molecules in the form of a hydride and in the process, become reduced (NADH, NADPH). For example, the reaction $A + \text{NAD}^+ \rightarrow B + \text{NADH}$ occurs where B is more oxidized than A, and the electrons are transferred by adding a hydride to NAD⁺ to yield the reduced cofactor, NADH.

The NAD⁺/NADH pair tends to be operative in energetic processes. For example, when glucose is oxidized, the electrons are “carried” by NADH to the electron transport system, which resides in the cell membrane. Oxidation of NADH to NAD⁺ releases electrons to the electron transport chain. The reduction of oxygen to water completes the circuit, and the energy released is used to energize the cell membrane by establishing a proton charge and concentration gradient across the membrane. Continually energizing the membrane then allows for oxidative ATP formation to occur, where the ATP produced is then hydrolyzed to thermodynamically drive biosynthesis. NADP⁺/NADPH, in turn, are usually involved in oxidative or reductive biosynthesis. For example, the amino acid synthesis reaction catalyzed by glutamate dehydrogenase is



The reactions that utilize NAD⁺/NADH and NADP⁺/NADPH are called dehydrogenases. As an aside, when the carrier is denoted as NAD(P)⁺ or NAD(P)H in a particular dehydrogenase-catalyzed reaction, this means that the enzyme is either promiscuous or it is uncertain as to which version of the carrier is used by the enzyme. It could also indicate that when the dehydrogenase was isolated and characterized from a source, there could have been a mixture of isozymes present.

Many cellular dehydrogenase-catalyzed reactions produce NADH while fewer produce NADPH. In *E. coli*, the hexose monophosphate (HMP) pathway and the isocitrate dehydrogenase in the Krebs cycle are key sources of NADPH production. Organisms tend to differ in the specificity of their dehydrogenases. The easily manipulated workhorse, *E. coli*, is reported to have dehydrogenases with high specificity meaning a particular enzyme works exclusively with NAD⁺/NADH or NADP⁺/NADPH [15]. Thus, if there is an imbalance between synthetic and energetic electron flows within a cell, there may be little “slop” in the system that can help to rebalance energy production with biosynthesis. Rather, transhydrogenase activity is used to convert NADH to NADPH, or vice versa. Transhydrogenase activity has been reported to account for about 35–45% of NADPH production under aerobic growth in wild-type *E. coli* [15].

Based on few NADPH supply sources and high dehydrogenase specificity, one can envision that if *E. coli* is compelled to conduct an abnormal synthesis that requires a lot of NADPH, then other NADPH-requiring biosynthetic systems will be impaired. If these other systems, in turn, provide important precursors, then product yield and formation kinetics will be compromised. Therefore, a number of strategies are now under investigation for managing cofactor cycling, and more will emerge in the near future for redox and other cofactors. Some examples follow that pertain to NADPH balancing.

Abolishing pyruvate kinase activity is thought to divert carbon flow through the hexose monophosphate (HMP) pathway [16]. This pathway is a significant source of NADPH and pentose production in *E. coli*. Thus, this host cell background was hypothesized to support enhanced therapeutic DNA production, and increased copy number was reported [17].

While also having the attribute of low acetate production, the redistribution of metabolite trafficking provided by pyruvate kinase deficiency may not be optimal for other product syntheses. Thus, another strategy such as amplifying transhydrogenase activity can be considered. Two transhydrogenases from *E. coli* have been characterized by Sauer et al. [15]. The reduction of NADP⁺ with NADH is reported to be performed by the proton-translocating PntAB, while the UdhA form is thought to contend with excess NADPH production. PntAB is membrane-associated while UdhA is cytosolic. Amplifying PntAM

would have the effect of loosening the dehydrogenase specificity, and the regulation of expression would appear to be consistent with balancing redox [15].

A localized approach, but one with system-wide impact was reported by Martinez et al. [18]. They replaced the native NAD-dependent glyceraldehyde 3-phosphate dehydrogenase, which is a glycolytic enzyme, with a NADP-dependent alternative from *Clostridium acetobutylicum*. When considered “on paper,” the replacement increases the stoichiometry of NADPH formation from glucose. To test the altered host cell, synthesis of lycopene and epsilon-caprolactone in the modified strain was compared to the unmodified strain. The modified strains exhibited higher productivity than the parent strains. Flux determinations indicated a reduced reliance on the HMP pathway, which further affirmed the impact of the enzyme change.

Other approaches have been taken that focus entirely on genetic regulation within the bacterial cell to ensure that it is set up to accommodate metabolic flux down a particular pathway. Some of these are more radical and others are more elegant in nature. The more radical approaches are to integrate synthetic or genetically altered regulatory circuits to *supplant* native systems. Examples include efforts to completely rewire transcription factors in yeast. Stephanopoulos and coworkers used DNA libraries and mutagenesis to create yeast cells that tolerate high ethanol concentrations [19]. In another case, an entire genome was reshuffled to generate cells that were protected from the overproduction of acid [20]. A more elegant approach is to initiate and maintain the required synthesis reactions based on an intracellular signaling molecule cueing on the metabolic state of the cell. Here, Farmer and Liao [21] demonstrated the minimally altered rewiring of the native regulatory circuit for the automated and sustained generation of lycopene (a plant-derived antioxidant and pigment). Also, Tsao and coworkers [22] used a similar approach to make sure all the cells in the reactor were on the same page—they used the AI-2 autoinduction system to key the synthesis of their recombinant protein of interest. That is, when the cells were at just the right cell density, they turned on the synthesis of their product so that by the end of the culture, they all made the right amount of protein and generally all at the same time! Indeed, there are many activities focused on genetic regulation of the specific system. These researchers hope to ensure that the efforts taken to identify, clone, and activate new pathways and synthesis capabilities are realized in practice.

4.9 Final Remarks

In summary, bacterial systems are the workhorse of modern biotechnology. The tools exist for their genetic manipulation. Also, industrial bioreactors attempt to create microenvironments suitable for bacterial growth and product expression. Through the exploitation of their rapid growth rates and biosynthetic capabilities, bacteria have served as miniature cell “factories” for the synthesis of many products and processes that are now on the market. With a more comprehensive understanding of their biosynthetic and biodegradative pathways (as well as their regulation!), next-generation processes and products will certainly come to fruition. The recent and ongoing work on imbedding long and foreign pathways into *E. coli* provides one example of the future. Recent work provides some guidance on what challenges to expect as well as potential remedies as the synthetic capability of microbes is harnessed further. As we move forward from “it works” to “it works really well,” cofactor cycling will be increasingly important.

References

1. Fuqua, C. and E.P. Greenberg. 2002. Listening in on bacteria: Acyl-homoserine lactone signalling. *Nat. Rev. Mol. Cell Biol.* **3**: 685–695.
2. Lupp, C., M. Urbanowski, E.P. Greenberg, and E.G. Ruby. 2003. The *Vibrio fischeri* quorum-sensing systems *ain* and *lux* sequentially induce luminescence gene expression and are important for persistence in the squid host. *Mol. Microbiol.* **50**: 319–331.

3. March, J.C., G. Rao, and W.E. Bentley. 2003. Biotechnological applications of green fluorescent protein. *Appl. Microbiol. Biotechnol.* **62**: 303–315.
4. Kostov, Y., C.R. Albano, and G. Rao. 2000. All solid-state GFP sensor. *Biotechnol. Bioeng.* **70**: 473–477.
5. Bukau, B. 1993. Regulation of the *Escherichia coli* heat-shock response. *Mol. Microbiol.* **9**: 671–680.
6. Taga, M.E., S.T. Miller, and B.L. Bassler. 2003. Lsr-mediated transport and processing of AI-2 in *Salmonella typhimurium*. *Mol. Microbiol.* **50**: 1411–1427.
7. Bailey, J.E. 1991. Toward a science of metabolic engineering. *Science* **252**: 1668–1675.
8. Khosravi, M., D.A. Webster, and B.C. Stark. 1990. Presence of the bacterial hemoglobin gene improves alpha-amylase production of a recombinant *Escherichia coli* strain. *Plasmid* **24**: 190–194.
9. Majewski, R.A. and M.M. Domach. 1990. Simple constrained-optimization view of acetate overflow in *Escherichia coli*. *Biotechnol. Bioeng.* **35**: 732–738.
10. Hofmeyr, J.H. 1989. Control-pattern analysis of metabolic pathways. Flux and concentration control in linear pathways. *Eur. J. Biochem.* **186**: 343–354.
11. Holms, H. 1996. Flux analysis and control of the central metabolic pathways in *Escherichia coli*. *FEMS Microbiol. Rev.* **19**: 85–116.
12. Fell, D.A. and H.M. Sauro. 1985. Metabolic control and its analysis. Additional relationships between elasticities and control coefficients. *Eur. J. Biochem.* **148**: 555–561.
13. Meerman, H.J. and G. Georgiou. 1994. Construction and characterization of a set of *E. coli* strains deficient in all known loci affecting the proteolytic stability of secreted recombinant proteins. *Biotechnology (NY)* **12**: 1107–1110.
14. Douglas J. Pitera, D.J., C.J. Paddon, J. D. Newman, and J.D. Keasling. 2007. Balancing a heterologous mevalonate pathway for improved isoprenoid production in *Escherichia coli*. *Metab. Eng.* **9**: 193–207
15. Sauer U., F. Canonaco, S. Heri, A. Perrenoud, and E. Fischer. 2004. The soluble and membrane-bound transhydrogenases UdhA and PntAB have divergent functions in NADPH metabolism of *Escherichia coli*. *J. Biol. Chem.* **279**(8): 6613–6619.
16. Ponce, E., A. Martinez, F. Bolivar, and F. Valle. 1998. Stimulation of glucose catabolism through the pentose pathway by the absence of the two pyruvate kinase isoenzymes in *Escherichia coli*. *Biotechnol. Bioeng.* **58**: 292–295.
17. D. Cunningham, Z. Liu, N. Domagalski, R. Koepsel, M.M. Atai, and M.M. Domach. 2009. Pyruvate kinase deficient *Escherichia coli* exhibits increased plasmid copy number and cyclic AMP. *J. Bacteriol.* **191**(9): 3041–3049.
18. Martínez, I., J. Zhu, H. Lin, G.N. Bennett, and K.-Y. San. 2008. Replacing *Escherichia coli* NAD-dependent glyceraldehyde 3-phosphate dehydrogenase (GAPDH) with a NADP-dependent enzyme from *Clostridium acetobutylicum* facilitates NADPH dependent pathways. *Metab. Eng.* **10**(6): 352–355.
19. Alper, H., Moxley, J., Nevoigt, E., Fink, G.R., and Stephanopoulos, G. 2006. Engineering yeast transcription machinery for improved ethanol tolerance and production. *Science* **314**(5805): 1565–1568.
20. Patnaik, R., Louie, S., Gavrilovic, V., Perry, K., Stemmer, W.P., Ryan, C.M., and del Cardayre, S. 2002. Genome shuffling of *Lactobacillus* for improved acid tolerance. *Nat. Biotechnol.* **20**(7): 707–712.
21. Farmer, W.R. and Liao, J.C. 2000. Improving lycopene production in *Escherichia coli* by engineering metabolic control. *Nat. Biotechnol.* **18**(5): 533–537.
22. Tsao, C.-Y., Hooshangi, S., Wu, H.-C., Valdes, J.J., and W. E. Bentley. 2010. Autonomous induction of recombinant proteins by minimally rewiring native quorum sensing Regulon of *E. coli*. *Metab. Eng.* **12**:291–297.

6

DNA Vaccines Production and Engineering

Michael M. Domach
Carnegie Mellon

Jonathan W. Meade
Carnegie Mellon

Mohammad A. Ataai
University of Pittsburgh

6.1	Introduction	6-1
6.2	DNA Vaccine Plasmid Design	6-5
6.3	Issues in Plasmid Design	6-5
6.4	DNA Vaccine Production at a Large Scale.....	6-5
6.5	Prospects for Improvement.....	6-6
6.6	Final Remarks.....	6-8
	References.....	6-9

6.1 Introduction

To set the stage for DNA vaccines, the spectrum of current vaccines are summarized first. The so-called “first generation” vaccines are comprised of attenuated or inactivated microorganisms or viruses. As the name suggests, an attenuated virus or microbe will replicate in the body at an impaired rate, thereby providing the advantage of antigen amplification, which can then promote a strong immune response. The attenuation however entails removing pathogenicity factors beforehand. Inactivated microbes and viruses simply expose the body’s immune system to antigenic material from sources killed by heat beforehand or by other means. These vaccines are considered to be safer than attenuated preparations.

Because only a small portion of an immunogenic macromolecule serves as the antigenic determinant that actually invokes an immune response, a next logical step was to produce the active “ingredient” while discarding the other components of the intact organism. Hepatitis B vaccine produced in *Escherichia coli* is one success story. *E. coli* is transformed to synthesize the hepatitis B surface antigen (HbsAg), and the recombinant protein is purified to produce the vaccine. The first vaccine became available in 1981.

Human papillomavirus (HPV) vaccine provides a more recent example. HPV is an agent of cervical cancer, which is the second most prevalent cause of cancer-related death in women across the world. Infection with HPV types 16 and 18 accounts for roughly 70% of cervical cancer cases and the majority of genital warts are the result of infections from HPV types 6 and 11. The approach taken was to produce a virus-like particle (VLP), which entails the self-assembly of a major capsid protein. One challenge posed to those working on this approach was to obtain correct self-assembly such that the VLP was viewed as the real agent by the immune system. In the process developed by Merck, yeast is transformed to produce the capsid protein. The isolated parts are then combined to self-assemble into pentameric structures, which in turn assemble further in VLPs. The product of this technology is known by the tradename, Gardasil®, and it offers the advantage of not containing any viral DNA.

Using and producing synthetic peptides and protein fragments as potential vaccines are another line of investigation. Success has been achieved with hoof and mouth disease (e.g., Doel et al., 1988; Wang et al., 2002). Challenges include contending with the quick clearance of small proteins from the body. Additionally, when outbreaks occur, a dual treatment and antispread, vaccination strategy is desirable, which has generated different antibody and vaccine mixtures.

In addition to microbes, plants have been shown to be potential producers of protein fragments or subunits. Indeed, a plant-produced vaccine for poultry against Newcastle disease virus was developed by Dow where modified tobacco plants were used to produce the subunit vaccine (<http://www.nature.com/nbt/journal/v24/n3/full/nbt0306-233.html>). Concerns over “pharma cropping” have, however, resulted in cautious adoption of the technology although much ongoing research continues in academic laboratories or in contained commercial facilities.

The alternative to producing, isolating, and then injecting immunogenic material into a patient is to have the patient transiently produce an antigen. This is the intent of DNA vaccines. DNA vaccines are circular, super-coiled plasmids that generally contain: (i) a gene that encodes the target antigen(s), (ii) an antibiotic resistance gene that enables the selection of plasmid-bearing cells, and (iii) a bacterial origin of replication (Herweijer and Wolff, 2003). The target gene’s promoter is designed to be active in the recipient’s cells, but it is not expressed in bacteria during plasmid production. Thus, transient expression of the antigen occurs following administration, and then the DNA and antigen are cleared. The advantages of DNA vaccines include their stability, low toxicity, and fewer side effects than when virus-based components are used. Additionally, they can be rapidly redesigned to deal with mutations or in response to epidemics. Production can also quickly occur because bacteria are the production vehicle as opposed to eggs or other slower, less scalable sources.

DNA vaccines were first tested in patients with HIV infection (MacGregor et al., 1998) followed by testing as preventive vaccines for HIV (Boyer et al., 2000). In early trials involving humans, where deep muscle injection was a common administration protocol, the immune responses to DNA vaccines were found to be less than expected. In contrast, early vaccines and administration protocols showed good efficacy in animals, and especially promising results in small animals. More recently, delivery via gene guns (US Military) and electroporation have been found to significantly increase antibody response compared to when naked DNA is injected. For example, clinical trial NCT00859729 addresses the treatment of prostate cancer and entails testing the efficacy of a DNA vaccine administered intradermally in combination with electroporation (<http://clinicaltrials.gov/ct2/show/NCT00859729>). The improved outcomes sought in humans will presumably occur due to lowering the barrier presented by the cellular uptake of DNA.

The exploration of alternative delivery methods and some signs of success have generated the renewed interest in DNA vaccines. Apart from full vaccination, one can also envision that DNA vaccines can serve as immune system primers, such that effective vaccination may require a lower “booster” dosage for a virus-based vaccine. Lowering the dosage of virus-based components, in turn, is expected to lower the probability of adverse side effects. Thus, it is likely that DNA vaccine products will find increased use in animal health products, and they will play a role in managing human health that ranges from immune system “priming” to full vaccination. Currently, four DNA plasmid preparations are licensed for veterinary applications, some of which address human diseases such as melanoma cancer (Williams et al., 2009). Concerning the current status for human use, Kutzler and Weiner (2008) documented the following clinical trials: 72 Phase I, 20 Phase II, and 2 Phase III. [Table 6.1](#) provides a cross section of the clinical trial landscape as of June 2010.

Owing to the rekindled interest, this chapter will review the engineering issues associated with producing DNA vaccines. The reader might also keep in mind that the production of DNA by bacteria also serves other purposes. For example, basic experimentation with mammalian cells often first requires the production of DNA by bacteria. The more efficient the DNA production is, the fewer times the process of DNA generation by bacteria must be done to generate a stockpile. The greater the stockpile, the more replicates, variations, and experiments that can then be performed without having to do a new round of DNA preparation.

TABLE 6.1 Survey of Ongoing Clinical Trials and Tracking Links, June 2010^a

Disease ^b	Dates	Type of Vaccine/Method	Sponsor	Status	Test Subject
AIDS ^c	Clinical Trials 10/09/01	Gag and Pol using a Biojector	NIAID, VRC	Ongoing	21 men and women
HIV ^d	Started 08/09/02	Biological: pGA2/JS2 plasmid DNA vaccine	NIAID	Completed Nov 2008	30 uninfected humans
Liver cancer ^e	Started 08/06/04	Adenoviral vector and plasmid sargramostim hepatocellular adjuvant	National Cancer Institute (NCI)	Completed Feb 2009	3–25 men and women
Kidney cancer ^f	Started 11/12/04	Human prostate-specific antigen plasmid DNA vaccine	National Cancer Institute (NCI)	Ongoing	18 men and women
Prostate cancer ^g	Started Mar-05	Biological: pTVG-HP with rhGM-CSF	University of Wisconsin, Madison	Completed Aug 2008	22 male 18 and older
HIV ^h	Started 08/05/05	Biological: HIV-1 gag DNA (with bupivacaine) IL-15 DNA, IL-12 DNA, sodium chloride injection	Wyeth	Terminated/Failed on December 2007	Adults with HIV
Multiple sclerosis ⁱ	2005–2006	BHT-3009 injection	Montreal Neurological Institute	Success—safe and well tolerated	30 patients
Dengue fever ^j	Clinical Trials 02/09/06	Biological: D1ME (dengue-1 premembrane/envelope)	U.S. Army Medical Research and Material	Completed June 2009	24 men and women
West Nile Fever ^k	Started 3/1/2006	Drug: VRC-WNV DNA020-00-VP	NIAID; National Institutes of Health	Completed Dec 2007	30 men and women
H5N1 Avian Influenza ^l	First human trial 12/21/06	Hemagglutinin (H) gene	VRC, NIAID	Ongoing	Human volunteers
Melanoma ^m	Started 4/1/2007	Biological: Xenogeneic tyrosinase DNA vaccine TriGrid delivery for intramuscular electroporation	Ichor Medical Systems/Memorial Sloan-Kettering CC	Ongoing	25 men and women
Chronic hepatitis B (HBV) ⁿ	Trial started 08/08/07	Genetic: a mixed plasmid DNA (HB-110) Drug: Adefovir	Genexine Co., Ltd.	Ongoing and Recruiting	27 men and women
Lymphoma ^o	Started 10/1/2007	Biological: plasmid DNA vaccine therapy Other: flow cytometry, immunoenzyme technique	Memorial Sloan-Kettering CC National Cancer Institute	Ongoing and Recruiting	18 men and women
HIV ^p	Started 10/17/08	Biological: PENNVAX-B GENEVAX IL-12-4532, IL-15 adjuvant	University of Pennsylvania	Ongoing and Recruiting	38 adults with HIV
Metastatic breast cancer ^q	Clinical trials 12/11/08	Biological: Mammaglobin-A DNA vaccine	Washington University School of Medicine	Ongoing until 2011	15 female

(Continued)

TABLE 6.1 (Continued) Survey of Ongoing Clinical Trials and Tracking Links, June 2010^a

Disease ^b	Dates	Type of Vaccine/Method	Sponsor	Status	Test Subject
H1N1 Influenza ^c	Clinical trials 08/24/09	Hemagglutinin	NIAID VRC	Ongoing	20 human
Malaria ^d	Announced 04/12/10	Adenovirus-vectored vaccine	Naval Medical Research Center	4/15 human subjects protected	Adult volunteers
Flu H5N1 & H1N1 ^e	Announced 06/15/10	VGX-3400X (hemagglutinin [HA] antigen, neuraminidase [NA] antigen, nucleoprotein [NP])	Inovio Pharmaceuticals, Inc.	Success	30 healthy subjects
CEA FrC ^u	Announced 6/17/2010	Anti-CEA DNA vaccine (ACVA) with a CEA/pDom fusion gene	Cancer Research UK New Agents Committee	Ongoing	Patients with CEA cancers
Metastatic melanoma ^v	2001 Phase 1 2003 Phase 2 2007 Phase 3	Allovectin-7 [®] , a plasmid/lipid complex containing the DNA sequences encoding HLA-B7 and β 2 microglobulin	Vical	Ongoing	375 patients in Phase 3

^a Prepared by Steven Yi, chemical engineering undergraduate, Carnegie Mellon.

^b Links for tracking

^c <http://www.niaid.nih.gov/news/newsreleases/2001/Pages/vaccinemade.aspx>

^d <http://clinicaltrials.gov/ct2/show/NCT00043511?term=dna±vaccines&cond=HIV&rank=1>

<http://www.liebertonline.com/doi/abs/10.1089/aid.2006.22.678?journalCode=aid>

^e <http://clinicaltrials.gov/ct/show/NCT00093548>

^f <http://clinicaltrials.gov/ct2/show/NCT00096629?term=dna±vaccines&rank=39>

^g <http://clinicaltrials.gov/ct2/show/NCT00582140?term=dna±vaccines&rank=77>

^h <http://clinicaltrials.gov/ct2/show/NCT00195312?term=dna±vaccines&cond=HIV&rank=4>

ⁱ <http://archneur.ama-assn.org/cgi/content/abstract/64.10.nct70002v1?maxtoshow=&HITS=10&hits=10&RESULTFORMAT=&fulltext=BHT-3009&searchid=1&FIRSTINDEX=0&resourcetype=HWCIT>

^j <http://clinicaltrials.gov/ct2/show/NCT00290147?term=dna±vaccines&rank=3>

^k <http://clinicaltrials.gov/ct2/show/NCT00300417?term=dna±vaccines&rank=108>

^l <http://www.niaid.nih.gov/news/newsreleases/2007/pages/fludnavax.aspx>

^m <http://clinicaltrials.gov/ct2/show/NCT00471133?term=dna±vaccines&rank=2>

ⁿ <http://clinicaltrials.gov/ct2/show/study/NCT00513968?term=dna±vaccines&rank=25>

^o <http://clinicaltrials.gov/ct2/show/NCT00561756?term=dna±vaccines&rank=42>

^p <http://clinicaltrials.gov/ct2/show/NCT00775424?term=dna±vaccines&cond=%22HIV±Infections%22&rank=13>

^q <http://clinicaltrials.gov/ct2/show/NCT00807781?term=dna±vaccines&rank=1>

^r <http://www.niaid.nih.gov/news/newsreleases/2009/Pages/CandidateDNAvaccine.aspx>

^s <http://www.medicalnewstoday.com/articles/186959.php>

^t <http://biotechstocktrader.com/inovio-immunizes-first-subject-in-flu-dna-vaccine-trial-009/>

^u <http://science.cancerresearchuk.org/research/who-and-what-we-fund/browse-by-location/southampton/university-of-southampton/grants/christian-ottensmeier-5634-a-cancer-research-uk-phase>

^v http://www.vical.com/products/cancer_therapies/allovectin-7.htm

6.2 DNA Vaccine Plasmid Design

The plasmids used as vaccines typically contain the ColE1 origin of replication (Grabherr and Bayer, 2002). Such plasmids utilize *E. coli* replication enzymes (e.g., Tomizawa, 1984). As part of the replication initiation process, a plasmid RNA transcript (RNA II) hybridizes with the template DNA strand at the plasmid's origin of replication. The RNA–DNA complex serves as the substrate for RNase H, which cleaves the hybridized preprimer RNA to produce a RNA primer. This RNA primer is then used for DNA synthesis by DNA polymerase I. ColE1-type plasmids control their copy number with two plasmid-encoded inhibitors, “RNA I” and a protein inhibitor (Tomizawa, 1984; Tomizawa and Som, 1984). RNA I inhibits the initiation of plasmid DNA replication by preventing the processing of a plasmid transcript (RNA II) to form an RNA primer for DNA polymerase I. The binding between RNA I and RNA II is a second-order reaction and the inhibitor protein, referred to as either Rom (Tomizawa, 1984) or Rop (Cesareni et al., 1982), increases the binding rate constant (Tomizawa and Som, 1984). DNA vectors typically lack the *rom* gene and thus attain higher copy numbers. Furthermore, increasing the temperature to 42°C increases the copy number by threefold. The higher temperature “melts” the interactions between RNA I and II thereby further diminishing the negative control over replication.

6.3 Issues in Plasmid Design

Using antibiotic selection to isolate and/or maintain plasmid-containing bacteria is not recommended by the US FDA, especially when β -lactamase activity is involved. Thus, at the minimum, plasmids that possess a kanamycin-resistance marker are often used in preparations that are intended for human use. Alternately, genes encoding non-antibiotic resistance markers on the plasmid that offset chromosomal-encoded toxicity elements are used. One example is the plasmid pNTC8485, which encodes an antisense RNA that “neutralizes” the expression of chromosomal-encoded levansucrase. Unless “neutralized” by the plasmid-encoded function, levansucrase activity generates toxicity to the host when sucrose is present. For more details including up-to-date plasmid maps, see <http://www.natx.com/PDFs/MammalianExpressionVectorsAntibiotic%20Free.pdf>.

The “metabolic burden” the plasmid can impose on a host cell such as *E. coli*, as reflected by a reduction in growth rate and thus increased production time, can be traced, in part, to plasmid design. For example, the plasmid-encoded selectable marker β -lactamase, which encodes ampicillin resistance, has been reported to account for 18% of total cellular protein (Rozkov et al., 2004). Much lower levels of β -lactamase activity are needed for the selection of plasmid-containing cells; hence, even if the level attained is less than 18% of total cellular protein, there tends to be a lot of “overkill” in the constitutive marker expression from many plasmids. Synthesis of such high levels of a protein acting as a selectable marker also consumes a substantial amount of cellular resources, which negatively impacts the yield and kinetics of plasmid DNA synthesis in cells. The antisense RNA selection strategy used in pNTC8485 and other complementation schemes can be viewed as addressing the burden issue as well as working around the need for antibiotics.

6.4 DNA Vaccine Production at a Large Scale

One effective method now used for producing plasmid DNA involves using a two-stage process (Williams et al., 2009). Cells are first grown at low temperature (30°C) in a fed-batch process using glycerol as the carbon and energy source. Glycerol is often used to avoid the production of acetate during growth; the production of acetate, which can become inhibitory as it accumulates, is much lower for growth on glycerol as compared to when glucose is used. The use of low temperature, in turn, restricts the plasmid replication rate to a low level, which lessens the metabolic burden exerted by plasmid synthesis during the propagation phase. The combined effects of growth on glycerol and using low temperature result in a low specific

growth rate (0.1 h^{-1}). Thereafter, elevating temperature increases the plasmid replication rate, which raises the value of plasmid/cell. A very effective “double bang” effect can be envisioned to occur in this second stage based on Equation 6.1, which accounts for the time-dependent level of a cellular constituent

$$dP/dt = r_s - \mu P \quad (6.1)$$

In Equation 6.1, P , r_s , and μ refer to plasmid DNA/cell, intrinsic synthesis rate, and specific growth rate, respectively. Thus, when temperature is increased, *de novo* synthesis in terms of r_s increases several fold while μ -driven cytoplasmic dilution decreases somewhat. The combination results in a significantly increased rate of plasmid DNA accumulation per cell. Overall, reduced kinetics during the cell propagation phase is traded off against lessened acetate toxicity and metabolic burden.

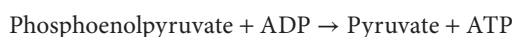
6.5 Prospects for Improvement

Wild bacteria contain plasmids which can provide some benefits for either individual cell or population survival. The conjugative F plasmid, for example, enables the transfer of genetic material between cells of *E. coli*. The copy number of F plasmids, or their derivatives, though is quite low, and in the single digits zone. Other hybrid plasmids attain copy numbers on the order of 100, and this value is now considered to be in the realm of “high copy number.” The aim of attaining much higher copy numbers translates the desired outcome far from what occurs in nature, or has been achieved thus far conventionally in the lab. Questions thus arise on how further increases may be achieved and what the actual limits may be.

Host fitness is one area that has received less attention than plasmid design. Here, the idea is whether metabolic engineering can be used to make *E. coli* more tolerant of plasmid synthesis at a very high level. Some leads come from adaptation studies where investigators compared the levels of gene expression or enzyme activities in plasmid-containing cells to those lacking plasmid. Other leads come from pursuing metabolism-inspired hypotheses. For example, a gene in a particular metabolic pathway related to DNA synthesis such as ribose production is amplified in order to assess whether the “burden” is reduced. Here, “burden” can be quantified by the extent that growth rate is *not* impacted when a high copy number plasmid is hosted. Some reports are summarized below that start to form a metabolic picture of what host improvements might be desirable.

Ow et al. (2006) found that one adaption to plasmid presence entailed increasing expression from *zwf* (encodes glucose-6-phosphate dehydrogenase) by 1.2-fold while the expression from phosphoglucose isomerase was decreased by 1.8-fold. Thus, if it is assumed that expression correlates with enzyme activity, their results suggest that one adaptation involves increasing the hexose monophosphate (HMP) pathway/glycolysis ratio by approximately a factor of 2. In another study, Birnbaum and Bailey (1991) found that *E. coli* expressed less pyruvate kinase (Pyk) and more phosphoenolpyruvate carboxylase (Ppc) as plasmid copy number increased. That such adaptive changes in fluxes allow *E. coli* to contend with plasmid presence is suggested further by the work of Flores et al. (2004). They found that when glucose was the carbon and energy source, *E. coli* (JM101) exhibited less burden when the HMP pathway gateway enzyme, glucose-6-phosphate dehydrogenase, was overexpressed. The metabolic burden, as indicated by the reduction in growth rate, was reduced when the expression of glucose-6-phosphate dehydrogenase was increased by 3.4-fold. Wang et al. also reported in 2006 that amplifying the HMP enzyme, ribose-5-phosphate isomerase A increased the copy number of a ColE1 plasmid in *E. coli*.

To explore further the patterns described above, Cunningham et al. (2009) explored whether the copy number of a pUC plasmid was elevated in a mutant of *E. coli* deficient in Pyk. Note that Pyk catalyzes the reaction below



This mutant was originally constructed by Ponce et al. (1998) and it is typically referred to as PB25. The PB25 mutant is a low acetate producer, and some reports indicate that the flux through the pentose-producing, HMP pathway is much higher than in the wild type (Ponce et al., 1998). Such a change in metabolic fluxes due to the Pyk deficiency makes sense from the metabolic and control standpoints. Pyk deficiency can result in phosphoenolpyruvate (PEP) accumulation, and some have reported such an outcome (Ponce et al., 1998). Elevated PEP, in turn, can influence the activity of phosphofructokinase, which is an enzyme that operates early in glycolysis. Because the importation rate of glucose and growth rate of PB25 is about the same as the wild type, the imported glucose has to go somewhere in PB25 when the flux through glycolysis is impeded via PEP-mediated feedback. One possible outcome is the imported glucose can instead be shunted through the HMP pathway, which increases pentose production.

Increased HMP flux also elevates the production of another HMP pathway-associated product, NADPH. The extra NADPH produced via the HMP pathway can then be used to contend with the increased reductive biosynthesis load imposed by increased DNA precursor synthesis. Furthermore, increasing one of the few sources of NADPH in *E. coli* is an important factor because the dehydrogenases in *E. coli* are reported to exhibit little cross reactivity between NAD^+/NADH and $\text{NADP}^+/\text{NADPH}$ (Fuhrer and Sauer, 2009). Thus, no transfer of reductant availability from NADH to NADPH via “slop” in the system can occur and provide a means for making up for shortfalls in NADPH production. However, transhydrogenase activity, which converts NADH into NADPH, may also help to balance redox metabolism in *E. coli*. It has been reported that during normal growth, up to 40% of the NADPH used in reductive biosynthesis can be derived from the NADH produced in catabolic reactions (Fuhrer and Sauer, 2009).

Finally, while ^{13}C NMR studies of PB25 differ in some respects, they all reveal that the mutant has increased Ppc flux. This makes sense from two standpoints. First, the mutation can cause an increase in PEP, the substrate for the Ppc-catalyzed reaction. Second, maintaining flux through the Krebs cycle can be accomplished when pyruvate production is curtailed by increasing the Ppc-catalyzed, anaplerotic reaction $\text{PEP} \rightarrow \text{oxaloacetate}$.

The above are metabolic arguments, and any comprehensive examination and redesign of host cell metabolism should also consider whether the host cell’s DNA replication enzymes may provide a limitation. One group has examined this question. Williams et al. (2009) have reported that plasmid yield or host growth rate was not altered when a wide range of DNA replication enzymes were amplified. Thus, at this juncture, it does not appear that the DNA replication machinery of a host cell is the main limitation. Rather, the combination of residual negative control over replication, excessive marker production, and imbalanced precursor/cofactor fluxes constitute the initial space over which to optimize a comprehensive design for a DNA vaccine production.

To experimentally test whether PB25 central metabolism may support greater plasmid production than the wild type while not suffering from a large reduction in growth rate, Cunningham et al. (2009) contrasted the synthesis of a high copy number plasmid in PB25 to that of the wild-type JM101. The idea here was PB25 may “bundle” the advantageous traits or adaptations found piecewise in the work described above. “Bundling” entails PB25 simultaneously provides elevated HMP pathway and Ppc fluxes and lessened Pyk flux. The pGFPuv plasmid was used, which is a pUC-type plasmid that lacks *rom*.

Experiments were performed starting with extremely dilute inoculum. The dilute starting point provided the opportunity for many cell generations to occur at a fixed specific growth rate such that the copy number (or expression of green fluorescent protein) per cell reached an asymptotic limit. The origin of such a limit can be seen by integrating Equation 6.1

$$P(t) = r_s/\mu - (r_s/\mu - P(0))e^{-\mu t} \quad (6.2)$$

As $\mu t = \ln(2) \times \text{number of generations} = 0.693 \times N_G \sim 5$, the amount of an intracellular constituent per cell (or per total cell mass) reaches a constant. Overall, these experiments were designed to allow for true balanced growth to be obtained for all cell constituents, and then maintained for 2–4 generations, well before glucose exhaustion and entry into the stationary phase occurred.

TABLE 6.2 Copy Number and Growth Rate Comparison for Isothermal and Temperature-Shifted Growth

Strain	Isothermal at 37°C		After temperature shift 37°C to 42°C	
	Growth Rate (h ⁻¹)	Copy Number	Growth Rate (h ⁻¹)	Copy Number ^a
JM101	0.76	129	0.61	519
PB25	0.59	537	0.56	1217

^a Determined immediately before stationary phase; about four generations post-shift.

The copy number results are summarized in Table 6.2 (Cunningham et al., 2009). When growth occurred at 37°C, the plasmid content of PB25 was about fourfold greater than the wild type. The plasmid content of PB25 when the temperature was increased from 37°C to 42°C was about 10-fold greater than that in the wild-type cells grown at 37°C. The specific growth rates of PB25 at 37°C and 42°C were similar (0.59 vs 0.56 h⁻¹), while a greater relative reduction in growth rate (ca 20%) was found for the wild-type cells growing on either glucose or glycerol. The plasmid yield from PB25 was 35 mg/g cell dry weight, which is in the “ball park” of that achieved from slower, fed-batch processes that use glycerol (Williams et al., 2009). The higher growth rate of PB25 on glucose (0.6 h⁻¹), however, represents a much higher amount of productivity as compared to when the growth rate is 0.1 h⁻¹, as maintained for growth on glycerol. Finally, the plasmid isolated from PB25 was found to be primarily in the supercoiled form, which is in accord with FDA requirements.

6.6 Final Remarks

Developing vaccines against cancer and infectious diseases are now major goals for biotech and pharmaceutical companies. Amongst the new vaccine candidates are DNA vaccines. All vaccines must balance efficacy against safety, while being economical to produce and thus disseminate. The last aspect is especially important to improving the delivery of healthcare to developing nations.

DNA vaccines are considered safe, and much ongoing work is now aimed at improving efficacy or reducing the cost of production. Given that a number of successful animal products now exist, at the minimum it can be expected that more DNA vaccines will be developed that are aimed at managing animal health. Improving delivery, in turn, will contribute to raising the likelihood that DNA vaccines will become an important tool for managing human health.

Concerning the production of DNA vaccines in bacteria such as *E. coli*, at this juncture the limit posed by host cell DNA replication machinery does not appear to have been reached yet. Rather, the residual negative control over replication and the metabolism of wild-type host cells are the first-level factors that can be adjusted in order to improve yield. To speculate a bit, after the first-level factors are addressed, DNA replication capacity, DNA-membrane interactions, and the increased presence of macromolecules in the cellular cytosol may emerge as the next issues with which to contend. Another important issue that may arise is as the copy number is increased, and redefines what now is considered to be “high,” the coding errors that accumulate in the replicated DNA may increase. Such errors could lead to lower vaccine efficacy or other problems unless the host strain’s editing mechanisms are augmented. The stability of the plasmids could also present a problem depending on the coding sequences used and the sizes of the plasmids.

Along the way as new work is performed on the problems associated with DNA vaccines, technological refinements and innovations will occur in plasmid and host cell design. These developments may have useful “spin offs.” From a basic standpoint, much more will be learned about how metabolism and its regulation integrates with DNA replication in bacteria such as *E. coli*. Developing new selection methods for plasmid-containing cells that do not rely on antibiotics will not only comply with FDA

recommendations and requirements but also lower the metabolic burden imposed on host cell. In the end, the wider adoption of antibiotic-free methodologies will reduce the reliance on antibiotic selection in research. That would represent one step forward toward slowing the evolution of microbes toward antibiotic resistance. Ongoing trials that seek to improve the delivery of DNA vaccines into patients may also open the door for the delivery of other drugs through such novel administration protocols.

References

- Birnbaum S. and J.E. Bailey. 1991. Plasmid presence changes the relative levels of many host cell proteins and ribosome components in recombinant *Escherichia coli*. *Biotechnol. Bioeng.* 37:736–745.
- Boyer J.D., A.D. Cohen, S. Vogt, K. Schumann, B. Nath, L. Ahn, K. Lacy et al. 2000. Vaccination of sero negative volunteers with a human immunodeficiency virus type1 env/revDNA vaccine induces antigen-specific proliferation and lymphocyte production of beta-chemokines. *J. Infect. Dis.* 181(2):476–483.
- Cesareni G., M.A. Muessing, and P. Polisky. 1982. Control of ColE1 DNA replication: The rop gene product negatively affects the transcription from the replication primer promoter. *Proc. Natl. Acad. Sci. USA* 79:6313–6317.
- Cunningham D., Z. Pan, R. Koepsel, M.M. Ataai, and M.M. Domach, 2009. Pyruvate kinase-deficient *Escherichia coli* exhibits increased plasmid copy number and cyclic AMP. *J. Bacteriol.* 191(9):3041–3049.
- Doel T.R., C. Gale, G. Brooke, and R. Dimarchi, 1988. Immunization against foot-and-mouth disease with synthetic peptides representing the C-terminal region of VP1. *J. Gen. Virol.* 69:2403–2406.
- Flores S., R. de Anda-Herrera, G. Gosset, and F.G. Bolivar. 2004. Growth-rate recovery of *Escherichia coli* cultures carrying a multicopy plasmid, by engineering of the pentose-phosphate pathway. *Biotechnol. Bioeng.* 87:485–494.
- Fuhrer T. and U. Sauer. 2009. Different biochemical mechanisms ensure network-wide balancing of reducing equivalents in microbial metabolism. *J. Bacteriol.* 191:2112–2121.
- Grabherr R. and Bayer K. 2002. Impact of targeted vector design on Co/E1 plasmid replication. *Trends Biotechnol.* 20(6):257–260.
- Herweijer H. and J.A. Wolff. 2003. Progress and prospects: Naked DNA gene transfer and therapy. *Gene Therapy* 10:453–458.
- Kutzler M.A. and D.B. Weiner. 2008. DNA vaccines: ready for prime time? *Nat. Rev. Genet.* 9(10):776–788.
- MacGregor R.R., J.D. Boyer, K.E. Ugen, K.E. Lacy, S.J. Gluckman, M.L. Bagarazzi, M.A. Chattergoon et al. 1998. First human trial of a DNA-based vaccine for treatment of human immunodeficiency virus type1 infection: Safety and host response. *J. Infect. Dis.* 178:92–100.
- Ow D.S.-W., P.M. Nissom, R. Philp, S.K.-W. Oh, and M.G.-S. Yap. 2006. Global transcriptional analysis of metabolic burden due to plasmid maintenance in *Escherichia coli* DH5a during batch fermentation. *Enzyme Microb. Technol.* 39:391–398.
- Ponce E., A. Martinez, F. Bolivar, and F. Valle. 1998. Stimulation of glucose catabolism through the pentose pathway by the absence of the two pyruvate kinase isoenzymes in *Escherichia coli*. *Biotechnol. Bioeng.* 58:292–295.
- Rozkov A., C.A. Avignone-Rossa, P.F. Ertl, P. Jones, R.D. O’Kennedy, J.J. Smith, J.W. Dale, and M.E. Bushell. 2004. Characterization of the metabolic burden on *Escherichia coli* DH1 cells imposed by the presence of a plasmid containing a gene therapy sequence. *Biotechnol. Bioeng.* 88:909–915.
- Tomizawa J. 1984. Control of ColE1 plasmid replication: Enhancement of binding of RNA I to the primer transcript by the Rom protein. *Cell* 38:861–870.
- Tomizawa J. and T. Som. 1984. Control of ColE1 plasmid replication: Enhancement of binding of RNA I to the primer transcript by the Rom protein. *Cell* 38:871–878.
- Vermij P. and E. Waltz. 2006. USDA approves the Wrst plant-based vaccine. *Nat. Biotechnol.* 24:233–234.
- Wang C.Y., T.Y. Chang, A.M. Walfield, J.Y. Shen, S.P. Chen, M.C. Li, Y.L. Lin et al. 2002. Effective synthetic peptide vaccine for foot-and-mouth disease in swine. *Vaccine* 20(19–20):2603–2610.

- Wang Z., L. Xiang, J. Shao, A. Węgrzyn, and G. Węgrzyn. 2006. Effects of the presence of ColE1 plasmid DNA in *Escherichia coli* on the host cell metabolism. *Microbial Cell Factories* 5:34.
- Williams J.A., J. Luke, S. Langtry, S. Anderson, C.P. Hodgson, and A.E. Carnes. 2009. Generic plasmid DNA production platform incorporating low metabolic burden seed-stock and fed-batch fermentation processes. *Biotechnol Bioeng.* 103(6):1129–1143.



Transport Phenomena and Biomimetic Systems

Robert J. Fisher

*SABRE Institute and Massachusetts
Institute of Technology*

Robert A. Peattie

Tufts University

- 7 **Biomimetic Systems: Concepts, Design, and Emulation** *Robert J. Fisher*7-1
Concepts of Biomimicry • Biomimicry and Tissue Engineering • Biomimetic
Membranes for Ion Transport • Assessing Mass Transfer Resistances in Biomimetic
Reactors • Electro-Enzymatic Membrane Reactors as Electron Transfer Chain
Biomimetics • References
- 8 **Transport/Reaction Processes in Biology and Medicine** *E.N. Lightfoot* 8-1
Introduction • Macroscopic Approximations: Allometry • Orders of Magnitude and
Characteristic Time Constants • Time Constant Ratios • Systems of Multiple Time
Constants • Pseudocontinuum Models • More Complex Situations • References
- 9 **Microvascular Heat Transfer** *James W. Baish* 9-1
Introduction and Conceptual Challenges • Basic Concepts • Vascular Models • Models
of Perfused Tissues • Parameter Values • Solutions of Models • Defining
Terms • References
- 10 **Fluid Dynamics for Bio Systems: Fundamentals and Model Analysis** *Robert A.
Peattie and Robert J. Fisher*.....10-1
Introduction • Elements of Theoretical Hydrodynamics • Pulsatile Flow • Models and
Computational Techniques • References

- 11 Animal Surrogate Systems** *Michael L. Shuler, Sarina G. Harris, Xinran Li, and Mandy B. Esch*..... **11-1**
 Background • Cell Culture Analog Concept • Prototype CCAs • Models of Barrier Tissues and Their Use with μ CCAs • Future Prospects • Defining Terms • References
- 12 Arterial Wall Mass Transport: The Possible Role of Blood Phase Resistance in the Localization of Arterial Disease** *John M. Tarbell and Yuchen Qiu*..... **12-1**
 Steady-State Transport Modeling • Damköhler Numbers for Important Solutes • Sherwood Numbers in the Circulation • Nonuniform Geometries Associated with Atherogenesis • Discussion • Possible Role of Blood Phase Transport in Atherogenesis • References
- 13 Transport Phenomena and the Microenvironment** *Robert J. Fisher and Robert A. Peattie* **13-1**
 Introduction • Tissue Microenvironments • Reacting Systems and Bioreactors • Illustrative Example: Control of Hormone Diseases via Tissue Therapy • References
- 14 Transport and Drug Delivery through the Blood–Brain Barrier and Cerebrospinal Fluid** *Bingmei M. Fu*..... **14-1**
 Introduction • Drug Delivery through the Blood–Brain Barrier • Drug Delivery through the Cerebrospinal Fluid • Acknowledgments • References
- 15 Interstitial Transport in the Brain: Principles for Local Drug Delivery** *W. Mark Saltzman*..... **15-1**
 Introduction • Implantable Controlled Delivery Systems for Chemotherapy • Drug Transport after Release from the Implant • Application of Diffusion–Elimination Models to Intracranial BCNU Delivery Systems • Limitations and Extensions of the Diffusion–Elimination Model • New Approaches to Drug Delivery Suggested by Modeling • Conclusion • References
- 16 Surfactant Transport and Fluid–Structure Interactions during Pulmonary Airway Reopening** *David Martin, Anne-Marie Jacob, and Donald P. Gaver III*..... **16-1**
 Introduction • Fluid–Structure Interactions in the Lung • Acknowledgment • References

The intention of this section is to couple the concepts of transport phenomena with chemical reaction kinetics and thermodynamics to introduce the field of reaction engineering. This essential information is needed to design and control engineering devices, particularly flow reactor systems. Through extension of these concepts, combined with materials design, to mimic biological systems in form and function, the field of biomimicry has evolved. The development of biomimetic systems is a rapidly emerging technology with expanding applications. Specialized journals devoted to exploring both the analysis of existing biological materials and processes, and the design and production of synthetic analogs that mimic biological properties are now emerging. These journals blend a biological approach with a materials/engineering science viewpoint covering topics that include: analysis of the design criteria used by organisms in the selection of specific biosynthetic materials and structures; analyses of the optimization criteria used in natural systems; the development of systems modeled on biological analogs; and applications of “intelligent” or “smart” materials in areas such as biosensors, robotics, and aerospace. This biomimicry theme is prevalent throughout all the chapters in this section, including one specifically devoted to these concepts with explicit examples of applications to reacting and transport processes.

The field of transport phenomena traditionally encompasses the subjects of momentum transport (viscous flow), energy transport (heat conduction, convection, and radiation), and mass transport (diffusion). In this section the media in which the transport occurs is regarded as continua; however, some molecular explanations are discussed. The continuum approach is of more immediate interest to engineers, but both approaches are required to thoroughly master the subject. The current emphasis in engineering education is on understanding basic physical principles versus “blind” use of empiricism. Consequently, it is imperative that the reader seek further edification in classical transport phenomena

texts; general (Bird et al., 2002; Deen, 1996), with chemically reactive systems (Rosner, 1986), and more specifically, with a biologically oriented approach (Fournier, 1999; Lightfoot, 1974). The laws (conservation principles, etc.) governing such transport will be seen to influence: (1) the local rates at which reactants encounter one another; (2) the temperature field within body regions (or compartments in pharmacokinetics modeling); (3) the volume (or area) needed to accomplish the desired turnover or transport rates; and (4) the amount and fate of species involved in mass transport and metabolic rates. For biomedical systems such as dialysis, in which only physical changes occur, the same general principles, usually with more simplifications, are used to design and analyze these devices. The transport laws governing nonreactive systems can often be used to make rational predictions of the behavior of “analogous” reacting systems. The importance of relative time scales will be discussed throughout this section by all authors. It is particularly important to establish orders-of-magnitude and to make realistic limiting calculations. Dimensional analysis and pharmacokinetic modeling techniques are especially attractive for these purposes; in fact, they may permit unifying the whole of biological transport (see other sections of this handbook and Enderle et al. (1999) and Fisher (1999)). As the reader progresses, the importance of transport phenomena in applied biology becomes steadily more apparent. “In all living organisms, but most especially the higher animals, diffusional and flow limitations are of critical importance; moreover, we live in a very delicate state of balance with respect to these two processes” (Lightfoot, 1974).

Each chapter in this section is somewhat self-contained. Similar concepts are brought forth and reinforced through applications and discussions. However, to further enhance the benefits obtained by the reader, it is prudent to first discuss some elementary concepts; the most relevant being control volume selection and flow reactors.

When applying the conservation laws to fluid matter treated as a continuum, the question arises as to the amount of matter to be considered. Typically this decision is based on convenience and/or level of detail required. There is no single choice. Many possibilities exist that can lead to the same useful predictions. The conservation laws of continuum dynamics can be applied to the fluid contained in a volume of arbitrary size, shape, and state of motion. The volume selected is termed a “control volume.” The simplest is one where every point on its surface moves with the local fluid velocity. It is called a “material” control volume since, in the absence of diffusion across its interface, it retains the material originally present within its control surface. Although conceptually simple, they are not readily used since they move through space, change their volume, and deform. An analysis of the motion of material control volumes is usually termed “Lagrangian” and time derivatives are termed “material” or “substantial” derivatives.

Another simple class of control volumes is defined by surfaces fixed in physical space, through which the fluid flows. These “fixed” control volumes are termed “Eulerian” and may be either macroscopic or differential in any or all directions. The fluid contained within an Eulerian control volume is said to be, in thermodynamic terms, an “open” (flow) system.

The most general type of control volume is defined by surfaces that move “arbitrarily,” that is, not related to the local fluid velocity. Such control volumes are used to analyze the behavior of nonmaterial “waves” in fluids, as well as moving phase boundaries in the presence of mass transfer across the interface (Crank, 1956; Fisher, 1989).

Characterization of the mass transfer processes in bioreactors, as used in cell or tissue culture systems, is essential when designing and evaluating their performance. Flow reactor systems bring together various reactants in a continuous fashion while simultaneously withdrawing products and excess reactants. These reactors generally provide optimum productivity and performance (Freshney, 2000; Levenspiel, 1989; Shuler and Kargi, 2001). They are classified as either tank- or tube-type reactors. Each represents extremes in the behavior of the gross fluid motion. Tank-type reactors are characterized by instant and complete mixing of the contents and are therefore termed perfectly mixed, or backmixed, reactors. Tube-type reactors are characterized by the lack of mixing in the flow direction and are termed plug flow, or tubular, reactors. The performance of actual reactors, though not fully

represented by these idealized flow patterns, may match them so closely that they can be modeled as such with negligible error. Others can be modeled as combinations of tank- and tube type over various regions.

An idealized backmixed reactor is analyzed as follows. Consider a stirred vessel containing a known fluid volume, into which multiple streams may be flowing that contain reactants, enzymes (bio-catalysts), nutrients, reaction medium, and so on. When all these components are brought together in the vessel, under properly controlled conditions such as temperature, pressure, and concentrations of each component, the desired reactions occur. The vessel is well mixed to promote good contacting of all components and hence an efficient reaction scheme can be maintained. The well-mixed state is achieved when samples withdrawn from different locations, including the exit, at the same instance in time are indistinguishable. The system is termed “lumped” versus “distributed,” as in a plug flow system where location matters. The response characteristics of a backmixed reactor are significantly different from those of a plug flow reactor. How reaction time variations affect performance and how quickly each system responds to upsets in the process conditions are key factors. The backmixed system is far more sluggish than the plug flow system. To evaluate the role of reaction time variations, the concept of residence time and how it is determined must be discussed. A brief analysis of a batch reactor will be useful in understanding the basic principles involved.

In batch systems, there is no flow in or out. The feed (initial charge) is placed in the reactor at the start of the process and the products are withdrawn all at once at some later time. Spatial uniformity of composition is assumed since vigorous mixing is typically applied. If accomplished (ideally), then the time for reaction is readily determined. This is significant since the conversion of reactants to products is a function of time, and can be obtained from knowledge of the reaction rate and its dependence upon composition and process variables. Since these other factors are typically controlled at a constant value, the time for reaction is the key parameter in the reactor design process. In a batch reactor the concentration of reactants is time dependent and, therefore, the rate of reaction as well. Conversion is now related to reaction time through the use of calculus. For this system, residence time, equal to the processing time, is the time for reaction.

In a backmixed reactor, the conversion of reactants is controlled by the average length of time fluid elements remain in the reactor (their residence time). The ratio of the volume of fluid in the tank to the volumetric flow rate of the exit stream determines the residence time. Recall that in an ideal system of this type, operating at steady state, concentrations in the vessel are uniform and equal to those in the exit stream and thus the reaction rate is maintained at a constant value. Conversion of individual reactants and yield of specific products can be determined simply by multiplying the appropriate rate of interest by the residence time. With imperfect mixing, fluid elements have a distribution of residence times and the performance of the reactor is clearly altered.

The analysis of the plug flow reactor system is based on the premise that there is no mixing in the flow direction and thus no interaction between neighboring fluid elements as they traverse the length of the reactor. This idealization permits use of the results obtained from the analysis of the batch reactor system. Each fluid element in the tubular reactor functions as a small batch reactor, undisturbed by its neighboring elements, and its reaction time is well defined as the ratio of tube length to the volume averaged fluid velocity. The concentration varies along the length of the reactor (also, rate), and can be simply related to reaction time. The mathematical analysis and prediction of performance is similar to that for a batch reactor. This analysis shows that the plug flow configuration yields higher conversions than the backmixed vessel, given equal residence times and the same processing conditions. However, the plug flow reactor responds more quickly to system upsets and is more difficult to control.

Most actual reactors deviate from these idealized systems primarily because of nonuniform velocity profiles, channeling and bypassing of fluids, and the presence of stagnant regions caused by reactor shape and internal components such as baffles, heat-transfer coils, and measurement probes. Disruptions to the flow path are common when dealing with heterogeneous systems, particularly when solids are present. To model these actual reactors, various regions are compartmentalized and

represented as combinations of plug flow and backmixed elements. For illustration, a brief discussion of recycle, packed bed, and fluidized-bed reactor systems follows.

Recycle reactors are basically plug flow reactors with a portion of the exit stream recycled to the inlet, which provides multiple passes through the reactor to increase conversion. It is particularly useful in bio-catalytic reactor designs, in which the use of a packed bed is desired because of physical problems associated with contacting and subsequent separation of the phases. The recycle reactor provides an excellent means to obtain backmixed behavior from a physically configured tubular reactor. Multiple reactors of various types, combined in series and/or parallel arrangements, can improve performance and meet other physical requirements. Contact patterns using multiple entries into a single reactor can emulate these situations. A system demonstrating this characteristic is a plug flow reactor with uniform side entry. If these entry points are distributed along the length with no front entry, the system will perform as a single backmixed system. The significance is that backmixed behavior is obtained without continual stirring or the use of recycle pumps. Furthermore, if these side entry points are limited to only a portion of the reactor length, then the system functions as backmixed reactors in series with plug flow reactors.

Special consideration needs to be given to heterogeneous reactors, in which interaction of the phases is required for the reactions to proceed. In these situations, the rate of reaction may not be the deciding factor in the reactor design. The rate of transport of reactants and/or products from one phase to another can limit the rate at which products are obtained. For example, if reactants cannot get to the surface of a solid catalyst faster than they would react at the surface, then the overall (observed) rate of the process is controlled by this mass transfer step. To improve the rate, the mass transfer must be increased. It would be useless to make changes that would affect only the surface reaction rate. Furthermore, if products do not leave the surface rapidly, they may block reaction sites and thus limit the overall rate. Efficient contacting patterns need to be utilized. Hence, fluidized-bed reactors (two-phase backmixed emulator), trickle-bed systems (three-phase packed-bed emulator), and slurry reactors (three-phase backmixed emulator) have evolved as important bioreactors. They are readily simulated, designed, scaled up, and modified to meet specific contacting demands in cell and tissue culture systems (Shuler and Kargi, 2001).

Flow reactors of all shapes, sizes, and uses are encountered in all phases of life. Examples of interest to bioengineers include: the pharmaceutical industry, to produce aspirin, penicillin, and other drugs; the biomass processing industry, to produce alcohol, enzymes and other specialty proteins, and value-added products; and the biotechnologically important tissue and cell culture systems. The type of reactor used depends on the specific application and on the scale desired. The choice is based on a number of factors. The primary ones are the reaction rate (or other rate-limiting process), the product distribution specifications, and the catalyst or other material characteristics, such as chemical and physical stability.

An interesting example of a reactor type useful for a transport rate process is one utilizing impinging jet technology. Here, process intensification concepts are exploited for the general area of microfluidics. The objective is to form nanoparticles via controlled crystallization. Intense mixing is obtained in the unstable super-saturated phase region for a solvent/antisolvent crystallization process, developing a "bottom-up" approach for size control (Panagiotou and Fisher, 2008; Panagiotou et al., 2009). Many pharmaceutical agents can be produced in this manner and/or when coupled with chemical reactions in both miscible and multiphase systems (Baldyga and Bourne, 1999; Brennen, 2005; Gradl and Peukert, 2009; Johnson and Prud'homme, 2003; Rabinow, 2004, 2005; Schwarzer and Peukert, 2004).

Selection of the appropriate reactor type when living systems are present requires more thorough discussions since, in these systems, the solid phase may change its dimensions as the reaction proceeds. Particles that increase in size, such as growing cell clusters, can fall out of the reaction zone and alter flow patterns within the vessel. This occurs when gravity overcomes fluid buoyancy and drag forces. In some instances, this biomass growth is the desired product; however, the substances produced by reactions catalyzed by the cellular enzymes are usually the desired products. By reproducing themselves, these cells provide more enzymes and thus productivity increases are possible. Note, however,

that there are both advantages and disadvantages to using these whole cell systems versus the enzymes directly. The cell membrane can be a resistance for transport; the consumption of reactant as a nutrient for cell processes reduces the efficiency of raw material usage; and special precautions must be taken to maintain a healthy environment and thus productivity (Freshney, 2000; Johnson et al., 2009; Lewis and Colton, 2004). The payoff, however, is that the enzymes within their natural environment are generally more active and safer from poisons or other factors that could reduce their effectiveness. Interesting examples are microbial fermentation processes, as discussed earlier. Backmixed flow reactors are used in these applications. They are best suited to maintain the cell line at a particular stage in its life cycle to obtain the desired results. The uniform and constant environment provided for the cells minimizes the adjustments that they need to make concerning nutrient changes, metabolic wastes, and so forth, such that production can proceed at a constant rate. The term “chemostat” is used when referring to backmixed reactors used in biotechnology applications. These are typically tank-type systems with mechanical agitation. All the reactor types discussed earlier, however, are applicable. Recall that mixed flow characteristics can be obtained in tubular reactors if recycle and/or side entry is employed. Thus, an air lift system using a vertical column with recycle and side entry ports is a popular design.

The design, analysis, and simulation of reactors thus become an integral part of the bioengineering profession. The study of chemical kinetics, particularly when coupled with complex physical phenomena, such as the transport of heat, mass, and momentum, is required to determine or predict reactor performance. It thus becomes imperative to uncouple and unmask the fundamental phenomenological events in reactors and to subsequently incorporate them in a concerted manner to meet the objectives of specific applications. This need further emphasizes the role played by the physical aspects of reactor behavior in the stability and controllability of the entire process. The following chapters in this section demonstrate the importance of all the concepts presented in this introduction.

References

- Baldyga, J. and Bourne, J.R. 1999. *Turbulent Mixing and Chemical Reactions*, John Wiley and Sons, Ltd, Chichester, England.
- Bird, R.B., Stewart, W.E., and Lightfoot, E.N. 2002. *Transport Phenomena*, 2nd Edition, John Wiley and Sons, New York.
- Brennen, C.E. 2005. *Fundamentals of Multiphase Flow*, Cambridge University Press, New York.
- Crank, J. 1956. *The Mathematics of Diffusion*, Oxford University Press, Oxford.
- Deen, W.M. 1996. *Analysis of Transport Phenomena*, Oxford Press, New York.
- Enderle, J., Blanchard, S., and Bronzino, J.D., Eds. 1999. *Introduction to Biomedical Engineering*, Academic Press, New York.
- Fisher, R.J. 1989. Diffusion with immobilization in membranes: Part II, in *Biological and Synthetic Membranes*, Butterfield, A., Ed., Alan R. Liss, Inc., New York, 138–151.
- Fisher, R.J. 1999. *Compartmental Analysis*, in *Introduction to Biomedical Engineering*, Academic Press, New York, Chap. 8.
- Fournier, R.L. 1999. *Basic Transport Phenomena in Biomedical Engineering*, Taylor & Francis, Philadelphia.
- Freshney, R.I. 2000. *Culture of Animal Cells*, 4th Edition, Wiley-Liss, New York.
- Gratl, J. and Peukert, W. 2009. Simultaneous 3-D observation of different kinetic sub-processes for precipitation in a T-mixer, *Chem. Eng. Sci.*, 64, 709–720.
- Johnson, A.E., Fisher, R.J., Weir, G.C. and Colton, C.K. 2009. Oxygen consumption and diffusion in assemblages of respiring spheres: Performance enhancement of a bioartificial pancreas, *Chem. Eng. Sci.*, 64(22), 4470–4487.
- Johnson, B. and Prud'homme, R. 2003. Chemical processing and micro-mixing in confined impinging jets, *AIChE J.*, 49(9), 2264–2282.
- Levenspiel, O. 1989. *The Chemical Reactor Omnibook*, Oregon State University Press, Corvallis, OR.

- Lewis, A.S. and Colton, C.K. 2004. Tissue engineering for insulin replacement in diabetes, in Ma, P.X. and Elisseeff, J., Eds., *Scaffolding in Tissue Engineering*, Marcel Dekker, New York.
- Lightfoot, E.N. 1974. *Transport Phenomena and Living Systems*, John Wiley and Sons, New York.
- Panagiotou, T. and Fisher, R.J. 2008. Form nanoparticles via controlled crystallization: A bottom-up approach, *Chem. Eng. Prog.*, 10(Oct.), 33–39.
- Panagiotou, T., Mesite, S. and Fisher, R. J. 2009. Production of norfloxacin nano-suspensions using microfluidics reaction technology (MRT) through solvent/anti solvent crystallization, *Ind. Eng. Chem. Res.*, 48(4), 1761–1771.
- Rabinow, B. 2004. Nanosuspensions in drug delivery, *Nat. Rev.-Drug Discov.*, 3, 785–796.
- Rabinow, B. 2005. Pharmacokinetics of drugs administered in nanosuspensions, *Discov. Med.*, 5(25), 74–79.
- Rosner, D.E. 1986. *Transport Processes in Chemically Reacting Flow Systems*, Butterworth Publishers, Boston, MA.
- Schwarzer, H.C. and Peukert, W. 2004. Tailoring particle size through nanoparticle precipitation, *Chem. Eng. Commun.*, 191, 580–608.
- Shuler, M.L. and Kargi F. 2001. *Bioprocess Engineering: Basic Concepts*, 2nd Edition, Prentice-Hall, Englewood Cliffs, NJ.

7

Biomimetic Systems: Concepts, Design, and Emulation

7.1	Concepts of Biomimicry.....	7-2
	Morphology and Properties Development • Molecular Engineering of Thin Films and Nanocapsules • Biotechnology, Bioreaction Engineering, and Systems Development	
7.2	Biomimicry and Tissue Engineering.....	7-4
	Integrated Systems • Blood-Brain Barrier • Vascular System • Implants	
7.3	Biomimetic Membranes for Ion Transport	7-8
	Active Transport Biomimetics • Mechanism for Facilitated Diffusion in Fixed Carrier Membranes • Jumping Mechanism in Immobilized Liquid Membranes	
7.4	Assessing Mass Transfer Resistances in Biomimetic Reactors	7-11
	Uncoupling Resistances • Use in Physiologically Based Pharmacokinetics Models and Cell Culture Analog Systems	
7.5	Electro-Enzymatic Membrane Reactors as Electron Transfer Chain Biomimetics.....	7-13
	Mimicry of <i>In Vivo</i> Coenzyme Regeneration Processes • Electro-Enzymatic Production of Lactate from Pyruvate	
	References.....	7-14

Robert J. Fisher
*SABRE Institute and
Massachusetts Institute
of Technology*

Humans have always been fascinated by the phenomenological events, both biological and physical in nature, that are revealed to us by our environment. Our innate curiosity drives us to study these observations and understand the fundamental basis of the mechanisms involved. Practical outcomes are the development of predictive capabilities of occurrence and the control of these events and their subsequent consequences; our safety and comfort being major incentives. Furthermore, we wish to design processes that mimic the beneficial aspects associated with their natural counterparts. Experience has taught us that these natural processes are complex and durable and that adaptability with multifunctionality is a must for biological systems to survive. Evolution, aiding these living systems to adapt to new environmental challenges, occurs at the molecular scale. Our need to be molecular scientists and engineers is thus apparent. Knowledge of the molecular building blocks used in the architectural configurations of both living and nonliving systems, along with an understanding of their design and the processes used for implementation, is essential for control and utilization. The ability to mimic demonstrates a sufficient knowledge base to design systems requiring controlled functionality. To perfect this approach, a series of sensor/reporter systems must be available. A particularly attractive feature of living systems is their unique ability to diagnose and repair localized damages through a continuously distributed sensor

network with inter- and intracellular communication capabilities. Mimicry of these networks is an integral component of many emerging research thrust areas, in particular, tissue engineering. Significant emphasis has been toward the development of intelligent membranes, specifically using sensor/reporter technology. A successful approach has been to couple transformation and separation technologies with detection and control systems.

The concept of intelligent barriers and substrates, such as membranes, arises from the coupling of this sensor/reporter technology with controlled chemistry and reaction engineering, selective transport phenomena, and innovative systems design. Engineered membrane mimetics are required to respond and adapt to environmental stresses, whether intentionally imposed or stochastic in nature. These intelligent membranes may take the form of polymeric films, composite materials, ceramics, supported liquid membranes, or as laminates. Their important feature is specific chemical functionality, engineered to provide selective transport, structural integrity, controlled stability and release, and sensor/reporter capabilities. Applications as active transport and electron transfer chain mimics, and their use in studying the consequences of environmental stresses on enzymatic functions, create valuable insights into cellular mechanisms.

Advanced materials, designed through knowledge gained from analysis of biological systems, have been instrumental in the progression and success of many tissue engineering applications. Their biocompatibility, multifunctionality, and physiochemical properties are essential attributes. When incorporated with living cells, for example, in organ/tissue constructs, integrated systems biology behavioral mimicry can be accomplished. This is particularly useful for drug efficacy and toxicity screening tests and thus minimizing the use of animals for these studies. For example, having an effective blood-brain barrier (BBB) mimetic, a realistic blood substitute, and cell culture analogs (CCAs) for the various organs needed for a useful animal surrogate system promotes more rapid development of therapeutic drugs. These biomimetic studies influence all phases, that is, the design, development, and delivery characteristics, of this effort. The design, applicability, and performance of these systems are briefly discussed in subsequent sections in this chapter and in greater depth in other chapters throughout this handbook.

7.1 Concepts of Biomimicry

Discoveries that have emerged from a wide spectrum of disciplines, ranging from biotechnology and genetics to polymer and molecular engineering, are extending the design and manufacturing possibilities for mimetic systems that were once incomprehensible. Understanding of the fundamental concepts inherent in natural processes has led to a broad spectrum of new processes and materials modeled on these systems (Srinivasan et al., 1991). Natural processes, such as active transport systems functioning in living systems, have been successfully mimicked and useful applications in other fields, such as pollution prevention, have been demonstrated (Thoresen and Fisher, 1995). Understanding the mechanisms at the molecular level, which living systems utilize, is needed before success at the macroscale can be assured. Multifunctionality, hierarchical organization, adaptability, reliability, self-regulation, and reparability are the key elements that living systems rely upon and that we must mimic to develop “intelligent systems.” Successes to date have been based on the use of techniques associated with research advances made in areas such as molecular engineering of thin films and nanocapsules, neural networks, reporter/sensor technology, morphology and properties developments in polymer blends, transport phenomena in stationary and reacting flow systems, cell culture and immobilization technologies, controlled release and stability mechanisms for therapeutic agents, and environmental stress analyses. A few examples in the bioengineering field are molecular design of supported liquid membranes to mimic active transport of ions; noninvasive sensors to monitor *in vivo* glucose concentrations; detection of microbial contamination by bioluminescence; immunomagnetic capture of pathogens; improved encapsulation systems; carrier molecules for targeting, imaging, and controlled release of pharmaceuticals; *in situ* regeneration of coenzymes electrochemically; and measurement of transport and failure mechanisms in “smart”

composites. All these successes were accomplished through interdisciplinary approaches, essentially using three major impact themes: morphology and properties development; molecular engineering of thin films and nanocapsules; and biotechnology, bioreaction engineering, and systems development.

7.1.1 Morphology and Properties Development

Polymer blends are a major focus of this research area (Weiss et al., 1995). Technology, however, has outpaced a detailed understanding of many facets of this science, which impedes the development and application of new materials. The purpose of this research is to develop the fundamental science that influences the phase behavior, phase architecture, and morphology and interfacial properties of polymer blends. The main medical areas where polymers and composites (polymeric) have found wide use are artificial organs, the cardiovascular system, orthopedics, dental sciences, ophthalmology, and drug delivery systems. Success has been related to the wide range of mechanical properties, transformation processes (shape possibilities), and low production costs. The limitation has been their interaction with living tissue. To overcome the biological deficiencies of synthetic polymers and to enhance the mechanical characteristics, a class of bioartificial polymeric materials has been introduced based on blends, composites, and interpenetrating polymer networks of both synthetic and biological polymers. Preparations from biopolymers such as fibrin, collagen, and hyaluronic acid with synthetic polymers such as polyurethane, poly(acrylic acid), and poly(vinyl alcohol) are available (Giusti et al., 1993; Luo and Prestwich, 2001).

7.1.2 Molecular Engineering of Thin Films and Nanocapsules

The focus in the thin-film research impact area is to develop a fundamental understanding of how morphology can be controlled in (1) organic thin-film composites prepared by Langmuir–Blodgett (LB) monolayer and multilayer techniques and (2) the molecular design of membrane systems using ionomers and selected supported liquids. Controlled structures of this nature will find immediate application in several aspects of smart materials development, particularly in microsensors.

The ability to form nanosized particles and/or emulsions that encapsulate active ingredients is an essential skill applicable to many facets of the engineering biosciences. Nanotechnologies have a major impact on drug delivery, molecular targeting, medical imaging, biosensor development, and in the cosmetic, personal care products, and nutraceuticals industries, to mention only a few. New techniques utilize high shear fields to obtain particle sizes in the range of 50–100 nm; about the size of the turbulent eddies developed. Stable emulsions can be formed with conventional mixing equipment where high shear elongation flow fields are generated near the tip of high-speed blades, but only in the range 500 nm and larger. High shear stresses can also be generated by forcing the components of the microemulsion to flow through a microporous material. The resultant solution contains average particle sizes as small as 50 nm. Units that incorporate jet impingement on a solid surface or with another jet also perform in this size range. Molecular self-assembly systems using novel biocompatible synthetic polymer compounds are also under development. These have been used successfully to encapsulate chemotherapeutic drugs and perfluorocarbons (PFC) (Kumar et al., 2005). The high oxygen solubility of PFCs makes them attractive as blood surrogates and also as additives in immuno-isolation tissue encapsulation systems to enhance gas transport (Johnson et al., 2009). Using nanoencapsulation techniques, these compounds can be dispersed throughout microencapsulating matrices and/or in tissue extracellular matrix (ECM) scaffold systems.

Surfaces, interfaces, and microstructures play an important role in many research frontiers. Exploration of structural property relationships at the atomic and molecular level, investigating elementary chemical and physical transformations occurring at phase boundaries, applying modern theoretical methods for predicting chemical dynamics at surfaces, and integration of this knowledge into models that can be used in process design and evaluation are within the realm of surface and

interfacial engineering. These concepts are also important in drug design and delivery. Both crystal size and its morphology impact type and rate of uptake, its partitioning characteristics, and efficacy. Through proper selection of processing conditions, the method used to obtain the supersaturation state and its magnitude, and use of surface active agents, one can control product properties. A particular polymorph can be formed by controlling/directing the self-assembly mechanisms. Furthermore, stability with respect to both crystal size and morphology is possible (Rabinow, 2004, 2005; Schwarzer and Peukert, 2004; Panagiotou and Fisher, 2008; Panagiotou et al., 2009).

The control of surface functionality by proper selection of the composition of the LB films and/or the self-assembling (amphiphatic) molecular systems can mimic many functions of a biologically active membrane. An informative comparison is that between inverted erythrocyte ghosts (Dinno et al., 1991; Matthews et al., 1993) and their synthetic mimics when environmental stresses are imposed on both systems. These model systems can assist in mechanistic studies to understand the functional alterations that result from ultrasound, EM fields, and UV radiation. The behavior of carrier molecules and receptor site functionality must be mimicked properly along with simulating disturbances in the proton motive force (PMF) of viable cells. Use of ion/electron transport ionomers in membrane-catalyst preparations is beneficial for programs such as electro-enzymatic synthesis and metabolic pathway emulation (Fisher et al., 2000; Chen et al., 2004). Development of new membranes used in artificial organs and advances in micelle reaction systems have resulted from these efforts.

7.1.3 Biotechnology, Bioreaction Engineering, and Systems Development

Focus for this research area is on: (1) sensor/receptor reporter systems and detection methods; (2) transport processes in biological and synthetic membranes; (3) biomedical and bioconversion process development; and (4) smart film/intelligent barrier systems. These topics require coupling with the previously discussed areas and the use of biochemical reaction engineering techniques. Included in all of these areas is the concept of metabolic engineering; the modification of the metabolism of organisms to produce useful products. Extensive research in bioconversion processes is currently being directed to producing important pharmaceuticals. Expanded efforts are also needed in the field of cell and tissue engineering, that is, the manipulation or reconstruction of cell and tissue function using molecular approaches (Johnson et al., 2009).

7.2 Biomimicry and Tissue Engineering

Before we can develop useful *ex vivo* and *in vitro* systems for the numerous applications in tissue engineering, we must have an appreciation of cellular function *in vivo*. Knowledge of the tissue microenvironment and communication with other organs is essential. The key questions that must therefore be addressed in the realm of tissue engineering are thus, how can tissue function be built, reconstructed, and/or modified? To answer these, we develop a standard approach based on the following axioms (Palsson, 2000): (1) in organogenesis and wound healing, proper cellular communications, with respect to each other's activities, are of paramount concern since a systematic and regulated response is required from all participating cells; (2) the function of fully formed organs is strongly dependent on the coordinated function of multiple cell types with tissue function based on multicellular aggregates; (3) the functionality of an individual cell is strongly affected by its microenvironment (within 100 μm of the cell, that is, the characteristic length scale); (4) this microenvironment is further characterized by (i) neighboring cells, that is, cell-cell contact and presence of molecular signals (soluble growth factors, signal transduction, trafficking, etc.), (ii) transport processes and physical interactions with the ECM, and (iii) the local geometry, in particular its effects on microcirculation. The importance of the microcirculation is that it connects all microenvironments to the whole-body environment. Most metabolically active cells in the body are located within a few hundred micrometers from a capillary.

This high degree of vascularization is necessary to provide the perfusion environment that connects every cell to a source and sink for respiratory gases, a source of nutrients from the small intestine, the hormones from the pancreas, liver, and glandular system, clearance of waste products via the kidneys and liver, delivery of immune system respondents, and so forth. The engineering of these functions *ex vivo* is the domain of bioreactor design, a topic discussed briefly in the introductory comments to this book and also in Chapters 10 and 13. These cell culture devices must appropriately simulate and provide these macroenvironmental functions while respecting the need for the formation of microenvironments. Consequently, they must possess perfusion characteristics that allow for uniformity down to the 100 μm length scale. These are stringent design requirements that must be addressed with a high priority to properly account for the role of neighboring cells, the ECM, cyto-/chemokine and hormone trafficking, geometry, the dynamics of respiration, and the transport of nutrients and metabolic by-products for each tissue system considered. These dynamic, chemical, and geometric variables must be duplicated as accurately as possible to achieve proper mimicry. Since this is a difficult task, a significant portion of Chapter 10 in this book is devoted to developing methods to describe the microenvironment. Using the tools discussed there we can develop systems to control microenvironments for *in vivo*, *ex vivo*, or *in vitro* applications.

The approach taken here to achieve the desired microenvironments is through use of novel membrane systems. They are designed to possess unique features for the specific application of interest and in many cases to exhibit stimulant/response characteristics. These so-called “intelligent” or “smart” membranes are the result of biomimicry, that is, having biomimetic features. Through functionalized membranes, typically in concerted assemblies, these systems respond to external stresses (chemical and/or physical in nature) to eliminate the threat either by altering stress characteristics or by modifying and/or protecting the cell/tissue microenvironment. An example is a microencapsulation motif for beta cell islet clusters to perform as a pancreas. This system uses multiple membrane materials, each with its unique characteristics and performance requirements, coupled with nanospheres dispersed throughout the matrix, which contain additional materials for enhanced transport and/or barrier properties and respond to specific stimuli (Galletti et al., 2000; Lewis and Colton, 2004; Peattie et al., 2004; Johnson et al., 2009).

The communication of every cell with its immediate environment and other tissues is a key requisite for successful tissue function. This need establishes important spatial-temporal characteristics and a significant signaling/information processing network (Lauffenburger and Linderman, 1993). Understanding this network and the information it contains is what the tissue engineer wishes to express and manage. For example, to stimulate the beginning of a specific cellular process appropriate signals to the nucleus are delivered at the cell membrane and transmitted through the cytoplasm by a variety of signal transduction mechanisms. Some signals are delivered by soluble growth factors that may originate from the circulating blood or from neighboring cells. The signal networking process is initiated after these molecules bind to selective receptors. The microenvironment is also characterized by cellular composition, the ECM, molecular dynamics (nutrients, metabolic waste products, and respiratory gases traffic in and out of the microenvironment in a highly dynamic manner), and local geometry (size scale of approximately 100 μm). Each of these can also provide the cell with important signals (dependent upon a characteristic time and length scale) to initiate specific cell functions for the tissue system to perform in a coordinated manner. If this arrangement is disrupted, cells that are unable to provide tissue function are obtained. Further discussions on this topic are presented in other chapters in this handbook devoted to cellular communications.

7.2.1 Integrated Systems

The interactions brought about by communications between tissue microenvironments and the whole-body system, via the vascular network, provide a basis for the systems biology approach taken to

understand the performance differences observed *in vivo* versus *in vitro*. The response of one tissue system to changes in another (due to signals generated, such as metabolic products or hormones) must be properly mimicked by coupling individual CCA systems through a series of microbioreactors if whole-body *in vivo* responses are to be meaningfully predicted. The need for microscale reactors is obvious when we consider the limited amount of tissue/cells available for these *in vitro* studies. This is particularly true when dealing with the pancreatic system where intact islets must be used (vs. individual beta cells) for induced insulin production by glucose stimulation (however, see Johnson et al. (2009) for a promising new approach). Their supply is extremely limited and maintaining viability and functionality is quite complex since the islet clusters *in vivo* are highly vascularized and this feature is difficult to maintain in preservation protocols or reproduce in mimetic systems. Therefore, the time scale for their usefulness is limited. Furthermore, one needs to minimize the amount of serum used (the communication fluid flowing through and between these biomimetic reactors), since in many cases, the serum obtained from actual patients must be used for proper mimicry. An animal surrogate system, primarily for drug toxicity studies, is currently being developed using this CCA concept (Shuler et al., 1996). A general CCA system is one of three topics selected to illustrate these system interaction concepts in subsequent subsections in this chapter and others in this handbook. Another is associated with the use of compartmental analysis in understanding the distribution and fate of molecular species, particularly pharmaceuticals, and the third is the need for facilitated transport across the BBB, due to its complexities, when these species are introduced into the whole body by systemic administration.

Compartmental analysis and modeling was first formalized in the context of isotropic tracer kinetics to determine distribution parameters for fluid-borne species in both living and inert systems, particularly useful for determining flow patterns in reactors and tissue uptake parameters (Fisher, 2000). Over time, it has evolved and grown as a formal body of theory (Michaels, 1988; Fisher, 2000). Models developed using compartmental analysis techniques are a class of dynamic, that is, differential equation, models derived from mass balance considerations. These compartmental models are widely used for quantitative analysis of the kinetics of “materials” in physiologic systems. These materials can be either exogenous, such as a drug or a tracer, or endogenous, such as a reactant (substrate) or a hormone. Kinetics include processes such as production, distribution, transport, utilization, and substrate–hormone control interactions.

7.2.2 Blood–Brain Barrier

Many drugs, particularly water-soluble or high-molecular-weight compounds, do not enter the brain following traditional systemic administration methods because their permeation rate through blood capillaries is very slow. This BBB severely limits the number of drugs that are candidates for treating brain disease. New strategies for increasing the permeability of brain capillaries to drugs are constantly being tested and are discussed elsewhere in other chapters of this handbook. A seemingly effective technique, of particular interest for this section is to utilize specific nutrient transport systems in brain capillaries to facilitate drug transport. For example, certain metabolic precursors are transported across endothelial cells by the neutral amino acid transport system and therefore, analog compounds could be used as both chaperones and targeting species. Also, direct delivery into the brain tissue by infusion, implantation of a drug-releasing matrix, and transplantation of drug-secreting cells are being considered. These approaches provide sustained drug delivery that can be confined to specific sites, localizing therapy to a given region. As they provide a localized and continuous source of active drug molecules, the total drug dosage can be less than with systemic administration. Polymeric implants, for controlled drug release, can also be designed to protect unreleased drug from degradation in the body and to permit localization of extremely high doses at precisely defined locations in the brain. Infusion systems require periodic refilling. This usually requires the drug to be stored in a liquid reservoir at body temperature and therefore many drugs are not suitable for this application since they are not stable under these conditions.

Coupling of these approaches, using nanosphere technologies to entrap the drug (sometimes modified for enhanced encapsulation stability) along with surface modifications of the spheres for specific targeting, has a higher probability of success to enhance transport into the brain. Proof-of-concept experiments can be conducted using a valid BBB model as an effective biomimetic. An *in vitro* coculture system comprised of porcine brain capillary endothelial cells (BCEC) with porcine astrocytes is widely accepted as a valid BBB model. Using standard cell culturing techniques, the astrocytes are seeded on the bottom of permeable membrane filters with BCEC seated on the top. This configuration permits communication between the two cell lines without disruption of the endothelial cell monolayer. The filters are suspended in a chamber of fluid such that an upper chamber is formed analogous to the lumen of a brain capillary blood vessel. BBB permeability is determined from the measurement of transendothelial electrical resistance (TEER), a standard technique that measures the cell layer's ability to resist the passage of a low electrical current. It essentially represents the passages of small ions and is the most sensitive measure of BBB integrity. The nanospheres can be used to encapsulate the radioactive-labeled drug and tested for their toxicity to the BBB using TEER and noting if loss of barrier properties are observed. Inulin (5200 Da) is used as a marker species to represent potential pharmaceutical drug candidates and when used without nanosphere encapsulation, provides a reasonable control. For example, its transport across the BBB is quite slow; less than 2% after 4 h of exposure. In proof-of-concept experiments, for the same time period and drug concentrations, more than 16% of the inulin within the nanospheres crossed the BBB (Kumar et al., 2005). Although mechanistic details are lacking, this greater than eightfold increase in rate represents a dramatic increase and supports the premise that nanosphere encapsulation can facilitate drug delivery across the BBB and further illustrates the usefulness of this BBB biomimetic system.

7.2.3 Vascular System

Nutrient supply and gas exchange can become limiting in high cell density situation, as in tissue emulsion *in vitro*, due to lack of an effective vasculature mimetic system to provide *in vivo* perfusion conditions. Many different system configurations/designs have been considered to overcome these deficiencies, such as cellulose and gel-foam sponge matrix materials, filter-well inserts, and mimetic membranes in novel bioreactor systems (Freshney, 2000). Of particular interest here is the use of synthetic polymer capillary fibers (hollow fibers) in perfusion chambers where they can support cell growth on their outer surfaces and are gas and nutrient permeable. Medium, saturated with 5% CO₂ in air, is pumped through the lumen of the capillary fibers (in a bundle configuration) and cells attached and growing on the outer surface of the fibers, fed by diffusion from the perfusate, can reach tissue-like cell densities. Different polymers and ultrafiltration properties provide molecular cut-offs at 10–100 kDa, regulating macromolecule diffusion. It is now possible for the cells to behave as they would *in vivo*. For example, in such cultures, choriocarcinoma cells release more human chorionic gonadotrophin than they would in conventional monolayer culture and colonic carcinoma cells produce elevated levels of carcinoembryonic antigen (Freshney, 2000). Unfortunately, sampling cells and determining cell density are difficult from these commercially available chambers. New configurations are presently being designed and tested to overcome these limitations and are discussed in Chapters 10 and 13 in this book.

7.2.4 Implants

The transport of mass to and within a tissue is determined primarily by convection and diffusion processes that occur throughout the whole-body system. The design of systems, for example, in cellular therapy, must consider methods to promote this integrated process and not just deal with the transport issues of the device itself. An encapsulated tissue system implant must develop an enhanced localized vasculature. This may be accomplished by (1) recruiting vessels from the preexisting network of the

host vasculature and/or (2) stimulating new vessel growth resulting from an angiogenic response of host vessels to the implant (Jain, 1994; Peattie et al., 2004). Therefore, when considering implantation of encapsulated tissue/cells, it would be prudent to design the implant to have this biomimetic characteristic; to elicit an angiogenic response from a component of and/or in the matrix itself. For example, it is known that hyaluronic hydrogels can be synthesized to be biodegradable and that these degradation products stimulate microvessel growth. Also, any biocompatible matrix could be loaded with cytokines that would diffuse out on their own and/or be released via degradation mechanisms from microcapsules dispersed throughout the ECM. A recent study (Peattie et al., 2004) demonstrated these facts and identified synergistic behaviors. In summary, cross-linked hyaluronic acid (HA) hydrogels were evaluated for their ability to elicit new microvessel growth *in vivo* when loaded with one of two cytokines, vascular endothelial growth factor (VEGF) or basic fibroblast growth factor (bFGF). HA film samples were surgically implanted in the ear pinnae of mice, and the samples retrieved 7 or 14 days postimplantation. Histologic analysis showed that all groups receiving an implant demonstrated significantly more microvessel density than control groups undergoing surgery but receiving no implant. Moreover, aqueous administration of either growth factor produced substantially more vessel growth than an HA implant with no cytokine. However, the most striking result obtained was a dramatic synergistic interaction between HA and VEGF. New vessel growth was quantified by a metric developed during that study; that is, a dimensionless neovascularization index (NI). This index is defined to represent the number of additional vessels present postimplant in a treatment group, minus the additional number due to the surgical procedure alone, normalized by the contralateral count. Presentation of VEGF in cross-linked HA generated vessel density of NI = 6.7 at day 14. This was more than twice the effect of the sum of HA alone (NI = 1.8) plus VEGF alone (NI = 1.3). This was twice the vessel density generated by coaddition of HA and bFGF (NI = 3.4). New therapeutic approaches for numerous pathologies could be notably enhanced by this localized, synergistic angiogenic response produced by the release of VEGF from cross-linked HA films.

7.3 Biomimetic Membranes for Ion Transport

Cells must take nutrients from their extracellular environment to grow and/or maintain metabolic activity. The selectivity and rate that these molecular species enter can be important in regulatory processes. The mechanisms involved depend upon the size of the molecules to be transported across the cell membrane. These biological membranes consist of a continuous double layer of molecules creating a hydrophobic interspace in which various membrane proteins are imbedded. Individual lipid molecules are able to diffuse rapidly within their own monolayer; however, they rarely “flip-flop” spontaneously between these two monolayers. These molecules are amphoteric and assemble spontaneously into bilayers when placed in water. Sealed compartments are thus formed, which reseal if torn.

The topic of membrane transport is discussed in detail in many texts (Alberts et al., 1989; Freshney, 2000). The following discussion is limited to membrane transport of small molecules, hence excluding macromolecules such as polypeptides, polysaccharides, and polynucleotides. The lipid bilayer is a highly impermeable barrier to most polar molecules and thus prevents the loss of the water-soluble contents of the cell interior. Consequently, cells have developed special means to transport these species across their membranes. Specialized transmembrane proteins accomplish this, each responsible for the transfer of a specific molecule or group of closely related molecules. The mechanism can be either energy independent, as in passive and facilitated diffusion, or energy dependent, as in active transport and group translocation.

In passive diffusion, molecules are transported with (or “down”) a concentration gradient that is thermodynamically favorable and can occur spontaneously. Facilitated diffusion utilizes a carrier molecule, imbedded in the membrane, that can combine specifically and reversibly with the molecule to be transported. This carrier protein undergoes conformational changes when the target molecule

binds and again when it releases that molecule on the transverse side of the membrane. This binding is dependent on favorable thermodynamics related to the concentration of free versus bound species. An equilibrium is established, as in a Langmuir isotherm, on both sides of the membrane. Thus, the rate of transport is proportional to concentration differences maintained on each side of the membrane and the direction of flow is down this gradient. Active transport is similar to facilitated transport in that a carrier protein is necessary; however, it occurs against (up) a concentration gradient, which is thermodynamically unfavorable and thus requires energy. Group translocation requires chemical modification of the substance during the process of transport. This conversion process traps the molecule on a specific side of the membrane due to its asymmetric nature and the essential irreversibility of the transformation. These complexities lead to difficulties in mimicry; thus, research in this area is slow in developing.

Several energy sources are possible for active transport, including electrostatic or pH gradients of the PMF, secondary gradients derived from the PMF by other active transport systems, and by the hydrolysis of ATP. The development of these ion gradients enables the cell to store potential energy in the form of these gradients.

It is essential to realize that simple synthetic lipid bilayers, that is, protein-free, can mimic only passive diffusion processes since they are impermeable to ions but freely permeable to water. Thermodynamically, virtually any molecule should diffuse across a protein-free, synthetic lipid bilayer down its concentration gradient. However, it is the rate of diffusion that is of concern, which is highly dependent upon the size of the molecule and its relative solubility in oil (i.e., the hydrophobic interior of the bilayer). Consequently, small nonpolar molecules such as O_2 readily diffuse. If small enough, uncharged polar molecules such as CO_2 , ethanol, and urea can diffuse rapidly, whereas glycerol is more difficult and glucose is essentially excluded. Water, because it has such a small volume and is uncharged, diffuses rapidly even though it is polar and relatively insoluble in the hydrophobic phase of the bilayer. Charged particles, on the other hand, no matter how small, such as Na^+ and K^+ , are essentially excluded. This is due to the charge and the high degree of hydration preventing them from entering the hydrocarbon phase. Quantitatively, water permeates the bilayer at a rate 10^3 faster than urea, 10^6 faster than glucose, and 10^9 faster than small ions such as K^+ . Thus, only nonpolar molecules and small uncharged polar molecules can cross the cellular lipid membrane directly by simple (passive) diffusion; others require specific membrane transport proteins, as either carriers or channels. Synthetic membranes can be designed for specific biomedical applications that can mimic the transport processes discussed earlier. Membrane selectivity and transport are enhanced with the aid of highly selective complexing agents, impregnated as either fixed site or mobile carriers. To use these membranes to their full potential, the mechanism of this diffusion needs to be thoroughly understood. The following subsections provide some insight for this behavior.

7.3.1 Active Transport Biomimetics

Extensive theoretical and experimental work has previously been reported for supported liquid membrane systems (SLMS) as effective mimics of active transport of ions (Cussler et al., 1989; Kalachev et al., 1992; Thoresen and Fisher, 1995; Stockton and Fisher, 1998). This was successfully demonstrated using di-(2-ethyl hexyl)-phosphoric acid as the mobile carrier dissolved in *n*-dodecane, supported in various inert hydrophobic microporous matrices (e.g., polypropylene), with copper and nickel ions as the transported species. The results showed that a pH differential between the aqueous feed and strip streams, separated by the SLMS, mimics the PMF required for the emulated active transport process that occurred. The model for transport in an SLMS is represented by a five-step resistance-in-series approach, as follows: (1) diffusion of the ion through a hydrodynamic boundary layer; (2) desolvation of the ion, where it expels the water molecules in its coordination sphere and enters the organic phase via ion exchange with the mobile carrier at the feed/membrane interface; (3) diffusion of the ion-carrier complex across the SLMS to the strip/membrane interface; (4) solvation of the ion as it enters

the aqueous strip solution via ion exchange; and (5) transport of the ion through the hydrodynamic boundary layer to the bulk stripping solution. A local Peclet number is used to characterize the hydrodynamics and the mass transfer occurring at each fluid/SLMS interface. The SLMS itself is modeled as a heterogeneous surface with mass transfer and reaction occurring only at active sites; in this case, the transverse pores. Long-term stability and toxicity problems limit their application (as configured above) in the biomedical arena. Use in combination with fixed-site carrier membranes as entrapping barriers has great potential and is an active research area. Some success has been obtained using (1) reticulated vitreous carbon as the support matrix and nafion, for the thin-film "active barrier" and (2) an ethylene-acrylic acid ionomer, utilizing the carboxylic acid groups as the fixed-site carriers. The most probable design for biomedical applications appears to be a laminate composite system that incorporates less toxic SLMSs and highly selective molecularly engineered thin-film entrapping membranes. Use of fixed-site carrier membranes in these innovative designs requires knowledge of transport characteristics. Cussler et al. (1989) have theoretically predicted a jumping mechanism for these systems. Kalachev et al. (1992) have shown that this mechanism can also occur in an SLMS at certain carrier concentrations. This mechanism allows for more efficient transport than common facilitated diffusion. Stability over time and a larger range of carrier concentrations where jumping occurs make fixed carrier membranes attractive for biomedical applications. A brief discussion of these jumping mechanisms follows.

7.3.2 Mechanism for Facilitated Diffusion in Fixed Carrier Membranes

A theory for the mechanism of diffusion through a membrane using a fixed carrier covalently bound to the solid matrix was developed previously (Cussler et al., 1989). The concept is that the solute molecule jumps from one carrier to the next in sequence. Facilitated diffusion can occur only if these "chained" carriers are reasonably close to each other and have some limited mobility. The advantages of using a chained carrier in a solid matrix versus a mobile carrier in a liquid membrane are that the stability is improved; there is no potential for solvent loss from the system, and the transport may actually be enhanced. Their theory is compared to that for the mobile carriers in the SLMS. For the fixed carrier (chained) system, the assumptions of fast reactions and that they take place only at the interface, are also used. The major difference is that the complex formed cannot diffuse across the membrane since the carrier is covalently bound to the polymer chain in the membrane. Although the complex does not diffuse in the classical random walk concept, it can "jiggle" around its equilibrium position. This movement can bring it into contact range with an uncomplexed carrier also "jiggling," and result in a reversible interaction typical to normal receptor/ligand surface motion. It is assumed that no uncomplexed solute can pass through the membrane; it would be immobilized and taken from the diffusion process. The transport process that is operable is best explained by viewing the chained carrier membrane as a lamella structure where each layer is of thickness L . Every carrier can move a distance X around its neutral position and is a length L away from its neighbors. Diffusion can occur only over the distance X . Therefore, there is a specific concentration where a solute flux is first detected, termed percolation threshold, occurring when $L = X$. This threshold concentration is estimated as $C = 1/(L^3 N_a)$, where C is the average concentration, L is the distance between carrier molecules, and N_a is Avogadro's number. In summary, the mechanism is that of intramolecular diffusion; each chained carrier having limited mobility within the membrane. A carrier at the fluid membrane interface reacts with the species to be transported and subsequently comes in contact with an uncomplexed carrier and reacts with it, repeating this transfer process across the entire width of the membrane.

7.3.3 Jumping Mechanism in Immobilized Liquid Membranes

Facilitated diffusion was studied in immobilized liquid membranes using a system composed of a micro-porous nitrocellulose film impregnated with tri-*n*-octylamine (TOA) in *n*-decane (Kalachev et al., 1992).

Experiments were monitored by measuring the conductivity of the feed and strip streams. The transport of ions (cobalt and iron) from an acidic feed (HCl) to a basic strip solution (NH₄OH) was accomplished. Their results suggest that there are three distinct transport regimes operable in the membrane. The first occurs at short times and exhibits very little ion transport. This initial time is termed the ion penetration time and is simply the transport time across the membrane. At long times, a rapid increase in indiscriminate transport is observed. At this critical time and beyond, there are stability problems; that is, loss of solvent from the pores leading to the degradation of the membrane and the formation of channels that compromise the ion selective nature of the system and its barrier properties.

Recall that their experiments were for a selective transport with (not against) the ion gradient. It is only in the intermediate time regime that actual facilitated transport occurs. In this second region, experiments were conducted using a cobalt feed solution for various times and carrier concentrations; all experiments showed a peak in flux. The velocity of the transported species can be obtained from these results and the penetration time versus carrier concentration is available. At the threshold carrier concentration, these researchers claim that the mechanism of transport is by jumping as proposed earlier for fixed-site carriers. The carrier molecules are now close enough to participate in a "bucket brigade" transport mechanism. The carrier molecules use local mobility, made possible by a low viscous solution of *n*-decane, to oscillate, passing the transported species from one to another. This motion results in faster transport than common facilitated transport, which relies on the random walk concept and occurs at lower TOA concentrations. It is in this low concentration region that the carrier molecules are too far apart to participate in the jumping scheme. At higher concentrations, well above the threshold value, the increased viscosity interferes with carrier mobility; the jumping is less direct or does not occur because of the increased bonding sites and hence removal of the species from the transport process.

7.4 Assessing Mass Transfer Resistances in Biomimetic Reactors

7.4.1 Uncoupling Resistances

Characterization of mass transfer limitations in biomimetic reactors is essential when designing and evaluating their performance. When used in CCA systems, the proper mimicry of the role of intrinsic kinetics and transport phenomena cannot be overemphasized. Lack of the desired similitude will negate the credibility of the phenomenological observations as pertaining to toxicity and/or pharmaceutical efficacy. The systems must be designed to allow manipulation, and thus control, of all interfacial events. The majority of material transfer studies for gaseous substrates are based on the assumption that the primary resistance is at the gas/liquid interface. Studies examining the use of hollow fiber membranes to enhance gas/liquid transport have been successfully conducted (Grasso et al., 1995). The liquid/cell interfacial resistance is thus uncoupled from that of the gas/liquid interface and they can now be examined separately to evaluate their potential impacts. A reduction in the mean velocity gradient, while maintaining a constant substrate flux into the liquid, resulted in a shift in the limiting resistance from the gas/liquid to the liquid/cell interface. This shift manifested itself as an increase in the Monod apparent half-saturation constant for the chemo-autotrophic methanogenic microbial system selected as a convenient analog. The result of these studies significantly influences the design and/or evaluation of reactors used in the biomedical engineering (BME) research area, especially for the animal surrogate or CCA systems. Although a reactor can be considered as well mixed based on spatial invariance in cell density, it was demonstrated that significant mass transfer resistance may remain at the liquid/cellular boundary layer.

There are three major points to be stressed. First, the liquid/cellular interface may contribute significantly to mass transfer limitations. Second, when mass transfer limitations exist, the intrinsic bio-kinetics parameters cannot be determined. In biochemical reactor design, intrinsic parameters are essential to adequately model the system performance. Furthermore, without an understanding of the

intrinsic biokinetics, one cannot accurately study transport mechanisms across biological membranes. The determination of passive or active transport across membranes is strongly affected by the extent of the liquid/cellular interfacial resistance.

7.4.2 Use in Physiologically Based Pharmacokinetics Models and Cell Culture Analog Systems

The potential toxicity of, and/or the action of, a pharmaceutical is tested primarily using animal studies. Since this technique can be problematic from both a scientific and ethical basis (Gura, 1997), alternatives have been sought. *In vitro* methods using isolated cells (Del Raso, 1993) are inexpensive, quick, and generally present no ethical issues. However, the use of isolated cell cultures does not fully represent the full range of biochemical activity as in the whole organism. Tissue slices and engineered tissues have also been studied but not without their inherent problems, such as the lack of interchange of metabolites among organs and the time-dependent exposure within the animal. An alternative to both *in vitro* and animal studies is the use of computer models based on physiologically based pharmacokinetics (PBPK) models (Connolly and Anderson, 1991). These models mimic the integrated, multicompartiment nature of animals and thus can predict the time-dependent changes in blood and tissue concentrations of the parent chemical and its metabolites. The obvious limitations lie in that a response is based on assumed mechanisms; therefore, secondary and “unexpected” effects are not included. Furthermore, parameter estimation is difficult. Consequently, the need for animal surrogates or CCA systems is created. The pioneering work of M.L. Shuler’s group at Cornell University (Sweeney et al., 1995; Shuler et al., 1996; Mufti and Shuler, 1998; also in Chapter 11 and the introductory comments of this book) and many others has led to the following approach.

These CCA systems are physical representations of the PBPK structure where cells or engineered tissues are used in organ compartments. The fluid medium that circulates between compartments acts as a “blood surrogate.” Small-scale bioreactors housing the appropriate cell types are the physical compartments that represent organs or tissues. This concept combines attributes of PBPK and *in vitro* systems. Furthermore, it is an integrated system that can mimic dose release kinetics, conversion into specific metabolites from each organ, and the interchange of these metabolites between compartments. Since the CCA system permits dose exposure scenarios that can replicate those of animal studies, it works in conjunction with a PBPK as a tool to evaluate and modify proposed mechanisms. Thus, bioreactor design and performance evaluation testing is crucial to the success of this animal surrogate concept. Efficient transfer of substrates, nutrients, stimulants, and so on from the gas phase across all interfaces may be critical for the efficacy of certain biotransformation processes and in improving blood compatibility of biosensors monitoring the compartments. Gas/liquid mass transfer theories are well established for microbial processes (Cussler, 1984). However, biotransformation processes also involve liquid/cellular interfacial transport. In these bioreactor systems, a gaseous species is transported across two interfaces. Each could be a rate-determining step and can mask intrinsic kinetics modeling studies associated with cellular growth and/or substrate conversion and product formation.

A methanogenic chemo-autotrophic process was selected for study because of its relative simplicity and strong dependence on gaseous nutrient transport, thus establishing a firm quantitative base case (Grasso et al., 1995). The primary objective was to compare the effect of fluid hydrodynamics on mass transfer across the liquid/cellular interface of planktonic cells and the subsequent impact upon growth kinetics. Standard experimental protocol to measure the gas/liquid resistance was employed (Cussler, 1984; Grasso et al., 1995). The determination of the liquid/cellular resistance is more complex. The thickness of the boundary layer was calculated under various hydrodynamic conditions and combined with molecular diffusion and mass action kinetics to obtain the transfer resistance. Microbial growth kinetics associated with these hydrodynamic conditions can also be examined. Since Monod models are commonly applied to describe chemo-autotrophic growth kinetics (Ferry, 1993), the half-saturation

constant can be an indicator of mass transfer limitations. The measured (apparent) value will be greater than the intrinsic value, as demonstrated in these earlier studies and mentioned previously.

7.5 Electro-Enzymatic Membrane Reactors as Electron Transfer Chain Biomimetics

7.5.1 Mimicry of *In Vivo* Coenzyme Regeneration Processes

In many biosynthesis processes, a coenzyme is required in combination with the base enzymes to function as high efficiency catalysts. A regeneration system is needed to repeatedly recycle the coenzyme to reduce operating costs in continuous *in vitro* synthesis processes, mimicking the *in vivo* regenerative process involving an electron transfer chain system. Multiple reaction sequences are initiated, as in metabolic cycles. NAD(H) is one such coenzyme. Because of its high cost, much effort has focused on improving the NAD(H) regeneration process (Chenault and Whitesides, 1987), with electrochemical methods receiving increased attention. The direct regeneration on an electrode has proven to be extremely difficult (Paxinos et al., 1991). Either acceleration of protonation or inhibition of intermolecular coupling of NAD⁺ is required. Redox mediators have permitted the coupling of enzymatic and electrochemical reactions; the mediator accepts the electrons from the electrode and transfers them to the coenzyme via an enzymatic reaction, and thus regeneration/recycling of the coenzyme during a biosynthesis reaction can be accomplished (Hoogvliet et al., 1988). The immobilization of mediator and enzyme on electrodes can reduce the separation procedure, increase the selectivity, and stabilize the enzyme activity (Fry et al., 1994). Various viologen mediators and electrodes have been investigated for the NADH system in batch configurations (Kunugi et al., 1990). The mechanism and kinetics were investigated by cyclic voltammetry, rotating disk electrode, and impedance measurement techniques. The performance of electrochemical regeneration of NADH on an enzyme-immobilized electrode for the biosynthesis of lactate in a packed bed flow reactor (Fisher et al., 2000; Chen et al., 2004) is selected as a model system to illustrate an electron transfer chain biomimetic.

7.5.2 Electro-Enzymatic Production of Lactate from Pyruvate

The reaction scheme is composed of a three-reaction sequence: (1) the NADH-dependent enzymatic (lactate dehydrogenase: LDH) synthesis of lactate from pyruvate; (2) the regeneration of NADH from NAD⁺ and enzymatic (lipoamide dehydrogenase: LipDH) reaction with the mediator (methyl viologen); and (3) the electrochemical (electrode) reaction. The methyl viologen (MV²⁺) accepts electrons from the cathode and donates them to the NAD⁺ via the LipDH reaction. The regenerated NADH in solution is converted to NAD⁺ in the enzymatic (LDH) conversion of pyruvate to lactate. A key feature of this system is the *in situ* regeneration of the coenzyme NADH. A flow-by porous reactor utilizes the immobilized enzyme system (LipDH and methyl viologen as a mediator) within the porous graphite cathodes, encapsulated by a cation exchange membrane (Nafion, 124). The free-flowing fluid contains the pyruvate/lactate reaction mixture, the LDH, and the NADH/NAD⁺ system. Lactate yields up to 70% have been obtained when the reactor system was operated in a semibatch (i.e., recirculation) mode for 24 h, as compared to only 50% when operated in a simple batch mode for 200 h. The multipass, dynamic input operating scheme permitted optimization studies to be conducted on system parameters. This includes concentrations of all components in the free solution (initial and dynamic input values could be readily adjusted through recycle conditioning), flow rates, and electrode composition and their transport characteristics. By varying the flow rates through this membrane reactor system, operating regimes can be identified that determine the controlling mechanism for process synthesis (i.e., mass transfer vs. kinetics limitations). Procedures for operational map development are thus established.

References

- Alberts, B., D. Bray, J. Lewis, M. Raff, K. Roberts, and J. D. Watson. 1989. *Molecular Biology of the Cell*, 2nd ed., Garland, New York.
- Chen, X., J.M. Fenton, R.J. Fisher, and R.A. Peattie. 2004. Evaluation of in-situ electro-enzymatic regeneration of co-enzyme NADH in packed bed membrane reactors: Biosynthesis of lactate, *J. El. Chem. Soc.*, 151(2):236–242.
- Chenault, H. K. and G. M. Whitesides. 1987. Regeneration of nicotinamide cofactors for use in organic synthesis, *Appl. Biochem. Biotechnol.* 14:147–197.
- Connolly, R.B. and M.E. Anderson. 1991. Biologically based pharmacodynamic models: Tool for toxicological research and risk assessment, *Annu. Rev. Pharmacol. Toxicol.*, 31:503.
- Cussler, E.L. 1984. *Diffusion: Mass Transfer in Fluid Systems*, Cambridge University Press, New York.
- Cussler, E., R. Aris, and A. Bhowm. 1989. On the limits of facilitated diffusion, *J. Membr. Sci.*, 43:149–164.
- Del Raso, N.J. 1993. *In vitro* methodologies for enhanced toxicity testing, *Toxicol. Lett.*, 68:91.
- Dinno, M.A., R.J. Fisher, J.C. Matthews, L.A. Crum, and W. Kennedy. 1991. Effects of ultrasound on membrane bound ATPase activity, *J. Acous. Soc. Am.* 90(4):2258–2262.
- Ferry, J.G. 1993. *Methanogenesis*, Chapman and Hall, New York.
- Fisher, R.J. 2000. Compartmental analysis, Chapter 8 in *Introduction to Biomedical Engineering*, (Editors) J. Enderle, S. Blanchard and J. Bronzino, Academic Press, Orlando, FL.
- Fisher, R.J., J.M. Fenton, and J. Iranmahboob 2000. Electro-enzymatic synthesis of lactate using electron transfer chain biomimetic membranes, *J. Membr. Sci.*, 177:17–24.
- Freshney, R.I. 2000. *Culture of Animal Cells*, 4th Edition, Wiley-Liss, New York.
- Fry, A.J., S.B. Sobolov, M.D. Leonida, and K.I. Vivodov. 1994. Immobilization of mediator and enzymes on electrodes for NADH regeneration, *Denki Kagaku*, 62:1260.
- Galletti, P.M., C.K. Colton, M. Jaffrin, and G. Reach 2000. Artificial pancreas, Chapter 134 in *Bio Medical Engineering Handbook*, 2nd Ed, (Editor) J. Bronzino, CRC Press, Boca Raton, FL.
- Giusti, P., L. Lazzeri, and L. Lelli. 1993. Bioartificial polymeric materials, *TRIP*, 1(9):21–25.
- Grasso, K., K. Strevett, and R. Fisher. 1995. Uncoupling mass transfer limitations of gaseous substrates in microbial systems, *Chem. Eng. J.*, 59:195–204.
- Gura, T. 1997. Systems for identifying new drugs are faulty, *Science*, 273:1041.
- Hoogvliet, J.C., L.C. Lievense, C. V. Kijk, and C. Veeger. 1988. Regeneration of co-enzymes in biosynthesis reactions, *Eur. J. Biochem.*, 174:273.
- Jain, R.K. 1994. *Transport Phenomena in Tumors, Advances in Chemical Engineering*, Vol. 19, pp. 129–194, Academic Press, Inc., San Diego.
- Johnson, A.E., R.J. Fisher, G.C. Weir, and C.K. Colton. 2009. Oxygen consumption and diffusion in assemblages of respiring spheres: Performance enhancement of a bioartificial pancreas, *Chem. Eng. Sci.*, 64(22):4470–4487.
- Kalachev, A.A., L.M. Kardivarenko, N.A. Plate, and V.V. Bargreev. 1992. Facilitated diffusion in immobilized liquid membranes: Experimental verification of the jumping mechanism and percolation threshold in membrane transport, *J. Membr. Sci.*, 75:1–5.
- Kumar, R., R. Tyagi, V.S. Parmar, A.C. Watterson, J. Kumar, J. Zhou, M. Hardiman, R. Fisher, and C.K. Colton. 2005. Perfluorinated amphiphilic polymers as nano probes for imaging and delivery of therapeutics for Cancer, *Polym Prepr.*, 45(2):230–233.
- Kunugi, S., K. Ikeda, T. Nakashima, and H. Yamada. 1990. Enzyme electrode based on gold-plated polyester cloth, *Poly Bull*, 24:247.
- Lauffenburger, D.A. and J.J. Linderman. 1993. *Receptors: Models for Binding, Trafficking, and Signaling*. Oxford University Press, New York.
- Lewis, A.S. and C.K. Colton. 2004. Tissue engineering for insulin replacement in diabetes, in *Scaffolding in Tissue Engineering*, (Editors) Ma, P.X. and Elisseeff, J., Marcel Dekker, New York.

- Luo, Y. and G.D. Prestwich. 2001. Hyaluronic acid-*N*-hydroxysuccinimide: A useful intermediate for bioconjugation, *Bioconjug. Chem.*, 12:1085–1088.
- Michaels, A.L. 1988. Membranes, membrane processes and their applications: Needs, unsolved problems, and challenges of the 1990s, *Desalination*, 77:5–34.
- Matthews, J.C., W.L. Harder, W.K. Richardson, R.J. Fisher, A.M. Al-Karmi, L.A. Crum, and M.A. Dinno. 1993. Inactivation of firefly luciferase and rat erythrocyte ATPase by ultrasound, *Membr. Biochem.*, 10:213–220.
- Mufti, N.A. and M.L. Shuler. 1998. Different *in vitro* systems affect CYP1A1 activity in response to 2,3,7,8-tetrachlorodibenzo-*p*-dioxin, *Toxicol. In Vitro*, 12:259.
- Palsson, B. 2000. Tissue engineering, Chapter 12 in *Introduction to Biomedical Engineering*, (Editors). J. Enderle, S. Blanchard, and J. Bronzino, Academic Press, Orlando, FL.
- Panagiotou, T. and R.J. Fisher. (2008 October). Form nanoparticles via controlled crystallization: A “bottom-up” approach, *Chem. Eng. Prog.*, 10:33–39.
- Panagiotou, T., S. Mesite, and R.J. Fisher. 2009. Production of norfloxacin nano-suspensions using Microfluidics Reaction Technology (MRT) through solvent/anti solvent crystallization, *Ind. Eng. Chem. Res.*, 48(4):1761–1771.
- Paxinos, A.S., H. Gunther, D.J.M. Schmedding, and H. Simon. 1991. Direct electron transfer from modified glassy carbon electrodes carrying covalently immobilised mediators to a dissolved viologen accepting pyridine nucleotide oxidoreductase and dihydrolipoamide dehydrogenase, *Bioelectro. Bioenerg.*, 25:425–436.
- Peattie, R.A., A.P. Nayate, M.A. Firpo, J. Shelby, R.J. Fisher, and G.D. Prestwich. 2004. Stimulation of *in vivo* angiogenesis by cytokine-loaded hyaluronic acid hydrogel implants, *Biomaterials*, 25:2789–2798.
- Rabinow, B. 2004. Nanosuspensions in drug delivery, *Nat Rev-Drug Discov.*, 3:785–796.
- Rabinow, B. 2005. Pharmacokinetics of drugs administered in nanosuspensions, *Discov Med.*, 5(25):74–79.
- Schwarzer, H.C. and W. Peukert. 2004. Tailoring particle size through nanoparticle precipitation, *Chem. Eng. Comm.*, 191:580–608.
- Shuler, M.L., A. Ghanem, D. Quick, M.C. Wang, and P. Miller. 1996. A self-regulating cell culture analog device to mimic animal and human toxicological responses, *Biotechnol. Bioeng.*, 52:45.
- Srinivasan, A.V., G.K. Haritos, and F.L. Hedberg. 1991. Biomimetics: Advancing man-made materials through guidance from nature, *Appl. Mechanics Reviews*, 44:463–482.
- Stockton, E. and R.J. Fisher. 1998. Designing biomimetic membranes for ion transport, *Proc. NEBC/IEEE Trans.*, 24(4):49–51.
- Sweeney, L.M., M.L. Shuler, J.G. Babish, and A. Ghanem. 1995. A cell culture analog of rodent physiology: Application to naphthalene toxicology, *Toxicol. In Vitro*, 9:307.
- Thoresen, K. and R.J. Fisher. 1995. Use of supported liquid membranes as biomimetics of active transport processes, *Biomimetics*, 3(1):31–66.
- Weiss, R.A., C. Beretta, S. Sasonga, and A. Garton. 1995. Applications for ionomers, *Appl. Polym. Sci.*, 41:491.

8

Transport/Reaction Processes in Biology and Medicine

8.1	Introduction	8-1
8.2	Macroscopic Approximations: Allometry.....	8-2
8.3	Orders of Magnitude and Characteristic Time Constants	8-3
8.4	Time Constant Ratios	8-5
	Classification of Blood Vessels • Simultaneous Diffusion and Chemical Reaction	
8.5	Systems of Multiple Time Constants.....	8-7
	Importance of Boundary Conditions • Pharmacokinetics and Related Processes • Hemodialysis • Gene Expression in Prokaryotes • Exercise and Type II Diabetes	
8.6	Pseudocontinuum Models	8-15
	Tissue Oxygenation • Pulmonary Structure and Function • Pulmonary Blood-Gas Matching	
8.7	More Complex Situations.....	8-17
	Stochastic Behavior of Genetic Regulation • Cellular Crowding • The Dual Nature of Oxygen • Self-Organization and Emergence	
	References.....	8-18

E.N. Lightfoot
University of Wisconsin

8.1 Introduction

Transport phenomena, and particularly mass transfer and chemical reaction, govern a great variety of physiological and pathological processes, and they supplement in a nontrivial way genetic factors in both organism development and species evolution. For humans and other mammals, of primary interest here, the body may in fact be viewed as a complex and hierarchical transport/reaction system supplying the needs of genes and protecting them from the external environment. This is suggested in [Figure 8.1](#) where four major organs are seen to interact directly with the external environment and, via an extremely complex series of mass transport processes, with other organs, all body cells, and ultimately their genes. These processes range from convective transport via blood and pulmonary gases to extremely complex forced diffusion mechanisms at the cellular and subcellular level.

Our purpose here is to suggest effective bases for modeling and manipulating selected subsystems of living bodies, and it must be recognized at the outset that a complete description is impossible. Just a glance at an atlas of the human anatomy will make this clear. The body will always be what Malcolm Gladwell [26] calls a mystery: a problem for which no complete solution exists. Our approach is to suggest approximations simple enough to be soluble, testable, and hopefully of some utility: what Gladwell calls

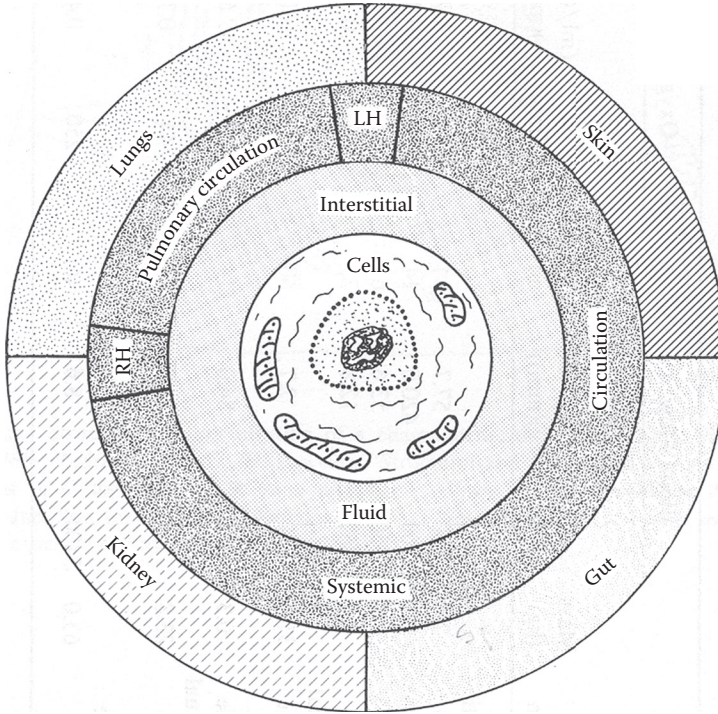


FIGURE 8.1 Mammalian topology.

puzzles. A major review of multiscale modeling in biological systems is provided by Bassingthwaight et al. [3], and we must settle for a much shorter discussion here. We start with macroscopically available parameters and proceed to more detailed descriptions.

8.2 Macroscopic Approximations: Allometry

We begin with observable relationships between macroscopic quantities, and express these by equations of the *allometric* form [14]:

$$P = aM^b$$

Here, “ P ” is some property to be predicted, “ M ” is a known property, and “ a ” and “ b ” are constants either already known or to be determined. Most commonly, M is the mass of the body or organ under consideration. The correlation of basal metabolic rates with body mass shown in Figure 8.2 is perhaps the most commonly available example, and it may be seen that even here data scatter is large. Under basal conditions, fat is the primary body fuel, and heat generation is about 4.7 kcal/mmol oxygen (STP). It is suggested that only recent correlations be used, for example, those of White and Seymour [62] or Roberts et al. [44]. Variants abound, and many are unreliable. Many mechanisms have been suggested as responsible for this correlation, but it should really be regarded as empirical. However, a few remarks are in order.

A primary reason that *basal metabolic rates* increase slower than linearly with body mass is that the proportion of highly active organs, for example, brain, liver, and kidney, falls with increase in total mass. Thus, total brain mass for most mammals increases more slowly than body mass [14,50, Table 3.4, p. 48]:

$$M_{\text{Brain}} = 0.011M^{0.76}$$

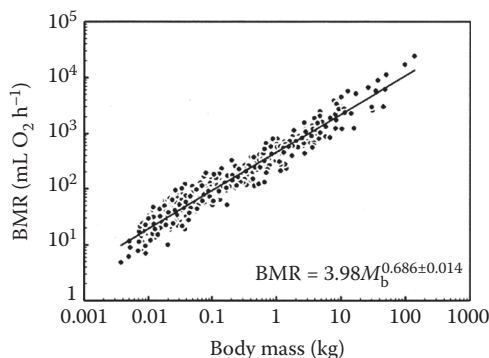


FIGURE 8.2 Basal metabolic rate.

TABLE 8.1 Brain Allometry

Species	Mammals	Monkeys	Great Apes	Humans
Coefficient (a)	0.01	0.02–0.03	0.03–0.04	0.08–0.09
Exponent (b)	0.7	0.66	0.66	0.66

Here, both masses are in kilograms. However, *overall* brain oxygen consumption per unit mass is invariant at about [39–41]

$$R_{O_2}(\text{brain}) = 3.72 \times 10^{-5} \text{ mmols O}_2/\text{mL}_s$$

The activity of liver and kidney, as well as their proportionate mass, do fall off with increasing size, but this is at least in part because more ducts and mechanical support are needed for larger animals.

However, primate brains are much bigger than those for other mammals, and ours are bigger yet (see Table 8.1 [49]).

It may be seen from comparing the table entry for mammals with the above equation that allometric correlations are far from exact. The real message of this table is that species differences can be very large, and that our major asset relative to other animals is mental. All species deviate from the mean in some respect, and this must be expected.

For most species maximum metabolic rate is about 10 times basal [33, p. 212]. However, some very athletic animals have much higher ratios of maximal to basal rates: pronghorn antelopes can achieve ratios of 65, and alligators can reach 40. A very informative discussion of diet, metabolic rates, and temperature control is provided in Chapter 14 of Reference 32.

It is also extremely important to determine in so far as possible the conditions under which the data presented have been determined and for which they will be used. A recently identified example of major uncertainty is that of gender differences between male and female rats and mice [56]. Planning and interpreting animal experiments are primary applications of allometry, but they must be used with care.

It is also clear that we must take a deeper look, and we begin immediately below.

8.3 Orders of Magnitude and Characteristic Time Constants

During almost all serious creative endeavors, the potential parameter space of interest is unmanageably large, and it is often desirable to limit initial consideration to *orders of magnitude* of probable relevance. Even the term “order of magnitude” is unfortunately heuristic, and success here depends in the last analysis on experience and judgment of the investigators. We try here to provide helpful examples based

TABLE 8.2 Commonly Used Diffusion Lengths

Shape	Parameter	Formula	Completion
Sphere	Radius R	$\ell^2 = R^2/6$	>0.99 complete
Cylinder	Radius R	$R^2/4$	>0.99
Slab	Half thickness L	$L^2/2$	>0.93

upon our own experience. Time constants prove to be of particular importance, and we use these as the primary basis for examples here.

We shall moreover consider just three types of time constants: mean residence times, t_m , diffusional times, $\ell^2/D_{im} = t_{dif}$, and reaction times, $c_i/R_i = t_{rxn}$. Here, “ t ” is time, “ ℓ ” is a characteristic length, “ D_{im} ” is a characteristic diffusivity of species “ i ” through mixture “ m ,” “ c_i ” is local molar concentration of species “ i ,” and R_i is the local molar rate of production of “ i ” by chemical reaction.

Mean residence time is only well defined for a volume V with impermeable surfaces except for one inlet and one outlet, with time-independent volumetric flow rate Q through it, and negligible diffusion across the inlet and outlet. Under these circumstances, mean residence time is given by [48,11, p. 756] (see Table 8.2)

$$t_m = V/Q$$

Characteristic length squared for the diffusional time constants are usually adapted to system shape.

Degrees of completion are calculated for uniform initial concentration and zero concentrations on the object boundary surface. Many other situations are described in such references as the venerable but still useful Reference 17.

As an example, we consider transients in the alveoli of the human lung: irregular sacs at the distal ends of the branching pulmonary system. To ensure a conservative estimate, we shall treat them as flat plates of half thickness 0.0105 cm, and we note that effective diffusivity of oxygen in pulmonary air is close to 0.2 cm²/s. The diffusional response time here is then

$$t_{dif} = (0.015\text{cm})^2/(0.2 \times 2\text{cm}^2/\text{s}) = 0.56\text{ms}$$

This is very short compared to the 1 s residence time of alveolar blood and the 1/12 of a minute between breaths. We may assume the alveolar gas to be well mixed.

It must be kept in mind that intracellular properties may differ substantially from those in saline solutions of the same ionic strength. This is in large part because cell interiors are crowded and contain membranes that limit mass transport. They also contain structures such as mitochondria that are impermeable to many diffusing metabolites. A few representative examples are supplied in Table 8.3.

TABLE 8.3 Intracellular Diffusion Coefficients

Compound	MW	Radius AA	Diffusivity (10 ⁻⁷ cm ² /s)		Ratio Water/Cell
			Water	Cells	
Sorbitol	182	2.5	94	50	1.9
Methylene blue	320	3.7	40	15	2.6
Sucrose	324	4.4	52	20	2.6
Eosin	648	6	40	8	5
Dextran	3600	12	18	3.5	5
Inulin	5500	13	15	3	5
Dextran	10,000	23.3	9.2	2.5	3.7
Dextran	24,000	35.5	6.3	1.5	4.2
Actin	43,000	23.2	5.3	0.03	167
Bovine serum albumin	68,000	36	6.9	0.1	65–71

Source: Adapted from Mastro, A. M. et al. 1984. PNAS, 81, 3414–3418.

Most of the systems of interest to us involve more than one time constant, and that is even true of our simple example of alveolar transients: these are really only of interest by way of comparison with blood circulation and breathing rates.

8.4 Time Constant Ratios

Many biological transport processes are primarily determined by ratios of time constants, and it is useful to look at them in this light. Moreover, examination of graphs in such texts as *Transport Phenomena* shows that the abscissas of a great many are themselves ratios of time constants, and recognizing this can often provide useful insight. Very often, for example, the behavior of both physiological and well-designed artificial systems tends to cluster about abscissa magnitudes of the order of unity. We now look at some specific examples.

8.4.1 Classification of Blood Vessels

We base our analysis on the canine data of Table 8.4 [16 and since reproduced in many newer sources, e.g., 25]. These are reasonably representative of their human counterpart except in lacking the larger arteries. The latter are of no interest to the present discussion as we are here concerned only in transport of respiratory gases and other small solutes between blood and surrounding tissue. Note that a Schmidt number of 1000 is used in this table. This is reasonable at the order-of-magnitude level of discussion.

We can extrapolate the information in this table by recognizing that most arteries end in binary branches, and to a surprisingly good approximation, they follow Murray's law:

$$R_2^3 = R_1^3/2$$

Here, R_2 is the radius of the two daughter arteries and R_1 that of the mother [52, p. 61], and it is shown by Fung [25, p. 118] that this tends to minimize the cost of blood flow: arteries serve primarily as transporters for blood and many other metabolites, and both construction and operation use a great deal of metabolic energy. Moreover, their diameters are continually controlled to maintain a desired wall shear stress ([25, p. 494] and [52, p. 67]). Veins parallel arteries and are larger in diameter. They provide storage as well as transport, and their diameters can be adjusted in responses to changes in blood volume.

We limit discussion to the interplay of flow and transverse mass transport, and we now estimate the utility of the various vessels to transmit dissolved substances to their walls by diffusion. We begin by looking at the last column in the table.

TABLE 8.4 Classification of Blood Vessels

Vessel	D (cm)	L	$\langle v \rangle$ Mean	L/D	Re Mean	Sc Assumed	L/D ReSc
Ascending aorta	1.5	5	20	3.333333	4500	1000	7.40741E-07
Descending aorta	1.3	20	20	15.38462	3400	1000	4.52489E-06
Adominal aorta	0.9	15	15	16.66667	1250	1000	1.33333E-05
Femoral artery	0.4	10	10	25	1000	1000	0.000025
Carotid artery	0.5	15		30		1000	
Arteriole	0.005	0.15	0.75	30	0.09	1000	0.33333333
Capillary	0.0006	0.06	0.07	100	0.001	1000	100
Venule	0.004	0.15	0.35	37.5	0.035	1000	1.071428571
Inferior vena cava	1	30	25	30	700	1000	4.28571E-05
Main pulmonary artery	1.7	3.5	70	2.058824	3000	1000	6.86275E-07

Source: Abstracted from Fung, Y. C. 1997. *Biomechanics: Circulation*, Springer, New York, Table 3.1:1, p.110.

$$\begin{aligned} L/D\text{ReSc} &= (L/D)(\mu/D \langle v \rangle \rho)(D_{\text{im}}\rho/\mu) \\ &= (L/\langle v \rangle)/(D^2/D_{\text{im}}) \end{aligned}$$

Here, $\langle v \rangle$ is the mean or flow average velocity [11, 2.3–20, p. 51]. Now

$$L/\langle v \rangle = t_m; \quad D^2/D_{\text{im}} = 16t_{\text{diff}}$$

We may thus write

$$t_m/t_{\text{diff}} = 16L/D\text{ReSc}$$

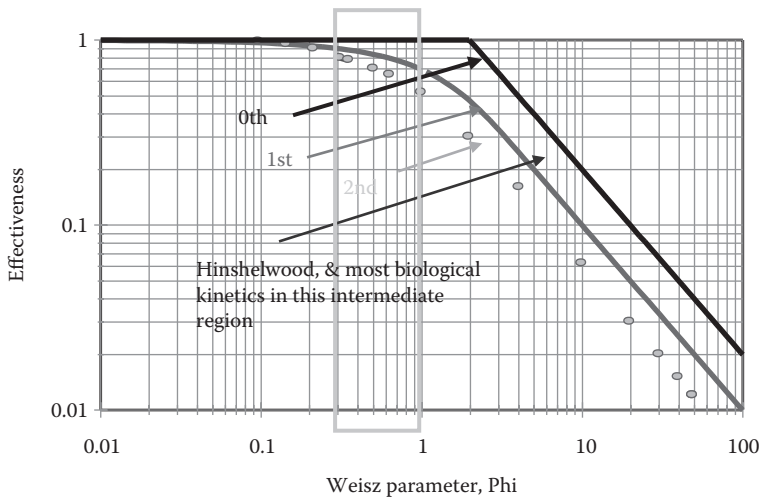
for small solutes such as gases.

It is now clear that only capillaries, and to a small degree arterioles and venules, are capable of transferring solutes between themselves and surrounding tissue. These three classes have long been known as the microcirculation because they are invisible to the naked eye. We now see a functional basis for this classification.

8.4.2 Simultaneous Diffusion and Chemical Reaction

We now base our discussion on a variant of the familiar effectiveness chart with an abscissa containing only observable quantities [59], Figure 8.3. Here, effectiveness factors are shown as a function of a Weisz modulus

$$\Phi = \frac{\langle R_i \rangle (V/S)^2}{c_i D_{\text{im}}}$$



$$\Phi = \frac{\langle R_i \rangle (V/S)^2}{c_{i0} D_{\text{im}}} \equiv \frac{T_{\text{dif}}}{T_{\text{rxn}}}$$

FIGURE 8.3 Effectiveness factors.

Downloaded by [JCR JCR] at 10:33 01 August 2015

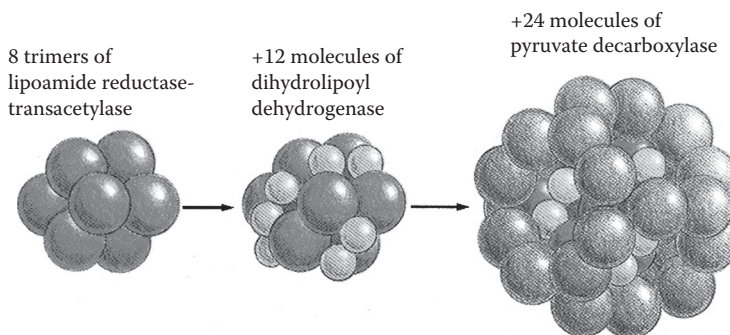


FIGURE 8.4 The pyruvate dehydrogenase complex.

for a porous catalyst in the form of a slab. Here, $\langle R \rangle$ is the observed rate of reaction of species “i” per unit volume, $\langle S/V \rangle$ is the observable specific surface of the catalyst (half thickness for a slab), c_i is the concentration of species “i” in the feed to the catalyst, and D_{im} is the effective diffusivity of species “i” through the catalyst matrix. Lines are shown for zeroth and first-order irreversible reaction and dots for second order. Michaelis–Menten and most biological kinetics are represented in the small region between zero and first order. To our present order of approximation, this graph is also valid for other shapes: $V/S = R/3$ for spheres; $R/2$ for cylinders.

It was shown by Weisz [59] that biological systems, and also well-designed industrial catalysts, tend to exhibit Weisz parameters between 1/3 and 1. However, as suggested in Figure 8.4 [1], biological systems tend to be much more complex. Putting catalysts for successive reactions adjacent to one another as in Figure 8.4 can make up for thermodynamically unfavorable intermediates, as suggested, for example, by Weisz [59], and nesting them decreases the chance for escape. The advantages of complex parallel reactions are discussed by Lane [32, p. 26] in connection with the Krebs cycle.

8.5 Systems of Multiple Time Constants

The mean residence time of solute in a flow system is of course only a partial description and corresponds to the first temporal moment [11, 23.6–3, p. 756] of exit tracer concentration for a pulse tracer input. It says nothing about the distribution of exit concentration as a function of time or the effect of the internal flow behavior. However, there are many circumstances where the shape is of no importance, and we begin by identifying some of these.

8.5.1 Importance of Boundary Conditions

We show an example of shape insensitivity by comparing the behavior of the two commonly used models shown in Figure 8.5: continuous stirred tank reactors, CSTRs, and plug flow reactors, PFRs. Here, the mean residence time of the test system is again defined as t_m .

The upper graph in this figure shows that the shapes of the exit tracer distributions for a pulse input are very different for these two systems. However, the responses to exponentially decaying input tracer concentrations

$$c_{in}(t) = c_0 e^{-t/t_0}$$

are much more interesting. Here, t_0 is the decay constant for the input stream. If

$$t_m = t_0$$

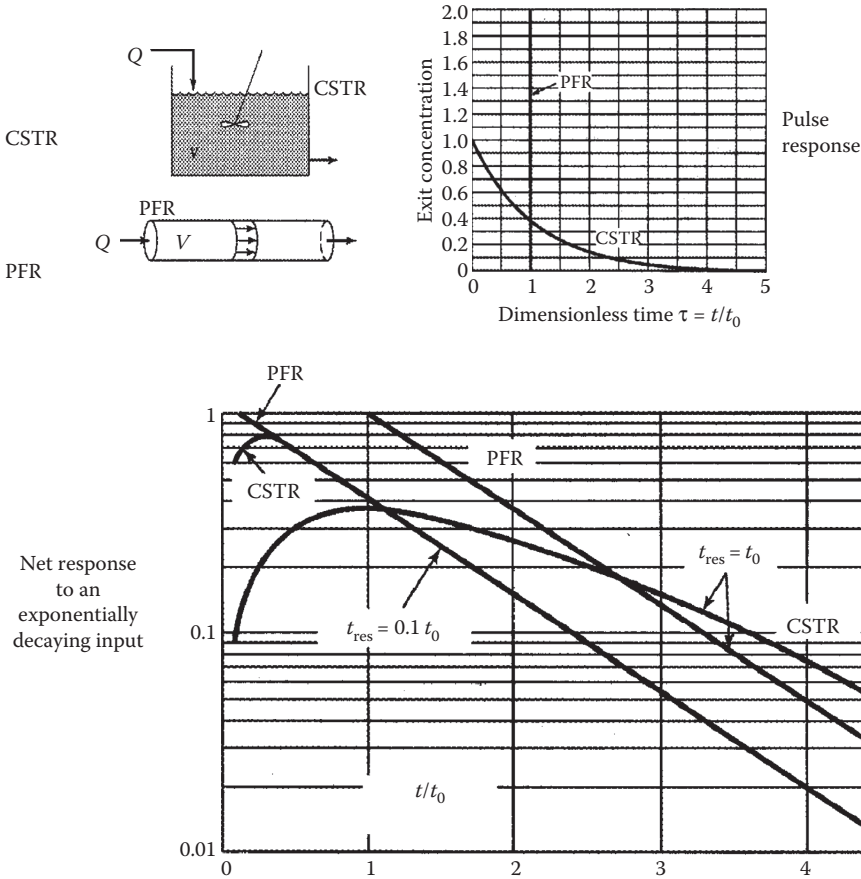


FIGURE 8.5 Universality.

the responses of the two flow systems are still quite different. However, if

$$t_m \ll t_0$$

the PFR and CSTR responses are indistinguishable, except at very short observer times. Moreover, they are simple decaying exponentials.

This simplification results from *time constant separation*, and it is characteristic of physiological, as opposed to pathological, systems. It is shown, for example, in glycolysis [30], Figure 8.6. There are 10 reactions shown here, and seven of them are so rapid that they may be considered instantaneous. System behavior is then controlled by three reactions, labeled HK, PFK, and PK, which are much slower.

8.5.2 Pharmacokinetics and Related Processes

The time scale separation characteristic of physiological systems is responsible for the success of many macroscopic descriptions and notably pharmacokinetics: that branch of pharmacology dealing with the absorption, distribution, metabolism, and elimination of drugs and toxins [43, 60 with others constantly appearing]. The body is now approximated by a network of mixing tanks as suggested in Figure 8.7. Here, each box shown is assumed to be in complete equilibrium, internally and with the venous blood leaving it. Models of this general type had long been used by anesthesiologists, the diving community,

Downloaded by [JCR JCR] at 10:33 01 August 2015

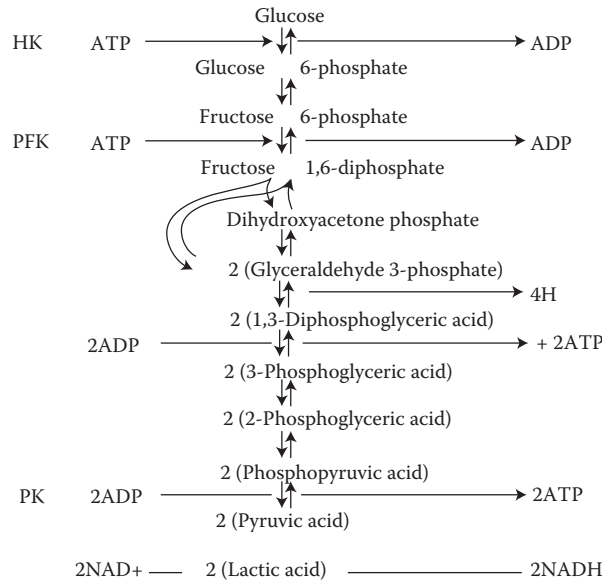


FIGURE 8.6 Glycolysis.

and others, but each box was completely empirical and characterized only by an assumed mean residence time t_m . The residence times were chosen empirically to fit observation.

A major step forward was made by two chemical engineers, the late Ken Bischoff [12] and Bob Dedrick [13], who identified the boxes as organs or groups of organs and predicted their mean residence times from actual physiological data. It was now possible to make *a priori* predictions and to

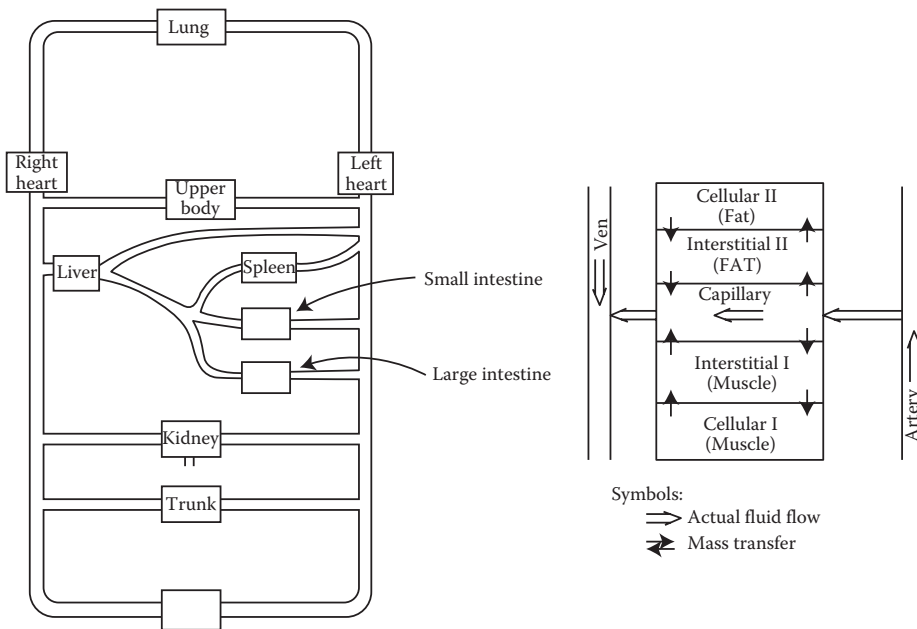


FIGURE 8.7 Pharmacokinetic approximations.

Downloaded by [JCR JCR] at 10:33 01 August 2015

explain the physiology upon which the resulting models were based. It was even possible to allow for concentration dependence of residence times and thus to describe the behavior of nonlinear systems with confidence.

Unfortunately, we shall have space here only for two simple examples, but the texts suggested above and others that may become available can extend this discussion enormously. An important related area is that of whole organ models [4]. See also References 29,55.

8.5.3 Hemodialysis

We first turn our attention to the amelioration of end-stage kidney disease by dialysis of blood against electrolyte solutions containing a healthy balance of metabolites [11, p. 733]. The nephrons that are to be supplemented and a sketch of a typical dialyzer are shown in Figure 8.8. The flat plate dialyzer shown is normally replaced by bundles of hollow fibers, and sometimes by the patient's peritoneal membrane. The dialyzing solution is normally prepared at the patient's side by dilution of a concentrate with carefully purified water, and accurate temperature control is needed for control as the dialysate composition is monitored by conductivity.

The system model is shown in Figure 8.9, and the conservation equations for the two compartments are

$$\begin{aligned} V_T dc_T/dt &= G - Q(c_T - c_B) \\ V_B dc_B/dt &= Q(c_T - c_B) - Clc_B \end{aligned}$$

Here, V_T is the total amount of tissue fluid, excluding that of the blood, V_B is that in the blood, c_T is the concentration of the metabolite of interest in the tissue, and c_B is that in the blood, G is the total rate of metabolite formation (assumed constant), and Cl is the "clearance of the dialyzer": the fraction of

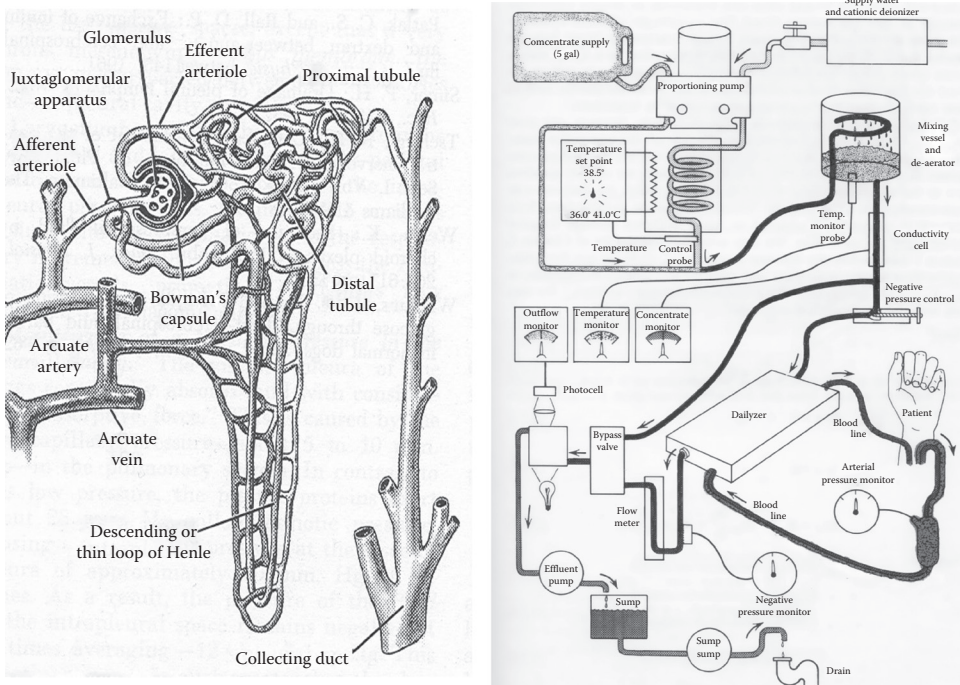


FIGURE 8.8 Hemodialysis.

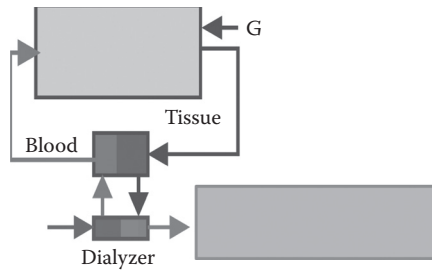


FIGURE 8.9 Dialysis model.

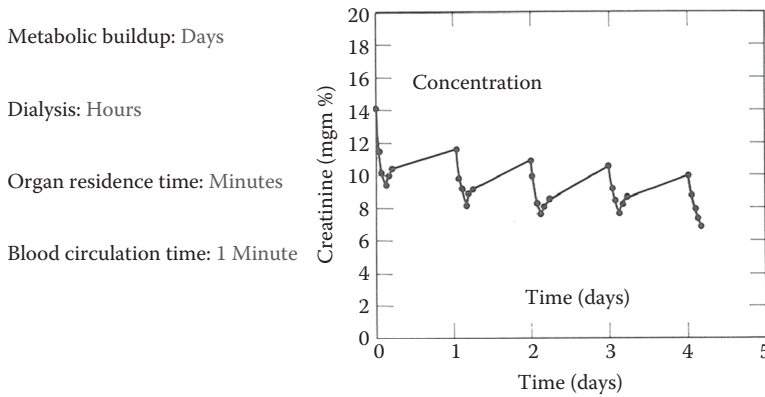


FIGURE 8.10 Test of creatinine modeling.

metabolite removed in one pass. Since the dialysate enters metabolite-free, clearance may be considered a property of the dialyzer and treated as a constant. Initially, the metabolite concentrations in blood and tissue may be considered equal.

Shown in Figure 8.10 are data for creatinine in a test dialyzer. The needed parameters are obtained to fit data for the first of the five dialyses shown. It may be seen from this and the four subsequent dialyses that the model fit is excellent. Clearly, the model is greatly simplified: neither the body tissue nor the blood is a simple mixing tank. Moreover, the rate of metabolite formation is far from constant. Rather the goodness of fit is due to excellent time constant separation: metabolite formation (day), dialysis (hour), organ residence time (minutes), and blood circulation (1 min).

Generally, time scales more than about a factor three or less than about one-third relative to that of primary interest can be assumed never to take place or to be instantaneous, respectively. Note that

$$e^3 = 20.1$$

These “rules of thumb” for order-of-magnitude analysis are clearly met in this example. However, it is always wise to check such assumptions to the extent possible and the creatinine data do this very nicely here.

8.5.4 Gene Expression in Prokaryotes

We next consider the dynamics of gene expression in bacterial cells as suggested in Figure 8.11. Here, a regulator, a protein molecule, must diffuse from an arbitrary initial position to activate a gene, that may

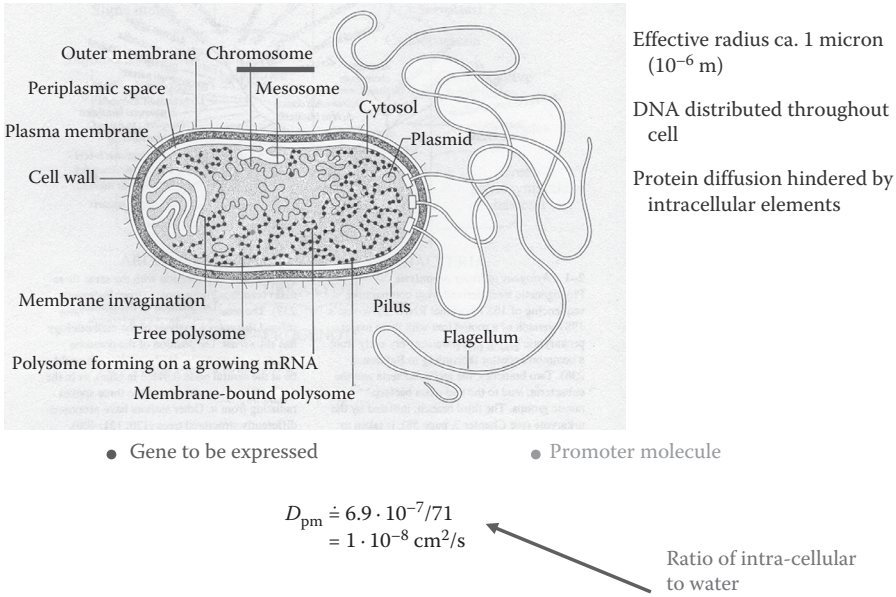


FIGURE 8.11 Gene expression in a bacterial cell.

also be anywhere in the cell [9,37]. We assume that this operation is a diffusion-controlled reaction that can be described by three sequential steps:

1. Sampling the entire region of the cell. For our present purposes, the regulator, the active portion of the gene, and the cell will all be treated as spherical. The radii of both the regulator and gene are taken as 2.5 nm and that of the cell as 1 micron. These simplifications are only reasonable at the order-of-magnitude level, but we shall find them to suffice. The time required for this process is of the order

$$T_{cell} \sim R_{cell}^2 / 6D_{PC}$$

Now, the diffusivity of the regulator through the cytoplasm will be far lower than in saline solution. We take it here to be that of serum albumin (see Table 8.3):

$$D_{PC} = 10^{-8} \text{ cm}^2/\text{s}; \quad T_{cell} \sim 10^{-8} \text{ cm}^2 / 6 \times 10^{-8} \text{ cm}^2\text{s}^{-1} = (s/6)$$

This is very fast.

- 2,3. Diffusion to the gene, now treated as a sphere of the combined radii of 5 nm, across a boundary layer. Here, we will use the expression for mass flux of the regulator protein reaching the gene from large surroundings across this surface (author):

$$N_p = \frac{D_{PC}C_{p\infty}}{(R_p + R_G)} \left[1 + 1/\sqrt{\pi\tau} \right]; \quad \tau = tD_{PC}/(R_p + R_G)^2$$

We first note that the transient term

$$1/\sqrt{\pi 10^{10} t/s}$$

Downloaded by [JCR JCR] at 10:33 01 August 2015

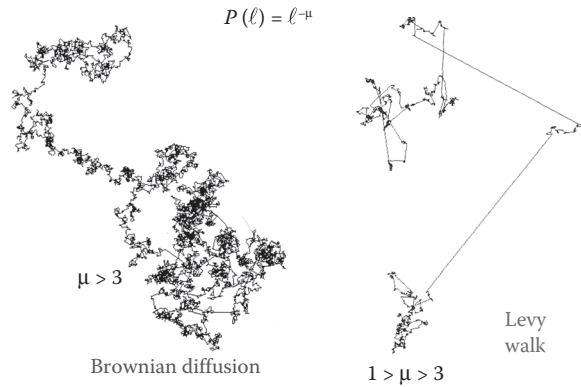


FIGURE 8.12 Dispersion models.

may be safely ignored. Now the probability P of finding the regulator still diffusing freely in the cytoplasm is given by a mass balance:

$$V_{\text{cell}} \frac{dc_p}{dt} = A_{\text{sph}} N_p; \quad d \ln cP/dt = 3D_{\text{PC}} [(R_p + R_G)/R_{\text{cell}}^3] = 1/T_{\text{rxn}}$$

Then

$$T_{\text{rxn}} = \left[\frac{1.5 \times 10^{-14}}{(10^{-4})^3} \right]^{-1} \text{ s} = 67 \text{ s}$$

This is by far the longest of the three characteristic times, and it governs the reaction. The above order-of-magnitude-based procedure is far simpler than the numerical approach used by the initial investigators [9], and it leads to the same result.

However, gene expression was found experimentally to be much faster than predicted. The authors suggested this speed resulted from weak adsorption of the regulator on all sections of the gene. As a result it could move in a one-dimensional dispersion along the gene on contact, then release itself, and sample other regions. This explanation seems to have been accepted and not examined further. We see then that dispersion in biological systems can be much more complicated than has been observed in more conventional situations.

One major example that has been substantiated is foraging, for example, for food supplies that are not uniformly distributed [53]. An example shown in Figure 8.12 contrasts Brownian dispersion with a Levy walk. It has been found that a great many species, from large animals to microscopic organisms, use something very close to a Levy walk [10,36,53] with a “mu” parameter close to the optimum magnitude of 2. Here, the probability P of a “jump” of length “ ℓ ” is shown as

$$P(\ell) = \ell^{-\mu}$$

Application of Levy walk theory in biology is still new, and medical applications are not yet known to this author. However, it would be surprising if it did not prove useful in studying epidemics and other dynamic disease situations.

8.5.5 Exercise and Type II Diabetes

Time constants can be useful even for nonlinear systems, but analysis here must be simplified. We use diabetes control by patients here as an important system, and one too complex for detailed modeling. A comparison of glucose removal from the blood stream between diabetic and nondiabetic (“normal”) patients is given in Figure 8.13.

We start by noting that blood glucose levels following meals for diabetics reach a plateau an hour or two after a meal and then decrease very slowly. This decrease can be greatly accelerated, and extended, by several minutes of moderate aerobic exercise as suggested in Figure 8.14 (data of author). Muscle contraction acts much like insulin in moving the glucose transporters, “GLUT4,” to the surface of muscle cells [36,38,46,47, and many newer]. A practical test of this effect is shown in Figure 8.15 (data of author). Here, 20–30 min brisk walks were taken about 2 h after breakfast in addition to normal doses

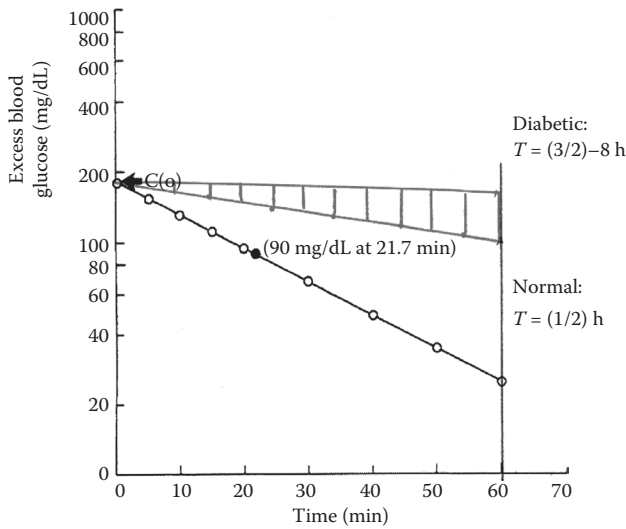


FIGURE 8.13 Glucose tolerance test.

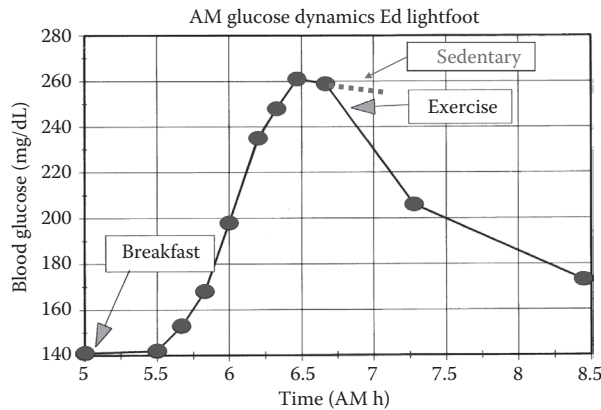


FIGURE 8.14 Glucose dynamics.

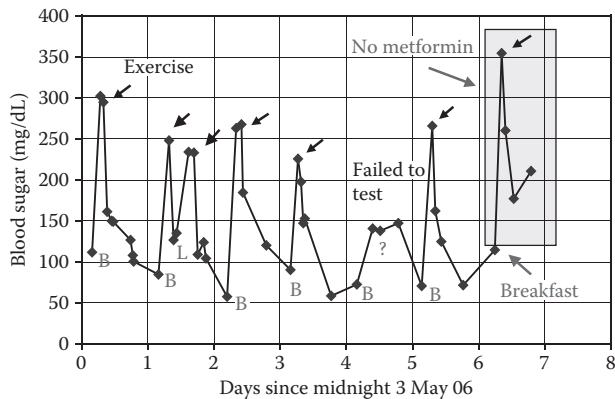


FIGURE 8.15 Effect of exercise versus metformin therapy.

of metformin: the primary means of control at that time. It is clear that the exercise was having a major effect for the entire day. Metformin was omitted on the last day, and it can be seen that the exercise had a substantially greater effect than the metformin.

8.6 Pseudocontinuum Models

Once we have been oriented at the order-of-magnitude level, it is time to develop the increasingly accurate descriptions needed to attack ever-more difficult problems. Over time, these descriptions become more complex and reliable, but they require more data and more sophisticated processing. The older and simpler models are, therefore, still useful. We suggest this by briefly reviewing the development of models for oxygenation of tissue. Development of biological systems can also follow rather simple mathematical rules that lessen the amount of information needed from the genes. We have already provided one example, the branching of arteries, and here we shall briefly discuss the fractal organization of the lungs. Finally, we briefly discuss the interaction of blood and gas flow in the lungs: a complex matching of two quite different systems that must work closely together.

8.6.1 Tissue Oxygenation

Our purpose here is to introduce and briefly describe oxygen transport and metabolism in parallel hexagonal cylinders of oxygen-demanding tissues surrounding individual capillaries. These are typical of such metabolically active systems as heart muscle or the gray matter of the brain, and modeling their behavior has received a great amount of attention [see 6–8,27]. We begin with the somewhat simplified model shown in Figure 8.16 [4, p. 35] where the hexagons have been simplified to circular cylinders as first suggested by August Krogh. One may then integrate the diffusion equations for blood and tissue. A wide variety of equations of state have been used for both blood and tissue, and it is perhaps most important to note that the metabolism of oxygen is very close to zero order. Moreover, the early simple models showed that axial dispersion and the models used for flow and diffusion within the capillaries are normally of secondary importance. This is borne out by more detailed calculations, and the profiles shown in Figure 8.16 are probably still reasonably representative of physiological operation and for general orientation [however, see 3].

They are not reliable for detailed studies however, and they fail to give a complete picture. They fail to show the interaction now known to occur between adjacent “cylinders,” they require a now unnecessary geometric simplification, and they use obsolete data for parameter estimates [18,19]. The problem of selecting a modeling strategy is discussed at length by Bassingthwaite et al. [3].

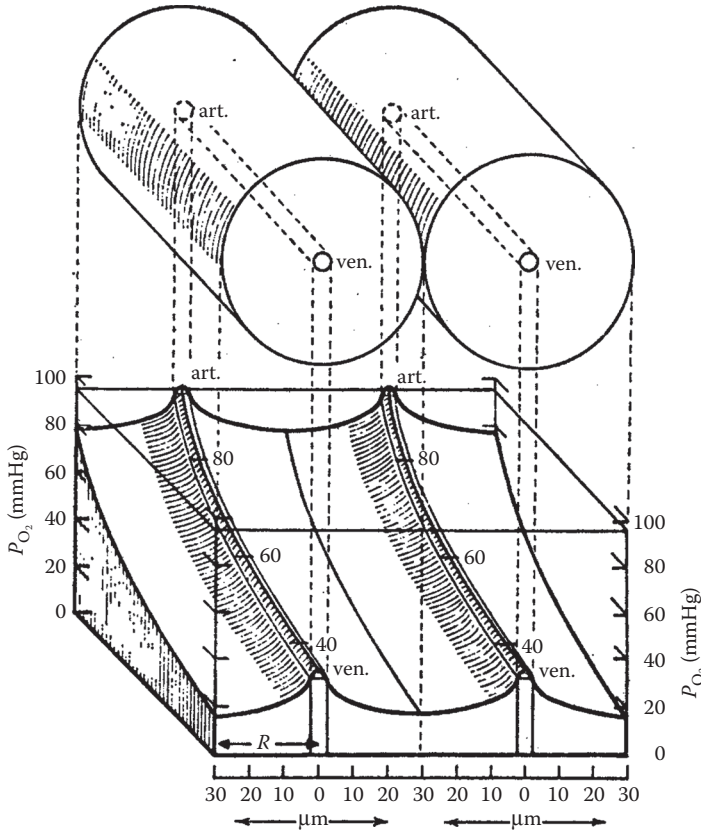


FIGURE 8.16 Tissue.

8.6.2 Pulmonary Structure and Function

We now turn to the pulmonary system sketched in [Figure 8.17](#), a combination of convective airways and the alveolar sacs where pulmonary gases are transferred to and from the blood. As with the pulmonary blood vessels, there is a sharp transition between diffusive (in the alveoli) and convective transport in the larger airways. However, to quote Bassingthwaight et al. [5, pp. 49–60], “the lung has two dominant features: irregularity and richness of structure.” They then go on to describe this structure in some detail. It was first suggested by Mandelbrot [34] that to a good first approximation the lung is a space-filling fractal.

The diameters of the first 11 branches fall off exponentially with branch number in both the right and left lungs [5], and the flow is complex and laminar. Axial dispersion [29] is appreciable here but less than that for parabolic flow, and it decreases steadily. It is negligible for subsequent branches. There is no appreciable diffusion across these large ducts, but deposition of aerosols is quite significant, and it is currently an active area of research (Google). Size distribution is complex in the smaller airways, but shows very little species dependence [5, p. 57].

Net transport in this dead-ended system is achieved by cyclic expansion and compression of the alveolar sacs, and only a small fraction of the pulmonary gases, primarily oxygen, carbon dioxide, and water, are exchanged in a single breath. This system is much less efficient than the lungs of birds [see 58,63] or the gills of fish, but it does provide a bit of stability. The major differences in oxygen transport in each of these three vertebrates reflect in large part their evolutionary history [58]. The mammalian airway system is very close to a space-filling fractal structure [34], a fact that decreases the genetic demands in development quite significantly [57].

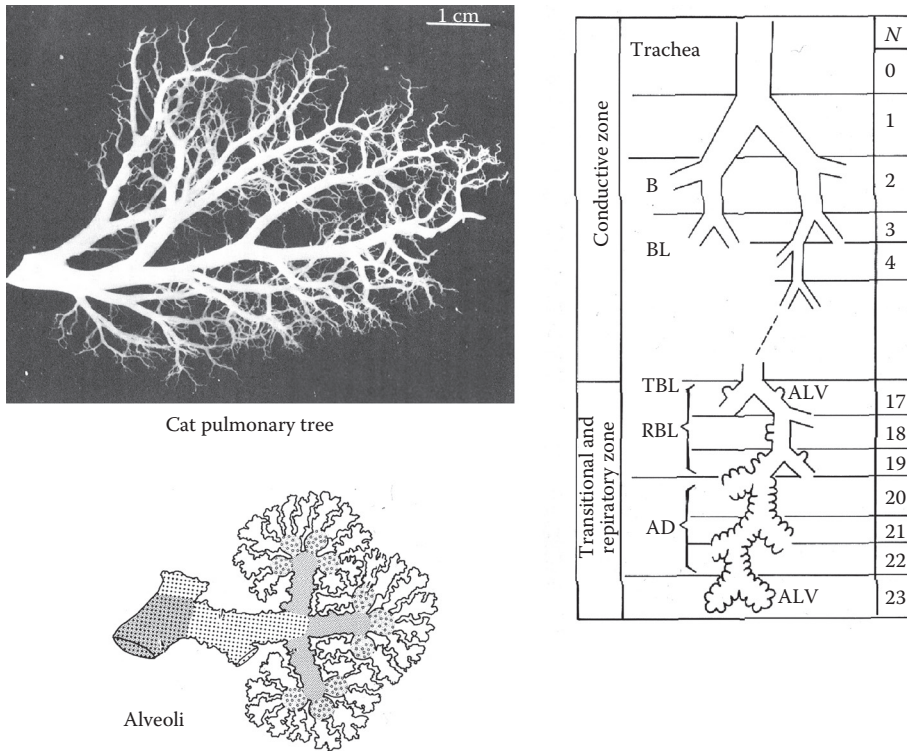


FIGURE 8.17 Pulmonary organization oxygenation.

8.6.3 Pulmonary Blood-Gas Matching

We end our series of specific examples by noting that even in healthy individuals there is a natural tendency for blood to concentrate in the lower regions of the lungs and air in the upper. Such maldistribution can cause serious problems. This is basically a problem in process control, but its diagnosis is achieved by measuring the response of the pulmonary system to a series of volatile tracers with different solubilities in blood [e.g., 45].

8.7 More Complex Situations

It is time now to bring this discussion to a close, and it may be noted that we have proceeded from very simple processes chosen to give some appreciation for the “design strategy” on which we are based and on to less detailed descriptions of more complex processes. We are far more complex than any man-made machines, but safety factors and other “design principles” are not so different from those used by engineers. It should not, therefore, come as a surprise to find that some awkward compromises also proved necessary. We introduce just a few of them here as a reminder: many of our common medical problems arise in self-organization at three levels: individual development, species evolution, and group interactions. Some of the simpler ones include the following.

8.7.1 Stochastic Behavior of Genetic Regulation

The erratic fluctuations of gene expression can produce abnormal reaction sequences, and these can even be taken advantage of by invading pathogens. Describing these situations requires sophisticated stochastic modeling [2,28,45,51].

8.7.2 Cellular Crowding

An important related area that we unfortunately do not have space for is that of whole-organ models [e.g., 61]. It has recently been found that identical genes in apparently identical cells can do very different things. In addition to the stochastic effect just introduced is an element of noisiness that can result from crowding [22,33,42,54]. Moreover, it appears that this problem becomes worse with age.

8.7.3 The Dual Nature of Oxygen

Although the aerobic metabolisms of vertebrates confer many advantages, the formation of peroxides and other highly active oxygen compounds are extremely dangerous [31,54, Chap. 8].

8.7.4 Self-Organization and Emergence

These topics become very important in dealing with invading organisms [10,15, 20–22,26].

Finally, we note that essentially all aspects of complexity theory find medical applications.

References

1. Alberts, B. M. et al. 2002. *The Molecular Biology of the Cell*, Garland, New York, NY.
2. Arkin, A., J. Ross, and H. H. McAdams. 1998. Stochastic kinetic analysis of developmental pathway bifurcation in λ -infected *Escherichia coli* cells, *Genetics*, 149, 1633–1648.
3. Bassingthwaighte, J. B., H. J. Chizeck, and L. E. Atlas. 2006. Strategies and tactics in multiscale modeling of cell-to-organ systems, *Proc IEEE*, 94, 819–831.
4. Bassingthwaighte, J. B., C. Goresky, and J. Linehan. 1998. *Whole Organ Approaches to Cellular Metabolism: Permeation, Cellular Uptake and Product Formation*, Springer, New York, NY.
5. Bassingthwaighte, J. B., L. S. Liebovitch, and B. J. West. 1994. *Fractal Physiology*, Medical and Technical Publishers, Oxford.
6. Beard, D. A. 2001. The computational framework for generating transport models from data bases of microvasculature anatomy, *Ann Biomed Eng*, 29, 837–843.
7. Beard, D. A. and J. B. Bassingthwaighte. 2001. Modeling advection and diffusion of oxygen in complex vascular networks, *Ann Biomed Eng*, 29, 298–310.
8. Beard, D. A. and F. Wu. 2009. Apparent diffusivity and Taylor dispersion of water and solutes in capillary beds, *Bull Math Biol*, 71, 1366–1377.
9. Berg, O. G., and P. H. Von Hippel. 1985. Diffusion controlled macromolecular interactions, *Ann Rev Biophys Biophys Chem*, 14, 131–160.
10. Bertrand, S., J. M. Burgos, F. Gerlotti, and J. Atiquipa. 2005. Levy trajectories of Peruvian purse-seiners as an indicator of the spatial distribution of anchovy (*Engraulis ringens*), *J Marine Sci*, 62, 477–482.
11. Bird, R. B., W. E. Stewart, and E. N. Lightfoot. 2007. *Transport Phenomena*, revised 2nd ed, Wiley, New York, NY.
12. Bischoff, K. B. 1967. Applications of a mathematical model for drug distribution in mammals. In: D. Hershey (ed.), *Chemical Engineering in Medicine and Biology*, Plenum, New York, NY.
13. Bischoff, K. B., and R. L. Dedrick. 1968. Thiopental pharmacokinetics, *J. Pharma. Sci.*, 57(8):1345–1351.
14. Calder, W. A. I. 1996. *Size, Function and Life History*, Dover, Mineola, NY.
15. Camazine, S., J.-L. Deneubourg, N. F. Franks, J. Sneyd, G. Theraulaz, and E. Bonabeau. 2003, 2nd printing. *Self-Organization in Biological Systems*, Princeton Studies in Complexity, Princeton, NJ.
16. Caro, C. G., T. J. Pedley, and S. A. Seed. 1974. Mechanics of the circulation. In: A. C. Guyton (ed.). *Cardiovascular Physiology*, Medical and Technical Publishers, Oxford, UK.

17. Carslaw, H. S., and J. C. Jaeger. 1959. *Conduction of Heat in Solids*, 2nd ed., Oxford University Press/Clarendon Press, Oxford, UK.
18. Dash, R. K., and J. B. Bassingthwaite. 2006. Simultaneous blood-tissue exchange of oxygen, carbon dioxide, bicarbonate, and hydrogen iron, *Ann Biomed Eng*, 34, 1129–1148.
19. Dash, R. K., and J. B. Bassingthwaite. 2010. Erratum to: Blood HbO₂, and HbCO₂ dissociation curves at varied O₂, CO₂, pH, 2,3DPG and temperature levels, *Ann Biomed Eng*, 38, 1683–1670.
20. Eigen, M. 1987. *Stufen zum Leben*, Piper, Munich.
21. Eigen, M. and R. Winkler-Oswatitsch. 1992. *Steps toward Life: A Perspective on Evolution*, Oxford University Press/Clarendon Press, Oxford, UK.
22. Ellis, R. J. 2001. Macromolecular crowding: Obvious but unappreciated. *Trends in Biomed Sci*, 26, 597–604.
23. El Samad, H., M. Khammash, L. Petsold, and D. Gillespie. 2005. Stochastic modelling of gene regulatory networks, *Int J Robust Non-Linear Contr*, 15, 691–711.
24. Feltz, B. 2006. *Self-Organization and Emergence in Life Sciences*, Springer, New York, NY.
25. Fung, Y. C. 1997. *Biomechanics: Circulation*, Springer, New York, NY.
26. Gladwell, M. 2007. Open secrets. *New Yorker* (January 8): 44.
27. Goldman, D. and A. S. Popel. 2001. A computational study of the effect of vasomotion on oxygen transport from capillary networks, *J Theor Biol*, 209, 189–199.
28. Hobbs, S. H. and E. N. Lightfoot. 1979. A Monte Carlo simulation of convective dispersion in the large airways, *Resp Physiol*, 37, 273–292.
29. Hoppensteadt, F. C. and C. H. Peskin. 2001. *Modeling and Simulation in Medicine and the Life Sciences*, 2nd ed, Springer, New York, NY.
30. Joshi, A. and B. O. Palsson. 1989. Metabolic dynamics in the human red cell. Part III. metabolic dynamics, *J Theor Biol*, 142, 41–68.
31. Lane, N. 2005. *Power, Sex and Suicide*, Oxford University Press/Clarendon Press, Oxford, UK.
32. Lane, N. 2009. *Life Ascending*, Norton/Symantec, Mountain View, CA.
33. Maamar, H., A. Raj, and D. Dubnau. 2007. Noise in gene expression determines cell fate in *Bacillus subtilis*, *Science*, 317(July), 526–529.
34. Mandelbrot, B. B. 1983. *The Fractal Geometry of Nature*, Freeman, Gordonsville, VA.
35. Mastro, A. M., M. Babich, W. D. Taylor, and A. D. Keith. 1984. Diffusion of a small molecule in the cytoplasm of mammalian cells, *PNAS*, 81, 3414–3418.
36. Neshet, I, I. E. Karl, and K. M. Kipnis. 1985. Dissociation of the effect(s) of insulin and contraction on glucose transport in rat epitochlearis muscle, *Am J Physiol*, 249, C226–232.
37. Pedraza, J. M. and J. Paulsson. 2008. Effects of molecular memory and bursting on gene expression. *Science*, 319(Jan), 339–343.
38. Pereira, L. O. and A. H. Lancha. 2004. Effect of insulin and contraction upon glucose transport in skeletal muscle, *Prog Biophys Mol Biol*, 84, 1–27.
39. Pearson, H. 2008. The cellular hullabaloo, *Nature*, 453, 150–153.
40. Popel, A. S. 1989. Theory of oxygen transport to tissue, *Crit Rev Biomed Eng*, 17, 257–321.
41. Purves, M. J. 1972. *Physiology of the Cerebral Circulation*, Cambridge University Press, Cambridge.
42. Raj, A. and A. van Oudenaarden. 2009. Single molecule approaches to stochastic gene expression, *Ann Rev Biophys*, 38, 255–270.
43. Ritschel, W. and G. L. Kearns. 2004. *Handbook of Basic Pharmacokinetics*, APhA, Washington, DC.
44. Roberts, M. S., E. N. Lightfoot, and W. P. Porter. 2010 May–June. A new model for the body size-metabolism relationship, 83(3):395–405.
45. Roca, J. and P. D. Wagner. 1993. Principles and information content of the multiple inert gas elimination technique, *Thorax*, 49, 815–824.
46. Rose, A. J. and E. A. Richter. 2005. Skeletal muscle glucose uptake during exercise, *Physiology*, 20, 260–270.

47. Ruzzin, J. and J. Jensen. 2005. Contraction activates glucose uptake and glycogen synthase in muscles from dexamethazone treated rats, *Am J Physiol*, 289, E241–E250.
48. Spalding, D. B. 1958. A note on mean residence times in steady flows of arbitrary complexity, *Chem Eng Sci*, 9, 74–77.
49. Stahl, W. R. 1965. Organ weights in primates and other mammals, *Science*, 50, 1038–1042.
50. Stiles, J. 2008. *The Fundamentals of Brain Development: Integrating Nature and Nurture*, Harvard, Cambridge, MA.
51. Thattai, M. and A. van Oudenaarden. 2001. Intrinsic noise in gene regulatory networks, *PNAS*, 98, 8614–8619.
52. Turner, J. S. 2007. *The Tinkerer's Accomplice*, Harvard, Cambridge, MA.
53. Viswanathan, G. M., S. Y. Buldyrev, S. Havlin, M. G. E. da Luz, E. P. Raposo, and H. E. Stanley. 1999. Optimizing the success of random searches, *Nature*, 401, 911–914.
54. Wagner, A. 2005. *Robustness and Evolvability in Living Systems*, Princeton University Press, Princeton, NJ.
55. Wagner, P. D. 2008. The multiple inert gas elimination technique, *Intensive Care Med*, 34, 994–1001.
56. Wald, C. and C. Wu. 2010. Of mice and women: The bias in animal models, *Science*, 327, 1571–1572.
57. Warburton, D. 2008. Order in the lung. *Nature*, 453, 733–734.
58. Ward, P. D. 2006. *Out of Thin Air*, Joseph Henry Press, Washington, DC.
59. Weisz, P. B. 1973. Diffusion and reaction: An interdisciplinary excursion, *Science*, 179, 4533–440.
60. Welling, P. 1997. *Pharmacokinetics*, American Chemical Society, Washington, DC.
61. West, J. B. 2008. *Respiratory Physiology*, Lippincott, Williams and Wilkins.
62. White, C. F., and R. S. Seymour. 2003. Mammalian basic metabolism rate is proportional to body mass $2/3$, *PNAS*, 100, 4046–4049.
63. Willmer, P. G. S. and I. Johnston. 2000. *Environmental Physiology of Animals*, Blackwell, Hoboken, NJ.

10

Fluid Dynamics for Bio Systems: Fundamentals and Model Analysis

Robert A. Peattie
Tufts University

Robert J. Fisher
*SABRE Institute and
Massachusetts Institute
of Technology*

10.1	Introduction	10-1
10.2	Elements of Theoretical Hydrodynamics.....	10-3
	Elements of Continuum Mechanics • Flow in Tubes	
10.3	Pulsatile Flow	10-9
	Hemodynamics in Rigid Tubes: Womersley's Theory • Hemodynamics in Elastic Tubes • Turbulence in Pulsatile Flow	
10.4	Models and Computational Techniques	10-14
	Approximations to the Navier-Stokes Equations • Computational Fluid Dynamics	
	References.....	10-16

10.1 Introduction

Biological processes within living systems are significantly influenced by the flow of liquids and gases. Biomedical engineers must therefore understand hydrodynamic phenomena [1] and the vital role they play in the biological processes that occur within the body [2]. In particular, engineers are concerned with perfusion effects in the cellular microenvironment, and the ability of the circulatory and respiratory systems to provide a whole-body communication network with dynamic response capabilities. Understanding the fundamental principles of fluid flow involved in these processes is also essential for describing transport of mass and heat throughout the body, as well as understanding how tissue function can be built, reconstructed, and/or modified for clinical applications.

From a geometric and flow standpoint, the body may be considered a network of highly specialized and interconnected organ systems. The key elements of this network for transport and communication are its pathway (the circulatory system) and its medium (blood). Of interest for engineering purposes are the ability of the circulatory system to transport oxygen and carbon dioxide, glucose, other nutrients and metabolites, and signal molecules to and from the tissues, as well as to provide an avenue for stress-response agents from the immune system, including cytokines, antibodies, leukocytes, and macrophages, and system repair agents such as stem cells and platelets. The bulk transport capability provided by convective flow helps to overcome the large diffusional resistance that would otherwise be offered by such a large entity as the human body. At rest, the mean blood circulation time is of the order of 1 min. Therefore, given that the total amount of blood circulating is about 76–80 mL/kg (5.3–5.6 L for a 70 kg “standard male”), the flow from the heart to this branching network is about 95 mL/s. This and other order of magnitude estimates for the human body are available elsewhere, for example, Refs. [2–4].

Although the fluids most often considered in biofluid mechanics studies are blood and air, other fluids such as urine, perspiration, tears, ocular aqueous and vitreous fluids, and the synovial fluid in the joints can also be important in evaluating tissue system behavioral responses to induced chemical and physical stresses. For purposes of analysis, these fluids are often assumed to exhibit Newtonian behavior, although the synovial fluid and blood under certain conditions can be non-Newtonian. Since blood is a suspension, it has interesting properties; it behaves as a Newtonian fluid for large shear rates, but is highly non-Newtonian for low shear rates. The synovial fluid exhibits viscoelastic characteristics that are particularly suited to its function of joint lubrication, for which elasticity is beneficial. These viscoelastic characteristics must be accounted for when considering tissue therapy for joint injuries.

Further complicating analysis is the fact that blood, air, and other physiologic fluids travel through three-dimensional passageways that are often highly branched and distensible. Within these pathways, disturbed or turbulent flow regimes may be mixed with stable, laminar regions. For example, blood flow is laminar in many parts of a healthy circulatory system in spite of the potential for peak Reynolds numbers (defined below) of the order of 10,000. However, “bursts” of turbulence are detected in the aorta during a fraction of each cardiac cycle. An occlusion or stenosis in the circulatory system, such as the stenosis of a heart valve, will promote such turbulence. Airflow in the lung is normally stable and laminar during inspiration, but less so during expiration, and heavy breathing, coughing, or an obstruction can result in fully turbulent flow, with Reynolds numbers of 50,000 a possibility.

Although elasticity of vessel walls can significantly complicate fluid flow analysis, biologically it provides important homeostatic benefits. For example, pulsatile blood flow induces accompanying expansions and contractions in healthy elastic-wall vessels. These wall displacements then influence the flow fields. Elastic behavior maintains the norm of laminar flow that minimizes wall stress, lowers flow resistance, and thus energy dissipation, and fosters maximum life of the vessel. In combination with pulsatile flow, distensibility permits strain relaxation of the wall tissue with each cardiac cycle, which minimizes the probability of vessel failure and promotes extended “on-line” use.

The term *perfusion* is used in engineering biosciences to identify the rate of blood supplied to a unit quantity of an organ or tissue. Clearly, perfusion of *in vitro* tissue systems is necessary to maintain cell viability along with functionality to mimic *in vivo* behavior. Furthermore, it is highly likely that cell viability and normoperative metabolism are dependent on the three-dimensional structure of the microvessels distributed through any tissue bed, which establishes an appropriate microenvironment through both biochemical and biophysical mechanisms. This includes transmitting both intracellular and long-range signals along the scaffolding of the extracellular matrix.

The primary objective of this chapter is to summarize the most important concepts of fluid dynamics, as hydrodynamic and hemodynamic principles have many important applications to physiology, pathophysiology, and tissue engineering. In fact, the interaction of fluids and supported tissue is of paramount importance to tissue development and viability, both *in vivo* and *in vitro*. The strength of adhesion and dynamics of detachment of mammalian cells from engineered biomaterials and scaffolds are important subjects of ongoing research [5], as are the effects of shear on receptor–ligand binding at the cell–fluid interface. Flow-induced stress has numerous critical consequences for cells, altering transport across the cell membrane, receptor density and distribution, binding affinity and signal generation with subsequent trafficking within the cell [6]. In addition, design and use of perfusion systems such as membrane biomimetic reactors and hollow fibers is most effective when careful attention is given to issues of hydrodynamic similitude. Similarly, understanding the role of fluid mechanical phenomena in arterial disease and subsequent therapeutic applications is clearly dependent on the appreciation of hemodynamics.

Understanding of fluid phenomena is also crucial for processing and transport applications not taking place within living systems. For example, the ability to generate nanoscale entities, as in emulsions and suspensions, requires knowledge of multiphase flow and turbulent mixing concepts. Typical uses are (1) “bottom-up” drug crystal size control, (2) permeation enhancement materials for dispersion

into immunoprotective barrier membranes, as in improving oxygen supply to encapsulated cells/tissue systems, and (3) creating chaperones for specific targets as in imaging and/or drug delivery. For further details and other important applications, the reader will find the following sources more appropriate [7–17].

A thorough treatment of the mathematics needed for model development and analysis is beyond the scope of this volume, and is presented in numerous sources [1,2]. Herein, the goal is to provide a physical understanding of the important issues relevant to hemodynamic flow and transport. Solution methods are summarized, and the benefits associated with use of computational fluid dynamics (CFD) packages are described. In particular, quantifying hemodynamic events can require invasive experimentation and/or extensive model and computational analysis.

10.2 Elements of Theoretical Hydrodynamics

It is essential that engineers understand both the advantages and the limitations of mathematical theories and models of biological phenomena, as well as the assumptions underlying those models. Mechanical theories often begin with Newton's second law ($\mathbf{F} = m\mathbf{a}$). When applied to continuous distributions of Newtonian fluids, Newton's second law gives rise to the *Navier–Stokes equations*. In brief, these equations provide an expression governing the motion of fluids such as air and water for which the rate of motion is linearly proportional to the applied stress producing the motion. Below, the basic concepts from which the Navier–Stokes equations have been developed are summarized along with a few general ideas about boundary layers and turbulence. Applications to the vascular system are then treated in the context of pulsatile flow. It is hoped that this very generalized approach will allow the reader to appreciate the complexities involved in an analytic solution to pulsatile phenomena, a necessity for properly describing vascular hemodynamics for clinical evaluations.

10.2.1 Elements of Continuum Mechanics

The theory of fluid flow, together with the theory of elasticity, makes up the field of continuum mechanics, the study of the mechanics of continuously distributed materials. Such materials may be either solid or fluid, or may have intermediate viscoelastic properties. Since the concept of a continuous medium, or continuum, does not take into consideration the molecular structure of matter, it is inherently an idealization. However, as long as the smallest length scale in any problem under consideration is significantly larger than the size of the molecules making up the medium and the mean free path within the medium, for mechanical purposes, all mass may safely be assumed to be continuously distributed in space. As a result, the density of materials can be considered to be a continuous function of spatial position and time.

10.2.1.1 Constitutive Equations

The response of any fluid to applied forces and temperature disturbances can be used to characterize the material. For this purpose, functional relationships between applied stresses and the resulting rate of strain field of the fluid are needed. Fluids that are homogeneous and isotropic, and for which there is a linear relationship between the state of stress within the fluid s_{ij} and the rate of strain tensor ξ_{ij} , where i and j denote the Cartesian coordinates x , y , and z , are called *Newtonian*. In physiologic settings, Newtonian fluids normally behave as if incompressible. For such fluids, it can be shown that

$$s_{ij} = -P\delta_{ij} + 2\mu\xi_{ij} \quad (10.1)$$

with μ being the dynamic viscosity of the fluid and $P = P(x, y, z)$ the fluid pressure.

10.2.1.2 Conservation (Field) Equations

In vector notation, conservation of mass for a continuous fluid is expressed through

$$\frac{\partial \rho}{\partial t} + \nabla \cdot \rho \mathbf{u} = 0 \quad (10.2)$$

where ρ is the fluid density and $\mathbf{u} = \mathbf{u}(x, y, z)$ is the vector velocity field. When the fluid is incompressible, density is constant and Equation 10.2 reduces to the well-known *continuity condition*, $\nabla \cdot \mathbf{u} = 0$. The continuity condition can also be expressed in terms of Cartesian velocity components (u, v, w) as $\partial u/\partial x + \partial v/\partial y + \partial w/\partial z = 0$.

The basic equation of Newtonian fluid motion, the Navier–Stokes equations, can be developed by substitution of the constitutive relationship for a Newtonian fluid, P-1, into the Cauchy principle of momentum balance for a continuous material [18]. In writing the second law for a continuously distributed fluid, care must be taken to correctly express the acceleration of the fluid particle to which the forces are being applied through the *material derivative* $D\mathbf{u}/Dt$, where $D\mathbf{u}/Dt = \partial\mathbf{u}/\partial t + (\mathbf{u} \cdot \nabla)\mathbf{u}$. That is, the velocity of a fluid particle may change for either of two reasons: because the particle accelerates or decelerates with time (*temporal acceleration*) or because the particle moves to a new position, at which the velocity has a different magnitude and/or direction (*convective acceleration*).

A flow field for which $\partial/\partial t = 0$ for all possible properties of the fluid and its flow is described as *steady*, to indicate that it is independent of time. However, the statement $\partial\mathbf{u}/\partial t = 0$ does not imply $D\mathbf{u}/Dt = 0$, and similarly $D\mathbf{u}/Dt = 0$ does not imply that $\partial\mathbf{u}/\partial t = 0$.

Using the material derivative, the Navier–Stokes equations for an incompressible fluid can be written in vector form as

$$\frac{D\mathbf{u}}{Dt} = \mathbf{B} - \frac{1}{\rho}\nabla P + \nu\nabla^2\mathbf{u} \quad (10.3)$$

where ν is the fluid kinematic viscosity $= \mu/\rho$.

Expanded in full, the Navier–Stokes equations are three simultaneous, nonlinear scalar equations, one for each component of the velocity field. In Cartesian coordinates, Equation 10.3 takes the form

$$\frac{\partial u}{\partial t} + u\frac{\partial u}{\partial x} + v\frac{\partial u}{\partial y} + w\frac{\partial u}{\partial z} = B_x - \frac{1}{\rho}\frac{\partial P}{\partial x} + \nu\left(\frac{\partial^2 u}{\partial x^2} + \frac{\partial^2 u}{\partial y^2} + \frac{\partial^2 u}{\partial z^2}\right) \quad (10.4a)$$

$$\frac{\partial v}{\partial t} + u\frac{\partial v}{\partial x} + v\frac{\partial v}{\partial y} + w\frac{\partial v}{\partial z} = B_y - \frac{1}{\rho}\frac{\partial P}{\partial y} + \nu\left(\frac{\partial^2 v}{\partial x^2} + \frac{\partial^2 v}{\partial y^2} + \frac{\partial^2 v}{\partial z^2}\right) \quad (10.4b)$$

$$\frac{\partial w}{\partial t} + u\frac{\partial w}{\partial x} + v\frac{\partial w}{\partial y} + w\frac{\partial w}{\partial z} = B_z - \frac{1}{\rho}\frac{\partial P}{\partial z} + \nu\left(\frac{\partial^2 w}{\partial x^2} + \frac{\partial^2 w}{\partial y^2} + \frac{\partial^2 w}{\partial z^2}\right) \quad (10.4c)$$

Flow fields may be determined by solution of the Navier–Stokes equations, provided \mathbf{B} is known. This is generally not a difficulty, since the only body force normally significant in hemodynamic applications is gravity. For an incompressible flow, there are then four unknown dependent variables, the three components of velocity and the pressure P , and four governing equations, the three components of the Navier–Stokes equations and the continuity condition. It is important to emphasize that this set of equations is *not* sufficient to calculate the flow field when the flow is compressible or involves temperature changes, since pressure, density, and temperature are then interrelated, which introduces new dependent variables to the problem.

Solution of the Navier–Stokes equations also requires that boundary conditions, and sometimes initial conditions as well, be specified for the flow field of interest. By far the most common boundary condition in physiologic and other engineering flows is the so-called *no-slip condition*, requiring that the layer of fluid elements in contact with a boundary have the same velocity as the boundary itself. For an unmoving, rigid wall, as in a pipe, this velocity is zero. However, in the vasculature, vessel walls expand and contract during the cardiac cycle.

Flow patterns and accompanying flow field characteristics depend largely on the values of governing dimensionless parameters. There are many such parameters, each relevant to specific types of flow settings, but the principle parameter of steady flows is the *Reynolds number*, Re , defined as $Re = \rho UL/\mu$, where U is a characteristic velocity of the flow field and L is a characteristic length. Both U and L must be selected for the specific problem under study, and in general, both will have different values in different problems. For pipe flow, U is most commonly selected to be the mean velocity of the flow with L being the pipe diameter.

It can be shown that the Reynolds number represents the ratio of inertial forces to viscous forces in the flow field. Flows at sufficiently low Re therefore behave as if highly viscous, with little to no fluid acceleration possible. At the opposite extreme, high Re flows behave as if lacking viscosity. One consequence of this distinction is that very high Reynolds number flow fields may at first seem to contradict the no-slip condition, in that they seem to “slip” along a solid boundary exerting no shear stress. This dilemma was first resolved in 1905 with Prandtl’s introduction of the *boundary layer*, a thin region of the flow field adjacent to the boundary in which viscous effects are important and the no-slip condition is obeyed [19–21].

10.2.1.3 Turbulence and Instabilities

Flow fields are broadly classified as either *laminar* or *turbulent* to distinguish between smooth and irregular motion, respectively. Fluid elements in laminar flow fields follow well-defined paths indicating smooth flow in discrete layers or “laminae,” with minimal exchange of material between layers due to the lack of macroscopic mixing. The transport of momentum between system boundaries is thus controlled by molecular action, and is dependent on the fluid viscosity.

In contrast, many flows in nature as well as engineered applications are found to fluctuate randomly and continuously, rather than streaming smoothly, and are classified as turbulent. These turbulent flows are characterized by a vigorous mixing action throughout the flow field, which is caused by *eddies* of varying size within the flow [7,14,15]. Because of these eddies fluctuate randomly, the velocity field is not constant in time. Although turbulent flows do not meet the aforementioned definition for steady, the velocity at any point presents a statistically distinct time-average value that is constant. Turbulent flows are therefore described as *stationary*, rather than truly unsteady.

Physically, the two flow states are linked, in the sense that any flow can be stable and laminar if the ratio of inertial to viscous forces is sufficiently small. Turbulence results when this ratio exceeds a *critical value*, above which the flow becomes unstable to perturbations and breaks down into fluctuations.

Fully turbulent flow fields have four defining characteristics [7,21,22]: they fluctuate *randomly*, they are *three-dimensional*, they are *dissipative*, and they are *dispersive*. The *turbulence intensity* I of any flow field is defined as the ratio of velocity fluctuations u' to time-average velocity \bar{u} , $I = u'/\bar{u}$.

Steady flow in straight, rigid pipes is characterized by only one dimensionless parameter, the Reynolds number. It was shown by Osborne Reynolds that for $Re < 2000$, incidental disturbances in the flow field are damped out and the flow remains stable and laminar. For $Re > 2000$, brief bursts of fluctuations appear in the velocity separated by periods of laminar flow. As Re increases, the duration and intensity of these bursts increases until they merge together into full turbulence. Laminar flow may be achieved with Re as large as 20,000 or greater in extremely smooth pipes, but it is unstable to flow disturbances and rapidly becomes turbulent if perturbed.

Since the Navier–Stokes equations govern all the behavior of any Newtonian fluid flow, it follows that turbulent flow patterns should be predictable through analysis based on those equations. However,

although turbulent flows have been investigated for more than a century and the equations of motion analyzed in great detail, no general approach to the solution of problems in turbulent flow has been found. Statistical studies invariably lead to a situation in which there are more unknown variables than equations, which is called the *closure problem* of turbulence. Efforts to circumvent this difficulty have included phenomenologic concepts such as *eddy viscosity* and *mixing length* (i.e., Kolmogorov scale), as well as analytical methods that include dimensional analysis and asymptotic invariance studies [7,14,15,21,22].

10.2.2 Flow in Tubes

Flow in a tube is the most common fluid dynamic phenomenon in the physiology of living organisms, and is the basis for transport of nutrient molecules, respiratory gases, hormones, and a variety of other important solutes throughout the bodies of all complex living plants and animals. Only single-celled organisms, and multicelled organisms with small numbers of cells, can survive without a mechanism for transporting such molecules, although even these organisms exchange materials with their external environment through fluid-filled spaces. Higher organisms, needing to transport molecules and materials over larger distances, rely on organized systems of directed flows through networks of tubes to carry fluids and solutes. In human physiology, the circulatory system, which consists of the heart, the blood vessels of the vascular tree, and the “working” fluid blood, serves to transport blood throughout the body tissues. It is perhaps the most obvious example of an organ system dedicated to creating and sustaining flow in a network of tubes. However, flow in tubes is also a central characteristic of the respiratory, digestive, and urinary systems. Furthermore, the immune system utilizes systemic circulatory mechanisms to facilitate transport of antibodies, white blood cells, and lymph throughout the body, while the endocrine system is critically dependent on blood flow for delivery of its secreted hormones to the appropriate target organs or tissues. In addition, reproductive functions are also based on fluid flow in tubes. Thus, seven of the ten major organ systems depend on flow in tubes to fulfill their functions.

10.2.2.1 Steady Poiseuille Flow

The most basic state of motion for fluid in a pipe is one in which the motion occurs at a constant rate, independent of time. The pressure–flow relation for laminar, steady flow in round tubes is called *Poiseuille’s law*, after J.L.M. Poiseuille, the French physiologist who first derived the relation in 1840 [23]. Accordingly, steady flow through a pipe or channel that is driven by a pressure difference between the pipe ends of just sufficient magnitude to overcome the tendency of the fluid to dissipate energy through the action of viscosity is called *Poiseuille flow*.

Strictly speaking, Poiseuille’s law applies only to steady, laminar flow through pipes that are straight, rigid, and infinitely long, with uniform diameter, so that effects at the pipe ends may be neglected without loss of accuracy. However, although neither physiologic vessels nor industrial tubes fulfill all those conditions exactly, Poiseuille relationships have proven to be of such widespread usefulness that they are often applied even when the underlying assumptions are not met. As such, Poiseuille flow can be taken as the starting point for analysis of cardiovascular, respiratory, and other physiologic flows of interest.

A straight, rigid round pipe is shown in [Figure 10.1](#), with x denoting the pipe axis and a the pipe radius. Flow in the pipe is governed by the Navier–Stokes equations, which for these conditions reduce to $d^2u/dr^2 + (1/r)(du/dr) = -\kappa/\mu$, with the conditions that the flow field must be symmetric about the pipe center line, that is, $du/dr|_{r=0} = 0$, and the no-slip boundary condition applies at the wall, $u = 0$ at $r = a$. Under these conditions, the velocity field solution is $u(r) = (\kappa/4\mu)(a^2 - r^2)$.

The velocity profile described by this solution has the familiar parabolic form known as Poiseuille flow ([Figure 10.1](#)). The velocity at the wall ($r = a$) is clearly zero, as required by the no-slip condition, while as expected on physical grounds, the maximum velocity occurs on the axis of the tube ($r = 0$) where $u_{\max} = \kappa a^2/4\mu$. At any position between the wall and the tube axis, the velocity varies smoothly with r , with no step change at any point.

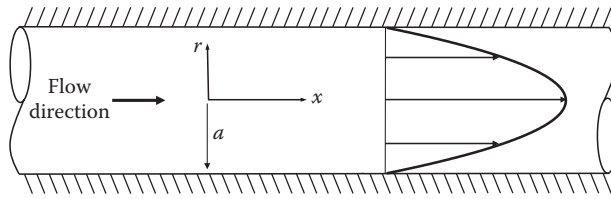


FIGURE 10.1 Parabolic velocity profile characteristic of Poiseuille flow in a round pipe of radius a . x , r —coordinate system with origin on the pipe centerline.

From physical analysis, it can be shown that the parabolic velocity profile results from a *balance* of the forces on the fluid in the pipe. The pressure gradient along the pipe accelerates fluid in the forward direction through the pipe, while at the same time, viscous shear stress retards the fluid motion. A parabolic profile is created by the balance of these effects.

Although the velocity profile is important and informative, in practice, one is therefore apt to be more concerned with measurement of the *discharge rate*, or total rate of flow in the pipe, Q , which can far more easily be accessed. The volume flow rate is given by area-integration of the velocity across the tube cross-section:

$$Q = \int_A \mathbf{u} \cdot d\mathbf{A} = \frac{\partial P}{\partial x} \frac{\pi a^4}{8\mu} \tag{10.5}$$

which is Poiseuille’s law.

For convenience, the relation between pressure and flow rate is often reexpressed in an Ohm’s law form, *driving force* = *flow* \times *resistance*, or $\partial P/\partial x = Q \cdot (8\mu/\pi a^4)$, from which the resistance to flow, $8\mu/\pi a^4$, is seen to be inversely proportional to the fourth power of the tube radius.

A further point about Poiseuille flow concerns the area-average velocity, U . Clearly, $U = Q/\text{cross-sectional area} = (\pi\kappa a^4/8\mu)/\pi a^2 = \kappa a^2/8\mu$. But, as was pointed out, the maximum velocity in the tube is $u_{\max} = \kappa a^2/4\mu$. Hence, $U = u_{\max}/2 = (1/2)u|_{r=0} = (1/2)u_{CL}$.

Finally, the shear stress exerted by the flow on the wall can be a critical parameter, particularly when it is desired to control the wall’s exposure to shear. From the solution for $u(r)$, it can be shown that wall shear stress, τ_w , is given by

$$\tau_w = -\mu \left. \frac{du}{dr} \right|_{r=a} = \frac{\partial P}{\partial x} \frac{a}{2} = \frac{4\mu Q}{\pi a^3} \tag{10.6}$$

To summarize, Poiseuille’s law, Equation 10.5, provides a relation between the pressure drop and net laminar flow in any tube, while Equation 10.6 provides a relation between the flow rate and wall shear stress. Thus, physical forces on the wall may be calculated from knowledge of the flow fields.

10.2.2.2 Entrance Flow

It can be shown that a Poiseuille velocity profile is the velocity distribution that minimizes energy dissipation in steady laminar flow through a rigid tube. Consequently, it is not surprising that if the flow in a tube encounters a perturbation that alters its profile, such as a branch vessel or a region of stenosis, immediately downstream of the perturbation the velocity profile will be disturbed away from a parabolic form, perhaps highly so. However, if the Reynolds number is low enough for the flow to remain stable as it convects downstream from the site of the original distribution, a parabolic form is gradually recovered. Consequently, at a sufficient distance downstream, a fully developed parabolic velocity profile again emerges.

Downloaded by [JCR JCR] at 10:34 01 August 2015

Both blood vessels and bronchial tubes of the lung possess an enormous number of branches, each of which produces its own flow disturbance. As a result, many physiologic flows may not be fully developed over a significant fraction of their length. It therefore becomes important to ask, what length of tube is required for a perturbed velocity profile to recover its parabolic form, that is, how long is the entrance length in a given tube? This question can be formally posed as: if x is the coordinate along the tube axis, for what value of x does $u|_{r=0} = 2U$? Through dimensional analysis it can be shown that $x/d = \text{const} \times (\rho dU/\mu) = \text{const} \times \text{Re}$, where d is the tube diameter. Thus, the length of tube over which the flow develops is $\text{const} \times \text{Re} \times d$. The constant must be determined by experiment, and is found to be in the range 0.03–0.04.

Since the entrance length, in units of tube diameters, is proportional to the Reynolds number and the mean Reynolds number for flow in large tubes such as the aorta and trachea is of the order of 500–1000, the entrance length in these vessels can be as much as 20–30 diameters. In fact, there are few segments of these vessels even close to that length without a branch or curve that perturbs their flow. Consequently, flow in these vessels can be expected to almost never be fully developed. In contrast, flow in the smallest bronchioles, arterioles, and capillaries may take place with $\text{Re} < 1$. As a result, their entrance length is $\ll 1$ diameter, and flow in them will virtually always be nearly or fully developed.

10.2.2.3 Mechanical Energy Equation

Flow fields in tubes with more complex shapes than simple straight pipes, such as those possessing bends, curves, orifices, and other intricacies, are often analyzed with an *energy balance* approach, since they are not well described by Poiseuille's law. Understanding such flow fields is important to establish dynamic similitude parameters for *in vitro* studies and perfusion devices, as well as for *in vivo* studies of curved and/or branched vessel flows. For any system of total energy E , the *first law of thermodynamics* states that any change in the energy of the system ΔE must appear as either heat transferred to the system in unit time Q or as work done by the system W , so that $\Delta E = Q - W$. Here a sign convention is taken such that Q , when positive, represents heat transferred *to* the system and W , when positive, is the work done *by* the system on its surroundings. The general form of the energy equation for a fluid system is

$$\dot{Q} - \dot{W}_s = \frac{d}{dt} \int_V \left(\frac{U^2}{2} + gz + e \right) \rho dV + \int_S \left(\frac{p}{\rho} + \frac{U^2}{2} + gz + e \right) \rho \mathbf{u} \cdot d\mathbf{S} \quad (10.7)$$

where W_s , the “shaft work,” represents work done on the fluid contained within a volume V bounded by a surface S by pumps, turbines, or other external devices through which power is often transmitted by means of a shaft; $U^2/2$ is the kinetic energy per unit mass of the fluid within V , gz is its potential energy per unit mass, with z the vertical coordinate and g gravitational acceleration, e is its internal energy per unit mass, and the density ρ is assumed to be constant.

The general equation can be simplified greatly when the flow is steady, since the total energy contained within any prescribed volume is then constant, and $d/dt = 0$. Applying Equation 10.7 to steady flow through a control volume whose end faces are denoted 1 and 2, respectively, then gives

$$\frac{p_1}{\gamma} + \beta_1 \frac{U_1^2}{2g} + z_1 + h_p = \frac{p_2}{\gamma} + \beta_2 \frac{U_2^2}{2g} + z_2 + h_l \quad (10.8)$$

where p_1 and p_2 are the pressures at faces 1 and 2, z_1 and z_2 are the vertical positions of those faces, $\gamma = \rho g$, h_p represents head supplied by a pump, and the coefficients β_1 and β_2 are kinetic energy correction factors introduced to simplify notation. Calculations show that $\beta = 1$ when the velocity is uniform across the section and $\beta = 2$ for laminar Poiseuille flow. Mechanical energy lost from the system is lumped together as a single term called *head loss*, h_l . For flow in a rigid pipe of length L and diameter d , h_l is well represented by $h_l = f(L/d)(U^2/2g)$, where f is called the *friction factor* of the pipe, and depends on both the pipe roughness and the flow Reynolds number. It can be shown that for laminar flow,

$f = 64/\text{Re}$. Then, $h_L = (32\mu LU/\gamma d^2)$. Forms that h_L can take on in turbulent flows are given in a variety of texts [24,25].

It is worth repeating that Equation 10.8 is only correct when the fluid density is constant, as is normally the case in tissue and engineering applications and even for air flow in the lung. Compressibility effects require separate energy considerations.

10.3 Pulsatile Flow

Flow in a straight, round tube driven by an axial pressure gradient that varies in time is the basis for blood transport in the arterial tree as well as respiratory gas transport in the trachea and bronchi. When the flow is confined within a tube of *rigid*, undeformable walls, its direction will always be parallel to the tube axis, so that there will only be an axial component of velocity $\mathbf{u} = (u(r,t), 0, 0)$ (Figure 10.2). Since all the fluid elements in the tube will then respond to any change in the pressure magnitude instantaneously and in unison, regardless of axial position, the velocity profile will be the same at all positions along the tube. It is as if all the fluid in the tube moves as a single rigid body.

As a result of the flow field acceleration and decelerations in pulsatile flows, a special type of boundary layer known as the *Stokes layer* develops. When the pressure gradient varies sinusoidally in time, as the pressure increases to its maximum, the flow increases, and as the pressure decreases, the flow does also. If the oscillations are of very low frequency, the velocity field will essentially be in phase with the pressure gradient and the boundary layers will have adequate time to grow into the tube core region. In the limit of very low frequency, the velocity field must therefore approach that of a steady Poiseuille flow. As frequency increases, however, the pressure gradient changes more rapidly and the flow begins to lag behind it due to the inertia of the fluid. The Stokes layers then become confined to a region near the wall, lacking the time required for further growth. In addition, the flow amplitude decreases with increasing oscillation frequency, as pressure gradient reversals occur more and more rapidly. In the limit of very high frequency, fluid in the tube center hardly moves at all and the Stokes layers are confined to a very thin region along the wall.

Because of the inertia of the fluid, the Stokes layer thickness, δ , is inversely related to the flow frequency, with $\delta \propto (\nu/\omega)^{1/2}$, where ω is the flow angular frequency (in rad/s).

10.3.1 Hemodynamics in Rigid Tubes: Womersley’s Theory

The rhythmic contractions of the heart produce a pressure distribution in the arterial tree that includes both a steady component, P_s , and a purely oscillatory component, P_{osc} , as does the velocity field.

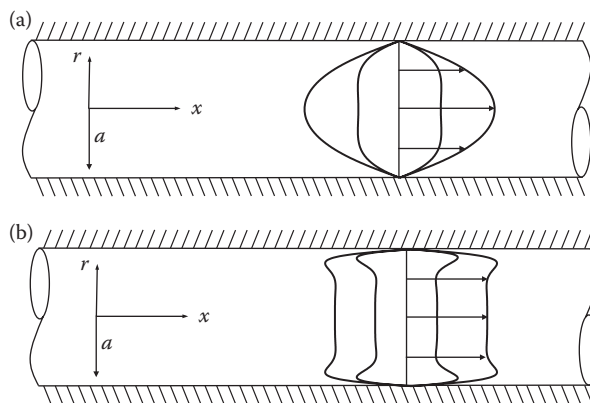


FIGURE 10.2 Representative velocity profiles of laminar, oscillatory flow in a straight, rigid tube, at four phases of the flow cycle. (a) $a = 3$, (b) $a = 13$.

Downloaded by [JCR JCR] at 10:34 01 August 2015

In contrast, flow in the trachea and bronchi has no steady component, and thus is purely oscillatory. It is common practice to refer to these components of pressure and flow as *steady* and *oscillatory*, respectively, and to use the term *pulsatile* to refer to the superposition of the two. A very useful feature of these flows, when they occur in rigid tubes, is that the governing equation (Equation 10.10) is linear, since the flow field is unidirectional and independent of axial position. The steady and oscillatory components can therefore be decoupled from each other, and analyzed separately. This gives

$$\begin{aligned} P(x,t) &= P_s(x) + P_{\text{osc}}(x,t) \\ u(r,t) &= u_s(r) + u_{\text{osc}}(r,t) \end{aligned} \quad (10.9)$$

The oscillatory component of this flow may be analyzed assuming the flow to be fully developed, so that entrance effects may be neglected, and to be driven by a purely oscillatory pressure gradient, $-(1/\rho)(\partial P/\partial x) = K \cos(\omega t) = \text{Re}(Ke^{i\omega t})$, where $i = \sqrt{-1}$ and here “Re” indicates the Real part of $Ke^{i\omega t}$. It is also convenient to introduce a new dimensionless parameter, the Womersley number, α [26], defined as $\alpha = a(\omega/\nu)^{1/2}$. Thus defined, α represents the ratio of the tube radius to the Stokes layer thickness.

The velocity field is then governed by

$$\frac{\partial u}{\partial t} = -\frac{1}{\rho} \frac{\partial P}{\partial x} + \nu \left(\frac{\partial^2 u}{\partial r^2} + \frac{1}{r} \frac{\partial u}{\partial r} \right) \quad (10.10)$$

subject to the no-slip boundary condition at the tube wall, which for a round tube takes the form $\mathbf{u} = 0$ for $r = a$.

The particular solution to equation 10.10 under this condition is most easily expressed in terms of complex *ber* and *bei* functions, which themselves are defined through [27] $\text{ber}(r) + i \cdot \text{bei}(r) = J_0(r \cdot i\sqrt{i})$, where J_0 represents the complex Bessel function of the first kind. Then

$$u(r,t) = \frac{K}{\omega} (B \cos \omega t + (1 - A) \sin \omega t) \quad (10.11)$$

where

$$A = \frac{\text{ber}\alpha \cdot \text{ber}\alpha \frac{r}{a} + \text{bei}\alpha \cdot \text{bei}\alpha \frac{r}{a}}{\text{ber}^2\alpha + \text{bei}^2\alpha} \quad (10.12a)$$

and

$$B = \frac{\text{bei}\alpha \cdot \text{ber}\alpha \frac{r}{a} - \text{ber}\alpha \cdot \text{bei}\alpha \frac{r}{a}}{\text{ber}^2\alpha + \text{bei}^2\alpha} \quad (10.12b)$$

Representative velocity profiles derived from these expressions are shown in [Figure 10.2](#) for two values of α , at four phases of the flow cycle. In these figures, the radial position, r , has been normalized by the tube radius, a . At $\alpha = 3$ (Figure 10.2a), a value that under resting conditions can occur in the smallest arteries and larger arterioles as well as the middle airways, Stokes layers can occupy a significant fraction of the tube radius. The velocity at the wall is zero, as required by the no-slip condition, and as in steady flow the velocity varies smoothly with r , with no step change at any point. However, even at this

low α , the velocity profile resembles a parabola only during peak flow rates. At other flow phases, a more uniform profile forms across the tube core.

In contrast, at $\alpha = 13$ (Figure 10.2b), which characterizes rest state flow in the aorta and trachea, the velocity profile of the pipe core is nearly uniform at all flow phases. Flow in the boundary layer is out of phase with that in the core, and flow reversals are possible in the Stokes layer. These changes in the velocity fields result from the inertia of the fluid, since as the flow frequency increases, less time is available in each flow cycle to accelerate the fluid.

To these flow fields of course must be added a steady component if the flow field is pulsatile rather than purely oscillatory.

As with steady flows, it is important to be able to use these expressions for the velocity field to determine the instantaneous total volume flow rate, Q_{inst} , or equivalently the instantaneous mean velocity, U_{inst} , since $Q_{\text{inst}} = U_{\text{inst}} \times \text{pipe area}$. Following Reference 28, it can be shown that the mean velocity is

$$\begin{aligned} U(t) &= \frac{K}{\omega} \left(\frac{2D}{\alpha} \cos \omega t + \left(\frac{1-2C}{\alpha} \right) \sin \omega t \right) \\ &= \frac{K}{\omega} \sigma \cos(\omega t - \delta) \end{aligned} \tag{10.13}$$

where

$$C = \frac{\text{ber}\alpha \cdot \text{bei}'\alpha - \text{bei}\alpha \cdot \text{ber}'\alpha}{\text{ber}^2\alpha + \text{bei}^2\alpha} \tag{10.14a}$$

$$D = \frac{\text{ber}\alpha \cdot \text{ber}'\alpha + \text{bei}\alpha \cdot \text{bei}'\alpha}{\text{ber}^2\alpha + \text{bei}^2\alpha} \tag{10.14b}$$

$$\sigma^2 = \left(\frac{1-2C}{\alpha} \right)^2 + \left(\frac{2D}{\alpha} \right)^2 \tag{10.14c}$$

$$\tan \delta = \frac{(1-2C/\alpha)}{(2D/\alpha)}. \tag{10.14d}$$

The oscillatory shear stress at the wall, $\tau_{w,\text{osc}}$, is given by $\tau_{w,\text{osc}} = -\mu (\partial u_{\text{osc}}/\partial r)|_{r=a}$.

This results in

$$\tau_{w,\text{osc}} = \text{Re} \left[\frac{\rho K a \sqrt{i}}{\alpha} \frac{J_1 \left(a \sqrt{-(i\omega/\nu)} \right)}{J_0 \left(a \sqrt{-(i\omega/\nu)} \right)} \cdot e^{i\omega t} \right]. \tag{10.15}$$

As with the oscillatory flow rate, the oscillatory wall shear stress lags the pressure gradient, reaching a maximum during peak flow.

10.3.2 Hemodynamics in Elastic Tubes

Because of the mathematical complexity of analysis of pulsatile flows in elastic tubes, and the variety of physical phenomena associated with them, space does not permit a full description of this topic. The

reader is instead referred to a number of excellent sources for a more complete treatment [29–31]. Here we only briefly summarize the most important features of these flows, to give the reader a sense of the richness of the physics underlying them.

In brief, in a tube with a nonrigid wall, any pressure change within the tube will lead to localized bulging of the tube wall in the high pressure region (Figure 10.3). Fluid can then flow in the radial direction into the bulge. Hence, not only is the radial velocity v no longer zero, but both u and v can no longer be independent of x even far from the tube ends. Thus the flow field is governed by the continuity condition along with the full Navier–Stokes equations. Assuming axial symmetry of the tube, these become

$$\frac{\partial u}{\partial x} + \frac{\partial v}{\partial r} + \frac{v}{r} = 0 \tag{10.16}$$

$$\begin{aligned} \frac{\partial u}{\partial t} + u \frac{\partial u}{\partial x} + v \frac{\partial u}{\partial r} &= -\frac{1}{\rho} \frac{\partial P}{\partial x} + \nu \left(\frac{\partial^2 u}{\partial x^2} + \frac{\partial^2 u}{\partial r^2} + \frac{1}{r} \frac{\partial u}{\partial r} \right) \\ \frac{\partial v}{\partial t} + u \frac{\partial v}{\partial x} + v \frac{\partial v}{\partial r} &= -\frac{1}{\rho} \frac{\partial P}{\partial r} + \nu \left(\frac{\partial^2 v}{\partial x^2} + \frac{\partial^2 v}{\partial r^2} + \frac{1}{r} \frac{\partial v}{\partial r} - \frac{v}{r^2} \right) \end{aligned} \tag{10.17}$$

The most important consequence of this is that even if the inlet pressure gradient depends only on t , within the tube the pressure gradient depends on x as well as t . An oscillatory pressure gradient applied at the tube entrance therefore propagates down the tube in a wave motion. Both the pressure and the velocity fields therefore take on wave characteristics.

The speed with which these waves travel down the tube can be expected to depend on the fluid inertia, that is, on its density, and on the wall stiffness. If the wall thickness is small compared to the tube radius and the effect of viscosity is neglected, the wave speed c_0 is given by the Moen–Korteweg formula $c_0 = (Eh/\rho d)^{1/2}$, where E is the stiffness, or Young’s modulus, of the tube wall and h is its thickness. As can be expected on physical grounds, the wave speed increases as the wall stiffness rises until when E becomes infinite, the wall is rigid. Thus, oscillatory motion in a *rigid* tube, in which all the fluid moves together in bulk, may be thought of as resulting from a wave traveling with infinite speed, so that any change in the pressure gradient is felt throughout the whole tube instantaneously. In an *elastic* tube, by contrast, pressure changes are felt locally at first and then propagate downstream at finite speed.

Because of the action of the pressure and shear stress on the wall position and displacement, oscillatory flow in an elastic tube is inherently a *coupled* problem, in the sense that it is not possible in general to determine the fluid motion without also determining the resulting wall motion; the two are intrinsically linked. It can be shown [29] that the motion of the *wall* is governed by

$$\frac{\partial^2 \zeta}{\partial t^2} = \frac{E}{(1 - \sigma^2)\rho_w} \left(\frac{\partial^2 \zeta}{\partial x^2} + \frac{\sigma}{a} \frac{\partial^2 \eta}{\partial x} \right) - \frac{\tau_w}{\rho_w h} \tag{10.18a}$$

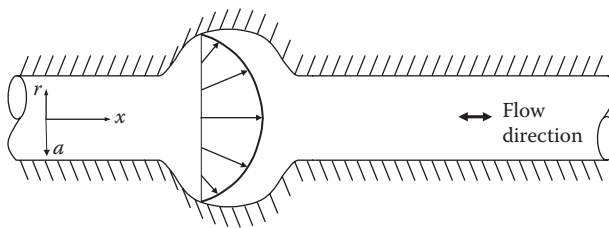


FIGURE 10.3 Local bulging of the tube wall at regions of high pressure in pulsatile flow in an elastic tube.

Downloaded by [JCR JCR] at 10:34 01 August 2015

$$\frac{\partial^2 \eta}{\partial t^2} = \frac{P_w}{\rho_w h} - \frac{E}{(1 - \sigma^2) \rho_w a} \left(\frac{\eta}{a} + \sigma \frac{\partial \zeta}{\partial x} \right) \tag{10.18b}$$

where ζ and η are the axial and radial displacement of the wall, respectively (both of which may vary with axial position x), P_w and τ_w are the fluid pressure and shear stress at the wall, ρ_w is the wall density, and σ is the Poisson's ratio, a wall material property. Equations 10.18a and b indicate the coupling of the wall and fluid motions, since they explicitly describe ζ and η , which are properties of the *wall*, in terms of P_w and τ_w , which are themselves properties of the *flow*. In addition, coupling is imposed by the no-slip boundary condition, since the layer of fluid in contact with the wall must have the same velocity as the wall. Hence, $(\partial \zeta / \partial t) = u(x, a, t)$, the axial component of velocity at the wall, and $(\partial \eta / \partial t) = v(x, a, t)$, the radial component of velocity at the wall.

With these governing equations and boundary conditions in place, and if the input pressure distribution that drives the flow field is known, it is possible to develop a formal solution for the axial velocity. For an oscillatory flow, the input pressure would normally be expected to be of a sinusoidal form $P(x, r, t) = \text{const} \cdot e^{i\omega t}$. Following Reference 29, the method of characteristics shows the pressure distribution throughout the tube to be $P(x, r, t) = A(x, r) e^{i\omega(t-x/c)}$, where c is the wave speed in the fluid and A is the pressure amplitude. Since the fluid must be taken to be viscous, c is not equal to c_0 , the inviscid fluid wave speed. Instead, $c = c_0 (2/(1 - \sigma^2)z)^{1/2}$, with z a parameter of the problem that depends on a , ω , ν , σ , ρ , ρ_w , and h . It can also be shown that the pressure amplitude A depends on x , but not on r , and therefore the pressure is uniform across any axial position in the tube [29]. Under these conditions, the solution for u , the principal velocity component of interest, can be stated as

$$u(x, r, t) = \text{Re} \left\{ \frac{A}{\rho c} \left[1 - G \frac{J_0 \left(r \sqrt{-(i\omega/\nu)} \right)}{J_0 \left(a \sqrt{-(i\omega/\nu)} \right)} \right] \cdot e^{i\omega(t-x/c)} \right\} \tag{10.19}$$

with G a factor that modifies the velocity profile shape compared to that in a rigid tube due to the wall elasticity. G is given by

$$G = \frac{2 + z(2\nu - 1)}{z(2\nu - g)} \tag{10.20}$$

with

$$g = \frac{2J_1 \left(a \sqrt{-(i\omega/\nu)} \right)}{\left(a \sqrt{-\frac{i\omega}{\nu}} \right) J_0 \left(a \sqrt{-(i\omega/\nu)} \right)}. \tag{10.21}$$

It is apparent from inspection of Equation 10.19 that the difference between the velocity field in a rigid tube and that in an elastic tube is contained in the factor G . However, since G is complex, and both its real and imaginary parts depend on the flow frequency ω , the difference is by no means readily evident. The reader is referred to Reference 29 for detailed depiction of representative velocity profiles. Nevertheless, it is important to note here that because the pressure distribution in an elastic tube takes the form of a traveling wave, *two separate* periodic oscillations can be derived from Equation 10.19. The first is that at any given axial position in the tube, the velocity profile varies sinusoidally with time, just as it does in a rigid tube. The second, however, is that at any instant of time during the flow cycle, the velocity field also varies sinusoidally in space. Fluid flows *away* from regions in which the pressure is greatest and *toward*

regions in which it is least. In a rigid tube, there is only one region of maximum pressure, the upstream tube end, and only one region of minimum pressure, the downstream end. Between them, the pressure varies linearly with axial position x . In contrast, in an elastic tube, the pressure varies *sinusoidally* with x , so that many high pressure regions can exist along the tube, and these lead to a series of flow reversals at any specific time.

A final word about oscillatory flow in an elastic tube concerns the possibility of *wave reflections*. In a rigid tube, there is no wave motion as such, and flow arriving at an obstruction or branch is disturbed in some way, but otherwise progresses through the obstruction. In contrast, the wave nature of flow in an elastic tube leads to entirely different behavior at an obstacle. At an obstruction such as a bifurcation or a branch, some of the energy associated with pressure and flow is transmitted through the obstruction, while the remainder is *reflected*. This leads to a highly complex pattern of superposing primary and reflected pressure and flow waves, particularly in the arterial tree since blood vessels are elastic and vessel branchings are ubiquitous throughout the vascular system. Such wave reflections may be analyzed in terms of transmission line theory [18,29].

10.3.3 Turbulence in Pulsatile Flow

Transition to turbulence in oscillatory pipe flows occurs through fundamentally different mechanisms than transition in steady flows, for two reasons. The first is that the oscillatory nature of the flow leads to a unique base state, the most important feature of which is the formation of an oscillatory Stokes layer on the tube wall. This layer has its own stability characteristics, which are not comparable to the stability characteristics of the boundary layer of steady flow. The second reason is that temporal deceleration destabilizes the whole flow field, so that perturbations of the Stokes layer can cause the flow to break down into unstable, random fluctuations. Instability often occurs during the deceleration phase of the flow cycle, and is immediately followed by relaminarization as the net flow decays to zero prior to reversal. Because of these characteristics, during deceleration phases of the flow cycle instabilities are observable in the Stokes layer even at much lower Reynolds numbers than those for which they would be found in steady flow [32].

Since the Stokes layer thickness δ itself depends on the flow frequency, transition to turbulence depends on the Womersley number as well as the Reynolds number. Experimental measurements of the velocity made in rigid tubes by noninvasive optical techniques [32] have shown that over a range of values of $\alpha \geq 8$, the flow was found to be fully laminar for $Re_\delta \leq 500$, where Re_δ is the Reynolds number based on the Stokes layer thickness rather than tube diameter. That is, $Re_\delta = U\delta/\nu$. For $500 < Re_\delta < 1300$, the core flow remained laminar while the Stokes layer became unstable during the deceleration phase of fluid motion. This turbulence was most intense in an annular region near the tube wall. These results are in accord with theoretical predictions of instabilities in Stokes layers [33,34]. For higher values of Re_δ , instability can be expected to spread across the tube core.

10.4 Models and Computational Techniques

10.4.1 Approximations to the Navier–Stokes Equations

The Navier–Stokes equations, Equations 10.3 and 10.4, together with the continuity condition, provide a complete set of governing equations for the motion of an incompressible Newtonian fluid. If appropriate boundary and initial conditions can be specified for the motion of such a fluid in a given flow system, in principle, a full set of governing equations and conditions for the system will be known. It may then be expected that the fluid motion can be deduced simply by solution of the resulting boundary value problem. Unfortunately, however, the mathematical difficulties resulting from the nonlinear character of the acceleration terms $D\mathbf{u}/Dt$ in the Navier–Stokes equations are so great that only a very limited number of

exact solutions have ever been found. The simplest of these pertain to cases in which the velocity has the same direction at every point in the flow field, as in the steady and pulsatile pipe flows discussed earlier.

Accordingly, there is a strong incentive to seek conditions under which one or more of the terms in Equation 10.3 are negligible or nearly so, and therefore an approximate and much simpler governing equation can be generated by neglecting them altogether. For example, the Reynolds number represents the ratio of inertial to viscous forces in the flow field. Accordingly, in flows for which $Re \gg 1$, it can be shown that the viscous term $\nu \nabla^2 \mathbf{u}$ is very much smaller than the acceleration $D\mathbf{u}/Dt$. Consequently, it can be omitted from the governing equation, which leads to solutions that are approximately valid at least outside the boundary layer. Conversely, when $Re \ll 1$, the viscous term $\nu \nabla^2 \mathbf{u}$ is much larger than the acceleration $D\mathbf{u}/Dt$.

In summary, these approximations show that viscosity is important in three situations:

1. When the overall Reynolds number is *low*, since then viscous effects act over the full flow field.
2. When the overall Reynolds number is *high*, since then viscosity is important in thin boundary layers.
3. When the flow is *enclosed*, as in a pipe flow, since then the available diffusion time is very large, and viscous effects can become important in the whole flow after some initial region or time.

An alternative approach to seeking simplifications to the Navier–Stokes equations is to accept the full set of equations, but approximate each term in the equation with a simpler form that permits solutions to be developed. Although the resulting equations are only *approximately* correct, the advent of modern digital computers has allowed them to be written with great fineness, so that highly accurate solutions are achieved. These techniques are called *computational fluid dynamics* (CFD).

10.4.2 Computational Fluid Dynamics

The steady improvement in computer speed and memory capabilities since the 1950s has made it possible for CFD to become a very powerful and versatile tool for the analysis of complex problems of interest in the engineering biosciences. By providing a cost-effective means to simulate real flows in detail, CFD permits studying complex problems combining thermodynamics, chemical reaction kinetics, and transport phenomena with fluid flow aspects. In addition, such problems often arise in highly complex geometries. Consequently, they may be far too difficult to study accurately without computational model approaches [35,36].

Furthermore, CFD offers a means for testing flow conditions that are unachievable or prohibitively expensive to test experimentally. For example, most flow loops and wind tunnels are limited to a fixed range of flow rates and governing parameter values. Such limits generally do not apply to CFD analyses. Moreover, flow under a wide range of parameter values may be tested with far less cost than performing repeated experiments.

A representative example of widespread interest to biomedical engineers is the analysis of hemodynamics in blood vessel models. When analyzing biologic responses to flow, or before employing newly developed surgical procedures, characterization studies need to be conducted to substantiate applicability. Cellular metabolic rates in encapsulated and free states, as well as pertinent transport phenomena, can be evaluated in anatomically realistic vessel configurations. These data, coupled with computational fluid dynamics modeling, provide the basis for redesign/reconfigurations as apropos. CFD is a very powerful and versatile tool for an analysis of this type.

At present, computational fluid dynamics methods are finding many new and diverse applications in bioengineering and biomimetics. For example, CFD techniques can be used to predict (1) velocity and stress distribution maps in complex reactor performance studies as well as in vascular and bronchial models; (2) strength of adhesion and dynamics of detachment for mammalian cells; (3) transport properties for nonhomogeneous materials and nonideal interfaces; (4) multicomponent diffusion rates using the Maxwell–Stefan transport model, as opposed to the limited traditional Fickian approach,

incorporating interactive molecular immobilizing sites, and (5) materials processing capabilities useful in encapsulation technology and designing functional surfaces.

Although a full description of CFD techniques is beyond the scope of this chapter, thorough descriptions of the methods and procedures may be found in many texts, for example, Refs. [37–39].

References

1. Bird RB, Stewart WE, Lightfoot EN, 2002. *Transport Phenomena*, 2nd edn. Wiley, New York.
2. Lightfoot EN, 1974. *Transport Phenomena and Living Systems*, Wiley-Interscience, New York.
3. Cooney DO, 1976. *Biomedical Engineering Principles*, Dekker, New York.
4. Lightfoot EN, Duca KA, 2000. The roles of mass transfer in tissue function. In: Bronzino JD (ed) *The Biomedical Engineering Handbook*, 2nd edn. CRC Press, Boca Raton, Chapter 115.
5. Goldstein AS, DiMilla, PA, 1997. Application of fluid mechanic and kinetic models to characterize mammalian cell detachment in a radial-flow chamber, *Biotech. Bioeng.* 55:616.
6. Lauffenburger DA, Linderman JJ, 1993. *Receptors: Models for Binding, Trafficking, and Signaling*, Oxford University Press, New York.
7. Baldyga J, Bourne JR, 1999. *Turbulent Mixing and Chemical Reactions*, John Wiley and Sons, Ltd, Chichester, England.
8. Johnson B, Prud'homme R, 2003. Chemical processing and micro-mixing in confined impinging jets. *AIChE J.* 49(9):2264–82.
9. Lewis AS, Colton CK, 2004. Tissue engineering for insulin replacement in diabetes. In: Ma PX and Elisseff J (eds.) *Scaffolding in Tissue Engineering*, Marcel Dekker, New York.
10. Schwarzer HC, Peukert W, 2004. Tailoring particle size through nanoparticle precipitation, *Chem. Eng. Comm.* 191:580–608.
11. Rabinow B, 2004. Nanosuspensions in drug delivery, *Nature Reviews-Drug Discovery* 3:785–96.
12. Rabinow B, 2005. Pharmacokinetics of drugs administered in nanosuspensions, *Discovery Medicine* 5(25):74–79.
13. Brennen CE, 2005. *Fundamentals of Multiphase Flow*, Cambridge University Press, NY.
14. Panagiotou T, Fisher RJ, 2008. Form nanoparticles via controlled crystallization: A bottom-up approach, *Chem. Eng. Prog.* 10(Oct.):33–39.
15. Panagiotou T, Mesite S, Fisher RJ, 2009. Production of norfloxacin nano-suspensions using microfluidics reaction technology (MRT) through solvent/anti solvent crystallization, *Ind. Eng. Chem. Res.* 48(4):1761–71.
16. Johnson AE, Fisher RJ, Weir GC, Colton CK, 2009. Oxygen consumption and diffusion in assemblages of respiring spheres: Performance enhancement of a bioartificial pancreas, *Chem. Eng. Sci.* 64(22):4470–87.
17. Gradl J, Peukert W, 2009. Simultaneous 3-D observation of different kinetic sub-processes for precipitation in a T-mixer, *Chem. Eng. Sci.* 64:709–20.
18. Fung YC, 1997. *Biomechanics: Circulation*, Springer-Verlag, New York.
19. Lamb H, 1945. *Hydrodynamics*. Dover Publishing, Inc., New York.
20. Schlichting H, 1979. *Boundary Layer Theory*, 7th edn. McGraw-Hill, New York.
21. Hinze JO, 1986. *Turbulence*, (Reissued). McGraw-Hill, New York.
22. Tennekes H, Lumley JL, 1972. *A First Course in Turbulence*, MIT Press, Cambridge.
23. Poiseuille JLM, 1840. Recherches experimentales sur le mouvement des liquides dans les tubes de tres petits diametres; 1. Influence de la pression sur la quantite de liquide qui traverse les tubes de tres petits diametres, *Comptes Rendus* 11:961.
24. Fox RW, McDonald AT, 1992. *Introduction to Fluid Mechanics*, 4th edn. John Wiley and Sons, New York.
25. Roberson JA, Crowe CT, 1997. *Engineering Fluid Mechanics*, 6th edn. John Wiley and Sons, New York.

26. Womersley JR, 1955. Method for the calculation of velocity, rate of flow and viscous drag in arteries when the pressure gradient is known, *J. Physiol.* 127:553.
27. Dwight HB, 1961. *Tables of Integrals and Other Mathematical Data*, McMillan Publishing Co., New York.
28. Gerrard JH, 1971. An experimental investigation of pulsating turbulent water flow in a tube, *J. Fluid Mech.* 46(1):43.
29. Zamir M, 2000. *The Physics of Pulsatile Flow*, AIP Press, Springer-Verlag, New York.
30. Womersley JR, 1955. Oscillatory motion of a viscous liquid in a thin-walled elastic tube—I: The linear approximation for long waves, *Phil. Mag.* 46:199.
31. Atabek SC, Lew HS, 1966. An experimental investigation of pulsating turbulent water flow in a tube, *Biophys. J.* 6:481.
32. Eckmann DM, Grotberg JB, 1991. Experiments on transition to turbulence in oscillatory pipe flow, *J. Fluid Mech.* 222:329.
33. Davis SH, von Kerczek C, 1973. A reformulation of energy stability theory, *Arch. Rat. Mech. Anal.* 52:112.
34. von Kerczek C, Davis SH, 1974. Linear stability theory of oscillatory Stokes layers, *J. Fluid Mech.* 62:753.
35. Rahmani RK, Keith TG, Ayasoufi A, 2006. Numerical simulation and mixing study of pseudoplastic fluids in an industrial helical static mixer, *J. Fluids Eng.* 128:467.
36. Kumar V, Shirke V, Nigam KDP, 2008. Performance of Kenics static mixer over a wide range of Reynolds number, *Chem. Eng. J.* 139:284.
37. Fletcher CA, 1991. *Computational Techniques for Fluid Dynamics*, Volume I, 2nd edn. Springer-Verlag, Berlin.
38. Fletcher CA, 1991. *Computational Techniques for Fluid Dynamics*, Volume II, 2nd edn. Springer-Verlag, Berlin.
39. Chung TJ, 2002. *Computational Fluid Dynamics*, Cambridge University Press, Cambridge.

Animal Surrogate Systems

Michael L. Shuler

Cornell University

Sarina G. Harris

Cornell University

Xinran Li

Cornell University

Mandy B. Esch

Cornell University

11.1	Background.....	11-1
	Limitations of Animal Studies • Alternatives to Animal Studies	
11.2	Cell Culture Analog Concept	11-2
11.3	Prototype CCAs.....	11-3
11.4	Models of Barrier Tissues and Their Use with μ CCAs.....	11-5
11.5	Future Prospects	11-8
	Defining Terms	11-8
	References.....	11-8

11.1 Background

Animal surrogate or cell culture analog (CCA) systems mimic the biochemical response of an animal or human when challenged with a chemical or drug. A true animal surrogate is a device that replicates the circulation, metabolism, and absorption of a chemical and its metabolites using interconnected multiple compartments to represent key organs. These compartments make use of engineered tissues or cell cultures. Physiologically based pharmacokinetic models (PBPK) guide the design of the device. The animal surrogate, particularly a human surrogate, can provide important insights into toxicity and efficacy of a drug or chemical when it is impractical or imprudent to use living animals (or humans) for testing. The combination of a CCA and PBPK provides a rational basis to relate molecular mechanisms to whole-animal response.

11.1.1 Limitations of Animal Studies

The primary method used to test the potential toxicity of a chemical or action of a pharmaceutical is to use animal studies, predominantly with rodents. However, animal studies are problematic. The primary difficulties are that the results may not be meaningful to the assessment of the human response (Gura, 1997). Because of the intrinsic complexity of a living organism and the inherent variability within a species, animal studies are difficult to use to identify unambiguously the underlying molecular mechanism for action of a chemical. The lack of a clear relationship among all of the molecular mechanisms to whole-animal response makes extrapolation across species difficult. This factor is particularly crucial when extrapolation of rodent data to humans is an objective. Further, without a good mechanistic model, it is difficult to rationally extrapolate from high doses to low doses. However, this disadvantage due to complexity can be an advantage; the animal is a “black box” and provides response data even when the mechanism of action is unknown. Further disadvantages reside in the high cost of animal studies, the long period of time often necessary to secure results, and the potential ethical problems in animal studies.

11.1.2 Alternatives to Animal Studies

In vitro methods using isolated cells (e.g., Del Raso, 1993) are inexpensive, quick, and have almost no ethical constraints (except the use of human embryonic stem cells). Because the culture environment can be specified and controlled, the use of isolated cells facilitates interpretation in terms of a biochemical mechanism. Since human cells can be used as well as animal cells, cross-species extrapolation is facilitated.

However, these techniques are not fully representative of human or animal response. Typical *in vitro* experiments expose isolated cells to a static dose of a chemical or drug. It is difficult to relate this static exposure to specific doses in a whole animal. The time-dependent change in the concentration of a chemical in an animal's organ cannot be replicated. If one organ modifies a chemical or prodrug that acts elsewhere, these actions would not be revealed by normal *in vitro* tests. Another related approach is the use of isolated cell cultures in a flow system such as a microphysiometer (McConnell et al., 1992; Cooke and O'Kennedy, 1999). Cells are cultured in a microscale (2.8 μL) flow cell, and changes in pH, measured electronically, report changes in cell physiology. An important use of this technology is the analysis or response of membrane-bound receptors in mammalian cells.

A major limitation of the use of cell cultures is that isolated cells do not fully represent the full range of biochemical activity of the corresponding cell type in a whole animal. Engineered tissues, especially cocultures (Bhatia et al., 1998), can provide a more authentic environment that can improve cell function. Another alternative is the use of tissue slices, typically from the liver (Olinga et al., 1997). However, tissue slices require the sacrifice of the animal, there is intrinsic variability, and biochemical activities can decay rapidly after harvest. The use of isolated tissue slices also does not reproduce interchange of metabolites among organs and the time-dependent exposure that occurs within an animal.

An alternative to both animal and *in vitro* studies is the use of computer models based on PBPK models (Connolly and Andersen, 1991). PBPK models can be applied to both humans and animals. Because PBPK models mimic the integrated, multicompartiment nature of animals, they can predict the time-dependent changes in blood and tissue concentrations of a parent chemical or its metabolites. Although construction of a robust, comprehensive PBPK is time-consuming, once the PBPK is in place, many scenarios concerning exposure to a chemical or treatment strategies with a drug can be tested quickly and inexpensively. Since PBPKs can be constructed for both animals and humans, cross-species extrapolation is facilitated. There are, however, significant limitations in relying solely on PBPK models. PBPK models can only provide a response based on assumed mechanisms, and secondary and unexpected effects are not included. A further limitation is the difficulty in estimating parameters, particularly kinetic parameters.

None of these alternatives to animal studies predict the human response to chemicals or drugs satisfactorily.

11.2 Cell Culture Analog Concept

A CCA is a physical replica of the structure of a PBPK where cells or engineered tissues are used in organ compartments to achieve the metabolic and biochemical characteristics of the animal. The cell culture medium circulates between compartments and acts as a "blood surrogate." Small-scale bioreactors with the appropriate cell types in the physical device represent organs or tissues.

The CCA concept combines attributes of a PBPK and other *in vitro* systems, but unlike other *in vitro* systems, the CCA is an integrated system that can mimic dose dynamics and allows for conversion of a parent compound into metabolites and the interchange of metabolites between compartments. Because volume ratios of organs and compound residence times are replicated physiologically correctly, CCA systems allow for dose exposure scenarios that can replicate the exposure scenarios used in animal studies.

A CCA is intended to work in conjunction with a PBPK as a tool to test and refine mechanistic hypotheses. The PBPK can be made an exact replica of the CCA; the predicted response and measured CCA response should exactly match if the PBPK contains a complete and accurate description of the molecular mechanisms. In the CCA, all flow rates, the number of cells in each compartment, and the levels of each enzyme can be measured independently, so no adjustable parameters are required. If the PBPK predictions and CCA results disagree, then the description of the molecular mechanisms is incomplete. The CCA and PBPK can be used in an iterative manner to test modifications in the proposed mechanism. When the PBPK is extended to describe the whole animal, failure to predict animal response would be due to inaccurate description of transport (particularly within an organ), inability to accurately measure kinetic parameters such as *in vivo* enzyme levels or activities, or the presence of *in vivo* metabolic activities that are not present in the cultured cells or tissues.

The goal is predicting human pharmacological response to drugs or assessing risk due to chemical exposure. A PBPK that can make an accurate prediction of both animal CCA and animal experiments would be "validated." If we use the same approach to construct a human PBPK and CCA for the same compound, then we would have a rational basis to extrapolate animal response to predict human response when human experiments would be inappropriate. Further, since the PBPK is mechanistically based, it would provide a basis for extrapolation to low doses. The CCA/PBPK approach complements animal studies by potentially providing an improved basis for extrapolation to humans.

CCAs can also simulate synergistic or antagonistic behaviors of drugs or chemicals. If a PBPK for compound A and a PBPK for compound B are combined, then the response to any mixture of A and B should be predictable since the mechanisms for response to both A and B are included. Since CCAs are relatively inexpensive, many combinations of compounds A and B with different concentrations can be tested. Synergistic and antagonistic behaviors would be apparent from the behaviors of the cells and tissues cultured within the CCA device.

CCAs used in combination with PBPKs and validated with animal models provide a basis for predicting the human response to mixtures of drugs or chemicals.

11.3 Prototype CCAs

A simple three-component CCA mimicking rodent response to a challenge by naphthalene was developed and tested by Sweeney et al. (1995). While this prototype system did not fulfill the criteria for a CCA of physically realistic organ residence times or ratio of cell numbers in each organ, it did contain multiple compartments and was operated with fluid recirculation, which is necessary to capture the effects of metabolites. Rat hepatoma (H4IIE) cells and lung (L2) cells were used for the liver and the lung compartment, respectively. No cells were required in the "other tissue" compartment in this model since no metabolic reactions were postulated to occur elsewhere for naphthalene or its metabolites. The H4IIE cells contained enzyme systems for activation of naphthalene (cytochrome P450IA1) to the epoxide form and conversion to dihydrodiol (epoxide hydrolase) and conjugation with glutathione (glutathione-S-transferase). The L2 cells had no enzymes for naphthalene activation. Cells were cultured in glass vessels as monolayers. Experiments with this system using lactate dehydrogenase (LDH) release and glutathione levels as dependent parameters supported a hypothesis where naphthalene is activated in the "liver" and reactive metabolites circulate to the "lung," causing glutathione depletion and cell death as measured by LDH release. Increasing the level of cytochrome p450 activity in the "liver" by increasing cell numbers or by preinducing H4IIE cells led to increased death of L2 cells. Experiments with "liver"-blank, "lung"- "lung," and "lung"-blank combinations all supported the hypothesis of a circulating reactive metabolite as the cause of L2 cell death.

The prototype system (Sweeney et al., 1995) was difficult to operate, nonphysiologic, and made time course experiments difficult. An alternative system using packed bed reactors for the "liver" and "lung" compartments that was easier to operate was therefore developed and tested (Ghanem and Shuler, 2000a).

This system successfully allowed time course studies and was physiological with respect to the ratio of “liver” to “lung” cells. While liquid residence times improved in this system, they were still not physiologic (i.e., 114 s vs. an *in vivo* value of 21 s in the liver and 6.6 s vs. an *in vivo* lung value of about 1.5 s) due to physically limited flow through the packed beds. Unlike the prototype system, no response to naphthalene was observed.

This difference in response of the two CCA designs was explained through the use of PBPK models of each CCA (Ghanem and Shuler, 2000b). In the prototype system, the large liquid residence times in the liver and the lung allowed the formation of large amounts of naphthol from naphthalene oxide and presumably the conversion of naphthol into quinones that were toxic. In the packed bed system, liquid residence times were sufficiently small so that the predicted naphthol level was negligible. Thus, the PBPK provided a mechanistic basis to explain the differences in response of the two experimental configurations.

Using another simple CCA, Mufti and Shuler (1998) demonstrated that the response of human hepatoma cells (HepG2) to exposure to dioxin (2,3,7,8-tetrachlorodibenzo-*p*-dioxin) is dependent on how the dose is delivered. The induction of cytochrome p450IA1 activity was used as a model response for exposure to dioxin. Data were evaluated to estimate dioxin levels giving cytochrome P450IA1 activity 0.01% of maximal induced activity. Such an analysis mimics the type of analysis used to estimate the risk due to chemical exposure. The “allowable” dioxin concentration was 4×10^{-3} nM using a batch spinner flask, 4×10^{-4} nM using a one-compartment system with continuous feed, and 1×10^{-5} nM using a simple two-compartment CCA. Further, the response could be correlated to an estimate of the amount of dioxin bound to the cytosolic Ah receptor with a simple model for two different human hepatoma cell lines. This work illustrates the potential usefulness of a CCA approach in risk assessment.

Ma et al. (1997) have discussed an *in vitro* human placenta model for drug testing. This was a two-compartment perfusion system using human trophoblast cells attached to a chemically modified polyethylene terephthalate fibrous matrix as a cell culture scaffold. This system is a CCA in the same sense as the two-compartment system used to estimate the response to dioxin.

Integration of cell culture and microfabrication to form CCA or CCA-like systems has advanced rapidly in the last 10 years. The use of microfabricated devices allows for relatively high-throughput studies that are inexpensive, conserve scarce reagents and tissues, and facilitate automated collection and processing of data. The construction of a simple microscale CCA with multiple cell types and recirculating flow has been accomplished by Sin et al. (2004). The three-compartment system (“liver”–“lung”–other tissue) uses monolayer cultures of HepG2-C3A cells in the “liver” compartment and L2 cells in the “lung” compartment. While monolayer cultures are a poor representation of the physiology of real tissues, this system demonstrates that an “animal-on-a-chip” model is possible. A dissolved oxygen sensor using a fluorescent ruthenium complex was integrated into the system, demonstrating the potential to build real-time sensors into such a device.

The use of a microscale CCA for studying the toxicity of environmental contaminant has been demonstrated using naphthalene as a model toxicant. A silicon-based, microfabricated CCA with four chambers (“liver”–“lung”–“fat”–other tissue) was used for two studies (Viravaidya et al. 2004a, Viravaidya and Shuler, 2004b). These studies demonstrated that naphthalene is converted in the liver by P450IA1 into a reactive metabolite that circulates to the lung compartment. Further, the experiments show that 1,2-naphthalenediol and 1,2-naphthoquinone are the primary reactive metabolites that cause reduction in glutathione levels and cell death in the lung. Excess levels of 1-naphthol are converted to 1,2-naphthalenediol, a result that is consistent with those obtained in a prior study using the macroscale packed bed CCA (Ghanem and Shuler, 2000b). Naphthaquinone and naphthalenediol can be intraconverted through redox cycling generating reactive oxygen species. Naphthaquinone addition is toxic by itself. The addition of a fat compartment modulates the toxicity, providing significant, but partial, protection. These studies, together, demonstrate the utility of microscale CCAs for the simulation of the toxicity of toxicants present in the environment.

More recent studies with microscale CCAs have demonstrated their capability to capture the effects of cancer drugs. Using a 3-D μ CCA device in which liver and colon cells were encapsulated in matrigel, the cytotoxic effects of Tegafur, a cancer drug that metabolizes in the liver to 5-fluorouracil (5-FU), was tested. The metabolite 5-FU acts as a chemotherapeutic agent for colon cancer. Operating the device without liver cells, Tegafur itself was effectively nontoxic to colon cancer cells (HCT-116). Adding liver cells (HepG2/C3A) to the system caused Tegafur to be converted to 5-FU by cytochrome P450 enzymes. The drug now exerted a significant toxic effect on HCT-116 cells (Sung and Shuler, 2009). This level of toxicity on HCT-116 cells was neither observed in 96-well plate experiments (with colon cells only) nor in μ CCA experiments in which liver cells were absent. Results observed *in vitro* have previously only been seen in animal experiments or clinical studies involving humans. They confirm that μ CCA devices are able to reproduce part of the liver metabolism and its consequences on HCT-116 cells.

Tatosian and Shuler (2009) first demonstrated that microscale CCAs could be used to simulate the synergistic effects of cancer drugs. In addition to the two uterine cancer cell lines MES-SA and its MDR variant MES-SA/DX-5, the device used for this study contained HepG2/C3A, representing the liver and metabolism of drugs, a megakaryoblast cell line (MEG-01), representing cells responsible for platelet formation, and a "normal" tissue compartment. Experiments were conducted with doxorubicin as the chemotherapeutic and two MDR suppressors, cyclosporine and nicardipine. Cyclosporine is used clinically as an immune system suppressor and nicardipine is a β -channel blocker. When either cyclosporine or nicardipine was added in addition to doxorubicin, the proliferation of the MDR cells was reduced from treatment with doxorubicin alone. More strikingly, when a combination of nicardipine and cyclosporine was used in place of a higher concentration of either MDR modulator alone, the MDR cell growth rate became negative. This synergistic interaction of the two modulators was not observed when using multiwell plate assays.

Examples of other devices with multicompartments that attempt to emulate aspects of human physiology include Chao et al. (2009), Vozzi et al. (2009), and Zhang et al. (2009). Chao et al. (2009) used a μ CCA-type device with primary human liver cells to predict hepatic clearance of model drug compounds. Vozzi et al. (2009) used a related system to probe the interaction of murine hepatocytes with human vasculature endothelial cells (HUVECs) showing enhanced albumin and urea synthesis due to coculture within the system. Zhang et al. (2009) constructed a μ CCA with four different cell types with local release of growth factors within a single compartment.

Simplifying the operation of μ CCAs is an important step toward the development and use of multiorgan devices. Sung et al. (2010) employed a novel, multilayer design, which enhanced the usability of the devices while allowing hydrogel-cell cultures of multiple types. Gravity-induced flow enabled pumpless operation and prevented bubble formation. Three cell lines representing the liver, tumor tissue, and marrow were cultured in a three-chamber μ CCA that was used to test the toxicity of the anticancer drug, 5-FU. The result was analyzed with a PK-PD model of the device, and compared with the result obtained in static cell culture. Each cell type exhibited differential responses to 5-FU, and the responses in the microfluidic environment were different from those in the static environment, but similar to what was anticipated from animal studies.

The above examples illustrate successful attempts to mimic the metabolic response of animals to drugs and environmental toxicants in integrated systems. The development of future CCAs will greatly benefit from engineered tissues that capture the authentic behavior of cells.

11.4 Models of Barrier Tissues and Their Use with μ CCAs

While the number of drug leads is increasing, the capacity to increase animal and human clinical studies is limited. It is imperative that preclinical testing and predictions for human response become more accurate. CCAs could become important tools contributing to this end. Because barrier tissues can alter the physical and chemical properties of drugs as well as significantly influence a drug's bioavailability,

CCAs of tissues such as the skin, the gastrointestinal tract epithelium, and the lung epithelium are useful additions to the already existing models.

While only a few μ CCAs that contain barrier tissue compartments have been developed so far, in principle, any *in vitro* model of a barrier tissue that was previously developed for drug testing with conventional methods could be adapted for use with μ CCAs.

One of the first reports on the use of engineered cells by Gay et al. (1992) describes the use of a living skin equivalent as an *in vitro* dermatotoxicity model. The living skin equivalent consists of a coculture of human dermal fibroblasts in a collagen-containing matrix overlaid with human keratinocytes that have formed a stratified epidermis. Mitochondrial function was used to assess the toxicity of 18 different chemicals. Eleven compounds classified as nonirritating had minimal or no effect on mitochondrial activity. For seven known human skin irritants, the concentration that inhibited mitochondrial activity by 50% corresponded to the threshold value for each of these compounds to cause irritation on human skin. However, living skin equivalents did not fully mimic the barrier properties of human skin. For example, the permeability of water was 30-fold greater in the living skin equivalent than in human skin. In a study by Kriwet and Parenteau (1996) the permeabilities of 20 different compounds in *in vitro* skin models was reported. Comparisons indicate that skin cultures are slightly more permeable (two- or three-fold) for highly lipophilic substances and considerably more permeable (about 10-fold) for polar substances than human-cadaver or freshly excised human skin.

Validation of four *in vitro* tests for skin corrosion by the European Center for the Validation of Alternative Methods (ECVAM) has led to a combination of *in vitro* tests becoming mandatory for determining skin corrosion of chemicals in the European Union (Fentem and Botham 2002). These *in vitro* tests included a combination of rat skin electrical resistance measurements and commercial reconstituted skin equivalents (EpiDermTM and EpiSkinTM). After a series of prevalidation studies, the protocols have been further improved, resulting in the development of the EpiSkin model that has been validated as the stand-alone method of distinguishing irritants from nonirritants according to EU standards (Kato et al. 2010). These developed skin equivalents are reconstructed human epidermal models. A skin model based on a cell line would be cheaper and more readily available. Suhonen et al. (2003) assessed a stratified rat epidermal keratinocyte cell line grown on a collagen gel at an air-liquid interface by measuring the permeability coefficients of 18 test compounds across the cell layer. The permeabilities were on average twofold greater than for human cadaver epidermis (range 0.3–5.2-fold difference). This cell culture model tended to overpredict the permeability of lipophilic solutes.

So far, the only μ CCA that includes a skin compartment is that developed by Brand et al. (2000). Dorsal skin from male hairless mice was used in a perfusion system that contained a chamber with Hep-G2 liver cells in a compartment downstream of the skin compartment. The system was operated with a syringe pump and subjected to paroxovanadium [VO(O₂)₂ 1, 10 phenanthroline] bpV(phen). A net 22% increase in glucose consumption was measured in the Hep-G2 cells, demonstrating that the system is capable of simulating the uptake of the compound through skin. The authors also show that the system can be used with Caco-2 cell to construct a model of the intestinal epithelium (Brand et al. 2000).

One of the most used cell-based assays is the Caco-2 cell model of the intestine. This model can be used to determine the oral availability of a drug or chemical. Caco-2 cell cultures are derived from a human colon adenocarcinoma cell line. Artursson et al. (2001) reviewed the use of the Caco-2 cell line for the prediction of drug permeability and concluded that Caco-2 monolayers best predict the permeabilities of drugs that exhibit passive transcellular transport. For drug molecules transported by carrier proteins, the expression of the specific transport system in the Caco-2 monolayer needs to be characterized. The cell line, C2Bbe1, is a clonal isolate of Caco-2 cells that is more homogeneous in apical brush border expression than the Caco-2 cell line. These cells form a polarized monolayer with an apical brush border morphologically comparable to the human colon. Tight junctions around the cells act to restrict passive diffusion by the paracellular route mimicking the transport resistance in the intestine. Hydrophobic solutes pass primarily by the transcellular route and hydrophilic compounds by the paracellular route. Yu and Sinko (1997) have demonstrated that the substratum (e.g., membrane) properties

upon which the monolayer forms can become important in estimating the barrier properties of such *in vitro* systems. The barrier effects of the substratum need to be separated from the intrinsic property of the monolayers. Further, Anderle et al. (1998) have shown that the chemical nature of substratum and other culture conditions can alter transport properties. Sattler et al. (1997) provide one example (with hypericin) of how this model system can be used to evaluate effects of formulation (e.g., use of cyclodextrin or liposomes) on oral bioavailability. Another example is the application of the Caco-2 system to transport of paclitaxel across the intestine (Walle and Walle, 1998). Rapid passive transport was partially counterbalanced by an efflux pump (probably P-glycoprotein) limiting oral bioavailability.

Models that simulate first-pass metabolism combine Caco-2 cells with hepatic cells in transwells in which Caco-2 cells are cultured on porous membranes and HepG2/C3A cells are cultured in the chamber beneath. With such systems, the two-organ response can be partially recreated. For example, Caco-2 cells transport the toxin benzo[*a*]pyrene (B[*a*]P) and its metabolites back to the apical side, thereby preventing liver cells toxicity (Choi H et al. 2004). Thus, the known low bioavailability of the B[*a*]P was replicated *in vitro*. To reduce nutrient depletion over the course of 48-h experiments, a simple fluidic circuit that connects the two tissue compartments with each other can be constructed. Using such a system, the synergistic two-organ response to a challenge with 3-methylcholanthrene (3-MC) could be simulated (Choi SH et al. 2004). The induced activity of the enzyme CYP1A1/2 was more elevated than would have been expected from the individual cell cultures.

Mahler et al. have incorporated a Caco-2/MTX-HT29 coculture model into a CCA that contained several other organ compartments. When operated in the presence of liver cells, the uptake and metabolism of acetaminophen could be successfully simulated (Mahler et al., 2009). Both epithelial cells and liver cells metabolize acetaminophen, resulting in a dose-dependent decrease in liver cell viability. The results were within the range of those generated by a study of acetaminophen digestion in mice (Gujral et al. 2002).

Another barrier of interest for drug delivery studies is the blood-brain barrier (BBB). The BBB is formed by the endothelial cells of brain capillaries. The primary characteristics of the BBB are its high resistance to chemical diffusion and transport due to the presence of complex tight junctions that inhibit paracellular transport and its low endocytic activity. Several *in vitro* models of the BBB have been developed, and several authors have reviewed the models and their possible uses as permeability and toxicity screens (Reinhardt and Gloor, 1997; Gumbleton and Audus, 2001; Lundquist and Renftel, 2002). The most common *in vitro* BBB model consists of a monolayer of primary isolated brain capillary endothelial cells, primary isolated endothelial cells from elsewhere in the body, or an endothelial cell line cultured on a membrane insert. The endothelial cells are often cocultured with astrocytes or astroglial cells. In cocultures, the barrier properties of the BBB model increase.

The biggest challenge with *in vitro* BBB models is obtaining endothelial cell cultures that display extensive tight junctions as observed *in vivo*. According to de Boer et al. (1999), the large number of *in vitro* models and the accompanying diversity in laboratory techniques makes quantitative comparisons between models difficult. An example of an *in vitro* BBB system applied to a toxicological study is described by Glynn and Yazdanian (1998) who used bovine brain microvessel endothelial cells grown on porous polycarbonate filters to compare the transport of nevirapine, a reverse transcriptase inhibitor to other HIV antiretroviral agents. Nevirapine was the most permeable antiretroviral agent and hence may have value in HIV treatment in reducing levels of HIV in the brain.

The model developed by Stanness with endothelial cells and astrocytes cocultured on opposite sides of "capillaries" in a hollow-fiber reactor incorporates continuous physiological perfusion of the endothelial cells (Stanness et al., 1996). Harris and Shuler present a unique membrane, an order of magnitude thinner than those available commercially, for close contact coculture of endothelial and astrocytes (Harris and Shuler 2003; Harris Ma, 2004). The microfabricated membrane allows for the integration of the BBB model with other CCA compartments within microfluidic platforms.

Other barrier tissues that research has focused on are the bronchial and the eye epithelium. An epithelial/fibroblast coculture model of the bronchial epithelium was used to examine ozone toxicity (Lang

et al. 1998). Huh et al. have used a microfluidic system to simulate the bronchial epithelium and were able to simulate and acoustically detect cellular-level lung injury induced by fluid mechanical stresses (Huh et al. 2007). Pasternak and Miller (1996) have tested a system to predict eye irritation, combining perfusion and a tissue model consisting of MDCK (Madin–Darby canine kidney) epithelial cells cultured on a semiporous cellulose ester membrane filter. The system could be fully automated using measurement of transepithelial electrical resistance (TER) as an end point. A decrease in TER is an indicator of cell damage and damage of the barrier function of the cell layer. The system was tested using nonionic surfactants and predicted the relative ocular toxicity of these compounds. The perfusion system mimics some dose scenarios (e.g., tearing) more easily than a static system and provides a more consistent environment for the cultured cells. A major advantage is that the TER can be measured throughout the entire exposure protocol without physically disturbing the tissue model and introducing artifacts in the response.

CCAs based on the concepts described here and incorporating advanced-engineered models of barrier tissues could become a powerful tool for testing the bioavailability of pharmaceuticals.

11.5 Future Prospects

The most serious bottleneck in pharmaceutical development is the ability to complete ADMET (adsorption–distribution–metabolism–elimination–toxicity) studies early enough in the development process to focus resources on the best drug candidates. Of particular importance are human surrogates that can improve the probability that a drug will be successful in clinical trials. Such trials may cost more than a 100 million dollars and success at the rate of one in three rather than current values (about one in ten) would offer significant economic advantage.

Over the last 4 years, the development of integrated devices that combine cell culture and microfabrication makes the commercial applications to pharmaceutical evaluation a real possibility (see Freedman, 2004, for discussion). However, the authenticity of engineered tissues remains a hurdle. While tissue with low levels of vascularization (e.g., skin and cartilage) can be mimicked reasonably well, vascularized tissues (e.g., liver) are still quite challenging. As improvements in tissue engineering occur, one of the first applications will be in testing of chemicals and pharmaceuticals. Over the next 10 years, we expect CCA-type systems to become industrially important in preclinical testing of pharmaceuticals and in evaluating chemicals (and chemical mixtures) for toxicity.

Defining Terms

Animal surrogate: A physiologically based cell or tissue multicompartimented device with fluid circulation to mimic metabolism and fate of a drug or chemical.

Engineered tissues: Cell culture mimic of a tissue or organ; often combines a polymer scaffold and one or more cell types.

Physiologically based pharmacokinetic model (PBPK): A computer model that replicates animal physiology by subdividing the body into a number of anatomical compartments, each compartment interconnected through the body fluid systems; used to describe the time-dependent distribution and disposition of a substance.

Tissue slice: A living organ is sliced into thin sections for use in toxicity studies; one primary organ can provide material for many tests.

References

- Anderle P, Niederer E, Werner R, Hilgendorf C, Spahn-Langguth H, Wunderu-Allenspach H, Merkle HP, Langguth P. 1998. P-Glycoprotein (P-gp) mediated efflux in Caco-2 cell monolayers: The influence of culturing conditions and drug exposure on P-gp expression levels. *J. Pharm. Sci.* 87:757.

- Artursson P, Palm K, Luthman K. 2001. Caco-2 monolayers in experimental and theoretical predictions of drug transport. *Adv. Drug Del. Rev.* 46:27.
- Bhatia SN, Balis UJ, Yarmush ML, Toner M. 1998. Microfabrication of hepatocyte/fibroblast co-cultures: Role of homotypic cell interactions. *Biotechnol. Prog.* 14:378.
- Brand RM, Hannah TL, Mueller C, Cetin Y, Hamel FG. 2000. A novel system to study the impact of epithelial barriers on cellular metabolism. *Ann. Biomed. Eng.* 28:1210.
- Chao P, Maguire T, Novik E. 2009. Evaluation of a microfluidic based cell culture platform with primary human hepatocytes for the prediction of hepatic clearance in human. *Biochem. Pharmacol.* 78(6):625.
- Choi H, Nishikawa M, Sakoda A, Sakai, Y. 2004. Feasibility of a simple double-layered coculture system incorporating metabolic processes of the intestine and liver tissue: Application to the analysis of benzo[a]pyrene toxicity. *Toxicol. In Vitro* 18:393.
- Choi SH, Fukuda O, Sakoda A, Sakai Y. 2004. Enhanced cytochrome P450 capacities of Caco-2 and Hep G2 cells in new coculture system under the static and perfused conditions: Evidence for possible organ-to-organ interactions against exogenous stimuli. *Mater. Sci. Eng. C* 24:333.
- Connolly RB, Andersen ME. 1991. Biologically based pharmacodynamic models: Tool for toxicological research and risk assessment. *Annu. Rev. Pharmacol. Toxicol.* 31:503.
- Cooke D, O'Kennedy R. 1999. Comparison of the detrazolium salt assay for succinate dehydrogenase with the cytosensor microphysiometer in the assessment of compound toxicities. *Anal. Biochem.* 274:188-194.
- de Boer AG, Gaillard PJ, Breimer, DD. 1999. The transference of results between blood-brain barrier cell culture systems. *Eur. J. Pharm. Sci.* 8:1.
- Del Raso NJ. 1993. *In vitro* methodologies for enhanced toxicity testing. *Toxicol. Lett.* 68:91
- Fentem JH, Botham PA. 2002. ECVAM's activities in validating alternative tests for skin corrosion and irritation. *Altern. Lab. Anim.* 30(Suppl 2):61.
- Freedman, DH. 2004. The silicon guinea pig. *Technol. Rev.* 107(June):62.
- Gay R, Swiderek M, Nelson D, Ernesti A. 1992. The living skin equivalent as a model *in vitro* for ranking the toxic potential of dermal irritants. *Toxic. In Vitro* 6:303.
- Ghanem A, Shuler, ML. 2000a. Characterization of a perfusion reactor utilizing mammalian cells on microcarrier beads. *Biotechnol. Prog.* 16:471-479.
- Ghanem A, Shuler ML. 2000b. Combining cell culture analogue reactor designs and PBPK models to probe mechanisms of naphthalene toxicity. *Biotechnol. Prog.* 16:334.
- Glynn SL, Yazdaniyan Y. 1998. *In vitro* blood-brain barrier permeability of nevirapine compared to other HIV antiretroviral agents. *J. Pharm. Sci.* 87:306.
- Gujral JS, Knight TR, Farhood A, Bajt ML, Jaeschke H. 2002. Mode of cell death after acetaminophen overdose in mice: Apoptosis or oncotic necrosis? *Toxicol. Sci.* 67(2):322.
- Gumbleton M, Audus KL. 2001. Progress and limitations in the use of *in vitro* cell cultures to serve as a permeability screen for the blood-brain barrier. *J. Pharm. Sci.* 90:1681.
- Gura T. 1997. Systems for identifying new drugs are often faulty. *Science* 273:1041.
- Harris Ma S. 2004. A physiologically based *in vitro* model of the blood-brain barrier utilizing a nanofabricated membrane. PhD Thesis. Cornell University, Ithaca, New York.
- Harris S, Shuler ML. 2003. Growth of endothelial cells on microfabricated silicon nitride membranes for an *in vitro* model of the blood-brain barrier. *Biotechnol. Bioprocess Eng.* 8:246.
- Huh D, Fujioka H, Tung Y, Futai N, Paine III R, Grotberg JB, Takayama S. 2007. Acoustically detectable cellular-level lung injury induced by fluid mechanical stresses in microfluidic airway systems. *PNAS* 104:18886.
- Katoh M, Hamajima F, Ogasawara T, Hata K. 2010. Assessment of human epidermal model LabCyte EPI-MODEL for *in vitro* skin irritation testing according to European Centre for the Validation of Alternative Methods (ECVAM)-validated protocol. *J. Toxicol. Sci.* 34(3):327.
- Kriwet K, Parenteau NL. 1996. *In vitro* skin models. *Cosmetics Toiletries* 111(Feb):93.

- Lang DS, Jorres RA, Mucke M, Siegfried W, Magnussen H. 1998. Interactions between human broncho-epithelial cells and lung fibroblasts after ozone exposure *in vitro*. *Toxicol. Lett.* 96,97:13.
- Lundquist S, Renftel M. 2002. The use of *in vitro* cell culture models for mechanistic studies and as permeability screens for the blood-brain barrier in the pharmaceutical industry—Background and current status in the drug discovery process. *Vasc. Pharmacol.* 38:335.
- Ma T, Yang S-T, Kniss DA. 1997. Development of an *in vitro* human placenta model by the cultivation of human trophoblasts in a fiber-based bioreactor system. *Am. Inst. Chem. Eng. Ann. Mtg.*, Los Angeles, CA, Nov. 16–21.
- Mahler GJ, Esch MB, Glahn RP, Shuler ML. 2009. Characterization of a gastrointestinal tract microscale cell culture analog used to predict drug toxicity. *Biotechnol Bioeng.* 104(1):193.
- McConnell HM, Owicki JC, Parce JW, Miller DL, Baxter GT, Wada HG, Pitchford S. 1992. The cytometer microphysiometer: Biological applications of silicon technology. *Science* 257:1906.
- Mufti NA, Shuler ML. 1998. Different *in vitro* systems affect CYP1A1 activity in response to 2,3,7,8-tetrachlorodibenzo-*p*-dioxin. *Toxicol. In Vitro* 12:259.
- Olinga, P, Meijer DKF, Slooff, MJH, Groothuis, GMM. 1997. Liver slices in *in vitro* pharmacotoxicology with special reference to the use of human liver tissue. *Toxicol. In Vitro* 12:77.
- Pasternak AS, Miller WM. 1996. Measurement of trans-epithelial electrical resistance in perfusion: Potential application for *in vitro* ocular toxicity testing. *Biotechnol. Bioeng.* 50:568.
- Reinhardt CA, Gloor SM. 1997. Co-culture blood-brain barrier models and their use for pharmacotoxicological screening. *Toxicol. In Vitro.* 11:513.
- Sattler S, Schaefer U, Schneider W, Hoelzl J, Lehr C-M. 1997. Binding, uptake, and transport of hypericin by Caco-2 cell monolayers. *J. Pharm. Sci.* 86:1120.
- Sin A, Chin KC, Jamil MF, Kostov Y, Rao G, Shuler ML. 2004. The design and fabrication of three-chamber microscale cell culture analog devices with integrated dissolved oxygen sensors. *Biotechnol. Prog.* 20:338.
- Stanness KA, Guatteo E, Janigro D. 1996. A dynamic model of the blood-brain barrier “*in vitro*.” *NeuroToxicol.* 17:481.
- Suhonen TM, Pasonen-Seppanen S, Kirjavainen M, Tammi M, Tammi R, Urtti A. 2003. Epidermal cell culture model derived from rat keratinocytes with permeability characteristics comparable to human cadaver skin. *Eur. J. Pharm. Sci.* 20:107.
- Sung JH, Kam, C, Shuler ML. 2010. A microfluidic device for a pharmacokinetic–pharmacodynamic (PK–PD) model on a chip. *Lab Chip* 10:446.
- Sung JH, Shuler ML 2009. A micro cell culture analog (microCCA) with 3-D hydrogel culture of multiple cell lines to assess metabolism-dependent cytotoxicity of anti-cancer drugs. *Lab Chip* 9:1385.
- Sweeney LM, Shuler ML, Babish JG, Ghanem A. 1995. A cell culture analog of rodent physiology: Application to naphthalene toxicology. *Toxicol. In Vitro* 9:307.
- Tatosian DA, Shuler ML. 2009. A novel system for evaluation of drug mixtures for potential efficacy in treating multidrug resistant cancers. *Biotechnol. Bioeng.* 103:187.
- Walle UK, Walle T. 1998. Taxol transport by human intestinal epithelial Caco-2 cells. *Drug Metabol. Disposit.* 26:343.
- Yu H, Sinko PJ. 1997. Influence of the microporous substratum and hydrodynamics on resistances to drug transport in cell culture systems: Calculation of intrinsic transport parameters. *J. Pharm. Sci.* 86:1448.
- Viravaidya K, Sin A, Shuler ML. 2004a. Development of a microscale cell culture analog to probe naphthalene toxicity. *Biotechnol. Prog.* 20:316.
- Viravaidya K, Shuler ML. 2004b. Incorporation of 3T3-L1 cells to mimic bioaccumulation in a microscale cell culture analog device for toxicity studies. *Biotechnol. Prog.* 20:590.
- Vozzi F, Heinrich JM, Bader A, Ahluwali AD. 2009. Connected culture of murine hepatocytes and HUVEC in a multicompartimental bioreactor. *Tissue Eng Part A* 15(6):1291.
- Zhang C, Zhao Z, Abdul Rahim NA, van Noort D, Yu H. 2009. Towards a human-on-chip: Culturing multiple cell types on a chip with compartmentalized microenvironments. *Lab Chip.* 9(22):3185.

13

Transport Phenomena and the Microenvironment

13.1	Introduction	13-1
13.2	Tissue Microenvironments	13-3
	Specifying Performance Criteria • Estimating Tissue Function • Communication • Cellularity • Dynamics • Geometry • System Interactions: Reaction and Transport Processes	
13.3	Reacting Systems and Bioreactors.....	13-9
	Reactor Types • Design of Microreactors • Scale-Up and Operational Maps	
13.4	Illustrative Example: Control of Hormone Diseases via Tissue Therapy	13-11
	Transport Considerations • Selection of Diabetes as Representative Case Study • Encapsulation Motif: Specifications, Design, and Evaluation	
	References.....	13-16

Robert J. Fisher
*SABRE Institute and
Massachusetts Institute
of Technology*

Robert A. Peattie
Tufts University

13.1 Introduction

The evolving technologies and advances in the engineering biosciences are expected to have significant impact in the fields of pharmaceutical engineering (drug production, delivery, targeting, and metabolism), molecular engineering (biomaterial design and biomimetics), biomedical reaction engineering (microreactor design, animal surrogate systems, artificial organs, and extracorporeal devices), and metabolic process control (receptor–ligand binding, signal transduction, and trafficking). Since the understanding of the cell/tissue environment will help produce major developments in all of these areas, the ability to characterize, control, and ultimately manipulate the microenvironment is critical. The key challenges, as identified by many sources (e.g., Palsson, 2000), are (1) proper reconstruction of the microenvironment for the development of tissue function, (2) scale-up to generate a significant amount of properly functioning microenvironments to be of clinical importance, (3) automating cellular therapy systems/devices to operate and perform at clinically meaningful scales, and (4) implementation in the clinical setting in concert with all the cell handling and preservation procedures required to administer cellular therapies. The direction of this chapter is toward supporting efforts to address these issues. Thus, the primary objective is to introduce the fundamental concepts needed to reconstruct tissues *ex vivo* and produce cells of sufficient quantity that maintain stabilized performance for extended time periods of clinical relevance. The delivery of cellular therapies, as a goal, was selected as one representative theme for illustration.

Before we can develop useful *ex vivo* and *in vitro* systems for the numerous applications sought, we must first have an appreciation of cellular function *in vivo*. Knowledge of the tissue microenvironment and communication with other organs is essential. We need to understand how tissue function can be

built, reconstructed, and/or modified. Our approach is based on the following axioms (Palsson, 2000): (1) in organogenesis and wound healing, proper cellular communications, with respect to each other's activities, are of paramount concern since a systematic and regulated response is required from all participating cells; (2) the function of fully formed organs is strongly dependent on the coordinated function of multiple cell types with tissue function based on multicellular aggregates; (3) the functionality of an individual cell is strongly affected by its microenvironment (within 100 μm of the cell, i.e., the characteristic length scale); (4) this microenvironment is further characterized by (i) neighboring cells, that is, cell-cell contact and presence of molecular signals (soluble growth factors, signal transduction, trafficking, etc.), (ii) transport processes and physical interactions with the extracellular matrix (ECM), and (iii) the local geometry, in particular its effects on microcirculation.

The importance of the microcirculation is that it connects all the microenvironments in every tissue to their larger whole-body environment. Most metabolically active cells in the body are located within a few hundred micrometers from a capillary. This high degree of vascularity is necessary to provide the perfusion environment that connects every cell to a source and sink for respiratory gases, a source of nutrients from the small intestine, the hormones from the pancreas, liver, and glandular system, clearance of waste products via the kidneys and liver, delivery of immune system respondents, and so forth (Jain, 1994). Further, the three-dimensional (3-D) arrangement of microvessels in any tissue bed is critical for efficient functioning. This *in vivo* network develops in response to physical and chemical (molecular) clues and thus reproduction of the microenvironment with its attendant signal molecule capabilities is an essential feature of an engineered tissue system.

The engineering of these functions *ex vivo* is within the domain of bioreactor design (Freshney, 2000; Shuler, 2000), a topic discussed briefly in this chapter and elsewhere in this handbook. Cell culture devices must possess perfusion characteristics that allow for uniformity down to the 100 μm length scale. These are stringent design requirements that must be addressed with a high priority to properly account for the role of neighboring cells, the ECM, cyto-/chemokine and hormone trafficking, cell-ECM geometric factors, respiratory dynamics, and transport of nutrients and metabolic by-products for each tissue system considered. To achieve proper reconstitution of the cellular microenvironment, these dynamic, chemical, and geometric variables must be duplicated as accurately as possible. Since this is a difficult task, significant effort is devoted to developing quantitative methods to describe the cell-scale microenvironment. Once available, these methods can be used to develop an understanding of the key problems associated with any given phenomenological event, formulate solution strategies, and analyze experimental results. It is important to stress that most useful analyses in tissue engineering are performed with approximate calculations based on physiological and cell biological data, basically, determining tissue "specification sheets." Such calculations are useful for interpreting organ physiology, and providing a starting point for more extensive experimental and computational programs needed to identify the specific needs of a given tissue system (examples are given below). Using the tools obtained from studying subjects such as biomimetics (materials behavior, membrane development, and similitude/simulation techniques), transport phenomena (mass, heat, and momentum transfer), reaction kinetics, and reactor performance/design, systems that control microenvironments for *in vivo*, *ex vivo*, or *in vitro* applications can be developed.

The emphasis taken here to achieve these desired tissue microenvironments is through use of novel membrane systems designed to possess unique features for the specific application of interest, and in many cases to exhibit stimulant/response characteristics. These so-called "intelligent" or "smart" membranes are the result of biomimicry, that is, they have biomimetic features. Through functionalized membranes, typically in concerted assemblies, these systems respond to external stresses (chemical and/or physical in nature) to eliminate the threat either by altering stress characteristics or by modifying and/or protecting the cell/tissue microenvironment. An example (to be discussed further later in this chapter) is a microencapsulation motif for beta cell islet clusters to perform as an artificial pancreas. This system uses multiple membrane materials, each with its unique characteristics and performance requirements, coupled with nanospheres dispersed throughout the matrix, which contain additional

materials to enhance transport and/or barrier properties, and initiate and/or respond to specific stimuli. This chapter is structured to develop an understanding of the technologies required to design systems of this nature and to ensure their stable performance.

13.2 Tissue Microenvironments

The communication of every cell with its immediate environment and other tissues establishes important spatial-temporal characteristics and develops a significant signaling/information processing network. The microenvironment is further characterized by cellular composition, the ECM, molecular dynamics (nutrients, metabolic waste products, and respiratory gases traffic in and out of the microenvironment in a highly dynamic manner), and local geometric factors (size scale of $\sim 100\ \mu\text{m}$). Each of these can also provide the cell with important signals (dependent upon a characteristic time and length scale) to initiate specific cell functions for the tissue system to perform in a coordinated manner. If this arrangement is disrupted, cells that are unable to provide tissue function are obtained. Further discussions on this topic are presented in later sections devoted to cellular communications.

13.2.1 Specifying Performance Criteria

Each tissue or organ undergoes its own unique and complex developmental program. There are, however, a number of common features of each component of the microenvironment that will be discussed in subsequent sections. The idea is to establish general criteria to guide the design of systems possessing these requisite global characteristics and functionality. Two representative tissue microenvironments (blood and bone) are selected here for a brief comparison to illustrate common features and distinctions.

13.2.2 Estimating Tissue Function

Blood: Interpretation of the physiological respiratory function of blood has been aided by insightful yet straightforward approximating calculations to establish basic functionalities and biologic design specifications. For example, blood needs to deliver about 10 mM of oxygen per minute to the body. Given a gross circulation rate of about 5 L/min, the delivery rate to tissues is about 2 mM oxygen per L during each pass through its circulatory system. The basic requirements that circulating blood must meet to deliver adequate oxygen to tissues are determined by the following: blood leaving the lungs has a partial pressure of oxygen between 90–100 mm Hg and drops to about 35–40 mm Hg in the venous blood at rest and to about 27 mm Hg during strenuous exercise. Thus, the required oxygen delivered to the tissues is accomplished through a partial pressure drop of about 55 mm Hg, on average. Unfortunately, the solubility of oxygen in aqueous media is low; its solubility given by a Henry's law relationship, where the liquid phase concentration is linearly proportional to its partial pressure. This equilibrium coefficient is about 0.0013 mM/mm Hg. Consequently, the amount of oxygen that can be delivered by this mechanism is limited to roughly 0.07 mM, significantly below the required 2 mM. The solubility of oxygen in blood must therefore be enhanced by some other mechanism, by a factor of about 30 at rest and 60 during strenuous exercise. This, of course, is accomplished by hemoglobin within red blood cells. However, to see how this came about, let us probe a little further. Enhancement could be obtained by putting an oxygen binding protein into the perfusion fluid. To stay within the vascular bed, this protein would have to be 50–100 kDa in size. With only a single binding site, the required protein concentration is 500–1000 g/L, which is too concentrated from both an osmolarity and a viscosity (10 \times) standpoint and clearly impractical. Furthermore, circulating proteases will lead to a short plasma half-life for these proteins. By increasing to four sites per oxygen-carrying molecule, the protein concentration is reduced to 2.3 mM and confining it within a protective cell membrane solves the escape, viscosity, and proteolysis problems. Obviously, nature has solved these problems since these are characteristics of hemoglobin within red blood cells. Furthermore, a more elaborate kinetics study of the binding characteristics of

hemoglobin shows that a positive cooperativity exists and can provide the desired oxygen transfer capabilities both at rest and under strenuous exercise.

These functions of blood establish standards that are difficult to mimic. When designing systems for *in vivo* applications promoting angiogenesis and minimizing diffusion lengths help alleviate oxygen delivery problems. Attempting to mimic this behavior in perfusion reactors, whether as extracorporeal devices or as production systems, is more complex since a blood substitute (e.g., perfluorocarbons in microemulsions) is typically needed. Performance, functionality, toxicity, and transport phenomena issues must be addressed. In summary, to maintain tissue viability and function within devices and microcapsules, methods are being developed to enhance mass transfer, especially that of oxygen. These methods include use of vascularizing membranes, *in situ* oxygen generation, use of thinner encapsulation membranes, and enhancing oxygen-carrying capacity in encapsulated materials. All these topics are addressed in subsequent sections throughout this chapter.

Bone marrow microenvironment: Perfusion rates in human bone marrow cultures are set by determining how often the media should be replenished. A dynamics similarity analysis with the *in vivo* situation is therefore appropriate. With a cell density of about 500 million cells/mL, blood perfusion through bone marrow *in vivo* is about 0.08 mL/cm³/minute, that is, a cell-specific perfusion rate of about 2.3 mL/10 million cells/day. Cell densities on the order of one million cells/mL are typical for starting cultures; 10 million cells would be placed in 10 mL of culture media containing about 20% serum (vol/vol). To accomplish a full daily media exchange would correspond to replacing the serum at 2 mL/10 million cells/day, which is similar to the number calculated previously. These conditions were used in the late 1980s and lead to the development of prolific cell cultures of human bone marrow. Subsequent scale-up produced a clinically meaningful number of cells that are currently undergoing clinical trials.

13.2.3 Communication

Tissue development is regulated by a complex set of events in which cells of the developing organ interact with each other and with other organs and tissue microenvironments. The vascular system connects all the microenvironments in every tissue to their larger whole-body environment. As discussed previously, a high degree of vascularity is necessary to transport signal molecules through this communication network at the rate and quantity required.

Cellular communication within tissues: Cells within tissues communicate with each other for a variety of important reasons, such as localizing cells within the microenvironment, directing cellular migration, and initiating growth factor-mediated developmental programs (Long, 2000). This communication is accomplished via three primary methods: (1) cells secrete a wide variety of soluble signal and messenger molecules, including Ca²⁺, hormones, paracrine and autocrine agents, catecholamines, growth and inhibitory factors, eicosanoids, chemokines, and many other types of cytokines, (2) via direct cell–cell contact, and (3) secreted proteins that alter the ECM chemical milieu. Each of these communication techniques differ in terms of their specificity, and their characteristic time and length scales, thus suitable to convey a particular type of message. These information exchanges are mediated by well-defined, highly specific receptor–ligand interactions that stimulate or control cell activities. For example, the appearance of specific growth factors leads to proliferation of cells expressing receptors for these growth factors. Further, chemical gradients exist that signal cells to move along tracts of molecules into a defined tissue area. High concentrations of the attractant or other signals then serve to localize cells by stopping their sojourn.

Soluble growth factors: Growth factors are a critical component of the tissue microenvironment inducing multifunctional behavior (Freshney, 2000). Their role in the signal processing network is particularly important for this chapter. They are small proteins in the size range of 15–20 kDa with a relatively high chemical stability. Initially, growth factors were discovered as active factors that originated in biological fluids and were known as colony-stimulating factors. It is now known that growth factors are

produced by a signaling cell and secreted to reach target cells through autocrine and paracrine mechanisms. They bind to their receptors, found in cellular membranes, with high affinities and trigger a complex signal transduction process. Typically, the receptor complex changes in such a way that its intracellular components take on catalytic activities. These receptor–ligand complexes are internalized in some cases with a typical time constant for internalization of the order 15–30 min. It has been shown that 10,000–70,000 growth factor molecules need to be consumed to stimulate cell division in complex cell cultures. Growth factors propagate a maximum distance of about 200 μm from their secretion source. Minimum time constants for the signaling processes are about 20 min. However, much longer times are encountered if the growth factor is sequestered. The kinetics of these processes are complex and detailed analyses can be found elsewhere (Lauffenburger and Linderman, 1993) since they are beyond the scope of this chapter.

Direct cell-to-cell contact: Direct contact between adjacent cells is common in epithelially derived tissues, and can also occur with osteocytes and both smooth and cardiac myocytes. Contact is maintained through specialized membrane structures, including desmosomes, tight junctions, and gap junctions, each of which incorporates cell adhesion molecules, surface proteins, cadherins, and connexins. Tight junctions and desmosomes are thought to bind adjacent cells cohesively, preventing fluid flow between cells. *In vivo* they are found, for example, in intestinal mucosal epithelium, where their presence prevents leakage of the intestinal contents through the mucosa. In contrast, gap junctions form direct cytoplasmic bridges between adjacent cells. The functional unit of a gap junction, called a connexon, is ~ 1.5 nm in diameter, and thus will allow molecules below about 1 kDa to pass between cells.

These cell-to-cell connections permit mechanical forces to be transmitted through tissue beds. A rapidly growing body of literature details how fluid mechanical shear forces influence cell and tissue adhesion functions (a topic discussed more thoroughly in other chapters), and it is known that signals are transmitted to the nucleus by cell stretching and compression. Thus, the mechanical role of the cytoskeleton in affecting tissue function by transducing and responding to mechanical forces is becoming better understood.

Extracellular matrix and cell–tissue interactions: The ECM is the chemical microenvironment that interconnects all the cells in the tissue and their cytoskeletal elements. The multifunctional behavior of the ECM is an important facet of tissue performance since it provides tissue with mechanical support. The ECM also provides cells with a substrate in which to migrate, as well as serving as a storage site for signal and communications molecules. A number of adhesion and ECM receptor molecules located on the cell surface play a major role in facilitating cell–ECM communications by transmitting instructions for migration, replication, differentiation, and apoptosis. Consequently, the ECM is composed of a large number of components that have varying mechanical and regulatory capabilities that provide its structural, dynamic, and informational functions. It is constantly being modified. For instance, ECM components are degraded by metalloproteases. About 3% of the matrix in cardiac muscle is turned over daily.

The composition of the ECM determines the nature of the signals being processed and in turn can be governed or modified by the cells comprising the tissue. The ECM can direct all cellular fate processes, providing a means for cells to communicate with signals that are more stable and may be more specific and stronger than those delivered by the diffusion process needed with growth factors. A summary of the components of the ECM and their functions for various tissues is given in Palsson (2000).

Many research groups are attempting to construct artificial ECMs. The scaffolding for these matrices has taken the form of polymer materials that can be surface modified for desired functionalities. In some cases, they are designed to be biodegradable, allowing the cells to replace this material with its natural counterpart as they establish themselves and their tissue function. The major obstacle is that the properties of this matrix are difficult to specify since the properties of natural ECMs are complex and not fully known. Furthermore, two-way communication between cells is difficult to mimic since the information contained within these conversations is also not fully known. At this time, the full spectrum of ECM functionalities can only be provided by the cells themselves.

Communication with the whole-body environment: The importance of the vascular system and in particular, the microcirculation, cannot be overemphasized. This network is needed to connect all the micro-environments in every tissue to their larger whole-body environment. A complex vascular morphology is established such that most metabolically active cells in the body are located within a few hundred micrometers from a capillary. This high degree of vascularity is necessary to provide the perfusion environment that connects every cell to a source and sink for respiratory gases, a source of nutrients from the small intestine, the hormones from the pancreas, liver, and glandular system, clearance of waste products via the kidneys and liver, delivery of immune system respondents, and so forth (Freshney, 2000; Jain, 1994; other chapters in this handbook). Transport of mass (and heat) in normal and neoplastic tissues occurs primarily by convection and diffusion processes that take place throughout the whole circulatory system and ECM (Fournier, 1999; Jain, 1994). The design of *in vivo* systems therefore must consider methods to promote this communication process, not only deal with the transport issues of the device itself. The implanted tissue system vasculature must therefore consist of (1) vessels recruited from the preexisting network of the host vasculature and (2) vessels resulting from the angiogenic response of host vessels to implanted cells (Hosack et al., 2008; Jain, 1994; Peattie et al., 2004, Riley et al., 2006). Although the implant vascular originates from the host vasculature, its organization may be completely different depending on the tissue type, its growth rate, and its location. The architecture may be different not only among varying tissue types but also between an implant and any spontaneous tissue outgrowth originating from growth factor stimuli, from the implant or as a whole-body response.

A blood-borne molecule or cell that enters the vasculature reaches the tissue microenvironment and individual cells via (i) distribution through the vascular tree, (ii) convection and diffusion across the microvascular wall, (iii) convection and diffusion through the interstitial fluid and ECM, and (iv) transport across the cell membrane (Lightfoot, 1974). The sojourn of molecules through the vasculature is governed by the morphology of that network (i.e., the number, length, diameter, and geometrical arrangement of various blood vessels) and the blood flow rate (determining perfusion performance). Transport across vessel walls to interstitial space and across cell membranes depends on the physical properties of the molecules (e.g., size, charge, and configuration), physiological properties of these barriers (e.g., transport pathways), and driving force (e.g., concentration and pressure gradients). Furthermore, specific or nonspecific binding to tissue components can alter the transport rate of molecules through a barrier by hindering the species and/or changing the transport parameters (Fisher, 1989).

Since the convective component of the transport processes via blood depends primarily on local blood flow in the tissue, coupled with vascular morphology of the tissue, hydrodynamics must be considered in designing for performance. In addition, perfusion rate requirements must take into account diffusional boundary layers along with the geometric factors of tissues and implants. In general, implant volume changes as a function of time more rapidly than for normal tissue due to tissue outgrowth, fibrotic tissue formation, and macrophage attachment. All these effects contribute to increased diffusion paths and nutrient consumption. Even with these distinctions between different tissues, the mathematical models of transport in normal, neoplastic, and implanted tissues both with and without barriers, whether *in vivo*, *ex vivo*, or *in vitro*, are identical. The only differences lie in the selection of physiological, geometric, and transport parameters. Furthermore, similar transport analyses can be applied to extracorporeal and novel bioreactor systems and their associated scale-up studies. Examples include artificial organs, animal surrogate systems, and the coupling of compartmental analysis with cell culture analogs in drug delivery and efficacy testing. Designing appropriate bioreactor systems for these applications is a challenge for tissue engineering teams collaborating with reaction engineering experts.

13.2.4 Cellularity

The number of cells found in the tissue microenvironment can be estimated as follows. The packing density of cells is on the order of a billion cells/cm³; tissues typically form with a porosity of between 0.5 and 0.7 and therefore have a cell density of ~100–500 million cells/cm³. Thus, an order of magnitude

estimate for a cube with a 100 μm edge, the mean intercapillary length scale, is about 500 cells. For comparison, simple multicellular organisms have about 1000 cells. Of course, the cellularity of the tissue microenvironment is dependent upon the tissue and the cell types composing it. At the extreme, ligaments, tendons, aponeuroses, and their associated dense connective tissue are acellular. Fibrocartilage is at the low end of cell-containing tissues, with about one million cells/ cm^3 or about 1 cell per characteristic cube. This implies that the microenvironment is simply one cell maintaining its ECM.

In most tissue microenvironments, many cell types are found in addition to the predominate cells that characterize that tissue. Leukocytes and immune system cells, including lymphocytes, monocytes, macrophages, plasma cells, and mast cells, can be demonstrated in nearly all tissues and organs, particularly during periods of inflammation. Precursor cells and residual undifferentiated cell types are present in most tissues as well, even in adults. Such cell types include mesenchymal cells (connective tissues), satellite cells (skeletal muscle), and pluripotential stem cells (hematopoietic tissues). Endothelial cells make up the wall of capillary microvessels, and thus are present in all perfused tissues.

13.2.5 Dynamics

In most tissues and organs, the microenvironment is constantly changing due to the transient nature of the multitude of events occurring. Matrix replacement, cell motion, perfusion, oxygenation, metabolism, and cell signaling all contribute to a continuous turnover. Each of these events has its own characteristic time constant. It is the relative magnitude of these time constants that dictate which processes can be considered in a pseudo-steady state with respect to the others. Determining the dynamic parameters of the major events (estimates available in Lightfoot, 1974; Long, 2000; Palsson, 2000) is imperative for successful modeling and design studies.

Time scaling of the systemic differential equations governing the physicochemical behavior of any tissue is extremely valuable in reducing the number of dependent variables needed to predict responses to selected perturbations and to evaluate system stability. In many cell-based systems, overall dynamics are controlled by transport and/or reaction rates. Controlling selected species transport then becomes the major issue since, under certain conditions, transport resistances may be beneficial. For example, when substrate inhibition kinetics is observed, performance is enhanced as the substrate transport rate is restricted. Furthermore, multiple steady states, with subsequent hysteresis problems, have been observed in these encapsulated systems as well as in continuous, suspension cell cultures (Bruns et al., 1973; Europa et al., 2000; Fisher et al., 2000). Consequently, perturbations in the macroenvironment of an encapsulated cell/tissue system can force the system to a new, less desired, steady state where cellular metabolism as measured by, for example, glucose consumption and amino acid synthesis is altered. Simply returning the macroenvironment to its original state may not be effective in returning the cellular system to its original (desired) metabolic state. The perturbation magnitudes that force a system to seek a new steady state, and subsequent hysteresis lags, are readily estimated from basic kinetics and mass transfer studies (Bruns et al., 1973; Europa et al., 2000). However, incorporation of intelligent behavior into an encapsulation system permits mediation of this behavior. This may be accomplished by controlling the cell/tissue microenvironment through the modification of externally induced chemical, biological (as in a macrophage or T cell), or physical stresses, and through selectively and temporally releasing therapeutic agents or signal compounds to modify cellular metabolism. Various novel bioreactor systems that are currently available as “off-the-shelf” items can be modified to perform these tasks in appropriate hydrodynamic flow fields, with controlled transport and/or contacting patterns, and at a microscale of relevance.

13.2.6 Geometry

Geometric similitude is important in attempting to mimic *in vivo* tissue behavior in engineered devices. The shape and size of any given tissue bed must be known to aid in the design of these devices since

geometric parameters help establish constraints for both physical and behavioral criteria. Many micro-environments are effectively 2-D surfaces (Palsson, 2000). Bone marrow has a fractal cellular arrangement with an effective dimensionality of 2.7, whereas the brain is a 3-D structure. These facts dictate the type of culture technique (high density, as obtained with hollow fiber devices, versus the conventional monolayer culture) to be used for best implant performance. For example, choriocarcinoma cells release more human chorionic gonadotrophin when using this type of high-density culture (Freshney, 2000).

13.2.7 System Interactions: Reaction and Transport Processes

The interactions brought about by communications between tissue microenvironments and the whole-body system, via the vascular network, provide a basis for the systems biology approach taken to understand the performance differences observed *in vivo* versus *in vitro*. The response of one tissue system to changes in another due to signals generated, metabolic product accumulation, or hormone appearances must be properly mimicked by coupling individual cell culture analog systems through a series of micro-bioreactors if whole-body *in vivo* responses are to be meaningfully predicted. The need for microscale reactors is obvious given the limited amount of tissue or cells available for many *in vitro* studies. This is particularly true when dealing with the pancreatic system (Galletti et al., 2000; Lewis and Colton, 2004) where intact Langerhans islets must be used rather than individual beta cells for induced insulin production by glucose stimulation. Their supply is extremely limited and maintaining viability and functionality is quite complex since the islet clusters *in vivo* are highly vascularized and this feature is difficult to reproduce in preservation protocols.

The coupling of reaction kinetics with transport processes is necessary to develop effective bioreactor systems. Further discussion of this topic is given later in this chapter. See Sections 13.3 and 13.4 for reactor design specifications and mass transfer analysis in encapsulation motifs, respectively. Heat and momentum transport are major topics discussed in other chapters in this handbook. Brief comments on the necessity for these studies are presented as follows.

In all living organisms, and especially the higher animals, diffusion and flow limitations are of critical importance. In adapting problem-solving strategies for mathematical analysis and modeling of specific physiologic transport problems, it becomes particularly important to establish orders of magnitude and to make realistic limiting calculations. Especially attractive for these purposes are dimensional analysis and pharmacokinetic modeling; it seems in fact that these may permit unifying the whole of biological mass transport. Distributed-parameter transport modeling is also helpful. To obtain useful models, one must set very specific goals and work toward them by systematically comparing theory and experiment. Particularly important are the estimation of transport properties and the development of specialized conservation equations, as for ultrathin membranes, about which only limited information is known. Thus, analysis of physiologic transport stands in strong contrast to classical areas of transport phenomena (Bird et al., 2002; Brodkey and Hershey, 1988; Deen, 1996; Fournier, 1999; Lightfoot, 1974; Rosner, 1986).

Mass transfer lies at the heart of physiology and provides major constraints on the metabolic rates and anatomy of living organisms, from the organization of organ networks to molecular intracellular structures. Limitations on mass transfer rates are major constraints for nutrient supply, waste elimination, and information transmission. The primary functional units of metabolically active muscle and brain, liver lobules, and kidney nephrons have evolved to just eliminate significant mass transfer limitations in the physiological state (Lightfoot, 1974). Turnover rates of highly regulated enzymes are just less than diffusion limitations. Signal transmission rates are frequently mass transport limited (Lauffenburger and Linderman, 1993) and very ingenious mechanisms have evolved to speed these processes (Palsson, 2000). Consequently, understanding tissue mass transport is important to accurately interpret transport-based experiments that involve complex interactions of transport and reaction processes, and further, our ability to design effective devices and biosensors.

Models for microvascular heat transfer are useful for understanding tissue thermoregulation, for optimizing thermal therapies such as hypothermia treatment, for modeling thermal regulatory response at the tissue level, for assessing microenvironment hazards that involve tissue heating, for using thermal means of diagnosing vascular pathologies, and for relating blood flow to heat clearance in thermal methods of blood perfusion measurement (Jain, 1994). For example, the effect of local hypothermia treatment is determined by the length of time that the tissue is held at an elevated temperature, normally 43°C or higher. Since the tissue temperature depends on the balance between the heat added by artificial means and the tissue's ability to clear that heat, an understanding of the means by which the blood transports heat is essential for assessing the tissue's response to any thermal perturbation. The thermal regulatory system and the metabolic needs of tissues can change the blood perfusion rates in some tissues by a factor 25 (Baish, 2000). More expensive reviews and tutorials on microvascular heat transfer may be found elsewhere (Baish, 2000; Cooney, 1976; Jain, 1994).

Biological processes within living systems are significantly influenced by the flow of liquids and gases. Consequently, understanding the basic pressure and flow mechanisms involved in biofluid processes is essential for our ability to design biomimetic systems. Simulations using computational fluid dynamics (CFD) models to develop the necessary similitude and performance predictions, and the experimental evaluations of prototype devices, are crucial for successful *in vivo* implantation applications. Even for systems intended to remain *in vitro*, the effects of physiological fluids must be anticipated. Other complex devices, such as the development of bioreactors as surrogate systems, also need design guidance from CFD methods. The interaction of fluids and supported tissue is paramount in tissue engineering and the control of the microenvironment. The strength of adhesion and dynamics of detachment of mammalian cells from engineered biomaterials scaffolds is an important ongoing research, as is the effects of shear on receptor–ligand binding at cell–fluid interfaces. In addition to altering transport across the cell membrane, and possibly more important, receptor location, binding affinity and signal generation, with subsequent trafficking within the cell (Lauffenburger and Linderman, 1993), can be changed.

Furthermore, the analysis and design of reactors is highly dependent upon knowing the nonideal flow patterns that exist within the vessel. In principle, if we have a complete velocity distribution map for the fluid, then we are able to predict the behavior of any given vessel as a reactor. Once considered an impractical approach, this is now obtainable by computing the velocity distribution using CFD-based procedures in which the full conservation equations are solved for the reactor geometry of interest. Both the nonlinear nature of these equations themselves and appropriate nonlinear constitutive relationships can readily be taken into consideration.

13.3 Reacting Systems and Bioreactors

Chemical reactions, usually closely coupled with transport phenomena, sustain and support life processes. Combining these with thermodynamics identifies the area of reaction engineering. Knowledge of the fundamentals involved is essential for our understanding of these reacting systems and ability to design and control engineering devices, such as the novel flow reactor systems needed by tissue engineers. These systems provide the required experimental conditions, that is, appropriate flow fields, with controlled transport and/or contacting patterns, and at a microscale of relevance.

The coupling of encapsulation technologies with cell culture techniques permits the extended use of these bioreactors with complex tissue systems such as islet clusters. Existing reactor systems are also useful in obtaining the basic transport and reaction kinetics parameters necessary to design the novel devices required for biomedical applications. In summary, the relevance of this work to the biotechnology and healthcare-based industries is in the development of artificial organ systems, extracorporeal devices to bridge transplantation, biosensors, drug design, discovery, development, and controlled delivery systems. Furthermore, the control and stabilization of metabolic processes has a major impact

on many research programs, including the development of animal surrogate systems for toxicity testing and biotechnological processes for the production of pharmaceuticals.

13.3.1 Reactor Types

Characterization of the mass transfer processes in bioreactors, as used in cell/tissue culture systems is essential when designing and evaluating their performance. Flow reactor systems bring together various reactants in a continuous fashion while simultaneously withdrawing products and excess reactants. These reactors generally provide optimum productivity and performance. They are classified as either tank- or tube-type reactors. Each represents extremes in the behavior of the gross fluid motion within the vessel. Tank-type reactors are characterized by instant and complete mixing of the contents and are therefore termed perfectly mixed, or back-mixed, reactors. Tube-type reactors are characterized by lack of mixing in the flow direction and are called plug flow or tubular reactors. The performance of actual reactors, though not fully represented by these idealized flow patterns, may match them so closely that they can be modeled as such with negligible error. Others can be modeled as combinations of tank and tube type over various regions.

Also in use are batch systems, where there is no flow in or out. The feed (initially charged) is placed in the reactor at the start of the process and the products are withdrawn (all at once) some time later. Reaction time is thus readily determined. This is significant since conversion is a function of time and can be obtained from the knowledge of the reaction rate and its dependence upon concentration and process variables. Since operating conditions such as temperature, pressure, and concentration (under certain circumstances) are typically controlled at a constant value, the time for reaction is the key parameter in the reactor design process. However, in a batch reactor, the concentration of reactants change with time and, therefore, the rate of reaction does as well. The performance of reactors can be predicted using rate expressions and straightforward mathematical tools.

Most actual reactors deviate from these idealized systems primarily because of nonuniform velocity profiles, channeling and bypassing of fluids, and the presence of stagnant regions caused by reactor shape and internal components such as baffles, heat transfer coils, and measurement probes. Disruptions to the flow path are common when dealing with heterogeneous systems, particularly when solids are present, as when using encapsulated systems. To model these actual reactors, various regions are compartmentalized and represented as combinations of plug flow and back-mixed elements. The study of biochemical kinetics, particularly when coupled with complex physical phenomena, such as the transport of heat, mass, and momentum, is required to determine or predict reactor performance. It is imperative to uncouple and unmask fundamental phenomenological events in reactors and to subsequently incorporate them in a concerted manner to meet objectives of specific applications. This need further emphasizes the role played by the physical aspects of reactor operation in process stability and controllability.

13.3.2 Design of Microreactors

Microscale reaction systems are often desirable for biomedical and biotechnological applications, in which the component substrates may be expensive or available only in very small quantities. This is particularly true when it is desired to conduct reactions with living cells. The advantages of microreactors are briefly summarized below. An important point to bear in mind is that these microscale systems, by their very nature, are differential reactors, that is, very low single-pass conversions. Although this single-pass analysis is quite beneficial when intermediate species kinetics studies are required, multiple passes and subsequent reservoir dynamics may be needed for higher conversion experimental programs. A few of the intrinsic qualities of microreactors are as follows: minimizes reactant (serum) requirements; minimizes the quantity of cells or biocatalysts and support material; short contact time reactions can be studied more reliably at reduced flow rate; extends the duration of experimental times,

that is, longer continuous operation with small resource consumption; “aging” studies, both accelerated and long term, are more easily conducted; minimizes transport effects; coping with both mixing and flow distribution problems is less formidable and the data are more amenable to analysis; compatibility with spectroscopic systems; *in situ* studies utilizing advanced spectroscopic techniques are easier to conduct since size restrictions are reduced; and control of aseptic environment operating in a biohazard/laminar flow hood is easily implemented, as is the optimum placement of ancillary equipment.

Design criteria and performance expectations are consistent with the principles of process intensification (PI) methods. The application of this PI philosophy to numerous systems has proven its value, on both a technology and economic basis. Some insight into the virtues obtainable can be found in a description of the “bottom-up” approach to the formation of nanocrystals (Panagiotou and Fisher, 2008).

13.3.3 Scale-Up and Operational Maps

These are complex topics requiring a thorough background in chemical reaction engineering. An extensive literature has been published on the art and technology of scale-up. Here, our objective is only to direct readers to some of the sources most pertinent to bioreactors; works worthy of attention are textbooks on biomedical engineering (Fournier, 1999; Palsson, 2000) and cell culture methods (Freshney, 2000).

The use of various membrane configurations coupled with bioreactors has led to multiple functionality improvements and innovations. Implementation as guard beds, recycle conditioning vessels (with solids separations capabilities), *in situ* extraction systems, and slip-stream (and/or bypass) reactors for “biocatalyst” activity maintenance are but a few important examples representing successful applications when using living systems operating in controlled microenvironments.

The biosynthesis of lactate from pyruvate (Chen et al., 2004) is an illustrative example of the use of reactor hydrodynamic characterization and mass transport studies to improve performance through identification of operating regimes in which selected mechanisms dominate. Exploitation of this knowledge can then enhance the contribution from the desired phenomena. The operational protocols to enter these regimes, once they are documented, are termed operational maps. The multipass, dynamic input operating scheme used in that study permitted system parameter optimization studies to be conducted, including concentrations of all components in the free solution, flow rates, and electrode composition and their transport characteristics. Operating regimes that determined the controlling mechanism for process synthesis (e.g., mass transfer vs. kinetics limitations) were readily identified by varying system variables and operating conditions. Thus, procedures for developing operational maps were established and implemented.

13.4 Illustrative Example: Control of Hormone Diseases via Tissue Therapy

The treatment of autoimmune disorders with cell/tissue therapy has shown significant promise. A successful implant comprises cells or tissue surrounded by a biocompatible matrix permitting the entry of small molecules such as oxygen, nutrients and electrolytes and the exit of toxic metabolites, hormones, and other small bioactive compounds, while excluding antibodies and T cells, thus protecting the encapsulated cells/tissue. Systems of this type are currently being evaluated for the treatment of a variety of disorders, including type I diabetes mellitus, Hashimoto’s disease (thyroiditis), and kidney failure. Several key issues need to be addressed before the clinical use of this technology can be realized: tissue supply, maintenance of cell viability and functionality, and protection from immune rejection. Viability and metabolic functionality are controlled by the transport of essential biochemical signal molecules, nutrients, and respiratory gases. In particular, maintenance of sufficient oxygen levels in the encapsulation device is critical to avoid local domains of necrotic and/or hypometabolic cells. Oxygen transport can be enhanced through several means, including the selection of optimal encapsulation

configurations, promotion of vascularization at the implantation site, and seeding at an optimal cell density. Despite research efforts directed in these areas, oxygen transport remains one of the major limitations in maintaining cell viability and functionality. To improve this situation, recent efforts have focused on the design of a novel nanotechnology-based encapsulation motif containing specific oxygen carriers. Such a motif will ensure complete metabolic functionality of the encapsulated cells and allow the cells to retain functionality over extended time, that is, months as opposed to weeks.

13.4.1 Transport Considerations

Our emphasis here is to describe the issues relevant to development of encapsulation motifs for tissue/cellular systems that help control their microenvironments. The objective is to discuss and utilize mechanisms by which molecular transport occurs through complex media. Experimental protocols focus on the selective transport of solute molecules to evaluate proposed mechanisms and establish performance criteria. Numerous models have been postulated to explain these phenomenological observations and to develop methodologies to predict performance, thereby facilitating the design of successful encapsulation systems. Issues that need to be incorporated into these models include (1) interfacial phenomena between the bulk fluid and the outer membrane surfaces and/or along a pore wall, (2) sorption into the membrane matrix itself with diffusion possibly affected by immobilization at specific interactive sites, (3) free and/or fixed site diffusion within the matrix and if appropriate, through the porous regions, whether as distinct pores, microchannels, or other nonhomogeneous discrete areas, and (4) any chemical reactions that could alter the nature of the diffusing species or the media itself.

Two models developed previously from the analysis of transport in hydrogel membranes (Fang et al., 1998; Yasuda and Lamaze, 1971) describe the various aspects of importance to us. Both pore and sorption mechanisms may be active but their classification, and thus characterization, is based upon which, if either, dominates. When considering a pore mechanism, the solute is envisioned as passing through fluid filled micropores (or channels) in the membrane. For molecules and their mean free path much smaller than these opening, a simple Fickian diffusion model will suffice. Knudsen diffusion will be considered when the pore size is smaller than the mean free path yet still larger than molecular diameter. As the pore and molecular sizes approach each other, hindered diffusion occurs where physical/chemical interactions of significant magnitude, not simply elastic collisions, play a dominant role in transport rates. It is in this region that interactions at the molecular level, such as surface adsorption (physical or chemisorption), absorption into the matrix (solubility), and molecular transformation, become major phenomenological factors. Consideration must now be given to rate events, extent of reaction, equilibrium partitioning, irreversibility, site proximity, degree of saturation, and desorption. Migration rates along fiber or crystalline components in the matrix (and/or pore surface) are dependent upon energetics as well as site proximity, where a shunt pathway could be established to enhance transport if close enough. Otherwise, random adsorption events should hinder the transport process, analogous to diffusion with immobilization (Fisher, 1989). However, once reaction sites are fully saturated, a normal diffusive zone can be established. The influence of chemical reactive sites can be determined following prior analyses (Cussler, 1984) when appropriate, as in functionalized surfaces and/or sites distributed throughout a membrane. In contrast, in porous materials possessing microchannels, but lacking a well-defined pore structure, the dominate phase is the fluid that fills these voids. This situation is analogous to that in a swollen fibrous media, in which solute can diffuse readily but encounters fibers in its sojourn through the membrane. These encounters have a random aspect due to the nonhomogeneous nature of the membrane. They could be passive, as in elastic collisions, or active through affinity interactions as in the pore concept described above.

Transport through nonporous materials requires solute to be absorbed (solubilized) in the matrix material. Solute molecules are, thus, subject to thermodynamic equilibrium factors at the fluid–solid interfaces, as well as the nature of the fluid and solid phases themselves. These include ion strength, degree of solute hydration, and other interactive forces. Once the solute is within the membrane, a simple

Fickian diffusion mechanism may take place. Furthermore, all the other affinity events, as discussed for the pore model, could occur at interactive sites establishing a more complex transport process.

Combinations of these mechanisms may be observed in any membrane system that has distinct fluid, amorphous, crystalline, and/or functionalized regions, whether classified as porous or nonporous. Membranes may be characterized with respect to these mechanistic events, as modeled based on experimental transport measurements. The analysis tools used to interpret these results are briefly discussed later in the context of this example case study.

13.4.2 Selection of Diabetes as Representative Case Study

The National Institute of Diabetes and Digestive and Kidney Diseases (NIDDKD) estimates that there are 16 million people (nearly one in 17) that have diabetes in the United States alone. It is one of the most common and widespread diseases, with as high as 6% of the world population suffering from diabetes. In addition to the primary symptom, loss of blood glucose regulation, complications, and sequelae of diabetes include blindness, cardiovascular disease, and loss of peripheral nerve function. When including these complications, diabetes is the fourth most important cause of mortality in the United States and the main cause of permanent blindness. The American Diabetes Association estimates that diabetics consume 15% of U.S. healthcare costs (more than twice their percentage of the population), that is, the total cost of diabetic morbidity and mortality is more than \$90 billion per year. At least 50% of that figure attributed to direct medical costs for the care of diabetic patients. Although most of the affected individuals are not dependent upon interventional insulin replacement, NIDDKD estimates that 800,000 diabetics do require this treatment to manage blood glucose regulation. Insulin delivery is not a cure, however. Restoration of normal glucose regulation by improved insulin therapy techniques that regulate insulin delivery offers the hope of circumventing the need for injection treatments and eliminating the serious debilitating secondary complications. Consequently, many research paths are being followed to determine how normal pancreatic functions can be returned to the body. These include whole-pancreas transplants, human and animal islet transplantation, fetal tissue exchange and creation of artificial beta cells, each with its pros and cons. The two major problems are the lack of sufficient organs or cells to transplant and the rejection of transplants. Since there is a severe shortage of adult pancreases, that is, 1000 patients per available organ, alternatives such as islet cell transplantation are being sought. Cell transplantation, if it could be successfully achieved, would help with both of these major problems. Use of either “artificial” islets, potentially grown from stem or beta cells themselves, or xenogenic islet clusters, in combination with designed materials for immunoisolation functionality could lead to restoration of normoperative glycemic control without the need for insulin therapy.

13.4.3 Encapsulation Motif: Specifications, Design, and Evaluation

The goal of ongoing research programs is to improve the success rate of pancreatic islet cell transplantation and thus provide a better means to regulate glucose levels for diabetic patients. This is being accomplished through immunoisolation and immunoalteration technologies implemented using intelligent membrane encapsulation systems. These systems exist as multilayered microcapsules that utilize semipermeable membranes that permit transport of nutrients, insulin, and metabolic waste products while excluding antibody and T-cell transport (Johnson et al., 2009; Lewis and Colton, 2004).

The immunoisolative capabilities of the encapsulation motif are based upon a size-exclusion principle whereby antibodies (primarily IgM and IgG) and complement proteins of the immune system are unable to reach the implanted cells. In order to activate the complement pathway in which antibodies bind specific complement proteins and ultimately destroy the implanted cells through lysis, one IgM molecule (MW = 800 kDa; ~30 nm diameter) and one molecule of complement protein C1q (MW = 410 kDa, ~30 nm diameter) must bind together. Alternatively, two IgG molecules (MW = 150 kDa each, ~20 nm total diameter) bind in concert with C1q to destroy the implant cells. Encapsulating cells in materials

with a molecular weight cut-off of roughly 200 kDa therefore shields cell surface antigens from exposure to these antibodies.

It is important to also consider the ability of implanted cells to shed antigens into the surrounding host tissues, triggering another type of immune response. Many such shed antigens are comprised of major histocompatibility complex (MHC) antigens, which are too small (57–61 kDa) to be retained by the encapsulation motif. Activation of the immune system in this manner recruits macrophages, which release reactive oxygen species in an attempt to destroy the implanted cells. The inclusion of reactive sites within the matrix that function as free radical scavengers is thus desirable to protect the cells from these toxic compounds. This may be possible using nanosphere technologies, whether active ingredient-loaded or by their own characteristics, dispersing them throughout the microsized beads. Simultaneously, nanosphere technology may also be designed to augment respiratory gas exchange (Johnson et al., 2009). The solubility of O₂ in water or blood plasma is ~2 mL O₂ per 100 mL of solution at standard temperature and pressure, which is at least an order of magnitude low for encapsulation purposes. Thus, selected O₂ carriers, such as perfluorocarbons, could be incorporated into the nanospheres or as microemulsions into the matrix of the encapsulating motif.

Transport to and from encapsulated cells of nutrients, respiratory gases, and similar small molecules is not affected by pore sizes commonly found in encapsulation motifs. However, transport of desired proteins, synthesized by the cells, out of the encapsulation matrix can be limited by the pore size of the material. Large secreted proteins (e.g., MW ~ 660 kDa) will be blocked by the MW cut-offs needed to shield the implanted cells from antibodies, whereas the diffusion of MW = 28 kDa and smaller proteins will not. Consequently, the molecular weight cut-off of the encapsulation material must be carefully chosen when transport of a secreted natural compound such as insulin is desired.

The hypothesis underlying this effort is that macromolecular biomaterial encapsulation materials can be engineered that would promote islet cluster viability while simultaneously facilitating desirable biologic responses. For encapsulation materials to be physiologically functional for metabolite transport and hormone secretion, their most important properties need to be biocompatibility and selective semipermeability. However, to promote implant longevity as well as augment tissue interstitium transport and exchange characteristics, an equally important subcharacteristic is the ability to stimulate neovascularization and vascular in-growth *in situ*. Approaches such as biodegradation of a sacrificial outer layer that either releases or “generates” growth factors to promote angiogenesis are currently being studied (Hosack et al., 2008; Riley et al., 2006). Thus, a single encapsulating material will not in general possess the spectrum of properties for a successful implantation. The design of a multilayer motif, in which each layer is selected to contribute specific functions, must be considered.

One must also account for the possibility that in certain situations increased transport resistances may be beneficial. For example, when substrate inhibition kinetics behavior is observed, performance is improved as the substrate transport rate is restricted. Mammalian cells can establish multiple steady states, with subsequent hysteresis effects, while in continuous culture at the same dilution rate and feed medium. Consequently, perturbations in the macroenvironment of an encapsulated cell/tissue system can force the system to a new, less desired, steady state with altered cellular metabolism. Simply returning the macroenvironment to its original state may not be effective in returning the cellular system to its original metabolic state, and hence predicted performance is unfavorable. The magnitudes of the macroenvironment perturbations forcing the system to seek a new steady state may be estimated from models developed simulating experimentally measured metabolism. Such behavior can be mediated by the encapsulation motif through its control of the cell/tissue microenvironment. In principle, the intelligent behavior of a proposed encapsulation system will allow the maintenance of the desired microenvironment through modification of stresses and release of necessary compounds. Characterization of the required materials in this motif and subsequent efficacy testing with appropriate cell/tissue systems is an integral component of these efforts. Fortunately, the majority of materials that must meet these objectives (desired functionalities) are currently available. Examples include hydrogels and their composite systems that incorporate ionomers and other functional entities. A thorough discussion of the

techniques used to characterize these materials can be found in many sources (e.g., Crank, 1956; Cussler, 1984; Deen, 1996; Sokolnicki, 2004; Sokolnicki et al., 2005). The key points are summarized as follows.

Physical and transport parameters: A variety of physical parameters may be measured or calculated as necessary for the analysis and interpretation of transport measurements. The hydrated encapsulation matrix or membrane volume is obtained using a water displacement technique. The porosity can be estimated through a simple mass balance. Membrane morphology studies are usually conducted using SEM, an available, simple, and straightforward method to determine physical characteristics of the membranes. Along with the equilibrium weight swelling ratio porosity measurement technique, surface morphology can be examined by SEM to determine the type and structure of the void space. System dimensions are obtained by direct measurement and/or simple calculations.

The membrane permeability is determined using a pseudo-steady state analysis based on Fick's law, equilibrium partitioning to the membrane surface, and the observed concentration difference across the membrane. The instantaneous flux, j , through the matrix or membrane (in a diffusion cell apparatus) is then given by

$$-j = \frac{[P]}{l}(C_D - C_R) \quad (13.1)$$

where l is the total length of the membrane and C_D and C_R are the concentrations within the donor cell and the receptor cell, respectively (Cussler, 1984). The parameter P is the membrane permeability and is defined as $P = D \cdot H$, where the partition coefficient, H , is the ratio of solute at/on the membrane surface to those free in solution, and D is the effective diffusion coefficient in the membrane. Using a time-variant mass balance for each compartment and subject to the initial condition, $(C_{0,D} - C_{0,R}) = (C_{1,D} - C_{1,R})$ at $t = 0$, the solution obtained provides a method to interpret transport measurements and calculate the permeability:

$$P = \frac{1}{\beta t} \cdot \ln \frac{(C_{0,D} - C_{0,R})}{(C_{1,D} - C_{1,R})} \quad (13.2)$$

The parameter β is a physical constant containing the dimensions of the diffusion cell and the membrane.

Measurements of dextran transport can be used to validate the effectiveness of a pore model for a given motif. Investigation of the relation between molecular size and rate of transport can establish whether diffusion is hindered due to pore walls or simply due to collisions with fibers in the diffusion path (Sokolnicki et al., 2005). To determine the unhindered diffusion rate of dextran molecules in water, the diffusivity at infinite dilution (Davidson and Deen, 1988; Labraun and Junter, 1994), must be calculated using the Stokes–Einstein equation:

$$D_o = kT / (6\pi\eta_w r_H) \quad (13.3)$$

where r_H , the hydrodynamic radii of the dextran molecules, is obtained using the Stokes–Einstein correlation based on molecular weight, k is the Boltzmann's constant, T is the absolute temperature, and η_w is the viscosity of water at that temperature. Calculated diffusion coefficients of various molecular-weight dextrans in water at dilute and semidilute concentrations are reported in the literature (Callaghan and Pinder, 1983). A ratio of D_{eff} to D_o less than one indicates that a hindered diffusion process is present. If this ratio is dependent on molecular size, then pore (or microchannel) dimensions dominate versus collisions with individual fibers.

When using a horizontal diffusion cell, the diffusivity of a solute through a particular membrane can only be determined directly from these experimental transport measurements under select conditions, that is, if the partition coefficient and all physical parameters of the membrane and apparatus

are known. Although membrane external dimensions can often be measured with reasonable accuracy, pore characteristics are typically lumped into an apparatus parameter that must be determined by calibration experiments and is accordingly subject to experimental error. Consequently, permeability determination is not a fundamental process. Its usefulness is restricted to applications within a data collection regime. Extensions to predict performance and provide better design protocols for novel applications requires that the fundamental parameters, diffusivity and partition coefficients, be known. Both can be obtained from desorption experiments, but data analysis from such experiments is more complicated, particularly when the motif geometry is nonspherical. One can use this technique to estimate both parameters, and then conduct adsorption tests to provide a direct measure of the partition coefficients, thereby providing redundancy checks for all three parameters, P , D , and H . Even with this more extensive data analysis program, one can only obtain effective diffusivities since the internal membrane structure is usually quite complex.

Marker species, such as vitamin B12, bovine serum albumin (BSA), and lysozyme, are generally selected to provide a reasonable range in size and properties for the solutes in desorption experiments. Membranes are initially saturated with one solute, and then immersed in a buffer solution of known volume. The mathematical analysis of the resulting desorption is based on an infinite sheet of uniform thickness placed in a solution, allowing the solute to diffuse from the sheet. Since membrane diameters are more than 100 times greater than the thickness, assumption of an infinite sheet is appropriate. The solution to this model system was developed by Crank (1956) in a form expressing the total amount of solute, M_t , in the solution at time t as a fraction of the amount after infinite time, M_∞ . An infinite series form is obtained where D_{eff} appears in the exponential terms and can be recovered using a nonlinear fitting routine. The number of terms retained in the summation is dependent on the magnitude of time and the relative spacing of the system eigenvalues. The calculated diffusion coefficients are then compared to those in pure solvent and establish a basis to identify a hindered diffusion mechanism. An analysis of the adsorption behavior of the marker molecules in the membranes assists in the investigation of the mass transport phenomena by identifying if solute–matrix (fiber) interactions are significant.

The ability to execute a research program to obtain the requisite data to evaluate and implement designed encapsulation motifs, for example, develop a prototype from experimental data for clinical testing, is dependent upon coordinating all the efforts described above. This includes using the various novel bioreactor systems discussed earlier to perform these tasks in appropriate flow fields, with controlled transport and/or contacting patterns, and at a microscale of relevance. Concerted programs will help in attaining the goal of understanding the microenvironment of encapsulated systems to control and optimize tissue function.

References

- Baish, J.W., 2000. Microvascular heat transfer, Chapter 8 In: *The Biomedical Engineering Handbook*, Bronzino JD (ed). 2nd Edition, CRC Press, Boca Raton, FL.
- Bird, R.B., W.E. Stewart, and E.N. Lightfoot, 2002. *Transport Phenomena*, 2nd Edition, Wiley, New York.
- Brodkey, R.S. and H.C. Hershey, 1988. *Transport Phenomena: A Unified Approach*. McGraw-Hill, New York.
- Bruns D., J. Bailey, and D. Luss, 1973, Steady state multiplicity and stability of enzymatic reaction systems. *Biotech Bioeng*, 15, 1131.
- Callaghan, P.T. and D.N. Pinder, 1983. A pulsed field gradient NMR study of self-diffusion in a polydisperse polymer system: Dextran in water. *Macromolecules*, 16, 968.
- Chen, X., J.M. Fenton, R.J. Fisher and R.A. Peattie, 2004. Evaluation of in-situ electro-enzymatic regeneration of co-enzyme NADH in packed bed reactors: Biosynthesis of lactate. *J Electro Chem Soc*, 151, 2.
- Cooney, D.O., 1976. *Biomedical Engineering Principles*. Dekker, New York.
- Crank, J., 1956. *The Mathematics of Diffusion*. Oxford University Press, London, UK.
- Cussler, E.L., 1984. *Diffusion: Mass Transfer in Fluid Systems*. Cambridge Press, New York.

- Davidson, M.G. and W.M. Deen, 1988. Hindered diffusion of water-soluble macromolecules in membranes. *Macromolecules*, 21, 3474.
- Deen, W.M., 1996. *Analysis of Transport Phenomena*. Oxford Press, New York.
- Europa A.F., A. Grambhir, P.C. Fu, and W.S. Hu, 2000. Multiple steady states with distinct cellular metabolism in continuous culture of mammalian cells. *Biotech Bioeng*, 67, 25.
- Fang, Y., Q. Cheng, and X.-B. Lu, 1998. Kinetics of *in vitro* drug release from chitosan/gelatin hybrid membranes. *J App Polymer Sci*, 68, 1751.
- Fisher, R.J., 1989. Diffusion with immobilization in membranes: Transport and failure mechanisms; Part II—Transport mechanisms, In: *Biological and Synthetic Membranes*, A. Butterfield (ed). Alan R. Liss Co., New York.
- Fisher R.J, S.C. Roberts, and R.A. Peattie, 2000. *Ann Biomed Eng*, 28(S1):39.
- Fournier, R.L., 1999. *Basic Transport Phenomena in Biomedical Engineering*. Taylor & Francis, Philadelphia.
- Freshney, R.I., 2000. *Culture of Animal Cells: A Manual of Basic Technique*, 4th Edition, Wiley-Liss, New York.
- Galletti, P.M., C.K.Colton, M. Jaffrin and G. Reach, 2000. Artificial pancreas, Chapter 134 In: *The Biomedical Engineering Handbook*, 2nd Edition, J. D. Bronzino (ed). CRC Press, Boca Raton, FL.
- Hosack, L.W., M.A. Firpo, J.A. Scott, G.D. Prestwich, and R.A. Peattie, 2008. Microvascular maturity elicited in tissue treated with cytokine-loaded hyaluronan-based hydrogels. *Biomaterials*, 29, 2336–47.
- Jain, R.K., 1994. Transport phenomena in tumors, *Advances in Chemical Engineering*, Vol. 19, pp. 129–194, Academic Press, Inc, Orlando, FL.
- Johnson, A.E., R.J. Fisher, G.C. Weir and C.K. Colton, 2009. Oxygen consumption and diffusion in assemblages of respiring spheres: Performance enhancement of a bioartificial pancreas. *Chem Eng Sci*, 64(22), 4470–87.
- Lauffenburger, D.A. and J.J. Linderman, 1993. *Receptors: Models for Binding, Trafficking, and Signaling*, Oxford University Press, New York.
- Lewis, A.S. and C.K. Colton, 2004. Tissue engineering for insulin replacement in diabetes, In: *Scaffolding in Tissue Engineering*, P. Ma and J. Elisseeff (eds). Marcel Dekker, New York.
- Lightfoot, E.N., 1974. *Transport Phenomena and Living Systems*, John Wiley and Sons, New York.
- Long, M.W., 2000. Tissue microenvironments, Chapter 118 In: *The Biomedical Engineering Handbook*, 2nd Edition, Vol. II, J. D. Bronzino (ed). CRC Press, Boca Raton, FL.
- Palsson, B., 2000. Tissue engineering, Chapter 12 In: *Introduction to Biomedical Engineering*, J. Enderle, S. Blanchard and J. Bronzino (eds). Academic Press, Orlando, FL.
- Panagiotou, T. and R.J. Fisher, 2008. Form nanoparticles via controlled crystallization: A bottom-up approach. *Chem Eng Prog*, 10(Oct.), 33–39.
- Peattie, R.A., A.P. Nayate, M.A. Firpo, J. Shelby, R.J. Fisher, and G.D. Prestwich. 2004. Stimulation of *in vivo* angiogenesis by cytokine-loaded hyaluronic acid hydrogel implants. *Biomaterials*, 25, 2789–98.
- Riley, C.M., P.W. Fuegy, M.A. Firpo, X.Z. Shu, G.D. Prestwich, and R.A. Peattie. 2006. Stimulation of *in vivo* angiogenesis using dual growth factor-loaded crosslinked glycosaminoglycan hydrogels. *Biomaterials*, 27, 5935–43.
- Rosner, D.E., 1986. *Transport Processes in Chemically Reacting Flow Systems*. Butterworth Publishers, Boston.
- Shuler, M.J., 2000. Animal surrogate systems, Chapter 97 In: *The Biomedical Engineering Handbook*, 2nd Edition, Vol. II, J. D. Bronzino (ed). CRC Press, Boca Raton, FL.
- Sokolnicki, A.M., 2004. MS Thesis, Mass transport parameters of bacterial cellulose membranes, Tufts University, Boston, MA.
- Sokolnicki, A.M., R.J. Fisher, T.P. Harrah and D.L. Kaplan, 2005. Permeability of bacterial cellulose membranes. *J Membr Sci*, 6793, 1–13.
- Yasuda, H. and C.E. Lamaze, 1971. Permselectivity of solutes in homogeneous water-swollen polymer membranes. *J Macromol Sci Phys Part B*, 5, 111.

14

Transport and Drug Delivery through the Blood–Brain Barrier and Cerebrospinal Fluid

14.1	Introduction	14-1
	Barriers in the Central Nervous System • Blood–Brain Barrier • Transport Pathways across the Blood–Brain Barrier • Brain–CSF Barrier	
14.2	Drug Delivery through the Blood–Brain Barrier	14-7
	Permeability of the Blood–Brain Barrier • Determination of the Blood–Brain Barrier Permeability <i>In Vivo</i> and <i>Ex Vivo</i> • <i>In Vitro</i> Blood–Brain Barrier Models • Transport Models for the Paracellular Pathway of the Blood–Brain Barrier • Strategies for Drug Delivery through the Blood–Brain Barrier	
14.3	Drug Delivery through the Cerebrospinal Fluid	14-18
	Production and Circulation of the Cerebrospinal Fluid • Radioimmunotherapy Delivered through the Cerebrospinal Fluid	
	Acknowledgments	14-20
	References	14-21

Bingmei M. Fu
*City College of the City
University of New York*

14.1 Introduction

The most complicated organ in our body is the brain. It contains 100 billion neurons and 1 trillion glial cells (nonnerve supporting cells in the brain, including astrocytes, oligodendrocytes, microglia, and ependymal cells). Along with a tremendous amount of blood vessels, these cells and surrounding extracellular matrix form highly complex, though well-organized 3-D interconnecting arrays. The movement of ions across neuronal membrane, through voltage-gated channels, conducts the information along the neuron axon at a speed up to 400 km/h. The release of neurotransmitter into the synaptic space between adjacent nerve cells mediates the communication between neurons. In order to perform its highly complicated tasks, the brain needs a substantial amount of energy to maintain electrical gradients across neuronal membranes and consequently requires a sufficient supply of oxygen and nutrients. Although it only accounts for 2% of the body weight, the brain uses 20% of the blood supply. The blood is delivered through a complex network of blood vessels that runs >650 km and passes a surface area of ~20 m². The mean distance between adjacent capillaries is ~40 μm, which allows almost instantaneous equilibration in the brain tissue surrounding the microvessels for small solutes such as glucose, amino acids, vitamins, oxygen, and so on. However, unlike peripheral microvessels in other organs where there is a relatively free small solute exchange between blood and tissue, the microvessels in the brain

(cerebral microvessels) constrain the movement of molecules between blood and the brain tissue [1,2]. This unique characteristic provides a natural defense against toxins circulating in the blood, however, it also prevents the delivery of therapeutic agents to the brain.

14.1.1 Barriers in the Central Nervous System

The vascular barrier system in the brain consists of the blood–brain barrier (BBB) and the blood–cerebrospinal fluid (CSF) barriers. There is another barrier, the brain–CSF barrier, between brain tissue and the CSF. The locations of these barriers are demonstrated in Figure 14.1 [3]. The blood–brain barrier is the name for the wall of the cerebral microvessels in the brain parenchyma. At the surface of the brain parenchyma, microvessels running in the pia mater are called pial microvessels, which are often used as *in vivo* models for studying the BBB permeability. Owing to its unique structure that will be discussed in the next section, the BBB maintains very low permeability to water and solutes. In the middle of the brain parenchyma, there are ventricular cavities (ventricles) filled with CSF secreted by the epithelial cells of choroid plexus [4]. The choroid plexus is a highly vascular tissue with leaky, fenestrated capillaries covered with ependymal epithelium, which has relatively tight junctions. The multicell layer between the blood and the CSF in the choroid plexuses is called the blood–CSF barrier.

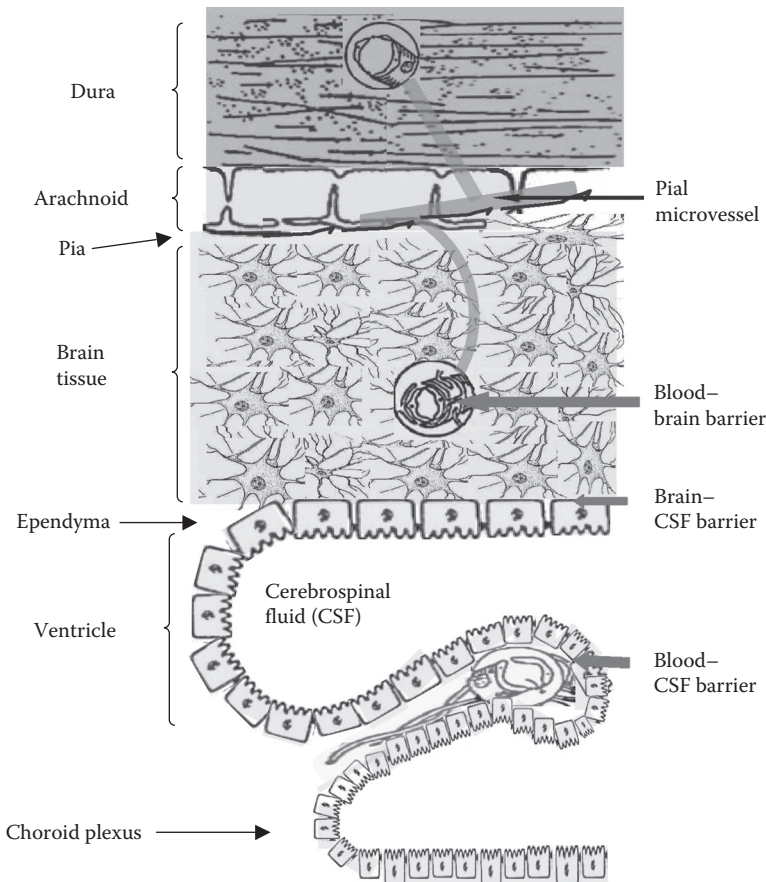


FIGURE 14.1 Locations of barriers in the brain. (Modified from Abbott NJ, 2004. *Neurosci Int.* 45:545.)

Since the area of the BBB is about 1000 times that of the blood–CSF barrier, it is more important to circumvent the impermeability of the BBB for delivering drugs to the brain [5,6]. The total surface area of the BBB constitutes by far the largest interface for blood–brain exchange, which is between 12 and 18 m² for the average human adult [7]. Unlike these two tight blood barriers, the interface between the CSF and brain tissue along the ependymal surface of the ventricles and that between pia mater and brain tissue, the so-called brain–CSF barriers, are rather leaky, implying a possible route for drug delivery to the brain. The CSF is formed by the choroid plexuses of the ventricles, passes the ventricles to the subarachnoid space over the pia mater, and finally is absorbed to the venules in the dura mater through arachnoid microvilli and arachnoid granulations [8,9].

14.1.2 Blood–Brain Barrier

The BBB is a unique dynamic regulatory interface between the cerebral circulation and the brain tissue, and it is essential for maintaining the microenvironment within brain. No other body organ so absolutely depends on a constant internal microenvironment as does the brain. In the brain, the extracellular concentrations of amino acids and ions such as Na⁺, K⁺, and Ca²⁺ must be retained in very narrow ranges [2]. If the brain is exposed to big chemical variations in these molecules, neurons would cease to function properly because some amino acids serve as neurotransmitters and certain ions modify the threshold for neuronal firing. The BBB also protects the central nervous system (CNS) from blood-borne neuroactive solutes, such as glutamate, glycine, norepinephrine, epinephrine, and peptide hormones [10], which can increase with physiological changes (e.g., diet and stress) and pathological changes (e.g., injury and diseases). In addition, the BBB plays a key role in facilitating the brain uptake of essential nutrients like glucose, hormones, and vitamins, and larger molecules like insulin, leptin, and iron to sustain brain growth and metabolism [11].

The term “blood–brain barrier” was coined by Lewandowsky in 1900 while he demonstrated that neurotoxic agents affected brain function only when directly injected into the brain but not when injected into the systemic circulation [12]. Nevertheless, the first experimental observation of this vascular barrier between the cerebral circulation and the CNS should date back to the 1880s, when Paul Ehrlich discovered that certain water-soluble dyes, like trypan blue, after being injected into the systemic circulation, were rapidly taken by all organs except the brain and spinal cord [13]. Ehrlich interpreted these observations as a lack of the affinity of the CNS for the dyes. However, subsequent experiments performed by Edwin Goldmann, an associate of Ehrlich, demonstrated that the same dyes, when injected directly into the CNS, stained all types of cells in the brain tissue but not any other tissues in the rest of the body [14]. It took an additional 70 years until this barrier was first localized to cerebral microvascular endothelial cells by electron-microscopic studies performed by Reese and Karnovsky [15]. Although the concept of the BBB has continued to be refined over the past few decades, the recent understanding of the basic structure of the BBB is built on the general framework established by their studies in the late 1960s; more specifically, the BBB exists primarily as a selective diffusion barrier at the level of cerebral capillary endothelium.

The anatomical structure of the BBB is shown in Figure 14.2b. For comparison, the cross-sectional view of a peripheral microvessel (a typical microvessel in nonbrain organs) is also shown in Figure 14.2a. For both peripheral microvessels and the BBB, the circumference of the microvessel lumen is surrounded by endothelial cells, the opposing membranes of which are connected by tight junctions. At the luminal surface of the endothelial cell, there is a rather uniform fluffy glycocalyx layer [16–19], which is mainly composed of heparan sulfate proteoglycan, chondroitin sulfate proteoglycan, and hyaluronic acid [20]. This mucopolysaccharide structure is highly hydrated in electrolytic solution and contains large numbers of solid-bound fixed negative charges due to the polyanionic nature of its constituents abundant in glycoproteins, acidic oligosaccharides, terminal sialic acids, proteoglycan, and glycosaminoglycans aggregates [21]. Pericytes attach to the abluminal membrane of the endothelium at irregular intervals. In a peripheral microvessel, there is a loose and irregular basal lamina (or basement membrane) surrounding the pericytes. In contrast, in the BBB, pericytes and endothelial cells are ensheathed

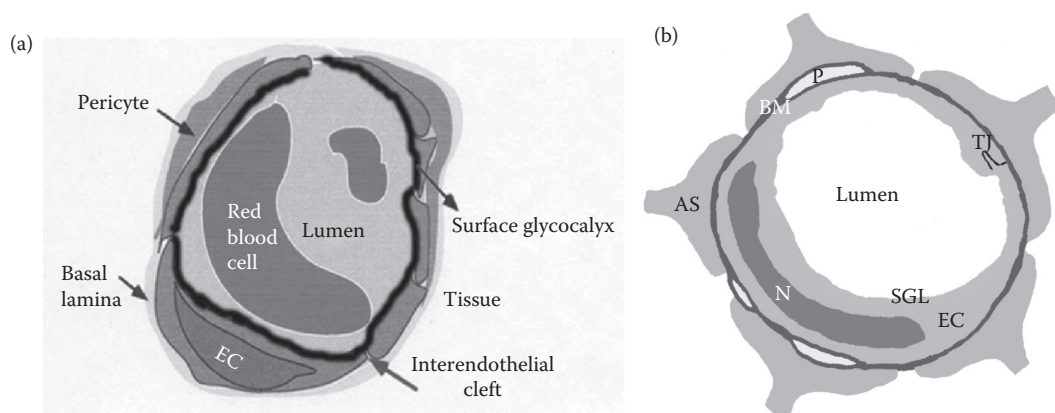


FIGURE 14.2 Schematic of the cross-sectional view of (a) a peripheral microvessel (the microvessel in nonbrain organs), and (b) the blood–brain barrier (BBB) or cerebral microvessel (the microvessel in the brain). In addition to other structures as in a peripheral microvessel, the BBB is wrapped by astrocyte foot processes (AS, green). BM, basement membrane (or basal lamina); EC, endothelial cell; N, nucleus of endothelial cell; P, pericytes; SGL, surface glycocalyx layer; TJ, tight junction.

by a very uniform basement membrane of 20–40 nm thickness, which is composed of collagen type IV, heparin sulfate proteoglycans, laminin, fibronectin, and other extracellular matrix proteins [22]. The basal lamina is contiguous with the plasma membranes of astrocyte end-feet, which wraps almost the entire abluminal surface of the endothelium [2].

In addition to the anatomical structures, the BBB differs from the peripheral microvessels in the following aspects. The mitochondrial content of the endothelial cells forming the BBB is greater than that of such cells in all nonneural tissues. It is suggested that this larger metabolic work capacity may be used to maintain the unique structural characteristics of the BBB, and/or by metabolic pumps that may require energy to maintain the differences in composition of the cerebral circulation and the brain tissue [23]. The BBB has high electrical resistance, much less fenestration, and more intensive junctions, which are responsible for restricting paracellular passage of water and polar solutes from the peripheral circulation entering into the CNS [24,25]. Between adjacent endothelial membranes, there are junctional complexes that include adherens junctions (AJs), tight junctions (TJs), and possibly gap junctions [26]. The structure of the junction complexes between endothelial cells is shown in Figure 14.3 [27,28]. Both AJs and TJs act to restrict paracellular transport across the endothelium while gap junctions mediate intercellular communication. AJs are ubiquitous in the vasculature and their primary component is vascular endothelial (VE)-cadherin. They basically mediate the adhesion of endothelial cells to each other and contact inhibition during vascular growth and remodeling. Although disruption of AJs at the BBB can lead to increased permeability, TJ is the major junction that confers the low paracellular permeability and high electrical resistance [29]. The tight junction complex includes two classes of transmembrane molecules: occludins and claudins. These transmembrane proteins from adjacent endothelia cells interact with each other and form seals in the spaces between adjacent endothelial cells. The cytoplasmic tails of the transmembrane proteins are linked to the actin cytoskeleton via a number of accessory proteins such as members of the zonula occludens family, ZO-1, ZO-2, and ZO-3.

A number of grafting and cell culture studies have suggested that the ability of cerebral endothelial cells to form the BBB is not intrinsic to these cells, but the cellular milieu of the brain somehow induces the barrier property into the blood vessels. It is believed that all components of the BBB are essential for maintaining functionality and stability of the BBB. Pericytes seem to play a key role in angiogenesis, structural integrity, and maturation of cerebral microvessels [30]. The extracellular matrix of the basal lamina appears to serve as an anchor for the endothelial layer via interaction of laminin and other matrix proteins

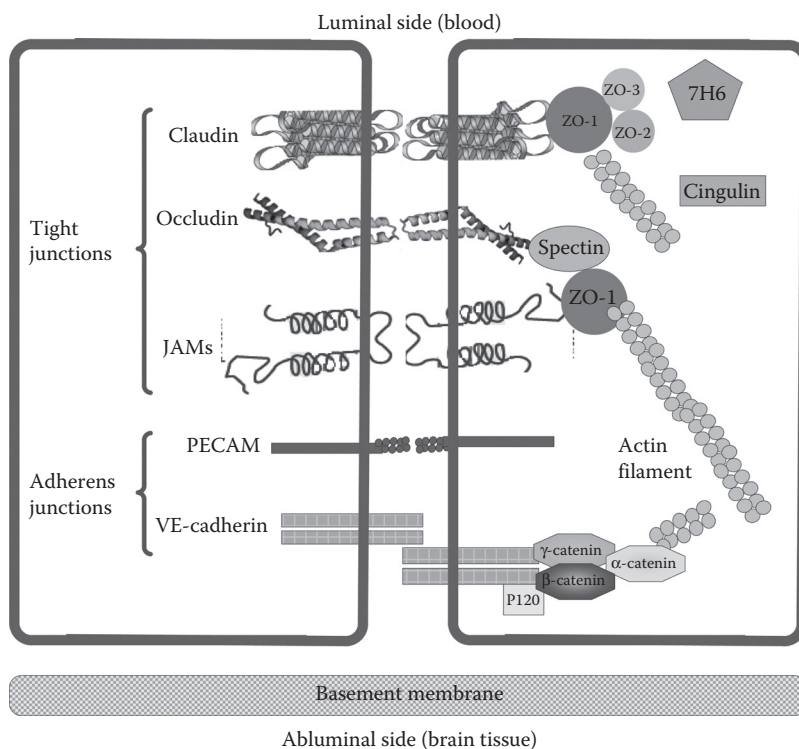


FIGURE 14.3 Schematic of junctional complex in the paracellular pathway of the BBB. (Modified from Kim JH et al. 2006. *J Biochem Mol Biol.* 39(4):339.)

with endothelial integrin receptors [31]. It was suggested that astrocytes are critical in the development and/or maintenance of unique features of the BBB. Additionally, astrocytes may act as messengers to or in conjunction with neurons in the moment-to-moment regulation of the BBB permeability [30].

14.1.3 Transport Pathways across the Blood–Brain Barrier

The BBB endothelial cells differ from those in peripheral microvessels in that they contain more intensive tight junctions, sparse pinocytotic vesicular transport, and many fewer fenestrations. The transport of substances from the capillary blood into the brain tissue depends on the molecular size, lipid solubility, binding to specific transporters, and electrical charge [32]. Figure 14.4 summarizes the transport routes across the BBB [33]. Compared to the peripheral microvessel wall, the additional structure of the BBB and tighter endothelial junctions greatly restrict hydrophilic molecules transport through the gaps between the cells, that is, the paracellular pathway of the BBB, route A in Figure 14.4. In contrast, small hydrophobic molecules such as O_2 and CO_2 diffuse freely across plasma membranes following their concentration gradients, that is, the transcellular lipophilic diffusion pathway, route C in Figure 14.4. The BBB permeability to most molecules can be estimated on the basis of their octanol/water partition coefficients [34]. For example, diphenhydramine (Benadryl), which has a high partition coefficient, can easily cross the BBB, whereas water-soluble loratadine (Claritin) is not able to penetrate the BBB and has little effect on the CNS [35].

However, the octanol/water partition coefficients do not completely reflect BBB permeability to solutes. Some solutes with low partition coefficients that easily enter into the CNS generally cross the BBB by active or facilitated transport mechanisms, which rely on ion channels, specific transporters,

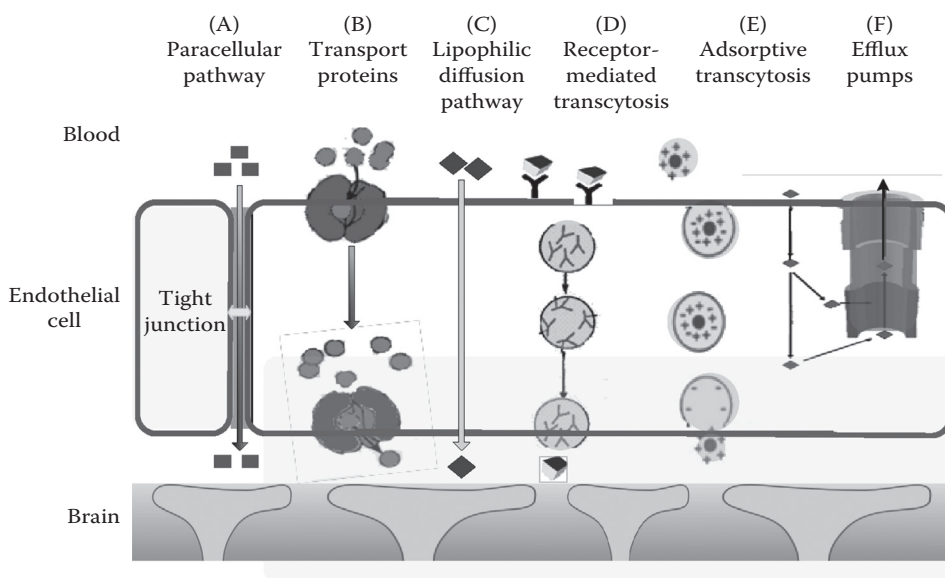


FIGURE 14.4 Transport pathways across the brain endothelial cell. (Modified from Neuwelt EA, 2004. *Neurosurgery* 54(1):131.)

energy-dependent pumps, and a limited amount of receptor-mediated transcytosis (RMT). Glucose, amino acids, and small intermediate metabolites, for example, are ushered into brain tissue via facilitated transport mediated by specific transport proteins (route B in Figure 14.4), whereas larger molecules, such as insulin, transferrin, low-density lipoprotein (LDL), and other plasma proteins, are carried across the BBB via receptor-mediated (route D) or adsorptive transcytosis (route E). Some small molecules with high octanol/water partition coefficients are observed to poorly penetrate the BBB. Recent studies suggested that these molecules are actively pumped back into blood by efflux systems (route F in Figure 14.4). These efflux systems greatly limit drug delivery across the BBB. For instance, P-glycoprotein (P-gp), which is a member of the adenosine triphosphate-binding cassette family of exporters, has been demonstrated to be a potent energy-dependent transporter. P-gp contributes greatly to the efflux of xenobiotics from brain to blood and has increasingly been recognized as having a protective role and being responsible for impeding the delivery of therapeutic agents [36]. The organic anion transporters and glutathione-dependent multidrug resistance-associated proteins (MRP) also contribute to the efflux of organic anions from the CNS, and many drugs with the BBB permeability that are lower than predicted are the substrates for these efflux proteins [2,28,33,37]. While the brain endothelium is the major barrier interface, the transport activity of the surrounding pericytes [38], basement membrane, and astrocyte foot processes (Figure 14.2b) [39] also contribute to the BBB barrier function under physiological conditions, and may act as a substitute defense if the primary barrier at the endothelium is compromised [40].

14.1.4 Brain–CSF Barrier

Although the brain lacks a lymphatic drainage [41], it has a lymph-like fluid compartment, the CSF, which fills the complex interconnected ventricles within the brain, and subarachnoid space around the brain (Figure 14.5). The CSF is secreted mainly by the choroids plexus in the walls of the lateral ventricles and flows constantly and unidirectionally from the lateral ventricles through the interventricular foramina into the third, then to the fourth ventricles, finally into subarachnoid space before draining into lymphatics and veins in sagittal sinus through arachnoid villi [42]. Although the barrier between the blood and the normal brain tissue is tight and macromolecules penetration

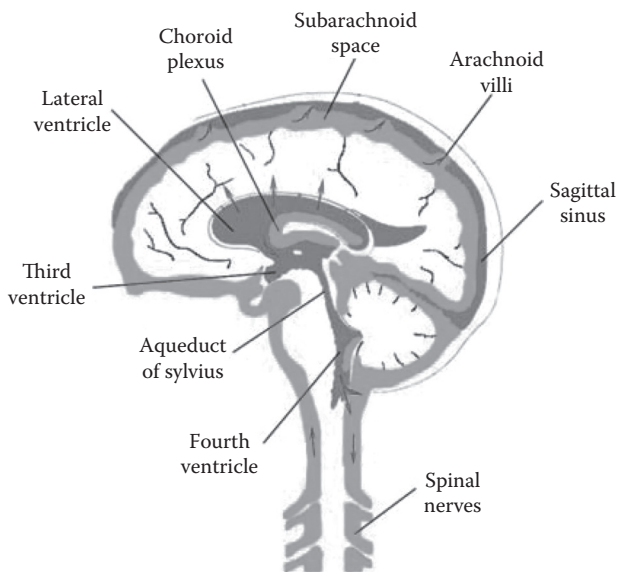


FIGURE 14.5 Circulation of the cerebrospinal fluid (CSF) and the brain–CSF barrier. (Modified from Abbott NJ et al. 2010. *Neurobiol Dis.* 37:13.)

into CSF is hampered by tight junctions in the blood–CSF barrier [43], the transfer of macromolecules (e.g., antibodies) between the CSF in the subarachnoid space and the meninges, as well as in the ependymal lining lateral ventricles (brain–CSF barrier) is relatively free. The total exchange area of the brain–CSF barrier was estimated to be at least 1800 cm² [44,45]. If considering the extensive basolateral infolding (toward blood side) and the lush apical membrane microvilli (toward CSF side), the total exchange area can be the same order of magnitude as the entire BBB [46].

14.2 Drug Delivery through the Blood–Brain Barrier

The endothelial cells lining microvessel walls provide the rate-limiting barrier to extravasations of plasma components of all sizes from electrolytes to proteins. In addition to the tight junction of the microvessel endothelium, there is a uniform and narrow matrix-like basement membrane layer (20–40 nm) sandwiched between the vessel wall and the astrocyte processes ensheathing the cerebral microvessel (Figure 14.2b). To develop effective and efficient methods for drug delivery to the brain through the BBB with the largest contact area with brain tissue, we need to understand the mechanism by which these structural components, as well as transporters, receptors, efflux pumps, and other components at the endothelium and astrocyte foot processes control the permeability of the BBB to water and solutes.

14.2.1 Permeability of the Blood–Brain Barrier

Same as a peripheral microvessel, the wall of the BBB can be viewed as a membrane. The membrane transport properties are often described by Kedem–Katchalsky equations derived from the theory of irreversible thermodynamics [47]:

$$J_s = PRT\Delta C + (1 - \sigma_f)CJ_v$$

$$J_v = L_p(\Delta p - \sigma_d RT\Delta C)$$

where J_s and J_v are the solute and volumetric fluxes and ΔC and Δp are the concentration and pressure difference across the membrane. L_p , the hydraulic conductivity, describes the membrane permeability to water. P , the diffusive permeability, describes the permeability to solutes. σ_f is the solvent drag or ultrafiltration coefficient that describes the retardation of solutes due to membrane restriction, and σ_d , the reflection coefficient, describes the selectivity of membrane to solutes. In many transport processes, σ_f is equal to σ_d [47] and thus we often use σ , the reflection coefficient, to represent both of them. These three coefficients can be determined both experimentally and theoretically. In addition to these quantitative coefficients, there are other less quantitative permeability indicators for the BBB, for example, brain uptake index (BUI), and brain efflux index (BEI) [2]. In the following sections, *in vivo* and *in vitro* experiments for determining permeability of the BBB are introduced, as well as the mathematical models.

14.2.2 Determination of the Blood–Brain Barrier Permeability *In Vivo* and *Ex Vivo*

Several *in vivo* and *ex vivo* rat models have been used for the study of the transport across the BBB, including pharmacokinetic methods [48–50], intracerebral microdialysis [51], positron emission tomography (PET) [52], magnetic resonance imaging (MRI) [53], the intravital microscopy study [54], occluding single microvessel measurement [55], and single microvessel fluorescence imaging method [56].

Pharmacokinetic methods are used to evaluate the delivery of a molecule from the systemic circulation into the brain, where the amount of solute delivered to the brain can be expressed by percentage of injected dose delivered per gram of the brain. Generally, a small volume of buffered Ringer's solution containing the radiolabeled compound of interest and a radiolabeled diffusible reference compound as an internal standard (such as ^3H -water) is injected into the common carotid artery, or the internal carotid artery, or the venule depending on different techniques. Then, the animal is sacrificed 5–15 s after injection, and the brain tissue and the injection solution are analyzed to calculate the BUI, which is the ratio of radiolabeled test compound/ ^3H reference in the brain, divided by the ratio of radiolabeled test compound/ ^3H reference in the injection mixture [2]. Another permeability indicator, BEI, can also be determined using this method. $\text{BEI} = (\text{amount of test compound injected into the brain} - \text{amount of test compound remaining in the brain}) / \text{amount of test compound injected into the brain}$. The assumptions of these models are (1) the reference compound is freely diffusible across the BBB; (2) the drug does not back-diffuse from the brain to blood; and (3) no metabolism of the compounds occurs before decapitation. The advantage of these pharmacokinetic methods is speed with which many compounds can be assessed in a short time, which is ideal in the high-throughput setting. The major disadvantages are (1) brain extraction only occurs over a limited time, making it difficult to accurately determine the BUI [2] and (2) the driving force for the transport is unknown.

Intracerebral microdialysis involves direct sampling of brain interstitial fluid by a dialysis fiber implanted into the brain parenchyma. The concentration of compound that has permeated into the brain following oral, intravenous, or subcutaneous administration can be monitored over time within the same animal. Any drug that enters the brain interstitial fluid will permeate into the physiological solution within the probe, and the solution may be subsequently assayed by an appropriate technique. The major advantage of this technique is that it provides pharmacokinetic profiles of drugs in the brain without killing animals at different time points. One limitation of this technique is that it greatly relies on and is limited by the sensitivity of the assay technique [51], since the solute concentrations may be extremely low in the dialysate. Another major disadvantage is that insertion of the probe can result in chronic BBB disruption.

More recently, various imaging techniques, including PET and MRI, have been used to determine BBB permeability in humans. PET is a noninvasive tracer technique used to quantify the BBB extravasations. MRI is also a noninvasive technique, but it is more qualitative than quantitative. The major disadvantages for these techniques include their inherent costs, labor intensity, relatively low

resolution (100 μm to 1 mm per pixel), and inability to differentiate between parent compound and metabolites [56,57].

All of the above-mentioned methods only measure certain indexes of relative permeability for the drug uptake to brain since they cannot determine the driving force for the efflux. Because it is hard to measure the BBB permeability in brain parenchyma, the microvessels in pia dura at the surface of brain (Figure 14.1) are often used in *in vivo* BBB permeability study. Although pial microvessels do not have the entire ensheathment of astrocytes as those cerebral microvessels in the parenchyma, the pial and cerebral microvessels appear to have many morphophysiological properties in common. These include ultrastructural characteristics, permeability of cell junctions to electron-dense tracers, transendothelium electrical resistance, and molecular properties of endothelium. For these reasons, pial microvessels are often used in the BBB permeability studies [58].

Gaber et al. [54] suggested a method to measure clearance or leakage of drug out of the pial microvessels rather than “true” permeability of the microvessels to solute. However, this method cannot determine the driving force, the concentration difference of the test solute across the BBB. The occluding single microvessel measurement is done directly on one single exposed pial microvessel after the frontal craniotomy removing a small section of the skull and the dura mater [55]. This method has well-controlled conditions, including known concentration difference, across the microvessel wall. However, recent study suggests that the exposed rat pial microvessels become leaky to both small and large molecules within 20–60 min following the craniotomy and the permeability of the exposed microvessels rises sharply after 160 min [59].

To quantify the permeability of intact rat pial microvessels and overcome the above-mentioned disadvantages, Yuan et al. [56] developed a noninvasive method, without exposing the cortex, to measure the solute permeability (P) of postcapillary venules on rat pia mater to various-sized solutes. The pial microvessels were observed by a high numerical aperture objective lens through a section of frontoparietal bones thinned with a microgrinder (revised surgical method from Reference 55). P was measured on individual pial venular microvessels with the perfused fluorescence tracer solution through the carotid artery by using highly sensitive quantitative fluorescence microscope imaging method. The major procedures are shown in Figures 14.6 and 14.7. The measured data plotted as permeability versus solute radius for the rat pial microvessels are shown in Figure 14.8. The measured permeability data for rat mesenteric microvessels are from Reference 60 for a small molecule, sodium fluorescein, an intermediate-sized molecule, α -lactalbumin, and a large molecule, albumin. Figure 14.8 shows that the solute permeability of rat pial microvessels is about an order of magnitude lower than that of rat mesenteric microvessels, from 1/11 for a small solute, sodium fluorescein, to 1/6 for a large solute, albumin or dextran 70k. The permeability data is also plotted for a small molecule, Lucifer Yellow, measured by [55,59] using an open-skull method.

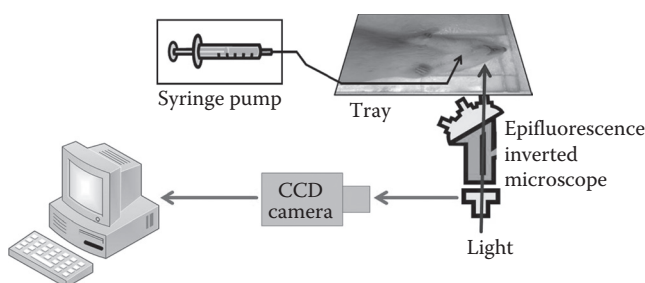


FIGURE 14.6 Schematic for the *in vivo* permeability measurement of rat pial microvessels. The fluorescence solution was injected into the brain via a carotid artery with a syringe pump. The fluorescence images were captured by a CCD camera, which was connected to an inverted microscope. The image analysis software was then used to measure the fluorescence intensity for the region of interest in each image.

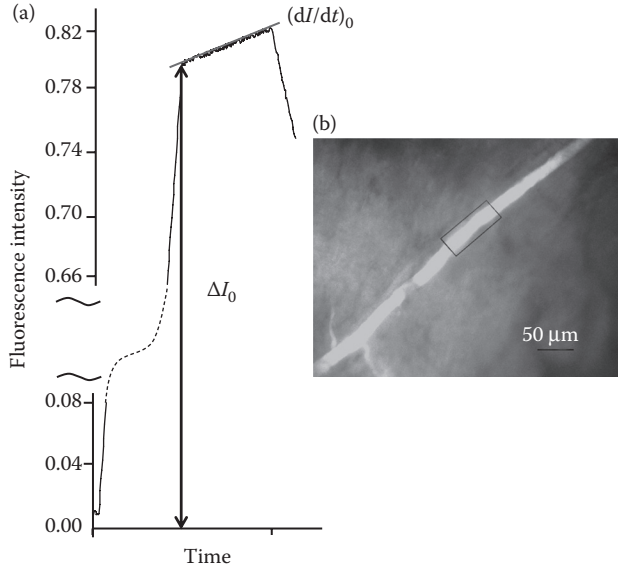


FIGURE 14.7 Quantitative fluorescence imaging method for the measurement of solute permeability in a rat pial microvessel. The images were collected during the *in vivo* experiments and the fluorescence intensity was analyzed off-line. When the fluorescence labeled test solute was injected into the carotid artery, the pial microvessel lumen filled with fluorescent solute (red frame in b), producing ΔI_0 . With continued perfusion, the measured fluorescence intensity increased indicating further transport of the solute out of the microvessel and into the surrounding tissue. The initial solute flux into the tissue was measured from the slope $(dI/dt)_0$ (a). The solute permeability P was calculated by $P = 1/\Delta I_0 (dI/dt)_0 r/2$. Here, r is the microvessel radius. The scale bar in (b) is 50 μm . (Redrawn from Yuan W et al. 2009. *Microvasc Res.* 77:166.)

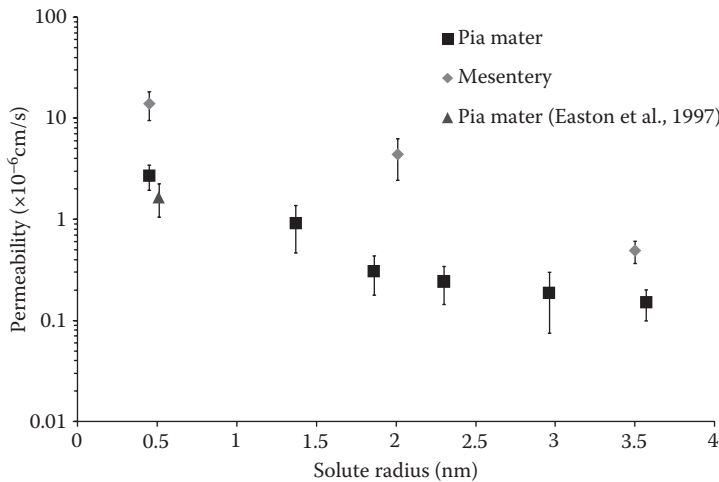


FIGURE 14.8 The pial microvessel permeability to various sized solutes versus solute radius (black squares) measured by a noninvasive method (Yuan et al., 2009) and the comparison between the measured data from Easton et al., 1997 (triangle) and those measured in mesenteric microvessels (diamonds). (Redrawn from Yuan W et al. 2009. *Microvasc Res.* 77:166.)

Downloaded by [JCR JCR] at 10:34 01 August 2015

14.2.3 *In Vitro* Blood–Brain Barrier Models

The development of *in vitro* models for the BBB has enabled the study of transport phenomena at the molecular and cellular levels. The aim of such *in vitro* BBB models is to functionally resemble as many as possible the unique characteristics of the BBB. Compared with *in vivo* animal models, the *in vitro* models are relatively accessible, flexible, reproducible, and abundantly available. Previous investigations showed that the permeability of the *in vitro* BBB models to various compounds such as sucrose, retinoic acid, retinol, haloperidol, caffeine, and mannitol was comparable to the permeability data obtained from *in vivo* models [61].

To characterize the transport properties of *in vitro* BBB models, the solute permeability P of the *in vitro* BBB was determined by measuring the flux of the selected tracer. The most commonly used cell culture substrate consists of a porous membrane support submerged in the culture medium (Transwell apparatus). The Transwell system is characterized by a horizontal side-by-side or vertical diffusion system. During the experiment, the flux of tracers into the abluminal compartment of the Transwell system is recorded as a function of the time and the solute permeability P is calculated from the slope of the flux. The tracers used in the transport experiments are labeled by a fluorescent dye or isotope whose intensity can be measured quantitatively. Another index, transendothelial electrical resistance (TEER), or the ionic conductance of the monolayer, is also a measurement of the “tightness” of the *in vitro* BBB models.

So far, two major types of *in vitro* BBB models have been developed: endothelial cell monolayer and coculture of endothelial cells with glial cells (the nonnerve cells in the brain). The cells for these models are basically obtained from primary/subpassaged or immortalized cell cultures. The origins of the cells are also very diverse: human, primate, bovine, porcine, rodent, and murine species.

The brain capillary endothelial cells (BCEC) have been used to establish tissue culture systems ever since the technique of culturing highly purified populations of microvascular cells became available in the early 1980s. The first endothelial monolayers were established using BCEC grown on culture dishes, microcarriers (e.g., dextran beads), and various kinds of filters, including nylon mesh and polycarbonate. These cultured BCEC cells keep their endothelial phenotypes and provide a simple model for studying the permeability of the BBB. For instance, they express angiotensin-converting enzyme, von Willebrand factor, and internalize acetylated LDL. However, they were reported to lose many BBB-specific features they possessed *in vivo*. For instance, they lack specific brain endothelial markers γ -glutamyl transpeptidase, marker enzyme alkaline phosphatase [62], and glucose transporter system [63]. Moreover, the permeability of the BCEC monolayer to sucrose was reported to be from 10^{-4} to 10^{-5} cm/s compared with 10^{-6} cm/s *in vivo*. The TEER for endothelial monolayer was also found to be pretty low, from 20 to $1400 \Omega \cdot \text{cm}^2$, compared with more than $2000 \Omega \cdot \text{cm}^2$ *in vivo*. So the BCEC monolayer alone is not a well-characterized model for the BBB. The major reason for this may be the lack of *in situ* environment and brain-derived signals.

In the human body, the BBB is almost completely ensheathed by surrounding tissue, mostly astrocyte foot processes. Experimental results from electron microscopic techniques show that astrocytes do have significant effects on the formation of the unique BBB phenotype of brain endothelial cells [64,65]. They induce the formation of the tight junctions between endothelial cells and increase paracellular integrity of the BBB. To better mimic the *in vivo* BBB, a model with coculture of BCEC and astrocyte was developed. This coculture model was characterized on the basis of specific cell-type properties and specific BBB properties by electron microscopic evaluation and immune-histochemistry methods [66]. The results showed that BCEC displayed (1) characteristic endothelial cell morphology; (2) expression of endothelial cell markers (i.e., CD51, CD62P, CD71, and cadherin 5); (3) tight junction formation between the cells; and (4) expression of typical barrier marker γ -glutamyl-transpeptidase (γ -GTP) and P-glycoprotein (P-gp) and transferrin receptors. Astrocytes displayed characteristic astrocyte morphology and expressed glial fibrillary acidic protein (GFAP). Transmission electron microscopy showed evidence of tight junction formation between the endothelial cells and few pinocytotic vesicles. A 15-fold

increase in γ -glutamyl transpeptidase activity was measured in the endothelial cells cocultured with astrocytes [67]. The permeability of the coculture system to several tracers was reported to be lower than the endothelial monolayer. These results indicate that the coculture system is a better model to study the transport across the BBB.

Primary BCEC have the closest resemblance to the BBB phenotype *in vivo*, and exhibit excellent characteristics of the BBB at early passages [57]. They, however, have inherent disadvantages such as being extremely time consuming and costly to generate, being easily contaminated by other neurovascular unit cells, losing their BBB characteristics over passages, and requiring high technical skills for extraction from brain tissue [68,69]. An immortalized mouse brain endothelial cell line, bEnd3, has recently been under investigation for *in vitro* BBB models because of its numerous advantages over primary cell culture: the ability to maintain BBB characteristics over many passages, easy growth and low cost, formation of functional barriers, and amenability to numerous molecular interventions [69–73]. Previous real time polymerase chain reaction (RT-PCR) analysis showed that bEnd3 cells express the tight junction proteins ZO-1, ZO-2, occludin, and claudin-5, and junctional adhesion molecules [69,74]. They also maintained the functionality of the sodium- and insulin-dependent stereospecific facilitative transporter GLUT-1 and the P-glycoprotein efflux mechanism [74], formed fairly tight barriers to radio-labeled sucrose, and responded like primary cultures to disrupting stimuli [69].

To characterize the transport properties of *in vitro* BBB models, Malina et al. [75] and others [76–84] measured the diffusive permeability of endothelial cell monolayer and coculture of endothelial cells with astrocytes to fluorescence or isotope-labeled tracers, for example, sucrose, inulin, and mannitol. Sahagun et al. [85] reported the ratio between abluminal concentration and luminal concentration of different-sized dextrans (4k, 10k, 20k, 40k, 70k, and 150k) across mouse brain endothelial cells. Gaillard and de Boer [66] measured the permeability of sodium fluorescein and fluorescein isothiocyanate (FITC)-labeled dextran 4k across a coculture of calf BCEC with rat astrocytes. Many investigators have measured the TEER of brain endothelial monolayers and cocultures as an indicator of ion permeability [86–89].

To seek for *in vitro* BBB models that are more accessible than animals for investigating drug transport across the BBB, Li et al. [90] characterized the junction protein expression and quantified the TER and permeability to water (L_p) and solutes (P) of four *in vitro* BBB models: bEnd3 monoculture, bEnd3 coculture with astrocytes, coculture with two BM substitutes: collagen type I and IV mixture, and Matrigel. Collagen type IV network is the basic framework of native BM [91,92] and Matrigel is a soluble and sterile extract of BM derived from the EHS tumor, which has been widely used as a reconstituted BM in studying cell morphogenesis, differentiation, and growth [93]. Their results show that L_p and P of the endothelial monoculture and coculture models are not different from each other. Compared with *in vivo* permeability data from rat pial microvessels, P of the endothelial monoculture and coculture models are not significantly different from *in vivo* data for dextran 70k, but they are 2–4 times higher for small solutes TAMRA and dextran 10k. This suggests that the endothelial monoculture and all of the coculture models are fairly good models for studying the transport of relatively large solutes (drugs or drug carriers) across the BBB.

14.2.4 Transport Models for the Paracellular Pathway of the Blood–Brain Barrier

Transport across the BBB includes both paracellular and transcellular pathways [94]. While large molecules cross the BBB through transcellular pathways, water and small hydrophilic solutes cross the BBB through the paracellular pathway [25]. The paracellular pathway of the BBB is formed by the endothelial surface glycocalyx, tight junction openings, the BM filled with extracellular matrix, and the openings between adjacent astrocyte foot processes (Figure 14.2b). In addition to the endothelial tight junctions, the BM and the astrocyte foot processes provide a significant resistance to water and solute transport across the BBB.

The breakdown of the BBB and increased permeability are widely observed in many brain diseases such as stroke, traumatic head injury, brain edema, Alzheimer’s disease, AIDS, brain cancer, meningitis, and so on [95–101]. Although numerous biochemical factors are found to be responsible for the breakdown of the BBB in disease, the quantitative understanding of how these factors affect the structural components of the BBB to induce BBB leakage is poor. On the other hand, the design of therapeutic drugs with better transport properties across the BBB relies greatly on this understanding. Therefore, it is important to investigate how the structural components in the paracellular pathway of the BBB affect its permeability to water and solutes through mathematical modeling.

Extended from a previous three-dimensional model for studying the transport across the peripheral microvessel wall with endothelium only [102,103], Li et al. [40] developed a new model for the transport across the BBB, which included the BM and wrapping astrocyte foot processes. The simplified model geometry is shown in Figure 14.9. This is the enlarged view for the part near the tight junction shown in Figure 14.2b. At the luminal side, there is an endothelial surface glycocalyx layer (SGL) with a thickness of L_f from 100 to 400 nm under normal physiological conditions [16–19,104]. Between adjacent endothelial cells, there is an interendothelial cleft with a length of $L \sim 500$ nm and a width of $2B \sim 20$ nm [104,105]. In the interendothelial cleft, there is a L_{jun} (~ 10 nm) thick junction strand with a continuous

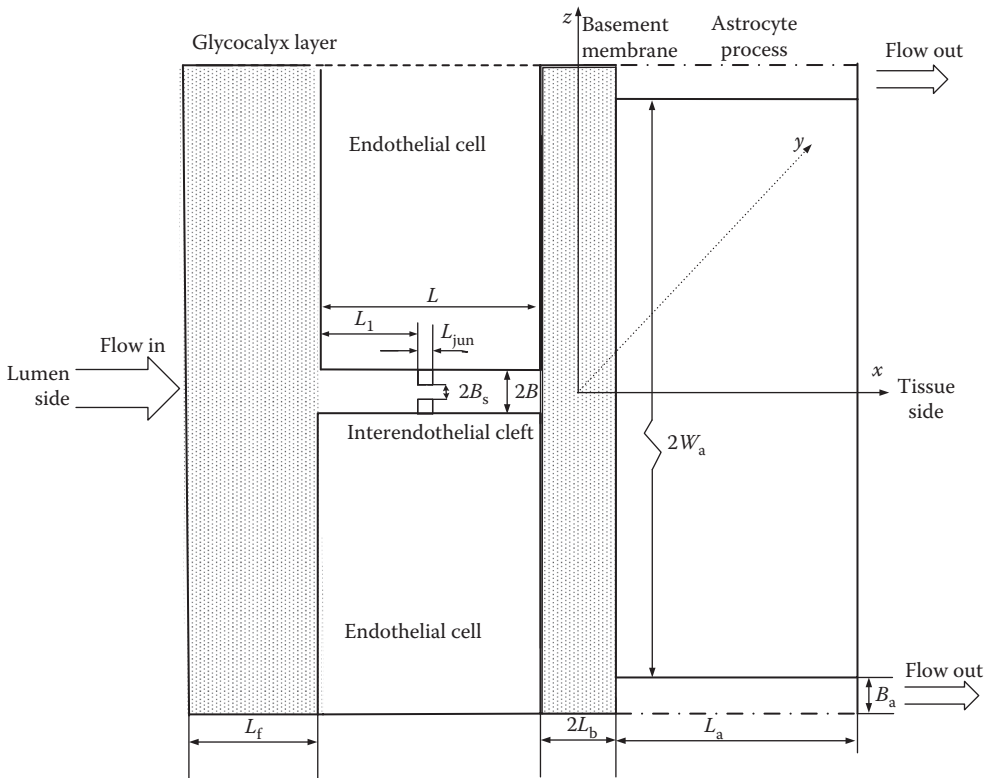


FIGURE 14.9 Model geometry for the paracellular pathway of the BBB (not in scale). The thickness of the endothelial surface glycocalyx layer is L_f . The interendothelial cleft has a length of L and a width of $2B$. The length of the tight junction strand in the interendothelial cleft is L_{jun} . The width of the small continuous slit in the junction strand is $2B_s$. The distance between the junction strand and luminal front of the cleft is L_1 . The width of the basement membrane is $2L_b$, and the length of the astrocyte foot processes is $2W_a$. The cleft between astrocyte foot processes has a length of L_a and a width of $2B_a$. The surface glycocalyx layer and the endothelial cells are defined as the endothelium only while the BBB is defined to include the endothelium, the basement membrane and the astrocytes. (Redrawn from Li G, Yuan W, Fu BM, 2010. *J. Biomech.* 43:2133–2140.)

Downloaded by [JCR JCR] at 10:34 01 August 2015

slit-like opening of width $2B_s$, which varies depending on the location of the cerebral microvessels (from ~ 1 to 10 nm). The distance between the junction strand and luminal front of the cleft is L_j . At the tissue side of the cleft, a BM separates the endothelium and the astrocyte foot processes. The thickness of the BM is $2L_b$ (20–40 nm) and the length of the astrocyte foot processes is $2W_a$ (~ 5000 nm). Between adjacent astrocyte foot processes, there is a cleft with length L_a (~ 1000 nm) and width $2B_a$ (20–2000 nm). The anatomic parameters for the BBB structural components were obtained from the electron microscopy studies in the literature.

Unlike the peripheral microvessel wall, the endothelium of the BBB has negligible large discontinuous breaks in the junction strand of the interendothelial cleft and the small slit in the junction strand is assumed continuous [25]. As a result, the cross-sectional BBB geometry is the same along the axial direction (y direction in Figure 14.9) and thus the model could be simplified to 2-D (in x, z plane). It could be further simplified to a unidirectional flow in each region due to very narrow clefts and the BM. In addition, the curvatures of the BM and the endothelium can be neglected because their widths are much smaller than the diameter of the microvessel. The fluid flow in the cleft regions of the BBB were approximated by the Poiseuille flow while those in the endothelial SGL and BM by the Darcy and Brinkman flows, respectively. Diffusion equations in each region were solved for the solute transport. After solving for the pressure, water velocity, and solute concentration profiles, the hydraulic conductivity L_p and solute permeability P can be calculated.

Figure 14.10a shows the model predictions for L_p as a function of tight junction opening B_s when the BM has different fiber densities. K_b is Darcy permeability in the BM. When the fiber density in the BM is the same as that in the SGL, $K_b = 3.16 \text{ cm}^2$. The small dash-dash in Figure 14.10a shows the case of peripheral microvessels with only endothelium. When B_s increases from 0.5 to 2 nm, L_p will increase by ~ 20 -fold. In contrast, when the endothelium is wrapped by the BM and the astrocytes as for the BBB, increase in B_s from 0.5 to 2 nm only induces fivefold increase in L_p when the fiber density in the BM is the same as that in the SGL (dash-dot-dash line). If the fiber density in the BM is 10 times of that in the SGL, the increase is only 1.6-fold in L_p (solid line), while if the fiber density in the BM is 1/10 of that in the SGL, the increase is 12-fold in L_p (large dash-dash line). Even at a large B_s of 5 nm, when the BM is filled with the same density fibers as in the SGL, the BBB permeability is only 17% of that of endothelium only. This percentage can be as low as 2% if the fiber density in the BM is 10 times of that in the SGL. Figure 14.10b shows the model predictions for L_p as a function of the endothelial SGL thickness L_f . The dashed line is for the case of endothelium only while the solid line for that of the BBB. We can see the decrease in L_f from 400 to 0 nm increases L_p by 3-fold in the case of endothelium only, while in the case of the BBB, the increase is only 25% in L_p with the protection of the BM and the astrocytes. Similar results are predicted for the solute permeability [40]. These results indicate that the BM and astrocytes of the BBB provide a great protection to the CNS under both physiological and pathological conditions. However, on the other hand, these unique structures also impede the drug delivery to the brain through the BBB.

14.2.5 Strategies for Drug Delivery through the Blood–Brain Barrier

A large number of people in the world are now suffering from CNS diseases. The total number of patients with CNS diseases is reported to be larger than that with cardiovascular diseases [5]. While the BBB serves as a natural defense that safeguards the brain against the invasion of various circulating toxins and infected cells, it also provides a significant impediment toward the delivery of diagnostic and therapeutic agents to the brain via the systemic route. Essentially, almost 100% of large-molecule drugs, including peptides, recombinant proteins, monoclonal antibodies, RNA interference (RNAi)-based drugs, and gene therapies, and more than 98% of small-molecule drugs cannot penetrate the brain microvessel wall by themselves [2,5].

Various methods such as intracerebral implantation, microdialysis, convection-enhanced distribution (CED), osmotic shock, and chemical modification of the BBB have been developed for delivering

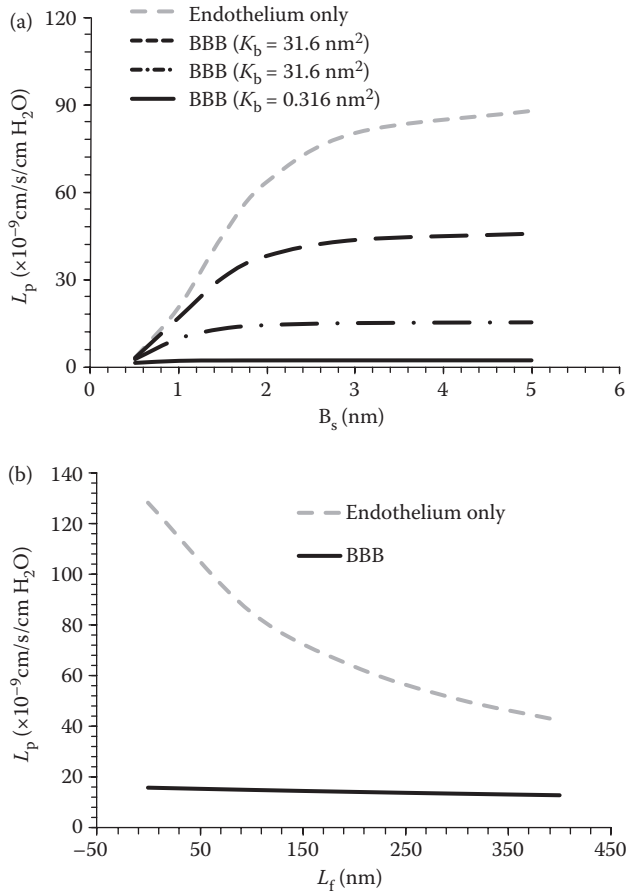


FIGURE 14.10 Model predictions for hydraulic conductivity L_p (a) as a function of B_s , the half width of the small slit in the junction strand under two cases: when considering transport across the endothelium only (endothelium only, dashed line), and when considering transport across the entire BBB (BBB). In the BBB case, three different fiber densities were considered for the basement membrane: the same as the fiber density in the surface glycocalyx layer ($K_b = 3.16 \text{ cm}^2$, the dash-dot-dash line), 10 times lower ($K_b = 31.6 \text{ cm}^2$, the dashed line) and higher ($K_b = 0.316 \text{ cm}^2$, the solid line); (b) as a function of the surface glycocalyx layer thickness L_f . (Redrawn from Li G, Yuan W, Fu BM, 2010. *J Biomech.* 43:2133–2140.)

drugs into the brain. However, the applications of these methods are limited and they can only partially keep with the demands of modern therapies. For instance, the efficiency of intracerebral implantation, microdialysis, and CED methods are low since their major transport mechanisms are diffusion and convection of interstitial fluid. The penetration distances of drugs delivered by the first two methods are reported to be $<1 \text{ mm}$ with simple diffusion [106]. CED has been shown in laboratory experiments to deliver high-molecular-weight proteins 2 cm from the injection site in the brain parenchyma after 2 h of continuous infusion [107]. However, the success of CED relies on precise placement of the catheters and other infusion parameters for delivery into the correct location in the brain parenchyma. For effective treatment of the CNS diseases, therapeutic agents have to reach the specific regions of the brain at an adequate amount. As discussed earlier, due to the abundance and the largest contact area of the BBB for blood–brain exchange, it is more reasonable to develop strategies for drug delivery through the BBB.

As shown in [Figure 14.4](#), we can directly deliver therapeutic agents through paracellular pathway (route A), lipophilic diffusion pathway (route C), or through transporters at the BBB by closely mimicking their substrates (route B), or mount the drugs on the ligands of the specific receptors expressed at the BBB (e.g., LDL receptor-related protein) for transcytosis (Trojan horse approach or RMT route D), as well as using cationized proteins, peptides, and nanoparticle carriers for adsorptive-mediated transcytosis (AMT, route E). The following summarizes the delivery strategies through these routes, respectively.

14.2.5.1 Delivery through Paracellular Pathway (Route A)

To increase the hydrophilic drug delivery from the blood to the brain tissue, we can transiently open the barriers in the paracellular pathway of the BBB, for example, the cleft opening ($2B$ in [Figure 14.9](#)), the tight junction opening ($2B_s$), the BM width ($2L_b$), or degrade the fiber matrix in the endothelial surface glycocalyx and in the BM. Osmotic shock by intracarotid administration of a hyperosmotic mannitol causes endothelial cells to shrink and increase $2B$, $2B_s$, and $2L_b$. Subsequent administration of drugs can increase their concentrations in the brain to a therapeutic level [108,109]. Physical means such as application of electric and magnetic fields can increase the drug brain uptake. Focused ultrasound, guided by MRI, combined with microbubbles injected into the blood stream has been shown to disrupt the BBB and increase the distribution of Herceptin in brain tissue by 50% in mice [110–112]. Application of inflammatory agents such as bradykinin analog can open the tight junction of the BBB and increase the drug transport to the brain [113,114]. However, these approaches are relatively costly and nonpatient friendly. They may also enhance tumor dissemination after BBB disruption and damage the neurons by allowing the passage of unwanted blood components into the brain [115].

14.2.5.2 Delivery through Lipophilic Diffusion Pathway (Route C)

Some molecules, for example, alcohol, nicotine, and benzodiazepine, can freely enter the brain through route C in [Figure 14.4](#). Their ability to passively (diffusion by concentration differences across the cell membrane) cross the BBB depends on the molecular weight (<500 Da), charge, (low hydrogen bonding capabilities) and lipophilicity [116]. Therefore, if we can modify the drugs through medicinal chemistry, for example, reduce the relative number of polar groups, or incorporate them with a lipid carrier, we can enhance their brain uptake [2,117]. Modification of antioxidants with pyrrolopyrimidines increases their ability to access target cells in the CNS [118]. Covalently attaching 1-methyl-1,4-dihyronicotinate to a hydroxymethyl group can enhance the delivery of ganciclovir (Cytovene, an antiviral medication) to the brain [119,120]. However, the modification that helps for the drug delivery to the brain often results in loss of the therapeutic function of a drug. In addition, increase of lipophilicity of a drug can result in making it a substrate for the efflux pump P-glycoprotein (route F in [Figure 14.4](#)) [115].

14.2.5.3 Delivery through Transporter-Mediated Pathway (Route B)

The brain requires a tremendous amount of essential substances for survival and function, for example, glucose, insulin, hormones, and LDL. These nutrients and substances are transported into the brain, not by paracellular or lipophilic diffusion pathway as described earlier, but by specific transporters or receptors at the BBB. Drugs can be modified to take advantage of the native BBB nutrient transporter systems, or by being conjugated to ligands that recognize receptors expressed at the BBB for the RMT. This physiological approach is by far recognized as the most likely successful drug delivery method to the brain.

Peptides and small molecules may use specific transporters expressed on the luminal and basolateral sides of the endothelial cells to cross into the brain. So far, at least eight different nutrient transporters have been identified to transport a group of nutrients with similar structures. Drugs can be modified to closely mimic the endogenous carrier substrates of these transporters and be transported through the specific transporter-mediated transcytosis. Dopamine can be used to treat Parkinson's disease, but itself is nonbrain penetrant. Instead, dopamine's metabolic precursor, L-Dopa, if delivered by a neutral amino acid carrier through its transporter at the BBB, shows a clear clinical benefit on patients with Parkinson's disease [6,121]. To use a BBB transporter for drug delivery, several important factors must

be considered: the kinetics and structural binding requirements of the transporter, therapeutic compound manipulation so that the compound binds but also remains active *in vivo*, and actual transport of the compound into the brain instead of just binding to the transporter [115].

14.2.5.4 Delivery through Receptor-Mediated Pathway (Route D)

Instead of by transporters, larger essential molecules are delivered into the brain by specific receptors highly expressed at the endothelial cells of the BBB. The RMT includes three steps: receptor-mediated endocytosis of the molecule at the luminal side of the endothelium (blood side), transport through the endothelial cytoplasm, and exocytosis of the molecule at the abluminal side of the endothelium (brain side). Although the exact mechanisms of RMT have not been well understood, drug delivery targeting three receptors, the insulin receptor, the transferrin receptor, and the LDL receptor, has been in use since the start of this century [121,122]. More and more receptors have been targeted for the drug delivery since then [115]. This physiological approach is often called a molecular Trojan horse since the therapeutic compounds are conjugated to the specific ligands or the antibodies, which can be recognized and delivered through transcytosis by the specific matching receptors at the endothelial cell membrane. In addition to molecular Trojan horses, drugs can be packaged to liposomes and other nanoparticles coated with targeting molecules such as antibodies to the specific receptors to improve the drug-loading capacity.

Although the Trojan horses for the BBB drug delivery are very promising in delivering large peptides and recombinant proteins such as neurotrophins, enzymes, and monoclonal antibodies [122], the traffic is limited by the number and carrying capacity of the receptors, as well as by the number of drug molecules that can attach to each antibody [123]. In addition, Gosk et al. [124] showed that using anti-transferrin mAb for drug delivery through the systemic administration, although the total amount of the drug in the brain is high, most of it stays associated with brain microvessel endothelial cells instead of in the brain parenchyma. Due to the high affinity of the antibodies, it is a challenge to dissociate from their specific receptors. Furthermore, widespread distribution of the receptors on peripheral organs would limit the specific delivery to the brain, and on the other hand, may induce additional toxicity.

14.2.5.5 Delivery through Adsorptive-Mediated Pathway (Route E)

AMT involves endocytosis and exocytosis of charged substances by the endothelial cells of the BBB. Its mechanism is different from that of the RMT, which needs specific matching receptors and ligands. Kumagai et al. [125] observed that polycationic proteins such as protamine could not only bind to the endothelial cell surface but also penetrate the BBB. Mixing protamine, poly-l-lysine or other cationic molecules with proteins (e.g., albumin) largely increased the BBB permeability to these proteins. These findings can be explained by AMT triggered by electrostatic interactions between the positively charged proteins and negatively charged membrane regions at the brain endothelium. At normal physiological pH, the luminal surface of the cerebral endothelium and the surrounding BM (see Figure 14.2b) carry negative charge [126] and provide the necessary environment for delivering positively charged drugs and drug carriers. Recently, a quantitative *in vivo* animal study by Yuan et al. [127] found that the charge density of the endothelial surface glycocalyx and that of the BM in rat pial microvessels are ~ 30 mEq/L. In another *in vitro* cell culture study, Yuan et al. [72] found the similar charge density on the surface of a cell monolayer of bEnd3, an immortalized mouse cerebral microvessel endothelial cell line.

To efficiently deliver a therapeutic protein or peptide across the BBB, the simplest way is to cationize the protein or peptide by amidation of its carboxylic acid groups, as well as glutamic and aspartic acid side chain groups with positively charged amines [128]. The degree of cationization of a protein or peptide may be critical for its pharmacokinetic fate. Cationization enhances delivery while inducing potential toxicity and immunogenicity of these proteins. PEGylation of cationized molecules can minimize the immunogenicity of these molecules. Positively charged cell-penetrating peptides (CPPs) are often used as the drug carriers for the brain delivery. Commonly used CPPs are penetratin, transportan, Syn-B,

and Tat [128]. Brain uptake of enkephalin analog dalargin was enhanced several hundred fold after they were carried by the CPPs [129]. Decoration of CPPs on the surface of liposome and biopolymer-based nanoparticles containing drugs has been shown to promote their uptake by the brain and entrance to the cytoplasm of neurons [130]. The drawbacks through AMT are lack of tissue selectivity, although the BBB may contain higher concentrations of negative charges than other tissues, and possible disruption of the BBB and binding of polycationic substances to the negatively charged plasma proteins and other anionic sites resulting in toxicity [131].

14.3 Drug Delivery through the Cerebrospinal Fluid

As described in the introduction, unlike the BBBs that have very low permeability to water and solutes, the brain–CSF barrier (see [Figure 14.1](#)), the interface between the brain tissue and CSF, is relatively leaky, allowing passage of macromolecules (e.g., antibodies) at certain degree. Although the exchange area of the brain–CSF barrier was estimated to be at least 1800 cm², the total exchange area can be the same order of magnitude as the entire BBB if the infolding and microvilli of the ependyma (the epithelial cells forming the brain–CSF barrier) are taken into consideration. Therefore, delivery through the brain–CSF barrier is very promising for treating certain types of brain diseases.

14.3.1 Production and Circulation of the Cerebrospinal Fluid

The CSF is actively secreted by ependymal cells, the epithelial cells lining the highly vascularized choroid plexus (see [Figures 14.1](#) and [14.5](#)). The rate of secretion in humans is ~500 mL/day. The CSF circulates from the lateral ventricles through the interventricular foramina into the third ventricle, then down the narrow aqueduct of sylvius into the fourth ventricle, where it exits through two lateral apertures and one median aperture. It then flows through the cerebellomedullary cistern down the spinal cord and into the subarachnoid space over the cerebral hemispheres ([Figure 14.5](#)). Finally, the CSF passes from the subarachnoid space into venous blood of sinus sagittalis superior in dura mater through arachnoid villi and arachnoid granulations. Drainage into the lymphatic system also occurs [8,42].

The human brain contains only 135–150 mL of CSF, so the CSF flow is rapid due to a high secretion rate of 500 mL/day. The high producing rate is achieved because the structure of choroid plexus is superbly adapted to the secretion [9]. First, the choroid plexus has abundant blood supply. Compared to the average blood supply in the cerebral cortex, which is 0.35–0.4 mL/min/g in a rat, the blood supply to the lateral ventricle choroid plexus is about ~4 mL/min/g, a 10-fold more [132]. Second, in contrast to the cerebral capillaries (the BBB), the capillaries in the choroid plexus are fenestrated and provide much less resistance to the substances transport from the blood to the epithelial cells lining the choroid plexus. Third, the choroid epithelium is a leaky type of epithelium and permits the material passage between the interstitial space and the CSF. Fourth, the choroidal epithelial cells possess numerous microvilli on the apical (CSF) side and extensive infolding at the basolateral (blood) side, which increase the surface area for contact between epithelia and the interstitium at one side, and epithelia and the CSF at the other side. Fifth, the choroid epithelial cells have rich mitochondria, suggesting that the production of ATP is sufficient to sustain normal secretion of CSF. Because of its rapid refreshing rate, broad contact area with the brain tissue, and relatively leaky barrier between the CSF and the brain, the CSF is becoming a very good candidate for drug delivery to the CNS system.

14.3.2 Radioimmunotherapy Delivered through the Cerebrospinal Fluid

For delivery through the CSF, drugs can be infused intraventricularly using a plastic reservoir called an Ommaya reservoir implanted subcutaneously in the scalp and connected to the ventricles within the brain via an outlet catheter [133] ([Figure 14.11](#)). Compared to vascular drug administration, CSF

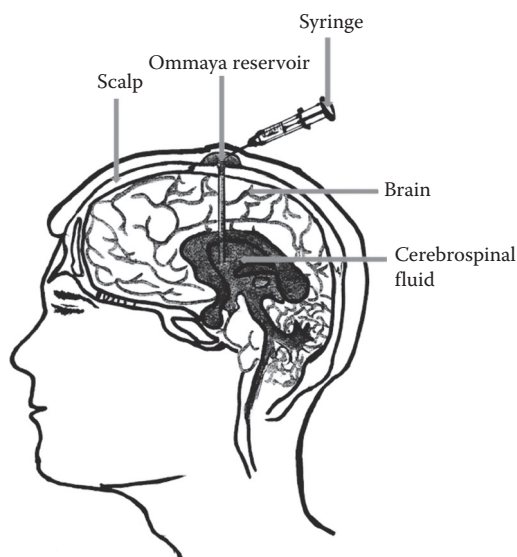


FIGURE 14.11 Drug delivery to the brain through cerebrospinal fluid.

delivery has several advantages: first, it bypasses the BBB and immediately enhances the CSF drug concentrations; second, it potentially reduces the systemic toxicity since the drug directly goes to the CNS; third, the half life of a drug can be longer since there is less enzymatic degrading activity in the CSF; fourth, the CSF can freely exchange molecules with the extracellular fluid of the brain parenchyma, delivering drugs into the CSF is more likely resulting in therapeutic CNS drug concentrations. The following presents a successful example for brain cancer treatment by delivering isotope-labeled therapeutic antibodies (radioimmunotherapy) through the CSF.

Tumor cells can invade the CSF and disseminate throughout the neuroaxis by the constant flow of CSF which travels from the ventricles to the spinal canal and over the cortical convexities. Involvement of the leptomeninges (LM) by any cancer is a serious complication with significant morbidity and mortality [134–136]. Its frequency is increasing as patients live longer and as neuroimaging modalities improve, approaching 5% in solid tumors such as breast cancer and lung cancer [135]. Neuroblastoma is the most common extracranial tumor of the sympathetic nervous system, occurring predominantly in early childhood and accounting for 6.7% of childhood cancer. With increasing period of remission, CNS metastasis (both parenchymal and LM), though rare in the past [136], has substantially increased in the past decade. Antibody-based radioimmunotherapy (RIT) administered through the CSF has clinical potential in the treatment of cancers metastatic to the LM or brain. ^{131}I -labeled monoclonal antibodies (mAbs) targeting GD2 (e.g., mAb 3F8) or B7H3 (e.g., mAb 8H9) when administered through an Ommaya reservoir have proven safe in phase I clinical trials [137]. Patients with relapsed neuroblastoma in the CNS (brain or LM), when treated with salvage regimens containing either intra-Ommaya ^{131}I -3F8 or ^{131}I -8H9, have survived for extended periods of time.

Given the unique physiology of the CSF compartment, as well as the well-defined kinetic/radiochemical properties of monoclonal antibodies, RIT delivered through the CSF can be optimized. An optimization model will help understand the complex dynamics of antibody and radiation dose delivered to tumor cells and to normal brain, and provide a tool to define the critical parameters in order to improve effectiveness and safety of ^{131}I -MoAb RIT administered through the CSF. In addition, since different isotopes have distinct microdosimetric properties, their biologic effect in CSF RIT can be simulated and compared. These critical parameters of CSF dynamics and mAb pharmacokinetics can

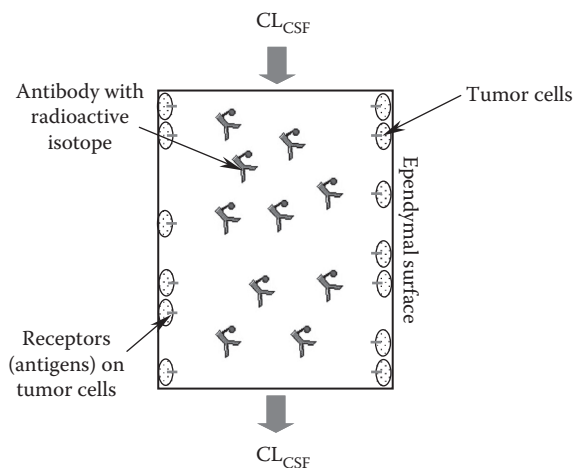


FIGURE 14.12 Schematic of pharmacokinetic model for radioimmunotherapy delivered through CSF administration. CL_{CSF} represents the flow rate of the cerebrospinal fluid. (Redrawn from Lv Y, Cheung NK, Fu BM, 2009. *J Nuclear Med.* 50(8):1324.)

be manipulated by pharmacologic interventions and genetic engineering, respectively, and be tested *in vivo* using rat or mice with LM xenografts. The long-term plan is to bring these concepts to human phase I and II studies.

Recently, Lv et al. [138] developed a pharmacokinetic model to evaluate the role of kinetic and transport parameters of RIT in maximizing the therapeutic ratio, the ratio of the area under the curve for the concentration of the bound antibodies versus time [$AUC(C_{IAR})$], to that for unbound antibodies [$AUC(C_{IA})$]. The CSF space was simplified as a single compartment and considered the binding of antibodies to antigens on tumor cells lining the surface of the CSF space (Figure 14.12). Mass conservation was applied to set up the equations for C_{IAR} , C_{IA} , and other pharmacokinetic variables and a Runge–Kutta method was used to solve the equations. This model agreed with the measured data in 10 of 14 patients in the phase I trial of intra-Ommaya RIT using ^{131}I -3F8 [133]. Using this model, several predictions were made: (1) Increasing the affinity of antibodies to antigens greatly increases $AUC(C_{IAR})$ but not $AUC(C_{IA})$. (2) For the same amount of isotope administered, the smaller antibody dosage and the higher specific activity improves therapeutic ratio. (3) When the isotope half life is 0.77 h, increasing the antibody association constant enhances $AUC(C_{IAR})$ much more than decreasing the dissociation constant even if overall affinity is unchanged. However, when the half life reaches 240 h, decreasing dissociation constant would slightly enhance $AUC(C_{IAR})$. (4) Decreasing the CSF bulk flow rate increases $AUC(C_{IAR})$. (5) At the same amount of antibody administered by continuous infusion and by split administrations, one can improve $AUC(C_{IAR})$ by up to 1.8-fold and 1.7-fold, respectively, compared to that by the single bolus administration. The improved therapeutic ratio by optimized kinetic and transport parameters may enhance clinical efficacy of this new treatment modality through the CSF.

Acknowledgments

The author would like to thank the funding support from NSF CBET-0754158, NIH 1SC1GM086286-01A1, and 1U54CA137788-01. She would also like to thank Dr. Guanglei Li, Dr. Wei Yuan, Ms Lingyan Shi, and Ms Lin Zhang for their assistance in preparing Figures 14.1, 14.2b, 14.3 through 14.6, and 14.11.

References

1. Abbott NJ, 1992. Comparative physiology of the blood-brain barrier. In: Bradbury MWB (ed) *Physiology and Pharmacology of the Blood-Brain Barrier*. Springer, Heidelberg. p. 371.
2. Pardridge WM, 1998. CNS drug design based on principles of blood-brain barrier transport. *J Neurochem*. 70:1781.
3. Abbott NJ, 2004. Evidence for bulk flow of brain interstitial fluid: Significance for physiology and pathology. *Neurosci Int*. 45:545.
4. Brown PD, Davies SL, Speake T, Millar ID, 2004. Molecular mechanisms of cerebrospinal fluid production. *Neurosci*. 129:957.
5. Pardridge WM, 2006. *Introduction to the Blood-Brain Barrier: Methodology, Biology and Pathology*. Cambridge University Press, Cambridge.
6. Pardridge WM, 2007. Drug targeting to the brain. *Pharm Res*. 24:1733.
7. Nag S, Begley DJ, 2005. Blood-brain barrier, exchange of metabolites and gases. In: Kalimo H (ed) *Pathology and Genetics. Cerebrovascular Diseases*. ISN Neuropath. Press, Basel. p. 22.
8. Culter RWP, Page L, Galicich J, Watters GV, 1968. Formation and absorption of cerebrospinal fluid in man. *Brain* 91:707.
9. Redzic ZB, Segal MB, 2004. The structure of the choroid plexus and the physiology of the choroid plexus epithelium. *Adv Drug Del Rev*. 56:1695.
10. Smith QR, 2000. Transport of glutamate and other amino acids at the blood-brain barrier. *J Nutr*. 130:1016.
11. Zhang Y, Pardridge WM, 2001. Rapid transferrin efflux from brain to blood across the blood-brain barrier. *J Neurochem*. 76:1597.
12. Lewandowsky M, 1900. Zur lehre von der cerebrospinalflussigkeit. *Z Klin Med*. 40:480.
13. Ehrlich P, 1885. *Das Sauerstoffbedurfnis Des Organismus*. Hireschwald. Berlin.
14. Goldmann E, 1913. Vitalfarbung am zentralnervensystem. *Abhandl Kongil Preuss Akad Wiss*. 1:1.
15. Reese TS, Karnovsky MJ, 1967. Fine structural localization of a blood-brain barrier to exogenous peroxidase. *J Cell Biol*. 34(1):207.
16. Adamson RH, Clough G, 1992. Plasma proteins modify the endothelial cell glycocalyx of frog mesenteric microvessels. *J Physiol*. 445:473.
17. Squire JM, Chew M, Nneji G, Neal C, Barry J, Michel C, 2001. Quasi-periodic substructure in the microvessel endothelial glycocalyx: A possible explanation for molecular filtering? *J Struct Biol*. 136(3):239.
18. Ueno M, Sakamoto H, Liao YJ, Onodera M, Huang CL, Miyanaka H, Nakagawa T, 2004. Blood-brain barrier disruption in the hypothalamus of young adult spontaneously hypertensive rats. *Histochem Cell Biol*. 122(2):131.
19. Vink H, Duling BR, 1996. Identification of distinct luminal domains for macromolecules, erythrocytes, and leukocytes within mammalian capillaries. *Circ Res*. 79(3):581.
20. Henry CB, Duling BR, 1999. Permeation of the luminal capillary glycocalyx is determined by hyaluronan. *Am J Physiol Heart Circ Physiol* 277(2):H508.
21. Tarbell JM, Pahakis MY, 2006. Mechanotransduction and the glycocalyx. *J Int Med*. 259(4):339.
22. Farkas E, Luiten PGM, 2001. Cerebral microvascular pathology in aging and Alzheimer's disease. *Prog Neurobiol*. 64(6):575.
23. Oldendorf WH, Cornford ME, Brown WJ, 1977. The large apparent work capability of the blood-brain barrier: A study of the mitochondrial content of capillary endothelial cells in brain and other tissues of the rat. *Ann Neurol*. 1:409.
24. Butt AM, Jones HC, Abbott NJ, 1990. Electrical resistance across the blood-brain barrier in anaesthetized rats: A developmental study. *J Physiol*. 429:47.
25. Hawkins BT, Davis TP, 2005. The blood-brain barrier/neurovascular unit in health and disease. *Pharmacol Rev*. 57:173.

26. Simard M, Arcuino G, Takano T, Liu QS, Nedergaard M, 2003. Signaling at the gliovascular interface. *J Neurosci.* 23(27):9254.
27. Kim JH, Park JA, Lee SW, Kim WJ, Yu YS, Kim KW, 2006. Blood-neural barrier: Intercellular communication at glio-vascular interface. *J Biochem Mol Biol.* 39(4):339.
28. Abbott NJ, Patabendige AAK, Dolman DEM, Yusof SR, Begley DJ, 2010. Structure and function of the blood-brain barrier. *Neurobiol Dis.* 37:13.
29. Romero IA, Radewicz K, Jubin E, Michel CC, Greenwood J, Couraud PO, Adamson P, 2003. Changes in cytoskeletal and tight junctional proteins correlate with decreased permeability induced by dexamethasone in cultured rat brain endothelial cells. *Neurosci Lett.* 344(2):112.
30. Ballabh P, Braun A, Nedergaard M, 2004. The blood-brain barrier: An overview: Structure, regulation, and clinical implications. *Neurobiol Dis.* 16:1.
31. Hynes RO, 1992. Integrins: Versatility, modulation, and signaling in cell adhesion. *Cell.* 69:11.
32. Moody DM, 2006. The blood-brain barrier and blood-cerebral spinal fluid barrier. *Semin Cardiothorac Vasc Anesth.* 10(2):128.
33. Neuwelt EA, 2004. Mechanisms of disease: The blood-brain barrier. *Neurosurgery* 54(1):131.
34. Sawchuk RJ, Elmquist WF (2000) Microdialysis in the study of drug transporters in the CNS. *Adv Drug Deliv Rev.* 45:295.
35. Kay GG, 2000. The effects of antihistamines on cognition and performance. *J Allergy Clin Immunol.* 105:S622.
36. Schuetz EG, Schinkel AH, Relling MV, Schuetz JD, 1996. P-glycoprotein: A major determinant of rifampicin-inducible expression of cytochrome P4503A in mice and humans. *Proc Natl Acad Sci USA.* 93:4001.
37. Begley DJ, 2007. Structure and function of the blood-brain barrier. In: Touitou E, Barry BW (eds) *Enhancement in Drug Delivery.* CRC Press. Boca Raton, FL. p. 575.
38. Shimizu S, 2008. A novel approach to the diagnosis and management of meralgia paresthetica. *Neurosurgery.* 63(4):E820.
39. Wolburg-Buchholz K, Mack AF, Steiner E, Pfeiffer F, Engelhardt B, Wolburg H, 2009. Loss of astrocyte polarity marks blood-brain barrier impairment during experimental autoimmune encephalomyelitis. *Acta Neuropathol.* 18(2):219.
40. Li G, Yuan W, Fu BM, 2010. A model for water and solute transport across the blood-brain barrier. *J. Biomech.* 43:2133–2140.
41. Davson H, Segal MB, 1995. *Physiology of the CSF and Blood-Brain Barriers.* CRC Press, Boca Raton, FL.
42. Guyton AC, Hall JE, 2000. *Textbook of Medical Physiology.* 10th Edition. Philadelphia: Saunders. p. 709.
43. Smith DE, Johanson CE, Keep RF, 2004. Peptide and peptide analog transport systems at the blood-CSF barrier. *Adv Drug Deliv Rev.* 56:1765.
44. Barta P, Dazzan P, 2003. Hemispheric surface area: Sex, laterality and age effects. *Cereb Cortex.* 13:364.
45. Blasberg RG, Patlak CS, Shapiro WR, 1977. Distribution of methotrexate in the cerebrospinal fluid and brain after intraventricular administration. *Cancer Treat Rep.* 61:633.
46. Keep RF, Jones HC, 1990. A morphometric study on the development of the lateral ventricle choroid plexus, choroid plexus capillaries and ventricular ependyma in the rat. *Brain Res Dev Brain Res.* 56:47.
47. Curry FE, 1984. Mechanics and thermodynamics of transcapillary exchange. In: Renkin EM and Michel CC (eds.) *Handbook of Physiology. The Cardiovascular System.* The American Physiology Society, Bethesda. Sect.2 (vol IV, pt1):309.
48. Cornford EM, Young D, Paxton JW, Sofia RD, 1992. Blood-brain barrier penetration of felbamate. *Epilepsia.* 33:944.
49. van Uiterl RL, Sage JI, Levy DE, Duffy TE, 1981. Comparison of radio-labeled butanol and iodoantipyrine as cerebral blood flow markers. *Brain Res.* 222:365.

50. Zlokovic BV, Begley DJ, Djuricic BM, Mitrovic DM, 1986. Measurement of solute transport across the blood-brain barrier in the perfused guinea pig brain: Method and application to *N*-methyl-alpha-aminoisobutyric acid. *J Neurochem.* 46:1444.
51. de Lange EC, de Boer BA, Breimer DD, 1999. Microdialysis for pharmacokinetic analysis of drug transport to the brain. *Adv Drug Deliv Rev.* 36:211.
52. Elsinga PH, Hendrikse NH, Bart J, Vaalburg W, van Waarde A, 2004. PET Studies on P-glycoprotein function in the blood-brain barrier: How it affects uptake and binding of drugs within the CNS. *Curr Pharm Des.* 10:1493.
53. Wang R, Ashwal S, Tone B, Tian HR, Badaut J, Rasmussen A, Obenaus A, 2007. Albumin reduces blood-brain barrier permeability but does not alter infarct size in a rat model of neonatal stroke. *Pediatr Res.* 62:261.
54. Gaber MW, Yuan H, Killmar JT, Naimark MD, Kiani MF, Merchant TE, 2004. An intravital microscopy study of radiation-induced changes in permeability and leukocyte-endothelial cell interactions in the microvessels of the rat pia mater and cremaster muscle. *Brain Res Brain Res Protoc.* 13:1.
55. Easton AS, Fraser PA, 1994. Variable restriction of albumin diffusion across inflamed cerebral microvessels of the anaesthetized rat. *J Physiol.* 475:147.
56. Yuan W, Lv Y, Zeng M, Fu BM, 2009. Non-invasive measurement of solute permeability in cerebral microvessels of the rat. *Microvasc Res.* 77:166.
57. Nicolazzo JA, Charman SA, Charman WN, 2006. Methods to assess drug permeability across the blood-brain barrier. *J Pharm Pharmacol.* 58:281.
58. Allt G, Lawrenson JG, 1997. Is the pial microvessel a good model for blood-brain barrier studies? *Brain Res Rev.* 24:67.
59. Easton AS, Sarker MH, Fraser PA, 1997. Two components of blood-brain barrier disruption in the rat. *J Physiol.* 503 (Pt 3):613.
60. Fu BM, Shen S, 2004. Acute VEGF effect on solute permeability of mammalian microvessels in vivo. *Microvasc Res.* 68:51.
61. Franke H, Galla HJ, Beuckmann CT, 1999. An improved low-permeability in vitro-model of the blood-brain barrier: Transport studies on retinoids, sucrose, haloperidol, caffeine and mannitol. *Brain Res.* 818(1):65.
62. Meyer J, Mischeck U, Veyhl M, Henzel K, Galla HJ, 1990. Blood-brain barrier characteristic enzymatic properties in cultured brain capillary endothelial cells. *Brain Res.* 514(2):305.
63. Hemmila JM, Drewes LR, 1993. Glucose transporter (GLUT1) expression by canine brain microvessel endothelial cells in culture: An immunocytochemical study. *Adv Exp Med Biol.* 331:13.
64. Abbott NJ, 2002. Astrocyte-endothelial interactions and blood-brain barrier permeability. *J Anat* 200(6):629.
65. Haseloff RE, Blasig IE, Bauer HC, Bauer H, 2005. In search of the astrocytic factor(s) modulating blood-brain barrier functions in brain capillary endothelial cells in vitro. *Cell Mol Neurobiol.* 25(1):25.
66. Gaillard PJ, de Boer AG, 2000. Relationship between permeability status of the blood-brain barrier and *in vitro* permeability coefficient of a drug. *Eur J Pharm Sci.* 12(2):95.
67. Demeuse B, Kerkhofs A, Struys-Ponsar C, Knoops B, Remacle C, de Aguilar PV, 2002. Compartmentalized coculture of rat brain endothelial cells and astrocytes: A syngenic model to study the blood-brain barrier. *J Neurosci Methods.* 121(1):21.
68. Deli MA, Abraham CS, Kataoka Y, Niwa M, 2005. Permeability studies on *in vitro* blood-brain barrier models: Physiology, pathology, and pharmacology. *Cell Mol Neurobiol.* 25(1):59.
69. Brown RC, Morris AP, O'Neil RG, 2007. Tight junction protein expression and barrier properties of immortalized mouse brain microvessel endothelial cells. *Brain Res.* 1130(1):17.
70. Soga N, Connolly JO, Chellaiah M, Kawamura J, Hruska KA, 2001. Rac regulates vascular endothelial growth factor stimulated motility. *Cell Commun Adhes.* 8(1):1.

71. Yoder EJ, 2002. Modifications in astrocyte morphology and calcium signaling induced by a brain capillary endothelial cell line. *Glia* 38(2):137.
72. Yuan W, Li G, Fu BM, 2010. Effect of surface charge of immortalized mouse cerebral endothelial cell monolayer on transport of charged solutes. *Ann Biomed Eng.* 38(4):1463.
73. Tyagi N, Moshal KS, Sen U, Vacek TP, Kumar M, Hughes WM Jr., Kundu S, Tyagi SC, 2009. H2S protects against methionine-induced oxidative stress in brain endothelial cells. *Antioxid Redox Signal* 11(1):25.
74. Omidi Y, Campbell L, Barar J, Connell D, Akhtar S, Gumbleton M, 2003. Evaluation of the immortalised mouse brain capillary endothelial cell line, bEnd3, as an *in vitro* blood-brain barrier model for drug uptake and transport studies. *Brain Res.* 990(1-2):95.
75. Malina KC, Cooper I, Teichberg VI, 2009. Closing the gap between the in-vivo and in-vitro blood-brain barrier tightness. *Brain Res.* 1284:12.
76. Bowman P D, Ennis SR, Rarey KE, Betz AL, Goldstein GW, 1983. Brain microvessel endothelial cells in tissue culture: A model for study of blood-brain barrier permeability. *Ann Neurol.* 14(4):396.
77. Thompson SE, Cavitt J, Audus KL, 1994. Leucine-enkephalin effects on paracellular and trans-cellular permeation pathways across brain microvessel endothelial-cell monolayers. *J Cardiovasc Pharmacol.* 24(5):818.
78. Salvetti F, Cecchetti P, Janigro D, Lucacchini A, Benzi L, Martini C, 2002. Insulin permeability across an *in vitro* dynamic model of endothelium. *Pharm Res.* 19(4):445.
79. Karyekar CS, Fasano A, Raje S, Lu RL, Dowling TC, Eddington ND, 2003. Zonula occludens toxin increases the permeability of molecular weight markers and chemotherapeutic agents across the bovine brain microvessel endothelial cells. *J Pharm Sci.* 92(2):414.
80. Hamm S, Dehouck B, Kraus J, Wolburg-Buchholz K, Wolburg H, Risau W, Cecchelli R, Engelhardt B, Dehouck MP, 2004. Astrocyte mediated modulation of blood-brain barrier permeability does not correlate with a loss of tight junction proteins from the cellular contacts. *Cell Tissue Res.* 315(2):157.
81. Kemper EM, Boogerd W, Thuis I, Beijnen JH, van Tellingen O, 2004. Modulation of the blood-brain barrier in oncology: Therapeutic opportunities for the treatment of brain tumours? *Cancer Treatment Rev.* 30(5):415.
82. Boveri M, Berezowski V, Price A, Slupek S, Lenfant AM, Benaud C, Hartung T, Cecchelli R, Prieto P, Dehouck MP, 2005. Induction of blood-brain barrier properties in cultured brain capillary endothelial cells: Comparison between primary glial cells and C6 cell line. *Glia* 51(3):187.
83. Kraus J, Voigt K, Schuller AM, Scholz M, Kim KS, Schilling M, Schabitz WR, Oschmann P, Engelhardt B, 2008. Interferon-beta stabilizes barrier characteristics of the blood-brain barrier in four different species in vitro. *Multiple Sclerosis* 14(6):843.
84. Poller B, Gutmann H, Krahenbuhl S, Weksler B, Romero I, Couraud PO, Tuffin G, Drewe J, Huwyler J, 2008. The human brain endothelial cell line hCMEC/D3 as a human blood-brain barrier model for drug transport studies. *J Neurochem.* 107(5):1358.
85. Sahagun G, Moore SA, Hart MN, 1990. Permeability of neutral vs. anionic dextrans in cultured brain microvascular endothelium. *Am J Physiol.* 259(1 Pt 2):H162.
86. Santaguida S, Janigro D, Hossain M, Oby E, Rapp E, Cucullo L, 2006. Side by side comparison between dynamic versus static models of blood-brain barrier in vitro: A permeability study. *Brain Res.* 1109:1.
87. de Vries HE, BlomRoosmalen MCM, van Oosten M, de Boer AG, van Berkel TJC, Breimer D D, Kuiper J, 1996. The influence of cytokines on the integrity of the blood-brain barrier in vitro. *J Neuroimmunol.* 64(1):37.
88. Cucullo L, McAllister MS, Kight K, Krizanac-Bengez L, Marroni M, Mayberg MR, Stanness KA, Janigro D, 2002. A new dynamic *in vitro* model for the multidimensional study of astrocyte-endothelial cell interactions at the blood-brain barrier. *Brain Res.* 951(2):243.
89. Zhang Y, Li CSW, Ye YY, Johnson K, Poe J, Johnson S, Bobrowski W, Garrido R, Madhu C, 2006. Porcine brain microvessel endothelial cells as an *in vitro* model to predict *in vivo* blood-brain barrier permeability. *Drug Metab Disp.* 34(11):1935.

90. Li G, Simon M, Shi Z, Cancel L, Tarbell JM, Morrison B, Fu BM, 2010. Permeability of endothelial and astrocyte cocultures: *In vitro* blood-brain barrier models for drug delivery. *Ann Biomed Eng.* 38(8):2499.
91. Engvall E, 1995. Structure and function of basement membranes. *Int J Dev Biol* 39(5):781.
92. Miosge N, 2001. The ultrastructural composition of basement membranes in vivo. *Histol Histopathol.* 16(4):1239.
93. Kleinman HK, Martin GR, 2005. Matrigel: Basement membrane matrix with biological activity. *Semin Cancer Biol.* 15(5):378.
94. Pardridge WM, 2005. Molecular biology of the blood-brain barrier. *Mol Biotechnol.* 30(1):57.
95. Dietrich WD, Alonso O, Halley M, 1994. Early microvascular and neuronal consequences of traumatic brain injury: A light and electron microscopic study in rats. *J Neurotrauma.* 11(3):289.
96. Fukuda K, Tanno H, Okimura Y, Nakamura M, Yamaura A, 1995. The blood-brain barrier disruption to circulating proteins in the early period after fluid percussion brain injury in rats. *J Neurotrauma.* 12(3):315.
97. Baldwin SA, Fugaccia I, Brown DR, Brown LV, Scheff SW, 1996. Blood-brain barrier breach following cortical contusion in the rat. *J Neurosurg.* 85(3):476.
98. Barzo P, Marmarou A, Fatouros P, Corwin F, Dunbar J, 1996. Magnetic resonance imaging-monitored acute blood-brain barrier changes in experimental traumatic brain injury. *J Neurosurg.* 85(6):1113.
99. Baskaya MK, Rao AM, Dogan A, Donaldson D, Dempsey RJ, 1997. The biphasic opening of the blood-brain barrier in the cortex and hippocampus after traumatic brain injury in rats. *Neurosci Lett.* 226(1):33.
100. Beaumont A, Marmarou A, Hayasaki K, Barzo P, Fatouros P, Corwin F, Marmarou C, Dunbar J, 2000. The permissive nature of blood brain barrier (BBB) opening in edema formation following traumatic brain injury. *Acta Neurochir Suppl.* 76:125.
101. Cernak I, Vink R, Zapple DN, Cruz MI, Ahmed F, Chang T, Fricke ST, Faden AI, 2004. The pathobiology of moderate diffuse traumatic brain injury as identified using a new experimental model of injury in rats. *Neurobiol Dis.* 17(1):29.
102. Fu BM, Chen B, 2003. A model for the structural mechanisms in the regulation of microvessel permeability by junction strands. *ASME J Biomech Eng.* 125:620.
103. Fu BM, Tsay R, Curry FE, Weinbaum S, 1994. A junction-orifice-entrance layer model for capillary permeability: Application to frog mesenteric capillaries. *ASME J Biomech Eng.* 116:502.
104. Schulze C, Firth JA, 1992. Interendothelial junctions during blood-brain-barrier development in the rat—Morphological changes at the level of individual tight junctional contacts. *Dev Brain Res* 69(1):85.
105. Adamson RH, Lenz JE, Zhang X, Adamson GN, Weinbaum S, Curry FE, 2004. Oncotic pressures opposing filtration across non-fenestrated rat microvessels. *J Physiol-Lond.* 557:889.
106. Mak M, Fung L, Strasser JF, Saltzman WM, 1995. Distribution of drugs following controlled delivery to the brain interstitium. *J Neurooncol* 26(2):91.
107. Bobo RH, Laske DW, Akbasak A, Morrison PF, Dedrick RL, Oldfield EH, 1994. Convection-enhanced delivery of macromolecules in the brain. *Proc Natl Acad Sci USA.* 91(6):2076.
108. Kroll RA, Neuwelt EA, 1998. Outwitting the blood-brain barrier for therapeutic purposes: Osmotic opening and other means. *Neurosurgery.* 42(5):1083.
109. Doolittle ND, Abrey LE, Ferrari N, Hall WA, Laws ER, McLendon RE, Muldoon LL et al., 2002. Targeted delivery in primary and metastatic brain tumors: Summary report of the seventh annual meeting of the Blood-Brain Barrier Disruption Consortium. *Clin Cancer Res.* 8(6):1702.
110. Hynynen K, McDannold N, Vykhodtseva N, Jolesz FA, 2001. Noninvasive MR imaging-guided focal opening of the blood-brain barrier in rabbits. *Radiology.* 220(3):640.
111. Hynynen K, McDannold N, Vykhodtseva N, Raymond S, Weissleder R, Jolesz FA, Sheikov N, 2006. Focal disruption of the blood-brain barrier due to 260-kHz ultrasound bursts: A method for molecular imaging and targeted drug delivery. *J Neurosurg.* 105(3):445.

112. Kinoshita M, 2006. Targeted drug delivery to the brain using focused ultrasound. *Top Magn Reson Imaging*. 17(3):209.
113. Dean RL, Emerich DF, Hasler BP, Bartus RT, 1999. Cereport (RMP-7) increases carboplatin levels in brain tumors after pretreatment with dexamethasone. *Neuro Oncol*. 1(4):268.
114. Borlongan CV, Emerich DF, 2003. Facilitation of drug entry into the CNS via transient permeation of blood brain barrier: Laboratory and preliminary clinical evidence from bradykinin receptor agonist, *Cereport*. *Brain Res Bull*. 60(3):297.
115. Gabathuler R, 2010. Approaches to transport therapeutic drugs across the blood-brain barrier to treat brain diseases. *Neurobiol Dis*. 37(1):48.
116. Lipinski CA, 2000. Drug-like properties and the causes of poor solubility and poor permeability. *J Pharmacol Toxicol Methods*. 44(1):235.
117. Shashoua VE, Hesse GW, 1996. N-docosaehexaenoyl, 3 hydroxytyramine: A dopaminergic compound that penetrates the blood-brain barrier and suppresses appetite. *Life Sci*. 58(16):1347.
118. Sawada GA, Williams LR, Lutzke BS, Raub TJ, 1999. Novel, highly lipophilic antioxidants readily diffuse across the blood-brain barrier and access intracellular sites. *J Pharmacol Exp Ther*. 288(3):1327.
119. Bodor N, Farag HH, Brewster ME 3rd, 1981. Site-specific, sustained release of drugs to the brain. *Science* 214(4527):1370.
120. Brewster ME, Raghavan K, Pop E, Bodor N, 1994. Enhanced delivery of ganciclovir to the brain through the use of redox targeting. *Antimicrob Agents Chemother* 38(4):817.
121. Pardridge WM, 2003. Blood-brain barrier drug targeting: The future of brain drug development. *Mol Interv*. 3(2):90.
122. Pardridge WM, 2006. Molecular Trojan horses for blood-brain barrier drug delivery. *Curr Opin Pharm*. 6(5):494.
123. Miller G, 2002. Drug targeting. Breaking down barriers. *Science* 297(5584):1116.
124. Gosk S, Vermehren C, Storm G, Moos T, 2004. Targeting anti-transferrin receptor antibody (OX26) and OX26-conjugated liposomes to brain capillary endothelial cells using *in situ* perfusion. *J Cereb Blood Flow Metab*. 24(11):1193.
125. Kumagai AK, Eisenberg JB, Pardridge WM, 1987. Adsorptive-mediated endocytosis of cationized albumin and a beta-endorphin-cationized albumin chimeric peptide by isolated brain capillaries. Model system of blood-brain barrier transport. *J Biol Chem*. 262(31):15214.
126. Lawrenson JG, Reid AR, Allt G, 1997. Molecular characteristics of pial microvessels of the rat optic nerve. Can pial microvessels be used as a model for the blood-brain barrier? *Cell Tissue Res*. 288, 259–65.
127. Yuan W, Li G, Zeng M, Fu BM, 2010. Modulation of the blood-brain barrier permeability by plasma glycoprotein orosomucoid. *Microvasc. Res*. 80(1):148–157.
128. Hervé F, Ghinea N, Scherrmann JM, 2008. CNS delivery via adsorptive transcytosis. *AAPS J*. 10(3):455.
129. Rousselle C, Clair P, Smirnova M, Kolesnikov Y, Pasternak GW, Gac-Breton S, Rees AR, Scherrmann JM, Temsamani J, 2003. Improved brain uptake and pharmacological activity of dalargin using a peptide-vector-mediated strategy. *J Pharmacol Exp Ther*. 306(1):371.
130. Liu L, Guo K, Lu J, Venkatraman SS, Luo D, Ng KC, Ling EA, Mochhala S, Yang YY, 2008. Biologically active core/shell nanoparticles self-assembled from cholesterol-terminated PEG-TAT for drug delivery across the blood-brain barrier. *Biomaterials* 29(10):1509.
131. Lockman PR, Koziara JM, Mumper RJ, Allen DD, 2004. Nanoparticle surface charges alter blood-brain barrier integrity and permeability. *J Drug Target*. 12(9–10):635.
132. Szmydynger-Chodobska J, Chodobski A, Johanson CE, 1994. Postnatal developmental changes in blood flow to choroid plexuses and cerebral cortex of the rat. *Am J Physiol*. 266(5 Pt 2):R1488.
133. Kramer K, Humm JL, Souweidane MM, Zanzonico PB, Dunkel IJ, Gerald WL, Khakoo Y et al., 2007. Phase I study of targeted radioimmunotherapy for leptomeningeal cancers using intra-Ommaya 131-I-3F8. *J Clin Oncol*. 25:5465–5470.

134. Bruno MK, Raizer J, 2005. Leptomeningeal metastases from solid tumors (meningeal carcinomatosis). *Cancer Treat Res.* 125:31.
135. Gleissner B, Chamberlain MC, 2006. Neoplastic meningitis. *Lancet Neurol.* 5:443.
136. Grossman SA, Spence A, 1999. NCCN clinical practice guidelines for carcinomatous/lymphomatous meningitis. *Oncology.* 13:144.
137. Kramer K, Kushner B, Heller G, Cheung NK, 2001. Neuroblastoma metastatic to the central nervous system. The Memorial Sloan-Kettering Cancer Center Experience and a Literature Review. *Cancer.* 91:1510.
138. Lv Y, Cheung NK, Fu BM, 2009. A pharmacokinetic model for radioimmunotherapy delivered through cerebrospinal fluid for the treatment of leptomeningeal metastases. *J Nuclear Med.* 50(8):1324.

15

Interstitial Transport in the Brain: Principles for Local Drug Delivery

15.1	Introduction	15-1
15.2	Implantable Controlled Delivery Systems for Chemotherapy.....	15-2
15.3	Drug Transport after Release from the Implant.....	15-4
15.4	Application of Diffusion–Elimination Models to Intracranial BCNU Delivery Systems.....	15-7
15.5	Limitations and Extensions of the Diffusion–Elimination Model.....	15-9
	Failure of the Model in Certain Situations	
15.6	New Approaches to Drug Delivery Suggested by Modeling..	15-12
15.7	Conclusion	15-12
	References.....	15-12

W. Mark Saltzman
Yale University

15.1 Introduction

Traditional methods for delivering drugs to the brain are inadequate. Many drugs, particularly water-soluble or high-molecular-weight compounds, do not enter the brain following systemic administration because they permeate through blood capillaries very slowly. This blood–brain barrier (BBB) severely limits the number of drugs that are candidates for treating brain disease.

Several strategies for increasing the permeability of brain capillaries to drugs have been tested. Since the BBB is generally permeable to lipid-soluble compounds that can dissolve and diffuse through endothelial cell membranes [1,2], a common approach for enhancing brain delivery of compounds is chemical modification to enhance lipid solubility [3]. Unfortunately, lipidization approaches are not useful for drugs with molecular weight larger than 1000. Another approach for increasing permeability is the entrapment of drugs in liposomes [4], but delivery may be limited by liposome stability in the plasma and uptake at other tissue sites.

Specific nutrient transport systems in brain capillaries can be used to facilitate drug entry into the brain. L-Dopa (L-3,4-dihydroxyphenylalanine), a metabolic precursor of dopamine, is transported across endothelial cells by the neutral amino acid transport system [5]. L-Dopa permeates through capillaries into the striatal tissue, where it is decarboxylated to form dopamine. Therefore, systemic administration of L-dopa is often beneficial to patients with Parkinson’s disease. Certain protein modifications, such as cationization [6] and anionization [7], produce enhanced uptake in the brain. Modification of drugs [8,9] by linkage to an antitransferrin receptor antibody also appears to enhance transport into the brain. This approach depends on receptor-mediated transcytosis of transferrin–receptor complexes by brain endothelial cells; substantial uptake also occurs in the liver.

The permeability of brain capillaries can be transiently increased by intra-arterial injection of the hyperosmolar solutions, which disrupt interendothelial tight junctions [10]. But BBB disruption affects capillary permeability throughout the brain, enhancing permeability to all compounds in the blood, not just the agent of interest. Intraventricular therapy, where agents are administered directly into the cerebrospinal fluid (CSF) of the ventricles, results in high concentrations within the brain tissue, but only in regions immediately surrounding the ventricles [11,12]. Because the agent must diffuse into the brain parenchyma from the ventricles, and because of the high rate of clearance of agents in the CNS into the peripheral circulation, this strategy cannot be used to deliver agents deep into the brain.

Because of the difficulty in achieving therapeutic drug levels by systemic administration, methods for direct administration of drugs into the brain parenchyma have been tested. Drugs can be delivered directly into the brain tissue by infusion, implantation of a drug-releasing matrix, or transplantation of drug-secreting cells [13]. These approaches provide sustained drug delivery that can be limited to specific sites, localizing therapy to a brain region. Because these methods provide a localized and continuous source of active drug molecules, the total drug dose can be less than needed with systemic administration. With polymeric controlled release, the implants can also be designed to protect unreleased drug from degradation in the body and to permit localization of extremely high doses (up to the solubility of the drug) at precisely defined locations in the brain. Infusion systems require periodic refilling; the drug is usually stored in a liquid reservoir at body temperature and many drugs are not stable under these conditions.

This chapter describes the transport of drug molecules that are directly delivered into the brain. For purposes of clarity, a specific example is considered: polymeric implants that provide controlled release of chemotherapy. The results can be extended to other modes of administration [13,14] and other types of drug agents [15].

15.2 Implantable Controlled Delivery Systems for Chemotherapy

The kinetics of drug release from a controlled release system are usually characterized *in vitro*, by measuring the amount of drug released from the matrix into a well-stirred reservoir of phosphate buffered water or saline at 37°C. Controlled release profiles for some representative anticancer agents are shown in Figure 15.1; all of the agents selected for these studies—1,3-bis(2-chloroethyl)-1-nitrosourea (BCNU), 4-HC, cisplatin, and taxol—are used clinically for chemotherapy of brain tumors. The controlled release period can vary from several days to many months, depending on properties of the drug, the polymer, and the method of formulation. Therefore, the delivery system can be tailored to the therapeutic situation by manipulation of implant properties.

The release of drug molecules from polymer matrices can be regulated by diffusion of drug through the polymer matrix or degradation of the polymer matrix. In many cases (including the release of BCNU, cisplatin, and 4HC from the degradable matrices shown in Figure 15.1), drug release from biodegradable polymers appears to be diffusion-mediated, probably because the time for polymer degradation is longer than the time required for drug diffusion through the polymer. In certain cases, linear release, which appears to correlate with the polymer degradation rate, can be achieved; this might be the case for taxol release from the biodegradable matrix (Figure 15.1), although the exceedingly low solubility of taxol in water may also contribute substantially to the slowness of release.

For diffusion-mediated release, the amount of drug released from the polymer is proportional to the concentration gradient of the drug in the polymer. By performing a mass balance on drug molecules within a differential volume element in the polymer matrix, a conservation equation for drug within the matrix is obtained:

$$\frac{\partial C_p}{\partial t} = D_p \nabla^2 C_p \quad (15.1)$$

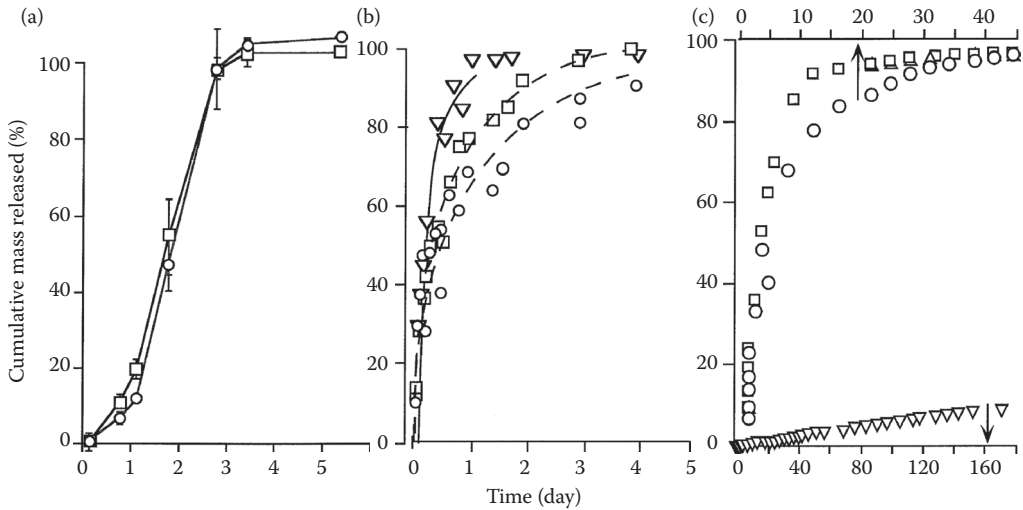


FIGURE 15.1 Controlled release of anticancer compounds from polymeric matrices. (a) Release of cisplatin (circles) from a biodegradable copolymer of fatty acid dimers and sebacic acid, p(FAD:SA), initially containing 10% drug. (b) Release of BCNU from EVAc matrices (circles), polyanhydride matrices p(CPP:SA) (squares), and p(FAD:SA) (triangles) matrices initially containing 20% drug. (c) Release of BCNU (squares), 4HC (circles), and taxol (triangles) from p(CPP:SA) matrices initially containing 20% drug. Note that panel (c) has two time axes: the lower axis applies to the release of taxol and the upper axis applies to the release of BCNU and 4HC. (Adapted from Dang, W. and W.M. Saltzman, *Journal of Biomaterials Science, Polymer Edition*, 1994, 6(3):291–311; Dang, W., *Engineering Drugs and Delivery Systems for Brain Tumor Therapy*. 1993, The Johns Hopkins University: Baltimore, MD.)

where C_p is the local concentration of drug in the polymer and D_p is the diffusion coefficient of the drug in the polymer matrix. This equation can be solved, with appropriate boundary and initial conditions, to obtain the cumulative mass of drug released as a function of time; the details of this procedure are described elsewhere [18]. A useful approximate solution, which is valid for the initial 60% of release, is

$$M_t = 4M_o \sqrt{\frac{D_{i;p}t}{\pi L^2}} \tag{15.2}$$

where M_t is the cumulative mass of drug released from the matrix, M_o is the initial mass of drug in the matrix, and L is the thickness of the implant. By comparing Equation 15.2 to the experimentally determined profiles, the rate of diffusion of the agent in the polymer matrix can be estimated (Table 15.1).

TABLE 15.1 Diffusion Coefficients for Chemotherapy Drug Release from Biocompatible Polymer Matrices

Drug	Polymer	Initial Loading (%)	D_p (cm ² /s)
Cisplatin	P(FAD:SA)	10	6.8×10^{-9}
BCNU	EVAc	20	1.6×10^{-8}
BCNU	P(FAD:SA)	20	6.9×10^{-8}
BCNU	P(CPP:SA)	20	2.3×10^{-8} (panel b) 2.0×10^{-8} (panel c)
4HC	P(CPP:SA)	20	3.1×10^{-10}
Taxol	P(CPP:SA)	20	n.a.

Note: Diffusion coefficients were obtained by comparing the experimental data shown in Figure 15.1 to Equation 15.2 and determining the best value of the diffusion coefficient to represent the data. n.a., not applicable.

15.3 Drug Transport after Release from the Implant

Bypassing the BBB is necessary, but not sufficient for effective drug delivery. Consider the consequences of implanting a delivery system, such as one of the materials characterized above, within the brain. Molecules released into the interstitial fluid in the brain extracellular space (ECS) must penetrate into the brain tissue to reach tumor cells distant from the implanted device. Before these drug molecules can reach the target site, however, they might be eliminated from the interstitium by partitioning into brain capillaries or cells, entering the CSF, or being inactivated by extracellular enzymes. Elimination always accompanies dispersion; therefore, regardless of the design of the delivery system, one must understand the dynamics of both processes in order to predict the spatial pattern of drug distribution after delivery.

The polymer implant is surrounded by biological tissue, composed of cells and an ECS filled with extracellular fluid (ECF). Immediately following implantation, drug molecules escape from the polymer and penetrate the tissue. Once in the brain tissue, drug molecules: (1) diffuse through the tortuous ECS in the tissue; (2) diffuse across semipermeable tissue capillaries to enter the systemic circulation and, therefore, are removed from the brain tissue; (3) diffuse across cell membranes by passive, active, or facilitated transport paths, to enter the intracellular space; (4) transform, spontaneously or by an enzyme-mediated pathway, into other compounds; and (5) bind to fixed elements in the tissue. Each of these events influence drug therapy: diffusion through the ECS is the primary mechanism of drug distribution in brain tissue; elimination of the drug occurs when it is removed from the ECF or transformed, and binding or internalization may slow the progress of the drug through the tissue.

A mass balance on a differential volume element in the tissue [19] gives a general equation describing drug transport in the region near the polymer [20]:

$$\frac{\partial C_i}{\partial t} + \bar{v} \cdot \nabla C_i = D_b \nabla^2 C_i + R_e(C_i) - \frac{\partial B}{\partial t} \quad (15.3)$$

where C is the concentration of the diffusible drug in the tissue surrounding the implant (g/cm^3 tissue), v is the fluid velocity (cm/s), D_b is the diffusion coefficient of the drug in the tissue (cm^2/s), $R_e(C)$ is the rate of drug elimination from the ECF ($\text{g}/\text{s}\text{-cm}^3$ tissue), B is the concentration of drug bound or internalized in cells (g/cm^3 tissue), and t is the time following implantation. In deriving this equation, the conventions developed by Nicholson [21], based on volume-averaging in a complex medium, and Patlak and Fenstermacher [20] were combined. In this version of the equation, the concentrations C and B and the elimination rate $R_e(C)$ are defined per unit volume of tissue. D_b is an effective diffusion coefficient, which must be corrected from the diffusion coefficient for the drug in water to account for the tortuosity of the ECS.

When the binding reactions are rapid, the amount of intracellular or bound drug can be assumed to be directly proportional, with an equilibrium coefficient K_{bind} , to the amount of drug available for internalization or binding:

$$B = K_{\text{bind}} C \quad (15.4)$$

Substitution of Equation 15.4 into Equation 15.3 yields, with some simplification:

$$\frac{\partial C_i}{\partial t} = \frac{1}{1 + K_{\text{bind}}} (D_b \nabla^2 C_i + R_e(C_i) - \bar{v} \cdot \nabla C_i) \quad (15.5)$$

The drug elimination rate, $R_e(C)$, can be expanded into the following terms:

$$R_e(C_t) = k_{\text{bbb}} \left(\frac{C_t}{\epsilon_{\text{ecs}}} - C_{\text{plasma}} \right) + \frac{V_{\text{max}} C_t}{K_m + C_t} + k_{\text{ne}} C_t \quad (15.6)$$

where k_{bbb} is the permeability of the BBB (defined based on concentration in the ECS), C_{plasma} is the concentration of drug in the blood plasma, V_{max} and K_m are Michaelis–Menton constants, and k_{ne} is a first-order rate constant for drug elimination due to nonenzymatic reactions. For any particular drug, some of the rate constants may be very small, reflecting the relative importance of each mechanism of drug elimination. If it is assumed that the permeability of the BBB is low ($C_{\text{pl}} \ll C$) and the concentration of drug in the brain is sufficiently low so that any enzymatic reactions are in the first-order regime ($C \ll K_m$), Equation 15.6 can be reduced to

$$-R_e(C_t) = \frac{k_{\text{bbb}}}{\epsilon_{\text{ecs}}} C_t + \frac{V_{\text{max}}}{K_m} C_t + k_{\text{ne}} C_t = k_{\text{app}} C_t \quad (15.7)$$

where k_{app} is a lumped first-order rate constant. With these assumptions, Equation 15.4 can be simplified by definition of an apparent diffusion coefficient, D^* , and an apparent first-order elimination constant, k^* :

$$\frac{\partial C_t}{\partial t} = D^* \nabla^2 C_t + k^* C_t - \frac{\bar{v} \cdot \nabla C_t}{1 + K_{\text{bind}}} \quad (15.8)$$

where $k^* = k_{\text{app}}/(1 + K_{\text{bind}})$ and $D = D_b/(1 + K_{\text{bind}})$.

Boundary and initial conditions are required for solution of differential Equation 15.8. If a spherical implant of radius R is implanted into a homogeneous region of the brain, at a site sufficiently far from anatomical boundaries, the following assumptions are reasonable:

$$C_t = 0 \quad \text{for } t = 0; \quad r > R \quad (15.9)$$

$$C_t = C_i \quad \text{for } t > 0; \quad r = R \quad (15.10)$$

$$C_t = 0 \quad \text{for } t > 0; \quad r \rightarrow \infty \quad (15.11)$$

In many situations, drug transport due to bulk flow can be neglected. This assumption (v is zero) is common in previous studies of drug distribution in brain tissue [20]. For example, in a previous study of cisplatin distribution following continuous infusion into the brain, the effects of bulk flow were found to be small, except within 0.5 mm of the site of infusion [22]. In the cases considered here, since drug molecules enter the tissue by diffusion from the polymer implant, not by pressure-driven flow of a fluid, no flow should be introduced by the presence of the polymer. With fluid convection assumed negligible, the general governing equation in the tissue, Equation 15.8, reduces to

$$\frac{\partial C_t}{\partial t} = D^* \nabla^2 C_t + k^* C_t \quad (15.12)$$

The no-flow assumption may be inappropriate in certain situations. In brain tumors, edema and fluid movement are significant components of the disease. In addition, some drugs can elicit cytotoxic edema. Certain drug/polymer combinations can also release drugs in sufficient quantity to create density-induced fluid convection.

Equation 15.12, with conditions 15.9 through 15.11, can be solved by Laplace transform techniques [13] to yield

$$\frac{C_t}{C_i} = \frac{1}{2\zeta} \left\{ \exp[-\phi(\zeta - 1)] \operatorname{erfc} \left[\frac{\zeta - 1}{2\sqrt{\tau}} - \phi\sqrt{\tau} \right] + \exp[\phi(\zeta - 1)] \operatorname{erfc} \left[\frac{\zeta - 1}{2\sqrt{\tau}} + \phi\sqrt{\tau} \right] \right\} \quad (15.13)$$

where the dimensionless variables are defined as follows:

$$\zeta = \frac{r}{R}; \quad \tau = \frac{D^*t}{R^2}; \quad \phi = R\sqrt{\frac{k^*}{D^*}} \quad (15.14)$$

The differential equation also has a steady-state solution, which is obtained by solving Equation 15.12 with the time derivative set equal to zero and subject to the boundary conditions 15.9 and 15.10:

$$\frac{C_t}{C_i} = \frac{1}{\zeta} \exp[-\phi(\zeta - 1)] \quad (15.15)$$

Figure 15.2 shows concentration profiles calculated using Equations 15.13 and 15.15. In this situation, which was obtained using reasonable values for all of the parameters, steady state is reached approximately 1 h after implantation of the delivery device. The time required to achieve steady state depends

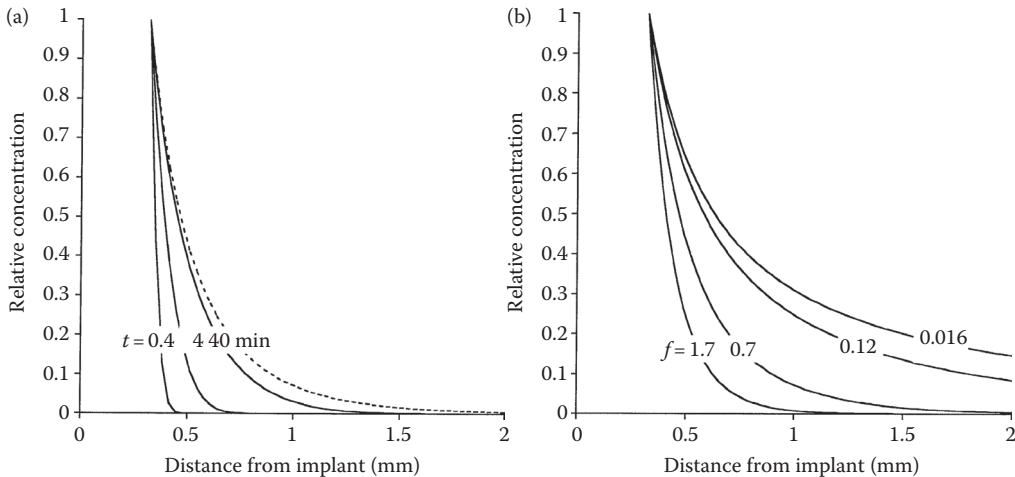


FIGURE 15.2 Concentration profiles after implantation of a spherical drug-releasing implant. (Panel a, transient) Solid lines represent the transient solution to Equation 15.12 (i.e., Equation 15.13) with the following parameter values: $D^* = 4 \times 10^{-7}$ cm²/s; $R = 0.032$ cm; $k^* = 1.9 \times 10^{-4}$ s⁻¹ ($t^{1/2} = 1$ h). The dashed line represents the steady-state solution (i.e., Equation 15.15) for the same parameters. (Panel b, steady state) Solid lines in this plot represent Equation 15.15 with the following parameters: $D^* = 4 \times 10^{-7}$ cm²/s; $R = 0.032$ cm. Each curve represents the steady-state concentration profile for drugs with different elimination half-lives in the brain, corresponding to different dimensionless moduli, f : $t^{1/2} = 10$ min ($f = 1.7$); 1 h (0.7); 34 h (0.12); and 190 h (0.016).

Downloaded by [JCR JCR] at 10:35 01 August 2015

on the rate of diffusion and elimination, as previously described [23], but will be significantly <24 h for most drug molecules.

15.4 Application of Diffusion–Elimination Models to Intracranial BCNU Delivery Systems

The preceding mathematical analysis, which assumes diffusion and first-order elimination in the tissue, agrees well with experimental concentration profiles obtained after implantation of controlled release polymers (Figure 15.3). At 3, 7, and 14 days after implantation of a BCNU-releasing implant, the concentration profile at the site of the implant was very similar. The parameter values (obtained by fitting Equation 15.15 to the experimental data) were consistent with parameters obtained using other methods [24], suggesting that diffusion and first-order elimination were sufficient to account for the pattern of drug concentration observed during this period. Parameter values were similar at 3, 7, and 14 days, indicating that the rates of drug release, drug dispersion, and drug elimination did not change during this period. This equation has been compared to concentration profiles measured for a variety of molecules delivered by polymer implants to the brain—dexamethasone [23], molecular weight fractions of dextran [25], nerve growth factor in rats [26,27], BCNU in rats [24], rabbits [28], and monkeys [29]. In each of these cases, the steady-state diffusion–elimination model appears to capture most of the important features of drug transport.

This model can be used to develop guidelines for the design of intracranial delivery systems. Table 15.2 lists some of the important physical and biological characteristics of a few compounds that have been considered for interstitial delivery to treat brain tumors. When the implant is surrounded by

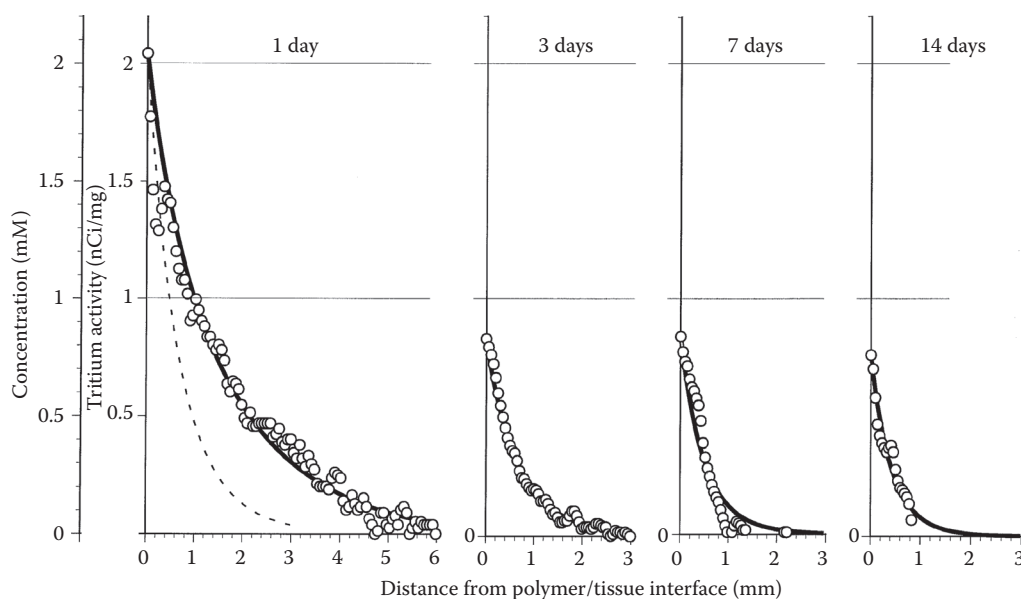


FIGURE 15.3 Concentration profiles after implantation of a BCNU-releasing implant. Solutions to Equation 15.15 were compared to experimental data obtained by quantitative autoradiographic techniques. The solid lines in the three panels labeled 3, 7, and 14 days were all obtained using the following parameters: $R = 0.15$ cm; $f = 2.1$; and $C_1 = 0.81$ mM. The solid line in the panel labeled 1 day was obtained using the following parameters: $R = 0.15$ cm; $f = 0.7$; and $C_1 = 1.9$ mM. (Modified from Fung, L. et al., *Pharmaceutical Research*, 1996, 13:671–682.)

TABLE 15.2 Implant Design Applied to Three Chemotherapy Compounds

	BCNU	4HC	Methotrexate
Molecular weight (daltons)	214	293	454
Solubility (mM)	12	100	100
Log ₁₀ K	1.53	0.6	-1.85
k* (h)	70	70	1
D* (10 ⁻⁷ cm ² /s)	14	14	5
Toxic concentration in culture (μM)	25	10	0.04
Maximum release rate (mg/day)	1.2	14	17
Implant lifetime at max rate (day)	0.85	0.07	0.06
Maximum concentration in tissue for 1-week-releasing implant (mM)	1.5	1.1	1.8
RT (mm)	1.3	2.5	5

Note: K is the octanol:water partition coefficient, k is the rate of elimination due to permeation through capillaries, and D_i is the diffusion coefficient of the drug in the brain. The following values are assumed, consistent with our results from polymer delivery to rats and rabbits: radius of spherical implant $R = 1.5$ mm; mass of implant $M = 10$ mg; drug loading in implant load = 10%.

tissue, the maximum rate of drug release is determined by the solubility of the drug, C_s , and the rate of diffusive transport through the tissue:

$$\left(\frac{dM_t}{dt}\right)_{\max} = (\text{Maximum flux}) \times (\text{Surface area}) = -D^* \frac{\partial C_t}{\partial r} \Big|_R 4\pi R^2 \quad (15.16)$$

Evaluating the derivative in Equation 15.16 from the steady-state concentration profile (Equation 15.15) yields

$$\left(\frac{dM_t}{dt}\right)_{\max} = 8\pi \dot{D}^* C_s R \quad (15.17)$$

Regardless of the properties of the implant, it is not possible to release drug into the tissue at a rate faster than determined by Equation 15.17. If the release rate from the implant is less than this maximum rate, C_i (the concentration in the tissue immediately outside the implant) is less than the saturation concentration, C_s . The actual concentration C_i can be determined by balancing the release rate from the implant (dM_t/dt , which can be determined from Equation 15.2 provided that diffusion is the mechanism of release from the implant) with the rate of penetration into the tissue obtained by substituting C_i for C_s in Equation 15.17:

$$C^* = \frac{dM_t}{dt} \left(\frac{1}{8\pi D^* R} \right) \quad (15.18)$$

The effective region of therapy can be determined by calculating the distance from the surface of the implant to the point where the concentration drops below the cytotoxic level (estimated as the cytotoxic concentration determined from *in vitro* experiments). Using Equation 15.15, and defining the radial distance for effective treatment as R_T , yields

$$\frac{C_{\text{cytotoxic}}}{C_i} = \frac{R}{R_T} \exp \left\{ -R \sqrt{\frac{k^*}{D^*}} \left(\frac{R_T}{R} - 1 \right) \right\} \quad (15.19)$$

Alternately, an effective penetration distance, d_p , can be defined as the radial position at which the drug concentration has dropped to 10% of the peak concentration:

$$0.10 = \frac{R}{d_p} \exp \left\{ -R \sqrt{\frac{k^*}{D^*}} \left(\frac{d_p}{R} - 1 \right) \right\} \quad (15.20)$$

These equations provide quantitative criteria for evaluating the suitability of chemotherapy agents for direct intracranial delivery (Table 15.2).

15.5 Limitations and Extensions of the Diffusion–Elimination Model

15.5.1 Failure of the Model in Certain Situations

The previous section outlined one method for the analysis of drug transport after implantation of a drug-releasing device. A simple pseudo-steady-state equation (Equation 15.15) yielded simple guidelines (Equations 15.16 through 15.19) for device design. Because the assumptions of the model were satisfied over a substantial fraction of the release period (days 3–14, based on the data shown in Figure 15.3), this analysis may be useful for predicting the effects of BCNU release from biodegradable implants. Pseudo-steady-state assumptions are reasonable during this period of drug release, presumably because the time required to achieve steady state (which is on the order of minutes) is much less than the characteristic time associated with changes in the rate of BCNU release from the implant (which is on the order of days).

But experimental concentration profiles measured 1 day after implantation were noticeably different: the peak concentration was substantially higher and the drug penetration into the surrounding tissue was deeper (see the left-hand panel of Figure 15.3). This behavior cannot be easily explained by the pseudo-steady-state models described above. For example, if the difference observed at 1 day represents transient behavior, the concentration observed at a fixed radial position should increase with time (Figure 15.2); in contrast, the experimental concentration at any radial position on day 1 is higher than the concentration measured at that same position on subsequent days.

15.5.1.1 Effect of Drug Release Rate

Alternately, the observed difference at 1 day might be due to variability in the rate of BCNU release from the polymer implant over this period, with transport characteristics in the tissue remaining constant. When similar BCNU-releasing implants are tested *in vitro*, the rate of drug release decreased over time (Figure 15.1). Equation 15.18 predicts the variation in peak concentration with release rate; the twofold higher concentration observed at the interface on day 1 (as compared to days 3 through 14) could be explained by a twofold higher release rate on day 1. But the effective penetration distance, d_p , does not depend on release rate. Experimentally measured penetration distances are ~1.4 mm on days 3, 7, and 14 and ~5 mm on day 1. This difference in penetration is shown more clearly in the day 1 panel of Figure 15.3: the dashed line shows the predicted concentration profile if k^* and D^* were assumed equal to the values obtained for days 3, 7, and 14. Changes in the rate of BCNU release are insufficient to explain the differences observed experimentally.

15.5.1.2 Determinants of Tissue Penetration

Penetration of BCNU is enhanced at day 1 relative to penetration at days 3, 7, and 14. For an implant of fixed size, penetration depends only on the ratio of elimination rate to diffusion rate: k^*/D^* . Increased penetration results from a decrease in this ratio (Figure 15.2), which could occur because of either a decreased rate of elimination (smaller k^*) or an increased rate of diffusion (larger D^*). But there are

no good reasons to believe that BCNU diffusion or elimination are different on day 1 than on days 3 through 14. With its high lipid solubility, BCNU can diffuse readily through brain tissue. In addition, elimination of BCNU from the brain occurs predominantly by partitioning into the circulation; since BCNU can permeate the capillary wall by diffusion, elimination is not a saturable process. Perhaps the enhanced penetration of BCNU is due to the presence of another process for drug dispersion, such as bulk fluid flow, which was neglected in the previous analysis.

The diffusion/elimination model compares favorably with available experimental data, but the assumptions used in predicting concentration profiles in the brain may not be appropriate in all cases. Deviations from the predicted concentration profiles may occur due to extracellular fluid flows in the brain, complicated patterns of drug binding, or multistep elimination pathways. The motion of interstitial fluid in the vicinity of the polymer and the tumor periphery may not always be negligible, as mentioned above. The interstitial fluid velocity is proportional to the pressure gradient in the interstitium; higher interstitial pressure in tumors—due to tumor cell proliferation, high vascular permeability, and the absence of functioning lymphatic vessels—may lead to steep interstitial pressure gradients at the periphery of the tumor [30]. As a result, interstitial fluid flows within the tumor may influence drug transport. A drug at the periphery of the tumor must overcome outward convection to diffuse into the tumor. Similarly, local edema after surgical implantation of the polymer may cause significant fluid movement in the vicinity of the polymer. More complete mathematical models that include the convective contribution to drug transport are required.

15.5.1.3 Effect of Fluid Convection

When bulk fluid flow is present ($v \neq 0$), concentration profiles can be predicted from Equation 15.8, subject to the same boundary and initial conditions (Equations 15.9 through 15.11). In addition to Equation 15.8, continuity equations for water are needed to determine the variation of fluid velocity in the radial direction. This set of equations has been used to describe concentration profiles during microinfusion of drugs into the brain [14]. Relative concentrations were predicted by assuming that the brain behaves as a porous medium (i.e., velocity is related to pressure gradient by Darcy's law). Water introduced into the brain can expand the interstitial space; this effect is balanced by the flow of water in the radial direction away from the infusion source and, to a lesser extent, by the movement of water across the capillary wall.

In the presence of fluid flow, penetration of drug away from the source is enhanced (Figure 15.4). The extent of penetration depends on the velocity of the flow and the rate of elimination of the drug. These calculations were performed for macromolecular drugs, which have limited permeability across the brain capillary wall. The curves indicate steady-state concentration profiles for three different proteins with metabolic half-lives of 10 min, 1 h, and 33.5 h. In the absence of fluid flow, drugs with longer half-lives penetrate deeper into the tissue (solid lines in Figure 15.4 were obtained from Equation 15.15). This effect is amplified by the presence of flow (dashed lines in Figure 15.4).

During microinfusion, drug is introduced by pressure-driven fluid flow from a small catheter. Therefore, pressure gradients are produced in the brain interstitial space, which lead to fluid flow through the porous brain microenvironment. Volumetric infusion rates of 3 $\mu\text{L}/\text{min}$ were assumed in the calculations reproduced in Figure 15.4. Since loss of water through the brain vasculature is slight, the velocity can be determined as a function of radial position:

$$v_r = \frac{q}{4\pi r^2 \varepsilon} \quad (15.21)$$

where q is the volumetric infusion rate and ε is the volume fraction of the interstitial space in the brain (approximately 0.20). Fluid velocity decreases with radial distance from the implant (Table 15.3), but at all locations within the first 20 mm of the implant site, predicted velocity was much greater than the velocities reported previously during edema or tumor growth in the brain.

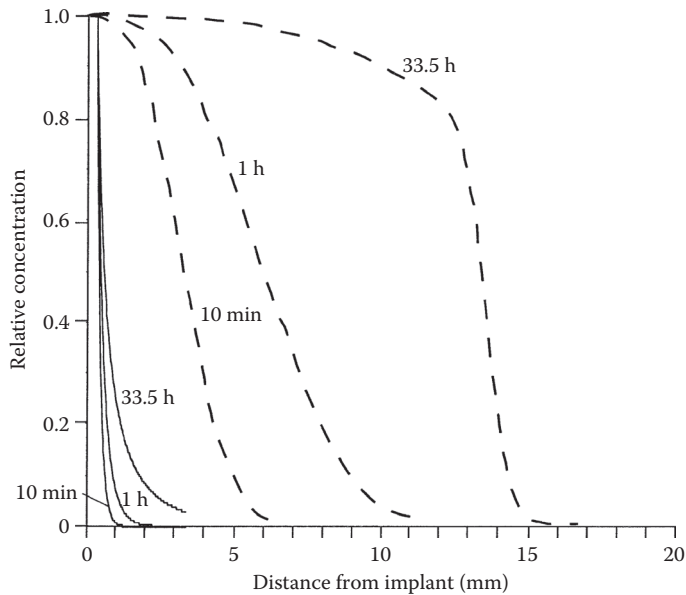


FIGURE 15.4 Concentration profiles predicted in the absence (solid lines) and presence (dashed lines) of interstitial fluid flow. Solid lines were obtained from Equation 15.15 with the following parameter values: $R = 0.032$ cm; $D = 4 \times 10^{-7}$ cm²/s; and $k^* = \ln(2)/t^{1/2}$, where $t^{1/2}$ is 10 min, 1 h, or 33.5 h as indicated on the graph. Dashed lines were obtained from Reference 14 using the same parameter values and an infusion rate of 3 μ L/min. The dashed line indicating the interstitial flow calculation for the long-lived drug ($t^{1/2} = 33.5$ h) was not at steady state, but at 12 h after initiation of the flow.

TABLE 15.3 Interstitial Fluid Velocity as a Function of Radial Position during Microinfusion

Radial Position (mm)	Interstitial Velocity (μ m/s)
2	5.0
5	0.8
10	0.2
20	0.05

Source: Calculated by method reported in Morrison, P.F. et al., *American Journal of Physiology*, 1994. 266:R292–R305.

The profiles predicted in Figure 15.4 were associated with the introduction of substantial volumes of fluid at the delivery site. Flow-related phenomena are probably less important in drug delivery by polymer implants. Still, this model provides useful guidelines for predicting the influence of fluid flow on local rates of drug movement. Clearly, the effect of flow velocity on drug distribution is substantial (Figure 15.4). Even relatively low flows, perhaps as small as 0.03 μ m/s, are large enough to account for the enhancement in BCNU penetration observed at day 1 in Figure 15.3.

15.5.1.4 Effect of Metabolism

The metabolism, elimination, and binding of drug are assumed to be first-order processes in our simple analysis. This assumption may not be realistic in all cases, especially for complex agents such as proteins. The metabolism of drugs in normal and tumor tissues is incompletely understood. Other cellular factors

(e.g., the heterogeneity of tumor-associated antigen expression and multidrug resistance) that influence the uptake of therapeutic agents may not be accounted for by our simple first-order elimination.

Finally, changes in the brain that occur during the course of therapy are not properly considered in this model. Irradiation can be safely administered when a BCNU-loaded polymer has been implanted in monkey brains, suggesting the feasibility of adjuvant radiotherapy. However, irradiation also causes necrosis in the brain. The necrotic region has a lower perfusion rate and interstitial pressure than tumor tissue; thus, the convective interstitial flow due to fluid leakage is expected to be smaller. Interstitial diffusion of macromolecules is higher in tumor tissue than in normal tissue, as the tumor tissue has larger interstitial spaces [31]. The progressive changes in tissue properties—due to changes in tumor size, irradiation, and activity of chemotherapy agent—may be an important determinant of drug transport and effectiveness of therapy in the clinical situation.

15.6 New Approaches to Drug Delivery Suggested by Modeling

Mathematical models, which describe the transport of drug following controlled delivery, can predict the penetration distance of drug and the local concentration of drug as a function of time and location. The calculations indicate that drugs with slow elimination will penetrate deeper into the tissue. The modulus f , which represents the ratio of elimination to diffusion rates in the tissue, provides a quantitative criterion for selecting agents for interstitial delivery. For example, high-molecular-weight dextrans were retained longer in the brain space, and penetrated a larger region of the brain than low-molecular-weight molecules following release from an intracranial implant [25]. This suggests a strategy for modifying molecules to improve their tissue penetration by conjugating active drug molecules to inert polymeric carriers. For conjugated drugs, the extent of penetration should depend on the modulus f for the conjugated compound as well as the degree of stability of the drug-carrier linkage.

The effects of conjugation and stability of the linkage between drug and carrier on enhancing tissue penetration in the brain have been studied in a model system [32]. Methotrexate (MTX)-dextran conjugates with different dissociation rates were produced by linking MTX to dextran (molecular weight 70,000) through a short-lived ester bond (half-life ≈ 3 days) and a longer-lived amide bond (half-life > 20 days). The extent of penetration for MTX-dextran conjugates was studied in three-dimensional human brain tumor cell cultures; penetration was significantly enhanced for MTX-dextran conjugates and the increased penetration was correlated with the stability of the linkage. These results suggest that modification of existing drugs may increase their efficacy against brain tumors when delivered directly to the brain interstitium.

15.7 Conclusion

Controlled release polymer implants are a useful new technology for delivering drugs directly to the brain interstitium. This approach is already in clinical use for treatment of tumors [33], and could soon impact treatment of other diseases. The mathematical models described in this chapter provide a rational framework for analyzing drug distribution after delivery. These models describe the behavior of chemotherapy compounds very well and allow prediction of the effect of changing properties of the implant or the drug. More complex models are needed to describe the behavior of macromolecules, which encounter multiple modes of elimination and metabolism and are subject to the effects of fluid flow. In addition, variations on this approach may be useful for analyzing drug delivery in other situations.

References

1. Lieb, W. and W. Stein, Biological membranes behave as non-porous polymeric sheets with respect to the diffusion of non-electrolytes. *Nature*, 1969. 224:240-249.
2. Stein, W.D., *The Movement of Molecules across Cell Membranes*. 1967, Academic Press: New York.

3. Simpkins, J., N. Bodor, and A. Enz, Direct evidence for brain-specific release of dopamine from a redox delivery system. *Journal of Pharmaceutical Sciences*, 1985. 74:1033–1036.
4. Gregoriadis, G., The carrier potential of liposomes in biology and medicine. *The New England Journal of Medicine*, 1976. 295:704–710.
5. Cotzias, C.G., M.H. Van Woert, and L.M. Schiffer, Aromatic amino acids and modification of parkinsonism. *The New England Journal of Medicine*, 1967. 276:374–379.
6. Triguero, D., J.B. Buciak, J. Yang, and W.M. Pardridge, Blood-brain barrier transport of cationized immunoglobulin G: Enhanced delivery compared to native protein. *Proceedings of the National Academy of Sciences USA*, 1989. 86:4761–4765.
7. Tokuda, H., Y. Takakura, and M. Hashida, Targeted delivery of polyanions to the brain. *Proceedings of the International Symposium on Control. Rel. Bioact. Mat.*, 1993. 20:270–271.
8. Friden, P., L. Walus, G. Musso, M. Taylor, B. Malfroy, and R. Starzyk, Anti-transferrin receptor antibody and antibody-drug conjugates cross the blood-brain barrier. *Proceedings of the National Academy of Sciences USA*, 1991. 88:4771–4775.
9. Friden, P.M., L.R. Walus, P. Watson, S.R. Doctrow, J.W. Kozarich, C. Backman, H. Bergman, B. Hoffer, F. Bloom, and A.-C. Granholm, Blood-brain barrier penetration and *in vivo* activity of an NGF conjugate. *Science*, 1993. 259:373–377.
10. Neuwelt, E., P. Barnett, I. Hellstrom, K. Hellstrom, P. Beaumier, C. McCormick, and R. Weigel, Delivery of melanoma-associated immunoglobulin monoclonal antibody and Fab fragments to normal brain utilizing osmotic blood-brain barrier disruption. *Cancer Research*, 1988. 48:4725–4729.
11. Blasberg, R., C. Patlak, and J. Fenstermacher, Intrathecal chemotherapy: Brain tissue profiles after ventriculocisternal perfusion. *The Journal of Pharmacology and Experimental Therapeutics*, 1975. 195:73–83.
12. Yan, Q., C. Matheson, J. Sun, M.J. Radeke, S.C. Feinstein, and J.A. Miller, Distribution of intracerebrally administered neurotrophins in rat brain and its correlation with Trk receptor expression. *Experimental Neurology*, 1994. 127:23–36.
13. Mahoney, M.J. and W.M. Saltzman, Controlled release of proteins to tissue transplants for the treatment of neurodegenerative disorders. *Journal of Pharmaceutical Sciences*, 1996. 85(12):1276–1281.
14. Morrison, P.F., D.W. Laske, H. Bobo, E.H. Oldfield, and R.L. Dedrick, High-flow microinfusion: Tissue penetration and pharmacodynamics. *American Journal of Physiology*, 1994. 266:R292–R305.
15. Haller, M.F. and W.M. Saltzman, Localized delivery of proteins in the brain: Can transport be customized? *Pharmaceutical Research*, 1998. 15:377–385.
16. Dang, W. and W.M. Saltzman, Controlled release of macromolecules from a biodegradable polyanhydride matrix. *Journal of Biomaterials Science, Polymer Edition*, 1994. 6(3):291–311.
17. Dang, W., *Engineering Drugs and Delivery Systems for Brain Tumor Therapy*. 1993, The Johns Hopkins University: Baltimore, MD.
18. Wyatt, T.L. and W.M. Saltzman, Protein delivery from non-degradable polymer matrices, in *Protein Delivery-Physical Systems*, L. Saunders and W. Hendren, Editors. 1997, Plenum Press: New York, NY. pp. 119–137.
19. Bird, R.B., W.E. Stewart, and E.N. Lightfoot, *Transport Phenomena*. 1960, New York: John Wiley & Sons. 780.
20. Patlak, C. and J. Fenstermacher, Measurements of dog blood-brain transfer constants by ventriculocisternal perfusion. *American Journal of Physiology*, 1975. 229:877–884.
21. Nicholson, C., Diffusion from an injected volume of a substance in brain tissue with arbitrary volume fraction and tortuosity. *Brain Research*, 1985. 333:325–329.
22. Morrison, P. and R.L. Dedrick, Transport of cisplatin in rat brain following microinfusion: An analysis. *Journal of Pharmaceutical Sciences*, 1986. 75:120–128.
23. Saltzman, W.M. and M.L. Radomsky, Drugs released from polymers: Diffusion and elimination in brain tissue. *Chemical Engineering Science*, 1991. 46:2429–2444.

24. Fung, L., M. Shin, B. Tyler, H. Brem, and W.M. Saltzman, Chemotherapeutic drugs released from polymers: Distribution of 1,3-bis(2-chloroethyl)-1-nitrosourea in the rat brain. *Pharmaceutical Research*, 1996. 13:671–682.
25. Dang, W. and W.M. Saltzman, Dextran retention in the rat brain following controlled release from a polymer. *Biotechnology Progress*, 1992. 8:527–532.
26. Krewson, C.E., M. Klarman, and W.M. Saltzman, Distribution of nerve growth factor following direct delivery to brain interstitium. *Brain Research*, 1995. 680:196–206.
27. Krewson, C.E. and W.M. Saltzman, Transport and elimination of recombinant human NGF during long-term delivery to the brain. *Brain Research*, 1996. 727:169–181.
28. Strasser, J.F., L.K. Fung, S. Eller, S.A. Grossman, and W.M. Saltzman, Distribution of 1,3-bis(2-chloroethyl)-1-nitrosourea (BCNU) and tracers in the rabbit brain following interstitial delivery by biodegradable polymer implants. *The Journal of Pharmacology and Experimental Therapeutics*, 1995. 275(3):1647–1655.
29. Fung, L.K., M.G. Ewend, A. Sills, E.P. Sapos, R. Thompson, M. Watts, O.M. Colvin, H. Brem, and W.M. Saltzman, Pharmacokinetics of interstitial delivery of carmustine, 4-hydroperoxycyclophosphamide, and paclitaxel from a biodegradable polymer implant in the monkey brain. *Cancer Research*, 1998. 58:672–684.
30. Jain, R.K., Barriers to drug delivery in solid tumors. *Scientific American*, 1994. 271(1): 58–65.
31. Clauss, M.A. and R.K. Jain, Interstitial transport of rabbit and sheep antibodies in normal and neoplastic tissues. *Cancer Research*, 1990. 50:3487–3492.
32. Dang, W.B., O.M. Colvin, H. Brem, and W.M. Saltzman, Covalent coupling of methotrexate to dextran enhances the penetration of cytotoxicity into a tissue-like matrix. *Cancer Research*, 1994. 54:1729–1735.
33. Brem, H., S. Piantadosi, P.C. Burger, M. Walker, R. Selker, N.A. Vick, K. Black et al. Placebo-controlled trial of safety and efficacy of intraoperative controlled delivery by biodegradable polymers of chemotherapy for recurrent gliomas. *Lancet*, 1995. 345:1008–1012.



Physiological Modeling, Simulation, and Control

Joseph L. Palladino
Trinity College

- 17 Modeling Strategies and Cardiovascular Dynamics** *Joseph L. Palladino, Gary M. Drzewiecki, and Abraham Noordergraaf*..... **17-1**
Introduction • Modeling Heart Dynamics • Modeling Muscle Dynamics • Modeling Heart Function during Hypertrophy • Summary • References
- 18 Compartmental Models of Physiological Systems** *Claudio Cobelli, Giovanni Sparacino, Maria Pia Saccomani, Gianna Maria Toffolo, and Andrea Caumo* **18-1**
Introduction • Definitions and Concepts • The Compartmental Model
• A Priori Identifiability • Parameter Estimation • Optimal Experiment Design • Validation • References
- 19 Cardiovascular Models and Control** *Madhusudan Natarajan, Fernando Casas, and W.D. Timmons*..... **19-1**
The Utility and Limitations of Desktop Patients • History of CV Modeling
• CV Modeling • Conclusions • References • Further Information
- 20 Respiratory Models and Control** *Chi-Sang Poon*..... **20-1**
Structure of the Respiratory Control System • Chemoreflex Models • Models of RCPG
• Optimization Models • Self-Tuning Regulator Models • Conclusion • Nomenclature
• References
- 21 Biomimetic Approaches to Physiological Control** *James J. Abbas and Amit Abraham*..... **21-1**
Introduction • Biomimetics: Inspiration, Ideas, and Performance Targets from Nature
• Neural Network Basics • Neural Network Control Systems • Summary
• Acknowledgments • Defining Terms • References • Further Information

- 22 Methods and Tools for Identification of Physiologic Systems** *Vasilis Z. Marmarelis*..... 22-1
 Parametric Approach • Nonparametric Approach • Modular Approach • Synergistic Use of Parametric and Nonparametric Approaches • Acknowledgment • References
- 23 Modeling Vascular Vibrations: Autoregulation and Vascular Sounds** *Gary M. Drzewiecki, John K-J. Li, and Abraham Noordergraaf*..... 23-1
 Autoregulating Windkessel Dynamics May Cause Low Frequency Oscillations • Theory and Acoustic Classification of Vascular Sounds in the Diseased Artery • References
- 24 External Control of Movements** *Dejan B. Popović and Mirjana B. Popović*..... 24-1
 Introduction • Control Methods for Multi-Input/Multi-Output Systems • Components of the Motor System in a Human Body • Modeling for the Design of an Analytic Controller of Movement • Nonanalytic Modeling of Movements • Defining Terms • References • Further Reading • Periodicals
- 25 The Fast Eye Movement Control System** *John Denis Enderle*..... 25-1
 Introduction • Saccade Characteristics • Westheimer Saccadic Eye Movement Model • Robinson's Model of the Saccade Controller • A Linear Homeomorphic Saccadic Eye Movement Model • 1995 Linear Homeomorphic Saccadic Eye Movement Model • 2009 Linear Homeomorphic Saccadic Eye Movement Model • Neural Input • Monkey Data and Results • Human Data and Results • Postinhibitory Rebound Burst and Post-Saccade Phenomena • Time-Optimal Controller • Saccade Neural Pathways • Saccade Control Mechanism • Conclusion • Defining Terms • References • Further Information
- 26 A Comparative Approach to Analysis and Modeling of Cardiovascular Function** *John K-J. Li, Ying Zhu, and Abraham Noordergraaf*..... 26-1
 Introduction • Dimensional Analysis of Physiological Function • Invariant Numbers and Their Physiological Applications • Comparative Analysis of the Mammalian Circulatory System • Metabolic Turn-Over Rate and Cardiac Work • Comparative Pulse Transmission Characteristics • Optimal Design Features • References
- 27 A Biomedical and Biophysical Approach to the Science in Cardiopulmonary Resuscitation** *Gerrit J. Noordergraaf, Igor W.F. Paulussen, Alyssa Venema, Gert Jan Scheffer, and Abraham Noordergraaf*..... 27-1
 Introduction • Basic Models and Methods in CPR: Its Fundamental Characteristics • Variations in CPR Technique Based on Physiological Expectations and Modeling • From Clinical Experiments to Biomedical and Biophysical Understanding • Current Developments • Summary • References
- 28 Kinematic Modeling of Left Ventricular Diastolic Function** *Leonid Shmuylovich, Charles S. Chung, and Sándor J. Kovács*..... 28-1
 Introduction • Solution of the DF Problem via Kinematic Modeling • Cardiovascular Physiology in the Phase Plane • Conclusion • References

Preface

The complexities of physiological systems often lead to the creation of new models to aid in the understanding of measured experimental data and to predict new features of the system under study. Models may serve to compactly summarize known system properties, including bio-mechanical, chemical, and electrical phenomena. Experiments carried out on the model yield new information that casts light on unknown mechanisms underlying these properties and stimulate the formulation of new questions and the design of new experiments. Further, such quantitative description often leads to a better understanding of the physical mechanisms underlying both normal and pathological system performance. Ultimately, modeling may facilitate clinical diagnosis of system failure at an early stage of disease development.

Models begin conceptually; for example, the concept that a blood vessel behaves as a fluid-filled pipe. Concepts may be developed into physical models, for example, using a latex tube to describe a blood

vessel, upon which experiments are performed. Often, concepts are realized as mathematical models, whereby the concept is described by physical laws, transformed into a set of mathematical equations, and solved via a computer. Simulations, distinct from models, are descriptions that mimic the physiological system. The quantitative nature of physiological models allows them to be employed as components of systems for the study of physiological control, illustrated in several of this section's chapters.

Chapter 17 describes the iterative process of physiological modeling and presents three widely different modeling approaches in cardiovascular dynamics. The first is a compact model of the canine left ventricle. Its modular design facilitates its application in larger cardiovascular system models, for example, one used to predict net blood flow during closed-chest cardiopulmonary resuscitation. Next, a large-scale, distributed muscle model shows how mechanical description of muscle structure can predict a molecular mechanism responsible for heart muscle's complex mechanical function, that is, structure predicts function. Finally, an approach for predicting ventricular hypertrophy based on cardiac function is presented, with function predicting structure.

Chapter 18 shows how compartmental models, vital to the field of pharmacokinetics, may be used to describe physiological systems. The production, distribution, transport, and interaction of exogenous materials, such as drugs or tracers, and endogenous materials, such as hormones, are described. Examples of both linear and nonlinear compartmental models are presented, as well as parameter estimation, optimal experiment design, and model validation.

Chapter 19 demonstrates the importance of cardiovascular modeling in designing drug delivery control systems, such as intravenous infusion pumps for pharmacological agents. The chapter begins with a review of segmental and transmission line models of the arterial system, and time-varying elastance descriptions of the left ventricle. The authors make an argument for employing nonlinear cardiovascular-linked pharmacological models to aid in controller design since data from these models can improve, and reduce the number of, animal and human experiments, and can be used to simulate human conditions not easily produced in animals.

Chapter 20 presents models used to study the continual interaction of the respiratory mechanical system and pulmonary gas exchange. Traditionally, the respiratory system is described as a chemostat—ventilation increases with increased chemical stimulation. Alternatively, the author proposes that quantitative description of the “respiratory central pattern generator,” a network of neuronal clusters in the brain, is a much more sophisticated and realistic approach. A study of this dynamic, optimized controller of a nonlinear plant is interesting both from physiological and engineering perspectives, the latter due to applications of these techniques for new, intelligent control system design.

Chapter 21 introduces the use of biomimetics for physiological control. As the name suggests, the field of biomimetics studies imitates nature's mechanisms and processes, providing “inspiration, ideas and performance targets from nature.” For example, neural networks have been used to describe the control of arm movements with electrical stimulation and the adaptive control of arterial blood pressure.

Chapter 22 surveys methods of system identification in physiology, the process of extracting model components from experimental data. Identification typically estimates unknown parameters within the specified model using experimental data and advanced computational techniques. Estimation may be either parametric, where algebraic or difference equations represent static or dynamic systems, or nonparametric, where analytical (convolution), computational (look-up tables), or graphical (phase-space) techniques characterize the system. This chapter also presents a hybrid modular approach to estimation.

Chapter 23 shows how modeling can propose mechanisms to explain experimentally observed vibrations in the cardiovascular system. A control system characterized by a slow and delayed change in resistance due to smooth muscle activity is presented. Experiments on this model show oscillations in the input impedance frequency spectrum, and flow and pressure transient responses to step inputs consistent with experimental observations. This autoregulation model supports the theory that low-frequency oscillations in heart rate and blood pressure variability spectra (Mayer waves) find their origin in the intrinsic delay of flow regulation. A second example presents acoustic classification of vascular

sounds in diseased arteries. A modeling-based study characterizes the sounds detected by physicians in the carotid artery during routine physical examinations, for the purpose of more accurate diagnosis of carotid artery disease via auscultation.

Chapter 24 presents models to describe the control of human movement, primarily the dynamics of human extremities. Presented are the challenges associated with control methods for multiple input/output systems, modeling muscle contraction, joints and other components of the human motor system, and parameter estimation. This chapter presents several models for limb movement control.

Chapter 25 describes physiological models of the fast eye movement, or saccade, that enables the eye to move quickly from one image to another. This common eye movement is encountered when scanning from the end of one line of printed text to the start of another. Early quantitative models helped define important characteristics of saccades. Increasingly complex models of the oculomotor plant were derived using improved models of the rectus eye muscle. Finally, application of system control theory and simulation methods led to a saccade generator model in close agreement with experimental data.

Chapter 26 adopts a comparative approach using biological scaling laws to compare the cardiovascular systems of different mammals. Allometry, the change of proportions with increase of size, and dimensional analysis is used to develop allometric relations for important cardiovascular parameters such as stroke volume, peripheral resistance, and heart efficiency. Optimal cardiovascular design is also discussed.

Chapter 27 presents a biomedical approach toward understanding the mechanics of cardiopulmonary respiration (CPR). A review of the literature reveals two competing theories—the cardiac pump and the thoracic pump. The authors give evidence for why closed-chest CPR has such poor clinical outcomes, and present a mathematical model of the system that provides insight for improving these clinical outcomes.

Chapter 28 offers a kinematic approach to model left ventricular diastolic function. The authors point out that kinematics-based models are species independent since they are based on classical laws of motion. They also show how such models can be validated via routine clinical methods.

18

Compartmental Models of Physiological Systems

Claudio Cobelli
University of Padua

Giovanni Sparacino
University of Padua

Maria Pia
Saccomani
University of Padua

Gianna Maria
Toffolo
University of Padua

Andrea Caumo
*San Raffaele Scientific
Institute*

18.1	Introduction	18-1
18.2	Definitions and Concepts.....	18-2
18.3	The Compartmental Model.....	18-3
	Theory • The Linear Model • The Nonlinear Model • Use in Simulation and Indirect Measurement	
18.4	A Priori Identifiability.....	18-7
18.5	Parameter Estimation	18-8
	Fisher Approach • Bayes Approach • Population Approaches	
18.6	Optimal Experiment Design.....	18-11
18.7	Validation.....	18-12
	References.....	18-12

18.1 Introduction

Compartmental models are a class of dynamic (i.e., differential equation), models derived from mass balance considerations, which are widely used for quantitatively studying the kinetics of materials in physiological systems. Materials can be either exogenous, such as a drug or a tracer, or endogenous, such as a substrate or a hormone, and kinetics include processes such as production, distribution, transport, utilization, and substrate–hormone control interactions.

Compartmental modeling was first formalized in the context of isotopic tracer kinetics. Over the years it has evolved and grown as a formal body of theory (Carson et al. 1983; Godfrey, 1983; Jacquez 1996; Cobelli et al., 2000; Cobelli and Carson, 2008).

Compartmental models have been widely employed for solving a broad spectrum of physiological problems related to the distribution of materials in living systems in research, diagnosis, and therapy, at whole-body, organ, and cellular levels. Examples and references can be found in books (Gibaldi and Perrier, 1982; Carson et al., 1983; Jacquez, 1996; Cobelli et al., 2000; Carson and Cobelli, 2013; Cobelli and Carson, 2008) and reviews (Carson and Jones, 1979; Cobelli, 1984; Cobelli and Caumo, 1998; Cobelli et al., 2007, 2009). Purposes for which compartmental models have been developed include

- Identification of system structure, that is, models to examine different hypotheses regarding the nature of specific physiological mechanisms.
- Estimation of unmeasurable quantities, that is, estimating internal parameters and variables of physiological interest.
- Simulation of the intact system behavior where ethical or technical reasons do not allow direct experimentation on the system itself.

- Prediction and control of physiological variables by administration of therapeutic agents, that is, models to predict an optimal administration of drug in order to keep one or more physiological variables within desirable limits.
- Cost/effectiveness optimization of dynamic clinical tests, that is, models to obtain maximal information from the minimum number of blood samples withdrawn from a patient.
- Diagnosis, that is, models to augment quantitative information from laboratory tests and clinical symptoms, thus improving the reliability of diagnosis.
- Teaching, that is, models to aid in the teaching of many aspects of physiology, clinical medicine, and pharmacokinetics.

The use of compartmental models of physiological systems has been greatly facilitated by the availability of specific software packages which can be used both for simulation and identification, such as ADAPT and SAAM-II; see the websites <http://bmsr.usc.edu/Software/ADAPT/ADAPT.html> and <http://depts.washington.edu/saam2> for specific information.

18.2 Definitions and Concepts

Let us start with some definitions. A *compartment* is an amount of material that acts as though it is well-mixed and kinetically homogeneous. A *compartmental model* consists of a finite number of compartments with specified interconnections among them. The interconnections represent fluxes of material which physiologically represent transport from one location to another or a chemical transformation, or both, or control signals. An example of a simple two-compartment model is illustrated in Figure 18.1, where the compartments are represented by circles and the interconnections by arrows.

Given the introductory definitions, it is useful before explaining *well-mixed* and *kinetic homogeneity* to consider possible candidates for compartments. Consider the notion of a compartment as a physical space. Plasma is a candidate for a compartment; a substance such as plasma glucose could be a compartment. Zinc in bone could be a compartment also, as could thyroxine in the thyroid. In some experiments, different substances could be followed in plasma: plasma glucose, lactate, and alanine provide examples. Thus, in the same experiment, there can be more than one plasma compartment, one for each of the substances being studied. This notion extends beyond plasma. Glucose and glucose-6-phosphate could be two different compartments inside a liver cell. Thus, a physical space may actually represent more than one compartment.

In addition, one must distinguish between compartments that are accessible and nonaccessible for measurement. Researchers often try to assign physical spaces to the nonaccessible compartments. This

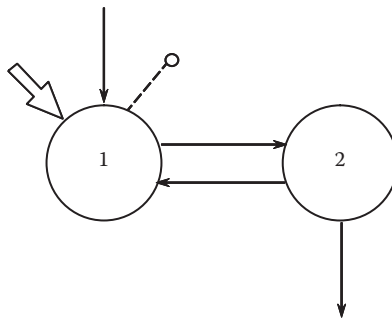


FIGURE 18.1 A two-compartment model. The substance enters *de novo* compartment 1 (arrow entering a compartment from “outside”) and irreversibly leaves from compartment 2 (arrow leaving a compartment to the “outside”). Material exchanges occur between compartments 2 and 1 and compartments 1 and 2 and are represented by arrows. Compartment 1 is the accessible compartment; test input and measurement (output) are denoted by a large arrow and a dashed line with a bullet, respectively.

is a very difficult problem that is best addressed once one realizes that the definition of a compartment is actually a theoretical construct, which may in fact lump material from several different physical spaces in a system; to equate a compartment with a physical space depends upon the system under study and assumptions about the model.

With these notions of what might constitute a compartment, it is easier to define the concepts of well-mixed and kinetic homogeneity. What *well-mixed* means is that any two samples taken from the compartment at the same time would have the same concentration of the substance being studied and therefore be equally representative. Thus, the concept of well mixed relates to uniformity of information contained in a single compartment.

Kinetic homogeneity means that every particle in a compartment has the same probability of taking the pathways leaving the compartment. Since, when a particle leaves a compartment, it does so because of metabolic events related to transport and utilization, it means that all particles in the compartment have the same probability of leaving due to one of these events.

The notion of a compartment, that is, lumping material with similar characteristics into collections that are homogeneous and behave identically, is what allows one to reduce a complex physiological system into a finite number of compartments and pathways. The required number of compartments depends both on the system being studied and on the richness of the experimental configuration. A compartmental model is clearly unique for each system studied, since it incorporates known and hypothesized physiology and biochemistry. It provides the investigator with insights into the system structure and is as good as the assumptions that are incorporated in the model.

18.3 The Compartmental Model

18.3.1 Theory

Figure 18.2 represents the i th compartment of an n -compartment model; $q_i \geq 0$ denotes the mass of the compartment. The arrows represent fluxes into and out of the compartment: the input flux into the compartment from outside the system, for example, *de novo* synthesis of material and exogenous test input, is represented by $u_i \geq 0$; the flux to the environment and, therefore, out of the system by f_{0i} ; the flux from compartment i to j by f_{ij} , and the flux from compartment j to i by f_{ji} . All fluxes are greater than or equal to zero. The general equations for the compartmental model are obtained by writing the mass balance equation for each compartment:

$$\dot{q}_i = \sum_{j \neq i}^n f_{ij} - \sum_{j \neq i}^n f_{ji} - f_{0i} + u_i, \quad q_i(0) = q_{i0} \tag{18.1}$$

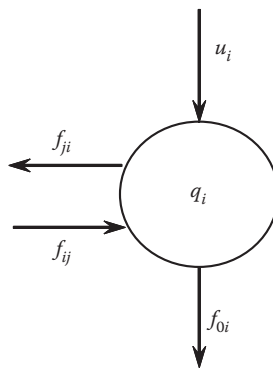


FIGURE 18.2 The i th compartment of an n -compartment model.

The input fluxes u_i are generally constant or functions of only time. The fluxes f_{ji} , f_{ij} , and f_{0i} can be functions of q_1, \dots, q_n and sometimes also of time (for the sake of simplicity, we will ignore this dependence). It is always possible to write

$$f_{ij}(\mathbf{q}) = k_{ij}(\mathbf{q})q_j \quad (18.2)$$

where $\mathbf{q} = (q_1, \dots, q_n)^T$ is the vector of the compartmental masses. As a result, Equation 18.1 can be written as

$$\dot{q}_i = \sum_{j=1}^n k_{ij}(\mathbf{q})q_j - \left(\sum_{\substack{j=1 \\ j \neq i}}^n k_{ij}(\mathbf{q}) + k_{0i}(\mathbf{q}) \right) q_i + u_i, \quad q_i(0) = q_{i0} \quad (18.3)$$

The k_{ij} 's are called *fractional transfer coefficients*. Equation 18.3 describes the generic *nonlinear* compartmental model. If the k_{ij} 's do not depend on the compartmental masses q_i 's, the model becomes *linear*.

Defining $k_{ii}(\mathbf{q}) = -\left(\sum_{\substack{j=1 \\ j \neq i}}^n k_{ji}(\mathbf{q}) + k_{0i}(\mathbf{q}) \right)$ we can now write Equation 18.3 as

$$\dot{q}_i = \sum_{j=1}^n k_{ij}(\mathbf{q})q_j + u_i, \quad q_i(0) = q_{i0} \quad (18.4)$$

and the model of the whole system as

$$\dot{\mathbf{q}} = \mathbf{K}(\mathbf{q})\mathbf{q} + \mathbf{u}, \quad \mathbf{q}(0) = \mathbf{q}_0 \quad (18.5)$$

where \mathbf{K} is the $n \times n$ *compartmental matrix* (hereafter, let us drop the dependence on \mathbf{q} , for simplicity of notation) and $\mathbf{u} = (u_1, \dots, u_n)^T$ is the vector of input fluxes into the compartments from outside the system.

For the linear case, \mathbf{K} is constant and one has

$$\dot{\mathbf{q}} = \mathbf{K}\mathbf{q} + \mathbf{u}, \quad \mathbf{q}(0) = \mathbf{q}_0 \quad (18.6)$$

The entries of the compartmental matrix \mathbf{K} , for both the nonlinear 5 and the linear 6 model, satisfy

$$k_{ii} \leq 0, \quad \text{for all } i \quad (18.7)$$

$$k_{ij} \geq 0, \quad \text{for all } i \neq j \quad (18.8)$$

$$\sum_{i=1}^n k_{ij} = \sum_{\substack{i=1 \\ i \neq j}}^n k_{ij} + k_{jj} = -k_{0j} \leq 0, \quad \text{for all } j \quad (18.9)$$

\mathbf{K} is thus a (column) diagonally dominant matrix. This is a very important property, and in fact the stability properties of compartmental models are closely related to the diagonal dominance of the compartmental matrix. For instance, in the linear model, Equation 9.6, one can show that all eigenvalues

have nonpositive real parts and that there are no purely imaginary eigenvalues: this means that all solutions are bounded and if there are oscillations they are damped. The qualitative theory of linear and nonlinear compartmental models has been reviewed in Jacquez and Simon (1993), where some stability results on nonlinear compartmental models are also presented.

18.3.2 The Linear Model

The linear model, Equation 18.6, has become very useful in applications due to an important result: the kinetics of a tracer in a constant steady-state system, linear or nonlinear, are linear with constant coefficients. An example is shown in Figure 18.3 where the three-compartment model by Cobelli et al. (1984b) for studying tracer glucose kinetics in steady state at the whole-body level is depicted. Linear compartmental models in conjunction with tracer experiments have been extensively used in studying distribution of materials in living systems at whole-body, organ, and cellular level. Examples and references can be found in Carson et al. (1983), Jacquez (1996), Cobelli et al. (2000), and Carson and Cobelli (2013).

An interesting application of linear compartmental models at the organ level is in describing the exchange of materials between blood, interstitial fluid, and cell of a tissue from multiple tracer indicator dilution data. Compartmental models provide a finite difference approximation in the space dimension of a system described by partial differential equations, which may be more easily resolvable from the data. These models are discussed in Jacquez (1996), and an example of a model describing glucose transport and metabolism in the human skeletal muscle can be found in Saccomani et al. (1996).

18.3.3 The Nonlinear Model

Almost all the biological models are nonlinear dynamic systems, including, for example, saturation or threshold processes. In particular, nonlinear compartmental models, Equation 18.5, are frequently found in biomedical applications. For such models the entries of \mathbf{K} are functions of \mathbf{q} , most commonly k_{ij} is a function of only a few components of \mathbf{q} , often q_i or q_j . Examples of k_{ij} function of q_i or q_j are the Hill and the Langmuir nonlinearities described, respectively, by

$$k_{ij}(q_j) = \frac{\alpha q_j(t)^{h-1}}{\beta + q_j(t)^h} \tag{18.10}$$

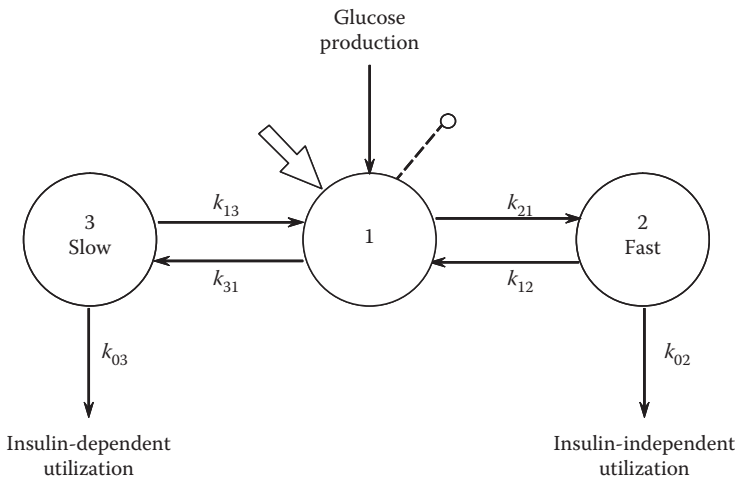


FIGURE 18.3 The linear compartmental model of glucose kinetics by Cobelli et al. (1984b).

Downloaded by [JCR JCR] at 10:36 01 August 2015

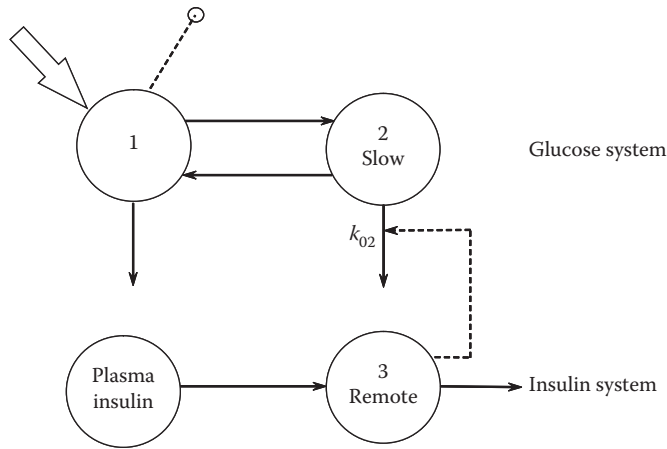


FIGURE 18.4 The nonlinear compartmental model of insulin control on glucose distribution and metabolism by Caumo and Cobelli (1993). The dashed line denotes a control signal.

$$k_{ij}(q_j) = 1 - \frac{q_i}{\gamma} \quad (18.11)$$

where α , β , γ are positive reals, and h is a positive integer. For $h = 1$, Equation 18.10 turns into the widely used Michaelis–Menten equation.

Other interesting examples arise in describing substrate–hormone control systems. For instance, the model of Figure 18.4 has been proposed (Caumo and Cobelli, 1993; Vicini et al., 1997) to describe the control of insulin on glucose distribution and metabolism during a glucose perturbation, which brings the system out of steady state. The model assumes compartmental descriptions for glucose and insulin kinetics, interacting via a control signal that emanates from the remote insulin compartment and affects the transfer rate coefficient, k_{02} , which is responsible for insulin-dependent glucose utilization. In this case one has

$$k_{02}(q_3) = \delta + q_3 \quad (18.12)$$

where δ is a constant.

Additional examples and references on nonlinear compartmental models can be found in Carson et al. (1983), Godfrey (1983), Jacquez (1996), and Carson and Cobelli (2013).

18.3.4 Use in Simulation and Indirect Measurement

Models such as those described by Equation 18.5 can be used for *simulation*. Assuming that both the matrix \mathbf{K} and initial state $\mathbf{q}(0)$ are known, it is possible to predict the behavior of the state vector \mathbf{q} for any possible input function \mathbf{u} .

A major use of compartmental models is in the *indirect measurement* of physiological parameters and variables. For instance, given data obtained from m compartments, which are accessible to measurement (usually m is a small fraction of the total number of compartments n), a model is used to estimate parameters not directly measurable and predict quantities related to nonaccessible compartments. In this case \mathbf{K} is unknown and input–output experiments are performed to generate data to determine \mathbf{K} . These data can be usually be described by a linear algebraic equation

$$\mathbf{y} = \mathbf{C}\mathbf{q} \quad (18.13)$$

where $\mathbf{y} = (y_1, \dots, y_m)^T$ is the vector of the m model outputs and \mathbf{C} is the $m \times n$ observation matrix. If model outputs are concentrations, the entries of \mathbf{C} are the inverse of the volumes of the m compartments accessible to measurement. Real data are noisy, thus an error term \mathbf{v} is usually added to \mathbf{y} in Equation 18.13 to describe the actual measurements \mathbf{z}

$$\mathbf{z} = \mathbf{y} + \mathbf{v} \quad (18.14)$$

\mathbf{v} is usually given a probabilistic description; for example, errors are assumed to be independent and often Gaussian. Equation 18.13 and Equation 18.14, together with Equation 18.5 or Equation 18.6, define the compartmental model of the system, that is, the model structure and the input–output experimental configuration.

The identification techniques described in the following section are aimed to determine the entries of \mathbf{K} (and often also those of \mathbf{C}) from the data vector \mathbf{z} of Equation 18.14.

18.4 A Priori Identifiability

Let us assume that a compartmental model structure has been postulated to describe the physiological system, that is, the number of compartments and the connections among them have been specified. This is the most difficult step in compartmental model building.

The structure can reflect a number of facts: there may be some a priori knowledge about the system, which can be incorporated in the structure; one can make specific assumptions about the system, which are reflected in the structure; by testing via simulation one can arrive at a structure that is needed to fit the data. The result at this stage is a nonlinear, Equation 18.5, or linear, Equation 18.6, where parameters of the compartmental matrix \mathbf{K} and those of the observation matrix \mathbf{C} , Equation 18.13, are usually unknown. Before performing the experiment or, if the experiment was already completed, before numerically estimating the model parameters from the experimental data, the following question arises: does the data contain enough information to unequivocally estimate (e.g., via least squares or maximum likelihood) all the unknown parameters of the postulated model structure? This question, set in the ideal context of error-free model structure and noise-free measurements, is usually referred to as the a priori *global identifiability*. Despite its theoretical nature, it is an essential, but often overlooked, prerequisite for model parameter estimation from real data. In particular, if it turns out in such an ideal context that some model parameters are not identifiable from the data, there is no way that the parameters can be identified in a real situation, with errors in the model structure and noise in the data.

A priori identifiability thus examines whether, given the ideal noise-free data \mathbf{y} , Equation 18.13, and the error-free compartmental model structure, Equations 18.5 and 18.6, it is possible to make unique estimates of all the unknown model parameters. A model can be *uniquely (globally) identifiable*—that is, all its parameters have one solution—or *nonuniquely (locally) identifiable*—that is, one or more of its parameters has more than one but a finite number of possible values—or *nonidentifiable*—that is, one or more of its parameters has an infinite number of solutions. For instance, the model of Figure 18.1 is uniquely identifiable, while that of Figure 18.3 is *nonidentifiable*.

A priori identifiability is also crucial in qualitative experiment design (Saccomani and Cobelli, 1992), which studies the input–output configuration necessary to ensure unique estimation of the unknown parameters. In fact, it allows distinguishing among those experiments that cannot succeed and those that might and, among the latter, may help in determining the minimal input–output configuration to ensure estimation of the unknown parameters. This is of particular relevance for physiological systems, where the number and sites of application of inputs and outputs are severely constrained by ethical and technical reasons.

The identifiability problem is in general a difficult task, since it requires solving a system of nonlinear algebraic equations with a number of terms and nonlinearity degree increasing with the model

order. For linear compartmental models various specific methods, for example, based on transfer function, similarity transformation, and graph topology, have been developed (Cobelli and DiStefano, 1980; Walter, 1982; Carson et al., 1983; Godfrey, 1983; Jacquez, 1996). Explicit identifiability results on catenary and mamillary compartmental models (Cobelli et al., 1979) and on the three-compartmental model (Norton, 1982) are available. The introduction of computer algebraic algorithms has considerably simplified the complexity of the problem (Audoly et al., 1998).

For nonlinear compartmental models the problem is more difficult. Some results are available based on the local state isomorphism theorem (Walter, 1982; Chappell and Godfrey, 1992; Chapman et al., 2003), on the revisited Taylor series approach (Joly-Blanchard and Denis-Vidal, 1998) and on differential algebra (Ollivier, 1990; Ljung and Glad, 1994; Audoly et al., 2001; Saccomani et al., 2003; Verdière et al., 2005). In particular, the introduction of concepts of differential algebra has been an important factor for addressing identifiability of nonlinear (compartmental and noncompartmental) models previously thought to be intractable. However, in the last few years, there were many software tools developed to perform parameter estimation from actual data, but essentially no tools to perform model identifiability tests. Only recently, a computer algebra software tool, DAISY, based on a differential algebra algorithm (Saccomani et al., 2003), has been released (Bellu et al., 2007) and it is freely available on the web site <http://daisy.dei.unipd.it>. DAISY is designed to automatically check identifiability of (linear and) nonlinear dynamic models described by polynomial or rational functions with given initial conditions. This is a very useful tool for biological and physiological systems that often exhibit nongeneric initial conditions; for example, a model of radiotracer kinetics is characterized by zero initial conditions. Although being based on rather sophisticated mathematics, the software does not require expertise on mathematical modeling by the medical/biological investigator to tackle problems which are hard and computationally intensive to test identifiability of nonlinear models (Saccomani et al., 2010).

From the above considerations, it follows that if a model is a priori uniquely identifiable, then identification techniques can be used to estimate from the noisy data \mathbf{z} , Equation 18.14, the numerical values of the unknown parameters. Conversely, if a model is either a priori nonuniquely identifiable or nonidentifiable, numerical estimation may lead to parametric values which are ambiguous and thus not informative about the biological system under study; this is particularly critical when dealing with physiological systems where a different numerical estimate can characterize a pathological state from a normal one. In this case, to solve the problem, different strategies can be used, for example, derivation of bounds for nonidentifiable parameters (DiStefano, 1983), model reparametrization (parameter aggregation), incorporation of additional knowledge, or design of a more informative experiment. An example on the use of some of these approaches for dealing with the nonidentifiable model of glucose kinetics of Figure 18.3 is given in Cobelli and Toffolo (1987).

In conclusion, a priori unique identifiability is a prerequisite for well posedness of parameter estimation and for reconstructability of state variables in compartments not accessible to measurement. It is a necessary but not sufficient condition to guarantee successful estimation of model parameters from real input-output data.

18.5 Parameter Estimation

Given a uniquely identifiable compartmental model, one can proceed by estimating the values of the unknown parameters from the experimental data. Assuming, for the sake of simplicity, that the model is linear and that only one output variable is observed, that is, $m = 1$, by integrating Equation 18.6 one can obtain the explicit solution for the model output, that is, $y(t) = g(t, \theta)$, where θ is a p -dimension vector which contains the p unknown parameters of the model. For instance, if the model of Figure 18.1 is used to describe the kinetics of a tracer after the administration of a pulse of known amplitude D (i.e., $u(t) = D\delta(t)$ and $q_1(0) = q_2(0) = 0$), the vector θ is a four-dimension vector containing the fractional

transfer coefficients k_{01} , k_{12} , k_{21} , and the volume V of the accessible compartment, while the accessible tracer concentration profile $y(t)$ is

$$y(t) = g(t, \theta) = \frac{D}{V} \left(\frac{k_{21} + k_{01} + \sqrt{(k_{12} + k_{21} + k_{01}) + 4k_{12}k_{01}}}{2\sqrt{(k_{12} + k_{21} + k_{01}) + 4k_{12}k_{01}}} e^{-(k_{12} + k_{21} + k_{01} + \sqrt{(k_{12} + k_{21} + k_{01}) + 4k_{12}k_{01}})t} + \frac{k_{12} + k_{01} + \sqrt{(k_{12} + k_{21} + k_{01}) + 4k_{12}k_{01}}}{2\sqrt{(k_{12} + k_{21} + k_{01}) + 4k_{12}k_{01}}} e^{-(k_{12} + k_{21} + k_{01} - \sqrt{(k_{12} + k_{21} + k_{01}) + 4k_{12}k_{01}})t} \right) \quad (18.15)$$

In practical cases, experimental data are collected at N discrete time instants t_1, \dots, t_N , so that discrete time measurements $y(t_k) = g(t_k, \theta)$ are available. Letting $\mathbf{z} = (z(t_1), \dots, z(t_N))^T$ to denote the vector of the noisy samples of the output, according to Equation 18.14 one has

$$\mathbf{z} = \mathbf{g}(\theta) + \mathbf{v} \quad (18.16)$$

where $\mathbf{g}(\theta) = (g(t_1, \theta), \dots, g(t_N, \theta))^T$, while $\mathbf{v} = (v(t_1), \dots, v(t_N))^T$ denotes the vector of the (additive) measurement error samples. Moreover, explicit solution of Equations 18.5 or 18.6 is often nonavailable. Thus, $\mathbf{g}(\theta)$ is obtained by numerical integration of Equations 18.5 or 18.6.

Estimates of θ can be determined by several methods. These methods can be divided into two major categories. In the so-called Fisher estimation approach, only the data vector \mathbf{z} of Equation 18.16 is supplied to the estimator in order to estimate the unknown model parameters θ . The second approach, known as the Bayes estimation approach, takes into account not only \mathbf{z} but also some statistical information that is a priori available on the unknown parameter vector θ .

18.5.1 Fisher Approach

In the Fisher approach, parameter estimates can be obtained by nonlinear least squares or maximum likelihood together with their precision, such as, a measure of a posteriori or numerical identifiability. Details and references on parameter estimation of physiological system models can be found in Carson et al. (1983) and Landaw and DiStefano (1984). Weighted nonlinear least squares is mostly used, in which an estimate $\hat{\theta}$ of the model parameter vector θ is determined as

$$\hat{\theta} = \arg \min_{\theta} [\mathbf{z} - \mathbf{g}(\theta)]^T \mathbf{W} [\mathbf{z} - \mathbf{g}(\theta)] \quad (18.17)$$

where \mathbf{W} is an $N \times N$ matrix of weights. In order to numerically solve Equation 18.17, both direct and gradient-type search methods are implemented in estimation schemes.

A correct knowledge of the error structure is needed in order to have a correct summary of the statistical properties of the estimates. This is a difficult task. Measurement errors are usually independent, and often a known distribution, for example, Gaussian, is assumed. Many properties of least squares hold, approximately, for a wide class of distributions if weights are chosen optimally, that is, equal to the inverse of the variances of the measurement errors, or at least inversely proportional to them if variances are known up to a proportionality constant, that is, \mathbf{W}^{-1} is equal or proportional to Σ_v , the $N \times N$ covariance matrix of the measurement error \mathbf{v} . Under these circumstances, an asymptotically correct approximation of the covariance matrix of the estimation error $\tilde{\theta} = \theta - \hat{\theta}$ can be used to evaluate the precision of parameter estimates:

$$\text{cov}(\tilde{\theta}) \cong \sigma^2 (\mathbf{S}^T \mathbf{W} \mathbf{S})^{-1} \quad (18.18)$$

where matrix \mathbf{S} is the $N \times p$ Jacobian matrix of $\mathbf{g}(\theta)$ calculated at $\hat{\theta}$ and σ^2 is the scale factor (possibly estimated a posteriori) such that $\Sigma_v = \sigma^2 \mathbf{W}^{-1}$. The approximation of Equation 18.18 becomes exact for a sufficiently large sample size and decreasing variances of the measurement error. If measurement errors are Gaussian, then this approximation is the Cramer–Rao lower-bound (inverse of the Fisher information matrix), that is, the optimally weighted least squares estimator is equivalent to the maximum likelihood estimator. Care must be taken in not using lower-bound variances as true parameter variances. Several factors corrupt these variances, for example, inaccurate knowledge of error structure, or a limited data set. Monte Carlo studies are needed to assess the robustness of the Cramer–Rao lower-bound in specific practical applications.

To examine the quality of model predictions to observed data, in addition to visual inspection, various statistical tests on residuals are available to check for presence of systematic misfitting, nonrandomness of the errors, and accordance with assumed experimental noise. Model order estimation, that is, number of compartments in the model, is also relevant here, and for linear compartmental models, criteria such as F-test, and those based on the parsimony principle such as the Akaike and Schwarz criteria, can be used if measurement errors are Gaussian.

18.5.2 Bayes Approach

Bayes estimators assume that the parameter vector is the realization of a random vector θ , the a priori probability distribution of which $p_\theta(\theta)$ is available, for example, from preliminary population studies. Starting from the knowledge of both the model of Equation 18.16 and the probability distribution of the noise vector \mathbf{v} , one can calculate the likelihood function $p_{z|\theta}(z|\theta)$ (i.e., the probability distribution of the measurement vector in dependence of the parameter vector). From $p_\theta(\theta)$ and $p_{z|\theta}(z|\theta)$, the a posteriori probability distribution $p_{\theta|z}(\theta|z)$ (i.e., the probability distribution of the parameter vector given the data vector) can be determined by exploiting the Bayes theorem:

$$p_{\theta|z}(\theta | \mathbf{z}) = \frac{p_{z|\theta}(\mathbf{z} | \theta)p_\theta(\theta)}{\int p_{z|\theta}(\mathbf{z} | \theta)p_\theta(\theta)d\theta} \quad (18.19)$$

From the function of Equation 18.19 several estimators can be defined. For instance, the maximum a posteriori (MAP) estimate is found by determining the value of θ , which renders $p_{\theta|z}(\theta|z)$ maximum, while the mean square (MS) estimate is defined as the expected value of θ , given the data vector:

$$\hat{\theta} = E[\theta | \mathbf{z}] = \int \theta p_{\theta|z}(\theta | \mathbf{z})d\theta \quad (18.20)$$

When \mathbf{v} and θ are uncorrelated and Gaussian, both the MS and MAP estimates are given by

$$\hat{\theta} = \arg \min_{\theta} [\mathbf{z} - \mathbf{g}(\theta)]^T \sum_{\mathbf{v}}^{-1} [\mathbf{z} - \mathbf{g}(\theta)] + [\theta - \mu_\theta]^T \sum_{\theta}^{-1} [\theta - \mu_\theta] \quad (18.21)$$

where μ_θ and Σ_θ are, respectively, the a priori expected value (size p) and covariance matrix (size $p \times p$) of vector θ . The concepts previously considered in the Fisher approach, that is, determination of a confidence interval of the parameter estimates and choice of model order, can be addressed in the Bayes approach as well. Bayes estimation can be of relevant interest, since when statistical information on the unknown parameters of the model is a priori available and exploited, a possibly significant improvement in the parameter estimates precision with respect to Fisher estimation can be obtained; see Cobelli et al. (1999) and Sparacino et al. (2000) for an example of application.

However, in most cases the handling of $p_{\theta|z}(\theta|z)$ and its integration in Equation 18.20 is analytically intractable and the sophisticated but computationally demanding numerical simulation techniques called Markov chain Monte Carlo must be used to determine Bayesian parameter estimates and their confidence intervals; see, for example, Pillonetto et al. (2002) and Magni et al. (2001) for two recent applications.

18.5.3 Population Approaches

So far, even if homogenous experimental data sets in M different individuals were available, for example, because the same input–output experiment to identify a compartmental model with a given structure was repeated in M homogenous individuals, model identification in each individual is attacked independently. In the literature, alternative parameter estimation approaches, called “population” approaches, have also been devised to identify simultaneously the M individual models starting from the ensemble of the M sets of experimental data. Both deterministic and Bayesian approaches are available (Beal and Sheiner, 1982; Steimer et al., 1984; Davidian and Giltinan, 1995; Sheiner and Wakefield, 1999; Lunn et al., 2002). Albeit complicated, both theoretically and algorithmically, they are particularly appealing when only few or particularly noisy data are available for each of the subjects under study, as it often happens in pharmacokinetic/pharmacodynamic research or epidemiological studies. In fact, thanks to the fact that “poor” individual data sets can borrow strength from the others, population parameter estimation approaches often allow for more satisfactory results achieved than standard single-subject parameter estimation approaches; see, for example, the compartmental model applications recently made in Vicini et al. (1998), Vicini and Cobelli (2001), and Bertoldo et al. (2004).

18.6 Optimal Experiment Design

At this point, one has a compartmental model structure, a description of the measurement error, and a numerical value of the parameters together with the precision with which they can be estimated. It is now appropriate to address the optimal experiment design issue. The rationale of optimal experiment design is to act on design variables such as number of test input and outputs, form of test inputs, number of samples and sampling schedule, and measurement errors so as to maximize, according to some criterion, the precision with which the compartmental model parameters can be estimated (DiStefano, 1981; Carson et al., 1983; Landaw and DiStefano, 1984; Walter and Pronzato, 1990).

In the Fisher approach, the Fisher information matrix J , which is the inverse of the lower bound of the covariance matrix, is treated as a function of the design variables and usually the determinant of J (this is called D-optimal design) is maximized in order to maximize precision of parameter estimates, and thus numerical identifiability.

The optimal design of sampling schedules, that is, the determination of the number and location of discrete-time points where samples are collected, has received much attention as it is the variable which is less constrained by the experimental situation. Theoretical and algorithmic aspects have been studied, and software is available, for both the single- and multioutput case (DiStefano, 1981; Landaw and DiStefano, 1984; Cobelli et al., 1985). Optimal sampling schedules are usually obtained in an iterative manner: one starts with the model obtained from pilot experiments and the program computes optimal sampling schedules for subsequent experimentation. An important result for single-output linear compartmental models is that D-optimal design usually consists of independent replicates at P distinct time points, where P is the number of parameters to estimate.

Optimal sampling schedule design has been shown, for example, to improve precision as compared to schedules designed by intuition or other convention and to optimize the cost effectiveness of a dynamic clinical test by reducing the number of blood samples withdrawn from a patient without significantly deteriorating their precision (Cobelli and Ruggeri, 1989; 1991).

The optimal input design problem has been relatively less studied, but some results are available on optimal equidose rectangular inputs (including the impulse) for parameter estimation in compartmental models (Cobelli and Thomaseth, 1987; 1988a, b).

In a Bayes estimation context, optimal experiment design is a more difficult task (see Walter and Pronzato, (1990) for a survey). Applications of this have thus been fewer than those with a Fisher approach, also because the numerical implementation of the theoretical results is much more demanding.

Finally, some results on optimal experiment design in a population parameter estimation context have also been recently presented (Hooker et al., 2003).

18.7 Validation

Validation involves assessing whether or not the compartmental model is adequate for its purpose. This is a difficult and highly subjective task in modeling of physiological systems, because intuition and understanding of the system play an important role. It is also difficult to formalize related issues such as model credibility, that is, the use of the model outside its established validity range. Some efforts have been made, however, to provide some formal aids for assessing the value of models of physiological systems (Carson et al., 1983; Cobelli et al., 1984a). A set of validity criteria have been explicitly defined, such as empirical, theoretical, pragmatic, and heuristic validity, and validation strategies have been outlined for two classes of models, broadly corresponding to simple and complex models. This operational classification is based on a priori identifiability and leads to clearly defined strategies as both complexity of model structure and extent of available experimental data are taken into account. For simple models, quantitative criteria based on identification, for example, a priori identifiability, precision of parameter estimates, and residual errors can be used in addition to physiological plausibility. In contrast with simple models, complex simulation models are essentially incomplete, as there will naturally be a high degree of uncertainty with respect to both structure and parameters. Therefore, validation will necessarily be based on less solid grounds. The following aids have been suggested: increasing model testability through model simplification; improved experimental design and model decomposition; adaptive fitting based on qualitative and quantitative feature comparison and time-course prediction; and model plausibility.

References

- Audoly, S., Bellu, G., D'Angio', L., Saccomani, M.P., and Cobelli, C. 2001. Global identifiability of nonlinear models of biological systems. *IEEE Trans. Biom. Eng.* 48: 55–65.
- Audoly, S., D'Angio', L., Saccomani, M.P., and Cobelli, C. 1998. Global identifiability of linear compartmental models. A computer algebra algorithm. *IEEE Trans. Biom. Eng.* 45: 36–47.
- Beal, S.L. and Sheiner, L.B. 1982. Estimating population kinetics. *Crit. Rev. Biomed. Eng.* 8: 195–222.
- Bellu, G., Saccomani, M.P., Audoly, S., and D'Angio', L. 2007. DAISY: A new software tool to test global identifiability of biological and physiological systems. *Comput. Methods Programs Biomed.* 88: 52–61.
- Bertoldo, A., Sparacino, G., and Cobelli, C. 2004. "Population" approach improves parameter estimation of kinetic models from dynamic PET data. *IEEE Trans. Med. Imag.*, 23: 297–306.
- Carson, E.R. and Cobelli, C. 2013. *Modeling Methodology for Physiology and Medicine*, 2nd Edition, Elsevier, London, UK.
- Carson, E.R., Cobelli, C., and Finkelstein, L. 1983. *The Mathematical Modelling of Metabolic and Endocrine Systems*. John Wiley & Sons, New York.
- Carson, E.R. and Jones, E.A. 1979. The use of kinetic analysis and mathematical modeling in the quantitation of metabolic pathways *in vivo*: Application to hepatic anion metabolism. *New Engl. J. Med.* 300: 1016–1027 and 1078–1986.
- Caumo, A. and Cobelli, C. 1993. Hepatic glucose production during the labelled IVGTT: Estimation by deconvolution with a new minimal model. *Am. J. Physiol.* 264: E829–E841.

- Chapman, M.J., Godfrey, K.R., Chappell, M.J., and Evans, N.D. 2003. Structural identifiability of non-linear systems using linear/non-linear splitting. *Int. J. Control.* 76: 209–216.
- Chappell, M.J. and Godfrey, K.R. 1992. Structural identifiability of the parameters of a nonlinear batch reactor model. *Math. Biosci.* 108: 245–251.
- Cobelli, C. 1984. Modeling and identification of endocrine-metabolic systems. Theoretical aspects and their importance in practice. *Math. Biosci.* 72: 263–281.
- Cobelli, C. and Carson, E.R. 2008. *Introduction to Modelling in Physiology and Medicine.* Academic Press, San Diego.
- Cobelli, C., Carson, E.R., Finkelstein, L., and Leaning, M.S. 1984a. Validation of simple and complex models in physiology and medicine. *Am. J. Physiol.* 246: R259–R266.
- Cobelli, C. and Caumo, A. 1998. Using what is accessible to measure that which is not: Necessity of model of system. *Metabolism*, 47: 1009.
- Cobelli, C., Caumo A., and Omenetto, M. 1999. Minimal model SG overestimation and SI underestimation: Improved accuracy by a Bayesian two-compartment model. *Am. J. Physiol.* 277: E481–488.
- Cobelli, C., Dalla Man, C., Sparacino, G., Magni, L., De Nicolao, G., and Kovatchev, B.P. 2009. Diabetes: Models, signals, and control. *IEEE Rev Biomed Eng* 2: 54–96.
- Cobelli, C. and DiStefano III, J.J. 1980. Parameter and structural identifiability concepts and ambiguities: A critical review and analysis. *Am. J. Physiol.* 239: R7–R24.
- Cobelli, C., Foster, D.M., and Toffolo, G. 2000. *Tracer Kinetics in Biomedical Research: From Data to Model.* Plenum Publishing Corp., New York, NY.
- Cobelli, C., Lepschy, A., and Romanin Jacur, G. 1979. Identifiability results on some constrained compartmental systems. *Math. Biosci.* 47: 173–196.
- Cobelli, C. and Ruggeri, A. 1989. Optimal design of sampling schedules for studying glucose kinetics with tracers. *Am. J. Physiol.* 257: E444–E450.
- Cobelli, C. and Ruggeri, A. 1991. A reduced sampling schedule for estimating the parameters of the glucose minimal model from a labelled IVGTT. *IEEE Trans. Biom. Eng.* 38: 1023–10218.
- Cobelli, C., Ruggeri, A., DiStefano III, J.J., and Landaw, E.M. 1985. Optimal design of multioutput sampling schedules: Software and applications to endocrine-metabolic and pharmacokinetic models. *IEEE Trans. Biom. Eng.* 32: 249–256.
- Cobelli, C. and Thomaseth, K. 1987. The minimal model of glucose disappearance: Optimal input studies. *Math. Biosci.* 83: 127–155.
- Cobelli, C. and Thomaseth, K. 1988a. On optimality of the impulse input for linear system identification. *Math. Biosci.* 89: 127–133.
- Cobelli, C. and Thomaseth, K. 1988b. Optimal equidose inputs and role of measurement error for estimating the parameters of a compartmental model of glucose kinetics from continuous-and discrete-time optimal samples. *Math. Biosci.* 89: 135–147.
- Cobelli, C. and Toffolo, G. 1987. Theoretical aspects and practical strategies for the identification of unidentifiable compartmental systems. In *Identifiability of Parametric Models*, Walter, E., Ed., Pergamon, Oxford, pp. 85–91.
- Cobelli, C., Toffolo, G., and Ferrannini, E. 1984b. A model of glucose kinetics and their control by insulin. Compartmental and noncompartmental approaches. *Math. Biosci.* 72: 291–315.
- Cobelli, C., Toffolo, G.M., Dalla Man, C., Campioni, M., Denti, P., Caumo, A., Butler, P., and Rizza, R.A. 2007. Assessment of beta-cell function in humans, simultaneously with insulin sensitivity and hepatic extraction, from intravenous and oral glucose tests. *Am J Physiol Endocrinol Metab* 293: E1–E15.
- Davidian, M. and Giltinan, D. 1995. *Nonlinear Models for Repeated Measurement Data.* Chapman and Hall, New York.
- DiStefano III, J.J. 1981. Optimized blood sampling protocols and sequential design of kinetic experiments. *Am. J. Physiol.* 9: R259–R265.

- DiStefano III, J.J. 1983. Complete parameter bounds and quasi identifiability conditions for a class of unidentifiable linear systems. *Math. Biosci.* 65: 51–68.
- Gibaldi, M. and Perrier, D. 1982. *Pharmacokinetics*. 2nd ed., Marcel Dekker, New York.
- Godfrey, K. 1983. *Compartmental Models and Their Application*. Academic Press, London.
- Hooker, A.C., Foracchia, M., Dodds, M.G., and Vicini, P. 2003. An evaluation of population D-optimal designs via pharmacokinetic simulations. *Ann. Biomed. Eng.* 31: 98–111.
- Jacquez, J.A. 1996. *Compartmental Analysis in Biology and Medicine*. 3rd ed., Biomedware, Ann Arbor, MI.
- Jacquez, J.A. and Simon, C.P. 1993. Qualitative theory of compartmental systems. *Siam. Rev.*, 35: 43–718.
- Joly-Blanchard, G. and Denis-Vidal, L. 1998. Some remarks about identifiability of controlled and uncontrolled nonlinear systems. *Automatica* 34: 1151–1152.
- Landaw, E.M. and DiStefano III, J.J. 1984. Multiexponential, multicompartmental, and noncompartmental modeling. II. Data analysis and statistical considerations. *Am. J. Physiol.* 246: R665–R677.
- Ljung, L. and Glad, T. 1994. On global identifiability for arbitrary model parametrizations. *Automatica*, 30: 265–276.
- Lunn, D.J., Best, N., Thomas, A., Wakefield, J., and Spiegelhalter, D. 2002. Bayesian analysis of population PK/PD models: General concepts and software. *J. Pharmacokinetic. Pharmacodynam.* 29: 271–307.
- Magni, P., Bellazzi, R., Nauti, A., Patrini, C., and Rindi, G. 2001. Compartmental model identification based on an empirical Bayesian approach: The case of thiamine kinetics in rats. *Med. Biol. Eng. Comput.* 39: 700–706.
- Norton, J.P. 1982. An investigation of the sources of non-uniqueness in deterministic identifiability. *Math. Biosci.* 60: 89–108.
- Ollivier, F. 1990. Le problème l'identifiabilité structurelle globale: étude théorique, méthodes effectives et bornes de complexité. Thèse de Doctorat en Science, École Polytechnique.
- Pillonetto, G., Sparacino, G., Magni, P., Bellazzi, R., and Cobelli, C. 2002. Minimal model $S(I) = 0$ problem in NIDDM subjects: Nonzero Bayesian estimates with credible confidence intervals. *Am. J. Physiol. Endocrinol. Metab.* 282: E564–E573.
- Saccomani, M.P., Audoly, S., Bellu, G., and D'Angiò, L. 2010. Testing global identifiability of biological and biomedical models with the DAISY software. *Comp. Biol. Med.* 40: 402–407.
- Saccomani, M.P., Audoly, S., and D'Angiò, L. 2003. Parameter identifiability of nonlinear systems: The role of initial conditions. *Automatica* 39: 619–632.
- Saccomani, M.P., Bonadonna, R., Bier, D.M., De Fronzo, R.A., and Cobelli, C. 1996. A model to measure insulin effects on glucose transport and phosphorylation in muscle: A three-tracer study. *Am. J. Physiol.* 33: E170–E185.
- Saccomani, M.P. and Cobelli, C. 1992. Qualitative experiment design in physiological system identification. *IEEE Contr. Syst. Mag.* 12: 18–23.
- Sheiner, L. and Wakefield, J. Population modelling in drug development. 1999. *Stat. Meth. Med. Res.* 8: 183–193.
- Sparacino, G., Tombolato, C., and Cobelli, C. 2000. Maximum-likelihood versus maximum a posteriori parameter estimation of physiological system models: The C-peptide impulse response case study. *IEEE Trans. Biom. Eng.* 47: 801–811.
- Steimer, J.L., Mallet, A., Golmard, J.L., and Boisvieux, J.F. 1984. Alternative approaches to estimation of population pharmacokinetic parameters: Comparison with the nonlinear mixed-effect model. *Drug Metab. Rev.* 15: 265–292.
- Verdière, N., Denis-Vidal, L., Joly-Blanchard, G., and Domurado, D. 2005. Identifiability and estimation of pharmacokinetic parameters for the ligands of the macrophage mannose receptor. *Int. J. Appl. Math. Comput. Sci.* 15: 4 517–526.
- Vicini, P., Barrett, P.H., Cobelli, C., Foster, D.M., and Schumitzky, A. 1998. Approaches to population kinetic analysis with application to metabolic studies. *Adv. Exp. Med. Biol.* 445: 103–113.

- Vicini, P. and Cobelli, C. 2001. The iterative two-stage population approach to IVGTT minimal modeling: Improved precision with reduced sampling. Intravenous glucose tolerance test. *Am. J. Physiol. Endocrinol. Metab.* 280: E179–E186.
- Vicini, P., Sparacino, G., Caumo, A., and Cobelli, C. 1997. Estimation of hepatic glucose release after a glucose perturbation by nonparametric stochastic deconvolution. *Comp. Meth. Progr. Biomed.* 52: 147.
- Walter, E. 1982. *Identifiability of State Space Models*. Springer-Verlag, Berlin.
- Walter, E. and Pronzato, L. 1990. Qualitative and quantitative experiment design for phenomenological models: A survey. *Automatica* 26: 195–213.

IV

Stem Cell Engineering: An Introduction

David V. Schaffer

University of California, Berkeley

- 29 Engineering the Pluripotent Stem Cell Niche for Directed Mesoderm Differentiation** *Céline L. Bauwens, Kelly A. Purpura, and Peter W. Zandstra*29-1
Introduction • Embryoid Body Differentiation: Capturing Aspects of Embryonic Development • Mesoderm Development: Similarities between the Embryo and the EB • ESC Differentiation: Strategies to Promote Mesoderm Subpopulations • Engineering the PSC Niche to Guide Mesoderm Development • Conclusion • Acknowledgments • References
- 30 Cell Mechanobiology in Regenerative Medicine: Lessons from Cancer** *Badriprasad Ananthanarayanan and Sanjay Kumar* 30-1
Introduction • Stem Cell Mechanobiology • Mechanobiology of Cell Proliferation • Mechanobiology of Cell Motility • Mechanobiology of Angiogenesis • Perspective: Three-Dimensional Material Systems for Investigating Mechanobiology • Conclusions • Acknowledgments • References
- 31 Systems-Engineering Principles in Signal Transduction and Cell-Fate Choice** *Karin J. Jensen, Anjun K. Bose, and Kevin A. Janes*31-1
Introduction • Autocrine and Paracrine Signaling in Cell-Fate Determination • Signaling Dynamics in Cell-Fate Determination • Computational Modeling of Cell-Fate Determination • Conclusions and Future Directions • References
- 32 Biomaterial Scaffolds for Human Embryonic Stem Cell Culture and Differentiation** *Stephanie Willerth and David V. Schaffer* 32-1
Introduction • Biomaterial Scaffolds for Maintaining hESCs in an Undifferentiated State • Biomaterials for Promoting hESC Differentiation into Specific Lineages • Conclusions • References
- 33 Stem Cells and Regenerative Medicine in the Nervous System** *Shelly Sakiyama-Elbert* 33-1
Stem Cell Sources • Applications • Conclusions • References

- 34 Stem Cells and Regenerative Medicine for Treating Damaged Myocardium** *Rohini Gupta, Kunal Mehtani, Kimberly R. Kam, and Kevin E. Healy*..... **34-1**
 Introduction • Natural Cells of the Myocardium • The ECM of the Myocardium • Types of Stem Cells • Direct Stem Cell Transplantation in the Clinic • Biomaterials for Transplantation of CSC • Experimental Observation of Biomaterials for Stem Cell Transplantation into the Heart • Biomaterials Used to Engineer “Heart Patch” *In Vitro* • Aligned Biomaterials for CSC • Summary • References
- 35 Stem Cells and Hematopoiesis** *Krista M. Fridley and Krishnendu Roy* **35-1**
 Introduction • Hematopoietic Development and Sources of Hematopoietic Stem Cells • The HSC Niche • Identification of HSCs • Plasticity of HSCs • Clinical Therapies with HSCs • Generation of Hematopoietic Cells in Culture • Summary • References
- 36 Synthetic Biomaterials and Stem Cells for Connective Tissue Engineering** *Ameya Phadke and Shyni Varghese* **36-1**
 Emergence of Stem Cells in Regenerative Medicine • Role of the Extracellular Microenvironment • Biomaterial-Mediated Repair of Connective Tissue • Conclusions and Future Directions • Acknowledgments • References
- 37 Derivation and Expansion of Human Pluripotent Stem Cells** *Sean P. Palecek* **37-1**
 Applications of Human Pluripotent Stem Cells • Deriving Human Embryonic Stem Cells • Deriving Induced Pluripotent Stem Cells • Characterizing Human Pluripotent Stem Cells • Expansion of Human Pluripotent Stem Cells • Large-Scale Expansion of Human Pluripotent Stem Cells • Summary • References
- 38 Bioreactors for Stem Cell Expansion and Differentiation** *Carlos A.V. Rodrigues, Tiago G. Fernandes, Maria Margarida Diogo, Cláudia Lobato da Silva, and Joaquim M.S. Cabral* **38-1**
 Introduction • Bioprocess Development and Selection • Bioreactor Configurations • Bioreactor Systems for Stem Cell Culture • Future Directions • References

Stem cells are in many ways like other cells. They proliferate, remain quiescent, apoptose, senesce, adhere, and migrate. However, they have two more properties that have been the crux of considerable biomedical attention and imagination: the capacity to self-renew or proliferate in an immature state, and the ability to differentiate into one or more specialized lineages. If these cellular talents can be sufficiently understood and controlled, they can yield insights into mechanisms of organismal development and adult homeostasis, and serve as the basis for cell replacement therapies to treat injured and diseased tissues and organs.

The field of stem cells is both mature and new. It originated with the discovery of hematopoietic stem cells by McCulloch and Till in the 1960s (Becker et al., 1963), which lie at the heart of the development of bone marrow transplant (Thomas et al., 1957) based treatments for a broad range of blood and other disorders for the past few decades. Multipotent stem cells with the capacity to differentiate into a subset of adult lineages have since been discovered in numerous additional adult tissues, including skeletal muscle (Muir et al., 1965), intestine (Troughton and Trier, 1969, Winton and Ponder, 1990), brain (Altman, 1962, Gage, 2000), and numerous others. In addition, pluripotent mouse (Evans and Kaufman, 1981) and subsequently human (Thomson et al., 1998) embryonic stem (ES) cells were derived with the capacity to differentiate into every cell of an adult organism. In addition to investigating mechanisms by which such immature cells undergo differentiation, the field has become increasingly interested in the phenomenon that mature cells can de-differentiate or be reprogrammed into an immature state. Initially, somatic cell nuclear transfer demonstrated that the genome from a differentiated mammalian cell could be reprogrammed to an embryonic state by

factors present in oocyte cytoplasm (Wilmut et al., 1997). More recently, it was shown that a differentiated mammalian cell can be induced into pluripotency through the overexpression of just four transcription factors (Takahashi and Yamanaka, 2006). Finally, just as basic advances in hematopoietic stem cell biology have occurred in parallel to clinical translation of bone marrow transplant and cord blood-based therapies, the Food and Drug Administration has recently approved clinical trials to explore the therapeutic potential of human ES cell-derived cells to treat spinal cord injury and age-related macular degeneration.

Understanding the properties and processes of stemness, differentiation, and reprogramming at a molecular level will progressively advance our knowledge of human development. In addition, learning how to control these processes will increasingly aid the translation of stem cell biology toward regenerative medicine, further building upon the clinical success of blood stem cells (Appelbaum, 2003). Alternatively, stem cells are increasingly being utilized as the basis for high-throughput drug discovery and toxicology screens to enhance the therapeutic potential of traditional pharmaceuticals. However, in general, clinical translation does face a number of challenges. While the potential of many stem cell classes to differentiate into one or more lineages is recognized, their proliferation and differentiation must be more precisely controlled to both maximize the production of therapeutically relevant cells, and for cell replacement therapies minimize contamination with residual cells that can give rise to tumors or other side effects. Furthermore, the continued development of robust processes to scale up the production of desired cells in high yield and purity is required. Finally, engrafting the resulting differentiated in vivo typically results in extremely low viability, so better means to enhance their functional integration into the target tissue must be developed.

How can engineers make contributions to address these challenges? This section of the *CRC Handbook of Biomedical Engineering* provides a broad view of engineering efforts in a number of these areas. For example, the analysis or reverse engineering of complex systems can yield an understanding of how complex behaviors arise from the collective interactions of numerous interacting parts. In the field of stem cells, such complex systems occur both outside and inside the cell. Specifically, in both developing embryos and adult tissues, stem cells reside within highly complex microenvironments or niches in which they are continuously exposed to signals including small molecules, soluble proteins, extracellular matrix proteins and proteoglycans, proteins immobilized to the extracellular matrix, signals immobilized on the surface of adjacent cells, and mechanical properties of the tissue. Controlling stem cell expansion and differentiation, either in vitro or in vivo, requires a precise understanding of these complex, interacting cues.

In Chapter 30, Bauwens et al. describe the temporal evolution of cell differentiation state and overall tissue structure in the early developing embryo, as well as some parallels with ES cell differentiation within embryoid bodies. Furthermore, they present the biochemical and biophysical signals that guide this process, and that can be harnessed to differentiate an ES cell into a therapeutically valuable cell type such as a cardiomyocyte. It is well recognized within the stem cell biology field that biochemical signals such as growth factors, morphogens, and cytokines regulate stem cell fate and function, but it is becoming increasingly appreciated that biophysical cues can also play key roles (Keung et al., 2010). In Chapter 30, Ananthanarayanan and Kumar discuss how mechanical cues regulate cellular processes such as proliferation and migration, as well as highlight parallels for how what has been learned about the mechanobiology of tumors can be applied to stem cells.

A stem cell residing within such complex repertoires of biochemical and biophysical signals must sense this extracellular regulatory information, though the activation of receptors on the surface and interior of cells, process these signals via the activation of complex signal transduction networks, and thereby transform inputs into outputs or fate decisions. These signal transduction processes are dense and highly interconnected, and individual molecular interactions within them are often nonlinear in nature. Janes and colleagues have made considerable advances in developing data-driven modeling approaches to elucidate key features of signal transduction processes that in general drive fate choices (Janes et al., 2006, Janes and Lauffenburger, 2006), and in Chapter 31, Jensen et al. describe how these

methods and principles can be applied to understand cellular signal processing events that drive stem cell fate decisions.

In addition to the analysis of complex systems, engineers are versed in applying basic information toward the synthesis or forward engineering of approaches to control the behavior of such systems. For example, the broadest activities of engineers in this field have been focused on applying the advances in biomaterials development over the past several decades to better control stem cell behavior. In Chapter 32, Willerth and Schaffer describe recent efforts to develop culture systems that can support the indefinite expansion of human ES cells, potentially by emulating the microenvironment that pluripotent cells experience during their brief window of existence in early embryogenesis. Advances by the scientific community in general over the past decade have led to increasingly defined culture systems for growing human ES cells, starting from co-culture with feeder cells in the presence of serum to growth on synthetic substrates in defined medium. In general, such better-defined systems enhance the reproducibility, safety, and scalability of stem cell culture as the field moves toward the clinic.

In parallel with progress on expanding immature pluripotent stem cells, systems to support their differentiation into therapeutically valuable lineages must be developed. Within Chapter 33, Sakiyama-Elbert describes a number of important considerations in the application of stem cell therapies to the central nervous system, including cell sources, disease and injury targets, and practical issues associated with cell differentiation and implantation. In Chapter 34, Gupta provides an in-depth analysis of the design of stem cell-based cardiac therapies, including sources of resident and exogenous cells, as well as natural and synthetic biomaterials for the differentiation and importantly for the implantation of cells to enhance their viability and engraftment.

Fridley and Roy (Chapter 35) provide a strong overview of the best characterized of stem and progenitor cells, those of the hematopoietic system. This chapter highlights recent advances in the understanding of the cellular and molecular composition of the hematopoietic stem cell niche, as well as approaches to build upon this basic information to direct stem cell differentiation into blood cell lineages. Moreover, in Chapter 36, Padkhe and Varghese provide deep insights into the development of advanced materials that can interface with stem cells for the repair of connective tissues, including bone, cartilage, tendons, and ligaments.

Furthermore, numerous stem cell applications will require large numbers of cells, requiring the continuing development of scalable technologies for cell expansion and differentiation. Palecek (Chapter 37) reviews considerable advances in the derivation and characterization of human pluripotent stem cells, as well as the development of bioreactors and culture systems for their large-scale expansion. Furthermore, in Chapter 38, Rodrigues and colleagues provide a strong overview of numerous classes of bioreactor systems for cell expansion and differentiation, as well as principles for their implementation to a number of multipotent and ES cell types.

In addition to highlighting many recent advances, these articles describe the need for future work. The progressive identification of key biochemical and biophysical regulatory signals will benefit basic stem cell and developmental biology, as well as regenerative medicine, and the application of quantitative approaches will deepen our understanding of intracellular mechanisms that govern cellular decisions. In parallel, the application of this basic information will aid the development of bioactive materials and ideally synthetic microenvironments to control and aid cell expansion, differentiation, and implantation. Furthermore, these engineered culture systems will increasingly become integrated into large-scale culture systems as stem cells progressively move toward the clinic. The growing recognition of stem cells as an important and exciting field will continue to draw investigators with diverse backgrounds—from biology, engineering, and the physical sciences—and thereby enable further progress in these and other new directions.

References

- Altman, J. 1962. Are new neurons formed in the brains of adult mammals? *Science*, 135, 1127–1128.
- Appelbaum, F. R. 2003. The current status of hematopoietic cell transplantation. *Ann Rev Med*, 54, 491–512.
- Becker, A. J., McCulloch, E. A., and Till, J. E. 1963. Cytological demonstration of the clonal nature of spleen colonies derived from transplanted mouse marrow cells. *Nature*, 197, 452–454.
- Evans, M. J. and Kaufman, M. H. 1981. Establishment in culture of pluripotential cells from mouse embryos. *Nature*, 292, 154–156.
- Gage, F. H. 2000. Mammalian neural stem cells. *Science*, 287, 1433–1438.
- Janes, K. A., Gaudet, S., Albeck, J. G., Nielsen, U. B., Lauffenburger, D. A., and Sorger, P. K. 2006. The response of human epithelial cells to TNF involves an inducible autocrine cascade. *Cell*, 124, 1225–1239.
- Janes, K. A. and Lauffenburger, D. A. 2006. A biological approach to computational models of proteomic networks. *Curr Opin Chem Biol*, 10, 73–80.
- Keung, A. J., Kumar, S., and Schaffer, D. V. 2010. Presentation counts: microenvironmental regulation of stem cells by biophysical and material cues. *Annu Rev Cell Dev Biol*, 26, 533–556.
- Muir, A. R., Kanji, A. H., and Allbrook, D. 1965. The structure of the satellite cells in skeletal muscle. *J Anat*, 99, 435–444.
- Takahashi, K. and Yamanaka, S. 2006. Induction of pluripotent stem cells from mouse embryonic and adult fibroblast cultures by defined factors. *Cell*, 126, 663–676.
- Thomas, E. D., Lochte, H. L., Lu, W. C., and Ferrebee, J. W. 1957. Intravenous infusion of bone marrow in patients receiving radiation and chemotherapy. *New Engl Econ Rev*, 257, 491–496.
- Thomson, J. A., Itskovitz-Eldor, J., Shapiro, S. S., Waknitz, M. A., Swiergiel, J. J., Marshall, V. S., and Jones, J. M. 1998. Embryonic stem cell lines derived from human blastocysts. *Science*, 282, 1145–1147.
- Troughton, W. D. and Trier, J. S. 1969. Paneth and goblet cell renewal in mouse duodenal crypts. *J Cell Biol*, 41, 251–268.
- Wilmut, I., Schnieke, A. E., McWhir, J., Kind, A. J., and Campbell, K. H. 1997. Viable offspring derived from fetal and adult mammalian cells. *Nature*, 385, 810–813.
- Winton, D. J. and Ponder, B. A. 1990. Stem-cell organization in mouse small intestine. *Proc R Soc Lond B Biol Sci*, 241, 13–18.

30

Cell Mechanobiology in Regenerative Medicine: Lessons from Cancer

Badriprasad
Ananthanarayanan
*University of California,
Berkeley*

Sanjay Kumar
*University of California,
Berkeley*

30.1	Introduction	30-1
30.2	Stem Cell Mechanobiology	30-3
30.3	Mechanobiology of Cell Proliferation	30-4
30.4	Mechanobiology of Cell Motility	30-7
30.5	Mechanobiology of Angiogenesis	30-8
30.6	Perspective: Three-Dimensional Material Systems for Investigating Mechanobiology	30-9
30.7	Conclusions.....	30-10
	Acknowledgments.....	30-10
	References.....	30-10

30.1 Introduction

The stem cell “niche” refers to the collective set of cell-extrinsic inputs that controls the functions of stem cells *in vivo*.^{1,2} The key regulatory mechanisms within the niche include presentation of soluble and immobilized molecules such as growth factors and cytokines, direct interactions with other cells (e.g., stromal cells), and adhesion to the extracellular matrix (ECM). These diverse inputs are regulated and integrated in a temporally and spatially dynamic fashion to control self-renewal and differentiation, the two hallmark properties of stem cells. Traditionally, the field has approached this subject from a paradigm that is largely biochemical in nature, focusing on the regulatory roles of soluble and membrane-bound ligands on stem cell behavior. While it is clear that these inputs are indeed important, it is also increasingly being recognized that mechanical and other types of biophysical interactions between cells with their extracellular milieu can profoundly influence stem cell behavior. This idea is an extension of a broader awareness that many cell types can sense and apply forces to their surroundings,³ and that the mechanical interactions of cells with their environment are critical regulators of function in physiology and disease, a concept now widely referred to as “cellular mechanobiology.”^{4,5} Early efforts in this area have demonstrated that, similar to other cell types in tissue, stem cells are also influenced by mechanical forces and that biophysical signaling can control stem cell self-renewal and differentiation.^{6–8} These effects are mediated by intracellular signaling pathways that transduce force cues into biochemical signals that in turn drive fundamental cellular processes such as cell adhesion, motility, proliferation, and differentiation.^{9,10}

Despite the growing interest in the mechanobiology of stem cells, our understanding of how these effects may be incorporated into a broader understanding of stem cell biology or leveraged to enhance stem cell-based therapies remains very limited. In addition, the mechanistic details of force transduction

processes in stem cells are still incompletely understood. By contrast, there is a comparatively more advanced literature on the effects of mechanical signaling on a variety of other non-stem cells. In particular, it is now well accepted that dysfunctional interactions between cells and their ECM play a significant role in the initiation and progression of some solid tumors,^{11,12} and that mechanical forces can influence malignant transformation, migration, and proliferation of cancer cells in culture.^{13,14} Several recent studies have illuminated the role of mechanical signaling from native and engineered ECMs in the initiation and spread of cancer, such as malignant transformation,^{15,16} migration,¹⁷ and proliferation.¹⁸ Indeed, it is possible to conceptualize the various stages in the progression of cancer in the form of a “force journey” in which mechanical interactions with the environment influence cellular behavior in concert with genetic and epigenetic cues.¹³ This raises the possibility that one might draw upon an understanding of tumor cell mechanobiology to formulate instructive analogies to stem cell mechanobiology, and that this in turn might offer important clues about mechanisms and therapeutic applications.

While the biology of cancer and that of stem cells may appear at first sight to be unrelated, there are in fact several important similarities (Figure 30.1). First, many of the molecular mechanisms known to process force cues are not unique to tumor cells and indeed are critical to the function of many normal cell types, including stem and progenitor cells. These include integrin-mediated adhesion to the ECM, establishment and stabilization of cell structure by the cytoskeleton, generation of cell–ECM tractional forces by actomyosin complexes, and regulation of cytoskeletal assembly and mechanics by Rho-family GTPases.^{10,19} Second, many of the processes that contribute to tumor growth, such as cell motility, ECM remodeling, and assembly of angiogenic vessels, are often critical to the success of tissue engineering and regenerative medicine strategies.⁸⁰ Finally, the hallmark ability of stem cells to undergo either self-renewal or differentiation bears direct mechanistic relevance to tumors inasmuch as tumor

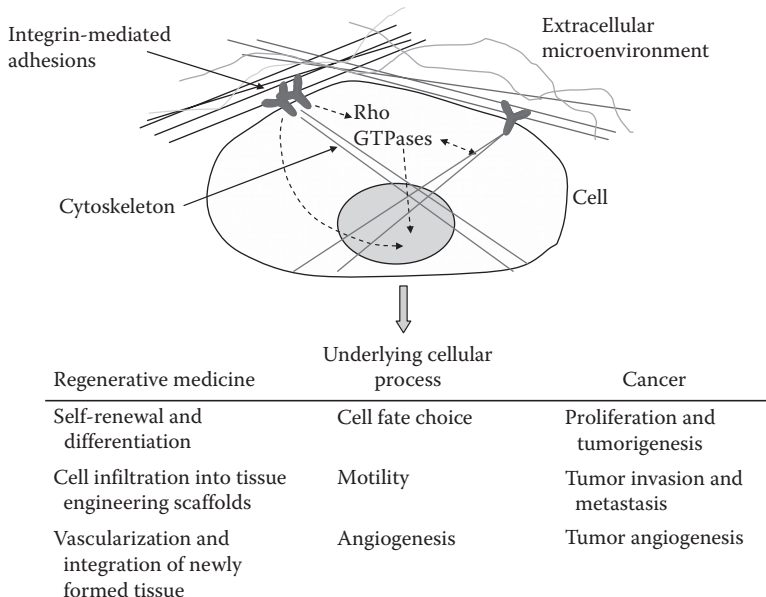


FIGURE 30.1 Similarities between cell–ECM mechanobiology of stem cells and cancer. A cell in its native microenvironment receives biophysical and biochemical inputs through integrin-mediated adhesions, initiating signaling cascades that direct the architecture and dynamics of the cellular cytoskeleton and in turn influence cellular contractility and force generation. These reciprocal relationships ultimately result in transcriptional programs effected by proteins such as the Rho family GTPases, thereby governing cell fate, motility, and angiogenesis. These fundamental cellular processes underlie phenomena of interest in regenerative medicine as well as in cancer.

growth frequently reflects profound dysregulation of cell-cycle progression, proliferation, differentiation, and death. This analogy has recently been articulated in a more literal way through the discovery of a privileged population of “cancer stem cells” within certain tumors, which often bear striking similarities to endogenous tissue stem cells.^{20–24} The cancer stem cell concept argues that a subpopulation of cells within the tumor mass is largely responsible for sustaining tumor growth through continuous self-renewal, and that this process may be arrested if these cells can be directed toward an alternative fate choice (e.g., death or differentiation).

In this chapter, we seek to explore mechanistic and functional connections between tumor cell mechanobiology and stem cell mechanobiology, with the goal of using the former to guide understanding of the latter. We begin with a brief overview of the mechanobiology of stem cells and the molecular mechanisms that mediate the effects of mechanical signaling. We then focus on the mechanobiology of three critical cellular processes that have historically been investigated in the context of cancer but are equally applicable to stem cell biology: proliferation, motility, and angiogenesis. Finally, we offer a perspective on biomaterial systems that can enable investigation of stem cell and cancer mechanobiology in three-dimensional (3D) topologies, which are an important feature of many native tissue environments and are increasingly recognized to be critical to *in vivo* cell behavior.

30.2 Stem Cell Mechanobiology

Mammalian tissues exhibit a wide range of mechanical properties, ranging from soft tissues such as brain and fat to hard tissue such as cartilage and bone. In fact, there are often significant mechanical heterogeneities within a single tissue, as observed within the hippocampus of the brain.²⁵ The presence of these mechanical heterogeneities within the *in vivo* niche begs the question of whether they give rise to signals that can directly or indirectly modulate stem cell behavior, and this has recently begun to be addressed with the use of culture systems based on natural or synthetic polymeric matrices.^{26–28} These material systems can be engineered to exhibit a wide range of elastic moduli, in contrast to traditionally used glass or plastic surfaces which are many orders of magnitude stiffer than most physiological tissues.

Several excellent reviews have covered the effects of mechanical signaling on stem cell fate,^{6–8} so we will limit our focus to a few particularly illustrative examples. Dynamic mechanical loading is widely observed for mature tissues in the musculoskeletal system and vasculature, but has also been observed to be important in the early stages of development.²⁹ For example, application of force to the *Drosophila* embryo induces expression of *twist*, a gene central to the regulation of germ-layer formation and patterning.³⁰ Similarly, tensile forces in the cell cortex can promote the sorting of progenitor cells and organization of germ layers in the gastrulating zebrafish embryo.³¹ At the cellular level, direct force application promotes myogenesis over adipogenesis in lung embryonic mesenchymal stem cells (MSCs),³² down-regulates pluripotency markers in mouse embryonic stem cells (mESCs),³³ and inhibits differentiation of human embryonic stem cells (hESCs).³⁴ Similarly, forces associated with shear flow, which have long been understood to be critical for the normal function of vascular endothelial and smooth muscle cells, are now recognized to also control the differentiation of stem cells into cardiovascular lineages³⁵ and the development of hematopoietic stem cells.^{36,37}

The mechanical properties of the microenvironment have been shown to affect stem cell differentiation in dramatic ways even in the absence of directly applied forces. For example, when MSCs are shape-constrained through the use of micropatterned ECM islands and cultured in media permissive of multiple lineages, cells forced to adopt rounded shapes preferentially undergo adipogenesis, whereas cells allowed to spread more fully preferentially undergo osteogenesis.³⁸ Further, when MSCs are cultured on ECMs of varying stiffness under similar permissive media conditions, softer substrates (0.1–1 kPa) induce neurogenic differentiation, stiffer (8–17 kPa) substrates promote muscle formation, while the stiffest (25–40 kPa) substrates produce bone cells.³⁹ In other words, MSCs appear to differentiate into tissue types whose stiffness approximates that of the underlying ECM. In both cases, inhibition of actomyosin contractility abrogates ECM stiffness-dependent differences in MSC

differentiation. More recently, ECM stiffness has been shown to regulate the proliferation of MSCs, with softer substrates inducing a quiescent state but not compromising the ability of cells to resume proliferation when transferred to stiff ECMs or to differentiate when treated with the appropriate factors.⁴⁰ Mechanosensitivity of stem cell differentiation has also been reported for tissues commonly regarded as protected from large external forces, such as the brain. For example, neural stem cells (NSCs) from the adult rat hippocampus differentiate optimally into neurons on soft substrates (~10 Pa), with stiffer substrates (~10 kPa) increasing glial differentiation.⁴¹ This trend has subsequently been observed for hippocampal NSCs encapsulated in 3D alginate scaffolds⁴² and for NSCs derived from other regions of the central nervous system,^{43,44} although the precise relationship appears to depend on the tissue and the species source and the ECM ligand.

While the mechanistic details of the above effects remain to be completely elucidated, a large number of proteins and protein complexes have been implicated in the processing of force signals. The primary force sensors are often located in the plasma membrane—for example, G-protein-coupled receptors,⁴⁵ ion channels,^{46,47} and integrins.⁴⁸ Indeed, the mechanosensitive growth and maturation of focal adhesions into structured complexes that contain a variety of cytoskeletal and signaling proteins represents one of the most important and well-studied ECM-mediated signaling pathways.^{19,49,50} Another important class of proteins is the Rho family of GTPases, whose canonical members Rho, Rac, and Cdc42 serve as key control points for cytoskeletal assembly and dynamics.^{51–53} These pathways directly influence the extent and nature of cell-generated forces, in part by regulating the assembly of actin stress fibers and bundles as well as the phosphorylation of nonmuscle myosin motor proteins that drive contraction of these structures.⁵⁴ Rho family proteins and actomyosin contractility have also been shown to mediate the mechanosensitive differentiation of MSCs and NSCs.^{38,39,128} Together, these mechanosensitive pathways may contribute to the regulation of gene expression via transcription factors⁵⁵ as well as other indirect or epigenetic pathways⁵⁶ to direct, restrict, or impose selective pressure on stem cell fate choices.

30.3 Mechanobiology of Cell Proliferation

Self-renewal, the process by which a cell divides to generate daughter cells with developmental potentials that are indistinguishable from those of the mother cell, is one of the hallmark features of stem cells.⁵⁷ In other words, self-renewal involves mobilization of processes that promote proliferation concurrent with inhibition of differentiation into a less proliferative or terminally differentiated cell type. The factors that affect self-renewal of stem cells from different tissues and at different stages of development continue to be elucidated.⁵⁸ However, it is clearly recognized that the niche plays a central role in the maintenance of stem cells *in vivo*. It has been suggested that the subversion of these normal maintenance signals from the niche is one of the mechanisms through which cancer stem cells gain unlimited proliferative capacities.⁵⁹ Indeed, many of the signaling networks that are known to be essential for the self-renewal of stem cells, including the Notch, Wnt, and Hedgehog pathways, were originally identified as oncogenes based on their role in tumor formation.^{60,61} This intimate connection between stemness and the proliferative properties of cancer raises the possibility that mechanisms identified as oncogenic in cancer might also facilitate stem cell self-renewal. Before exploring commonalities in signaling between the mechanobiology of tumor cell proliferation and the mechanobiology of stem cell self-renewal, we will discuss potential mechanisms that may underlie the mechanosensitivity of stem cell self-renewal.

There is evidence that some of the pathways that regulate self-renewal are sensitive to mechanical forces. The Wnt pathway is known to be important for the physiological adaptation of bone mass and structure to mechanical loading.⁶² Both pulsatile fluid flow⁶³ and mechanical strain⁶⁴ have been shown to activate the Wnt/ β -catenin pathway in bone cells, which results in nuclear translocation of β -catenin and increased proliferation. This pathway has also been implicated in tumorigenesis⁶⁵ and in controlling self-renewal of stem cells.⁶⁶ Similarly, mechanical forces have been shown to induce the expression of proteins of the Hedgehog family in smooth muscle cells⁶⁷ and chondrocytes.⁶⁸ The mechanosensitivity of these pathways has not yet been explored in the context of stem cell self-renewal.

There is a significant body of evidence supporting the role of mechanical forces in controlling proliferation, and it is becoming clear that several of these effects are communicated through cell–matrix focal adhesions. As we described earlier, these structures serve as organizing centers for both mechanotransductive and mitogenic signaling elements and grow and mature upon application of force. For example, focal adhesion kinase (FAK),⁶⁹ extracellular-signal-regulated kinase (ERK), and kinases of the Src family strongly promote proliferation and are all known to localize to focal adhesions.⁴⁹ Further, the Rho GTPases, previously mentioned for their role in organizing the cellular cytoskeleton, also play a direct role in controlling cell-cycle progression.^{53,70,71} The effect of mechanical signaling on cell-cycle control was tested directly in a recent study in which cells from various tissues were cultured on variable-stiffness ECMs.⁷² Compliant ECMs that mimic physiological tissue stiffness inhibited progression through the cell cycle (Figure 30.2), but highly stiff ECMs that mimic the stiffening associated with pathological matrix remodeling accelerated cell-cycle progression through various mechanisms including a FAK-Rac-cyclin D1 pathway. Rho GTPases have been shown to mediate the mechanosensitivity of mesenchymal stem cell differentiation in response to matrix elasticity³⁹ and cell shape.³⁸ Thus, mechanosensitive pathways known to be important in cancer and other cells may have direct roles in establishing self-renewal or directing differentiation.

Seminal work by Bissell and colleagues established that the tumor microenvironment plays a critical role in the formation and spread of tumors.^{11,12,73} Later, Wang and colleagues showed that the stiffness of the ECM regulates the proliferative ability of normal cells, but that malignant transformation decreases this sensitivity to ECM mechanics, possibly allowing for anchorage-independent and uncontrolled proliferation.⁷⁴ This observation is reminiscent of the classical soft agar assay, in which cells are judged to be successfully transformed if they develop an ability to proliferate on soft, nonadhesive ECMs. The hypothesis that mechanics can mediate malignant transformation was tested directly in a landmark

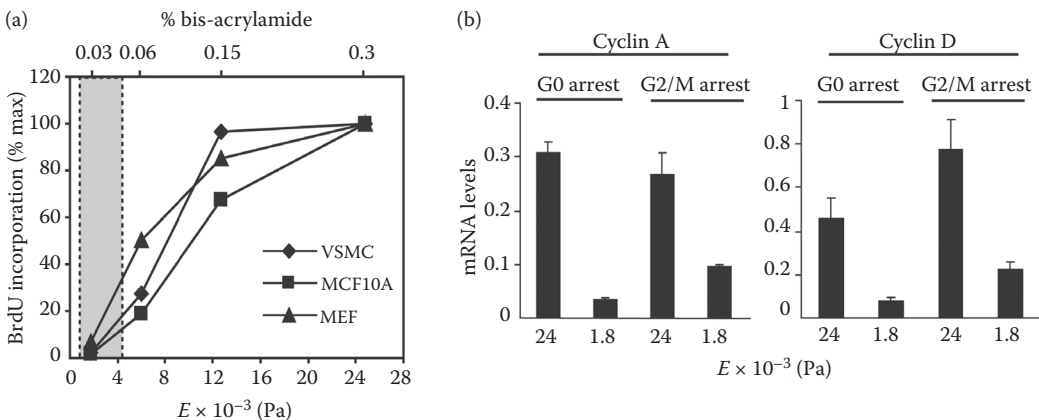


FIGURE 30.2 Mechanobiological control of cell-cycle progression. In this study, the effect of substrate stiffness on cell-cycle progression was assessed in mouse embryonic fibroblasts (MEFs), vascular smooth muscle cells (VSMCs), and MCF10A mammary epithelial cells. (a) Effect of substrate stiffness on cell proliferation. Increasing substrate stiffness results in a greater fraction of BrdU-positive cells for all cell types upon stimulation with mitogens. The shaded area highlights the range of elastic moduli measured in mouse mammary glands and arteries (data not shown). (b) Effect of substrate stiffness on expression of cell-cycle checkpoint genes. MEFs were synchronized at G0 (by 48 h serum starvation) or at G2/M (by treatment with 5 mg/mL nocodazole for 24 h) and then reseeded on hydrogels of varying stiffness and stimulated with 10% fetal bovine serum (FBS). Induction of cyclin A and cyclin D1 expression depended strongly on matrix stiffness regardless of whether cells entered G1 phase from G0 or G2/M, with higher stiffness substrates promoting increased cell-cycle progression. (Reproduced with permission from Klein, E.A. et al. *Current Biology* 2009, 19(18), 1511–1518.)

study by Weaver and colleagues, who showed that culturing nontumorigenic mammary epithelial cells on ECMs of tumor-like stiffness induces dysplasia, proliferation, and activation of oncogenic signaling pathways.¹⁶ The recent finding that breast tumorigenesis is accompanied by crosslinking and stiffening of the collagenous matrix even in premalignant tissue verifies that this phenomenon is relevant to tumorigenesis *in vivo*. These effects are mediated by increased signaling through integrins and focal adhesions, and may be suppressed by the inhibition of lysyl oxidase (LOX).¹⁵ A complementary set of studies with breast epithelial tumor cells in 3D collagen matrices has also elucidated the role of FAK, ERK, and Rho in the promotion of a proliferative and invasive phenotype in response to increased collagen density.^{75,76} Our laboratory recently tested the link between ECM stiffness and the pathophysiology of malignant brain tumors *in vitro*.¹⁸ When we cultured human glioblastoma multiforme (GBM) cells on

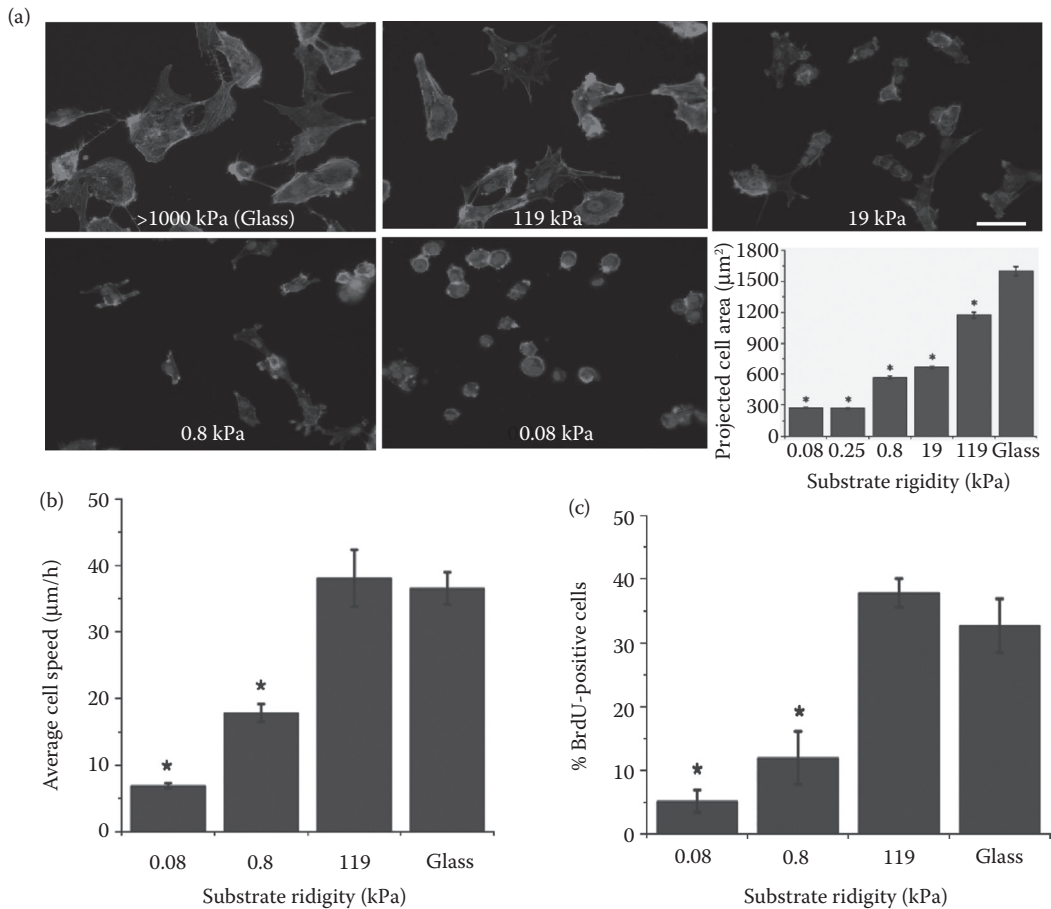


FIGURE 30.3 Mechanobiological control of glioma cell behavior. The effect of mechanics on the morphology, motility, and proliferation of U373 MG glioblastoma multiforme tumor cells was assessed by plating cells on variable-stiffness polyacrylamide substrates coated with fibronectin. (a) Effect on cell morphology and adhesion. Cell morphology shows a steep dependence on substrate stiffness, with cells spreading extensively and forming well-defined focal adhesions and stress fibers on glass or stiff substrates, but not on softer substrates. Immunofluorescence images depict nuclear DNA (blue), F-actin (green), and the proliferation marker Ki67 (red). (b) Effect on motility. Increasing substrate stiffness increases the speed of random cell migration. (c) Effect on proliferation. Substrate stiffness also influences proliferation, with a greater fraction of BrdU-positive cells seen on stiffer substrates. (Reproduced with permission from Ulrich, T.A. et al. *Cancer Research* 2009, 69(10), 4167–4174.)

variable-stiffness ECMs coated with fibronectin, we found that ECM stiffness strongly regulates cellular morphology, motility, and proliferation (Figure 30.3). Increasing ECM stiffness resulted in a higher fraction of dividing cells, as determined by bromodeoxyuridine (BrdU) incorporation. Thus, proliferative signals generated by mechanosensitive pathways have been shown to influence the formation and progression of cancer, and bear investigation in the context of stem cell self-renewal. Mechanoregulation of self-renewal is important not just in niche-mediated maintenance of adult stem cell populations, but also for engineering stem cell therapies where control of cell fate is essential.

30.4 Mechanobiology of Cell Motility

Cell motility is a fundamental process that contributes to development, tissue homeostasis, wound healing, and a wide variety of pathological processes.^{77,78} In embryonic development, movements of single cells and multicellular sheets contribute to segregation and patterning and establish the highly specified architecture of developing tissues.⁷⁷ Migration of progenitor cell populations is essential in tissues that undergo continuous regeneration during adult life such as the skin, intestinal epithelia, and the brain, where large-scale movements of neural progenitors along defined paths are observed.⁷⁸ Further, cell migration is essential during all phases of tissue repair and regeneration, including recruitment of leukocytes as part of the inflammatory response, reentry of cells into the wound area, and revascularization of the tissue.⁷⁹ Similarly, cell migration is essential for the success of regenerative therapies such as scaffold-based tissue engineering.^{27,80} Indeed, cell infiltration into the scaffold has long been recognized as an important consideration in the design of tissue engineering scaffolds. This has spurred a significant interest in optimizing pore size within scaffolds, for example, for bone tissue engineering,⁸¹ to allow sufficient cell penetration without compromising bulk mechanical properties. Similarly, significant efforts have been devoted to the development of synthetic matrices that can be proteolytically degraded by migrating cells.^{82–84} Despite these advances in scaffold engineering, the field could benefit from a greater understanding of the mechanisms that govern cell motility in synthetic ECMs to efficiently design tissue engineering scaffolds for regenerative medicine.

Cell migration on two-dimensional (2D) substrates has been described as a physically integrated molecular process in which the cell undergoes cycles consisting of morphological polarization and membrane extension, attachment at the leading edge, contraction of the cell body, and finally detachment of the trailing edge.⁸⁵ In this mode of motility, known as mesenchymal motility, the cell must be able to physically exert force on the substratum through cell–matrix adhesions. This depends not only on the strength of these adhesions⁸⁶ but also on the mechanical compliance of the substrate, which determines the response to cell-applied forces. It has now been clearly established that the migration speed of a variety of cell types depends on the elasticity of the underlying substrate.^{87–89} For example, we recently showed that the average speed of random migration of glioma cells significantly increases when the matrix stiffness is increased (Figure 30.3).¹⁸ This trend was also observed for glioma cells cultured on variable-stiffness hydrogels composed of hyaluronic acid, thereby extending our previous observations to a brain-mimetic ECM platform.¹²⁹ Inhibition of nonmuscle myosin II-based contractility ablates this stiffness sensitivity and rescues motility on soft substrates, indicating a tight balance between protrusive and contractile forces within cells. The phenomenon of “durotaxis” describes cell motion in response to variations in substrate stiffness, with many cell types displaying a trend to migrate toward stiffer regions.^{90,91} Therefore, engineering the mechanical properties of the matrix may enable better infiltration of stem cells into scaffolds for tissue engineering applications.

Several novel insights into the mechanisms of cell migration have been deduced from recent studies on tumor invasion and metastasis.^{92,93} Perhaps the most intriguing of these is the recognition that tumor cells can exhibit several different modes of motility, differing not only in their average speeds but also in their requirement for cell–ECM adhesions, contractile force generation, and ECM remodeling via proteolysis. As tumor cells invade the surrounding matrix, they often exhibit mesenchymal motility, which is typically accompanied by pericellular proteolysis by secreted and membrane-associated enzymes such

as matrix metalloproteases (MMPs). These enzymes can degrade the surrounding matrix to clear steric barriers against migration. However, in the absence of proteolytic abilities, or when proteolysis is specifically blocked by pharmacological agents, tumor cells have been observed to switch to an “amoeboid” form of motility in which cells depend primarily on contractile forces generated by the actomyosin cytoskeleton to extrude themselves through existing pores and channels in the ECM.^{94–96} Amoeboid motility is often viewed as independent of protease activity and the strength of cell–matrix adhesions, permitting tumor cells to escape strategies directed against mesenchymal motility. These findings have obvious clinical relevance in therapies targeting cancer metastasis, but they are also relevant for tissue engineering. The exact nature of stem cell motility in tissue engineering scaffolds will dictate whether strong cell–ECM adhesions are required, or whether degradability by cellular proteases is an important design requirement. Further investigation of these questions should facilitate the formulation of more precise strategies for engineering stem cell behavior in synthetic scaffolds.

30.5 Mechanobiology of Angiogenesis

Vascularization is crucial for the viability of engineered tissue replacements.⁹⁷ The therapeutic potential of stem cells in medicine hinges on the ability to generate functional replacements of diseased cell types in the body; however, the efficacy of any stem cell-based therapy will ultimately depend on the extent of vascularization, innervation, and functional integration of the newly formed tissue. Since oxygen and nutrient supply and waste removal depend critically on the vasculature,⁹⁸ angiogenesis represents an important step in the success of regenerative therapies using stem cells. It is not surprising, therefore, that a significant amount of work in the development of scaffolds for tissue engineering has been focused on the controlled delivery of growth factors that promote angiogenesis.^{27,99,100} Although soluble signaling via growth factors from the vascular-endothelial growth factor (VEGF)¹⁰¹ and angiopoietin¹⁰² families represent the primary mechanisms governing angiogenesis in mammalian tissue, it has also been recognized that solid-state biochemical and physical signals from the ECM play an important role.^{103,104}

Angiogenesis is also clearly an important step in the progression of cancer.^{105,106} As a tumor grows and spreads, it outstrips the capacity of diffusion to supply the oxygen and nutrients needed for continued proliferation and expansion. Some tumors acquire the ability to circumvent this limitation by directing the host vasculature to extend new blood vessels. This “angiogenic switch” has received increasing attention in recent years as a potential point for therapeutic intervention to limit the growth of tumors. Indeed, antiangiogenic interventions such as a monoclonal antibody against VEGF (e.g., bevacizumab, commercially marketed as Avastin) have shown clinical success in the treatment of colorectal cancer in combination with chemotherapy.¹⁰⁷ These successes have spurred interest in the diverse mechanisms that promote angiogenesis, including the role played by ECM-mediated mechanical signaling.¹⁰⁴

Initial work in the mechanobiology of angiogenesis concerned the effects of mechanical signaling on the growth of endothelial cells. For example, it was found that fibronectin density governs cell shape and cell fate, directing proliferation when cells are spread on high fibronectin density substrates, but triggering apoptosis on rounded cells on low-density substrates.¹⁰⁸ The connection between cell shape and cell fate was established conclusively in a landmark study by Ingber, Whitesides, and colleagues, who used microcontact-printed fibronectin ECMs to control cell shape independently of matrix density and soluble factors, and showed that cell shape can independently drive proliferation, differentiation, and death.¹⁰⁹ Further work has focused on the development of microvasculature, such as the formation and structure of capillary networks, as a function of ECM density and stiffness. For example, it has been shown that the density of the collagenous matrix in which endothelial cells are cultured influences their ability to form branched capillaries with small lumens, resembling those found *in vivo*.¹¹⁰ Similarly, the density of fibrin matrix surrounding endothelial cells cultured on beads has been shown to govern the extent of capillary network formation.¹¹¹ Both these results implicate cellular force generation due to actomyosin contractility as an important process through which cells sense and respond to mechanical forces in their environment. In addition to these angiogenic effects, mechanical signaling

is also known to be important in force-dependent neovascularization via enlargement and elongation of existing blood vessels. For example, in an *in vivo* model of wound healing, neovascularization was found to depend on the ability of cells to stress and contract the collagenous matrix.¹¹²

Mechanistically, the transduction of mechanical force into angiogenic signals is known to partly follow the canonical routes of force transduction outlined previously, including the generation of cytoskeletal tension through the actomyosin apparatus and the activity of GTPases such as Rho.¹¹³ In addition, it has recently been discovered that there may be direct crosstalk between force-mediated signaling and the classical VEGF signaling pathways that govern angiogenesis. In a recent study, it was determined that p190RhoGAP, an endogenous inhibitor of Rho GTPase activation, controls capillary network formation both *in vitro* and *in vivo* by sequestering transcription factors that govern sensitivity to VEGF via expression of the VEGFR2 receptor gene.⁵⁵ Further, p190RhoGAP activity may be decreased by increasing the stiffness of the substrate, resulting in increased Rho activation as well as promotion of VEGFR2 gene expression and VEGF-based angiogenesis. Thus, study of the mechanobiology of angiogenesis has revealed several interesting regulatory effects and their mechanisms. These studies can inform the design of material scaffolds and clinical protocols, which, by promoting angiogenesis and vascularization, might enable better integration of stem cell-derived engineered tissues *in vivo*.

30.6 Perspective: Three-Dimensional Material Systems for Investigating Mechanobiology

A large amount of the existing knowledge on cell–ECM interactions has been derived from *in vitro* studies using cells cultured on 2D surfaces. Although these studies have revealed a great deal about the mechanisms of cell adhesion, migration, and force transduction, it is becoming increasingly recognized that cells in their native 3D ECM exhibit behavior that is distinct from that seen in 2D.^{114,115} For instance, cell–matrix adhesions in 3D display strikingly different morphology, effects on matrix organization, and protein recruitment patterns compared to those observed in 2D.¹¹⁶ These fundamental differences in cell–ECM contacts result in a functionally different behavioral phenotype for cells in 3D matrices. This fact has been recognized for the last two decades in the context of the formation and growth of tumors,^{11,117,118} and is beginning to be apparent in the context of stem cell self-renewal and differentiation. For example, hESCs cultured in a medium conditioned by fibroblast feeders were shown to undergo self-renewal in 3D scaffolds of crosslinked hyaluronic acid, but not on 2D surfaces of the same material.¹¹⁹ Similarly, directed differentiation of mESCs into hematopoietic lineages has been shown to be more efficient in 3D culture.¹²⁰ Since mechanical communication between cells and the ECM is largely channeled through cell–ECM adhesions, it follows that force sensing and transduction and the concomitant effects on cellular physiology should also depend on the dimensionality of the matrix.¹²¹ For example, we recently delineated the effects of one important aspect of 3D culture—cellular confinement in narrow spaces—by building a novel microfabricated polyacrylamide gel system, where tumor cells confined within narrow channels migrated faster than in wide channels or on flat surfaces of the same ECM stiffness, due to more efficient polarization of cell-generated traction forces.¹³⁰ Therefore, it is essential that cell–ECM mechanical signaling be explored in physiologically relevant 3D models.

Traditional approaches to study cell–ECM biology in 3D have focused on natural ECM proteins that form gels under physiological conditions, for example, collagen I and Matrigel. While these materials do partially recapitulate the rich biochemical milieu to which cells are exposed in native environments, they offer a fairly limited range of mechanical properties. Further, the mechanics, microstructure, and biochemistry of these gels are intimately linked, in that changing the bulk density of the gel-forming proteins simultaneously varies all the above properties, making it difficult to attribute observed differences in cell behavior unambiguously to chemical or mechanical stimuli. Further, many of these native biomaterials are inappropriate for stem cell-based regenerative medicine, because they are typically derived from animal sources and therefore suffer from batch-to-batch variability and pose unacceptable

risks with respect to pathogenicity and immunogenicity. Therefore, there has been a significant drive toward the development of semisynthetic and synthetic 3D model ECMs that can be used to study cancer and stem cell biology and might potentially be appropriate for therapeutic use.^{27,28,122–124} Several synthetic polymer systems have been developed that can be crosslinked to varying extents, and by inclusion of full-length proteins or short peptides, can mimic the native ECM and also permit independent variation of matrix stiffness and adhesive functionality. Taking a cue from the recent tissue engineering efforts,^{125,126} we recently developed a system for studying cell–matrix mechanobiology in 3D based on mixtures of collagen I and agarose, a biologically inert polysaccharide that forms a filamentous meshwork and serves to stiffen collagen gels with modest effects on their fibrous architecture.¹²⁷ This hybrid system allows the study of cell mechanobiology in 3D while uncoupling the effects of matrix structure and mechanics from biochemistry. Studies of invasion of spheroids of glioma cells implanted in these gels revealed that increasing agarose concentrations created increasingly stiff gels but progressively slowed and eventually stopped invasion. This result was somewhat surprising, given that increasing stiffness was found to increase glioma cell motility on 2D surfaces (Figure 30.3). However, it appears that steric barriers created by the agarose meshwork present an obstacle to cell migration in 3D and limit the ability of the cells to contract and remodel collagen fibers, combining to prevent glioma invasion.¹³¹ This study illustrates clearly that some aspects of cellular behavior, such as the dependence of motility on the porosity and degradability of the matrix, can only be captured in 3D environments. Therefore, the development of material systems that can increasingly mimic native 3D ECM while retaining independent control of various design parameters such as stiffness, porosity, biochemical functionality, and degradability is crucial for facilitating studies on the mechanobiology of stem cells and cancer.

30.7 Conclusions

Biophysical interactions of stem cells with the extracellular milieu in their native niches as well as in engineered tissue constructs represent an important class of inputs governing cell behavior. Some of the mechanisms by which cells detect and process these inputs are conserved among many cell types, including stem cells, normal cells, and tumor cells. Therefore, a comparative study of these mechanisms may allow us to leverage our knowledge of the mechanobiology of normal cells and cancer to accelerate our understanding of the processes that control stem cell fate and design more effective strategies for regenerative medicine.

Acknowledgments

We apologize to the many authors whose work could not be cited because of space limitations. Sanjay Kumar wishes to acknowledge the support of a UC Berkeley Stem Cell Center Seed Grant, the Arnold and Mabel Beckman Young Investigator Award, an NSF Research Award (CMMI-0727420), an NIH Physical Sciences in Oncology Center Grant (1U54CA143836), and the NIH Director's New Innovator Award (1DP2OD004213)—a part of the NIH Roadmap for Medical Research.

References

1. Fuchs, E.; Tumber, T.; Guasch, G., Socializing with the neighbors: Stem cells and their niche. *Cell* 2004, 116(6), 769–778.
2. Moore, K. A.; Lemischka, I. R., Stem cells and their niches. *Science* 2006, 311(5769), 1880–1885.
3. Discher, D. E.; Janmey, P.; Wang, Y. L., Tissue cells feel and respond to the stiffness of their substrate. *Science* 2005, 310(5751), 1139–1143.
4. Ingber, D. E., Mechanobiology and diseases of mechanotransduction. *Annals of Medicine* 2003, 35(8), 564–577.
5. Vogel, V.; Sheetz, M., Local force and geometry sensing regulate cell functions. *Nature Reviews Molecular Cell Biology* 2006, 7(4), 265–275.

6. Keung, A. J.; Healy, K. E.; Kumar, S.; Schaffer, D. V., Biophysics and dynamics of natural and engineered stem cell microenvironments. *Wiley Interdisciplinary Reviews: Systems Biology and Medicine* 2009, 2(1), 49–64.
7. Discher, D. E.; Mooney, D. J.; Zandstra, P. W., Growth factors, matrices, and forces combine and control stem cells. *Science* 2009, 324(5935), 1673–1677.
8. Guilak, F.; Cohen, D. M.; Estes, B. T.; Gimble, J. M.; Liedtke, W.; Chen, C. S., Control of stem cell fate by physical interactions with the extracellular matrix. *Cell Stem Cell* 2009, 5(1), 17–26.
9. Ingber, D. E., Cellular mechanotransduction: Putting all the pieces together again. *FASEB J.* 2006, 20(7), 811–827.
10. Chen, C. S., Mechanotransduction—a field pulling together? *Journal of Cell Science* 2008, 121(20), 3285–3292.
11. Bissell, M. J.; Radisky, D., Putting tumours in context. *Nature Reviews Cancer* 2001, 1(1), 46–54.
12. Nelson, C. M.; Bissell, M. J., Of extracellular matrix, scaffolds, and signaling: Tissue architecture regulates development, homeostasis, and cancer. *Annual Review of Cell and Developmental Biology* 2006, (22), 287–309.
13. Kumar, S.; Weaver, V., Mechanics, malignancy, and metastasis: The force journey of a tumor cell. *Cancer and Metastasis Reviews* 2009, 28(1), 113–127.
14. Butcher, D. T.; Alliston, T.; Weaver, V. M., A tense situation: Forcing tumour progression. *Nature Reviews Cancer* 2009, 9(2), 108–122.
15. Levental, K. R.; Yu, H. M.; Kass, L.; Lakins, J. N.; Egeblad, M.; Erler, J. T.; Fong, S. F. T. et al., Matrix crosslinking forces tumor progression by enhancing integrin signaling. *Cell* 2009, 139(5), 891–906.
16. Paszek, M. J.; Zahir, N.; Johnson, K. R.; Lakins, J. N.; Rozenberg, G. I.; Gefen, A.; Reinhart-King, C. A. et al., Tensional homeostasis and the malignant phenotype. *Cancer Cell* 2005, 8(3), 241–254.
17. Zaman, M. H.; Trapani, L. M.; Sieminski, A. L.; MacKellar, D.; Gong, H.; Kamm, R. D.; Wells, A.; Lauffenburger, D. A.; Matsudaira, P., Migration of tumor cells in 3D matrices is governed by matrix stiffness along with cell-matrix adhesion and proteolysis. *Proceedings of the National Academy of Sciences of the United States of America* 2006, 103(29), 10889–10894.
18. Ulrich, T. A.; de Juan Pardo, E. M.; Kumar, S., The mechanical rigidity of the extracellular matrix regulates the structure, motility, and proliferation of glioma cells. *Cancer Research* 2009, 69(10), 4167–4174.
19. Geiger, B.; Spatz, J. P.; Bershadsky, A. D., Environmental sensing through focal adhesions. *Nature Reviews Molecular Cell Biology* 2009, 10(1), 21–33.
20. Al-Hajj, M.; Wicha, M. S.; Benito-Hernandez, A.; Morrison, S. J.; Clarke, M. F., Prospective identification of tumorigenic breast cancer cells. *Proceedings of the National Academy of Sciences of the United States of America* 2003, 100(7), 3983–3988.
21. Reya, T.; Morrison, S. J.; Clarke, M. F.; Weissman, I. L., Stem cells, cancer, and cancer stem cells. *Nature* 2001, 414(6859), 105–111.
22. Singh, S. K.; Hawkins, C.; Clarke, I. D.; Squire, J. A.; Bayani, J.; Hide, T.; Henkelman, R. M.; Cusimano, M. D.; Dirks, P. B., Identification of human brain tumour initiating cells. *Nature* 2004, 432(7015), 396–401.
23. Visvader, J. E.; Lindeman, G. J., Cancer stem cells in solid tumours: Accumulating evidence and unresolved questions. *Nature Reviews Cancer* 2008, 8(10), 755–768.
24. Bonnet, D.; Dick, J. E., Human acute myeloid leukemia is organized as a hierarchy that originates from a primitive hematopoietic cell. *Nature Medicine* 1997, 3(7), 730–737.
25. Elkin, B. S.; Azeloglu, E. U.; Costa, K. D.; Morrison, B., Mechanical heterogeneity of the rat hippocampus measured by atomic force microscope indentation. *Journal of Neurotrauma* 2007, 24(5), 812–822.
26. Saha, K.; Pollock, J. F.; Schaffer, D. V.; Healy, K. E., Designing synthetic materials to control stem cell phenotype. *Current Opinion in Chemical Biology* 2007, 11(4), 381–387.
27. Lutolf, M. P.; Hubbell, J. A., Synthetic biomaterials as instructive extracellular microenvironments for morphogenesis in tissue engineering. *Nature Biotechnology* 2005, 23(1), 47–55.
28. Lutolf, M. P.; Gilbert, P. M.; Blau, H. M., Designing materials to direct stem-cell fate. *Nature* 2009, 462(7272), 433–441.

29. Ghosh, K.; Ingber, D. E., Micromechanical control of cell and tissue development: Implications for tissue engineering. *Advanced Drug Delivery Reviews* 2007, 59(13), 1306–1318.
30. Farge, E., Mechanical induction of twist in the *Drosophila* foregut/stomodaeal primordium. *Current Biology* 2003, 13(16), 1365–1377.
31. Krieg, M.; Arboleda-Estudillo, Y.; Puech, P. H.; Kafer, J.; Graner, F.; Muller, D. J.; Heisenberg, C. P., Tensile forces govern germ-layer organization in zebrafish. *Nature Cell Biology* 2008, 10(4), 429–436.
32. Yang, Y.; Beqaj, S.; Kemp, P.; Ariel, I.; Schuger, L., Stretch-induced alternative splicing of serum response factor promotes bronchial myogenesis and is defective in lung hypoplasia. *Journal of Clinical Investigation* 2000, 106(11), 1321–1330.
33. Chowdhury, F.; Na, S.; Li, D.; Poh, Y.C.; Tanaka, T. S.; Wang, F.; Wang, N., Material properties of the cell dictate stress-induced spreading and differentiation in embryonic stem cells. *Nature Materials* 2010, 9(1), 82–88.
34. Saha, S.; Lin, J.; De Pablo, J. J.; Palecek, S. P., Inhibition of human embryonic stem cell differentiation by mechanical strain. *Journal of Cellular Physiology* 2006, 206(1), 126–137.
35. Illi, B.; Scopece, A.; Nanni, S.; Farsetti, A.; Morgante, L.; Biglioli, P.; Capogrossi, M. C.; Gaetano, C., Epigenetic histone modification and cardiovascular lineage programming in mouse embryonic stem cells exposed to laminar shear stress. *Circulation Research* 2005, 96(5), 501–508.
36. North, T. E.; Goessling, W.; Peeters, M.; Li, P. L.; Ceol, C.; Lord, A. M.; Weber, G. J. et al., Hematopoietic stem cell development is dependent on blood flow. *Cell* 2009, 137(4), 736–748.
37. Adamo, L.; Naveiras, O.; Wenzel, P. L.; McKinney-Freeman, S.; Mack, P. J.; Gracia-Sancho, J.; Suchy-Dicey, A. et al., Biomechanical forces promote embryonic haematopoiesis. *Nature* 2009, 459(7250), 1131–U120.
38. McBeath, R.; Pirone, D. M.; Nelson, C. M.; Bhadiraju, K.; Chen, C. S., Cell shape, cytoskeletal tension, and RhoA regulate stem cell lineage commitment. *Developmental Cell* 2004, 6(4), 483–495.
39. Engler, A. J.; Sen, S.; Sweeney, H. L.; Discher, D. E., Matrix elasticity directs stem cell lineage specification. *Cell* 2006, 126(4), 677–689.
40. Winer, J. P.; Janmey, P. A.; McCormick, M. E.; Funaki, M., Bone marrow-derived human mesenchymal stem cells become quiescent on soft substrates but remain responsive to chemical or mechanical stimuli. *Tissue Engineering Part A* 2009, 15(1), 147–154.
41. Saha, K.; Keung, A. J.; Irwin, E. F.; Li, Y.; Little, L.; Schaffer, D. V.; Healy, K. E., Substrate modulus directs neural stem cell behavior. *Biophysical Journal* 2008, 95(9), 4426–4438.
42. Banerjee, A.; Arha, M.; Choudhary, S.; Ashton, R. S.; Bhatia, S. R.; Schaffer, D. V.; Kane, R. S., The influence of hydrogel modulus on the proliferation and differentiation of encapsulated neural stem cells. *Biomaterials* 2009, 30(27), 4695–4699.
43. Seidlits, S. K.; Khaing, Z. Z.; Petersen, R. R.; Nickels, J. D.; Vanscoy, J. E.; Shear, J. B.; Schmidt, C. E., The effects of hyaluronic acid hydrogels with tunable mechanical properties on neural progenitor cell differentiation. *Biomaterials* 2010, 31(14), 3930–3940.
44. Leipzig, N. D.; Shoichet, M. S., The effect of substrate stiffness on adult neural stem cell behavior. *Biomaterials* 2009, 30(36), 6867–6878.
45. Chachisvilis, M.; Zhang, Y. L.; Frangos, J. A., G protein-coupled receptors sense fluid shear stress in endothelial cells. *Proceedings of the National Academy of Sciences of the United States of America* 2006, 103(42), 15463–15468.
46. Martinac, B., Mechanosensitive ion channels: Molecules of mechanotransduction. *Journal of Cell Science* 2004, 117(12), 2449–2460.
47. Kung, C., A possible unifying principle for mechanosensation. *Nature* 2005, 436(7051), 647–654.
48. Katsumi, A.; Orr, A. W.; Tzima, E.; Schwartz, M. A., Integrins in mechanotransduction. *Journal of Biological Chemistry* 2004, 279(13), 12001–12004.
49. Berrier, A. L.; Yamada, K. M., Cell-matrix adhesion. *Journal of Cellular Physiology* 2007, 213(3), 565–573.
50. Chen, C. S.; Tan, J.; Tien, J., Mechanotransduction at cell-matrix and cell-cell contacts. *Annual Review of Biomedical Engineering* 2004, 6, 275–302.

51. Nobes, C. D.; Hall, A., Rho, Rac, and Cdc42 GTPases regulate the assembly of multimolecular focal complexes associated with actin stress fibers, lamellipodia, and filopodia. *Cell* 1995, 81(1), 53–62.
52. Burridge, K.; Wennerberg, K., Rho and Rac take center stage. 2004, 116(2), 167–179.
53. Etienne-Manneville, S.; Hall, A., Rho GTPases in cell biology. *Nature* 2002, 420(6916), 629–635.
54. Pellegrin, S.; Mellor, H., Actin stress fibres. *Journal of Cell Science* 2007, 120(20), 3491–3499.
55. Mammoto, A.; Connor, K. M.; Mammoto, T.; Yung, C. W.; Huh, D.; Aderman, C. M.; Mostoslavsky, G.; Smith, L. E. H.; Ingber, D. E., A mechanosensitive transcriptional mechanism that controls angiogenesis. *Nature* 2009, 457(7233), 1103–U57.
56. Le Beyec, J.; Xu, R.; Lee, S. Y.; Nelson, C. M.; Rizki, A.; Alcaraz, J.; Bissell, M. J., Cell shape regulates global histone acetylation in human mammary epithelial cells. *Experimental Cell Research* 2007, 313(14), 3066–3075.
57. Molofsky, A. V.; Pardal, R.; Morrison, S. J., Diverse mechanisms regulate stem cell self-renewal. *Current Opinion in Cell Biology* 2004, 16(6), 700–707.
58. Morrison, S. J.; Spradling, A. C., Stem cells and niches: Mechanisms that promote stem cell maintenance throughout life. *Cell* 2008, 132(4), 598–611.
59. Li, L. H.; Neves, W. B., Normal stem cells and cancer stem cells: The niche matters. *Cancer Research* 2006, 66(9), 4553–4557.
60. Pardal, R.; Clarke, M. F.; Morrison, S. J., Applying the principles of stem-cell biology to cancer. *Nature Reviews Cancer* 2003, 3(12), 895–902.
61. Al-Hajj, M.; Clarke, M. F., Self-renewal and solid tumor stem cells. *Oncogene* 2004, 23(43), 7274–7282.
62. Bonewald, L. F.; Johnson, M. L., Osteocytes, mechanosensing and Wnt signaling. *Bone* 2008, 42(4), 606–615.
63. Santos, A.; Bakker, A. D.; Zandieh-Doulabi, B.; de Blicke-Hogervorst, J. M. A.; Klein-Nulend, J., Early activation of the beta-catenin pathway in osteocytes is mediated by nitric oxide, phosphatidylinositol-3 kinase/Akt, and focal adhesion kinase. *Biochemical and Biophysical Research Communications* 2010, 391(1), 364–369.
64. Armstrong, V. J.; Muzylak, M.; Sunters, A.; Zaman, G.; Saxon, L. K.; Price, J. S.; Lanyon, L. E., Wnt/beta-catenin signaling is a component of osteoblastic bone cell early responses to load-bearing and requires estrogen receptor alpha. *Journal of Biological Chemistry* 2007, 282(28), 20715–20727.
65. Taipale, J.; Beachy, P. A., The Hedgehog and Wnt signaling pathways in cancer. *Nature* 2001, 411(6835), 349–354.
66. Reya, T.; Duncan, A. W.; Ailles, L.; Domen, J.; Scherer, D. C.; Willert, K.; Hintz, L.; Nusse, R.; Weissman, I. L., A role for Wnt signalling in self-renewal of haematopoietic stem cells. *Nature* 2003, 423(6938), 409–414.
67. Morrow, D.; Sweeney, C.; Birney, Y. A.; Guha, S.; Collins, N.; Cummins, P. M.; Murphy, R.; Walls, D.; Redmond, E. M.; Cahill, P. A., Biomechanical regulation of hedgehog signaling in vascular smooth muscle cells *in vitro* and *in vivo*. *American Journal of Physiology-Cell Physiology* 2007, 292(1), C488–C496.
68. Wu, Q. Q.; Zhang, Y.; Chen, Q., Indian hedgehog is an essential component of mechanotransduction complex to stimulate chondrocyte proliferation. *Journal of Biological Chemistry* 2001, 276(38), 35290–35296.
69. Zhao, J.; Guan, J. L., Signal transduction by focal adhesion kinase in cancer. *Cancer and Metastasis Reviews* 2009, 28(1–2), 35–49.
70. Welsh, C. F.; Roovers, K.; Villanueva, J.; Liu, Y. Q.; Schwartz, M. A.; Assoian, R. K., Timing of cyclin D1 expression within G1 phase is controlled by Rho. *Nature Cell Biology* 2001, 3(11), 950–957.
71. Olson, M. F.; Ashworth, A.; Hall, A., An essential role for Rho, Rac, and Cdc42 GTPases in cell-cycle progression through G(1). *Science* 1995, 269(5228), 1270–1272.
72. Klein, E. A.; Yin, L. Q.; Kothapalli, D.; Castagnino, P.; Byfield, F. J.; Xu, T. N.; Levental, I.; Hawthorne, E.; Janmey, P. A.; Assoian, R. K., Cell-cycle control by physiological matrix elasticity and *in vivo* tissue stiffening. *Current Biology* 2009, 19(18), 1511–1518.

73. Boudreau, N.; Sympson, C. J.; Werb, Z.; Bissell, M. J., Suppression of ICE and apoptosis in mammary epithelial cells by extracellular matrix. *Science* 1995, 267(5199), 891–893.
74. Wang, H. B.; Dembo, M.; Wang, Y. L., Substrate flexibility regulates growth and apoptosis of normal but not transformed cells. *American Journal of Physiology-Cell Physiology* 2000, 279(5), C1345–C1350.
75. Provenzano, P. P.; Inman, D. R.; Eliceiri, K. W.; Keely, P. J., Matrix density-induced mechanoregulation of breast cell phenotype, signaling and gene expression through a FAK-ERK linkage. *Oncogene* 2009, 28(49), 4326–4343.
76. Provenzano, P. P.; Inman, D. R.; Eliceiri, K. W.; Knittel, J. G.; Yan, L.; Rueden, C. T.; White, J. G.; Keely, P. J., Collagen density promotes mammary tumor initiation and progression. *BMC Medicine* 2008, 6, 11.
77. Locascio, A.; Nieto, M. A., Cell movements during vertebrate development: Integrated tissue behaviour versus individual cell migration. *Current Opinion in Genetics & Development* 2001, 11(4), 464–469.
78. Hatten, M. E., Central nervous system neuronal migration. *Annual Review of Neuroscience* 1999, 22, 511–539.
79. Martin, P., Wound healing—aiming for perfect skin regeneration. *Science* 1997, 276(5309), 75–81.
80. Griffith, L. G.; Naughton, G., Tissue engineering—current challenges and expanding opportunities. *Science* 2002, 295(5557), 1009–1014.
81. Karageorgiou, V.; Kaplan, D., Porosity of 3D biomaterial scaffolds and osteogenesis. *Biomaterials* 2005, 26(27), 5474–5491.
82. Luo, Y.; Shoichet, M. S., A photolabile hydrogel for guided three-dimensional cell growth and migration. *Nature Materials* 2004, 3(4), 249–253.
83. Lutolf, M. P.; Lauer-Fields, J. L.; Schmoekel, H. G.; Metters, A. T.; Weber, F. E.; Fields, G. B.; Hubbell, J. A., Synthetic matrix metalloproteinase-sensitive hydrogels for the conduction of tissue regeneration: Engineering cell-invasion characteristics. *Proceedings of the National Academy of Sciences of the United States of America* 2003, 100(9), 5413–5418.
84. Mann, B. K.; Gobin, A. S.; Tsai, A. T.; Schmedlen, R. H.; West, J. L., Smooth muscle cell growth in photopolymerized hydrogels with cell adhesive and proteolytically degradable domains: Synthetic ECM analogs for tissue engineering. *Biomaterials* 2001, 22(22), 3045–3051.
85. Lauffenburger, D. A.; Horwitz, A. F., Cell migration: A physically integrated molecular process. *Cell* 1996, 84(3), 359–369.
86. Palecek, S. P.; Loftus, J. C.; Ginsberg, M. H.; Lauffenburger, D. A.; Horwitz, A. F., Integrin-ligand binding properties govern cell migration speed through cell-substratum adhesiveness. *Nature* 1997, 385(6616), 537–540.
87. Pelham, R. J.; Wang, Y. L., Cell locomotion and focal adhesions are regulated by substrate flexibility. *Proceedings of the National Academy of Sciences of the United States of America* 1997, 94(25), 13661–13665.
88. Peyton, S. R.; Putnam, A. J., Extracellular matrix rigidity governs smooth muscle cell motility in a biphasic fashion. *Journal of Cellular Physiology* 2005, 204(1), 198–209.
89. Engler, A.; Bacakova, L.; Newman, C.; Hategan, A.; Griffin, M.; Discher, D., Substrate compliance versus ligand density in cell on gel responses. *Biophysical Journal* 2004, 86(1), 617–628.
90. Lo, C. M.; Wang, H. B.; Dembo, M.; Wang, Y. L., Cell movement is guided by the rigidity of the substrate. *Biophysical Journal* 2000, 79(1), 144–152.
91. Wong, J. Y.; Velasco, A.; Rajagopalan, P.; Pham, Q., Directed movement of vascular smooth muscle cells on gradient-compliant hydrogels. *Langmuir* 2003, 19(5), 1908–1913.
92. Friedl, P.; Wolf, K., Tumour-cell invasion and migration: Diversity and escape mechanisms. *Nature Reviews Cancer* 2003, 3(5), 362–374.
93. Sahai, E., Mechanisms of cancer cell invasion. *Current Opinion in Genetics & Development* 2005, 15(1), 87–96.

94. Sahai, E.; Marshall, C. J., Differing modes of tumour cell invasion have distinct requirements for Rho/ROCK signalling and extracellular proteolysis. *Nature Cell Biology* 2003, 5(8), 711–719.
95. Wolf, K.; Mazo, I.; Leung, H.; Engelke, K.; von Andrian, U. H.; Deryugina, E. I.; Strongin, A. Y.; Bocker, E. B.; Friedl, P., Compensation mechanism in tumor cell migration: Mesenchymal-amoeboid transition after blocking of pericellular proteolysis. *Journal of Cell Biology* 2003, 160(2), 267–277.
96. Friedl, P.; Wolf, K., Proteolytic interstitial cell migration: A five-step process. *Cancer and Metastasis Reviews* 2009, 28(1–2), 129–135.
97. Laschke, M. W.; Harder, Y.; Amon, M.; Martin, I.; Farhadi, J.; Ring, A.; Torio-Padron, N. et al., Angiogenesis in tissue engineering: Breathing life into constructed tissue substitutes. *Tissue Engineering* 2006, 12(8), 2093–2104.
98. Carmeliet, P., Angiogenesis in health and disease. *Nature Medicine* 2003, 9(6), 653–660.
99. Zisch, A. H.; Lutolf, M. P.; Hubbell, J. A., Biopolymeric delivery matrices for angiogenic growth factors. *Cardiovascular Pathology* 2003, 12(6), 295–310.
100. Richardson, T. P.; Peters, M. C.; Ennett, A. B.; Mooney, D. J., Polymeric system for dual growth factor delivery. *Nature Biotechnology* 2001, 19(11), 1029–1034.
101. Ferrara, N.; Gerber, H. P.; LeCouter, J., The biology of VEGF and its receptors. *Nature Medicine* 2003, 9(6), 669–676.
102. Davis, S.; Yancopoulos, G. D., The angiopoietins: Yin and yang in angiogenesis. In *Vascular Growth Factors and Angiogenesis*, Lena Claesson-Welsh (Ed.), 1999; Vol. 237, pp. 173–185.
103. Ingber, D. E.; Folkman, J., How does extracellular-matrix control capillary morphogenesis. *Cell* 1989, 58(5), 803–805.
104. Ingber, D. E., Mechanical signalling and the cellular response to extracellular matrix in angiogenesis and cardiovascular physiology. *Circulation Research* 2002, 91(10), 877–887.
105. Carmeliet, P.; Jain, R. K., Angiogenesis in cancer and other diseases. *Nature* 2000, 407(6801), 249–257.
106. Folkman, J.; Bach, M.; Rowe, J. W.; Davidoff, F.; Lambert, P.; Hirsch, C.; Goldberg, A.; Hiatt, H. H.; Glass, J.; Henshaw, E., Tumor angiogenesis—therapeutic implications. *New England Journal of Medicine* 1971, 285(21), 1182–1186
107. Ferrara, N., Vascular endothelial growth factor: Basic science and clinical progress. *Endocrine Reviews* 2004, 25(4), 581–611.
108. Ingber, D. E., Fibronectin controls capillary endothelial-cell growth by modulating cell-shape. *Proceedings of the National Academy of Sciences of the United States of America* 1990, 87(9), 3579–3583.
109. Chen, C. S.; Mrksich, M.; Huang, S.; Whitesides, G. M.; Ingber, D. E., Geometric control of cell life and death. *Science* 1997, 276(5317), 1425–1428.
110. Sieminski, A. L.; Hebbel, R. P.; Gooch, K. J., The relative magnitudes of endothelial force generation and matrix stiffness modulate capillary morphogenesis *in vitro*. *Experimental Cell Research* 2004, 297(2), 574–584.
111. Kniazeva, E.; Putnam, A. J., Endothelial cell traction and ECM density influence both capillary morphogenesis and maintenance in 3-D. *American Journal of Physiology-Cell Physiology* 2009, 297(1), C179–C187.
112. Kilarski, W. W.; Samolov, B.; Petersson, L.; Kvanta, A.; Gerwins, P., Biomechanical regulation of blood vessel growth during tissue vascularization. *Nature Medicine* 2009, 15(6), 657–664.
113. Moore, K. A.; Polte, T.; Huang, S.; Shi, B.; Alsberg, E.; Sunday, M. E.; Ingber, D. E., Control of basement membrane remodeling and epithelial branching morphogenesis in embryonic lung by Rho and cytoskeletal tension. *Developmental Dynamics* 2005, 232(2), 268–281.
114. Yamada, K. M.; Cukierman, E., Modeling tissue morphogenesis and cancer in 3D. *Cell* 2007, 130(4), 601–610.

115. Cukierman, E.; Pankov, R.; Yamada, K. M., Cell interactions with three-dimensional matrices. *Current Opinion in Cell Biology* 2002, 14(5), 633–639.
116. Cukierman, E.; Pankov, R.; Stevens, D. R.; Yamada, K. M., Taking cell-matrix adhesions to the third dimension. *Science* 2001, 294(5547), 1708–1712.
117. Jacks, T.; Weinberg, R. A., Taking the study of cancer cell survival to a new dimension. *Cell* 2002, 111(7), 923–925.
118. Debnath, J.; Brugge, J. S., Modelling glandular epithelial cancers in three-dimensional cultures. *Nature Reviews Cancer* 2005, 5(9), 675–688.
119. Gerecht, S.; Burdick, J. A.; Ferreira, L. S.; Townsend, S. A.; Langer, R.; Vunjak-Novakovic, G., Hyaluronic acid hydrogel for controlled self-renewal and differentiation of human embryonic stem cells. *Proceedings of the National Academy of Sciences of the United States of America* 2007, 104(27), 11298–11303.
120. Liu, H.; Roy, K., Biomimetic three-dimensional cultures significantly increase hematopoietic differentiation efficacy of embryonic stem cells. *Tissue Engineering* 2005, 11(1–2), 319–330.
121. Pedersen, J. A.; Swartz, M. A., Mechanobiology in the third dimension. *Annals of Biomedical Engineering* 2005, 33(11), 1469–1490.
122. Griffith, L. G.; Swartz, M. A., Capturing complex 3D tissue physiology *in vitro*. *Nature Reviews Molecular Cell Biology* 2006, 7(3), 211–224.
123. Hutmacher, D. W., Biomaterials offer cancer research the third dimension. *Nature Materials* 2010, 9(2), 90–93.
124. Tibbitt, M. W.; Anseth, K. S., Hydrogels as extracellular matrix mimics for 3D cell culture. *Biotechnology and Bioengineering* 2009, 103(4), 655–663.
125. Balgude, A. P.; Yu, X.; Szymanski, A.; Bellamkonda, R. V., Agarose gel stiffness determines rate of DRG neurite extension in 3D cultures. *Biomaterials* 2001, 22(10), 1077–1084.
126. Batorsky, A.; Liao, J. H.; Lund, A. W.; Plopper, G. E.; Stegemann, J. P., Encapsulation of adult human mesenchymal stem cells within collagen-agarose microenvironments. *Biotechnology and Bioengineering* 2005, 92(4), 492–500.
127. Ulrich, T. A.; Jain, A.; Tanner, K.; MacKay, J. L.; Kumar, S., Probing cellular mechanobiology in three-dimensional culture with collagen-agarose matrices. *Biomaterials* 2010, 31(7), 1875–1884.
128. Keung, A. J.; de Juan Pardo, E. M.; Schaffer, D. V.; Kumar, S., Rho GTPases mediate the mechanosensitive lineage commitment of neural stem cells. *Stem Cells* 2011, 29(11), 1886–1897.
129. Ananthanarayanan, B.; Kim, Y.; Kumar, S., Elucidating the mechanobiology of malignant brain tumors using a brain matrix-mimetic hyaluronic acid hydrogel platform. *Biomaterials* 2011, 32(31), 7913–7923.
130. Pathak, A.; Kumar, S., Independent regulation of tumor cell migration by matrix stiffness and confinement. *Proceedings of the National Academy of Sciences* 2012, 109(26), 10334–10339.
131. Ulrich, T. A.; Lee, T. G.; Shon, H. K.; Moon, D. W.; Kumar, S., Microscale mechanisms of agarose-induced disruption of collagen remodeling. *Biomaterials* 2011, 32(24), 5633–5642.



Tissue Engineering

John P. Fisher
University of Maryland

Antonios G. Mikos
Rice University

- 39 Strategic Directions** *Peter C. Johnson*..... **39-1**
Introduction • Previous Approaches to the Assignment of Strategic
Directions in Tissue Engineering • Tools in the Identification of Strategic
Directions • Summary • References
- 40 Silks** *Monica A. Serban and David L. Kaplan*..... **40-1**
Introduction to Silks • Tissue Engineering Applications of Silks • Concluding
Remarks • References
- 41 Calcium Phosphates** *Kemal Sariibrahimoglu, Joop G.C. Wolke, Sander C.G.
Leeuwenburgh, and John A. Jansen*.....**41-1**
Introduction • Physicochemical Properties of CaP Compounds • CaP Blocks/
Granules • CaP Cements • Conclusion • References
- 42 Engineered Protein Biomaterials** *Andreina Parisi-Amon and
Sarah C. Heilshorn* **42-1**
Engineered Protein Biomaterials as an Alternative to “Traditional”
Biomaterials • Synthesis of Engineered Protein Biomaterials • Design of Engineered
Protein Biomaterials • Applications of Engineered Protein Biomaterials • References
- 43 Synthetic Biomaterials** *Joshua S. Katz and Jason A. Burdick*..... **43-1**
Introduction • Choice of Monomer • Polymerization Mechanisms • Biomaterial
Degradation • Poly(ethylene glycol) • Poly(esters) • Poly(anhydrides) • Poly(ortho
esters) • Poly(urethanes) • Pseudo Poly(amino acids) • Poly(acrylates) and
Poly(methacrylates) • Non-Polymeric Synthetic Biomaterials • Conclusions • References

- 44 Growth Factors and Morphogens: Signals for Tissue Engineering**
A. Hari Reddi **44-1**
 Introduction • Tissue Engineering and Morphogenesis • The Bone Morphogenetic Proteins • Growth Factors • BMPs Bind to Extracellular Matrix • Clinical Applications • Challenges and Opportunities • Acknowledgments • References
- 45 Signal Expression in Engineered Tissues** *Martha O. Wang and John P. Fisher* **45-1**
 Introduction • Biology of Osteoblasts • Biology of Chondrocytes • Signaling Pathway Overview • Anabolic Growth Factors/Cytokines • Catabolic Growth Factors/Cytokines • Hormones • Mechanotransduction • Dual Growth Factor Studies • Conclusion • References
- 46 Pluripotent Stem Cells** *Todd C. McDevitt and Melissa A. Kinney* **46-1**
 Origin and Derivation of Embryonic Stem Cells • Characteristics • Alternate Derivation Methods • Propagation • Differentiation • Clinical Outlook
 • Conclusion • References
- 47 Hematopoietic Stem Cells** *Ian M. Kaplan, Sebastien Morisot, and Curt I. Civin* ... **47-1**
 Introduction: The Hematopoietic Hierarchy • The Hematopoietic Lineage Commitment Process • Hematopoietic Stem Cells • Sources of Hematopoietic Stem Cells for Clinical Transplantation • *Ex Vivo* Expansion of HSCs • Conclusion • References
- 48 Mesenchymal Stem Cells** *Pamela C. Yelick and Weibo Zhang* **48-1**
 Definition • Cell Characteristics • Potential Therapeutic Applications • Potential Concerns • Conclusion • References
- 49 Nanobiomaterials for Tissue Engineering** *Pramod K. Avti, Sunny C. Patel, Pushpinder Uppal, Grace O'Malley, Joseph Garlow, and Balaji Sitharaman* **49-1**
 Introduction • Nanobiomaterials to Improve Bulk and Surface Properties of Tissue Engineering Scaffolds • Nanobiomaterials for Therapeutic Delivery • Nanobiomaterials to Image the Process of Tissue Formation • Continuing and Future Developments
 • Abbreviations • References
- 50 Biomimetic Approaches in Tissue Engineering** *Indong Jun, Min Sup Kim, Ji-Hye Lee, Young Min Shin, and Heungsoo Shin* **50-1**
 Introduction • Biomimetic Surface Modifications • Growth Factor-Presenting Materials • Biomimetic Hydrogels and Controlled Cell Interactions • Composite Scaffolds Used to Mimic Specific Cellular Environments • Scaffolds Mimicking the Structure of ECM • Conclusions • References
- 51 Molecular Biology Techniques** *X.G. Chen, Y.L. Fang, and W.T. Godbey* **51-1**
 Histochemistry • Gel Electrophoresis • Restriction Enzymes • Other DNA Modification Enzymes • The Polymerase Chain Reaction • Blotting • References
- 52 Biomaterial Mechanics** *Kimberly M. Stroka, Leann L. Norman, and Helim Aranda-Espinoza* **52-1**
 Introduction • Cellular Mechanotransduction • Mechanics of Biomaterials • Potential Target and Applications • Summary • References
- 53 Mechanical Conditioning** *Elaine L. Lee and Horst A. von Recum* **53-1**
 Why Do We Need Mechanical Conditioning? • Cellular Response to Mechanical Stimuli versus the Living Cell as a Mechanical Structure • Mechanotransduction and Mechanical Conditioning Terminology • Current Technologies—Advantages and Disadvantages • Upcoming Technologies • Conclusion • References
- 54 Micropatterned Biomaterials for Cell and Tissue Engineering** *Murugan Ramalingam and Ali Khademhosseini* **54-1**
 Introduction • Surface Modification and Patterning Approaches • Techniques for Chemical Patterning and Applications to Cell Studies • Techniques for Topographical Patterning and Applications to Cell Studies • Techniques for Three-Dimensional Patterning and Applications to Tissue Engineering • Concluding Remarks • References

- 55 **Drug Delivery** *Prinda Wanakule and Krishnendu Roy* 55-1
Introduction • Mechanisms of Drug Delivery • Drugs of Interest in Tissue Engineering • Drug Delivery in Tissue Engineering • Outlook • References
- 56 **Gene Therapy** *C. Holladay, M. Kulkarni, W. Minor, and Abhay Pandit* 56-1
Introduction • Delivery Technique (Vector) • Systemic and Local Gene Delivery • Therapeutic Preclinical or Clinical Trials • Summary • Acknowledgments • References
- 57 **Nanotechnology-Based Cell Engineering Strategies for Tissue Engineering and Regenerative Medicine Applications** *Joaquim Miguel Oliveira, João Filipe Mano, and Rui Luís Reis* 57-1
Introduction • Cell Engineering Strategies • Concluding Remarks • References
- 58 **Cell Encapsulation** *Stephanie J. Bryant* 58-1
Introduction • Gelation Mechanisms Employed in Cell Encapsulation • Hydrogel Structure and Degradation • Concluding Remarks • References
- 59 **Coculture Systems for Mesenchymal Stem Cells** *Song P. Seto and Johnna S. Temenoff* 59-1
Introduction • Cells of Interest • Overview of Coculture Methods • Cocultures with Chondrocytes • Osteoblast Coculture with MSCs • Myoblast Coculture with MSCs • Communication between Mesenchymal and Endothelial Lineages • Future Outlook • Acknowledgments • References
- 60 **Tissue Engineering Bioreactors** *Sarindr Bhumiratana, Elisa Cimetta, Nina Tandon, Warren Grayson, Milica Radisic, and Gordana Vunjak-Novakovic* 60-1
Introduction • Overview of the Field • Principles of Bioreactor Design • Microscale Technologies • Cardiac Tissue Engineering Bioreactors • Vascular Bioreactors • Bone Tissue Engineering Bioreactor • Cartilage Tissue Engineering Bioreactors • Tendon/Ligament Tissue Engineering Bioreactors • Summary and Challenges • Acknowledgment • References
- 61 **Shear Forces** *Jose F. Alvarez-Barreto, Samuel B. VanGordon, Brandon W. Engebretson, and Vasillios I. Sikavitsas* 61-1
Introduction: Cells and Shear Forces • Effect of Shear Forces on Tissue-Specific Cells • References
- 62 **Vascularization of Engineered Tissues** *Monica L. Moya and Eric M. Brey* 62-1
Introduction • Neovascularization • Strategies for Vascularizing Engineered Tissues • Conclusions • References
- 63 **Biomedical Imaging of Engineered Tissues** *Nicholas E. Simpson and Athanassios Sambanis* 63-1
Introduction • Optical Imaging • Radiation-Based Imaging • Ultrasound • Infrared Imaging • Nuclear Magnetic Resonance • Conclusion • Acknowledgments • References
- 64 **Multiscale Modeling of *In Vitro* Tissue Cultivation** *Kyriacos Zygorakis* 64-1
Introduction • Model Detail and Abstraction • Cell Proliferation and Migration • Cell Population Dynamics and Mass Transport • Continuous, Discrete, and Hybrid Models for Tissue Growth • A Modeling Framework for *In Vitro* Tissue Cultivation • Components of the Hybrid Multiscale Model • Results and Discussion • References
- 65 **Bone Engineering** *Lucas A. Kinard, Antonios G. Mikos, and F. Kurtis Kasper* 65-1
Introduction • References
- 66 **Dental and Craniofacial Bioengineering** *Hemin Nie and Jeremy J. Mao* 66-1
Introduction • Clinical Challenges of Dental, Oral, and Craniofacial Bioengineering • Bone Regeneration • Tooth Regeneration • Soft-Tissue Regeneration • Concluding Remarks • Acknowledgments • References

- 67 Tendon and Ligament Engineering** *Nicholas Sears, Tyler Touchet, Hugh Benhardt, and Elizabeth Cosgriff-Hernández*.....67-1
 Introduction • Structure of Fibrous Connective Tissues • Current Ligament
 Reconstructive Techniques • Engineered Tendon and Ligament Grafts • Mechanical
 Stimulation • *In Vivo* Models to Demonstrate Efficacy • Key Challenges and Critical
 Issues • References
- 68 Cartilage Tissue Engineering** *Emily E. Coates and John P. Fisher* 68-1
 Cartilage Tissue: Composition, Function, and Disease • Cartilage Tissue
 Engineering • Zonal Cartilage Engineering • Stem Cells in Cartilage Tissue Engineering
 • Dynamic Culture Systems for Cartilage Engineering • Acknowledgments • References
- 69 TMJ Engineering** *Michael S. Detamore* 69-1
 Introduction • Structure and Function of TMJ Tissues • Tissue Engineering
 Approaches • Looking to the Future in TMJ Tissue Engineering • References
- 70 Interface Tissue Engineering** *Helen H. Lu, Nora Khanarian, Kristen Moffat,
 and Siddarth Subramony*..... 70-1
 Introduction • Interface Scaffold Design for Ligament-to-Bone Interface Tissue Engineering
 • Interface Scaffold Design for Tendon-to-Bone Interface Tissue Engineering • Stratified
 Scaffold Design for Cartilage-to-Bone Interface Tissue Engineering • Summary and Future
 Directions • References
- 71 The Bioengineering of Dental Tissues** *Rena N. D'Souza, Katherine R. Regan,
 Kerstin M. Galler, and Songtao Shi*71-1
 Introduction • The Tooth and Its Supporting Structures • Genetic Control of
 Tooth Development • Tooth Regenerative Strategies • Conclusion
 • Acknowledgments • References
- 72 Tissue Engineering of the Urogenital System** *In Kap Ko, Anthony Atala, and
 James J. Yoo*..... 72-1
 Introduction • Fundamental Components of Urogenital Tissue Engineering • Engineering
 Specific Urogenital Structures • Perspective • Acknowledgment • References
- 73 Vascular Tissue Engineering** *Laura J. Suggs*..... 73-1
 Introduction • Cell Source • Scaffolds/Extracellular Matrix • Growth Factor
 Signaling • Vascular Grafts and Medial Equivalents • Engineered Vascular
 Networks • Conclusions • References
- 74 Neural Engineering** *Yen-Chih Lin and Kacey G. Marra*.....74-1
 Overview of the Anatomy of the Nervous System • Peripheral Nerve Repair • CNS
 Repair • Animal Models of Nervous System Injury Research • Overall Summary of
 Neural Tissue Engineering • References
- 75 Tumor Engineering: Applications for Cancer Biology and
 Drug Development** *Joseph A. Ludwig and Emily Burdett*..... 75-1
 Introduction • Cancer Fundamentals and Relationship to Tissue Engineering • Preclinical
 Drug Evaluation • Advanced 3D Models of Cancer • Tools for Creation of a Bioengineered
 Tumor Model • Applications of Advanced 3D Cancer Models • Conclusions • References

39

Strategic Directions

Peter C. Johnson
*Avery-Dennison
Medical Solutions
Scintellix, LLC*

39.1 Introduction	39-1
39.2 Previous Approaches to the Assignment of Strategic Directions in Tissue Engineering.....	39-2
39.3 Tools in the Identification of Strategic Directions	39-3
Identification of Concepts Having General Criticality • Cohesive Technology Opportunity Stratification • Modulators of Strategy	
39.4 Summary.....	39-8
References.....	39-9

39.1 Introduction

Properly identified strategic directions for technology development optimize our ability to bring robustly engineered tissues to humanity. They guide our work within the dual envelopes of technical possibility and social/commercial acceptability. As we have learned, the effective engineering of human tissues represents a challenge of the highest order (Table 39.1). In order to make effective progress, some marshalling of resources and establishment of common directions are becoming ever more essential. A reasoned declaration of strategy is now more necessary for our field than ever.

Strategy implies the efficient application of resources toward a common end. It begins with the end in sight and works backwards to define tactics, boundary conditions and a temporal sequence that together, enable the end to be reached. What is this “end” in the field of tissue engineering? Simply stated, it is the creation of reproducible tissue replacement/augmentation technologies that are safe, effective, and economically attractive for use in day-to-day healthcare across the entire population.

Strategy, although forward-looking, is limited by what is known at the point in time when it is crafted. It is axiomatic that “best laid plans” are commonly thwarted by either a misappreciation of challenges or by the emergence of previously unknown accelerators of development. Nonetheless, what is important about strategy is its capacity—when well designed—to bring key stakeholders together into a common understanding of goals, tactics, and limitations. The set of stakeholders who have a vested interest in tissue engineering success is quite broad—and their interests are diverse (Table 39.2). The development of a comprehensive strategy for the field requires that their needs as a group be carefully considered.

The complete aggregation of these stakeholders in a robust strategic planning exercise has never been achieved, though such processes are now being designed. In harmony with the nature of a *Bioengineering Handbook*, this piece will therefore not provide a specific set of strategic directions for the field but rather, a system through which strategic directions can be defined. The techniques presented here can be used not only to support pan-stakeholder strategy development but also the strategic directions of individual investigators and their laboratory teams.

TABLE 39.1 Components of the Overall Challenge Facing the Field of Tissue Engineering

Challenge Component	Concern
Intellectual	Can we attract and retain sufficient multidisciplinary talent having the imagination and tenacity to overcome present technical limitations? Can we sufficiently unify the focus of tissue engineers to meet technical goals?
Technical	Can cells be reproducibly sourced and tissues be manufactured to specification? Can we master the requirements for both 2D and 3D tissues, the latter as perfusable systems?
Regulatory	Can engineered tissues exhibit safety and efficacy thresholds that will trigger FDA clearance for marketing?
Commercial	Can engineered tissues replace existing technologies with enhanced function and lower cost?
Social	Will caregivers and patients embrace engineered tissues as solutions to multiple healthcare problems?

TABLE 39.2 Stakeholders

Stakeholders	Primary Concerns
Patients	Safety, efficacy, cost
Caregivers	Safety, efficacy, cost, ease of use, improvement upon other technology
Payers	Safety, efficacy, cost-effectiveness
Scientists/engineers	Technically possible
Research funding agencies	Probability of technical success and successful application in humans
Regulatory bodies	Safety and efficacy
Investors/companies/employees	Commercial profitability
General public	Understandability and acceptability as a technology; nonthreatening

Note: The stakeholders in the field of tissue engineering represent a complex set of capabilities and interests, all of which must be considered in the assignment of strategic directions for the field.

39.2 Previous Approaches to the Assignment of Strategic Directions in Tissue Engineering

While there have been several scholarly assessments of the state of technical and commercial development in tissue engineering, formal, pan-stakeholder strategic directions have seldom been a focus of such work.¹⁻⁹ In a 2007 publication,³ Johnson et al. reviewed a general, primarily technical strategy for the field. Using Hoshin strategic assessment methodology, the authors surveyed the worldwide editorial board of the journal, *Tissue Engineering*. By putting forth a goal of strong clinical penetration of tissue engineering technologies by the year 2021, they were able to elicit those steps that the editors felt were required to achieve the goal. They then compared the relative dominance of the identified steps (Table 39.3) and incorporated an assessment of present progress (Table 39.4) to further stratify the steps by priority. The result is shown in Table 39.5.

This study had the advantage of inclusion of international participants but was limited to a single component of the stakeholder pool—scientists and engineers. Although certainly not causal, the article presaged the recent explosion of literature in the angiogenesis,¹⁰ stem cell,¹¹ and systems biology categories. Since these were deemed the most critical positive influencers of the other steps, it remains to be seen how technical accomplishments in the field will accelerate as a consequence. The article also identifies technology development funding as a critical element but perhaps surprisingly, only as a follower to the other strategic steps. A cohesive story and preliminary data, after all, are always requirements for

TABLE 39.3 Relative Dominance of Strategic Steps

Strategic Step	Relative Dominance
Stem cell science	12
Molecular biology/systems biology	11
Clinical understanding/interaction	10
Cell sourcing and cell/tissue interaction	10
Angiogenic control	9
Immunologic understanding and control	7
Standardized models	5
Regulatory transparency	5
Multidisciplinary understanding/cooperation	5
Manufacturing/scale up	4
Enhanced biomaterial functionality	4
Expectation management/communication	2
Pharmacoeconomic/commercial pathway	1
Multilevel funding	0

Note: All of the strategic steps listed are considered to be critical to the achievement of the goal. However, their relative dominance is shown on the right as the number of other steps over which they are felt to be stronger in a pairwise comparison.³

TABLE 39.4 Strategic Steps: Progress to Date (2007)

Strategic Step	Progress to Date (2007)
Multidisciplinary understanding/cooperation	6.5
Expectation management/communication	5.5
Multilevel funding	4.8
Enhanced biomaterial functionality	4.8
Standardized models	4.8
Clinical understanding/Interaction	4.5
Regulatory transparency	4.5
Molecular biology/systems biology	4.0
Cell sourcing and cell/tissue characterization	3.8
Stem cell science	3.8
Pharmacoeconomic/commercial pathway	3.8
Manufacturing/scale up	3.5
Immunologic understanding and control	3.5
Angiogenic control	2.8

Note: Progress was semi quantitatively assigned using a continuous scale from 1 = No Progress to 10 = Fully Complete.³

funding to occur. Future articles of this type would do well to enhance inclusion of the stakeholder pool along the lines outlined in [Table 39.1](#).

39.3 Tools in the Identification of Strategic Directions

39.3.1 Identification of Concepts Having General Criticality

It is often difficult to physically assemble a significant number of representatives of the stakeholder pools shown in [Table 39.1](#) in order to gain their feedback on the elements of strategic direction for a field.

TABLE 39.5 Normalized Dominance of Strategic Steps

Normalized Dominance of Strategic Steps	Ratio of Dominance/ Progress
Angiogenic control	3.3
Stem cell science	3.2
Molecular biology/systems biology	2.8
Cell sourcing and cell/tissue characterization	2.7
Clinical understanding/interaction	2.2
Immunologic understanding and control	2.0
Manufacturing/scale up	1.1
Regulatory transparency	1.1
Standardized models	1.1
Enhanced biomaterial functionality	0.8
Multidisciplinary understanding/cooperation	0.8
Expectation management/communication	0.4
Pharmacoeconomic/commercial pathway	0.3
Multilevel funding	0.0

Note: When the Relative Dominance number in Table 39.3 is divided by the Progress number in Table 39.4, a normalization of strategic step priority is achieved. This approach enables the identification of the sequence of steps that will be the most efficient in the achievement of the goal.³

TABLE 39.6 Generally Critical Concepts for Tissue Engineering

 Concepts Having General Criticality for Tissue Engineering

Clinical need
Degree of improvement over alternative therapy
Technical feasibility
Cost effectiveness
Likelihood to pass the regulatory process
Likelihood to be reimbursed
Manufacturability
Ease of distribution
Potential for general use
Likelihood of caregiver adoption
Degree to which free of biological risk

As previously discussed, online or mailed survey instruments may be effectively used to gain information from these groups. Table 39.6 depicts an example set of Generally Critical Concepts (GCC) that might be gleaned from a comprehensive survey of all stakeholder groups (in the author's estimation).

While good general directions can be gleaned in this fashion, it is difficult to determine specific technology development directions from them, such as which tissue or which clinical indication would be best to focus on at any point in time.

39.3.2 Cohesive Technology Opportunity Stratification

A follow-on methodology known as Cohesive Technology Opportunity Stratification (CTOS) can be used to leverage agreed-upon concepts having General Criticality in order to provide this functionality.

Briefly described, CTOS assembles GCC, weights them by their importance relative to one another and incorporates these weights into an algorithm-driven technology stratification spreadsheet. In the

latter, intensity of fit scales are developed under each Generally Critical Concept to allow assignment of a value to any technology being assessed. In addition, the weight of the GCC is multiplied by the scalar assignment in each column and these are summed for all GCCs as shown in [Figure 39.1](#). Weights and scales are ideally assigned/developed together by representatives of all stakeholder groups. An example of how weights are assigned is shown in [Table 39.7](#) (author's impressions are only shown).

While the assignment of weights in this example are the author's alone, they were assigned with a general appreciation for the points of view of the stakeholder groups in [Table 39.1](#). If these values were to be ratified in a formal pan-stakeholder survey and assignment, the relative criticality of concepts would be illuminating. For example, the likeliness of reimbursement, the ability to pass regulatory review, cost-effectiveness and absence of biological risk loom large in the assessment of any technology. Conversely, technical feasibility weighs in only weakly as a deciding element. This is because tissue engineering, to be successful as an applied medical discipline, must begin any assessment of its strategic direction at the "end." That is, any tissue engineering technology must pass through the same hurdles (reimbursement, regulation, cost-effectiveness, risk) as do present, nontissue engineering technologies. Another way to put this is that the most technically feasible tissue engineering technology is of little worth to humanity if it cannot pass through these critical hurdles that enable commercialization.

[Figure 39.1](#) shows the aforementioned Technology Stratification Spreadsheet. Note that the spreadsheet has both "Perfect" and "Threshold" entries. The Perfect technology would achieve the highest scalar scores for each of the GCCs. The Threshold technology values (numerics assigned by the author only) represent the minimum that would be acceptable for a tissue engineering technology to reach human use. Note that both the weighting and stratification mechanisms are time and progress-sensitive. Should there be changes in reimbursement or regulatory systems or if technology advanced rapidly to reduce risk and enhance cost-effectiveness, scalar and weight values could change, perhaps also changing the Threshold value for acceptable technology. These tools are simply provided as examples of ways in which the processing of strategic directions can be made more objective.

Also to be noted in [Figure 39.1](#) is that assigning scalar values for each GCC assesses several tissue targets for development. These are then processed according to the multiplication (by weight) and summation algorithm. Note the tissues that fall above and below the Threshold level at this point in time (author's numeric assignments only). A general assessment of the stakeholder pools in tissue engineering is presently underway and will be the topic of a future report. Until then, any stratification of this type must be considered tentative.

An analysis of this type takes into consideration the circumstances of the time of the analysis and perhaps a short look into the future only. As such, the tissue targets deemed most worthy of development today can change over time, as factors such as technical feasibility, reimbursability, regulatory clearance potential and the like change. The numbers shown in this analysis represent the best guess of the author only. In a formal strategic planning session, all stakeholder groups would agree upon these. In this analysis, there is no surprise that the tissues deemed most readily developable in today's timeframe have almost all demonstrated some degree of commercial momentum. Also, the temporal progression from 1D (cell) to 2D (planar sheets of cells and matrix) and 3D (vascularized organs or organoids) tissue development appears to hold up as a function of construct complexity.

39.3.3 Modulators of Strategy

As previously alluded, strategic direction represents a best guess as to the optimal course a field of endeavor can pursue, given present and immediate future restraints. However, what if these restraints are underestimated? Or better, what if new discoveries are made that bypass present restraints? Under these circumstances, a revisitation of strategy will be called for immediately, as the game will have changed. Modulators of strategy can come in many forms. [Table 39.8](#) illustrates several such unexpected modulators, both inhibitors and accelerators. It is important to watch for these, since they can have a major impact on the timing of development of the essential technology bases of the field.

Strategic Selection of Tissue Engineering Solutions

Criteria	Clinical Need	Degree of Improvement Upon Alternate Therapy	Technical Feasibility	Cost Effectiveness	Likelihood to Pass the Regulatory Process	Likelihood to Be Reimbursed	Manufacturability	Ease of Distribution	Potential for General Use	Likelihood of Caregiver Adoption	Degree To Which Free of Biological Risk	Total
	0 = None 1 = Minimal 2 = Clear 3 = Extensive 3	0 = None 1 = Minimal 2 = Clear 3 = Extensive 6	0 = Not Feasible 1 = Possible 2 = Probable 3 = Certain 1	0 = Not Cost Effective 1 = Possible 2 = Probable 3 = Certain 7	0 = Impossible 1 = Possible 2 = Probable 3 = Certain 9	0 = Impossible 1 = Possible 2 = Probable 3 = Certain 10	0 = Impossible 1 = Possible 2 = Probable 3 = Certain 3	0 = Impossible 1 = Possible 2 = Probable 3 = Certain 2	0 = None 1 = Minimal 2 = Clear 3 = Extensive 3	0 = Impossible 1 = Possible 2 = Probable 3 = Certain 4	0 = High Risk 1 = Medium 2 = Low 3 = None 7	
Solutions												
Perfect	3	3	3	3	3	3	3	3	3	3	3	165.0
Skin Equivalents	2.5	1.8	3	1.8	3	3	3	2.5	1.7	1.8	2	131.2
Ligament	3	2.5	2.5	1.8	2	2.3	2.5	3	3	2.7	2	127.4
Cartilage	3	2.5	2.5	1.5	2.3	2	2	3	3	2.7	2	123.5
Bladder	2.5	3	2.7	2	2	2	2	2	1.8	2.5	2	119.6
Vessels	3	3	2	1.8	1.8	1.8	2	2	2	2	2	113.8
Bone (Long)	3	2.3	2	1.8	2	2	2	2	2	2	2	113.4
Myocardial Stem Cells	3	2.5	0.8	1.7	1.8	2.2	2	2	2.5	2.5	1	109.4
Stem Cells (Tendon)	2	2	2.3	2	2	2	2.5	2.5	2.5	2.5	1	109.3
Threshold	2	2	2	2	2	2	2	1	1.5	2	2	106.5
Bone (Craniofacial)	1.6	2	2	1	1.5	1.5	2	2	2	2.5	2	94.3
Kidney	3	3	0.5	1	1	1.5	1.5	1	2	2	2	93.0
Heart Valve	2.5	1.8	2.3	1	1	1	2	2	2	2	2	84.6
Skeletal Muscle	1.3	1.5	1.5	1	1	1	1	1	2	2	2	73.4
Liver (Whole or Segment)	2.5	2	0.5	1	0.8	1	0.8	0.8	2	2	1.5	72.7
Neural Tissue	1.5	1.8	1	1	1	1	1	1	1.5	1.5	1.5	68.3

FIGURE 39.1 Example of comprehensive technology opportunity stratification, taking into consideration weighted General Critical Concepts and scalars. Each assigned scalar for each GCC is multiplied by the weight of that GCC and these are summed across all GCCs to provide the total. (Numbers assigned here are by the author only as an example.)

TABLE 39.7 Assignment of Weights to Generally Critical Concepts

	Clinical Need	Degree of Improvement upon Alternate Therapy	Technical Feasibility	Cost Effectiveness	Likelihood to Pass the Regulatory Process	Likelihood to Be Reimbursed	Manufacturability	Ease of Distribution	Potential for General Use	Likelihood of Care-giver Adoption	Degree to Which Free of Biological Risk	Weight
Clinical need									1	1	1	3
Degree of improvement upon alternate therapy	1		1				1	1	1	1		6
Technical feasibility	1											1
Cost effectiveness	1	1	1				1	1	1	1		7
Likelihood to pass the regulatory process	1	1	1	1			1	1	1	1	1	9
Likelihood to be reimbursed	1	1	1	1	1		1	1	1	1	1	10
Manufacturability	1		1					1				3
Ease of distribution	1		1									2
Potential for general use			1				1	1				3
Likelihood of caregiver adoption			1				1	1	1			4
Degree to which free of biological risk		1	1	1			1	1	1	1		7

Note: The GCCs in the leftmost column are compared to all other GCCs in the topmost column. If the leftmost column GCC is more critical than the topmost row GCC, a “1” is placed in the cell. If the reverse, the cell is left blank. The rightmost column depicts the summed weight of relative criticality of leftmost column GCCs.

TABLE 39.8 Modulators of Strategy

Inhibitors	Accelerators
Enhanced risk aversion of regulatory bodies	New evidence supporting the safety and efficacy of engineered tissues
Federal restrictions on stem cell research	New, enhanced federal financial and legal support for stem cell research
New evidence that tissue vascularization cannot be maintained in vitro	Identification of genes responsible for the modular vascularization of tissues in any environment
Limited interdisciplinary understanding and cooperation	New educational methodologies that enable standardized cross-disciplinary understanding

Note: Example inhibitors and accelerators of strategy are shown. Each type can substantially alter the verity of previously described strategic directions. In the event that any such modulator is material, a new assessment of strategic directions should be undertaken.

In Table 39.8, one of the identified Inhibitors of strategy is “Limited Interdisciplinary Understanding and Cooperation.” This has recently been formally investigated in a survey of the membership of the Tissue Engineering and Regenerative Medicine Society, North American chapter (TERMIS-NA)¹² that was carried out by that organization’s Industry Committee. In an attempt to understand the hurdles to commercialization of tissue engineering technologies, members were asked to assign themselves to one of the following groups, based upon their present employment:

- Academia
- A Start-Up Company (i.e., having products in early development)
- A Development Stage Company (i.e., having products in late development or early sales)
- An Established Company (i.e., ongoing, predictable product sales and growth)

In an online survey, sets of group-specific feasible hurdles were presented to participants. They were asked to identify the most difficult hurdles not only for their group *but for all other groups, as well*. This enabled the authors to determine what each group identified as its critical hurdles to product commercialization. In addition, it enabled the authors to determine the degree to which cross-disciplinary understanding (or its lack) might contribute to the modulation of strategy.

The authors also asked survey participants to characterize the intensity of the difficulties of their hurdles, relative to the perceived hurdles of other groups.

The results are interesting. Not only did all groups assess their own hurdles as significantly more difficult than those of other groups but there was an approximately 40% error in the assessment of the specific difficult hurdles of other groups. In other words, in a field such as ours that needs technology to be handed off to ever better structured commercial entities in order to reach the marketplace, there are multiple barriers to understanding—probably a clearly Inhibitory modulator. The Industry Committee of TERMIS-NA is using these data to structure its educational programs to rectify this situation—an example of action that may provide an Acceleratory modulation of strategy. Clearly, of all the Inhibitors and Accelerators of strategy, the human element looms largest.

39.4 Summary

The development of strategic directions is not a rote exercise though it can be approached objectively. Reduced to its essentials, it is very similar to the way in which design engineers clarify the nuanced elements of successful products. They do this by first asking any and every person who may be impacted by the technology to offer their opinion regarding form and function. They then stratify features by priority for inclusion in the ultimate product.

Tissue engineering products have the potential to deeply impact the future of medicine. However, not all potential tissue engineering products have the same probability of technical or commercial success. Leveraging stakeholder understanding to identify GCCs that serve as success filters sets the stage for the rational stratification of potential products. Any such analysis represents only the reality of a point in time and certainly should not inhibit creative endeavor among investigators. However, the exercise creates a sense of inclusion for stakeholders, enhances mutual understanding by all parties and creates a mechanism for structured information sharing among investigators and others. Through greater and more structured information sharing, new and more rapid permutations of ideas may ensue. Ironically, the greatest benefit of this process may be the enhancement of the potential for *serendipity* in both technical and commercial development.

References

1. Advancing Tissue Science and Engineering: A Multi-Agency Strategic Plan, U.S. Government Multi-Agency Tissue Engineering Science (MATES) Interagency Working Group, National Science and Technology Council, 2007. Web site: <http://tissueengineering.gov/welcome-s.htm>.
2. McIntire, LV, Ed. *WTEC Panel on Tissue Engineering Research*, Academic Press, San Diego, 2003.
3. Johnson, PC, Mikos, AG, Fisher, JP, and Jansen, JA. Strategic directions in tissue engineering, *Tissue Eng.* 2007 Dec; 13(12):2827–37.
4. Lysaght, MJ, Jaklenec, A, and Deweerd, E. Great expectations: Private sector activity in tissue engineering, regenerative medicine, and stem cell therapeutics, *Tissue Eng. Part A* 2008 Feb; 14(2):305–15.
5. Lysaght, MJ and Hazlehurst, AL. Tissue engineering: The end of the beginning, *Tissue Eng.* 2004 Jan–Feb; 10(1–2):309–20.
6. Lysaght, MJ and Hazlehurst, AL. Private sector development of stem cell technology and therapeutic cloning, *Tissue Eng.* 2003 June; 9(3):555–61.
7. Lysaght, MJ and Reyes, J. The growth of tissue engineering, *Tissue Eng.* 2001 Oct; 7(5):485–93. Review.
8. Lysaght, MJ, Nguy, NA, and Sullivan, K. An economic survey of the emerging tissue engineering industry, *Tissue Eng.* 1998 Fall; 4(3):231–8.
9. Lysaght, MJ. Product development in tissue engineering, *Tissue Eng.* 1995 Summer; 1(2):221–8.
10. Johnson, PC and Mikos, AG. *Advances in Tissue Engineering: Volume 1—Angiogenesis*, Mary Ann Liebert, Inc., Publishers, New Rochelle, NY, 2010.
11. Johnson, PC and Mikos, AG. *Advances in Tissue Engineering: Volume 2—Stem Cells*, Mary Ann Liebert, Inc., Publishers, New Rochelle, NY, 2010.
12. Johnson, PC, Bertram, TA, Tawil, B, and Hellman, KB. Hurdles in tissue engineering/regenerative medicine product commercialization: A survey of North American academia and industry, *Tissue Eng., Part A* 2011 Jan; 17(1–2):5–15.

42

Engineered Protein Biomaterials

Andreina
Parisi-Amon
Stanford University
Sarah C.
Heilshorn
Stanford University

42.1	Engineered Protein Biomaterials as an Alternative to “Traditional” Biomaterials	42-1
42.2	Synthesis of Engineered Protein Biomaterials	42-3
42.3	Design of Engineered Protein Biomaterials	42-5
	Crosslinking Domains • Structural Domains • Degradation Domains • ECM Cell-Binding Domains • Cell–Cell Adhesion Domains • Cell-Directive Domains	
42.4	Applications of Engineered Protein Biomaterials	42-11
	References.....	42-11

42.1 Engineered Protein Biomaterials as an Alternative to “Traditional” Biomaterials

Materials that are ideal for *in vitro* cell studies and *in vivo* transplantation studies, en route to clinical translation, aim to mimic the complex milieu of biochemical and biomechanical signals found in the extracellular matrix (ECM) while remaining biocompatible and biodegradable. Protein engineering of biomaterials relies on the designer to dictate precise protein polymer sequences using amino acid building blocks, which in turn dictate the material’s structure and functionality. Coupled with recombinant technology, which permits direct genetic fusion of multiple peptide functionalities into a single protein, protein engineering aims to produce modular biomaterials that meet the goals of biocompatibility and biodegradability while enabling predictable cell–material interactions that dictate cell responses.

Deriving inspiration from nature, scientists have designed protein-engineered biomaterials that include specific peptide domains to direct crosslinking, material structure, degradation, cell-binding, growth factor-binding, and cell-signaling. The fusion of these various peptide domains to create a full-length, protein-engineered biomaterial results in an inherently modular design strategy. Combinatorial variation in domain choices and sequences creates a family of scaffolds with properties customized for different cell types and tissue engineering applications (Figure 42.1). The DNA sequence of the designed protein is then encoded in a recombinant DNA plasmid that is transformed into a host organism, which translates and transcribes the protein. The engineered protein is then harvested and purified for use as a biomaterial.

As seen in Figure 42.1, many peptide domains used in protein-engineered biomaterials are derived from amino acid sequences found in the natural ECM. Naturally existing biomaterials such as collagen and Matrigel (a complex mixture of biomacromolecules primarily consisting of laminin) clearly have physiologically relevant biofunctionalities, as they are harvested directly from mammalian sources. However,

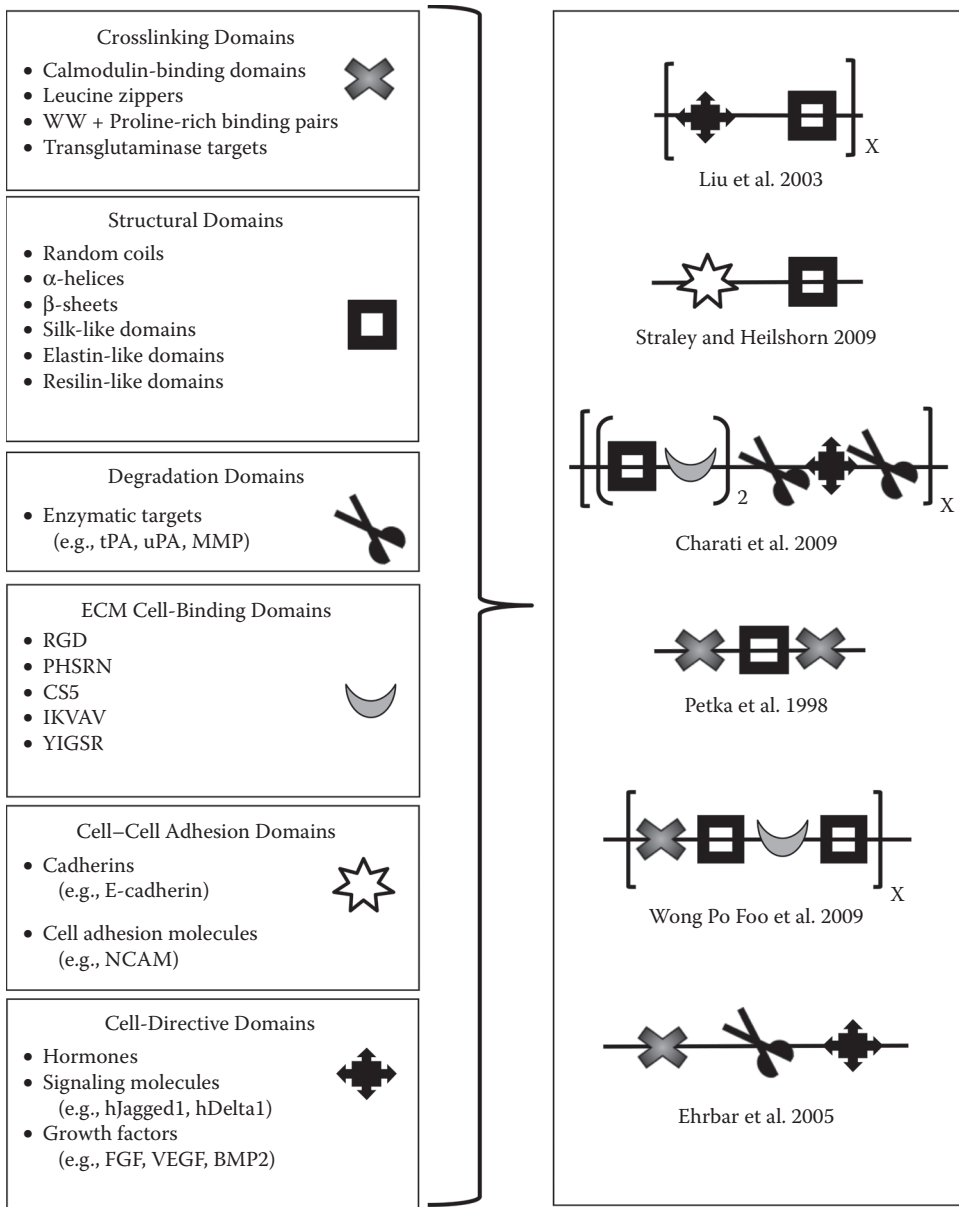


FIGURE 42.1 In the modular protein engineering design strategy, multiple peptide domains are fused together to design novel, multifunctional, recombinant protein polymers with specific properties.

while the complex biochemical compositions of these materials are valued for their ability to initiate multiple cellular signaling pathways, their compositions also make naturally derived materials nonideal, as their properties cannot be easily tailored. Moreover, harvesting and processing of these materials may destroy their higher-order structures (such as fibers) while also producing undesirable batch-to-batch variability. In addition, some natural materials are known to cause high levels of immunogenic response and can have additional clinical translation difficulties due to their mammalian origins. Borrowing bio-functional peptide domains from natural ECM proteins and including them within engineered proteins enables the creation of multifunctional biomaterials that address many of these concerns.

An alternative approach to create tailorable biomaterials is the use of synthetic polymers such as PEG (polyethylene glycol), PMMA (poly(methyl methacrylate)), PHEMA (poly(2-hydroxyethyl methacrylate)), and PLGA (poly(lactic-co-glycolic acid)) derivatives. While these materials are easily tailored, they are usually bio-inert without further modification. As such, these materials can only achieve biofunctionality with the incorporation of additional components such as ECM-derived peptides and proteins. Often however, these functional peptides play a role in the mechanical structure, making it difficult to independently tune the biofunctionality and mechanical properties of the biomaterial (Thompson et al. 2006). In addition, the synthetic chemistries inherent to these materials may carry the risk of toxic crosslinkers, activating agents, and degradation fragments (Williams et al. 2005, Seymour et al. 1987).

While protein-engineered biomaterials overcome some of the concerns associated with natural and synthetic biomaterials, they also have their own limitations. Before these materials can be considered for clinical translation, the laboratory-scale synthesis and purification processes typically used during the biomaterial design phase must be optimized to achieve efficient scale-up of production. Although the materials are generally made from protein building blocks native to the human body, rendering them cytocompatible and bioresorbable, they may nonetheless trigger an immunogenic response, particularly due to their synthesis in a foreign host organism. For example, proteins made in Gram-negative bacteria, such as *Escherichia coli* (*E. coli*), must be sufficiently purified to remove endotoxin, a lipopolysaccharide that can trigger an innate immune response (Rietschel et al. 1994). Even with these challenges, protein-engineered materials constitute an exciting area of biomaterials research given their exquisite design control that enables the creation of novel biomimetic cell scaffolds. In this chapter, we will focus on recent developments in the field of engineered protein biomaterials and highlight opportunities for future advances.

42.2 Synthesis of Engineered Protein Biomaterials

Following the design of a specific protein polymer (which is discussed in the following section), a variety of methods can be used to synthesize and purify the protein. Solid-phase synthesis is the process by which novel proteins are manually created through the sequential addition of individual amino acids (Kates and Albericio 2000). While this process has become more optimized and commonplace over the past several years, the resulting proteins are limited in length and the process is too time consuming and expensive to scale-up to the high levels of production needed for potential therapies. Instead, with the discovery of molecular cloning in the 1970s, scientists have been able to harness the protein factories that exist in nature—cells (Porro et al. 2005). Mammalian (Nagaoka et al. 2002), insect (Tomita et al. 1999), plant (Karg and Kallio 2009), fungal (yeast) (Graf et al. 2009), and bacterial (Zerbs et al. 2009) cells have all been used for recombinant protein synthesis, each with their advantages and disadvantages. Irrespective of the host, the creation of a protein through the cellular processes of transcription and translation is inherently advantageous, as it provides efficient molecular-level control of the protein synthesis. Furthermore, built-in accuracy and error-checking mechanisms by the ribosome ensure that the desired protein sequence is being produced (Zaher and Green 2009).

Choosing which host to use is a key step in recombinant protein synthesis, as it determines the complexity of the protein sequence that can be produced, as well as the efficiency with which the production can take place. Microorganisms such as *E. coli* and *Saccharomyces cerevisiae* (yeast), with their relative ease of genetic modification, low cost of culture, and high growth rates compared to mammalian cells, are often chosen as the host. In fact, for simple protein structures, prokaryotic *E. coli* is often the first host of choice due to its simplicity and versatility. However, for more complex proteins that require post-transcriptional processing for correct structure and resulting function, eukaryotic yeast, such as *S. cerevisiae* and *Pichia pastoris* are more often chosen, as they combine the high growth rate and simplicity of a single-celled microorganism with the organelles needed for specialized folding and modification.

Once the host is chosen, the exact nucleotide sequence must be designed, while keeping in mind that various hosts may have different tolerances to specific sequences. While some basic tenets are known,

such as the fact that highly repetitive sequences have an increased susceptibility of resulting in unwanted recombination events (Bzymek and Lovett 2001), it is difficult to predict *a priori* which sequences will have high translational efficiency and yield, therefore making sequence design an iterative process. To that end, scientists are working to create sequence design programs that use host-specific algorithms to improve expression (Gao et al. 2004). Once designed, the completed sequence is synthesized and introduced into the host cell for production. Culture conditions, such as pH, temperature, and oxygen abundance also play a complex role in the yield of protein production.

After protein production, the product must be collected from the cell, either through secretion or cell lysis, and then purified such that only the protein of interest remains. Purification can be achieved through various chromatographic methods, in which the product-containing solution is run through a resin-packed column that takes advantage of specific properties of the target protein, such as size, charge, hydrophobicity, or ligand binding. The basic process includes binding or capturing the protein of interest to the resin, allowing all impurities to run through, and then releasing the purified product for collection (Nilsson et al. 1997). Often multiple iterations are required to isolate the target protein with the desired level of purity. To scale up the process for larger yields, chromatographic methods are often deemed too expensive and time-intensive; therefore, alternative techniques utilizing differential target protein solubility are often developed. For example, target proteins that include an elastin-like sequence typically exhibit lower critical solution temperature behavior, whereby the protein forms a highly concentrated coacervate at elevated temperatures while most other contaminating proteins remain in solution (McPherson et al. 1996). This thermodynamic phenomenon can be exploited to purify the target protein through a simple sequence of centrifugations at alternating temperatures above and below the target protein's lower critical solution temperature (Meyer and Chilkoti 1999). Finally, additional purification may be needed to make the product cytocompatible for proteins expressed in Gram-negative bacteria such as *E. coli*. These target proteins are often contaminated with residual amounts of endotoxin (i.e., lipopolysaccharide), a component of the bacterial cell wall that can activate an innate immune

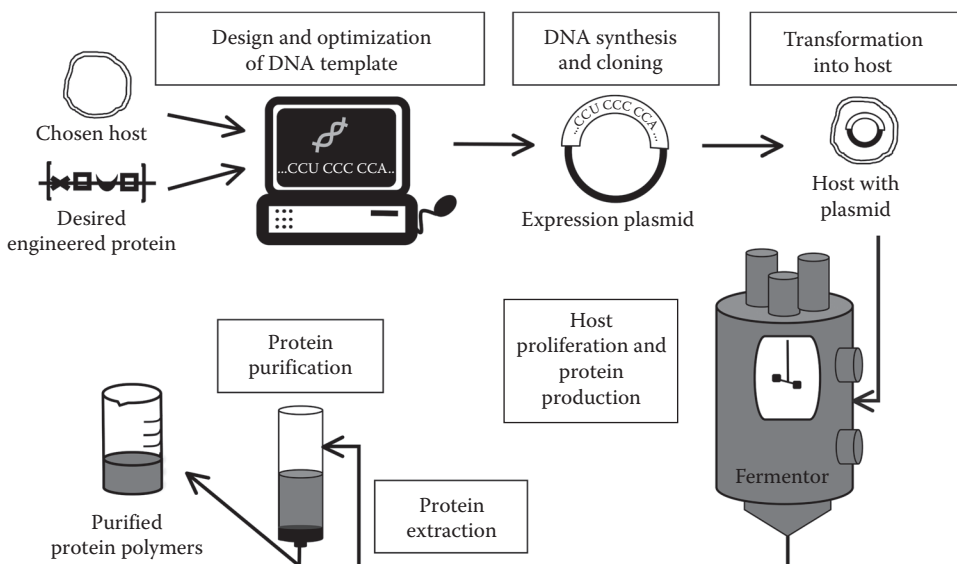


FIGURE 42.2 Design and synthesis of recombinantly engineered protein polymers. First, an expression host and target amino acid sequence are chosen. This information is used to design a DNA template that encodes the engineered protein polymer. After synthesis and cloning of the DNA template into a recombinant expression plasmid, the plasmid is introduced into the host organism. A fermentor is used to control environmental parameters during host proliferation and protein expression. Following protein extraction and purification, a pure sample of engineered protein polymer remains.

response. Several techniques have been developed for efficient endotoxin purification, with the most commonly used being an affinity-based column (Petsch and Anspach 2000).

Through iterative optimization, the use of microorganism hosts for recombinant protein engineering provides an economical and efficient method to synthesize engineered proteins in therapeutic quantities (Figure 42.2). Optimized protocols and laboratory-scale fermentors enable the growth of high-density cultures in volumes from 1 to 200 L, enabling the production of multigram protein yields (Heilshorn et al. 2003, Chow et al. 2006, Welsh and Tirrell 2000, Shiloach and Fass 2005).

42.3 Design of Engineered Protein Biomaterials

The inherent modularity of the peptide building-block design strategy of protein-engineered biomaterials provides the ability not only to design materials emulating a specific biological niche, but also to create a versatile family of materials simply through the inclusion or removal of singular peptide domains. The domains that are fused together to create full-length proteins can be classified by the functionalities they convey to the final product (Figure 42.1). For example, many biologically inspired domains can interact directly with cells through the promotion of cell–ligand interactions, cell–cell adhesion mimicry, or behavioral instruction (i.e., regulation of proliferation, differentiation, etc.). Alternatively, other domains can affect material properties, such as degradability and elastic modulus (i.e., the stiffness of a material), which may further direct cell behavior (Discher et al. 2005). Other selected domains can impart specific structural motifs, such as random coils (Davis et al. 2009), coiled-coils (Stevens et al. 2004), β -sheets (Marini et al. 2002), and hierarchical self-assembling domains (Chung et al. 2010) to the protein polymers, which affect the material's microstructure.

Historically, these peptides were identified by isolating domains of interest from naturally evolved proteins. The tripeptide RGD sequence (arginine–glycine–aspartic acid), a commonly used cell-adhesion domain, is a prime example of this. RGD was isolated in 1983 from the extracellular and plasma protein fibronectin and was identified as the minimal sequence necessary to promote cell-attachment properties (Pierschbacher and Ruoslahti 1984). Other commonly used domains include elastin-like sequences, which are derived from the protein elastin found in connective tissue (Meyer and Chilkoti 2002), and recombinant-silks (Prince et al. 1995). Both of these peptide domains are used to confer their unique mechanical properties (i.e., resilience, elasticity, and strength) to the resulting biomaterial.

More recently, the design of protein-engineered biomaterials has not been limited to domains found in nature. As computational design (Hin Yan Tong et al. 2002) and high-throughput screens (Sidhu et al. 2003) are increasingly being used in peptide development, the variety and specificity of domains available for biomaterials design are rapidly expanding. The design process, however, is not always straightforward. For example, the functionality of a given peptide can be affected by the context of the fully assembled protein, that is, the identity of the flanking peptide domains (Heilshorn et al. 2005). As such, the activity of the domains in each protein composition must be evaluated after the initial design phase. Another complication in peptide selection is the lack of clarity surrounding exactly which properties are imperative for specific niches. Because protein-engineered biomaterials are synthesized to include rationally chosen domains, this design strategy enables iterative testing and optimization of cell–material interactions to overcome both of the limitations discussed above. To illustrate this inherent design flexibility, the sections below give several specific examples of peptide domains identified from naturally evolved proteins, through computational design, or by high-throughput screening to confer specific biomaterial functionalities.

42.3.1 Crosslinking Domains

The inclusion of crosslinking domains enables the formation of a network from the individual designed protein polymer chains, forming two- and three-dimensional material structures with the desired mechanical integrity for supporting cells. Because many cellular behaviors, including spreading,

signaling, and gene transcription, are known to be responsive to the stiffness of the biomaterial, it is critical to exert control over this design variable in order to direct cell growth and differentiation (Discher et al. 2005). The monodispersity of recombinant proteins, resulting in polymers with identical composition, allows for the tight regulation of the frequency and distance between crosslinking sites, with higher crosslinking densities generating stiffer materials (Welsh and Tirrell 2000). Several crosslinking strategies exist for protein-engineered biomaterials, including enzymatic covalent crosslinking, chemical covalent crosslinking, and physical (i.e., noncovalent) crosslinking via peptide domains that associate through electrostatic or hydrophobic/hydrophilic interactions.

An example of enzymatic covalent crosslinking is the use of the enzyme transglutaminase (TGase). TGase is found naturally in the processes of wound healing and ECM stabilization, where it catalyzes covalent bond formation between lysine (K) and glutamine (Q) residues through a calcium-dependent reaction (Greenberg et al. 1991). Through a process of rational peptide design and screening, several amino acid sequences were identified to have high specificity and tight binding to TGase (Hu and Messersmith 2003). In one example, these optimized TGase crosslinking peptides were included as domains within a family of engineered proteins with varying molecular weights between the lysine-containing domains, resulting in a family of biomaterials with a fourfold range in modulus, from 4 to 16 kPa (Davis et al. 2010).

The binding of calmodulin protein to calmodulin-binding domains (CBDs) is another calcium-dependent crosslinking reaction, although this strategy results in physical (rather than covalent) crosslinks. Upon binding four calcium ions, calmodulin undergoes a conformational change, allowing it to bind to the hundreds of CBDs found in other proteins. This binding is reversible upon the depletion of calcium ions. The myriad of both natural and engineered CBDs improves the versatility of this binding method, as calmodulin–CBD pairs can be chosen with binding affinities that range over five-orders of magnitude and with differing calcium dependencies, ultimately enabling control over the material's modulus and the reversibility of network formation (Topp et al. 2006).

Leucine zippers comprise another interesting crosslinking domain that allows for reversible self-assembly, in this case through the noncovalent association of coiled-coil domains (Petka et al. 1998). Naturally evolved leucine zippers function as DNA-binding domains in various transcriptional regulatory proteins. The motif has been well characterized and is known for its heptad amino acid repeat with hydrophobic amino acids at positions one and four and charged amino acids at positions five and seven (Landschulz et al. 1988). At specific pH and temperature conditions, the zipper peptide folds into a helical structure with both hydrophobic residues on one face, promoting interhelical interactions between multiple folded zippers and leading to association. Connecting concatenated zipper motifs by a hydrophilic amino acid sequence creates a triblock co-polymer that utilizes the natural protein–protein interactions for the formation of a hydrogel, where the zipper domains provide the physical crosslinks (Petka et al. 1998). This system lends itself to independent tuning of both the hydrophilic domain (length, composition, and charge density) as well as the zipper domain (electrostatic charge), thereby fine-tuning the overall properties of the gelation phase diagram. Recently, additional functionality has been imparted into leucine zipper hydrogels through the incorporation of folded globular proteins. For example, the inclusion of an alcohol dehydrogenase with aldo–keto reductase activity (AdhD) into a leucine zipper protein polymer led to a thermostable, self-assembling hydrogel with enzymatic activity (Wheeldon et al. 2008).

WW and proline-rich domains represent another example of associating peptides that have been used to design protein-engineered hydrogels. Numerous WW domains, so named for their conserved tryptophan (W) residues, have been identified in intracellular proteins and also derived computationally (Russ et al. 2005). WW domains bind to proline-rich sequences, which are divided into several different classes with varying dissociation constants. The design of protein block copolymers containing multiple WW or proline-rich domains connected by hydrophilic peptide spacers enabled the formation of a mixing-induced, two-component hydrogel (Wong Po Foo et al. 2009). The large library of various WW and proline-rich domains allowed for modulation of the crosslinking strength, and hence hydrogel viscoelastic properties, based on the binding affinity of the chosen domains. In addition, the use of

transient physical crosslinks to form the protein hydrogel resulted in a shear-thinning and self-healing biomaterial, which is required for injectable therapeutic applications.

42.3.2 Structural Domains

In addition to the density of crosslinking sites, the mechanical properties of a protein-engineered biomaterial can also be controlled by including various structural peptide domains in the primary sequence. Elastomeric proteins contain domains that cause them to exhibit rubber-like elasticity, enabling them to undergo high levels of reversible deformation under high stress (Tamburro et al. 2010). Elastin and silk are elastomeric proteins that have been extensively studied and whose desirable mechanical properties have been incorporated into many different biomaterials. In addition to their structural properties, elastin-inspired polymers have been explored for use as injectable biomaterials and implantable scaffolds due to their biocompatibility and thermal sensitivity (Cappello et al. 1990). Through a combination of protein sequence selection and spinning conditions, silk fibers have an outstanding combination of mechanical properties—high strength, elasticity, and resistance to compression failure—that is highly desirable for biomaterials (Gosline et al. 1999). In addition, they have been found to have tunable degradation rates and to be biocompatible (Park et al. 2010). Attempting to harness these properties, researchers have succeeded in designing multiple versions of recombinant silk through expression in host systems, such as yeast, *E. coli*, and mammalian cells (Fahnestock and Bedzyk 1997, Asakura et al. 2003).

A recent addition to the library of structural domains included in protein-engineered biomaterials is resilin. This protein enables many insects to fly, jump, and vocalize, both by storing energy in sound-producing organs and by constraining vibrations during flight. Natural resilin from locusts and dragonflies has demonstrated a remarkable fatigue lifetime and up to 92% resilience (ability to recover after deforming under applied stress) (Tamburro et al. 2010, Elvin et al. 2005). Resilin-derived peptide sequences were observed to have no stable secondary structure and instead underwent continuous interconversion between extended (poly-L-proline II) and folded (β -turn) conformations, allowing resilin to act as an entropic spring. The structural resilin domain has been incorporated into engineered protein biomaterials combining multiple biofunctional domains, including the RGD ligand for cell binding, a matrix metalloproteinase-sensitive sequence for proteolytic degradation, and a heparin-binding domain for the binding and controlled release of growth factors (Charati et al. 2009). The crosslinked material was found to be both highly elastic and to promote cell attachment and proliferation, making it an ideal candidate for mechanically demanding tissue engineering applications.

Another way to use proteins as structural domains is to harness their self-associative interactions to create specifically shaped nanostructures. For example, structures such as hollow cages may be used as drug or gene delivery materials (Uchida et al. 2007), while self-assembled compact structures, such as M13 bacteriophages, can be used to display a high density of a cell-binding peptide (Chung et al. 2010). While the above examples utilized protein self-assembly to form naturally evolved structures, scientists can also mix and match various peptide domains to form novel self-assembling nanostructures. As an example, several rigid α -helical peptide domains that either dimerize or trimerize were fused together at specific angles to create a family of engineered proteins that self-assembled into both cage-like and filamentous nanostructures (Padilla et al. 2001).

42.3.3 Degradation Domains

For many tissue engineering applications, the ideal biomaterial will eventually fully degrade, thereby promoting cell invasion and allowing the injured site to be completely replaced by new host tissue. The ability to degrade can be incorporated into protein-engineered biomaterials by incorporating peptide domains that undergo proteolytic degradation in response to cell-secreted protease enzymes. Matrix metalloproteinases (MMPs), such as collagenase, are proteases that have been recognized as key in cell

migration (Moses 1997, Gailit and Clark 1994). Seminal work proving the concept of engineered biodegradation was performed using synthetic PEG polymers crosslinked by synthesized peptides that served as proteolytic MMP-target sites (West and Hubbell 1999). Building on this work, the use of proteolytic target peptides to enable biodegradation has been extended to a wide range of synthetic polymeric biomaterials and recombinant protein-engineered biomaterials.

The designed biomaterial degradation rate can be tailored by controlling the concentration of protease degradation sites within the engineered protein or by altering the amino acid sequence of the protease target site. As an example, elastin-like domains were alternated with proteolytic target sites that degrade in response to tissue plasminogen activator (tPA) or urokinase plasminogen activator (uPA), enzymes produced by endothelial and neuronal cells (Straley and Heilshorn 2009b). Altering the three flanking residues upstream of the proteolytic target site resulted in a family of engineered proteins with 97% sequence homology, identical mechanical properties, and a 200-fold range in protease degradation rate. Engineered proteins with differing degradation kinetics were patterned to form composite biomaterials that sequentially degraded to reveal internally patterned three-dimensional structures. The engineered proteins were further modified to enable the release of two encapsulated small molecules with distinct spatial and temporal delivery profiles (Straley and Heilshorn 2009b).

The well-planned placement of proteolytic degradation sites has also been utilized to control the release of tethered growth factors such as vascular endothelial growth factor (VEGF) (Ehrbar et al. 2005). In this example, a plasmin cleavage site was placed between the VEGF and a crosslinking domain that enabled tethering of the recombinant engineered protein to a fibrin biomaterial. This design enabled slow, plasmin-induced release of the VEGF that could be predictably tuned through implementation of a simple mathematical model. Clearly there are a multitude of variations that can be conceived from this framework, using different degradation sites and various growth factors, cytokines, or other signaling molecules. An especially interesting scenario would be one in which multiple growth factors are tethered into a single biomaterial and released in a timed manner to emulate a specific developmental pathway. These examples show great promise for the advent of biomaterials that not only degrade in response to cell-secreted proteases, but also undergo three-dimensional pattern formation or biochemical release to further direct cell behavior.

42.3.4 ECM Cell-Binding Domains

A central role of the ECM is to mediate cellular adhesion through peptide ligands that are recognized by various cell-surface receptors, most notably integrins. Integrins are a class of heterodimeric, transmembrane receptors that exist in a variety of sub-unit combinations. Many cell types present several different integrin receptor combinations on their cell surfaces at different times (Plow et al. 2000). Integrin–ligand binding induces multiple intracellular signaling cascades that can influence cell morphology, migration, gene expression, and differentiation. To recreate these cell-binding events in engineered materials, peptides identified as cell-binding domains from ECM proteins are commonly incorporated into synthetic polymeric and protein-engineered biomaterials. Exemplifying the complexity often found in natural systems, certain peptide ligands are substrates for multiple integrins, certain integrins are receptors for multiple peptide ligands, and certain peptide ligands are present in multiple ECM proteins (Ruoslahti and Pierschbacher 1987, Ruoslahti 1988). Given this complexity, the presentation of peptide ligands within engineered biomaterials offers an opportunity to mechanistically study integrin signaling responses. By presenting various cell-binding domains within an engineered protein biomaterial, scientists often can control the identity and concentration of peptide ligands without altering other material properties such as mechanical stiffness. For example, two different fibronectin-derived peptide ligands, RGD and REDV, were included as cell-binding domains interspersed with elastin-like domains to form two different protein-engineered biomaterials with different integrin specificities. In a direct comparison, human umbilical vein endothelial cells were observed to spread more rapidly and adhere more strongly to the RGD-containing proteins (Liu et al. 2004).

In a second example, the activity of the RGD domain was studied in combination with the so-called “synergy site” of fibronectin, PHSRN. Each cell-binding domain was fused to a serine esterase to enable covalent linkage of the engineered protein to a self-assembled monolayer (Eisenberg et al. 2009). While both domains were observed to independently mediate adhesion, RGD presented a much higher binding affinity. However, at relatively low ligand densities, the co-presentation of PSHRN with RGD led to more efficient cell adhesion than the presentation of RGD alone, confirming the synergistic interaction of these two binding domains.

In addition to exerting control over cell adhesion, ECM cell-binding domains can also be employed to influence cell morphology and phenotype. For example, the cell-binding domain IKVAV, naturally found at the end of the $\alpha 1$ chain of laminin, has been utilized to promote neurite outgrowth from neuronal cells on protein-engineered biomaterials (Nakamura et al. 2009). Similarly, the IKVAV domain has also been implicated in promoting endothelial cell migration and angiogenic behavior (Nakamura et al. 2008). In a direct comparison of RGD and IKVAV cell-binding domains incorporated within self-assembling β -sheet hydrogels, the RGD domain promoted firm endothelial cell adhesion and a traditional cobblestone-like cell morphology, while the IKVAV domain promoted minimal cell adhesion and a spindle-shaped, elongated cell morphology (Jung et al. 2009). These results corroborate previous findings that suggest the IKVAV domain may promote a more migratory endothelial cell phenotype (Schnaper et al. 1993).

Often, the minimal amino acid sequence known to induce integrin binding may have a slightly altered functionality compared to the exact same sequence presented within the context of the full-length, naturally evolved protein. Similarly, when ECM cell-binding domains are incorporated into protein-engineered biomaterials, the context of the flanking amino acid residues can greatly impact the functionality. Often, the minimal amino acid sequence is flanked by spacer sequences to enhance conformational flexibility or a larger amino acid sequence derived from the natural ECM protein. Even in these cases, amino acid choice quite distal to the ECM cell-binding domain can alter cellular response, as observed by differential strengths of cell adhesion to two engineered proteins containing identical REDV domains and different elastin-like domains (Heilshorn et al. 2005). Recently, this ability to alter peptide ligand conformational stability has been utilized to modulate integrin specificity and ultimately differentiation of mesenchymal stem cells (Martino et al. 2009).

These few examples demonstrate how optimization of ligand identity, ligand concentration, and ligand stability can be used to impart cell-instructive properties to protein-engineered biomaterials. As additional mechanistic insight is gained into the actions of integrin signaling (both in response to single ligands or combinations of ligands), the development of cell-instructive biomaterials is expected to increase.

42.3.5 Cell–Cell Adhesion Domains

Cell–cell interactions mediate many aspects of cell behavior, including proliferation, migration, and differentiation. These interactions range from stable cell–cell junctions formed within epithelial linings to the transient influence of immune cells on white blood cells during infection. These cell–cell interactions are generally mediated through cell–cell adhesion proteins presented on the cell surface such as selectins, cadherins, and members of the immunoglobulin (Ig) superfamily (Cooper 2000). Similar to the integrin-binding domains described above, cell–cell binding domains can be incorporated into protein-engineered biomaterials to mimic the action of cell–cell interactions and exert control over cell behavior.

As an example, E-cadherin forms calcium-dependent cell–cell adhesion homophilic interactions that are needed for tissue morphogenesis and the maintenance of organized solid tissues (Nagaoka et al. 2010). The E-cadherin extracellular domain was fused to the heavy chain, crystallizable fragment (Fc) of the IgG antibody to form an engineered protein that could be easily tethered to tissue-culture plastic surfaces through adsorption of the Fc region, resulting in presentation of the E-cadherin domain. Hepatocyte culture on this substrate induced cellular responses typical of increased cell–cell interactions, including decreased proliferation and promotion of the differentiated phenotype (Nagaoka et al.

2002). Embryonic stem cells cultured on these E-cadherin-mimetic surfaces did not form colonies, retained their pluripotency, displayed increased proliferation, and had higher transfection efficiency than cells in colony-forming cultures (Nagaoka et al. 2006).

The Ig superfamily includes both cell surface and soluble proteins involved in many roles of cell recognition, binding, and adhesion, all linked by the common “Ig fold” structure of immunoglobulins. Some members of the superfamily, such as the Neural Cell Adhesion Molecule (NCAM), fall in the cell–cell adhesion domain category. NCAM is found on the surfaces of most neural cells and is involved in cell–cell interactions during brain development, synaptic plasticity, and regeneration (Cambon et al. 2004). Peptides encompassing different portions of NCAM have been identified and found to influence neurite growth (Soroka et al. 2002). These peptides are promising for use in biomaterials focused on neural regeneration; for example, recently a fusion protein was created that combines an elastin-like sequence and the P2 peptide of NCAM (Straley and Heilshorn 2009a).

42.3.6 Cell-Directive Domains

The category of cell-directive domains includes hormones, growth factors, cytokines, and other signaling molecules. These molecules generally act in a cell-type specific and context-dependent manner to modulate many cell processes, including proliferation, differentiation, migration, adhesion, and gene expression (Silva et al. 2009).

For example, growth factors such as VEGF, fibroblast growth factor (FGF), and bone morphogenetic protein-2 (BMP2) have been studied extensively for their important roles in wound healing, angiogenesis, and bone formation, respectively. While growth factors often have been blended with or tethered to synthetic materials to impart biofunctionality, the recombinant synthesis strategy of producing protein-engineered biomaterials enables the direction incorporation of growth factor domains within the primary polymeric backbone. One such example was discussed previously in Section 42.3.3, where a VEGF domain was fused to a proteolytic target domain and a crosslinking domain (Ehrbar et al. 2005). A second example is the linking of FGF to the RGD cell-binding domain of fibronectin, resulting in a fusion protein with enhanced angiogenic activity (Hashi et al. 1994). Another family of cell-directive molecules includes the hDelta1 and hJagged1 domains, which make up part of the Notch signaling pathway that is key in cell developmental fate decision-making (Beckstead et al. 2006). Both of these functional domains have been interspersed within elastin-like structural domains to create a family of covalently crosslinkable proteins for Notch activity modulation (Liu et al. 2003).

An interesting example within this category is the p21 peptide, which induces cell cycle arrest by interfering with proliferating cell nuclear antigen function and inhibiting cyclin-dependent-kinase activity (Mutoh et al. 1999). This peptide is being investigated for potential cancer therapeutics to target tumor cells and prevent their continued proliferation. The p21 peptide was fused to the C-terminus of an elastin-like domain to render the engineered protein thermally responsive (Massodi et al. 2010). At temperatures below the critical solution temperature, the engineered protein remains soluble, while at higher temperature a reversible aggregate is formed. Thermal induction of aggregation may enable specific targeting of the p21 peptide to a heated solid tumor. In addition, a cell penetrating peptide was fused to the N-terminus of the engineered protein, resulting in increased cellular uptake by cancerous cells (Massodi et al. 2010).

The six peptide domain categories described above are the functionalities most commonly incorporated into protein-engineered biomaterials. Despite the large library of potential peptide domains that are included in these categories, the immense diversity of other potential peptide functionalities has only begun to be realized. Recently, a wide variety of other peptide functionalities, such as inorganic precipitation domains (Wong Po Foo et al. 2006), enzymatic domains (Lu et al. 2010), and enzymatic inhibitor domains (Roberge et al. 2002) have been successfully designed into protein-engineered biomaterials. As the protein-engineered biomaterials field continues to mature, it is expected that an increasing diversity of multifunctional, cell-responsive biomaterials will continue to be developed for a variety of applications.

42.4 Applications of Engineered Protein Biomaterials

The two most common applications of protein-engineered biomaterials are (i) use as an ECM-mimetic for studies of cell–environment interactions and (ii) various potential clinical uses. Due to their modular design and exact biosynthesis, protein-engineered biomaterials are ideal platforms for reductionist biological studies. Protein-engineered biomaterials are highly reproducible, engineered matrices that may represent a more physiologically relevant *in vitro* environment compared to traditional cell culture on rigid tissue-culture polystyrene. Because matrix biochemistry, biophysics, and dimensionality (i.e., two- versus three-dimensional environments) are all known to impact cell behavior, utilizing a reproducible cell culture platform that attempts to recreate key aspects of the *in vivo* ECM may lead to more physiologically relevant results. In addition, insights gained from these fundamental investigations of cell response will lead to enhanced understanding of cell–peptide domain interactions, thereby informing the design of future protein-engineered biomaterials.

Protein-engineered biomaterials aimed for use in the clinic include space-filling and structural implants for tissue engineering, as well as injectable materials that function as cell carriers, endogenous cell recruiters, or delivery systems for drugs, growth factors, and other signaling molecules. While many exciting and promising research projects are underway, the barrier to entering clinical trials is high, as the final product must prove to be efficacious and safe, as well as cost-effective with scalable production. As with all biomaterials, a panel of preclinical and clinical safety studies, including potential negative immune system responses, must be performed prior to potential commercialization. Another critical consideration is the ease of use of the material in a clinical setting and the roles of the physician and the patient in deploying the biomaterial. For example, an implant whose use requires a more invasive and time consuming surgery, a disadvantage for both the patient's health and the physician's time, is much less likely to be adopted than a material that can be implanted through a comparatively less invasive injection.

A current example of a protein-engineered biomaterial entering the clinical landscape is that of NuCore® Injectable Nucleus, which is being investigated as a replacement for disc tissue lost due to herniation or surgery to reduce disc degeneration, with the goal of easing the associated back and leg pain. The material is a fusion protein combining silk-like and elastin-like domains, one of which is altered to allow enable chemical crosslinking (Boyd and Carter 2006). The properties of the material have been designed to closely emulate the pH, complex modulus, and protein and water content of natural disc tissue (Boyd and Carter 2006). Initially developed by Protein Polymer Technologies, Inc., NuCore was approved by the United States Food and Drug Administration (FDA) for Investigational Device Exemption (IDE) feasibility studies in 2006 under the direction of Spine Wave, Inc. Results of a 2-year follow-up pilot clinical study were promising, showing NuCore to be biocompatible and effective in reducing the back and leg pain that accompanies herniated lumbar discs requiring surgery (Berlemann and Schwarzenbach 2009).

The continued progress of protein-engineered biomaterials, such as NuCore, toward clinical approval is very encouraging and exciting for the entire field. With the wide-variety of multi-functional, protein-engineered biomaterials that are currently the subject of intense research and preclinical trials and the immense future potential to include new biofunctionalities into these materials, it seems imminent that this class of materials will bring forward a new realm of therapies as they enter clinical use in the near future.

References

- Asakura, T., Nitta, K., Yang, M. et al. 2003. Synthesis and characterization of chimeric silkworm silk. *Biomacromolecules*, 4: 815–20.
- Beckstead, B. L., Santosa, D. M., and Giachelli, C. M. 2006. Mimicking cell-cell interactions at the biomaterial-cell interface for control of stem cell differentiation. *J Biomed Mater Res A*, 79: 94–103.

- Berlemann, U. and Schwarzenbach, O. 2009. An injectable nucleus replacement as an adjunct to microdiscectomy: 2 year follow-up in a pilot clinical study. *Eur Spine J*, 18: 1706–12.
- Boyd, L. M. and Carter, A. J. 2006. Injectable biomaterials and vertebral endplate treatment for repair and regeneration of the intervertebral disc. *Eur Spine J*, 15 Suppl 3: S414–21.
- Bzymek, M. and Lovett, S. T. 2001. Instability of repetitive DNA sequences: The role of replication in multiple mechanisms. *Proc Natl Acad Sci USA*, 98: 8319–25.
- Cambon, K., Hansen, S. M., Venero, C. et al. 2004. A synthetic neural cell adhesion molecule mimetic peptide promotes synaptogenesis, enhances presynaptic function, and facilitates memory consolidation. *J Neurosci*, 24: 4197–204.
- Cappello, J., Crissman, J., Dorman, M. et al. 1990. Genetic engineering of structural protein polymers. *Biotechnol Prog*, 6: 198–202.
- Charati, M. B., Ifkovits, J. L., Burdick, J. A., Linhardt, J. G., and Kiick, K. L. 2009. Hydrophilic elastomeric biomaterials based on resilin-like polypeptides. *Soft Matter*, 5: 3412–6.
- Chow, D. C., Dreher, M. R., Trabbic-Carlson, K., and Chilkoti, A. 2006. Ultra-high expression of a thermally responsive recombinant fusion protein in *E. coli*. *Biotechnol Prog*, 22: 638–46.
- Chung, W.-J., Merzlyak, A., and Lee, S. 2010. Fabrication of engineered M13 bacteriophages into liquid crystalline films and fibers for directional growth and encapsulation of fibroblasts. *Soft Matter*, 6: 4454–9.
- Cooper, G. M. 2000. The cell surface: Cell–cell interactions. *The Cell: A Molecular Approach*. 2nd Edition ed. Sunderland, MA: Sinaur Associates.
- Davis, N. E., Ding, S., Forster, R. E., Pinkas, D. M., and Barron, A. E. 2010. Modular enzymatically cross-linked protein polymer hydrogels for *in situ* gelation. *Biomaterials*, 31: 7288–97.
- Davis, N. E., Karfeld-Sulzer, L. S., Ding, S., and Barron, A. E. 2009. Synthesis and characterization of a new class of cationic protein polymers for multivalent display and biomaterial applications. *Biomacromolecules*, 10: 1125–34.
- Discher, D. E., Janmey, P., and Wang, Y. L. 2005. Tissue cells feel and respond to the stiffness of their substrate. *Science*, 310: 1139–43.
- Ehrbar, M., Metters, A., Zammaretti, P., Hubbell, J. A., and Zisch, A. H. 2005. Endothelial cell proliferation and progenitor maturation by fibrin-bound VEGF variants with differential susceptibilities to local cellular activity. *J Control Release*, 101: 93–109.
- Eisenberg, J. L., Piper, J. L., and Mrksich, M. 2009. Using self-assembled monolayers to model cell adhesion to the 9th and 10th type III domains of fibronectin. *Langmuir*, 25: 13942–51.
- Elvin, C. M., Carr, A. G., Huson, M. G. et al. 2005. Synthesis and properties of crosslinked recombinant pro-resilin. *Nature*, 437: 999–1002.
- Fahnestock, S. R. and Bedzyk, L. A. 1997. Production of synthetic spider dragline silk protein in *Pichia pastoris*. *Appl Microbiol Biotechnol*, 47: 33–9.
- Gailit, J. and Clark, R. A. F. 1994. Wound repair in the context of extracellular matrix. *Current Opinion in Cell Biology*, 6: 717–25.
- Gao, W., Rzewski, A., Sun, H., Robbins, P. D., and Gambotto, A. 2004. UpGene: Application of a web-based DNA codon optimization algorithm. *Biotechnol Prog*, 20: 443–8.
- Gosline, J. M., Guerette, P. A., Ortlepp, C. S., and Savage, K. N. 1999. The mechanical design of spider silks: From fibroin sequence to mechanical function. *Journal of Experimental Biology*, 202: 3295–303.
- Graf, A., Dragosits, M., Gasser, B., and Mattanovich, D. 2009. Yeast systems biotechnology for the production of heterologous proteins. *FEMS Yeast Research*, 9: 335–48.
- Greenberg, C. S., Birkbichler, P. J., and Rice, R. H. 1991. Transglutaminases: Multifunctional cross-linking enzymes that stabilize tissues. *FASEB J*, 5: 3071–7.
- Hashi, H., Hatai, M., Kimizuka, F., Kato, I., and Yaoi, Y. 1994. Angiogenic activity of a fusion protein of the cell-binding domain of fibronectin and the basic fibroblast growth-factor. *Cell Structure and Function*, 19: 37–47.
- Heilshorn, S. C., Dizio, K. A., Welsh, E. R., and Tirrell, D. A. 2003. Endothelial cell adhesion to the fibronectin CS5 domain in artificial extracellular matrix proteins. *Biomaterials*, 24: 4245–52.

- Heilshorn, S. C., Liu, J. C., and Tirrell, D. A. 2005. Cell-binding domain context affects cell behavior on engineered proteins. *Biomacromolecules*, 6: 318–23.
- Hin Yan Tong, A., Drees, B., Nardelli, G. et al. 2002. A combined experimental and computational strategy to define protein interaction networks for peptide recognition modules. *Science*, 295: 321–4.
- Hu, B. H. and Messersmith, P. B. 2003. Rational design of transglutaminase substrate peptides for rapid enzymatic formation of hydrogels. *J Am Chem Soc*, 125: 14298–9.
- Jung, J. P., Nagaraj, A. K., Fox, E. K. et al. 2009. Co-assembling peptides as defined matrices for endothelial cells. *Biomaterials*, 30: 2400–10.
- Karg, S. R. and Kallio, P. T. 2009. The production of biopharmaceuticals in plant systems. *Biotechnology Advances*, 27: 879–94.
- Kates, S. A. and Albericio, F. 2000. *Solid-Phase Synthesis: A Practical Guide*, New York, Marcel Dekker, Inc.
- Landschulz, W. H., Johnson, P. F., and Mcknight, S. L. 1988. The leucine zipper: A hypothetical structure common to a new class of DNA binding proteins. *Science*, 240: 1759–64.
- Liu, C. Y., Apuzzo, M. L. J., and Tirrell, D. A. 2003. Engineering of the extracellular matrix: Working toward neural stem cell programming and neurorestoration—Concept and progress report. *Neurosurgery*, 52: 1154–65.
- Liu, J. C., Heilshorn, S. C., and Tirrell, D. A. 2004. Comparative cell response to artificial extracellular matrix proteins containing the RGD and CS5 cell-binding domains. *Biomacromolecules*, 5: 497–504.
- Lu, H. D., Wheeldon, I. R., and Banta, S. 2010. Catalytic biomaterials: Engineering organophosphate hydrolyase to form self-assembling enzymatic hydrogels. *Protein Eng Des Sel*, 23: 559–66.
- Marini, D. M., Hwang, W., Lauffenburger, D. A., Zhang, S. G., and Kamm, R. D. 2002. Left-handed helical ribbon intermediates in the self-assembly of a beta-sheet peptide. *Nano Lett*, 2: 295–9.
- Martino, M. M., Mochizuki, M., Rothenfluh, D. A. et al. 2009. Controlling integrin specificity and stem cell differentiation in 2D and 3D environments through regulation of fibronectin domain stability. *Biomaterials*, 30: 1089–97.
- Massodi, I., Moktan, S., Rawat, A., Bidwell, G. L., 3rd and Raucher, D. 2010. Inhibition of ovarian cancer cell proliferation by a cell cycle inhibitory peptide fused to a thermally responsive polypeptide carrier. *Int J Cancer*, 126: 533–44.
- McPherson, D. T., Xu, J., and Urry, D. W. 1996. Product purification by reversible phase transition following *Escherichia coli* expression of genes encoding up to 251 repeats of the elastomeric pentapeptide GVGVP. *Protein Expr Purif*, 7: 51–7.
- Meyer, D. E. and Chilkoti, A. 1999. Purification of recombinant proteins by fusion with thermally-responsive polypeptides. *Nat Biotechnol*, 17: 1112–5.
- Meyer, D. E. and Chilkoti, A. 2002. Genetically encoded synthesis of protein-based polymers with precisely specified molecular weight and sequence by recursive directional ligation: Examples from the elastin-like polypeptide system. *Biomacromolecules*, 3: 357–67.
- Moses, M. A. 1997. The regulation of neovascularization by matrix metalloproteinases and their inhibitors. *Stem Cells*, 15: 180–9.
- Mutoh, M., Lung, F. D., Long, Y. Q. et al. 1999. A p21(Waf1/Cip1)carboxyl-terminal peptide exhibited cyclin-dependent kinase-inhibitory activity and cytotoxicity when introduced into human cells. *Cancer Res*, 59: 3480–8.
- Nagaoka, M., Ise, H., and Akaike, T. 2002. Immobilized E-cadherin model can enhance cell attachment and differentiation of primary hepatocytes but not proliferation. *Biotechnol Lett*, 24: 6.
- Nagaoka, M., Jiang, H. L., Hoshiba, T., Akaike, T., and Cho, C. S. 2010. Application of recombinant fusion proteins for tissue engineering. *Ann Biomed Eng*, 38: 683–93.
- Nagaoka, M., Koshimizu, U., Yuasa, S. et al. 2006. E-cadherin-coated plates maintain pluripotent ES cells without colony formation. *PLoS One*, 1: e15.
- Nakamura, M., Mie, M., Mihara, H., and Kobatake, E. 2009. Construction of a multi-functional extracellular matrix protein that increases number of N1E-115 neuroblast cells having neurites. *J Biomed Mater Res B Appl Biomater*, 91: 425–32.

- Nakamura, M., Mie, M., Mihara, H., Nakamura, M., and Kobatake, E. 2008. Construction of multi-functional extracellular matrix proteins that promote tube formation of endothelial cells. *Biomaterials*, 29: 2977–86.
- Nilsson, J., Stahl, S., Lundeberg, J., Uhlen, M., and Nygren, P. A. 1997. Affinity fusion strategies for detection, purification, and immobilization of recombinant proteins. *Protein Expr Purif*, 11: 1–16.
- Padilla, J. E., Colovos, C., and Yeates, T. O. 2001. Nanohedra: Using symmetry to design self assembling protein cages, layers, crystals, and filaments. *Proc Natl Acad Sci USA*, 98: 2217–21.
- Park, S. H., Gil, E. S., Shi, H. et al. 2010. Relationships between degradability of silk scaffolds and osteogenesis. *Biomaterials*, 31: 6162–72.
- Petka, W. A., Harden, J. L., Mcgrath, K. P., Wirtz, D., and Tirrell, D. A. 1998. Reversible hydrogels from self-assembling artificial proteins. *Science*, 281: 389–92.
- Petsch, D. and Anspach, F. B. 2000. Endotoxin removal from protein solutions. *J Biotechnol*, 76: 97–119.
- Pierschbacher, M. D. and Ruoslahti, E. 1984. Cell attachment activity of fibronectin can be duplicated by small synthetic fragments of the molecule. *Nature*, 309: 30–3.
- Plow, E. F., Haas, T. A., Zhang, L., Loftus, J., and Smith, J. W. 2000. Ligand binding to integrins. *J Biol Chem*, 275: 21785–8.
- Porro, D., Sauer, M., Branduardi, P., and Mattanovich, D. 2005. Recombinant protein production in yeasts. *Mol Biotechnol*, 31: 245–59.
- Prince, J. T., Mcgrath, K. P., Digriolamo, C. M., and Kaplan, D. L. 1995. Construction, cloning, and expression of synthetic genes encoding spider dragline silk. *Biochemistry*, 34: 10879–85.
- Rietschel, E. T., Kirikae, T., Schade, F. U. et al. 1994. Bacterial endotoxin: Molecular relationships of structure to activity and function. *FASEB J*, 8: 217–25.
- Roberge, M., Peek, M., Kirchofer, D., Dennis, M. S., and Lazarus, R. A. 2002. Fusion of two distinct peptide exosite inhibitors of Factor VIIa. *Biochem J*, 363: 387–93.
- Ruoslahti, E. 1988. Fibronectin and its receptors. *Annu Rev Biochem*, 57: 375–413.
- Ruoslahti, E. and Pierschbacher, M. D. 1987. New perspectives in cell adhesion: RGD and integrins. *Science*, 238: 491–7.
- Russ, W. P., Lowery, D. M., Mishra, P., Yaffe, M. B., and Ranganathan, R. 2005. Natural-like function in artificial WW domains. *Nature*, 437: 579–83.
- Schnaper, H. W., Kleinman, H. K., and Grant, D. S. 1993. Role of laminin in endothelial cell recognition and differentiation. *Kidney Int*, 43: 20–5.
- Seymour, L. W., Duncan, R., Strohal, J., and Kopecek, J. 1987. Effect of molecular weight (Mw) of N-(2-hydroxypropyl) methacrylamide copolymers on body distribution and rate of excretion after subcutaneous, intraperitoneal, and intravenous administration to rats. *J Biomed Mater Res*, 21: 1341–58.
- Shiloach, J. and FASS, R. 2005. Growing E. coli to high cell density—A historical perspective on method development. *Biotechnol Adv*, 23: 345–57.
- Sidhu, S. S., Bader, G. D., and Boone, C. 2003. Functional genomics of intracellular peptide recognition domains with combinatorial biology methods. *Curr Opin Chem Biol*, 7: 97–102.
- Silva, A. K., Richard, C., Bessodes, M., Scherman, D., and Merten, O. W. 2009. Growth factor delivery approaches in hydrogels. *Biomacromolecules*, 10: 9–18.
- Soroka, V., Kiryushko, D., Novitskaya, V. et al. 2002. Induction of neuronal differentiation by a peptide corresponding to the homophilic binding site of the second Ig module of the neural cell adhesion molecule. *J Biol Chem*, 277: 24676–83.
- Stevens, M. M., Allen, S., Sakata, J. K. et al. 2004. pH-dependent behavior of surface-immobilized artificial leucine zipper proteins. *Langmuir*, 20: 7747–52.
- Straley, K. S. and Heilshorn, S. C. 2009a. Design and adsorption of modular engineered proteins to prepare customized, neuron-compatible coatings. *Front Neuroeng*, 2: 9.
- Straley, K. S. and Heilshorn, S. C. 2009b. Dynamic, 3D-pattern formation within enzyme-responsive hydrogels. *Adv Mater*, 21: 4148.

- Tamburro, A. M., Panariello, S., Santopietro, V. et al. 2010. Molecular and supramolecular structural studies on significant repetitive sequences of resilin. *Chembiochem*, 11: 83–93.
- Thompson, M. T., Berg, M. C., Tobias, I. S. et al. 2006. Biochemical functionalization of polymeric cell substrata can alter mechanical compliance. *Biomacromolecules*, 7: 1990–5.
- Tomita, M., Yoshizato, K., Nagata, K., and Kitajima, T. 1999. Enhancement of secretion of human procollagen I in mouse HSP47-expressing insect cells. *J Biochem*, 126: 1118–26.
- Topp, S., Prasad, V., Cianci, G. C., Weeks, E. R., and Gallivan, J. P. 2006. A genetic toolbox for creating reversible Ca²⁺-sensitive materials. *J Am Chem Soc*, 128: 13994–5.
- Uchida, M., Klem, M. T., Allen, M. et al. 2007. Biological containers: Protein cages as multifunctional nano-platforms. *Adv Mater*, 19: 1025–1042.
- Welsh, E. R. and Tirrell, D. A. 2000. Engineering the extracellular matrix: A novel approach to polymeric biomaterials. I. Control of the physical properties of artificial protein matrices designed to support adhesion of vascular endothelial cells. *Biomacromolecules*, 1: 23–30.
- West, J. L. and Hubbell, J. A. 1999. Polymeric biomaterials with degradation sites for proteases involved in cell migration. *Macromolecules*, 32: 241–244.
- Wheeldon, I. R., Gallaway, J. W., Barton, S. C., and Banta, S. 2008. Bioelectrocatalytic hydrogels from electron-conducting metallopolypeptides coassembled with bifunctional enzymatic building blocks. *Proc Natl Acad Sci USA*, 105: 15275–80.
- Williams, C. G., Malik, A. N., Kim, T. K., Manson, P. N., and Elisseff, J. H. 2005. Variable cytocompatibility of six cell lines with photoinitiators used for polymerizing hydrogels and cell encapsulation. *Biomaterials*, 26: 1211–8.
- Wong Po Foo, C., Patwardhan, S. V., Belton, D. J. et al. 2006. Novel nanocomposites from spider silk-silica fusion (chimeric) proteins. *Proc Natl Acad Sci USA*, 103: 9428–33.
- Wong Po Foo, C. T., Lee, J. S., Mulyasmita, W., Parisi-Amon, A., and Heilshorn, S. C. 2009. Two-component protein-engineered physical hydrogels for cell encapsulation. *Proc Natl Acad Sci USA*, 106: 22067–72.
- Zaher, H. S. and Green, R. 2009. Quality control by the ribosome following peptide bond formation. *Nature*, 457: 161–6.
- Zerbs, S., Frank, A. M., and Collart, F. R. 2009. Bacterial systems for production of heterologous proteins. *Methods Enzymol*, 463: 149–68.

Synthetic Biomaterials

43.1	Introduction	43-1
43.2	Choice of Monomer.....	43-2
43.3	Polymerization Mechanisms	43-2
43.4	Biomaterial Degradation	43-4
	Hydrolytic Degradation • Enzymatic Degradation • Stimuli-Responsive Degradation • Degradation By-Products	
43.5	Poly(ethylene glycol)	43-6
43.6	Poly(esters).....	43-7
	Poly(α -esters) • Poly(propylene fumarate) • Other Poly(esters)	
43.7	Poly(anhydrides)	43-10
43.8	Poly(ortho esters).....	43-11
43.9	Poly(urethanes)	43-11
43.10	Pseudo Poly(amino acids).....	43-12
43.11	Poly(acrylates) and Poly(methacrylates).....	43-13
43.12	Non-Polymeric Synthetic Biomaterials.....	43-14
43.13	Conclusions.....	43-16
	References.....	43-16

Joshua S. Katz

*Dow Chemical
Company*

Jason A. Burdick

*University of
Pennsylvania*

43.1 Introduction

Synthetic biomaterials have been developed over the last century for a range of applications, including for dental fillings, bone cements, prosthetics, and contact lenses (Griffith 2000, Langer and Tirrell 2004, Ratner and Bryant 2004). In recent years, synthetic biomaterials have evolved to address problems in the field of tissue engineering, namely as three-dimensional scaffolding material to provide structure during tissue formation. This chapter will begin with an overview of the development and properties of synthetic biomaterials for tissue engineering and then focus on the various classes of materials that have been developed. The specific focus will be on synthetic polymers and primarily those that undergo degradation.

When designing and using synthetic biomaterials for tissue engineering applications, it is important to consider many criteria (Drury and Mooney 2003, Lutolf and Hubbell 2005, Shin et al. 2003). This includes the specific tissue of interest (e.g., cartilage versus liver) with respect to the healing potential, cell sources for repair, and vascularization. The scaffold should degrade in accordance with tissue healing (to facilitate, but not impede tissue growth) and into non-toxic by-products. The processing of the polymer must be possible into the desired structure, including as hydrogels, fibrous scaffolds, or macroporous materials. It may also be desirable to incorporate cells, growth factors, and other molecules to aid in the healing response. The bulk mechanical properties are also of concern depending on the local tissue loading and the influence of mechanical properties on cell behavior. With these criteria in mind, nearly endless compositions have been investigated for many tissue types. This chapter will cover materials that exhibit a range of properties and cell and tissue interactions.

The evolution of materials for use in tissue engineering began with various natural materials (e.g., collagen, fibrin), then turned to synthetic materials used for other biomedical applications (e.g., sutures), and now to more complex materials and scaffolds. Added complexity may include control over materials in both time and space, as well as the inclusion of biological components that can lead to optimal cellular signaling. However, the development of new materials opens up questions related to bulk properties, as well as the *in vivo* tissue response and cellular interactions. The overall goal is to better understand the materials toward their use in clinical applications for tissue repair.

43.2 Choice of Monomer

The most significant factor in determining the material properties of a polymer is the structure of the monomer(s) selected for polymerization. Monomer choice dictates both side chain and backbone structure, the latter which determines the polymer classification. Even minor changes to the chemical modification of a monomer (and the resulting polymer) can have drastic effects on polymer solubility, mechanical strength, crystallinity, and sensitivity to degradation. Consequently, the choice of monomer also often dictates the manner in which the material can be processed for biomedical applications.

As a general rule, hydrophilic polymers are processed into hydrogels whereas hydrophobic polymers are processed into solid, porous scaffolds (e.g., foams or fibrous structures). Hydrogels are water-swollen networks held together by cross-links (either chemical or physical, depending on the material) between the polymers. In the absence of cross-links, the polymers typically would simply dissolve. Because water is ubiquitous in these materials, it is important that hydrolysis be controlled to better manipulate degradation timing with tissue formation. Hydrogels are generally soft materials because of their high water content and are therefore generally more suitable for soft tissue applications.

In contrast, hydrophobic polymers must be processed into three-dimensional porous scaffolds to support cell and tissue population, as well as nutrient and waste transport. This topic will be discussed in more detail in other chapters. Water does not penetrate hydrophobic materials extensively, so swelling is generally negligible. As hydrophobic materials can span a large range of material properties, they have potential for applications in both hard and soft tissue engineering. Generally, poly(ethylene glycols) (PEGs) and some of the poly(acrylates) and poly(methacrylates) are used as hydrophilic materials, while there are many examples of hydrophobic materials, which will be discussed in more detail below.

43.3 Polymerization Mechanisms

In addition to monomer selection determining polymer behavior, the ultimate structure of the polymer, such as its molecular weight, polydispersity, and degree of branching can also have profound effects on the material properties. These characteristics can be controlled through the polymerization mechanism and corresponding choice of initiators, terminating molecules, and reaction conditions. Polymers are generally synthesized through one of two mechanisms: step growth or chain growth polymerization (Odian 2004).

The vast majority of polymers produced are synthesized using a step growth mechanism. In step growth polymerizations, all monomeric species are equally able to react with other monomers in a stepwise manner, slowly building dimers, trimers, tetramers, etc. In addition, small oligomers can react with each other (e.g., dimer + trimer \rightarrow pentamer). Because all monomers are able to react at the beginning of polymerization, at early time points, while conversion is high, the molecular weights remain low. Only at very high conversion it is possible to obtain high molecular weight species. For polymerization to proceed, monomers must contain at least two reactive groups (where the presence of more than two reactive groups enables branching and/or cross-linking). Monofunctional monomers cause chain termination and can be used to control the molecular weight of the final polymer. In addition, for copolymer systems in which multiple monomers react with each other (e.g., "A" only reacts with "B" and "B"

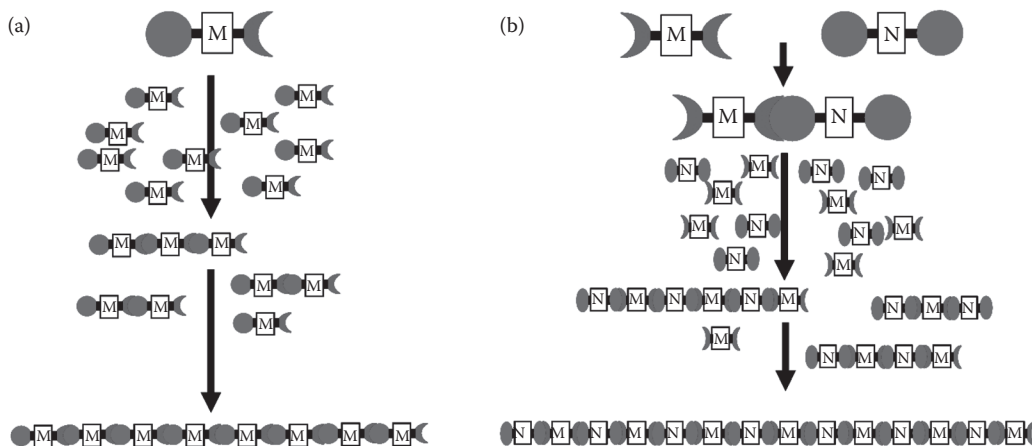


FIGURE 43.1 Step growth polymerization. In step growth polymerization, monomers slowly react with each other until ultimately a high molecular weight species is formed. Monomers can react with themselves (a), or with a complementary monomer (b), forming an alternating copolymer.

only reacts with “A”), molecular weight can be controlled through the monomer feed ratio. Schematics of both types of step-growth polymerization can be found in Figure 43.1.

In contrast to step growth polymerizations, chain growth polymerizations require activation of monomer by an initiator species. The active initiator reacts with a monomer, forming a bond and transferring the reactive point to the end of the monomer, allowing it to react with another, quickly forming a chain (Figure 43.2). Consequently, unlike with step growth polymerizations, even at very low conversions, the polymers present may be of high molecular weight. The most common chain growth polymerization is free radical polymerization. In free radical polymerizations, a radical is introduced to the system through an initiator that activates in the presence of light or heat, or through reductive/oxidative mechanisms. As free radicals are very unstable, the active initiator quickly reacts with monomer (usually a vinyl monomer), transferring the radical to the monomer, which can then react with another monomer, growing the chain. Growth is halted by the reaction of the free radical with another species present in solution to quench the radical such as inhibitors, oxygen, other free radicals, or scission of another polymer’s backbone. Free radical polymerization is used to produce both linear polymers that can be further processed into structural materials or to cross-link materials directly into a structure, such as a hydrogel.

In more recent years, a significant amount of research has involved the development of catalysts for controlling chain growth polymerizations such that high molecular weights and narrow polydispersities can be obtained. In these reactions, known as “living polymerizations” the catalysts stabilize the growing reactive chain end, enabling slow and uniform growth of the polymers. Consequently, the

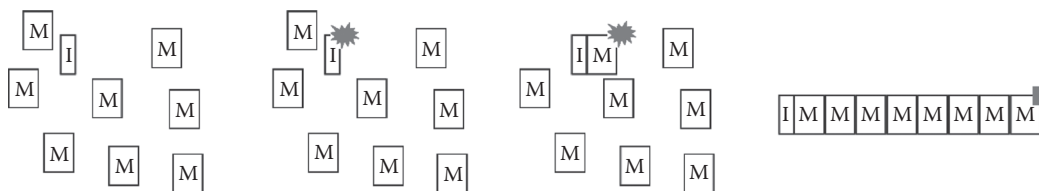


FIGURE 43.2 Chain growth polymerization. In chain growth polymerization, an initiator molecule is activated and rapidly transfers its activity to a monomer, which continues to react with more monomers in succession until a termination reaction occurs.

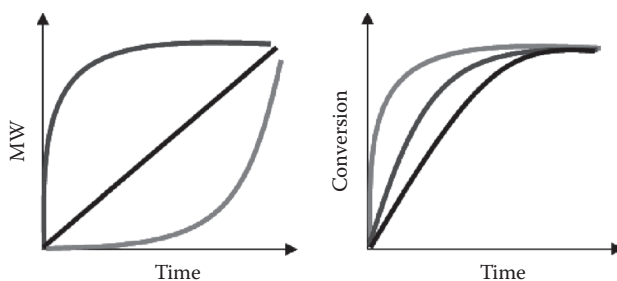


FIGURE 43.3 Progression of polymer molecular weight and monomer conversion with time for step growth (red), chain growth (blue), and living (black) polymerizations.

molecular weight changes are linear with time and conversion. In addition, due to the high stability of the growing chain ends, living polymerizations allow for the synthesis of high-fidelity diblock copolymers. Figure 43.3 demonstrates the molecular weight and monomer conversion profiles for all three typical polymerization mechanisms.

43.4 Biomaterial Degradation

To facilitate the replacement of synthetic scaffold materials with natural tissue, many materials are now being processed and designed to degrade under physiological conditions. Degradation can also be used as a tool to deliver molecules (e.g., growth factors) or cells to aid in the tissue healing and to manipulate material properties with time. This section explores the various routes of degradation that have been used in synthetic materials for tissue engineering.

43.4.1 Hydrolytic Degradation

The vast majority of degradable synthetic materials degrade *in vivo* through water hydrolysis of polymer bonds. Classically, degradation and erosion of a biomaterial have been described in one of two ways, namely surface erosion or bulk erosion. Which mode of erosion a material undergoes is dictated by both the ability of water to penetrate the material (hydrophobicity) and the rate of bond hydrolysis (lability). Materials that are highly hydrophobic but also exhibit relatively labile bonds undergo surface erosion because the fast degradation at the surface is more rapid than water penetration into the material. Consequently, surface eroding materials exhibit a relatively linear decrease in mass with time (depending on the sample geometry), as the hydrolyzed portion of the material, located solely at the water–material interface, becomes free to dissolve into the surrounding solution. In contrast, materials that undergo slow hydrolysis and are more hydrophilic are more susceptible to bulk degradation. In bulk-degrading materials, little mass loss is observed at (relatively) early time points until enough of the material has degraded throughout, leading to nearly complete dissolution of the polymer. The slow degradation rate enables penetration of water throughout the material, allowing uniform hydrolysis. However, at early times, as the majority of the material remains intact, even those portions that have been hydrolyzed remain with the material, trapped from escape, and hence the minimal mass loss. However, practically all materials exhibit some combination of bulk and surface erosion, leading to hybrid degradation profiles (Figure 43.4).

43.4.2 Enzymatic Degradation

Few synthetic materials are susceptible to recognition and degradation by endogenous enzymes found in human tissues. Consequently, several groups have recently begun to incorporate synthetic peptides

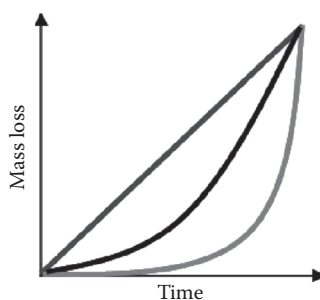


FIGURE 43.4 Mass loss profile for idealized bulk eroding (red) and surface eroding (blue) polymeric materials. The actual mass loss profile is a hybrid of the two profiles, shown in black.

containing consensus sequences sensitive to proteolytic enzymes, such as matrix metalloproteinases (MMP) (Lutolf et al. 2003). Using solid phase peptide synthesis, these specialty peptides are designed to cross-link hydrogels. Most of this work has focused on natural materials or PEG-based hydrogels. Several approaches have been taken to fabricate these gels, including the use of multi-arm PEGs with bifunctional peptides cross-linking them or building large repeating PEG-peptide-PEG macromers that then crosslink using UV light (Lutolf and Hubbell 2005, Miller et al. 2010). The MMP peptides were coupled to the PEG using a Michael-type addition through terminal cysteines on the peptide and vinyl groups on the PEGs. Once the gels have been formed, surrounding cells (either encapsulated or at the surface) produce MMPs as they migrate into and through the gel, slowly degrading the synthetic network and allowing it to be replaced by new tissue.

43.4.3 Stimuli-Responsive Degradation

Another potential route to inducing degradation is through the cleavage of reduction-sensitive linkages, such as disulfide bonds (Cerritelli et al. 2007, Lee and Park 1998). The vast majority of research in this field has focused on nano-sized drug delivery vehicles, as most reduction occurs inside endosomal and lysosomal compartments of cells. As the extracellular environment is generally non-reductive in nature, reductive degradation is unlikely to find significant use as a degradation route for materials being developed for tissue engineering applications, as in such applications, the materials are not taken up by cells. Alternatively, light is now being used as a trigger for polymer degradation, where ultraviolet light exposure of incorporated *o*-nitrobenzyl moieties can lead to polymer cleavage (Katz and Burdick 2010, Kloxin et al. 2009). This provides precise spatial and temporal control over material properties and user-dictated degradation.

43.4.4 Degradation By-Products

When designing a biodegradable implant, it is important to keep in mind the products of the material's degradation (Nair and Laurencin 2007). Most materials undergoing hydrolysis liberate large amounts of acid as the degradation products. For rapidly degrading materials, such a large local concentration of acid could prove to be toxic, interfering with the intended application of the material while inducing inflammation. In addition, as many materials' degradation profiles are affected by pH, the generation of acids (or bases) locally could significantly alter the continued degradation of the material. The choice of monomer must be considered when designing synthetic polymers as it will be a component of the degradation products and care should be taken to understand the resulting cell and tissue interactions with degradation. Generally, the quantity and timing of degradation product release, as well as monomer toxicity, correlates to cytotoxicity and the *in vivo* inflammatory response.

43.5 Poly(ethylene glycol)

PEG (also known as poly(ethylene oxide)) is one of the most widely used materials in tissue engineering (Drury and Mooney 2003). As a result of its extreme hydrophilicity, PEG is highly resistant to protein adsorption and therefore works well as a non-fouling, non-immunogenic surface in a biological environment. This makes PEG materials a “blank slate” so that cellular interactions can be precisely controlled through added features (e.g., peptides). Furthermore, because it is one of the few synthetic hydrophilic materials available, it has become a prime candidate for use in many soft tissue applications, where hydrogels are preferable to hard materials.

PEG is synthesized by the ring-opening polymerization of ethylene oxide and very narrow molecular weight distributions can be obtained through the use of living catalysts (Figure 43.5). The choice of initiator determines the end group chemistry, which is important for enabling post-functionalization of the polymer to allow for cross-linking into networks and chemical functionalization of the resulting material. The use of a multifunctional initiator allows for multi-branched PEGs. Many PEGs are commercially available with alcohol termini, ranging in molecular weight from a few hundred Daltons to several million. The most common functionality added to PEG to process it into a three-dimensional biomaterial is the acrylate group which enables polymerization and (if more than one acrylate per polymer) cross-linking through free radical routes. Hydrogels of PEG diacrylate are non-degradable under physiological conditions on time scales of interest for tissue engineering. To address this issue, several groups have added short polyesters to the PEG termini prior to acrylation (Metters et al. 2000, Sawhney et al. 1993). These short polyester chains provide a route to hydrolytic degradation, the kinetics of which can be tuned by the choice of polyester and number of groups incorporated.

Although beneficial in that it resists nearly all non-specific binding, PEG materials are limited because of the inability of cells to attach to these gels and grow. To address this issue, multi-functional PEGs are now being developed and used that incorporate a route to present a biologically relevant ligand to enhance cell interactions (Burdick and Anseth 2002, Hern and Hubbell 1998). PEG hydrogels have also been investigated that degrade via enzymes or through light (as discussed above) and have found utility for a wide range of tissue engineering applications.

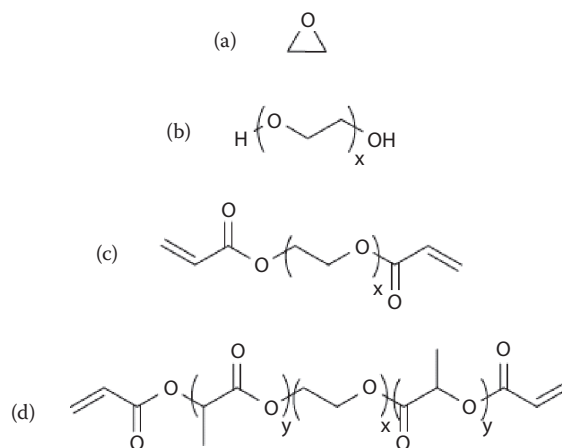


FIGURE 43.5 Poly(ethylene glycol) is synthesized by the ring-opening polymerization of ethylene oxide (a) and has the structure shown in (b). PEG can be modified with acrylate groups for cross-linking (c) or with short poly(ester) chains and acrylate groups for crosslinking and degradability (d).

43.6 Poly(esters)

43.6.1 Poly(α -esters)

The poly(α -esters) are a class of thermoplastic polymers that are widely used in surgical implant materials (Nair and Laurencin 2007) and are likely the most investigated hydrophobic polymer class used in tissue engineering applications. The properties of this class of material vary widely depending on the polymer molecular weight, hydrophobicity of the monomer, and the degree of crystallinity of the resulting polymer. Poly(α -esters) can be synthesized through either step or living chain growth polymerizations. Step growth polymers are formed by the condensation of alcohols and carboxylic acids (or activated esters). To produce robust polymers, high temperature and vacuum are required to remove the water by-product. Even with such extreme conditions, however, the synthesis of high molecular weight species is fairly limited. In contrast, living polymerization can be achieved through the ring opening polymerization of lactones (Labet and Thielemans 2009). These reactions proceed at relatively low temperatures (as low as room temperature has been achieved) and monodisperse, high molecular weight polymers can be obtained. The most common catalyst for chain growth polymerization of lactones is stannous octoate, though many other electron rich catalysts such as alkyl aluminums and heterocyclic carbenes have been employed to provide further control over the reaction progression and to produce multi-block polymers. Figure 43.6 shows the structures of the monomers and polymers to be discussed in the next section.

The glycolide monomer is the smallest unit in the poly(α -ester) series. The resulting polymer, poly(glycolic acid) is crystalline with a T_g in the range of 40°C and melting temperature over 200°C. As a result of its high crystallinity, it has a very strong tensile modulus, making it a promising candidate for many tissue engineering applications. Its ability to form fibers has also made it a strong candidate for bioresorbable sutures. Poly(glycolic acid) is a bulk degrading polymer, breaking down into naturally occurring glycine. However, owing to the rapidly produced acidic degradation products, poly(glycolic acid) may be limited to only a few *in vivo* applications (Li 1999, Nair and Laurencin 2007).

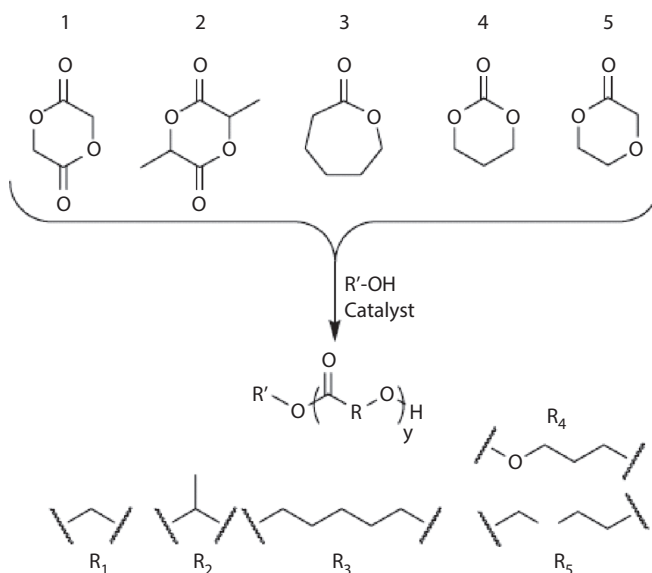


FIGURE 43.6 Cyclic lactones undergo ring-opening polymerization to form the poly(α -esters). Monomers shown are (1) glycolide, (2) lactide, (3) caprolactone, (4) trimethylene carbonate, and (5) dioxanone.

Lactic acid is a naturally occurring chiral molecule whose polymer properties vary significantly based on the chirality of the monomer feed. Enantiomerically pure monomer feeds (all D-lactide or L-lactide) produce highly crystalline polymers. As L-lactide is the naturally occurring species, poly(L-lactic acid) (PLLA) is more often used for medical applications. These polymers have a T_g around 60°C and melt at temperatures slightly lower than poly(glycolic acid), around 175°C. As a result of the crystalline nature of the polymer—and that it is more hydrophobic than poly(glycolic acid)—degradation is relatively slower, with resorption taking several years. In contrast to PLLA, polymers made from a racemic mixture of monomer are amorphous in nature, with a T_g approximately 5°C less than the optically pure polymers. Owing to the amorphous nature, these polymers are significantly softer than PLLA and hydrolyze in a manner of months. In all cases, these polymers undergo primarily bulk degradation and produce lactic acid as their degradation product (Li 1999).

Significant research has also been conducted on copolymers of lactic and glycolic acid (PLGA), an FDA-approved biomaterial. These polymers degrade relatively rapidly (weeks to months), as they do not benefit from the crystalline stability afforded materials of the homopolymers and have the added hydrophilicity from the glycolide. The degradation rate depends on the actual polymer composition, molecular weight, and how the material has been processed. Applications of PLGA range from tissue engineering scaffolds, to fast-degrading sutures, to drug-delivery vehicles (Li 1999).

Several larger cyclic monomers have also been used for the production of more hydrophobic polyesters. Poly(dioxanone) (PDN) and poly(caprolactone) (PCL) are polyesters with significantly reduced glass transition temperatures, PDN being around -5°C and PCL being as low as -60°C. PDN has a melting temperature of around 110°C, whereas the melting temperature of PCL is closer to 60°C. Both polymers undergo bulk degradation over very long periods of time, their rates limited by their hydrophobicity and crystallinity. Consequently, these polymers are potentially useful for applications requiring the long-term presence of the material, such as long-term releasing drug-delivery devices or slow-growth tissue regeneration (Nair and Laurencin 2007).

Similar to the poly(α -esters), both in structure and route of preparation, is poly(trimethylene carbonate) (PTMC). PTMC is a soft amorphous polymer that is highly elastic. Unlike the poly(α -esters), PTMC does not undergo bulk degradation, but rather is subject to surface-erosion. Interestingly, the rate of surface erosion is significantly higher in an *in vivo* setting compared with *in vitro* (Zhang et al. 2006). This enhanced rate of degradation is caused by the ability of PTMC to undergo enzymatic degradation in addition to simple hydrolysis. PTMC is one of the very few completely synthetic materials that can be subject to enzymatic hydrolysis, making it a particularly interesting candidate for materials development.

43.6.2 Poly(propylene fumarate)

Poly(propylene fumarate) (PPF) is a classical example of a degradable poly(ester) synthesized by step-growth polymerization. There are several methods for synthesis of the polymer including transesterification of a fumaric ester or direct esterification of 1,2-propanediol and fumaric acid using an acidic catalyst (Gresser et al. 1995, Suggs et al. 1997). Both fumaric acid and 1,2-propanediol are known to be biocompatible, translating to minimal adverse responses to the material *in vivo* (Nair and Laurencin 2007). An advantage of the PPF structure is an unsaturated double bond in each repeat unit of the polymer (Figure 43.7). This double bond enables further polymerization and cross-linking of PPF polymers following casting into a desired shape (i.e., a tissue defect). PPF can also be used as a biodegradable cross-linker for other vinyl monomers, such as *N*-vinyl pyrrolidone or methyl methacrylate (Frazier et al. 1997, Gresser et al. 1995). These two added benefits—cross-linking and copolymerization—have enabled a broad spectrum of material properties accessible to PPF materials. However, research with PPF has mainly been centered on applications in bone tissue engineering, and as a result, in order to better mimic bone, it is often combined in a composite with beta-tricalcium phosphate (Temenoff and Mikos 2000, Wolfe et al. 2002).

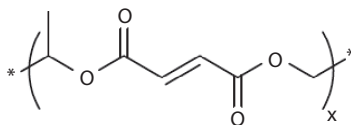


FIGURE 43.7 Structure of poly(propylene fumarate). The unsaturated double bond enables further polymerization and cross-linking of the polymer.

43.6.3 Other Poly(esters)

In addition to ring-opening polymerization and transesterification reactions, condensation reactions can also afford polyesters, though with less control over the molecular weight and polydispersity of the resulting polymers. These materials are obtained by the condensation of alcohols and carboxylic acids or activated esters. One such example material that has been explored for tissue engineering is a copolymer of sebacic acid and glycerol, shown in Figure 43.8 (Wang et al. 2003). Synthesized in the melt, high temperature, and vacuum facilitates condensation and removal of water. If allowed to proceed to completion, the material cures owing to the three alcohols on glycerol providing a route to cross-linking. Others have stopped the reaction prior to curing and in a second step, acrylated the polymer, which could then be cross-linked following radical initiation (Ifkovits et al. 2008). Poly(glycerol-co-sebacate) is an elastomeric material, making it a suitable candidate for tissue engineering of soft flexible tissues such as muscle.

Recently, a new class of poly(esters), poly(β -amino esters) (PBAEs), has been developed (Anderson et al. 2006). Originally designed as a potential gene-delivery vehicle, PBAEs have demonstrated promise in the field of tissue engineering as scaffold materials (Brey et al. 2010). PBAEs are synthesized through step-growth polymerization via Michael-type addition of an amine across the vinyl bond of an acrylate (Figure 43.9). The use of diacrylate monomers allows for polymerization (each amine can add to two double bonds, linking the monomers). These polymers are synthesized in the bulk without the production of by-products. The monomer (diacrylate and amine) ratios are set to ensure that the polymer end-groups are acrylates, allowing for radical cross-linking of the material. A large combinatorial library of PBAEs was screened for mechanical and degradation properties, and the choice of monomers can have a significant effect on both. Although all formulations were found to bulk degrade, the most hydrophilic polymers were found to degrade too quickly for applications in tissue engineering, indicating the need for at least a moderate hydrophobicity to the material to have applicability in tissue engineering.

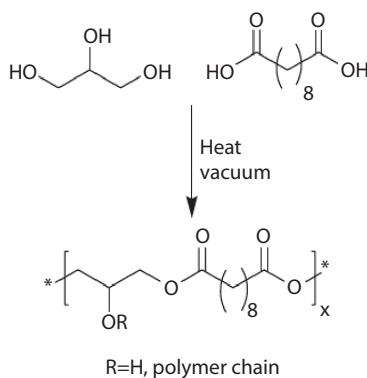


FIGURE 43.8 Glycerol and sebacic acid esterify to form poly(glycerol sebacate), an elastomeric material.

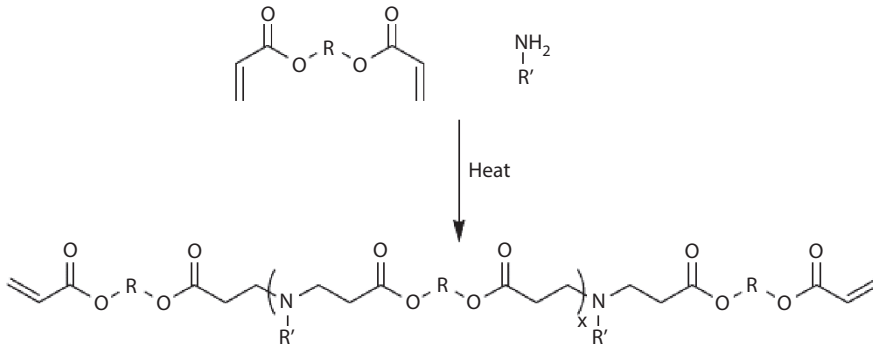


FIGURE 43.9 Acrylates and primary amines react by Michael addition to form poly(β -amino esters). The mechanical and degradation properties of the PBAEs vary greatly based on the R and R' groups.

43.7 Poly(anhydrides)

The major class of surface-eroding polymers is poly(anhydrides) (Kumar et al. 2002). More sensitive to hydrolytic cleavage than esters, the anhydride backbone is able to degrade relatively quickly, allowing less time for water penetration into the material and, therefore, the resulting surface-eroding profile. The use of hydrophobic moieties surrounding the anhydride linkage further limits water penetration into the bulk. Poly(anhydrides) are synthesized predominantly by condensation reactions of carboxylic acids or their activated derivatives—activated esters or acyl chlorides, though ring opening polymerization of adipic anhydride has also been achieved (Albertsson and Lundmark 1988, Kumar et al. 2002). Various catalysts that coordinate the carbonyl have been introduced that accelerate the synthesis and also afford higher molecular weight polymers. The range of monomers that have been investigated for poly(anhydride) synthesis and applications is vast, ranging from simple aliphatic diacids (i.e., sebacic acid or adipic acid) which degrade in a matter of weeks to bulky aromatic diacids such as 1,3-bis(*p*-carboxyphenoxy) propane which must be used as copolymers to reduce brittleness (Kumar et al. 2002). Such a copolymer is shown in Figure 43.10. Others have made poly(anhydrides) from fatty acids and amino acids or with branches (Domb 1990, Domb et al. 1995, Maniar et al. 1990). In one particularly interesting example, poly(anhydrides) were synthesized with a salicylic acid-based monomer, degrading into the common analgesic drug (Erdmann and Uhrich 2000).

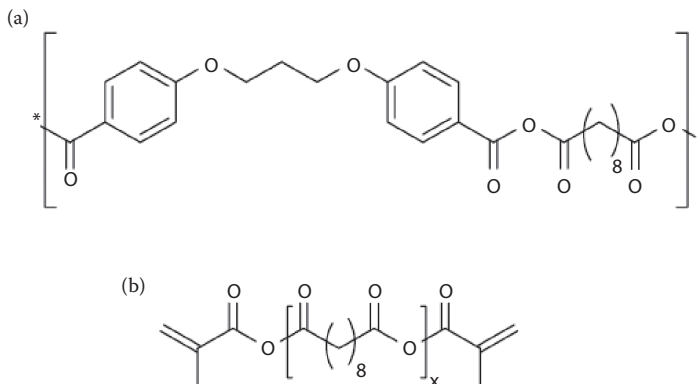


FIGURE 43.10 Poly(anhydrides). (a) Poly(1,3-bis(*p*-carboxyphenoxy)propane-co-sebacate), an aliphatic-aromatic copoly(anhydride). (b) Methacrylated poly(sebacate), which can undergo cross-linking through the methacrylate groups.

Poly(anhydrides) made inroads in the field of biomaterials through their use in drug-delivery applications (Kumar et al. 2002). Because they surface erode, a linear release of encapsulated drugs could be achieved, allowing for constant, sustained drug concentrations *in vivo*. Poly(anhydrides), however, are somewhat limited in their applications as their processing can be difficult owing to high degrees of crystallinity, leading to poor solubility in most solvents, and any hydrophilic candidate would hydrolyze at a rate too fast for any practical application. To address this concern, methacrylated poly(anhydrides), which begin soft and moldable and can then be cross-linked into a defect, have also been developed and investigated for tissue engineering applications (Muggli et al. 1999).

43.8 Poly(ortho esters)

Another major class of surface-eroding polymers is the poly(ortho esters) (POE; Figure 43.11) (Heller et al. 2002). Four classes of POEs have been developed for applications in controlled drug delivery, as they exhibit linear release profiles of encapsulated contents. The POE structure is a carbon bonded to three oxygens, two of which are part of the backbone of the polymer. They exhibit pH-dependent hydrolysis, cleaving to yield alcohols and esters, though the esters often further hydrolyze to the corresponding alcohol and acid. POE I was the first POE developed, a copolymer of tetrahydrofuran and a diol. However, because POE I degrades into hydroxybutyric acid (from butyrolactone), which further catalyzes (and accelerates) degradation, focus was turned to other POEs. POE II is a far more stable POE than POE I, and through the choice of diol, the material properties of the polymer can be tuned from glassy to semi solid. However, because of the extreme hydrophobicity of this POE II, there was little control over the very slow degradation rate, limiting their applicability. POE III is a semi-solid polymer; however, it was limited in development by difficulties in obtaining reproducible synthetic results. The most advanced POE is POE IV, a modified version of POE II to address the slow hydrolysis. POE IV is a copolymer of POE II and short PLA or PGA segments. The PLA or PGA offers a route to facile hydrolysis and the production of either lactic or glycolic acid further catalyzes the decay of the POE. By controlling the amount of PLA or PGA added, the degradation rate can be easily tuned.

43.9 Poly(urethanes)

Poly(urethanes) are a class of polymer that have been explored for many applications in the materials science field (Santerre et al. 2005). As a result of their ability to form segmented block copolymers, a wide range of material properties is accessible, making them a particularly attractive class of polymers. Polyurethanes are synthesized by the polycondensation of diols and diisocyanates. To form segmented diblock copolymers, polymeric diols (e.g., PEG or a polyester) are used as a small percentage of the diol feed (with the remainder being a low molecular weight diol or diamine called a chain extender). Figure 43.12 shows a poly(urethane) with a poly(ester) segment. Upon condensation, the polymeric diol forms

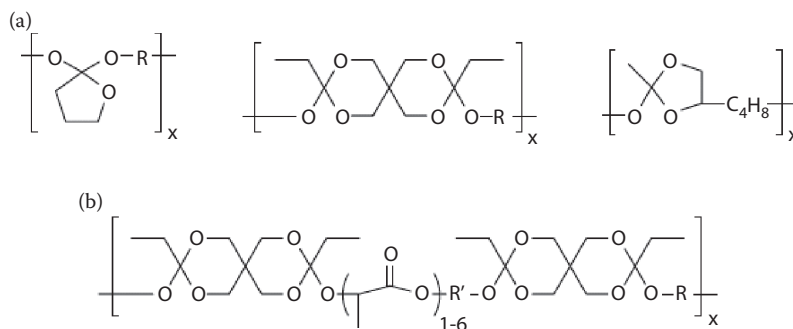


FIGURE 43.11 The poly(orthoesters). (a) left to right: POE-I, POE-II, and POE-III. (b) POE-IV.

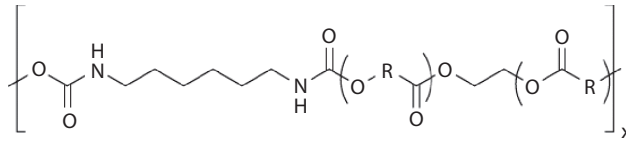


FIGURE 43.12 The general structure of a poly(urethane), synthesized from hexamethylene diisocyanate and a poly(ester) diol.

one block (soft segment), while the small diol/diamine in conjunction with the diisocyanate forms the other (hard segment). One limitation to the use of poly(urethanes) for tissue engineering applications, however, has been the severe toxicity associated with the degradation products of the most common diisocyanate monomers. To address these concerns about toxicity, more recently, several biocompatible diisocyanates have been developed, including lysine diisocyanate, based on the natural amino acid and hexamethylene diisocyanate. Used in conjunction with biocompatible soft segments such as PCL or PEG, these materials hold much promise for the engineering of many tissues (Loh et al. 2008). Specific functionalities have also been explored for incorporation in poly(urethanes) through the use of sugars (i.e., sucrose), amino acids or even drugs as part of the hard segment or the polymer (Santerre et al. 2005).

43.10 Pseudo Poly(amino acids)

To better mimic natural materials, tyrosine has been used as a base for the development of a series of polymers that offer much promise for tissue engineering applications (Bourke and Kohn 2003). Desaminotyrosyl-tyrosine alkyl esters can be processed into a variety of polymers including poly(carbonates) and poly(arylates). The backbone structure contains an amide bond (linking the tyrosine and desaminotyrosine) and the carbonate or arylate (ester) bond (Figure 43.13). The polymers are produced by step growth polymerization and usually have a polydispersity between 1.4 and 1.8. Having a biphenolic monomer structure lends the polymer the ability to have the robust mechanical properties that are accessible for other commercial plastics, whereas the use of tyrosine as the base for the monomer enables biocompatibility. Varying the side chain alkyl length and diacid linkage (for arylates) further enhances the mechanical properties. Indeed, different versions of these polymers can range from amorphous to liquid crystalline. As a result of the hydrophobicity of the backbone, the water content of

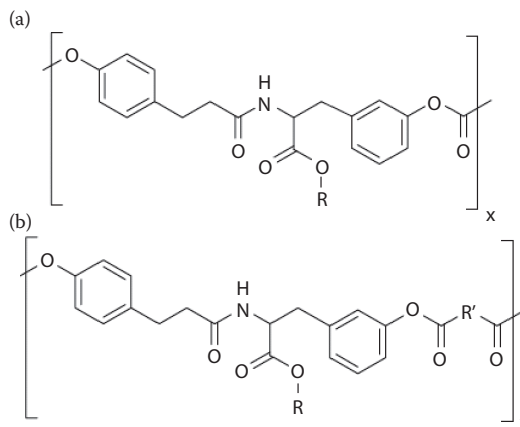


FIGURE 43.13 Pseudo poly(amino acids). Poly(carbonate) (a) and poly(arylate) (b) desaminotyrosyl-tyrosine copolymers. The R group is usually an alkyl chain.

the polymers is also quite low, remaining at only a few percent, leading to very slow degradation times. In addition, because the monomers themselves are relatively water insoluble, mass loss is also very slow, even though there is some bulk degradation. The degradation products also have fewer equivalents of acid compared with the poly(α -esters), which should lead to less inflammation at a site of implantation. To increase the water content, PEG has been incorporated into the backbone of the polymer through the ether or carbonate linkages. In addition, the inclusion of PEG increased the degradation rate of the polymer and decreased the mechanical stiffness. These PEGylated materials are being further explored for self-assembly for drug delivery and soft tissue engineering applications and in medical devices (Johnson et al. 2010, Sheihet et al. 2007, Yu and Kohn 1999).

43.11 Poly(acrylates) and Poly(methacrylates)

In addition to the use of acrylates as a route to cross-linking PEG as described above, small molecule acrylates can also be polymerized to form materials useful for tissue engineering. Poly(methacrylates) were first developed for use as bone cements and dental sealants, forming hard, hydrophobic, insoluble materials upon cross-linking (Anseth et al. 1995, Mousa et al. 2000). More recently, (meth)acrylates have been developed for more advanced tissue engineering applications. The properties of poly(acrylates) and poly(methacrylates) are highly influenced by the pendant side group (Figure 43.14). When the side chains are hydrophilic, such as hydroxyethyl, short chains of PEG or the free acid, the resulting materials are highly hydrophilic and form hydrogels upon cross-linking (Guvendiren et al. 2009). Conversely, saturated hydrocarbon or aromatic ring (i.e., butyl methacrylate or benzyl methacrylate) side chains lend the polymer a hydrophobic character, insolubility in water, and depending on the exact side chain, the polymer can also be quite crystalline. As the backbone of poly(acrylates) and poly(methacrylates) are saturated hydrocarbons, there is no route for degradation of the backbone polymer in a physiological environment. Consequently, hydrophobic materials are very slowly degrading *in vivo*. Hydrophilic poly(acrylates) and poly(methacrylates) are generally water soluble unless cross-linked, and cross-linked versions can only degrade when degradable units are included in the cross-linker.

Responsive (meth)acrylates have also been developed, offering responses to light and pH. 2-Nitrobenzyl (meth)acrylate is a light-sensitive, protected form of (meth)acrylic acid (Doh and Irvine

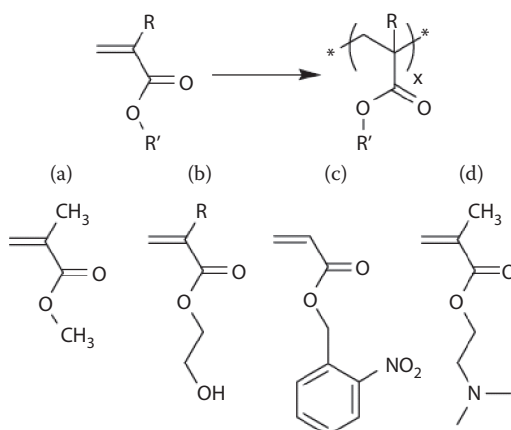


FIGURE 43.14 (Top) Acrylates (R=H) and methacrylates (R=CH₃) polymerize to form poly(acrylates) and poly(methacrylates), which have saturated hydrocarbon backbones. (Bottom) Four common (meth)acrylate monomers. (a) Methyl methacrylate is a hydrophobic monomer commonly used in bone cements. (b) 2-Hydroxyethyl(meth)acrylate is a hydrophilic monomer used in soft tissue engineering. (c) 2-Nitrobenzyl acrylate is a protected form of acrylic acid and deprotects upon exposure to UV light. (d) 2-Dimethylaminoethyl methacrylate is a pH-sensitive monomer.

2004). When polymerized, due to the presence of the 2-nitrobenzyl group, the polymer is highly hydrophobic. However, on exposure to UV light, the 2-nitrobenzyl moiety is cleaved, producing (meth)acrylic acid, which is highly hydrophilic. This polymer (or copolymers of it) has been useful for producing materials where UV light can be used to spatially and temporally alter the hydrophilicity of the material. Poly(methacrylates) containing secondary and tertiary amines in their side chains offer pH responsiveness (Lee et al. 1999). At elevated (and neutral) pH, the amines are uncharged, lending a hydrophobic character to the polymer. However, on dropping the pH, the polymer quickly becomes charged through protonation of the amines, making the material hydrophilic. These materials offer a route to enhanced cellular delivery of drugs and proteins, as only in the lower pH of the endosome does the polymer become charged, making the delivery vehicle dissolve or swell and release its contents (Hu et al. 2007).

Poly(acrylates) and poly(methacrylates) are synthesized through chain growth or living mechanisms. The most common route to their preparation is free radical polymerization. However, to obtain higher molecular weights with more narrow dispersities, living routes (either living radical or anionic) must be used, which stabilize the reactive, growing species. There are several well-established living radical polymerization routes. Atom transfer radical polymerization uses a transition metal catalyst (usually copper) that sits in equilibrium between two oxidation states to coordinate and stabilize the growing radical (Coessens et al. 2001). As the non-radical oxidation state is preferred in the equilibrium, the progression of the reaction is stabilized, leading to fewer side and termination reactions compared with normal free radical polymerization. Homolytic scission of an alkyl-halide bond by the catalyst initiates the reaction, and the halide is carried throughout the polymerization, remaining present even at termination. Two other living radical polymerization routes are reversible addition-fragmentation chain transfer (RAFT) and nitroxide-mediated polymerizations (NMP). RAFT stabilizes growing radicals through the reversible addition and fragmentation of the radical across the C-S double bond of a chain transfer agent, a di- or tri-thiocarbonyl compound (Moad et al. 2005). The reduction in number of actively growing species (compared with temporarily dormant species) allows for the reaction to proceed in a living manner. NMP stabilizes the reaction by temporarily deactivating the growing polymer chain and a nitroxide scavenger reversibly accepting the free radical (Sciannone et al. 2008). As nitroxide radicals are very stable, side reactions are diminished and the number of growing chains at any given time is reduced. However, NMP is somewhat limited by the number of commercially available initiators. The full details of these mechanisms are beyond the scope of this chapter, but several excellent reviews, referenced above, have been written on atom transfer radical polymerization, RAFT, and NMP.

43.12 Non-Polymeric Synthetic Biomaterials

Although the majority of synthetic materials explored for applications in tissue engineering are polymers, several research groups have explored the use of non-polymeric synthetic materials that can be processed into materials conducive to tissue engineering applications.

As a greater class, poly(peptides) are generally considered to be natural materials. However, with the advent and optimization of solid phase synthesis techniques, many peptides now being explored for tissue engineering can be considered synthetic. In addition, while in the natural sphere peptides are usually confined to containing only the canonical 20 L-amino acids, solid phase synthesis has allowed for the facile introduction of many other unnatural amino acids, further increasing the possible sequences available. Synthetic peptides have generally been explored in two arenas: in conjunction with other materials to enhance their properties or as stand-alone self-assembling materials. Many biologically relevant proteins have short consensus sequences that can be synthesized to modify non-bioactive materials. The most common sequence is the RGD (arginine-glycine-aspartic acid), an integrin-binding domain from the extracellular matrix protein fibronectin (Hersel et al. 2003, Hubbell 1995). Many variations of this three-amino acid sequence have been explored to couple the peptide to various materials and to enhance its binding properties. Cysteine residues can be used to couple the peptide to synthetic materials containing maleimide, vinyl sulfone, or acrylate groups through Michael addition. Multiple

cysteine residues have also been used to lock the RGD into a specific conformation through introduction of a disulfide bridge in the peptide. Many other peptides have been explored as well to enhance specific functionality of a biomaterial, including IKVAV and YIGSR (laminin peptides). In addition to introducing side functionality to materials, short peptides have also been used to cross-link synthetic and natural materials, providing a route for cellular remodeling of scaffolds. For example, many groups have explored the use of MMP-sensitive peptides to cross-link hydrogels, where cross-links are cleaved by cellular produced MMPs (Khetan et al. 2009, Lutolf et al. 2003).

Non-naturally occurring peptides have also been developed that self-assemble into hydrogels through non-covalent interactions within the peptides (Charati et al. 2009). Such peptides have been engineered on multiple length scales, ranging from short oligomers that can interact and assemble through pi-stacking of aromatic residues to large peptides containing helical domains that interact, providing a route to physical cross-linking. Many of these larger peptides are too large to produce using solid phase routes and therefore require synthesis using molecular biology techniques, limiting the choice of amino acids and sequences to those that are naturally occurring. Recently there have been several advances in improving molecular biology to enable the addition of unnatural amino acids through directed evolution of tRNA-tRNA synthetase pairs toward the desired unnatural amino acid (Wang and Schultz 2005). However, such advances still do not offer the same variety that can be obtained through solid phase techniques.

In addition to synthesizing self-assembling peptides, several groups have begun to look at peptide derivatives for applications in medicine, for example a class of materials known as peptide amphiphiles (Cui et al. 2010, Hartgerink et al. 2002). An example peptide amphiphile is shown in Figure 43.15. These materials are surfactant hybrids of peptides and lipids. Under physiological conditions, the peptide amphiphiles self assemble, undergoing a hydrophobic condensation of the lipid tail and hydrophobic amino acid residues while being stabilized in solution by the hydrophilic peptide residues at the terminus of the amphiphile. Most often the peptide amphiphiles assemble to form long fibers in solution, where entanglement of the fibers causes gelation of the material. Use of consensus sequences (such as those described above) in the peptide portion of the material allows for the creation of bioactive hydrogels that promote cell infiltration and growth.

Moving still a little further away from basic poly(peptide) structure are poly(peptoids), developed by the Barron group at Stanford University (Kirshenbaum et al. 1998, Patch and Barron 2002). Unlike typical peptides, poly(peptoids) have a structure in which rather than being on the α -carbon, the amino acid side chain is attached to the amine itself, forming a tertiary amine (Figure 43.16). Similar to synthetic peptides, they can be synthesized in a facile manner on a solid phase peptide synthesizer. The Barron group has found that these materials can be good mimics for naturally occurring peptides while avoiding significant recognition by the immune system and offering enhanced biostability. This is an example

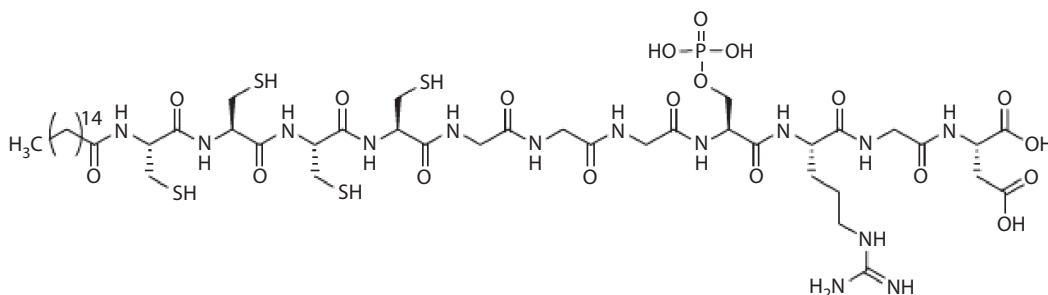


FIGURE 43.15 A self-assembling peptide amphiphile. Upon exposure to salts, the amphiphile self-assembles into fibers, entangling to form a gel. The fibers can be stabilized by oxidation of the SH groups on the cysteines. The RGD head of the amphiphile encourages cell binding and the phosphate encourages mineralization. (Adapted from Hartgerink, J. D., E. Beniash, and S. I. Stupp 2002. *Proceedings of the National Academy of Sciences of the United States of America*. 99: 5133–38.)

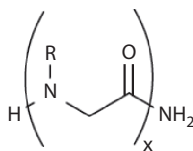


FIGURE 43.16 The basic structure of a poly(peptoid), in which the R group of the peptide is attached to the amine rather than the α -carbon.

of materials that have enhanced complexity and may lead to more improved structures for tissue engineering applications in the future.

43.13 Conclusions

As chemistry advances our ability to design novel monomers and routes to polymerization, the quality and quantity of materials available for research in tissue engineering will continue to increase. Early, classical polymers and polymeric materials have pushed open the door for the development of and advances in tissue engineering as a field. However, while these classical polymers have been utilized for early applications in the field, as research progresses, it appears as though further advances in the smart design of polymers and their resulting materials will better enhance our ability to improve, restore, and replace damaged tissue function.

References

- Albertsson, A. C. and S. Lundmark 1988. Synthesis of poly(adipic anhydride) by use of ketene. *Journal of Macromolecular Science-Chemistry*. A25: 247–58.
- Anderson, D. G., C. A. Tweedie, N. Hossain et al. 2006. A combinatorial library of photocrosslinkable and degradable materials. *Advanced Materials*. 18: 2614–18.
- Anseth, K. S., S. M. Newman, and C. N. Bowman 1995. Polymeric dental composites: Properties and reaction behavior of multimethacrylate dental restorations. *Advances in Polymer Science*. 122: 177–217.
- Bourke, S. L. and J. Kohn 2003. Polymers derived from the amino acid L-tyrosine: Polycarbonates, polyarylates and copolymers with poly(ethylene glycol). *Advanced Drug Delivery Reviews*. 55: 447–66.
- Brey, D. M., C. Chung, K. D. Hankenson, J. P. Garino, and J. A. Burdick 2010. Identification of osteoconductive and biodegradable polymers from a combinatorial polymer library. *Journal of Biomedical Materials Research Part A*. 93A: 807–16.
- Burdick, J. A. and K. S. Anseth 2002. Photoencapsulation of osteoblasts in injectable RGD-modified PEG hydrogels for bone tissue engineering. *Biomaterials*. 23: 4315–23.
- Cerritelli, S., D. Velluto, and J. A. Hubbell 2007. PEG-SS-PPS: Reduction-sensitive disulfide block copolymer vesicles for intracellular drug delivery. *Biomacromolecules*. 8: 1966–72.
- Charati, M. B., J. L. Ifkovits, J. A. Burdick, J. G. Linhardt, and K. L. Kiick 2009. Hydrophilic elastomeric biomaterials based on resilin-like polypeptides. *Soft Matter*. 5: 3412–16.
- Coessens, V., T. Pintauer, and K. Matyjaszewski 2001. Functional polymers by atom transfer radical polymerization. *Progress in Polymer Science*. 26: 337–77.
- Cui, H. G., M. J. Webber, and S. I. Stupp 2010. Self-assembly of peptide amphiphiles: From molecules to nanostructures to biomaterials. *Biopolymers*. 94: 1–18.
- Doh, J. and D. J. Irvine 2004. Photogenerated polyelectrolyte bilayers from an aqueous-processible photoresist for multicomponent protein patterning. *Journal of the American Chemical Society*. 126: 9170–71.
- Domb, A. J. 1990. Biodegradable polymers derived from amino-acids. *Biomaterials*. 11: 686–89.

- Domb, A. J. and R. Nudelman 1995. Biodegradable polymers derived from natural fatty-acids. *Journal of Polymer Science Part A-Polymer Chemistry*. 33: 717–25.
- Drury, J. L. and D. J. Mooney 2003. Hydrogels for tissue engineering: Scaffold design variables and applications. *Biomaterials*. 24: 4337–51.
- Erdmann, L. and K. E. Uhrich 2000. Synthesis and degradation characteristics of salicylic acid-derived poly(anhydride-esters). *Biomaterials*. 21: 1941–46.
- Frazier, D. D., V. K. Lathi, T. N. Gerhart, and W. C. Hayes 1997. Ex vivo degradation of a poly(propylene glycol-fumarate) biodegradable particulate composite bone cement. *Journal of Biomedical Materials Research*. 35: 383–89.
- Gresser, J. D., S. H. Hsu, H. Nagaoka et al. 1995. Analysis of a vinyl pyrrolidone poly(propylene fumarate) resorbable bone-cement. *Journal of Biomedical Materials Research*. 29: 1241–47.
- Griffith, L. G. 2000. Polymeric biomaterials. *Acta Materialia*. 48: 263–77.
- Guvendiren, M., S. Yang, and J. A. Burdick 2009. Swelling-induced surface patterns in hydrogels with gradient crosslinking density. *Advanced Functional Materials*. 19: 3038–45.
- Hartgerink, J. D., E. Beniash, and S. I. Stupp 2002. Peptide-amphiphile nanofibers: A versatile scaffold for the preparation of self-assembling materials. *Proceedings of the National Academy of Sciences of the United States of America*. 99: 5133–38.
- Heller, J., J. Barr, S. Y. Ng, K. S. Abdellauoi, and R. Gurny 2002. Poly(ortho esters): Synthesis, characterization, properties and uses. *Advanced Drug Delivery Reviews*. 54: 1015–39.
- Hern, D. L. and J. A. Hubbell 1998. Incorporation of adhesion peptides into nonadhesive hydrogels useful for tissue resurfacing. *Journal of Biomedical Materials Research*. 39: 266–76.
- Hersel, U., C. Dahmen, and H. Kessler 2003. RGD modified polymers: Biomaterials for stimulated cell adhesion and beyond. *Biomaterials*. 24: 4385–415.
- Hu, Y., T. Litwin, A. R. Nagaraja et al. 2007. Cytosolic delivery of membrane-impermeable molecules in dendritic cells using PH-responsive core-shell nanoparticles. *Nano Letters*. 7: 3056–64.
- Hubbell, J. A. 1995. Biomaterials in tissue engineering. *Bio-Technology*. 13: 565–76.
- Ifkovits, J. L., R. F. Padera, and J. A. Burdick 2008. Biodegradable and radically polymerized elastomers with enhanced processing capabilities. *Biomedical Materials*. 3: 034104.
- Johnson, P. A., A. Luk, A. Demtchouk et al. 2010. Interplay of anionic charge, poly(ethylene glycol), and iodinated tyrosine incorporation within tyrosine-derived polycarbonates: Effects on vascular smooth muscle cell adhesion, proliferation, and motility. *Journal of Biomedical Materials Research Part A*. 93A: 505–14.
- Katz, J. S. and J. A. Burdick 2010. Light-responsive biomaterials: Development and applications. *Macromolecular Bioscience*. 10: 339–48.
- Khetan, S., J. S. Katz, and J. A. Burdick 2009. Sequential crosslinking to control cellular spreading in 3-dimensional hydrogels. *Soft Matter*. 5: 1601–06.
- Kirshenbaum, K., A. E. Barron, R. A. Goldsmith et al. 1998. Sequence-specific polypeptoids: A diverse family of heteropolymers with stable secondary structure. *Proceedings of the National Academy of Sciences of the United States of America*. 95: 4303–08.
- Kloxin, A. M., A. M. Kasko, C. N. Salinas, and K. S. Anseth 2009. Photodegradable hydrogels for dynamic tuning of physical and chemical properties. *Science*. 324: 59–63.
- Kumar, N., R. S. Langer, and A. J. Domb 2002. Polyanhydrides: An overview. *Advanced Drug Delivery Reviews*. 54: 889–910.
- Labet, M. and W. Thielemans 2009. Synthesis of polycaprolactone: A review. *Chemical Society Reviews*. 38: 3484–504.
- Langer, R. and D. A. Tirrell 2004. Designing materials for biology and medicine. *Nature*. 428: 487–92.
- Lee, A. S., A. P. Gast, V. Butun, and S. P. Armes 1999. Characterizing the structure of PH dependent poly-electrolyte block copolymer micelles. *Macromolecules*. 32: 4302–10.
- Lee, H. and T. G. Park 1998. Reduction/oxidation induced cleavable/crosslinkable temperature-sensitive hydrogel network containing disulfide linkages. *Polymer Journal*. 30: 976–80.

- Li, S. M. 1999. Hydrolytic degradation characteristics of aliphatic polyesters derived from lactic and glycolic acids. *Journal of Biomedical Materials Research*. 48: 342–53.
- Loh, X. J., K. B. C. Sng, and J. Li 2008. Synthesis and water-swelling of thermo-responsive poly(ester urethane)s containing poly(epsilon-caprolactone), poly(ethylene glycol) and poly(propylene glycol). *Biomaterials*. 29: 3185–94.
- Lutolf, M. P. and J. A. Hubbell 2005. Synthetic biomaterials as instructive extracellular microenvironments for morphogenesis in tissue engineering. *Nature Biotechnology*. 23: 47–55.
- Lutolf, M. P., J. L. Lauer-Fields, H. G. Schmoekel et al. 2003. Synthetic matrix metalloproteinase-sensitive hydrogels for the conduction of tissue regeneration: Engineering cell-invasion characteristics. *Proceedings of the National Academy of Sciences of the United States of America*. 100: 5413–18.
- Maniar, M., X. D. Xie, and A. J. Domb 1990. Polyanhydrides. 5. Branched polyanhydrides. *Biomaterials*. 11: 690–94.
- Metters, A. T., K. S. Anseth, and C. N. Bowman 2000. Fundamental studies of a novel, biodegradable PEG-b-PLA hydrogel. *Polymer*. 41: 3993–4004.
- Miller, J. S., C. J. Shen, W. R. Legant et al. 2010. Bioactive hydrogels made from step-growth derived PEG-peptide macromers. *Biomaterials*. 31: 3736–43.
- Moad, G., E. Rizzardo, and S. H. Thang 2005. Living radical polymerization by the raft process. *Australian Journal of Chemistry*. 58: 379–410.
- Mousa, W. F., M. Kobayashi, S. Shinzato et al. 2000. Biological and mechanical properties of PMMA-based bioactive bone cements. *Biomaterials*. 21: 2137–46.
- Muggli, D. S., A. K. Burkoth, and K. S. Anseth 1999. Crosslinked polyanhydrides for use in orthopedic applications: Degradation behavior and mechanics. *Journal of Biomedical Materials Research*. 46: 271–78.
- Nair, L. S. and C. T. Laurencin 2007. Biodegradable polymers as biomaterials. *Progress in Polymer Science*. 32: 762–98.
- Odian, G. 2004. *Principles of polymerization*. Hoboken, NJ: John Wiley & Sons, Inc.
- Patch, J. A. and A. E. Barron 2002. Mimicry of bioactive peptides via non-natural, sequence-specific peptidomimetic oligomers. *Current Opinion in Chemical Biology*. 6: 872–77.
- Ratner, B. D. and S. J. Bryant 2004. Biomaterials: Where we have been and where we are going. *Annual Review of Biomedical Engineering*. 6: 41–75.
- Santerre, J. P., K. Woodhouse, G. Laroche, and R. S. Labow 2005. Understanding the biodegradation of polyurethanes: From classical implants to tissue engineering materials. *Biomaterials*. 26: 7457–70.
- Sawhney, A. S., C. P. Pathak, and J. A. Hubbell 1993. Bioerodible hydrogels based on photopolymerized poly(ethylene glycol)-co-poly(alpha-hydroxy acid) diacrylate macromers. *Macromolecules*. 26: 581–87.
- Sciannamea, V., R. Jerome, and C. Detrembleur 2008. In-situ nitroxide-mediated radical polymerization (NMP) processes: Their understanding and optimization. *Chemical Reviews*. 108: 1104–26.
- Sheihet, L., K. Piotrowska, R. A. Dubin, J. Kohn and D. Devore 2007. Effect of tyrosine-derived triblock copolymer compositions on nanosphere self-assembly and drug delivery. *Biomacromolecules*. 8: 998–1003.
- Shin, H., S. Jo, and A. G. Mikos 2003. Biomimetic materials for tissue engineering. *Biomaterials*. 24: 4353–64.
- Suggs, L. J., R. G. Payne, M. J. Yaszemski, L. B. Alemany, and A. G. Mikos 1997. Synthesis and characterization of a block copolymer consisting of poly(propylene fumarate) and poly(ethylene glycol). *Macromolecules*. 30: 4318–23.
- Temenoff, J. S. and A. G. Mikos 2000. Injectable biodegradable materials for orthopedic tissue engineering. *Biomaterials*. 21: 2405–12.
- Wang, L. and P. G. Schultz 2005. Expanding the genetic code. *Angewandte Chemie-International Edition*. 44: 34–66.
- Wang, Y. D., Y. M. Kim, and R. Langer 2003. In vivo degradation characteristics of poly(glycerol sebacate). *Journal of Biomedical Materials Research Part A*. 66A: 192–97.

- Wolfe, M. S., D. Dean, J. E. Chen et al. 2002. In vitro degradation and fracture toughness of multilayered porous poly(propylene fumarate)/beta-tricalcium phosphate scaffolds. *Journal of Biomedical Materials Research*. 61: 159–64.
- Yu, C. and J. Kohn 1999. Tyrosine-PEG-derived poly(ether carbonate)s as new biomaterials—Part I: Synthesis and evaluation. *Biomaterials*. 20: 253–64.
- Zhang, Z., R. Kuijjer, S. K. Bulstra, D. W. Grijpma, and J. Feijen 2006. The in vivo and in vitro degradation behavior of poly(trimethylene carbonate). *Biomaterials*. 27: 1741–48.

Nanobiomaterials for Tissue Engineering

Pramod K. Avti
Stony Brook University

Sunny C. Patel
Stony Brook University

Pushpinder Uppal
Stony Brook University

Grace O'Malley
Stony Brook University

Joseph Garlow
Stony Brook University

Balaji Sitharaman
Stony Brook University

49.1	Introduction	49-1
49.2	Nanobiomaterials to Improve Bulk and Surface Properties of Tissue Engineering Scaffolds.....	49-2
	Nanofibrous Scaffolds • Nanobiomaterial-Incorporated Polymer Scaffolds	
49.3	Nanobiomaterials for Therapeutic Delivery.....	49-5
49.4	Nanobiomaterials to Image the Process of Tissue Formation... ..	49-9
49.5	Continuing and Future Developments.....	49-13
	Abbreviations	49-13
	References.....	49-15

49.1 Introduction

Tissue engineering (TE) is an emerging interdisciplinary field that seeks to restore, improve and maintain normal tissue or organ functions. To these ends, one or more of the following three components: progenitor cells, signaling molecules, and engineered biomaterials or scaffolds are applied (Langer and Vacanti, 1993). The advancement of TE requires new biomaterials to deliver important biochemical moieties (e.g., growth factors) to the engineered tissues, to direct tissue growth, and to improve monitoring and evaluating of the regenerating tissue.

Nanotechnology-based approaches are currently being pursued for a variety of biomedical applications. Nanotechnology is a relatively new field of science broadly defined as research and technology development at length scales between 1 and 100 nm to create materials, gain fundamental insights into their properties, and to use the nanoscale materials as components or building blocks to create novel structures, or devices (Rodgers et al., 2006). At these length scales, materials show unique properties and functions. However, in certain cases, the length scales for these novel properties maybe under 1 nm (down to 0.1 nm for atomic and molecular manipulation) or over 100 nm (up to 300 nm in case of nanopolymers and nanocomposites). Nanotechnology is a convergent technology in which, the boundaries separating discrete disciplines become blurred. Biochemists, materials scientists, electrical engineers, and molecular biologists may all be considered experts in the field if they are involved in the development of nanosized structures.

Specifically for TE, nanotechnology-based approaches allow the synthesis of unique nanobiomaterials having nanoscale features that can mimic the natural extracellular matrix to affect the cellular functions (e.g., adhesion, mobility, and differentiation) (Harrison and Atala, 2007; Kim and Fisher, 2007). Further, these nanobiomaterials could be developed with multifunctional capabilities as delivery agents of signaling molecules and genes as well as efficient imaging probes to noninvasively monitor implanted cells, and the process of tissue regeneration in tissue-engineered constructs. This chapter provides the reader

a perspective of nanobiomaterials for TE. It discusses the various nanobiomaterials been developed to (a) improve bulk and surface properties of TE scaffolds; (b) deliver biochemical moieties (e.g., genes, growth factors); and (c) image the process of tissue formation.

49.2 Nanobiomaterials to Improve Bulk and Surface Properties of Tissue Engineering Scaffolds

Nanobiomaterial-based approaches have been used in the developments of two types of TE structures: (1) Nanofibrous scaffolds and (2) Nanobiomaterial-incorporated polymer composite scaffolds.

49.2.1 Nanofibrous Scaffolds

Scaffolds are porous biomaterials and play a pivotal role in the TE paradigm by providing temporary structural support, guiding cells to grow, assisting the transport of essential nutrients and waste products, and facilitating the formation of functional tissues and organs. Nanofiber scaffolds are TE scaffolds with nanoscopic structure and morphologies fabricated using natural and synthetic materials. These materials are biodegradable or nonbiodegradable polymers and generally biocompatible. Some examples of the natural materials used as starting materials for the development of nanofiber scaffolds are self-assembling polypeptides, DNA, RNA, carbohydrates, peptides, collagen, fibrin, glycosaminoglycans, fibrinogen, gelatin, elastin, silk, hyaluronan, and chitosan (Matthews et al., 2002; Min et al., 2004; Silva et al., 2004; Bhattarai et al., 2005; Li et al., 2005; Hamdi et al., 2009; Carneiro et al., 2010). Examples of synthetic materials include poly(ethylene glycol) (PEG), poly(vinyl alcohol) (PVA), poly(hydroxyethyl methacrylate), poly(lactic acid) (PLA), poly(glycolic acid), poly(lactic-*co*-glycolic acid) (PLGA), poly(ϵ -caprolactone) (PCL), poly(methyl methacrylate) (PMMA), poly(propylene fumarate) (PPF) (Ding et al., 2002; Kenawy et al., 2003; Gupta et al., 2005; Kim et al., 2005; Chen et al., 2008; Choi et al., 2008; Corey et al., 2008; Powell and Boyce, 2008). Nanofiber scaffolds have special characteristics such as high surface area to volume ratio, functional groups for high density functionalization, and high porosities. The nanofibers can also mimic natural extracellular matrix (ECM). The fabrication techniques used in synthesizing these scaffolds are phase separation (Smith and Ma, 2004), melt-blowing, template synthesis, electrospinning (Li et al., 2002), and self-assembly (Whitesides and Boncheva, 2002). Among these methods, nanofibers obtained from electrospinning and self-assembly have widespread applications in bone, skin, neural, cartilage, vascular heart, and lung TE (Pham et al., 2006; Rubenstein et al., 2007; Chew et al., 2008; Venugopal et al., 2008).

The electrospinning method allows the fabrication of solid, hollow, or core-shell nanofiber scaffolds, where the nanofibers can be randomly arranged or aligned along a particular direction (Bini et al., 2004; Corey et al., 2007). The hollow fiber scaffolds (Figure 49.1) are suitable for loading drugs, and enzymes to improve tissue regeneration (Bini et al., 2004).

The core-shell fibers are also well suited for drug-delivery applications as the core helps in loading the drug and the shell controls release kinetics. Synthetic and overexpressed peptide and protein precursors have been widely used as starting materials for the development of self-assembled nanofiber scaffolds (Koide et al., 2005; Kotch and Raines, 2006; Paramonov et al., 2006; Woolfson and Ryadnov, 2006; Gauba and Hartgerink, 2007). For instance, elastin is a self-assembling polymeric protein with good mechanical strength properties with potential applications for vascular TE (Bellingham et al., 2003; Miao et al., 2005; Daamen et al., 2007). Recently, recombinant (synthetic) polypeptides of elastin were self-assembled to form novel macromolecular nanostructures (Bellingham et al., 2003; Vieth et al., 2007). Self-assembled nanofiber scaffolds are well-suited to incorporate cell signaling molecules that can affect progenitor cell behavior such as their attachment, differentiation, and proliferation (Hofmann et al., 2006; Meinel et al., 2006, 2009). The complexity of the self-assembly techniques leads to low yields and relatively high cost; its main limitations compared to the electrospinning method. Table 49.1 lists some of the recent advances in the development of nanofibrous scaffolds for TE.

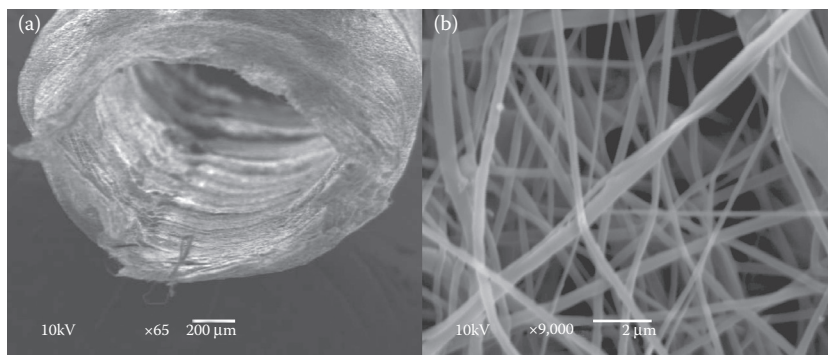


FIGURE 49.1 SEM imaging of micro- and nanofiber electrospun poly(1-caprolactone)/poly(D,L-lactic-co-glycolic acid) tubular scaffolds designed for regenerating sciatic nerve transections. (a) Tube lumen and (b) zoomed details of the tube wall. Both nano- and microfibers are visible. Fiber links are obtained via partial solvent evaporation and polymer annealing subsequent to electrospinning in order to increase the overall prosthesis mechanical properties. (Reprinted from *Biomaterials* 26(31), Bhattarai N. et al. Electrospun chitosan based nanofibers and their cellular compatibility, 6176–84. Copyright 2005, with permission from Elsevier.)

TABLE 49.1 Nanofibrous Scaffolds

Nanofiber Material	Intended Application	Functions and Biological Response/Improvements	Reference
PLGA	Neural TE	Neurite formation and elongation	Lee et al. (2009)
	Bladder tissue engineering	Increased bladder cell adhesion and growth, increased production of elastin, and collagen proteins enhance in urinary bladder wall replacement	Pattison et al. (2005)
PGS	Retinal transplantation	Improved the growth of graft-host cells without signs of inflammation	Pritchard et al. (2010)
	Vascular regeneration	Decreased thrombogenicity (platelet adhesion and aggregation) and inflammatory response when used as blood contacting surface	Motlagh et al. (2006)
	Cardiac tissue engineering	Bioinert, biocompatible, wide degradation properties, good mechanical properties matching the physical characteristics of heart tissue	Chen et al. (2008)
PEG	Cartilage regeneration	Improved cellularity, collagen and glycosaminoglycan content	Mahmood et al. (2006)
	Wound healing	Fibronectin-coupled PEG are cytocompatible, improves proliferation and migration of fibroblasts both <i>in vitro</i> and <i>in vivo</i>	Ghosh et al. (2006)
PLLA	Neural tissue engineering	Improves neurite growth, elongation, and differentiation	Corey et al. (2007); Yang et al. (2004, 2005)
	Cardiac tissue engineering	Increased contractile machinery (sarcomeres) in cardiomyocytes	Zong et al. (2005)
	Bone tissue engineering	Increased osteoblast adhesion, proliferation, mineralization, and protein marker expression	Woo et al. (2003, 2006)
CNFs	Neural tissue engineering	Increased elastic modulus, neuronal cell adhesion, neurite extension, and decreased astrocyte adhesion	McKenzie et al. (2004)
	Vascular tissue engineering	Supports the aggregation and enhances the migration ability of endothelial cells	Han et al. (2009)

continued

TABLE 49.1 (continued) Nanofibrous Scaffold

Nanofiber Material	Intended Application	Functions and Biological Response/Improvements	Reference
Peptide nanofibers	Bone tissue engineering	Increased osteoblast adhesion, enhanced mineral deposition, decreased fibroblast adhesion	Khang et al. (2006); Price et al. (2003)
	Bladder tissue regeneration	Promotes bladder smooth muscle cells attachment, matrix production and spindled morphology	Harrington et al. (2006)
	Neural regeneration	IKVAV-Peptide nanofibers increased the neural progenitor cells attachment, migration, neurite outgrowth and undergo selective and rapid differentiation.	Silva et al. (2004)
	Vascular tissue regeneration	Heparin binding-peptide nanofibers influenced the tube formation in endothelial cells	Rajangam et al. (2006, 2008)
	Cardiac tissue engineering	Heparin binding-peptide nanofibers restored the hemodynamic functions in acute myocardial infarction	Rajangam et al. (2006, 2008)
PCL	Skin grafting	Improved growth, longevity of keratinocytes and fibroblasts during wound healing	Reed et al. (2009)
	Vascular tissue engineering	Modulated smooth muscle cells behavior to express contractile phenotype, attained spindle shape, oriented and directional migration	Xu et al. (2004)
	Cardiac tissue engineering	Enhanced cardiomyocytes attachment, growth and proliferation. Increased synchronized contraction and contractile machinery (actin, tropomyosin, cardiac troponin)	Ishii et al. (2005); Shin et al. (2004)
	Bone tissue engineering	Improved cellular adhesion, penetration into the scaffold thereby releasing ECM and helps in differentiation	Yoshimoto et al. (2003); Shin et al. (2004); Li et al. (2005a,b)
Polyurethane	Skin grafting	Increased rate of epithelialization, well organized dermis formation	Khil et al. (2003)
Chitin nanofiber	Skin tissue engineering	Promoted keratinocyte and fibroblast cellular attachment and proliferation	Noh et al. (2006)
SF	Skin tissue engineering	Highly porous, high surface area and improved mechanical properties of SFs responsible for use in wound dressing material and skin regeneration application	Kim et al. (2003)
PET	Vascular tissue engineering	Increased hydrophobicity of scaffold enables endothelial cells to attain polygonal morphology and express cell adhesion markers PECAM, ICAM, VCAM responsible for vascularization	Ma et al. (2005)

49.2.2 Nanobiomaterial-Incorporated Polymer Scaffolds

Nanoparticles have also been incorporated into porous scaffolds to improve their bulk and surface properties. A large number of porous scaffolds do not possess mechanical properties (a bulk property) necessary for *in vivo* applications (Mistry and Mikos, 2005). Thus, nanobiomaterials are incorporated into these scaffolds to improve their mechanical properties. For instance, carbon nanotubes have high Young's modulus (~1 TPa), and therefore, have been incorporated as reinforcing agents into porous polymer scaffolds to improve their mechanical properties (Lukic et al., 2005; Shi et al., 2005) (Figure 49.2).

Further, organic or inorganic nanomaterials have also been incorporated to induce bioactive properties (a surface property) into the scaffolds. The rationale here is that the physical interface between biological systems (e.g., proteins, DNA) and nanobiomaterials share a number of common (e.g., similar size scales) as well as complementary (e.g., inorganic/organic versus biological composition) attributes. Since, the

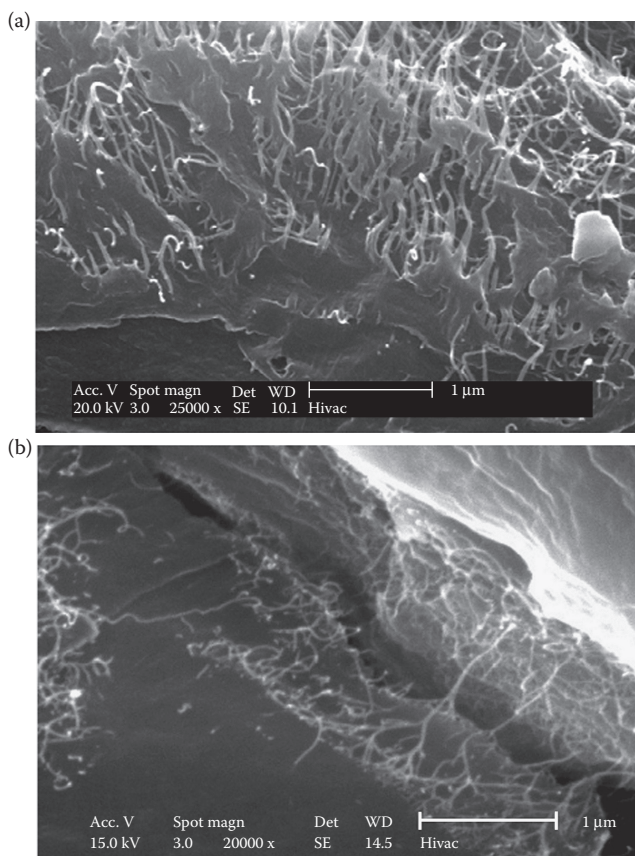


FIGURE 49.2 SEM images of single-walled carbon nanotubes (SWCNTs) incorporated polymer scaffolds. (a) SWCNT bundles pulled out of the fracture surface from SWCNT polymer scaffold (0.05% by weight of SWCNT was dispersed in the scaffold). (b) Crack region propagation is prevented by spanning the SWCNT bundles. (Shi, X. et al. Rheological behaviour and mechanical characterization of injectable poly(propylene fumarate)/single-walled carbon nanotube composites for bone tissue engineering. *Nanotechnology*. 16: S531–8. Copyright 2005 IOP Science.)

nanoscale interactions in tissues (e.g., protein–protein interaction) are crucial for controlling many cellular functions such as cell–cell interactions, migration, proliferation, and ECM production (Benoit and Anseth, 2005), the nanomaterials could affect these interactions to achieve the desired result. For instance, incorporating ceramic nanoparticles into polymer scaffolds has been shown to induce bioactive properties into the scaffolds (Liu et al., 2006). The bioactive properties are induced by the ceramic nanoparticles by improving the adsorption characteristics of proteins such as fibronectin, vitronectin, laminin, and collagen involved in osteoblast functions (Webster et al., 1999, 2000, 2001). Some of the common fabrication techniques to incorporate nanoparticles into scaffolds include solvent casting, salt leaching, and freeze drying. Using all these methods, the individual nanoparticles are randomly distributed into the scaffolds. More examples of the nanoparticle-incorporated scaffolds examples and their applications are listed in [Table 49.2](#).

49.3 Nanobiomaterials for Therapeutic Delivery

Controlled production and/or delivery of tissue-inducing macromolecules such as cytokines and growth factors are widely applied strategies in regenerative medicine. The physical and chemical properties of a large number of nanobiomaterials make them suitable for a variety of therapeutic and drug-delivery

applications in TE (Figure 49.3). The external surfaces of the nanobiomaterials can be covalently or noncovalently functionalized with biological moieties that target specific cell or tissues types and/or pharmaceutical agents. Here, the nanobiomaterials target a specific cell or tissue type, and act as biological cargo vehicles to transport, and deliver therapeutic agents via a biochemical or biophysical stimulus (Langer and Tirrell, 2004).

Furthermore, the nanobiomaterial themselves can be used as a therapeutic agent by exploiting their unique physical properties (Shi et al., 2010). For example, the strong optical absorption properties of SWCNTs and gold nanoparticles render them capable of generating acoustic waves upon irradiation. These waves have shown to affect the process of osteoinduction (Green et al., 2009). Other advantages of using nanobiomaterials for therapeutic purposes, and as delivery vehicles include their nanoscale dimensions, which enhance their retention and permeability in the regenerating tissues (Gannon et al.,

TABLE 49.2 Nanobiomaterial-Based Polymer/Composite Scaffolds

Nanoparticle Material	Intended Applications	Function and Biological Improvements	Reference
<i>n</i> -HA/PA, <i>n</i> -HA/PA/ MSC	Bone Tissue engineering	Enhanced osteogenesis than pure <i>n</i> -HA/PA scaffolds	Wang et al. (2007)
Bioactive-glass ceramic nanoparticles	Bone tissue engineering	Higher amount of mineral deposited on the composite scaffold, which increased with increasing time of incubation	Peter et al. (2010)
Bioglass-based glass-ceramic pellets	General applications	Bioactive and resorbable nanofibrous coatings can be used to tailor the surface topography of bioactive glass-ceramics	Bretcanu et al. (2009)
Mesoporous bioactive glasses	Bone tissue engineering	<i>In vitro</i> bioactivity of these MBGs scaffolds was dependent on the chemical composition	Zhu et al. (2008), Yan et al. (2006)
Forsterite	Bone tissue engineering	Significantly promoted cell proliferations, cell adhesion, spread, and growth on the surface of the nanostructured forsterite ceramic	Kharaziha and Fathi (2010)
Chitosan–nanohydroxyapatite	Bone tissue engineering	Well-developed structure morphology, physicochemical properties and superior cytocompatibility seen in chitosan– <i>n</i> HA porous scaffolds	Thein-Han and Misra (2009)
HA and PEG/PBT	Bone tissue engineering	Increased Young's modulus, tensile strength, and elongation at break of composite scaffold	Liu et al. (1998)
HA/PLLA	Bone tissue engineering	Increased compressive modulus and protein adsorption	Wei and Ma (2004)
HA/PLGA	Bone tissue engineering	Stimulated cell proliferation and osteogenic differentiation	Kim et al. (2006)
HA/PLGA	Bone tissue engineering	<i>In vivo</i> bone formation after 8 weeks of implantation to critical size defects in rat skulls	Kim et al. (2007)
POC	Cardiac tissue engineering	Decreased porosity caused a rise in the elastic modulus, ECM proteins promoted cell adhesion in a protein-type- and concentration-dependent manner	Hidalgo-Bastida et al. (2007)
Cellulose acetate, regenerated cellulose	Cardiac tissue engineering	Cellulose acetate and regenerated cellulose surfaces promoted cardiac cell growth, enhanced cell connectivity (gap junctions) and electrical functionality	Entcheva et al. (2004)
Fibrin	Cardiac tissue engineering	Dense fibrin scaffolds had mechanical properties closer to native myocardium than fibrin gels	Robinson et al. (2008), Thomson et al. (2010)
PF	Cardiac tissue engineering	PF hydrogel biomaterial can be used as an <i>in situ</i> polymerizable biomaterial for stem cells and their cardiomyocyte derivatives	Shapira-Schweitzer et al. (2009)

TABLE 49.2 (continued) Nanobiomaterial-Based Polymer/Composite Scaffolds

Nanoparticle Material	Intended Applications	Function and Biological Improvements	Reference
Fibrin, Collagen	Neural tissue engineering	Cells showed high viability after printing, which was equivalent to that of manually plated cells, cells printed within 1 mm from the border of VEGF releasing fibrin gel showed GF-induced changes in their morphology	Lee et al. (2010)
SWCNT/PPF	Bone tissue engineering	Significantly improved flexural and compressive modulus, compressive offset yield strength, flexural strength	Shi et al. (2006)
HA/collagen dip-coated in aqueous ferrofluids containing iron oxide nanoparticles	Bone tissue engineering	Magnetic scaffolds supported adhesion and proliferation of human bone marrow stem cells <i>in vitro</i>	Bock et al. (2010)
Gold colloid/chitosan film	Skin tissue engineering	Significantly increased the attachment of keratinocytes and promote their growth; a good candidate for wound dressing in skin tissue engineering	Zhang et al. (2009)
Silver and collagen type 1	Neural tissue engineering	Superior functionality of the nano-silver-collagen scaffold in the adsorption to laminin and subsequent regeneration of damaged peripheral nerves	Ding et al. (2010)
Titanium, CoCrMo	Vascular stent applications	Vascular stents composed of nanometer compared with micron-sized metal particles invoked cellular responses important for improved vascular stent applications	Choudhary et al. (2006)
Titanium	Vascular stent applications	Enhanced endothelial and vascular smooth muscle cell functions compared with those of conventional-sized particles	Choudhary et al. (2007)
Titanium	Bone tissue engineering	Superior compressive strength, and osteoconductivity of PMMA composite	Goto et al. (2005)
Titanium	Bone tissue engineering	Enhanced cellular adhesion	Webster et al. (1999), Kay et al. (2002)
Titanium	Bone tissue engineering	Increased osteogenic functions in PLGA composite scaffolds	Webster and Smith (2005), Liu et al. (2005, 2006)
Surface-modified alumoxane, PPF/PF-DA	Bone tissue engineering	Demonstrated feasibility of fabricating degradable nanocomposite scaffolds for bone tissue engineering by photo-crosslinking fumarate-based polymers, alumoxane nanoparticles	Mistry et al. (2009)
Aluminum	Bone tissue engineering	Increased flexural, and compressive strength of PPF composite scaffold	Horch et al. (2004)
Polyurethane	Cardiac tissue engineering	Cells cultured on laminin and collagen IV exhibited preferential attachment	Alperin et al. (2005)
PGS	Cardiac tissue engineering	Showed a wide range of degradability	Chen et al. (2008)
PGS	Cardiac tissue engineering	Strain amplifications were lower in ALH versus rectangular honeycomb scaffolds, appearing to be inversely correlated with previously measured strains-to-failure	Jean and Engelmayr (2010)
Alginate	Cardiac tissue engineering	Immobilized RGD peptide promoted cell adherence to the matrix, prevented cell apoptosis and accelerated cardiac tissue regeneration	Shachar et al. (2011)

continued

TABLE 49.2 (continued) Nanobiomaterial-Based Polymer/Composite Scaffolds

Nanoparticle Material	Intended Applications	Function and Biological Improvements	Reference
PEG	Neural tissue engineering	Initial presence of fibrin did not influence the cell-fate decisions of the encapsulated precursor cells (fibrin degraded enzymatically)	Namba et al. (2009)
PVA/PAA IPN films, PDMS	Neural tissue engineering	Glial fibrillary acidic protein immunoreactivity in animals receiving coated implants was significantly lower compared to that of uncoated implants, neurite extension of rat pheochromocytoma cells was clearly greater on PVA/PAA IPN films than on PDMS substrates	Lu et al. (2009)
Melanin	Neural tissue engineering	Enhanced Schwann cell growth and neurite extension compared to collagen films <i>in vitro</i> ; induced an inflammation response that was comparable to silicone implants; implants were significantly resorbed after 8 weeks	Bettinger et al. (2009)
Silica/PCL	Bone tissue engineering	Similar mechanical properties of natural bone	Yoo and Rhee (2004)
PCL, PCL/Matrigel	Neural tissue engineering	Covalently functionalized PCL/Matrigel nanofibrous scaffolds promoted the proliferation and neurite outgrowth of NPCs compared to PCL	Ghasemi-Mobarakeh et al. (2010)
PCL	Neural tissue engineering	Cells on nanowire surfaces expressed key neuronal markers and demonstrated neuronal phenotypic behavior as compared to the cells on control surfaces, significantly higher cell adhesion, proliferation and viability of cells cultured on nanowire surfaces	Bechara et al. (2010)
PCL/gelatin	Neural tissue engineering	Increased hydrophilicity of nanofibrous scaffolds and yielded better mechanical properties compared to PCL alone	Gupta et al. (2009)
PCL	Cardiac tissue engineering	Low stiffness in the range of 300–400 kPa for soft-tissue engineering achieved; high density of cells was recorded after 4 days of culture. Fusion and differentiation observed as early as 6 days <i>in vitro</i> and was confirmed after 11 days	Yeong et al. (2010)
PCL	Cardiac tissue engineering	Honeycomb structures and the pore sizes influenced the morphology, cytoskeletal organization and focal adhesion of the cardiac myocytes	Arai et al. (2008)
PLGA	Bone tissue engineering	Collagen mineralization process induced the formation of nanosize carbonated hydroxyapatite, while nanosize hydroxyapatite is formed during PLGA mineralization	Liao et al. (2008)
PLLA	Bladder tissue engineering	Provided an optimal microenvironment for facilitating cell-matrix penetration and retention of myogenic-differentiated BMSCs	Tian et al. (2010)
	Cardiac tissue engineering	Better cell adhesion and mature cytoskeleton structure with well-defined periodic units in the contractile machinery (sarcomeres) in PLLA, superior response in PLLA, CM cell density was lower on hydrophilic and faster degrading electrospun scaffolds	Zong et al. (2005)
	Neural tissue engineering	Directed neuronal stem cell elongation and its neurite outgrowth is parallel to the direction of PLLA fibers	Yang et al. (2005)
	Bone tissue engineering	Dual-scale scaffold structures provided a better choice for tissue engineering and 3-D cell culture applications with	Cheng and Kisaalita (2010)

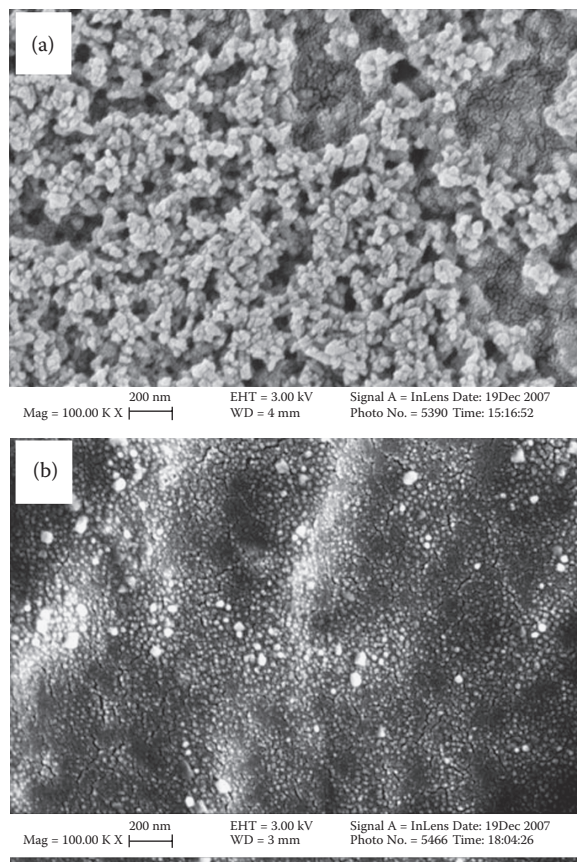


FIGURE 49.3 Nano-HA-PLGA-peptide drug delivery system. SEM images of the (a) HA-PLGA nanoparticles with peptides physically adsorbed on the nanoparticles and (b) HA/PLGA nanoparticles with peptides covalently immobilized on the nanoparticles. (Liu, H. and T. J. Webster. Ceramic/polymer nanocomposites with tunable drug delivery capability at specific disease sites. *J Biomed Mater Res A*. 93(3): 1180–92. Copyright 2010 Wiley Interscience. Reproduced with permission.)

2007). Additionally, in case of certain types of nanomaterials (e.g., nanorods or nanotubes), their large aspect ratio allows attachment of multiple functional groups for the targeted delivery of multiple therapeutic entities. [Table 49.3](#) represents some of the developed nanobiomaterial systems for delivery and therapeutic applications.

49.4 Nanobiomaterials to Image the Process of Tissue Formation

The limitations of standard diagnostic tools and techniques for detecting, and monitoring the process of tissue regeneration in small animals are well known (Greco, 2008). The most robust technique for the evaluation of *de novo* tissue formation, neo-vascularization or monitoring the fate of transplanted cells is histological analysis. Because histology is an endpoint evaluation, and large variation is observed, it is difficult to assess temporal results in a statistically significant manner. In search of alternatives, much progress has been made on new approaches for noninvasive *in vivo* imaging using positron emission tomography (PET), magnetic resonance imaging (MRI), and x-ray computed tomography (CT).

These imaging modalities offer scientists the spatial and temporal information in a faster and more convenient manner. For each imaging modality, substantial attention has been devoted to the

development of contrast agents. Novel nanobiomaterial-based contrast agents may enhance molecular imaging by improving detection sensitivity and selectivity. The strategies developed for design of these nanobiomaterial-based contrast agents for imaging tissue regeneration include encapsulation or coating of medically relevant metal ions within hollow nanomaterials (Figure 49.4), the functionalization of the exterior surface of the nanobiomaterials with a variety of imaging agents (e.g., organic

TABLE 49.3 Nanobiomaterial-Based Drug Delivery System in Tissue Engineering

Nanoparticle System	Intended Application	Delivery	Function and Biological Improvements	Reference
Dendrimer	Bone tissue engineering	Gene delivery	LacZ gene transduction in human chondrocyte-like cell without cytotoxic effect and morphological changes	Ohashi et al. (2001)
	Bone tissue engineering	Gene delivery	Increased nucleus penetration and enhanced gene transfection using dexamethasone conjugated PAMAM	Choi et al. (2006)
	Bone tissue engineering	Gene delivery	Targeted delivery of antiarthritic drug with folate-PAMAM dendrimer	Chandrasekar et al. (2007)
	Bone tissue engineering	Gene delivery	Improved bone formation in a rat bone-defect model using magnetic rhBMP-2 liposomes	Matsuo et al. (2003)
	Bone tissue engineering	Gene delivery	Enhanced bone formation in cranial defect on rabbit model using cationic liposome loading BMP-2 cDNA plasmids	Ono et al. (2004)
Liposome	Bone tissue engineering	Gene delivery	Critical size defect healing in rat model	Park et al. (2003)
Micelle	Bone tissue engineering	Gene delivery	Improved efficiency, and less toxic transfection toward primary osteoblast cells using polyplex micelles	Kanayama et al. (2006)
	Bone tissue engineering	Gene delivery	Allowed adherence of aldehyde-terminated PEG-PLA block polymer to a tissue surface <i>in vivo</i>	Murakami et al. (2007)
PEGylation	Bone tissue engineering	Gene delivery	Extended half-life of BSA with PEG-PLGA nanoparticle	Li et al. (2001)
	Neurons tissue engineering	Drug delivery	TTC was conjugated to nanoparticles using neutravidin, and the resulting nanoparticles were shown to selectively target neuroblastoma cells <i>in vitro</i>	Townsend et al. (2007)
		Drug delivery	The amount of lipid coverage affected its drug release kinetics	Chan et al. (2009)
		Gene delivery	Variable transfection activity can be achieved over extended periods of time upon release of pDNA and nonviral gene delivery vectors from electrospun coaxial fiber mesh scaffolds	Saraf et al. (2010)
	Bone tissue engineering	Gene delivery	Showed effective gene release with AMPEG/PCL nanoparticle with low density of primary amine groups	Jang et al. (2006)
Bone tissue engineering	Gene delivery	Demonstrated higher DNA protection to enzymatic degradation and higher reporter gene expression with PEG-cationized gelatin	Kushibiki and Tabata (2005)	
Polymeric	Intra ocular	Device delivery	Photo-crosslinked PPF-based matrices showed promise as long-term delivery devices for intraocular drug delivery.	Haesslein et al. (2006)

TABLE 49.3 (continued) Nanobiomaterial-Based Drug Delivery System in Tissue Engineering

Nanoparticle System	Intended Application	Delivery	Function and Biological Improvements	Reference
Polymeric nanoparticle + DNA	Ophthalmic	Drug delivery	Combination of the nanoparticles with bioadhesive polymers increased the ocular drug bioavailability	Langer et al. (1997)
	Cancer treatment	Drug delivery	Surface functionalization of NPs with the A10 PSMA Apt significantly enhanced delivery of NPs to tumors versus equivalent NPs lacking the A10 PSMA Apt	Cheng et al. (2007)
	Tumor treatment	Drug delivery	PEO-modified poly-1 nanoparticles could provide increased therapeutic benefit by delivering the encapsulated drug to solid tumors	Potineni et al. (2003)
		Drug delivery	NPs with methoxyl surface groups might be an ideal candidate for drug delivery applications	Salvador-Morales et al. (2009)
	Horomone therapy	Hormone delivery	Blood glucose levels of diabetic rats can be effectively controlled by oral SS-ILP administration	Morishita et al. (2006)
	Hormone therapy	Hormone delivery	Particle size and delivery site are very important factors for ILP with respect to increasing the bioavailability of insulin following oral administration.	Morishita et al. (2004), Huang and Wang (2006)
	Bone tissue engineering	Gene delivery	Increased DNA penetration into the cells and luciferase activity with DNA-PEG-gelatin nanoparticle	Hosseinkhani and Tabata (2006)
	Bone tissue engineering	Gene delivery	Up to 70% high DNA encapsulation efficiency with sustained release both <i>in vitro</i> and <i>in vivo</i>	Cohen et al. (2000)
	Bone tissue engineering	Gene delivery	PLGA nanoparticle with tetracycline with affinity for HA	Choi et al. (2005)
	Tissue specific	Gene delivery	Variations in nanoparticle peptide coating density can alter the tissue-specificity of gene delivery <i>in vivo</i>	Harris et al. (2010)
Bone tissue engineering	Gene delivery	Polymerized nanogel with stability in aqueous media, low toxicity, and enhanced DNA uptake in HeLa cell	McAllister et al. (2002)	
Bone tissue engineering	Gene delivery	Penetration of PLGA-VEGF nanoparticle carrier in myocardial cells and successful <i>in vivo</i> angiogenesis	Yi et al. (2006)	
Bone tissue engineering	Gene delivery	Higher gene expression level with smaller size of PLGA	Prabha et al. (2002)	
Nanosized inorganic material	Bone tissue engineering	Gene delivery	Enhanced DNA internalization of DNA mediated by folate receptor binding, improved gene transfection rate subsequently	Mansouri et al. (2006)
	Bone tissue engineering	Gene delivery	<i>In vitro</i> DNA transfection using DNA-chitosan nanoparticle	Erbacher et al. (1998)
	Bone tissue engineering	Gene delivery	Co-precipitated DNA with calcium phosphate nanocomposites onto the cell-culture surface enhanced b-gal expression level in MG-63 and Saos-2 cells	Shen et al. (2004)
Nanosized metallic material	Renal regeneration	Gene delivery	Synthesized shRNA that is specific to the p53 gene was efficiently delivered into HEK293 and HeLa human cell lines	Ryou et al. (2010)

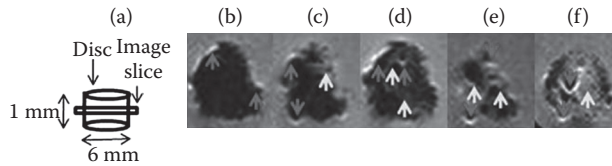


FIGURE 49.4 MRI of Gadonanotube-reinforced biodegradable polymer nanocomposites. (a) Schematic of the sample arrangement within the MRI. Representation two-dimensional images through a nanocomposite disc after (b) 2 h, (c) 24 h, (d) 3 days, (e) 5 days, and (f) 7 days. The higher (white) pixel intensities within the dark disc represent regions of higher water concentration. The MRI showed enhanced water penetration, which increased with time. Beyond day 1, the discs swelled considerably, the dark parts on the MRI slowly disappeared, and by day 5, there was an increase in image brightness throughout the disc indicating that the water was homogenously distributed throughout the sample. (Sitharaman, B. et al. Magnetic resonance imaging studies on gadonanotube-reinforced biodegradable polymer nanocomposites. *J Biomed Mater Res A*. 93(4): 1454–62. Copyright 2010 Wiley Interscience. Reproduced with permission.)

dyes, radiopharmaceuticals), and exploiting the intrinsic physical properties of the nanobiomaterials (e.g., intrinsic fluorescence of quantum dots). The charge and the nature of coating material determine the stability, biodistribution, metabolism, pharmacokinetics, and pharmacodynamics of these imaging agents (Corot et al., 2006). Table 49.4 lists some of the recent advances in the development of nanobio-material-based imaging systems for TE.

TABLE 49.4 Nanobiomaterials Based Imaging in Tissue Engineering

Imaging System	Nanoparticle/Polymer Materials	Functions and Biological Response/Improvements	Reference
MRI	Perfluorocarbons-conjugated RGD-peptide nanoparticles	Vascular disease specific targeting, easy cellular internalization, molecular imaging, cellular tracking and <i>in vivo</i> imaging	Kok et al. (2011)
	SPION nanoparticles in agar based stem cell implants	Cellular tracking of labeled stem cells and noninvasive <i>in vivo</i> MRI during cartilage regeneration	Nedopil et al. (2010)
	SPION (Ferridex) nanoparticles in chondrocyte-hydrogel constructs	Approach towards understanding the fate of chondrocyte labeled iron oxide nanoparticles in tissue-engineering constructs for cartilage tissue regeneration	Ramaswamy et al. (2009)
	SPION (Ferrumoxide)	SPION labeled BMSCs do not undergo differentiation <i>in vivo</i> and provides nontoxic MRI contrast agents	Balakumaran et al. (2010)
	SPION	Direct injection of SPION-ESCs into infarct myocardium improves cardiac functions	Au et al. (2009)
	Gadolinium-SWCNTs nanoparticles	Gadolinium catalyzed SWCNTs reinforced PLGA nanocomposites is used for noninvasive MRI and to study the fate of the nanoparticles upon degradation from polymer scaffolds	Sitharaman et al. (2010); Van der Zande et al. (2011)
microPET	[¹⁸ F]FB-PEG-RGD	These particles have fast blood clearance rates, rapid and high uptake by tumors, lower organ accumulation, and image the process of angiogenesis	Chen et al. (2004)

TABLE 49.4 (continued) Nanobiomaterials Based Imaging in Tissue Engineering

Imaging System	Nanoparticle/Polymer Materials	Functions and Biological Response/ Improvements	Reference
Optical imaging	Rare earth doped nanoparticles conjugated with human serum albumin and RGD peptide	Biocompatible, and biologically targetable nanoshell complexes useful for disease targeting and NIR imaging	Naczynski et al. (2010)
	Gold nanoparticles-conjugated to dye labeled targeting peptides and PEG	Noninvasive NIR imaging to study the protease activity mediated disease progression.	Mu et al. (2010)
	Silicon nanocrystals coated with amphiphilic polymers	Stable and bright photoluminescence in the pH range of 7–10 for biological tissue imaging	Hessel et al. (2010)
CT	Gold nanoparticles functionalized with glutamic acid	Targeting damaged bone tissue	Zhang et al. (2010)

49.5 Continuing and Future Developments

Nanobiomaterials show promise and potential towards the development of tools and techniques for TE. A number of nanobiomaterials have been investigated for applications in cellular and molecular imaging/sensing such as *in vivo* monitoring and tracking of transplanted cells and engineered tissues; therapeutic drug-delivery to deliver genes, signaling proteins, and growth factors; improving the bulk and surface properties of TE scaffolds. In a number of these applications, nanobiomaterials have been used in combination with other biomaterials and have demonstrated suitability in enabling components of various electronic, biochemical, and mechanical structures, devices or implants for TE.

Advancements in synthesis of high-quality nanobiomaterials and the availability in bulk quantities for a number of these nanobiomaterials have facilitated research and the development of a number of nanobiomaterial-driven biomedical technologies. For some TE applications, products that utilize nanobiomaterials *in vitro* are already commercially available. For example, Invitrogen Inc. (Carlsbad, California), has developed miniaturized sensor systems that utilizes quantum dots to detect a wide variety of proteins and antibodies *in vitro*. Nanoprobes Inc. (Yaphank, New York) has developed proprietary technology utilizes the stability and unique structure of gold nanoparticles for immunoassays in a variety of tissues. However, progress has been slow in developing nanobiomaterial-based products for *in vivo* TE applications. The *in vivo* toxicity and biodistribution of a large number of nanobiomaterials still needs to be thoroughly understood before their translation into clinic. Additionally, high costs and time constraints associated with nanobiomaterial production and processing (purification and sorting) are barriers for some applications. However, these costs are highly dependent on the specific application of a particular nanobiomaterial. Nevertheless, the development of nanobiomaterial-based TE technologies represents a challenging, but potentially rewarding opportunity to develop the next generation biomedical products.

Abbreviations

ALH	Accordion-like honeycomb
ALP	Alkaline phosphatase
AMPEG	Amine-terminated methoxy poly(ethylene glycol)
Apt	A10 RNA aptamer
BMP	Bone morphogenetic protein
BMSC	Bone marrow mesenchymal stem cells
BSA	Bovine serum albumin
CG	Chitosan-gelatin

CH	Pure chitosan scaffolds
CH1	nHA-chitosan scaffold
CM	Chitosan scaffolds of varying% nHA weight
CNFs	Carbon nanofibers
CPC	Calcium phosphate cement
CT	Computed tomography
DOTA	1,4,7,10-tetraazacyclododecane-N,N',N'',N'''-tetraacetic acid
ECM	Extracellular matrix
ESCs	Embryonic stem cells
FB	Fluorobenzoyl
GF	Growth factor
HA	Hydroxyapatite
HA-coll	Hyaluronic acid-collagen
HBDC	Human bone-derived cells
HCA	Hydroxylcarbonate apatite
hMSC	Human mesenchymal stem cell
ICAM	Inter-cellular adhesion molecule
IPNs	Interpenetrating polymer networks
IKVAV	Isolucine lysine-valine-alanine-valine
MBGs	Mesoporous bioactive glass
microPET	micro Positron emission tomography
MMA	Methylmethacrylate
MPEG	Methoxy poly(ethylene glycol)
MSCs	Marrow stem cells or mesenchymal stem cells
n-HA/PA	Nano-hydroxyapatite/polyamide
nHA	Chitosan-nanohydroxyapatite
nBGC	Bioactive glass ceramic nanoparticles
NIR	Near infrared
NP	Nanoparticles
NSC	Neural stem cells
NT-3	Neurotrophin-3
P3HB	Poly(3-hydroxybutyrate)
PAMAM	Polyamidoamine
PBT	Poly(butylene terephthalate)
PCL	Poly(1-caprolactone)
PDMS	Poly-(dimethylsiloxane)
pDNA	Plasmid DNA
PECAM	Platelet endothelial cell adhesion molecule
PEG	Poly(ethylene glycol)
PEI-HA	Poly(ethylenimine)-hyaluronic acid
PEO	Poly(ethylene oxide)
PET	Polyethylene terephthalate
PF	PEGylated fibrinogen
PHBV	Poly(3-hydroxybutyrate-co-hydroxyvalerate)
PGS	Poly(glycerol-co-sebacic acid)
PLA	Poly(lactic acid)
PLGA	Poly(D,L-lactic-co-glycolic acid)
PLLA	Poly(L-lactic acid)
PMMA	Poly(methyl methacrylate)
POC	Poly(1,8-octanediol-co-citric acid)

PPF	Poly(propylene fumarate)
PPF/PF-DA	Poly(propylene fumarate)/propylene fumarate-diacrylate
Ppy	Polypyrrole
PSMA	Prostate specific membrane antigen
PVA/PAA	Poly(vinyl alcohol)/poly(acrylic acid)
RGD	L-arginine, glycine, and L-aspartic acid peptide
rh	Recombinant human
SBF	Simulated body fluid
SEM	Scanning electron microscope
SF	Silk fibroin
SPION	Super paramagnetic iron oxide nanoparticles
SPM	Sulfopropylmethacrylate
SS-ILP	Super small-insulin-loaded polymer microparticle
SWCNT	Single-walled carbon nanotubes
TTC	Tetanus toxin C
VCAM	Vascular cell adhesion molecule
VEGF	Vascular endothelial growth factor

References

- Alperin, C., P. W. Zandstra, and K. A. Woodhouse. 2005. Polyurethane films seeded with embryonic stem cell-derived cardiomyocytes for use in cardiac tissue engineering applications. *Biomaterials* 26(35): 7377–86.
- Arai, K., M. Tanaka, S. Yamamoto, and M. Shimomura. 2008. Effect of pore size of honeycomb films on the morphology, adhesion and cytoskeletal organization of cardiac myocytes. *Colloids and Surfaces A: Physicochem Eng Aspects* 313–314: 530–35.
- Au, K. W., S. Y. Liao, Y. K. Lee, W. H. Lai, K. M. Ng, Y. C. Chan, M. C. Yip et al. 2009. Effects of iron oxide nanoparticles on cardiac differentiation of embryonic stem cells. *Biochem Biophys Res Commun* 379(4): 898–903.
- Balakumaran, A., E. Pawelczyk, J. Ren, B. Sworder, A. Chaudhry, M. Sabatino, D. Stroncek, J. A. Frank, and P. G. Robey. 2010. Superparamagnetic iron oxide nanoparticles labeling of bone marrow stromal (mesenchymal) cells does not affect their “stemness”. *PLoS One* 5(7): e11462.
- Bechara, S. L., A. Judson, and K. C. Papat. 2010. Template synthesized poly(3-caprolactone) nanowire surfaces for neural tissue engineering. *Biomaterials* 31: 3492–501.
- Bellingham, C. M., M. A. Lillie, J. M. Gosline, G. M. Wright, B. C. Starcher, A. J. Bailey, K. A. Woodhouse, and F. W. Keeley. 2003. Recombinant human elastin polypeptides self-assemble into biomaterials with elastin-like properties. *Biopolymers* 70(4): 445–55.
- Benoit, D. S., and K. S. Anseth. 2005. Heparin functionalized PEG gels that modulate protein. *Biochem Eng Biotechnol* 94: 1–22.
- Bettinger, C. J., J. P. Bruggeman, A. Misra, J. T. Borenstein, and R. Langer. 2009. Biocompatibility of biodegradable semiconducting melanin films for nerve tissue engineering. *Biomaterials* 30(17): 3050–57.
- Bhattarai, N., D. Edmondson, O. Veiseh, F. A. Matsen, and M. Zhang. 2005. Electrospun chitosan based nanofibers and their cellular compatibility. *Biomaterials* 26(31): 6176–84.
- Bini, T. B., S. Gao, X. Xu, S. Wang, S. Ramakrishna, and K. W. Leong. 2004. Peripheral nerve regeneration by microbraided poly(L-lactide-co-glycolide) biodegradable polymer fibers. *J Biomed Mater Res A* 68(2): 286–95.
- Bock, N., A. Riminucci, C. Dionigi et al. 2010. A novel route in bone tissue engineering: Magnetic biomimetic scaffolds. *Acta Biomater* 6: 786–96.
- Bretcanu, O., S. K. Misra, D. M. Yunos, A. R. Boccaccini, I. Roy, T. Kowalczyk, S. Blonski, and T. A. Kowalewski. 2009. Electrospun nanofibrous biodegradable polyester coatings on Bioglass®-based glass-ceramics for tissue engineering. *Mater Chem Phys* 118: 420–26.

- Carneiro, K. M., F. A. Aldaye, and H. F. Sleiman. 2010. Long-range assembly of DNA into nanofibers and highly ordered networks using a block copolymer approach. *J Am Chem Soc* 132(2): 679–85.
- Chan, J. M., L. Zhang, K. P. Yuet, G. Liao, J. W. Rhee, R. Langer, and O. C. Farokhzad. 2009. PLGA–lecithin–PEG core–shell nanoparticles for controlled drug delivery. *Biomaterials* 30(8): 1627–34.
- Chandrasekar, D., R. Sistla, F. J. Ahmad, R. K. Khar, and P. V. Diwan. 2007. The development of folate–PAMAM dendrimer conjugates for targeted delivery of anti-arthritic drugs and their pharmacokinetics and biodistribution in arthritic rats. *Biomaterials* 28(3): 504–12.
- Chen, F. X., Li, X. Mo, C. He, H. Wang, and Y. Ikada. 2008. Electrospun chitosan–P(LLA–CL) nanofibers for biomimetic extracellular matrix. *J Biomater Sci Polym Ed* 19: 677–91.
- Chen, Q. Z., A. Bismarck, U. Hansen, S. Junaid, M. Q. Tran, S. E. Harding, N. N. Ali, and A. R. Boccaccini. 2008. Characterisation of a soft elastomer poly(glycerol sebacate) designed to match the mechanical properties of myocardial tissue. *Biomaterials* 29(1): 47–57.
- Chen, V. J. and P. X. Ma. 2004. Nano-fibrous poly(L-lactic acid) scaffolds with interconnected spherical macropores. *Biomaterials* 25: 2065–73.
- Chen, X., R. Park, Y. Hou, V. Khankaldyyan, I. Gonzales-Gomez, M. Tohme, J. R. Bading, W. E. Laug, and P. S. Conti. 2004. MicroPET imaging of brain tumor angiogenesis with 18F-labeled PEGylated RGD peptide. *Eur J Nucl Med Mol Imaging* 31(8): 1081–9.
- Chen, X., Y. Hou, M. Tohme, R. Park, V. Khankaldyyan, I. Gonzales-Gomez, J. R. Bading, W. E. Laug, and P. S. Conti. 2004. Pegylated Arg–Gly–Asp peptide: 64Cu labeling and PET imaging of brain tumor alphavbeta3-integrin expression. *J Nucl Med* 45(10): 1776–83.
- Cheng, J., B. A. Teply, I. Sherifi, J. Sung, G. Luther, F. X. Gu, E. Levy-Nissenbaum, A. F. Radovic-Moreno, R. Langer, and O. C. Farokhzad. 2007. Formulation of functionalized PLGA–PEG nanoparticles for *in vivo* targeted drug delivery. *Biomaterials* 28(5): 869–76.
- Cheng, K. and W. S. Kisaalita. 2010. Exploring cellular adhesion and differentiation in a micro-/nano-hybrid polymer scaffold. *Biotechnol Prog* 26(3): 838–46.
- Chew, S. Y., R. Mi, A. Hoke A, and K. W. Leong. 2008. The effect of the alignment of electrospun fibrous scaffolds on Schwann cell maturation. *Biomaterials* 29: 653–61.
- Choi, J. S., K. S. Ko, J. S. Park, Y. H. Kim, S. W. Kim, and M. Lee. 2006. Dexamethasone conjugated poly(amidoamine) dendrimer as a gene carrier for efficient nuclear translocation. *Int J Pharm* 320(1/2): 171–8.
- Choi, J. S., S. J. Lee, G. J. Christ, A. Atala, and J. J. Yoo. 2008. The influence of electrospun aligned poly(varepsilon-caprolactone)/collagen nanofiber meshes on the formation of self-aligned skeletal muscle myotubes. *Biomaterials* 29: 2899–906.
- Choi, S. W., W. S. Kim, and J. H. Kim. 2005. Surface-functionalized nanoparticles for controlled drug delivery. *Methods Mol Biol* 303: 121–31.
- Choudhary, S., M. Berhe, K. M. Haberstroh, and T. J. Webster. 2006. Increased endothelial and vascular smooth muscle cell adhesion on nanostructured titanium and CoCrMo. *Int J Nanomed* 1(1): 41–9.
- Choudhary, S., K. M. Haberstroh, and T. J. Webster. 2007. Enhanced functions of vascular cells on nanostructured Ti for improved stent applications. *Tissue Eng* 13(7): 1421–30.
- Cohen, H., R. J. Levy, J. Gao, I. Fishbein, V. Kousaev, S. Sosnowski, S. Slomkowski, and G. Golomb. 2000. Sustained delivery and expression of DNA encapsulated in polymeric nanoparticles. *Gene Ther* 7(22): 1896–905.
- Corey, J. M., C. C. Gertz, B. S. Wang, L. K. Birrell, S. L. Johnson, D. C. Martin, and E. L. Feldman. 2008. The design of electrospun PLLA nanofiber scaffolds compatible with serum-free growth of primary motor and sensory neurons. *Acta Biomater* 4(4): 863–75.
- Corey, J. M., D. Y. Lin, K. B. Mycek, Q. Chen, S. Samuel, E. L. Feldman, and D. C. Martin. 2007. Aligned electrospun nanofibers specify the direction of dorsal root ganglia neurite growth. *J Biomed Mater Res A* 83(3): 636–45.
- Corot, C., P. Robert, J. M. Idée, and M. Port. 2006. Recent advances in iron oxide nanocrystal technology for medical imaging. *Adv Drug Deliv Rev* 58(14): 1471–504.

- Daamen, W. F., J. H. Veerkamp, J. C. van Hest, and T. H. van Kuppevelt. 2007. Elastin as a biomaterial for tissue engineering. *Biomaterials* 28(30): 4378–98.
- Ding, B., H. Y. Kim, S. C. Lee, C.-L. Shao, D.-R. Lee, S.-J. Park, G.-B. Kwag, and K.-J. Choi. 2002. Preparation and characterization of a nanoscale poly(vinyl alcohol) fiber aggregate produced by an electrospinning method. *J Polym Sci B-Polym Phys* 40: 1261–8.
- Ding, T., Z. J. Luo, Y. Zheng, X. Y. Hu, and Z. X. Ye. 2010. Rapid repair and regeneration of damaged rabbit sciatic nerves by tissue-engineered scaffold made from nano-silver and collagen type I. *Injury* 41: 522–7.
- Entcheva, E., H. Bien, L. Yin, C. Y. Chung, M. Farrell, and Y. Kostov. 2004. Functional cardiac cell constructs on cellulose-based scaffolding. *Biomaterials* 25: 5753–62.
- Erbacher, P., S. Zou, T. Bettinger, A. M. Steffan, and J. S. Remy. 1998. Chitosan-based vector/DNA complexes for gene delivery: Biophysical characteristics and transfection ability. *Pharm Res* 15(9): 1332–9.
- Gannon, C. J., P. Cherukuri, B. I. Jakobson, L. Cognet, J. S. Kanzius, C. Kittrell, R. B. Weisman et al. 2007. Carbon nanotube-enhanced thermal destruction of cancer cells in a noninvasive radiofrequency field. *Cancer* 110(12): 2654–65.
- Gaub, V. and J. D. Hartgerink. 2007. Self-assembled heterotrimeric collagen triple helices directed through electrostatic interactions. *J Am Chem Soc* 129: 2683–90.
- Ghasemi-Mobarakeh, L., M. P. Prabhakaran, M. Morshed, M. H. Nasr-Esfahani, and S. Ramakrishna. 2010. Bio-functionalized PCL nanofibrous scaffolds for nerve tissue engineering. *Mater Sci Eng C* 30: 1129–36.
- Ghosh, K., X. D. Ren, X. Z. Shu, G. D. Prestwich, and R. A. Clark. 2006. Fibronectin functional domains coupled to hyaluronan stimulate adult human dermal fibroblast responses critical for wound healing. *Tissue Eng* 12(3): 601–13.
- Goto, K., J. Tamura, S. Shinzato, S. Fujibayashi, M. Hashimoto, M. Kawashita, T. Kokubo, and T. Nakamura. 2005. Bioactive bone cements containing nano-sized titania particles for use as bone substitutes. *Biomaterials* 26(33): 6496–505.
- Greco, G. N. (ed.). 2008. *Tissue Engineering Research Trends*. Nova Science Publishers, New York.
- Green, D. E., J. P. Longtin, and B. Sitharaman. 2009. The effect of nanoparticle-enhanced photoacoustic stimulation on multipotent marrow stromal cells. *ACS Nano* 3(8): 2065–72.
- Gupta, D., J. Venugopal, M. P. Prabhakaran, V. R. Dev, S. Low, A. T. Choon, and S. Ramakrishna. 2009. Aligned and random nanofibrous substrate for the *in vitro* culture of Schwann cells for neural tissue engineering. *Acta Biomater* 5(7): 2560–9.
- Gupta, P., C. Elkins, T. E. Long, and G. L. Wilkes. 2005. Electrospinning of linear homopolymers of poly(methyl methacrylate): Exploring relationships between fiber formation, viscosity, molecular weight and concentration in a good solvent. *Polymer* 46: 4799.
- Haesslein, A., H. Ueda, M. C. Hacker, S. Jo, D. M. Ammon, R. N. Borazjani, J. F. Kunzler, J. C. Salamone, and A. G. Mikos. 2006. Long-term release of fluocinolone acetonide using biodegradable fumarate-based polymers. *J Control Release* 114(2): 251–60.
- Hamdi, H., A. Furuta, V. Bellamy, A. Bel, E. Puymirat, S. Peyrard, O. Agbulut, and P. Menasché. 2009. Cell delivery: Intramyocardial injections or epicardial deposition? Ahead-to-head comparison. *Ann Thorac Surg*. 87(4): 1196–203.
- Han, Z., H. Kong, J. Meng, C. Wang, S. Xie, and H. Xu. 2009. Electrospun aligned nanofibrous scaffold of carbon nanotubes-polyurethane composite for endothelial cells. *J Nanosci Nanotechnol* 9(2): 1400–2.
- Harrington, D. A., E. Y. Cheng, M. O. Guler, L. K. Lee, J. L. Donovan, R. C. Claussen, and S. I. Stupp. 2006. Branched peptide-amphiphiles as self-assembling coatings for tissue engineering scaffolds. *J Biomed Mater Res A* 78(1): 157–67.
- Harris, T. J., J. J. Green, P. W. Fung, R. Langer, D. G. Anderson, and S. N. Bhatia. 2010. Tissue-specific gene delivery via nanoparticle coating. *Biomaterials* 31(5): 998–1006.
- Harrison, B. S. and A. Atala. 2007. Carbon nanotube applications for tissue engineering. *Biomaterials* 28(2): 344–53.

- Hessel, C. M., M. R. Rasch, J. L. Hueso, B. W. Goodfellow, V. A. Akhavan, P. Puvanakrishnan, J. W. Tunnel, and B. A. Korgel. 2010. Alkyl passivation and amphiphilic polymer coating of silicon nanocrystals for diagnostic imaging. *Small* 6(18): 2026–34.
- Hidalgo-Bastida, L. A., J. J. A. Barry, N. M. Everitt, F. R. Rose, L. D. Buttery, I. P. Hall, W. C. Claycomb, and K. M. Shakesheff. 2007. Cell adhesion and mechanical properties of a flexible scaffold for cardiac tissue engineering. *Acta Biomater* 3(4): 457–62.
- Hofmann, S., S. Knecht, R. Langer, D. L. Kaplan, G. Vunjak-Novakovic, H. P. Merkle, and L. Meinel. 2006. Cartilage-like tissue engineering using silk scaffolds and mesenchymal stem cells. *Tissue Eng* 12(10): 2729–38.
- Horch, R. A., N. Shahid, A. S. Mistry, M. D. Timmer, A. G. Mikos, and A. R. Rarron. 2004. Nanoreinforcement of poly(propylene fumarate)- based networks with surface modified alumoxane nanoparticles for bone tissue engineering. *Biomacromolecules* 5: 1990–8.
- Hosseinkhani, H. and Y. Tabata. 2006. Self assembly of DNA nanoparticles with polycations for the delivery of genetic materials into cells. *J Nanosci Nanotechnol* 6(8): 2320–8.
- Huang, Y. Y. and C. H. Wang. 2006. Pulmonary delivery of insulin by liposomal carriers. *J Control Release* 113(1): 9–14.
- Ishii, O., M. Shin, T. Sueda, and J. P. Vacanti. 2005. *In vitro* tissue engineering of a cardiac graft using a degradable scaffold with an extracellular matrix-like topography. *J Thorac Cardiovasc Surg* 130: 1358–63.
- Jang, J. S., S. Y. Kim, S. B. Lee, K. O. Kim, J. S. Han, and Y. M. Lee. 2006. Poly(ethylene glycol)/poly(1-caprolactone) diblock copolymeric nanoparticles for non-viral gene delivery: The role of charge group and molecular weight in particle formation, cytotoxicity and transfection. *J Control Release* 113(2): 173–82.
- Jean, A. and G. C. Engelmayr Jr. 2010. Finite element analysis of an accordion-like honey comb scaffold for cardiac tissue engineering. *J Biomech* 31 July 2010. Ahead of print.
- Kanayama, N., S. Fukushima, N. Nishiyama, K. Itaka, W. D. Jang, K. Miyata, Y. Yamasaki, U. I. Chung, and K. Kataoka. 2006. A PEG based biocompatible block cationic polymer with high buffering capacity for the construction of polyplex micelles showing efficient gene transfer toward primary cells. *Chem Med Chem* 1(4): 439–44.
- Kay, S., A. Thapa, K. M. Haberstroh, and T. J. Webster. 2002. Nanostructured polymer/nanophase ceramic composites enhance osteoblast and chondrocyte adhesion. *Tissue Eng* 8(5): 753–61.
- Kenawy, E. R., J. M. Layman, J. R. Watkins, G. L. Bowlin, J. A. Matthews, D. G. Simpson, and G. E. Wnek. 2003. Electrospinning of poly(ethyleneco-vinyl alcohol) fibers. *Biomaterials* 24(6): 907–13.
- Khang, D., M. Sato, R. L. Price, A. E. Ribbe, and T. J. Webster. 2006. Selective adhesion and mineral deposition by osteoblasts on carbon nanofiber patterns. *Int J Nanomed* 1(1): 65–72.
- Kharaziha, M. and M. H. Fathi. 2010. Improvement of mechanical properties and biocompatibility of forsterite bioceramic addressed to bone tissue engineering materials. *J Mech Behav Biomed Mater* 3(7): 530–7.
- Khil, M. S., D. I. Cha, H. Y. Kim, I. S. Kim, and N. Bhattarai. 2003. Electrospun nanofibrous polyurethane membrane as wound dressing. *J Biomed Mater Res B Appl Biomater* 67: 675–9.
- Kim, S. S., K. M. Ahn, M. S. Park, J. H. Lee, C. Y. Choi, and B. S. Kim. 2007. A poly(lactide-co-glycolide)/hydroxyapatite composite scaffold with enhanced osteoconductivity. *J Biomed Mater Res A* 80(1): 206–15.
- Kim, H. S., K. Kim, H. J. Jin, and I. J. Chin. 2005. Morphological characterization of electrospun nano-fibrous membranes of biodegradable poly(L-lactide) and poly(lactide-co-glycolide). *Macromol Symp* 224: 145.
- Kim, K. and J. P. Fisher. 2007. Nanoparticle technology in bone tissue engineering. *J Drug Target* 15(4): 241–52.
- Kim, S. H., Y. S. Nam, T. S. Lee, and W. H. Park. 2003. Silk fibroin nanofiber Electrospinning, properties, and structure. *Polym J* 35: 185–90.
- Kim, S. S., P. M. Sun, O. Jeon, Yong Choi C, and B. S. Kim. 2006. Poly(lactide-co-glycolide)/hydroxyapatite composite scaffolds for bone tissue engineering. *Biomaterials* 27(8): 1399–409.
- Koide, T., D. L. Homma, S. Asada, and K. Kitagawa. 2005. Self-complementary peptides for the formation of collagen-like triple helical supramolecules. *Bioorg Med Chem Lett* 15: 5230–3.

- Kok, M. B., A. de Vries, D. Abdurrachim, J. J. Prompers, H. Gröll, K. Nicolay, and G. J. Strijkers. 2011. Quantitative (1)H MRI, (19)F MRI, and (19)F MRS of cell-internalized perfluorocarbon paramagnetic nanoparticles. *Contrast Media Mol Imaging* 6(1): 19–27.
- Kotch, F. W. and R. T. Raines. 2006. Self-assembly of synthetic collagen triple helices. *Proc Natl Acad Sci USA* 103: 3028–33.
- Kushibiki, T. and Y. Tabata. 2005. Preparation of poly(ethylene glycol)-introduced cationized gelatin as a non-viral gene carrier. *J Biomater Sci Polym Ed* 16(11): 1447–61.
- Langer, K., E. Mutschler, G. Lambrecht, D. Mayer, G. Troschau, F. Stieneker, and J. Kreuter. 1997. Methyl methacrylate sulfopropyl methacrylate copolymer nano particles for drug delivery: Part III: Evaluation as drug delivery system for ophthalmic applications. *Int J Pharm.* 158(2): 219–31.
- Langer, R. and D. A. Tirrell. 2004. Designing materials for biology and medicine. *Nature* 428 (6982): 487–92.
- Langer, R. and Vacanti, J. P. 1993. Tissue engineering. *Science* 260(5110): 920–6.
- Lee, J. Y., C. A. Bashur, A. S. Goldstein, and C. E. Schmidt. 2009. Polypyrrole-coated electrospun PLGA nanofibers for neural tissue applications. *Biomaterials* 30(26): 4325–35.
- Lee, Y. B., S. Polio, W. Lee, G. Dai, L. Menon, R. S. Carroll, and S. S. Yoo. 2010. Bio-printing of collagen and VEGF-releasing fibrin gel scaffolds for neural stem cell culture. *Exp Neurol* 223(2): 645–52.
- Li, M. Y., M. J. Mondrinos, M. R. Gandhi, F. K. Ko, A. S. Weiss, and P. I. Leikes. 2005. Electrospun protein fibers as matrices for tissue engineering. *Biomaterials* 26(30): 5999–6008.
- Li, W. J., C. T. Laurencin, E. J. Caterson, R. S. Tuan, and F. K. Ko. 2002. Electrospun nanofibrous structure: A novel scaffold for tissue engineering. *J Biomed Mater Res* 60(4): 613–21.
- Li, W. J., R. Tuli, X. Huang, P. Laquerriere, and R. S. Tuan. 2005a. Multilineage differentiation of human mesenchymal stem cells in a three-dimensional nanofibrous scaffold. *Biomaterials* 26(5): 5158–66.
- Li, W. J., R. Tuli, C. Okafor, A. Derfoul, K. G. Danielson, D. J. Hall, and R. S. Tuan. 2005b. A three-dimensional nanofibrous scaffold for cartilage tissue engineering using human mesenchymal stem cells. *Biomaterials* 26(6): 599–609.
- Li, Y.-P., Y.-Y. Pei, X.-Y. Zhang, Z.-H. Gu, Z. H. Zhou, W.-F. Yuan, J.-J. Zhao, J.-H. Zhu, and X.-J. Gao. 2001. PEGylated PLGA nanoparticles as protein carriers: synthesis, preparation and biodistribution in rats. *J Control Release* 71: 203–11.
- Liao, S., R. Murugan, C. K. Chan, and S. Ramakrishna. 2008. Processing nanoengineered scaffolds through electrospinning and mineralization suitable for biomimetic bone tissue engineering. *J Mech Behav Biomed Mater* 1(3): 252–60.
- Liu, H., E. B. Slamovich, and T. J. Webster. 2005. Increased osteoblast functions on nanophase titania dispersed in poly-lactic-coglycolic acid composites. *Nanotechnology* 16(7): S601–S608.
- Liu, H., E. B. Slamovich, and T. J. Webster. 2006. Increased osteoblast functions among nanophase titania/poly(lactide-co-glycolide) composites of the highest nanometer surface roughness. *J Biomed Mater Res A* 78A(4): 798–807.
- Liu, H. and T. J. Webster. 2010. Ceramic/polymer nanocomposites with tunable drug delivery capability at specific disease sites. *J Biomed Mater Res A* 93(3): 1180–92.
- Liu, Q., J. R. de Wijn, and C. A. van Blitterswijk. 1998. Composite biomaterials with chemical bonding between hydroxyapatite filler particles and PEG/PBT copolymer matrix. *J Biomed Mater Res A* 40(3): 490–7.
- Lu, Y., D. Wang, T. Li, X. Zhao, Y. Cao, H. Yang, and Y. Y. Duan. 2009. Poly(vinyl alcohol)/poly(acrylic acid) hydrogel coatings for improving electrode–neural tissue interface. *Biomaterials* 30(25): 4143–51.
- Lukic, B., J. W. Seo, R. R. Bacsa, S. Delpeux, F. Béguin, G. Bister, A. Fonseca et al. 2005. Catalytically grown carbon nanotubes of small diameter have a high Young's modulus. *Nano Lett* 5(10): 2074–7.
- Ma, Z., M. Kotaki, T. Yong, W. He, and S. Ramakrishna. 2005. Surface engineering of electrospun polyethylene terephthalate (PET) nanofibers towards development of a new material for blood vessel engineering. *Biomaterials* 26: 2527–36.
- Mahmood, T. A., V. P. Shastri, C. A. van Blitterswijk, R. Langer, and J. Riesle. 2006. Evaluation of chondrogenesis within PEGT: PBT scaffolds with high PEG content. *J Biomed Mater Res A* 79(1): 216–22.

- Mansouri, S., Y. Cuie, F. Winnik, Q. Shi, P. Lavigne, M. Benderdour, E. Beaumont, and J. C. Fernandes. 2006. Characterization of folate–chitosan–DNA nanoparticles for gene therapy. *Biomaterials* 27(9): 2060–5.
- Matsuo, T., T. Sugita, T. Kubo, Y. Yasunaga, M. Ochi, and T. Murakami. 2003. Injectable magnetic liposomes as a novel carrier of recombinant human BMP-2 for bone formation in a rat bone defect model. *J Biomed Mater Res A* 66(4): 747–54.
- Matthews, J. A., G. E. Wnek, D. G. Simpson, and G. L. Bowlin. 2002. Electrospinning of collagen nanofibers. *Biomacromolecules* 3(2): 232–8.
- McAllister, K., P. Sazani, M. Adam, M. J. Cho, M. Rubinstein, R. J. Samulski, and J. M. DeSimone. 2002. Polymeric nanogels produced via inverse microemulsion polymerization as potential gene and anti-sense delivery agents. *J Am Chem Soc* 124(51): 15198–207.
- McKenzie, J. L., M. C. Waid, R. Shi, and T. J. Webster. 2004. Decreased functions of astrocytes on carbon nanofiber materials. *Biomaterials* 25(7–8): 1309–17.
- Meinel, L., O. Betz, R. Fajardo, S. Hofmann, A. Nazarian, E. Cory, M. Hilbe et al. 2006. Silk based biomaterial to heal critical sized femur defects. *Bone* 39: 922–31.
- Meinel, A. J., K. E. Kubow, E. Klotzsch, M. Garcia-Fuentes, M. L. Smith, V. Vogel, H. P. Merkle, and L. Meinel. 2009. Optimization strategies for electronspun silk fibroin tissue engineering scaffolds. *Biomaterials* 30(17): 3058–67.
- Miao, M., J. T. Cirulis, S. Lee, and F. W. Keeley. 2005. Structural determinants of cross-linking and hydrophobic domains for self-assembly of elastin-like polypeptides. *Biochemistry* 44(43): 14367–75.
- Min, B. M., G. Lee, S. H. Kim, Y. S. Nam, T. S. Lee, and W. H. Park. 2004. Electrospinning of silk fibroin nanofibers and its effect on the adhesion and spreading of normal human keratinocytes and fibroblasts *in vitro*. *Biomaterials* 25(7–8):1289–97.
- Mistry, A. S., S. H. Cheng, T. Yeh, E. Christenson, J. A. Jansen, and A. G. Mikos. 2009. Fabrication and *in vitro* degradation of porous fumarate-based polymer/alumoxane nanocomposite scaffolds for bone tissue engineering. *J Biomed Mater Res A* 89(1): 68–79.
- Mistry, A. S. and A. G. Mikos. 2005. Tissue engineering strategies for bone regeneration. *Adv Biochem Eng Biotechnol* 94:1–22.
- Morishita, M., T. Goto, K. Nakamura, A. M. Lowman, K. Takayama, N. A. Peppas. 2006. Novel oral insulin delivery systems based on complexation polymer hydrogels: Single and multiple administration studies in type 1 and 2 diabetic rats. *J Control Release* 110(3): 587–94.
- Morishita, M., T. Goto, N. A. Peppas, J. I. Joseph, M. C. Torjman, C. Munsick, K. Nakamura, T. Yamagata, K. Takayama, and A. M. Lowman. 2004. Mucosal insulin delivery systems based on complexation polymer hydrogels: Effect of particle size on insulin enteral absorption. *J Control Release* 97(1): 115–24.
- Motlagh, D., Y. Yang, K. Y. Lui, A. R. Webb, and G. A. Ameer. 2006. Hemocompatibility evaluation of poly(glycerol-sebacate) *in vitro* for vascular tissue engineering. *Biomaterials* 27(24): 4315–24.
- Mu, C. J., D. A. LaVan, R. S. Langer, and B. R. Zetter. 2010. Self-assembled gold nanoparticles molecular probes for detecting proteolytic activity *in vivo*. *ACS Nano* 4(3): 1511–20.
- Murakami, Y., M. Yokoyama, T. Okano, H. Nishida, Y. Tomizawa, M. Endo, and H. Kurosawa. 2007. A novel synthetic tissue-adhesive hydrogel using a crosslinkable polymeric micelle. *J Biomed Mater Res A* 80(2): 421–7.
- Naczynski, D. J., T. Andelman, D. Pal, S. Chen, R. E. Riman, C. M. Roth, and P. V. Moghe. 2010. Albumin nanoshell encapsulation of near-infrared-excitable rare-Earth nanoparticles enhances biocompatibility and enables targeted cell imaging. *Small* 6(15): 1631–40.
- Namba, R. M., A. A. Cole, K. B. Bjugstad, and M. J. Mahoney. 2009. Development of porous PEG hydrogels that enable efficient, uniform cell-seeding and permit early neural process extension. *Acta Biomater* 5(6): 1884–97.
- Nedopil, A. J., L. G. Mandrussow, and H. E. Daldrup-Link. 2010. Implantation of ferumoxides labeled human mesenchymal stem cells in cartilage defects. *J Vis Exp* 38: 1793.

- Noh, H. K., S. W. Lee, J. M. Kim, J. E. Oh, K. H. Kim, C. P. Chung, S. C. Choi, W. H. Park, and B. M. Min. 2006. Electrospinning of chitin nanofibers: Degradation behavior and cellular response to normal human keratinocytes and fibroblasts. *Biomaterials* 27(21): 3934–44.
- Ohashi, S., T. Kubo, T. Ikeda, Y. Arai, K. Takahashi, Y. Hirasawa, M. Takigawa, E. Satoh, J. Imanishi, and O. Mazda. 2001. Cationic polymer-mediated genetic transduction into cultured human chondrosarcoma-derived HCS-2/8 cells. *J Orthop Sci* 6(1): 75–81.
- Ono, I., T. Yamashita, H. Y. Jin, Y. Ito, H. Hamada, Y. Akasaka, M. Nakasu, T. Ogawa, and K. Jimbow. 2004. Combination of porous hydroxyapatite and cationic liposomes as a vector for BMP-2 gene therapy. *Biomaterials* 25(19): 4709–18.
- Paramonov, S. E., H. W. Jun, and J. D. Hartgerink. 2006. Self-assembly of peptide-amphiphile nanofibers: The roles of hydrogen bonding and amphiphilic packing. *J Am Chem Soc* 128(22): 7291–98.
- Park, J., J. Ries, K. Gelse, F. Kloss, K. von der Mark, J. Wiltfang, F. W. Neukam, and H. Schneider. 2003. Bone regeneration in critical size defects by cell-mediated BMP-2 gene transfer: A comparison of adenoviral vectors and liposomes. *Gene Ther* 10(13): 1089–98.
- Pattison, M. A., S. Wurster, T. J. Webster, and K. M. Haberstroh. 2005. Three-dimensional, nano-structured PLGA scaffolds for bladder tissue replacement applications. *Biomaterials* 26(15): 2491–500.
- Peter, M., N. S. Binulala, S. V. Naira, N. Selvamurugana, H. Tamura, and R. Jayakumara. 2010. Novel biodegradable chitosan–gelatin/nano-bioactive glass ceramic composite scaffolds for alveolar bone tissue engineering. *Chem Eng J* 158: 353–61.
- Pham, Q. P., U. Sharma, and A. G. Mikos. 2006. Electrospinning of polymeric nanofibers for tissue engineering applications: A review. *Tissue Eng* 12: 1197–211.
- Potinen, A., D. M. Lynn, R. Langer, and M. M. Amiji. 2003. Poly(ethyleneoxide)-modified poly(β -aminoester) nanoparticles as pH-sensitive biodegradable system for paclitaxel delivery. *J Control Release* 86(2–3): 223–34.
- Powell, H. M. and S. T. Boyce. 2008. Fiber density of electrospun gelatin scaffolds regulates morphogenesis of dermal-epidermal skin substitutes. *J Biomed Mater Res A* 84: 1078–86.
- Prabha, S., W. Z. Zhou, J. Panyam, and V. Labhasetwar. 2002. Sizedependency of nanoparticle-mediated gene transfection: Studies with fractionated nanoparticles. *Int J Pharm* 244(1/2): 105–15.
- Price, R. L., M. C. Waid, K. M. Haberstroh, and T. J. Webster. 2003. Selective bone cell adhesion on formulations containing carbon nanofibers. *Biomaterials* 24(11): 1877–87.
- Pritchard, C. D., K. M. Arnér, R. A. Neal, W. L. Neeley, P. Bojo, E. Bachelder, J. Holz et al. 2010. The use of surface modified poly(glycerol-co-sebacic acid) in retinal transplantation. *Biomaterials* 31(8): 2153–62.
- Rajangam, K., M. S. Arnold, M. A. Rocco, and S. I. Stupp. 2008. Peptide amphiphile nanostructure-heparin interactions and their relationship to bioactivity. *Biomaterials* 29(23): 3298–305.
- Rajangam, K., H. A. Behanna, M. J. Hui, X. Han, J. F. Hulvat, J. W. Lomasney, and S. I. Stupp. 2006. Heparin binding nanostructures to promote growth of blood vessels. *Nano Lett* 6(9): 2086–90.
- Ramaswamy, S., J. B. Greco, M. C. Uluer, Z. Zhang, Z. Zhang, K. W. Fishbein, and R. G. Spencer. 2009. Magnetic resonance imaging of chondrocytes labeled with superparamagnetic iron oxide nanoparticles in tissue-engineered cartilage. *Tissue Eng Part A* 15(12): 3899–910.
- Reed, C. R., L. Han, A. Andraday, M. Caballero, M. C. Jack, J. B. Collins, S. C. Saba, E. G. Lobo, B. A. Cairns, and J. A. van Aalst. 2009. Composite tissue engineering on polycaprolactone nanofiber scaffolds. *Ann Plast Surg* 62(5): 505–12.
- Robinson, P. S., S. L. Johnson, M. C. Evans, V. H. Barocas, and R. T. Tranquillo. 2008. Functional tissue-engineered valves from cell-remodeled fibrin with commissural alignment of cell-produced collagen. *Tissue Eng Part A* 14(1): 83–95.
- Rodgers, P., A. L. Chun, S. Cantrill, and J. Thomas. 2006. Small is different. *Nature Nanotechnol* 1(1): 1–9.
- Rubenstein, D., D. Han, S. Goldgraben, H. El-Gendi, P. I. Gouma, and M. D. Frame. 2007. Bioassay chamber for angiogenesis with perfused explanted arteries and electrospun scaffolding. *Microcirculation* 14(7): 723–37.

- Ryou, S. M., S. Kim, H. H. Jang, J. H. Kim, J. H. Yeom, M. S. Eom, J. Bae, M. S. Han, and K. Lee. 2010. Delivery of shRNA using gold nanoparticle–DNA oligonucleotide conjugates as a universal carrier. *Biochem Biophys Res Commun* 398(3): 542–6.
- Salvador-Morales, C., L. Zhang, R. Langer, and O. C. Farokhzad. 2009. Immuno compatibility properties of lipid–polymer hybrid nanoparticles with heterogeneous surface functional groups. *Biomaterials* 30(12): 2231–40.
- Saraf, A., L. S. Baggett, R. M. Raphael, F. K. Kasper, and A. G. Mikos. 2010. Regulated non-viral gene delivery from coaxial electrospun fiber mesh scaffolds. *J Control Release* 143(1): 95–103.
- Shachar, M., O. Tsur-Gang, T. Dvir, J. Leor, and S. Cohen. 2011. The effect of immobilized RGD peptide in alginate scaffolds on cardiac tissue engineering. *Acta Biomater* 7(1): 152–62.
- Shapira-Schweitzer, K., M. Habib, L. Gepstein, and D. Seliktar. 2009. A photopolymerizable hydrogel for 3-D culture of human embryonic stem cell-derived cardiac myocytes and rat neonatal cardiac cells. *J Mol Cell Cardiol* 46(2): 213–24.
- Shen, H., J. Tan, and W. M. Saltzman. 2004. Surface-mediated gene transfer from nanocomposites of controlled texture. *Nat Mater* 3(8): 569–74.
- Shi, J., A. R. Votruba, O. C. Farokhzad, and R. Langer. 2010. Nanotechnology in drug delivery and tissue engineering: from discovery to applications. *Nano Lett* 10(9): 3223–30.
- Shi, X., J. L. Hudson, P. P. Spicer, J. M. Tour, R. Krishnamoorti, and A. G. Mikos. 2005. Rheological behaviour and mechanical characterization of injectable poly(propylene fumarate)/single-walled carbon nanotube composites for bone tissue engineering. *Nanotechnology* 16: S531–8.
- Shi, X., J. L. Hudson, P. P. Spicer, J. M. Tour, R. Krishnamoorti, and A. G. Mikos. 2006. Injectable nanocomposites of single-walled carbon nanotubes and biodegradable polymers for bone tissue engineering. *Biomacromolecules* 7(7): 2237–42.
- Shin, M., O. Ishii, T. Sueda, and J. P. Vacanti. 2004. Contractile cardiac grafts using a novel nanofibrous mesh. *Biomaterials* 25: 3717–23.
- Shin, M., H. Yoshimoto, and J. P. Vacanti. 2004. *In vivo* bone tissue engineering using mesenchymal stem cells on a novel electrospun nanofibrous scaffold. *Tissue Eng* 10(1/2): 33–41.
- Silva, G. A., C. Czeisler, K. L. Niece, E. Beniash, D. A. Harrington, J. A. Kessler, and S. I. Stupp. 2004. Selective differentiation of neural progenitor cells by high-epitope density nanofibers. *Science* 303(5662): 1352–5.
- Sitharaman, B., M. Van Der Zande, J. S. Ananta, X. Shi, A. Veltien, X. F. Walboomers, L. J. Wilson, A. G. Mikos, A. Heerschap, and J. A. Jansen. 2010. Magnetic resonance imaging studies on gadonanotube-reinforced biodegradable polymer nanocomposites. *J Biomed Mater Res A* 93(4): 1454–62.
- Smith, L. A. and P. X. Ma. 2004. Nano-fibrous scaffolds for tissue engineering. *Coll Surf B Biointerf* 39: 125–31.
- Thein-Han, W. W. and R. D. K. Misra. 2009. Biomimetic chitosan- nanohydroxyapatite composite scaffolds for bone tissue engineering. *Acta Biomaterialia* 5: 1182–97.
- Thomson, K. S., G. Robinson, F. S. Korte et al. 2010. Cell-seeded fibrin scaffolds for cardiac tissue engineering. *Biophys J* 98(3): 718a.
- Tian, H., S. Bharadwaj, Y. Liu, H. Ma, P. X. Ma, Z. Atala, and Y. Zhang. 2010. Myogenic differentiation of human bone marrow mesenchymal stem cells on a 3D nano fibrous scaffold for bladder tissue engineering. *Biomaterials* 31(5): 870–7.
- Townsend, S. A., G. D. Evrony, F. X. Gu, M. P. Schulz, R. H. Brown Jr, and R. Langer. 2007. Tetanus toxin C fragment-conjugated nanoparticles for targeted drug delivery to neurons. *Biomaterials* 28(34): 5176–84.
- van der Zande, M., B. Sitharaman, X. F. Walboomers, L. Tran, J. S. Ananta, A. Veltien, L. J. Wilson et al. 2011. *In vivo* Magnetic resonance imaging of the distribution pattern of gadonanotubes released from a degrading poly(Lactic-Co-Glycolic Acid) scaffold. *Tissue Eng Part C Methods* 17(1): 19–26.
- Venugopal, J. R., S. Low, A. T. Choon, A. B. Kumar, and S. Ramakrishna. 2008. Nanobioengineered electrospun composite nanofibers and osteoblasts for bone regeneration. *Artif Organs* 32: 388–97.
- Venugopal, J., S. Low, A. T. Choon, A. B. Kumar, and S. Ramakrishna. 2008. Electrospun-modified nanofibrous scaffolds for the mineralization of osteoblast cells. *J Biomed Mater Res A* 85(2): 408–17.

- Vieth, S., C. M. Bellingham, F. W. Keeley, S. M. Hodge, and D. Rousseau. 2007. Microstructural and tensile properties of elastinbased polypeptides crosslinked with genipin and pyrroloquinoline quinone. *Biopolymers* 85(3): 199–206.
- Wang, H., Y. Li, Y. Zuo, J. Li, S. Ma, and L. Cheng. 2007. Biocompatibility and osteogenesis of biomimetic nanohydroxyapatite/polyamide composite scaffolds for bone tissue engineering. *Biomaterials* 28: 3338–48.
- Webster, T. J., C. Ergun, R. H. Doremus, R. W. Siegel, and R. Bizios. 2000. Specific proteins mediate enhanced osteoblast adhesion on nanophase ceramics. *J Biomed Mater Res* 51(3): 475–83.
- Webster, T. J., L. S. Schadler, and R. W. Siegel, and R. Bizios. 2001. Mechanisms of enhanced osteoblast adhesion on nanophase alumina involve vitronectin. *Tissue Eng* 7(3): 291–301.
- Webster, T. J., R. W. Siegel, R. Bizios. 1999. Osteoblast adhesion on nanophase ceramics. *Biomaterials* 10(13): 1221–27.
- Webster, T. J. and T. A. Smith. 2005. Increased osteoblast function on PLGA composites containing nanophase titania. *J Biomed Mater Res A* 74(4): 677–86.
- Wei, G. and P. X. Ma. 2004. Structure and properties of nanohydroxyapatite/polymer composite scaffolds for bone tissue engineering. *Biomaterials* 25(19): 4749–57.
- Whitesides, G. M. and M. Boncheva. 2002. Beyond molecules: Self-assembly of mesoscopic and macroscopic components. *Proc Natl Acad Sci USA* 99: 4769–74.
- Woo, K. M., V. J. Chen, and P. X. Ma. 2003. Nano-fibrous scaffolding architecture selectively enhances protein adsorption contributing to cell attachment. *J Biomed Mater Res A* 67(2): 531–7.
- Woo, K. M., J. H. Jun, V. J. Chen, J. Seo, J. H. Baek, H. M. Ryoo, G. S. Kim, M. J. Somerman, and P. X. Ma. 2007. Nano-fibrous scaffolding promotes osteoblast differentiation and biomineralization. *Biomaterials* 28(2): 335–43.
- Woolfson, D. N. and M. G. Ryadnov. 2006. Peptide-based fibrous biomaterials: Some things old, new and borrowed. *Curr Opin Chem Biol* 10: 559–67.
- Xu, C. Y., R. Inai, M. Kotaki, and S. Ramakrishna. 2004. Aligned biodegradable nanofibrous structure: A potential scaffold for blood vessel engineering. *Biomaterials* 25: 877–86.
- Yan, X., X. Huang, C. Yu, H. Deng, Y. Wang, Z. Zhang, S. Qiao, G. Lu, and D. Zhao. 2006. The in-vitro bioactivity of mesoporous bioactive glasses. *Biomaterials* 27(18): 3396–403.
- Yang, F., C. Y. Xu, M. Kotaki, S. Wang, S. Ramakrishna S. 2004. Characterization of neural stem cells on electrospun poly(L-lactic acid) nanofibrous scaffold. *J Biomater Sci Polym Ed.* 15(12): 1483–97.
- Yang, F., R. Murugan, S. Wang, and S. Ramakrishna. 2005. Electrospinning of nano/micro scale poly(L-lactic acid) aligned fibers and their potential in neural tissue engineering. *Biomaterials* 26: 2603–10.
- Yeong, W. Y., N. Sudarmadji, H. Y. Yu, C. K. Chua, K. F. Leong, S. S. Venkatraman, Y. C. Boey, and L. P. Tan. 2010. Porous polycaprolactone scaffold for cardiac tissue engineering fabricated by selective laser sintering. *Acta Biomater* 6: 2028–34.
- Yi, F., H. Wu, and G. L. Jia. 2006. Formulation and characterization of poly(D, L-lactide-co-glycolide) nanoparticle containing vascular endothelial growth factor for gene delivery. *J Clin Pharm Ther* 31(1): 43–8.
- Yoo, J. J., and S. H. Rhee. 2004. Evaluations of bioactivity and mechanical properties of poly (ε-caprolactone)/silica nanocomposite following heat treatment. *J Biomed Mater Res A* 68(3): 401–10.
- Yoshimoto, H., Y. M. Shin, H. Terai, and J. P. Vacanti. 2003. A biodegradable nanofiber scaffold by electrospinning and its potential for bone tissue engineering. *Biomaterials* 24(12): 2077–82.
- Zhang, Y., H. He, W. J. Gao, S. Y. Lu, Y. Liu, and H. Y. Gu. 2009. Rapid adhesion and proliferation of keratinocytes on the gold colloid/chitosan film scaffolds. *Mater Sci Eng C* 29(3): 908–12.
- Zhang, Z., R. D. Ross, and R. K. Roeder. 2010. Preparation of functionalized gold nanoparticles as a targeted X-ray contrast agent for damaged bone tissue. *Nanoscale* 2(4): 582–6.
- Zhu, Y., C. Wu, Y. Ramaswamy et al. 2008. Preparation, characterization and *in vitro* bioactivity of mesoporous bioactive glasses (MBGs) scaffolds for bone tissue engineering. *Microporous and Mesoporous Materials* 112: 494–503.
- Zong, X., H. Bien, C. Y. Chung, L. Yin, D. Fang, B. S. Hsiao, B. Chu, and E. Entcheva. 2005. Electrospun fine-textured scaffolds for heart tissue constructs. *Biomaterials* 26(26): 5330–8.

50

Biomimetic Approaches in Tissue Engineering

Indong Jun

Hanyang University

Min Sup Kim

Hanyang University

Ji-Hye Lee

Hanyang University

Young Min Shin

Hanyang University

Heungsoo Shin

Hanyang University

50.1	Introduction	50-1
50.2	Biomimetic Surface Modifications	50-3
50.3	Growth Factor-Presenting Materials.....	50-5
50.4	Biomimetic Hydrogels and Controlled Cell Interactions	50-6
50.5	Composite Scaffolds Used to Mimic Specific Cellular Environments	50-8
50.6	Scaffolds Mimicking the Structure of ECM.....	50-10
50.7	Conclusions.....	50-11
	References.....	50-12

50.1 Introduction

Tissue engineering aims to direct regeneration or repair of damaged tissue through the use of cells, biomaterials, and bioactive signals. During the last several decades, many tissue engineering products have been in clinical use for treating patients suffering from tissue loss or dysfunction in skin, bone, or cartilage, and increasing numbers of clinical trials are currently waiting for approval and commercialization to treat more challenging diseases in nerves and pancreatic tissue (Place et al., 2009). Previously developed tissue engineering products include biomaterial derived from natural as well as synthetic origins, growth factors stimulating tissue morphogenesis, differentiated or progenitor cells, or combinations of these. In particular, for full recovery of biological function of engineered tissues, the strategy of implanting a combination of biomaterials, cells, and growth factors together has been considered the most feasible compared to separate applications of the individual components (Huebsch and Mooney, 2009). However, this strategy has often failed due to lack or absence of an ideal biomaterial that is able to actively control the many functions of native cellular microenvironments.

The roles of biomaterials in tissue engineering are diverse as shown in [Figure 50.1](#); they primarily provide structural support (scaffolds) for cell adhesion and expansion during *ex vivo* cultivation of biopsied cells prior to transplantation (Shin et al., 2003). Cells isolated from patients or donors could be directly injected into patients, and, in some circumstances, biomaterials, including fibrin or collagen, have been coinjected to prevent initial cell loss and to improve graft survival rate (Wang and Guan, 2010a). In some cases, application of cells can be excluded and the scaffold alone can be implanted in order to recruit endogenous progenitors and to prompt them to undergo repair and regeneration processes (Shin et al., 2003). In either approach, appropriate porosity and pore distribution within scaffolds are imperative for the free exchange of gases and cellular by-products, and the scaffolds themselves should be degraded by coordination of tissue in-growth and remodeling with minimal adverse effects. Additionally, scaffolds have been utilized as carriers of tissue-specific chemokines and morphogens (Lee and Shin, 2007). Many of these growth factors are proteins that have a low circulation

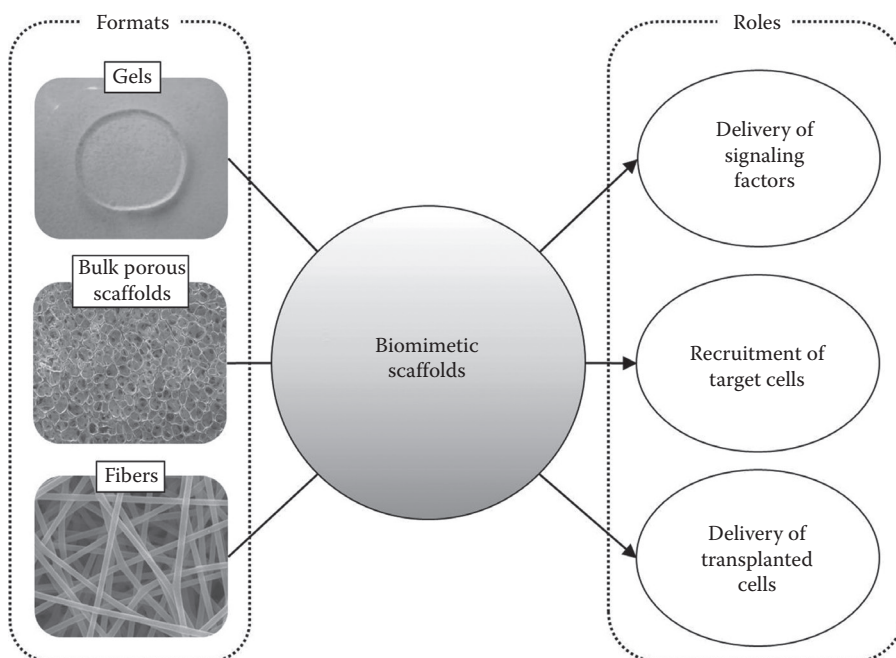


FIGURE 50.1 Major roles and formats of biomimetic scaffolds in tissue engineering.

half-life in blood, resulting in abrupt denaturation and loss of biological activities upon systemic injection. Dosage optimization is also important for the retention of therapeutic concentration during specific regeneration or the occurrence of repair events (it could be days or months depending on target tissues). Scaffolds have been designed to incorporate several growth factors and to control their temporal and spatial presentations in order to maximize tissue regeneration. In addition to these relatively simple roles, regeneration of complex tissues requires more defined chemical, mechanical, and physiological characteristics of scaffolds; this has become more evident with improved knowledge of the regulatory mechanisms of the cellular microenvironment in normal tissues that actively govern cell homeostasis and survival (Marklein and Burdick, 2010). In particular, utilization of embryonic and adult stem cells as cell sources has been a major paradigm in tissue engineering, and being able to design scaffolds to precisely control key functions of stem cells may have enormous impact on the full exploitation of their therapeutic potential.

Under normal conditions, cells have intimate contact with neighboring cells via mechanical binding of membrane-bound proteins, allowing for the operation of metabolic machinery via interactions with soluble factors. The main components in cellular microenvironment and how they are interacting with cells are illustrated in [Figure 50.2](#). In addition, cells are surrounded by the extracellular matrix (ECM), conglomerates of biomacromolecules, including polysaccharides and proteins, which provide structural support and trigger biochemical signaling. Many biomacromolecules in the ECM are crosslinked and assembled as fibrous bundles, which are also involved in multiple bindings with residing cells to control diverse cellular activities. The key cellular components involved in adhesion are proteins that exist on the cell surface. Several classes of cell adhesion proteins have been identified, including cadherins, selectins, immunoglobulin-like adhesion molecules, and integrins. Among them, integrins are one of the major glycoproteins able to sense external signals through specific binding with numerous ligands (Hynes, 2002). Some domains, such as the arginine–glycine–aspartic acid (RGD) domain, can specifically bind to integrins, which are widely used to modulate cell adhesion and proliferation on scaffolds (Shin et al., 2003; Marklein and Burdick, 2010). Extracellular domains of transmembrane receptors

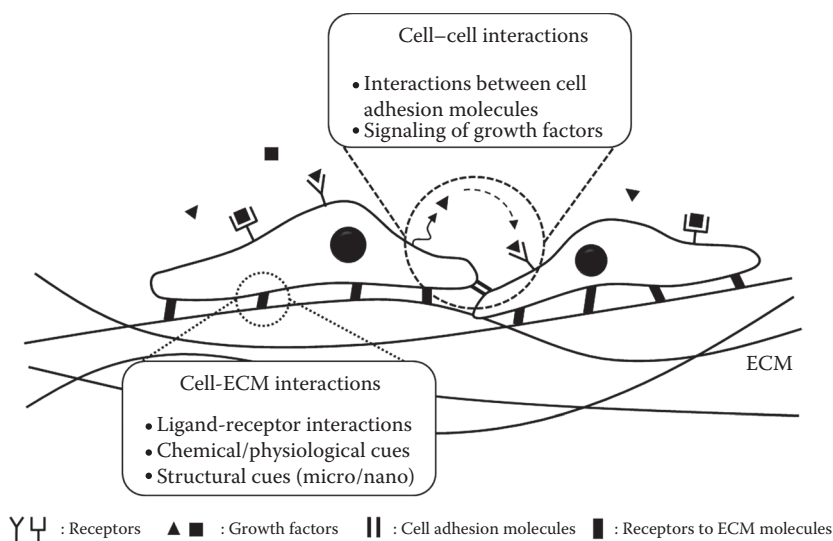


FIGURE 50.2 Main components in cellular microenvironment.

have specific ligands for receptor-mediated binding, presumably regulating a myriad of cell functions; these have attracted significant attention in scaffold design. Recent reports have demonstrated that not only chemical composition and conformation of proteins and polysaccharides within the context of the cellular microenvironment, but also the overall organization and mechanical properties of the ECM are involved in the regulation of intrinsic cell properties (Engler et al., 2006; Huebsch et al., 2010). For example, subtle changes in the presentation of spatially distributed ligands on a nanometer scale can modulate the clustering of transmembrane receptors and subsequently affect intercellular signaling. Intrinsic elasticity within the cellular environment directs the specificity of the stem cell lineage from soft to hard tissue.

In this chapter, biomimetic approaches in tissue engineering are defined as combined efforts to design scaffolds with defined features that mimic structure and function of the native cellular microenvironment (compared to conventional scaffolds). Particularly, this chapter will focus on the most widely reported themes in biomimetic scaffold design, how they have been exploited in several tissue engineering applications, and the remaining challenges for their use. The main strategies covered in the chapter are summarized in [Figure 50.3](#).

50.2 Biomimetic Surface Modifications

The appropriate cellular environment properly regulates cell survival, including adhesion, spreading, proliferation, and differentiation activities. During the development of a tissue engineering strategy, as a structural platform to support tissue homeostasis, biodegradable poly(α -hydroxy)esters such as poly(lactic-*co*-glycolic acid) (PLGA), poly(L-lactide) (PLLA), and polycaprolactone (PCL) have been widely used as scaffolds due to their biocompatibilities and good mechanical properties (Jeong et al., 2005, 2008; Hutmacher, 2000; Jin et al., 2009). Even though these materials have been useful in the fabrication of controlled porous and/or nanofibrous structures, active control of cellular behaviors has been limited due to the absence of cellular interactivity (Shin et al., 2003; Cheung et al., 2007). In fact, these materials are hydrophobic and lack surface functional groups to modulate cell-material interactions. Therefore, surface modification techniques to immobilize hydrophilic groups and to further incorporate bioactive molecules have attracted significant attention (Furth et al., 2007).

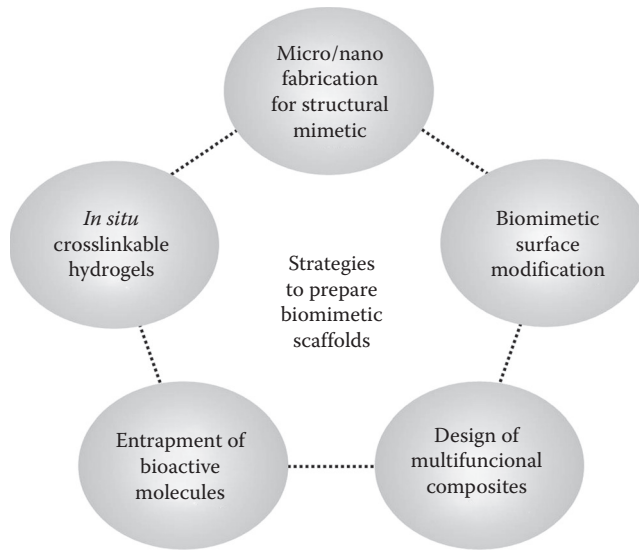


FIGURE 50.3 Strategies to prepare biomimetic scaffolds.

The most simple surface modification technique is physical protein adsorption. In these processes, proteins are physically adsorbed onto the scaffold surface via ionic bonding and electrostatic interactions, and the substrates with adsorbed proteins are simply and easily obtained through dipping into a protein solution (Wilson et al., 2005). For example, PLLA film and nanofibrous mesh were immersed in a 20 g/mL fibronectin and laminin solution for 12 h; the protein-coated substrates exhibited four times greater adhesion of mouse skeletal muscle cells (C2C12) than did the nonmodified substrates (Cui et al., 2003). However, the interactions between the materials and the physically adsorbed proteins are relatively weak and are insufficient to organize long-term cellular behaviors because the proteins can be easily detached from the material surface. To address the problem of physical protein adsorption, covalent immobilization of proteins has also been attempted. To accomplish covalent immobilization, the surfaces of synthetic polymers were pretreated via several processes to enhance the surface functional groups so that covalent immobilization is more favorable, since most synthetic polymers used as scaffolding materials are relatively inert. One previous approach involved surface etching (aminolysis), in which carboxyl (–COOH) groups were simply exposed on the surface by immersing scaffolds in an alkaline solution such as 0.1 or 1 M NaOH, and amide bonds were formed with primary amine groups in most proteins (Zhu et al., 2002). Previously, PLLA films were immersed in 1 M NaOH, and then gelatin was covalently conjugated with EDC/NHS chemistry. The gelatin-conjugated PLLA films accelerated the proliferation of chondrocytes as well as the expressions of collagen type II and GAG (Cui et al., 2003).

Introduction of surface functional groups can be achieved using plasma treatment by altering exposure power, time, and types of gases. High-energy plasma generates free radicals on the surfaces of scaffolds in the presence of argon gas, and superoxide is generated on the surfaces. The activated surfaces sequentially react with acrylic acid (AAc), and AAc-grafted surfaces exhibiting COOH group are finally obtained. Klee et al. (2003) previously obtained PVDF–PAAc films by exposing cells to argon plasma (900 W, 30 s) and 20% AAc, and a twofold increase in human osteoblasts over an 8-day period of cultivation was observed after fibronectin conjugation. In addition, AAc was grafted onto PCL films after argon plasma exposure, and collagen was subsequently conjugated on the AAc–PCL films, directing significant enhancement of human dermal fibroblast and myoblast proliferation on the substrates (Cheng and Teoh, 2004). AAc–PLCL films have also been prepared using gamma-ray irradiation (5–15 kGy), and gelatin (2 mg/mL) was further immobilized on the films, which modulated human mesenchymal

stem cells (hMSCs) behaviors, including adhesion, spreading, proliferation, and differentiation (Shin et al., 2008). Recently, electron beams, as a source for precise control of high resolution and power, have also been used to induce graft polymerization of AAc (Sun et al., 2004).

As previously mentioned, a potential strategy to enhance cell interactivity using tissue engineering scaffolds is secondary immobilization of adhesion-related proteins. Since major proteins involved in the construction of ECM environments, such as fibronectin, collagen, laminin, and vitronectin, play roles in modulating cell behaviors, they are popular targets of immobilization. For instance, fibronectin was conjugated on PLLA, PCL, and silicone rubber scaffolds and exhibited significantly enhanced survivals for osteoblasts, chondrocytes, and myoblasts (Volcker et al., 2001; Bhati et al., 2001; Lan et al., 2005; Cronin et al., 2004; Klee et al., 2003). Similarly, specific domains present in these proteins have been widely used to enhance cell interactivity using scaffolds (Kim and Park, 2006). The RGD derived from fibronectin peptide has been widely conjugated on prefunctionalized scaffolds; the scaffolds can successfully organize adhesion and proliferation of osteoblasts, myoblasts, fibroblasts, hMSCs, as well as osteogenic differentiation of osteoblasts (Smith and Ma, 2004; Hill et al., 2006; Shin et al., 2010). In addition, nonintegrin-mediated sequences, including Tyr-Ile-Gly-Ser-Arg (YIGSR) peptide, derived from laminin, also control adhesion and proliferation of cells similar to that of the RGD peptide; YIGSR peptide-immobilized polyurethane-polyethylene glycol (PEG) reduced platelet deposition and facilitated endothelialization (Jun and West, 2005). Similarly, when the Arg-Glu-Asp-Val (REDV) peptide was conjugated on a lactide-polyethylene glycol base scaffold, adhesion of human umbilical vein endothelial cells (HUVEC) was enhanced (Park et al., 2010a). Tissue engineering scaffolds functionalized with bioactive molecules have been used in many tissues, including defective bone, cartilage, muscle, and nerve. RGD peptide-conjugated nanofibers modulated differentiation of osteoblasts and showed significant potential to trigger faster bone growth (Shin et al., 2010). Moreover, collagen-modified PLLA scaffolds were shown to facilitate proliferation of chondrocytes for 20 days, suggesting that it would potentially be a more favorable cartilage regeneration system (Ma et al., 2005). In addition, biomimicked nanofibers with collagen demonstrated greater nerve regeneration, with a two times higher survival of neural stem cells (Li et al., 2008). Therefore, incorporation of a variety of ECM proteins and peptides could be the simplest method for modulating a wide range of cellular activities and tissue responses.

50.3 Growth Factor-Presenting Materials

Growth factors play a crucial role in information transfer between cells and their ECM in tissue regeneration. Growth factors can also stimulate or inhibit cellular proliferation, differentiation, migration, adhesion, and gene expression. Therefore, many researchers have been interested in the delivery of growth factors to regulate cellular metabolism in order to regenerate the desired tissue from the cells (Babensee et al., 2000). However, many growth factors are rapidly degraded and deactivated by enzymes or other chemical and physical degrading reactions occurring at body temperature and hence have short biological half-lives (Lee et al., 2000). To address these problems, polymeric materials have been frequently used to allow for controlled, sustained, and localized delivery of growth factors, providing the necessary spatial and temporal gradients to regulate cellular metabolism. Polymeric delivery vehicles (as scaffolds) allow for controlled kinetics and dosing of growth factor release, while also protecting the protein from degradation (Tayalia and Mooney, 2009). Growth factors could be incorporated within the scaffolds by simple mixing during the preparation of the scaffolds or could be reversibly introduced by exploiting physiological interactions. Heparin is commonly used as a natural polymer to capture many growth factors in their heparin-binding domains. Another strategy to introduce growth factors in an engineered cellular environment is direct immobilization of growth factors onto scaffolds. However, some growth factors are sensitive to conformational changes, and forced presentation of an active domain during the immobilization process may be a major concern.

Nonetheless, the simplest method for encapsulating growth factors into a polymer matrix is by mixing the factors with the polymer prior to the gelation or crosslinking process. In hydrogels, growth

factors are typically encapsulated, and their encapsulation and release profiles from gels are controlled by crosslinking density or shape and by the density of pores in the polymer network. Also, the biological activity and distribution of growth factors after gelation are critical factors. Murphy et al. (2000) fabricated three-dimensional (3D), porous scaffolds of the copolymer 85:15 poly(lactide-co-glycolide), including vascular endothelial growth factor (VEGF), into a gas foaming/particulate leaching process, from which VEGF was released slowly and maintained its biological activity over a 15 day period. In another study, epidermal growth factor (EGF) delivery vehicles were made of chitosan, and, during *in vivo* testing, EGF released from the chitosan hydrogels accelerated the decrease of skin defects compared to those of groups without EGF (Alemdaroglu et al., 2006). There have been other studies performed with growth factors encapsulated or imbedded within scaffolds for effective neopithelialization and bone formation using bFGF and bone morphogenetic protein-2 (BMP-2), respectively (Miyoshi et al., 2005; Pitukmanorom et al., 2008).

Although physical entrapment of growth factors within scaffolds may be simple and easy, control over release kinetic can sometimes be difficult to achieve. In ECM, heparin is a highly sulfated glycosaminoglycan, with lysine-rich heparin-binding domains that are capable of high-affinity binding to several growth factors, including fibroblast growth factors (FGF), VEGF, BMP-2, and others. The interactions between heparin and heparin-binding growth factors are reversible depending on the physiological properties of the surrounding environment. Thus, various growth factor delivery systems have exploited heparin to actively capture and liberate heparin-binding growth factors. Patel et al. (2007) fabricated heparin conjugated PLLA nanofibers, and these nanofibers stored and released bFGF in a controlled manner. Using these nanofibers, they determined that released bFGF enhanced neurite outgrowth from DRG tissues and migration of fibroblasts compared to groups without bFGF. Similar studies have demonstrated that heparin immobilization onto scaffolds is effective for the controlled release of bFGF and other heparin-binding growth factors (Jeon et al., 2006; Freeman et al., 2008).

As described above, growth factors regulate cellular behaviors, and many researchers have focused on regenerating the desired tissue from cells in *in vivo* experiments targeted for wound healing, angiogenesis, and regeneration of bone and nerve. Although the majority of studies using growth factors were based on a system in which growth factors are released in a soluble form, Choi et al. (2008) fabricated EGF immobilized on PCL-PEG copolymer nanofibers for the purpose of treating diabetic ulcers. The EGF-nanofibers showed enhanced *in vivo* wound healing activities compared to those of control groups (without EGF) or those of EGF solutions alone, indicating that this particular growth factor can be activated from an immobilized state. Hosseinkhani et al. (2007) fabricated a self-assembled peptide-amphiphile (PA) to induce enhanced ectopic bone formation through the controlled release of BMP-2. During *in vivo* testing, the injection of PA together with BMP-2 into the back subcutis of rats resulted in significant bone formation around the injection site compared to those of BMP-2 injection alone or PA injection alone. Heparin-conjugated fibrin gel was also effective for the controlled delivery of nerve growth factor (NGF); after *in vivo* testing of rats, groups receiving heparin and NGF demonstrated that controlled release of NGF factors enhanced significant peripheral nerve regeneration (Lee et al., 2003). Another study combined heparin and PA to deliver VEGF and bFGF, demonstrating that the released dual-growth factors induced greater blood vessel formation compared to those of groups with monogrowth factor (Rajangam et al., 2006).

50.4 Biomimetic Hydrogels and Controlled Cell Interactions

Hydrogels are 3D networks of polymeric chains which are formed via covalent or noncovalent crosslinking reactions. They provide a favorable environment for cell growth due to high biocompatibility and could be used as an injectable format to fill tissue defects. Moreover, many hydrogels are resistant to nonspecific protein adsorption and therefore have been widely studied as potential platforms for the incorporation of proteins and peptides in ECM to control cell-scaffolds interactions. The capability to absorb large amounts of water allows for the entrapment and sustainability of the release of growth

factors or chemokines for suitable tissue growth via diffusion-mediated mechanisms (Lutolf, 2009; Slaughter et al., 2009).

Early work with PEG hydrogels focused on immobilization of cell-adhesive and nonadhesive peptide sequences derived from ECM proteins to modulate cell adhesion, spreading, and proliferation. The peptide sequences Arg-Gly-Asp (RGD, fibronectin), Tyr-Ile-Gly-Ser-Arg (YIGSR, laminin), Ile-Lys-Val-Ala-Val (IKVAV, fibrinogen), Ile-Lys-Leu-Leu-Ile (IKLLI), and Pro-Asp-Ser-Gly-Arg (PDSGR) were widely studied for specific cell-matrix interactions (Meiners and Mercado, 2003). The pioneering work with these themes was reported by Hubbell and his colleagues, suggesting that incorporation of the cell-adhesive peptide domain is critical for *in vitro* neurite extension and *in vivo* bone formation (Hubbell, 1999). Other types of hydrogels have also been synthesized. Recent work by Benton et al. (2009) reported that valvular interstitial cells cultured within hydrogels composed of PEG-norbornene as a photo-polymerizable polymer along with various concentrations of RGD peptide (0 ~ 2000 μM) increased the projected area and spreading of the cells with increasing peptide concentration. Hydrogels can serve as a reservoir to entrap growth factors and regulate cellular behavior. For example, precursor solutions consisting of primary hepatocytes, thermosensitive PEG-DA, thiolated heparin, and hepatocyte growth factor (HGF) (capable of binding with heparin via electrostatic interactions) were used to prepare hydrogels to control the release of HGF. As a result, the encapsulated primary hepatocytes produced statistically increased levels of albumin and urea as an important factor of liver metabolism (Kim et al., 2010b). These results indicate that hydrogels coupled with appropriate signals can provide an optimal cellular growth environment. In addition, in an ischemia model, a microbead-like hydrogel system incorporating HGF was injected into the hind limb, revealing relatively higher levels of ischemic leg limb perfusion, alpha SMA expression, and blood vessel formation (Ruvinov et al., 2010).

One of the most interesting features of hydrogels is their versatility of mechanical properties with minimal alteration of other environmental factors. Analysis with alginate hydrogels using diverse stiffness suggests that the mechanics of adhesive substrates may regulate the cell proliferation and transfection efficiency of nonviral vectors (Kong et al., 2005). Acrylamide gels with immobilized collagen possess a broad range of elasticity, which has been used to demonstrate that stem cells can be differentiated into myogenic, neurogenic, and osteogenic lineages upon elasticity sensing. Recently, modified gelatin with 3-(4-hydroxyphenyl) propionic acid (HPA) was synthesized and prepared as a hydrogel via enzyme polymerization using H_2O_2 and horseradish peroxidase (HRP). hMSCs were cultured with gelatin-modified hydrogels prepared as soft (281 Pa) and hard (841 Pa) types; it was reported that the neurogenic differentiation within 3D gelatin hydrogels showed different levels of several neurogenic differentiation markers such as β 3-tubulin, NFH, NFL, and MAP2 (Wang et al., 2010b). These results suggest that biomimetic hydrogels with tunable mechanical properties can serve as useful tools to address fundamental questions regarding the mechanobiological regulation of cellular microenvironments of various cell types and as regulators of specific cell functions for tissue regeneration. Cellular behaviors, including cell adhesion, spreading, differentiation, and ECM deposition, are known to be dictated by micro- or nanoscale arrangements and by geographical patterns of the underlying matrices. Under physiological conditions, muscle tissue has anisotropic alignment, and many studies have shown that differentiation of myoblasts is affected by these anisotropically patterned hydrogels. For example, myocytes cultured on nanoscale-patterned anisotropic PEG hydrogels showed greater expression of connexin 43 protein and increased conduction velocity of connexin gap junctions, an important parameter in the characterization of biologically functional cardiac tissue formation (Kim et al., 2010a). In addition, cultured myoblasts revealed higher differentiation characteristics on PDMS hydrogels using a master mold and fabricated using electron-beam lithography (EBL) to form an array of 120 nm diameter pits of 100 nm depth and 300 nm pitch in hexagonal and square arrangements than they did on nonpatterned hydrogels with respect to the expression of α -actinin, a characteristic gene of myogenic differentiation (Shimizu et al., 2009). In addition to muscle cells, Matthew et al. reported that hMSCs cultured on nanoscale symmetry hydrogels or with disorder patterning showed higher bone mineralization on a

substrate with disordered patterns (Dalby et al., 2007). These results indicate that providing geometrical signals to hydrogels may synergistically guide tissue formation.

Cells cultured on the surfaces of hydrogels may be useful as an *in vitro* defined culture system to investigate the physiology and pathophysiology of both cells and tissues. The two-dimensional culture system, however, does not provide a microenvironment close to that *in vivo* and therefore may not represent an accurate model. The main drawbacks of the two-dimensional culture hydrogel system are the insufficient regulation of 3D architecture and the variations in biochemical cues from those of the *in vivo* environment, which may alter metabolism and reduce the functionalities of cells (Lutolf et al., 2009; Tibbitt and Anseth, 2009).

The movements and polarizations of cells are dynamically controlled by degradation of crosslinked ECM biomolecules in the vicinity of cells in response to specific enzymes secreted by the cells themselves. Specifically, matrix metalloproteinases (MMP) cause a disruption in the physical barrier inside the ECM, which may allow for cellular invasion, intravasation, extravasation, and migration. Although encapsulation of cells in natural hydrogels such as collagen and fibrin can be successful, these natural hydrogels can be degraded by secreted enzymes, including collagenase, stromelysin, and gelatinase, to enhance 3D migration; thus they are intrinsically lacking in mechanical properties. To address this problem, synthetic hydrogels that mimic proteolytic degradation properties have been developed. Using a Michael-type addition reaction, 4-arm-PEG-tetravinyl sulfone, mono-cysteine adhesion peptide, and bis-cysteine MMP substrate peptide (GPQGIWGQK) were combined to prepare hydrogels with encapsulated human foreskin fibroblasts (HFF). The hydrogels were degraded in response to proteases secreted from HFF residing within the hydrogels, resulting in free cell migration into the partially degraded hydrogel network (Lutolf et al., 2003). Similarly, using hydrogels consisting of PEG-DA, cell-adhesive peptide (CGRGDS), primary chick aortas cells, and MMP-sensitive peptide, researchers demonstrated that the angiogenic sprout of an aorta was regulated by the MMP-susceptibility of the hydrogel backbone (Miller et al., 2010). Recently, more advanced approaches have been reported, in which the angiogenic growth factor VEGF was genetically modified to have a terminal thiol group that was covalently incorporated into the hydrogel through photopolymerization, with a proteolytic sequence as a spacer. When subcutaneously implanted into male Lewis rats *in vivo*, the hydrogels were degraded by the activity of the proteases secreted by the cells, and the VEGF was released in response to the proteolytic enzymes that controlled the release rate (Phelps et al., 2010).

50.5 Composite Scaffolds Used to Mimic Specific Cellular Environments

In the development of scaffolds for tissue regeneration, the use of composite materials with diverse chemical and physical properties may be plausible to mimic the complex cellular microenvironment. In general, composite scaffolds can be prepared using a simple combination of both natural and synthetic polymers and both organic and inorganic materials, which are desired for their unique properties. Here, we will briefly discuss composite scaffolds used in bone, muscle, and neural tissue regeneration.

As discussed in the previous section, one major drawback of using synthetic polymers as a scaffold material is the limited cellular interaction capability due to the absence of a bioactive domain. Immobilization of proteins and peptides present in the ECM may partially alleviate these problems. The preparation of composite materials by physically mixing synthetic biodegradable polymers with natural polymers such as chitosan or collagen has been sought as an alternative strategy. In a study of composite materials by Ghasemi-Mobarakeh et al. (2008), poly(ϵ -caprolactone) and gelatin were mixed in a 70:30 ratio and electrospun to fabricate random and aligned fibers. The results showed increased neural cell proliferation in gelatin-containing fibers in both random and aligned structures. It was also reported that the introduction of gelatin into synthetic polymers affected differentiation of hMSCs (Rim et al., 2009). The incorporation of gelatin into a poly[(L-lactide)-*co*-(ϵ -caprolactone)] (PLCL) matrix increased the cellularity and controlled morphology of cultured hMSCs as a function of the concentration of

gelatin in the matrix compared to those of PLCL-only nanofibers. Moreover, under osteogenic differentiation conditions, the expression of osteogenic differentiation-associated genes, alkaline phosphatase activity, and calcium deposition were enhanced in the gelatin-containing PLCL nanofibers compared to those of the PLCL group, indicating that physical mixing of natural and synthetic polymers can regulate many cell functions, including adhesion and osteogenic differentiation of stem cells. A similar approach was applied to the development of scaffolds for cardiac tissue engineering, in which three different materials were combined to mimic the chemical and mechanical properties of myocardium; PLCL was used as a basic matrix to provide stable mechanical properties and elasticity, PLGA was incorporated to retard the overall degradation rate of the matrix, and collagen was added to improve the bioactivities of the scaffolds (Park et al., 2005). Other groups developed composites of synthetic and natural polymers for articular cartilage regeneration in which thin knitted PLGA meshes were used as a skeleton for mechanical support and collagen was incorporated as a thick layer on both sides of the PLGA skeleton to increase the overall thickness. The results showed improved syntheses of aggrecan and type-2 collagen on the composite forms when the chondrocytes were cultured for 8 weeks (Dai et al., 2010). These results suggest that composites of natural and synthetic polymers can easily recapitulate appropriate cellular events for successful tissue regeneration.

It is well known that proliferation or differentiation of nerve or muscle tissue can be enhanced by electrical stimulation, which is in part attributed to the propagation of action potentials upon stimulation. To exploit these physiological events, composites of biodegradable polymers with electroconductive materials have been investigated for effective transmission of electrical signals to the cells cultured on them. PLCL and polyaniline, one of the widely used electrically conductive materials, were mixed to fabricate the nanofiber meshes, illustrating that myotube formation was accelerated when the myoblasts were cultured on polyaniline-containing nanofibers compared to that of PLCL-only nanofibers, even without electrical stimulation (Jun et al., 2009). Another electroconductive polymer, polypyrrole, was also used as a composite with other synthetic polymers. For example, polypyrrole was incorporated as particles into polylactide scaffolds, and the fibroblasts cultured on them with various intensities of DC current showed controlled proliferation in a current-dependent manner (Shi et al., 2004).

Unlike other tissues, bone is composed of over 70% inorganic constituents rich in calcium and phosphate ions. This unique chemical composition has been known to influence bone development and repair. Therefore, composites of synthetic polymer matrices with bone-like inorganic chemicals have been widely used to facilitate bone formation. For example, when hydroxyapatites were incorporated into PLGA nanofibers, the osteogenic differentiation of hMSCs was better than that in cells cultured on pure PLGA nanofibers, as shown by their osteoconductive effect (Lee et al., 2010). The composite nanofibers of tricalcium phosphates and PLLA were also reported as a scaffold for the culture of adipose-derived stem cells (ADSC), demonstrating enhanced cellular proliferation and ALP activity, suggesting that chemicals with structures similar to bone can modulate the osteogenic differentiation of ADSC (McCullen et al., 2009). Instead of using composites, carbonated hydroxyapatite crystals can be formed in simulated body fluid (SBF); PCL nanofibers were incubated in SBF solution to produce a bone-like mineral film, which can also control cell adhesion and proliferation (Araujo et al., 2008). The composites of calcium phosphates can be formulated as a gel as well as a solid type of scaffold. When hydroxyapatite and tricalcium phosphate or biphasic calcium phosphate (BCP) were mixed with fibrin gel and subsequently injected into sheep muscle, formation of mineralized bone was observed 6 months after implantation (Le Nihouannen et al., 2008). Similarly, biphasic calcium phosphate/PLGA composite scaffolds improved the regeneration of alveolar bone 24 weeks after implantation (Ajdukovic et al., 2007).

Although tissue engineering approaches have led to regeneration or repair of damaged tissue, the success is often only partial; the original biological function is often not regained due to limited integration with native tissue or incomplete recovery of chemical and biological compositions of the tissue interface. Geometrically, the tissue interface, that is, cartilage–bone, tendon/ligament–bone, or muscle–tendon, is placed between two dissimilar tissues; however, the chemical composition, orientation, and structure of the ECMs exhibit profound differences. In order to engineer such a complicated tissue structure,

biphasic scaffolds are also required for effective regeneration of two types of tissues and their interfaces. For example, polycaprolactone (PCL)-poly(glycolic acid) (PGA) hybrid scaffolds were fabricated for reconstruction of the tooth and gingival interface. The scaffolds were fabricated using a 3D printing technique; PGA was targeted for the periodontal ligament region, and PCL was targeted for bone regeneration. The human gingival fibroblasts and human periodontal ligament cells were separately seeded onto each side of the scaffold, and the *in vivo* results showed that the formed structure appeared to be similar to those of tooth cementum-like tissue, ligament, and bone (Park et al., 2010b). To mimic the epithelium (collagen-rich connective tissue/muscle layer that exists in hollow organs), collagen matrices were stitched onto PGA scaffolds using threaded collagen fibers. Urothelial and bladder smooth muscle cells were seeded onto composite scaffolds, and the construct formed a bladder tissue-like structure, showing histological evidence of the presence of both layers 4 weeks after *in vivo* implantation into mice (Eberli et al., 2009). Osteochondral composite scaffolds were also developed for the treatment of defects in both bone and cartilage; the upper layer of the scaffolds was made of a mixture of hyaluronic acid and collagen, and the bottom layer was of collagen with a high composition of hydroxyapatite. In addition, the intermediate layer was composed of collagen with a relatively lower content of hydroxyapatite. When bone marrow stem cells were seeded onto the scaffolds, the cells differentiated into different types of cells in response to the local chemical composition of the matrix. Chondrocytes were seen on the upper layer, with osteoblasts on the bottom (Tampieri et al., 2008). Composite scaffolds of multiple components may also be useful for other applications. For example, tripolyphosphate was mixed with PLGA to neutralize the acidic degradation product of PLGA after *in vivo* implantation (Xie et al., 2010). Incorporation of PEO into a nanofibrous system was effective for control and porosity of fibers after coelectrospinning using 50% EtOH (Ionescu et al., 2010). Thus, the method to prepare composite combined scaffolds is useful for mimicking the complex microenvironment of the body through full exploitation of mechanical, chemical, and physiological properties of the constituent materials.

50.6 Scaffolds Mimicking the Structure of ECM

In tissue engineering, the regeneration of tissue can be obtained through the cultivation of cells on the appropriate scaffolds. These scaffolds play the role of the native ECM and mimic its fibrous and porous structures (size: from micro- to nanometer), which are composed of various biomolecules. Thus, scaffolds with various structural alterations have been developed to modulate cellular behaviors via property control, including morphology, porosity, pore density, surface, and mechanical properties.

Generally, control over pore structure and distribution and micro/nanoscale structures have been achieved using several scaffold-preparation methods, including salt leaching, phase separation, peptide assembly, knitting fibers, and electrospinning. Kang et al. (2006) fabricated gelatin scaffolds with dual pores using a modified overrun process for closed pores and a particle-leaching technique (NaCl and sucrose) for open pores. These gelatin scaffolds could also easily modulate the distribution and shapes of dual pores. A report by Liu et al. (2000) showed that the pore shape of macroporous poly(2-hydroxyethyl methacrylate) (p(HEMA)) hydrogels with NaCl was dependent on the concentration of NaCl. They found that the swelling ratio increased with increasing equilibrium water content and hydrogel porosity. Cooper et al. (2005) developed a PLGA graft with microfibrillar scaffolds for the anterior cruciate ligament (ACL). These PLGA grafts had easily controllable architecture, porosity, degradability, and mechanical properties for regeneration of the ligament. Moreover, their microfibrillar scaffolds exhibited optimal pore diameters (175–233 micron) for ligament tissue ingrowth, and initial mechanical properties of the construct approximated those of the native ligament. The arrangement of fibers regulates the overall mechanical properties and matrix deposition patterns of cultured cells. A 3D weaving technique was used to generate anisotropic 3D woven structures for cartilage tissue constructs, and these scaffolds showed mechanical properties on the same order of magnitude as values for native articular cartilage, as measured by compressive, tensile, and shear testing. Moreover, they observed that the developed scaffolds had the potential for direct implantation *in vivo* with biological support without requiring cultivation *in vitro* (Moutos et al., 2007).

Biomolecules with distinct hydrophobic and hydrophilic domains such as peptides can form self-assembled nanostructures via weak interactions, such as hydrogen bonding, hydrophobic interactions, and Van der Waals interactions. For application as a cell culture substrate and drug delivery vehicle, self-assembled nanostructures could easily be functionalized by incorporating peptide sequences that direct cell behavior into the buildup molecule. Gelain et al. (2007) developed self-assembling peptide nanofibers that were able to be utilized as a cell culture substrate and drug delivery vehicles for the regeneration of peripheral nerve and cardiomyocytes. Electrospinning is an additional method of producing nano/microscale fibers, and it provides a simple and versatile method to fabricate nanofibrous scaffolds with various biocompatible polymers. This method has been widely modified for nonwoven and oriented fiber development for cell culture substrates and for tubular fibers used as vehicles in the delivery of therapeutic proteins. Using nonwoven and oriented fibers, researchers investigated the control of cellular responses according to polymer composition, porosity, physical properties, and fiber morphology. Also, using tubular fibers, they investigated the delivery efficiencies of drug or protein target cells and tissues. Kim et al. (2010c) fabricated a polycaprolactone-gelatin (PG) composite of nonwoven fibers and evaluated its physical properties based on the content of gelatin in the fibers. They observed enhanced myogenesis on the PG composite nonwoven fibers with increasing contents of gelatin. The electrospinning process is advantageous for controlling porosity and fiber diameter, major parameters in the regulation of cell function. For example, a study using nonwoven fibers that were able to control porosity using PCL and water-soluble PEO particles in which the porosity of nonwoven fibers was effectively modulated by leaching PEO particles demonstrated that nonwoven fibers with high porosity induced higher differentiation of osteoblasts (Ekaputra et al., 2008). Polyethersulfone nonwoven fibers with various fiber diameters used to investigate the behaviors of neural stem cells on fibers were effective in modulating differentiation and migration of neural stem cells as a function of fiber diameter (Christopherson et al., 2009).

There is an increasing body of evidence that suggesting that surface geometry and topography affect the regulatory mechanisms of certain type of cells. Charest et al. (2007) developed topographic patterns on scaffolds consisting of embossed ridges and grooves or arrays of holes to investigate the differentiation of myoblasts. They observed higher alignment of myoblasts on grooves and the highest degree of differentiation at 5 ~ 25 μm patterns. Also, they found that microscale topography modulates myoblast alignment but did not have an effect on cell density. To mimic the mechanical properties of the ventricular myocardium recognized as anisotropic tissue, microfabrication techniques were used to create an accordion-like honeycomb microstructure in poly(glycerol sebacate). These scaffolds show similar mechanical properties and microstructures to the native myocardium, which may be dictated by the fiber orientation (Engelmayr et al., 2008). Using an electrospinning technique, oriented fibers can be produced easily by modulating the velocity of the collecting drum. These oriented fibers allowed for the induction of fibroblast migration (Kurpinski et al., 2010), differentiation of human coronary artery smooth muscle cells (Xu et al., 2004) and cardiomyocytes (Zong et al., 2005) and have been further utilized as vascular graft materials (Hashi et al., 2007).

50.7 Conclusions

The detailed understanding of regulatory mechanisms of cellular interaction with the microenvironment and how these mutual communications translate to the development, repair, and regeneration of certain types of tissues has long been a goal of many biologists and medical scientists. Although the goal has not been completely achieved and many challenges still remain, the gradual understanding in the field has spurred scientists in material engineering to create novel biomaterials that can be recognized by cells and that are responsive to cellular secretions and production in ways similar to those occurring in the native cellular microenvironment. These materials can be used in many biological applications, particularly holding great potential as scaffolds for tissue engineering. With conventional properties such as biocompatibility and degradability, the scaffold should be designed to manipulate the fates of

implanted and endogenous cells and to actively modulate tissue regeneration. Biomimetic approaches discussed in this chapter and other creative methods to be developed would definitely open a new era for redefining new roles for biological scaffold.

References

- Ajdukovic, Z., Ignjatovic, N., Petrovic, D. et al. 2007. Substitution of osteoporotic alveolar bone by biphasic calcium phosphate/poly-DL-lactide-co-glycolide biomaterials. *J Biomater Appl* 21: 317–28.
- Alemdaroglu, C., Degim, Z., Celebi, N. et al. 2006. An investigation on burn wound healing in rats with chitosan gel formulation containing epidermal growth factor. *Burns* 32: 319–27.
- Araujo, J. V., Martins, A., Leonor, I. B. et al. 2008. Surface controlled biomimetic coating of polycaprolactone nanofiber meshes to be used as bone extracellular matrix analogues. *J Biomater Sci Polym Ed* 19: 1261–78.
- Babensee, J. E., Mcintire, L. V., and Mikos, A. G. 2000. Growth factor delivery for tissue engineering. *Pharmaceut Res* 17: 497–504.
- Benton, J. A., Fairbanks, B. D., and Anseth, K. S. 2009. Characterization of valvular interstitial cell function in three dimensional matrix metalloproteinase degradable PEG hydrogels. *Biomaterials* 30: 6593–603.
- Bhati, R. S., Mukherjee, D. P., Mccarthy, K. J. et al. 2001. The growth of chondrocytes into a fibronectin-coated biodegradable scaffold. *J Biomed Mater Res* 56: 74–82.
- Charest, J. L., Garcia, A. J., and King, W. P. 2007. Myoblast alignment and differentiation on cell culture substrates with microscale topography and model chemistries. *Biomaterials* 28: 2202–10.
- Cheng, Z. and Teoh, S. H. 2004. Surface modification of ultra thin poly (epsilon-caprolactone) films using acrylic acid and collagen. *Biomaterials* 25: 1991–2001.
- Cheung, H. Y., Lau, K. T., Lu, T. P. et al. 2007. A critical review on polymer-based bio-engineered materials for scaffold development. *Composites Part B-Eng* 38: 291–300.
- Choi, J. S., Leong, K. W., and Yoo, H. S. 2008. *in vivo* wound healing of diabetic ulcers using electrospun nanofibers immobilized with human epidermal growth factor (EGF). *Biomaterials* 29: 587–96.
- Christopherson, G. T., Song, H., and Mao, H. Q. 2009. The influence of fiber diameter of electrospun substrates on neural stem cell differentiation and proliferation. *Biomaterials* 30: 556–64.
- Cooper, J. A., Lu, H. H., Ko, F. K. et al. 2005. Fiber-based tissue-engineered scaffold for ligament replacement: Design considerations and *in vitro* evaluation. *Biomaterials* 26: 1523–32.
- Cronin, E. M., Thurmond, F. A., Bassel-Duby, R. et al. 2004. Protein-coated poly(L-lactic acid) fibers provide a substrate for differentiation of human skeletal muscle cells. *J Biomed Mater Res Part A* 69A: 373–81.
- Cui, Y. L., Hou, X., Qi, A. D. et al. 2003. Biomimetic surface modification of poly(L-lactic acid) with gelatin and its effects on articular chondrocytes *in vitro*. *J Biomed Mater Res A* 66: 770–8.
- Dai, W., Kawazoe, N., Lin, X. et al. 2010. The influence of structural design of PLGA/collagen hybrid scaffolds in cartilage tissue engineering. *Biomaterials* 31: 2141–52.
- Dalby, M. J., Gadegaard, N., Tare, R. et al. 2007. The control of human mesenchymal cell differentiation using nanoscale symmetry and disorder. *Nat Mater* 6: 997–1003.
- Eberli, D., Freitas Filho, L., Atala, A. et al. 2009. Composite scaffolds for the engineering of hollow organs and tissues. *Methods* 47: 109–15.
- Ekaputra, A. K., Prestwich, G. D., Cool, S. M. et al. 2008. Combining electrospun scaffolds with electro-sprayed hydrogels leads to three-dimensional cellularization of hybrid constructs. *Biomacromolecules* 9: 2097–103.
- Engelmayr, G. C., JR., Cheng, M., Bettinger, C. J. et al. 2008. Accordion-like honeycombs for tissue engineering of cardiac anisotropy. *Nat Mater* 7: 1003–10.
- Engler, A. J., Sen, S., Sweeney, H. L. et al. 2006. Matrix elasticity directs stem cell lineage specification. *Cell* 126: 677–89.

- Freeman, I., Kedem, A., and Cohen, S. 2008. The effect of sulfation of alginate hydrogels on the specific binding and controlled release of heparin-binding proteins. *Biomaterials* 29: 3260–8.
- Furth, M. E., Atala, A., and Van Dyke, M. E. 2007. Smart biomaterials design for tissue engineering and regenerative medicine. *Biomaterials* 28: 5068–73.
- Gelain, F., Horii, A., and Zhang, S. G. 2007. Designer self-assembling peptide scaffolds for 3-D tissue cell cultures and regenerative medicine. *Macromol Biosci* 7: 544–51.
- Ghasemi-Mobarakeh, L., Prabhakaran, M. P., Morshed, M. et al. 2008. Electrospun poly(epsilon-caprolactone)/gelatin nanofibrous scaffolds for nerve tissue engineering. *Biomaterials* 29: 4532–9.
- Hashi, C. K., Zhu, Y., Yang, G. Y. et al. 2007. Antithrombogenic property of bone marrow mesenchymal stem cells in nanofibrous vascular grafts. *Proc Natl Acad Sci USA* 104: 11915–20.
- Hill, E., Boontheekul, T., and Mooney, D. J. 2006. Regulating activation of transplanted cells controls tissue regeneration. *Proc Natl Acad Sci USA* 103: 2494–9.
- Hosseinkhani, H., Hosseinkhani, M., Khademhosseini, A. et al. 2007. Bone regeneration through controlled release of bone morphogenetic protein-2 from 3-D tissue engineered nano-scaffold. *J Contr Rel* 117: 380–6.
- Hubbell, J. A. 1999. Bioactive biomaterials. *Curr Opin Biotechnol* 10: 123–9.
- Huebsch, N., Arany, P. R., Mao, A. S. et al. 2010. Harnessing traction-mediated manipulation of the cell/matrix interface to control stem-cell fate. *Nat Mater* 9: 518–26.
- Huebsch, N. and Mooney, D. J. 2009. Inspiration and application in the evolution of biomaterials. *Nature* 462: 426–32.
- Hutmacher, D. W. 2000. Scaffolds in tissue engineering bone and cartilage. *Biomaterials* 21: 2529–43.
- Hynes, R. O. 2002. Integrins: Bidirectional, allosteric signaling machines. *Cell* 110: 673–87.
- Ionescu, L. C., Lee, G. C., Sennett, B. J. et al. 2010. An anisotropic nanofiber/microsphere composite with controlled release of biomolecules for fibrous tissue engineering. *Biomaterials* 31: 4113–20.
- Jeon, O., Kang, S. W., Lim, H. W. et al. 2006. Long-term and zero-order release of basic fibroblast growth factor from heparin-conjugated poly(L-lactide-co-glycolide) nanospheres and fibrin gel. *Biomaterials* 27: 1598–607.
- Jeong, S. I., Kwon, J. H., Lim, J. I. et al. 2005. Mechano-active tissue engineering of vascular smooth muscle using pulsatile perfusion bioreactors and elastic P1cl scaffolds. *Biomaterials* 26: 1405–11.
- Jeong, S. I., Lee, A. Y., Lee, Y. M. et al. 2008. Electrospun gelatin/poly(L-lactide-co-epsilon-caprolactone) nanofibers for mechanically functional tissue-engineering scaffolds. *J Biomater Sci Polym Ed* 19: 339–57.
- Jin, J., Jeong, S. I., Shin, Y. M. et al. 2009. Transplantation of mesenchymal stem cells within a poly(lactide-co-epsilon-caprolactone) scaffold improves cardiac function in a rat myocardial infarction model. *Eur J Heart Fail* 11: 147–53.
- Jun, H. W. and West, J. L. 2005. Modification of polyurethaneurea with Peg and Yigrs peptide to enhance endothelialization without platelet adhesion. *J Biomed Mater Res B Appl Biomater* 72: 131–9.
- Jun, I., Jeong, S., and Shin, H. 2009. The stimulation of myoblast differentiation by electrically conductive sub-micron fibers. *Biomaterials* 30: 2038–47.
- Kang, H. G., Kim, S. Y., and Lee, Y. M. 2006. Novel porous gelatin scaffolds by overrun/particle leaching process for tissue engineering applications. *J Biomed Mater Res B Appl Biomater* 79B: 388–97.
- Kim, D. H., Lipke, E. A., Kim, P. et al. 2010a. Nanoscale cues regulate the structure and function of macroscopic cardiac tissue constructs. *Proc Natl Acad Sci USA* 107: 565–70.
- Kim, M., Lee, J. Y., Jones, C. N. et al. 2010b. Heparin-based hydrogel as a matrix for encapsulation and cultivation of primary hepatocytes. *Biomaterials* 31: 3596–603.
- Kim, M. S., Jun, I., Shin, Y. M. et al. 2010c. The development of genipin-crosslinked poly(caprolactone) (PCL)/gelatin nanofibers for tissue engineering applications. *Macromol Biosci* 10: 91–100.
- Kim, T. G. and Park, T. G. 2006. Biomimicking extracellular matrix: Cell adhesive Rgd peptide modified electrospun poly(D,L-lactic-co-glycolic acid) nanofiber mesh. *Tissue Eng* 12: 221–33.

- Klee, D., Ademovic, Z., Bosserhoff, A. et al. 2003. Surface modification of poly(vinylidene fluoride) to improve the osteoblast adhesion. *Biomaterials* 24: 3663–70.
- Kong, H. J., Liu, J. D., Riddle, K. et al. 2005. Non-viral gene delivery regulated by stiffness of cell adhesion substrates. *Nat Mater* 4: 460–4.
- Kurpinski, K. T., Stephenson, J. T., Janairo, R. R. et al. 2010. The effect of fiber alignment and heparin coating on cell infiltration into nanofibrous Plla scaffolds. *Biomaterials* 31: 3536–42.
- Lan, M. A., Gersbach, C. A., Michael, K. E. et al. 2005. Myoblast proliferation and differentiation on fibronectin-coated self assembled monolayers presenting different surface chemistries. *Biomaterials* 26: 4523–31.
- Le Nihouannen, D., Saffarzadeh, A., Gauthier, O. et al. 2008. Bone tissue formation in sheep muscles induced by a biphasic calcium phosphate ceramic and fibrin glue composite. *J Mater Sci Mater Med* 19: 667–75.
- Lee, A. C., Yu, V. M., Lowe, J. B. et al. 2003. Controlled release of nerve growth factor enhances sciatic nerve regeneration. *Exp Neurol* 184: 295–303.
- Lee, J. H., Rim, N. G., Jung, H. S. et al. 2010. Control of osteogenic differentiation and mineralization of human mesenchymal stem cells on composite nanofibers containing poly[lactic-co-(glycolic acid)] and hydroxyapatite. *Macromol Biosci* 10: 173–82.
- Lee, K. Y., Peters, M. C., Anderson, K. W. et al. 2000. Controlled growth factor release from synthetic extracellular matrices. *Nature* 408: 998–1000.
- Lee, S. H. and Shin, H. 2007. Matrices and scaffolds for delivery of bioactive molecules in bone and cartilage tissue engineering. *Adv Drug Deliv Rev* 59: 339–59.
- Li, W., Guo, Y., Wang, H. et al. 2008. Electrospun nanofibers immobilized with collagen for neural stem cells culture. *J Mater Sci Mater Med* 19: 847–54.
- Liu, Q., Hedberg, E. L., Liu, Z. W. et al. 2000. Preparation of macroporous poly(2-hydroxyethyl methacrylate) hydrogels by enhanced phase separation. *Biomaterials* 21: 2163–9.
- Lutolf, M. P. 2009. Spotlight on hydrogels. *Nat Mater* 8: 451–3.
- Lutolf, M. P., Gilbert, P. M., and Blau, H. M. 2009. Designing materials to direct stem-cell fate. *Nature* 462: 433–41.
- Lutolf, M. P., Lauer-Fields, J. L., Schmoekel, H. G. et al. 2003. Synthetic matrix metalloproteinase-sensitive hydrogels for the conduction of tissue regeneration: Engineering cell-invasion characteristics. *Proc Natl Acad Sci USA* 100: 5413–8.
- Ma, Z., Gao, C., Gong, Y. et al. 2005. Cartilage tissue engineering Plla scaffold with surface immobilized collagen and basic fibroblast growth factor. *Biomaterials* 26: 1253–9.
- Marklein, R. A. and Burdick, J. A. 2010. Controlling stem cell fate with material design. *Adv Mater* 22: 175–89.
- McCullen, S. D., Zhu, Y., Bernacki, S. H. et al. 2009. Electrospun composite poly(L-lactic acid)/tricalcium phosphate scaffolds induce proliferation and osteogenic differentiation of human adipose-derived stem cells. *Biomed Mater* 4: 035002.
- Meiners, S. and Mercado, M. L. T. 2003. Functional peptide sequences derived from extracellular matrix glycoproteins and their receptors—Strategies to improve neuronal regeneration. *Mol Neurobiol* 27: 177–95.
- Miller, J. S., Shen, C. J., Legant, W. R. et al. 2010. Bioactive hydrogels made from step-growth derived Peg-peptide macromers. *Biomaterials* 31: 3736–43.
- Miyoshi, M., Kawazoe, T., Igawa, H. H. et al. 2005. Effects of bfgf incorporated into a gelatin sheet on wound healing. *J Biomater Sci Polym Ed* 16: 893–907.
- Moutos, F. T., Freed, L. E., and Guilak, F. 2007. A biomimetic three-dimensional woven composite scaffold for functional tissue engineering of cartilage. *Nat Mater* 6: 162–7.
- Murphy, W. L., Peters, M. C., Kohn, D. H. et al. 2000. Sustained release of vascular endothelial growth factor from mineralized poly(lactide-co-glycolide) scaffolds for tissue engineering. *Biomaterials* 21: 2521–7.

- Park, C. H., Hong, Y. J., Park, K. et al. 2010a. Peptide-grafted lactide-based poly(ethylene glycol) porous scaffolds for specific cell adhesion. *Macromol Res* 18: 526–32.
- Park, C. H., Rios, H. F., Jin, Q. et al. 2010b. Biomimetic hybrid scaffolds for engineering human tooth-ligament interfaces. *Biomaterials* 31: 5945–52.
- Park, H., Radisic, M., Lim, J. O. et al. 2005. A novel composite scaffold for cardiac tissue engineering. *In Vitro Cell Dev Biol Anim* 41: 188–96.
- Patel, S., Kurpinski, K., Quigley, R. et al. 2007. Bioactive nanofibers: Synergistic effects of nanotopography and chemical signaling on cell guidance. *Nano Lett* 7: 2122–8.
- Phelps, E. A., Landazuri, N., Thule, P. M. et al. 2010. Bioartificial matrices for therapeutic vascularization. *Proc Natl Acad Sci USA* 107: 3323–8.
- Pitukmanorom, P., Yong, T. H., and Ying, J. Y. 2008. Tunable release of proteins with polymer-inorganic nanocomposite microspheres. *Adv Mater* 20: 3504–9.
- Place, E. S., Evans, N. D., and Stevens, M. M. 2009. Complexity in biomaterials for tissue engineering. *Nat Mater* 8: 457–70.
- Rajangam, K., Behanna, H. A., Hui, M. J. et al. 2006. Heparin binding nanostructures to promote growth of blood vessels. *Nano Lett* 6: 2086–90.
- Rim, N. G., Lee, J. H., Jeong, S. I. et al. 2009. Modulation of osteogenic differentiation of human mesenchymal stem cells by poly[(L-lactide)-co-(epsilon-caprolactone)]/gelatin nanofibers. *Macromol Biosci* 9: 795–804.
- Ruvinov, E., Leor, J., and Cohen, S. 2010. The effects of controlled Hgf delivery from an affinity-binding alginate biomaterial on angiogenesis and blood perfusion in a hindlimb ischemia model. *Biomaterials* 31: 4573–82.
- Shi, G., Rouabhia, M., Wang, Z. et al. 2004. A novel electrically conductive and biodegradable composite made of polypyrrole nanoparticles and polylactide. *Biomaterials* 25: 2477–88.
- Shimizu, K., Fujita, H., and Nagamori, E. 2009. Alignment of skeletal muscle myoblasts and myotubes using linear micropatterned surfaces ground with abrasives. *Biotechnol Bioeng* 103: 631–8.
- Shin, H., Jo, S., and Mikos, A. G. 2003. Biomimetic materials for tissue engineering. *Biomaterials* 24: 4353–64.
- Shin, Y. M., Kim, K. S., Lim, Y. M. et al. 2008. Modulation of spreading, proliferation, and differentiation of human mesenchymal stem cells on gelatin-immobilized poly(L-lactide-co-caprolactone) substrates. *Biomacromolecules* 9: 1772–81.
- Shin, Y. M., Shin, H., and Lim, Y. M. 2010. Surface modification of electrospun poly(L-lactide-co-epsilon-caprolactone) fibrous meshes with a rgd peptide for the control of adhesion, proliferation and differentiation of the preosteoblastic cells. *Macromol Res* 18: 472–81.
- Slaughter, B. V., Khurshid, S. S., Fisher, O. Z. et al. 2009. Hydrogels in regenerative medicine. *Adv Mater* 21: 3307–29.
- Smith, L. A. and Ma, P. X. 2004. Nano-fibrous scaffolds for tissue engineering. *Coll Surf B-Biointerfaces* 39: 125–31.
- Sun, H., Wirsén, A. and Albertsson, A. C. 2004. Electron beam-induced graft polymerization of acrylic acid and immobilization of arginine-glycine-aspartic acid-containing peptide onto nanopatterned polycaprolactone. *Biomacromolecules* 5: 2275–80.
- Tampieri, A., Sandri, M., Landi, E. et al. 2008. Design of graded biomimetic osteochondral composite scaffolds. *Biomaterials* 29: 3539–46.
- Tayalia, P. and Mooney, D. J. 2009. Controlled growth factor delivery for tissue engineering. *Adv Mater* 21: 3269–85.
- Tibbitt, M. W. and Anseth, K. S. 2009. Hydrogels as extracellular matrix mimics for 3D cell culture. *Biotechnol Bioeng* 103: 655–63.
- Volcker, N., Klee, D., Hocker, H. et al. 2001. Functionalization of silicone rubber for the covalent immobilization of fibronectin. *J Mater Sci Mater Med* 12: 111–9.
- Wang, F. and Guan, J. 2010a. Cellular cardiomyoplasty and cardiac tissue engineering for myocardial therapy. *Adv Drug Deliv Rev* 62: 784–97.

- Wang, L. S., Chung, J. E., Chan, P. P. Y. et al. 2010b. Injectable biodegradable hydrogels with tunable mechanical properties for the stimulation of neurogenic differentiation of human mesenchymal stem cells in 3D culture. *Biomaterials* 31: 1148–57.
- Wilson, C. J., Clegg, R. E., Leavesley, D. I. et al. 2005. Mediation of biomaterial-cell interactions by adsorbed proteins: A review. *Tissue Eng* 11: 1–18.
- Xie, S., Zhu, Q., Wang, B. et al. 2010. Incorporation of tripolyphosphate nanoparticles into fibrous poly(lactide-co-glycolide) scaffolds for tissue engineering. *Biomaterials* 31: 5100–9.
- Xu, C. Y., Inai, R., Kotaki, M. et al. 2004. Aligned biodegradable nanotubular structure: A potential scaffold for blood vessel engineering. *Biomaterials* 25: 877–86.
- Zhu, Y., Gao, C., Liu, X. et al. 2002. Surface modification of polycaprolactone membrane via aminolysis and biomacromolecule immobilization for promoting cytocompatibility of human endothelial cells. *Biomacromolecules* 3: 1312–9.
- Zong, X. H., Bien, H., Chung, C. Y. et al. 2005. Electrospun fine-textured scaffolds for heart tissue constructs. *Biomaterials* 26: 5330–8.

51

Molecular Biology Techniques

51.1	Histochemistry.....	51-1
	Hematoxylin and Eosin • Toluidine Blue • Crystal Violet • Alkaline Phosphatase Assay • Oil Red O	
51.2	Gel Electrophoresis.....	51-4
	Agarose Gel Electrophoresis • Polyacrylamide Gel Electrophoresis • SDS-PAGE	
51.3	Restriction Enzymes	51-9
	Introduction to the Technique • Technical Considerations	
51.4	Other DNA Modification Enzymes.....	51-10
	DNA Ligase • Blunting Enzymes • Calf Intestinal Phosphatase	
51.5	The Polymerase Chain Reaction.....	51-14
	The Traditional Polymerase Chain Reaction • Real-Time Quantitative PCR	
51.6	Blotting.....	51-20
	The Southern Blot • The Northern Blot • The Western Blot • The Eastern Blot	
	References.....	51-24

X.G. Chen
Tulane University

Y.L. Fang
Tulane University

W.T. Godbey
Tulane University

Biomedical engineering covers many facets, from chemistry for the development of biodegradable tissue scaffolds, to physics to describe the mechanical properties of an implanted material, to biology for the manipulation of cells for implantation as well as the understanding of the host organism that will receive the implant, to mathematics for analysis and modeling applications. This chapter will focus on molecular biology techniques that are commonly employed in biomedical engineering. It will cover different ways of analyzing proteins, RNA, and DNA, as well as an introduction to DNA manipulation techniques that are used in genetic engineering.

The chapter is by no means a comprehensive presentation of techniques; only a small subset of the most common techniques is presented. In doing so, a technique will be introduced and broadly described, followed by some technical considerations one might want to keep in mind when performing the laboratory procedures. For more detailed protocols, the reader might be interested in consulting one of several laboratory manuals that have done an excellent job of compiling and explaining a broad range of molecular biology techniques. These manuals include *Molecular Cloning: A Laboratory Manual* by Sambrook and Russell, *Conn's Biological Stains: A Handbook of Dyes, Stains and Fluorochromes for Use in Biology and Medicine* by Horobin, Kiernan, and Kiernan, and *Gene Cloning* by Lodge, Lund, and Minchin.

51.1 Histochemistry

Cells and tissues are relatively colorless under microscopy. To aid with visualization and analysis, a variety of stains have been developed to enhance the details of structures of particular interest. Stains

can also be used to detect and determine the location of specific substances in a sample. In this section, five stains used in common practice are introduced and outlined.

51.1.1 Hematoxylin and Eosin

51.1.1.1 Introduction to the Technology

The dyes hematoxylin and eosin (H&E) are typically used together because the cellular structures that they label are complimentary. Hematoxylin is obtained via extraction from logwood. Eosin is an artificial stain.

The extracted form of hematoxylin is not endowed with staining ability until it has been oxidized into hematein. There are two common methods used for the oxidation. "Ripening" is one strategy that leaves hematoxylin in the air and under light, thus allowing oxidation to take place naturally. Although the process is slow, the oxidized product can maintain an enduring property of staining. The second common strategy shortens the time of reaction via the use of oxidizing agents such as sodium iodate. This method makes hematein available whenever it is needed, but the resulting solution may suffer from over-oxidization or later degradation by natural oxidation (Bancroft and Gamble, 2008). The addition of a mordant to a sample stained with hematein will yield a positively charged complex that will bind to negatively charged structures in the prepared sample, including nuclear chromatin. A mordant in this case is a substance that has an affinity with a particular dye that will help to form an insoluble material upon interaction with the dye (Bourne and Danielli, 1970). Mordants often used in hematein staining are metal salts including aluminum, iron, copper, and chromium salts. Although oxidation and the use of a mordant are required to convert hematoxylin into a positively charged hematein complex, hematoxylin itself is said to be a nuclear stain.

There are several forms of eosin that are commercially available. One of the most popular types, eosin Y, is soluble in both water and alcohol. As opposed to hematoxylin, eosin is an anionic stain that forms a complex with acidophilic sites such as the cytoplasm, connective tissue fibers, and collagen fibers, which will be stained red or pink (Cormack, 2001). Usually acetic acid is added to eosin solutions to act as an accelerant to enhance staining.

51.1.1.2 Technical Considerations

The following is a simple procedure for staining using H&E (Nagy, 2008, Dhein et al., 2005, Bronner-Fraser, 1996):

1. *Dewaxing and rehydration:* For samples that have been embedded in paraffin, sectioned, and mounted on slides, the mounted sections are soaked in xylene to dissolve the wax. Several immersions in a series of ethanol/water solutions with descending percentages of ethanol (100%, 95%, 80% then 70%) are sequentially performed to rehydrate the section for staining. Finally, the sections are washed with tap water and soaked in distilled water.
2. *Hematoxylin staining:* The section is next stained for 5 min using alum hematoxylin (50 g aluminum potassium sulfate, 11 g hematoxylin, 0.1 g sodium iodate, 1.0 g citric acid and 50 g chloral hydrate) and washed by tap water. It is recommended that the slide is next dipped in a solution of acid alcohol (ethanol containing 1% hydrochloric acid) to sharpen the contrast of the stain. After rinsing with tap water, the section may change from light red to gray-blue if the tap water is alkaline. This process is commonly known as "bluing."
3. *Eosin counterstaining:* The treated section is immersed in an eosin solution (2.5 g eosin, 0.5 mL glacial acetic acid and 495 mL water) for 3 min and rinsed with tap water.
4. *Dehydration and mounting:* The stained section is immersed in a series of ethanol/water solutions with increasing percentages of ethanol (70%, 80%, 95%, and 100%) to remove water because the presence of water can refract light and prevent clear observation of fine structures under microscopy. Xylene is an effective clearing agent and is suggested to be employed to allow the refraction coefficient of the tissue to increase. The resulting slide can then be mounted for preservation using a medium such as Permount.

51.1.2 Toluidine Blue

51.1.2.1 Introduction to the Technology

Toluidine blue is a synthetic dye that is frequently used as a nuclear stain. It is a typical alkaline dye and the cation in it has affinity for acidic substances contained in cell and tissue samples. For example, toluidine blue can be used to detect cell nuclei by staining the nucleic acids therein. The dye is also used for staining mucin and mast cells (Humason, 1972).

In histology, stains can be categorized into two groups: orthochromatic and metachromatic. Orthochromatic stains pass on the color themselves to specific components in cells or tissues. Fast green and Orange G are two orthochromatic dyes. Metachromatic stains take on a different color after binding to their targets. Methylene blue is an example of a metachromatic dye (Krishnamurthy, 1999, Humason, 1972). Toluidine blue can be either orthochromatic or metachromatic, depending on the chemical reaction that takes place during the staining process. When toluidine blue reacts with lignin, a molecule common used by some plants to make their cell walls stronger, the dye will take on the orthochromatic blue color. However, when the dye reacts with sulfated proteoglycans such as those found in mast cells and basophilic granules, the dye will metachromatically stain the structures purple/red at acid pH.

51.1.2.2 Technical Considerations

A brief protocol for the use of toluidine blue for the detection of mast cells follows (Humason, 1972):

1. Slides are deparaffinized and immersed in alcohol in the same fashion as that described for H&E staining.
2. Slides are immersed for 1–2 min in the staining solution, comprised of 0.2 g toluidine blue O in 100 mL or 60% ethanol in water.
3. Tap water is used for rinsing.
4. The samples are dehydrated in acetone.
5. Xylene is added for the purpose of clearing tissues followed by slide mounting.

Toluidine blue can also be used to locate cells in a biodegradable three-dimensional matrix when hydrolysis is a concern (Godbey et al., 2004):

1. Incubate the scaffold containing cells in 10% neutral-buffered formalin overnight
2. Rinse 3 × 15 min with phosphate-buffered saline.
3. Dehydrate the scaffolds by passing them 2 × 10 min through each of a series of dilutions of 70%, 80%, 90%, 95%, and 100% ethanol.
4. The scaffolds are now ready for embedding and sectioning. (JB-4 polymethacrylate embedding is recommended.)
5. Sections can then be stained using 1% toluidine blue in sodium acetate followed by rinsing with water.

51.1.3 Crystal Violet

51.1.3.1 Introduction to the Technology

Crystal violet is an excellent stain that is widely used in cytology, histology, and bacteriology. It is a typical basic dye that can be dissolved in both water and alcohol, allowing the staining of cell nuclei. Crystal violet staining is often used in the evaluation of cytotoxicity and growth inhibition assays.

51.1.3.2 Technical Considerations (Saotome et al., 1989)

1. Wash cells with PBS. The cells should not be fixed—this is an assay to be performed on intact cells.
2. Add 50 μL of 0.5% crystal violet in methanol to the cell culture.
3. Incubate for 10 min at room temperature.

4. Discard the staining solution and wash the culture gently with tap water.
5. Add 1% sodium dodecyl sulfate solution to the sample to solubilize the stain and agitate lightly.
6. Quantify via absorbance readings at 570 nm versus control cultures.

51.1.4 Alkaline Phosphatase Assay

51.1.4.1 Introduction to the Technology

Alkaline phosphatase is a specific enzyme that can remove the phosphate groups from nucleotides or proteins. The total level of serum alkaline phosphatase is a good indicator for the activity of a series of isoenzymes in liver and bone, and the placenta during pregnancy (Campbell et al., 1993). For the tissue engineer, the alkaline phosphatase assay is used as a marker of bone tissue production, including the osteogenic differentiation of stem or progenitor cells into bone cells.

51.1.4.2 Technical Considerations

A procedure for measuring alkaline phosphatase activity via a colorimetric assay follows (Holtorf et al., 2005):

1. Mix 80 μL of cell lysate with 20 μL of alkaline buffer solution (1.5 M 2-amino-2-methyl-1-propanol at pH 10.3).
2. Add 100 μL of p-nitrophenyl phosphate 100 \times stock substrate solution (100 \times stock is made by adding 40 mg of 4-nitrophenyl phosphate disodium salt hexahydrate into 10 mL of ddH₂O).
3. Incubate at 37°C for 1 h.
4. Stop the reaction with 100 μL of 0.3 M NaOH.
5. Measure absorbance at 405 nm.

51.1.5 Oil Red O

51.1.5.1 Introduction to the Technology

Oil red O is used to stain lipids, fatty acids, triglycerides, and cholesterol to make them visible under light microscopy. Like other lysochromes (fat stains), oil red O is more soluble in lipids than in its alcohol solvent which causes it to preferentially stay in lipid droplets (Kiernan, 1981). This stain is often used to demonstrate adipogenic differentiation of stem or progenitor cells.

51.1.5.2 Technical Considerations

Oil red O has an intense color and the staining procedure is convenient to perform on sectioned preparations (Humason, 1972):

1. Rinse the frozen section in 60% isopropanol for 30 s.
2. Stain the section by immersion in oil red O solution (0.7 g oil red O in 200 mL pure isopropanol) for 10 min.
3. Rinse the section in 60% isopropanol for few seconds and then wash in tap water for 2–3 min.
4. A hematoxylin counterstain can be performed at this point.

51.2 Gel Electrophoresis

Gel electrophoresis is widely used in molecular biology to separate macromolecules, such as polynucleotides or proteins, via physical characteristics such as size, shape, or isoelectric point. The technique has been an essential tool in the biosciences for analyzing protein molecular weights, determining the number of bases in a DNA fragment, preparing samples for blotting, visualizing results of the polymerase chain reaction, and more.

Both proteins and polynucleotides have electrostatic charges. When in the presence of an electric field, they will move toward the anode or cathode according to the net charge of the molecule. The gel matrix serves as a barrier to slow the movement of the macromolecules. Molecules with different sizes, shapes, or net charges will migrate at different rates through the matrix, thereby being sorted into different bands. Dyes, radiolabeling, or immunoblotting can be used to visualize the separated bands of macromolecules. The bands can be compared to a reference marker of the same material (nucleotide or protein) to ascertain fundamental information such as molecular weight.

51.2.1 Agarose Gel Electrophoresis

51.2.1.1 Introduction to the Technique

Agarose gel electrophoresis is often used to separate polynucleotides. Agarose is a polysaccharide isolated from seaweed, which is remarkably suitable for serving as gel matrix because of its neutral charge and relatively low degree of chemical complexity. Agarose melts and dissolves at a relatively high temperature and forms a gel matrix upon cooling. The gel is made in a buffer solution such as Tris-acetate-EDTA (TAE) to match the buffer that will be used for the electrophoresis procedure. Upon application of an electric field, polynucleotides of different sizes can pass through the porous agarose matrix at different rates according to their size because of the uniform negative charge distribution of the molecules. The resulting bands are visualized via the use of fluorescent molecules.

51.2.1.2 Technical Considerations

51.2.1.2.1 Concentration of Agarose

When used to separate polynucleotides, agarose is used at concentrations in the range of 0.3–2% (w/v). Agarose concentration determines pore size within the gel matrix, which in turn determines the optimal range of polynucleotide sizes that can be efficiently separated. The following table is a convenient way to determine the concentration of agarose to use for various DNA separations (Mitra, 2003):

Concentration of Agarose	Fragment Sizes (bp)
0.3%	5000–60,000
0.6%	1000–20,000
0.7%	800–10,000
0.9%	500–7000
1.2%	400–6000
1.5%	200–3000
2.0%	100–2000

51.2.1.2.2 Applied Voltage

The rate of polynucleotide movement is dependent upon applied voltage (Rapley and Walker, 1998). The higher the voltage, the faster the DNA moves. However, higher voltages are associated with higher currents within the gel, which translates into higher temperatures. High temperatures accelerate the migration rates of fragments in the sample, which would increase band widths and thereby reduce resolution. An inhomogeneous temperature distribution would produce convection and possibly mix fragments that are to be separated. If the temperatures are high enough, double-stranded fragments can denature and produce unexpected results. Therefore, an appropriate voltage should be used, or cooling methods should be employed when the high voltage is required.

Recommended voltage settings are as follows (Brown, 2000):

Recommended Voltage (V/cm) ^a	Fragment Sizes (bp)
5	≤1000
4–10	1000–12,000
1–2	≥12,000

^a cm refers to the distance from cathode to anode, in centimeters.

While it may be counterintuitive to use a lower voltage for larger fragment sizes, this is the usual practice to prevent streaking of the bands.

51.2.1.2.3 Visualization of Bands

Ethidium bromide (EB) is a DNA intercalating dye that fluoresces orange upon exposure to ultraviolet light. EB can be added to the hot agarose solution (~4 μL/100 mL of solution) before it is cooled to form the gel. Alternatively, EB can be added to the buffer reservoir closest to the anode just prior to turning on the electrical current for running the gel. Being positively charged, EB will migrate toward the cathode as the DNA migrates toward the anode. When the two molecules meet, the EB will bind to the DNA. One could also immerse the gel into a solution of buffer containing EB after the sample has been run. While soaking the gel after separation allows for less use of the neurotoxic and carcinogenic EB over time since the soaking solution can be reused, DNA can diffuse during the soak which will decrease the sharpness of the observed bands.

PicoGreen is another fluorophore that is used to bind to double-stranded DNA (dsDNA) for visualization of separated DNA bands after electrophoresis. This technique is sensitive enough to detect 1 ng of DNA even when RNA and protein contaminants are present (Kieleczawa, 2006). Because of its sensitivity, the dye can be used to quantify dsDNA concentrations. One must avoid contamination with divalent metal ions such as Mg²⁺, Ca²⁺, and Zn²⁺ because they can quench the fluorescence of the dye (Singer et al., 1997, Saunders et al., 1999).

51.2.1.2.4 DNA Loading Buffer

There are two or three main reasons for mixing a DNA sample with loading buffer before loading it into a gel for electrophoresis. First, loading buffer will contain an agent such as glycerol or ficoll to increase the density of the sample so that the sample will settle to the bottom of the well upon loading. Second, the loading buffer will contain one or more dyes to aid the user with monitoring the progress of migration without having to halt the electrophoretic process. A common dye pair is bromophenol blue/xylene cyanol, which will migrate at rates similar to 300 and 4000 base-pair DNA, respectively (Kumar and Garg, 2005). Third, some loading buffers will incorporate 6 mM EDTA, which serves as a chelating agent for divalent cations and therefore indirectly inhibits the action of many enzymes.

A recipe for a common 6× loading buffer (which will be used at 2 μL of loading buffer per 10 μL of DNA sample) follows (Sambrook and Russell, 2001):

- 0.25% (w/v) bromophenol blue
- 0.25% (w/v) xylene cyanol FF
- 30% (v/v) glycerol in water (15% Ficoll (w/v) can be used, instead)

51.2.2 Polyacrylamide Gel Electrophoresis

51.2.2.1 Introduction to the Technique

Polyacrylamide gel electrophoresis (PAGE) is an electrophoresis technique that can be used for separating small macromolecules such as proteins or small oligonucleotides. To form the cross-linked gel,

acrylamide monomers are polymerized with ethylene bisacrylamide, using tetramethylethylenediamine as the catalyst and ammonium persulfate as the initiator. Polyacrylamide gels can be classified into two categories: continuous and discontinuous systems. The continuous system has a single gel separating tanks containing the same buffer as that used in the gel. The separation of macro molecules occurs by the sieve effect. The discontinuous system contains two gels—a stacking gel and a separating gel—each made with a different buffer. The stacking gel operates by the concentration effect, where leading ions (generally Cl^-) move more quickly through the gel than does the protein sample. In contrast, trailing ions (commonly glycine in the electrophoresis buffer) migrate more slowly than the protein. Between the two ion layers the protein molecules are concentrated into a sharp band. The separating gel consists of smaller pores in which the sieve effect is the determining factor. After the protein moves from the stacking gel into the separating gel, the smaller pores separate the protein based on size (and shape, when the proteins are not denatured).

51.2.2.2 Technical Considerations

51.2.2.2.1 Pore Size

The pore size of gel can be controlled by monomer concentration (T) and cross-linker concentration (C). T and C could be calculated by the following equations (Hjerten, 1962):

$$T = \frac{a + b}{m} \times 100\%; \quad \text{and} \quad C = \frac{b}{a + b} \times 100\%,$$

where

a = the mass of acrylamide

b = the mass of ethylene bisacrylamide

m = the buffer volume

The following table can serve as a guide for preparing the appropriate polyacrylamide gels for protein separation (Hames, 1998):

M _r range of Proteins in the Sample	Acrylamide Concentration	
	%T	%C
25,000–300,000	5	2.6
15,000–100,000	10	2.6
12,000–50,000	15	2.6
13,000–1,000,000	3–30	8.4
14,000–210,000	5–20	2.6
14,000–330,000	8–15	1.0

51.2.2.2.2 Visualization of Bands

The separated polypeptide bands can be visualized through staining with Coomassie Brilliant Blue or silver salts (Roe, 2001). Coomassie blue staining follows three straightforward steps: fixation, staining, and destaining. Fixation locks the proteins inside the gel to prevent their diffusion during staining and destaining. Staining entails the submersion of the entire gel into a solution of a solvent mixture (45 mL water + 45 mL methanol + 10 mL glacial acetic acid) plus Coomassie Brilliant Blue (0.25 g), causing the entire gel to turn blue. Because of the methanol and acetic acid in the solution, the fixation and staining steps are performed simultaneously. Destaining entails the submersion of the gel into solvent solution without dye, which will remove dye molecules that are not bound to protein.

51.2.3 SDS-PAGE

Sodium dodecyl sulfate polyacrylamide gel electrophoresis (SDS-PAGE) is a technique used for analyzing proteins. SDS is a detergent with a hydrophobic, saturated 12-carbon tail and a sulfate head group (and sodium as a counterion) (Clark, 2005). When proteins are treated with SDS, the hydrocarbon tail binds to the polypeptides via the polypeptide backbones, leaving the sulfate head groups to interact with water. This interaction disrupts the secondary and tertiary structure of the proteins and they will denature. Approximately one SDS molecule will bind for every two amino acid residues, so the negatively charged dodecyl sulfate molecules can completely shield the charge of protein. While the overall charge will be roughly proportional to protein size, the charge to mass ratio will be the same for large versus small proteins (Figure 51.1). As a result of roughly equivalent charge concentrations, electrophoresis can be used to separate mixed samples of proteins based on size. Comparing the resulting bands to a set of standards will yield the approximate molecular weights of the proteins in a sample.

It is relatively easy to treat proteins with SDS. First, a 2× sample buffer—composed of 0.92 g SDS, 2 mL β-mercaptoethanol, 4.0 g glycerol, 0.3 g Tris, and 2 mL bromophenol blue (0.1% w/v in water)

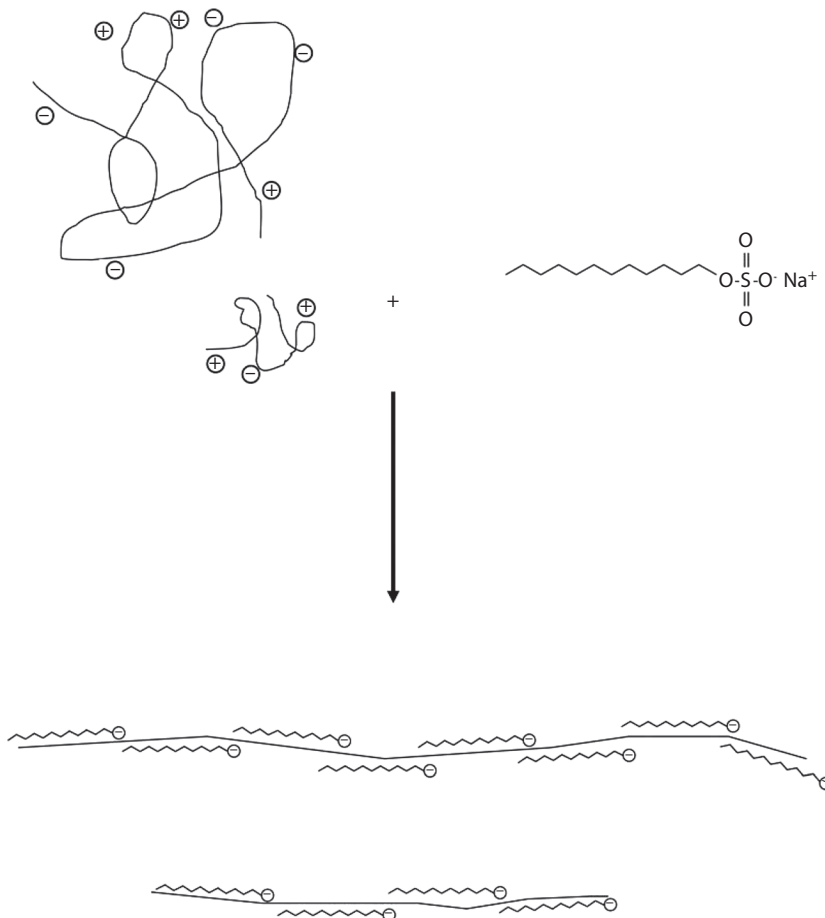


FIGURE 51.1 The action of SDS on proteins. Proteins in solution will fold and carry charges dependently upon their primary amino acid sequences. In the presence of SDS, they will denature and carry a uniform coating of negative charges. The charges of the amino acid side chains will be masked by the SDS. This example shows SDS molecules interacting with two proteins of different net charge and differing in mass by approximately twofold. The end result is two polypeptides with equal charge-to-mass ratios that can be separated by PAGE according to size.

in water to 20 mL total volume, with pH adjusted to 6.8 with HCl—is mixed with the protein sample at 1:1 buffer to sample (Walker, 1994). The β -mercaptoethanol is a reducing agent used to break any disulfide bonds within the proteins. Glycerol is used to increase the sample density, and bromophenol blue is used to aid with the visualization process during electrophoresis. Tris is used to buffer the pH of the mixture. The solution is then boiled for two minutes to completely denature the proteins. After the sample is cooled, it can then be placed into the wells of a polyacrylamide gel for electrophoresis.

51.3 Restriction Enzymes

51.3.1 Introduction to the Technique

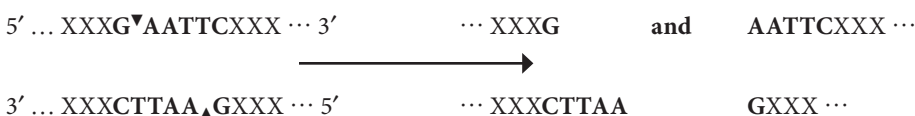
Restriction enzymes are bacterial endonucleases that get their name from the early finding that they restrict the propagation of bacteriophages on culture plates. Their native function is to cut dsDNA, such as what may be transduced into a bacterium by a bacteriophage, via the recognition of specific DNA sequences. Since the first restriction enzyme was isolated at 1968 (Menninger et al., 1968) this class of enzymes has been one of the most significant tools in molecular biology and has allowed the development of recombinant DNA technology. Custom stretches of DNA, such as engineered plasmids with bio-active promoter or exon sequences, can be formed though the cutting of target fragments from genomic or plasmid DNA followed by fragment transfer into a gene vector (a process that utilizes additional enzymes such as the Klenow fragment or DNA ligase). Another application of restriction enzymes is in verifying plasmid identities through affirmation of specific base sequences within the plasmids, and the distance between such sequences via the lengths of fragments that are generated by the cuts. In brief, restriction enzymes are indispensable tools for modern gene engineering.

There is a systematic way in which restriction enzymes are named (Smith and Nathans, 1973). The first three letters are in italics, and represent the genus and species names of the host bacterium. A nonitalicized letter may appear next, representing the particular strain from which the isolate was purified. The name will end with a roman numeral to indicate the order of discovery for multiple restriction enzymes arising from the same bacterium. For example, *EcoRI* was isolated from *Escherichia coli* RY13, while *HindIII* was isolated from *Haemophilus influenzae* strain **d**, and was the third enzyme isolated from this strain. (Note that the strain for *HindIII* can be found in older publications listed as Rd. The “R” is part of an R–M system, which denotes **R**estriction endonuclease versus **M**odification enzymes. The R and M strain designations are routinely dropped.)

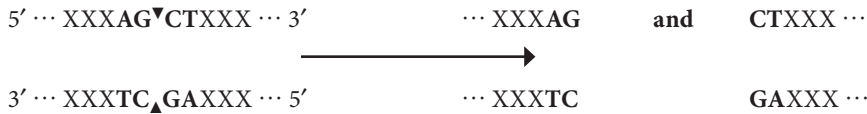
Restriction enzymes can be classified into three types, type I, II, or III, based on their enzymology and cofactor requirements (Wilson, 1988). Because types I and III cut DNA variably or with low efficiency, they are not typically used for genetic engineering. Type II enzymes can reproducibly and efficiently cleave specific nucleotide sequences (“restriction sites”), making them the most reliable set of restriction enzymes for DNA manipulation.

Type II restriction enzymes typically have two similar subunits that can recognize and cleave DNA in the presence of the cofactor Mg^{2+} (Pingoud and Jeltsch, 2001). The enzyme initially binds to the DNA recognition site directly or will bind randomly to the DNA and then linearly diffuse to the recognition site. Once at the recognition site, the conformation of the enzyme would change to allow for catalysis of the digestion reaction. After strand cleavage, the enzyme detaches from the DNA molecule or moves on to another recognition site on the same dsDNA (Pingoud and Jeltsch, 2001).

A restriction enzyme can produce one of two types of cuts: sticky or blunt. A sticky cut produces sticky ends, or two DNA overhangs that are complimentary to one another. *EcoRI* produces sticky ends as follows (triangles indicate cleavage points):



Blunt ends result when the DNA cuts are at the same position on both sides of the double strand. For example, an AluI cut would produce two blunt ends as follows:



Regardless of whether a blunt or sticky cut has been made, there will be a phosphate group on the 5' end and a hydroxyl group on the 3' end of each strands. This is important for ligation purposes. In general, sticky ends are easier to insert and ligate than are blunt ends.

51.3.2 Technical Considerations

It is a relatively simple matter to use restriction enzymes to cut DNA. All that is required is a suitable buffer (supplied by the company that provides the enzyme), any required cofactors for the enzyme being used (such as bovine serum albumin), some DNA, and the appropriate temperature for incubation of the reaction. In determining the correct amount of enzyme to use for a particular reaction, one should be aware of enzyme activity, which is reported as “units” of enzyme. One unit of commercial restriction enzyme is typically defined as the amount of enzyme needed to digest 1 μg of λ DNA in 1 h at optimal temperature (usually 37°C) in a total reaction volume of 50 μL (New England Biolabs, 2009a). As an example, if the restriction enzyme is supplied in glycerol at a concentration of 20,000 U/mL and one wishes to digest 1 μg of DNA, 0.05 μL of restriction enzyme would work for the particular reaction. However, measuring 0.05 μL of solution is impractical, so 0.5 μL is often used instead. While one could dilute the enzyme stock solution, this practice generally yields poor results and is not recommended.

A typical endonuclease digestion reaction takes place in 10 μL total volume. Volumes for the reaction are given below, in the order in which the reaction solution is mixed:

10.0 – Σ (all other reagents) μL	water
1.0 μL	10 \times buffer
x μL	10 \times additives (such as bovine serum albumin). $x = 0.0$ or 1.0
y μL	DNA, 1 μg (although 0.1 μg may be enough to faintly visualize large fragments)
0.5 μL	enzyme 1
(0.5 μL)	enzyme 2, if used)
10.0 μL	total volume

51.4 Other DNA Modification Enzymes

Restriction enzymes are often used for the construction of engineered plasmids. At this point in the chapter it might be useful to mention other enzymes that are commonly used for DNA manipulation, namely DNA ligase, blunting enzymes, and calf intestinal phosphatase.

51.4.1 DNA Ligase

51.4.1.1 Introduction to the Technique

For plasmid construction, simply putting two fragments with sticky ends together is not enough. There will still be a gap in the phosphodeoxyribose backbone unless steps are taken to conjugate the free 3' hydroxyl of one fragment with the 5' phosphate group of the next (Figure 51.2). This can be accomplished using a DNA ligase. T4 DNA ligase, isolated from bacteriophage T4-infected *Escherichia coli*, is a convenient choice for this purpose. It can catalyze the conjugation of the two end groups into a single

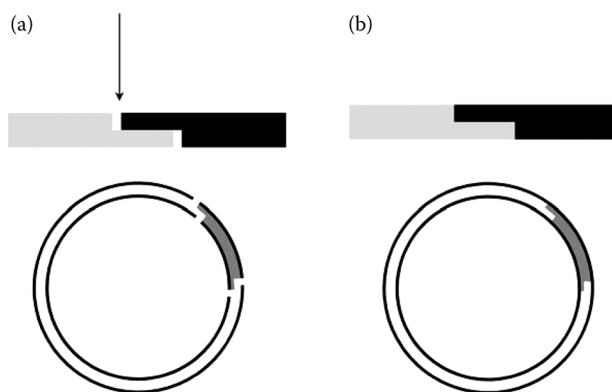


FIGURE 51.2 An overview of DNA ligase. (a) Although DNA fragments with sticky ends can fit like a puzzle piece into a vector with complimentary sticky ends, the plasmids cannot be replicated because of the molecular gaps between the two pieces. (b) DNA ligase seals the molecular gaps by creation of new phosphodiester bonds. Top—two DNA fragments with complimentary 5′ overhangs. The arrow indicates a discontinuous gap in the DNA backbone. Bottom—a larger view, showing the interaction of an insert with a plasmid vector.

phosphodiester bond (Figure 51.3). Blunt ends can also be recombined by T4 DNA ligase, but the efficiency of ligation is much lower than for sticky end ligation.

51.4.1.2 Technical Considerations

The ligation reaction takes place by mixing reaction buffer, the DNA to be ligated, and an appropriate amount of enzyme, and incubating at 16°C for 4–16 h (Sambrook and Russell, 2001). A 10× reaction buffer is supplied with commercial T4 DNA ligases. To determine the appropriate amount of enzyme, use the definition of one unit: the amount of DNA ligase needed to ligate 50% of HindIII fragments of λ DNA with a 5′ DNA termini concentration of 0.12 μM (300 $\mu\text{g}/\text{mL}$) in a 20 μL reaction volume in 30 min at 16°C using 1× T4 DNA ligase reaction buffer (New England Biolabs, 2009b). Thus the required amount of enzyme depends on the DNA content in the sample.

Following is a typical ligation reaction setup (Sambrook and Russell, 2001, New England Biolabs, 2009b):

10.0 – Σ (all other reagents) μL	water
1.0 μL	10 × T4 DNA ligase reaction buffer
x μL	vector DNA
y μL	insert DNA
1 μL	T4 DNA ligase (400,000 cohesive end units/ml)
10.0 μL total volume	

Note that the total concentration of vector plus insert should be 1–10 $\mu\text{g}/\text{mL}$.

51.4.2 Blunting Enzymes

51.4.2.1 Introduction to the Technique

Sometimes it is necessary to ligate fragments that do not have complementary base pair overhangs (the sticky ends do not match up). In this case T4 DNA ligase cannot be used for ligation because the fragments will not be held in close proximity to one another by hydrogen bonds. However, the fragments can be made to have blunt ends via the DNA polymerase activity or the exonuclease activity of either the Klenow fragment or T4 DNA polymerase.

The Klenow fragment is the large proteolytic fragment of *E. coli* DNA polymerase. This enzyme has 5′ to 3′ polymerization and 3′ to 5′ exonuclease activities, which are important to note with respect to the

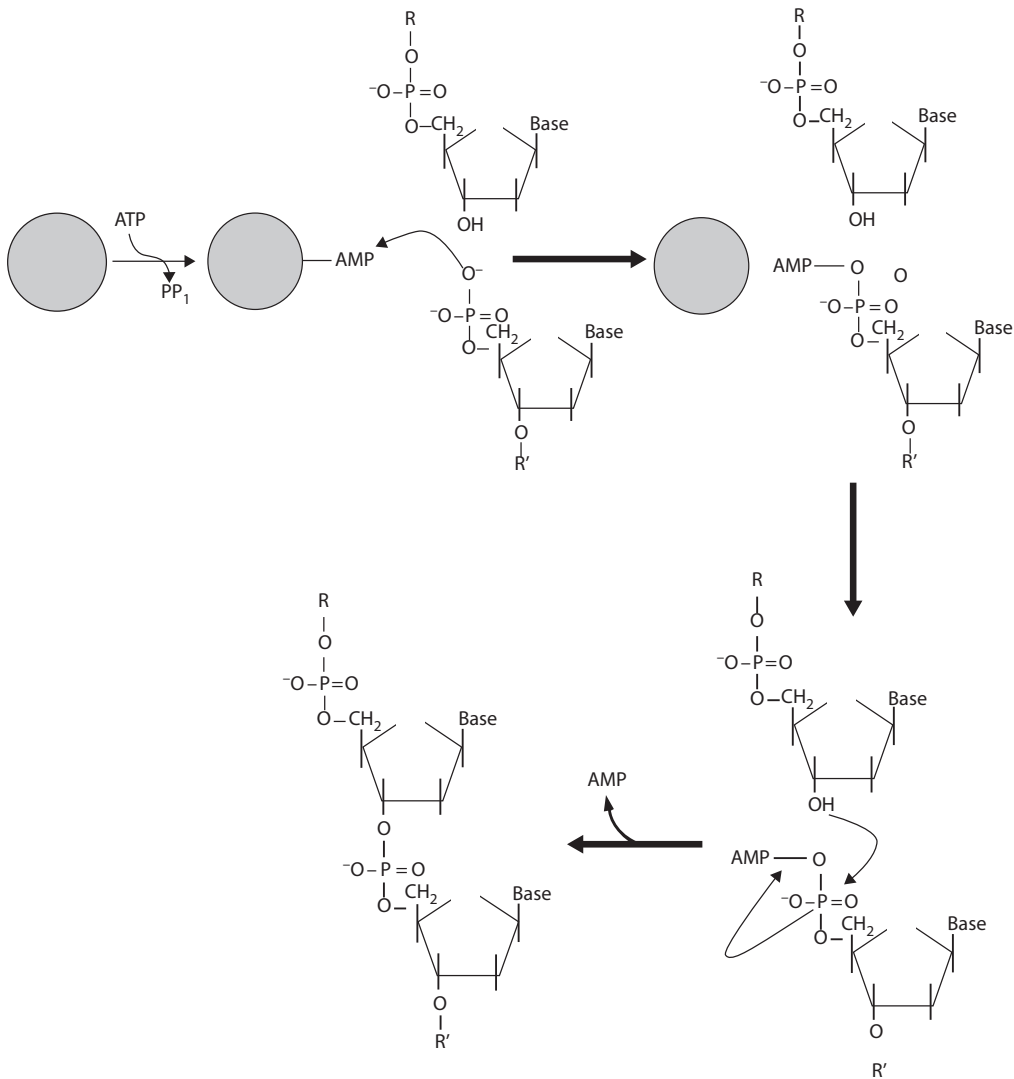


FIGURE 51.3 The mechanism of DNA ligase. After being activated by the addition of an AMP molecule by cleavage of an ATP, DNA ligase catalyzes attachment of a phosphate on a 5' DNA terminus to the phosphate of AMP, followed by the transfer of the terminal phosphate to the hydroxyl of a 3' DNA terminus and the release of the AMP molecule.

type of overhang the DNA fragment of interest has (Steitz, 1993). The Klenow fragment can utilize dNTPs to complementarily fill in the gap of a 5' overhang to form a blunt end (Sambrook and Russell, 2001). Although the Klenow fragment also has 3' to 5' exonuclease activity, it is not recommended for blunting 3' overhangs because of lower reaction efficiency (Sambrook and Russell, 2001). Versions of the enzyme are available that have lost their 3' to 5' exonuclease activity altogether (Derbyshire et al., 1988).

To make blunt ends out of DNA fragments having 3' overhangs, T4 DNA polymerase is recommended. T4 DNA polymerase is an enzyme isolated from bacteriophage T4-infected *E. coli*. Like the Klenow fragment, it also has 5' to 3' polymerization and 3' to 5' exonuclease activities (Sambrook and Russell, 2001). However, the activity of 3' to 5' exonuclease is 200-fold greater than that of the Klenow fragment.

After treatment with the Klenow fragment or T4 DNA polymerase, the resulting blunt-ended fragments can be cloned into an open blunt-ended vector using T4 DNA ligase.

51.4.2.2 Technical Considerations

Klenow Fragment (Sambrook and Russell, 2001)		T4 DNA Polymerase (Brown, 2000)	
Water	× μL	Water	× μL
10× buffer	2.5 μL	10 × buffer	2.5 μL
DNA	1 μg	DNA	1 μg
dNTP	133 μM final conc. ^a	BSA	1.25 μL 10× restriction enz.
Enzyme	1.0 μL	dNTP	100 μM final conc. ^b
Total	25 μL	Enzyme	1.0 μL
		Total	25 μL
Incubate 15 min at room temperature		Incubate 15–30 min at 15°C	

^a 133 μM final concentration = 1.66 μL of 2 mM dNTP

^b 100 μM final concentration = 1.25 μL of 2 mM dNTP

51.4.3 Calf Intestinal Phosphatase

51.4.3.1 Introduction to the Technique

Calf intestinal alkaline phosphatase (CIP) is a dimeric metalloenzyme whose function in genetic engineering is to dephosphorylate the 5' end of a plasmid vector after a restriction cut to prevent the plasmid from being ligated without a DNA insert (Eun, 1996). The DNA fragment to be inserted into the plasmid will not be exposed to CIP to preserve its 5' phosphate groups. The result of combining the unmodified insert with the dephosphorylated vector is that ligation will produce only vector-insert combinations, thus easing the burden of screening for plasmids containing the inserted DNA in subsequent steps.

51.4.3.2 Technical Considerations

CIP is a powerful enzyme, and many molecular biologists will avoid using it because it is hard to deactivate or remove completely from reaction mixtures, which would have a deleterious effect on subsequent ligation efforts. Others might suggest that the amount of enzyme needed is so small that simply dipping a pipette tip into stock enzyme solution will usually transfer enough enzyme for the reaction to take place. Incubation of a heat-killed restriction cut or blunting reaction mixture for 60 min at 37°C could suffice, with purification via gel electrophoresis, phenol extraction, or spin column taking place immediately after the incubation.

A more formal method of using CIP has the reaction mixture incubated in a two-step manner. The amount of enzyme and reaction time will depend on the amount and type of fragment end that is produced by restriction cutting. Details are given in the following table (Sambrook and Russell, 2001):

Terminus Type	Amount of CIP per Mole DNA Ends	Reaction Times and Temperatures
5'-overhang	0.01 unit	37°C for 30 min, then 37°C for 30 min ^a
3'-overhang	0.1–0.5 unit	37°C 15 min, then 55°C 45 min
Blunt end	0.1–0.5 unit	37°C 15 min, then 55°C 45 min

^a The procedure is to add the given amount of enzyme and incubate at the first time and temperature shown, then to add an additional aliquot of the same amount of enzyme and incubate at the second time and temperature.

After the final incubation, the enzyme should be inactivated or removed (or both). Inactivation can occur by heating the solution to 65°C for 30 min, or to 75°C for 10 min (Sambrook and Russell, 2001). Commercially available purification kits can be used to remove the enzyme and salts from the DNA solution.

51.5 The Polymerase Chain Reaction

51.5.1 The Traditional Polymerase Chain Reaction

51.5.1.1 Introduction to the Technique

The polymerase chain reaction (PCR) is a means to amplify a given stretch of nucleotides to determine their relative concentration in different cell samples, or to produce usable quantities of a sequence of nucleotides for DNA cloning. The technique allows for the amplification of a few copies (in theory, only one copy is needed) of a specific piece of DNA into perhaps billions of copies in a relatively short time. The procedure is relatively inexpensive, requiring only a thermocycler and the appropriate enzymes and reagents for processing. The first description of PCR was published in 1985 (Saiki et al., 1985), and has proven to be such an important technique that the Nobel Prize in 1993 was awarded to Kary Banks Mullis for its discovery.

PCR is an enzymatic process that is repeated over multiple cycles. The enzyme can be one of many commercially available versions of DNA polymerase, and it is used to catalyze the synthesis of a DNA sequence complementary to a single-stranded template to yield a double-stranded DNA fragment composed of the original DNA template plus the newly synthesized strand. Double-stranded DNA is required for DNA polymerase to bind to and commence synthesis of the complementary strand. This double-stranded region is provided by the binding of short (~20 base) primers to the single-stranded DNA template. The primers also give specificity to PCR because they are designed to bind only in regions flanking the particular DNA sequence of interest.

51.5.1.2 Technical Considerations

51.5.1.2.1 Cycle Parameters

One cycle of this traditional form of PCR contains three steps: denaturation, annealing, and elongation. Each of the three PCR steps takes place under a different temperature for specific reasons, as outlined below.

Denature: This step is performed at 90–98°C to separate dsDNA into single-stranded chains (ssDNA) (Saiki et al., 1988). Heating allows the DNA duplexes to melt through the dissociation of the hydrogen bond between the complementary bases in each strand. It is important to keep the temperature high in this step to prevent re-association of the strands, but it must be kept below 100°C to prevent the removal of water molecules from the DNA.

Anneal: The goal of this step is to permit association of the primers with the ssDNA fragments. The temperature used for this step is critical to the PCR process, and varies with the base composition of the dsDNA sequence being amplified. If the temperature is too low, the ssDNA fragments will reassociate and not be amplified. If the temperature is too high, then there will be too much energy in the system to allow for hydrogen bonding to hold primer and template strands together. There is a relatively small temperature range whereby the ssDNA fragments will associate with the primers preferentially over their complementary (and longer) ssDNA counterparts, typically 50–65°C. However, even this range is not exact enough because temperatures slightly too low will allow association of primers to sequences of DNA in a less-specific fashion (termed “nonspecific binding”), which will result in the amplification of unwanted DNA sequences. The optimal temperature for annealing can be determined by the following formula (Rychlik et al., 1990):

$$T_a = 0.3 \cdot T_m(\text{primer}) + 0.7 \cdot T_m(\text{product}) - 14.9,$$

where

T_a = annealing temperature, and

T_m = melting temperature of the primers or product, defined as the temperature at which 50% of the oligonucleotides and the associated complimentary strand are in duplex. T_m can be calculated by:

For short sequences (≤ 20 bases), such as primers,

$$T_m = 2(A + T) + 4(G + C),$$

where A , T , G , and C are the number of adenine, thymine, guanine, and cytosine bases in the sequence, respectively (Marmur and Doty, 1962).

For longer sequences, such as amplicons,

$$T_m = 81.5 + 16.6(\log M) + 0.41(\%G + \%C) - 0.63(\%formamide) - \left(\frac{600}{n}\right),$$

where M = the concentration of monovalent cations (such as Na^+ and K^+), $\%G$ and $\%C$ are the mole fractions of guanine and cytosine, respectively, $\%formamide$ = the percentage of formamide in the solution, and n = the number of nucleotides in the sequence (Newton and Graham, 1997).

Extend: This step allows the DNA polymerase to create a complimentary fragment to the template strand, yielding a dsDNA fragment with “new” DNA bases. Since the original dsDNA was separated into two ssDNA chains using the double-stranded primer/template pair as a primer, the net result will be twice as many dsDNA fragments of interest, with each fragment containing a newly synthesized DNA polymer. The extension step is carried out at the optimal temperature for the DNA polymerase being used. For instance, 72°C would be used for Taq DNA polymerase (Sambrook and Russell, 2001), because this is the temperature at which the parent organism, *Thermus aquaticus*, lives.

Theoretically, the number of fragments of the target DNA is doubled after each cycle, which implies an exponential relation between the number of cycles and the amount of PCR product. For instance, after 30 PCR cycles one could theoretically obtain up to 2^{30} copies of the target DNA sequence. This does not mean that one could easily perform 100 cycles of PCR to obtain 2^{100} copies of the original fragment. DNA polymerase uses deoxyribonucleotide triphosphates (dNTPs) as high-energy monomers for building the polymeric DNA copies, and the amount of starting materials required are infeasible due, in part, to the osmolarity of the solution that would contain them (or the cost of the system that would require greater volumes or reagents and enzyme).

51.5.1.2.2 Primer Design

Primers are the main determinant of PCR specificity, so great care must be taken for their proper design. There exist many computer programs, both free and for purchase, that were written to assist with the task of primers design. Outputs generally list many possibilities for primer sets so the investigator must be prepared to analyze the results for proper selection. Following are some guidelines to aid with selecting successful and unique primer sets (McPherson and Hames, 1995, Pelt-Verkuil et al., 2008, Newton and Graham, 1997):

1. Primers lengths should be in the range of 18 and 30 nucleotides. Shorter primers could decrease the specificity of the PCR and therefore cause amplification of sequences that are not of interest. Primers that are too long will require higher annealing temperatures, which could affect DNA polymerase activity during elongation.
2. The sequences of primer sets should not be complementary, which would lead to the self-annealing of primers into structures known as primer-dimers. Primer-dimers cannot bind to template DNA strands and are therefore useless for PCR.

3. One should avoid having complementary regions in any individual primer, otherwise hairpin structures could form within the primer itself.
4. Regions of repeated bases should be avoided, such as CCCCC or TTTTT. Such sequences are prone to mismatching.
5. The annealing temperatures of the two primers in a set should be roughly the same (within 5°C of each other).

51.5.2 Real-Time Quantitative PCR

As a cornerstone of modern molecular biology techniques, the polymerase chain reaction has undergone persistent development during the past 20 years. The advent of real-time quantitative PCR has brought the potential of the PCR into full play, allowing a shift from qualitative to quantitative analyses. It can measure the starting concentration of DNA, cDNA, or RNA templates. As opposed to traditional PCR, the process of real-time PCR is monitored via fluorescence readings once per replication cycle to allow for direct measurements of PCR amplifications without the need for postprocessing.

51.5.2.1 Introduction to the Technique

The introduction of fluorescent chemistries into reaction systems has made it possible to detect PCR product concentration through its relation to fluorescence intensity. The fluorescent chemistries that are used in real-time quantitative PCR will be introduced in detail later. First, a discussion of the DNA amplification process is needed to acquire a basic understanding of the principles underlying PCR.

The curve of DNA concentration versus cycle number typically has four distinct regions, termed the linear, early exponential, exponential, and plateau phases (Wong and Medrano, 2005). In the beginning of the process (generally the first 5 or 10 cycles), the amount of PCR product is insufficient to yield fluorescence emission above the background level. Baseline fluorescence is calculated at this stage. Upon entering the early exponential phase, the accumulated fluorescence intensity has increased to a level that exceeds background levels—ordinarily 10 times the standard deviation of the background levels observed. At this point the target (amplicon) can be reliably detected. The PCR cycle number at which the observed fluorescence first exceeds this value is referred to as the cycle threshold (C_t). The C_t value is what is used for subsequent calculations of relative and quantitative DNA or RNA concentrations.

In the exponential phase, the number of DNA copies increases exponentially under ideal reaction conditions. As the reaction cycles continue to increase, reagents are used and the efficiency of template amplification decreases. Amplification fails to occur in an exponential way, and the PCR enters into the plateau stage. Since it is the C_t value that will be used for analyses, log-linear and plateau data serve as little more than confirmation that the amplification process proceeded in a standard way.

In traditional PCR, the amplified target is detected by postprocessing that includes gel electrophoresis. Real-time PCR produces more reliable results than the traditional method because the error-generating steps of postprocessing are not performed. In addition, obtaining C_t data from the early exponential phase is associated with less variance than data obtained at the end of the exponential phase. Another advantage of real-time PCR is that it is not plagued by the problem of determining whether data from different samples were gathered from different phases of the amplification curve (where plateau values for all samples may be equal if the number of cycles used is high enough). Studies have supported the theoretical statement that the C_t value has a linear relation to the logarithm of the original DNA template concentration (Hilario and Mackay, 2007).

If one were to start with a greater amount of target DNA, a significant increase in fluorescence signal will appear more quickly, which would be reflected by a lower C_t value. The curve of fluorescence intensity versus cycle number for standard samples of known concentrations can be used to generate data that can be used to determine the starting concentrations of unknown samples. This technique is termed real-time quantitative PCR, or qPCR.

51.5.2.2 Fluorescence Chemistries

In the early stage of real-time qPCR development, sequence-unspecific detection based on DNA binding dyes like SYBR green was widely applied. SYBR green is a DNA-intercalating dye that dramatically increases in fluorescence when associated with dsDNA. During the PCR reaction set, as cycle number increases so does the accumulation of dsDNA, so there is more dsDNA around to bind the dye to make it fluorescent. Fluorescence intensity correlates with dsDNA concentration and will therefore increase proportionally with DNA amplification. This technique is useful for detecting the amplification of any dsDNA without designing probes (discussed below) so it is convenient and economical. However, dyes can also bind nonspecifically to any dsDNA such as primer dimers to possibly yield false-positive signals. To resolve this problem, dissociation curve analysis must be performed to address the possible presence of multiple PCR products via the number of first-derivative melting peaks (Osborn and Smith, 2005).

The technique that uses hydrolysis probes is an indirect means to detect PCR products. A pair of primers (the same primers as can be designed and used for the Traditional PCR method described earlier) is added to the system along with a sequence-specific probe—designed to bind between the two primers—that is labeled with a reporter dye on the 5′ end and a quencher dye on the 3′ end. Before the probe unfolds and binds to its DNA target sequence, the light energy emitted by the reporter can be absorbed by the quencher group, thus reducing observable reporter fluorescence intensity. However, after the probe has bound to its complimentary sequence on the target DNA strand, the extension step of PCR will utilize the 5′ to 3′ nuclease activity of the DNA polymerase and the probe will be degraded, thus releasing the nucleotides holding the reporter and quencher groups and separating the fluorophore from its quencher. Unshielded by the quencher dye, more of the emitted fluorescence signal can be observed. Every time a DNA strand is amplified a fluorescent molecule is released, so PCR product formation can be inferred through fluorescence. An advantage of this technique is that multiple probes, with different fluorophore/quencher pairs, can be used in the same tube to detect multiple DNA sequences in the same sample.

The molecular beacon technique also utilizes probes for hybridization. The beacons are comprised of a sequence-specific region flanked by two inverted repeats that will hybridize with each other to form a hairpin structure. They contain a fluorophore and a quencher that act as a fluorescence resonance energy transfer (FRET) pair. When the molecular beacon is in a hairpin structure the fluorophore and quencher that are bound to each end of the molecule will result in a reduction of fluorescence intensity via FRET. When the complementary sequence becomes exposed on the ssDNA molecule to be amplified after the melting step of PCR, the beacon will hybridize with the target DNA and transform into an open structure that includes the separation of the reporter and quencher. Reporter emission will then occur without energy transfer to the quencher. The molecular beacon probes have greater specificity than the hydrolysis probes mentioned above because of the presence of the complimentary flanking sequences that are used to form hairpins. This yields a situation where, thermodynamically, the probe bound to the ssDNA target complex must be more stable than probe bound to itself to form the hairpin for the hybridization to occur (Wong and Medrano, 2005).

Evolving from molecular beacons, fluorescence-labeled primers link both the PCR primer and detection mechanism together in the same molecule, thus allowing the fluorophore to directly appear in PCR products. Scorpion primers are one type of such primers. They are composed of a reporter dye on the 5′ end, internal complementary sequences for forming a hairpin loop, a quencher dye, a DNA-polymerase-blocker, and a primer complimentary to the DNA target sequence on the 3′ end (Figure 51.4a). Initially, the primer portion of the Scorpion probe binds to the target template and chain extension takes place. Then the probe transforms from a hairpin loop structure to an open structure after exposure to a second heat denaturing step, and the newly exposed bases on the probe are able to hybridize with the newly synthesized DNA after the extension step (Figure 51.4b through c) (Thelwell et al., 2000). The fluorophore, being on the 5′ end of the probe, is relocated to the far end of the probe–new DNA hybrid as the hairpin

denatures and the 5' end of the probe binds with the 3' end of the new DNA (Figure 51.4d). With the reporter molecule being far removed from the quencher molecule, fluorescence will be readily detectable. This unimolecular fluorescent chemistry has the advantage of rapid detection with fewer molecules versus methods utilizing primer-probe sets.

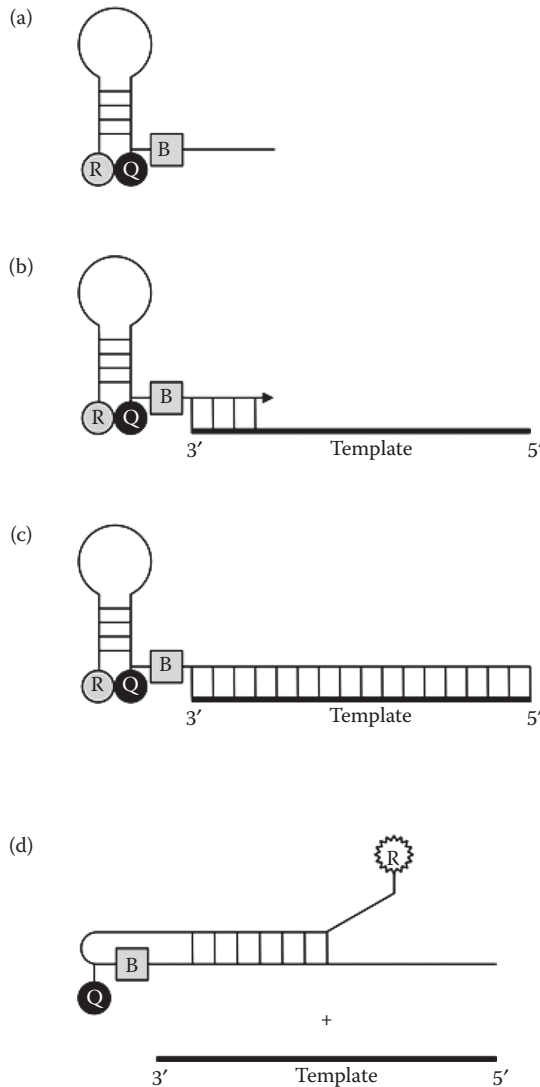


FIGURE 51.4 Scorpion primers. (a) Scorpion primers contain a reporter dye (R) on the 5' end, internal complementary sequences for forming a hairpin loop, a quencher dye (Q), a DNA-polymerase-blocker (B), and a primer complementary to the DNA target sequence on the 3' end of the primer. (b) The primer binds to the target DNA sequence via the 3' primer sequence. (c) DNA polymerase extends the primer to make a new sequence complementary to the DNA template. (d) After heating and denaturation, the scorpion primer is released from the DNA template and denatures to lose its hairpin structure. The internal sequence is free to bond with the new DNA bases, thus separating the reporter and the quencher and yielding an increase in detectable reporter fluorescence.

51.5.2.3 Technical Considerations

As with the traditional PCR method, real-time PCR also utilizes the repeated three steps of denature, anneal, and extend. The technical considerations presented earlier are also valid for this PCR method. However, there are differences between the two methods, which are noted below.

Fluorescent probes or DNA intercalating dyes are used in real-time PCR because an assessment of DNA concentration is made during each cycle via fluorescence intensity. As a result, primer design is slightly more complicated than that for traditional PCR. In particular, more attention must be paid to the possible secondary structures that the primers and probes can form, such as hairpins or primer-dimers. These structures are of especial concern when SYBR Green-based qPCR is being used, since short dsDNA fragments will result which will be detected by the intercalating dye.

The optimal amplicon size for real-time PCR is in the range of 50–150 base pairs. A larger target, in particular greater than 300 base pairs, will result in a delayed emergence of the C_t . Concerning probe design, the melting temperature of the probe is recommended to be 10°C higher than that of the primer set to obtain a priority for probe binding to the target. The probe should bind on the same strand and somewhat close to one of the primers to allow for detectible changes to the fluorescent signal soon after extension begins (Pestana et al., 2009).

Real-time PCR also requires a more complex thermocycler than does traditional PCR because a light source and a fluorescence detection system are required. Adding to the expense of real-time PCR are the costs of SYBR green or labeled primer/probe sets, a computer, and an analytical software package.

51.5.2.4 Quantification

There are two strategies for template quantification in real-time qPCR: absolute and relative. In the absolute quantification method, the amplification signal is associated with DNA copy number by employing a calibration curve (Pestana et al., 2009). A series of diluted standards of known concentrations, determined by light absorption at 260 nm using a spectrophotometer, are prepared and used to obtain the calibration curve (Walker and Rapley, 2009). The standards should be the same material as the samples of unknown concentration. Samples concentrations can be determined via matching their C_t values against the calibration curve. In absolute quantification it is assumed that all standards and samples have equal amplification efficiencies. Taking into account the difficulty related to preparing reliable standards for quantification, the absolute quantification strategy requires considerable effort. It is highly recommended that a fresh calibration curve is generated for each experiment, especially in cases where data are collected and compared on different days or in different laboratories.

In the relative quantification method, a calibrator is utilized to measure the relative change of samples in gene expression. The calibrator can be an endogenous control, an exogenous control, or a reference gene (Dorak, 2006).

When a standard curve is used for relative quantification, the sample quantities are calculated based on the standard curve and then reported as n -fold differences relative to the calibrator (which is defined as 1-fold). This method can be employed even though the amplification efficiencies of the calibrator and target genes may not be equal (Wong and Medrano, 2005). An endogenous control—typically a house-keeping gene such as β -actin, GAPDH, or 18s rRNA—is routinely introduced and amplified along with the gene of interest.

The comparative C_t method, another popular method of relative quantification, makes use of mathematical equations to calculate the relative differences between samples and the reference gene (Schmittgen and Livak, 2008). The values of C_t obtained in the early-exponential phase of PCR can reflect the amounts of the initial templates. Various models may take nonideal PCR efficiencies into account, but assume equal amplification kinetics for both the gene of interest and the reference gene. A standard curve is not required in this method, so it is a convenient way of testing a great number of samples. A variety of relative quantification methods have been proposed in recent years for the purpose of improving the accuracy of PCR product quantification, including those put forth by Pfaffl (2001),

Godbey et al. (2008), and Liu and Saint (2002), plus other models termed Amplification plot (Peirson et al., 2003), and Q-gene (Muller et al., 2002).

Real-time PCR has multiple advantages, including high sensitivity, great specificity, good reproducibility, and a wide dynamic quantification range (Dorak, 2006). In consideration of these advantages, the method is viewed as one of the most popular molecular biological techniques for analytical and quantitative study.

51.6 Blotting

51.6.1 The Southern Blot

51.6.1.1 Introduction to the Technique

The Southern blot is a useful technique for determining the presence of a specific sequence in DNA samples. While it is not used much for tissue engineering, the fundamental principle of separating a sample and then hybridizing a probe to a specific sequence is common to other blots that are useful to the tissue engineer. This technique is presented before the other blots for historical perspective.

The Southern blot is a basic molecular biological technique that was invented by the British biologist Edwin Mellor Southern in 1975 (Southern, 1975). It has been applied extensively for the detection of major gene arrangements, thus playing an important role in DNA chromatographic analysis, diagnosis of genetic diseases, and the analysis of PCR products.

51.6.1.2 Technical Considerations (Southern, 1975, Hoy, 2003)

1. *Preparation of sample:* DNA Genomic DNA is extracted directly from animal cells or tissues. The DNA obtained will be too long to be used in hybridization analyses, so the sample should be digested by restriction endonucleases into a series of smaller fragments.
2. *Gel electrophoresis:* Agarose gel electrophoresis is used to separate DNA fragments from step 1 by size. Fragments that have the same size will occupy the same band within the gel. The molecular weights of different fragments can be determined based on DNA molecular weight standards that are introduced into the gel adjacent to the sample.
3. *Pretreatment:* Before the DNA is transferred from the gel onto the blotting membrane, it is important to process the separated DNA beforehand because of the amount of time required to completely transfer DNA fragments. It takes much longer for fragments in excess of 10 kilobase pairs (kbp) to be transferred than small fragments (<1 kbp). When there are DNA fragments larger than 10 kbp, the gel should be treated with dilute HCl to depurinate the large fragments and break them into small pieces (Slater, 1986).

During steps 1 and 2, the DNA in the sample maintains a double-stranded configuration. However, single-stranded DNA is required for hybridization. To denature dsDNA into ssDNA, the gel is incubated with an alkaline solution (commonly sodium hydroxide), followed by neutralization via a buffer. After denaturing, binding between the negatively charged DNA and the positively charged membrane in step 4 will be enhanced. In addition, any residual RNA that may exist in the DNA sample will be hydrolyzed.

4. *Transfer:* The material used for the transfer membrane is an important factor for retaining DNA following transfer. Nitrocellulose was the first material to be used for nucleic acid blots. Buffers with high ionic strength are indispensable for the binding of nucleic acids to these membranes because nitrocellulose interacts with nucleic acids via hydrophobic interactions. As such, nitrocellulose does not have a strong affinity for nucleic acids, so DNA can easily dissolve into solution (particularly the small fragments). Nitrocellulose membranes are also quite brittle when dry, which complicates the procedure further. An alternative to the nitrocellulose membrane is the nylon membrane, which has stronger DNA binding capability than nitrocellulose because it

interacts with DNA via charge–charge interactions (Avison, 2007). Furthermore, it can be reused for detection of different nucleic acids sequences without preparing a new sample. The probe previously used is rinsed at high temperature and a different probe is later introduced to detect another sequence.

A large filter paper is soaked in saline–sodium citrate buffer (0.15 M NaCl, 0.015 M sodium citrate) and placed on a glass or plastic support. The gel strip is laid on top of the wet paper and covered by a sheet of nitrocellulose or nylon membrane. Many layers of dry filter paper (or paper towels) are placed on top of the membrane. Capillary action causes the movement of buffer through the membrane to the dry paper. The DNA fragments are carried along with the buffer, but the fragments are deposited on the membrane through the interactions just mentioned.

Electrophoretic transfer is also an effective strategy for performing the blotting procedure, and is especially suited for transferring large DNA fragments. One must keep in mind that the ionic strength of buffer is related to its conductance, so the buffer composition has an influence on electrophoretic transfer efficiency and the binding ability with membrane (Butler, 1991). A vacuum pump can also be used to facilitate the blot transfer. No matter which method is applied, the separation pattern of the DNA fragments is preserved as they travel from the gel to the membrane.

The membrane is next baked in an oven, placed in a vacuum or exposed to ultraviolet light to strengthen the attachment of the DNA that has been transferred.

5. *Pre-hybridization*: The membrane used to trap the restriction fragments can also bind the probe, which is also made from DNA. The membrane is therefore soaked in pre-hybridization solution containing salmon or herring sperm DNA to nonspecifically block all remaining DNA-binding sites on the membrane. The blocking DNAs are heterogenic with mammalian DNA, so they will not bind with the hybridization probe.
6. *Southern hybridization*: The labeled DNA probe should be denatured via heating to transform it into a ssDNA structure, then used to wash the filter membrane. If the sample DNA contains a sequence complementary to that of the probe, the probe will bind to the sample DNA. Hybridization is carried out in a salt buffer with comparatively high ionic strength. The stringency of the hybridization can be increased by increasing the hybridization temperature or decreasing the salt concentration (Gearhart, 2003, Walker and Rapley, 2000).
7. *Wash*: Excessive probe should be washed from the membrane with saline–sodium citrate buffer. During the wash process, if radiolabeled probes were used, the radioactive intensity of the membrane is monitored. Rinsing is halted when the radiation intensity of the membrane is within one- to two-fold that of background. If the membrane is not rinsed sufficiently there will be reduced contrast upon detection.
8. *Detection*: If a radioactive probe is used, hybridization can be detected via exposure of x-ray film to the membrane. Note that fluorescent and chromogenic probes are also available.

51.6.2 The Northern Blot

51.6.2.1 Introduction to the Technique

Inspired by the Southern blot, James Alwine, David Kemp, and George Stark at Stanford University developed the northern blot technique in 1977 (Alwine et al., 1977). The northern blot is used to analyze gene expression via RNA detection. It can be used to monitor transcriptional activity of an endogenous or exogenous gene in cells or tissues.

There are three significant advantages to use the northern blotting technique for measuring the level of RNA. First, one gene can sometimes generate different RNA species. Northern blotting can provide a comparison between multiple RNAs derived from a single gene, yielding detailed information including

size and relative copy number. Second, after an RNA sample has been bound to a membrane, multiple hybridizations with different probes can be performed to analyze the expression of several genes on the same RNA sample (Murray, 1991). Third, the technique is relatively simple to perform and all required equipments are inexpensive.

Northern blot analysis can also be associated with several drawbacks. Measures should be taken to prevent samples from being contaminated by RNase, a prevalent enzyme that is responsible for RNA degradation. The presence of RNases would affect data quality and render the quantification of gene expression unreliable. In addition, northern blotting is not as sensitive as other techniques such as nuclease protection assays or PCR. Although simple to perform, the technique is time consuming, especially when a great number of samples are to be analyzed, even though more than one gene can be detected per blot (Perdew et al., 2006).

51.6.2.2 Technical Considerations

The main procedure of northern blotting is very similar to that of Southern blotting in that both contain steps of sample preparation, gel electrophoresis, transfer from gel to membrane, probe hybridization, and detection. Northern blotting differs from the Southern procedure in the following ways:

1. *Preparation of sample:* Detergents are used to lyse cells and then solvents are required to extract RNA. RNA is separated from proteins and DNA by means of liquid-phase separation or oligo (dT) chromatography. Considering that RNase is ubiquitous, RNase inhibition must be performed to prevent RNA degradation. Guanidine isothiocyanate can be used lyse cells and simultaneously inactivate RNases (Bird and Smith, 2002). Because RNA molecules are comparatively small, there is no need to use restriction endonucleases to break the RNA into smaller fragments.
2. *Gel electrophoresis:* Denaturing agents are incorporated into the agarose gels to limit RNA secondary structures (as opposed to performing the gel electrophoresis first and denaturing in a subsequent step). Formaldehyde and glyoxal are two commonly used denaturants. Sodium hydroxide should be avoided because it tends to hydrolyze the 2'-hydroxyl groups of RNA. In addition, it has been reported that the use of ethidium bromide in gels can hinder the subsequent transfer of RNA from gel to membrane, thus an alternative such as alcidine orange should be used for RNA visualization (Coleman and Tsongalis, 2006).

51.6.3 The Western Blot

51.6.3.1 Introduction to the Technique

The western blot, also known as the immunoblot, is used to identify and relatively quantify the amount of a specific protein within a sample containing multiple proteins, such as what is obtained following cell lysis. An immunochemical assay is used for protein identification. The technique is often used to detect the downstream product of specific gene expression. Due to high sensitivity, efficiency, and convenience, the western blot has been widely used by researchers through the world.

There are three basic steps to the western blot procedure: separation of proteins by gel electrophoresis, transfer of the separated samples from the gel to a membrane, and probing the membrane with antibodies. Proteins carry highly variable charges which are not easy to separate by simple gel electrophoresis. Therefore, sodium dodecyl sulfate (SDS) is often applied to denature the proteins and apply a uniform negative charge concentration to all of the polypeptides. The polypeptides can then be separated via polyacrylamide gel electrophoresis according to size.

After gel electrophoresis, the polypeptides are transferred electrophoretically from the gel to a membrane which serves as a support for the immunoreactions to follow. The fractionated polypeptides are adsorbed onto the membrane by noncovalent bonds and then exposed to a primary antibody which will bind specifically to the protein in question. The primary antibody will be detected through the binding of a labeled secondary antibody. The label is visualized via staining or radioactive assay.

51.6.3.2 Technical Considerations

The main procedures of western blotting are similar to those of Southern and northern blotting, including gel electrophoresis, transfer to a membrane, and probe hybridization. However, there are differences of particular note:

1. *Gel electrophoresis*: The gel electrophoresis used for the western blot is SDS-PAGE. The proteins in the sample are denatured by mixing them with SDS and then boiling. Details for SDS-PAGE are given in Section 51.2.3.
2. *Transfer*: Typically, electrophoretic transfer is the more preferable method for western blotting due to its high efficiency. Electro-transfer of the separated polypeptides onto the membrane can be accomplished by either semi-dry blotting or tank transferring systems (Walker, 2002). Tank transferring is more convenient and efficient than semi-dry blotting, but semi-dry blotting is more suitable for large gels because fewer buffers are required. For semi-dry blotting, two stacks of filter paper pre-wet with buffer are placed into contact with the gel and membrane to form a sandwich. The membrane is on the side of the anode, while the gel is by the cathode. Applying an electric current will cause the polypeptides to be transferred from the gel to the membrane because of the SDS that was used to denature them while providing a uniform negative charge. The tank transfer system is similar, utilizing a blotting sandwich with filter paper, membrane and gel submerged in a tank. The polypeptides will be similarly transferred by applied electrical current.

Nitrocellulose or polyvinylidene difluoride membranes are often utilized for western blotting. Because of their moderate levels of protein retention and comparably low price, nitrocellulose membranes have been well accepted for basic detection. However, polyvinylidene difluoride membranes possess better protein retention, physical strength, and chemical resistance. Thus they are often used when reprobng or protein sequencing will be performed because they will not be affected by repeated washing with organic solvents.

3. *Blocking*: Before applying the probes, the membrane must be blocked with proteins that will not be recognized by the probes. Blocking buffer or even dry instant milk can be used. This step is necessary because the portions of the membrane that did not receive the electrically transferred sample would still be charged, which could lead to nonspecific binding of the primary antibody probe.
4. *Probe hybridization*: Unlike in Southern and northern blots, the probes of the western blot are antibodies. Primary antibodies specific for the target polypeptides are required, and can be produced from animal species that are different from the origin of the protein sample. For example, if we are investigating the expression of mouse protein XYZ, we might use a primary immunoglobulin G (IgG) antibody raised in rabbits termed rabbit anti-mouse XYZ. Secondary antibodies could be tagged as antibody–enzyme conjugates or ^{125}I -labeled antibodies. The secondary antibodies will detect the primary antibodies, and be raised in a species different from what produced the primary antibodies. In our example, we might use labeled goat anti-rabbit IgG.

There are many commercially available labeled secondary antibody products. The most common conjugated enzymes are alkaline phosphatase and horseradish peroxidase. Alkaline phosphatase, discussed earlier in the section on histochemistry, dephosphorylates the substrate 5-bromo-4-chloro-3-indolyl phosphate which can be oxidized by nitroblue tetrazolium. The resulting signal would appear as a blue/purple dye. Horseradish peroxidase can catalyze the oxidation of 4-(chloro-1-naphthol), in the presence of hydrogen peroxide, into an insoluble blue dye. Apart from using antibody–enzyme conjugates, secondary antibodies can be labeled with ^{125}I to permit detection by autoradiography.

51.6.4 The Eastern Blot

After the development of the Southern and northern blots, and after the western blotting technique was developed by Towbin in 1979 (Towbin et al., 1979), many scholars have attempted to use “Eastern” in

the name of their own blotting techniques. As examples, Wreschner et al. (Wreschner and Herzberg, 1984), and Ishikawa et al. (Taki et al., 1994, Ishikawa and Taki, 2000) have put forth techniques termed Middle Eastern blotting, Eastern–Western blotting, and Far-Eastern blotting, respectively. In 2001, Shan et al. (2001) proposed their own “Eastern blotting” technique for the visualization of small molecules by means of thin layer chromatography (TLC). In the technique, the TLC plate is dried, followed by blotting of small molecules to a poly(vinylidene fluoride) (PVDF) membrane (Crocker and Murray, 2003). In general, eastern blotting is used to analyze proteins, lipoproteins, or glycoproteins, to detect posttranslational protein modifications. Samples are separated via SDS-PAGE and transferred to PVDF or nitrocellulose membranes for detection and analysis. So far, however, the scientific community has not reached a consensus for the definition of eastern blotting. Some researchers insist that eastern blotting does not exist at all.

References

- Alwine, J. C., Kemp, D. J., and Stark, G. R. 1977. Method for detection of specific RNAs in agarose gels by transfer to diazobenzyloxymethyl-paper and hybridization with DNA probes. *Proc Natl Acad Sci USA*, 74: 5350–4.
- Avison, M. B. 2007. *Measuring Gene Expression*, New York; Abingdon [England], Taylor & Francis.
- Bancroft, J. D. and Gamble, M. 2008. *Theory and Practice of Histological Techniques*, Edinburgh; New York, Churchill Livingstone.
- Bird, R. C. and Smith, B. F. 2002. *Genetic Library Construction and Screening : Advanced Techniques and Applications*, Berlin; New York, Springer.
- Bourne, G. H. and Danielli, J. F. (ed.) 1970. *International Review of Cytology*, New York: Academic Press, Inc..
- Bronner-Fraser, M. (ed.) 1996. *Methods in Cell Biology*, San Diego: Academic Press, Inc.
- Brown, T. A. 2000. *Essential Molecular Biology: A Practical Approach*, Oxford; New York, Oxford University Press.
- Butler, J. E. 1991. *Immunochemistry of Solid-Phase Immunoassay*, Boca Raton, CRC Press.
- Campbell, G., Compston, J., and Crisp, A. 1993. *The Management of Common Metabolic Bone Disorders*, Cambridge [England]; New York, Cambridge University Press.
- Clark, D. P. 2005. *Molecular Biology*, Amsterdam; Boston, Elsevier Academic Press.
- Coleman, W. B. and Tsongalis, G. J. 2006. *Molecular Diagnostics: For the Clinical Laboratorian*, Totowa, NJ, Humana Press.
- Cormack, D. H. 2001. *Essential Histology*, Philadelphia, Lippincott Williams & Wilkins.
- Crocker, J. and Murray, P. 2003. *Molecular Biology in Cellular Pathology*, Chichester, West Sussex, England; Hoboken, NJ, John Wiley & Sons.
- Derbyshire, V. et al. 1988. Genetic and crystallographic studies of the 3',5'-exonucleolytic site of DNA polymerase I. *Science*, 240: 199–201.
- Dhein, S., Mohr, F. W., and Delmar, M. 2005. *Practical Methods in Cardiovascular Research*, Berlin; New York, Springer.
- Dorak, M. T. 2006. *Real-Time PCR*, New York, Taylor & Francis.
- Eun, H.-M. 1996. *Enzymology Primer for Recombinant DNA Technology*, San Diego, Academic Press.
- Gearhart, J. P. (ed.) 2003. *Pediatric Urology*, Totowa, Humana Press Inc.
- Godbey, W. T., Hindy, S. B., Sherman, M. E., and Atala, A. 2004. A novel use of centrifugal force for cell seeding into porous scaffolds. *Biomaterials*, 25: 2799–805.
- Godbey, W. T., Zhang, X., and CHANG, F. 2008. The importance of and a method for including transfection efficiency into real-time PCR data analyses. *Biotechnol Bioeng*, 100: 765–72.
- Hames, B. D. 1998. *Gel Electrophoresis of Proteins: A Practical Approach*, Oxford; New York, Oxford University Press.
- Hilario, E. and Mackay, J. 2007. *Protocols for Nucleic Acid Analysis by Nonradioactive Probes*, Totowa, NJ, Humana Press.

- Hjerten, S. 1962. "Molecular sieve" chromatography on polyacrylamide gels, prepared according to a simplified method. *Arch Biochem Biophys*, Suppl 1: 147–51.
- Holtorf, H. L., Jansen, J. A., and Mikos, A. G. 2005. Flow perfusion culture induces the osteoblastic differentiation of marrow stroma cell-scaffold constructs in the absence of dexamethasone. *J Biomed Mater Res A*, 72: 326–34.
- Hoy, M. A. 2003. *Insect Molecular Genetics: An Introduction to Principles and Applications*, Amsterdam; Boston, Academic Press.
- Humason, G. L. 1972. *Animal Tissue Techniques*, San Francisco, W. H. Freeman.
- Ishikawa, D. and Taki, T. 2000. Thin-layer chromatography blotting using polyvinylidene difluoride membrane (Far-Eastern blotting) and its applications. *Sphingolipid Metabolism and Cell Signaling, Pt B*, 312: 145–57.
- Kieleczawa, J. 2006. *DNA Sequencing II: Optimizing Preparation and Cleanup*, Sudbury, MA, Jones and Bartlett Publishers.
- Kiernan, J. A. 1981. *Histological and Histochemical Methods: Theory and Practice*, Oxford, England; New York, Pergamon Press.
- Krishnamurthy, K. V. 1999. *Methods in Cell Wall Cytochemistry*, Boca Raton, FL, CRC Press.
- Kumar, A. and Garg, N. 2005. *Genetic Engineering*, New York, Nova Biomedical Books.
- Liu, W. and Saint, D. A. 2002. A new quantitative method of real time reverse transcription polymerase chain reaction assay based on simulation of polymerase chain reaction kinetics. *Anal Biochem*, 302: 52–9.
- Marmur, J. and Doty, P. 1962. Determination of the base composition of deoxyribonucleic acid from its thermal denaturation temperature. *J Mol Biol*, 5: 109–18.
- McPherson, M. J. and Hames, B. D. 1995. *PCR 2 : A Practical Approach*, Oxford; New York, IRL Press at Oxford University Press.
- Menninger, J. R., Wright, M., Menninger, L., and Meselson, M. 1968. Attachment and detachment of bacteriophage lambda DNA in lysogenization and induction. *J Mol Biol*, 32: 631–7.
- Mitra, S. 2003. *Sample Preparation Techniques in Analytical Chemistry*, Hoboken, NJ, J. Wiley.
- Muller, P. Y., Janovjak, H., Miserez, A. R., and Dobbie, Z. 2002. Processing of gene expression data generated by quantitative real-time RT-PCR. *Biotechniques*, 32: 1372–4, 1376, 1378–9.
- Murray, E. J. 1991. *Gene Transfer and Expression Protocols*, Clifton, NJ, Humana Press.
- Nagy, L. E. 2008. *Alcohol: Methods and Protocols*, Totowa, NJ, Humana Press.
- New England Biolabs. 2009a. *Optimizing Restriction Endonuclease Reactions* [Online]. Available at http://www.neb.com/nebecomm/tech_reference/restriction_enzymes/setting_up_reaction.asp
- New England Biolabs. 2009b. *T4 DNA Ligase FAQ* [Online]. Available at <http://www.neb.com/nebecomm/products/faqproductM0202.asp>
- Newton, C. R. and Graham, A. 1997. *PCR*, Oxford, OX, UK New York, BIOS Scientific Publishers; Springer.
- Osborn, A. M. and Smith, C. J. 2005. *Molecular Microbial Ecology*, New York; Abingdon [England], Taylor & Francis.
- Peirson, S. N., Butler, J. N., and Foster, R. G. 2003. Experimental validation of novel and conventional approaches to quantitative real-time PCR data analysis. *Nucleic Acids Res*, 31: e73.
- Pelt-Verkuil, E. V., Belkum, A. V., and Hays, J. P. 2008. *Principles and Technical Aspects of PCR Amplification*, Dordrecht, Springer.
- Perdew, G. H., Vanden Heuvel, J. P., and Peters, J. M. 2006. *Regulation of Gene Expression: Molecular Mechanisms*, Totowa, NJ, Humana Press.
- Pestana, E. A., Adama Diallo, S. B., Crowther, J. R., and Viljoen, G. J. 2009. *Early, Rapid and Sensitive Veterinary Molecular Diagnostics—Real Time pcr Applications*, New York, Springer.
- Pfaffl, M. W. 2001. A new mathematical model for relative quantification in real-time RT-PCR. *Nucleic Acids Res*, 29: e45.
- Pingoud, A. and Jeltsch, A. 2001. Structure and function of type II restriction endonucleases. *Nucleic Acids Res*, 29: 3705–27.

- Rapley, R. and Walker, J. M. 1998. *Molecular Biomethods Handbook*, Totowa, NJ, Humana Press.
- Roe, S. 2001. *Protein Purification Techniques : A Practical Approach*, Oxford; New York, Oxford University Press.
- Rychlik, W., Spencer, W. J., and Rhoads, R. E. 1990. Optimization of the annealing temperature for DNA amplification in vitro. *Nucleic Acids Res*, 18: 6409–12.
- Saiki, R. K., Gelfand, D. H., Stoffel, S. et al. 1988. Primer-directed enzymatic amplification of DNA with a thermostable DNA polymerase. *Science*, 239: 487–91.
- Saiki, R. K., Scharf, S., Faloona, F. et al. 1985. Enzymatic amplification of beta-globin genomic sequences and restriction site analysis for diagnosis of sickle cell anemia. *Science*, 230: 1350–4.
- Sambrook, J. and Russell, D. W. 2001. *Molecular Cloning : A Laboratory Manual*, Cold Spring Harbor, NY, Cold Spring Harbor Laboratory Press.
- Saotome, K., Morita, H., and Umeda, M. 1989. Cytotoxicity test with simplified crystal violet staining method using microtitre plates and its application to injection-drugs. *Toxicology in Vitro*, 3: 317–21.
- Saunders, G. C., Parkes, H. C., and Laboratory of the Government Chemist (Great Britain) 1999. *Analytical Molecular Biology: Quality and Validation*, Cambridge, Published for Laboratory of the Government Chemist by the Royal Society of Chemistry.
- Schmittgen, T. D. and Livak, K. J. 2008. Analyzing real-time PCR data by the comparative C(T) method. *Nat Protoc*, 3: 1101–8.
- Shan, S. J., Tanaka, H., and Shoyama, Y. 2001. Enzyme-linked immunosorbent assay for glycyrrhizin using anti-glycyrrhizin monoclonal antibody and an eastern blotting technique for glucuronides of glycyrrhetic acid. *Anal Chem*, 73: 5784–90.
- Singer, V. L., Jones, L. J., Yue, S. T., and Haugland, R. P. 1997. Characterization of PicoGreen reagent and development of a fluorescence-based solution assay for double-stranded DNA quantitation. *Anal Biochem*, 249: 228–38.
- Slater, R. J. 1986. *Experiments in Molecular Biology*, Clinton, NJ, Humana Press.
- Smith, H. O. and Nathans, D. 1973. Letter: A suggested nomenclature for bacterial host modification and restriction systems and their enzymes. *J Mol Biol*, 81: 419–23.
- Southern, E. M. 1975. Detection of specific sequences among DNA fragments separated by gel electrophoresis. *J Mol Biol*, 98: 503–17.
- Steitz, T. A. 1993. *Structural Studies of Protein-Nucleic Acid Interaction : The Sources of Sequence-Specific Binding*, New York, NY, USA, Cambridge University Press.
- Taki, T., Handa, S., and Ishikawa, D. 1994. Blotting of glycolipids and phospholipids from a high-performance thin-layer chromatogram to a polyvinylidene difluoride membrane. *Analytical Biochemistry*, 221: 312–16.
- Thelwell, N., Millington, S., Solinas, A., Booth, J., and Brown, T. 2000. Mode of action and application of Scorpion primers to mutation detection. *Nucleic Acids Res*, 28: 3752–61.
- Towbin, H., Staehelin, T., and Gordon, J. 1979. Electrophoretic transfer of proteins from polyacrylamide gels to nitrocellulose sheets—Procedure and some applications. *Proc Natl Acad Sci USA*, 76: 4350–4.
- Walker, J. M. 1994. *Basic Protein and Peptide Protocols*, Totowa, NJ, Humana Press.
- Walker, J. M. 2002. *The Protein Protocols Handbook*, Totowa, NJ, Humana Press.
- Walker, J. M. and Rapley, R. 2000. *Molecular Biology and Biotechnology*, Cambridge, Royal Society of Chemistry.
- Walker, J. M. and Rapley, R. 2009. *Molecular Biology and Biotechnology*, Cambridge, Royal Society of Chemistry.
- Wilson, G. G. 1988. Type II restriction- modification systems. *Trends Genet*, 4: 314–8.
- Wong, M. L. and Medrano, J. F. 2005. Real-time PCR for mRNA quantitation. *Biotechniques*, 39: 75–85.
- Wreschner, D. H. and Herzberg, M. 1984. A new blotting medium for the simple isolation and identification of highly resolved messenger-RNA. *Nucl Acids Res*, 12: 1349–59.

Prinda
Wanakule

*University of Texas,
Austin*

Krishnendu Roy

*University of Texas,
Austin*

55.1	Introduction	55-1
55.2	Mechanisms of Drug Delivery.....	55-2
	Diffusion from Nondegradable Systems • Bioerosion • Stimuli-Responsive Systems • Overall Release Profiles	
55.3	Drugs of Interest in Tissue Engineering	55-6
	Drug Properties and Design Considerations	
55.4	Drug Delivery in Tissue Engineering	55-8
	Classical Drug Delivery Systems • Drug Delivery from Tissue Engineering Scaffolds and Matrices	
55.5	Outlook.....	55-13
	References.....	55-14

55.1 Introduction

The study and practice of tissue engineering requires a multidisciplinary approach in order to create new cells and tissues for the treatment of diseases (Langer and Vacanti 1993, Becker and Göpferich 2007). Drug delivery has proven to be an integral part in directing the development and differentiation of progenitor cells into functional tissues, specifically, the controlled delivery of pharmacologically active or bioactive agents, such as cytokines, growth factors, morphogens, and nucleic acids. By controlling the delivery of these drugs at different time points and concentrations, a direct effect is exerted on the cell proliferation, differentiation, or migration, with the potential for controlling the phenotype and functionality of developing tissues (Biondi et al. 2008, Boontheekul and Mooney 2003, Fisher et al. 2010, Langer and Vacanti 1993, Nomi et al. 2002, Saltzman and Olbricht 2002, Tabata 2003, Uebersax et al. 2009).

The goals of drug delivery, in general, are manifold, and include the targeting of drug to specific cells or sites in the body, overcoming tissue barriers associated with delivery routes, overcoming cellular barriers which control cellular uptake, and controlled release. Controlled release concepts encompass the ability to control release of bioactive molecules at target sites, the effective concentration of drug in the body, as well as its duration of activity.

In tissue engineering, controlled delivery encompasses “the provision of a bioactive molecule over time in a manner such that its biological activity can be productively harnessed” (Hubbell 2008). The use of controlled drug delivery, more so than the other goals of drug delivery, has come into greater use in tissue engineering in recent years (Biondi et al. 2008, Fisher et al. 2010, Uebersax et al. 2009). In this context, there are three major applications of drug delivery concepts that are being widely used to engineer tissue constructs: (a) spatially and temporally controlled delivery of proteins, peptides, lipids, and small molecules (e.g., growth factors, enzymes, and morphogens), (b) spatially patterned presentation of cell-signaling ligands, and (c) delivery of nucleic acids to direct progenitor cells to specific pathways (e.g., through either ectopic gene expression or targeted gene silencing).

While it is possible to directly infuse these bioactive molecules into culture flasks and plates (*in vitro*) or by injection (*in vivo*), this may be undesirable for several reasons. For example, many proteins and

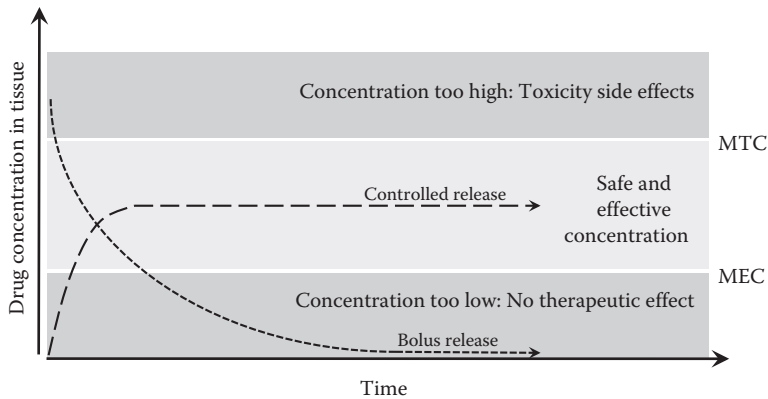


FIGURE 55.1 In classical drug delivery, controlled release systems aim to achieve a constant concentration of bioactive drug that is both safe and effective. MEC = minimum effective concentration; MTC = minimum toxic concentration.

peptides have short half-lives in serum or media due to inactivation by proteases and enzymes, and thus, need continual replenishment to maintain a certain minimum effective concentration (see Figure 55.1). Additionally, unconstrained repeated doses may result in toxic effects. Delivery of nucleic acids also poses the additional challenge of intracellular targeting. The controlled temporal and spatial release of these drugs could reduce the amount of expensive drug and chemical signals required, as well as the potential toxic effects (Hubbell 2008, Biondi et al. 2008, Boontheekul and Mooney 2003, Caldorera-Moore and Peppas 2009, Fisher et al. 2010, Saltzman and Olbricht 2002, Uebersax et al. 2009) and at the same time increase their bioavailability. This temporal and spatial control has also given rise to new possibilities and advances in tissue engineering, for example, the use of three-dimensional scaffolds to spatially differentiate cells into various “zones” consisting of different cell types (Mapili et al. 2005, Klein et al. 2009).

The objective of this chapter is to provide the reader with a basic understanding of drug delivery, an overview of controlled drug delivery technologies, as well as their applicability to and significance in the field of tissue engineering. We first begin by providing a brief review on the modes of drug delivery, or drug release, from drug delivery systems. Next, we move on to discuss some drugs of interest in tissue engineering applications, as well as their properties that affect the design of the delivery system. We then explore the methods used to control the release of drugs in tissue engineering, with special emphasis on the release of drugs from tissue engineering scaffolds and matrices. Finally, we provide an outlook on the future of drug delivery in tissue engineering, and follow with references.

55.2 Mechanisms of Drug Delivery

There are myriad mechanisms to direct the release of drugs in a controlled manner. We can classify the drug delivery mechanisms of special interest in tissue engineering into three main categories: diffusion from nondegradable systems, bioerodible systems, and stimuli-responsive systems. Several other strategies have been employed to create desirable release profiles; however, an exhaustive description is certainly beyond the scope of this chapter, and may be found in excellent reviews in the literature (Caldorera-Moore and Peppas 2009, Langer and Peppas 2003, Lavan et al. 2003, Saltzman and Olbricht 2002).

55.2.1 Diffusion from Nondegradable Systems

Diffusion is one of the most kinetically well-defined concepts of transport phenomena, and is especially applicable in the diffusion of drug molecules from nondegradable drug delivery systems (Truskey et al.

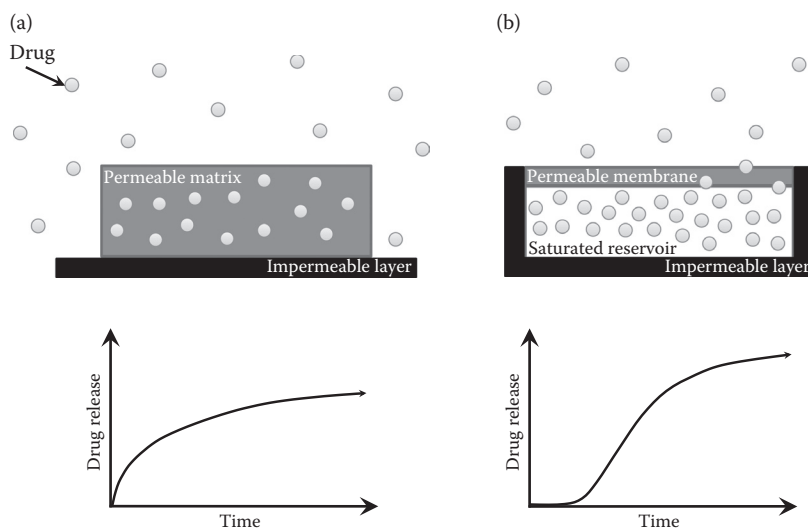


FIGURE 55.2 (a) Diffusion-driven release of drug from a matrix. (b) Diffusion-driven release of drug from a saturated reservoir through a membrane.

2004, Becker and Göpferich 2007). Thermodynamically driven, it is the result of the random walk of submicron particles, called Brownian motion. Although movement may seem random at the microscopic level, at the macroscopic level, movement of particles along a concentration gradient is observed. Fick's second law of diffusion describes the temporal and spatial net movement of particles by diffusion:

$$\frac{\partial C(x, y, z, t)}{\partial t} = \frac{\partial^2 C}{\partial x^2} + \frac{\partial^2 C}{\partial y^2} + \frac{\partial^2 C}{\partial z^2}$$

Numerous solutions for this equation have been derived in order to describe the diffusion of drug molecules from several types of drug delivery devices under several conditions; for details, we refer the reader to an excellent text by Truskey et al. (2004). However, the two main diffusive conditions of special interest in drug delivery for tissue engineering are the diffusion of drug from a polymer matrix and the diffusion of drug from a reservoir through a membrane (see Figure 55.2), both of which are predictably well defined. The solutions to the problem are highly dependent on the initial drug concentration and the geometry of the device, and as such, the diffusion of drug out of the system may be changed by altering the device geometry, and prolonged by increasing the initial concentration (Truskey et al. 2004, Becker and Göpferich 2007).

Along the same lines, however, the disadvantage of this system lies in its dependence on drug concentration to define the flux of drug out of the system. As the drug concentration decreases over time and there is less of a concentration gradient, the release rate also decreases over time. This is especially pronounced in the diffusion of drug from a polymer matrix. However, by using a highly saturated drug reservoir with diffusion of drug driven through a membrane, a constant release of drug may be achieved over an extended period of time—longer than may be typically achieved through use of a matrix alone (Truskey et al. 2004, Becker and Göpferich 2007, Hubbell 2008).

55.2.1.1 Diffusion from Swellable Polymers

Diffusion of drugs may also be controlled by the use of swellable polymers, including swellable cross-linked hydrogels. In this case, there is an increase in polymer chain mobility due to the uptake of a solvent, such as water, that decreases the glass transition of the polymer (T_g). Drugs that are entrapped

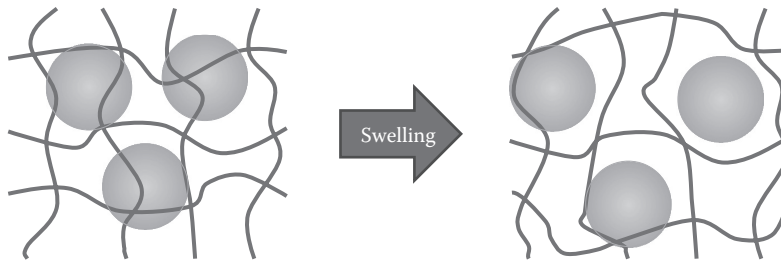


FIGURE 55.3 Diffusion of drug from a swellable polymer matrix. In the preswollen state, drug molecules are entrapped within the network structure. Swelling of the polymer network results in increased polymer chain mobility and pore size, increasing the rate of diffusion of drugs out of the network.

and immobilized by the nonswollen polymer matrix may then begin to diffuse out due to the increased flexibility, resulting in a heightened release rate. In order to achieve this, the pore size of the polymer matrix must be sufficiently small so as to restrict a drug of known hydrodynamic radius. Upon swelling, the pore size increases, thus allowing movement and diffusion of the drug out from the matrix (see Figure 55.3) (Becker and Göpferich 2007, Hubbell 2008, Lustig and Peppas 1988). The diffusion of drugs from swellable polymer matrices has been well studied for macroporous (pore size between 0.1 and 1.0 μm), microporous (100–1000 \AA), and nonporous (10–100 \AA) hydrogels by several groups, and tunable drug release profiles from swellable polymers have been achieved (Hubbell 2008, Annabi et al. 2010).

55.2.2 Bioerosion

By definition, bioerosion refers to the erosion of a polymer into water-soluble products under physiological conditions, including both physical and chemical processes (according to the European Society for Biomaterials Consensus Conference in 1986) (Williams 1986). As a side note, biodegradation refers to the degradation by biological molecules, such as enzymes, which will be covered in the following section on stimuli-responsive systems. The most common mechanism of bioerosion is by hydrolysis of a polymer backbone by neutral water; however, accelerated hydrolysis may occur in the presence of ion catalysts and acidic pH. Erosion may proceed by either surface erosion or bulk erosion (see Figure 55.4). In surface erosion, the rate at which water is able to penetrate the device is slower than the erosion rate.

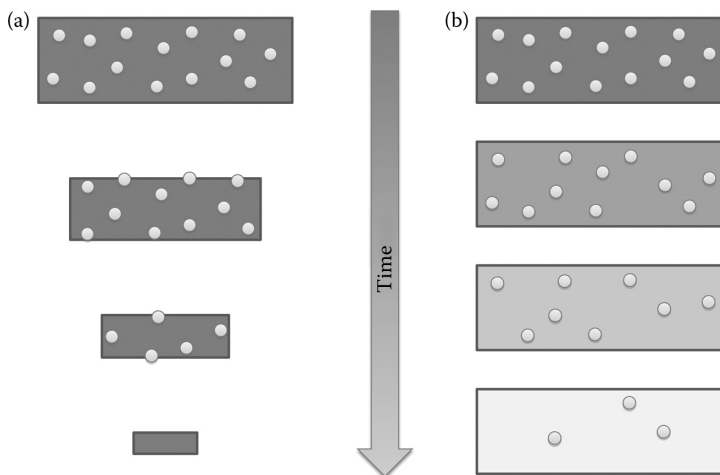


FIGURE 55.4 Surface erosion (a) and bulk erosion (b) of polymeric devices.

On the other hand, bulk erosion occurs when the rate of water penetration into the device is greater than the rate of erosion (Gombotz and Pettit 1995, Göpferich 1996, Steinbüchel and Matsumura 2003).

Bioerodible drug delivery systems have been designed to both provide a mechanism of controlled drug release and to eliminate the need for device extraction after the lifetime of the system. As the device erodes, drug that has been solubilized or suspended within the device is slowly released. In general, surface eroding systems (heterogeneous) have a release rate proportional to the surface erosion rate, are driven primarily by erosion rather than diffusion, and can be varied according to device geometry. Bulk eroding systems (homogeneous) are driven by a combination of erosion and diffusion kinetics, with first-order kinetics for the rate of erosion, as well as the permeability of the device. Several parameters affect the rate of hydrolysis, and thus, release rate, including lability of the polymer backbone, hydrophobicity or hydrophilicity of the polymer, morphology, and molecular weight (Gombotz and Pettit 1995, Göpferich 1996, Heller 1985, Jain et al. 2005, Steinbüchel and Matsumura 2003).

55.2.3 Stimuli-Responsive Systems

In recent decades, a greater interest in the stimuli-responsive subfield in controlled drug delivery has been developing as a means to deliver drug only when or where it is needed. These stimuli-responsive types of systems often rely on physicochemical changes due to disease pathology or the cell microenvironment. Common stimuli include pH, temperature, ions, enzymes, light, and biomolecules, all of which have been designed to illicit a response in drug carriers to trigger drug release (Caldorera-Moore et al. 2010, Caldorera-Moore and Peppas 2009, Fisher et al. 2010, Jia and Kiick 2009, Löwik et al. 2010, Wanakule and Roy 2012).

55.2.3.1 pH-Responsive Systems

Several hydrogel-based drug delivery systems with the ability to swell or shrink in response to pH changes have been developed as triggered-release delivery systems. The pH-triggered swelling and shrinking mechanisms are primarily due to the properties of the side chain pendant group, which are cationic or anionic (Caldorera-Moore and Peppas 2009, Khare and Peppas 1993, 1995). Anionic hydrogels are ionized at pHs above their pK_a , and thus exhibit high swelling at these higher pHs due to repulsion of the ionized groups (Khare and Peppas 1995). In contrast, cationic hydrogels are ionized at pHs below their pK_a , exhibiting high swelling below their pK_a (Khare and Peppas 1993).

Changes in pH exist throughout the body at the organ, tissue, and cellular level, and even due to various disease states. For example, pH-triggered drug delivery systems have been developed that are capable of triggering drug release when moving from the acidic gastric cavity to the more neutral small intestine (Gallardo et al. 2008, Liu and Basit 2010), where much drug absorption occurs, as well as from the neutral extracellular environment to the slightly more acidic early endosome (intracellular) (Boussif et al. 1995, Putnam et al. 2001). Thus, pH-responsive systems offer a versatile way in which to trigger drug release in response to environmental cues.

55.2.3.2 Enzyme-Responsive Systems

A relatively new strategy in drug delivery is to incorporate enzyme-sensitive components into the drug carriers, which are primarily hydrogel-based. Enzyme-degradable hydrogels have been shown to exhibit minimal release without the presence of enzyme, and triggered release in the presence of enzyme (Caldorera-Moore and Peppas 2009, Gobin and West 2002, Miyata et al. 2002, Peppas et al. 2000, Vartak and Gemeinhart 2007). This strategy has been used extensively in tissue engineering applications (Gobin and West 2002, Zisch et al. 2003a); however, it also provides an effective means of physiologically controlled release of drugs (Aimetti et al. 2009, Vartak and Gemeinhart 2007). Enzyme-responsive systems are suitable for site-specific delivery because enzymatic cleavage is highly specific, and many enzymes are upregulated in several diseases, such as various cancers and inflammatory diseases (Aimetti et al. 2009, Caldorera-Moore et al. 2010, Caldorera-Moore and Peppas 2009, Glangchai et al. 2008, Vartak and

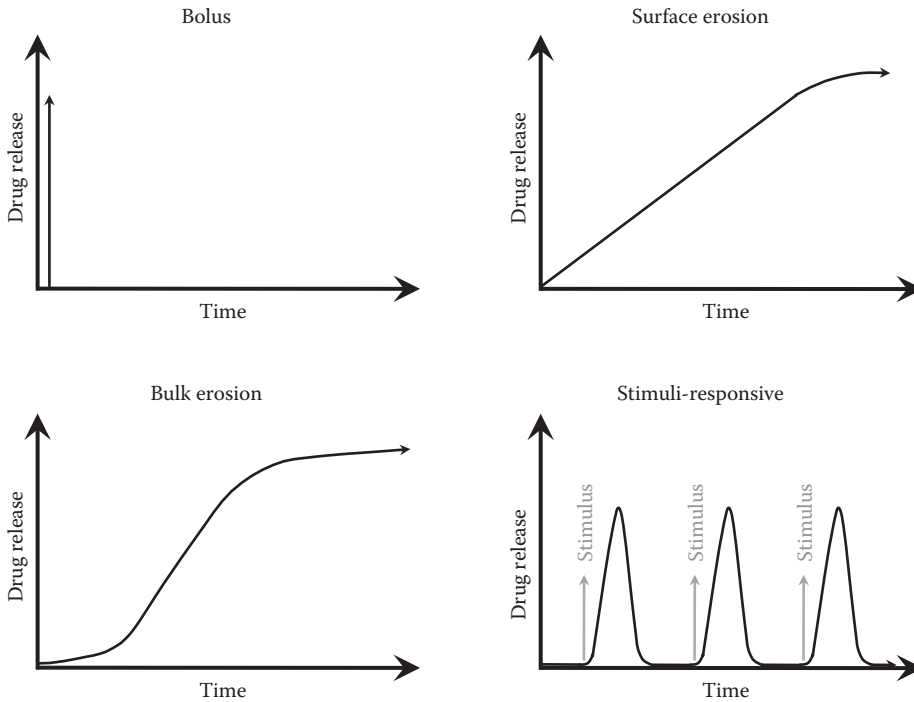


FIGURE 55.5 Release profiles of various delivery mechanisms. See Figure 55.2 for diffusion-driven release profiles.

Gemeinhart 2007). In most cases, enzyme-cleavable proteins, peptides, or extracellular matrix (ECM) components are incorporated into the hydrogel cross-links (Gobin and West 2002, Miyata et al. 2002, Zisch et al. 2003a). In another set-up, enzyme-degradable components are used as covalent linkers to conjugate drugs as pendant groups off the polymer backbone (Caldorera-Moore and Peppas 2009, Tauro et al. 2008). Upon encountering the enzyme, the cross-links are broken, releasing any encapsulated drug.

55.2.4 Overall Release Profiles

Oftentimes, the overall drug release mechanism may be due to a combination of the aforementioned modes. For example, diffusion plays a role in each of these mechanisms in that the drug must diffuse out of eroding scaffolds, or swollen matrices. Stimuli-responsive carriers may also release drug by stimuli-induced erosion or swelling. In choosing a release mechanism, the temporal requirements of drug in the system, as well as drug pharmacokinetics, must be considered.

There are several release profiles that may be achieved by the delivery systems described here (Figure 55.5). Several classical drug delivery systems were designed with the aim of achieving a zero order, or linear, release rate, which results in a constant level of drug in the tissues. However, newer drug delivery systems are designed to release drug when and where it is needed, thereby reducing side effects (Truskey et al. 2004, Hubbell 2008, Biondi et al. 2008, Becker and Göpferich 2007). Since spatial and temporal control over drug release is often required to guide the differentiation of cells into their appropriate niches, highly ordered systems with a combination of mechanisms may be required.

55.3 Drugs of Interest in Tissue Engineering

The primary drugs of interest for tissue engineering applications may be roughly divided into three groups: growth factors, adhesion factors, and nucleic acids. Growth factors are cell signaling proteins or

TABLE 55.1 Common Drugs or Bioactive Agents Used in Tissue Engineering

Abbreviation	Bioactive Agent	Application
BMP	Bone morphogenetic protein	Osteogenesis
PTH	Human parathyroid hormone	Osteogenesis
TGF- β	Transforming growth factor beta	Differentiation, anti-proliferation
HGF	Hepatocyte growth factor	Proliferation
G-CSF	Granulocyte colony-stimulating factor	Proliferation
GM-CSF	Granulocyte-macrophage colony-stimulating factor	Proliferation
VEGF	Vascular endothelial growth factor	Angiogenesis
FGF	Fibroblast growth factor	Angiogenesis
EPO	Erythropoietin	Angiogenesis
OPG	Osteoprotegerin	Angiogenesis
Ang1	Angiopoietin-1	Angiogenesis, vessel maturation
PDGF	Platelet-derived growth factor	Angiogenesis, vessel maturation
NGF	Nerve growth factor	Nerve regeneration
GDNF	Glial-derived neurotrophic factor	Nerve regeneration
	Fibronectin	Adhesion, cell substrate
	Vitronectin	Adhesion, cell substrate
	Fibrinogen	Adhesion, cell substrate
	Laminin	Adhesion, cell substrate
RGD	Arginine–Glycine–Asparagine	Adhesion
S1P	Sphingosine 1-phosphate	Chemoattractant
MIP3 α	Macrophage inflammatory protein 3 alpha	Chemoattractant

hormones that have an effect on cell differentiation, proliferation, and maturation through a process of ligand–receptor binding. Some examples of growth factors include bone morphogenetic proteins, vascular endothelial growth factors, and some cytokines. Adhesion factors are proteins and peptides that are typically bound to the ECM and relay mechanical stress feedback to the cell. Adhesion factors include vitronectin and fibronectin, as well as the fibronectin-derived peptide sequence, RGD. Some common proteins used in tissue engineering, as well as the intended function or purpose, are summarized in Table 55.1 (Hubbell 2008, Biondi et al. 2008, Chen and Mooney 2003, Haller and Saltzman 1998, Becker and Göpferich 2007, Robinson and Talmadge 2002, Tabata 2003, Zisch et al. 2003b). Nucleic acids (plasmid DNA, oligonucleotides, and siRNA) are used in tissue engineering primarily to direct progenitor cells into a specific phenotype or to express growth factors and morphogens *in situ* (Amiji 2005, Reynolds et al. 2004). A detailed discussion of this modality is beyond the scope of this chapter and can be found in the Gene Therapy (Chapter 56) and Cell Engineering (Chapter 57) chapters of this text. This chapter will predominantly focus on protein, peptide, and small-molecule drugs used directly as growth factors or adhesion factors.

55.3.1 Drug Properties and Design Considerations

Given that the majority of growth factors and adhesion factors are composed of bioactive proteins, or derivatives thereof, there are many considerations that must be made in order to design suitable systems for the delivery of these proteins in active forms. The most prominent consideration is the need to deliver the proteins in their native forms, that is, with their tertiary structure intact. Several methods of drug incorporation into delivery systems may cause protein denaturation from processing and encapsulation conditions, such as the application of heat, high shear forces, pH changes, UV, and exposure to organic solvents. Also considering that the majority of these proteins are hydrophilic, the choice of

delivery materials is important in that exposure to hydrophobic materials may cause protein denaturation (Manning et al. 1989, 2010, Wang 1999). Lastly, the conditions that lead to drug release must also be evaluated to verify that they do not damage the protein. For example, in the case of hydrolytically degradable polyester drug carriers, a slightly acidic microenvironment is often created, which could affect protein activity (Fu et al. 2000). The final conformation of the protein must be such that its bioactivity is not affected, and there are no forms present that may elicit ill effects or immunogenicity (Hubbell 2008).

Along the same lines, the biological environment that the protein drugs are exposed to, whether *in vitro* or *in vivo*, may affect the protein conformation and activity. Several components in serum, including enzymes and peptidases, cause protein degradation often within minutes, decreasing the half-life dramatically. Glomerular, or renal, filtration also plays a key role in decreasing the half-life of proteins. For example, *in vivo*, the half-lives of PDGF, bFGF, and VEGF are approximately 2, 3, and 50 min respectively. A common strategy to improve the circulating half-lives of these proteins is to encapsulate them within polymers, however, care must be taken to ensure that the encapsulating material does not cause protein agglomeration or activate clotting factors (Manning et al. 1989, 2010, Wang 1999). Another common strategy is the conjugation of poly(ethylene glycol), or PEG, referred to as PEGylation (Eliason 2001, Molineux 2002, Roberts et al. 2002, Sato 2002). PEGylation of proteins has been shown to increase circulation time *in vivo* and decrease the rate of protein degradation by enzymes (Molineux 2003, Yang et al. 2004).

Aside from classical cell culture flasks and dishes, there has recently been an increased usage of ECM-mimicking gel matrices to serve both as a cell scaffold and as a controlled drug delivery device (Gobin and West 2002, Lutolf et al. 2003). These bioinspired matrices may be either hybrid synthetic and biomaterial or biomaterial alone, offer improved compatibility and stability with proteins, and have been designed to mimic the ways in which growth factors are released in the body (Wee and Gombotz 1998, Sano et al. 1998, Ikada and Tabata 1998, Lutolf et al. 2003). In the body, growth factors are either stored within the ECM or secreted by cells for short-term signaling. The ECM serves as a responsive delivery system for these growth factors, which may be controlled dynamically by cell movement and secretion of enzymes that degrade the matrix (Gobin and West 2002, Hubbell 2008). Adhesion factors in the ECM also relay mechanical feedback to the cells, and help the cells migrate as controlled by cellular signals (Wacker et al. 2008, Jia and Kiick 2009, Saltzman and Baldwin 1998). These ECM-mimicking systems offer several advantages over classical systems, as we will discuss in the following section.

55.4 Drug Delivery in Tissue Engineering

Given the complex temporal and spatial control of drug delivery required in tissue engineering, several strategies have been developed to meet the needs of this growing field. The strategies may be roughly classified into four major categories:

1. Classical drug delivery systems for use in cell culture or *in vivo* at local sites
2. Drug delivery from tissue engineering scaffolds and matrices
3. Cells (genetically altered or otherwise) to produce drugs in the system
4. Biomimetic systems with conjugated drugs

The primary focus of this chapter will be to discuss in greater detail the first two strategies, the use of classical drug delivery systems, and especially the delivery of drugs from the cell scaffolds and matrices. The latter two strategies are discussed in great lengths within the Gene Therapy (Chapter 56), and Cell Engineering (Chapter 57), and Biomimetics (Chapter 50) chapters.

55.4.1 Classical Drug Delivery Systems

Several classical drug delivery systems for tissue engineering are still in use for a wide variety of applications. The majority of these systems are employed to provide a means of long-term, controlled

release of drugs into the local environment, whether *in vitro* or *in vivo*, for example, the use of poly(lactic-co-glycolic) acid (PLGA), microparticles for the controlled delivery of encapsulated growth factor. The required release profile may be chosen based on several factors including the rate of drug clearance from the system, pharmacokinetics, and stability. Thereafter, a system will be designed or chosen based on these requirements, considering parameters such as material properties, degradation rate, and device geometry. Generally, the major types of classical systems used include monolithic or slab-type systems, particulate systems, and gel-like systems.

55.4.1.1 Monolithic Systems

Monolithic polymer systems have a long history in drug delivery in that they were the first types of systems to be used for the controlled release of bioactive proteins and peptides. Among the first systems reported for controlled release was the polymeric membrane system composed of poly(ethylene-co-vinyl acetate) or EVAc, as described by Folkman and Langer in 1976 (Cao and Langer 2008). Although these systems were not biodegradable, the excellent controlled release profiles set the stage for an entirely new strategy of controlled release. In the following decade, several new biodegradable or bioerodible materials were developed with the aim of achieving sustained release *in vivo* without the need for removal after transplantation. Some of the materials included polyanhydrides (Jain et al. 2005), poly(ortho esters) (Heller 1985), and poly(α -hydroxyesters) (Lucke et al. 2002), with several more described in the literature. However, with the advent of these erodible systems came new unforeseen challenges due to the new intricacies of the system, including pH changes and side reactions with encapsulated drug due to the degraded products (Brunner et al. 1999, Fu et al. 2000, Van De Weert et al. 2000).

These early delivery systems were made in the form of monolithic devices because of their ease of manufacture by solvent casting, extrusion, and injection molding. These bulk devices were also able to carry a large payload of drug, and could be tailored for different release rates by changing material composition, drug loading, or including dispersants. As discussed in the previous section on the mechanisms of drug release, release from nondegradable systems is controlled primarily by diffusion. Erosion-controlled release provided more control over the release rate, which could be changed by the degradation rate, or by choosing between surface or bulk erosion. Monolithic devices based on the poly(lactic-co-glycolic acid) copolymer, PLGA, were and still are commonly used in the erodible systems because erosion may be well controlled by changing crystallinity, copolymer composition, and molecular weight (Athanasios et al. 1998, Fu et al. 2000, Mohamed and Van Der Walle 2008, Sánchez et al. 2003, Thissen et al. 2006, Van De Weert et al. 2000). Other monolithic devices have been based on cross-linked hydrogels, and will be discussed in more detail in the following sections.

55.4.1.2 Particulate Systems

Following the progress made in monolithic and erodible devices, microparticulate systems began to surface in the field. Whereas monolithic systems required surgical implantation *in vivo* and are associated with a strong drug gradient, particulate systems offered the possibility of an injectable system and more even distribution in the tissue *in vivo*, or in cell culture. Microparticles also provided the flexibility for cell microencapsulation, or combinatorial delivery from microparticle distribution within monolithic systems or gels (Truskey et al. 2004, Becker and Göpferich 2007, Singh et al. 2009). Aside from microparticles, nanoparticles, liposomes, and other similar particulate technologies have also been explored; however, microparticles have been most widely applied to tissue engineering, and some of these other technologies will be discussed in other chapters.

Microparticulate systems have been widely used for the delivery of growth factors for directing cell differentiation and proliferation. One application that has been extensively studied is the use of both EVAc and PLGA microparticles to deliver nerve growth factor (NGF) for supporting cellular therapy in neurodegenerative diseases (Haller and Saltzman 1998). PLGA microparticles are also still in use for delivery of several other proteins, including BMP-2 (Kempen et al. 2008) and interferon- α (Sánchez et al. 2003). Poly(phosphoester) microspheres with encapsulated NGF loaded within silicone nerve

conduits showed greater peripheral nerve regeneration as compared to conduits with free NGF loaded (Xu et al. 2003). Pfister et al. (2007) has reviewed other similar systems of NGF loaded microspheres for nerve regeneration. Excellent reviews may be found in the contemporary literature on the important considerations with protein encapsulation within polymer systems (Mohamed and Van Der Walle 2008, Van De Weert et al. 2000).

Hydrogel microparticles have also been used extensively to encapsulate proteins for drug delivery in tissue engineering. Some of the earliest hydrogel microparticle, or microgel, systems were the alginate beads, easily formed by dropping or spraying into cationic solutions, such as calcium (Wee and Gombotz 1998, Tønnesen and Karlsen 2002). Alginate microbeads are still widely used for delivery of FGF and osteogenic proteins (Lee et al. 2009, Moya et al. 2010a,b), as well as for microencapsulation of chondrocytes for coculture with bone marrow stem cells for osteogenic differentiation (Thompson et al. 2009). Along with alginate, microgels based on collagen (Nagai et al. 2010), gelatin (Li et al. 2010), and hyaluronan and its derivatives (Gaffney et al. 2010) are all used to deliver a variety of proteins.

Aside from encapsulation of proteins, much work has been done on the surface functionalization of microparticles for cellular interaction and proliferative effects. Surface modification of PLGA microspheres with an amine-terminated dendrimer improved long-term proliferation of chondrocytes without observed changes in the cell phenotype, as compared to monolayer culture systems (Thissen et al. 2006). Additionally, surface functionalization of polystyrene magnetic microbeads with the DLL4 notch ligand used in coculture has been shown to efficiently generate T cells from mouse bone marrow hematopoietic stem cells (Taqvi et al. 2006).

55.4.1.3 Gel-Based and Gel-Like Systems

Several gel-based and gel-like systems also offer the advantage of being injectable *in vivo*, taking on the shape of the tissue cavity. Additionally, the hydrophilic matrix structures of gels offer the advantage of high compatibility with the majority of proteins and peptides of interest in tissue engineering. Gelation occurs by several methods, including thermally- or pH-induced cross-linking (Zisch et al. 2003a,b), sol-gel transitions, and physical gelation. Early injectable gel-like systems include those composed of alginate, gelatin, and collagen (Wee and Gombotz 1998, Sano et al. 1998, Ikada and Tabata 1998). Although gel systems for protein delivery are a classical form of drug delivery, they have in recent decades gained much significance as a combinatorial tissue engineering substrate and drug delivery medium. As such, much attention will be directed toward these systems in the following section.

55.4.2 Drug Delivery from Tissue Engineering Scaffolds and Matrices

As the previous systems focused on controlled delivery strategies separate from a tissue engineering substrate, herein referred to as the substrate, much work has been done in using the substrate itself as a controlled release medium. Both scaffolds and matrices have been used to achieve desirable release strategies, where scaffolds refer to macro- or microporous substrates to provide structural support, and matrices refer to more or less continuous nanoporous substrates, such as gels. Several strategies may be used to achieve the desired effect, including the admixing of drugs within matrices, entrapment of drugs within matrices, covalent binding of drugs to the matrix, affinity binding of drugs to the matrix, and microparticles embedded in matrices for delivery of drug.

55.4.2.1 Drugs Admixed with Cell Substrate

A common form of drug delivery from the tissue engineering substrate is by simply admixing the drug with the cell substrate. As previously discussed, various mechanisms may be used to control the release, with the desired effect usually being prolongation of the release. In the case of prolongation, even a small degree of affinity between the substrate materials may serve to slow the release rate. Additionally, poorly soluble drugs may dissolve over time and provide a sustained release profile. The cell substrate may also

serve as a diffusion-limiting factor, providing drug release in a localized area of the scaffold, also known as zonal release.

Several examples of drugs admixed within a cell substrate have already resulted in commercial products, especially the release of bone morphogenetic proteins from collagen sponges and matrices (Seeherman and Wozney 2005). Aside from the collagen sponge, other substrates for BMP delivery have included calcium phosphate cement, both of which have shown excellent orthopedic tissue regeneration *in vivo* (Seeherman and Wozney 2005, Seeherman et al. 2006, 2008, 2010). Gelatin, a form of denatured collagen, has also been used both in its native self-assembled gel form and as a cross-linked gel to deliver growth factors. During fabrication, gelatin may be modified into either negatively or positively charged gels at physiological pH in order to create low-affinity electrostatic interactions with a protein drug (Thyagarajapuram et al. 2007, Young et al. 2005, Ikada and Tabata 1998). These low-affinity electrostatic interactions of proteins with gelatin have been shown to prolong release rates as compared to nonelectrostatic gelatin (Thyagarajapuram et al. 2007, Yamamoto et al. 2006, Ozeki and Tabata 2006, Guo et al. 2010).

Growth factors have also been admixed with hydrophobic polymers, such as PLGA, to provide a sustained release profile. For example, early work by Richardson et al., used combinatorial PLGA scaffold and particulate systems to achieve dual growth factor delivery. In this case, one growth factor (VEGF) is admixed with particulate polymer along with microsphere-encapsulated growth factor (PDGF), which is then processed into a porous cell scaffold. By successfully achieving sustained release of both growth factors, improved angiogenesis was observed as compared to either growth factor alone (Richardson et al. 2001).

55.4.2.2 Drugs Entrapped within Cell Substrate

It is also possible to engineer hydrogel cell carriers with structures capable of physically trapping drug molecules within the cell carrier's molecular structure, most commonly, with hydrogels. Hydrogels form somewhat of a three-dimensional network structure, where the molecular weight and structure of the cross-linking molecule determines the pore size. If the pore size of the hydrogel is sufficiently close to the size of the drug of interest, then the release of the drug from the matrix could then be inhibited by the network structure (Lustig and Peppas 1988). In this case, drug release would be driven either by polymer swelling or degradation of cross-links. Commonly, the drug is loaded with the polymer precursor solutions, and the hydrogel network is then reacted to form around the drug (Lin and Anseth 2009, Jia and Kiick 2009, Metters and Hubbell 2005).

Common materials used for these systems include PEG, fibrin, collagen, and hyaluronic acid (Suri and Schmidt 2009, Lin and Anseth 2009, Jia and Kiick 2009, Metters and Hubbell 2005, Lutolf et al. 2003, Sakiyama-Elbert and Hubbell 2000). A study by van de Wetering et al. illustrated the ability to tune the release of human growth hormone (hGH) from various PEG-based hydrogels using different cross-linked network architectures. Tighter cross-linked networks were able to significantly prolong the release of hGH over loosely formed networks (Van De Wetering et al. 2005). In addition to single-component hydrogel networks, hybrid hydrogels of interpenetrated networks or semi-interpenetrated networks are similarly able to form diverse network structures of varying pore sizes and cross-linking densities (Suri and Schmidt 2009).

Due to the tight nanoporous properties of these hydrogels, which may prevent cell intergrowth, these systems are often employed as particulate systems within a scaffold. Scott et al. created PEG-based scaffolds using a modular assembly system of hydrogel microspheres with encapsulated sphingosine 1-phosphate (S1P), microspheres for structural support, and porogen particles. The resulting macroporous scaffolds with incorporated S1P-loaded microspheres showed an approximate twofold increase in rate of cell migration into the scaffold as compared to scaffolds without S1P-loaded microspheres (Scott et al. 2010). Alternatively, cell ingrowth into such nanoporous hydrogels may be achieved by incorporating enzyme-cleavable moieties into the network structure, thus allowing a cell to easily infiltrate the hydrogel by secreting ECM-degrading enzymes. Examples of these ingrowth matrices with entrapped drug include fibrin-based matrices for controlled release of NGF (Sakiyama-Elbert and Hubbell 2000) and

PEG-based matrices with matrix metalloproteinase substrates as cross-linkers with entrapped rhBMP (Lutolf et al. 2003).

55.4.2.3 Covalent Binding of Drugs to Cell Substrate

It is oftentimes advantageous, if not required, to covalently bind drugs to the cell substrate itself. For example, adhesion peptides must be bound to the substrate in order to elicit the correct response in the cell for migration. Although adhesion sites are already present in naturally derived materials, such as collagen and fibrin, cell substrates composed of synthetic components (such as PEG) must include adhesion peptides to effectively promote cell adhesion and signaling. Scaffolds of naturally derived materials may also benefit from adhesion peptide or growth factor incorporation to provide a higher degree of control over cell migration and differentiation.

In a study by Hern and Hubbell, the cell adhesion peptide RGD (Arg–Gly–Asp) was covalently bound to PEG-based hydrogels either directly or using a PEG spacer arm, and compared to a nonadhesive control peptide (Hern and Hubbell 1998). Due to the greater steric availability of the adhesion peptide bound to the PEG spacer arm, specific mediation of cell spreading was observed in contrast to non-specific cell spreading observed in direct conjugation of the peptide to the scaffold. Wacker et al. compared S1P-induced endothelial cell migration in PEG hydrogels with either linear or cyclic RGD peptide sequences for implications in implant endothelialization speed following implantation (Wacker et al. 2008). Although linear RGD produced greater adhesion strength and long-term adhesion on exposure to shear stress from fluid flow, cyclic RGD produced a faster rate of endothelial cell migration. These studies illustrate the complexity in the incorporation of adhesion peptides into scaffolds, from determining the optimal conformation for steric availability, and finding the balance between high adhesion strength and higher migration rates for tissue regeneration.

In addition to covalent binding of adhesion peptides into cell substrates, drugs may also be covalently bound to the substrates in order to achieve directed differentiation, interaction, or promote migration of a specific cell phenotype. For example, vascularization of regenerated tissues is necessary for nutrient delivery *in vivo*, and requires high-order cell and tissue arrangement controlled by growth factors. Leslie-Barbick et al. were able to achieve endothelial cell tubulogenesis in 2D and 3D PEG-based scaffolds by covalently attaching VEGF and an RGD adhesion peptide, in comparison to RGD-immobilized scaffolds alone (Leslie-Barbick et al. 2009). Similarly, a study by Chiu and Radisic showed enhanced vascularization of endothelial cells in collagen scaffolds with immobilized VEGF and angiopoietin-1 over collagen scaffolds alone and soluble factor in collagen scaffolds alone (Chiu and Radisic 2010).

Furthermore, some drugs require binding to the substrate such that they are released only in response to cell ingrowth, for example, by enzymatic cleavage, providing on-demand delivery of the drug. In the case of bone regeneration, high concentrations of drug may result in overactivation of cells locally, and thus, abnormal tissue regeneration. By incorporating an enzyme-cleavable prodrug of a parathyroid hormone fragment into a cell ingrowth matrix, Arrighi et al. (2009) were able to circumvent osteoclast overactivation and show dose-dependent bone healing *in vivo*.

55.4.2.4 Affinity Binding of Drugs to Cell Substrate

Another strategy for binding drugs to a cell substrate involves the use of affinity binding molecules that have strong interactions with several growth factors and other proteins. A comprehensive review of the myriad molecules is outside the scope of this chapter, and we refer the reader to excellent reviews in the literature (Uebersax et al. 2009, Maxwell et al. 2005). Instead, we will focus on two groups of common affinity binding molecules: heparin/heparan sulfate and fibrin/fibrinogen. Other molecules of interest include laminins, collagens, glycosaminoglycans (GAGs), DNA, poly(amino acids), avidin-biotin (Baeza et al. 2010, Clapper et al. 2008, Segura et al. 2005), and other polysaccharides.

Heparan sulfate and heparin are GAGs that are present in a variety of tissues throughout the body, regulate many processes, and bind a variety of proteins or growth factors. There are several growth

factors that bind to both heparan sulfate and heparin, and are known as heparin binding growth factors (HBGFs). Commonly noted HBGFs include members of the families of FGF, HGF, and VEGFs. Heparan sulfate has been used in micropatterned PEG-based scaffolds for spatiotemporal release of growth factors and multilineage differentiation (Mapili et al. 2005), and widely in other applications (Woodruff et al. 2007, Pieper et al. 2002, Chintala et al. 1995). However, due to lower costs, heparin is more widely used in cell substrates for HBGFs, and has been incorporated into gels for osteogenic differentiation (Benoit et al. 2007, Benoit and Anseth 2005), endothelialization (Mcgonigle et al. 2008, Tae et al. 2006), nerve regeneration (Wood et al. 2009, 2010), and a variety of other applications (Uebersax et al. 2009, Kiick 2008, Nie et al. 2007, Zhang et al. 2006).

Fibrin and fibrinogen are proteins found in the blood that are critical in the clotting and wound sealing process; cleavage of fibrinogen by thrombin yields fibrin (Spicer and Mikos 2010, Uebersax et al. 2009, Sierra 1993). Fibrinogen is used primarily in fibrin glue systems, where a mixture of fibrinogen solution and calcium-rich thrombin solution are codelivered for surgical use as a sealant or hemostatic agent (Sierra 1993, Spicer and Mikos 2010), but has recently gained more interest as a cell substrate with protein immobilization capabilities (Spicer and Mikos 2010). Fibrin is widely used for its affinity binding characteristics with other proteins to slowly release growth factors, particularly VEGF and FGF, to loaded cells within the gel (Ehrbar et al. 2008, Losi et al. 2010). Work by the Swartz group used VEGF bound to fibrin-based matrices along with interstitial fluid flow in order to direct blood and lymphatic capillary morphogenesis, resulting in organized tubular structures (Helm et al. 2005, 2007). Hybrid PEG and fibrin matrices have also been used to create cell substrates with the ability to entrap, covalently conjugate, and affinity bind growth factors, and have tunable mechanical properties for directed differentiation (Drinnan et al. 2010, Zhang et al. 2010). PEG-based materials that mimic the fibrin clotting cascade, known as fibrin analogs, have also been created for tissue engineering applications (Ehrbar et al. 2007).

55.4.2.5 Particulate Systems within Cell Substrate

Microparticles, and to a lesser extent, nanoparticles, may often be incorporated into cell substrates to provide another mechanism of controlled drug release to the cells. The complexities in these systems are vast when considering the combinations of material properties, release profiles, release mechanisms, or substrate construct. In some cases, the particles may be hydrophobic and rely on hydrolysis to control the release of growth factors, as in the release of BMPs from PLGA microspheres in scaffolds and matrices (Ji et al. 2010, Gavenis et al. 2010, Li et al. 2009a, Wang et al. 2009). In other cases, the particles provide a facile means in which to provide controlled delivery of growth factors *in vivo*, for example, by injection (Li et al. 2009b, Sasaki et al. 2008, Inoue et al. 2006) or intratracheally (Hirose et al. 2008). Particles may also serve as cell carriers themselves, or assemble into a cell substrate at a later stage (Scott et al. 2010).

55.5 Outlook

The concepts of controlled release and controlled ligand presentation in tissue engineering are gaining increasing interest and are now considered to be integral to the success of tissue regeneration and cell engineering. The merging of the two complementary fields, tissue engineering and drug delivery, is providing exciting new directions in regenerative medicine. Although significant progress has been made in incorporating temporally controlled growth factor release from scaffolds, as well as in efficient presentation of adhesive ligands, there remain considerable challenges in mimicking the complex, spatially and temporally patterned microenvironments of tissues *in vivo*. The complicated milieu of growth factors, morphogens, extracellular matrix components, and cell signaling must be accurately reproduced if complex, functionally relevant tissue structures are to be regenerated and engineered. Future directions in tissue engineering therefore must incorporate and develop new drug delivery concepts where multiple bioactive agents can be available to progenitor cells in a highly spatially controlled manner and at levels and sequences relevant to the differentiation kinetics of specific tissues.

References

- Aimetti, A. A., A. J. Machen, and K. S. Anseth. 2009. Poly(ethylene glycol) hydrogels formed by thiol-ene photopolymerization for enzyme-responsive protein delivery. *Biomaterials* 30: 6048–54.
- Amiji, M. M. 2005. *Polymeric Gene Delivery: Principles and Applications*. Boca Raton, FL: CRC Press.
- Annabi, N., J. W. Nichol, X. Zhong et al. 2010. Controlling the porosity and microarchitecture of hydrogels for tissue engineering. *Tissue Eng Pt B Rev* 16: 371–83.
- Arrighi, I., S. Mark, M. Alvisi et al. 2009. Bone healing induced by local delivery of an engineered parathyroid hormone prodrug. *Biomaterials* 30: 1763–71.
- Athanasiou, K. A., C. M. Agrawal, F. A. Barber, and S. S. Burkhart. 1998. Orthopaedic applications for plaga biodegradable polymers. *Arthroscopy* 14: 726–37.
- Baeza, A., I. Izquierdo-Barba, and M. Vallet-Regí. 2010. Biotinylation of silicon-doped hydroxyapatite: A new approach to protein fixation for bone tissue regeneration. *Acta Biomater* 6: 743–49.
- Becker, C. and A. Göpferich. 2007. Drug delivery. In *Tissue Engineering*, ed. Fisher, J. P., A. G. Mikos and J. D. Bronzino (Eds.) 600. Boca Raton: CRC Press.
- Benoit, D. S. W. and K. S. Anseth. 2005. Heparin functionalized PEG gels that modulate protein adsorption for hmsc adhesion and differentiation. *Acta Biomater* 1: 461–70.
- Benoit, D. S. W., A. R. Durney, and K. S. Anseth. 2007. The effect of heparin-functionalized PEG hydrogels on three-dimensional human mesenchymal stem cell osteogenic differentiation. *Biomaterials* 28: 66–77.
- Biondi, M., F. Ungaro, F. Quaglia, and P. A. Netti. 2008. Controlled drug delivery in tissue engineering. *Adv Drug Deliv Rev* 60: 229–42.
- Boonthekul, T. and D. J. Mooney. 2003. Protein-based signaling systems in tissue engineering. *Curr Opin Biotechnol* 14: 559–65.
- Boussif, O., F. Lezoualc'h, M. A. Zanta et al. 1995. A versatile vector for gene and oligonucleotide transfer into cells in culture and *in vivo*: Polyethylenimine. *PNAS* 92: 7297–301.
- Brunner, A., K. Mäder, and A. Göpferich. 1999. Ph and osmotic pressure inside biodegradable microspheres during erosion. *Pharm Res* 16: 847–53.
- Caldorera-Moore, M., N. Guimard, L. Shi, and K. Roy. 2010. Designer nanoparticles: Incorporating size, shape and triggered release into nanoscale drug carriers. *Expert Opin Drug Deliv* 7: 479–95.
- Caldorera-Moore, M. and N. A. Peppas. 2009. Micro- and nanotechnologies for intelligent and responsive biomaterial-based medical systems. *Adv Drug Deliv Rev* 61: 1391–401.
- Cao, Y. and R. Langer. 2008. A review of Judah Folkman's remarkable achievements in biomedicine. *PNAS* 105: 13203.
- Chen, R. R. and D. J. Mooney. 2003. Polymeric growth factor delivery strategies for tissue engineering. *Pharm Res* 20: 1103–12.
- Chintala, S. K., R. R. Miller, and C. A. Mcdevitt. 1995. Role of heparan sulfate in the terminal differentiation of growth plate chondrocytes. *Arch Biochem Biophys* 316: 227–34.
- Chiu, L. L. Y. and M. Radisic. 2010. Scaffolds with covalently immobilized VEGF and angiopoietin-1 for vascularization of engineered tissues. *Biomaterials* 31: 226–41.
- Clapper, J. D., M. E. Pearce, C. A. Guymon, and A. K. Salem. 2008. Biotinylated biodegradable nanotemplated hydrogel networks for cell interactive applications. *Biomacromolecules* 9: 1188–94.
- Drinnan, C. T., G. Zhang, M. A. Alexander, A. S. Pulido, and L. J. Suggs. 2010. Multimodal release of transforming growth factor-beta1 and the bb isoform of platelet derived growth factor from pegylated fibrin gels. *J Control Release* 147: 180–86.
- Ehrbar, M., S. C. Rizzi, R. Hlushchuk et al. 2007. Enzymatic formation of modular cell-instructive fibrin analogs for tissue engineering. *Biomaterials* 28: 3856–66.
- Ehrbar, M., S. M. Zeisberger, G. P. Raebler et al. 2008. The role of actively released fibrin-conjugated VEGF for VEGF receptor 2 gene activation and the enhancement of angiogenesis. *Biomaterials* 29: 1720–29.

- Eliason, J. F. 2001. Pegylated cytokines: Potential application in immunotherapy of cancer. *BioDrugs* 15: 705–11.
- Fisher, O. Z., A. Khademhosseini, R. Langer, and N. A. Peppas. 2010. Bioinspired materials for controlling stem cell fate. *Acc Chem Res* 43: 419–28.
- Fu, K., D. W. Pack, A. M. Klibanov, and R. Langer. 2000. Visual evidence of acidic environment within degrading poly(lactic-co-glycolic acid) (PLGA) microspheres. *Pharm Res* 17: 100–16.
- Gaffney, J., S. Matou-Nasri, M. Grau-Olivares and M. Slevin. 2010. Therapeutic applications of hyaluronan. *Mol Biosyst* 6: 437–43.
- Gallardo, D., B. Skalsky, and P. Kleinebudde. 2008. Controlled release solid dosage forms using combinations of (meth)acrylate copolymers. *Pharm Dev Technol* 13: 413–23.
- Gavenis, K., U. Schneider, J. Groll, and B. Schmidt-Rohlfing. 2010. BMP-7-loaded PGLA microspheres as a new delivery system for the cultivation of human chondrocytes in a collagen type I gel: The common nude mouse model. *Int J Artif Organs* 33: 45–53.
- Glangchai, L. C., M. Caldorera-Moore, L. Shi, and K. Roy. 2008. Nanoimprint lithography based fabrication of shape-specific, enzymatically-triggered smart nanoparticles. *J Control Release* 125: 263–72.
- Gobin, A. S. and J. L. West. 2002. Cell migration through defined, synthetic ecm analogs. *FASEB J* 16: 751–53.
- Gombotz, W. R. and D. K. Pettit. 1995. Biodegradable polymers for protein and peptide drug delivery. *Bioconjug Chem* 6: 332–51.
- Göpferich, A. 1996. Mechanisms of polymer degradation and erosion. *Biomaterials* 17: 103–14.
- Guo, X., H. Park, S. Young et al. 2010. Repair of osteochondral defects with biodegradable hydrogel composites encapsulating marrow mesenchymal stem cells in a rabbit model. *Acta Biomater* 6: 39–47.
- Haller, M. F. and W. M. Saltzman. 1998. Nerve growth factor delivery systems. *J Control Release* 53: 1–6.
- Heller, J. 1985. Controlled drug release from poly(ortho esters). *Ann N Y Acad Sci* 446: 51–66.
- Helm, C.-L. E., M. E. Fleury, A. H. Zisch, F. Boschetti, and M. A. Swartz. 2005. Synergy between interstitial flow and VEGF directs capillary morphogenesis *in vitro* through a gradient amplification mechanism. *PNAS* 102: 15779–84.
- Helm, C.-L. E., A. Zisch, and M. A. Swartz. 2007. Engineered blood and lymphatic capillaries in 3-d VEGF-fibrin-collagen matrices with interstitial flow. *Biotechnol Bioeng* 96: 167–76.
- Hern, D. and J. Hubbell. 1998. Incorporation of adhesion peptides into nonadhesive hydrogels useful for tissue resurfacing. *J Biomed Mater Res* 39: 266–76.
- Hirose, K., A. Marui, Y. Arai et al. 2008. Novel approach with intratracheal administration of microgelatin hydrogel microspheres incorporating basic fibroblast growth factor for rescue of rats with monocrotaline-induced pulmonary hypertension. *J Thorac Cardiovasc Surg* 136: 1250–56.
- Hubbell, J. 2008. Controlled release strategies in tissue engineering. In *Tissue Engineering*, ed. Blitterswijk, C. A. V. and P. Thomsen (Eds.) 740. Boston: Elsevier/Academic Press.
- Ikada, Y. and Y. Tabata. 1998. Protein release from gelatin matrices. *Adv Drug Deliv Rev* 31: 287–301.
- Inoue, A., K. A. Takahashi, Y. Arai et al. 2006. The therapeutic effects of basic fibroblast growth factor contained in gelatin hydrogel microspheres on experimental osteoarthritis in the rabbit knee. *Arthritis Rheum* 54: 264–70.
- Jain, J. P., S. Modi, A. J. Domb, and N. Kumar. 2005. Role of polyanhydrides as localized drug carriers. *J Control Release* 103: 541–63.
- Ji, Y., G. P. Xu, Z. P. Zhang et al. 2010. BMP-2/PLGA delayed-release microspheres composite graft, selection of bone particulate diameters, and prevention of aseptic inflammation for bone tissue engineering. *Ann Biomed Eng* 38: 632–39.
- Jia, X. and K. L. Kiick. 2009. Hybrid multicomponent hydrogels for tissue engineering. *Macromol Biosci* 9: 140–56.
- Kempen, D. H. R., L. Lu, T. E. Hefferan et al. 2008. Retention of *in vitro* and *in vivo* BMP-2 bioactivities in sustained delivery vehicles for bone tissue engineering. *Biomaterials* 29: 3245–52.
- Khare, A. R. and N. A. Peppas. 1993. Release behavior of bioactive agents from pH-sensitive hydrogels. *J Biomater Sci Polym Ed* 4: 275–89.

- Khare, A. R. and N. A. Peppas. 1995. Swelling/deswelling of anionic copolymer gels. *Biomaterials* 16: 559–67.
- Kiick, K. L. 2008. Peptide- and protein-mediated assembly of heparinized hydrogels. *Soft Matter* 4: 29–37.
- Klein, T. J., J. Malda, R. L. Sah, and D. W. Huttmacher. 2009. Tissue engineering of articular cartilage with biomimetic zones. *Tissue Eng Part B Rev* 15: 143–57.
- Langer, R. and N. Peppas. 2003. Advances in biomaterials, drug delivery, and bionanotechnology. *AIChE J* 49: 2990–3006.
- Langer, R. and J. P. Vacanti. 1993. Tissue engineering. *Science* 260: 920–26.
- Lavan, D. A., T. McGuire, and R. Langer. 2003. Small-scale systems for *in vivo* drug delivery. *Nat Biotechnol* 21: 1184–91.
- Lee, M., W. Li, R. K. Siu et al. 2009. Biomimetic apatite-coated alginate/chitosan microparticles as osteogenic protein carriers. *Biomaterials* 30: 6094–101.
- Leslie-Barbick, J. E., J. J. Moon, and J. L. West. 2009. Covalently-immobilized vascular endothelial growth factor promotes endothelial cell tubulogenesis in poly(ethylene glycol) diacrylate hydrogels. *J Biomater Sci Polym Ed* 20: 1763–79.
- Li, B., T. Yoshii, A. E. Hafeman et al. 2009a. The effects of rhbmp-2 released from biodegradable polyurethane/microsphere composite scaffolds on new bone formation in rat femora. *Biomaterials* 30: 6768–79.
- Li, L., H. Okada, G. Takemura et al. 2009b. Sustained release of erythropoietin using biodegradable gelatin hydrogel microspheres persistently improves lower leg ischemia. *J Am Coll Cardiol* 53: 2378–88.
- Li, M., X. Liu, X. Liu, and B. Ge. 2010. Calcium phosphate cement with BMP-2-loaded gelatin microspheres enhances bone healing in osteoporosis: A pilot study. *Clin Orthop Relat Res* 468: 1978–85.
- Lin, C.-C. and K. S. Anseth. 2009. PEG hydrogels for the controlled release of biomolecules in regenerative medicine. *Pharm Res* 26: 631–43.
- Liu, F. and A. W. Basit. 2010. A paradigm shift in enteric coating: Achieving rapid release in the proximal small intestine of man. *J Control Release* 147: 242–45.
- Losi, P., E. Briganti, A. Magera et al. 2010. Tissue response to poly(ether)urethane-polydimethylsiloxane-fibrin composite scaffolds for controlled delivery of pro-angiogenic growth factors. *Biomaterials* 31: 5336–44.
- Löwik, D. W. P. M., E. H. P. Leunissen, M. Van Den Heuvel, M. B. Hansen, and J. C. M. Van Hest. 2010. Stimulus responsive peptide based materials. *Chem Soc Rev* 39: 3394–412.
- Lucke, A., J. Kiermaier, and A. Göpferich. 2002. Peptide acylation by poly(alpha-hydroxy esters). *Pharm Res* 19: 175–81.
- Lustig, S. and N. Peppas. 1988. Solute diffusion in swollen membranes. IX. Scaling laws for solute diffusion in gels. *J Appl Polym Sci* 36: 735–47.
- Lutolf, M. P., F. E. Weber, H. G. Schmoekel et al. 2003. Repair of bone defects using synthetic mimetics of collagenous extracellular matrices. *Nat Biotechnol* 21: 513–18.
- Manning, M. C., D. K. Chou, B. M. Murphy, R. W. Payne, and D. S. Katayama. 2010. Stability of protein pharmaceuticals: An update. *Pharm Res* 27: 544–75.
- Manning, M. C., K. Patel, and R. T. Borchardt. 1989. Stability of protein pharmaceuticals. *Pharm Res* 6: 903–18.
- Mapili, G., Y. Lu, S. Chen, and K. Roy. 2005. Laser-layered microfabrication of spatially patterned functionalized tissue-engineering scaffolds. *J Biomed Mater Res B* 75: 414–24.
- Maxwell, D. J., B. C. Hicks, S. Parsons, and S. E. Sakiyama-Elbert. 2005. Development of rationally designed affinity-based drug delivery systems. *Acta Biomater* 1: 101–13.
- McGonigle, J. S., G. Tae, P. S. Stayton, A. S. Hoffman, and M. Scatena. 2008. Heparin-regulated delivery of osteoprotegerin promotes vascularization of implanted hydrogels. *J Biomater Sci Polym Ed* 19: 1021–34.
- Metters, A. and J. A. Hubbell. 2005. Network formation and degradation behavior of hydrogels formed by michael-type addition reactions. *Biomacromolecules* 6: 290–301.
- Miyata, T., T. Uragami, and K. Nakamae. 2002. Biomolecule-sensitive hydrogels. *Adv Drug Deliv Rev* 54: 79–98.
- Mohamed, F. and C. F. Van Der Walle. 2008. Engineering biodegradable polyester particles with specific drug targeting and drug release properties. *J Pharm Sci* 97: 71–87.

- Molineux, G. 2002. Pegylation: Engineering improved pharmaceuticals for enhanced therapy. *Cancer Treat Rev* 28 Suppl A: 13–16.
- Molineux, G. 2003. Pegylation: Engineering improved biopharmaceuticals for oncology. *Pharmacotherapy* 23: 3S-8S.
- Moya, M. L., M.-H. Cheng, J.-J. Huang et al. 2010a. The effect of fgf-1 loaded alginate microbeads on neovascularization and adipogenesis in a vascular pedicle model of adipose tissue engineering. *Biomaterials* 31: 2816–26.
- Moya, M. L., M. R. Garfinkel, X. Liu et al. 2010b. Fibroblast growth factor-1 (fgf-1) loaded microbeads enhance local capillary neovascularization. *J Surg Res* 160: 208–12.
- Nagai, N., N. Kumasaka, T. Kawashima et al. 2010. Preparation and characterization of collagen microspheres for sustained release of VEGF. *J Mater Sci Mater Med* 21: 1891–98.
- Nie, T., A. Baldwin, N. Yamaguchi, and K. L. Kiick. 2007. Production of heparin-functionalized hydrogels for the development of responsive and controlled growth factor delivery systems. *J Control Release* 122: 287–96.
- Nomi, M., A. Atala, P. D. Coppi, and S. Soker. 2002. Principles of neovascularization for tissue engineering. *Mol Aspects Med* 23: 463–83.
- Ozeki, M. and Y. Tabata. 2006. Interaction of hepatocyte growth factor with gelatin as the carrier material. *J Biomater Sci Polym Ed* 17: 163–75.
- Peppas, N. A., P. Bures, W. Leobandung, and H. Ichikawa. 2000. Hydrogels in pharmaceutical formulations. *Eur J Pharm Biopharm* 50: 27–46.
- Pfister, L. A., M. Papaloizos, H. P. Merkle, and B. Gander. 2007. Nerve conduits and growth factor delivery in peripheral nerve repair. *J Peripher Nerv Syst* 12: 65–82.
- Pieper, J. S., T. Hafmans, P. B. Van Wachem et al. 2002. Loading of collagen-heparan sulfate matrices with bFGF promotes angiogenesis and tissue generation in rats. *J Biomed Mater Res* 62: 185–94.
- Putnam, D., C. A. Gentry, D. W. Pack, and R. Langer. 2001. Polymer-based gene delivery with low cytotoxicity by a unique balance of side-chain termini. *PNAS* 98: 1200–5.
- Reynolds, A., D. Leake, Q. Boese et al. 2004. Rational siRNA design for RNA interference. *Nat Biotechnol* 22: 326–30.
- Richardson, T. P., M. C. Peters, A. B. Ennett, and D. J. Mooney. 2001. Polymeric system for dual growth factor delivery. *Nat Biotechnol* 19: 1029–34.
- Roberts, M. J., M. D. Bentley, and J. M. Harris. 2002. Chemistry for peptide and protein pegylation. *Adv Drug Deliv Rev* 54: 459–76.
- Robinson, S. N. and J. E. Talmadge. 2002. Sustained release of growth factors. *In Vivo* 16: 535–40.
- Sakiyama-Elbert, S. E., and J. A. Hubbell. 2000. Controlled release of nerve growth factor from a heparin-containing fibrin-based cell ingrowth matrix. *J Control Release* 69: 149–58.
- Saltzman, W. M. and S. Baldwin. 1998. Materials for protein delivery in tissue engineering. *Adv Drug Deliv Rev* 33: 71–86.
- Saltzman, W. M. and W. L. Olbricht. 2002. Building drug delivery into tissue engineering. *Nat Rev Drug Discov* 1: 177–86.
- Sánchez, A., M. Tobío, L. González, A. Fabra, and M. J. Alonso. 2003. Biodegradable micro- and nanoparticles as long-term delivery vehicles for interferon-alpha. *Eur J Pharm Sci* 18: 221–29.
- Sano, A., T. Hojo, M. Maeda, and K. Fujioka. 1998. Protein release from collagen matrices. *Adv Drug Deliv Rev* 31: 247–66.
- Sasaki, N., T. Minami, K. Yamada et al. 2008. *In vivo* effects of intra-articular injection of gelatin hydrogen microspheres containing basic fibroblast growth factor on experimentally induced defects in third metacarpal bones of horses. *Am J Vet Res* 69: 1555–59.
- Sato, H. 2002. Enzymatic procedure for site-specific pegylation of proteins. *Adv Drug Deliv Rev* 54: 487–504.
- Scott, E. A., M. D. Nichols, R. Kuntz-Willits, and D. L. Elbert. 2010. Modular scaffolds assembled around living cells using poly(ethylene glycol) microspheres with macroporation via a non-cytotoxic porogen. *Acta Biomater* 6: 29–38.

- Seeherman, H. J., J. M. Archambault, S. A. Rodeo et al. 2008. Rrhbmp-12 accelerates healing of rotator cuff repairs in a sheep model. *J Bone Joint Surg Am* 90: 2206–19.
- Seeherman, H., R. Li, M. Boussein et al. 2006. Rrhbmp-2/calcium phosphate matrix accelerates osteotomy-site healing in a nonhuman primate model at multiple treatment times and concentrations. *J Bone Joint Surg Am* 88: 144–60.
- Seeherman, H. J., X. J. Li, M. L. Boussein, and J. M. Wozney. 2010. Rrhbmp-2 induces transient bone resorption followed by bone formation in a nonhuman primate core-defect model. *J Bone Joint Surg Am* 92: 411–26.
- Seeherman, H. and J. M. Wozney. 2005. Delivery of bone morphogenetic proteins for orthopedic tissue regeneration. *Cytokine Growth Factor Rev* 16: 329–45.
- Segura, T., B. C. Anderson, P. H. Chung et al. 2005. Crosslinked hyaluronic acid hydrogels: A strategy to functionalize and pattern. *Biomaterials* 26: 359–71.
- Sierra, D. H. 1993. Fibrin sealant adhesive systems: A review of their chemistry, material properties and clinical applications. *J Biomater Appl* 7: 309–52.
- Singh, A., S. Suri, and K. Roy. 2009. In-situ crosslinking hydrogels for combinatorial delivery of chemokines and sirna-DNA carrying microparticles to dendritic cells. *Biomaterials* 30: 5187–200.
- Spicer, P. P. and A. G. Mikos. 2010. Fibrin glue as a drug delivery system. *J Control Release* 148: 49–55.
- Steinbüchel, A. and S. Matsumura. 2003. *Biopolymers: Miscellaneous Biopolymers and Biodegradation of Synthetic Polymers*. Weinheim: Wiley-VCH.
- Suri, S. and C. E. Schmidt. 2009. Photopatterned collagen-hyaluronic acid interpenetrating polymer network hydrogels. *Acta Biomater* 5: 2385–97.
- Tabata, Y. 2003. Tissue regeneration based on growth factor release. *Tissue Eng* 9 Suppl 1: S5–15.
- Tae, G., M. Scatena, P. S. Stayton, and A. S. Hoffman. 2006. PEG-cross-linked heparin is an affinity hydrogel for sustained release of vascular endothelial growth factor. *J Biomater Sci Polym Ed* 17: 187–97.
- Taqvi, S., L. Dixit, and K. Roy. 2006. Biomaterial-based notch signaling for the differentiation of hematopoietic stem cells into t cells. *J Biomed Mater Res A* 79: 689–97.
- Tauro, J. R., B.-S. Lee, S. S. Lateef, and R. A. Gemeinhart. 2008. Matrix metalloprotease selective peptide substrates cleavage within hydrogel matrices for cancer chemotherapy activation. *Peptides* 29: 1965–73.
- Thissen, H., K.-Y. Chang, T. A. Tebb et al. 2006. Synthetic biodegradable microparticles for articular cartilage tissue engineering. *J Biomed Mater Res A* 77: 590–98.
- Thompson, A. D., M. W. Betz, D. M. Yoon, and J. P. Fisher. 2009. Osteogenic differentiation of bone marrow stromal cells induced by coculture with chondrocytes encapsulated in three-dimensional matrices. *Tissue Eng Pt A* 15: 1181–90.
- Thyagarajapuram, N., D. Olsen, and C. R. Middaugh. 2007. The structure, stability, and complex behavior of recombinant human gelatins. *J Pharm Sci* 96: 3363–78.
- Tønnesen, H. H. and J. Karlsen. 2002. Alginate in drug delivery systems. *Drug Dev Ind Pharm* 28: 621–30.
- Truskey, G. A., F. Yuan, and D. F. Katz. 2004. *Transport Phenomena in Biological Systems*. Upper Saddle River: Pearson/Prentice Hall.
- Uebersax, L., H. P. Merkle, and L. Meinel. 2009. Biopolymer-based growth factor delivery for tissue repair: From natural concepts to engineered systems. *Tissue Eng Pt B Rev* 15: 263–89.
- Van De Weert, M., W. E. Hennink, and W. Jiskoot. 2000. Protein instability in poly(lactic-co-glycolic acid) microparticles. *Pharm Res* 17: 1159–67.
- Van De Wetering, P., A. T. Metters, R. G. Schoenmakers, and J. A. Hubbell. 2005. Poly(ethylene glycol) hydrogels formed by conjugate addition with controllable swelling, degradation, and release of pharmaceutically active proteins. *J Control Release* 102: 619–27.
- Vartak, D. G. and R. A. Gemeinhart. 2007. Matrix metalloproteases: Underutilized targets for drug delivery. *J Drug Target* 15: 1–20.
- Wacker, B. K., S. K. Alford, E. A. Scott et al. 2008. Endothelial cell migration on RGD-peptide-containing PEG hydrogels in the presence of sphingosine 1-phosphate. *Biophys J* 94: 273–85.

- Wanakule, P. and K. Roy. 2012. Disease-responsive drug delivery: The next generation of smart delivery devices. *Curr Drug Metab* 13: 42–9.
- Wang, C.-K., M.-L. Ho, G.-J. Wang et al. 2009. Controlled-release of rhbmp-2 carriers in the regeneration of osteonecrotic bone. *Biomaterials* 30: 4178–86.
- Wang, W. 1999. Instability, stabilization, and formulation of liquid protein pharmaceuticals. *Int J Pharm* 185: 129–88.
- Wee, S. and W. Gombotz. 1998. Protein release from alginate matrices. *Adv Drug Deliv Rev* 31: 267–85.
- Williams, D. F. 1986. Definitions in biomaterials. Proceedings of The European Society for Biomaterials Consensus Conference in Chester, England.
- Wood, M. D., M. R. Macewan, A. R. French et al. 2010. Fibrin matrices with affinity-based delivery systems and neurotrophic factors promote functional nerve regeneration. *Biotechnol Bioeng* 106: 970–79.
- Wood, M. D., A. M. Moore, D. A. Hunter et al. 2009. Affinity-based release of glial-derived neurotrophic factor from fibrin matrices enhances sciatic nerve regeneration. *Acta Biomater* 5: 959–68.
- Woodruff, M. A., S. N. Rath, E. Susanto et al. 2007. Sustained release and osteogenic potential of heparan sulfate-doped fibrin glue scaffolds within a rat cranial model. *J Mol Histol* 38: 425–33.
- Xu, X., W.-C. Yee, P. Y. K. Hwang et al. 2003. Peripheral nerve regeneration with sustained release of poly(phosphoester) microencapsulated nerve growth factor within nerve guide conduits. *Biomaterials* 24: 2405–12.
- Yamamoto, M., Y. Takahashi, and Y. Tabata. 2006. Enhanced bone regeneration at a segmental bone defect by controlled release of bone morphogenetic protein-2 from a biodegradable hydrogel. *Tissue Eng* 12: 1305–11.
- Yang, B.-B., P. K. Lum, M. M. Hayashi, and L. K. Roskos. 2004. Polyethylene glycol modification of filgrastim results in decreased renal clearance of the protein in rats. *J Pharm Sci* 93: 1367–73.
- Young, S., M. Wong, Y. Tabata, and A. G. Mikos. 2005. Gelatin as a delivery vehicle for the controlled release of bioactive molecules. *J Control Release* 109: 256–74.
- Zhang, G., C. T. Drinnan, L. R. Geuss, and L. J. Suggs. 2010. Vascular differentiation of bone marrow stem cells is directed by a tunable three-dimensional matrix. *Acta Biomater* 6: 3395–403.
- Zhang, L., E. M. Furst, and K. L. Kiick. 2006. Manipulation of hydrogel assembly and growth factor delivery via the use of peptide-polysaccharide interactions. *J Control Release* 114: 130–42.
- Zisch, A. H., M. P. Lutolf, M. Ehrbar et al. 2003a. Cell-demanded release of VEGF from synthetic, biointeractive cell ingrowth matrices for vascularized tissue growth. *FASEB J* 17: 2260–62.
- Zisch, A. H., M. P. Lutolf, and J. A. Hubbell. 2003b. Biopolymeric delivery matrices for angiogenic growth factors. *Cardiovasc Pathol* 12: 295–310.

56

Gene Therapy

C. Holladay

National University of
Ireland, Galway

M. Kulkarni

National University of
Ireland, Galway

W. Minor

National University of
Ireland, Galway

Abhay Pandit

National University of
Ireland, Galway

56.1	Introduction	56-1
56.2	Delivery Technique (Vector)	56-2
	Viral • Nonviral • Scaffolds • Cell-Mediated Gene Therapy	
56.3	Systemic and Local Gene Delivery.....	56-6
	Dose	
56.4	Therapeutic Preclinical or Clinical Trials.....	56-8
	Bone • Diabetic Wound Healing • Lower-Limb Ischemia • Myocardial Infarction • Cancer	
56.5	Summary.....	56-18
	Acknowledgments.....	56-19
	References.....	56-19

56.1 Introduction

The area of gene therapy is considered to have its roots in the early 1960s with the birth of genetic transformation of eukaryotic cells *in vitro* (Friedmann, 1992), although it could be argued that it was the transformation of pneumococcal cells in the 1940s that really inspired the concept (Avery et al., 1944). Another critical leap was made in the early 1980s with the work of Spradling and Rubin in *Drosophila*, where exogenous DNA sequences were introduced into germ line cells in order to correct a genetic defect (Rubin and Spradling, 1982, Spradling and Rubin, 1982). In the subsequent years, gene therapy has been proposed for a variety of genetic diseases (Friedmann, 1989) as well as other, more organ-specific pathologies.

Gene therapy broadly encompasses any technique used to regulate eukaryotic protein expression by manipulation of the genetic machinery. This includes everything from delivery of DNA sequences to miRNA interference of mRNA translation to delivery of cells with altered genomes.

This can take the form of permanently inserting a gene into a nonspecific location on a chromosome in order to replace a nonfunctional gene, regulating a specific gene, temporarily placing a gene in the nucleus to be expressed for a short period, replacing an original, impaired gene or gene promoter with a functioning sequence using homologous recombination, or repairing an impaired gene using selective reverse mutation to return a gene to normal function.

Unlike drug delivery, a cell transfected by gene delivery to produce a specific protein can continuously release the bioactive chemical. Epigenetic promoters can even be used so that expression will only occur under certain conditions. Gene vectors can be tailored to preferentially transfect specific cells. In contrast, local drug injections expose the drug to the surrounding area, possibly causing unnecessary side effects.

The aim of this work is to provide a general overview of the field as well as the recent advances and techniques. To that end, the vectors used in gene therapy, the advantages and disadvantages of systemic vs. local delivery, and a variety of examples of clinical and preclinical studies using gene therapy for the treatment of disease will be discussed.

56.2 Delivery Technique (Vector)

The genes must enter the nucleus of a cell to be effective. Gene therapy vectors are not required, but greatly increase transfection efficiency. Genes can be delivered to a host through modified viruses, lipid or polymer complexes, cells modified *ex vivo*, or released from a scaffold. These methods are described in detail below (see Figure 56.1).

56.2.1 Viral

Viral gene delivery exploits the highly evolved ability of viruses to infect cells and thereby deliver exogenous nucleic acids.

While there may be other drawbacks associated with their use, viruses represent the most effective method for introducing exogenous DNA into eukaryotic cells. As early as the 1960s, evidence existed that viruses could be used to genetically modify cells (Friedmann, 1992). By the mid-1980s, evidence existed that nearly 100% efficiency could be obtained with available viral systems. Over the last few decades, a variety of different viruses have become common tools cited in gene therapy literature. Both retroviruses (such as Moloney murine leukemia virus, lentivirus and simian immunodeficiency virus) and DNA viruses (which include adenovirus and adeno-associated virus [AAV]) have been applied in both *in vitro* and *in vivo* gene-therapy studies.

56.2.1.1 Adenovirus

Adenoviruses are DNA viruses commonly used in gene therapy which do not incorporate their DNA into the host's genome.

As a result, it will not be duplicated with the host DNA and cell division will produce daughter cells without the transfected genetic material. This makes the effects of the adenovirus temporary, but removes the risk of damage to the host's genome. Gendicine, a cancer treatment using adenovirus delivered

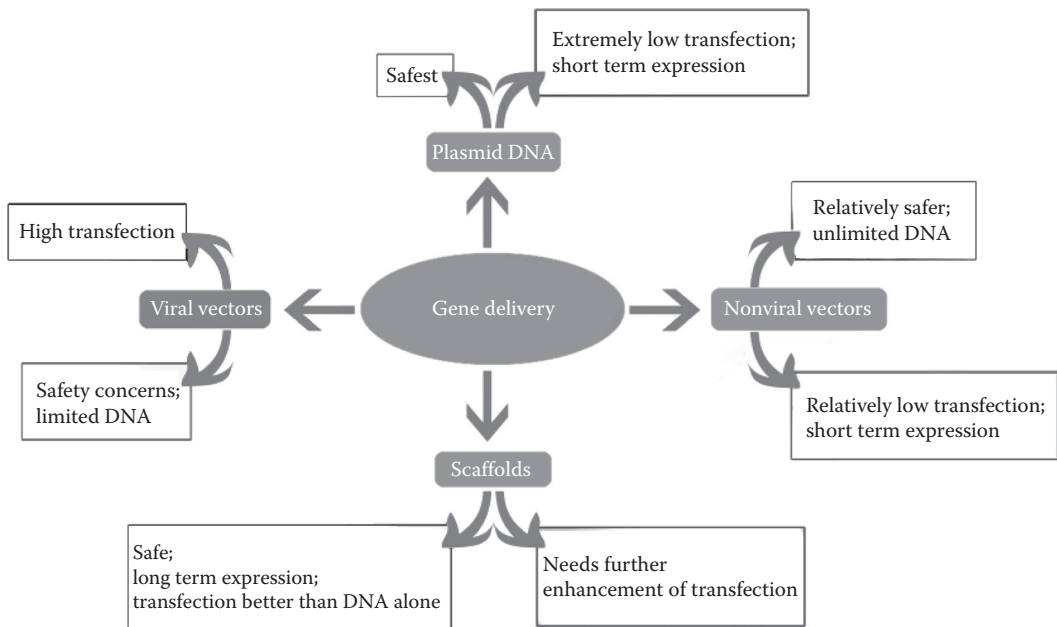


FIGURE 56.1 Vectors of gene delivery.

Downloaded by [JCR JCR] at 10:40 01 August 2015

gene therapy has been licensed in China, but not approved in the European Union or the United States (Pearson et al., 2004). Adenovirus vectors were used in the 1999 gene therapy that resulted in the death of a patient, Jesse Gelsinger. This was the first, and as of yet, only death as the result of gene therapy in the United States. After the death of Mr. Gelsinger, an altered, genetically crippled version of the adenovirus has been used in gene therapy trials (Pollner, 2000).

The major advantages of adenoviral vectors compared to other viral vectors include ease of manipulation, relatively large transgene cloning capacity, and the ability to produce high titers (Vinge et al., 2008). These vectors are relatively efficient, *in vitro* and *in vivo*, and capable of transfecting nondividing cells (Davis et al., 2008). An additional advantage of adenoviruses is that they can be made replication deficient to improve safety and can be “guttled” to increase the cloning capacity. The major disadvantage of these vectors is the inflammatory and immune response seen upon *in vivo* delivery, as this limits the gene expression time and can induce further complications (Vinge et al., 2008). Guttled adenoviruses have lower immunogenicity, but they still trigger a reasonably significant cellular immune response (Davis et al., 2008). Coating adenoviruses with polyethylene glycol (PEG) has been suggested as a strategy to reduce the immune response to the proteins in the viral capsid. This method could also allow control of targeting by masking certain receptor-binding domains and presenting others (Gray and Samulski, 2008).

56.2.1.2 Adeno-Associated Virus

The AAV is a very small virus incapable of replication in a host cell without the assistance of a helper-virus.

AAVs are the most difficult of all the viral delivery vectors to produce, but new production techniques are increasing the ease of mass producing these small vectors. AAVs have been shown to be able to transfect quiescent cells.

AAVs are single-stranded DNA viruses (unlike adenoviruses which are double-stranded DNA viruses) (Gray and Samulski, 2008). They are somewhat analogous to gutted adenovirus in that they are usually incapable of replication in a host cell without the assistance of a helper virus (Davis et al., 2008). The recombinant AAVs used in gene therapy lack the ability to integrate into host genomes, persisting instead as episomal DNA in target cells (Lyon et al., 2008). Thus, there is theoretically a negligible risk of mutagenesis although long-term clinical trials would be required to confirm this. Importantly, no AAV serotype has been found to cause human disease (Davis et al., 2008). However, AAV vectors do elicit immune responses *in vivo* and some argue that they can cause insertional mutagenesis (Hacein-Bey-Abina et al., 2003) and their cloning capacity is also somewhat limited (4–5 kb) (Davis et al., 2008, Vinge et al., 2008).

Another feature, which could be advantageous or disadvantageous depending on the application, is that the expression kinetics of AAVs are relatively slow. Transgene expression generally peaks between 2 and 4 weeks after transfection (Lyon et al., 2008). Self-complementary AAVs have higher transfection levels—sometimes reported as more than 100 times over normal AAVs—but the packaging capacity of the virus is necessarily halved (~2.3 kb), which limits the applicability of such vectors (Gray and Samulski, 2008). A final concern is that 20–40% of the human population has antibodies to AAV2 serotype and thus can neutralize the vectors, drastically reducing transfection. It is also possible that, with repeated treatment, patients could develop antibodies to the vectors and thus the treatment would lose effectiveness over time (Lyon et al., 2008).

56.2.1.3 Retrovirus

Retroviruses are RNA carrying viruses that use reverse transcriptase to create DNA for incorporation into the host's genome.

A complication arising from the use of retroviruses in genetic engineering is that they add DNA to a random section of the altered chromosome. There is a small chance that the new genetic material will be inserted within gene or gene promoter, disrupting gene production.

Lentivirus has shown reasonable promise for cardiac applications because it can transduce nondividing cells like cardiomyocytes (Davis et al., 2008). The sequence delivered by the lentivirus integrates into host genome, which means that transfection is “stable” but also introduces the risk of mutagenesis, carcinogenesis, and immune response induction (Haider et al., 2008). Another disadvantage of lentivirus is that only low titres can be prepared (Davis et al., 2008). Furthermore, lentiviruses are less stable than other vectors and thus are more difficult to work with (Davis et al., 2008). A final drawback is that these vectors have very high efficiency *in vitro* (80–100%) but only up to about 30% efficiency *in vivo* (Davis et al., 2008).

56.2.2 Nonviral

While viral systems are among the most effective agents available for gene transfer, they have associated health risks, high production costs, and a variety of other drawbacks. Thus, the gene therapy field has focused on the development of nonviral gene delivery systems. A variety of agents have been investigated.

While viral systems are among the most effective agents available for gene transfer, they have associated health risks, high production costs, and a variety of other drawbacks. Thus, the gene therapy field has focused on the development of nonviral gene delivery systems. A variety of agents have been investigated (see Figure 56.2).

56.2.2.1 Naked DNA

DNA can transfect a cell without a delivery vector when simply injected intramuscularly or intravenously. However, this technique has a much lower efficiency than other methods. To improve transfection efficiency, physical methods can be used to improve gene delivery. Electroporation using an electric current or calcium ions temporarily increases the permeability of the plasma membrane and allows DNA to pass into the cell (Neumann et al., 1982). Sonoporation uses ultrasonic sound to

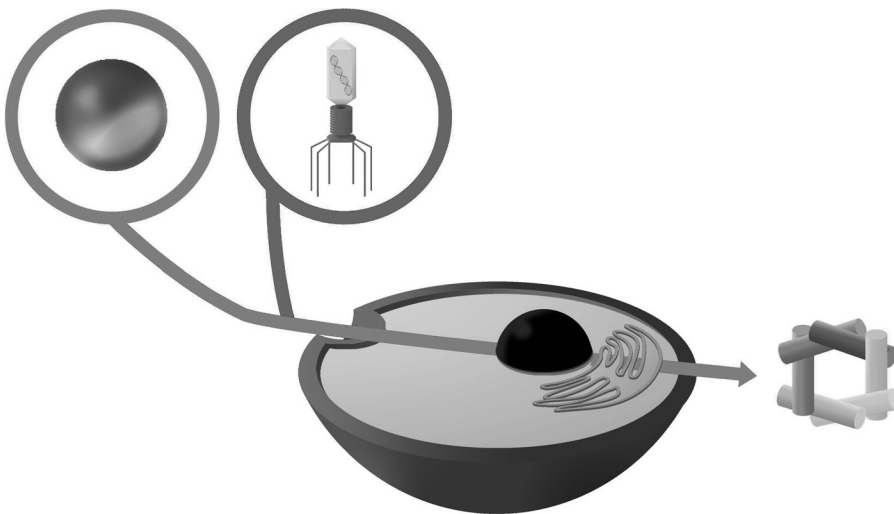


FIGURE 56.2 Hypothesized route of polymeric or liposomal complex internalization in a eukaryotic cell. Initially, particles bind to the surface of the cell. This can occur via charge interaction or ligand binding. A pit forms and becomes an endosome. This endosome then combines with an acidic lysosome. This swelling may be responsible for the bursting of the endosomal membrane and release of the complexes. These complexes then may enter the nucleus via nuclear pores. Once in the nucleus, normal transcription and translation are hypothesized to occur. It should be noted that at each step the vast majority of complexes are likely degraded or excreted, leaving only a very small fraction that actually reaches the nucleus. (From Dennig, J. and Duncan, E. 2002. *Journal of Biotechnology*, 90, 339–347; Dufes, C., Uchegbu, I. F., and Schatzlein, A. G. 2005. *Advanced Drug Delivery Reviews*, 57, 2177–2202.)

induce a similar increase in permeability of the plasma membrane and allowing large molecules to pass into the cell (Song et al., 2007).

56.2.2.2 Lipids

Lipoplexes are complexes arising from the combination of nucleic acids and lipids which form condensed structures capable of passing through cell membranes.

Under normal conditions, DNA is too negatively charged from the phosphates within its chemical structure to pass through a cell membrane. Naked DNA either requires a membrane to be chemically or electrically disrupted or enters the cell during cytokinesis. Lipoplexes and polyplexes form a positively charged sheath around a plasmid and allow the DNA to pass through the plasma membrane. Anion and neutral lipids can be used to form lipoplexes, but cationic lipids have increased lipoplex stability and cellular uptake and are more popular. Unfortunately, lipoplexes formed with cationic lipids exhibit cell toxicity at high levels. This dose-dependent toxicity limits the genetic load that can be delivered and, until it can be solved, limits the therapeutic uses of lipoplexes.

Lipoplexes are commonly used in gene therapy to transfer genetic material into a cancer cell, either by suppressing oncogenes or activating tumor suppression control genes. Lipoplexes have also been used to successfully transfect respiratory endothelial cells leading to studies to treat respiratory diseases such as cystic fibrosis.

56.2.2.3 Polymers

Polyplexes are complexes arising from the interaction between nucleic acids and polymers, where the polymers condense the nucleic acids and mediate their passage through the cell membrane.

Polyplexes are similar to lipoplexes in that most of the interactions between the polymer and the genetic sequence are ionic chemical interactions. Most polymers used for DNA complexation are cationic and interact with the anionic phosphates in nucleic acid.

In most cases, the DNA used in polyplexes and lipoplexes is not inserted into the host genome, but is delivered in plasmid form which, when inserted into the nucleus, is transcribed along with the genome. In addition to minimizing the risk of mutating a healthy gene with random insertion, using a noninserting plasmid means that the gene therapy will only cause a temporary alteration of gene expression. While this is a limitation when the desired effect in gene therapy is the replacement of a defective gene, it does allow gene therapy to be used when a permanent alteration to gene expression is not desired. For example, transient gene therapy can be used to increase the growth of nerve axons or increase the healing of a diabetic patient without resulting in a permanent increase in the natural growth rate of cells.

56.2.3 Scaffolds

Scaffolds can also be used as a delivery device for genetic information. As gene therapy has applications for tissue engineering and regenerative medicine, combining gene therapy with tissue-engineered scaffolds (a biocompatible framework for growing tissue on and within it) is a natural approach. Scaffolds can be used to control the dose and duration of exposure. They can be used with cell-mediated gene therapy to localize the delivery of the altered cells. As previously mentioned, many vectors for gene delivery have dose-dependent cytotoxicity or immune response. Using scaffolds as a secondary release mechanism causes a gradual release while keeping the high transfection efficiency of the other vectors (Jawad et al., 2007) (Simpson et al., 2007). Scaffold-mediated gene therapy is used in the treatment of cancer as well as regenerative medicine. In this case, the goal is either to increase the expression of antioncogenes or by using gene therapy to modify immune cells to more readily attack tumor cells. Gene delivery scaffolds can be inserted near cancer cells or into the dead space remaining after a tumor is removed (Kusumoto et al., 2001).

56.2.4 Cell-Mediated Gene Therapy

Cell-mediated gene therapy relies upon the delivery of cells genetically modified *ex vivo* to modulate the protein expression for therapeutic purposes.

Cell-mediated gene therapy differs from other vector-mediated techniques in a variety of ways. First, the genetic manipulation occurs *ex vivo*, before the cells are implanted. Second, the transgene production depends entirely on the viability of the implanted cells, so the delivery technique of the cell suspension must be carefully considered. Finally, the source, preparation, and characterization of the cells represent an additional level of complication. There are several important implications of these differences, as compared to vector-mediated gene delivery. For example, the cell type that produces the transgene depends on the experimental or therapeutic strategy rather than on the vector or administration technique used. The isolation and expansion of these cells may determine the overall efficacy of the treatment as the viability of the cells is critical. Intelligent choice of cell type may also augment the efficacy of the therapy; for example, using stem cells to deliver factors to infarcted myocardium means that the paracrine benefits of stem cells in such a situation are included in addition to the benefits associated with the gene therapy (Baraniak and McDevitt, 2010).

A significant advantage of *ex vivo* gene delivery is that selection protocols can be used to select the transfected cells over the unmodified cells, essentially eliminating the importance of transfection efficiency. Furthermore, the immunogenicity of the vector is less problematic as it does not have to be introduced *in vivo*. While it is possible that *ex vivo* manipulation could alter the expression of molecules such as MHC class I or II on the cell surface, these effects tend to be less problematic than, for example, the immune response to systemically administered virus (Shayakhmetov et al., 2010). However, the potential danger of tumorigenicity is not eliminated. As the vector is not introduced into the host, it is unlikely to induce tumor formation in the host tissue; however, the transplanted cells are genetically modified to permanently express the transgene which implies a modification in their genetic structure. Insertional mutagenesis is thus quite likely, which can lead to the uncontrolled proliferation of these cells (Themis et al., 2003, Shi et al., 2001, Haviernik and Bunting, 2004, Ali et al., 1994).

As the delivery technique is so critical to the success of cell-mediated therapy, significant research has gone into development of an “optimal” cell delivery technique. The simplest method, injection of cell suspension, offers minimal opportunity to augment the survival rate of the cells or to direct their engraftment. Indeed, very low retention rates of injected cells have been observed in certain settings (Pons et al., 2009). The use of biomaterial scaffolds presents a solution to both of these concerns, as the cells can be physically protected and their migration limited by using a cell-seeded scaffold to deliver the modified cells (Sales et al., 2007, Jawad et al., 2007, Simpson et al., 2007). Modification and functionalization of the scaffold can further enhance the viability and control the differentiation of the implanted cells (Hosseinkhani et al., 2006a,b, 2005, 2008, Hosseinkhani and Tabata, 2006, Hosseinkhani, 2006, Zhang et al., 2006, Simpson et al., 2007). Considering the benefits associated with the incorporation of the scaffold, as well as the potential for added functionality, the future of effective cell-mediated gene therapy will likely include scaffold-based delivery.

56.3 Systemic and Local Gene Delivery

While the administration technique and the actual gene therapy vector may seem less important than the gene being delivered, they can have a significant impact. Certain administration techniques are more effective than others and the choice of local or systemic delivery may determine the efficacy of the therapy.

The successful treatment of certain diseases requires systemic gene delivery. However, the viral and nonviral vectors administered systemically, mostly by intravenous injection, meet with a number of barriers that hinder their ability to reach the target tissues, including interactions with proteins and cells in blood, serum stability, first pass metabolism in liver, nonspecific delivery to unintended tissues

and/or attacked by macrophages, digestive enzymes such as proteases and nucleases, suffer destruction by immune responses. A number of studies have investigated the methods to determine and modulate the viral tropism (Ylosmaki et al., 2008, Michelfelder and Trepel, 2009, Tan et al., 2007, Yang et al., 2009, Li et al., 2008a, Bakker et al., 2001). In case of nonviral vectors, a number of approaches have shown promising results. Generally, when naked DNA is used for systemic delivery, large doses are employed. However, a study has shown successful delivery to kidney when comparatively much lower dose is administered via inferior vena cava (Wu et al., 2005). For liposomal systems, PEGylation is a commonly used method which increases the circulation time by protecting them from attack by macrophages. Various such stealth technologies have been described (Immordino et al., 2006). PEGylated nanoparticles have shown promising results for systemic nonviral delivery (Kaul and Amiji, 2004, 2005). A wide range of targeting strategies such as peptide (Li and Huang, 2006, Zhang et al., 2008a), antibody (Zhang et al., 2008b, Peer et al., 2008) or antibody fragment (Kim et al., 2008) linkage or substrates for specific receptors (Hattori et al., 2004), have been employed for targeted delivery to tissue/cells of interest.

Some diseased conditions only need local gene therapy and the use of tissue engineered scaffolds becomes more evident in these cases. Tissue-engineered scaffolds can act as reservoir or depot systems to keep the gene vectors from having systemic effect while, at the same time, release the genes in a controlled manner for extended periods of protein expression (Kulkarni et al., 2010) or suppression. A number of studies have shown localized sustained release of DNA (Guo et al., 2006, Chun et al., 2005, Chen et al., 2007a). Tissue-engineered scaffolds also provide protection to the DNA which partially explains the enhancement of the transfection observed by delivery via gene activated matrices (GAM) (Bonadio et al., 1999a, Bonadio, 2000). The enhanced efficacy and therapeutic benefits has been observed in various studies employing tissue engineered scaffolds with either plasmid DNA alone (Andree et al., 2001) or complexed with liposomes/polymers (Winn et al., 2005b, Peng et al., 2009, Wang et al., 2009) or with virus (Breen et al., 2008).

56.3.1 Dose

When considering a treatment regimen, the dose of the therapeutic agent is an extremely important issue. It can, in fact, represent the difference between massive therapeutic benefit and complete ineffectiveness. A further consideration is that in gene delivery, a higher dose is not necessarily associated with a higher level of transgene expression. As with many biological systems, there appears to be both an upper and lower limit or a "window" of efficacy (Bonadio et al., 1999b).

Comparing the dose of viral and nonviral therapies is not trivial. As the transfection efficiency of viruses is far higher than that observed with nonviral vectors, far less virus is required to stimulate comparable levels of transgene expression. In general, the transfection efficiency of a vector is inversely related to the required dose (Holladay et al., 2009). The cytotoxicity of the vector is another important consideration. Naked plasmid DNA elicits very little immune or inflammatory response, while many polymers and viruses are significantly antigenic (Breunig et al., 2007). Thus, the maximum dose of a virus might be determined by the host response to the vector rather than the optimal transgene expression. Indeed, viral therapies are now regarded with caution after isolated incidences of fatalities and other "serious adverse events" (SAEs) were associated with viral clinical trials (Lyon et al., 2008, Lehrman, 1999, Marshall, 2000, Check, 2003, Porteus et al., 2006). The earliest fatality reported to be associated with a viral clinical trial used one of the highest doses cited in the literature, 3.8×10^{13} virus particles of an adenovirus variant (Lehrman, 1999). Naked plasmids, conversely, can be administered in very high doses but are unlikely to induce significant transgene expression. For example, 4 mg of plasmid induced no adverse reactions in an early angiogenic clinical trial (Kalka et al., 2000) as was a total of 8 mg delivered over the course of a more recent angiogenic clinical trial (Shigematsu et al., 2010). The doses of nonviral vectors are generally lower than naked plasmid, as most vectors have some antigenicity. The most popular nonviral vector used in clinical trials are cationic lipid/plasmid complexes (Edelstein et al., 2007).

Comparing animal studies to human clinical trials is also problematic, as differences in size and weight logically translate to differences in optimal dose. The doses used in clinical trials do not always reflect this, however. For example, in the cardiac area, approximately the same average dose of naked plasmid (~0.75 mg) is used in rats, pigs, and humans, despite orders of magnitude differences in overall mass.

56.4 Therapeutic Preclinical or Clinical Trials

A wide range of disease states have been investigated as potential candidates for gene therapy. Some of the areas with more significant recent advances are discussed, including gene therapy for bone regeneration, diabetic wound healing, lower-limb ischemia, myocardial infarction, and cancer.

56.4.1 Bone

The regeneration of bone tissue presents an interesting problem for the tissue-engineering and biomaterials field. Bone defects are relatively common, whether due to injury, disease, or as a by-product of surgery. While many types of fractures and small defects can be fully regenerated without intervention, others require replacement or other therapy in order to heal. The natural healing process involves primarily osteoinduction—the stimulation of bone tissue formation by undifferentiated or progenitor cell types. The other major method of bone tissue formation depends on osteoconduction, where bone tissue forms over a surface. This is more commonly observed in response to implants than in natural bone regeneration (Albrektsson and Johansson, 2001). The current gold standard in bone tissue engineering is the use of autografts (Ahlmann et al., 2002). Essentially, bone from a less critical area (i.e., pelvis) is harvested and used to replace the missing bone elsewhere. This has obvious drawbacks, as two injury sites result, and the harvest site must then regenerate. Allografts—bone harvested from donors—are an alternative, but in order to minimize the chance of immune rejection, fresh allografts are freeze-dried, frozen, gamma irradiated or treated with ethylene oxide. This significantly decreases the osteoinductive and osteoconductive properties of the allografts (Keating and McQueen, 2001). However, allografts are a commercially available alternative to autografts. Xenografts, bone harvested from animals, represents a third option. There are a number of bovine-derived bone substitutes available on the market, such as Cerabone®, Endobon®, and Osteograf® (Gisep, 2002, Tadic and Epple, 2004). As these xenografts are composed of the natural hydroxyapatite structure which is common to all vertebrates, they are osteoconductive. However, they do not possess the osteoinductive properties of autografts, which may be largely due to the presence of natural signaling molecules on unmodified bone. Tissue engineering products for bone regeneration are available commercially, OP-1® and INFUSE®, which use recombinant human bone morphogenic protein-7 (rhBMP-7) and recombinant human bone morphogenic protein-2 (rhBMP-2), respectively.

Gene therapy approaches for the regeneration of bone predominantly focus on the upregulation of growth factors such as bone morphogenic protein 2 (BMP-2). Naked plasmid DNA delivery has been shown to improve bone formation, epithelialization and the formation of blood vessels, as discussed in [Table 56.1](#). Viral gene delivery has been shown to induce bone formation when adenovirus encoding BMP-2 was injected into mouse skeletal muscle (Musgrave et al., 1999).

Scaffold-based approaches have found a significant benefit to be associated with loading the plasmid (naked or complexed) or virus into a biomaterial. Higher transfection efficiencies have been observed as compared to direct delivery of the vector (Winn et al., 2005a). In fact, the delivery and transgene expression profiles were found to depend on the complexation reagent, implying a potential mechanism for control of transfection and gene expression (Winn et al., 2005a, Xie et al., 2001). The term “Gene Activated Matrix,” often abbreviated as GAM, has emerged as a descriptor for some of the collagen-scaffold-based systems used for the delivery of plasmid DNA (Fang et al., 1996, Bonadio et al., 1999b). These matrices were found to significantly increase bone regeneration when used to deliver a secreted peptide

TABLE 56.1 Summary of Therapeutic Trials Using Gene Therapy for Bone Tissue Engineering

Mode of Delivery	Gene	Reference
Adenovirus	BMP-2	Egermann et al., 2006a,b, Baltzer et al., 2000
Adenovirus	BMP-2	Musgrave et al., 1999
Polylactic coglycolic acid/ polypropylene fumarate scaffold	BMP-7	Rivard et al., 1995
Retrovirus	BMP-4, BMP-6	Jane et al., 2002
Retrovirus	MDS1-EVI1, PRDM16, SETBP1	Schwarzwaelder et al., 2006, Ott et al., 2006
Naked DNA/ Electroporation	BMP-4	Kishimoto et al., 2002
Lipoplex	LIM Mineralization Protein (LMP-1)	Yoon and Boden, 2004, Sangadala et al., 2003, Minamide et al., 2003, Kim et al., 2003, Viggeswarapu et al., 2002, 2005, 2001, Minamide et al., 2001, Boden et al., 1998, Liu et al., 2010
Collagen calcium- phosphate scaffold	VEGF	Keeney et al., 2010
Collagen scaffold	BMP-2 or secreted peptide fragment of human parathyroid hormone (hPTH 1-34)	Fang et al., 1996
Collagen scaffold	Secreted peptide fragment of human parathyroid hormone (hPTH 1-34)	Bonadio et al., 1999b
Cell-mediated	BMP-7	Nussenbaum et al., 2005
Cell-mediated	BMP-2	Blum et al., 2003
Cell-mediated	BMP-2	Wang et al., 2003
Cell-mediated	BMP-2	Laurencin et al., 2001
Cell mediated	BMP-2	Jiang et al., 2009

fragment of human parathyroid hormone (hPTH) in the treatment of critical gap defects. Collagen calcium-phosphate scaffolds, which naturally have osteoconductive properties, were found to act as both a reservoir system and a transfection reagent when used to deliver VEGF plasmid (Keeney et al., 2010). Filling of the femoral cavity was increased in the groups treated with the plasmid, implying a beneficial effect of VEGF upregulation in the regenerating bone and suggesting a potential gene of interest for future studies. Functionalized decellularized, or demineralized bone has also been studied as a carrier for cell-mediated gene therapy (Wang et al., 2003).

While efficacy has been established in a variety of preclinical studies, gene therapy for bone regeneration is still in development. Scaffold-mediated delivery of genes or cells may represent a major future direction in the field, whether the scaffold is used simplistically as a delivery vehicle or is functionalized with osteoinductive or osteoconductive factors such as calcium phosphate or recombinant growth factors.

56.4.2 Diabetic Wound Healing

Wound healing is a classic example of a complex and highly intricate response in the repair and regeneration of damaged tissue. Under physiological conditions, normal adult skin has a considerable capacity for structural and functional repair via a highly orchestrated process tightly regulated by growth factors and cytokines (Werner and Grose, 2003) and characterized by distinct but overlapping phases of wound healing, namely hemostasis, inflammation, proliferation, and remodeling (Diegelmann and Evans, 2004). When the wounds fail to progress through the normal phases of healing and enter to a

state of chronic pathologic inflammation, they are termed as “chronic,” “impaired,” or “compromised” (Menke et al., 2007). Diabetes is one of most common causes of chronic wounds, others being venous and pressure ulcers (Mustoe et al., 2006, Nwomeh et al., 1998). Diabetes is a major health problem and disease prevalence is growing at a phenomenal rate. Management of diabetic foot disease is very expensive and the cost of managing the diabetic foot complications is estimated to be in billions of US dollars (Giurini and Lyons, 2005, Dorresteijn et al., 2010, Wukich, 2010). In Europe, the average cost per episode is €6,650 for leg ulcers and €10,000 for foot ulcers, which accounts for 2–4% of healthcare budgets (Gottrup et al., 2010). The altered molecular mechanisms leading to chronic healing are being extensively studied (Blakytyn and Jude, 2006, 2009, Brem and Tomic-Canic, 2007, Galkowska et al., 2006), unraveling the pathogenesis of diabetic wound healing and opening new avenues, complementary to the standard treatment protocol, for successful management of diabetic ulcers. To date, a number of studies have investigated the role of growth factors and cytokines, such as VEGF, FGF, PDGF, TGF- α , IGF-1, NGF, GM-CSF, in the management of diabetic wounds either as individual factors (Fernandez-Montequin et al., 2007, 2009, Saba et al., 2002, Pandit et al., 2000, Mustoe et al., 1991, Judith et al., 2010, Li et al., 2008b, Matsuda et al., 1998, Fang et al., 2010) or as combination of factors (Kiritsy et al., 1995, Greenhalgh et al., 1993, Brown et al., 1994, Davidson et al., 1997, Jazwa et al., 2010b, Cao et al., 2010). In recent years, gene therapy is being investigated extensively in recent years, majorly due to failure to achieve the clinical promise of growth factors/cytokines delivery despite of intensive research (Eming et al., 2004). The limited success of growth factors/cytokines delivery can be attributed to a number of factors which include their short half-lives, degradation by proteases, toxicity at high doses and lack of effective delivery (Steed, 1998, Grinnell et al., 1992, Barrick et al., 1999, Lauer et al., 2000, Bowler, 2002). A number of studies have shown promising results in normalizing various pathological aspects of diabetic wound healing. Some recent salient examples have been details in [Table 56.2](#).

Recently, tissue-engineered biological dressings have gained significant attention, not only because they fill the wound gap by extracellular matrix and induce expression of cytokines and growth factors which accelerate wound healing (Veves et al., 2001), but also due to the fact that they provide opportunity to combine other wound therapeutics such as antimicrobial agents, growth factors and/or cytokines as recombinant proteins, genes, or live cells (Andreadis and Geer, 2006, Horch et al., 2005, Supp and Boyce, 2005). One such tissue-engineered scaffold which employs human platelet-derived growth factor (PDGF)-B with replication-defective adenovirus in bovine collagen gel (GAM501) is being investigated in human patients. The clinical phase I/II results of this study showed that 93% of patients had a positive-biologic response to GAM501, as assessed by a decrease in ulcer size and GAM501 did not appear to have any toxicity at doses that showed biologic activity (Mulder et al., 2009).

56.4.3 Lower-Limb Ischemia

Peripheral arterial disease (PAD) is an increasingly common disease, affecting approximately 4.3% of people over the age of 40 in the United States (Selvin and Erlinger, 2004), and 12–20% of people over the age of 65 (Bakal et al., 2000). The most severe form of this disease is critical limb ischemia (CLI) which affects 0.05–0.1% of people worldwide (Shigematsu et al., 2010). Current treatment strategies include surgical and endovascular revascularization, but more than one in four patients will require major amputation within a year of treatment and current mortality rates exceed 20% per annum (Shigematsu et al., 2010). Thus, this is an excellent candidate for gene therapy trials as the current gold standard of treatment has extremely limited success.

Delivery of angiogenic genes is the most popular gene therapy treatment for CLI. VEGF, HGF, eNOS and FGF have all been investigated as potential angiogenic genes in preclinical and clinical trials (see [Table 56.3](#)).

Randomized, multi-center meta-analyses have indicated significant improvements in odds ratios associated with angiogenic gene therapy (Haro et al., 2009). In a recent trial involving diabetic patients, an apparent improvement was observed, but due to the small numbers the primary end point of

TABLE 56.2 Summary of Therapeutic Trials Using Gene Therapy for Diabetic Wound Healing

Vector	Gene	Animal Model	Wound Type	Significant Finding	Reference
Viral vectors					
AAV vector	Simultaneous transfer of VEGF-A and fibroblast growth factor 4	C57BLKS mice homozygous for a mutation in the leptin receptor (<i>Lepr^{db}</i>)	Full-thickness excisional circular wounds (4 mm in diameter)	Simultaneous delivery VEGF-A and FGF-4 gene therapy leads to significantly faster wound closure, increased granulation tissue formation, vascularity and dermal matrix deposition	Jazwa et al., 2010a
rAAV	Ang-1 (angiopoietin-1)	C57BL/KsJ <i>Lepr^{db}</i> mice	full-thickness longitudinal incisions (4 cm) on dorsum	Ang-1 gene transfer improves the delayed wound repair in diabetes by stimulating angiogenesis, apparently without VEGF involvement	Bitto et al., 2008
Adenovirus	c-Met gene	Organ cultured human diabetic corneas	5-mm epithelial wounds	Recombinant AV-driven c-met transduction into diabetic corneas appears to restore HGF signaling, normalize diabetic marker patterns, and accelerate wound healing	Saghizadeh et al., 2010
Adenovirus in fibrin scaffold	Endothelial nitric oxide synthase (eNOS)	Alloxan-induced diabetic New Zealand white rabbits	6-mm punch biopsy wounds on the ears	Fibrin delivery of AdeNOS resulted in enhanced eNOS expression, inflammatory response, and a faster rate of re-epithelialization	Breen AM, 2008
Adenovirus vector (ADV/VEGF165)	VEGF 165	BKS.Cg-m +/+ <i>Lepr^{db}</i> type 2 diabetic mice	Full-thickness excisional wounds, 1.4 cm in diameter on the dorsum	ADV/VEGF165 improves healing enhancing tensile stiffness and/or increasing epithelialization and collagen deposition, as well as by decreasing time to wound closure	Brem et al., 2009
Adenovirus	Placenta growth factor (PIGF)	Streptozotocin induced diabetic C57Bl/6 male mice	6 mm-diameter full-thickness punch biopsy wound	PIGF gene transfer improved granulation tissue formation, maturation, and vascularization, as well as monocytes/macrophages local recruitment	Cianfarani et al., 2006
Adenovirus	Platelet-derived growth factor (PDGF)-B	C57BLKS/J-m +/+ <i>Lepr(db)</i> and streptozotocin induced	8 mm full-thickness flank wounds	Adenoviral-mediated gene therapy with PDGF-B significantly enhanced wound healing and neovascularization in diabetic wounds with augmentation of EPC recruitment	Keswani et al., 2004

continued

TABLE 56.2 (continued) Summary of Therapeutic Trials Using Gene Therapy for Diabetic Wound Healing

Vector	Gene	Animal Model	Wound Type	Significant Finding	Reference
Lentivirus	Stromal-derived growth factor-1 α (SDF-1 α).	BKS.Cg-m ^{+/+} Lepr ^{db} /J mice	8-mm full-thickness wound	SDF-1 α treatment exhibited a decrease in wound surface area with more cellular wounds and increased granulation tissue volume and resulted in complete epithelialization at 2 weeks	Badillo et al., 2007
Lentivirus	Platelet-derived growth factor (PDGF)-B	<i>db/db</i> mice	2 \times 2-cm full-thickness dermal wound	Statistically significant increase in angiogenesis and substantially thicker, more coherently aligned collagen fibers	Lee et al., 2005, Man et al., 2005
Non-Viral Vectors					
Naked plasmid injection	HSP47	Alloxan-induced diabetic rat	Excisional skin wounds	Increased collagen I production around the wound during repair process	Wang and Li, 2009
Plasmid vector with electroporation	Hypoxia-inducible factor 1 α (HIF-1 α)	BKS.Cg-m ^{+/+} Lepr ^{db} /J mice	5-mm full-thickness circular excisional wounds on the dorsum	Electroporation with HIF-1 α increased levels of HIF-1 α mRNA on day 3 and increased levels of VEGF, PLGF, PDGF-B, and ANGPT2 mRNA on day 7 and ten folds increase in circulating angiogenic cells after HIF-1 α treatment	Liu et al., 2008
Plasmid vector with electroporation	Keratinocyte growth factor-1 (KGF-1)	BKS.Cg-m. Lepr ^{db-db} mice	Excisional wounds	Results showed improvement in healing rate, quality of epithelialization and density of new blood vessels	Marti et al., 2004, 2008
Sonoporation of minicircle DNA	VEGF ₁₆₅	Streptozotocin-Induced diabetic C57BL/6J mice	6 mm punch biopsy wounds on the dorsum	Sonoporation of minicircle-VEGF ₁₆₅ resulted in Accelerated wound closure with markedly increased skin blood perfusion and CD31 expression and full restoration of normal architecture	Yoon et al., 2009
Plasmid pellet (1% methyl cellulose)	HOXA3	<i>db/db</i> mice	8-mm full thickness excisional wound on the dorsum	HOXA3 accelerates wound repair by mobilizing endothelial progenitor cells and attenuating the excessive inflammatory response of chronic wounds	Mace et al., 2009

DNA/ Methylcellulose Pellets	Sonic hedgehog (Shh)	C57BLKS/J-m ^{+/+} Lepr ^{db} mice	8 mm full-thickness excisional skin wounds	Topical gene therapy resulted in acceleration of wound recovery with increased wound vascularity	Asai et al., 2006
Gold particles and gene gun	Rat opioid growth factor receptor (OGFr) complementary DNA	Adult male rats	3-mm corneal abrasions	Excess OGFr delays reepithelialization, whereas attenuation of OGFr accelerates repair of the corneal surface	Zagon et al., 2006
RGDK-lipopeptide	rhPDGF-B	Streptozotocin-Induced Diabetic Sprague-Dawley Rats	2.1 cm (radii) circular dorsal skin incision to the level of the loose subcutaneous tissues	A single subcutaneous administration of the electrostatic complex of RGDK-lipopeptide and rhPDGF-B plasmid is capable of healing incisional wounds in streptozotocin-induced diabetic rats with significantly higher degree of epithelization, keratization, fibrocollagenation and blood vessel formation	Bhattacharyya et al., 2009
Lipofectin and Lipofectamine 2000	Human insulin-like growth factor (hIGF)-1 (with keratinocytes)	Streptozotocin-Induced Diabetic Yorkshire pigs	Full-thickness excisional wounds (15 × 1.5 × 0.8 cm) on the dorsum	Nonviral gene transfer increased IGF-1 expression in diabetic wounds by up to 900-fold and 83% wound closure achieved with combined gene and cell therapy	Hirsch et al., 2008
Plasmid/ liposome	aFGF	Db/db mouse	Excisional and incisional	Accelerated closure of excisional wounds and increased wound breaking strength in incisional wounds	Sun et al., 1997
Plasmid in PEG-PLGAPEG tri-block co-polymer	TGFβ1	Db/db mouse	7 x 7 mm excisional	Enhanced closure, re-epithelialization and cell proliferation	Lee et al., 2003

TABLE 56.3 Summary of Selected Trials Using Angiogenic Gene Therapy to Treat CLI

Gene	Delivery Method	Dose	Reference
VEGF-121	Adenovirus	$4 \times 10^{9.5}$ – 4×10^{10} particles	Rajagopalan et al., 2001
HGF	Hemagglutinating virus of Japan (HVJ)-liposome	20–40 μ g	Taniyama et al., 2001
FGF-1	Naked plasmid (clinical trial)	0.5–32 mg in total (16 mg per injection maximum, 2 injections in some cases)	Comerota et al., 2002
eNOS	Naked plasmid	500 μ g	Namba et al., 2003
VEGF-165	Naked plasmid (clinical trial)	0.4–2 mg	Shyu et al., 2003
FGF-1	Naked plasmid (clinical trial)	0.5, 2, 4 mg	Baumgartner et al., 2009
VEGF-165	Naked plasmid (case study)	2 mg	Isner et al., 1996
VEGF-165	Naked plasmid (clinical trial)	2 mg	Isner et al., 1998
VEGF-165	Naked plasmid (clinical trial)	4 mg	Baumgartner et al., 1998
VEGF-165	Adenovirus and naked plasmid	2×10^{10} pfu or 2 mg plasmid	Makinen et al., 2002
VEGF-165	Naked plasmid (clinical trial)	2 mg	Kusumanto et al., 2006

reduction in the number of amputations was not observed (Kusumanto et al., 2006). Overall, while there does appear to be a small but significant improvement, the therapeutic potential originally envisioned by Baumgartner et al. has not yet been achieved (Baumgartner et al., 1998). Improvements such as polymeric transfection reagents or biomaterial-based systems which improve the specificity of the gene delivery could represent future directions for this area.

56.4.4 Myocardial Infarction

There are two predominant forms of ischemic heart disease, namely acute damage due to myocardial infarction (MI) and chronic damage due to restricted perfusion of tissue due to atherosclerosis. These two forms of heart disease accounts for 35% of deaths reported in the United States every year (Guyton and Hall, 2000) and approximately a third of deaths worldwide, making it the most common cause of death in developed countries (Gray and Samulski, 2008).

Cardiac gene therapy has been under investigation for more than two decades. In the 1990s, trials established that cardiac tissue could be genetically modified with viruses, naked plasmids and liposomes (Acsadi et al., 1991, Barnes et al., 1993, Guzman et al., 1993, French et al., 1994, Baru et al., 1995, Nabel, 1995). Since then, gene therapy has been proposed as a treatment for conditions ranging myocarditis to advanced congestive heart failure. The goals of cardiac gene therapy are essentially to minimize damage, to promote regeneration, or some combination thereof. The late Dr. Jeffrey Isner and his colleagues were responsible for much of the ground-breaking work in the area, conducting a number of clinical trials starting in 1995, focusing on delivery of vascular endothelial growth factor (VEGF-A) plasmid (Isner, 1998, Losordo et al., 1998, 2002, Ashare et al., 1999, Lathi et al., 1999, Symes et al., 1999, Schwarz et al., 2000, Henry et al., 2001, Vale et al., 2001, Fortuin et al., 2003, Yoon et al., 2005). A variety of other genes have been investigated since, although no major breakthroughs in clinical studies have yet been reported. A variety of viral vectors have been employed as well as naked plasmids and lipid or polymer-mediated delivery (see Table 56.4).

A variety of cardiac disorders have been treated with adenoviral systems, including cardiomyopathy (Bathgate et al., 2008), ventricular arrhythmia (Prunier et al., 2008), and, most significantly, damage after myocardial infarction (Shah et al., 2001, White et al., 2000) (Gupta et al., 2008a, Pleger et al., 2007). Adenovirus vectors have been used to study calcium handling in the myocardium by modulating expression of sarcoplasmic reticulum Ca^{2+} ATPase pump (SERCA2a) (del Monte et al., 2001, Miyamoto et al., 2000, Schmidt et al., 2000, Gupta et al., 2008b). Myocardial delivery of a variety of growth factors with adenovirus has also been investigated, including human hepatocyte growth factor (hHGF) (Chen et al., 2007b), placental growth factor (PlGF) (Roncal et al., 2008), human vascular endothelial growth

TABLE 56.4 Summary of Reported Gene Therapy Clinical Trials

Mode of Delivery	Gene	Lead Author	Reference
Naked plasmid	VEGF-A165	Ripa	Ripa et al., 2006
Naked plasmid	VEGF-A165	Gyongyosi	Gyongyosi et al., 2005
Naked plasmid	VEGF-A165	Kastrup	Kastrup et al., 2005
Naked plasmid	VEGF-A165	Losordo	Losordo et al., 1998
Naked plasmid	VEGF-A165 and GSF (granulocyte stimulating factor)	Wang	Wang et al., 2007
Naked plasmid	VEGF-C	Vale	Vale et al., 2001
Lipid-mediated	VEGF-A165	Hedman	Hedman et al., 2003, 2008
AAV	SERCA2a	Hajjar	Hajjar et al., 2008
Adenovirus	HGF	Yuan	Yuan et al., 2008b
Adenovirus	FGF	Lyon, Flynn, Rosengart, Grines, Kapur	Lyon et al., 2008, Flynn and O'Brien, 2008, Rosengart et al., 1999, Kapur and Rade, 2008, Grines et al., 2002

TABLE 56.5 Summary of *In Vivo* Preclinical Cardiac Studies Using Viral Gene Therapy

Mode of Delivery	Gene	Reference
Adenovirus	SERCA2a	Prunier et al., 2008, Gupta et al., 2008b, Sabbah et al., 2003, del Monte et al., 2001, Schmidt et al., 2000, Miyamoto et al., 2000
Adenovirus	Human HGF	Miyagawa et al., 2006, Chen et al., 2007b
Adenovirus	PlGF	Roncal et al., 2008
Adenovirus	VEGF	Guerrero et al., 2008
Adenovirus	HGF	Yuan et al., 2008a
AAV	IL-10	Nonaka-Sarukawa et al., 2008
AAV	Antisense phospholamban (asPLB)	Zhao et al., 2008
Lentivirus	Angiotensin converting enzyme 2 (ACE2)	Sarkissian et al., 2008

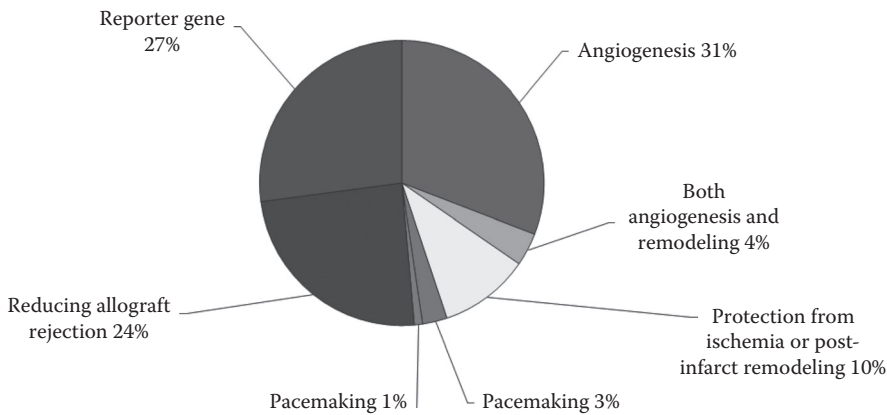
factor (VEGF) (Guerrero et al., 2008). A summary of selected preclinical studies using viruses to transfect the myocardium is described in Table 56.5.

Approximately half of the ongoing and completed clinical trials in cardiac gene therapy have used adenoviral vectors. The adenovirus-based clinical trials with the acronym AGENT were the largest and first myocardial gene therapy trials conducted on humans (Kapur and Rade, 2008, Grines et al., 2002). VEGF delivery via adenoviral vectors was demonstrated by Rosengart et al. to be safe, with clinically significant therapeutic effects (Rosengart et al., 1999). However, Phase II and III clinical trials in humans were largely inconclusive (Lyon et al., 2008).

Naked plasmid delivery accounts for about 41% of the reported clinical trials (Holladay et al., 2009), while lipid and cell-mediated gene delivery account for approximately 3% and 2%, respectively. The success rate has been relatively high considering that the transfection efficiency of non-viral gene delivery techniques is much lower than that of viruses. Neither treatment technique has significantly improved cardiac function in large-scale clinical trials, but both have shown promise. A wide variety of genes have been investigated in non-viral preclinical trials, as shown in Table 56.6, but clinical trials have focused solely on VEGF (Holladay et al., 2009) (Figure 56.3).

TABLE 56.6 Summary of *In Vivo* Cardiac Studies Using Lipid- or Polymer-Mediated Delivery of Plasmid DNA

Gene	Lead Author	Reference
Anti-angiotensin converting enzyme (ACE) siRNA	Kim	Kim et al., 2007
IL-4	Furukawa	Furukawa et al., 2005, 2008
IL-10	Sen, Hong, Oshima, Furukawa	Sen et al., 2001, Hong et al., 2002, Oshima et al., 2002, 2007, Furukawa et al., 2005, 2008
Antisense cyclin-dependent kinase cdk2, E2F decoy	Kawauchi	Kawauchi et al., 2000
Cis element decoy against NFkB	Sawa	Sawa et al., 1997
Heat-shock protein (HSP70)	Suzuki	Suzuki et al., 1997
Heat-shock protein (HSP70)	Jayakumar	Jayakumar et al., 2000
Heat-shock protein (HSP70)	Jayakumar	Jayakumar et al., 2001
eNOS	Iwata	Iwata et al., 2001
VEGF-A165	Pelisek	Pelisek et al., 2003
VEGF-A121	Wang	Wang et al., 2004

**FIGURE 56.3** Summary of genes studied in preclinical cardiac trials.

Another growing area of interest in myocardial gene therapy is cell-mediated delivery of therapeutics, as summarized in [Table 56.7](#). *Ex vivo* transfection of cells such as mesenchymal stem cells or skeletal myoblasts has been shown to improve cardiac function in a variety of preclinical models. Overexpression of elastin fragments (Mizuno et al., 2005b,a), VEGF (Ye et al., 2007, Suzuki et al., 2001, Yang et al., 2007), HGF (Miyagawa et al., 2006), adrenomedullin (Jo et al., 2007, Nagaya et al., 2003), MHC class I (Geissler et al., 2000), hyperpolarization-activated cyclic nucleotide-gated (HCN) channels (Potapova et al., 2004), and β_2 -adrenergic receptor (Edelberg et al., 1998) have all been investigated using cell-mediated gene therapy.

One of the disadvantages of cell injection is that great precision is required for the effective administration of the cells. Furthermore, very low retention rates are generally observed using these techniques. While the reason for this is not completely understood, it is likely that inflammation, nutrient limitations, and damage due to the injection procedure could be responsible. Scaffold-based cell therapy approaches for the treatment of the myocardium could present a possible solution to this problem. A number of recent studies have described using cell-seeded scaffolds instead of cell injections for cell-based therapy of the myocardium cells. Delivery of cardiomyocytes (Zimmermann et al., 2004), mesenchymal stem

TABLE 56.7 Summary of Studies Using Cell-Mediated Delivery of Therapeutics

Gene	Lead Author	Reference
Elastin	Mizuno	Mizuno et al., 2005b
Elastin	Mizuno	Mizuno et al., 2005a
VEGF-A165 and Ang-1	Ye	Ye et al., 2007
VEGF-A165	Suzuki	Suzuki et al., 2001
HGF	Miyagawa	Miyagawa et al., 2006
VEGF-A165	Yang	Yang et al., 2007
Adrenomedullin (AM)	Jo Ji	Jo et al., 2007
Adrenomedullin (AM)	Nagaya	Nagaya et al., 2003
MHC class I	Geissler	Geissler et al., 2000
Hyperpolarization-activated cyclic nucleotide-gated (HCN) channels	Potapova	Potapova et al., 2004
β 2-Adrenergic receptor	Edelberg	Edelberg et al., 1998
VEGF, PDGF	Das	Das et al., 2009
VEGF	Goncalves	Goncalves et al., 2010
VEGF, HGF, SDF-1, Akt1	Blumenthal	Blumenthal et al., 2010

cells (Xiang et al., 2006, Potapova et al., 2008, Wei et al., 2008), fibroblasts (Kellar et al., 2005) and bone marrow cells (Chachques et al., 2007) has been achieved. The observed benefits included significant improvements in ejection fraction (Chachques et al., 2007, Kellar et al., 2005), increases in infarcted wall thickness (Chachques et al., 2007), higher levels of angiogenic and cardioprotective factors (Wei et al., 2008) and improved electrical properties (Potapova et al., 2008). The use of biomaterial scaffolds to deliver genetically modified cells has also been demonstrated using a fibrin gel to deliver VEGF-expressing cardiac fibroblasts (Goncalves et al., 2010) and polyurethane to deliver skeletal myoblasts expressing a variety of different factors (Blumenthal et al., 2010). The use of scaffold-based gene therapy without a cellular component represents a potential new direction for cardiac gene therapy. A proof-of-concept study used fibrin glue as a delivery vehicle for plasmid DNA encoding pleiotrophin. Enhanced neovasculation was found to be associated with the therapy, but overall functional effects were not reported (Christman et al., 2005).

While the progress of gene therapy approaches for myocardial regeneration may be closer to clinical realization than some other areas, significant advances remain to be made. The role of nonviral approaches, especially cell and scaffold-mediated, are likely to be key to clinical translation of many therapies.

56.4.5 Cancer

Gene therapy can treat cancer by directly reducing the amount of tumor cells by lysing them with oncolytic viruses (Norman and Lee, 2005), regulating the expression of bioactive molecules that affect cell growth and development (Duval et al., 2006), or by inciting the immune system to react against antigens found in tumor cells (Clarke et al., 2010). These therapies can be combined, but the limiting size of the capsid and the dose-dependent responses to gene therapy make this difficult. It is more likely to combine a single technique with standard therapies. Gene therapy treatments are still in the early clinical trial phase, and while some trials show partial patient improvement, they have not resulted in full regression. Such trials are shown in [Table 56.8](#).

The systemic administration of cytokines show a clinical response in treating cancer (Lotze et al., 1986, Shau et al., 1990, Motzer et al., 1998, Ozer et al., 1998), but natural toxicity makes administering cytokines as a treatment unfeasible. Cytokine gene therapy is one of the methods being developed

TABLE 56.8 Clinical Trials of Gene Therapy Treating Cancer

Type of Cancer	Gene	Mode of Delivery	Reference
Melanoma	IL-2	Cell-mediated	Duval et al., 2006
	GM-CSF	Cell-mediated	Kusumoto et al., 2001
Renal cancer	GM-CSF	Cell-mediated	Tani et al., 2004
	IL-2	Cell-mediated	Uemura et al., 2006
Small-cell lung cancer	IL-2	Adenovirus	Griscelli et al., 2003
	P-53	Adenovirus	Chiappori et al., 2010
Prostate	IL-2	Adenovirus	Trudel et al., 2003
	— — — — —	Wild-type reovirus	Norman and Lee, 2005
Breast	IL-2	Adenovirus	Stewart et al., 1999
Solid tumors	TNF	Adenovirus	Gregorc et al., 2009
Sarcoma	TNF	Adenovirus	Mundt et al., 2004

for a more efficient, less toxic use of cytokines. Not only does this result in a more gradual, continuous exposure to cytokines, but the use of promoters give more control over the rate or duration of cytokine production (Lopez et al., 2004).

Tumor-associated antigens (TAAs) are chemical markers to identify tumor cells and can be used to specifically target tumor cells. Antitumor immunotherapy involves inciting the immune system, usually cytotoxic T cells (CTC), to attack cells with TAAs. Viruses are encoded with transgenes for TAAs and are administered to infect host cells. The immune response to the viral load will lead to specific immune responses against the transgene product, causing the virus to act as a vaccine (Woo et al., 2006).

Oncolytic virus therapy exploits tumor cells' susceptibility to viruses to target them and transfect only the tumor cells. By using viruses very unlikely to transfect healthy human cells, the viruses specificity makes it a useful anticancer agent. Some wild-type viruses, such as the reovirus, can be used as an oncolytic virus (Comins et al., 2008).

56.5 Summary

To conclude, gene therapy can be administered using effective but immunogenic viruses or less antigenic nonviral techniques with associated lower levels of transfection. Gradual, continuous release can be mediated by the use of scaffolds as reservoirs. Another alternative is cells already altered *ex vivo*. Gene therapy is currently limited to clinical trials and more basic research, but multiple treatments are showing marked improvement with acceptable side effects.

The future of gene therapy requires a significant decrease in side effects while providing effective treatment. This is necessary both to compete against other therapies and to obtain regulatory approval. As new methods of avoiding dangerous doses, such as the gradual release of vectors with scaffolds, become more widespread, gene therapy will become a more viable form of treatment. Further research into nonviral vectors will develop new materials with limited cytotoxicity and high transfection efficiency. As viruses become less necessary for gene therapy the stigma against them will no longer hurt gene therapy when it comes to patient approval and regulation.

The use of scaffolds will likely become more pronounced in gene therapy as it integrates with other therapies. Scaffolds can support increased loads of DNA or cells transfected *in vitro*, leading to increased expression, or the scaffold can be designed for a slow degradation, resulting in long-term modified gene expression. They are improving to where a high DNA complex load, highly controlled and adjustable degradation rate, biocompatibility, angiogenic properties, and differentiation induction can be achieved in the same structure without sacrificing any of the desired qualities.

Acknowledgments

This material is based upon works supported by the Science Foundation Ireland under grant no. 07/SRC/B1163.

Health Research Board (HRB/2008/188) for financial support of this work.

References

2008. First gene therapy clinical trial for heart failure. *Molecular Therapy*, 16, 1353–1353.
- Acsadi, G., Jiao, S., Jani, A., Duke, D., Williams, P., Chong, W., and Wolff, J. A. 1991. Direct gene-transfer and expression into rat-heart in vivo. *New Biologist*, 3, 71–81.
- Ahlmann, E., Patzakis, M., Roidis, N., Shepherd, L., and Holtom, P. 2002. Comparison of anterior and posterior iliac crest bone grafts in terms of harvest-site morbidity and functional outcomes. *Journal of Bone and Joint Surgery-American Volume*, 84A, 716–720.
- Albrektsson and Johansson 2001. Osteoinduction, osteoconduction and osseointegration. *European Spine Journal*, 10, S96-S101-S101.
- Ali, M., Lemoine, N. R., and Ring, C. J. A. 1994. The use of Dna viruses as vectors for gene-therapy. *Gene Therapy*, 1, 367–384.
- Andreadis, S. T. and Geer, D. J. 2006. Biomimetic approaches to protein and gene delivery for tissue regeneration. *Trends in Biotechnology*, 24, 331–337.
- Andree, C., Voigt, M., Wenger, A., Erichsen, T., Bittner, K., Schaefer, D., Walgenbach, K. J., Borges, J., Horch, R. E., Eriksson, E., and Stark, G. B. 2001. Plasmid gene delivery to human keratinocytes through a fibrin-mediated transfection system. *Tissue Eng*, 7, 757–766.
- Asai, J., Takenaka, H., Kusano, K. F., II, M., Luedemann, C., Curry, C., Eaton, E., Iwakura, A., Tsutsumi, Y., Hamada, H., Kishimoto, S., Thorne, T., Kishore, R., and Losordo, D. W. 2006. Topical sonic hedgehog gene therapy accelerates wound healing in diabetes by enhancing endothelial progenitor cell-mediated microvascular remodeling. *Circulation*, 113, 2413–2424.
- Ashare, A. B., Maysky, M., Vale, P. R., Losordo, D. W., Symes, J. F., and Isner, J. M. 1999. Quantitative evaluation of gene therapy for myocardial angiogenesis. *Journal of Nuclear Medicine*, 40, 760.
- Avery, O. T., Mcleod, C. M., and Mccarty, M. 1944. Studies on the chemical nature of the substance inducing transformation of pneumococcal types. *Journal of Experimental Medicine*, 79, 137–158.
- Badillo, A. T., Chung, S., Zhang, L., Zoltick, P., and Liechty, K. W. 2007. Lentiviral gene transfer of Sdf-1alpha to wounds improves diabetic wound healing. *Journal of Surgery and Research*, 143, 35–42.
- Bakal, C., Becker, G., Clement, D. L., Cronenwett, J., Durand-Zaleski, I., Diehm, C., Harris, K., Hiatt, W. R., Hunink, M., Isner, J., Lammer, J., Norgren, L., Novo, S., Ricco, J. B., Verstraete, M., and White, J. 2000. Management of peripheral arterial disease (Pad). *European Journal of Vascular and Endovascular Surgery*, 19 Suppl A, S115–S143.
- Bakker, A. C., Van DE Loo, F. A., Joosten, L. A., Bennink, M. B., Arntz, O. J., Dmitriev, I. P., Kashentsera, E. A., Curiel, D. T., and Van DEN Berg, W. B. 2001. A tropism-modified adenoviral vector increased the effectiveness of gene therapy for arthritis. *Gene Therapy*, 8, 1785–1793.
- Baltzer, A. W. A., Lattermann, C., Whalen, J. D., Wooley, P., Weiss, K., Grimm, M., Ghivizzani, S. C., Robbins, P. D., and Evans, C. H. 2000. Genetic enhancement of fracture repair: healing of an experimental segmental defect by adenoviral transfer of the Bmp-2 gene. *Gene Therapy*, 7, 734–739.
- Baraniak, P. R. and Mcdevitt, T. C. 2010. Stem cell paracrine actions and tissue regeneration. *Regenerative Medicine*, 5, 121–143.
- Barnes, P. F., Abrams, J. S., LU, S. Z., Sieling, P. A., Rea, T. H., and Modlin, R. L. 1993. Patterns of cytokine production by Mycobacterium-reactive human T-cell clones. *Infection and Immunity*, 61, 197–203.
- Barrick, B., Campbell, E. J., and Owen, C. A. 1999. Leukocyte proteinases in wound healing: Roles in physiologic and pathologic processes. *Wound Repair Regen*, 7, 410–422.

- Baru, M., Axelrod, J. H., and Nur, I. 1995. Liposome-encapsulated DNA-mediated gene-transfer and synthesis of human factor-IX in mice. *Gene*, 161, 143–150.
- Bathgate, R. A. D., Lekgabe, E. D., Mcguane, J. T., SU, Y., Pham, T., Ferraro, T., Layfield, S., Hannan, R. D., Thomas, W. G., Samuel, C. S., and DU, X. J. 2008. Adenovirus-mediated delivery of relaxin reverses cardiac fibrosis. *Molecular and Cellular Endocrinology*, 280, 30–38.
- Baumgartner, I., Chronos, N., Comerota, A., Henry, T., Pasquet, J. P., Finiels, F., Caron, A., Dedieu, J. F., Pilsudski, R., and Delaã RE, P. 2009. Local gene transfer and expression following intramuscular administration of Fgf-1 plasmid DNA in patients with critical limb ischemia. *Molecular Therapy*, 17, 914–921.
- Baumgartner, I., Pieczek, A., Manor, O., Blair, R., Kearney, M., Walsh, K., and Isner, J. M. 1998. Constitutive expression of phvegf165 after intramuscular gene transfer promotes collateral vessel development in patients with critical limb ischemia. *Circulation*, 97, 1114–1123.
- Bhattacharyya, J., Mondal, G., Madhusudana, K., Agawane, S. B., Ramakrishna, S., Gangireddy, S. R., Madhavi, R. D., Reddy, P. K., Konda, V. R., Rao, S. R., Udaykumar, P., and Chaudhuri, A. 2009. Single subcutaneous administration of Rgdk-lipo-peptide:rhpdgf-B gene complex heals wounds in streptozotocin-induced diabetic rats. *Molecular Pharmacology*, 6, 918–927.
- Bitto, A., Minutoli, L., Galeano, M. R., Altavilla, D., Polito, F., Fiumara, T., Calo, M., LO Cascio, P., Zentilin, L., Giacca, M., and Squadrito, F. 2008. Angiopoietin-1 gene transfer improves impaired wound healing in genetically diabetic mice without increasing Vegf expression. *Clinical Science (Lond)*, 114, 707–718.
- Blakytyn, R. and Jude, E. 2006. The molecular biology of chronic wounds and delayed healing in diabetes. *Diabetes Medicine*, 23, 594–608.
- Blakytyn, R. and Jude, E. B. 2009. Altered molecular mechanisms of diabetic foot ulcers. *International Journal of Low Extreme Wounds*, 8, 95–104.
- Blum, J. S., Barry, M. A., Mikos, A. G., and Jansen, J. A. 2003. *In vivo* evaluation of gene therapy vectors in ex vivo-derived marrow stromal cells for bone regeneration in a rat critical-size calvarial defect model. *Human Gene Therapy*, 14, 1689–1701.
- Blumenthal, B., Golsong, P., Poppe, A., Heilmann, C., Schlensak, C., Beyersdorf, F., and Siepe, M. 2010. Polyurethane scaffolds seeded with genetically engineered skeletal myoblasts: A promising tool to regenerate myocardial function. *Artificial Organs*, 34(2), E46–E54.
- Boden, S. D., Liu, Y. S., Hair, G. A., Helms, J. A., HU, D., Racine, M., Nanes, M. S., and Titus, L. 1998. Lmp-1, a Lim-domain protein, mediates Bmp-6 effects on bone formation. *Endocrinology*, 139, 5125–5134.
- Bonadio, J. 2000. Tissue engineering via local gene delivery: Update and future prospects for enhancing the technology. *Advances in Drug Delivery Reviews*, 44, 185–194.
- Bonadio, J., Smiley, E., Patil, P., and Goldstein, S. 1999a. Localized, direct plasmid gene delivery in vivo: prolonged therapy results in reproducible tissue regeneration. *Nature Medicine*, 5, 753–759.
- Bonadio, J., Smiley, E., Patil, P., and Goldstein, S. 1999b. Localized, direct plasmid gene delivery in vivo: prolonged therapy results in reproducible tissue regeneration. *Nature Medicine*, 5, 753–759.
- Bowler, P. G. 2002. Wound pathophysiology, infection and therapeutic options. *Annals in Medicine*, 34, 419–427.
- Breen, A., Dockery, P., O'brien, T., and Pandit, A. 2008. The use of therapeutic gene enos delivered via a fibrin scaffold enhances wound healing in a compromised wound model. *Biomaterials*, 29, 3143–3151.
- Breen AM, D. P., O'Brien T, Pandit AS 2008. The use of therapeutic gene enos delivered via a fibrin scaffold enhances wound healing in a compromised wound model. *Biomaterials*, 29, 3143–3151.
- Brem, H., Kodra, A., Golinko, M. S., Entero, H., Stojadinovic, O., Wang, V. M., Sheahan, C. M., Weinberg, A. D., Woo, S. L., Ehrlich, H. P., and Tomic-Canic, M. 2009. Mechanism of sustained release of vascular endothelial growth factor in accelerating experimental diabetic healing. *Journal of Investigative Dermatology*, 129, 2275–2287.
- Brem, H. and Tomic-Canic, M. 2007. Cellular and molecular basis of wound healing in diabetes. *Journal of Clinical Investigation*, 117, 1219–1222.
- Breunig, M., Lungwitz, U., Liebl, R., and Goepferich, A. 2007. Breaking up the correlation between efficacy and toxicity for nonviral gene delivery. *Proceedings of the National Academy of Sciences of the United States of America*, 104, 14454–14459.

- Brown, R. L., Breeden, M. P., and Greenhalgh, D. G. 1994. Pdgf and Tgf-alpha act synergistically to improve wound healing in the genetically diabetic mouse. *Journal of Surgical Research*, 56, 562-70.
- Cao, L., Arany, P. R., Kim, J., Rivera-Feliciano, J., Wang, Y. S., He, Z., Rask-Madsen, C., King, G. L., and Mooney, D. J. 2010. Modulating Notch signaling to enhance neovascularization and reperfusion in diabetic mice. *Biomaterials*, 34, 9048-9056.
- Chachques, J. C., Trainini, J. C., Lago, N., Masoli, O. H., Barisani, J. L., Cortes-Morichetti, M., Schussler, O., and Carpentier, A. Year. Myocardial assistance by grafting a new bioartificial upgraded myocardium (Magnum clinical trial): One year follow-up. In: *3rd International Conference on Cell Therapy for Cardiovascular Diseases*, 2007 New York, NY, pp. 927-934.
- Check, E. 2003. Cancer risk prompts US to curb gene therapy. *Nature*, 422, 7-7.
- Chen, J., Huang, S. W., Lin, W. H., and Zhuo, R. X. 2007a. Tunable film degradation and sustained release of plasmid DNA from cleavable polycation/plasmid DNA multilayers under reductive conditions. *Small*, 3, 636-643.
- Chen, X. H., Minatoguchi, S., Kosai, K., Yuge, K., Takahashi, T., Arai, M., Wang, N. Y., Misao, Y., Lu, C. J., Onogi, H., Kobayashi, H., Yasuda, S., Ezaki, M., Ushikoshi, H., Takemura, G., Fujiwara, T., and Fujiwara, H. 2007b. *In vivo* hepatocyte growth factor gene transfer reduces myocardial ischemia - reperfusion injury through its multiple actions. *Journal of Cardiac Failure*, 13, 874-883.
- Chiappori, A. A., Soliman, H., Janssen, W. E., Antonia, S. J., and Gabrilovich, D. I. 2010. Ingn-225: A dendritic cell-based p53 vaccine (Ad.p53-DC) in small cell lung cancer: Observed association between immune response and enhanced chemotherapy effect. *Expert Opin Biol Ther*, 10, 983-991.
- Christman, K. L., Fang, Q. Z., Yee, M. S., Johnson, K. R., Sievers, R. E., and Lee, R. J. 2005. Enhanced neovasculature formation in ischemic myocardium following delivery of pleiotrophin plasmid in a biopolymer. *Biomaterials*, 26, 1139-1144.
- Chun, K. W., Lee, J. B., Kim, S. H., and Park, T. G. 2005. Controlled release of plasmid DNA from photo-cross-linked pluronic hydrogels. *Biomaterials*, 26, 3319-3326.
- Cianfarani, F., Zambruno, G., Brogelli, L., Sera, F., Lacal, P. M., Pesce, M., Capogrossi, M. C., Failla, C. M., Napolitano, M., and Odorisio, T. 2006. Placenta growth factor in diabetic wound healing: Altered expression and therapeutic potential. *American Journal of Pathology*, 169, 1167-1182.
- Clarke, J. M., Morse, M. A., Lyerly, H. K., Clay, T., and Osada, T. 2010. Adenovirus vaccine immunotherapy targeting Wt1-expressing tumors. *Expert Opinion in Biological Therapy*, 10, 875-883.
- Comerota, A. J., Throm, R. C., Miller, K. A., Henry, T., Chronos, N., Laird, J., Sequeira, R., Kent, C. K., Bacchetta, M., Goldman, C., Salenius, J. P., Schmieder, F. A., and Pilsudski, R. 2002. Naked plasmid Dna encoding fibroblast growth factor type 1 for the treatment of end-stage unreconstructible lower extremity ischemia: Preliminary results of a phase I trial. *Journal of Vascular Surgery*, 35, 930-936.
- Comins, C., Heinemann, L., Harrington, K., Melcher, A., DE Bono, J., and Pandha, H. 2008. Reovirus: Viral therapy for cancer 'as nature intended'. *Clinical Oncology (R Coll Radiol)*, 20, 548-554.
- Das, H., George, J. C., Joseph, M., Das, M., Abdulhameed, N., Blitz, A., Khan, M., Sakthivel, R., Mao, H. Q., Hoit, B. D., Kuppasamy, P., and Pompili, V. J. 2009. Stem cell therapy with overexpressed Vegf and Pdgf genes improves cardiac function in a rat infarct model. *Plos One*, 4(10), e7325.
- Davidson, J. M., Broadley, K. N., and Quagliano, D. 1997. Reversal of the wound healing deficit in diabetic rats by combined basic fibroblast growth and transforming factor-beta1 therapy. *Wound Repair Regeneration*, 5, 77-88.
- Davis, J., Westfall, M. V., Townsend, D., Blankinship, M., Herron, T. J., Guerrero-Serna, G., Wang, W., Devaney, E., and Metzger, J. M. 2008. Designing heart performance by gene transfer. *Physiological Reviews*, 88, 1567-1651.
- Del Monte, F., Williams, E., Lebeche, D., Schmidt, U., Rosenzweig, A., Gwathmey, J. K., Lewandowski, E. D., and Hajjar, R. J. 2001. Improvement in survival and cardiac metabolism after gene transfer of sarcoplasmic reticulum Ca2 + -ATPase in a rat model of heart failure. *Circulation*, 104, 1424-1429.

- Dennig, J. and Duncan, E. 2002. Gene transfer into eukaryotic cells using activated polyamidoamine dendrimers. *Journal of Biotechnology*, 90, 339–347.
- Diegelmann, R. F. and Evans, M. C. 2004. Wound healing: An overview of acute, fibrotic and delayed healing. *Frontiers in Bioscience*, 9, 283–289.
- Dorresteijn, J. A., Kriegsman, D. M., and Valk, G. D. 2010. Complex interventions for preventing diabetic foot ulceration. *Cochrane Database Systems Reviews*, 1, Cd007610.
- Dufes, C., Uchegbu, I. F., and Schatzlein, A. G. 2005. Dendrimers in gene delivery. *Advanced Drug Delivery Reviews*, 57, 2177–2202.
- Duval, L., Schmidt, H., Kaltoft, K., Fode, K., Jensen, J. J., Sorensen, S. M., Nishimura, M. I., and Von DER Maase, H. 2006. Adoptive transfer of allogeneic cytotoxic T lymphocytes equipped with a Hla-A2 restricted Mart-1 T-cell receptor: A phase I trial in metastatic melanoma. *Clinical Cancer Research*, 12, 1229–1236.
- Edelberg, J. M., Aird, W. C., and Rosenberg, R. D. 1998. Enhancement of murine cardiac chronotropy by the molecular transfer of the human beta(2) adrenergic receptor cDNA. *Journal of Clinical Investigation*, 101, 337–343.
- Edelstein, M. L., Abedi, M. R., and Wixon, J. 2007. Gene therapy clinical trials worldwide to 2007—An update. *The Journal of Gene Medicine*, 9, 833–842.
- Egermann, M., Baltzer, A. W., Adamaszek, S., Evans, C., Robbins, P., Schneider, E., and Lill, C. A. 2006a. Direct adenoviral transfer of bone morphogenetic protein-2 cDNA enhances fracture healing in osteoporotic sheep. *Human Gene Therapy*, 17, 507–517.
- Egermann, M., Lill, C. A., Griesbeck, K., Evans, C. H., Robbins, P. D., Schneider, E., and Baltzer, A. W. 2006b. Effect of Bmp-2 gene transfer on bone healing in sheep. *Gene Therapy*, 13, 1290–1299.
- Eming, S. A., Krieg, T., and Davidson, J. M. 2004. Gene transfer in tissue repair: status, challenges and future directions. *Expert Opinion in Biological Therapy*, 4, 1373–1386.
- Fang, J. M., Zhu, Y. Y., Smiley, E., Bonadio, J., Rouleau, J. P., Goldstein, S. A., Mccauley, L. K., Davidson, B. L., and Roessler, B. J. 1996. Stimulation of new bone formation by direct transfer of osteogenic plasmid genes. *Proceedings of the National Academy of Sciences of the United States of America*, 93, 5753–5758.
- Fang, Y., Shen, J., Yao, M., Beagley, K. W., Hambly, B. D., and Bao, S. 2010. Granulocyte–macrophage colony-stimulating factor enhances wound healing in diabetes via upregulation of proinflammatory cytokines. *British Journal of Dermatology*, 162, 478–486.
- Fernandez-Montequin, J. I., Infante-Cristia, E., Valenzuela-Silva, C., Franco-Perez, N., Savigne-Gutierrez, W., Artaza-Sanz, H., Morejon-Vega, L., Gonzalez-Benavides, C., Eliseo-Musenden, O., Garcia-Iglesias, E., Berlanga-Acosta, J., Silva-Rodriguez, R., Betancourt, B. Y., and Lopez-Saura, P. A. 2007. Intralesional injections of Citoprot-P (recombinant human epidermal growth factor) in advanced diabetic foot ulcers with risk of amputation. *International Wound Journal*, 4, 333–343.
- Fernandez-Montequin, J. I., Valenzuela-Silva, C. M., Diaz, O. G., Savigne, W., Sancho-Soutelo, N., Rivero-Fernandez, F., Sanchez-Penton, P., Morejon-Vega, L., Artaza-Sanz, H., Garcia-Herrera, A., Gonzalez-Benavides, C., Hernandez-Canete, C. M., Vazquez-Proenza, A., Berlanga-Acosta, J., and Lopez-Saura, P. A. 2009. Intra-lesional injections of recombinant human epidermal growth factor promote granulation and healing in advanced diabetic foot ulcers: multicenter, randomised, placebo-controlled, double-blind study. *International Wound Journal*, 6, 432–443.
- Flynn, A. and O'brien, T. 2008. Alferminogene tadenovec, an angiogenic Fgf4 gene therapy for coronary artery disease. *Drugs*, 11, 283–293.
- Fortuin, F. D., Vale, P., Losordo, D. W., Symes, J., Delaria, G. A., Tyner, J. J., Schaer, G. L., March, R., Snell, R. J., Henry, T. D., Van Camp, J., Lopez, J. J., Richenbacher, W., Isner, J. M., and Schatz, R. A. 2003. One-year follow-up of direct myocardial gene transfer of vascular endothelial growth factor-2 using naked plasmid deoxyribonucleic acid by way of thoracotomy in no-option patients. *American Journal of Cardiology*, 92, 436–439.
- French, B. A., Mazur, W., Geske, R. S., and Bolli, R. 1994. Direct *in vivo* gene-transfer into porcine myocardium using replication-deficient adenoviral vectors. *Circulation*, 90, 2414–2424.

- Friedmann, T. 1989. Progress toward human gene therapy. *Science*, 244, 1275–1281.
- Friedmann, T. 1992. A brief history of gene therapy. *Nature Genetics*, 2, 93–98.
- Furukawa, H., Oshima, K., Tung, T., Cui, G. G., Laks, H., and Sen, L. 2005. Liposome-mediated combinatorial cytokine gene therapy induces localized synergistic immunosuppression and promotes long-term survival of cardiac allografts. *Journal of Immunology*, 174, 6983–6992.
- Furukawa, H., Oshima, K., Tung, T., Cui, G. G., Laks, H., and Sen, L. Y. 2008. Overexpressed exogenous IL-4 and IL-10 paradoxically regulate allogenic T-Cell and cardiac myocytes apoptosis through Fas/FasL pathway. *Transplantation*, 85, 437–446.
- Galkowska, H., Wojewodzka, U., and Olszewski, W. L. 2006. Chemokines, cytokines, and growth factors in keratinocytes and dermal endothelial cells in the margin of chronic diabetic foot ulcers. *Wound Repair and Regeneration*, 14, 558–565.
- Geissler, E. K., Graeb, C., Tange, S., Guba, M., Jauch, K. W., and Scherer, M. N. 2000. Effective use of donor Mhc class I gene therapy in organ transplantation: Prevention of antibody-mediated hyperacute heart allograft rejection in highly sensitized rat recipients. *Human Gene Therapy*, 11, 459–469.
- Gisep, A. 2002. Research on ceramic bone substitutes: Current status. *Injury-International Journal of the Care of the Injured*, 33, 88–92.
- Giurini, J. M. and Lyons, T. E. 2005. Diabetic foot complications: Diagnosis and management. *Int J Low Extreme Wounds*, 4, 171–182.
- Goncalves, G. A., Vassallo, P. F., Dos Santos, L., Schettert, I. T., Nakamuta, J. S., Becker, C., Tucci, P. J. F., and Krieger, J. E. 2010. Intramyocardial transplantation of fibroblasts expressing vascular endothelial growth factor attenuates cardiac dysfunction. *Gene Therapy*, 17, 305–314.
- Gottrup, F., Apelqvist, J., and Price, P. 2010. Outcomes in controlled and comparative studies on non-healing wounds: Recommendations to improve the quality of evidence in wound management. *J Wound Care*, 19, 237–268.
- Gray, S. J. and Samulski, R. J. 2008. Optimizing gene delivery vectors for the treatment of heart disease. *Expert Opinion on Biological Therapy*, 8, 911–922.
- Greenhalgh, D. G., Hummel, R. P., Albertson, S., and Breeden, M. P. 1993. Synergistic actions of platelet-derived growth factor and the insulin-like growth factors in vivo. *Wound Repair Regen*, 1, 69–81.
- Gregorc, V., Santoro, A., Bencicelli, E., Punt, C. J., Citterio, G., Timmer-Bonte, J. N., Caligaris Cappio, F., Lambiasi, A., Bordignon, C., and Van Herpen, C. M. 2009. Phase Ib study of Ngr-htnf, a selective vascular targeting agent, administered at low doses in combination with doxorubicin to patients with advanced solid tumours. *British Journal of Cancer*, 101, 219–224.
- Grines, C., Rubanyi, G. M., Kleiman, N. S., Marrott, P., and Watkins, M. W. Year. Angiogenic gene therapy with adenovirus 5 fibroblast growth factor-4 (Ad5fgf = 4): A new option for the treatment of coronary artery disease. In: *Workshop on Angiogenic Gene Therapy*, Dec 13–15, 2002 New York, New York. 24N–31N.
- Grinnell, F., Ho, C. H., and Wysocki, A. 1992. Degradation of fibronectin and vitronectin in chronic wound fluid: analysis by cell blotting, immunoblotting, and cell adhesion assays. *Journal of Investigative Dermatology*, 98, 410–416.
- Griscelli, F., Opolon, P., Saulnier, P., Mami-Chouaib, F., Gautier, E., Echchakir, H., Angevin, E., LE Chevalier, T., Bataille, V., Squiban, P., Tursz, T., and Escudier, B. 2003. Recombinant adenovirus shedding after intratumoral gene transfer in lung cancer patients. *Gene Therapy*, 10, 386–395.
- Guerrero, M., Athota, K., Moy, J., Mehta, L. S., Laguens, R., Crottogini, A., Borrelli, M., Corry, P., Schoenherr, D., Gentry, R., Boura, J., Grines, C. L., Raff, G. L., Shanley, C. J., and O'neill, W. W. 2008. Vascular endothelial growth factor-165 gene therapy promotes cardiomyogenesis in reperfused myocardial infarction. *Journal of Interventional Cardiology*, 21, 242–251.
- Guo, T., Zhao, J., Chang, J., Ding, Z., Hong, H., Chen, J., and Zhang, J. 2006. Porous chitosan-gelatin scaffold containing plasmid Dna encoding transforming growth factor-beta1 for chondrocytes proliferation. *Biomaterials*, 27, 1095–1103.
- Gupta, D., Molina, E. J., Palma, J., Gaughan, J. P., Long, W., and Macha, M. 2008a. Adenoviral beta-adrenergic receptor kinase inhibitor gene transfer improves exercise capacity, cardiac contractility, and

- systemic inflammation in a model of pressure overload hypertrophy. *Cardiovascular Drugs and Therapy*, 22, 373–381.
- Gupta, D., Palma, J., Molina, E., Gaughan, J. P., Long, W., Houser, S., and Macha, M. 2008b. Improved exercise capacity and reduced systemic inflammation after adenoviral-mediated Serca-2a gene transfer. *Journal of Surgical Research*, 145, 257–265.
- Guyton, A. C. and Hall, J. E. 2000. Unit IV: The circulation. *Textbook of Medical Physiology*. 10th ed. Philadelphia, Pennsylvania: W.B. Saunders Company.
- Guzman, R. J., Lemarchand, P., Crystal, R. G., Epstein, S. E., and Finkel, T. 1993. Efficient gene transfer into myocardium by direct-injection of adenovirus vectors. *Circulation Research*, 73, 1202–1207.
- Gyongyosi, M., Khorsand, A., Zamini, S., Sperker, W., Strehblow, C., Kastrup, J., Jorgensen, E., Hesse, B., Tagil, K., Botker, H. E., Ruzyllo, W., Teresinska, A., Dudek, D., Hubalewska, A., Ruck, A., Nielsen, S. S., Graf, S., Mundigler, G., Novak, J., Sochor, H., Maurer, G., Glogar, D., and Sylven, C. 2005. Noga-guided analysis of regional myocardial perfusion abnormalities treated with intramyocardial injections of plasmid encoding vascular endothelial growth factor A-165 in patients with chronic myocardial ischemia—Subanalysis of the Euroinject-One multicenter double-blind randomized study. *Circulation*, 112, I157–I165.
- Hacein-Bey-Abina, S., Von Kalle, C., Schmidt, M., LE Deist, F., Wulffraat, N., Mcintyre, E., Radford, I., Villeval, J.-L., Fraser, C. C., Cavazzana-Calvo, M., and Fischer, A. 2003. A serious adverse event after successful gene therapy for X-linked severe combined immunodeficiency. *The New England Journal of Medicine*, 348, 255–256.
- Haider, H. K., Elmadbouh, I., Jean-Baptiste, M., and Ashraf, M. 2008. Nonviral vector gene modification of stem cells for myocardial repair. *Molecular Medicine*, 14, 79–86.
- Hajjar, R. J., Zsebo, K., Deckelbaum, L., Thompson, C., Rudy, J., Yaroshinsky, A., Ly, H., Kawase, Y., Wagner, K., Borow, K., Jaski, B., London, B., Greenberg, B., Pauly, D. F., Patten, R., Starling, R., Mancini, D., and Jessup, M. 2008. Design of a phase 1/2 trial of intracoronary administration of Aav1/SERCA2a in patients with heart failure. *Journal of Cardiac Failure*, 14, 355–367.
- Haro, J., Acin, F., Lopez-Quintana, A., Florez, A., Martinez-Aguilar, E., and Varela, C. 2009. Meta-analysis of randomized, controlled clinical trials in angiogenesis: Gene and cell therapy in peripheral arterial disease. *Heart and Vessels*, 24, 321–328.
- Hattori, Y., Kawakami, S., Suzuki, S., Yamashita, F., and Hashida, M. 2004. Enhancement of immune responses by Dna vaccination through targeted gene delivery using mannosylated cationic liposome formulations following intravenous administration in mice. *Biochemistry and Biophysics Research Communication*, 317, 992–999.
- Haviernik, P. and Bunting, K. D. 2004. Safety concerns related to hematopoietic stem cell gene transfer using retroviral vectors. *Current Gene Therapy*, 4, 263–276.
- Hedman, M., Hartikainen, J., Syvanne, M., Stjernvall, J., Hedman, A., Kivela, A., Vanninen, E., Mussalo, H., Kauppila, E., Simula, S., Narvanen, O., Rantala, A., Peuhkurinen, K., Nieminen, M. S., Laakso, M., and Yla-Herttuala, S. 2003. Safety and feasibility of catheter-based local intracoronary vascular endothelial growth factor gene transfer in the prevention of postangioplasty and in-stent restenosis and in the treatment of chronic myocardial ischemia—Phase II results of the Kuopio Angiogenesis Trial (Kat). *Circulation*, 107, 2677–2683.
- Henry, T. D., Rocha-Singh, K., Isner, J. M., Kereiakes, D. J., Giordano, F. J., Simons, M., Losordo, D. W., Hendel, R. C., Bonow, R. O., Eppler, S. M., Zioncheck, T. F., Holmgren, E. B., and McCluskey, E. R. 2001. Intracoronary administration of recombinant human vascular endothelial growth factor to patients with coronary artery disease. *American Heart Journal*, 142, 872–880.
- Hirsch, T., Spielmann, M., Velandar, P., Zuhaili, B., Bleiziffer, O., Fossum, M., Steintraesser, L., Yao, F., and Eriksson, E. 2008. Insulin-like growth factor-1 gene therapy and cell transplantation in diabetic wounds. *Journal of Gene Medicine*, 10, 1247–1252.
- Holladay, C. A., O'Brien, T., and Pandit, A. 2009. Non-viral gene therapy for myocardial engineering. *Wiley Interdisciplinary Reviews: Nanomedicine and Nanobiotechnology*, 2, 232–248.

- Hong, Y. S., Laks, H., Cui, G. G., Chong, T., and Sen, L. Y. 2002. Localized immunosuppression in the cardiac allograft induced by a new liposome-mediated IL-10 gene therapy. *Journal of Heart and Lung Transplantation*, 21, 1188–1200.
- Horch, R. E., Kopp, J., Kneser, U., Beier, J., and Bach, A. D. 2005. Tissue engineering of cultured skin substitutes. *Journal of Cellular and Molecular Medicine*, 9, 592–608.
- Hosseinkhani, H. 2006. Dna nanoparticles for gene delivery to cells and tissue. *International Journal of Nanotechnology*, 3, 416–461.
- Hosseinkhani, H., Azzam, T., Kobayashi, H., Hiraoka, Y., Shimokawa, H., Domb, A. J., and Tabata, Y. 2006a. Combination of 3D tissue engineered scaffold and non-viral gene carrier enhance *in vitro* Dna expression of mesenchymal stem cells. *Biomaterials*, 27, 4269–4278.
- Hosseinkhani, H., Hosseinkhani, M., Gabrielson, N. P., Pack, D. W., Khademhosseini, A., and Kobayashi, H. 2008. Dna nanoparticles encapsulated in 3D tissue-engineered scaffolds enhance osteogenic differentiation of mesenchymal stem cells. *Journal of Biomedical Materials Research Part A*, 85A, 47–60.
- Hosseinkhani, H., Inatsugu, Y., Hiraoka, Y., Inoue, S., Shimokawa, H., and Tabata, Y. 2005. Impregnation of plasmid Dna into three-dimensional scaffolds and medium perfusion enhance *in vitro* Dna expression of mesenchymal stem cells. *Tissue Engineering*, 11, 1459–1475.
- Hosseinkhani, H. and Tabata, Y. 2006. Self assembly of Dna nanoparticles with polycations for the delivery of genetic materials into cells. *Journal of Nanoscience and Nanotechnology*, 6, 2320–2328.
- Hosseinkhani, H., Yamamoto, M., Inatsugu, Y., Hiraoka, Y., Inoue, S., Shimokawa, H., and Tabata, Y. 2006b. Enhanced ectopic bone formation using a combination of plasmid Dna impregnation into 3-D scaffold and bioreactor perfusion culture. *Biomaterials*, 27, 1387–1398.
- Immordino, M. L., Dosio, F., and Cattel, L. 2006. Stealth liposomes: Review of the basic science, rationale, and clinical applications, existing and potential. *International Journal of Nanomedicine*, 1, 297–315.
- Isner, J. M. 1998. Arterial gene transfer of naked Dna for therapeutic angiogenesis: Early clinical results. *Advanced Drug Delivery Reviews*, 30, 185–197.
- Isner, J. M., Baumgartner, I., Rauh, G., Schainfeld, R., Blair, R., Manor, O., Razvi, S., and Symes, J. F. 1998. Treatment of thromboangiitis obliterans (Buerger's disease) by intramuscular gene transfer of vascular endothelial growth factor: Preliminary clinical results. *Journal of Vascular Surgery*, 28, 964–975.
- Isner, J. M., Pieczek, A., Schainfeld, R., Blair, R., Haley, L., Asahara, T., Rosenfield, K., Razvi, S., Walsh, K., and Symes, J. F. 1996. Clinical evidence of angiogenesis after arterial gene transfer of phvegf165 in patient with ischaemic limb. *Lancet*, 348, 370–374.
- Iwata, A., Sai, S., Nitta, Y., Chen, M., DE Fries-Hallstrand, R., Dalesandro, J., Thomas, R., and Allen, M. D. 2001. Liposome-mediated gene transfection of endothelial nitric oxide synthase reduces endothelial activation and leukocyte infiltration in transplanted hearts. *Circulation*, 103, 2753–2759.
- Jane, J. A., Dunford, B. A., Kron, A., Pittman, D. D., Sasaki, T., Li, J. Z., Li, H. W., Alden, T. D., Dayoub, H., Hankins, G. R., Kallmes, D. F., and Helm, G. A. 2002. Ectopic osteogenesis using adenoviral bone morphogenetic protein (Bmp)-4 and Bmp-6 gene transfer. *Molecular Therapy*, 6, 464–470.
- Jawad, H., Ali, N. N., Lyon, A. R., Chen, Q. Z., Harding, S. E., and Boccaccini, A. R. 2007. Myocardial tissue engineering: A review. *Journal of Tissue Engineering and Regenerative Medicine*, 1, 327–342.
- Jayakumar, J., Suzuki, K., Khan, M., Smolenski, R. T., Farrell, A., Latif, N., Raisy, O., Abunasra, H., Sammut, I. A., Murtuza, B., Amrani, M., and Yacoub, M. H. 2000. Gene therapy for myocardial protection—Transfection of donor hearts with heat shock protein 70 gene protects cardiac function against ischemia – reperfusion injury. *Circulation*, 102, 302–306.
- Jayakumar, J., Suzuki, K., Sammut, I. A., Smolenski, R. T., Khan, M., Latif, N., Abunasra, H., Murtuza, B., Amrani, M., and Yacoub, M. H. 2001. Heat shock protein 70 gene transfection protects mitochondrial and ventricular function against ischemia – reperfusion injury. *Circulation*, 104, I303–I307.
- Jazwa, A., Kucharzewska, P., Leja, J., Zagorska, A., Sierpniowska, A., Stepniowski, J., Kozakowska, M., Taha, H., Ochiya, T., Derlacz, R., Vahakangas, E., Yla-Herttuala, S., Jozkowicz, A., and Dulak, J. 2010a. Combined vascular endothelial growth factor-A and fibroblast growth factor 4 gene transfer improves wound healing in diabetic mice. *Genetic Vaccines Therapy*, 8, 6.

- Jazwa, A., Kucharzewska, P., Leja, J., Zagorska, A., Sierpniowska, A., Stepniewski, J., Kozakowska, M., Taha, H., Ochiya, T., Derlacz, R., Vahakangas, E., Yla-Herttuala, S., Jozkowicz, A., and Dulak, J. 2010b. Combined vascular endothelial growth factor-A and fibroblast growth factor 4 gene transfer improves wound healing in diabetic mice. *Genetic Vaccines Therapy*, 8, 6.
- Jiang, X. Q., Zhao, J., Wang, S. Y., Sun, X. J., Zhang, X. L., Chen, J., Kaplan, D. L., and Zhang, Z. Y. 2009. Mandibular repair in rats with premineralized silk scaffolds and Bmp-2-modified bMSCs. *Biomaterials*, 30, 4522–4532.
- Jo, J. I., Nagaya, N., Miyahara, Y., Kataoka, M., Harada-Shiba, M., Kangawa, K., and Tabata, Y. 2007. Transplantation of genetically engineered mesenchymal stem cells improves cardiac function in rats with myocardial infarction: Benefit of a novel nonviral vector, cationized dextran. *Tissue Engineering*, 13, 313–322.
- Judith, R., Nithya, M., Rose, C., and Mandal, A. B. 2010. Application of a Pdgf-containing novel gel for cutaneous wound healing. *Life Science*, 87, 1–8.
- Kalka, C., Masuda, H., Takahashi, T., Gordon, R., Tepper, O., Gravereaux, E., Pieczek, A., Iwaguro, H., Hayashi, S.-I., Isner, J. M., and Asahara, T. 2000. Vascular endothelial growth factor165 gene transfer augments circulating endothelial progenitor cells in human subjects. *Circulation Research*, 86, 1198–1202.
- Kapur, N. K. and Rade, J. J. 2008. Fibroblast growth factor 4 gene therapy for chronic ischemic heart disease. *Trends in Cardiovascular Medicine*, 18, 133–141.
- Kastrup, J., Jorgensen, E., Ruck, A., Tagil, K., Glogar, D., Ruzyllo, W., Botker, H. E., Dudek, D., Drvota, V., Hesse, B., Thuesen, L., Blomberg, P., Gyongyosi, M., and Sylven, C. 2005. Direct intramyocardial plasmid vascular endothelial growth factor-A(165)-gene therapy in patients with stable severe angina pectoris—A randomized double-blind placebo-controlled study: The Euroinject One trial. *Journal of the American College of Cardiology*, 45, 982–988.
- Kaul, G. and Amiji, M. 2004. Biodistribution and targeting potential of poly(ethylene glycol)-modified gelatin nanoparticles in subcutaneous murine tumor model. *Journal of Drug Target*, 12, 585–591.
- Kaul, G. and Amiji, M. 2005. Tumor-targeted gene delivery using poly(ethylene glycol)-modified gelatin nanoparticles: *In vitro* and *in vivo* studies. *Pharmaceutical Research*, 22, 951–961.
- Kawauchi, M., Suzuki, J., Morishita, R., Wada, Y., Izawa, A., Tomita, N., Amano, J., Kaneda, Y., Ogihara, T., Takamoto, S., and Isobe, M. 2000. Gene therapy for attenuating cardiac allograft arteriopathy using ex vivo E2F decoy transfection by Hvj-Ave-liposome method in mice and nonhuman primates. *Circulation Research*, 87, 1063–1068.
- Keating, J. F. and McQueen, M. M. 2001. Substitutes for autologous bone graft in orthopaedic trauma. *Journal of Bone and Joint Surgery-British Volume*, 83B, 3–8.
- Keeney, M., Van DEN Beucken, J., Van DER Kraan, P. M., Jansen, J. A., and Pandit, A. 2010. The ability of a collagen/calcium phosphate scaffold to act as its own vector for gene delivery and to promote bone formation via transfection with Vegf(165). *Biomaterials*, 31, 2893–2902.
- Kellar, R. S., Shepherd, B. R., Larson, D. F., Naughton, G. K., and Williams, S. K. 2005. Cardiac patch constructed from human fibroblasts attenuates reduction in cardiac function after acute infarct. *Tissue Engineering*, 11, 1678–1687.
- Keswani, S. G., Katz, A. B., Lim, F. Y., Zoltick, P., Radu, A., Alae, D., Herlyn, M., and Crombleholme, T. M. 2004. Adenoviral mediated gene transfer of Pdgf-B enhances wound healing in type I and type II diabetic wounds. *Wound Repair and Regeneration*, 12, 497–504.
- Kim, H. S., Viggswarapu, M., Boden, S. D., Liu, Y. S., Hair, G. A., Louis-Ugbo, J., Murakami, H., Minamide, A., Suh, D. Y., and Titus, L. 2003. Overcoming the immune response to permit ex vivo gene therapy for spine fusion with human type 5 adenoviral delivery of the Lim mineralization protein-1 cDNA. *Spine*, 28, 219–226.
- Kim, K. S., Lee, Y. K., Kim, J. S., Koo, K. H., Hong, H. J., and Park, Y. S. 2008. Targeted gene therapy of Ls174 T human colon carcinoma by anti-Tag-72 immunoliposomes. *Cancer Gene Therapy*, 15, 331–340.
- Kim, W. J., Chang, C. W., Lee, M., and Kim, S. W. 2007. Efficient sirna delivery using water soluble lipopolymer for anti-angiogenic gene therapy. *Journal of Controlled Release*, 118, 357–363.

- Kiritsy, C. P., Antoniadis, H. N., Carlson, M. R., Beaulieu, M. T., and D'andrea, M. 1995. Combination of platelet-derived growth factor-BB and insulin-like growth factor-I is more effective than platelet-derived growth factor-BB alone in stimulating complete healing of full-thickness wounds in "older" diabetic mice. *Wound Repair Regeneration*, 3, 340–350.
- Kishimoto, K. N., Watanabe, Y., Nakamura, H., and Kokubun, S. 2002. Ectopic bone formation by electroporatic transfer of bone morphogenetic protein-4 gene. *Bone*, 31, 340–347.
- Kulkarni, M., Greiser, U., O'Brien, T., and Pandit, A. 2010. Liposomal gene delivery mediated by tissue-engineered scaffolds. *Trends in Biotechnology*, 28, 28–36.
- Kusumanto, Y. H., Van Weel, V., Mulder, N. H., Smit, A. J., Van DEN Dungen, J. J. A. M., Hooymans, J. M. M., Sluiter, W. J., Tio, R. A., Quax, P. H. A., Gans, R. O. B., Dullaart, R. P. F., and Hospers, G. A. P. 2006. Treatment with intramuscular vascular endothelial growth factor gene compared with placebo for patients with diabetes mellitus and critical limb ischemia: A double-blind randomized trial. *Human Gene Therapy*, 17, 683–691.
- Kusumoto, M., Umeda, S., Ikubo, A., Aoki, Y., Tawfik, O., Oben, R., Williamson, S., Jewell, W., and Suzuki, T. 2001. Phase 1 clinical trial of irradiated autologous melanoma cells adenovirally transduced with human GM-CSF gene. *Cancer Immunology and Immunotherapy*, 50, 373–381.
- Lathi, K. G., Cespedes, R. M., Losordo, D. W., Vale, P. R., Symes, J. F., and Isner, J. M. 1999. Direct intramyocardial gene therapy with Vegf for inoperable coronary artery disease: Preliminary clinical results. *Anesthesia and Analgesia*, 88, U78–U78.
- Lauer, G., Sollberg, S., Cole, M., Flamme, I., Sturzebecher, J., Mann, K., Krieg, T., and Eming, S. A. 2000. Expression and proteolysis of vascular endothelial growth factor is increased in chronic wounds. *Journal of Investigative Dermatology*, 115, 12–18.
- Laurencin, C. T., Attawia, M. A., Lu, L. Q., Borden, M. D., Lu, H. H., Gorum, W. J., and Lieberman, J. R. 2001. Poly(lactide-co-glycolide)/hydroxyapatite delivery of Bmp-2-producing cells: A regional gene therapy approach to bone regeneration. *Biomaterials*, 22, 1271–1277.
- Lee, J. A., Conejero, J. A., Mason, J. M., Parrett, B. M., Wear-Maggitti, K. D., Grant, R. T., and Breitbart, A. S. 2005. Lentiviral transfection with the Pdgf-B gene improves diabetic wound healing. *Plastic Reconstruction Surgery*, 116, 532–538.
- Lee, P. Y., Li, Z., and Huang, L. 2003. Thermosensitive hydrogel as a Tgf-beta1 gene delivery vehicle enhances diabetic wound healing. *Pharmaceutical Research*, 20, 1995–2000.
- Lehrman, S. 1999. Virus treatment questioned after gene therapy death. *Nature*, 401, 517–518.
- Li, D., Guang, W., Abuzeid, W. M., Roy, S., Gao, G. P., Sauk, J. J., and O'Malley, B. W., JR. 2008a. Novel adenoviral gene delivery system targeted against head and neck cancer. *Laryngoscope*, 118, 650–658.
- Li, H., Fu, X., Zhang, L., Huang, Q., Wu, Z., and Sun, T. 2008b. Research of Pdgf-BB gel on the wound healing of diabetic rats and its pharmacodynamics. *Journal of Surgery and Research*, 145, 41–48.
- Li, S. D. and Huang, L. 2006. Surface-modified Lpd nanoparticles for tumor targeting. *Annals of New York Academy of Sciences*, 1082, 1–8.
- Liu, H., Bargouti, M., Zughaier, S., Zheng, Z. M., Liu, Y. S., Sangadala, S., Boden, S. D., and Titus, L. 2010. Osteoinductive Lim mineralization protein-1 suppresses activation of NF-kappa B and selectively regulates Mapk pathways in pre-osteoclasts. *Bone*, 46, 1328–1335.
- Liu, L., Marti, G. P., Wei, X., Zhang, X., Zhang, H., Liu, Y. V., Nastai, M., Semenza, G. L., and Harmon, J. W. 2008. Age-dependent impairment of Hif-1alpha expression in diabetic mice: Correction with electroporation-facilitated gene therapy increases wound healing, angiogenesis, and circulating angiogenic cells. *Journal of Cell Physiology*, 217, 319–327.
- Lopez, C. A., Kimchi, E. T., Mauceri, H. J., Park, J. O., Mehta, N., Murphy, K. T., Beckett, M. A., Hellman, S., Posner, M. C., Kufe, D. W., and Weichselbaum, R. R. 2004. Chemoinducible gene therapy: A strategy to enhance doxorubicin antitumor activity. *Molecular Cancer Therapy*, 3, 1167–1175.
- Losordo, D. W., Vale, P. R., Hendel, R. C., Milliken, C. E., Fortuin, F. D., Cummings, N., Schatz, R. A., Asahara, T., Isner, J. M., and Kuntz, R. E. 2002. Phase 1/2 placebo-controlled, double-blind, dose-escalating

- trial of myocardial vascular endothelial growth factor 2 gene transfer by catheter delivery in patients with chronic myocardial ischemia. *Circulation*, 105, 2012–2018.
- Losordo, D. W., Vale, P. R., Symes, J. F., Dunnington, C. H., Esakof, D. D., Maysky, M., Ashare, A. B., Lathi, K., and Isner, J. M. 1998. Gene therapy for myocardial angiogenesis—Initial clinical results with direct myocardial injection of phvegf(165) as sole therapy for myocardial ischemia. *Circulation*, 98, 2800–2804.
- Lotze, M. T., Chang, A. E., Seipp, C. A., Simpson, C., Vetto, J. T., and Rosenberg, S. A. 1986. High-dose recombinant interleukin 2 in the treatment of patients with disseminated cancer. Responses, treatment-related morbidity, and histologic findings. *JAMA*, 256, 3117–3124.
- Lyon, A. R., Sato, M., Hajjar, R. J., Samulski, R. J., and Harding, S. E. 2008. Gene therapy: Targeting the myocardium. *Heart*, 94, 89–99.
- Mace, K. A., Restivo, T. E., Rinn, J. L., Paquet, A. C., Chang, H. Y., Young, D. M., and Boudreau, N. J. 2009. Hoxa3 modulates injury-induced mobilization and recruitment of bone marrow-derived cells. *Stem Cells*, 27, 1654–65.
- Makinen, K., Manninen, H., Hedman, M., Matsi, P., Mussalo, H., Alhava, E., and Yla-Herttuala, S. 2002. Increased vascularity detected by digital subtraction angiography after Vegf gene transfer to human lower limb artery: a randomized, placebo-controlled, double-blinded phase II study. *Molecular Therapy*, 6, 127–133.
- Man, L. X., Park, J. C., Terry, M. J., Mason, J. M., Burrell, W. A., Liu, F., Kimball, B. Y., Moorji, S. M., Lee, J. A., and Breitbart, A. S. 2005. Lentiviral gene therapy with platelet-derived growth factor B sustains accelerated healing of diabetic wounds over time. *Annals in Plastic Surgery*, 55, 81–86; discussion 86.
- Marshall, E. 2000. Biomedicine: Gene therapy on trial. *Science*, 288, 951–957.
- Marti, G., Ferguson, M., Wang, J., Byrnes, C., Dieb, R., Qaiser, R., Bonde, P., Duncan, M. D., and Harmon, J. W. 2004. Electroporative transfection with Kgf-1 Dna improves wound healing in a diabetic mouse model. *Gene Therapy*, 11, 1780–1785.
- Marti, G. P., Mohebi, P., Liu, L., Wang, J., Miyashita, T., and Harmon, J. W. 2008. Kgf-1 for wound healing in animal models. *Methods in Molecular Biology*, 423, 383–391.
- Matsuda, H., Koyama, H., Sato, H., Sawada, J., Itakura, A., Tanaka, A., Matsumoto, M., Konno, K., Ushio, H., and Matsuda, K. 1998. Role of nerve growth factor in cutaneous wound healing: Accelerating effects in normal and healing-impaired diabetic mice. *Journal of Experimental Medicine*, 187, 297–306.
- Menke, N. B., Ward, K. R., Witten, T. M., Bonchev, D. G., and Diegelmann, R. F. 2007. Impaired wound healing. *Clinical Dermatology*, 25, 19–25.
- Michelfelder, S. and Trepel, M. 2009. Adeno-associated viral vectors and their redirection to cell-type specific receptors. *Advances in Genetics*, 67, 29–60.
- Minamide, A., Boden, S. D., Viggewarapu, M., Hair, G. A., Oliver, C., and Titus, L. 2003. Mechanism of bone formation with gene transfer of the cDNA encoding for the intracellular protein Lmp-1. *Journal of Bone and Joint Surgery-American Volume*, 85A, 1030–1039.
- Minamide, A., Titus, L., Viggewarapu, M., Oliver, C., Hair, G., and Boden, S. D. 2001. Bone formation induced by Ad5-Lmp-1: Histological and immunohistochemical analysis. *Journal of Bone and Mineral Research*, 16, S477–S477.
- Miyagawa, S., Sawa, Y., Fukuda, K., Hisaka, Y., Taketani, S., Memon, I. A., and Matsuda, H. 2006. Angiogenic gene cell therapy using suicide gene system regulates the effect of angiogenesis in infarcted rat heart. *Transplantation*, 81, 902–907.
- Miyamoto, M. I., Del Monte, F., Schmidt, U., Disalvo, T. S., Kang, Z. B., Matsui, T., Guerrero, J. L., Gwathmey, J. K., Rosenzweig, A., and Hajjar, R. J. 2000. Adenoviral gene transfer of SERCA2a improves left-ventricular function in aortic-banded rats in transition to heart failure. *Proceedings of the National Academy of Sciences of the United States of America*, 97, 793–798.
- Mizuno, T., Mickle, D. A. G., Kiani, C. G., and Li, R. K. 2005a. Overexpression of elastin fragments in infarcted myocardium attenuates scar expansion and heart dysfunction. *American Journal of Physiology-Heart and Circulatory Physiology*, 288, H2819–H2827.

- Mizuno, T., Yau, T. M., Weisel, R. D., Kiani, C. G., and Li, R. K. 2005b. Elastin stabilizes an infarct and preserves ventricular function. *Circulation*, 112, I81–I88.
- Motzer, R. J., Rakhit, A., Schwartz, L. H., Olencki, T., Malone, T. M., Sandstrom, K., Nadeau, R., Parmar, H., and Bukowski, R. 1998. Phase I trial of subcutaneous recombinant human interleukin-12 in patients with advanced renal cell carcinoma. *Clinical Cancer Research*, 4, 1183–1191.
- Mulder, G., Tallis, A. J., Marshall, V. T., Mazingo, D., Phillips, L., Pierce, G. F., Chandler, L. A., and Sosnowski, B. K. 2009. Treatment of nonhealing diabetic foot ulcers with a platelet-derived growth factor gene-activated matrix (Gam501): Results of a phase 1/2 trial. *Wound Repair and Regeneration*, 17, 772–779.
- Mundt, A. J., Vijayakumar, S., Nemunaitis, J., Sandler, A., Schwartz, H., Hanna, N., Peabody, T., Senzer, N., Chu, K., Rasmussen, C. S., Kessler, P. D., Rasmussen, H. S., Warso, M., Kufe, D. W., Gupta, T. D., and Weichselbaum, R. R. 2004. A Phase I trial of TNFerade biologic in patients with soft tissue sarcoma in the extremities. *Clinical Cancer Research*, 10, 5747–5753.
- Musgrave, D. S., Bosch, P., Ghivizzani, S., Robbins, P. D., Evans, C. H., and Huard, J. 1999. Adenovirus-mediated direct gene therapy with bone morphogenetic protein-2 produces bone. *Bone*, 24, 541–547.
- Mustoe, T. A., O’Shaughnessy, K., and Kloeters, O. 2006. Chronic wound pathogenesis and current treatment strategies: A unifying hypothesis. *Plastic Reconstruction Surgery*, 117, 35S–41S.
- Mustoe, T. A., Pierce, G. F., Morishima, C., and Deuel, T. F. 1991. Growth factor-induced acceleration of tissue repair through direct and inductive activities in a rabbit dermal ulcer model. *Journal of Clinical Investigation*, 87, 694–703.
- Nabel, E. G. 1995. Gene therapy for cardiovascular disease. *Circulation*, 91, 541–548.
- Nagaya, N., Kangawa, K., Kanda, M., Uematsu, M., Horio, T., Fukuyama, N., Hino, J., Harada-Shiba, M., Okumura, H., Tabata, Y., Mochizuki, N., Chiba, Y., Nishioka, K., Miyatake, K., Asahara, T., Hara, H., and Mori, H. 2003. Hybrid cell – gene therapy for pulmonary hypertension based on phagocytosing action of endothelial progenitor cells. *Circulation*, 108, 889–895.
- Namba, T., Koike, H., Murakami, K., Aoki, M., Makino, H., Hashiya, N., Ogihara, T., Kaneda, Y., Kohno, M., and Morishita, R. 2003. Angiogenesis induced by endothelial nitric oxide synthase gene through vascular endothelial growth factor expression in a rat hindlimb ischemia model. *Circulation*, 108, 2250–2257.
- Neumann, E., Schaefer-Ridder, M., Wang, Y., and Hofschneider, P. H. 1982. Gene transfer into mouse lymphoma cells by electroporation in high electric fields. *EMBO Journal*, 1, 841–845.
- Nonaka-Sarukawa, M., Okada, T., Ito, T., Yamamoto, K., Yoshioka, T., Nomoto, T., Hojo, Y., Shimpo, M., Urabe, M., Mizukami, H., Kume, A., Keda, U., Shimada, K., and Ozawa, K. 2008. Adeno-associated virus vector-mediated systemic interleukin-10 expression ameliorates hypertensive organ damage in Dahl salt-sensitive rats. *Journal of Gene Medicine*, 10, 368–374.
- Norman, K. L., and Lee, P. W. 2005. Not all viruses are bad guys: The case for reovirus in cancer therapy. *Drug Discov Today*, 10, 847–855.
- Nussenbaum, B., Rutherford, R. B., and Krebsbach, P. H. 2005. Bone regeneration in cranial defects previously treated with radiation. *Laryngoscope*, 115, 1170–1177.
- Nwomeh, B. C., Yager, D. R., and Cohen, I. K. 1998. Physiology of the chronic wound. *Clinical and Plastic Surgery*, 25, 341–356.
- Oshima, K., Cui, G. G., Tung, T., Okotie, O., Laks, H., and Sen, L. Y. 2007. Exogenous IL-10 overexpression reduces perforin production by activated allogenic Cd8+ cells and prolongs cardiac allograft survival. *American Journal of Physiology-Heart and Circulatory Physiology*, 292, H277–H284.
- Oshima, K., Sen, L., Cui, G. G., Tung, T., Sacks, B. M., Arellano-Kruse, A., and Laks, H. 2002. Localized interleukin-10 gene transfer induces apoptosis of alloreactive T cells via Fas/FasL pathway, improves function, and prolongs survival of cardiac allograft. *Transplantation*, 73, 1019–1026.
- Ott, M. G., Schmidt, M., Schwarzwald, K., Stein, S., Siler, U., Koehl, U., Glimm, H., Kuhlcke, K., Schilz, A., Kunkel, H., Naundorf, S., Brinkmann, A., Deichmann, A., Fischer, M., Ball, C., Pilz, I., Dunbar, C., DU, Y., Jenkins, N. A., Copeland, N. G., Luthi, U., Hassan, M., Thrasher, A. J., Hoelzer, D., Von Kalle, C.,

- Seger, R., and Grez, M. 2006. Correction of X-linked chronic granulomatous disease by gene therapy, augmented by insertional activation of *Mds1-Evi1*, *Prdm16* or *Setbp1*. *Nature Medicine*, 12, 401–409.
- Ozer, H., Wiernik, P. H., Giles, F., and Tendler, C. 1998. Recombinant interferon-alpha therapy in patients with follicular lymphoma. *Cancer*, 82, 1821–1830.
- Pandit, A. S., Wilson, D. J., Feldman, D. S., and Thompson, J. A. 2000. Fibrin scaffold as an effective vehicle for the delivery of acidic fibroblast growth factor (Fgf-1). *Journal of Biomaterials Applications*, 14, 229–242.
- Pearson, S., Jia, H., Kandachi, K. 2004. China approves first gene therapy. *Nature Biotechnology*, 22(1), 3–4.
- Peer, D., Park, E. J., Morishita, Y., Carman, C. V., and Shimaoka, M. 2008. Systemic leukocyte-directed sirna delivery revealing cyclin D1 as an anti-inflammatory target. *Science*, 319, 627–630.
- Pelisek, J., Fuchs, A., Engelmann, M. G., Shimizu, M., Golda, A., Mekkaoui, C., Rolland, P. H., and Nikol, S. 2003. Vascular endothelial growth factor response in porcine coronary and peripheral arteries using nonsurgical occlusion model, local delivery, and liposome-mediated gene transfer. *Endothelium—Journal of Endothelial Cell Research*, 10, 247–255.
- Peng, L., Cheng, X., Zhuo, R., Lan, J., Wang, Y., Shi, B., and Li, S. 2009. Novel gene-activated matrix with embedded chitosan/plasmid Dna nanoparticles encoding Pdgf for periodontal tissue engineering. *Journal of Biomedical Material Research A*, 90, 564–576.
- Pleger, S. T., Boucher, M., Most, P., and Koch, W. J. 2007. Targeting myocardial beta-adrenergic receptor signaling and calcium cycling for heart failure gene therapy. *Journal of Cardiac Failure*, 13, 401–414.
- Pollner, F. 2000. Gene therapy trial and errors raise scientific, ethical, and oversight questions. *The Nih Catalyst*, 8, 1–1a.
- Pons, J., Huang, Y., Takagawa, J., Arakawa-Hoyt, J., Ye, J., Grossman, W., Kan, Y. W., and SU, H. 2009. Combining angiogenic gene and stem cell therapies for myocardial infarction. *The Journal of Gene Medicine*, 11, 743–753.
- Porteus, M. H., Connelly, J. P., and Pruett, S. M. 2006. A look to future directions in gene therapy research for monogenic diseases. *PLoS Genetics*, 2, e133.
- Potapova, I., Plotnikov, A., Lu, Z. J., Danilo, P., Valiunas, V., Qu, J. H., Doronin, S., Zuckerman, J., Shlapakova, I. N., Gao, J. Y., Pan, Z. M., Herron, A. J., Robinson, R. B., Brink, P. R., Rosen, M. R., and Cohen, I. S. 2004. Human mesenchymal stem cells as a gene delivery system to create cardiac pacemakers. *Circulation Research*, 94, 952–959.
- Potapova, I. A., Doronin, S. V., Kelly, D. J., Rosen, A. B., Schultdt, A. J. T., Lu, Z. J., Kochupura, P. V., Robinson, R. B., Rosen, M. R., Brink, P. R., Gaudette, G. R., and Cohen, I. S. 2008. Enhanced recovery of mechanical function in the canine heart by seeding an extracellular matrix patch with mesenchymal stem cells committed to a cardiac lineage. *American Journal of Physiology—Heart and Circulatory Physiology*, 295, H2257–H2263.
- Prunier, F., Kawase, Y., Gianni, D., Scapin, C., Danik, S. B., Ellinor, P. T., Hajjar, R. J., and Del Monte, F. 2008. Prevention of ventricular arrhythmias with sarcoplasmic reticulum Ca²⁺ ATPase pump overexpression in a porcine model of ischemia reperfusion. *Circulation*, 118, 614–624.
- Rajagopalan, S., Shah, M., Luciano, A., Crystal, R., and Nabel, E. G. 2001. Adenovirus-mediated gene transfer of Vegf121 improves lower-extremity endothelial function and flow reserve. *Circulation*, 104, 753–755.
- Ripa, R. S., Wang, Y., Jorgensen, E., Johnsen, H. E., Hesse, B., and Kastrup, J. 2006. Intramyocardial injection of vascular endothelial growth factor-A(165) plasmid followed by granulocyte-colony stimulating factor to induce angiogenesis in patients with severe chronic ischaemic heart disease. *European Heart Journal*, 27, 1785–1792.
- Rivard, C. H., Chaput, C. J., Desrosiers, E. A., Yahia, L. H., and Selmani, A. 1995. Fibroblast seeding and culture in biodegradable porous substrates. *Journal of Applied Biomaterials*, 6, 65–68.
- Roncal, C., Buysschaert, I., Chorianopoulos, E. K., Georgiadou, M., Meilhac, O., Demol, M., Michel, J. B., Vinckier, S., Moons, L., and Carmeliet, P. 2008. Beneficial effects of prolonged systemic administration of Pdgf on late outcome of post-ischaemic myocardial performance. *Journal of Pathology*, 216, 236–244.

- Rosengart, T. K., Lee, L. Y., Patel, S. R., Sanborn, T. A., Parikh, M., Bergman, G. W., Hachamovitch, R., Szulc, M., Kligfield, P. D., Okin, P. M., Hahn, R. T., Devereux, R. B., Post, M. R., Hackett, N. R., Foster, T., Grasso, T. M., Lesser, M. L., Isom, O. W., and Crystal, R. G. 1999. Angiogenesis gene therapy—Phase I assessment of direct intramyocardial administration of an adenovirus vector expressing Vegf121 cDNA to individuals with clinically significant severe coronary artery disease. *Circulation*, 100, 468–474.
- Rubin, G. M. and Spradling, A. C. 1982. Genetic transformation of *Drosophila* with transposable element vectors. *Science*, 218, 348–353.
- Saba, A. A., Freedman, B. M., Gaffield, J. W., Mackay, D. R., and Ehrlich, H. P. 2002. Topical platelet-derived growth factor enhances wound closure in the absence of wound contraction: an experimental and clinical study. *Annals of Plastic Surgery*, 49, 62–66; discussion 66.
- Sabbah, H. N., Sharov, V. G., Gupta, R. C., Mishra, S., Rastogi, S., Undrovinas, A. I., Chaudhry, P. A., Todor, A., Mishima, T., Tanhehco, E. J., and Suzuki, G. 2003. Reversal of chronic molecular and cellular abnormalities due to heart failure by passive mechanical ventricular containment. *Circulation Research*, 93, 1095–1101.
- Saghizadeh, M., Kramerov, A. A., Yu, F. S., Castro, M. G., and Ljubimov, A. V. 2010. Normalization of wound healing and diabetic markers in organ cultured human diabetic corneas by adenoviral delivery of c-Met gene. *Investigative Ophthalmology and Visual Science*, 51, 1970–1980.
- Sales, V. L., Mettler, B. A., Lopez-Illasaca, M., Johnson, J. A., and Mayer, J. E. 2007. Endothelial progenitor and mesenchymal stem cell-derived cells persist in tissue-engineered patch in vivo: Application of green and red fluorescent protein-expressing retroviral vector. *Tissue Engineering*, 13, 525–535.
- Sangadala, S., Titus, L., Viggewarapu, M., Liu, Y., Hair, G. A., Gibson, E., Oliver, C., and Boden, S. D. 2003. Use of Lmp-1 fusion protein to induce bone formation without risks of gene therapy. *Journal of Bone and Mineral Research*, 18, S185–S185.
- Sarkissian, S. D., Grobe, J. L., Yuan, L., Narielwala, D. R., Walter, G. A., Katovich, M. J., and Raizada, M. K. 2008. Cardiac overexpression of angiotensin converting enzyme 2 protects the heart from ischemia-induced pathophysiology. *Hypertension*, 51, 712–718.
- Sawa, Y., Morishita, R., Suzuki, K., Kagisaki, K., Kaneda, Y., Maeda, R., Kadoba, K., and Matsuda, H. 1997. A novel strategy for myocardial protection using *in vivo* transfection of cis element 'decoy' against NFkB binding site—Evidence for a role of NFkB in ischemia – reperfusion injury. *Circulation*, 96, 280–284.
- Schmidt, U., Del Monte, F., Miyamoto, M. I., Matsui, T., Gwathmey, J. K., Rosenzweig, A., and Hajjar, R. J. 2000. Restoration of diastolic function in senescent rat hearts through adenoviral gene transfer of sarcoplasmic reticulum Ca²⁺ + -ATPase. *Circulation*, 101, 790–796.
- Schwarz, E. R., Speakman, M. T., Patterson, M., Hale, S. S., Isner, J. M., Kedes, L. H., and Kloner, R. A. 2000. Evaluation of the effects of intramyocardial injection of Dna expressing vascular endothelial growth factor (Vegf) in a myocardial infarction model in the rat—Angiogenesis and angioma formation. *Journal of the American College of Cardiology*, 35, 1323–1330.
- Schwarzwaelder, K., Schmidt, M., Deichmann, A., Ott, M. G., Stein, S., Glimm, H., Siler, U., Hoelzer, D., Seger, R., Grez, M., and Von Kalle, C. 2006. Insertional activation of Mds1/Evi1, Prdm16 and Setbp1 in a successful chronic granulomatous disease (Cgd) gene therapy trial. *Blood*, 108, 3274.
- Selvin, E. and Erlinger, T. P. 2004. Prevalence of and risk factors for peripheral arterial disease in the United States: Results from the National Health and Nutrition Examination Survey, 1999–2000. *Circulation*, 110, 738–743.
- Sen, L., Hong, Y. S., Luo, H. M., Cui, G. G., and Laks, H. 2001. Efficiency, efficacy, and adverse effects of adenovirus- vs. liposome-mediated gene therapy in cardiac allografts. *American Journal of Physiology-Heart and Circulatory Physiology*, 281, H1433–H1441.
- Shah, A. S., White, D. C., Emani, S., Kypson, A. P., Lilly, R. E., Wilson, K., Glower, D. D., Lefkowitz, R. J., and Koch, W. J. 2001. *In vivo* ventricular gene delivery of a {beta}-adrenergic receptor kinase inhibitor to the failing heart reverses cardiac dysfunction. *Circulation*, 103, 1311–1316.

- Shau, H., Isacescu, V., Ibayashi, Y., Tokuda, Y., Golub, S. H., Fahey, J. L., and Sarna, G. P. 1990. A pilot study of intralymphatic interleukin-2. I. Cytotoxic and surface marker changes of peripheral blood lymphocytes. *J Biological Response Model*, 9, 71–80.
- Shayakhmetov, D. M., DI Paolo, N. C., and Mossman, K. L. 2010. Recognition of virus infection and innate host responses to viral gene therapy vectors. *Molecular Therapy*, 18, 1422–1429.
- Shi, W. F., Arnold, G. S., and Bartlett, J. S. 2001. Insertional mutagenesis of the adeno-associated virus type 2 (Aav2) capsid gene and generation of Aav2 vectors targeted to alternative cell-surface receptors. *Human Gene Therapy*, 12, 1697–1711.
- Shigematsu, H., Yasuda, K., Iwai, T., Sasajima, T., Ishimaru, S., Ohashi, Y., Yamaguchi, T., Ogihara, T., and Morishita, R. 2010. Randomized, double-blind, placebo-controlled clinical trial of hepatocyte growth factor plasmid for critical limb ischemia. *Gene Therapy*, 17, 1152–1161.
- Shyu, K. G., Chang, H., Wang, B. W., and Kuan, P. 2003. Intramuscular vascular endothelial growth factor gene therapy in patients with chronic critical leg ischemia. *American Journal of Medicine*, 114, 85–92.
- Simpson, D., Liu, H., Fan, T. H. M., Nerem, R., and Dudley, S. C. 2007. A tissue engineering approach to progenitor cell delivery results in significant cell engraftment and improved myocardial remodeling. *Stem Cells*, 25, 2350–2357.
- Song, Y., Hahn, T., Thompson, I. P., Mason, T. J., Preston, G. M., LI, G., Paniwnyk, L., and Huang, W. E. 2007. Ultrasound-mediated DNA transfer for bacteria. *Nucleic Acids Research*, 35, e129.
- Spradling, A. C. and Rubin, G. M. 1982. Transposition of cloned P elements into Drosophila germ line chromosomes. *Science*, 218, 341–347.
- Steed, D. L. 1998. Modifying the wound healing response with exogenous growth factors. *Clinical and Plastic Surgery*, 25, 397–405.
- Stewart, A. K., Lassam, N. J., Quirt, I. C., Bailey, D. J., Rotstein, L. E., Krajden, M., Dessureault, S., Gallinger, S., Cappe, D., Wan, Y., Addison, C. L., Moen, R. C., Gauldie, J., and Graham, F. L. 1999. Adenovector-mediated gene delivery of interleukin-2 in metastatic breast cancer and melanoma: Results of a phase 1 clinical trial. *Gene Therapy*, 6, 350–363.
- Sun, L., XU, L., Chang, H., Henry, F. A., Miller, R. M., Harmon, J. M., and Nielsen, T. B. 1997. Transfection with aFGF cDNA improves wound healing. *Journal of Investigative Dermatology*, 108, 313–318.
- Supp, D. M. and Boyce, S. T. 2005. Engineered skin substitutes: Practices and potentials. *Clinical Dermatology*, 23, 403–412.
- Suzuki, K., Murtuza, B., Smolenski, R. T., Sammut, I. A., Suzuki, N., Kaneda, Y., and Yacoub, M. H. 2001. Cell transplantation for the treatment of acute myocardial infarction using vascular endothelial growth factor-expressing skeletal myoblasts. *Circulation*, 104, I207–I212.
- Suzuki, K., Sawa, Y., Kaneda, Y., Ichikawa, H., Shirakura, R., and Matsuda, H. 1997. *In vivo* gene transfection with heat shock protein 70 enhances myocardial tolerance to ischemia – reperfusion injury in rat. *Journal of Clinical Investigation*, 99, 1645–1650.
- Symes, J. F., Losordo, D. W., Vale, P. R., Lathi, K. G., Esakof, D. D., Mayskiy, M., and Isner, J. M. Year. Gene therapy with vascular endothelial growth factor for inoperable coronary artery disease. In: *35th Annual Meeting of the Society-of-Thoracic-Surgeons*, Jan 24–29 1999 San Antonio, TX. 830–836.
- Tadic, D. and Epple, M. 2004. A thorough physicochemical characterisation of 14 calcium phosphate-based bone substitution materials in comparison to natural bone. *Biomaterials*, 25, 987–994.
- Tan, P. H., Xue, S. A., Wei, B., Holler, A., Voss, R. H., and George, A. J. 2007. Changing viral tropism using immunoliposomes alters the stability of gene expression: Implications for viral vector design. *Molecular Medicine*, 13, 216–226.
- Tani, K., Azuma, M., Nakazaki, Y., Oyaizu, N., Hase, H., Ohata, J., Takahashi, K., Oiwamonna, M., Hanazawa, K., Wakumoto, Y., Kawai, K., Noguchi, M., Soda, Y., Kunisaki, R., Watari, K., Takahashi, S., Machida, U., Satoh, N., Tojo, A., Maekawa, T., Eriguchi, M., Tomikawa, S., Tahara, H., Inoue, Y., Yoshikawa, H., Yamada, Y., Iwamoto, A., Hamada, H., Yamashita, N., Okumura, K., Kakizoe, T., Akaza, H., Fujime, M., Clift, S., Ando, D., Mulligan, R., and Asano, S. 2004. Phase I study of autologous tumor vaccines

- transduced with the GM-Csf gene in four patients with stage IV renal cell cancer in Japan: Clinical and immunological findings. *Molecular Therapy*, 10, 799–816.
- Taniyama, Y., Morishita, R., Hiraoka, K., Aoki, M., Nakagami, H., Yamasaki, K., Matsumoto, K., Nakamura, T., Kaneda, Y., and Ogihara, T. 2001. Therapeutic angiogenesis induced by human hepatocyte growth factor gene in rat diabetic hind limb ischemia model: Molecular mechanisms of delayed angiogenesis in diabetes. *Circulation*, 104, 2344–2350.
- Themis, M., May, D., Coutelle, C., and Newbold, R. F. 2003. Mutational effects of retrovirus insertion on the genome of V79 cells by an attenuated retrovirus vector: Implications for gene therapy. *Gene Therapy*, 10, 1703–1711.
- Trudel, S., Trachtenberg, J., Toi, A., Sweet, J., LI, Z. H., Jewett, M., Tshilias, J., Zhuang, L. H., Hitt, M., Wan, Y., Gaudie, J., Graham, F. L., Dancey, J., and Stewart, A. K. 2003. A phase I trial of adenovector-mediated delivery of interleukin-2 (AdIL-2) in high-risk localized prostate cancer. *Cancer Gene Therapy*, 10, 755–763.
- Uemura, H., Fujimoto, K., Tanaka, M., Yoshikawa, M., Hirao, Y., Uejima, S., Yoshikawa, K., and Itoh, K. 2006. A phase I trial of vaccination of Ca9-derived peptides for Hla-A24-positive patients with cytokine-refractory metastatic renal cell carcinoma. *Clinical Cancer Research*, 12, 1768–1775.
- Vale, P. R., Losordo, D. W., Milliken, C. E., McDonald, M. C., Gravelin, L. M., Curry, C. M., Esakof, D. D., Maysky, M., Symes, J. F., and Isner, J. M. 2001. Randomized, single-blind, placebo-controlled pilot study of catheter-based myocardial gene transfer for therapeutic angiogenesis using left ventricular electromechanical mapping in patients with chronic myocardial ischemia. *Circulation*, 103, 2138–2143.
- Veves, A., Falanga, V., Armstrong, D. G., and Sabolinski, M. L. 2001. Graftskin, a human skin equivalent, is effective in the management of noninfected neuropathic diabetic foot ulcers: A prospective randomized multicenter clinical trial. *Diabetes Care*, 24, 290–295.
- Viggeswarapu, M., Bargouti, M., Teklemariam, M., Baker, N., Rogers, C., Zhu, L., Titus, L., and Boden, S. D. 2005. Increasing Bmp responsiveness in human mesenchymal stem cells *in vitro* by addition of the osteoinductive Lmp-1 gene. *Journal of Bone and Mineral Research*, 20, S359–S359.
- Viggeswarapu, M., Boden, S. D., Liu, Y. S., Hair, G. A., Louis-Ugbo, J., Murakami, H., Kim, H. S., Mayr, M. T., Hutton, W. C., and Titus, L. 2001. Adenoviral delivery of Lim mineralization protein-1 induces new-bone formation *in vitro* and *in vivo*. *Journal of Bone and Joint Surgery-American Volume*, 83A, 364–376.
- Viggeswarapu, M., Kim, H., Boden, S. D., Hair, G. A., Oliver, C., and Titus, L. 2002. Overcoming the immune response to permit ex vivo gene therapy for spine fusion using human type 5 adenovirus to deliver Lim mineralization protein-1 (Lmp-1) cDNA. *Journal of Bone and Mineral Research*, 17, M45.
- Vinge, L. E., Raake, P. W., and Koch, W. J. 2008. Gene therapy in heart failure. *Circulation Research*, 102, 1458–1470.
- Wang, J. C., Kanim, L. E. A., Yoo, S., Campbell, P. A., Berk, A. J., and Lieberman, J. R. 2003. Effect of regional gene therapy with bone morphogenetic protein-2-producing bone marrow cells on spinal fusion in rats. *Journal of Bone and Joint Surgery-American Volume*, 85A, 905–911.
- Wang, W., LI, W., Ong, L. L., Lutzow, K., Lendlein, A., Furlani, D., Gabel, R., Kong, D., Wang, J., LI, R. K., Steinhoff, G., and MA, N. 2009. Localized and sustained Sdf-1 gene release mediated by fibronectin films: A potential method for recruiting stem cells. *International Journal of Artificial Organs*, 32, 141–149.
- Wang, Y. Z., Ripa, R. S., Jorgensen, E., Hesse, B., Mortensen, S., and Kastrup, J. 2007. Mobilization of haematopoietic and non-haematopoietic cells by granulocyte-colony stimulating factor and vascular endothelial growth factor gene therapy in patients with stable severe coronary artery disease. *Scandinavian Cardiovascular Journal*, 41, 397–404.
- Wang, Z. and Li, L. 2009. The plasmid encoding Hsp47 enhances collagen expression and promotes skin wound healing in an alloxan-induced diabetic model. *Cell Biology International*, 33, 705–710.
- Wang, Z. G., Ling, Z. Y., Ran, H. T., Hong, R., Zhang, Q. X., Huang, A. L., QI, L., Zhao, C. J., Tang, H. L., Lin, G., Peng, M. L., and PU, S. Y. 2004. Ultrasound-mediated microbubble destruction enhances Vegf gene delivery to the infarcted myocardium in rats. *Clinical Imaging*, 28, 395–398.

- Wei, H. J., Chen, C. H., Lee, W. Y., Chiu, I., Hwang, S. M., Lin, W. W., Huang, C. C., Yeh, Y. C., Chang, Y., and Sung, H. W. 2008. Bioengineered cardiac patch constructed from multilayered mesenchymal stem cells for myocardial repair. *Biomaterials*, 29, 3547–3556.
- Werner, S. and Grose, R. 2003. Regulation of wound healing by growth factors and cytokines. *Physiology Reviews*, 83, 835–870.
- White, D. C., Hata, J. A., Shah, A. S., Glower, D. D., Lefkowitz, R. J., and Koch, W. J. 2000. Preservation of myocardial beta-adrenergic receptor signaling delays the development of heart failure after myocardial infarction. *Proceedings of the National Academy of Sciences of the United States of America*, 97, 5428–5433.
- Winn, S. R., Chen, J. C., Gong, X., Bartholomew, S. V., Shreenivas, S., and Ozaki, W. 2005a. Non-viral-mediated gene therapy approaches for bone repair. *Orthodontics and Craniofacial Research*, 8, 183–190.
- Winn, S. R., Chen, J. C., Gong, X., Bartholomew, S. V., Shreenivas, S., and Ozaki, W. 2005b. Non-viral-mediated gene therapy approaches for bone repair. *Orthodontics and Craniofacial Research*, 8, 183–190.
- Woo, C. Y., Osada, T., Clay, T. M., Lyster, H. K., and Morse, M. A. 2006. Recent clinical progress in virus-based therapies for cancer. *Expert Opinion in Biological Therapy*, 6, 1123–1134.
- Wu, X., Gao, H., Pasupathy, S., Tan, P. H., Ooi, L. L., and Hui, K. M. 2005. Systemic administration of naked Dna with targeting specificity to mammalian kidneys. *Gene Therapy*, 12, 477–486.
- Wukich, D. K. 2010. Current concepts review: diabetic foot ulcers. *Foot and Ankle International*, 31, 460–467.
- Xiang, Z., Liao, R. L., Kelly, M. S., and Spector, M. 2006. Collagen-Gag scaffolds grafted onto myocardial infarcts in a rat model: A delivery vehicle for mesenchymal stem cells. *Tissue Engineering*, 12, 2467–2478.
- Xie, Y. B., Yang, S. T., and Kniss, D. A. 2001. Three-dimensional cell-scaffold constructs promote efficient gene transfection: Implications for cell-based gene therapy. *Tissue Engineering*, 7, 585–598.
- Yang, J. F., Zhou, W. W., Zheng, W., Ma, Y. L., Lin, L., Tang, T., Liu, J. X., Yu, J. F., Zhou, X. M., and Hu, J. G. 2007. Effects of myocardial transplantation of marrow mesenchymal stem cells transfected with vascular endothelial growth factor for the improvement of heart function and angiogenesis after myocardial infarction. *Cardiology*, 107, 17–29.
- Yang, L., Jiang, J., Drouin, L. M., Agbandje-Mckenna, M., Chen, C., Qiao, C., Pu, D., Hu, X., Wang, D. Z., Li, J., and Xiao, X. 2009. A myocardium tropic adeno-associated virus (Aav) evolved by Dna shuffling and *in vivo* selection. *Proceedings of the National Academy of Sciences USA*, 106, 3946–3951.
- Ye, L., Haider, H. K., Jiang, S., Tan, R. S., GE, R. W., Law, P. K., and Sim, E. K. W. 2007. Improved angiogenic response in pig heart following ischaemic injury using human skeletal myoblast simultaneously expressing Vegf(165) and angiopoietin-1. *European Journal of Heart Failure*, 9, 15–22.
- Ylosmaki, E., Hakkarainen, T., Hemminki, A., Visakorpi, T., Andino, R., and Saksela, K. 2008. Generation of a conditionally replicating adenovirus based on targeted destruction of E1A mrna by a cell type-specific Microrna. *Journal of Virology*, 82, 11009–11015.
- Yoon, C. S., Jung, H. S., Kwon, M. J., Lee, S. H., Kim, C. W., Kim, M. K., Lee, M., and Park, J. H. 2009. Sonoporation of the minicircle-Vegf(165) for wound healing of diabetic mice. *Pharmaceutical Research*, 26, 794–801.
- Yoon, S. T. and Boden, S. D. 2004. Spine fusion by gene therapy. *Gene Therapy*, 11, 360–367.
- Yoon, Y. S., Uchida, S., Masuo, O., Cejna, M., Park, J. S., Gwon, H. C., Kirchmair, R., Bahlman, F., Walter, D., Curry, C., Hanley, A., Isner, J. M., and Losordo, D. W. 2005. Progressive attenuation of myocardial vascular endothelial growth factor expression is a seminal event in diabetic cardiomyopathy—Restoration of microvascular homeostasis and recovery of cardiac function in diabetic cardiomyopathy after replenishment of local vascular endothelial growth factor. *Circulation*, 111, 2073–2085.
- Yuan, B., Zhang, Y. R., Zhao, Z., Wu, D. L., Yuan, L. Z., Wu, B., Wang, L. S., and Huang, J. 2008a. Treatment of chronic myocardial ischemia by adenovirus-mediated hepatocyte growth factor gene transfer in minipigs. *Science in China Series C-Life Sciences*, 51, 537–543.

- Yuan, B., Zhao, Z., Zhang, Y. R., Wu, C. T., Jin, W. G., Zhao, S., Wang, W., Zhang, Y. Y., Zhu, X. L., Wang, L. S., and Huang, J. 2008b. Short-term safety and curative effect of recombinant adenovirus carrying hepatocyte growth factor gene on ischemic cardiac disease. *In Vivo*, 22, 629–632.
- Zagon, I. S., Sassani, J. W., Malefyt, K. J., and Mclaughlin, P. J. 2006. Regulation of corneal repair by particle-mediated gene transfer of opioid growth factor receptor complementary DNA. *Archives in Ophthalmology*, 124, 1620–1624.
- Zhang, G., Wang, X., Wang, Z., Zhang, J., and Suggs, L. 2006. A PEGylated fibrin patch for mesenchymal stem cell delivery. *Tissue Engineering*, 12, 9–19.
- Zhang, H., Kusunose, J., Kheirloomoom, A., Seo, J. W., QI, J., Watson, K. D., Lindfors, H. A., Ruoslahti, E., Sutcliffe, J. L., and Ferrara, K. W. 2008a. Dynamic imaging of arginine-rich heart-targeted vehicles in a mouse model. *Biomaterials*, 29, 1976–1988.
- Zhang, Y., Wang, Y., Boado, R. J., and Pardridge, W. M. 2008b. Lysosomal enzyme replacement of the brain with intravenous non-viral gene transfer. *Pharmaceutical Research*, 25, 400–406.
- Zhao, X. Y., HU, S. J., LI, J., Mou, Y., Bian, K., Sun, J., and Zhu, Z. H. 2008. raav-asplb transfer attenuates abnormal sarcoplasmic reticulum Ca²⁺ -ATPase activity and cardiac dysfunction in rats with myocardial infarction. *European Journal of Heart Failure*, 10, 47–54.
- Zimmermann, W. H., Melnychenko, I., and Eschenhagen, T. 2004. Engineered heart tissue for regeneration of diseased hearts. *Biomaterials*, 25, 1639–1647.

Nanotechnology-Based Cell Engineering Strategies for Tissue Engineering and Regenerative Medicine Applications

Joaquim Miguel
Oliveira

University of Minho
ICVS/3B's

João Filipe Mano

University of Minho
ICVS/3B's

Rui Luís Reis

University of Minho
ICVS/3B's

57.1	Introduction	57-1
57.2	Cell Engineering Strategies.....	57-2
	Intracellular Delivery • Nanoparticles in Cell Engineering and Cellular Responses	
57.3	Concluding Remarks.....	57-7
	References.....	57-7

57.1 Introduction

We have been assisting a multitude of scientific achievements in the merging fields of cell- and tissue engineering and regenerative medicine (TERM), and thus there is a need to highlight the most recent and relevant works in these particular areas of research. Owing to the multidisciplinary nature of these fields, we were encouraged to briefly overview other important issues namely, those related with the application of nanotechnology principles in regenerative medicine. This particular topic is appealing since there is the need for developing more effective treatments to cure the several spontaneous and injuries-related diseases. Owing to the limited regenerative capacity of the body, scientists envision for example, nanoparticle systems for efficiently delivering specific drugs, bioactive agents, and genetic material, and to target-specific cells or even cellular compartments. In this chapter, the regenerative potential of different cells (and its sources), and their responsiveness to modulators are succinctly addressed. The cell engineering strategies that have been designed for targeting the regeneration or repair of specific body parts is also discussed herein. Focus is placed on the research dealing with new promising strategies, namely the use of nanocarriers, polymeric, and ceramic, for the control delivery of biomolecules intracellularly. These vehicles are aimed at modulating cell functions such as, adhesion, proliferation, and differentiation of cells. If this strategy on one side, allowed our group to envision regenerate bone by means of controlling stem cells differentiation *in vitro* while maintaining their cellular phenotype *in vivo* upon reimplantation, whereas on the other, we were able to apply the developed nanocarriers to cross other biological barriers such as the blood–brain barrier, opening up new possibilities for targeting the central nervous system (CNS).

57.2 Cell Engineering Strategies

In our body there are different cell types, which can be classified as: (i) germ cells, (ii) somatic cells, and (iii) stem cells. Germ cells are cells that give rise to gametes, both male and female. Somatic cells are the specialized ones and make up the adult body. In their differentiated state they may possess one or more copies of the genome, with the exception of erythrocytes which do not possess. Finally, stem cells can be defined as cells that possess the capacity to divide indefinitely, that is, proliferate in culture and potentially may also differentiate into functionally distinct cellular phenotypes (Spangrude 2003). Stem cells can be grouped according to the source or tissue of origin. Alternatively, they can also be classified for their capacity of differentiation as follows: (i) totipotent, that is, the cells can differentiate in all types of specialized cells of the body, including the entire fetus and placenta; (ii) pluripotent, it means that cells can differentiate in all cells constituting the three germ layers (ectoderm, mesoderm, and endoderm), but not the whole organism; (iii) multipotent, that is, the cells can only differentiate in a limited type of specialized cells; and (iv) unipotent, that is, these cells can only give rise to one differential cell lineage.

It is well-known that the identification of several stem cell sources and their isolation promise to revolutionize the concept of regenerative medicine (Conrad and Huss 2005), allowed us to develop numerous cell-based therapies. For cell therapy, either differentiated (e.g., autologous chondrocytes) (Risbud and Sittinger 2002) or undifferentiated (e.g., stem cells) cells (Spangrude 2003, Zeng and Rao 2007) can be used. An implantation at the injury site of freshly isolated cells (e.g., own-patient cells) or cultured cells (differentiated cells alone or in combination with stem cells, and with or without the presence of bioactive molecules) is a possibility.

Despite, the use of stem cells in clinical practice being limited it raises many problems and concerns, especially a subtype of stem cells, the embryonic stem (ES) cells. This problem is not only due to ethical/religious issues (McKay 2000, McLaren 2001), safety (Dawson et al. 2003, Rando 2006) or technical limitations, but also to the legislative/regulatory constraints (Spangrude 2003). Adult stem cells are seen as an alternative to ES cells, as their clinical use seems to be safe, without complications and major ethical issues (Pountos and Giannoudis 2005, Verfaillie 2002). Stem cells can proliferate and differentiate beyond the tissues in which they normally reside or may be artificially placed (Wright et al. 2001). In fact, it has been shown that bone marrow-derived stem cells can not only reconstitute the bone marrow but also are capable of forming several types of mesenchymal tissues, including bone (Trojani et al. 2006), muscle cells (Dezawa et al. 2004), lung and gut (Jiang et al. 2002). For example, cell-sheet transplantation has been proving to be a breakthrough therapeutic strategy for the treatment of myocardial infarction (Miyahara et al. 2006), among others. The intensive research efforts and technological advances allowed to identify and isolate different types of stem cells from germ cells, embryo, fetus (e.g., fetal blood, placenta, and umbilical cord blood), and adult tissues and organs (Anker et al. 2003, Barry and Murphy 2004, Bongso and Richards 2004, Fraser et al. 2006, Loebel et al. 2003, Romanov et al. 2003). In addition, it was reported that the isolation of stem cells derived from amniotic fluid that express embryonic and adult stem cell markers (De Coppi et al. 2007). The amniotic fluid-derived stem cells were found to be pluripotent, meaning that they have the potential to differentiate into cell types representing each embryonic germ layer, including cells of adipogenic, osteogenic, myogenic, endothelial, neuronal, and hepatic lineages.

Interestingly, differentiated cells can be reprogrammed to a pluripotent state by transfer of nuclear contents into oocytes, by fusion with ES cells, and for male germ cells by cell culture alone. Quite recently, Takahashi et al. (Takahashi et al. 2007, Takahashi and Yamanaka 2006) demonstrated that pluripotent stem cells can be directly generated from fibroblast cultures, the so-called induced pluripotent stem (iPs) cells by retrovirus-mediated transfection with four transcription factors, namely Oct3/4, Sox2, c-Myc, and Klf4, under ES cell culture conditions. The four factors, however, cannot fully explain iPs cell induction (Yamanaka 2008). Though, this step further has major implications in regenerative medicine as for the first time, it was possible to create pluripotent cells directly from the somatic cells of humans (Park et al. 2008).

Growth factors and other bioactive molecules may be provided to control cell's fate either from cultural media (Heng et al. 2004, Zhang and Li 2005) or simply by incorporating into the scaffold (Hosseinkhani et al. 2006, Kato et al. 2006), a temporary three-dimensional matrix (3D), which can be more advantageous from a practical point of view. Often, this process may take days or weeks until it forms a tissue similar to that which is aimed at repair or regeneration. With simple tissues, only one cell type may be required (e.g., chondrocytes in cartilage repair), but in other cases, more than one cell type is a must, as the tissue to be regenerated consists of multiple structures (e.g., osteochondral tissues) (Wendt et al. 2005, Mano and Reis 2007). Thus, this will require considerable sophistication with respect to the therapeutic strategy itself, and tissue-engineering (TE) solutions seem to be the most adequate ones. In the following subsections, we review the advances resulting from targeting therapeutics and intracellular delivery, and the benefits to therapies associated with this type of approach. The advantages of using nanocarriers to accomplish the site-directed manner of drug delivery aimed at controlling different cellular functions will be also addressed.

57.2.1 Intracellular Delivery

Intracellular delivery is now a commonplace subject in the advanced regenerative strategies and it is gaining a clinical significance. In particular, the current work is investigating the synthesis of smart nanocarriers for delivering drugs (Breunig et al. 2008, Faraji and Wipf 2009, Nishiyama and Kataoka 2006) as an alternative to traditional drug regimens. These have been designed not only to allow drug molecules or a genetic material to be attached or loaded within the nanocarriers but also to incorporate different functionalities for cellular and subcellular targetability, traceability, and stimuli-responsiveness (Oh et al. 2009, Onaca et al. 2009). These nanocarriers can reduce the uptake of toxic agents, avoid the secondary effects of certain drugs, and improve its bioavailability, that is, these systems allow for enhancing drug accumulation and solubility at the target site and decrease their clearance by the body, thus decreasing the dosage needs. Certain biological barriers such as cell membrane and blood-brain barrier are impermeable to biomolecules larger than 1 kDa (Bareford and Swaan 2007). Therefore, nanocarriers exhibiting high permeability may accommodate these macromolecules and improve the transport across these barriers (Allard et al. 2009, Smith and Gumbleton 2006).

Cellular internalization mechanism can be grouped as follows: (i) phagocytosis, that is, uptake of large particles (in the order of a few micrometers), which is restricted to specialized cells (e.g., macrophages) and (ii) pinocytosis, that is, molecules are taken up by cells by means of fluid-phase endocytosis, clathrin-assisted and receptor-mediated endocytosis (~120 nm), caveolin-assisted and receptor-mediated endocytosis (~60 nm), and clathrin and caveolin-independent endocytosis (~90 nm) (Alberola and Radler 2009, Bareford and Swaan 2007, Conner and Schmid 2003).

At the present moment, researchers are able to bioengineer the macromolecular complexes using the ability of all cells of our body toward internalizing certain macromolecules by means of endocytosis, a mechanism which retains them in transporting vesicles within the cell. Despite, there is a possibility of lysosomal degradation (e.g., hydrolytic and enzymatic degradation) of the drug delivery complexes upon internalization, thus most strategies should bear in mind this premise. In other cases, such a deleterious possibility can be advantageous namely, those involving an enzymatic release of therapeutics which are aimed at treating lysosomal storage diseases (e.g., Gaucher's disease), cancer, and Alzheimer's disease.

Another reported possibility is the lipid-raft endocytic internalization, which opens up the possibility of avoiding the degradative intracellular drug delivery route. By means of surface engineering of macromolecules with lipid-raft-associated ligands, cellular internalization and vesicular trafficking to nonlysosomal subcellular compartments became possible. Further details on the endocytic mechanisms for the targeted delivery of macromolecules and its intracellular fate can be found elsewhere (Bareford and Swaan 2007).

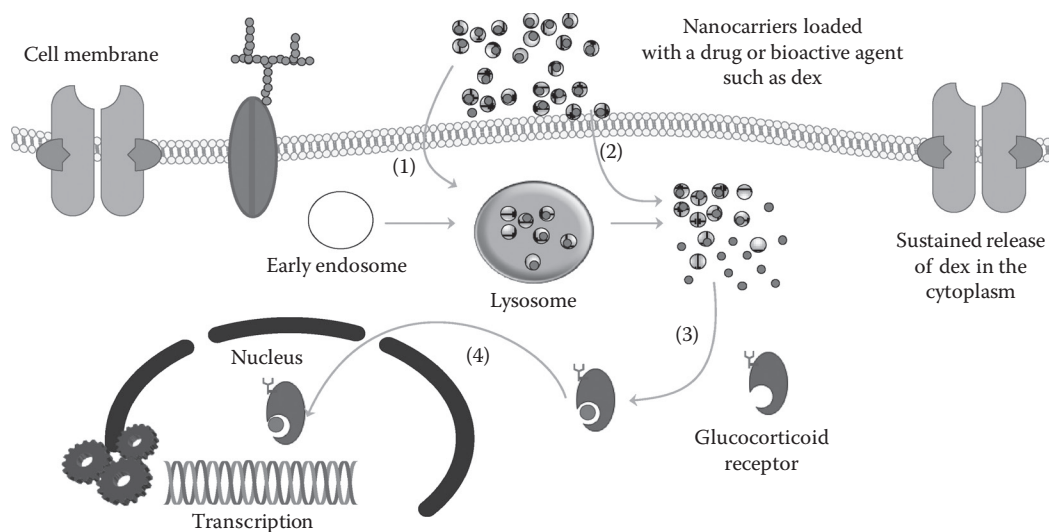


FIGURE 57.1 Scheme of the nanoparticles' intracellular reservoir for the sustained release of Dex aimed at modulating the osteogenic differentiation of stem cells. (1 and 2) Indicate the internalization contact and crossing of the cell membrane through different mechanisms; (2) dex release from nanoparticles into the cytoplasm; (3) interaction of dex with the glucocorticoid receptor in the cytoplasm; and (4) translocation of the complex receptor/drug into the nucleus, and mRNA transcription followed by protein translation from mRNA. (Adapted from Oliveira J. M. et al. 2010b. *Prog Polym Sci* 35:1163–94.)

Interestingly, our first study (Oliveira et al. 2008) on the surface engineering of macromolecules reported the modification of poly(amidoamine) dendrimers (PAMAM) with the water-soluble carboxymethylchitosan (CMChT), the so-called CMChT/PAMAM dendrimer nanoparticles. The developed nanoparticles were aimed at finding application as intracellular carriers to deliver bioactive molecules for controlling the fate of stem cells, namely their proliferation and differentiation. Figure 57.1 shows a scheme of the rationale proposed by our group for the intracellular drug delivery of dexamethasone (Dex) by means of using the CMChT/PAMAM dendrimer nanoparticles.

Our data showed that the dex-loaded CMChT/PAMAM dendrimer nanoparticles can be internalized by different cell types and play a crucial role in the regulation of osteogenesis *in vitro*, both in 2D and 3D culturing conditions (Oliveira et al. 2008, 2009). Applying the cell- and TE principles, we have demonstrated that the dex-loaded CMChT/PAMAM dendrimer nanoparticles may be beneficial as an intracellular nanocarrier, which supplied dex in a regimented manner *ex vivo* and promoted a superior ectopic *de novo* bone formation *in vivo* (Oliveira et al. 2010a). So far, this new approach evidenced the usefulness of the intracellular drug delivery for controlling the behavior of stem cells. The exceptional properties of the dendrimer nanoparticles, namely its biocompatibility and internalization efficiency, triggered their potential use for not only, producing the living tissues *in vitro* but also, for finding a wider application in CNS and gene therapy strategies (Oliveira 2010b), despite the need of conducting further fundamental studies.

57.2.2 Nanoparticles in Cell Engineering and Cellular Responses

The physicochemical properties of the nanoparticles can affect the internalization efficiency and cellular responses (Alberola and Radler 2009, Clift et al. 2010). Size, concentration, M_w and surface properties are some features of the nanocarriers that will dictate its ability for being taken up by the living cells (Allard et al. 2009, Cho et al. 2009, Chung et al. 2007, Lu et al. 2010, Oliveira et al. 2008, Pedraza et al. 2008). The shape of the nanoparticles has been shown to affect its cellular uptake and

their functions (Huang et al. 2010). In turn, the zeta potential of the cerium oxide nanoparticles also modulates its internalization ability by adenocarcinoma lung cells (A549) (Patil et al. 2007). However, the first step for optimizing drug delivery and targeting is to understand the mechanism of drug release from nanoparticles and its route of internalization by the cells. There are different techniques that allow us to study the targeting of nanoparticles to cells and their intracellular fate (Huth et al. 2006, Mady et al. 2009, Richardson et al. 2008, Torchilin 2005).

The genetically modified cells opened new possibilities in the field of TERM (Sheyn et al. 2010). In fact, the ability of small molecules to regulate the gene expression has potential therapeutic applications namely interfering RNA (siRNA), but its use is limited by inefficient delivery. Several solutions have been advanced to circumvent this problem, such as the use of stimuli-responsive nanocarriers which can improve their delivery efficiency. Many examples of pH-responsive systems are provided in literature (Checot et al. 2007, Hatakeyama et al. 2009, Schmaljohann 2006, Simões et al. 2001, Wang et al. 2005, Xu et al. 2010). An interesting work is related with the triggered release of adsorbed poly(ethylene glycol) (PEG)-b-polycation polymers from pH-dependent (PD) liposomes (Auguste et al. 2008). These were found to possibly protect from immune recognition (pH 7.4) and subsequent intracellular delivery of siRNA within the endosome (pH ~5.5). In this work, the polycationic blocks, based on either poly[2-(dimethylamino)ethyl methacrylate] or polylysine enabled the anchoring of the PEG protective block. By encapsulating siRNA, the authors have shown green fluorescent protein (GFP) silencing in the genetically modified, GFP-expressing human cervical epithelioid carcinoma (HeLa) cells and glyceraldehyde-3-phosphate dehydrogenase (GAPD) knockdown in the human umbilical vein endothelial cells (HUVEC). Akita and coworkers (Akita et al. 2010) reported on the *ex vivo* siRNA delivery to the primary mouse bone marrow-derived dendritic cells for finding applications as a cancer vaccine. In their studies, a successful endosomal escape was achieved by using a PD fusogenic peptide (GALA) modified on a lipid mixture that was optimized for endosomal fusion. Results showed that siRNA loaded in nanocarriers efficiently suppresses the endogenous gene expression and enhanced the dendritic cell-based vaccine potency *in vivo*. In turn, Potineni et al. (2003) reported on poly(ethylene oxide)-modified poly(b-amino ester) nanoparticles as a pH-sensitive biodegradable carrier for paclitaxel delivery. Pluronic/poly(ethylenimine) nanocapsules, which are cationic and thermally sensitive, have also been proposed as an siRNA delivery nanocarrier (Lee et al. 2008).

As previously discussed herein, the intracellular fate of macromolecular complexes is determined by the internalization mechanism and consequently by the intracellular trafficking. For targetability, caveolae-dependent endocytic route seems to be most promising since it does not transport the internalized material to endosomes and lysosomes where the internalized material can undergo degradation. Lee et al. (2007) revealed that the hyaluronic acid (HA) nanogels were selectively internalized by colorectal carcinoma cell line (HCT-116 cells) via the receptor-mediated endocytosis. In this work, siRNA was encapsulated into HA nanogels by means of using an inverse water-in-oil emulsion route. Their studies demonstrated that the HA/siRNA nanogels were up taken by HA receptor-positive cells (HCT-116 cells) having HA-specific CD44 receptors on the surface. The *in vitro* studies using glutathione (GSH) showed that the degradation/erosion of the disulfide-crosslinked HA nanogels, triggered by an intracellular reductive agent, controlled the release pattern of siRNA, which evidences the target-specific intracellular delivery of siRNA using degradable hyaluronic acid nanogels. The linking of different targeting ligands to nanocarriers have also been used for this purpose (Nakase et al. 2008, Santos et al. 2010, Shao et al. 2006).

For traceability, nanocarriers can be labeled by linking or encapsulating a probe. Several molecules can be used as markers or probes, namely histological and fluorescent dyes, radiotracers, and contrast agents (Burks et al. 2009, Domanski et al. 2004, Fretz et al. 2004, Huth et al. 2006, Straubinger et al. 1983, Sun et al. 2008). Our group followed a similar strategy and linked fluorescein isothiocyanate (FITC) to CMChT/PAMAM dendrimer nanoparticles to investigate the uptake and the mechanism of internalization by rat bone marrow stromal cells (Oliveira et al. 2008). To gain further insight into the internalization mechanism, it was used colchicine, an endocytic inhibitor that binds tightly to microtubules and causes microtubule depolymerization. This assay suggested that nanoparticles were taken up by cells through a mechanism that is not exclusively endocytic.

Succinctly, research dealing with the uptake and the intracellular behavior of stimuli-sensitive nano-carriers can be investigated by means of: (i) combining different inhibitors aimed at selectively blocking different pathways, (ii) using different permeabilizing agents, (iii) using fluorescent probes, which should be specific for the different endocytic routes, and (iv) using different types of cells, which internalize the stimuli-sensitive nanocarriers by means of different mechanisms (Douglas et al. 2008).

Now, let us focus on the cellular responses to different nanoparticles upon its internalization, namely dendrimers, quantum dots (QDs), core-shell cationic nanoparticles, liposomes, and magnetic nanoparticles (MNPs). For example, the cytotoxicity screening and applicability of CMChT/PAMAM dendrimer nanoparticles for CNS applications have been recently assessed using neurons, astrocytes, and oligodendrocytes (Salgado et al. 2010). Post-natal hippocampal neurons and cortical glial cells were able to internalize the FITC-labeled CMChT/PAMAM dendrimer nanoparticles with high efficiency. This work revealed that the binding of these nanoparticles to fluorescent probes for tracing purposes was also possible. We have found that cell viability was not significantly affected upon exposure to these nanoparticles. Moreover, it was possible to observe that neurons, astrocytes, oligodendrocytes, and microglial cells were able to internalize the CMChT/PAMAM dendrimer nanoparticles at different rates. The ongoing studies are focused on loading relevant drugs (e.g., methylprednisolone) for CNS-related applications into the CMChT/PAMAM dendrimer nanoparticles.

Shieh et al. (2008) reported a controllable and nontoxic gene transfection method, the photochemical internalization (PCI)-mediated gene delivery, by means of using polyamidoamine (PAMAM, G4) dendrimers surface modified with 5,10,15-tri(4-acetamidophenyl)-20-mono(4-carboxyl-phenyl) porphyrin (TAMCPP) as intracellular nanocarriers. TAMCPP conjugation do not increase the cytotoxicity of the PAMAM dendrimer below 20 μm , but significantly induced cell death after suitable irradiation. Under almost nontoxic PAMAM G4-TAMCPP-mediated PCI treatment, the expression of GFP could be markedly enhanced in HeLa cells. Therefore, the conjugate showed the potential as a nanocarrier for PCI-mediated gene therapy. For further details on the current state and achievements on the development of nanocarriers for light-induced gene transfection may be found elsewhere (Nishiyama and Kataoka 2006).

QDs have been proposed as ideal candidates for innumerable biological applications, including imaging and labeling of cells (Howarth et al. 2005, Prinzen et al. 2007, Smith et al. 2008, Xing et al. 2006). Since they provide outstanding features such as a small and uniform size and unique optical properties, they are powerful nanotools for the investigation of distinct cellular processes, like uptake, receptor trafficking, and intracellular delivery (Hild et al. 2008). Despite, there is a need to surface and modify the QDs, as they often present a certain degree of toxicity (Hezinger et al. 2008). For example, Chang et al. (2008) labeled the human bone mesenchymal stem cells (hADAS) with CdSe/ZnS QDs. In this study, cell proliferation assays demonstrated that peptide-1-labeled QD delivery protects hADAS from the damage caused by the internalization of QDs. They also concluded that the endo-/lysosome degradation of QDs may depend on different surface coatings and critically influence the differentiation of hADAS. Iron oxide (Fe_2O_3) nanoparticles, with different sizes and surface potentials, have also been proposed for labeling bone marrow-derived mesenchymal stem cells (Jo et al. 2010). This group has demonstrated that Fe_2O_3 -pullulan nanoparticles may be a promising nanotool for the magnetic resonance imaging (MRI) labeling of stem cells.

Genetic vaccination using core-shell cationic nanoparticles have been proposed (Castaldello et al. 2006). In this work, a hydrophilic tentacular shell bearing positively charged groups and PEG chains were covalently linked to a poly(methylmethacrylate) (PMMA) core by means of following an emulsion polymerization method. The *in vitro* studies demonstrated that nanoparticles reversibly adsorbed large amounts of DNA, preserved its functional structure, and were efficiently taken up by cells. *In vivo* studies revealed that nanoparticles were non toxic. In turn, intramuscular immunization using the nanoparticle loaded with a plasmid (pCV-tat), promoted significant antigen-specific humoral and long-lasting cellular responses, and significantly improved Th1-type T cell responses and cytotoxic T lymphocytes against human immunodeficiency virus (HIV)-1 Tat.

Thompson and coworkers (Thompson and Gross 1988) reported a system for efficiently packaging antibodies and other macromolecules into liposomes. The strategy was based on delivering the encapsulated molecules into living cells through liposome-cell fusion. Results have shown that antibodies maintained their ability to recognize and bind to their specific antigens. To determine if the antibodies were capable of interfering with cellular processes *in vivo*, the group measured the effects of liposome-introduced antiribosome antibodies on translation and antitubulin antibodies on mitosis. Their data demonstrated a significant inhibition and the antibodies could in fact, be used to interfere with specific functions at specific times. Other liposomal formulations namely Doxil[®] and Visudyne[®], have been approved for clinical use. Nevertheless, the aforementioned polymeric micelles have been attracting much attention as compared to stealth liposomes. This is mainly due to the secondary effects associated with the administration of PEG-liposome formulations, which often requires the preadministration of anti-histamine and anti-inflammatory drugs. In turn, it is believed that polymeric micelles might not cause toxicity problems such as those observed for stealth liposomes (Nishiyama and Kataoka 2006). In turn, Ito et al. (2005) showed that cell attachment can be stimulated by means of linking an Arg-Gly-Asp (RGD)-motif-containing peptide to magnetite cationic liposomes (MCLs).

MNPs have been shown as promising for finding an application for intracellular delivery, diagnostics, and therapy purposes (Shubayev et al. 2009). Despite, Pisanic Ii et al. (2007) reported that the intracellular delivery of moderate levels of Fe₂O₃ nanoparticles may adversely affect cell functioning. Actually, their cytotoxicity experiments demonstrated that an exposure to the increasing concentrations of anionic MNPs, from 0.15 to 15 mm of iron, resulted in a dose-dependent diminishing viability and capacity of rat pheochromocytoma (PC12) cells to extend neurites. They have concluded that more studies on Fe₂O₃ internalization are needed, to screen its biocompatibility.

57.3 Concluding Remarks

Nanotechnology has been showing great promise in intracellular drug delivery and human therapeutics and diagnose. A wide variety of nanotools exists already, and have been explored in cell- and TE strategies. Different materials, formulations, and methods of synthesis have been put forward. Despite, careful use a comprehensive research to understand better and assess their effects on cells, and assess its bio-safety prior administration to humans must be considered. We can envision particularly interesting applications of nanoparticles in drug delivery, namely those that relate to the central nervous system. Since many neuropharmacologic agents do not reach the brain due to the blood-brain barrier, it can be expected that the use of nanotools allow us to overcome these barrier challenges and establish new therapeutic possibilities, in the near future.

References

- Akita, H., Kogure, K., Moriguchi, R. et al. 2010. Nanoparticles for ex vivo siRNA delivery to dendritic cells for cancer vaccines: Programmed endosomal escape and dissociation. *J Control Release* 143:311–17.
- Alberola, A. P. and Radler, J. O. 2009. The defined presentation of nanoparticles to cells and their surface controlled uptake. *Biomaterials* 30:3766–70.
- Allard, E., Passirani, C., and Benoit, J.P. 2009. Convection-enhanced delivery of nanocarriers for the treatment of brain tumors. *Biomaterials* 30:2302–18.
- Anker, P. S., Noort, W. A., Scherjon, S. A. et al. 2003. Mesenchymal stem cells in human second-trimester bone marrow, liver, lung, and spleen exhibit a similar immunophenotype but a heterogeneous multilineage differentiation potential. *Haematologica* 88:845–52.
- Auguste, D. T., Furman, K., Wong, A. et al. 2008. Triggered release of siRNA from poly(ethylene glycol)-protected, pH-dependent liposomes. *J Control Release* 130:266–74.
- Bareford, L. M. and Swaan, P. M. 2007. Endocytic mechanisms for targeted drug delivery. *Adv Drug Deliv Rev* 59:748–58.

- Barry, F. P. and Murphy, J. M. 2004. Mesenchymal stem cells: Clinical applications and biological characterization. *Int J Biochem Cell Biol* 36:568–84.
- Bongso, A. and Richards, M. 2004. History and perspective of stem cell research. *Best Pract Res Clin Obstet Gynaecol* 18:827–42.
- Breunig, M., Bauer, S., and Goepferich, A. 2008. Polymers and nanoparticles: Intelligent tools for intracellular targeting? *Eur J Pharm Biopharm* 68:112–28.
- Burks, S. R., Barth, E. D., Halpern, H. J., Rosen, G. M., and Kao, J. P. Y. 2009. Cellular uptake of electron paramagnetic resonance imaging probes through endocytosis of liposomes. *Biochim Biophys Acta (BBA)—Biomembranes* 1788:2301–8.
- Castaldello, A., Brocca-Cofano, E., Voltan, R. et al. 2006. DNA prime and protein boost immunization with innovative polymeric cationic core-shell nanoparticles elicits broad immune responses and strongly enhance cellular responses of HIV-1 tat DNA vaccination. *Vaccine* 24:5655–69.
- Chang, J.C., Su, H.L., and Hsu, S.H. 2008. The use of peptide-delivery to protect human adipose-derived adult stem cells from damage caused by the internalization of quantum dots. *Biomaterials* 29:925–36.
- Checot, F., Rodriguez-Hernandez, J., Gnanou, Y., and Lecommandoux, S. 2007. pH-responsive micelles and vesicles nanocapsules based on polypeptide diblock copolymers. *Biomol Eng* 24:81–5.
- Cho, M., Cho, W.S., Choi, M. et al. 2009. The impact of size on tissue distribution and elimination by single intravenous injection of silica nanoparticles. *Toxicol Lett* 189:177–83.
- Chung, T.H., Wu, S.H., Yao, M. et al. 2007. The effect of surface charge on the uptake and biological function of mesoporous silica nanoparticles in 3T3-L1 cells and human mesenchymal stem cells. *Biomaterials* 28:2959–66.
- Clift, M. J. D., Rothen-Rutishauser, B., Brown, D. M. et al. 2010. The impact of different nanoparticle surface chemistry and size on uptake and toxicity in a murine macrophage cell line. *Toxicol Appl Pharmacol* 232:418–27.
- Conner, S. D. and Schmid, S. L. 2003. Regulated portals of entry into the cell. *Nature* 422:37–44.
- Conrad, C. and Huss, R. 2005. Adult stem cell lines in regenerative medicine and reconstructive surgery. *J Surgical Res* 124:201–08.
- Dawson, L., Bateman-House, A. S., Agnew, D. M. et al. 2003. Safety issues in cell-based intervention trials. *Fertil Steril* 80:1077–85.
- De Coppi, P., Bartsch, J. G., Siddiqui, M. M. et al. 2007. Isolation of amniotic stem cell lines with potential for therapy. *Nature Biotechnol* 25:100–6.
- Dezawa, M., Kanno, H., Hoshino, M. et al. 2004. Specific induction of neuronal cells from bone marrow stromal cells and application for autologous transplantation. *J Clin Invest* 113:1701–10.
- Domanski, D. M., Klajnert, B., and Bryszewska, M. 2004. Incorporation of fluorescent probes into PAMAM dendrimers. *Bioelectrochemistry* 63:193–7.
- Douglas, K. L., Piccirillo, C. A., and Tabrizian, M. 2008. Cell line-dependent internalization pathways and intracellular trafficking determine transfection efficiency of nanoparticle vectors. *Eur J Pharm Biopharm* 68:676–87.
- Faraji, A. H. and Wipf, P. 2009. Nanoparticles in cellular drug delivery. *Bioorg Med Chem* 17:2950–62.
- Fraser, J. K., Wulur, I., Alfonso, Z., and Hedrick, M. H. 2006. Fat tissue: An underappreciated source of stem cells for biotechnology. *Trends Biotechnol* 24:150–4.
- Fretz, M. M., Koning, G. A., Mastrobattista, E., Jiskoot, W., and Storm, G. 2004. OVCAR-3 cells internalize TAT-peptide modified liposomes by endocytosis. *Biochim Biophys Acta (BBA)—Biomembranes* 1665:48–56.
- Hatakeyama, H., Ito, E., Akita, H. et al. 2009. A pH-sensitive fusogenic peptide facilitates endosomal escape and greatly enhances the gene silencing of siRNA-containing nanoparticles in vitro and in vivo. *J Control Release* 139:127–32.
- Heng, B. C., Haider, H. K., Sim, E. K.W., Tong Cao, T., and Ng, S. C. 2004. Strategies for directing the differentiation of stem cells into the cardiomyogenic lineage in vitro. *Cardiovasc Res* 62:34–42.

- Hezinger, A. F. E., Tessmar, J., and Göpferich, A. 2008. Polymer coating of quantum dots—A powerful tool toward diagnostics and sensorics. *Eur J Pharm Biopharm* 68:138–52.
- Hild, W. A., Breunig, M., and Goepferich, A. 2008. Quantum dots—Nano-sized probes for the exploration of cellular and intracellular targeting. *Eur J Pharm Biopharm* 68:153–68.
- Hosseinkhani, H., Yamamoto, M., Inatsugu, Y. et al. 2006. Enhanced ectopic bone formation using a combination of plasmid DNA impregnation into 3-D scaffold and bioreactor perfusion culture. *Biomaterials* 27:1387–98.
- Howarth, M., Takao, K., Hayashi, Y., and Ting, A. Y. 2005. Targeting quantum dots to surface proteins in living cells with biotin ligase. *Proc Natl Acad Sci USA* 102:7583–8.
- Huang, X., Teng, X., Chen, D., Tang, F., and He, J. 2010. The effect of the shape of mesoporous silica nanoparticles on cellular uptake and cell function. *Biomaterials* 31:438–48.
- Huth, U. S., Schubert, R., and Peschka-Süss, R. 2006. Investigating the uptake and intracellular fate of pH-sensitive liposomes by flow cytometry and spectral bio-imaging. *J Control Release* 110:490–504.
- Ito, A., Ino, K., Kobayashi, T., and Honda, H. 2005. The effect of RGD peptide-conjugated magnetite cationic liposomes on cell growth and cell sheet harvesting. *Biomaterials* 26:6185–93.
- Jiang, Y., Jahagirdar, B. N., Reinhardt, R. L. et al. 2002. Pluripotency of mesenchymal stem cells derived from adult marrow. *Nature* 418:41–9.
- Jo, J.I., Aoki, I. and Tabata, Y. 2010. Design of iron oxide nanoparticles with different sizes and surface charges for simple and efficient labeling of mesenchymal stem cells. *J Control Release* 142:465–73.
- Kato, M., Namikawa, T., Terai, H. et al. 2006. Ectopic bone formation in mice associated with a lactic acid/dioxanone/ethylene glycol copolymer–tricalcium phosphate composite with added recombinant human bone morphogenetic protein-2. *Biomaterials* 27:3927–33.
- Lee, H., Mok, H., Lee, S., Oh, Y.K., and Park, T. G. 2007. Target-specific intracellular delivery of siRNA using degradable hyaluronic acid nanogels. *J Control Release* 119:245.
- Lee, S. H., Choi, S. H., Kim, S. H., and Park, T. G. 2008. Thermally sensitive cationic polymer nanocapsules for specific cytosolic delivery and efficient gene silencing of siRNA: Swelling induced physical disruption of endosome by cold shock. *J Control Release* 125:25–32.
- Loebel, D. A. F., Watson, C. M., De Young, R. A., and Tam, P. P. L. 2003. Lineage choice and differentiation in mouse embryos and embryonic stem cells. *Dev Biol* 264:1–14.
- Lu, S., Xia, D., Huang, G. et al. 2010. Concentration effect of gold nanoparticles on proliferation of keratinocytes. *Colloids Surf B: Biointerfaces* 81:406–11.
- Mady, M. M., Ghannam, M. M., Khalil, W. A., Müller, R., and Fahr, A. 2009. Efficiency of cytoplasmic delivery by non-cationic liposomes to cells in vitro: A confocal laser scanning microscopy study. *Phys Med* 25:88–93.
- Mano, J. F. and Reis, R. L. 2007. Osteochondral defects: Present situation and tissue engineering approaches. *J Tissue Eng Reg Med* 1: 261–73.
- McKay, R. 2000. Stem cells—Hype and hope. *Nature* 406:361–64.
- McLaren, A. 2001. Ethical and social considerations of stem cell research. *Nature* 414:129–31.
- Miyahara, Y., Nagaya, N., Kataoka, M. et al. 2006. Monolayered mesenchymal stem cells repair scarred myocardium after myocardial infarction. *Nat Med* 12:459–65.
- Nakase, I., Takeuchi, T., Tanaka, G., and Futaki, S. 2008. Methodological and cellular aspects that govern the internalization mechanisms of arginine-rich cell-penetrating peptides. *Adv Drug Deliv Rev* 60:598.
- Nishiyama, N. and Kataoka, K. 2006. Current state, achievements, and future prospects of polymeric micelles as nanocarriers for drug and gene delivery. *Pharmacol Ther* 112:630–48.
- Oh, J. K., Lee, D. I., and Park, J. M. 2009. Biopolymer-based microgels/nanogels for drug delivery applications. *Prog Polym Sci* 34:1261–82.
- Oliveira, J. M., Kotobuki, N., Marques, A. P. et al. 2008. Surface engineered carboxymethylchitosan/poly(amidoamine) dendrimer nanoparticles for intracellular targeting. *Adv Funct Mater* 18:1840–53.

- Oliveira, J. M., Kotobuki, N., Tadokoro, M. et al. 2010a. Ex vivo culturing of stromal cells with dexamethasone-loaded carboxymethylchitosan/poly(amidoamine) dendrimer nanoparticles promotes ectopic bone formation. *Bone* 46:1424–35.
- Oliveira, J. M., Salgado, A. J., Sousa, N., Mano, J. F., and Reis, R. L. 2010b. Dendrimers and derivatives as a potential therapeutic tool in regenerative medicine strategies—A review. *Prog Polym Sci* 35:1163–94.
- Oliveira, J. M., Sousa, R. A., Kotobuki, N. et al. 2009. The osteogenic differentiation of rat bone marrow stromal cells cultured with dexamethasone-loaded carboxymethylchitosan/poly(amidoamine) dendrimer nanoparticles. *Biomaterials* 30:804–13.
- Onaca, O., Ramona, E., Hughes, D. W., and Meier, W. 2009. Stimuli-responsive polymersomes as nanocarriers for drug and gene delivery. *Macromol Biosci* 9:129–39.
- Park, I.H., Zhao, R., West, J. A. et al. 2008. Reprogramming of human somatic cells to pluripotency with defined factors. *Nature* 451:141–6.
- Patil, S., Sandberg, A., Heckert, E., Self, W., and Seal, S. 2007. Protein adsorption and cellular uptake of cerium oxide nanoparticles as a function of zeta potential. *Biomaterials* 28:4600–7.
- Pedraza, C. E., Bassett, D. C., McKee, M. D. et al. 2008. The importance of particle size and DNA condensation salt for calcium phosphate nanoparticle transfection. *Biomaterials* 29:3384–92.
- Pisanic Ii, T. R., Blackwell, J. D., Shubayev, V. I., Fiñones, R. R., and Jin, S. 2007. Nanotoxicity of iron oxide nanoparticle internalization in growing neurons. *Biomaterials* 28:2572–81.
- Potineni, A., Lynn, D. M., Langer, R., and Amiji, M. M. 2003. Poly(ethylene oxide)-modified poly([beta]-amino ester) nanoparticles as a pH-sensitive biodegradable system for paclitaxel delivery. *J Control Release* 86:223–34.
- Pountos, I. and Giannoudis, P. V. 2005. Biology of mesenchymal stem cells. *Injury, Int J Care Injured* 36:5: S8–S12.
- Prinzen, L., Miserus, R.J. J. H. M., Dirksen, A. et al. 2007. Optical and magnetic resonance imaging of cell death and platelet activation using annexin A5-functionalized quantum dots. *Nano Lett* 7:93–100.
- Rando, T. A. 2006. Stem cells, ageing and the quest for immortality. *Nature* 441:1080–6.
- Richardson, S. C. W., Wallom, K.L., Ferguson, E. L. et al. 2008. The use of fluorescence microscopy to define polymer localisation to the late endocytic compartments in cells that are targets for drug delivery. *J Control Release* 127:1–11.
- Risbud, M. V. and Sittinger, M. 2002. Tissue engineering: Advances in in vitro cartilage generation. *Trends Biotechnol* 20:351–6.
- Romanov, Y. A., Svintsitskaya, V. A., and Smirnov, V. N. 2003. Searching for alternative sources of post-natal human mesenchymal stem cells: Candidate MSC-like cells from umbilical cord. *Stem Cells* 21:105–10.
- Salgado, A. J., Oliveira, J. M., Pirraco, R. P. et al. 2010. Carboxymethylchitosan/poly(amidoamine) dendrimer nanoparticles in central nervous systems-regenerative medicine: Effects on neuron/glial cell viability and internalization efficiency. *Macromol Biosci* 10:1130–40.
- Santos, A. O., da Silva, L. C. G., Bimbo, L. M. et al. 2010. Design of peptide-targeted liposomes containing nucleic acids. *Biochim Biophys Acta (BBA)—Biomembranes* 978:56–64.
- Schmaljohann, D. 2006. Thermo- and pH-responsive polymers in drug delivery. *Adv Drug Deliv Rev* 58:1655–70.
- Shao, K., Hou, Q., Duan, W. et al. 2006. Intracellular drug delivery by sulfatide-mediated liposomes to gliomas. *J Control Release* 115:150–7.
- Sheyn, D., Mizrahi, O., Benjamin, S. et al. 2010. Genetically modified cells in regenerative medicine and tissue engineering. *Adv Drug Deliv Rev* 62:683–98.
- Shieh, M.J., Peng, C.L., Lou, P.J. et al. 2008. Non-toxic phototriggered gene transfection by PAMAM-porphyrin conjugates. *J Control Release* 129:200–6.
- Shubayev, V. I., Pisanic Ii, T. R., and Jin, S. 2009. Magnetic nanoparticles for theragnostics. *Adv Drug Deliv Rev* 61:467–77.

- Simões, S., Slepushkin, V., Düzgünes, N., and Pedroso de Lima, M. C. 2001. On the mechanisms of internalization and intracellular delivery mediated by pH-sensitive liposomes. *Biochim Biophys Acta (BBA)—Biomembranes* 1515:23–37.
- Smith, A. M., Duan, H., Mohs, A. M., and Nie, S. 2008. Bioconjugated quantum dots for in vivo molecular and cellular imaging. *Adv Drug Deliv Rev* 60:1226–40.
- Smith, M. W. and Gumbleton, M. 2006. Endocytosis at the blood brain barrier: From basic understanding to drug delivery strategies. *J Drug Target* 14:191–214.
- Spangrude, G. J. 2003. Stem cells and tissue regeneration: When is a stem cell really a stem cell? *Bone Marrow Transplant* 32: S7–S11.
- Straubinger, R. M., Hong, K., Friend, D. S., and Papahadjopoulos, D. 1983. Endocytosis of liposomes and intracellular fate of encapsulated molecules: Encounter with a low pH compartment after internalization in coated vesicles. *Cell* 32:1069–79.
- Sun, C., Lee, J. S. H., and Zhang, M. 2008. Magnetic nanoparticles in MR imaging and drug delivery. *Adv Drug Deliv Rev* 60:1252–65.
- Takahashi, K., Okita, K., Nakagawa, M., and Yamanaka, S. 2007. Induction of pluripotent stem cells from fibroblast cultures. *Nat Protoc* 2:3081–9.
- Takahashi, K. and Yamanaka, S. 2006. Induction of pluripotent stem cells from mouse embryonic and adult fibroblast cultures by defined factors. *Cell* 126:663–76.
- Thompson, W. S. and Gross, R. H. 1988. Antibodies introduced into living cells with liposomes localize specifically and inhibit specific intracellular processes. *Gene Anal Tech* 5:73–9.
- Torchilin, V. P. 2005. Fluorescence microscopy to follow the targeting of liposomes and micelles to cells and their intracellular fate. *Adv Drug Deliv Rev* 57:95–109.
- Trojani, C., Boukhechba, F., Scimeca, J.C. et al. 2006. Ectopic bone formation using an injectable biphasic calcium phosphate/Si-HPMC hydrogel composite loaded with undifferentiated bone marrow stromal cells. *Biomaterials* 27:3256–64.
- Verfaillie, C. M. 2002. Adult stem cells: Assessing the case for pluripotency. *Trends in Cell Biol* 12:502–8.
- Wang, C.H., Wang, C.H., and Hsiue, G.H. 2005. Polymeric micelles with a pH-responsive structure as intracellular drug carriers. *J Control Release* 108:140–9.
- Wendt, D., Jakob, M., and Martin, I. 2005. Bioreactor-based engineering of osteochondral grafts: From model systems to tissue manufacturing. *J Biosci Bioeng* 100:489–94.
- Wright, D. E., Wagers, A. J., Gulati, A. P., Johnson, F. L., and Weissman, I. L. 2001. Physiological migration of hematopoietic stem and progenitor cells. *Science* 294:1933–6.
- Xing, Y., Smith, A. M., Agrawal, A., Ruan, G., and Nie, S. M. 2006. Molecular profiling of single cancer cells and clinical tissue specimens with semiconductor quantum dots. *Int. J. Nanomed* 1:473–81.
- Xu, S., Luo, Y., Graeser, R. et al. 2010. Development of pH-responsive core-shell nanocarriers for delivery of therapeutic and diagnostic agents. *Bioorg Med Chem Lett* 198:73.
- Yamanaka, S. 2008. Induction of pluripotent stem cells from mouse fibroblasts by four transcription factors. *Cell Prolif* 41:51–6.
- Zhang, J. and Li, L. 2005. BMP signaling and stem cell regulation. *Dev Biol* 284:1–11.
- Zeng, X. and Rao, M. S. 2007. Human embryonic stem cells: Long term stability, absence of senescence and a potential cell source for neural replacement. *Neuroscience* 145:1348–58.

Cell Encapsulation

58.1	Introduction	58-1
58.2	Gelation Mechanisms Employed in Cell Encapsulation	58-2
	Gelation via Noncovalent Interactions • Gelation via Covalent Crosslinking: Radical Chain Polymerization • Gelation via Covalent Crosslinking: Step Growth Polymerization	
58.3	Hydrogel Structure and Degradation.....	58-8
	The Role of Hydrogel Structure in Tissue Development • Modes of Degradation	
58.4	Concluding Remarks.....	58-11
	References.....	58-12

Stephanie J. Bryant
University of Colorado

58.1 Introduction

The general approach in tissue engineering is to culture cells in 3D scaffolds that serve as temporary cell supports for guiding new tissue growth. The scaffold may be prefabricated with high porosity whereby cells are seeded into the pores or the scaffold may be formed in the presence of cells thus directly encapsulating cells. In the former strategy, the size of the pores is generally much larger (~10–50 times) than that of a cell effectively presenting a 2D surface onto which cells adhere. However, cells interacting with surfaces in two dimensions is generally an unnatural interaction that can ultimately affect the fate of the cell (Gieni and Hendzel 2008). Rather, cells in their native environment are surrounded in *three* dimensions by an extracellular matrix with which to interact (Cukierman et al. 2001). Therefore, in the latter scaffold strategy, encapsulating cells in 3D scaffolds creates microenvironments that more closely resemble the architecture and mechanics of native tissues (Saha et al. 2007; Tibbitt and Anseth 2009). How cells interact with their extracellular environment influences many cellular functions such as proliferation, differentiation, and matrix synthesis, which are important for engineering living and functional tissues.

From a practical perspective, cell encapsulation strategies offer several additional advantages. For example, by suspending cells in a solution prior to solidification, cells can be uniformly distributed throughout the scaffold (Bryant and Anseth 2001b). Since the process of encapsulating cells is inherently mild and cell-friendly, it often can be employed as a means to deliver cells *in vivo* and minimally invasively whereby cells suspended in a liquid precursor solution are injected to the site of interest and cured *in situ* (Atala et al. 1993; Elisseff et al. 1999a; Passaretti et al. 2001). By curing the scaffold directly at the site of interest, the precursors are able to diffuse into the neighboring tissue and upon gelation create a bond between the scaffold and the tissue without the need for external fixatives. With these many advantages, it is not surprising that cell encapsulation strategies have received significant attention in recent years. However, developing scaffolds for cell encapsulation comes with stringent requirements, thus limiting the range of suitable precursors and processes by which scaffolds are formed.

The materials most commonly employed to encapsulate cells are hydrogels. Hydrogels are water swellable, yet water insoluble crosslinked polymeric networks that imbibe large amounts of water and

exhibit tissue-like elastic properties making them ideal candidates as scaffolds for tissue engineering. The earliest hydrogels used for cell encapsulations were naturally forming hydrogels based on proteins, such as collagen (Elsdale and Bard 1972) and fibrin (Sims et al. 1998), and polysaccharides, such as alginate (Lim and Sun 1980) and agarose (Dupuy et al. 1988). These early and seminal contributions demonstrated both the importance of culturing cells in a 3D environment over traditional 2D culture platforms and the ability for hydrogels to serve as suitable platforms for regenerating new tissue.

The advantages of natural hydrogels include their inherent biocompatibility, their ability to form via benign processes, and for those prepared from proteins the presentation of biological cues that promote cellular interactions with the hydrogel. However, natural hydrogels inherently suffer from batch-to-batch variations and a greater potential for contamination and are generally more difficult to control and tune. To overcome these shortcomings, synthetic hydrogels have become more widely studied for cell encapsulation. Synthetic hydrogels can be formed from synthetic polymers, providing purely 3D structural support for cells and tissue deposition, or from natural polymers, proteins, or peptides, which have been modified in such a way as to impart both biological functionality as well as control over the 3D environment. Strategies that combine synthetic polymers with natural polymers or their derivatives offer an ideal platform for tuning many of the macroscopic properties while simultaneously presenting biological cues in a controlled manner. The level of control afforded by synthetic hydrogels continues to increase as new chemistries and new strategies for hydrogel formation are developed and being designed with cell encapsulation in mind.

The following sections highlight (i) different gelation mechanisms and hydrogel chemistries, which have been successfully employed to encapsulate cells for a variety of tissue engineering applications and (ii) the role that hydrogel structure and the different modes of degradation have on directing cellular behavior in 3D.

58.2 Gelation Mechanisms Employed in Cell Encapsulation

Regardless of the gelation mechanism employed to encapsulate cells, the liquid precursors and gelation mechanisms must be suitable for cells. Since cells are suspended in the liquid precursor solution, there are several requirements. The precursors must be water-soluble and cyto-compatible. In general, hydrogel precursors are comprised of macromolecular monomers or macromers derived from biocompatible polymers instead of low molecular monomers, which are often cytotoxic (Schweikl et al. 2006). As a general rule, designing macromers with molecular weights that are 3000 Da or greater will minimize their cyto-toxicity. Finally, the aqueous solution must be buffered to a physiological osmolarity to prevent cell lysis.

The two primary mechanisms by which gelation occurs and are through noncovalent interactions, such as hydrophobic or ionic interactions, and through covalent crosslinking via chain or step growth polymerization. Examples of each gelation mechanism are shown in [Figure 58.1](#). Noncovalent interactions can be reversible or irreversible, while covalent crosslinks are generally irreversible. While gelation mechanisms via noncovalent interactions are typically benign, they often result in hydrogels with weak mechanical properties limiting their applications to areas where high stresses are not prevalent. On the other hand, hydrogels formed from covalent crosslinks cover a wide range of macroscopic properties making them highly tunable for tissue engineering applications. However, their gelation mechanisms require additional components that may introduce cyto-toxic species if the polymerization conditions are not carefully selected. Each gelation mechanism has its advantages and limitations. Therefore, choosing a cell encapsulation strategy will depend on a number of factors including, but not limited to, the type(s) of cells to be encapsulated, the tissue to be engineered, if cells are to be delivered *in vivo*, the clinical application, the ease of use, and of course, user preference. The following sections give several examples of cell encapsulation strategies that have successfully employed gelation mechanisms via noncovalent interactions with a specific focus on self-assembling polymers, covalent crosslinking via radical chain polymerization, and covalent crosslinking via step

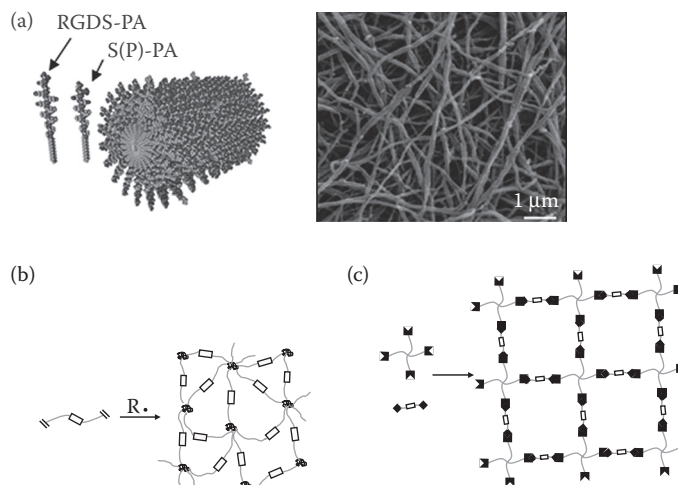


FIGURE 58.1 Examples of gelation mechanisms that have been successfully employed in cell encapsulation strategies: (a) self-assembling peptides that assemble via noncovalent interactions into cylindrical, micellar structures, and subsequently into nanofibers that form a macroscopic hydrogel, (b) radical chain polymerization whereby in this example a radical initiates polymerization of a divinyl macromolecular monomer leading to a covalently crosslinked network, and (c) step growth polymerization whereby in this example two distinctly different macromolecular monomers form a homogeneous crosslinked network. (Panel (a) is reprinted from *Biomaterials*, 31, Mata, A. et al. Bone regeneration mediated by biomimetic mineralization of a nanofiber matrix, 6004–12. Copyright 2010, with permission from Elsevier.)

growth polymerizations. While not comprehensive, references are provided to direct the reader to more complete reviews.

58.2.1 Gelation via Noncovalent Interactions

An interesting subset of hydrogels are those which self-assemble in aqueous solutions either spontaneously or in response to a stimuli, such as temperature. In general, these polymers are comprised of hydrophobic and hydrophilic segments that give rise to their unique behaviors in aqueous solutions. When designed properly, these amphiphilic polymers undergo a transition from a soluble polymer solution to a semisolid gel capable of entrapping large amounts of water and living cells. Two types of self-assembling hydrogels which are attractive for cell encapsulation are those formed from thermoresponsive polymers and self-assembling peptides.

Thermoresponsive hydrogels are one type of stimuli responsive hydrogel which when designed to undergo a sol–gel transition near body temperature, are particularly attractive for delivering cells *in vivo* and minimally invasively (Ruel-Gariepy and Leroux 2004; Klouda and Mikos 2008). In general, thermoresponsive polymers in aqueous solutions respond to changes in temperature because of a decrease in their overall hydrophilicity that leads to a decrease in the solubility of the polymer chains. This transition leads to unfavorable water–polymer interactions and thus thermodynamically promotes polymer–polymer and water–water interactions. For cell encapsulations and tissue engineering, designing thermoresponsive polymers that undergo a sol–gel transition when temperature is increased from ambient to physiological is most desirable.

Several polymers have been designed to exhibit thermoresponsive behavior near physiological temperatures with demonstrated suitability for cell encapsulation and tissue engineering. Two examples of common polymers are the triblock copolymer, poly(ethylene glycol)-*b*-poly(propylene glycol)-*b*-poly(ethylene glycol), commercially known as Pluronics[®] and poly(*N*-isopropylacrylamide) (pNiPAAm). Specifically,

Pluronic F-127 at a concentration above its critical micelle concentration forms a micellar liquid at room temperature but transforms to a macroscopic hydrogel near physiological temperature (Wanka et al. 1994) enabling *in vivo* delivery of cells (Saim et al. 2000). Hydrogels formed from Pluronics® have been successfully used to encapsulate several different cell types including chondrocytes (i.e., cartilage cells) (Cao et al. 1998), osteoblasts (i.e., bone cells) (Lippens et al. 2009), human mesenchymal stem cells (hMSCs) (Dang et al. 2006), intervertebral disc cells (Dang et al. 2006), and hepatocytes (Khattak et al. 2005). PNiPAAm, on the other hand, contains a hydrophilic amide bond and a hydrophobic isopropyl group within each repeat unit, which gives the polymer its remarkable ability to respond to changes in temperature, with a lower critical solution temperature (LCST) near physiological temperature (Schild 1992). However, in its collapsed form, much of the water is excluded from the pNiPAAm making it unsuitable for encapsulating cells. In addition, PNiPAAm forms a stable crosslinked polymer making it undesirable for applications in tissue engineering. To overcome these shortcomings, copolymers have been designed where NiPAAm is copolymerized with chemistries that impart hydrophilicity to enhance water retention and chemistries that are susceptible to degradation. This strategy offers a highly flexible platform from which to design polymers that self-assemble into hydrogels with tunable properties. For example, copolymers have been designed with a LCST near body temperature, enabling gelation upon injection into the body, but as the polymer degrades to a certain composition and molecular weight its LCST decreases to below body temperature inducing reverse gelation and solubilizing the hydrogel (Fujimoto et al. 2009). Copolymers containing pNiPAAm have been successfully employed to encapsulate hMSCs while maintaining their viability and multipotency (Pollock and Healy 2010; Wang et al. 2010).

A different subset of hydrogels which are formed from noncovalent interactions and which have been successfully employed in cell encapsulation is self-assembling polypeptides. In general, peptides are designed to contain hydrophobic and hydrophilic amino acids, which through noncovalent interactions facilitate self-assembly into higher order structures (Branco and Schneider 2009). The choice of amino acids and the length of the polypeptide dictate the self-assembly process. In addition, the mechanical properties and speed of self-assembly can be enhanced by increasing the degree of hydrophobicity (Caplan et al. 2002). Peptides have been designed with hydrophobic and ionic amino acids that self-assemble in physiological medium making them particularly attractive for encapsulating cells (Gelain et al. 2007; Cui et al. 2010). Self-assembly occurs because the charges on the polypeptide become shielded when placed in a physiological medium leading to an increase in the overall hydrophobicity of the peptide driving it to self-assemble. One example is a peptide containing a periodic repetition of alternating hydrophobic and ionic hydrophilic amino acids (i.e., lysine-leucine-aspartic acid-leucine (KLDL)...), which self-assemble into β -sheets and subsequently into nanofibers that form a macroscopic hydrogel (Gelain et al. 2007; Yang et al. 2010). These structures imbibe large amounts of water (>99% water) and are supportive of cell encapsulation and tissue growth as demonstrated by encapsulating chondrocytes and adult equine progenitor cells for cartilage tissue engineering (Kisiday et al. 2002, 2008). Another example is polypeptides comprised of hydrophobic alkyl chains and ionic peptides, which self-assemble into cylindrical, micellar structures in physiological medium (e.g., Figure 58.1a) (Mata et al. 2010) and which are also supportive of cell encapsulation (Cui et al. 2010). While these polypeptides are unnatural, they may be further modified with peptide sequences that are recognizable by cells (Gelain et al. 2006). For example, when the laminin epitope, isoleucine-lysine-valine-alanine-valine (IKVAV), was incorporated into the polypeptide, encapsulated neural progenitor cells rapidly differentiated into neurons (Silva et al. 2004). Peptide sequences that are susceptible to enzymatic cleavage have also been engineered into the polypeptides without sacrificing self-assembly processes, thus enabling cell migration (Galler et al. 2010).

Another class of self-assembling polypeptides that have been employed in cell encapsulation strategies is elastin-like-polypeptide (ELP) (MacEwan and Chilkoti 2010). This polypeptide is different from the aforementioned polypeptides in that it undergoes self-assembly in response to changes in temperature forming micelle-like structures. Its transition temperature can be tuned by varying the guest amino acid residue, X, within the repeating amino acid sequence, (VPGXG)_m and by the length of the polypeptide (Meyer and Chilkoti 2002). Further functionalization of the polypeptide via side groups

is possible without adversely affecting its thermal responsiveness. ELPs have been used to encapsulate chondrocytes leading to cartilage-like matrix deposition (Betre et al. 2002) and human adipose derived adult stem cells where the ELP hydrogel provided an environment that promoted chondrogenesis in the absence of chondrogenic factors (Betre et al. 2006).

Taken together, self-assembling polymers and polypeptides that form hydrogels have many advantages with respect to encapsulating cells, delivering cells *in vivo*, and recovering cells for further manipulation due to their reversible gelation (Huang et al. 2007). Their main shortcoming, however, is insufficient mechanical properties and lack stability for many tissue engineering applications (Klouda and Mikos 2008). To overcome this limitation, thermogelling polymers have been modified to contain reactive groups, such as acrylates or methacrylates, to permit subsequent chemical crosslinking (Hacker et al. 2008; Lee and Park 2009). In self-assembling peptides, the mechanical properties have been improved similarly by incorporating chemical crosslinks. For example, reacting a lysine-containing ELP with an organophosphorous crosslinker facilitated covalent crosslinking without adversely affecting cell viability during encapsulation (Lim et al. 2007). From a clinical perspective, the advantage of a dual gelation system is that immediately upon injection solidification occurs rapidly, thus entrapping the cells in place and which is then followed by chemical crosslinking to impart stability and mechanical integrity. The latter process may be designed to occur more slowly thus minimizing the potential cytotoxic effects of chemical crosslinking (described in more detail in the following sections). Nonetheless, self-assembling polymers and peptides offer an attractive platform for encapsulating cells under gentle gelation conditions.

58.2.2 Gelation via Covalent Crosslinking: Radical Chain Polymerization

Radical chain polymerizations are attractive for cell encapsulations because they are rapid, occurring on clinically relevant time scales, can be performed under mild conditions at physiological pH and temperature, and polymerized *in vivo* using minimally invasive procedures. Radical chain polymerization involves the polymerization of vinyl macromers through initiation, propagation, and termination to create crosslinked polymer networks (i.e., Figure 58.1b). For cell encapsulation strategies, macromers are typically comprised of biocompatible polymers that have been modified with two or more vinyl groups to enable crosslinking. The most common vinyl groups are acrylates, methacrylates, and fumarates. Initiation of the polymerization reaction requires an initiator molecule(s) and in certain instances an initiating signal such as temperature or exposure to light. The two most common initiating systems employed in cell encapsulations are redox initiating systems and photoinitiating systems.

Redox initiating systems are comprised of two components typically a peroxide oxidizing agent and an amine reducing agent, which react together to form active centers (e.g., radical anions) that initiate the polymerization reaction. The cytotoxicity of redox initiating systems has been primarily linked to changes in the pH of the initiators and to a lesser extent on the active centers, but is dependent on both initiator concentration and chemistry (Temenoff et al. 2003, 2004a). The cytotoxicity can be minimized by using low initiator concentrations and initiators dissolved in cell culture medium, which acts as a buffer to maintain a neutral pH, while still permitting polymerization (Temenoff et al. 2003, 2004a). The most common redox initiating system is ammonium persulfate and *N,N,N',N'*-tetramethylethylenediamine and which has been shown to lead to gelation times on clinically relevant times scales, <10 min (Temenoff et al. 2004a).

Photoinitiating systems are comprised of photoinitiator molecules and initiating light. Upon exposure to light, photoinitiator molecules absorb photons of light energy and dissociate into radicals that initiate the polymerization. The reaction conditions can be quite harsh on cells if not carefully chosen. Therefore, photoinitiators are typically selected based on their ability to dissociate into radicals by either long-wave ultraviolet light (~365 nm) or visible light (~400–700 nm). In addition, photoinitiator concentration, photoinitiator efficiency (a measure of the ability of a photoinitiator to dissociate into radicals), radical chemistry, and exposure time will affect cell viability during encapsulation (Bryant

et al. 2000; Williams et al. 2005). The most common UV photoinitiator used in cell encapsulations is the water soluble photoinitiator, 2-hydroxy-1-[4-(hydroxyethoxy)phenyl]-2-methyl-1-propanone also referred to as Irgacure® 2959, a registered trademark name of Ciba Specialty Chemical, for its cytocompatibility (Bryant et al. 2000). Other UV photoinitiators (e.g., 2,2-dimethoxy-2-phenylacetophenone) have been successfully employed in cell encapsulations but typically require low initiator concentrations and/or short polymerization times to minimize their cytotoxic effects (Bryant et al. 2000; Mann et al. 2001). One primary concern with using ultraviolet light in cell encapsulations is its potential adverse effects on DNA. DNA damage was reported in ~10% of cells immediately following their encapsulation by a UV photoinitiating system, but the damage appeared to be repaired within a few days postencapsulation (Fedorovich et al. 2009). An alternative is visible light photoinitiating systems, which are attractive for several reasons. Visible light is known to be less damaging to cells than UV light and visible light penetrates deeper through thick and dense materials, such as human tissue, making it possible to cure through tissues, for example, transdermally (Elisseff et al. 1999a). Examples of visible light photoinitiators, which have been used in cell encapsulations are eosin-Y and triethanolamine and camphorquinone (Cruise et al. 1998; Cruise et al. 1999; Ahmed et al. 2007). However, the shortcoming of visible light photoinitiators is their low photoinitiator efficiency; often requiring longer polymerization times. Because of these limitations, UV photoinitiating systems remain the most widely used in photopolymerizations involving cell encapsulations despite their potential drawbacks.

Numerous chemistries have been modified with acrylates and methacrylates to produce macromers suitable for cell encapsulations. Acrylates are known to have increased cytotoxicity over methacrylates, when small monomers are employed (Yoshii 1997). However, the author is not aware of any reports indicating differences in cytotoxicity between acrylates and methacrylates when macromolecular monomers are employed for cell encapsulations. Another main difference between acrylates and methacrylates is the methyl group on the methacrylate helps to stabilize the propagating radical resulting in generally slower rates of polymerization (Jager et al. 1997). However, reaction times for both acrylate- and methacrylate-based macromers can occur on clinically relevant timescales, on the order of seconds to several minutes. One of the most widely employed macromers for cell encapsulations is poly(ethylene glycol) diacrylate or dimethacrylate and its degradable form poly(α -hydroxy ester)-*b*-poly(ethylene glycol)-*b*-poly(α -hydroxy ester) di(meth)acrylate (Sawhney et al. 1993), which have been used to encapsulate numerous types of cells including islets (Hill et al. 1997; Weber et al. 2006), smooth muscle cells (Mann and West 2002), chondrocytes (Elisseff et al. 1999b; Bryant and Anseth 2003), osteoblasts (Burdick and Anseth 2002), neural precursor cells (Mahoney and Anseth 2006), hepatocytes (Tsang et al. 2007), and mesenchymal stem cells (Williams et al. 2003; Nuttelman et al. 2005). Other chemistries such as poly(vinyl alcohol), poly(2-hydroxyethyl methacrylate), and polysaccharides (e.g., hyaluronan, chondroitin sulfate, chitosan, etc.) enable functionalization with multiple (meth)acrylates offering an additional mechanism by which to control the resulting hydrogel properties (Martens and Anseth 2000; Smeds and Grinstaff 2001; Bryant et al. 2004b). For example, when neural progenitor cells were encapsulated in hydrogels containing the same concentration of hyaluronic acid, but which were prepared with varying degrees of methacrylate substitution, the differentiation of the progenitor cells was significantly impacted (Seidlits et al. 2010). A lower methacrylate substitution led to soft hydrogels, which promoted differentiation into neurons while higher methacrylate substitution led to stiffer hydrogels and differentiation into the undesirable cell type, astrocytes.

An alternative to using (meth)acrylate functionalized polymers for cell encapsulation is macromers containing fumarate (Yaszemski et al. 1996). Fumarate is a natural compound that contains a polymerizable vinyl group and an ester linkage that imparts degradability. The most common strategy has been to incorporate a single fumarate moiety into the backbone of a synthetic polymer, namely poly(ethylene glycol), which when reacted with a divinyl crosslinker (e.g., poly(ethylene glycol) diacrylate) leads to a crosslinked and biodegradable hydrogel. Fumarate-based macromers have been successfully used to encapsulate several types of cells including chondrocytes (Park et al. 2005) and marrow stromal cells for chondrogenesis (Park et al. 2009) and osteogenesis (Temenoff et al. 2004b).

58.2.3 Gelation via Covalent Crosslinking: Step Growth Polymerization

More recently, there have been significant efforts to design hydrogels that form via step growth polymerization (i.e., Figure 58.1c). One of the main advantages of a step growth polymerization is that the resulting hydrogel forms a homogeneous network structure, which is in contrast to the inhomogeneous structure formed by radical chain polymerization. These well-defined networks lead to improved mechanical properties and higher degrees of swelling over hydrogels formed from similar macromers under radical chain polymerization (Malkoch et al. 2006). Cell encapsulations have been successful in such hydrogels synthesized by Michael-type addition reactions (Lutolf et al. 2003; Shu et al. 2004), radical mediated thiol-ene photopolymerizations, a type of click reaction (Fairbanks et al. 2009), and copper-free “click” reactions (DeForest et al. 2009).

In Michael-type addition, the reaction occurs between thiols and unsaturated groups (e.g., vinyl sulfones and acrylates) under slightly basic conditions. While the basic environment does not adversely affect cells during encapsulation, the reactivity of thiolates (i.e., the reactive form of thiols) can be increased at neutral pH by altering the chemistry adjacent to the thiol (Lutolf et al. 2001; Shu et al. 2004). In cell encapsulation it is common to employ two distinct macromolecular monomers where one macromer contains three or more functional groups to enable crosslinking and the second macromer contains two functional groups. For example, synthetic extracellular matrix (sECM) including polysaccharides (e.g., hyaluronan and chondroitin sulfate) and proteins (e.g., gelatin) have been modified with multiple thiol groups and subsequently reacted with poly(ethylene glycol) diacrylate to create 3D environments with tunable chemistry (Serban and Prestwich 2008). For example, a hyaluronan sECM hydrogel containing encapsulated human adipose-derived stem cells supported their maturation into mature adipocytes *in vivo* (Flynn et al. 2009) while a hyaluronan and gelatin sECM hydrogel supported *in situ* delivery of mesenchymal stem cells for osteochondral repair (Liu et al. 2006). One of the attractive features of the Michael-type addition reaction is the ease with which peptides can be incorporated into the hydrogel. By simply functionalizing peptides with one or more cysteines (the amino acid containing a thiol side group) the peptide is readily incorporated into a network. Mono-cysteine peptides enable proteins to be tethered to the hydrogel backbone, while di-cysteine peptides become incorporated into the crosslinks of the network. This strategy has enabled facile fabrication of hydrogels comprised of cell adhesion ligands to permit cell attachment and of peptide crosslinks that are sensitive to matrix metalloproteinases (MMPs) (i.e., matrix-degrading enzymes) to enable cell-mediated degradation and migration (Lutolf et al. 2003).

Click reactions are highly selective and highly efficient orthogonal reactions that offer a reliable and modular platform for designing new chemistries (Kolb et al. 2001). Thiol-ene polymerizations are considered to be one type of click reaction (Hoyle and Bowman 2010) and offer an alternative to the base-catalyzed Michael-type addition reaction. The reaction undergoes a step-growth mechanism by alternating between propagation, where a thiyl radical propagates across the alkene, and chain transfer reactions that leads to the formation of a thioether linkages while simultaneously producing a thiyl radical (Cramer and Bowman 2001; Fairbanks et al. 2009). When a photoinitiator is employed, the reaction can be both spatially and temporally controlled (Fairbanks et al. 2009), while simultaneously forming a near ideal hydrogel network. By reacting –ene functionalized (e.g., norbornene) and thiol functionalized (e.g., peptides) *macromolecular* monomers with a cytocompatible photoinitiator and concentration, thiol-ene click reactions are suitable for encapsulating cells (Benton et al. 2009). For copper-free click reactions between azides and alkynes (Baskin et al. 2007), the development of a difluorinated cyclooctyne as the alkyne has enabled the reaction to proceed without the need for the cytotoxic metal catalyst making it possible to perform these types of click reactions *in vivo* (Agard et al. 2004; Baskin et al. 2007) and in the presence of cells (DeForest et al. 2009). For cell encapsulations, high molecular weight macromers have been designed to contain tetra-azides which when reacted with bis(cyclooctyne)-functionalized peptides within physiological medium enable encapsulation of cells. The reaction, however, was reported to take ~1 h, which is significantly slower than that reported for

radical initiated polymerizations (~10 min). Nonetheless, no additional components are required for this click reaction and high cell viability can be achieved after encapsulation.

Overall, a variety of strategies have been developed from which to create covalently crosslinked hydrogels for cell encapsulation. The strategies range from simple and versatile platforms for delivering cells *in situ* to complex 3D environments that are spatially and/or temporally controlled towards recapitulating the complex architecture of native tissues. While the polymerization and/or crosslinking reactions require additional components, utilizing macromolecular monomers and selecting appropriate reaction conditions has enabled cells to be encapsulated through a variety of gelation mechanisms without adversely affecting their viability.

58.3 Hydrogel Structure and Degradation

The molecular structure of the hydrogel controls many of the macroscopic properties important in developing a tissue engineering strategy including water content, mesh size (i.e., pore structure), mechanical properties, and degradation behavior. Because these properties are closely linked through the crosslinking density of the hydrogel, careful consideration of all properties must be taken into account when optimizing a hydrogel for a given application. For example, high mechanical strength is critical when designing a hydrogel for *in situ* placement within an articulating joint that is subjected to large stresses, however, the water content and diffusional capabilities are sacrificed. Incorporating degradation into the hydrogel allows for temporal changes to the hydrogel structure, but the rate of degradation must be tuned with elaboration of new tissue. This requirement is in contrast to prefabricated porous scaffolds where large pores (~200 μm) provide ample space for new tissue to be deposited prior to scaffold degradation. Therefore, an understanding of how the hydrogel structure impacts tissue development is critical to optimizing a hydrogel formulation for tissue engineering.

58.3.1 The Role of Hydrogel Structure in Tissue Development

The act of encapsulating and retaining cells within a 3D hydrogel requires that the mesh size of the hydrogel be sufficiently smaller than that of a cell. A typical mesh size or the average distance between crosslinks for poly(ethylene glycol)(PEG) hydrogels formed from di(meth)acrylate macromers ranges from ~4 to 20 nm (Bryant and Anseth 2001a). The relatively *small* dimensions of the polymer mesh impact a number of critical factors important to a successful tissue engineering strategy including morphology of the cells, the ability to form cell–cell contacts, diffusion of nutrients to the cells, and diffusion of extracellular matrix molecules for macroscopic tissue evolution. Since degradation directly impacts mesh size, engineering in degradable linkages is often necessary to support many of these critical factors, which would otherwise be hindered by a tight crosslinked network.

When cells are suspended in a liquid precursor solution prior to encapsulation, they naturally exhibit a round morphology. Upon encapsulation, the hydrogel network essentially surrounds each cell, entrapping them as single cells in a relatively tight mesh, and acting as a physical restraint that forces the cells to retain a round morphology. This round morphology can be observed in the examples in [Figure 58.2](#). For cells such as chondrocytes, a round morphology is essential to retaining their differentiated phenotype making hydrogels an ideal platform for culturing chondrocytes. However, for many types of cells the ability for a cell to spread (Chen et al. 1997) and/or form cell–cell contacts (Hosokawa et al. 2010) is critical to its survival and/or function. Therefore, tuning the hydrogel chemistry with proteins and/or peptides to promote cell attachment *and* to facilitate degradation are critical design features for many applications.

In addition to influencing the morphology of the encapsulated cells, the mesh size also impacts diffusion of molecules through the hydrogel. The mesh size is generally sufficiently large as to not hinder diffusion of small nutrients such as glucose and oxygen, but may impact diffusion of large growth factors and other important signaling factors especially when designing high moduli hydrogels. However,

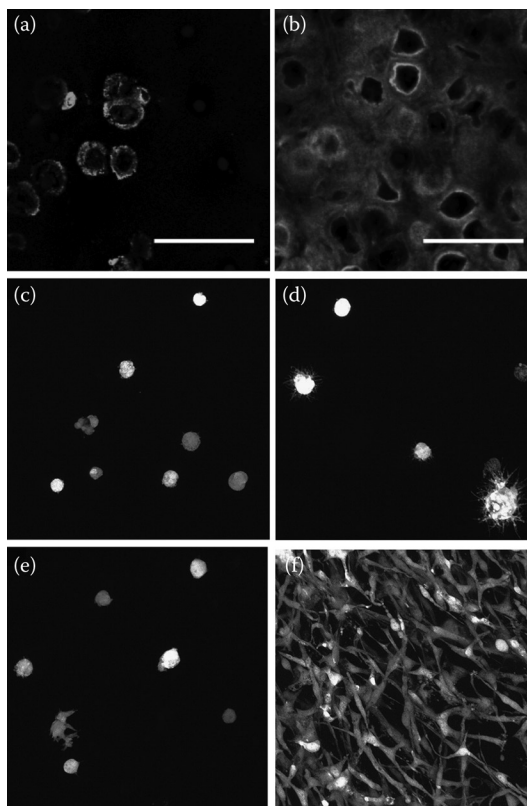


FIGURE 58.2 The impact of temporal changes in hydrogel structure via degradation in hydrolytically labile hydrogels (a,b) and enzymatically labile hydrogels (c–f). In panels a and b, bovine articular cartilage cells (i.e., chondrocytes) were encapsulated in hydrogels formed from poly(ethylene glycol) dimethacrylate macromers, which did not exhibit signs of degradation (a) and encapsulated in hydrogels formed from poly(lactic acid)-*b*-poly(ethylene glycol)-*b*-poly(lactic acid) dimethacrylate, which were completely degraded within 2 weeks (b). After 25 days, collagen type II deposited by the cartilage cells (gray) is localized to the pericellular region in nondegrading hydrogels (a), but is deposited throughout the extracellular matrix in degrading hydrogels (b). In panels c–f, murine myofibroblasts were encapsulated in poly(ethylene glycol) hydrogels formed from a step-growth polymerization containing either highly sensitive (c,d) or moderately sensitive (e,f) crosslinkers to MMPs. Panels c,e are three days postencapsulation and panels d,f are 21 days postencapsulation. Cells were transfected with a fluorescent protein for visualization. (Panels c–f are reprinted from *Biomaterials*, Patterson, J. and Hubbell, J. A. Enhanced proteolytic degradation of molecularly engineered PEG hydrogels in response to mmp-1 and mmp-2, doi:10.1016/j.biomaterials.2010.06.061. Copyright 2010, with permission from Elsevier.)

it is thought that a 3D culture system with some hindrances to diffusion is representative of the native tissue environment. Equally important is the impact that the mesh size will have on diffusion of newly synthesized tissue macromolecules. The extracellular matrix that makes up tissues is comprised of large macromolecules that can reach dimensions on nanometer length scales. For example, collagen, which is one of the most abundant extracellular matrix proteins found in the body, can reach dimensions up to several hundred nanometers in diameter (Svoboda et al. 1983; Moeller et al. 1995). In nondegrading hydrogels, many extracellular matrix molecules are restricted to regions immediately surrounding the cell. For example, collagen type II deposited by chondrocytes or chondrogenically differentiated mesenchymal stem cells was localized to the pericellular matrix throughout the course of culture (Bryant and Anseth 2003; Bryant et al. 2003; Sontjens et al. 2006). Similar findings were reported for collagen

type I and elastin deposited by vocal fold fibroblasts (Liao et al. 2008). The incorporation of degradable linkages into the hydrogel enables temporal increases in the gel mesh size permitting the deposition of these large matrix molecules into the extracellular space of the hydrogels (Bryant and Anseth 2003). For example, when chondrocytes were encapsulated in biodegradable poly(ethylene glycol) hydrogels, a macroscopic tissue developed. Figure 58.2a,b illustrates the impact that temporal changes in the gel structure have on a developing tissue. However, for many of the very large matrix macromolecules, the hydrogel must reach near complete degradation for macroscopic tissue development (Bryant et al. 2004a).

58.3.2 Modes of Degradation

The primary mechanisms by which hydrogels are designed to degrade is through hydrolysis, enzyme-mediated, or a combination. In enzyme mediated degradation schemes, degradation may occur through exogenous delivery of enzymes or through enzymes secreted by the cell. By explicitly programming degradable linkages into the polymer network and through careful selection of the chemistry, degradation can often be controlled and tuned to match tissue evolution. If degradation is too slow, tissue growth may be retarded as the extracellular matrix that is deposited by the cell quickly fills the pericellular space. If degradation is too fast, dissolution of the hydrogel may occur leading to a loss of cells and/or defects in the engineered tissue. Additionally, environmental factors should be taken into account as they may impact degradation kinetics (e.g., the *in vivo* environment).

The majority of hydrolytically labile hydrogels are designed to degrade through ester linkages that are located in the crosslink or backbone of the hydrogel. Examples of ester linkages which have been successfully employed in cell encapsulation include α -hydroxy esters (e.g., lactic acid and ϵ -caprolactone) (Bryant et al. 2003; Benoit et al. 2006), fumarates (Fisher et al. 2004; Temenoff et al. 2004b), and phosphoesters (Wang et al. 2003, 2005). For these hydrogels, degradation begins immediately upon exposing the hydrogel to an aqueous environment. Therefore, the rate of degradation and overall timing of degradation must be tuned for each cell type and tissue application. The degradation rate can be controlled through the chemistry of the degradable linker. For example, the ester linkage in poly(lactic acid) will have a higher degradation rate than the ester linkage in poly(caprolactone) resulting in degradation times that can vary substantially from days to months (Sawhney et al. 1993). Bimodal degradation schemes have also been investigated in an effort to temporally tune degradation for enhanced tissue deposition (Martens et al. 2003; Rice and Anseth 2004). For example, fast degrading linkages may allow for immediate tissue deposition, while slower degrading crosslinks may help to maintain mechanical integrity and a 3D structure during tissue maturation (Bryant et al. 2004a). Alternatively, hydrogels have been engineered with degradable linkages that are sensitive to enzymes not typically produced by cells enabling the user to define degradation. For example, caprolactone linkages, which degrade slowly via hydrolysis, may also degrade by the enzyme lipase at a much faster rate under appropriate enzyme concentrations. This strategy offers the ability to *turn on* and *turn off* degradation at defined periods of time. This temporal control over degradation has led to enhanced macroscopic tissue development for cartilage tissue engineering (Rice and Anseth 2007).

Alternatively, cell-mediated degrading hydrogels have been engineered as a mechanism where cells dictate degradation rather than the user setting *a priori* a fixed degradation rate. Hydrogels designed from natural biopolymers, such as hyaluronic acid (Smeds and Grinstaff 2001; Shu et al. 2004; Burdick et al. 2005; Masters et al. 2005) and chondroitin sulfate (Li et al. 2004; Bryant et al. 2005; Shu et al. 2006) can be degraded by cell-secreted hyaluronidases and chondroitinases, respectively. Another attractive strategy is to incorporate into the crosslinks of synthetic hydrogels short peptide sequences that represent the enzyme substrate site within a protein (Lutolf et al. 2003). Peptides that are collagen-based are the most widely investigated and are recognized by a number of MMPs, which are secreted by a variety of cell types. This strategy leads to local degradation (Lee et al. 2007), providing

a mechanism by which to maintain mechanical integrity during hydrogel degradation. While many MMPs will degrade multiple substrates, the rate of degradation can vary dramatically (Turk et al. 2001). Therefore, it is possible to select for a sequence that leads to fast or slow degradation (Patterson and Hubbell 2010). An example of a poly(ethylene glycol) hydrogel comprised of two different peptide substrates both of which are cleavable by MMPs secreted by cells, but which exhibit different degradation rates is shown in Figure 58.2c,f. These figures clearly demonstrate the impact that temporal differences in degradation can have on cellular behavior. Cells encapsulated in a hydrogel containing crosslinks that are highly susceptible to MMPs leads to cell proliferation, cell spreading, and the formation of cell–cell connections whereas crosslinks with low susceptibility essentially retain the cells in a rounded and isolated state.

In addition to controlling degradation via the choice of degradable linker, and so on, the presence of cells, as well as, the *in vivo* environment may also impact hydrogel degradation. While many ester linkages degrade via hydrolysis, they are also susceptible to cleavage by enzymes, that is, esterases, present in serum containing culture medium and the *in vivo* environment. For example, the overall degradation time was significantly reduced when poly(ethylene glycol) hydrogels containing poly(lactic acid) degradable linkages were degraded in cell culture medium containing serum compared to a phosphate buffered saline solution (Martens et al. 2003). However, degradation of poly(ethylene glycol)-based hydrogels containing fumarate as the degradable linker, was not enhanced in serum-containing medium suggesting the fumarate ester linkage may not be as susceptible to serum containing proteases (Temenoff et al. 2004a). The presence of cells and developing tissue *in vitro* has also been shown to affect the degradation behavior of hydrolytically labile hydrogels (Bryant et al. 2003). This observation is attributed to the fact that when tissue is deposited the hydrogel does not undergo large degrees of swelling and hence degradation is not as fast. The *in vivo* environment is also known to accelerate cleavage of ester linkages (Kuronon et al. 1979; Catiker et al. 2000) enhancing degradation of many hydrolytically labile hydrogels. Furthermore, the act of implanting a material in the body will lead to some degree of inflammation of which MMPs are known to be involved (Parks et al. 2004) and hence may affect the degradation behavior of MMP-susceptible hydrogels. Taken together, a better understanding of how the environment impacts the degradation behavior of a hydrogel will help to design strategies that are in tune with tissue development.

58.4 Concluding Remarks

Cell encapsulation strategies are an enabling technology for tissue engineering where cells are combined with a precursor solution prior to gelation offering ease of handling and facilitating minimally invasive delivery of cells *in situ*. In addition, there are numerous synthetic and natural chemistries from which to choose and/or combine enabling the fabrication of tailor made hydrogels that recapitulate many of the mechanical and biochemical characteristics of native tissue. As we gain better understandings of the native niche surrounding cells *in vivo*, there has been a paradigm shift from designing permissive environments from purely synthetic hydrogels to designing promoting environments that give cells biological cues to direct their fate and function. For example, biomimetic hydrogels offer a platform from which to fine-tune the macroscopic properties through manipulations in the bioinert and synthetic chemistry independently from the incorporation of biological recognition sites. In addition to creating a 3D environment suitable for cell and tissue growth, there are several practical aspects that need to be considered when developing a clinically relevant cell encapsulation strategy and which are worth noting. These considerations include an easily scalable process for manufacturing, the marketability, the acceptance by surgeons, patients, and healthcare providers, and the ability to receive food and drug administration (FDA) approval. Although there are stringent requirements to develop a successful strategy for encapsulating cells, there have been significant advances in cell encapsulations for a variety of cell types and tissues with many successes reported *in vitro* and *in vivo*. In summary, cell encapsulation holds great promise as an enabling technology for regenerating tissues.

References

- Agard, N. J., Prescher, J. A., and Bertozzi, C. R. 2004. A strain-promoted [3 + 2] azide-alkyne cycloaddition for covalent modification of biomolecules in living systems. *J Am Chem Soc* 126: 15046–47.
- Ahmed, T. A. E., Griffith, M., and Hincke, M. 2007. Characterization and inhibition of fibrin hydrogel-degrading enzymes during development of tissue engineering scaffolds. *Tissue Eng* 13: 1469–77.
- Atala, A., Cima, L. G., Kim, W. et al. 1993. Injectable alginate seeded with chondrocytes as a potential treatment for vesicoureteral reflux. *J Urol* 150: 745–47.
- Baskin, J. M., Prescher, J. A., Laughlin, S. T. et al. 2007. Copper-free click chemistry for dynamic *in vivo* imaging. *Proc Natl Acad Sci U S A* 104: 16793–97.
- Benoit, D. S. W., Durney, A. R., and Anseth, K. S. 2006. Manipulations in hydrogel degradation behavior enhance osteoblast function and mineralized tissue formation. *Tissue Eng* 12: 1663–73.
- Benton, J. A., Fairbanks, B. D., and Anseth, K. S. 2009. Characterization of valvular interstitial cell function in three dimensional matrix metalloproteinase degradable PEG hydrogels. *Biomaterials* 30: 6593–603.
- Betre, H., Ong, S. R., Guilak, F. et al. 2006. Chondrocytic differentiation of human adipose-derived adult stem cells in elastin-like polypeptide. *Biomaterials* 27: 91–99.
- Betre, H., Setton, L. A., Meyer, D. E., and Chilkoti, A. 2002. Characterization of a genetically engineered elastin-like polypeptide for cartilaginous tissue repair. *Biomacromolecules* 3: 910–16.
- Branco, M. C. and Schneider, J. P. 2009. Self-assembling materials for therapeutic delivery. *Acta Biomater* 5: 817–31.
- Bryant, S. J. and Anseth, K. S. 2001a. Hydrogel properties influence ecm production by chondrocyte photoencapsulated in poly(ethylene glycol) hydrogels. *J Biomed Mater Res* 59: 63–72.
- Bryant, S. J. and Anseth, K. S. 2001b. The effects of scaffold thickness on tissue engineered cartilage in photocrosslinked poly(ethylene oxide) hydrogels. *Biomaterials* 22: 619–26.
- Bryant, S. J. and Anseth, K. S. 2003. Controlling the spatial distribution of ECM components in degradable PEG hydrogels for tissue engineering cartilage. *J Biomed Mater Res* 64A: 70–79.
- Bryant, S. J., Arthur, J. A., and Anseth, K. S. 2005. Incorporation of tissue-specific molecules alters chondrocyte metabolism and gene expression in photocrosslinked hydrogels. *Acta Biomater* 1: 243–52.
- Bryant, S. J., Bender, R. J., Durand, K. L., and Anseth, K. S. 2004a. Encapsulating chondrocytes in degrading PEG hydrogels with high modulus: Engineering gel structural changes to facilitate cartilaginous tissue production. *Biotechnol Bioeng* 86: 747–55.
- Bryant, S. J., Davis-Arehart, K. A., Luo, N. et al. 2004b. Synthesis and characterization of photopolymerized multifunctional hydrogels: Water-soluble poly(vinyl alcohol) and chondroitin sulfate macromers for chondrocyte encapsulation. *Macromolecules* 37: 6726–33.
- Bryant, S. J., Durand, K. L., and Anseth, K. S. 2003. Manipulations in hydrogel chemistry control photoencapsulated chondrocyte behavior and their extracellular matrix production. *J Biomed Mater Res* 67A: 1430–36.
- Bryant, S. J., Nuttelman, C. R., and Anseth, K. S. 2000. Cytocompatibility of ultraviolet and visible light photoinitiating systems on cultured nih/3t3 fibroblasts *in vitro*. *J Biomater Sci Polym Ed* 11: 439–57.
- Burdick, J. A. and Anseth, K. S. 2002. Photoencapsulation of osteoblasts in injectable rgd-modified PEG hydrogels for bone tissue engineering. *Biomaterials* 23: 4315–23.
- Burdick, J. A., Chung, C., Jia, X. Q., Randolph, M. A., and Langer, R. 2005. Controlled degradation and mechanical behavior of photopolymerized hyaluronic acid networks. *Biomacromolecules* 6: 386–91.
- Cao, Y. L., Rodriguez, A., Vacanti, M. et al. 1998. Comparative study of the use of poly(glycolic acid), calcium alginate and pluronics in the engineering of autologous porcine cartilage. *J Biomater Sci Polym Ed* 9: 475–87.
- Caplan, M. R., Schwartzfarb, E. M., Zhang, S. G., Kamm, R. D., and Lauffenburger, D. A. 2002. Control of self-assembling oligopeptide matrix formation through systematic variation of amino acid sequence. *Biomaterials* 23: 219–27.

- Catiker, E., Gumusderelioglu, M., and Guner, A. 2000. Degradation of pla, plga homo- and copolymers in the presence of serum albumin: A spectroscopic investigation. *Polym Int* 49: 728–34.
- Chen, C. S., Mrksich, M., Huang, S., Whitesides, G. M., and Ingber, D. E. 1997. Geometric control of cell life and death. *Science* 276: 1425–28.
- Cramer, N. B. and Bowman, C. N. 2001. Kinetics of thiol-ene and thiol-acrylate photopolymerizations with real-time fourier transform infrared. *J Polym Sci Part A-Polym Chem* 39: 3311–19.
- Cruise, G. M., Hegre, O. D., Lamberti, F. V. et al. 1999. *In vitro* and *in vivo* performance of porcine islets encapsulated in interfacially photopolymerized poly(ethylene glycol) diacrylate membranes. *Cell Transplant* 8: 293–306.
- Cruise, G. M., Scharp, D. S., and Hubbell, J. A. 1998. Characterization of permeability and network structure of interfacially photopolymerized poly(ethylene glycol) diacrylate hydrogels. *Biomaterials* 19: 1287–94.
- Cui, H. G., Webber, M. J., and Stupp, S. I. 2010. Self-assembly of peptide amphiphiles: From molecules to nanostructures to biomaterials. *Biopolymers* 94: 1–18.
- Cukierman, E., Pankov, R., Stevens, D. R., and Yamada, K. M. 2001. Taking cell-matrix adhesions to the third dimension. *Science* 294: 1708–12.
- Dang, J. M., Sun, D. D. N., Shin-Ya, Y. et al. 2006. Temperature-responsive hydroxybutyl chitosan for the culture of mesenchymal stem cells and intervertebral disk cells. *Biomaterials* 27: 406–18.
- Deforest, C. A., Polizzotti, B. D., and Anseth, K. S. 2009. Sequential click reactions for synthesizing and patterning three-dimensional cell microenvironments. *Nat Mater* 8: 659–64.
- Dupuy, B., Gin, H., Baquey, C., and Ducassou, D. 1988. Insitu polymerization of a microencapsulating medium round living cells. *J Biomed Mater Res* 22: 1061–70.
- Elisseeff, J., Anseth, K., Sims, D. et al. 1999a. Transdermal photopolymerization for minimally invasive implantation. *Proc Natl Acad Sci USA* 96: 3104–07.
- Elisseeff, J., Anseth, K., Sims, D. et al. 1999b. Transdermal photopolymerization of poly(ethylene oxide)-based injectable hydrogels for tissue-engineered cartilage. *Plast Reconstr Surg* 104: 1014–22.
- Elsdale, T. and Bard, J. 1972. Collagen substrata for studies on cell behavior. *J Cell Biol* 54: 626.
- Fairbanks, B. D., Schwartz, M. P., Halevi, A. E. et al. 2009. A versatile synthetic extracellular matrix mimic via thiol-norbornene photopolymerization. *Adv Mater (Weinheim, Ger)* 21: 5005–10.
- Fedorovich, N. E., Oudshoorn, M. H., Van Geemen, D. et al. 2009. The effect of photopolymerization on stem cells embedded in hydrogels. *Biomaterials* 30: 344–53.
- Fisher, J. P., Jo, S., Mikos, A. G., and Reddi, A. H. 2004. Thermoreversible hydrogel scaffolds for articular cartilage engineering. *Journal of Biomedical Materials Research Part A* 71A: 268–74.
- Flynn, L., Prestwich, G. D., Semple, J. L., and Woodhouse, K. A. 2009. Adipose tissue engineering *in vivo* with adipose-derived stem cells on naturally derived scaffolds. *Journal of Biomedical Materials Research Part A* 89A: 929–41.
- Fujimoto, K. L., Ma, Z. W., Nelson, D. M. et al. 2009. Synthesis, characterization and therapeutic efficacy of a biodegradable, thermoresponsive hydrogel designed for application in chronic infarcted myocardium. *Biomaterials* 30: 4357–68.
- Galler, K. M., Aulisa, L., Regan, K. R., D'souza, R. N., and Hartgerink, J. D. 2010. Self-assembling multidomain peptide hydrogels: Designed susceptibility to enzymatic cleavage allows enhanced cell migration and spreading. *J Am Chem Soc* 132: 3217–23.
- Gelain, F., Bottai, D., Vescovi, A., and Zhang, S. G. 2006. Designer self-assembling peptide nanofiber scaffolds for adult mouse neural stem cell 3-dimensional cultures. *PLoS ONE* 1: e119.
- Gelain, F., Horii, A., and Zhang, S. G. 2007. Designer self-assembling peptide scaffolds for 3-d tissue cell cultures and regenerative medicine. *Macromol Biosci* 7: 544–51.
- Gieni, R. S. and Hendzel, M. J. 2008. Mechanotransduction from the ECM to the genome: Are the pieces now in place? *J Cell Biochem* 104: 1964–87.
- Hacker, M. C., Klouda, L., Ma, B. B., Kretlow, J. D., and Mikos, A. G. 2008. Synthesis and characterization of injectable, thermally and chemically gelable, amphiphilic poly(*n*-isopropylacrylamide)-based macromers. *Biomacromolecules* 9: 1558–70.

- Hill, R. S., Cruise, G. M., Hager, S. R. et al. 1997. Immunoisolation of adult porcine islets for the treatment of diabetes mellitus. The use of photopolymerizable polyethylene glycol in the conformal coating of mass-isolated porcine islets. *Ann NY Acad Sci* 831: 332–43.
- Hosokawa, K., Arai, F., Yoshihara, H. et al. 2010. Cadherin-based adhesion is a potential target for niche manipulation to protect hematopoietic stem cells in adult bone marrow. *Cell Stem Cell* 6: 194–98.
- Hoyle, C. E. and Bowman, C. N. 2010. Thiol-ene click chemistry. *Angew. Chem.-Int Ed* 49: 1540–73.
- Huang, X., Zhang, Y., Donahue, H. J., and Lowe, T. L. 2007. Porous thermoresponsive-co-biodegradable hydrogels as tissue-engineering scaffolds for 3-dimensional *in vitro* culture of chondrocytes. *Tissue Eng* 13: 2645–52.
- Jager, W. F., Lungu, A., Chen, D. Y., and Neckers, D. C. 1997. Photopolymerization of polyfunctional acrylates and methacrylate mixtures: Characterization of polymeric networks by a combination of fluorescence spectroscopy and solid state nuclear magnetic resonance. *Macromolecules* 30: 780–91.
- Khattak, S. F., Bhatia, S. R., and Roberts, S. C. 2005. Pluronic f127 as a cell encapsulation material: Utilization of membrane-stabilizing agents. *Tissue Eng* 11: 974–83.
- Kisiday, J., Jin, M., Kurz, B. et al. 2002. Self-assembling peptide hydrogel fosters chondrocyte extracellular matrix production and cell division: Implications for cartilage tissue repair. *Proc Natl Acad Sci USA* 99: 9996–10001.
- Kisiday, J. D., Kopesky, P. W., Evans, C. H. et al. 2008. Evaluation of adult equine bone marrow- and adipose-derived progenitor cell chondrogenesis in hydrogel cultures. *J Orthop Res* 26: 322–31.
- Klouda, L. and Mikos, A. G. 2008. Thermoresponsive hydrogels in biomedical applications. *Eur J Pharm Biopharm* 68: 34–45.
- Kolb, H. C., Finn, M. G., and Sharpless, K. B. 2001. Click chemistry: Diverse chemical function from a few good reactions. *Angew. Chem.-Int Ed* 40: 2004–21.
- Kurono, Y., Maki, T., Yotsuyanagi, T., and Ikeda, K. 1979. Esterase-like activity of human-serum albumin—structure-activity-relationships for the reactions with phenyl acetates and para-nitrophenyl esters. *Chem Pharm Bull* 27: 2781–86.
- Lee, H. and Park, T. G. 2009. Photo-crosslinkable, biomimetic, and thermo-sensitive pluronic grafted hyaluronic acid copolymers for injectable delivery of chondrocytes. *J Biomed Mater Res Part A* 88A: 797–806.
- Lee, S. H., Moon, J. J., Miller, J. S., and West, J. L. 2007. Poly(ethylene glycol) hydrogels conjugated with a collagenase-sensitive fluorogenic substrate to visualize collagenase activity during three-dimensional cell migration. *Biomaterials* 28: 3163–70.
- Li, Q., Williams, C. G., Sun, D. D. N. et al. 2004. Photocrosslinkable polysaccharides based on chondroitin sulfate. *J Biomed Mater Res Part A* 68A: 28–33.
- Liao, H. M., Munoz-Pinto, D., Qu, X. et al. 2008. Influence of hydrogel mechanical properties and mesh size on vocal fold fibroblast extracellular matrix production and phenotype. *Acta Biomater* 4: 1161–71.
- Lim, D. W., Nettles, D. L., Setton, L. A., and Chilkoti, A. 2007. Rapid cross-linking of elastin-like polypeptides with (hydroxymethyl)phosphines in aqueous solution. *Biomacromolecules* 8: 1463–70.
- Lim, F. and Sun, A. M. 1980. Microencapsulated islets as bioartificial endocrine pancreas. *Science* 210: 908–10.
- Lippens, E., Declercq, H., Molera, J. G. et al. 2009. Modified pluronic f127 hydrogel as a cell delivery system for bone tissue engineering. *Tissue Eng Part A* 15: 40.
- Liu, Y. C., Shu, X. Z., and Prestwich, G. D. 2006. Osteochondral defect repair with autologous bone marrow-derived mesenchymal stem cells in an injectable, in situ, cross-linked synthetic extracellular matrix. *Tissue Eng* 12: 3405–16.
- Lutolf, M. P., Lauer-Fields, J. L., Schmoekel, H. G. et al. 2003. Synthetic matrix metalloproteinase-sensitive hydrogels for the conduction of tissue regeneration: Engineering cell-invasion characteristics. *Proc Natl Acad Sci U S A* 100: 5413–18.
- Lutolf, M. P., Tirelli, N., Cerritelli, S., Cavalli, L., and Hubbell, J. A. 2001. Systematic modulation of michael-type reactivity of thiols through the use of charged amino acids. *Bioconjug Chem* 12: 1051–56.

- Macewan, S. R. and Chilkoti, A. 2010. Elastin-like polypeptides: Biomedical applications of tunable biopolymers. *Biopolymers* 94: 60–77.
- Mahoney, M. J. and Anseth, K. S. 2006. Three-dimensional growth and function of neural tissue in degradable polyethylene glycol hydrogels. *Biomaterials* 27: 2265–74.
- Malkoch, M., Vestberg, R., Gupta, N. et al. 2006. Synthesis of well-defined hydrogel networks using click chemistry. *Chem Commun (Camb)*: 2774–76.
- Mann, B. K., Gobin, A. S., Tsai, A. T., Schmedlen, R. H., and West, J. L. 2001. Smooth muscle cell growth in photopolymerized hydrogels with cell adhesive and proteolytically degradable domains: Synthetic ecm analogs for tissue engineering. *Biomaterials* 22: 3045–51.
- Mann, B. K. and West, J. L. 2002. Cell adhesion peptides alter smooth muscle cell adhesion, proliferation, migration, and matrix protein synthesis on modified surfaces and in polymer scaffolds. *J Biomed Mater Res* 60: 86–93.
- Martens, P. and Anseth, K. S. 2000. Characterization of hydrogels formed from acrylate modified poly(vinyl alcohol) macromers. *Polymer* 41: 7715–22.
- Martens, P. J., Bryant, S. J., and Anseth, K. S. 2003. Tailoring the degradation of hydrogels formed from multivinyl poly(ethylene glycol) and poly(vinyl alcohol) macromers for cartilage tissue engineering. *Biomacromolecules* 4: 283–92.
- Masters, K. S., Shah, D. N., Leinwand, L. A., and Anseth, K. S. 2005. Crosslinked hyaluronan scaffolds as a biologically active carrier for valvular interstitial cells. *Biomaterials* 26: 2517–25.
- Mata, A., Geng, Y. B., Henrikson, K. J. et al. 2010. Bone regeneration mediated by biomimetic mineralization of a nanofiber matrix. *Biomaterials* 31: 6004–12.
- Meyer, D. E. and Chilkoti, A. 2002. Genetically encoded synthesis of protein-based polymers with precisely specified molecular weight and sequence by recursive directional ligation: Examples from the elastin-like polypeptide system. *Biomacromolecules* 3: 357–67.
- Moeller, H. D., Bosch, U., and Decker, B. 1995. Collagen fibril diameter distribution in patellar tendon autografts after posterior cruciate ligament reconstruction in sheep—changes over time. *J Anat* 187: 161–67.
- Nuttelman, C. R., Tripodi, M. C., and Anseth, K. S. 2005. Synthetic hydrogel niches that promote hmsc viability. *Matrix Biol* 24: 208–18.
- Park, H., Guo, X., Temenoff, J. S. et al. 2009. Effect of swelling ratio of injectable hydrogel composites on chondrogenic differentiation of encapsulated rabbit marrow mesenchymal stem cells *in vitro*. *Biomacromolecules* 10: 541–46.
- Park, H., Temenoff, J. S., Holland, T. A., Tabata, Y., and Mikos, A. G. 2005. Delivery of tgf-beta 1 and chondrocytes via injectable, biodegradable hydrogels for cartilage tissue engineering applications. *Biomaterials* 26: 7095–103.
- Parks, W. C., Wilson, C. L., and Lopez-Boado, Y. S. 2004. Matrix metalloproteinases as modulators of inflammation and innate immunity. *Nat Rev Immunol* 4: 617–29.
- Passaretti, D., Silverman, R. P., Huang, W. et al. 2001. Cultured chondrocytes produce injectable tissue-engineered cartilage in hydrogel polymer. *Tissue Eng* 7: 805–15.
- Patterson, J. and Hubbell, J. A. 2010. Enhanced proteolytic degradation of molecularly engineered PEG hydrogels in response to mmp-1 and mmp-2. *Biomaterials* doi:10.1016/j.biomaterials.2010.06.061.
- Pollock, J. F. and Healy, K. E. 2010. Mechanical and swelling characterization of poly(*n*-isopropyl acrylamide-co-methoxy poly(ethylene glycol) methacrylate) sol-gels. *Acta Biomater* 6: 1307–18.
- Rice, M. A. and Anseth, K. S. 2004. Encapsulating chondrocytes in copolymer gels: Bimodal degradation kinetics influence cell phenotype and extracellular matrix development. *J Biomed Mater Res Part A* 70A: 560–68.
- Rice, M. A. and Anseth, K. S. 2007. Controlling cartilaginous matrix evolution in hydrogels with degradation triggered by exogenous addition of an enzyme. *Tissue Eng* 13: 683–91.
- Ruel-Gariepy, E. and Leroux, J. C. 2004. *In situ*-forming hydrogels—Review of temperature-sensitive systems. *Eur J Pharm Biopharm* 58: 409–26.

- Saha, K., Pollock, J. F., Schaffer, D. V., and Healy, K. E. 2007. Designing synthetic materials to control stem cell phenotype. *Curr Opin Chem Biol* 11: 381–87.
- Saim, A. B., Cao, Y. L., Weng, Y. L. et al. 2000. Engineering autogenous cartilage in the shape of a helix using an injectable hydrogel scaffold. *Laryngoscope* 110: 1694–97.
- Sawhney, A. S., Pathak, C. P., and Hubbell, J. A. 1993. Bioerodible hydrogels based on photopolymerized poly(ethylene glycol)-co-poly(alpha-hydroxy acid) diacrylate macromers. *Macromolecules* 26: 581–87.
- Schild, H. G. 1992. Poly (*n*-isopropylacrylamide)—experiment, theory and application. *Prog Polym Sci* 17: 163–249.
- Schweickl, H., Spagnuolo, G., and Schmalz, G. 2006. Genetic and cellular toxicology of dental resin monomers. *J Dent Res* 85: 870–77.
- Seidlits, S. K., Khaing, Z. Z., Petersen, R. R. et al. 2010. The effects of hyaluronic acid hydrogels with tunable mechanical properties on neural progenitor cell differentiation. *Biomaterials* 31: 3930–40.
- Serban, M. A. and Prestwich, G. D. 2008. Modular extracellular matrices: Solutions for the puzzle. *Methods* 45: 93–98.
- Shu, X. Z., Ahmad, S., Liu, Y. C., and Prestwich, G. D. 2006. Synthesis and evaluation of injectable, in situ crosslinkable synthetic extracellular matrices for tissue engineering. *J Biomed Mater Res Part A* 79A: 902–12.
- Shu, X. Z., Liu, Y. C., Palumbo, F. S., Lu, Y., and Prestwich, G. D. 2004. *In situ* crosslinkable hyaluronan hydrogels for tissue engineering. *Biomaterials* 25: 1339–48.
- Silva, G. A., Czeisler, C., Niece, K. L. et al. 2004. Selective differentiation of neural progenitor cells by high-epitope density nanofibers. *Science* 303: 1352–55.
- Sims, C. D., Butler, P. E., Cao, Y. L. et al. 1998. Tissue engineered neocartilage using plasma derived polymer substrates and chondrocytes. *Plast Reconstr Surg* 101: 1580–85.
- Smeds, K. A. and Grinstaff, M. W. 2001. Photocrosslinkable polysaccharides for *in situ* hydrogel formation. *J Biomed Mater Res* 54: 115–21.
- Sontjens, S. H. M., Nettles, D. L., Carnahan, M. A., Setton, L. A., and Grinstaff, M. W. 2006. Biodendrimer-based hydrogel scaffolds for cartilage tissue repair. *Biomacromolecules* 7: 310–16.
- Svoboda, E. L. A., Howley, T. P., and Deporter, D. A. 1983. Collagen fibril diameter and its relation to collagen turnover in 3 soft connective tissues in the rat. *Connect Tissue Res* 12: 43–48.
- Temenoff, J. S., Park, H., Jabbari, E. et al. 2004a. Thermally cross-linked oligo(poly(ethylene glycol) fumarate) hydrogels support osteogenic differentiation of encapsulated marrow stromal cells *in vitro*. *Biomacromolecules* 5: 5–10.
- Temenoff, J. S., Park, H., Jabbari, E. et al. 2004b. *In vitro* osteogenic differentiation of marrow stromal cells encapsulated in biodegradable hydrogels. *J Biomed Mater Res Part A* 70A: 235–44.
- Temenoff, J. S., Shin, H., Conway, D. E., Engel, P. S., and Mikos, A. G. 2003. *In vitro* cytotoxicity of redox radical initiators for cross-linking of oligo(poly(ethylene glycol) fumarate) macromers. *Biomacromolecules* 4: 1605–13.
- Tibbitt, M. W. and Anseth, K. S. 2009. Hydrogels as extracellular matrix mimics for 3D cell culture. *Biotechnol Bioeng* 103: 655–63.
- Tsang, V. L., Chen, A. A., Cho, L. M. et al. 2007. Fabrication of 3D hepatic tissues by additive photopatterning of cellular hydrogels. *FASEB J* 21: 790–801.
- Turk, B. E., Huang, L. L., Piro, E. T., and Cantley, L. C. 2001. Determination of protease cleavage site motifs using mixture-based oriented peptide libraries. *Nat Biotechnol* 19: 661–67.
- Wang, D. A., Williams, C. G., Li, Q. A., Sharma, B., and Elisseeff, J. H. 2003. Synthesis and characterization of a novel degradable phosphate-containing hydrogel. *Biomaterials* 24: 3969–80.
- Wang, D. A., Williams, C. G., Yang, F. et al. 2005. Bioresponsive phosphoester hydrogels for bone tissue engineering. *Tissue Eng* 11: 201–13.
- Wang, F., Li, Z. Q., Khan, M. et al. 2010. Injectable, rapid gelling and highly flexible hydrogel composites as growth factor and cell carriers. *Acta Biomater* 6: 1978–91.

- Wanka, G., Hoffmann, H. and Ulbricht, W. 1994. Phase-diagrams and aggregation behavior of poly(oxyethylene)-poly(oxypropylene)-poly(oxyethylene) triblock copolymers in aqueous-solutions. *Macromolecules* 27: 4145–59.
- Weber, L. M., He, J., Bradley, B., Haskins, K., and Anseth, K. S. 2006. PEG-based hydrogels as an *in vitro* encapsulation platform for testing controlled beta-cell microenvironments. *Acta Biomater* 2: 1–8.
- Williams, C. G., Kim, T. K., Taboas, A. et al. 2003. *In vitro* chondrogenesis of bone marrow-derived mesenchymal stem cells in a photopolymerizing hydrogel. *Tissue Eng* 9: 679–88.
- Williams, C. G., Malik, A. N., Kim, T. K., Manson, P. N., and Elisseff, J. H. 2005. Variable cytocompatibility of six cell lines with photoinitiators used for polymerizing hydrogels and cell encapsulation. *Biomaterials* 26: 1211–18.
- Yang, Y., Khoe, U., Wang, X. et al. 2010. Designer self-assembling peptide nanomaterials. *Nano Today* 4: 193–210.
- Yaszemski, M. J., Payne, R. G., Hayes, W. C., Langer, R., and Mikos, A. G. 1996. *In vitro* degradation of a poly(propylene fumarate)-based composite material. *Biomaterials* 17: 2127–30.
- Yoshii, E. 1997. Cytotoxic effects of acrylates and methacrylates: Relationships of monomer structures and cytotoxicity. *J Biomed Mater Res* 37: 517–24.

62

Vascularization of Engineered Tissues

Monica L. Moya
*University of
California, Irvine*

Eric M. Brey
*Illinois Institute of
Technology
Hines Veterans
Hospital*

62.1	Introduction	62-1
62.2	Neovascularization.....	62-1
	Angiogenesis • Vasculogenesis • Arteriogenesis	
62.3	Strategies for Vascularizing Engineered Tissues.....	62-4
	Prevascularized Constructs • Inducing Vascularization upon Implantation • Surgical Approaches	
62.4	Conclusions.....	62-11
	References.....	62-11

62.1 Introduction

Tissue engineering has received significant attention due to its potential to provide alternatives to traditional clinical options for organ replacement and tissue reconstruction. Although success has been achieved for some clinical applications, the ability to engineer tissues of sufficient size and complexity for many applications is limited by the ability to control vascularization. The specific dimensions depend on the metabolic needs of a given tissue, but tissues are generally limited to a few 100 μm in thickness in the absence of a blood supply. Currently most successful engineered tissues are thin (Griffith and Naughton, 2002, Morrison, 2009). Although neovascularization (new blood vessel formation) occurs in these tissues the extent would be insufficient to vascularize materials of large volumes. Engineering large, complex tissues requires the ability to stimulate extensive neovascularization in sufficient time to avoid necrosis. In addition, the presence of vessels within the scaffolds is not likely to be sufficient. The structure, functionality, and stability of the resultant vascular networks must be appropriate to support tissue function.

Neovascularization limitations in tissue engineering are well established and have been an active area of research over the last decade (Skalak et al., 2002). People have investigated a number of different approaches for enhancing network formation in engineered tissues, including using cells, growth factors, prevascularizing by cell self-assembly, material patterning, and surgical techniques (Figure 62.1). Despite this attention, the ability to rapidly and appropriately assemble networks in engineered tissues remains a significant challenge. In this chapter we will describe the state of the art in vascularizing engineered tissues, identifying recent advances and challenges yet to be addressed.

62.2 Neovascularization

Neovascularization can occur through three mechanisms that will be described in the following sections: vasculogenesis, angiogenesis, and arteriogenesis (Figure 62.2). These processes often do not occur independently *in vivo* and many signaling events are common to more than one mechanism (Cao et al.,

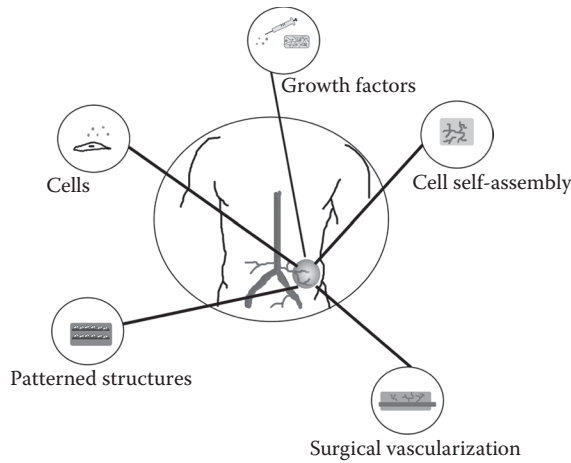


FIGURE 62.1 Approaches investigated for promoting vascularization of engineered tissues, includes patterning vessels into the polymer scaffold, seeding cells into the scaffolds that incorporate into new vessels and/or provide signals to induce vascularization, adding growth factors or growth factor delivery systems in the scaffold to promote vessel ingrowth, inducing cells to assemble into networks prior to implantation, and surgically implanting the materials in a location that optimizes vascularization.

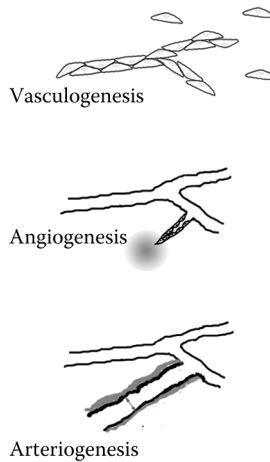


FIGURE 62.2 Neovascularization can occur via three mechanisms: vasculogenesis, angiogenesis, and arteriogenesis. Vasculogenesis is the organization of new vessels from precursor cells. Angiogenesis is the formation of new vessels from pre-existing vessels, typically occurring by sprouting of new vessels up a gradient of soluble factors. Arteriogenesis is the process by which arteries or arterioles are remodeled into larger vessels.

2005a). It is possible that all three modes of vascularization will need to be considered when developing strategies for vascularizing engineered tissues.

62.2.1 Angiogenesis

Angiogenesis, the predominant mechanism of neovascularization in adults, refers to the formation of new vessels from pre-existing vessels. In this section, the primary mechanisms of angiogenesis, the sprouting of new vessels from the existing vessels, is described. However, other mechanisms of angiogenesis

can occur, such as intussusception where an existing vessel is divided into two. Angiogenesis occurs during normal physiological processes, such as wound healing and the female reproductive cycle, and in disease states such as tumor growth and retinopathy (Nomi et al., 2002). Angiogenesis is initiated by soluble factors expressed by cells in response to a wide range of stimuli including hypoxia, mechanical stress, metabolic stress, and immune or inflammatory signals (Carmeliet and Jain, 2000, Montesano et al., 1986). Endothelial cells (ECs) are normally in a quiescent or nonproliferative state with a balance of both proangiogenic and antiangiogenic signals in the environment. The cells are activated when there is a shift in the balance toward factors that promote angiogenesis (Carmeliet and Jain, 2000).

A number of proangiogenic factors have been identified that contribute to this process, but members of the vascular endothelial growth factor (VEGF) and fibroblast growth factor (FGF) families have received the most attention. Receptors present on ECs are activated by interaction with these factors, resulting in the upregulation of proteases that degrade the underlying basement membrane (BM) and surrounding extracellular matrix (ECM). A change in the shape of ECs allows them to migrate into the surrounding matrix forming sprouts from the existing vessel (Nomi et al., 2002). Cells at the tips of the sprout migrate while cells behind the tip proliferate, allowing the sprout to elongate. For obvious reasons, angiogenesis research has primarily focused on ECs, but the initial stages of angiogenesis are a multicellular process. Mural cells are reduced relative to the amount found in stable vessels but are still present during the initial stages and may be involved in initiating microvascular development (Brey et al., 2004, Ozerdem and Stallcup, 2003, Yana et al., 2007, Gerhardt and Betsholtz, 2003). Other cells, such as macrophages and fibroblasts, may facilitate vessel invasion by breaking down the ECM ahead of the sprout (Anghelina et al., 2004, 2006, Sunderkotter et al., 1994).

Depending on the distribution of soluble (proteins) and insoluble (ECM/biomaterials) factors in the environment, a new branch may form from the sprouting vessel or the vessel can continue to elongate. The choice between elongation and sprouting appears to depend, at least in part, on the concentration gradient of VEGF (Gerhardt et al., 2003). The sprouts eventually join up with other sprouts to form a closed loop through which blood can flow. Under physiological angiogenesis, the newly formed vasculature is remodeled into a stable network tailored to the specific metabolic demands of the local tissue. During this time some of the vessels formed become mature and stable while other regress (Francis et al., 2008). Vessel maturation involves the production of new BM and an increase in the number of mural cells surrounding the tubes. These cells are recruited, in part, by the secretion of platelet-derived growth factor-BB (PDGF-BB) (Darland and D'Amore, 1999, Nomi et al., 2002, Gaengel et al., 2009) and angiopoietin-1 (Ang-1) (Aplin et al., 2009, Hoffmann et al., 2005). Mature vessels are less dependent on angiogenic factors for survival and are required for proper vascular network function (Abramsson et al., 2002). Once vessels are matured, the ECs return to their quiescent state. Currently a significant amount of research is focused on the role of soluble factors as well as insoluble factors in the extracellular microenvironment on neovascularization (Francis et al., 2008).

62.2.2 Vasculogenesis

Vasculogenesis, the process of vessel development primarily occurring during embryogenesis, is the formation of new blood vessels by progenitor cells. In adults, vasculogenesis occurs when angioblasts, or endothelial precursor cells (EPCs), home to tissues from the bone marrow or circulating blood. Stromal cell-derived factor-1 is a primary mediator involved in EPC trafficking to these tissues. The EPCs differentiate into ECs and organize into nascent endothelial tubes. The ECs then secrete signals similar to those involved in the maturation stage of angiogenesis to recruit mural cells for stabilization (Nomi et al., 2002, Carmeliet, 2003). Although vasculogenesis can occur in adults, the level of its contribution remains unclear (Carmeliet, 2000, van Weel et al., 2008). Results suggest that less than 5% of ECs in newly formed vessels result from the differentiation of circulating precursor cells (Cao et al., 2005a). Although the contribution of EPCs to neovascularization in adults appears low, studies suggest that increasing the homing and recruitment of EPCs to a given tissue can enhance neovascularization (Yamaguchi et al., 2003).

62.2.3 Arteriogenesis

Arteriogenesis is the process by which arteries or arterioles are remodeled into larger vessels. Although arteriogenesis is the process of remodeling existing vessels and there is no formation of new vessels, it is a process that may be essential for proper vascularization of engineered tissues. This process, also known as collateralization, occurs when ECs and smooth muscle cells (SMCs) are activated (due to increased shear stress or cytokines) and upregulate growth factors that stimulate SMC proliferation and recruitment of mononuclear cells. Cell proliferation leads to an increase in the thickness of the vessel wall (Carmeliet, 2000, van Weel et al., 2008). This process is more efficient at increasing blood flow in ischemic tissues due to the formation of high-conductance vessels rather than neovascularization which primarily produces capillaries with low volumetric flow (Scholz et al., 2002, Brey et al., 2005).

62.3 Strategies for Vascularizing Engineered Tissues

62.3.1 Prevascularized Constructs

One strategy that has been explored to vascularize engineered tissues is to produce a vascular network within the construct prior to implantation. The presence of the vascular network could accelerate tissue perfusion by inosculation with host vessels that invade the scaffold from the surrounding tissue. Prevascularized tissue may allow for the construction of larger tissues and has the potential to improve the survival and function of other cells present in the scaffold that may be especially sensitive to low oxygen concentration. Critical to this approach, however, is the rate of inosculation with the host vasculature and the stability and function of the preformed vascular networks. In the following sections, methods of constructing prevascularized tissues are discussed.

62.3.1.1 Cell Self-Assembly

It is well established that in the presence of appropriate soluble factors and scaffolds tuned to the correct stiffness, ECs seeded on, or in, the scaffolds will self organize into network structures (Figure 62.3). This phenomenon has been explored as an approach to create materials with vascular networks that inosculate with host vasculature to rapidly establish perfusion upon implantation. Although ECs alone were initially used in the early self-assembly systems (Montesano et al., 1983, Folkman and Haudenschild, 1980), a number of studies have shown the importance of additional cell types to the formation, stability, and function of the resultant networks. Often, mural cells are combined with ECs which are then cultured *in vitro* to allow three-dimensional (3D) capillary-like assembly via a vasculogenic-like process. This process has been applied to a number of scaffold materials, including collagen (Koike et al., 2004), fibrin (Chen et al., 2009, 2010), and poly(ethylene glycol) (PEG)-based hydrogels (Moon et al., 2010).

Materials containing self-assembled vessels consisting of ECs and mural cells have even been shown to establish connections with host vasculature that are stable for up to 1 year *in vivo* (Koike et al., 2004). Inosculation of prevascularized scaffolds has also been shown with synthetic gels but extremely small material volumes were used (5 μ l) (Moon et al., 2010). Researchers have demonstrated that this approach can be used to generate specific vascularized tissues with the addition of a third cell type, including skeletal (Levenberg et al., 2005) and cardiac muscles (Caspi et al., 2007). Others have combined ECs with a cell type other than mural cells to create vascularized skin (Gibot et al., Black et al., 1998) and bone (Unger et al., 2010) *in vitro* and demonstrated successful anastomosis of the vessels in these constructs upon implantation *in vivo*. These studies show that a nonvascular cell can provide signals essential to vascular stability.

Although promising, this strategy is highly dependent on the cell source and its feasibility for routine application relies on the availability of cells that can be easily harvested, cultured, and applied. A variety of ECs have been used in these self-assembly strategies, including mature and progenitor ECs, arterial and venous cells, and cells harvested from both macro and micro vessels. Differences in cell source used

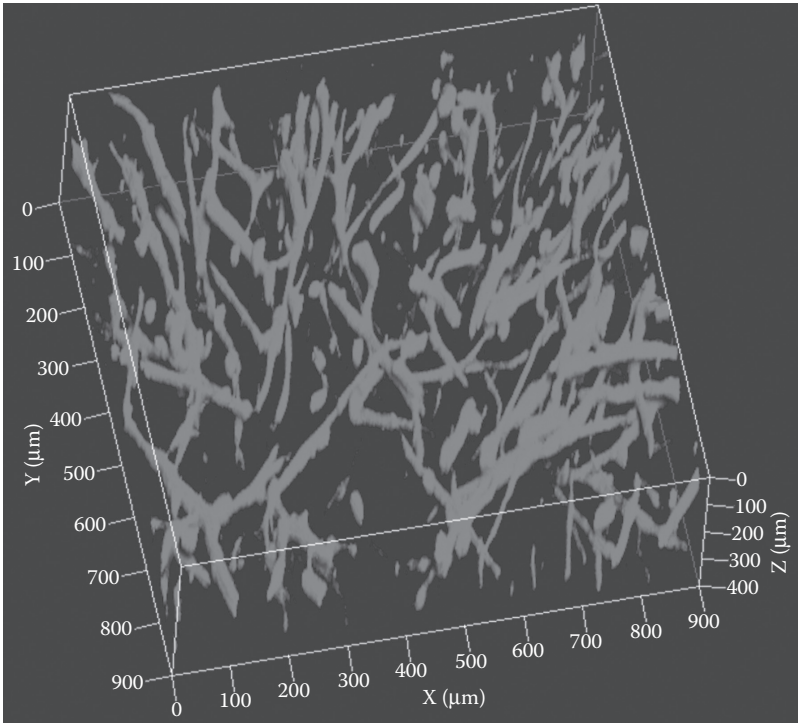


FIGURE 62.3 Three-dimensional confocal microscopy image of vascular networks formed in collagen gels.

can significantly influence the results. Chen et al. (2010) compared prevascularized constructs formed using human umbilical vein EC and EPCs isolated from cord blood. In both cases the ECs were interdispersed with fibroblasts in a fibrin matrix. Although the ECs formed vessel networks at a similar rate *in vitro*, *in vivo* the EPCs outperformed constructs made with human umbilical vein ECs by anastomosing with host vasculature at a faster rate. As anastomosis rate appears to vary between cell types, the success of these approaches will require an understanding of how efficiently the cell type used in a given application inosculates with host vessels.

As for any tissue engineering application, autologous cells would be the ideal source for these strategies. They would limit the immune response to prevascularized tissue constructs on implantation. However, this may pose an additional challenge as, outside of congenital defects and trauma patients, most of the individuals in the targeted population for these vascularization therapies are older with a variety of comorbidities, including diabetes, hypertension, a history of smoking, etc. These conditions are associated with a reduced capacity for vessel assembly (Francis-Sedlak et al., 2010), which may hinder the successful application of these approaches to the patient population in most need of interventions. Studies are needed that address the capabilities of cells from these specific patient populations to form networks and inosculate with host vasculature. Vascularization of scaffolds through self-assembly of ECs is a promising strategy, but requires significantly more research before clinical application. Regardless of clinical success, these cell-based constructs serve as an environment for controlled study of the complex interaction between cells and the ECM during vessel formation.

62.3.1.2 Patterned Structures

The techniques described above exploit the ability of ECs to assemble into networks on their own based on soluble and insoluble factors in the culture or bioreactor environment. At best, these networks can be described as immature vessels and their 3D complexity is primarily limited to interconnected small

vessels. Material and cell patterning technologies have been explored in an effort to engineer polymer scaffolds that mimic the complexity and microarchitecture of biological tissues.

Early efforts in vessel patterning focused on two-dimensional (2D) patterning on rigid substrates such as gold (Chen et al., 1998, Dike et al., 1999, Kaihara et al., 2000). Using microcontact printing, adhesive patterns of fibronectin could be created on the surface of gold (Chen et al., 1998). The spreading and proliferation of ECs were found to depend on the size and geometry of the adhesive patterns. Using this technique ECs cultured on 10- μm wide lines of fibronectin formed capillary tubular structures with a central lumen, whereas cells adhered to 30- μm lines of fibronectin formed monolayers (Dike et al., 1999). This study showed how patterning ECM proteins can be used to generate vascular structures in precise locations. However, the 2D nature of this approach and the materials used are not appropriate for tissue engineering applications.

Capillary networks consisting of vessels with diameters approaching 10 μm were etched into silicon and Pyrex surfaces using micromachining techniques (Kaihara et al., 2000). ECs and hepatocytes cultured on these 2D branched structures could be lifted off as cell monolayers and implanted. Although the hepatocytes survived following implantation, it is not clear how well the patterned vascular microstructure was maintained. Silicon wafers etched in this manner have been used as molds for the creation of vascular patterns within biodegradable cell adhesive poly(glycerol sebacate) elastomers (Fidkowski et al., 2005) and poly(lactic-co-glycolic acid) (PLGA) scaffolds (King et al., 2004). These networks contained inlet and outlet ports enabling perfusion. When the poly(glycerol sebacate) devices were seeded with ECs and perfused at physiological flow rates complete endothelialization was accomplished after 14 days and remained stable for 4 weeks in culture. This technique can be used to produce complex, high-resolution 2D patterns. However, their application is limited to patterning 2D with extension to 3D resulting from multilayer replication of the 2D patterns (Borenstein et al., 2007). Melt micromolding with thermal fusion bonding has been shown to enable fusion of patterned PLGA layers generated using the silicon molds (King et al., 2004).

Three-dimensional printing technologies have been used to create a vascularized “mini-liver” *in vitro* (Griffith et al., 1997). Using this approach 200- μm channels were created within biodegradable polymer scaffolds of poly(L-lactic acid) and PLGA. ECs attached and filled the channels after 5 weeks in static culture. When seeding mixed populations of hepatocytes and ECs into these scaffolds, the cells reorganized into structures that appeared similar to sinusoids. This approach provides an interesting example of generating 3D networks within a tissue parenchyma. Recently, this work has been combined with advanced bioreactor technologies to perfuse the tissue units with cell culture media (Domansky et al., 2010). Although complex 3D models of small vascularized tissues were created, research has not been performed to show how these vessels would interact with host tissue following implantation.

Micromolding has been used to generate channels within collagen gels by patterning a material that can be selectively degraded away from the bulk material (Chrobak et al., 2006). When lined with a monolayer of ECs, the channels served as functional, perfusable microvascular tubes with diameters between 75 and 150 μm after maturation and lengths spanning the entire collagen gel (5–7 mm), have been generated. These capillaries exhibited barrier function and resistance to leukocyte adhesion similar to capillaries *in vivo*. This technique of molding selectively degradable, or “sacrificial,” regions within materials has been used to generate channels with complex 3D geometries (Golden and Tien, 2007), but it is not clear how these complex geometries could be seeded with ECs.

Other approaches for creating microvascular patterns within scaffolds with high resolution have focused on laser-based patterning. Laser-guided direct writing was used to deposit multiple cells on various surfaces including biological gels with micron accuracy (Nahmias et al., 2005). This approach was used to pattern ECs on multilayers of Matrigel (a mouse tumor extract consisting of BM proteins) to generate 3D structures. The ECs elongated and formed tube-like structures along the patterns in a self-assembly process. Laser printing has also been used to directly deposit patterns of ECs onto Matrigel (Chen et al., 2006). Again, these initially unconnected EC patterns assembled into interconnected patterns.

Photopolymerizable polymers, such as many PEG-based hydrogels, can be easily patterned using non-contact photolithography. Interfacial photopolymerization of PEG has been shown to allow production of microvascular patterns within multilayered PEG hydrogels with feature sizes between 50 and 70 μm using simple photomasks (Papavasiliou et al., 2008). When using interfacial photopolymerization, the thickness of each layer can be controlled by polymerization conditions without the need of spacers or molds. This approach could be exploited to allow formation of 3D multilayered structures with distinct pattern formation in each layer. Microchannels have also been created within PEG hydrogels by patterning degradable polymers (Chiu et al., 2009a). The patterned region can be selectively degraded away due to the greater susceptibility of the patterned material to hydrolysis than the bulk hydrogel, resulting in channel formation. Using this approach, multilayered interconnected channels were fabricated through hydrolytic degradation of the patterned regions within distinct layers. The channels can be functionalized with cell adhesion sequences to support EC growth to form capillary-like channels (Chiu et al., 2011).

Patterning technologies are far from clinical application, but have been shown to allow precise control over the generation of vascular-like structures and microchannels within polymer scaffolds commonly used in tissue engineering. The majority of the research has used these structures as model networks for the study of vessel assembly or microfluidics. Questions remain as to how well these structures will function on the inevitable remodeling encountered following implantation. In addition, cell-sourcing issues described in the previous section are not avoided with these techniques.

62.3.2 Inducing Vascularization upon Implantation

Another approach relies on stimulating and guiding the body to provide the vasculature. Stimuli are delivered from the polymer scaffold to accelerate the invasion and organization of vessels. Prevascularized tissues may also benefit from such approaches as preformed vessel networks would still require that the host vasculature invades the scaffold and inosculates with the scaffold network. Strategies of inducing vascularization on implantation may prove to be more practical than creating a network within each construct prior to implantation. Although this approach is likely to prolong the time required for perfusion of the entire construct *in vivo*, it will likely reduce the *in vitro* construction phase.

62.3.2.1 Growth Factors

The process of neovascularization is an intricate temporal and spatial orchestration of many growth factors. Understanding their involvement in the processes of vessel formation, maturation, regression, and remodeling is crucial to designing optimized therapeutic strategies for inducing blood vessel growth. Several growth factors including, but not limited to, FGF-1, FGF-2, VEGF, and PDGF have demonstrated the ability to stimulate vessel formation in both clinical and basic research (Udelson et al., 2000, Hendel et al., 2000, Benjamin et al., 1998, Lokmic and Mitchell, 2008, Schumacher et al., 1998, Nikol et al., 2008). Methods currently used in clinical trials in which angiogenic proteins are under investigation as a treatment of ischemic tissues, primarily use large bolus injections which are not optimally effective. The short half lives of proteins *in vivo* mean these methods must rely on high levels of injected proteins which may lead to abnormal vasculature and severe side effects (Gu et al., 2004, August et al., 2006).

The success of growth factor-based strategies depends significantly on the method and timing of delivery. Several studies have indicated that a timeframe may exist for which these growth factors have an optimal effect (Cao and Mooney, 2007). The untimely removal of VEGF from a vascularizing tissue, prior to the formation of a mural cell coat, caused EC detachment from the vessel wall and vessel regression (Benjamin and Keshet, 1997). Administering PDGF-BB can disrupt EC-mural cell interactions but only when administered to immature vessels (Benjamin et al., 1998). These results indicate that the timing of both growth factor addition and removal may be critical to success.

In addition to timing, growth factor dose is important for stimulating the proper response. VEGF administered at high dosages can lead to vessels with chaotic structure and hyperpermeability (Ozawa et al., 2004). Continuous low levels of FGF-1 have been shown to promote vessel growth and, more

importantly, stabilize and prevent regression of vessels, a problem that may occur when delivering high concentrations of FGF-1 (Uriel et al., 2006). These studies suggest that low levels are optimal, but the actual dosage for each protein is likely to depend on the site of implantation, the presence of other angiogenic molecules, and the method of delivery (Lokmic and Mitchell, 2008).

One approach for overcoming the transient nature of proteins is to use gene therapies to prolong the duration of increased growth factor levels. Naked FGF-1 plasmid has been explored as a treatment for patients with critical limb ischemia and gave favorable results with regard to limb salvage (Nikol et al., 2008). Similarly, local intramuscular injection of naked VEGF plasmid in an animal limb ischemia model was demonstrated to increase tissue perfusion (Tsurumi et al., 1996). Incorporation of genes into polymer scaffolds can further prolong the effect, reducing the need for repeated application. Plasmid DNA encoding for VEGF delivered from PLGA scaffolds implanted subcutaneously into mice was found to be more effective at increasing blood vessel density than empty scaffolds (Jang et al., 2005). Hypoxia-inducible factor-1 α , a factor that indirectly stimulates angiogenesis by inducing the expression of VEGF, has been delivered *in vivo* by entrapment of peptide–DNA nanoparticles in a fibrin matrix (Trentin et al., 2006). This approach proved to be more efficient at stimulating angiogenesis than VEGF delivered in fibrin. Furthermore, the gene transfer of hypoxia-inducible factor- α increased the number of mature vessels formed.

Proteins have also been incorporated directly into polymer scaffolds to stimulate neovascularization. Growth factors have been added to both natural and synthetic polymers to generate vascularized tissues. As with other tissue engineering applications, poly(l-lactic acid), PLGA, and PEG have received significant attention (Takahiro et al., 2000). A variety of polymer properties (cross-linking, molecular weight, hydrophobicity, charge, etc.) can be modified to influence release kinetics (Pitt, 1990, Amsden and Turner, 1999). However, sometimes the fabrication process can interfere with the functionality of the proteins (Zisch et al., 2003). Natural polymers for delivery include alginate (Moya et al., 2009b, 2010), fibrin, collagen, chitosan, and gelatin (Young et al., 2005). Some ECM-based materials, such as fibrin, have both a natural ability to stimulate neovascularization and demonstrated success in delivering active biological molecules (Fasol et al., 1994, Pandit et al., 1998, 2000). To allow for better control of delivery of protein from fibrin matrices some researchers have focused on improving the retention of proteins through heparin adsorption (Pike et al., 2006, Sakiyama-Elbert and Hubbell, 2000) or covalent incorporation (Zisch et al., 2001). Proteins are typically incorporated in a form in which they readily diffuse from the scaffolds stimulating local vessels to sprout toward the implanted material. This leads to similar issues of transience seen in direct injection methods. When VEGF is covalently attached to the scaffolds its release is delayed, prolonging its biological function and reducing the risk of ectopic effects (Zisch et al., 2001). Scaffold-anchored VEGF has been shown to have improved activity and promote more extensive neovascularization relative to freely diffusing VEGF (Ehrbar et al., 2005). Covalent attachment to PEG-based hydrogels has shown similar improvements in vascularization (Seliktar et al., 2004). Collagen, which is normally not a very effective delivery conduit, modified with heparan sulfate demonstrates an ability to deliver FGF-2 and promote stable vascularization *in vivo* (Pieper et al., 2002). By attaching the protein of interest to a degradable scaffold the protein is prevented from being rapidly cleared from the body and local release can be controlled based on material degradation and tissue invasion.

Covalent attachment to the scaffold is not the only method for improving results. Sustained levels of proteins can also be attained by delivery from polymer microparticles. Delivery of FGF-1 from alginate microbeads results in both an increase in initial vessel invasion and a greater persistence of the vascularization in collagen scaffolds than a single-dose suspended within the material (Moya et al., 2009a,b, 2010) (Figure 62.4). In addition, by delivering FGF-1 from alginate the dose required to achieve vascularization is lower than what is required when the protein is suspended in the scaffold (Uriel et al., 2006, Moya et al., 2010). The FGF-1 studies described here and the VEGF studies in the previous section indicate that by control of growth factor transport in a polymer scaffold, a single growth factor can have a dramatic effect on neovascularization.

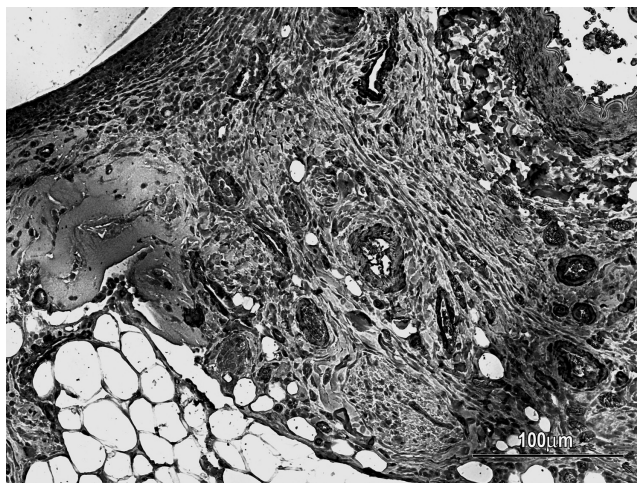


FIGURE 62.4 Immunohistochemical stain showing vessels formed in response to the sustained delivery of FGF-1. The brown stain indicates the presence of smooth muscle alpha actin-positive mural cells coating the vessels after 3 weeks of stimulation.

Although a single protein has been shown to enhance neovascularization when delivered appropriately, one growth factor may not be sufficient for the task of generating a stable, mature microvascular network in a large engineered tissue. Dual protein strategies have been developed to investigate whether temporally controlled delivery of two growth factors can further improve the response (Richardson et al., 2001, Peirce et al., 2004, Mandal and Kundu, 2009). Most research has focused on the sequential delivery of a protein that stimulates vessel sprouting and invasion followed by a factor involved in the recruitment of mural cells. Under some conditions vessels formed in response to VEGF alone may regress, but this regression can be inhibited by following VEGF delivery with angiopoietin-1 (Ang-1) (Peirce et al., 2004). Rapid release of VEGF followed by PDGF-BB leads to larger vessels and greater mural cell interactions in polymer scaffolds (Richardson et al., 2001). The combination of PDGF-BB with FGF-2 can increase arteriogenesis in models of tissue ischemia (Cao et al., 2003). Dual growth factor delivery approaches can also be combined with a cell-based strategy to improve results (Jay et al., 2010). Alginate microbeads containing VEGF and monocyte chemoattractant protein-1 (MCP-1) dispersed in a collagen/fibronectin scaffold along with human umbilical vein ECs were found to be an improvement over ECs alone. The addition of MCP-1 was incorporated due to its documented arteriogenic properties. However, MCP improved functional vessel formation as well as increased the number of SMC-coated vessels. This research shows that controlled delivery of multiple growth factors may enhance neovascularization over a single factor. However, the delivery methods still need to be optimized. In addition, it is not clear how many growth factors need to be delivered or which combinations should be used. Polymer systems that deliver multiple proteins with different release kinetics present a significant optimization challenge.

62.3.2.2 Cells

In Section 62.3.1, strategies for assembling networks of ECs in polymer scaffolds before implantation were described. However, the distribution of ECs throughout the scaffold without any particular structure can also accelerate vessel assembly. Cell-based strategies have been investigated clinically for the treatment of ischemic tissues (Amrani and Port, 2003). In both research and clinical trials, these cells have exhibited regenerative potential, but it is not clear how much this potential comes from the transplanted cells forming networks or if paracrine signals from the cells accelerate host neovascularization.

Stem cells are especially attractive for vascularization strategies because of their regenerative properties, expandability and potential to differentiate into multiple cell types. In one study, both

endothelial-like and smooth muscle-like vascular progenitor cells were differentiated from human embryonic bodies by exposure to PDGF or VEGF (Ferreira et al., 2007). When these cells were implanted in nude mice using Matrigel as a scaffold, microvessels formed and appeared to anastomose with the host vasculature. Similarly, ECs derived from human embryonic stem cells transplanted with a mouse mesenchymal precursor cell line in a fibronectin–collagen gel contributed to functional blood vessels formed *in vivo* that integrated with the host circulatory system (Wang et al., 2007). Transplanted stem cells may be more effective at promoting angiogenesis than injection of genes for ANG-1 and VEGF (Shyu et al., 2006).

Success for forming vessel networks *in vivo* has also been demonstrated using EPCs from human peripheral blood (Fuchs et al., 2009) particularly to address ischemia (Kawamoto et al., 2001, Kalka et al., 2000). Another source of adult stem cells that has similar proliferative potential but requires less invasive harvesting methods are adipose-derived stem cells from adipose stroma. These cells have demonstrated promising preclinical potential by differentiating into ECs and contributing to neovascularization upon implantation for the treatment of ischemia (Cao et al., 2005b, Miranville et al., 2004).

To further improve on the use of stem cells for inducing vascularization, stem cells transfected to secrete factors have also been examined for their ability to stimulate vascularization *in vivo*. In some of these studies, transfecting stem cells with growth factor genes for VEGF (Yang et al., 2010, Geiger et al., 2007) or FGF-2 (Guo et al., 2006) showed marked improvement over control groups using non-gene-transfected stem cells. This approach is attractive because it not only exploits the regenerative properties of stem cells but produces growth factors for targeted local delivery of angiogenic proteins. In combination with other vascularization strategies transfected cells have also demonstrated success at increasing vessel density (Yu et al., 2009). This method of using gene therapy to get cells to secrete angiogenic factors has also been used with other cell types such as islets to improve engraftment by overexpressing angiogenic factors to stimulate revascularization upon implantation (Su et al., 2007, Cheng et al., 2005b). To address the issue of heterogeneous expression levels in transduced cells, some researchers are focusing on developing methods for selecting out cells expressing desired levels (Misteli et al., 2010). Although gene modification of cells is a promising solution to integrate growth factors and cell delivery, long-term studies are needed to examine the effect of these cells actively remaining and secreting factors after desired vessel formation.

62.3.3 Surgical Approaches

Whether using growth factors, cells, or combinations of the two to promote neovascularization, the approaches can be very successful at generating microvascular networks in small volume scaffolds. Clinical application for the treatment of large defects requires a more complex vessel hierarchy within larger scaffold volumes. Techniques developed in the surgical sciences can be used to improve vascularization on implantation.

Prefabrication approaches developed in the field of reconstructive microsurgery can be exploited to enhance neovascularization (Uriel et al., 2008, Cheng et al., 2005a, 2006, 2009, 2010, Brey et al., 2007, Moya et al., 2010). In these approaches, the scaffolds are implanted in a “donor” tissue location that would promote greater neovascularization than the defect location. After a period of prefabrication time, the vascularized tissue can then be transferred to a recipient site. In one embodiment, scaffolds are implanted around a vascular pedicle. The pedicle allows *de novo* vascularization of the scaffolds that provides an option for transfer to the recipient defect with or without microsurgical techniques. Using a rodent vascular pedicle model, the alginate FGF-1 delivery strategy described in Section 62.3.2.1 greater overall vascularization is achieved when the beads are implanted around a vascular pedicle (Moya et al., 2010) than other vascularized beds (Moya et al., 2009a,b). These vascularized scaffolds along with the pedicle may be transferred to the recipient site and connected to host vessels using microsurgical techniques. It may be difficult to translate the pedicle model to clinical application, but large volumes of vascularized

tissues can be created by implantation of materials around microsurgically created vessel loops (Hofer et al., 2003, Mian et al., 2000, 2001, Tanaka et al., 2003, Staudenmaier et al., 2004, Demirtas et al., 2010).

Implantation of a tissue engineering construct into a highly vascularized donor location can be used to guide fabrication of large volumes of vascularized tissues with complex 3D shape (Cheng et al., 2009). The application of prefabricated or prelaminated flap has been widely applied in clinical cases (Guo and Pribaz, 2009, Mathy and Pribaz, 2009, Pribaz and Fine, 2001). This approach has been successfully applied clinically where the prefabricated vascularized tissue was easily transferred to the recipient location (Cheng et al., 2006). The use of established surgical approaches to enhance vascularization in large volume scaffolds has received little attention for applications in tissue engineering. When combined with a novel growth factor and/or cell strategy, surgical techniques may help optimize the volumes of scaffolds vascularized.

62.4 Conclusions

In order for tissue engineering to approach its vast clinical potential, researchers must continue to develop new and innovative methods for controlling neovascularization. This issue has received significant attention in recent years, and the studies in this chapter describe some of the progress that has been made. However, the challenge of generating stable, extensive, microvascular networks in large volumes of tissues still remains. Research up to this point has primarily resulted in vascularization of small volume scaffolds, which do not approach the clinical volumes needed. The continued development of novel approaches that consider specifically the issue of vascularizing large, complex tissues will lead to new tissue engineering interventions.

References

- Abramsson, A., Berlin, O., Papayan, H., Paulin, D., Shani, M., and Betsholtz, C. 2002. Analysis of mural cell recruitment to tumor vessels. *Circulation*, 105, 112–7.
- Amrani, D. L. and Port, S. 2003. Cardiovascular disease: Potential impact of stem cell therapy. *Expert Rev Cardiovasc Ther*, 1, 453–61.
- Amsden, B. and Turner, N. 1999. Diffusion characteristics of calcium alginate gels. *Biotechnol Bioeng*, 65, 605–10.
- Anghelina, M., Krishnan, P., Moldovan, L., and Moldovan, N. I. 2004. Monocytes and macrophages form branched cell columns in matrigel: Implications for a role in neovascularization. *Stem Cells Dev*, 13, 665–76.
- Anghelina, M., Krishnan, P., Moldovan, L., and Moldovan, N. I. 2006. Monocytes/macrophages cooperate with progenitor cells during neovascularization and tissue repair: Conversion of cell columns into fibrovascular bundles. *Am J Pathol*, 168, 529–41.
- Aplin, A. C., Fogel, E., and Nicosia, R. F. 2009. Ang-1 and MCP-1 cooperate in pericyte recruitment during angiogenesis. *FASEB J*, 23, 116.6.
- August, A. D., Kong, H. J., and Mooney, D. J. 2006. Alginate hydrogels as biomaterials. *Macromol Biosci*, 6, 623–33.
- Benjamin, L. E. and Keshet, E. 1997. Conditional switching of vascular endothelial growth factor (VEGF) expression in tumors: Induction of endothelial cell shedding and regression of hemangioblastoma-like vessels by VEGF withdrawal. *Proc Natl Acad Sci USA*, 94, 8761–6.
- Benjamin, L. E., Hemo, I., and Keshet, E. 1998. A plasticity window for blood vessel remodelling is defined by pericyte coverage of the preformed endothelial network and is regulated by PDGF-B and VEGF. *Development*, 125, 1591–8.
- Black, A. F., Berthod, F., L'heureux, N., Germain, L., and Auger, F. A. 1998. *In vitro* reconstruction of a human capillary-like network in a tissue-engineered skin equivalent. *FASEB J*, 12, 1331–40.

- Borenstein, J. T., Weinberg, E. J., Orrick, B. K., Sundback, C., Kaazempur-Mofrad, M. R., and Vacanti, J. P. 2007. Microfabrication of three-dimensional engineered scaffolds. *Tissue Eng*, 13, 1837–44.
- Brey, E. M., Cheng, M. H., Allori, A., Satterfield, W., Chang, D. W., Patrick, C. W., Jr., and Miller, M. J. 2007. Comparison of guided bone formation from periosteum and muscle fascia. *Plast Reconstr Surg*, 119, 1216–22.
- Brey, E. M., Mcintire, L. V., Johnston, C. M., Reece, G. P., and Patrick, C. W., Jr. 2004. Three-dimensional, quantitative analysis of desmin and smooth muscle alpha actin expression during angiogenesis. *Ann Biomed Eng*, 32, 1100–7.
- Brey, E. M., Uriel, S., Greisler, H. P., and Mcintire, L. V. 2005. Therapeutic neovascularization: Contributions from bioengineering. *Tissue Eng*, 11, 567–84.
- Cao, L. and Mooney, D. J. 2007. Spatiotemporal control over growth factor signaling for therapeutic neovascularization. *Adv Drug Deliv Rev*, 59, 1340–50.
- Cao, R., Brakenhielm, E., Pawliuk, R., Wariaro, D., Post, M. J., Wahlberg, E., Leboulch, P., and Cao, Y. 2003. Angiogenic synergism, vascular stability and improvement of hind-limb ischemia by a combination of PDGF-BB and FGF-2. *Nat Med*, 9, 604–13.
- Cao, Y., Hong, A., Schulten, H., and Post, M. J. 2005a. Update on therapeutic neovascularization. *Cardiovasc Res*, 65, 639–48.
- Cao, Y., Sun, Z., Liao, L., Meng, Y., Han, Q., and Zhao, R. C. 2005b. Human adipose tissue-derived stem cells differentiate into endothelial cells *in vitro* and improve postnatal neovascularization *in vivo*. *Biochem Biophys Res Commun*, 332, 370–9.
- Carmeliet, P. 2000. Mechanisms of angiogenesis and arteriogenesis. *Nat Med*, 6, 389–95.
- Carmeliet, P. 2003. Angiogenesis in health and disease. *Nat Med*, 9, 653–60.
- Carmeliet, P. and Jain, R. K. 2000. Angiogenesis in cancer and other disease. *Nature*, 407, 249.
- Caspi, O., Lesman, A., Basevitch, Y., Gepstein, A., Arbel, G., Habib, I. H. M., Gepstein, L., and Levenberg, S. 2007. Tissue engineering of vascularized cardiac muscle from human embryonic stem cells. *Circ Res*, 100, 263–72.
- Chen, C. S., Mrksich, M., Huang, S., Whitesides, G. M., and Ingber, D. E. 1998. Micropatterned surfaces for control of cell shape, position, and function. *Biotechnol Prog*, 14, 356–63.
- Chen, C. Y., Barron, J. A., and Ringeisen, B. R. 2006. Cell patterning without chemical surface modification: Cell-cell interactions between printed bovine aortic endothelial cells (BAEC) on a homogeneous cell-adherent hydrogel. *Appl Surf Sci*, 252, 8641–5.
- Chen, X., Aledia, A. S., Ghajar, C. M., Griffith, C. K., Putnam, A. J., Hughes, C. C., and George, S. C. 2009. Prevascularization of a fibrin-based tissue construct accelerates the formation of functional anastomosis with host vasculature. *Tissue Eng A*, 15, 1363–71.
- Chen, X., Aledia, A. S., Popson, S. A., Him, L. K., Hughes, C. C., and George, S. 2010. Rapid anastomosis of endothelial precursor cell-derived vessels with host vasculature is promoted by a high density of co-transplanted fibroblasts. *Tissue Eng*, 16(2), 585–94.
- Cheng, M. H., Brey, E. M., Allori, A., Satterfield, W. C., Chang, D. W., Patrick, C. W., Jr., and Miller, M. J. 2005a. Ovine model for engineering bone segments. *Tissue Eng*, 11, 214–25.
- Cheng, M. H., Brey, E. M., Allori, A. C., Gassman, A., Chang, D. W., Patrick, C. W., Jr., and Miller, M. J. 2009. Periosteum-guided prefabrication of vascularized bone of clinical shape and volume. *Plast Reconstr Surg*, 124, 787–95.
- Cheng, M. H., Brey, E. M., Ulusal, B. G., and Wei, F. C. 2006. Mandible augmentation for osseointegrated implants using tissue engineering strategies. *Plast Reconstr Surg*, 118, 1e–4e.
- Cheng, M. H., Uriel, S., Moya, M. L., Francis-Sedlak, M., Wang, R., Huang, J. J., Chang, S. Y., and Brey, E. M. 2010. Dermis-derived hydrogels support adipogenesis *in vivo*. *J Biomed Mater Res*, 92(3), 852–8.
- Cheng, Y., Zhang, J. L., Liu, Y. F., Li, T. M., and Zhao, N. 2005b. Islet transplantation for diabetic rats through the spleen. *Hepatobiliary Pancreat Dis Int*, 4, 203–6.
- Chiu, Y. C., Cheng, M. H., Uriel, S., and Brey, E. M. 2011. Materials for engineering vascularized adipose tissue. *J Tissue Viability*, 20(2), 37–48.

- Chiu, Y.-C., Larson, J. C., Perez-Luna, V. H., and Brey, E. M. 2009. Formation of microchannels in poly(ethylene glycol) hydrogels by selective degradation of patterned microstructures. *Chem Mater*, 21, 1677–82.
- Chrobak, K. M., Potter, D. R., and Tien, J. 2006. Formation of perfused, functional microvascular tubes in vitro. *Microvasc Res*, 71, 185–96.
- Darland, D. C. and D'Amore, P. A. 1999. Blood vessel maturation: Vascular development comes of age. *J Clin Invest*, 103, 157–8.
- Demirtas, Y., Engin, M. S., Aslan, O., Ayas, B., and Karacalar, A. 2010. The effect of “minimally invasive transfer of angiosomes” on vascularization of prefabricated/prelaminated tissues. *Ann Plast Surg*, 64, 491–5 10.1097/SAP.0b013e31819b6c6e.
- Dike, L., Chen, C., Mrksich, M., Tien, J., Whitesides, G., and Ingber, D. 1999. Geometric control of switching between growth, apoptosis, and differentiation during angiogenesis using micropatterned substrates. *In Vitro Cell Dev Biol Anim*, 35, 441–8.
- Domansky, K., Inman, W., Serdy, J., Dash, A., Lim, M. H., and Griffith, L. G. 2010. Perfused multiwell plate for 3D liver tissue engineering. *Lab Chip*, 10, 51–8.
- Ehrbar, M., Metters, A., Zammaretti, P., Hubbell, J. A., and Zisch, A. H. 2005. Endothelial cell proliferation and progenitor maturation by fibrin-bound VEGF variants with differential susceptibilities to local cellular activity. *J Control Release*, 101, 93–109.
- Fasol, R., Schumacher, B., Schlaudraff, K., Hauenstein, K.-H., and Seitelberger, R. 1994. Experimental use of a modified fibrin glue to induce site-directed angiogenesis from the aorta to the heart. *J Thorac Cardiovasc Surg*, 107, 1432–9.
- Ferreira, L. S., Gerecht, S., Shieh, H. F., Watson, N., Rupnick, M. A., Dallabrida, S. M., Vunjak-Novakovic, G., and Langer, R. 2007. Vascular progenitor cells isolated from human embryonic stem cells give rise to endothelial and smooth muscle like cells and form vascular networks in vivo. *Circ Res*, 101, 286–94.
- Fidkowski, C., Kaazempur-Mofrad, M. R., Borenstein, J., Vacanti, J. P., Langer, R., and Wang, Y. 2005. Endothelialized microvasculature based on a biodegradable elastomer. *Tissue Eng*, 11, 302–9.
- Folkman, J. and Haudenschild, C. 1980. Angiogenesis in vitro. *Nature*, 288, 551–6.
- Francis, M. E., Uriel, S., and Brey, E. M. 2008. Endothelial cell-matrix interactions in neovascularization. *Tissue Eng B Rev*, 14, 19–32.
- Francis-Sedlak, M. E., Moya, M. L., Huang, J.-J., Lucas, S. A., Chandrasekharan, N., Larson, J. C., Cheng, M.-H., and Brey, E. M. 2010. Collagen glycation alters neovascularization *in vitro* and *in vivo*. *Microvasc Res*, 80, 3–9.
- Fuchs, S., Ghanaati, S., Orth, C., Barbeck, M., Kolbe, M., Hofmann, A., Eblenkamp, M., Gomes, M., Reis, R. L., and Kirkpatrick, C. J. 2009. Contribution of outgrowth endothelial cells from human peripheral blood on *in vivo* vascularization of bone tissue engineered constructs based on starch polycaprolactone scaffolds. *Biomaterials*, 30, 526–34.
- Gaengel, K., Genove, G., Armulik, A., and Betsholtz, C. 2009. Endothelial-mural cell signaling in vascular development and angiogenesis. *Arterioscler Thromb Vasc Biol*, 29, 630–38.
- Geiger, F., Lorenz, H., Xu, W., Szalay, K., Kasten, P., Claes, L., Augat, P., and Richter, W. 2007. VEGF producing bone marrow stromal cells (BMSC) enhance vascularization and resorption of a natural coral bone substitute. *Bone*, 41, 516–22.
- Gerhardt, H. and Betsholtz, C. 2003. Endothelial-pericyte interactions in angiogenesis. *Cell Tissue Res*, 314, 15–23.
- Gerhardt, H. et al 2003. VEGF guides angiogenic sprouting utilizing endothelial tip cell filopodia. *J Cell Biol*, 161, 1163–77.
- Gibot, L., Galbraith, T., Huot, J., and Auger, F. A. 2010. A Preexisting microvascular network Benefits *in vivo* Revascularization of a microvascularized tissue-engineered skin substitute. *Tissue Eng A*, 16(10), 3199–206.
- Golden, A. P. and Tien, J. 2007. Fabrication of microfluidic hydrogels using molded gelatin as a sacrificial element. *Lab Chip*, 7, 720–5.

- Griffith, L. G. and Naughton, G. 2002. Tissue engineering—current challenges and expanding opportunities. *Science*, 295, 1009–14.
- Griffith, L. G., Wu, B., Cima, M. J., Powers, M. J., Chaignaud, B., and Vacanti, J. P. 1997. *In vitro* organogenesis of liver tissue. *Ann N Y Acad Sci*, 831, 382–97.
- Gu, F., Amsden, B., and Neufeld, R. 2004. Sustained delivery of vascular endothelial growth factor with alginate beads. *J Control Release*, 96, 463–72.
- Guo, L. and Pribaz, J. J. 2009. Clinical flap prefabrication. *Plast Reconstr Surg*, 124, e340–50.
- Guo, X., Zheng, Q., Kulbatski, I., Yuan, Q., Yang, S., Shao, Z., Wang, H., Xiao, B., Pan, Z., and Tang, S. 2006. Bone regeneration with active angiogenesis by basic fibroblast growth factor gene transfected mesenchymal stem cells seeded on porous beta-TCP ceramic scaffolds. *Biomed Mater*, 1, 93–9.
- Hendel, R. C., Henry, T. D., Rocha-Singh, K., Isner, J. M., Kereiakes, D. J., Giordano, F. J., Simons, M., and Bonow, R. O. 2000. Effect of intracoronary recombinant human vascular endothelial growth factor on myocardial perfusion: Evidence for a dose-dependent effect. *Circulation*, 101, 118–21.
- Hofer, S. O., Knight, K. M., Cooper-White, J. J., O'Connor, A. J., Perera, J. M., Romeo-Meeuw, R., Penington, A. J., Knight, K. R., Morrison, W. A., and Messina, A. 2003. Increasing the volume of vascularized tissue formation in engineered constructs: An experimental study in rats. *Plast Reconstr Surg*, 111, 1186–92; discussion 1193–4.
- Hoffmann, J. et al. 2005. Endothelial survival factors and spatial completion, but not pericyte coverage of retinal capillaries determine vessel plasticity. *FASEB J*, 19, 2035–6.
- Jang, J. H., Rives, C. B., and Shea, L. D. 2005. Plasmid delivery *in vivo* from porous tissue-engineering scaffolds: Transgene expression and cellular transfection. *Mol Ther*, 12, 475–83.
- Jay, S. M., Shepherd, B. R., Andrejecs, J. W., Kyriakides, T. R., Pober, J. S., and Saltzman, W. M. 2010. Dual delivery of VEGF and MCP-1 to support endothelial cell transplantation for therapeutic vascularization. *Biomaterials*, 31, 3054–62.
- Kaihara, S., Borenstein, J., Koka, R., Lalan, S., Ochoa, E. R., Ravens, M., Pien, H., Cunningham, B., and Vacanti, J. P. 2000. Silicon micromachining to tissue engineer branched vascular channels for liver fabrication. *Tissue Eng*, 6, 105–17.
- Kalka, C., Masuda, H., Takahashi, T., Kalka-Moll, W. M., Silver, M., Kearney, M., Li, T., Isner, J. M., and Asahara, T. 2000. Transplantation of ex vivo expanded endothelial progenitor cells for therapeutic neovascularization. *Proc Natl Acad Sci USA*, 97, 3422–7.
- Kawamoto, A. et al. 2001. Therapeutic potential of ex vivo expanded endothelial progenitor cells for myocardial ischemia. *Circulation*, 103, 634–7.
- King, K., Wang, C., Kaazempur-Mofrad, M., Vacanti, J., and Borenstein, J. 2004. Biodegradable microfluidics. *Adv Mater*, 16, 2007–12.
- Koike, N., Fukumura, D., Gralla, O., Au, P., Schechner, J. S., and Jain, R. K. 2004. Tissue engineering: Creation of long-lasting blood vessels. *Nature*, 428, 138–9.
- Levenberg, S. et al. 2005. Engineering vascularized skeletal muscle tissue. *Nat Biotech*, 23, 879–84.
- Lokmic, Z. and Mitchell, G. M. 2008. Engineering the microcirculation. *Tissue Eng B Rev*, 14, 87–103.
- Mandal, B. B. and Kundu, S. C. 2009. Calcium alginate beads embedded in silk fibroin as 3D dual drug releasing scaffolds. *Biomaterials*, 30, 5170–7.
- Mathy, J. A. and Pribaz, J. J. 2009. Prefabrication and prelamination applications in current aesthetic facial reconstruction. *Clin Plast Surg*, 36, 493–505.
- Mian, R., Morrison, W. A., Hurley, J. V., Penington, A. J., Romeo, R., Tanaka, Y., and Knight, K. R. 2000. Formation of new tissue from an arteriovenous loop in the absence of added extracellular matrix. *Tissue Eng*, 6, 595–603.
- Mian, R. A., Knight, K. R., Penington, A. J., Hurley, J. V., Messina, A., Romeo, R., and Morrison, W. A. 2001. Stimulating effect of an arteriovenous shunt on the *in vivo* growth of isografted fibroblasts: A preliminary report. *Tissue Eng*, 7, 73–80.
- Miranville, A., Heeschen, C., Sengenès, C., Curat, C. A., Busse, R., and Bouloumie, A. 2004. Improvement of postnatal neovascularization by human adipose tissue-derived stem cells. *Circulation*, 110, 349–55.

- Misteli, H., Wolff, T., Fuglistaler, P., Gianni-Barrera, R., Gurke, L., Heberer, M., and Banfi, A. 2010. High-throughput flow cytometry purification of transduced progenitors expressing defined levels of vascular endothelial growth factor induces controlled angiogenesis in vivo. *Stem Cells*, 28, 611–9.
- Montesano, R., Orci, L., and Vassalli, P. 1983. *in vitro* rapid organization of endothelial cells into capillary-like networks is promoted by collagen matrices. *J Cell Biol*, 97, 1648–52.
- Montesano, R., Vassalli, J. D., Baird, A., Guillemin, R., and Orci, L. 1986. Basic fibroblast growth factor induces angiogenesis in vitro. *Proc Natl Acad Sci*, 83, 7297–301.
- Moon, J. J., Saik, J. E., Poche, R. A., Leslie-Barbick, J. E., Lee, S. H., Smith, A. A., Dickinson, M. E., and West, J. L. 2010. Biomimetic hydrogels with pro-angiogenic properties. *Biomaterials*, 31, 3840–7.
- Morrison, W. A. 2009. Progress in tissue engineering of soft tissue and organs. *Surgery*, 145, 127–30.
- Moya, M. L., Cheng, M. H., Huang, J. J., Francis-Sedlak, M. E., Kao, S. W., Opara, E. C., and Brey, E. M. 2010. The effect of FGF-1 loaded alginate microbeads on neovascularization and adipogenesis in a vascular pedicle model of adipose tissue engineering. *Biomaterials*, 31, 2816–26.
- Moya, M. L., Garfinkel, M. R., Liu, X., Lucas, S., Opara, E. C., Greisler, H. P., and Brey, E. M. 2009a. Fibroblast growth factor-1 (FGF-1) loaded microbeads enhance local capillary neovascularization. *J Surg Res*, 160, 208–12.
- Moya, M. L., Lucas, S., Francis-Sedlak, M., Liu, X., Garfinkel, M. R., Huang, J. J., Cheng, M. H., Opara, E. C., and Brey, E. M. 2009b. Sustained delivery of FGF-1 increases vascular density in comparison to bolus administration. *Microvasc Res*, 78, 142–7.
- Nahmias, Y., Schwartz, R. E., Verfaillie, C. M., and Odde, D. J. 2005. Laser-guided direct writing for three-dimensional tissue engineering. *Biotechnol Bioeng*, 92, 129–36.
- Nikol, S. et al. 2008. Therapeutic angiogenesis with intramuscular NV1FGF improves amputation-free survival in patients with critical limb ischemia. *Mol Ther*, 16, 972–8.
- Nomi, M., Atala, A., Coppi, P. D., and Soker, S. 2002. Principals of neovascularization for tissue engineering. *Mol Aspects Med*, 23, 463–83.
- Ozawa, C. R., Banfi, A., Glazer, N. L., Thurston, G., Springer, M. L., Kraft, P. E., Mcdonald, D. M., and Blau, H. M. 2004. Microenvironmental VEGF concentration, not total dose, determines a threshold between normal and aberrant angiogenesis. *J Clin Invest*, 113, 516–27.
- Ozderdem, U. and Stallcup, W. B. 2003. Early contribution of pericytes to angiogenic sprouting and tube formation. *Angiogenesis*, 6, 241–9.
- Pandit, A., Ashar, R., Feldman, D., and Thompson, A. 1998. Investigation of acidic fibroblast growth factor delivered through a collagen scaffold for the treatment of full-thickness skin defects in a rabbit model. *Plast Reconstr Surg*, 101, 766–75.
- Pandit, A. S., Wilson, D. J., and Feldman, D. S. 2000. Fibrin scaffold as an effective vehicle for the delivery of acidic fibroblast growth factor (FGF-1). *J Biomater Appl*, 14, 229–42.
- Papavasiliou, G., Songprawat, P., Perez-Luna, V., Hammes, E., Morris, M., Chiu, Y. C., and Brey, E. 2008. Three-dimensional patterning of poly (ethylene Glycol) hydrogels through surface-initiated photopolymerization. *Tissue Eng C Methods*, 14, 129–40.
- Peirce, S. M., Price, R. J., and Skalak, T. C. 2004. Spatial and temporal control of angiogenesis and arterIALIZATION using focal applications of VEGF164 and Ang-1. *Am J Physiol Heart Circ Physiol*, 286, H918–25.
- Pieper, J. S., Hafmans, T., Van Wachem, P. B., Van Luyn, M. J., Brouwer, L. A., Veerkamp, J. H., and Van Kuppevelt, T. H. 2002. Loading of collagen-heparan sulfate matrices with bFGF promotes angiogenesis and tissue generation in rats. *J Biomed Mater Res*, 62, 185–94.
- Pike, D. B., Cai, S., Pomraning, K. R., Firpo, M. A., Fisher, R. J., Shu, X. Z., Prestwich, G. D., and Peattie, R. A. 2006. Heparin-regulated release of growth factors *in vitro* and angiogenic response *in vivo* to implanted hyaluronan hydrogels containing VEGF and bFGF. *Biomaterials*, 27, 5242–51.
- Pitt, C. G. 1990. The controlled parenteral delivery of polypeptides and proteins. *Int J Pharm*, 59, 173–96.
- Pribaz, J. J. and Fine, N. A. 2001. Prefabricated and prelaminated flaps for head and neck reconstruction. *Clin Plast Surg*, 28, 261–72, vii.

- Richardson, T. P., Peters, M. C., Ennett, A. B., and Mooney, D. J. 2001. Polymeric system for dual growth factor delivery. *Nat Biotechnol*, 19, 1029–34.
- Sakiyama-Elbert, S. E., and Hubbell, J. A. 2000. Development of fibrin derivatives for controlled release of heparin-binding growth factors. *J Control Release*, 65, 389–402.
- Scholz, D., Ziegelhoeffer, T., Helisch, A., Wagner, S., Friedrich, C., Podzuweit, T., and Schaper, W. 2002. Contribution of arteriogenesis and angiogenesis to postocclusive hindlimb perfusion in mice. *J Mol Cell Cardiol*, 34, 775–87.
- Schumacher, B., Pecher, P., Von Specht, B. U., and Stegmann, T. 1998. Induction of neovascularization in ischemic myocardium by human growth factors: First clinical results of a new treatment of coronary heart disease. *Circulation*, 97, 645–50.
- Seliktar, D., Zisch, A. H., Lutolf, M. P., Wrana, J. L., and Hubbell, J. A. 2004. MMP-2 sensitive, VEGF-bearing bioactive hydrogels for promotion of vascular healing. *J Biomed Mater Res A*, 68, 704–16.
- Shyu, K. G., Wang, B. W., Hung, H. F., Chang, C. C., and Shih, D. T. 2006. Mesenchymal stem cells are superior to angiogenic growth factor genes for improving myocardial performance in the mouse model of acute myocardial infarction. *J Biomed Sci*, 13, 47–58.
- Skalak, T. C., Little, C. D., Mcintire, L. V., Hirschi, K. K., Tranquillo, R. T., Post, M., and Ranieri, J. 2002. Vascular assembly in engineered and natural tissues. *Ann NY Acad Sci*, 961, 255–7.
- Staudenmaier, R., Hoang, T. N., Kleinsasser, N., Schurr, C., Frolich, K., Wenzel, M. M., and Aigner, J. 2004. Flap prefabrication and prelamination with tissue-engineered cartilage. *J Reconstr Microsurg*, 20, 555–64.
- Su, D., Zhang, N., He, J., Qu, S., Slusher, S., Bottino, R., Bertera, S., Bromberg, J., and Dong, H. H. 2007. Angiopoietin-1 production in islets improves islet engraftment and protects islets from cytokine-induced apoptosis. *Diabetes*, 56, 2274–83.
- Sunderkotter, C., Steinbrink, K., Goebeler, M., Bhardwaj, R., and Sorg, C. 1994. Macrophages and angiogenesis. *J Leukoc Biol*, 55, 410–22.
- Takahiro, M., Yumi, S., Yuji, H., Takehiko, S., and Yoshino, H. 2000. Protein encapsulation into biodegradable microspheres by a novel S/O/W emulsion method using poly(ethylene glycol) as a protein micronization adjuvant. *J Control Release*, 69, 435–44.
- Tanaka, Y., Sung, K. C., Tsutsumi, A., Ohba, S., Ueda, K., and Morrison, W. A. 2003. Tissue engineering skin flaps: Which vascular carrier, arteriovenous shunt loop or arteriovenous bundle, has more potential for angiogenesis and tissue generation? *Plast Reconstr Surg*, 112, 1636–44.
- Trentin, D., Hall, H., Wechsler, S., and Hubbell, J. A. 2006. Peptide-matrix-mediated gene transfer of an oxygen-insensitive hypoxia-inducible factor-1 α variant for local induction of angiogenesis. *Proc Natl Acad Sci USA*, 103, 2506–11.
- Tsurumi, Y., Takeshita, S., Chen, D., Kearney, M., Rossow, S. T., Passeri, J., Horowitz, J. R., Symes, J. F., and Isner, J. M. 1996. Direct intramuscular gene transfer of naked DNA encoding vascular endothelial growth factor augments collateral development and tissue perfusion. *Circulation*, 94, 3281–90.
- Udelson, J. E., Dilsizian, V., Laham, R. J., Chronos, N., Vansant, J., Blais, M., Galt, J. R., Pike, M., Yoshizawa, C., and Simons, M. 2000. Therapeutic angiogenesis with recombinant fibroblast growth factor-2 improves stress and rest myocardial perfusion abnormalities in patients with severe symptomatic chronic coronary artery disease. *Circulation*, 102, 1605–10.
- Unger, R. E., Ghanaati, S., Orth, C., Sartoris, A., Barbeck, M., Halstenberg, S., Motta, A., Migliaresi, C., and Kirkpatrick, C. J. 2010. The rapid anastomosis between prevascularized networks on silk fibroin scaffolds generated *in vitro* with cocultures of human microvascular endothelial and osteoblast cells and the host vasculature. *Biomaterials*, 31, 6959–67.
- Uriel, S., Brey, E. M., and Greisler, H. P. 2006. Sustained low levels of fibroblast growth factor-1 promote persistent microvascular network formation. *Am J Surg*, 192, 604–9.
- Uriel, S., Huang, J. J., Moya, M. L., Francis, M. E., Wang, R., Chang, S. Y., Cheng, M. H., and Brey, E. M. 2008. The role of adipose protein derived hydrogels in adipogenesis. *Biomaterials*, 29, 3712–9.

- Van Weel, V., Van Tongeren, R. B., Van Hinsbergh, V. W., Van Bockel, J. H., and Quax, P. H. 2008. Vascular growth in ischemic limbs: A review of mechanisms and possible therapeutic stimulation. *Ann Vasc Surg*, 22, 582–97.
- Wang, Z. Z., Au, P., Chen, T., Shao, Y., Daheron, L. M., Bai, H., Arzigian, M., Fukumura, D., Jain, R. K., and Scadden, D. T. 2007. Endothelial cells derived from human embryonic stem cells form durable blood vessels in vivo. *Nat Biotech*, 25, 317–8.
- Yamaguchi, J. et al. 2003. Stromal cell-derived factor-1 effects on ex vivo expanded endothelial progenitor cell recruitment for ischemic neovascularization. *Circulation*, 107, 1322–8.
- Yana, I. et al. 2007. Crosstalk between neovessels and mural cells directs the site-specific expression of MT1-MMP to endothelial tip cells. *J Cell Sci*, 120, 1607–14.
- Yang, F. et al. 2010. Genetic engineering of human stem cells for enhanced angiogenesis using biodegradable polymeric nanoparticles. *Proc Natl Acad Sci USA*, 107, 3317–22.
- Young, S., Wong, M., Tabata, Y., and Mikos, A. G. 2005. Gelatin as a delivery vehicle for the controlled release of bioactive molecules. *J Control Release*, 109, 256–74.
- Yu, J. X., Huang, X. F., Lv, W. M., Ye, C. S., Peng, X. Z., Zhang, H., Xiao, L. B., and Wang, S. M. 2009. Combination of stromal-derived factor-1 α and vascular endothelial growth factor gene-modified endothelial progenitor cells is more effective for ischemic neovascularization. *J Vasc Surg*, 50, 608–16.
- Zisch, A. H., Lutolf, M. P., and Hubbell, J. A. 2003. Biopolymeric delivery matrices for angiogenic growth factors. *Cardiovasc Pathol*, 12, 295–310.
- Zisch, A. H., Schenk, U., Schense, J. C., Sakiyama-Elbert, S. E., and Hubbell, J. A. 2001. Covalently conjugated VEGF—fibrin matrices for endothelialization. *J Control Release*, 72, 101–13.

73

Vascular Tissue Engineering

73.1	Introduction	73-1
	Significance • Cardiovascular Disease	
73.2	Cell Source	73-2
	Differentiated Cells • Endothelial Progenitors • Smooth Muscle Progenitors • Mesenchymal Stem Cells • Pluripotent Stem Cells	
73.3	Scaffolds/Extracellular Matrix	73-5
	Synthetic Scaffolds • Natural Scaffolds • Cell Assembly • Matrix and Culture Effects	
73.4	Growth Factor Signaling	73-7
73.5	Vascular Grafts and Medial Equivalents	73-9
73.6	Engineered Vascular Networks	73-10
73.7	Conclusions.....	73-12
	References.....	73-12

Laura J. Suggs
University of Texas, Austin

73.1 Introduction

73.1.1 Significance

Cardiovascular disease is the number one cause of death in developed countries. Over 60 million Americans suffer from some type of vascular disorder [1], and disease associated with small to medium size vessels is the chief killer in the United States [2]. Over 500,000 coronary artery bypass graft (CABG) surgeries were performed in 2000 [1]. Current options for graft replacements are either autologous vessels or synthetic materials. Synthetic materials, despite being readily available and relatively inexpensive, are associated with thrombogenicity and neo-intima formation in low-flow and small-diameter vessels. Autologous vessels exhibit better patency; however, about 60% of CABG patients do not possess suitable healthy vessels to serve as a graft [3]. Vascular tissue engineering holds promise for the rescue and regeneration of tissue following ischemia, the development of small diameter blood vessel substitutes and the creation of mature blood vessel networks.

The paradigm of tissue engineering constitutes a scaffold upon which cells can adhere, proliferate, and express their differentiated function, the cells themselves and any signals, soluble or otherwise, which the cell requires. Our current understanding of the interplay between the cells and their supporting scaffold has demonstrated a reciprocal interaction where the scaffold can inform and control tissue organization and cell differentiation, and the cells are able to remodel tissue engineering matrices to better approximate natural tissue. A successful vascular tissue engineering strategy would result in a physiologically functional blood vessel or vessel network to adequately perfuse diseased or injured tissue. This strategy would necessarily be devised across various disciplines and rely on an understanding of engineering principles and the life sciences.

One approach that has been successful in tissue engineering is to enhance cell adhesion to matrices and scaffolds in order to encourage cell attachment and proliferation. This strategy becomes problematic in the presence of blood due to the ability of flowing blood to recognize foreign surfaces. Traditional, permanent cardiovascular devices have been designed to be inert to cell and platelet adhesion. As a result, many researchers have attempted to approximate the blood vessel lumen by lining constructs with a functional endothelium. The endothelium, a single layer of endothelial cells (ECs), serves as the primary regulatory for blood coagulation and transport from the blood space to the tissue space. Investigators have also looked to known angiogenic mechanisms to control EC migration, adhesion, and function in the context of forming microvascular networks. Collectively, much work has been focused on the control or seeding of terminally differentiated cells within scaffolds, however, a dramatic increase in the understanding of stem and vascular progenitor cells has driven the exploration of these cell sources for vascular tissue engineering. Furthermore, a greater understanding of how cells interact with both soluble and insoluble, or matrix, signals has resulted in novel combination strategies for regeneration of a number of vascular deficiencies.

73.1.2 Cardiovascular Disease

With the average age increasing, the prevalence of cardiovascular disease has continued to expand. The primary cause is atherosclerosis, a thickening of the lining of the arteries (the intima). It most commonly affects the arteries of the heart, brain, and lower limbs, and subsequent ischemia results in functional deficits and tissue damage. Antithrombotic therapy, bypass grafting and therapeutic angiogenesis are potential treatments for vascular disease. Atherosclerosis is thought to begin with some type of injury to the ECs that line blood vessels. This injury may be mechanical, such as repeated stress on the cells; or chemical, including exposure to molecules such as oxidized low-density lipoprotein (LDL). Stress on the cells that line the arterial wall may be caused by hypertension. Elevated levels of lipids and cholesterol can be due to diet, genetic disposition, or diseases such as diabetes. In response to this injury, ECs initiate the healing process. As part of healing, ECs secrete agents which recruit additional cell types. Macrophages locate themselves within the intima and accumulate lipids to form foam cells. These cells then organize to form fatty streaks which will eventually become a fibrous atherosclerotic plaque. As these lesions grow, they can become calcified which reduces distensibility and can result in thrombosis at the site of the plaque.

Ischemic heart disease is the single most common cause of death. Ischemic heart disease, or reduced blood flow to the heart, is primarily brought on by atherosclerosis in the coronary circulation. Some deaths occur suddenly as a result of acute closure on the coronary arteries while some occur because of a progressive weakening of the heart muscle. Acute coronary occlusion can be a result of thrombus formation in an atherosclerotic vessel. This thrombus can occlude the vessel resulting in a cessation of blood flow to the corresponding region of the heart. The area of muscle that has no flow and cannot function is said to be infarcted. A formed thrombus can break loose, or embolize, and occlude a downstream vessel, again resulting in myocardial infarction. Cardiac failure can also result from chronic damage. Congestive heart failure is a result of ischemic heart muscle which has reduced contractility. Back pressure, or congestion, builds up in either the pulmonary or systemic circulation depending on which side of the heart is affected. In order to compensate for this decreased output, the heart increases the volume of blood which is being pumped, and the heart muscle becomes enlarged.

73.2 Cell Source

73.2.1 Differentiated Cells

Seeding of EC populations onto synthetic device surfaces was an early tissue engineering approach to limit thrombosis. Isolation and culture of a significant population of ECs for seeding as well

as their retention on a synthetic surface under blood shear is problematic. Pioneering work by Jarrell et al. proposed the isolation of microvessel endothelium from human adipose tissue from a lipo-aspirate [4]. They were able to collect a large fraction of cells that exhibited phenotypic characteristics of ECs. Subsequent high-density seeding onto synthetic graft surfaces was possible, but early clinic work did not demonstrate the necessary improvements over unseeded grafts [5]. Subsequent work with the stromal vascular fraction from adipose tissue has revealed a heterogeneous population containing ECs as well as a multipotent cell of mesenchymal lineage among others [6].

73.2.2 Endothelial Progenitors

Following work by Asahara and colleagues, investigators have identified endothelial progenitor cells (EPCs) from peripheral blood, bone marrow mononuclear cells, and umbilical cord blood. This early work reported the role of EPCs in enhancing postnatal vasculogenesis in a model of hind limb ischemia [7]. Subsequent preclinical work has evaluated the potential of EPCs for enhancing recovery in cardiac injury. The isolation of this cell population begins with an enrichment of CD34+ cells, which is also a marker for hematopoietic stem cells (HSCs), followed by tissue culture plastic adherence selection. Differentiation has been promoted through culture with vascular endothelial growth factor (VEGF) [8–9]. These cells share a number of other markers with HSCs including: VEGFR2/flk-1 +, Tek (Tie-2), cKit, Sca-1, CD133, and CD34 [7]. No marker to date has been definitive for the EPC. Bone marrow-derived CD34+ cells have been used to seed grafts in dogs with enhanced endothelialization, but the role of these cells is unclear as no correlation was seen between the number of cells and the degree of endothelialization [10].

Populations of EPCs with colony forming ability, endothelial colony forming cells (ECFCs) have been isolated through an extended culture process called late outgrowth. This process is also based on culture adherence and colony formation at 7–21 days. Unlike early outgrowth EPCs, ECFCs have the ability to form tubes. Markers of mature ECs have been used to characterize these cells and include: von Willebrand Factor (vWF), platelet endothelial cell adhesion molecule-1 (PECAM-1/CD31) and vascular endothelial-cadherin (VE-Cad), and by uptake of Dil-acetylated LDL and binding of lectin. ECFCs have been shown to incorporate into newly formed vasculature in animal models of ischemia. While both EPCs and ECFCs have been shown to improve neovascularization, they may have different roles in enhancing this process.

EPCs may also have the ability to mobilize toward sites of ischemia and participate in vasculogenesis [11]. The stem cell homing factor, granulocyte macrophage-colony stimulating factor has been administered systemically and enhanced the numbers of EPCs circulating in peripheral blood as well as the degree of neovascularization in a model of ischemia [12]. VEGF has also been shown to enhance the mobilization of EPCs to peripheral blood either directly in mice or via plasmid or recombinant protein in humans. Other factors that have been proposed as agents to increase the number of circulating EPCs include: Ang-1, placenta-derived growth factor (PlGF), erythropoietin and 3-hydroxy-3-methylglutaryl coenzyme A. While it is likely that increasing the number of circulating EPCs may enhance neovascularization at sites of ischemia, enhancing engraftment at the site of injury or onto a synthetic surface may also be necessary. Clinical trials with circulating EPCs (e.g., the START trial) did not show efficacy in patients with lower limb ischemia [13]. A potential engraftment factor may be stromal cell-derived factor (SDF)-1 α . SDF-1 α is involved in stem cell homing to the bone marrow compartment during HSC transplantation. Our group has used a polymeric delivery system to enhance stem cell homing via SDF-1 α localization in a mouse model of myocardial infarction [14]. Enhancing stem cell homing in this model increased the measured functional recovery. Engraftment of EPCs onto synthetic grafts may also be enhanced via an antibody capture technique. The use of a CD34 antibody localized to graft surfaces has been evaluated in a preliminary trial, the HEALING trial [15].

73.2.3 Smooth Muscle Progenitors

Analogous to ECs, smooth muscle cells (SMCs) for tissue engineering have often been derived from mature tissues such as aorta in order to be evaluated in animal models. Acquiring a sufficient number of autologous cells may limit clinical translation to humans, however. In the use of SMCs and their progenitors for tissue engineered vascular graft (TEVG) fabrication; it has been proposed that early passage cells may have an enhanced ability to produce extracellular matrix components which could result in higher strengths and improved performance [16]. Smooth muscle progenitor cells have been reported to reside in peripheral blood, and express markers characteristic of mature SMCs following cytokine stimulation. SMC-positive markers include: α -smooth muscle actin, myosin heavy chain, and calponin. It is important to note, however, that markers of angioblasts (CD34, Flk-1, Flt-1) [17], were also seen, suggesting that they retained markers of their origin from blood. Mesenchymal stem cells (MSCs) from bone marrow, as discussed below can also exhibit SMC phenotype following stimulation with transforming growth factor (TGF)- β . Mechanical stimulation of MSCs has been shown to upregulate markers of SMCs. Specifically, uniaxial cyclic strain of 2D cultures demonstrated upregulation of smooth muscle α -actin, calponin, as well as a number of collagen isoforms including collagen I [18].

73.2.4 Mesenchymal Stem Cells

MSCs are a stem cell population that are present in bone marrow, adipose tissue, or peripheral blood and can differentiate readily into terminal cells of the mesenchyme. Recent evidence suggests that MSCs can express phenotypic characteristics of endothelial, neural, smooth muscle, skeletal myoblasts, and cardiomyocytes [19–21]. Isolated, autologous bone marrow stem cells have been shown to contribute to cardiac muscle repair and formation of new blood vessels following tissue ischemia, based on the localization of genetic markers [21–22]. Cells of perivascular origin have also been isolated that share markers of both mural cells and MSCs including (CD146, NG-2, and PDGF-R β) [23,24]. These cells exhibited multilineage potential toward cells of the mesenchyme. The relationship among MSCs and mural cells including both pericytes and SMCs is still poorly understood, and it remains to be seen what cell population will be most effective for reapproximating the medial layer of TEVGs.

Clinical studies have been performed using autologous MSCs to seed the pores of synthetic grafts in an extracardiac total cavopulmonary position [25]. A 50/50 ratio of polylactic acid to polycaprolactone blend was used to construct the grafts along with other polymeric reinforcement. Safety was demonstrated at the 1 year follow-up in a total of 42 patients. It is unclear at this point what role the MSCs are playing within these constructs and whether or not they are differentiating toward the correct vascular cell type.

73.2.5 Pluripotent Stem Cells

Embryonic stem (ES) cells provide promise as a pluripotent cell source for vascular tissue engineering. If ES cells are to fulfill this potential, efficient, and scalable culture techniques to provide fully differentiated cell types must be developed. Clinical concerns over ES cell therapies include immunogenicity and tumorigenicity. Various strategies are currently being explored to “tailor” cells toward specific patients to circumvent problems associated with immune rejection [26,27]. Pluripotent adult stem cells have also been derived from postnatal cells using genetic manipulation. These cells are termed induced pluripotent stem cells and may provide an autologous cell source without the potential for immune rejection. They are genetically modified adult cells that behave in a similar manner to ES cells and are pluripotent [28]. Teratoma formation can still occur, however, the generation of tumors from pluripotent stem cells can be eliminated by using fully differentiated cells. Desired lineages can be enriched during differentiation using various strategies. These include induction using chemokines, co-culture with differentiated

cell types, as well as genetic manipulation on the starting ES cell population. Selection based on surface markers is possible, either with or without induction, using cell sorting techniques. Cells of mesodermal origin including osteoblasts, chondrocytes, cardiomyocytes, ECs, SMCs, and hematopoietic (blood) cells have all been generated from mouse ES cells [29–33].

73.3 Scaffolds/Extracellular Matrix

73.3.1 Synthetic Scaffolds

Polyglycolic acid (PGA), a well-characterized biodegradable polymer, has been investigated for use in many tissue engineering applications. Niklason was the first to show feasibility of PGA as a scaffold for vascular tissue engineering [34]. Her group seeded a porous, degradable, tubular PGA mesh scaffold with bovine aortic SMCs and cultured the grafts in a bioreactor with pulsatile flow through the lumen of the vessel. After 8 weeks, the PGA mesh had been partially replaced by a SMC medial layer and showed increased collagen and mechanical properties. ECs were then seeded on the luminal surface. These vessels showed promising results with burst strengths over 2000 mm Hg and patency of up to 4 weeks in a porcine model. Contraction was observed in response to serotonin, endothelin-1, and prostaglandin $F_{2\alpha}$.

Poly(ethylene glycol) (PEG) possesses several advantages as a biomaterial. In addition to being hydrophilic and biocompatible, it is resistant to protein adsorption and cell adhesion, and therefore is non-immunogenic with very few biological interactions when rendered insoluble or chemically conjugated to proteins. It can be modified to include a variety of reactive functional groups that can be utilized to impart new properties to PEG. For example, acrylated PEG will undergo photopolymerization and can do so in the presence of cells with minimal harmful effects [35]. Additionally, PEG can be modified to include biologically-relevant molecules such as adhesion peptides [36], growth factors [37], or proteolytically degradable enzymes.

PEG hydrogel-based TEVGs have the potential to combine the advantages of a synthetic scaffold with benefits such as specific cell-material interactions, including remodeling in response to tissue genesis. Publications by West's group described photopolymerizable PEG hydrogel extracellular matrix (ECM) analogs that mimic the properties of collagen [38,39]. These hydrogels included degradable sequences, sensitive to proteases such as collagenase and elastase, in the backbone of the polymer. They also incorporated grafted adhesive peptides, such as arginine-glycine-aspartic acid (RGD), in the network. The hydrogels degraded as cells produced proteolytic enzymes. The nonimmunogenic properties and biological function of these PEG-based hydrogels present an attractive scaffold alternative. They could lead to a TEVG that, when implanted, could encourage cell growth and function and would be completely replaced over time to create totally new tissue.

73.3.2 Natural Scaffolds

The first TEVG was developed by Weinberg and Bell [40]. This pioneering study proved feasibility of a TEVG based on a scaffold of natural materials and vascular cells. The graft was derived from a collagen gel supported by Dacron mesh and seeded with bovine aortic SMC, EC, and fibroblasts. Initially, a collagen gel containing SMCs was cast in a tubular shape. After a 1-week culture period, Dacron mesh was wrapped around the outside of this layer to provide mechanical strength. Another layer of collagen and fibroblasts was cast over this, and the inner lumen was lined with ECs. Functional and histological staining confirmed formation of an endothelial layer and production of prostacyclin and vWF. However, this graft did not exhibit sufficient mechanical strength. Several parameters were varied, such as collagen concentration, cell density, and culture time. Nevertheless, the highest reported burst strength was approximately 325 mm Hg. This was significantly less than typical physiologic pressures of 5000 mm Hg in the coronary artery and 2000 mm Hg in the saphenous vein.

Acellular matrices have been developed as an alternative to collagen gel-based TEVGs. The major advantage of an acellular approach is the elimination of the long culture time associated with cell-seeded scaffolds. One material of interest is small intestine submucosa (SIS), a matrix that has been mechanically treated to remove cells, leaving an intact scaffold composed mainly of collagen. SIS possesses mechanical properties suitable for a vascular graft, and better compliance than current autologous vessel grafts [41]. In one case, Huynh rolled sheets of porcine SIS around a mandrel to form a TEVG [42]. The SIS matrix was cross-linked with 1-ethyl-3(3-dimethylaminopropyl) carbodiimide hydrochloride, and the inner lining was coated with bovine fibrillar collagen derivatives and treated with heparin to prevent thrombosis. These grafts were implanted into rabbits and all remained patent until harvest after 90 days. Upon examination, infiltration of SMCs and ECs from surrounding tissue was apparent. Additionally, vessels showed physiologic activity in response to vasoactive agents. Preimplant burst strengths were ~930 mm Hg. Similar work by Roeder using the carotid artery in a canine model examined burst strengths of remodeled SIS grafts after 60 days [43]. This approach produced burst strengths of ~5000 mm Hg in the explanted vessels, equivalent to the burst strength of native vessels.

Another tactic has been to use de-cellularized arterial matrices as a scaffold for TEVGs. Advantages include blood compatibility and an ECM with correctly aligned collagen and elastin fibers. Native vessels are treated with trypsin and ethylenediaminetetraacetic acid to remove cells [44]. This leaves an intact matrix that can be used for implantation. Cells may be seeded in the matrix and conditioned under pulsatile flow [45]. Fibrosis was a problem in these types of grafts, and concern remains over immune response and disease transmission with the xenogenic materials used in acellular matrices.

73.3.3 Cell Assembly

L'Heureux et al. created a TEVG by rolling sheets of cells around a mandrel to form a layered construct [46]. No supportive scaffold was used. Human umbilical vein SMCs and human dermal fibroblasts were grown in culture flasks to super-confluency in high ascorbic acid conditions for 1 month. The cell sheets were then rolled around a mandrel to form tissue layers. After 8 weeks of culture in a bioreactor, the lumen was seeded with ECs and then cultured for another week. At the end of this period, ECs showed α -LDL uptake and vWF and SMCs showed positive staining for α -smooth muscle actin and desmin. Grafts showed circumferential alignment, significant ECM production, and burst strengths of about 2000 mm Hg. However, only a 50% patency rate was seen in a canine model after 1 week. Note that this was a xenograft implantation and one would expect a significant immune response. Other disadvantages included a total culture time of 3 months, and the fact that much of the graft's strength was attributed to the adventitial layer, not the medial layer as seen in native vessels.

73.3.4 Matrix and Culture Effects

The importance of matrix signaling has been demonstrated for both stem cells [47,48] as well as differentiated vascular cell types. Nikolovski et al. cultured SMCs on two different types of scaffolds, collagen, and PGA. They demonstrated that SMCs can sense the nature of the substrate and that SMCs proliferated to a greater degree on collagen, while SMCs exhibited greater differentiated function as measured by elastin production on PGA scaffolds. This result was confirmed not only on 2D substrates but also on 3-D scaffolds. The investigators hypothesized that the cells were "sensing" their substrate via the adsorbed protein layer and subsequently examined the composition of those proteins.

Prior work in our lab has demonstrated that an adult mesodermal progenitor cell, specifically human MSCs, seeded in a PEGylated fibrin gel within 48 h *in vitro* began to form vascular tube-like networks, in contrast to controls of unreactive PEG mixed with fibrinogen or fibrin alone [49]. These tubes stained positive for mature EC specific markers like CD31 and vWF. Real-time polymerase chain reaction

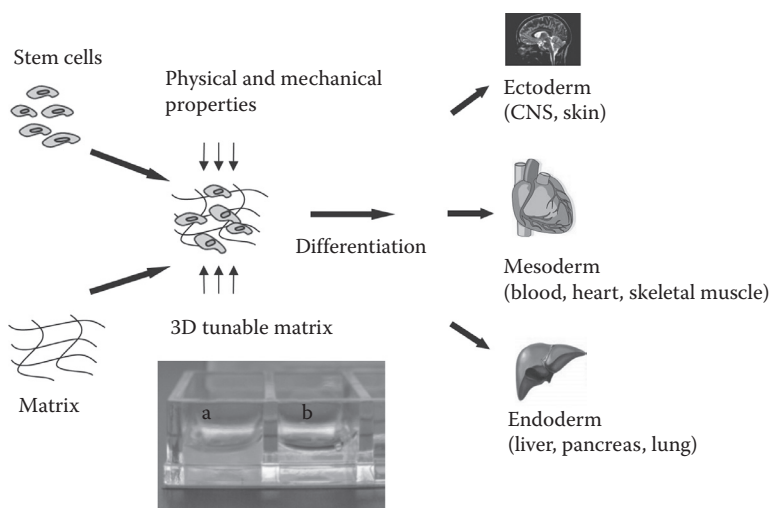


FIGURE 73.1 Schematic of a controlled 3D matrix culture system for directing stem cell differentiation. Picture denotes 3D cell culture matrix in 4-well chamber slide. (a) Fibrin (b) PEGylated fibrin. (Reproduced with permission from Zhang, G. et al. *Acta Biomater*, 2010.)

(RT-PCR) data also demonstrated that CD31 and vWF as well as VEGF mRNA was expressed in MSCs. This demonstrates that the composition of the culture substrate or matrix can not only control the differentiated function of cells but also drive stem cell differentiation toward an EC-like phenotype. Clearly, vascular tissue engineering depends on a number of factors including media composition as well as scaffold chemistry and physical characteristics. (Figure 73.1).

73.4 Growth Factor Signaling

The third component of a classical tissue engineering approach is any signaling imposed on target cells to induce or maintain the desired phenotype. In particular, soluble signals have been used either as a media supplement to support maturation of TEVGs as described below, as a localized cytokine on synthetic materials in order to control cell migration and growth, or as a delivered drug from degradable matrices to encourage blood vessel network formation. A number of cytokines are involved in the stimulation of vascular cells including ECs, SMCs, and their progenitors. One of the most widely studied factors in VEGF which includes the isoforms A–F and PlGF [50]. The family of VEGF peptides is a key player in the angiogenic response [51]. VEGF can exert activity directly on ECs to stimulate migration and proliferation in the formation of neovasculature. VEGF acts to induce mobilization of EPCs into peripheral blood as well as to induce differentiation from EPCs and ECFCs. Additionally, VEGF acts as a factor to increase blood vessel permeability.

The family of fibroblast growth factors (FGFs) is another group of potent factors controlling angiogenesis [52]. Over 22 members of the FGF family have been identified and many of them act on multiple cells types. FGF1 and FGF2 have been reported to act on ECs to enhance angiogenesis. In particular FGF1 and FGF2 can promote an angiogenic phenotype in culture [53]. FGFs can exert their activity through autocrine or paracrine pathways to promote angiogenesis. Molecular cross-talk exists between the FGF and VEGF families of growth factors, and they can act synergistically to promote blood vessel formation while retaining specific activities toward ECs [54].

Platelet-derived growth factor (PDGF) has a number of activities on vascular cells including mediating collagen synthesis by fibroblasts, mediating inflammation, regulating lymph development, and recruiting stem cell mobilization [55]. PDGF has also been shown to cause dramatic effects on SMCs and

their progenitors. PDGF promotes recruitment of pericytes during blood vessel development, thereby enhancing blood vessel stabilization and maturation [56]. The effects of PDGF on SMCs include enhancing proliferation, migration, and synthesis of matrix proteins. TGF- β 1 is a pleiotropic growth factor that has an indirect effect on the angiogenesis cascade by upregulating production of VEGF and basic fibroblast growth factor (bFGF) from SMCs [57]. Additionally, it has been hypothesized that TGF- β 1 may recruit inflammatory cells that release VEGF, bFGF, and PDGF-BB and thus further influence angiogenesis [58,59]. Furthermore, evidence has indicated that TGF- β 1 may induce SMC phenotype from a population of MSCs [60–62].

Other factors involved in regulating angiogenesis and blood vessel maturation include the angiopoietins; angiopoietin-1 and -2, hepatocyte growth factor (HGF), neurotrophin nerve growth factor, erythropoietin, and insulin-like growth factor as well as members of the hedgehog (Hh) family of proteins, particularly sonic hedgehog (Shh) which has demonstrated potent angiogenic activity.

Incorporation of cytokines into synthetic materials that retain graft strength and growth factor activity is a significant challenge. The vascular growth factors VEGF and FGF-1 have been delivered from cardiovascular implants using the native affinity of these factors for natural proteins such as fibrin and heparin. Commercially available fibrin adhesive has been embedded within expanded polytetrafluoroethylene (ePTFE) grafts [63,64]. The presence of cytokine-loaded fibrin alters the drug release profile to maintain activity over a longer timecourse. Heparin has also been used in the development of affinity matrices. In particular, heparin has been covalently bound to ePTFE and to polyester grafts via charge interaction [65,66]. Heparin has been used to slow growth factor release by incorporation in fibrin and embedding in synthetic grafts. Casper et al. used a low molecular weight heparin (LMWH) grafted to PEG followed by electrospinning into poly(lactic-co-glycolic acid) (PLGA) grafts. Heparin and FGF retention was higher with the conjugation versus LMWH alone [67]. Other matrix proteins that have been used to mediate growth factor release include albumin to localize VEGF [68] and combinations of gelatin and heparin to localize VEGF and FGF-2 to polyurethane grafts [69].

Incorporating cytokines into cardiovascular device coatings has the potential to mediate cell growth around the device. Analogous to EC seeding on vascular conduits, enhancing signaling from a synthetic surface may encourage EC growth and migration to enhance endothelialization. In particular, VEGF has been incorporated into hydrocarbon stent coatings, EC growth was enhanced, but restenosis in animal models was not reduced [70,71]. Phosphorylcholine coatings have been used in VEGF gene delivery strategy with success [72,73]. As is the case with EC seeding, the retention of migrated ECs on device surfaces is complicated by flowing blood and the underlying stiffness of the surface.

An alternative to incorporation of growth factors either within grafts or within device coatings is to tether growth factors directly onto surfaces. In particular, the challenge with this strategy is to retain growth factor activity following tethering. Pioneering work by Ito and Imanishi reported the immobilization of insulin directly onto polymeric substrates. Enhanced cell proliferation was demonstrated relative to controls of soluble or adsorbed insulin [74]. Surface-tethering of insulin also resulted in an increase in the degree of endothelialization on vascular grafts. Cells could be maintained in tissue culture without media supplementation of serum through the use of insulin delivered via surface-tethering to microcarriers. Surface-tethering of growth factors may provide some unique advantages over soluble signals including protection against normal enzymatic inactivation as well as the highly localized action of the growth factor activity. Immobilization of growth factors using the molecularly mobile, PEG may aggregate ligand–receptor complexes on the cell surface and augment receptor-mediated functions [75]. Similar immobilization strategies have been used to encourage EC or EPC engraftment on synthetic substrates [15,76].

Mann used an acryloyl-PEG-N-hydroxy succinimide (NHS) molecule to incorporate adhesion peptides into a PEG hydrogel [77]. Tethering growth factor (GFs) such as TGF- β 1 using the same acryloyl-PEG-NHS chemistry increased matrix production and elastic modulus. It is hypothesized that local presentation of the GF maintains bioactivity and promotes localized effects [37]. This same chemistry could incorporate other GFs to promote EC proliferation or activity [78]. Further, the cell adhesive domain arginine-glycine-aspartic acid-serine (RGDS) can be patterned within gels to promote EC tubulogenesis [79].

73.5 Vascular Grafts and Medial Equivalents

The seminal work on TEVGs by Weinberg and Bell in 1986 [80] was based on the observed contraction of a collagen by embedded fibroblasts. Contraction of 10–20-fold was possible and particular focus was directed toward the replacement of the contractile or medial layer of the TEVG. Several groups have attempted to improve upon the mechanical strength of collagen gel-based TEVGs using various methods. Tranquillo's group has investigated magnetically-oriented collagen gel fibrils and glycation cross-linking to increase mechanical strength [81,82]. They also looked at fibrin as an alternative to collagen and studied the effect of various media supplements, including ascorbic acid, TGF- β , insulin, and plasmin [83,84]. Seliktar conditioned collagen gel-based TEVGs with cyclic mechanical strain and noted increased mechanical strength through matrix metalloproteinase remodeling [85]. With the use of these methods, the burst strength of TEVGs has been increased above that of Weinberg and Bell, but is still a major concern for clinical translation.

The further refinement of TEVGs in 1999 by Niklason et al. demonstrated the increase and maintenance of burst strength of the construct. A major contributor to the success of this vessel was the pulsatile bioreactor culture system. An example of this is shown in Figure 73.2. Conditioning was performed at 165 beats/min and a radial strain of 5%. Previous work has shown that dynamic mechanical strain regulates the development of *in vitro* smooth muscle tissue [86]. The mechanical stresses imparted by the bioreactor, in addition to media supplements, contributed to vessel strength by increasing collagen synthesis *in vitro*. This idea is important for any TEVG that contains a SMC component. Further work to study the benefits of fibril alignment, cross-linking, and media supplements, as demonstrated by other groups, could lead to further improvements.

In a unique strategy, SMCs have been incorporated directly into electrospun poly(ester urethane) urea (PEUU) scaffolds [87]. Using this method, investigators could uniformly distribute a large number of cells within a material possessing the necessary strength and extensibility for use as a graft material. Using a combination of electrospinning and electrospraying maintained cell viability during processing even in the presence of organic solvents. Measured strengths were reduced by ~24%, but *in vivo* results have not yet been reported.

Media composition has been shown to be important for the bulk of cell seeding approaches described above. In particular, most rely on high concentrations of various factors in culture along with relative

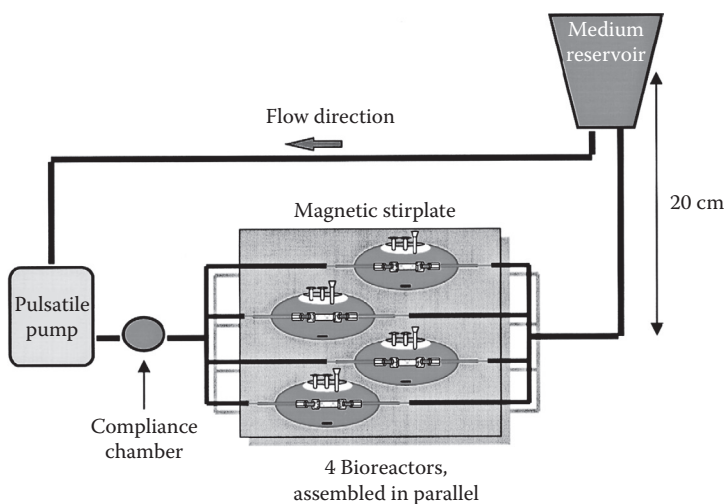


FIGURE 73.2 Biomimetic system for vessel culture. (Reproduced with permission from Niklason, L.E. et al., *Science*, 1999. 284(5413): 489–93.)

long periods of culture or mechanical conditioning in order to enhance burst strengths of TEVGs. For cell assembly as described by L'Heureux SMCs from human umbilical veins and fibroblasts from human dermis were cultured independently in culture supplemented with 50 $\mu\text{g}/\text{mL}$ of ascorbic acid. In Nicklason's work the media was supplemented with 20% fetal bovine serum, ascorbic acid, copper, and various amino acids. Typical *in vitro* culture times range from weeks to months. It would be desirable to reduce the culture times as well as to control the cytokine composition that the cells are exposed to locally following implantation. These goals have motivated work into optimizing signaling events either in culture or following implantation. Another problem that will have to be addressed in the future is cell source if fully differentiated cells are to be used. Autologous tissue is the best cell source to prevent an immune response, yet extended culture is necessary between cell harvest and graft implantation.

The greatest challenges that TEVGs currently face are thrombosis and insufficient mechanical strength; both of these could cause catastrophic failure of a graft *in vivo*. Compliance mismatch has been implicated as a problem in previous graft failures. Close matching of mechanical properties is of importance; however, exact matching may not be necessary. Currently used autologous vessel grafts have widely varied mechanical properties, yet have been successful as replacement tissue. A successful TEVG should mimic the native artery as closely as possible, both in character and function. Ideally, the ECM should contain similar amounts of collagen and elastin to the native artery, to ensure comparable strength and recoil. The graft should also contain a confluent layer of luminal ECs to prevent thrombosis. Additionally, for a graft to be commercially feasible, it will need to be cost effective and competitive with current graft therapies. None of the previously described TEVGs meet all the requirements for a successful, implantable replacement therapy. Clearly, there is room for further research in this area.

73.6 Engineered Vascular Networks

There is a significant interest in neovascularization of growth of new blood vessels following ischemia. Blood vessel obstruction in various tissues such as cardiac or skeletal muscle leads to tissue hypoxia and tissue necrosis. This is particular damaging in the heart due to the postmitotic state of the mature cardiac myocyte. The restoration of blood flow through ischemic tissues may regenerate new tissue or rescue existing tissue (as in the cardiac case) leading to improved function.

Strategies for enhancing vascularization are based on the use of angiogenic agents or vascular cells that can either encourage blood vessel growth from existing vessels (angiogenesis) or participate in the assembly of blood vessels (vasculogenesis). As noted previously, a number of different stem and progenitor cell populations including: MSCs, HSCs and EPCs have demonstrated potential for vascular cell differentiation. These cells have been delivered to ischemic tissues in various animal models as well as clinical trials. The infusion of autologous MSCs following myocardial infarction and reperfusion is still ongoing to evaluate functional recovery.

The extent to which stem cells can actually participate in new blood vessels may be very dependent on the cell type and microenvironment. Very detailed fluorescent cell labeling and confocal imaging of transplanted cells into skeletal muscle revealed that while MSCs could participate in neovascularization, the extent of transdifferentiation toward vascular cell types was minimal [88]. Our laboratory has demonstrated that while MSCs could readily transdifferentiate into vascular cells including ECs *in vitro*, the extent of transdifferentiation *in vivo* in a mouse MI model was not correlated with the extent of new blood vessel formation [49,89].

Recent studies have shown the importance of the contribution of multiple cell types including vascular progenitors when engineering vascularized tissue on synthetic matrices [90]. Constructs fabricated from 50/50 poly(L-lactic acid) (PLLA)/PLGA were seeded with mouse myoblasts and human embryonic ECs. The addition of an EC population increased implant vascularization and subsequent tissue viability. Blood vessel organization, however, has only been investigated *in vivo*, and it remains unclear the relative contribution of EPC types, whether providing a purely paracrine role or differentiating and incorporating into the newly formed blood vessels [91].

Combination strategies using multiple growth factors, stem cell populations or growth factor stimulation in combination with stem cell delivery may be necessary in order to provide a robust blood vessel network. Much can be learned from vascular biology with respect to the activity of various growth factors in the development of blood vessels. The action of cytokines can be dependent on concentration, timing and the context of the target cell. It is therefore of great importance to have growth factor presentation that is tightly controlled. A major challenge in growth factor delivery is the relatively short half-life of most therapeutic peptides as well as their sensitivity to processing. Scaffold delivery systems that can deliver multiple growth factors and/or stem cells are particularly challenging. Stem cell delivery is complicated by the typically low retention of viable cells as well as the lack of understanding regarding the mechanism for enhanced blood vessel formation. Tissue engineering advances may provide solutions for combination delivery with next generation scaffolds.

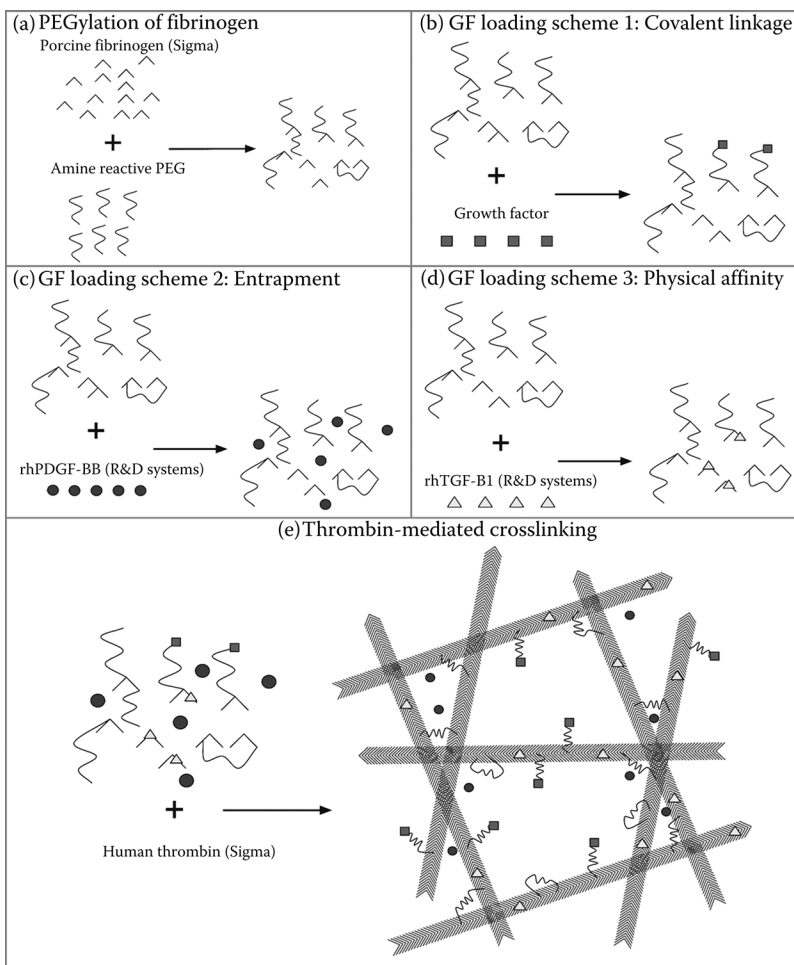


FIGURE 73.3 Schematic of 3 mechanisms to load growth factors (GFs) into PEGylated fibrin gels. (a) Depicts PEGylation of fibrinogen with amine reactive PEG. (b) Depicts conjugation of GF through homobifunctional PEG. (Adapted from Zhang, G. et al., *Tissue Eng*, 2007. **13**(8): 2063–71; Zhang, G. et al., *Tissue Eng*, 2006. **12**(1): 9–19.) (c) Depicts admixing of GFs into PEG and fibrinogen solution. (d) Depicts physical affinity of particular GFs with fibrinogen. (e) Depicts thrombin-mediated gelation of fibrinogen into PEGylated fibrin gels loaded with multiple GFs. (Reproduced with permission from Drinnan, C.T. et al., *J Control Release*, 2010.)

Examples of matrices that have been used for combination delivery include natural proteins such as type I collagen or fibrin to treat ischemic myocardium [92,93]. The native biologic activity of structural proteins may be particularly important for maintaining cell viability and differentiated function. Designed peptides based on charged α -linked side chains have been investigated as self-assembling matrices with the ability to recruit therapeutic cell populations in a mouse myocardial model. Endothelial and SMCs were identified following delivery [94,95]. A cardiomyocyte survival factor was also delivered via self-assembling peptide with measured induction of downstream signaling [96]. Investigators have correlated the matrix physical characteristics to the organization of formed vascular networks.

Pioneering work by Mooney and colleagues demonstrated the dual delivery of growth factors with distinct kinetics. Richardson et al. incorporated VEGF and PDGF-BB into a poly(lactic-co-glycolic acid) (PLGA) matrix and microspheres to present a controlled dual GF release [97]. Increased blood vessel size and distribution were demonstrated with the multiple GF release compared to individual GF release. Similarly, our laboratory has demonstrated that PEGylated fibrin can be loaded with growth factors using different mechanisms with varying release profiles (Figure 73.3). Specifically, a rapid release of PDGF-BB and delayed release of TGF- β 1 was demonstrated by two distinct mechanisms. These release profiles parallel vasculogenesis models for capillary tube stabilization and mural cell differentiation [98,99]. Further, differentiation of MSCs toward pericytes is predicted to require a similar GF cascade to form mature mural cells [62].

Our laboratory has also reported the combination delivery of stem cells with growth factor delivery. We looked specifically at the codelivery of HGF and MSCs in a mouse model of myocardial ischemia [89]. We demonstrated that delivery of both cells and HGF from PEGylated fibrin resulted in a 15-fold increase in cell retention with reduced fibrosis and enhanced ejection fraction as a measure of cardiac performance. An important conclusion of this study was that increases in blood vessel density could be produced through the release of the growth factor alone which was not necessarily correlated with improved cardiac output. While many growth factors are known to stimulate angiogenesis, the stabilization and maturation of newly formed vessels may be more complex and necessary for functional recovery.

73.7 Conclusions

Successful vascular tissue engineering strategies consider cell source, scaffold composition, as well as any additional signals that may be imposed during culture. Challenges that remain within this field are generally associated with defining the appropriate cell populations and controlling the effects of matrix composition and signaling upon the cells of interest. Cell source and the contribution of vascular progenitors in repair and blood vessel assembly are open questions. Identifying the correct cell population, scaffold characteristics and added signals for the development of blood vessels continues to be an important question within the field of vascular tissue engineering.

References

1. Schmedlen, R.H. et al., Tissue engineered small-diameter vascular grafts. *Clin Plast Surg*, 2003. **30**(4): 507–17.
2. Tu, J.V. et al., Use of cardiac procedures and outcomes in elderly patients with myocardial infarction in the United States and Canada. *N Engl J Med*, 1997. **336**(21): 1500–5.
3. Moneta, G.L. and J.M. Porter, Arterial substitutes in peripheral vascular surgery: A review. *J Long Term Eff Med Implants*, 1995. **5**(1): 47–67.
4. Williams, S.K., D.G. Rose, and B.E. Jarrell, Microvascular endothelial cell seeding of ePTFE vascular grafts: Improved patency and stability of the cellular lining. *J Biomed Mater Res*, 1994. **28**(2): 203–12.
5. Schmidt, S.P. et al., Evaluation of expanded polytetrafluoroethylene arteriovenous access grafts onto which microvessel-derived cells were transplanted to “improve” graft performance: Preliminary results. *Ann Vasc Surg*, 1998. **12**(5): 405–11.

6. Planat-Benard, V. et al., Plasticity of human adipose lineage cells toward endothelial cells: Physiological and therapeutic perspectives. *Circulation*, 2004. **109**(5): 656–63.
7. Asahara, T. and J.M. Isner, Endothelial progenitor cells for vascular regeneration. *J Hematother Stem Cell Res*, 2002. **11**(2): 171–78.
8. Gehling, U.M. et al., *In vitro* differentiation of endothelial cells from AC133-positive progenitor cells. *Blood*, 2000. **95**(10): 3106–12.
9. Boyer, M. et al., Isolation of endothelial cells and their progenitor cells from human peripheral blood. *J Vasc Surg*, 2000. **31**(1 Pt 1): 181–89.
10. Bhattacharya, V. et al., Enhanced endothelialization and microvessel formation in polyester grafts seeded with CD34(+) bone marrow cells. *Blood*, 2000. **95**(2): 581–85.
11. Ribatti, D., The discovery of endothelial progenitor cells. An historical review. *Leuk Res*, 2007. **31**(4): 439–44.
12. Cottler-Fox, M.H. et al., Stem cell mobilization. *Hematol Am Soc Hematol Educ Program*, 2003: 419–37.
13. van Royen, N. et al., START Trial: A pilot study on STimulation of ARTeriogenesis using subcutaneous application of granulocyte-macrophage colony-stimulating factor as a new treatment for peripheral vascular disease. *Circulation*, 2005. **112**(7): 1040–46.
14. Zhang, G. et al., Controlled release of stromal cell-derived factor-1 alpha *in situ* increases c-kit+ cell homing to the infarcted heart. *Tissue Eng*, 2007. **13**(8): 2063–71.
15. Aoki, J. et al., Endothelial progenitor cell capture by stents coated with antibody against CD34: The HEALING-FIM (Healthy Endothelial Accelerated Lining Inhibits Neointimal Growth-First In Man) Registry. *J Am Coll Cardiol*, 2005. **45**(10): 1574–79.
16. Grassl, E.D., T.R. Oegema, and R.T. Tranquillo, Fibrin as an alternative biopolymer to type-I collagen for the fabrication of a media equivalent. *J Biomed Mater Res*, 2002. **60**(4): 607–12.
17. Simper, D. et al., Smooth muscle progenitor cells in human blood. *Circulation*, 2002. **106**(10): 1199–204.
18. Park, J.S. et al., Differential effects of equiaxial and uniaxial strain on mesenchymal stem cells. *Biotechnol Bioeng*, 2004. **88**(3): 359–68.
19. Makino, S. et al., Cardiomyocytes can be generated from marrow stromal cells *in vitro*. *J Clin Invest*, 1999. **103**(5): 697–705.
20. Pittenger, M.F. et al., Multilineage potential of adult human mesenchymal stem cells. *Science*, 1999. **284**(5411): 143–47.
21. Toma, C. et al., Human mesenchymal stem cells differentiate to a cardiomyocyte phenotype in the adult murine heart. *Circulation*, 2002. **105**(1): 93–98.
22. Strauer, B.E. et al., Repair of infarcted myocardium by autologous intracoronary mononuclear bone marrow cell transplantation in humans. *Circulation*, 2002. **106**(15): 1913–18.
23. Abedin, M., Y. Tintut, and L.L. Demer, Mesenchymal stem cells and the artery wall. *Circ Res*, 2004. **95**(7): 671–76.
24. Tintut, Y. et al., Multilineage potential of cells from the artery wall. *Circulation*, 2003. **108**(20): 2505–10.
25. Isomatsu, Y. et al., Extracardiac total cavopulmonary connection using a tissue-engineered graft. *J Thorac Cardiovasc Surg*, 2003. **126**(6): 1958–62.
26. Menasche, P., The potential of embryonic stem cells to treat heart disease. *Curr Opin Mol Ther*, 2005. **7**(4): 293–99.
27. Oh, S.K. and A.B. Choo, Human embryonic stem cells: Technological challenges towards therapy. *Clin Exp Pharmacol Physiol*, 2006. **33**(5–6): 489–95.
28. Park, I.H. et al., Reprogramming of human somatic cells to pluripotency with defined factors. *Nature*, 2008. **451**(7175): 141–46.
29. Boheler, K.R. et al., Differentiation of pluripotent embryonic stem cells into cardiomyocytes. *Circ Res*, 2002. **91**(3): 189–201.
30. Hegert, C. et al., Differentiation plasticity of chondrocytes derived from mouse embryonic stem cells. *J Cell Sci*, 2002. **115**(Pt 23): 4617–28.

31. Kramer, J., C. Hegert, and J. Rohwedel, *In vitro* differentiation of mouse ES cells: Bone and cartilage. *Methods Enzymol*, 2003. **365**: 251–68.
32. Levenberg, S. et al., Endothelial cells derived from human embryonic stem cells. *Proc Natl Acad Sci USA*, 2002. **99**(7): 4391–96.
33. Wobus, A.M. et al., Embryonic stem cells as a model to study cardiac, skeletal muscle, and vascular smooth muscle cell differentiation. *Methods Mol Biol*, 2002. **185**: 127–56.
34. Niklason, L.E. et al., Functional arteries grown *in vitro*. *Science*, 1999. **284**(5413): 489–93.
35. Hill-West, J.L. et al., Prevention of postoperative adhesions in the rat by *in situ* photopolymerization of bioresorbable hydrogel barriers. *Obstet Gynecol*, 1994. **83**(1): 59–64.
36. Hern, D.L. and J.A. Hubbell, Incorporation of adhesion peptides into nonadhesive hydrogels useful for tissue resurfacing. *J Biomed Mater Res*, 1998. **39**(2): 266–76.
37. Mann, B.K., R.H. Schmedlen, and J.L. West, Tethered-TGF-beta increases extracellular matrix production of vascular smooth muscle cells. *Biomaterials*, 2001. **22**(5): 439–44.
38. Gobin, A.S. and J.L. West, Cell migration through defined, synthetic ECM analogs. *Faseb J*, 2002. **16**(7): 751–53.
39. Mann, B.K. et al., Smooth muscle cell growth in photopolymerized hydrogels with cell adhesive and proteolytically degradable domains: Synthetic ECM analogs for tissue engineering. *Biomaterials*, 2001. **22**(22): 3045–51.
40. Weinberg, C.B. and E. Bell, A blood vessel model constructed from collagen and cultured vascular cells. *Science*, 1986. **231**(4736): 397–400.
41. Roeder, R. et al., Compliance, elastic modulus, and burst pressure of small-intestine submucosa (SIS), small-diameter vascular grafts. *J Biomed Mater Res*, 1999. **47**(1): 65–70.
42. Huynh, T. et al., Remodeling of an acellular collagen graft into a physiologically responsive neovessel. *Nat Biotechnol*, 1999. **17**(11): 1083–86.
43. Roeder, R.A., G.C. Lantz, and L.A. Geddes, Mechanical remodeling of small-intestine submucosa small-diameter vascular grafts—A preliminary report. *Biomed Instrum Technol*, 2001. **35**(2): 110–20.
44. Bader, A. et al., Engineering of human vascular aortic tissue based on a xenogeneic starter matrix. *Transplantation*, 2000. **70**(1): 7–14.
45. Teebken, O.E. et al., Tissue engineering of vascular grafts: Human cell seeding of decellularised porcine matrix. *Eur J Vasc Endovasc Surg*, 2000. **19**(4): 381–86.
46. L'Heureux, N. et al., A completely biological tissue-engineered human blood vessel. *Faseb J*, 1998. **12**(1): 47–56.
47. Engler, A.J. et al., Matrix elasticity directs stem cell lineage specification. *Cell*, 2006. **126**(4): 677–89.
48. Engler, A.J. et al., Myotubes differentiate optimally on substrates with tissue-like stiffness: Pathological implications for soft or stiff microenvironments. *J Cell Biol*, 2004. **166**(6): 877–87.
49. Zhang, G. et al., A PEGylated fibrin patch for mesenchymal stem cell delivery. *Tissue Eng*, 2006. **12**(1): 9–19.
50. Roy, H., S. Bhardwaj, and S. Yla-Herttuala, Biology of vascular endothelial growth factors. *FEBS Lett*, 2006. **580**(12): 2879–87.
51. Shibuya, M., Differential roles of vascular endothelial growth factor receptor-1 and receptor-2 in angiogenesis. *J Biochem Mol Biol*, 2006. **39**(5): 469–78.
52. Presta, M. et al., Fibroblast growth factor/fibroblast growth factor receptor system in angiogenesis. *Cytokine Growth Factor Rev*, 2005. **16**(2): 159–78.
53. Wiedlocha, A. and V. Sorensen, Signaling, internalization, and intracellular activity of fibroblast growth factor. *Curr Top Microbiol Immunol*, 2004. **286**: 45–79.
54. Distler, J.H. et al., Angiogenic and angiostatic factors in the molecular control of angiogenesis. *Q J Nucl Med*, 2003. **47**(3): 149–61.
55. Alvarez, R.H., H.M. Kantarjian, and J.E. Cortes, Biology of platelet-derived growth factor and its involvement in disease. *Mayo Clin Proc*, 2006. **81**(9): 1241–57.

56. Wang, X.T., P.Y. Liu, and J.B. Tang, PDGF gene therapy enhances expression of VEGF and bFGF genes and activates the NF-kappaB gene in signal pathways in ischemic flaps. *Plast Reconstr Surg*, 2006. **117**(1): 129–37; discussion 138–9.
57. Isner, J.M. and A. Takayuki, Therapeutic angiogenesis. *Front Biosci*, 1998. **3**: e49–69.
58. Ahrendt, G., D.E. Chickering, and J.P. Ranieri, Angiogenic growth factors: A review for tissue engineering. *Tissue Eng*, 1998. **4**(2): 117–30.
59. Li, J., Y.P. Zhang, and R.S. Kirsner, Angiogenesis in wound repair: Angiogenic growth factors and the extracellular matrix. *Microsc Res Tech*, 2003. **60**(1): 107–14.
60. Seruya, M. et al., Clonal population of adult stem cells: Life span and differentiation potential. *Cell Transplant*, 2004. **13**(2): 93–101.
61. Wang, D. et al., Proteomic profiling of bone marrow mesenchymal stem cells upon transforming growth factor beta1 stimulation. *J Biol Chem*, 2004. **279**(42): 43725–34.
62. Ross, J.J. et al., Cytokine-induced differentiation of multipotent adult progenitor cells into functional smooth muscle cells. *J. Clin. Invest*, 2006. **116**(12): 3139–49.
63. Gosselin, C. et al., ePTFE coating with fibrin glue, FGF-1, and heparin: Effect on retention of seeded endothelial cells. *J Surg Res*, 1996. **60**(2): 327–32.
64. Greisler, H.P. et al., Enhanced endothelialization of expanded polytetrafluoroethylene grafts by fibroblast growth factor type 1 pretreatment. *Surgery*, 1992. **112**(2): 244–54; discussion 254–5.
65. Mohamed, M.S., M. Mukherjee, and V.V. Kakkar, Thrombogenicity of heparin and non-heparin bound arterial prostheses: An *in vitro* evaluation. *J R Coll Surg Edinb*, 1998. **43**(3): 155–57.
66. Begovac, P.C. et al., Improvements in GORE-TEX vascular graft performance by Carmeda BioActive surface heparin immobilization. *Eur J Vasc Endovasc Surg*, 2003. **25**(5): 432–37.
67. Casper, C.L. et al., Functionalizing electrospun fibers with biologically relevant macromolecules. *Biomacromolecules*, 2005. **6**(4): 1998–2007.
68. Crombez, M. et al., Improving arterial prosthesis neo-endothelialization: Application of a proactive VEGF construct onto PTFE surfaces. *Biomaterials*, 2005. **26**(35): 7402–9.
69. Masuda, S. et al., Vascular endothelial growth factor enhances vascularization in microporous small caliber polyurethane grafts. *Asaio J*, 1997. **43**(5): M530–34.
70. Swanson, N. et al., *In vitro* evaluation of vascular endothelial growth factor (VEGF)-eluting stents. *Int J Cardiol*, 2003. **92**(2–3): 247–51.
71. Swanson, N. et al., Vascular endothelial growth factor (VEGF)-eluting stents: *In vivo* effects on thrombosis, endothelialization and intimal hyperplasia. *J Invasive Cardiol*, 2003. **15**(12): 688–92.
72. Van Belle, E. et al., Passivation of metallic stents after arterial gene transfer of phVEGF165 inhibits thrombus formation and intimal thickening. *J Am Coll Cardiol*, 1997. **29**(6): 1371–79.
73. Walter, D.H. et al., Local gene transfer of phVEGF-2 plasmid by gene-eluting stents: An alternative strategy for inhibition of restenosis. *Circulation*, 2004. **110**(1): 36–45.
74. Ito, Y., G. Chen, and Y. Imanishi, Artificial juxtacrine stimulation for tissue engineering. *J Biomater Sci Polym Ed*, 1998. **9**(8): 879–90.
75. Li, J.S. et al., Enhancement of artificial juxtacrine stimulation of insulin by co-immobilization with adhesion factors. *J Biomed Mater Res*, 1997. **37**(2): 190–97.
76. Blindt, R. et al., A novel drug-eluting stent coated with an integrin-binding cyclic Arg-Gly-Asp peptide inhibits neointimal hyperplasia by recruiting endothelial progenitor cells. *J Am Coll Cardiol*, 2006. **47**(9): 1786–95.
77. Mann, B.K. and J.L. West, Cell adhesion peptides alter smooth muscle cell adhesion, proliferation, migration, and matrix protein synthesis on modified surfaces and in polymer scaffolds. *J Biomed Mater Res*, 2002. **60**(1): 86–93.
78. Leslie-Barbick, J.E., J.J. Moon, and J.L. West, Covalently-immobilized vascular endothelial growth factor promotes endothelial cell tubulogenesis in poly(ethylene glycol) diacrylate hydrogels. *J Biomater Sci Polym Ed*, 2009. **20**(12): 1763–79.

79. Moon, J.J. et al., Micropatterning of poly(ethylene glycol) diacrylate hydrogels with biomolecules to regulate and guide endothelial morphogenesis. *Tissue Eng Part A*, 2009. **15**(3): 579–85.
80. Weinberg, C.B. and E. Bell, A blood vessel model constructed from collagen and cultured vascular cells. *Science*, 1986. **231**(4736): 397–400.
81. Gorton, T.S., T.R. Oegema, and R.T. Tranquillo, Exploiting glycation to stiffen and strengthen tissue equivalents for tissue engineering. *J Biomed Mater Res*, 1999. **46**(1): 87–92.
82. Tranquillo, R.T. et al., Magnetically orientated tissue-equivalent tubes: Application to a circumferentially orientated media-equivalent. *Biomaterials*, 1996. **17**(3): 349–57.
83. Grassl, E.D., T.R. Oegema, and R.T. Tranquillo, Fibrin as an alternative biopolymer to type-I collagen for the fabrication of a media equivalent. *J Biomed Mater Res*, 2002. **60**(4): 607–12.
84. Neidert, M.R. et al., Enhanced fibrin remodeling *in vitro* with TGF-beta1, insulin and plasmin for improved tissue-equivalents. *Biomaterials*, 2002. **23**(17): 3717–31.
85. Seliktar, D., R.M. Nerem, and Z.S. Galis, The role of matrix metalloproteinase-2 in the remodeling of cell-seeded vascular constructs subjected to cyclic strain. *Ann Biomed Eng*, 2001. **29**(11): 923–34.
86. Kim, B.S. et al., Cyclic mechanical strain regulates the development of engineered smooth muscle tissue. *Nat Biotechnol*, 1999. **17**(10): 979–83.
87. Stankus, J.J. et al., Microintegrating smooth muscle cells into a biodegradable, elastomeric fiber matrix. *Biomaterials*, 2006. **27**(5): 735–44.
88. O'Neill, T.J.t. et al., Mobilization of bone marrow-derived cells enhances the angiogenic response to hypoxia without transdifferentiation into endothelial cells. *Circ Res*, 2005. **97**(10): 1027–35.
89. Zhang, G. et al., Enhancing efficacy of stem cell transplantation to the heart with a PEGylated fibrin biomatrix. *Tissue Eng Part A*, 2008. **14**(6): 1025–36.
90. Levenberg, S. et al., Engineering vascularized skeletal muscle tissue. *Nat Biotechnol*, 2005. **23**(7): 879–84.
91. Murayama, T. et al., Determination of bone marrow-derived endothelial progenitor cell significance in angiogenic growth factor-induced neovascularization *in vivo*. *Exp Hematol*, 2002. **30**(8): 967–72.
92. Liu, J. et al., Autologous stem cell transplantation for myocardial repair. *Am J Physiol Heart Circ Physiol*, 2004. **287**(2): H501–11.
93. Xiang, Z. et al., Collagen-GAG scaffolds grafted onto myocardial infarcts in a rat model: A delivery vehicle for mesenchymal stem cells. *Tissue Eng*, 2006. **12**(9): 2467–78.
94. Davis, M.E. et al., Injectable self-assembling peptide nanofibers create intramyocardial microenvironments for endothelial cells. *Circulation*, 2005. **111**(4): 442–50.
95. Narmoneva, D.A. et al., Self-assembling short oligopeptides and the promotion of angiogenesis. *Biomaterials*, 2005. **26**(23): 4837–46.
96. Davis, M.E. et al., Local myocardial insulin-like growth factor 1 (IGF-1) delivery with biotinylated peptide nanofibers improves cell therapy for myocardial infarction. *Proc Natl Acad Sci USA*, 2006. **103**(21): 8155–60.
97. Richardson, T.P. et al., Polymeric system for dual growth factor delivery. *Nat Biotechnol*, 2001. **19**(11): 1029–34.
98. Hirschi, K.K. et al., Endothelial cells modulate the proliferation of mural cell precursors via platelet-derived growth factor-BB and heterotypic cell contact. *Circ Res*, 1999. **84**(3): 298–305.
99. Hirschi, K.K., S.A. Rohovsky, and P.A. D'Amore, PDGF, TGF-B, and heterotypic cell-cell interactions mediate endothelial cell-induced recruitment of 10T1/2 cells and their differentiation to smooth muscle fate. *J Cell Biol*, 1998. **141**(3): 805–14.
100. Zhang, G., C.T. Drinnan, L.R. Geuss, and L.J. Suggs, Vascular differentiation of bone marrow stem cells is directed by a tunable three-dimensional matrix. *Acta Biomater*, 2010. **6**(9): 3395–403.
101. Drinnan, C.T., G. Zhang, M.A. Alexander, A.S. Pulido, and L.J. Suggs, Multimodal release of transforming growth factor-beta1 and the BB isoform of platelet derived growth factor from PEGylated fibrin gels. *J Control Release*, 2010. **147**(2): 180–5.

75

Tumor Engineering: Applications for Cancer Biology and Drug Development

75.1	Introduction	75-1
75.2	Cancer Fundamentals and Relationship to Tissue Engineering	75-2
75.3	Preclinical Drug Evaluation.....	75-4
	Monolayer Cell Culture • Animal Models • Tumor Explants	
75.4	Advanced 3D Models of Cancer.....	75-6
	Spheroids • Bioengineered Tumors	
75.5	Tools for Creation of a Bioengineered Tumor Model	75-8
	ECM Gels • Polymer Scaffolds • Signaling Molecules • Cocultures • Bioreactors	
75.6	Applications of Advanced 3D Cancer Models	75-12
	Improve Evaluation of New Cancer Drugs • Study the Impact of a 3D Microenvironment upon Angiogenesis • Create More Advanced Animal Models	
75.7	Conclusions.....	75-14
	References.....	75-14

Joseph A. Ludwig
University of Texas,
Houston
MD Anderson Cancer
Center

Emily Burdett
BioScience Research
Collaborative

75.1 Introduction

Though considerable progress has been made since the advent of the modern chemotherapy era, cancer remains a leading cause of death throughout the developed world. Within the United States alone, more than half a million people die of their malignancies each year, often despite receiving treatment that, unfortunately, fails to provide long-term control of tumor growth secondary to *de novo* or acquired drug resistance. While concerted efforts by academic institutions, the pharmaceutical industry, and governmental agencies such as the Food and Drug Administration (FDA) strive to rapidly transition promising therapies along the drug development pipeline from the lab bench to the bedside, a number of hurdles exist both preclinically and clinically.

A major one, which contributes to the drug development costs averaging more than 1.7 billion dollars per year for each FDA-approved drug,¹ is the inability to accurately predict in advance which preclinical drug candidates will ultimately prove beneficial in time-consuming and costly late-stage clinical trials. As oncologists and cancer biologists can attest to, though it is relatively easy to eradicate cancer within cell lines and animals, potential drug candidates tested with these model systems often show little or no efficacy when tested in humans. To close this void, preclinical models of cancer must improve to the

fullest extent possible to better replicate, *ex vivo*, the complexity that occurs naturally. Toward that end, applications previously intended for regenerative tissue engineering are finding new uses for the creation of bioengineered tumor models, that is, multicellular three-dimensional (3D) tumor-like constructs that rely upon nonnative biomimetic microenvironments or scaffolds to recapitulate defining cancer characteristics such as malignant transformation, invasion, or growth.

As described in the previous chapters, a diverse range of tissue engineering applications have emerged or are on the near horizon that promise to improve survival and/or quality of life either by supplanting worn out or defective human tissues or augmenting poorly functioning ones. Examples include biological substitutes for damaged joints, biosynthetic bone grafts or skin grafts, and many others. Unlike those applications however, which by and large are intended for regenerative purposes for eventual *in vivo* transplantation, bioengineered tumors serve an altogether different purpose—to provide a high fidelity *ex vivo* model of human tumor biology that cannot otherwise be studied as readily in patients (or animal models) for myriad reasons, including practical limitations in biopsy frequency, limited patient numbers (especially for rare tumor types), uncontrollable conditions (serum growth factors, immune surveillance, etc.) and restricted evaluation in humans to those drugs which are either FDA-approved or in clinical trials.

To obviate some of those inherent challenges, the nascent field of tumor bioengineering offers a multidisciplinary approach that draws upon lessons learned for regenerative bioengineering applications and applies them to the field of cancer biology. The result of this convergence is a greater capacity to define the precise contributions that 3D geometry, cell–cell interaction, tumor stroma, and drug diffusion have upon tumor growth, metastatic potential, and chemosensitivity that would not otherwise be possible using traditional two-dimensional (2D) monolayer cell growth. Ultimately, of course, the knowledge gained from 3D bioengineered tumor models should serve to improve the lives of cancer patients by explaining divergent preclinical and clinical drug responses.

Paralleling the overarching structure of this book, this chapter first discusses the fundamentals (with sections that focus on the relationship between cancer biology and tissue engineering as well as the current paradigm of preclinical drug testing), next describes advanced 3D models and enabling technologies used for bioengineered tumors, and finally highlights potential applications by which bioengineered tumors may contribute to our understanding of cancer biology. Though all models, including recent bioengineered tumor models used to understand cancer biology, will undoubtedly fall short of the goal of exactly mimicking the complex *in vivo* biology, considerable progress toward that goal has been made since traditional 2D culture was first used. Just as ancient Greek philosophers realized a spherical Earth better fit their experimental observations than the planar one originally conceptualized, cancer biologists have understood for some time that cancer cells grown in 3D culture often mimic *in vivo* conditions better than 2D monolayer cell culture upon plastic substratum. As the effects that spatial and temporal cues have upon the cancer phenotype are better comprehended, we anticipate the field of tissue engineering will play an ever-greater role in identifying novel targets amenable to biologically targeted cancer treatment.

75.2 Cancer Fundamentals and Relationship to Tissue Engineering

Though a comprehensive discussion of cancer biology is beyond the scope of this text, a brief introduction is in order, with particular attention to the remarkable overlap that exists between normal cellular processes that occur physiologically (and within tissue-engineered models) and anomalous ones, which are subverted by malignant cells during their malignant transformation. At its simplest, malignant tumors (as opposed to benign neoplasms) may be defined generically as an accumulation of dysfunctional cells, originally derived from a single corrupted normal cell, that gain the ability to invade and metastasize—often to the detriment of the host. A fuller understanding for those macroscopic events of

tumor growth and metastasis, however, can be attributed by and large to either somatic or spontaneous genetic errors that lead to amplification and/or upregulation of cancer-promoting genes (oncogenes) or loss of function mutations in tumor suppressor genes. This multistep process of tumorigenesis imbues malignant cells with several molecular hallmarks of cancer.

As described succinctly by Hanahan and Weinberg more than a decade ago, those hallmarks include the ability to evade apoptosis, self-sufficiency in growth signals, insensitivity to antigrowth signals, an unlimited replicative potential, as well as interactions at the tumor–stroma interface that promote angiogenesis, invasion, and metastasis.² Although such capabilities are invariably required for cancer formation, growth, and invasion, not all are unique to cancer and, given the appropriate setting, normal cells may transiently exhibit some of those same cancer-like features (Table 75.1).

For example, during embryogenesis human stem cells and their more differentiated progenitors expand at an incredible rate, forming organs and complex anatomical structures at a pace rivaling tumor formation. The capacity for brisk neoplasia can be similarly observed during hepatic regeneration following partial hepatectomy. Like their malignant counterparts, noncancerous human stems cells have

TABLE 75.1 Comparisons of Malignant Neoplasms, Wounds, and Bioengineered Tissues

	Cancers	Wounds	Bioengineered Tissues
Growth signals	Tumors often grow without reliance upon growth factors secondary to activating mutations in cognate receptors, receptor amplification, or upregulation of downstream pathways	Initial clot contains fibrin, fibronectin, and platelets as well as mitogens and chemoattractants that recruit the cells needed for wound healing	Growth factors can be used with synthetic scaffolds or hydrogels in an attempt to mimic the wound healing process and improve growth and survival of the cells of interest
Antigrowth signals	Can become insensitive to antigrowth signals and proliferate unhindered	Responsive, such that wounds normally avoid overgrowth (keloids being an exception)	Responsive to antigrowth signals
Tissue invasion	Can invade into and beyond natural tissue borders	Wounds are transiently invaded by a host of inflammatory cells (lymphocytes, macrophages, etc.) to form “granulation tissue”	Bioengineered tissues can be embedded <i>in vivo</i> for regenerative purposes. Though invasion does not occur, interaction with the host tissue can be helpful in maintaining implant viability, growth, and function
Distant spread	The ability to metastasize is a fundamental trait of cancers (as opposed to benign neoplasms)	Does not occur	Does not occur
Replication potential	Unlimited secondary to altered telomeres	Stem cells possess unlimited replication potential	Limited, although human mesenchymal stem cells have been used for regenerative purposes
Angiogenesis	Tumor cells and recruited cancer-associated fibroblasts often secrete VEGF and other growth factors to stimulate angiogenesis	Angiogenesis is a critical early physiological process necessary for wound healing	Bioengineered tissues have been designed to promote angiogenesis through addition of exogenous angiogenic factors. Required for long-term viability of <i>in vivo</i> tissue implants
Apoptosis	Can evade apoptosis through a process called anoikis	Occurs normally. Apoptosis plays an especially important role during embryogenesis	Occurs normally. Biomimetic scaffolds and ECMs can be provided in an attempt to avoid programmed cell death

the capacity for unlimited self-renewal, can often migrate to foreign locations with the body as needed, and can elicit physiological angiogenesis. Finally, as Dvorak highlighted more than two decades ago, numerous parallels exist between tumor formation and wound healing such that tumors can, in some sense, be described as “wounds that do not heal.”³ Both tumors and wounds lay a foundation of fibrin–fibronectin matrix and growth factors that serve as chemoattractants for inflammatory cells; mainly fibroblasts, lymphocytes, and endothelial cells. In the initial phases of both wound healing and tumor formation, angiogenesis is required to supply nutrients, exchange oxygen, and remove waste and, just as a wound’s fibrin-clot evolves to form highly cellular and vascularized granulation tissue, tumors coerce their surrounding stroma to further their capacity to grow and invade.

Perhaps what most distinguishes neoplasms (both malignant and benign) from normal physiological phenomena such as wound healing, embryogenesis, and tissue regeneration is that cancer’s cells have lost their homeostatic cues between the surrounding stroma and themselves, and therefore, continue to propagate without respect for their surrounding environment. Malignant neoplasms go one step further and not only fail to recognize normal cellular or tissue boundaries but can also grow within foreign environments such lymph nodes or bone (for carcinomas) or lung tissue (for sarcomas) through a process of anoikis (the ability for anchorage-independent cell growth). Analogous to the “seed and soil” example, it is now recognized that the intrinsic properties of the cancer cell (“seed”) and surrounding stroma (“soil”) are critical for tumor metastasis.

Given this dysfunctional bidirectional signaling that occurs between tumor and stroma, one might be tempted to mistakenly discount the impact that spatial and temporal cues have upon a cancer’s phenotype. However, most cancer cells grown *in vitro* still require a minimal supplement of growth factors, most often provided with the addition of fetal calf serum, and many cell types require plates specially coated with collagen or other matrix components to grow. Also, splitting cells too sparsely can limit cell growth by depriving them of required paracrine signaling. Thus, even cancer cells cannot entirely forgo their reliance upon stroma and extracellular matrix (ECM) for survival.

As has readily become apparent, a cancer’s phenotype is also critically dependent upon the presence or absence of adherent culture surfaces, the extracellular matrix, and the design and chemical makeup of extracellular scaffolding material, which together can promote 3D *in vitro* cancer growth that better replicates *in vivo* conditions. Tissue engineers have, of course, known of the marked impact the surrounding stroma and extracellular environment has upon cell and tissue growth from the very beginning of their collective effort to create *ex vivo* tissue. As a prelude to discussing how lessons learned from the tissue engineering field can be applied to the science of cancer biology to create improved higher fidelity 3D *ex vivo* tumor models, the limitations of current 2D monolayer culture and xenograft models are noted with special attention to their use for evaluation of potential antineoplastic agents.

75.3 Preclinical Drug Evaluation

75.3.1 Monolayer Cell Culture

Since the advent of *in vitro* immortalized cancer growth on traditional 2D monolayers, individual cell lines and diverse cancer panels have been widely used for evaluation of antineoplastic drug candidates.⁴ For example, more than two decades ago the National Cancer Institute established a panel of 60 unique cancer cell lines used to screen more than 100,000 compounds; many other cancer cell lines have been used with similar intent.^{4–7} Via a number of high-throughput technologies measuring the expression at the gene and protein level, correlations between expression and drug efficacy have been used to identify drugs with unique mechanisms of action and elucidated resistance mechanisms.^{4–6}

However, despite the undeniable scientific advances, 2D monolayer culture has generally failed to serve as a reliable predictor of clinical benefit for promising drugs that transition into the clinical arena.^{8,9} The reasons for this are myriad but the artificial growth environment itself is considered to be a likely culprit.⁴ The immortalization process tends to enrich for the most rapidly proliferating cancer

cells capable surviving on uncoated tissue culture plastic as opposed to ones that would naturally grow at a more subdued rates in the native 3D environment *in vivo*.⁷ Furthermore, although fetal calf serum is usually added to culture medium as a surrogate for missing growth factors, 2D monolayer culture lacks other critical features such as an ECM, human soluble signaling molecules, and a 3D architecture composed of stromal cells and irregular microvasculature.¹⁰ The influence of those factors on cancer cells have been thoroughly discussed elsewhere.¹⁰⁻¹⁵

For the reason that the vast majority of anticancer drugs work by indiscriminant targeting the processes responsible for cell division, rather than specific proteins or pathways responsible for other cancer traits (e.g., resistance to apoptosis, immortality, metastatic potential, growth factor independence), the recent trend in preclinical *in vitro* drug testing has been to move beyond traditional 2D culture models and rely more heavily upon emerging 3D ones or to animal models, though animal models have their own limitations noted below.

75.3.2 Animal Models

Of course an alternative to *in vitro* models that better reproduce the biological complexity of human tumors is to use tumor xenografts within an animal model. That strategy allows several of the 3D micro-environmental cues missing during monolayer growth to be replaced, albeit incompletely since major differences exist between human and animal tissues.¹⁶ By far the most widespread xenograft model employed for preclinical drug evaluation is the subcutaneous human tumor xenograft.¹⁷ Briefly summarized, human tumor cells are implanted subcutaneously in immunodeficient mice and allowed to grow sufficiently to be detectible by physical calipers or luminescent measures. Then experimental therapeutics are compared to placebo controls for potential efficacy and molecular pathways within responding or resistant xenografts can be interrogated to monitor if the drug effect occurred through the hypothesized mechanism of action.¹⁶ By evaluating drug pharmacokinetics and toxicity, animal models additionally serve as a necessary step prior to phase I human clinical trials.

Unfortunately, as with *in vitro* testing, the majority of drugs that appear promising in xenograft models fail to display equal efficacy in those early phase I/II trials.^{8,9,18} Again, this might be expected given the subtle differences that exist between the human and mouse 3D tumor microenvironment; such differences are likely to be especially pronounced using a foreign subcutaneous tumor placement rather than orthotopic site.^{16,17} Sophisticated animal models can be used to overcome some of these shortcomings, either by orthotopic xenograft placement or autochthonous tumor models whereby tumors arise within their expected locations induced by genetic manipulation and carcinogen exposure.¹⁹⁻²¹ Though biological data from those models are likely to be relevant to the human clinical experience, their added complexity and technical difficulty often precludes their extensive use. Moreover, not all cancer types can be adapted for orthotopic or autochthonous study. In summary, a critical role for animal models persists but they are not yet reliable enough to predict human drug response.

75.3.3 Tumor Explants

Tumor explants, typically millimeter size pieces tumor specimens directly transplanted in animals without transient *in vitro* culture, offers a third alternative for preclinical drug evaluation. Whereas standard *in vitro* culture often results in dedifferentiated cells that stray far from the original *in vivo* phenotype, tumor explants have the distinct advantage of maintaining cell differentiation in a near native state. This is especially helpful, as many of the signaling cascades targeted by biologically oriented therapies are likely to remain essentially unaltered within the explants and, thereby, provide a truer reflection of how the original tumors may have responded. In the rare instances when patients and their respective tumor explants were exposed to the same drug, strong correlations in drug efficacy have been reported.

Though explants probably offer the highest fidelity to native human tumors, they are also the most technically demanding and least commonly employed for cancer research. Since tumor explants are

derived from patients' tumors, there are obviously finite amounts available, all the limitations of animal models exist, and the cost of surgical tissue acquisition can be prohibitive unless the surgical resection is planned as part of routine clinical care.

75.4 Advanced 3D Models of Cancer

75.4.1 Spheroids

Advanced 3D cancer models have been developed with the intent of overcoming many of the challenges inherent in 2D monolayer culture, xenografts, and tumor explants. Since its invention in the early 1970s, the most commonly studied 3D cancer model has been the human tumor spheroid, defined as a small (<1 mm diameter), tightly bound spherical aggregate of cancer cells derived from a cancer cell line. Similar to the embryoid bodies often used in stem cell research, spheroids tend to form when transformed cells are maintained under nonadherent conditions. Most healthy adherent cell types will undergo a process called anoikis, or apoptosis triggered by lack of adherence to a surface, but cancer cells have developed mechanisms to resist this, and can therefore survive while suspended long term in cell culture media. The individual cells in suspension will then aggregate together and over time these loosely bound cell masses will develop into the more tightly bound spheroids. Because spheroids provide cancer cells with both a 3D architecture and extensive cell–cell contacts, they model the *in vivo* cellular environment much more effectively than 2D monolayers and exhibit many of the biological properties of solid tumors, including cell morphology,^{22,23} growth kinetics,²² gene expression,²² and drug response.^{23,24}

75.4.1.1 Spheroid Formation Techniques

Various methods can be used to induce spheroid formation. One method used by cancer biologists involves subjecting a cell suspension to constant mixing.^{25,26} This is most commonly done using a spinner flask, where a small rotor continually stirs the solution. The resulting sheer stress at the walls of the flask prevents cells from attaching or settling to the bottom, ultimately resulting in spheroid formation.^{25,26} The size and number of spheroids produced by this method is relatively consistent, and can be controlled by varying factors like cell density or stirring speed.^{27,28} The spinner flask is not appropriate for all applications, however, because the high sheer stresses encountered by the cells can damage them.²⁷ The rotary wall vessel reactor uses a similar method to produce spheroids, but is gentler on the cells because of lower sheer stress. In that system, a cell suspension is placed between an outer cylinder that rotates and an inner one held stationary, resulting in constant liquid motion around the inner cylinder. This was originally developed as a method to mimic microgravity but can successfully produce spheroids as well. Despite its advantages, the rotary wall vessel reactor requires expensive and cumbersome specialized equipment that confine its general use.^{27,28}

A simpler and more commonly used spheroid formation technique is liquid overlay, which involves plating a cell solution on a nonadherent surface. Because this method avoids shear stress problems and eliminates the need for specialized equipment, it is more accessible to the general oncological research community. Briefly, nonadherent tissue culture surfaces can be easily achieved by coating tissue culture plates with thin films of agar.²⁹ The agar prevents cells from adhering to the plate surface which leads to cell aggregation and eventual spheroid formation. Though other types of nonadherent coatings are available, agar remains popular because it is easy to use and inexpensive. Commercially available non-binding and low adhesion tissue culture plates are becoming widespread and produce similar results when used for spheroid culture. A disadvantage of the liquid overlay technique is that the resulting spheroids can be highly varied in size and number, a challenge to ensuring uniformity among experimental samples.²⁷ One way to avoid this problem is to produce individual spheroids within agar-coated 96 well plates; the concavity of the agar surface yields a single spheroid per well of consistent size and cell composition. Scaling up for high-throughput applications can be difficult using this method because

each spheroid is produced one at a time, yet the simplicity inherent in the liquid overlay culture method has made it extremely popular with cancer researchers.^{22–24,30}

Other techniques developed in recent years have sought to improve the consistency of spheroids even further though none of these have obtained mainstream popularity. One method, that grows spheroids within hanging drops of liquid, has been very successful in the creation of single spheroids of consistent size and cell number.^{27,31} As with other methods, this process is also difficult to scale up. Additionally, extra handling steps are required because cells can only be maintained in hanging drops for short time periods.²⁸ Other groups have created microfluidic chips where very small spheroids of defined geometry are formed within prefabricate microwells. This technique, along with various others, has only seen limited use due to the precise equipment requirements.³²

75.4.1.2 Spheroids as a Model of Tumor Microregions and Micrometastases

As with other 3D tissue models, diffusional gradients are present within the structure of tumor spheroids. But unlike models of healthy tissues, these gradients can often be beneficial in mimicking certain aspects of tumor biology. One of the hallmarks of cancer is the ability of a growing tumor to recruit a vasculature. However, this vasculature is not present during the early stages of formation of a nascent tumor or micrometastasis, and angiogenesis is only triggered when the tumor reaches a large enough size where hypoxia and lack of nutrients become detrimental to cells. Additionally, the angiogenesis that occurs during tumor formation is not the same carefully orchestrated process involved in the growth and healing of healthy tissues. Instead, the vasculature that forms within a tumor is often highly irregular. This results in an uneven blood supply throughout the tumor, and microregions often exist where the blood supply is not adequate to meet the cells' metabolic needs. Tumors therefore become heterogeneous tissues with marked variations in cell metabolic activity and even the presence of secondary necroses where the blood supply becomes too low. Because of this heterogeneity, many researchers consider tumor spheroids to be a good model of *in vivo* cancer biology because its 3D structure results in a similar metabolic distribution. In order for cells on the interior of a spheroid to remain viable, oxygen and nutrients must diffuse in while waste products diffuse out. The result is a stratified structure where cell viability decreases as distance from the spheroid surface increases.^{27,28} The outer rim of the spheroid is made up of rapidly proliferating cells where nutrients and oxygen are quickly supplied and waste products are just as quickly removed. The inner cell layers, conversely, are relatively quiescent and under higher metabolic stress due to hypoxia and accumulation of waste by-products. Since the limit of diffusion of small molecules like oxygen through the cell mass is only about 150–200 μm , spheroids with a diameter over about 500 μm will also contain a necrotic core.^{27,28} A spheroid system, therefore, effectively mimics the variation in physiological stress and oxygenation experienced by cells within nascent tumors, micrometastases, and avascular tumor microregions, which makes them a good model of the growth kinetics and heterogeneity found in some areas of solid tumors.^{28,33}

75.4.2 Bioengineered Tumors

Although they more effectively mimic the native state inherent in the host, tumor spheroids still suffer from several of the limitations present within 2D monolayer culture. They are devoid of their extracellular surroundings and lack environmental cues provided by an ECM, other cell types (such as fibroblasts, endothelial cells, etc.), and 3D scaffolding that would exist *in vivo*. In an attempt to overcome those limitations, the nascent scientific discipline of tumor bioengineering has emerged largely through cross-disciplinary collaboration between tissue engineers and cancer biologists who recognize the complementary strengths each discipline brings to the other.

As with any emerging scientific discipline, it remains difficult to precisely define the scope of research implied under the rubric of bioengineered tumors. Some prominent scientists have reasonably defined tumor engineering as “the construction of complex culture models that recapitulate aspects of the *in vivo* tumor microenvironment to study the dynamics of tumor development, progression, and therapy on

multiple scales.”³⁴ While that definition is certainly true, and accurately describes the end goal, it is a little ambiguous with respect to the requirement for “complexity,” as nonbioengineered tumor models may be equally complex. We propose a slightly different definition and suggest that bioengineered tumors require three fundamental traits:

1. Formation of 3D cellular structures that are more complex than would naturally occur in the absence of tissue-engineered conditions (i.e., beyond 2D culture and self-forming spheroids)
2. Reliance upon tissue engineering processes that enables the interaction between the cancer cells to be measured and precisely controlled
3. Recreation of aspects of tumor behavior (e.g., tumor growth kinetics, invasion, metastasis, angiogenesis, and drug sensitivity) that occurs *in vivo* with high fidelity

All three traits are required, as the presence of just one or two traits can be found within traditional cancer models. For example, tumor spheroids have higher 3D order and better mimic the *in vivo* tumor phenotype but form through innate biological programming independent of tissue engineering processes. Since 3D spheroids form spontaneously without the aid of external tissue engineering control, they obviously cannot be said to be “bioengineered.” Equally true, exotic tissue-engineered surfaces exist for 2D cell culture but lack any higher 3D cell architecture; in such cases, despite a clear reliance upon tissue engineering, the criteria are unmet because monolayer cultures lack tumor-like properties.³⁵

Within the definition proposed above, a number of enabling technologies formerly used in tissue engineering applications are being adapted for use in bioengineered tumors. Several key applications will be discussed herein after briefly describing the core technologies used within those applications.

75.5 Tools for Creation of a Bioengineered Tumor Model

75.5.1 ECM Gels

ECM gel culture is a widely used technique in the cancer biology field that has been used to study the effect of 3D growth on cancer cell behavior. In this scenario, tumor cells are suspended in a gel-like matrix. Over time, the individual cells will migrate toward one another and form spheroid-like structures within the gel. These spheroids are similar to traditional spheroids; however, they experience both cell–cell and cell–matrix interactions, which in many cases is a better mimic of their natural *in vivo* microenvironment.

Various materials have been used as a basis for gel culture, including collagen and alginate; however, recent research commonly employs Matrigel or similar crude ECM extracts. Matrigel is a biologically complex undefined mixture of ECM molecules and growth factors derived from the ESH mouse sarcoma cell line, which has proven to be a good platform for the growth of both cancerous and healthy cell types because of its diverse signaling and attachment capabilities. Numerous methods can be used for Matrigel embedding, including suspending cells within the matrix itself, as well as floating cells on top of a preformed matrix gel.

Gel embedding offers a variety of advantages over traditional spheroid culture. For one, the signaling environment offered by the Matrigel is much more similar to the complex signaling milieu encountered by tumor cells *in vivo*. Although more invasive cancers usually form disorganized cell masses within the gel, less invasive cancers (typically lower-grade ones which still resemble their cell type of origin) usually form complex structures reminiscent of the *in vivo* host tumor. For example, when breast carcinoma cells are placed within ECM gel culture, less invasive tumor types form ductal structures similar to those seen in native breast tissue. This demonstrates that signaling molecules and 3D structural environments act to encourage the cells to organize into their native structure; it also gives a system whereby the invasiveness of a given cancer cell line can be evaluated and compared to other cell lines. Additionally, for many tissue types, it offers the chance to compare the growth of cancerous cells to their cell type of origin.

Most adherent cell types will undergo anoikis, or apoptosis due to lack of adhesion, when placed in a nonadherent environment required for traditional spheroid formation. Gel embedding, however, offers adhesion sights to these healthy cells within the matrix. Like their cancerous counterparts, they will subsequently migrate together and often form tissue-like structures within the gel. Mina Bissel's laboratory at U.C. Berkley, which has pioneered much of the work in Matrigel embedding, has used these advantages to study various breast carcinoma cell lines and to compare them to native breast tissue.³⁶⁻³⁸

One disadvantage of using naturally derived sources, such as Matrigel, is the ill-defined and irreproducible nature of the mixture. Because the composition of Matrigel and other EHS-derived ECM gels is unknown, it can be hard to ensure that the signaling environment is a good mimic of the particular tumor type under study. In recent years, ECM extracts from a variety of specific tissue types have become available, so it is now possible to study select cancer types within their native ECM. To date, this has yet to be used extensively for 3D cancer cell culture. Some research is underway to develop artificial ECM gels that have a well-defined and tailored molecular makeup, and this may offer a viable alternative for 3D models when studying the particular effects of various biological molecules or inhibitors.

75.5.2 Polymer Scaffolds

As the tissue engineering field has made greater contributions toward the development of 3D cancer models, researchers have begun to use many of the polymer matrices developed for tissue culture as an alternative method to provide cancer cells with a 3D architecture. These polymer scaffolds offer the advantage of superior mechanical properties and more tunable characteristics such as porosity, degradation properties, mechanical strength, and surface functionality.

The majority of published work relating to bioengineered tumor models has focused on the interaction between cancer cells and polymer scaffolds. Polymers that have been investigated include porous chitosan,^{39,40} surface-modified poly(lactic acid) and poly(lactic-co-glycolic acid) (PLGA) microparticles,^{41,42} porous PLGA discs,⁴³ and alginate-l-lysine-alginate hydrogels.⁴⁴ Cancer cell lines were found to attach and proliferate on these materials and to form 3D structures that were histologically and morphologically similar to *in vivo* tumors. These models have been evaluated preliminarily as a platform to study cancer drug response and the creation of angiogenic factors under hypoxic conditions, and results suggest significant changes in comparison to 2D controls and greater similarity to the *in vivo* phenotype.

The polymer scaffold that is used in the creation of a bioengineered tumor serves many of the same roles as in traditional tissue engineering pursuits. First, it should provide a basic architecture for 3D cell growth and attachment. A 3D architecture, including both cell-cell and cell-matrix attachments, plays an important role in dictating cell behavior, including cell migration, proliferation rates, response to signaling molecules, and resistance to apoptosis. Second, researchers can use the polymer matrix as a means to mimic the mechanical strength and signaling capabilities provided by the ECM molecules *in vivo*. Signaling provided by ECM molecules has been investigated extensively in cancer biology and has been shown to modify both cancer cell signaling and drug response. Signaling through the β 1-integrin has been particularly well known for the effect it has on the phenotype of a wide variety of cancers. Although not as extensively studied, substrate stiffness has also been shown to exert an effect on cancer cell growth, especially as it pertains to cancer cell migration rates. A polymer matrix with mechanical properties tuned to match the *in vivo* tumor tissue and modified to mimic natural ECM signaling is therefore preferred when creating a bioengineered tumor model. Finally, a polymer scaffold must be biocompatible and maintain adequate porosity to allow for cancer cell migration and oxygen and nutrient transfer within the construct without sacrificing mechanical integrity. Some factors with less relevance when used to model cancer include scaffold immunogenicity and degradation rate, since patient implantation will not occur.

Although only a small number of materials have been investigated thus far in tumor models, many others could be adapted for that purpose or, at the very least, serve as an ideal starting place. As mentioned in the introduction, malignant cells rely upon their surrounding tissue environment or "soil"

for growth signals and often metastasize to specific locations conducive to tumor survival and growth. Therefore, to the extent bioengineered tissues replicate those environments, they may serve as an easily controlled model of tumor invasion and metastasis. As the science of bioengineered tumors evolves in parallel with the field of tissue engineering, new polymer scaffold materials used for tissue regeneration may be adapted to the specific needs of cancer-type-specific tumor models.

75.5.3 Signaling Molecules

In common with tissue regeneration/engineering, wound healing, and tumor growth, is the reliance upon various signaling molecules (proteins, peptides, or glycoprotein-related growth factors and cytokines) for a host of cellular effects, including chemotaxis, mitogenesis, morphogenesis, metabolism, and apoptosis.⁴⁵ As occurs physiologically, those effects are impacted by systemic exposures of hormones and circulating growth factors (growth hormone, insulin, insulin-like growth factor, etc.) as well as by localized, autocrine- and paracrine-induced, time and spatially dependent concentrations unique to a particular microenvironment. Malignant cells, to a certain extent, rely upon the same signaling cascades as do healing wounds and regenerating tissues but, as discussed previously, often acquire independence from specific growth factors through amplification or activating mutations of their cognate growth factor receptors, which clearly obviates the need for receptor–ligand binding for downstream pathway activation. In addition to heterotypic signaling (i.e., signaling by one cell type to affect another), cancer cells may acquire the capacity to manufacture growth factors directly and, thereby induce an autocrine positive feedback loop that reinforces tumor growth and invasion.^{46–48} A number of excellent reviews exist which thoroughly describe this phenomenon.

As discussed previously, ECM gels like Matrigel may serve as a biologically derived, albeit poorly defined, source for many of the growth factors needed for the purposes of tissue engineering or bioengineered tumors. Such gel-based systems, while adequate for providing uniform growth factor concentrations and even some temporal control over release parameters, are not as ideally suited for mimicking the local tumor microenvironment as are tunable, biocompatible polymer scaffolds. A number of modern approaches have sought to better orchestrate spatially dependent signaling by integrating signaling molecules within polymer scaffolds through covalent immobilization (using chemical crosslinking) or noncovalent methods such as growth factor-encapsulated, crosslinked microspheres⁴⁹ or nanoparticles.⁵⁰ Other methods of growth factor delivery include localized bolus injection,⁵¹ release from coated scaffolds,^{52,53} and release from within biodegradable polymer scaffolds.^{54–57}

Using “wound healing” as the paradigm for future development, a number of tissue-engineered models have naturally sought to replicate the temporal release of sequential growth factors. By extension to tumor bioengineering, cancer biologists may adapt such models as new tools in their arsenal to interrogate the tumor–ECM microenvironment. As this occurs, one would anticipate that biologically targeted therapies will evolve beyond antiangiogenic therapy to include ones aimed at disrupting the ECM–tumor interrelationship as well.

75.5.4 Cocultures

Just as in healthy tissues, tumors do not exist in isolation but are composed of an amalgamation of diverse cell types, including nonmalignant ones. In fact, cancer-associated fibroblasts (CAF), lymphocytes, endothelial cells, and macrophages together can routinely account for up to 90% of the tumor volume; presumably stimulated by the cancer-associated inflammatory state and a vigorous but ineffective immune response.

CAFs, the most prominent nonmalignant intratumoral cell type (especially within breast and pancreatic carcinomas),^{1,58} play a critical tumorigenic role by contributing superfluous signaling molecules, including hepatocyte growth factor (HGF), fibroblast growth factor (FGF), interleukin-6 (IL-6), and others.⁵⁹ In certain epithelial cancer types, they have been shown to produce insulin-like growth factor

1 (IGF-1), a potent stimulant of mitogenesis and tumorigenesis.^{60,61} CAFs may work in concert with endothelial cells by promoting angiogenic factors such as vascular endothelial growth factor (VEGF), platelet-derived growth factor (PDGF), and SDF-1 α .^{62,63} Even tissue invasion and metastasis can be encouraged by CAFs by contributing to the transforming growth factor- β (TGF- β)-mediated epithelial-to-mesenchymal transition, a process characterized by reduced cell adhesion, repressed expression of E-cadherin, and enhanced cell motility.^{64,65} Finally, proinvasion proteases such as matrix metalloproteases and plasminogen activators can be supplemented by CAFs to directly aid tumor invasion.⁶⁶

Other cell types with that have a multifaceted role in the tumor–host relationship include endothelial cells, tumor-infiltrating lymphocytes (TIL), pericytes, and others. Endothelial cells are required in order to produce enough vascularity within the tumor necessary to reach a significant size. Paradoxically, immune cells can simultaneously serve both to reinforce and suppress tumor growth and maintenance; some immune cells are responsible for detecting and eliminating irregular cells, such as those that have undergone a malignant transformation whereas others can be signaled to produce inflammatory molecules that can both aid in vascularization as well as increasing the rate of genetic changes that occur within the cells, thus aiding in tumor progression. The role that macrophages play in tumor progression has been studied extensively, and in some cases, they appear to be required in order for tumor progression to occur.

On account of the importance of stromal cells, some researchers have investigated 3D cocultures that combine cancer cells with one or more other cell types within their environment. These have taken many forms but the majority is spheroid cocultures (i.e., a cancer spheroid combined with a fibroblast spheroid or a cancer spheroid combined with a monolayer or suspension of stromal cells). As an example of one such approach, prostate cancer spheroids have been combined with osteoblasts to aid in understanding the effect of the bone microenvironment on prostate cancer metastases.

Although stromal cells play a vital role in dictating cancer cell behavior, incorporating them into a general tissue engineering strategy will be challenging. Culture conditions that can accommodate both cell types must be optimized, the scaffold/signaling environment must be compatible with both malignant and normal cell types, and the models systems must be able to account for differences in cell proliferation rates. With the complexity inherent in such a culture scheme, many tissue engineers simply try to mimic the signaling molecules expressed by stromal cells directly without attempting to achieve the real-world molecular cross-talk that occurs within patients' tissues and/or tumors.

75.5.5 Bioreactors

A fifth tool that may be invariably used in the development of a bioengineered tumor are bioreactors, which allow for careful monitoring of cell and tissue culture growth under highly controlled, reproducible, and sometimes automated conditions. Given the ability to precisely control pH, temperature, fluid pressure, shear stress, nutrient concentrations, waste removal, and diffusion of oxygen, it is not surprising that bioreactors have found a valuable functional niche both within industry and academia.⁶⁷ Depending upon the bioreactor type, some offer unique advantages over another. For example, the spinner-flask bioreactors may improve surface deposition of cells onto 3D scaffolds; rotating-wall vessel (RWV) bioreactors can mimic conditions of microgravity; and specialized reactors can provide mechanical stress under physiological conditions that mimic tissues exposed to repetitive weight bearing (e.g., cartilage and bones). Furthermore, unlike static culture methods, direct perfusion bioreactors (whereby culture medium flows steadily through porous scaffolds) excel in achieving both uniform cell seeding throughout the interior and exterior 3D compartments and homogeneous nutrient- and oxygen-gradients free of hypoxic and/or nutrient deficient regions typical of spheroids.

As experts in tissue engineering are aware for the reasons mentioned above, bioreactors are especially adept at producing 3D tissues that more closely resemble their normal or cancerous tissue counterparts. Specifically with respect to cancer, RWV bioreactors using prostate⁶⁸ or melanoma⁶⁹ cell lines can elicit 3D structures bearing close resemblance to *in vivo* tumor morphology. That bioreactors promise to

maintain certain cancer types in their native, differentiated state is perhaps the most important and potentially useful rationale for their use as preclinical models as opposed to comparatively inferior approaches such as monolayer, spheroid, or static 3D culture. This supposition stems from the fact that many of the recently FDA-approved anticancer therapeutics are aimed at specific molecular targets and/or pathways known to vary considerably depending upon the differentiation state; by extension, if the bioreactor-enabled preclinical 3D models are nearly equivalent to human tumors with respect to differentiation, then preclinical models should serve as better predictors of subsequent clinical efficacy.

75.6 Applications of Advanced 3D Cancer Models

75.6.1 Improve Evaluation of New Cancer Drugs

Though pharmacokinetic evaluation of drug absorption, metabolism, excretion, and toxicity in animals remains a mandatory step that precedes introduction into human clinical trials, a persistent Achilles' heel of animal and *in vitro* cancer models alike has been the general lack of predictive value with respect to drug efficacy.^{7,8,9,18,70–72} For lack of a better strategy, those traditional preclinical models have remained the most popular. Yet, mirroring a trend toward multidisciplinary “team” science, it has become increasingly common for cancer biologists and tissue engineers to work collaboratively, blending valuable aspects of 3D tissue engineering into well-established *in vitro* cancer models. By doing so, there has been some early success in achieving several principle goals of *ex vivo* cancer models: (1) better prediction in advance of human trials, which drugs will succeed in combating cancer, (2) help define the mechanism(s) by which drug resistance develops, and (3) investigate the impact the tumor–ECM interaction has upon drug sensitivity, cell differentiation, invasion, and metastasis.

As described earlier in this chapter, monolayer cultures have been woefully inadequate in meeting those goals. By mimicking some of the features of *in vivo* tumors (e.g., regions of local hypoxia or nutrient deprivation, slower cell proliferation, reliance upon spatial cues, and cell–cell interaction) tumor spheroids have had more success and paved the way for more advanced drug testing models.

Just as most *in vivo* tumors are considerably more chemoresistant than *in vitro* models of the same cancer type, so too are most cancer spheroids for several reasons.^{27,30} First, most drugs are limited by their diffusion when they are placed in static culture with a 3D tumor construct. Therefore, drugs in the interior of the construct are exposed to a lower drug concentration than drugs on the periphery, which can contribute to lower cell death. This has actually been exploited in several studies that examined large molecule and antibody therapies in order to understand how well they can diffuse into a tissue. Second, cell–cell attachments provided by the 3D structure and E-cadherin-mediated pathways can help to protect the cell against cell death and to avoid anoikis. Third, cell matrix attachments and the resulting 3D cell morphology can also play a role in altering the cell's phenotype and protect it from drug-induced apoptosis. Finally, cells within a 3D structure will often proliferate at a much lower rate than cells grown in monolayers. Because most cytotoxic drugs target the cell cycle, a lower proliferative rate results in lower overall cell death. A thorough description of the malignant cell lines tested in spheroid culture and a detailed assessment of the challenges associated in moving from monolayer to spheroid culture for purposes of drug testing are reviewed elsewhere.²⁸

Cell aggregates embedded within natural or synthetic ECM have proven particularly useful for teasing apart the impact cell–ECM interactions have upon differentiation and invasion.⁷³ One prominent example developed by Bissell and colleagues found that breast cells embedded within a laminin-rich ECM formed either organized polarized acinus-like structures or bizarre highly proliferative colonies when normal or malignant cells were, respectively, used as the source.⁷⁴ Since the effects of biologically targeted drugs are highly dependent upon their respective gene or protein targets, maintaining the differentiation status and expression profile of tumor models in a pattern closer to their *in vivo* counterpart would be expected to more accurately assess a drug candidate's clinical potential. This was conclusively demonstrated by Fischbach et al. using a 3D model of human oral squamous carcinoma

cells that were maintained on poly(lactide-co-glycolide) scaffolds; in that system, the oral cancer cells grown in 2D were sensitive to LY294002, a PI3-kinase inhibitor, whereas the same cells grown in 3D were resistant.^{43,75}

75.6.2 Study the Impact of a 3D Microenvironment upon Angiogenesis

In recognition that tumors must fully rely upon angiogenesis to grow beyond a microscopic size, anti-angiogenic small molecules and antibodies targeting VEGF and other endothelial growth factors have received intense scrutiny as a promising cancer therapy.^{76,77} Though such therapies have proven moderately successful, there remains considerable room for improvement and much remains to be learned to optimize antiangiogenic treatment. As nicely reviewed by Verbridge et al., bioengineered tumor models overcome many of the potential limitations of *in vitro*- and animal-based models of angiogenesis and are particularly useful for studying the impact that the cell-cell, cell-ECM, and 3D architecture have upon the angiogenic process.⁷⁸

To examine spatiotemporal control of angiogenesis, lithographic techniques have been used to build 3D microfluidic structures within a calcium alginate hydrogel seeded with cells.⁷⁹ The effect of cell-cell interaction upon blood vessel formation has been modeled by micropatterning techniques^{80,81} and the role of the ECM matrix has been extensively studied using a number of natural and synthetic biodegradable scaffolds that allow time-variable release of growth factors.^{82,83} Some, designed with covalently linked VEGF within the synthetic matrix, have even been used to assess the effect of cell-mediated growth factor release that occurs as endothelial cells invade and locally remodel the ECM.⁸⁴ Though less often considered, mechanical forces that increase cytoskeletal tension may favor capillary network formation by human endothelial cells.⁸⁵ Advanced 3D models using photo-cross-linked RGD-modified polyacrylamide⁸⁶ or ionic-cross-linked alginate hydrogels⁸⁷ can provide a novel means to alter the surrounding elasticity in ways not previously possible with traditional 2D monolayer culture.⁸⁸ Altered pH and temperature may also be used to change ECM stiffness but those parameters must of course remain within physiological ranges safe for cell survival.

75.6.3 Create More Advanced Animal Models

The most widely used animal model for studying cancer remains the subcutaneous human tumor xenograft and although this model has provided scientists with an incredible wealth of preclinical data, the foreign location of tumor growth also confounds the conclusions that can be drawn. Orthotopic models overcome this shortcoming by placing a given tumor within its tissue type of origin in the mouse but have their own challenges, as they are more technically demanding and have not been developed for all tissue types.

Given the clinical *raison d'être* for tissue engineering and regenerative medicine, and vast experience using implanted noncancerous tissues for that purpose, it should be no surprise that *ex vivo* tissue-engineered tumor models meant for xenograft use are better tumor biomimetics than human subcutaneous or orthotopic models. Cancer cells that are first grown on 3D structures prior to later *in vivo* implantation often maintain a more differentiated state; plus, the biodegradable polymer matrix offers a more reliable delivery vehicle for tumor cells than just media alone. Furthermore, the field of tissue engineering has also devoted considerable attention to resolving the issues of perfusion and hypoxia in an effort to avoid the substantial cell death that often occurs within days of *in vivo* tissue implantation.

In the oral squamous cell model described earlier, larger tumor sizes were observed when cells were grown initially in 3D culture, as opposed to 2D, prior to *in vivo* implantation.⁴³ Tissue-engineered human tumors could also theoretically be used to study cancers that metastasize to bone, such as prostate, colon, or breast cancer among others. As an example, in the first model, to integrate engineered bone into a murine model for the purpose of studying breast cancer metastasis, Rosenblatt et al. used silk scaffolds coated with bone morphogenetic protein-2 (BMP-2) and seeded with bone marrow stromal

cells as an implanted surrogate of human bone.^{89,90} As the fields of tissue engineering and cancer biology forge an even stronger alliance, tissue-engineered scaffolds and ECMs are likely to find widespread utility for improved *in vivo* models.

75.7 Conclusions

Given the substantial scientific overlap that exists between the scientific disciplines of tissue engineering and cancer biology, and exponential progress that both fields have made in the high-throughput post-genomic era, the stage has been set for potential convergence of the fields. That has, of course, already occurred before for other engineering disciplines, as concepts from electrical engineering have been applied to cancer biology in describing the aberrant cancer signaling cascades as dysfunctional “circuits” amenable to measurement and control. Similarly, the field of systems biology is rooted, in part, on concepts relating to control process engineering (i.e., stability, fragility, and feedback loops that can either blunt or magnify the input signals of mechanical systems), which from a biological perspective can be useful in deciphering how normal and malignant cells maintain homeostasis and evade apoptosis. Improved control and measurement of the cell–cell and cell–ECM relationship, a distinct advantage inherent in tissue engineering, will almost certainly enable the creation of better cancer models, which should serve to more reliably assess preclinical drug effectiveness, enable a better understanding of cancer biology, and allow a better glimpse of the role ECM plays in tumorigenesis.

References

1. Kalluri R, Zeisberg M. Fibroblasts in cancer. *Nat Rev Cancer* 2006; 6:392–401.
2. Hanahan D, Weinberg RA. The hallmarks of cancer. *Cell* 2000; 100:57–70.
3. Dvorak HF. Tumors: Wounds that do not heal. Similarities between tumor stroma generation and wound healing. *N Engl J Med* 1986; 315:1650–9.
4. Shoemaker RH. The NCI60 human tumour cell line anticancer drug screen. *Nat Rev Cancer* 2006; 6:813–23.
5. Holbeck SL. Update on NCI *in vitro* drug screen utilities. *Eur J Cancer* 2004; 40:785–93.
6. Monga M, Sausville EA. Developmental therapeutics program at the NCI: Molecular target and drug discovery process. *Leukemia* 2002; 16:520–6.
7. Ertel A, Verghese A, Byers SW, Ochs M, Tozeren A. Pathway-specific differences between tumor cell lines and normal and tumor tissue cells. *Mol Cancer* 2006; 5:55.
8. Johnson JI, Decker S, Zaharevitz D et al. Relationships between drug activity in NCI preclinical *in vitro* and *in vivo* models and early clinical trials. *Br J Cancer* 2001; 84:1424–31.
9. Voskoglou-Nomikos T, Pater JL, Seymour L. Clinical predictive value of the *in vitro* cell line, human xenograft, and mouse allograft preclinical cancer models. *Clin Cancer Res* 2003; 9:4227–39.
10. Mueller MM, Fusenig NE. Friends or foes—Bipolar effects of the tumour stroma in cancer. *Nat Rev Cancer* 2004; 4:839–49.
11. Bissell MJ, Radisky D. Putting tumours in context. *Nat Rev Cancer* 2001; 1:46–54.
12. Jacks T, Weinberg RA. Taking the study of cancer cell survival to a new dimension. *Cell* 2002; 111:923–5.
13. Wernert N. The multiple roles of tumour stroma. *Virchows Arch* 1997; 430:433–43.
14. Liotta LA, Kohn EC. The microenvironment of the tumour–host interface. *Nature* 2001; 411:375–9.
15. Zahir N, Weaver VM. Death in the third dimension: Apoptosis regulation and tissue architecture. *Curr Opin Genet Dev* 2004; 14:71–80.
16. Kung AL. Practices and pitfalls of mouse cancer models in drug discovery. *Adv Cancer Res* 2007; 96:191–212.
17. Teicher BA. Tumor models for efficacy determination. *Mol Cancer Ther* 2006; 5:2435–43.
18. Kelland LR. Of mice and men: Values and liabilities of the athymic nude mouse model in anticancer drug development. *Eur J Cancer* 2004; 40:827–36.

19. Killion JJ, Radinsky R, Fidler IJ. Orthotopic models are necessary to predict therapy of transplantable tumors in mice. *Cancer Metastasis Rev* 1998; 17:279–84.
20. Sharpless NE, Depinho RA. The mighty mouse: Genetically engineered mouse models in cancer drug development. *Nat Rev Drug Discov* 2006; 5:741–54.
21. Talmadge JE, Lenz BE, Klabansky R et al. Therapy of autochthonous skin cancers in mice with intravenously injected liposomes containing muramyltripeptide. *Cancer Res* 1986; 46:1160–3.
22. Lawlor ER, Scheel C, Irving J, Sorensen PH. Anchorage-independent multi-cellular spheroids as an *in vitro* model of growth signaling in Ewing tumors. *Oncogene* 2002; 21:307–18.
23. Myatt SS, Redfern CP, Burchill SA. p38MAPK-Dependent sensitivity of Ewing's sarcoma family of tumors to fenretinide-induced cell death. *Clin Cancer Res* 2005; 11:3136–48.
24. Kang HG, Jenabi JM, Zhang J et al. E-cadherin cell-cell adhesion in ewing tumor cells mediates suppression of anoikis through activation of the ErbB4 tyrosine kinase. *Cancer Res* 2007; 67:3094–105.
25. Sutherland RM, Inch WR, McCredie JA, Kruuv J. A multi-component radiation survival curve using an *in vitro* tumour model. *Int J Radiat Biol Relat Stud Phys Chem Med* 1970; 18:491–5.
26. Durand RE, Sutherland RM. Effects of intercellular contact on repair of radiation damage. *Exp Cell Res* 1972; 71:75–80.
27. Lin RZ, Chang HY. Recent advances in three-dimensional multicellular spheroid culture for biomedical research. *Biotechnol J* 2008; 3:1172–84.
28. Friedrich J, Ebner R, Kunz-Schughart LA. Experimental anti-tumor therapy in 3-D: Spheroids—old hat or new challenge? *Int J Radiat Biol* 2007; 83:849–71.
29. Yuhas JM, Li AP, Martinez AO, Ladman AJ. A simplified method for production and growth of multicellular tumor spheroids. *Cancer Res* 1977; 37:3639–43.
30. Friedrich J, Seidel C, Ebner R, Kunz-Schughart LA. Spheroid-based drug screen: Considerations and practical approach. *Nat Protoc* 2009; 4:309–24.
31. Timmins NE, Nielsen LK. Generation of multicellular tumor spheroids by the hanging-drop method. *Methods Mol Med* 2007; 140:141–51.
32. Wu LY, Di Carlo D, Lee LP. Microfluidic self-assembly of tumor spheroids for anticancer drug discovery. *Biomed Microdevices* 2008; 10:197–202.
33. Kunz-Schughart LA. Multicellular tumor spheroids: Intermediates between monolayer culture and *in vivo* tumor. *Cell Biol Int* 1999; 23:157–61.
34. Ghajar CM, Bissell MJ. Tumor engineering: The other face of tissue engineering. *Tissue Eng Part A*; 16:2153–6.
35. Burdett E, Kasper FK, Mikos AG, Ludwig JA. Engineering tumors: A tissue engineering perspective in cancer biology. *Tissue Eng Part B Rev* 2010; 16:351–9.
36. Lee GY, Kenny PA, Lee EH, Bissell MJ. Three-dimensional culture models of normal and malignant breast epithelial cells. *Nat Methods* 2007; 4:359–65.
37. Petersen OW, Ronnov-Jessen L, Howlett AR, Bissell MJ. Interaction with basement membrane serves to rapidly distinguish growth and differentiation pattern of normal and malignant human breast epithelial cells. *Proc Natl Acad Sci USA* 1992; 89:9064–8.
38. Wang F, Weaver VM, Petersen OW et al. Reciprocal interactions between beta1-integrin and epidermal growth factor receptor in three-dimensional basement membrane breast cultures: A different perspective in epithelial biology. *Proc Natl Acad Sci USA* 1998; 95:14821–6.
39. Dhiman HK, Ray AR, Panda AK. Characterization and evaluation of chitosan matrix for *in vitro* growth of MCF-7 breast cancer cell lines. *Biomaterials* 2004; 25:5147–54.
40. Dhiman HK, Ray AR, Panda AK. Three-dimensional chitosan scaffold-based MCF-7 cell culture for the determination of the cytotoxicity of tamoxifen. *Biomaterials* 2005; 26:979–86.
41. Sahoo SK, Panda AK, Labhasetwar V. Characterization of porous PLGA/PLA microparticles as a scaffold for three dimensional growth of breast cancer cells. *Biomacromolecules* 2005; 6:1132–9.
42. Horning JL, Sahoo SK, Vijayaraghavalu S et al. 3-D tumor model for *in vitro* evaluation of anticancer drugs. *Mol Pharm* 2008; 5:849–62.

43. Fischbach C, Chen R, Matsumoto T et al. Engineering tumors with 3D scaffolds. *Nat Methods* 2007; 4:855–60.
44. Coutu DL, Yousefi AM, Galipeau J. Three-dimensional porous scaffolds at the crossroads of tissue engineering and cell-based gene therapy. *J Cell Biochem* 2009; 108:537–46.
45. Chen FM, Zhang M, Wu ZF. Toward delivery of multiple growth factors in tissue engineering. *Biomaterials*; 31:6279–308.
46. Marek L, Ware KE, Fritzsche A et al. Fibroblast growth factor (FGF) and FGF receptor-mediated autocrine signaling in non-small-cell lung cancer cells. *Mol Pharmacol* 2009; 75:196–207.
47. Park M, Park H, Kim WH, Cho H, Lee JH. Presence of autocrine hepatocyte growth factor-Met signaling and its role in proliferation and migration of SNU-484 gastric cancer cell line. *Exp Mol Med* 2005; 37:213–9.
48. Sawhney RS, Cookson MM, Sharma B, Hauser J, Brattain MG. Autocrine transforming growth factor alpha regulates cell adhesion by multiple signaling via specific phosphorylation sites of p70S6 kinase in colon cancer cells. *J Biol Chem* 2004; 279:47379–90.
49. Chen F, Wu Z, Wang Q et al. Preparation and biological characteristics of recombinant human bone morphogenetic protein-2-loaded dextran-co-gelatin hydrogel microspheres, *in vitro* and *in vivo* studies. *Pharmacology* 2005; 75:133–44.
50. Chen FM, Ma ZW, Dong GY, Wu ZF. Composite glycidyl methacrylated dextran (Dex-GMA)/gelatin nanoparticles for localized protein delivery. *Acta Pharmacol Sin* 2009; 30:485–93.
51. Kawaguchi H, Nakamura K, Tabata Y et al. Acceleration of fracture healing in nonhuman primates by fibroblast growth factor-2. *J Clin Endocrinol Metab* 2001; 86:875–80.
52. Lind M, Overgaard S, Nguyen T, Ongpipattanakul B, Bunger C, Soballe K. Transforming growth factor-beta stimulates bone ongrowth. Hydroxyapatite-coated implants studied in dogs. *Acta Orthop Scand* 1996; 67:611–6.
53. Liu Y, Huse RO, de Groot K, Buser D, Hunziker EB. Delivery mode and efficacy of BMP-2 in association with implants. *J Dent Res* 2007; 86:84–9.
54. Uebersax L, Merkle HP, Meinel L. Biopolymer-based growth factor delivery for tissue repair: From natural concepts to engineered systems. *Tissue Eng Part B Rev* 2009; 15:263–89.
55. Sohler J, Vlugt TJ, Cabrol N, Van Blitterswijk C, de Groot K, Bezemer JM. Dual release of proteins from porous polymeric scaffolds. *J Control Release* 2006; 111:95–106.
56. Ginty PJ, Barry JJ, White LJ, Howdle SM, Shakesheff KM. Controlling protein release from scaffolds using polymer blends and composites. *Eur J Pharm Biopharm* 2008; 68:82–9.
57. Woo BH, Fink BF, Page R et al. Enhancement of bone growth by sustained delivery of recombinant human bone morphogenetic protein-2 in a polymeric matrix. *Pharm Res* 2001; 18:1747–53.
58. Ostman A, Augsten M. Cancer-associated fibroblasts and tumor growth—bystanders turning into key players. *Curr Opin Genet Dev* 2009; 19:67–73.
59. Pietras K, Ostman A. Hallmarks of cancer: Interactions with the tumor stroma. *Exp Cell Res* 2010; 316:1324–31.
60. Strnad H, Lacina L, Kolar M et al. Head and neck squamous cancer stromal fibroblasts produce growth factors influencing phenotype of normal human keratinocytes. *Histochem Cell Biol*; 133:201–11.
61. LeBedis C, Chen K, Fallavollita L, Boutros T, Brodt P. Peripheral lymph node stromal cells can promote growth and tumorigenicity of breast carcinoma cells through the release of IGF-I and EGF. *Int J Cancer* 2002; 100:2–8.
62. Orimo A, Weinberg RA. Stromal fibroblasts in cancer: A novel tumor-promoting cell type. *Cell Cycle* 2006; 5:1597–601.
63. Orimo A, Gupta PB, Sgroi DC et al. Stromal fibroblasts present in invasive human breast carcinomas promote tumor growth and angiogenesis through elevated SDF-1/CXCL12 secretion. *Cell* 2005; 121:335–48.
64. Bhowmick NA, Moses HL. Tumor-stroma interactions. *Curr Opin Genet Dev* 2005; 15:97–101.

65. Bhowmick NA, Neilson EG, Moses HL. Stromal fibroblasts in cancer initiation and progression. *Nature* 2004; 432:332–7.
66. Joyce JA, Pollard JW. Microenvironmental regulation of metastasis. *Nat Rev Cancer* 2009; 9:239–52.
67. Martin I, Wendt D, Heberer M. The role of bioreactors in tissue engineering. *Trends Biotechnol* 2004; 22:80–6.
68. Rhee HW, Zhou HE, Pathak S et al. Permanent phenotypic and genotypic changes of prostate cancer cells cultured in a three-dimensional rotating-wall vessel. *In Vitro Cell Dev Biol Anim* 2001; 37:127–40.
69. Licato LL, Prieto VG, Grimm EA. A novel preclinical model of human malignant melanoma utilizing bioreactor rotating-wall vessels. *In Vitro Cell Dev Biol Anim* 2001; 37:121–6.
70. Balis FM. Evolution of anticancer drug discovery and the role of cell-based screening. *J Natl Cancer Inst* 2002; 94:78–9.
71. Kerbel RS. Human tumor xenografts as predictive preclinical models for anticancer drug activity in humans: Better than commonly perceived-but they can be improved. *Cancer Biol Ther* 2003; 2:S134–9.
72. Sausville EA. Overview. Cancer drug discovery: Pathway promise or covalent certainty for drug effect— quo vadis? *Curr Opin Investig Drugs* 2000; 1:511–3.
73. Debnath J, Brugge JS. Modelling glandular epithelial cancers in three-dimensional cultures. *Nat Rev Cancer* 2005; 5:675–88.
74. Nelson CM, Bissell MJ. Modeling dynamic reciprocity: Engineering three-dimensional culture models of breast architecture, function, and neoplastic transformation. *Semin Cancer Biol* 2005; 15:342–52.
75. Fischbach C, Kong HJ, Hsiong SX, Evangelista MB, Yuen W, Mooney DJ. Cancer cell angiogenic capability is regulated by 3D culture and integrin engagement. *Proc Natl Acad Sci USA* 2009; 106:399–404.
76. Folkman J. Tumor angiogenesis: Therapeutic implications. *N Engl J Med* 1971; 285:1182–6.
77. Jain RK. Normalization of tumor vasculature: An emerging concept in antiangiogenic therapy. *Science* 2005; 307:58–62.
78. Verbridge SS, Chandler EM, Fischbach C. Tissue-engineered three-dimensional tumor models to study tumor angiogenesis. *Tissue Eng Part A*; 16:2147–52.
79. Choi NW, Cabodi M, Held B, Gleghorn JP, Bonassar LJ, Stroock AD. Microfluidic scaffolds for tissue engineering. *Nat Mater* 2007; 6:908–15.
80. Tan CP, Cipriany BR, Lin DM, Craighead HG. Nanoscale resolution, multicomponent biomolecular arrays generated by aligned printing with parylene peel-off. *Nano Lett* 2010; 10:719–25.
81. Tan CP, Seo BR, Brooks DJ, Chandler EM, Craighead HG, Fischbach C. Parylene peel-off arrays to probe the role of cell-cell interactions in tumour angiogenesis. *Integr Biol (Camb)* 2009; 1:587–94.
82. Hern DL, Hubbell JA. Incorporation of adhesion peptides into nonadhesive hydrogels useful for tissue resurfacing. *J Biomed Mater Res* 1998; 39:266–76.
83. Zisch AH, Lutolf MP, Hubbell JA. Biopolymeric delivery matrices for angiogenic growth factors. *Cardiovasc Pathol* 2003; 12:295–310.
84. Zisch AH, Lutolf MP, Ehrbar M et al. Cell-demanded release of VEGF from synthetic, biointeractive cell ingrowth matrices for vascularized tissue growth. *FASEB J* 2003; 17:2260–2.
85. Mammoto A, Connor KM, Mammoto T et al. A mechanosensitive transcriptional mechanism that controls angiogenesis. *Nature* 2009; 457:1103–8.
86. Ulrich TA, de Juan Pardo EM, Kumar S. The mechanical rigidity of the extracellular matrix regulates the structure, motility, and proliferation of glioma cells. *Cancer Res* 2009; 69:4167–74.
87. Genes NG, Rowley JA, Mooney DJ, Bonassar LJ. Effect of substrate mechanics on chondrocyte adhesion to modified alginate surfaces. *Arch Biochem Biophys* 2004; 422:161–7.
88. Mammoto T, Ingber DE. Mechanical control of tissue and organ development. *Development* 2010; 137:1407–20.
89. Moreau JE, Anderson K, Mauney JR, Nguyen T, Kaplan DL, Rosenblatt M. Tissue-engineered bone serves as a target for metastasis of human breast cancer in a mouse model. *Cancer Res* 2007; 67:10304–8.
90. Kuperwasser C, Dessain S, Bierbaum BE et al. A mouse model of human breast cancer metastasis to human bone. *Cancer Res* 2005; 65:6130–8.

VI

Artificial Organs

Donald R. Peterson

Texas A&M University—Texarkana

- 76 Artificial Heart and Circulatory Assist Devices** *Gerson Rosenberg* 76-1
Introduction • History of LVADs • Engineering Design of Blood Pumps • Conclusions • References
- 77 Cardiac Valve Prostheses** *Sivakkumar Arjunon, Neelakantan Saikrishnan, and Ajit P. Yoganathan* 77-1
Background • Brief History of Heart Valve Prostheses • Current Status of Heart Valve Replacement • Mechanical versus Bioprosthetic Heart Valves • Engineering Concerns and Hemodynamic Assessment of Prosthetic Heart Valves • Current Trends in Valve Design • Conclusion • References
- 78 Artificial Lungs** *Keith E. Cook, Timothy M. Maul, and William J. Federspiel* 78-1
Clinical Need for Artificial Lungs • Basic Principles of Operation • Cardiopulmonary Bypass • Extracorporeal Membrane Oxygenation • Total Artificial Lungs • Extracorporeal CO₂ Removal • Intravascular Respiratory Assist Catheters • Next-Generation Research and Development • References
- 79 Blood Substitutes** *Amy G. Tsai, Pedro Cabrales, and Marcos Intaglietta* 79-1
Biophysical Factors in Designing Blood Substitutes • Biological Reactions to Blood Transfusion • The Maintenance of Shear Stress • Historical Trends in the Development of Blood Substitutes • Large Hemoglobin Constructs • Naturally Occurring Large Hb Molecules • Fluorocarbons • Encapsulation of Hemoglobin • Plasma Expanders • Summary and Conclusions • Acknowledgments • References • Further Information
- 80 Liver Support Systems** *Matthew S. Chang and Robert S. Brown, Jr.* 80-1
Introduction • The Normal Liver • Liver Failure • The Ideal Liver Support Device • Components of a Liver Support Device • Nonbiologic Artificial Liver Support Devices • Bioartificial Liver Support Devices • Where We Are Now • Conclusions • Defining Terms • References • Further Information
- 81 Peritoneal Dialysis Equipment** *Carlo Crepaldi, Carla Estremadoyro, Francesca Katiana Martino, Maria Pia Rodighiero, and Claudio Ronco* 81-1
Introduction • The New Generation of Cyclers • The Ideal PD Machine • Prescription and Delivery of APD • Treatment Monitoring • Current and Future Trends in APD • ViWAK PD • AWAK PD • Experimental Approaches • Conclusions • References

82 Artificial Skin and Dermal Equivalents *Dennis P. Orgill, Raul Cortes, and Ioannis V. Yannas* **82-1**
The Vital Functions of Skin • Current Treatment of Massive Skin Loss • Two Conceptual Stages in the Treatment of Massive Skin Loss by Use of Artificial Skin • Design Principles for a Permanent Skin Replacement • Clinical Studies of a Permanent Skin Replacement (Artificial Skin) • Alternative Approaches: CEA and SE • Defining Terms • References • Further Information

Blood Substitutes

Amy G. Tsai
*University of California,
San Diego*

Pedro Cabrales
*University of California,
San Diego*

Marcos Intaglietta
*University of California,
San Diego*

79.1	Biophysical Factors in Designing Blood Substitutes.....	79-2
	Microhemodynamic Considerations • Oxygen Transport • Colloidal Osmotic Pressure • Summary	
79.2	Biological Reactions to Blood Transfusion.....	79-5
79.3	The Maintenance of Shear Stress.....	79-6
79.4	Historical Trends in the Development of Blood Substitutes....	79-7
	Pre-NO Developments of Hemoglobin-Based Materials • Post-NO Blood Substitutes Development and PEG-Hemoglobin	
79.5	Large Hemoglobin Constructs	79-8
79.6	Naturally Occurring Large Hb Molecules.....	79-9
79.7	Fluorocarbons	79-9
79.8	Encapsulation of Hemoglobin	79-10
79.9	Plasma Expanders.....	79-11
79.10	Summary and Conclusions	79-12
	Acknowledgments.....	79-13
	References.....	79-13
	Further Information.....	79-18

Blood substitutes received a major impetus for development when it was realized that the blood supply could become contaminated with the advent of the acquired immune-deficiency syndrome (AIDS). This motivation and concern has since faded as advances in blood testing have lowered the risk of human immunodeficiency virus (HIV) transmission by blood transfusion to less than one case in half a million transfusions. However, blood has a short shelf life (42 days) and special storage requirements (4°C), making blood transfusions accessibility problematic in emergencies or battlefield situations. The necessity for a blood substitute also remains since blood supply is limited; in fact, if the current donation trends continue, it is estimated that the United States alone will have an annual shortage of 4 million units of red blood cells (RBCs) by the year 2030 [88].

Blood transfusions treat insufficient oxygen-carrying capacity, so-called anemia. Whereas oxygen transport capacity is invariably restored by increasing circulating hemoglobin levels, transfusion does not stop the hypoxic and inflammatory cascade initiated during the anemia, and increasing evidence suggests that transfusion of allogeneic blood is not the optimal approach to blood volume (BV) restoration due to inherent toxicities [40].

The demand for blood products in civilian and armed forces medicine is currently satisfied by donor blood, a source projected to become significantly restricted and insufficient over time as age demographics change the proportion of older individuals. Additionally, this aging population will inevitably increase the demand for blood. Synthetic or bioengineered cellular blood components show promise; however, it could be many years before these products are ready to enter broad clinical use. Advances in recombinant methodology and stem cell manipulation may correct some of the upcoming deficits in blood products; however, production of clinical materials in quantities to restore oxygen-carrying

capacity in blood transfusion scenarios is unlikely to become available in the near future at costs within means of the healthcare system. Therefore, repeated and unrelated volunteer blood donors may remain the only source of cellular blood components for the next decade.

The development of blood substitutes is intertwined with our understanding of the function of blood. Early approaches primarily focused on mimicking blood's oxygen carrying capacity. Fluorinated hydrocarbons and metal complexes in the solution were tried but the oxygen transport properties and capacity of the hemoglobin molecule cannot be equaled. Much effort has been directed to modify the hemoglobin molecule to eliminate its kidney toxicity, extend its intravascular retention time, and to prevent its extravasation. These alterations of the hemoglobin molecule were done prior to the discovery of the role of nitric oxide (NO) in the circulation and the intrinsic capacity of hemoglobin to scavenge NO by facilitating its conversion from a bioactive material into nitrate, a bioinactive form (NO dioxygenase reaction).

The discovery of the role of NO in circulatory regulation introduced awareness that blood imparts shear stress to the endothelial cells lining blood vessels. These hemodynamic forces induce various functional stimuli to the vascular endothelium leading to the production of NO and alterations in a variety of functionally important factors, many of which are regulated by gene expression [24,95]. In this context, the role of blood viscosity and how this is affected by potential blood substitutes is becoming increasingly important.

Blood substitutes have evolved significantly from the initial approach of introducing an oxygen-carrying fluid in the circulation, and an understanding is beginning to emerge on how to optimize the physical properties of the oxygen-carrying fluid as well as its oxygen transport properties. However, oxygen-carrying blood substitutes have been consistently afflicted by negative effects due to their inherent toxicity, and taming toxicity has been the major goal of blood substitutes' development [2,3]. This was partially accomplished by conjugation of Hb with polyethylene glycol (PEG-Hb), producing a vasoinactive material that, however, delivers limited amounts of oxygen in clinically relevant conditions.

Toxicity considerations are not restricted to hemoglobin solutions but extend to encapsulation of hemoglobin in vesicles and perfluorocarbons (PFCs) in emulsions. These formulations appear to be less toxic than molecular hemoglobin solutions; however, they introduce into the circulation large amounts of phospholipids, whose long-range effects are not well known. Therefore, a major barrier to progress in this area remains the lack of a systematic analysis and understanding of the sources, nature, and extent of toxicity associated with the proposed blood substitutes. Furthermore, there is no universal gauge for comparing the extent of the toxicity. It is generally assumed that the gold standard of transfusion is blood; however, an evidence of transfusion-related adverse events, both short- and long-term, has led to clinical studies of its efficacy [50,79] and blood, *per se*, is increasingly recognized as a source of toxicity.

Blood transfusions and their outcome have primarily been evaluated clinically in terms of systemic parameters and blood substitutes have been formulated almost exclusively focusing on their oxygen transport properties without addressing ancillary effects that result from changing the flow properties of blood. The critical phenomena that determine the systemic outcome following altered blood composition are microscopic, and radicated in the microcirculation [83], the locale for the biophysical interaction between blood and tissue [47]. Furthermore, introducing a blood substitute into the circulation may turn out to never be complete without toxicity; therefore, it is critical to understand the nature and extent of toxicity, to arrive at a product that is an improvement over blood transfusions.

79.1 Biophysical Factors in Designing Blood Substitutes

79.1.1 Microhemodynamic Considerations

Blood exerts its functions in the microcirculation; therefore, it is important to insure that the introduction of a fluid into the circulation preserves the functionality of this compartment. In the physiological condition, blood flow provides oxygen and mechanical signals to the microvasculature, which serve to self-regulate the local blood flow. After severe blood losses, anemia or any condition that requires a

blood transfusion will result in compromised oxygenation and vascular shear stress, thus impairing the local vascular regulatory process. Consequently, when the transfusions are given, they do not achieve their intended goal, since they only increase oxygen-carrying capacity without restoring normal hydro-mechanical conditions of the microcirculation.

Notably, this aspect of fluid resuscitation has not been fully considered, even in the development of plasma expanders, which are comparatively simpler fluids whose primary purpose is that of restoring circulatory volume. This is due in part to the difficulty of defining a functioning microcirculation, an obstacle now overcome by the realization that the extent of functional capillary density (FCD) defines how well the microcirculation sustains the tissue. A defect of this parameter is that it is not readily observable in clinical conditions, being primarily available only from experimental studies.

Physiological studies show that FCD is determined by the maintenance of hydraulic capillary pressure above a given threshold (~ 15 mm Hg) [16]. Therefore, the management of BV with oxygen-carrying and noncarrying fluids must ensure that sufficient pressure is transmitted to the periphery to perfuse the capillaries. Failure of maintaining adequate FCD has no immediate repercussion on oxygen transport for the organism at rest, but is critically important for washing out the by-products of metabolism and the maintenance of acid-base balance and pH. Even in hemorrhagic shock, FCD is critical for its function in detoxifying the tissue, rather than for oxygen transport as shown by the experiments of Kerger et al. [46].

Sufficient capillary pressure to perfuse the capillaries requires sufficient central blood pressure, and how to achieve this is not always unequivocal. In hemorrhagic shock, vascular refilling improves heart function reestablishing blood pressure, and when this is insufficient, vasopressors are used. However, vasopressors, which are used in final option scenarios, act on the arteriolar circulation, increasing pressure upstream and lowering capillary pressure, thus being detrimental to FCD [29]; therefore, their extended use would eventually lead to the peripheral tissue and then organ failure.

Low-pressure resuscitation, which emphasizes vasodilatation and flow, is a mechanism that favors the recovery of FCD. The viscosity of the fluid introduced is also a factor. The viscosity of blood in normal conditions is 4–5 cP, and plasma viscosity about 1.2 cP, which is the viscosity of conventional plasma expanders. Blood viscosity is strongly dependent on hematocrit (Hct). If a blood substitute is used near the transfusion trigger, a condition when blood is called for due to a loss of oxygen-carrying capacity (usually when Hct is about 50%), the circulation will be significantly diluted. In this condition, circulating blood has significantly reduced viscosity, lowering the production of shear stress by blood on the endothelium, which reduces the bioavailability of NO, causing vasoconstriction.

Increasing plasma viscosity provides a mechanism for transmitting central blood pressure to the periphery in a hemodiluted organism, since this increases shear stress preferentially in the microcirculation, which in normal conditions has low Hct and blood viscosity [10]. This discovery has led to identifying a new class of BV substitution fluids, currently labeled supraplasma expanders, that enhance oxygen transport capacity by establishing a condition of supra perfusion, significantly enhancing flow.

79.1.2 Oxygen Transport

The microcirculation is adapted to a specific distribution of oxygen tension (pO_2) that is in part determined by the shape of the oxygen dissociation curve for hemoglobin. In this system, blood with specific pO_2 locates at specific microvascular sites as a result of the control of active mechanisms that sense pO_2 in tissue and blood, and partition oxygen delivery between the arteriolar and capillary circulation [44].

The pO_2 in blood is distributed so that the oxygen dissociation curve for hemoglobin has the steepest slope in the arterioles where the adrenergic sensor system has the highest density [76]. Arterioles ahead of this fulcrum deliver most of the oxygen to the tissues at rest. Capillary oxygen delivery becomes predominant in working tissue [78].

The relationship between pO_2 and blood oxygen saturation, defined by the value of $p50$ (pO_2 at which hemoglobin is 50% saturated) is important in determining how tissue is oxygenated. It is generally

assumed that a high p50 benefits tissue oxygenation because oxygen is more readily released. However, a high p50 causes a disproportionate increase in the oxygen released in the arterioles, which is a signal for vasoconstriction. Therefore, normal or lower p50 is preferable to avoid the constrictive stimulus. Low p50 constitutes a form of targeted oxygen delivery, since it causes oxygen to be delivered in tissue locations with low pO₂.

Sakai et al. [72] studied hemoglobin vesicles with p50 of 9, 16, and 30 mm Hg in the microcirculation of the hamster window model subjected to an 80% isovolumic blood exchange. Optimal p50, at which FCD and tissue pO₂ were maximal, and microvascular flow and diameter were maximal, corresponded to a p50 of 16 mm Hg. Baines et al. [6] compared oxygen delivery in isolated kidneys perfused with hemoglobin solutions with p50s at 11 and 35 mm Hg and found that the solution with the lower p50 delivered oxygen twice as effectively. Cabrales et al. introduced the allosteric effectors inositol hexaphosphate (IHP) and 5-hydroxymethyl-2-furfural (5HMF) into RBCs by electroporation to change the hemoglobin oxygen affinity, varying *in vitro* p50s from 10 to 50 mm Hg (normal p50 = 32 mm Hg, human blood). RBCs were used to transfuse awake hamsters, which were then subjected to 50% BV hemorrhage followed by a shock period of 1 h; the hamsters were then resuscitated with 25% BV with high or low p50 RBCs (Hct = 50%). After resuscitation, arteriolar diameter and flow were significantly lower for high p50 and FCD was significantly lower. There was no significant difference in arteriolar pO₂. Tissue pO₂, venular pO₂, and oxygen delivery were higher for high p50 RBCs. These results show that lowering blood p50 in resuscitation provides and improves microvascular function.

79.1.3 Colloidal Osmotic Pressure

Maintenance of an adequate circulating volume is the resultant of the Starling fluid exchange forces determined by the interplay of capillary and colloidal osmotic pressure. The capillary membrane has a reflection coefficient for albumin, the principal colloid in plasma, of almost 1, depending on the tissue and organ, which is sufficient to retain water in the circulation and maintain circulating volume. The corresponding osmotic pressure in healthy organs is approximately equal to capillary hydraulic pressure. Restituting BV to the circulation under ideal conditions would be done with a fluid having the same colloidal osmotic pressure as blood; however, this is a moving target because what has to be matched is capillary pressure, which may be low in the initial stages of resuscitation. If the resuscitation fluid has sufficient osmotic pressure, this situation is favorable to the resuscitation process because it enhances fluid absorption from the tissue into the circulation.

A blood substitute should also have a colloidal osmotic pressure that does not cause significant fluid shifts, because this changes the concentration of the oxygen carrier, Hct, and blood viscosity.

The colloidal osmotic pressure is related to viscosity of a molecular solution, since both depend on the number of particles per unit volume and particle volume. If the hemoglobin contained in RBCs is dissolved in plasma, the osmotic pressure would be extraordinarily high, in the range of several atmospheres. Since this depends on the number of molecules in solutions, polymerization of the Hb is a practical way to maintain concentration and controls the number of particles. An additional advantage of polymerization is that as the number of particles decreases and the particle dimensions increase, the vasoactivity of hemoglobin decreases. Furthermore, since viscosity is a function of the total volume of the solute (Einstein's equation), the viscosity tends to remain constant.

The colloidal osmotic pressure is ultimately dependent on the concentration of the solute. Therefore, a solute that traps or restricts the mobility of the solvent will decrease the effective solvent volume, increasing colloidal osmotic pressure. This effect is exhibited by formulations where colloids are conjugated with polyethylene glycol, yielding very large osmotic pressures at low concentrations. This effect critically limits the concentration at which they can be used; in the organism, they become further diluted as their presence pulls fluid from the tissue into the circulation. At the other end of the spectrum, encapsulating the oxygen carrier eliminates the material from the osmotic pressure considerations, creating a different set of problems, related to the extravasation of fluids.

In summary, a blood substitute colloidal osmotic pressure is important in determining vascular filling, an effect that feeds back in setting the *in vivo* concentration of the oxygen carrier.

79.1.4 Summary

The preceding discussion is a summary of consideration pertaining to the biophysical nature of the material to be introduced into the circulation for the purpose of carrying oxygen. Such materials are either solutes or a solute contained within some packet, or membrane such as liposomes, and so on. Their oxygen-carrying capacity and mode of oxygen loading and release are interrelated and affect circulatory function solely on the basis of the physical properties. It is notable that these considerations were not specifically accounted for in the original design of blood substitutes. A consequence of this is that a blood substitute must promote circulatory conditions favorable for oxygen transport. Conversely, the restoration of oxygen transport must overcome not only the deficit of the transporter, but also the loss of efficiency of the transport system. Given this background and the properties embodied in the originally developed blood substitutes, in retrospect, it would have been surprising if they had been successful.

Formulation of a blood substitute requires accepting several countercurrent ideas: (a) oxygen delivery is as important as open capillaries, (b) lowering blood viscosity is not universally beneficial, (c) a high-affinity oxygen carrier is more efficacious when oxygen delivery capacity is decreased, and (d) oncotic pressures should be matched to capillary pressure to prevent fluid shifts that alter the oxygen-carrying and delivery capacity. A central concept is that the transfusion trigger is also a 'viscosity trigger' indicating the threshold beyond which blood viscosity should not be allowed to decrease further and is actively controlled.

79.2 Biological Reactions to Blood Transfusion

The restitution of BV to a circulatory system that has been subjected to a loss is never a symmetrical process since even in ideal conditions, the blood that exits the circulation suffers alterations as soon as the event takes place. Once blood leaves the circulation, it must be anticoagulated, and it undergoes a number of biochemical changes that specifically affect microvascular function. These changes and their consequences on the ability of blood to restore microvascular function are exacerbated by storage and are documented in terms of their effects on microvascular function [85]. As a consequence, there is no fundamental gold standard for comparing volume restitution fluids.

Oxygen-carrying plasma expanders based on hemoglobin of small molecular dimensions cause vasoconstriction as repeatedly found with $\alpha\alpha$ -hemoglobin. This is due to NO scavenging and the oversupply of oxygen to the arteriolar vessel wall caused by facilitated diffusion of oxygen transported by molecular hemoglobin in the solution.

Vasoconstriction has also been attributed to the possibility that smaller molecules may pass through the endothelial barrier establishing an NO sink between the endothelium and smooth muscle [27,56]. Sakai et al. [69] compared the microvascular effects of molecular hemoglobin solutions of different molecular radii and found a direct correlation between increasing molecular dimension and decreasing pressor effect, as well as decreased vasoconstriction of small arteries and large arterioles. This study compared cross-linked Hb (XLHb), PEG-Hb, hydroxyethylstarch-conjugated XLHb, polymerized XLHb, and PEG-modified Hb-vesicles (PEG-HbV). Their molecular diameters were 7, 22, 47, 68, and 224 nm, respectively. Vasoconstriction and hypertension decreased progressively, being minimal with the bolus infusion of PEG-HbV.

The mechanism that determines this effect is linked to the balance between NO scavenging by hemoglobin and NO produced by shear stress. This process was elucidated by Tsai et al. [82] who showed that increased molecular dimensions lead to increased shear stress and NO bioavailability in the microvessel walls.

Blood transfusion or the introduction of blood substitutes is usually preceded by the anemic phase where blood is hemodiluted to maintain volume with non-oxygen-carrying crystalloids or colloids. This phase introduces changes in the mechanical and chemical environment of the endothelium, which propagate upon transfusion. These changes include activation of genetically controlled mechanisms such as endothelial impairment due to inflammatory reactions [80], activation of the endothelium, platelets, and neutrophils, and liberation of cytokines. At the cellular level, there may be endothelial swelling and increased endothelial permeability due to ischemic injury [55].

Once perfusion is recovered, vascular regulatory processes are not fully functional, such as endothelial nitric-oxide synthase (eNOS), which becomes uncoupled and instead of generating NO produces superoxide, contributing to oxidative stress and triggering an inflammatory cascade. The additive role of oxidative and nitrosative stress results in increased NO release from inducible NOS (iNOS) in perivascular tissue and from macrophages/monocytes. The NO generated by iNOS is metabolized to peroxynitrite, which is cytotoxic to tissues.

Cell-free hemoglobin in the circulation is the source of uncontrolled oxidative reactions with different oxidants/antioxidants. Hemoglobin reacts with oxygen and NO, generating reactive oxygen or nitrogen species that upon contact with the endothelium cause oxidative stress-related pathologies. This is a major source of toxicity related to the presence of large quantities of molecular hemoglobin solution in the circulation, which may be directly responsible for some of the pathologies evidenced in clinical trials [3,31].

79.3 The Maintenance of Shear Stress

Maintaining blood viscosity or increased plasma viscosity in reperfusion may be beneficial because basal levels of shear stress are necessary for the up regulation of superoxide dismutase (SOD) and NO that reduce oxidative damage [26]. Shear stress mitigates the effects of oxidative stresses caused by H₂O₂ and oxygen radicals [37]. Increased shear stress leads to increased or normalized NO production and suppression of endothelin-1 gene expression [62]. Therefore, normal shear stress is necessary for lowering peripheral vascular resistance via gene-expression-mediated mechanisms beyond the regulation of NO.

Normalization of NO production lowers oxygen requirement of the endothelium and parenchymal tissue [66]. Thus, normalized blood viscosity or increased plasma viscosity is beneficial not only due to the transfer of pressure to the microcirculation and improvement of microvascular flow and FCD, but also because of the mitigation or prevention of long-term (hours to days) endothelial damage triggered by programmed gene expression, and lowered potential damage due to hypoxia by reducing the tissue oxygen demand.

Blood and plasma viscosity are critical since lowered values increase oxygen delivery but decrease shear stress. Consequently, a blood substitute, beyond its effect in maintaining FCD, should be effective in preventing ischemia and apoptosis, which can be accomplished through the maintenance of adequate levels of shear stress.

Sakai et al. perfused narrow gas-permeable tubes with different blood substitutes and immersed the apparatus in an NO atmosphere. It was found that NO binding of deoxygenated hemoglobin solutions was reduced by PEGylation, by addition of high-molecular-weight hydroxyethyl starch (2.8 cP), and by encapsulation to form Hb-vesicles. It was conjectured that higher viscosity and particle size reduce lateral diffusion when particles are flowing, inhibiting the reaction with NO [70].

The effects of shear stress in the circulation are difficult to evaluate *in vivo*; however, they can be studied with significant resolution in endothelial cell cultures exposed to laminar flow. This approach has demonstrated many of the phenomena determined by shear stress first reported by Frangos et al. [28] and Grabowsky et al. [32]. The group of Chien [24] associated shear stress effects with gene expression and the group of Menu and coworkers [30] provided new data on the effects of shear stress associated

with the perfusion of blood substitutes, relating hemoglobin oxidation, heme oxygenase transcription, and interaction with endothelial-mediated vasoactive factor and inflammation.

79.4 Historical Trends in the Development of Blood Substitutes

79.4.1 Pre-NO Developments of Hemoglobin-Based Materials

Hemoglobin is an ideal oxygen carrier because it transports a large amount of hemoglobin, is not antigenic, and it loads and unloads oxygen reversibly, at room temperature, as a function of the oxygen concentration gradient that is exposed. Major commercial efforts attempted to convert hemoglobin solutions into blood substitutes, with several reaching phase III clinical trials. These initiatives focused on using chemical modifications that prevent excretion of the hemoglobin molecule by the kidney. In addition, since hemoglobin outside the RBC has a high affinity for oxygen, significant efforts were directed at correcting this problem, initially solved using agents that react at the binding site of 2,3 DPG, the allosteric factor that shifts the oxygen dissociation curve to the right [7]. In retrospect, this proved to be a futile endeavor since hemoglobin has a p50 of 12–14 mm Hg which current studies show to be ideally suited for oxygenating the tissue in anemic conditions. A result of this work was the stabilization of the tetrameric structure of the molecule, thus extending vascular retention. A definitive step was finding that much of the toxicity of hemoglobin solutions was due to the presence of RBC membrane elements, and that these could be removed by filtration [63] to produce the so-called stroma-free hemoglobin that is the basis of all hemoglobin solutions.

Polymerizing hemoglobin is another method for increasing retention time and preventing extravasation in the kidney. Glutaraldehyde is a suitable cross-linking agent; however, the polymerization reaction results in products with a distribution of molecular dimensions. Northfield Laboratories Inc., Evanston, IL developed pyridoxylated polymerized hemoglobin made from outdated human blood, PolyHeme. An extensive clinical trial in the United States dealing with trauma patients indicated that PolyHeme was not inferior to standard of care, however, neither was it superior. Furthermore, it presented adverse effects similar to those found with HemAssist; thus, production of this material was abandoned.

A novel polymerized hemoglobin product was HbOC-201 (Hemopure) manufactured by Biopure Corporation, Cambridge, MA. The novelty was that this product was made with bovine hemoglobin, which was found not to present complications due to its nonhuman origin. The significance of this is that all products depend on hemoglobin from human sources, and therefore do not provide a clear view of how the dwindling human supply and availability will be used to satisfy both the need for RBCs and the need for human hemoglobin. Hemopure is approved in South Africa for the treatment of anemic patients for the purpose of reducing the use of allogeneic RBCs. Biopure Corporation did not succeed in having the U.S. Navy carry out clinical trials with Hemopure due to an adverse-effect profile similar to that of the other products discussed, and the company was acquired by OPK Biotech LLC, Cambridge, MA that now produces the material for export to Russia, where it is approved.

A polymerized material was produced and tested by Hemosol Corporation, Mississauga, Canada (HemoLink), and recombinant hemoglobin products were produced by Optro, Somatogen, Eli Lilly, and Baxter Healthcare. All these products were found to potentially increase the risk of strokes and myocardial infarction.

Blood substitutes were critically reviewed by Chen et al. [23] who reached the conclusion: “Published animal studies and clinical trials carried out in a perioperative setting have demonstrated that these products successfully transport and deliver oxygen, but all may induce hypertension and lead to unexpectedly low cardiac outputs. Overall, these studies suggest that HBOCs resulted in only modest blood saving during and after surgery, no improvement in mortality and an increased incidence of adverse reactions” (p. 803). This assertion is supported by findings of the meta-analysis of Natanson et al. [57] who found that clinical trials associated with blood substitutes increased the risk of mortality by 30% and myocardial infarction 2.7-fold.

79.4.2 Post-NO Blood Substitutes Development and PEG–Hemoglobin

Awareness of the role of NO in blood transfusion emerged slowly. The group of Winslow and coworkers [65] was one of the first to investigate the NO-binding characteristics of different blood substitutes in an attempt to explain the unusual properties evidenced by PEG-Hb. This material was based on the PEGylation of protein concepts proposed by Abuchowski et al. [1] that were deployed to formulate an oxygen carrier by Iwashita [41]. The group of Acharya and coworkers developed a variation of the PEGylation method based on the reaction of maleimides with the thiol group of the cysteine residues of proteins, a reaction carried out at neutral pH in the refrigerator, yielding products with high homogeneity. Since Hb molecules have only two cysteine groups on their surface, additional thiol groups were introduced to obtain a product consisting of a protein core surrounded by five PEG chains of about 5 kDa.

Sangart Inc., San Diego, CA, developed a maleimide- conjugated PEG hemoglobin currently undergoing clinical trials in the United States and Europe [89]. This material, known as Hemospan, or MP4OX, is PEG-conjugated human hemoglobin. It has a low p50, in the range of 5 mm Hg, and comparatively high colloidal osmotic pressure (~50 mm Hg) at a concentration of 4 g/dL. PEG-Hb has several unusual properties. The most remarkable characteristic is that when administered in conditions of extreme hemodilution, at a circulating concentration of 1 g/dL, it produces a state of supraprefusion with high microvascular flow rates and FCD. This effect has also been observed with high-viscosity plasma expanders with the difference that these materials lower heart function, while PEG-Hb does not. The very low oxygen affinity of PEG-Hb led to the formulation of the oxygen autoregulation hypothesis, by which PEG-Hb is able to hide oxygen from the arteriolar sensors in charge of controlling the supply of oxygen by regulating blood flow.

The autoregulation hypothesis for the vasoactivity of molecular hemoglobin solutions probably accounts for some of the vasoactivity found with these solutions; however, it is difficult to envision how it operates in conditions of extreme hemodilution that present a generalized condition of hypoxia, which should be the prevailing regulatory signal controlling blood flow. The experiments of Tsai et al. [82] who measured perimicrovascular NO in conditions of extreme hemodilution show that shear stress and perivascular NO are significantly increased with PEG–albumin, a molecule with similar biophysical properties to PEG-Hb, and hyperviscous plasma. However, although PEG-Hb exhibits supraprefusion in extreme hemodilution, perivascular NO is not increased.

These contradictory results are in part explained by Kluger [49], who observed that increasing nitrite concentration in circulation increases NO bioavailability due to the reaction of hemoglobin with nitrite that oxidizes hemoglobin and produces NO [18,25]. The PEG–hemoglobin and nitrite results are especially interesting as hemoglobin conjugated with PEG produces NO from nitrite at an enhanced rate [53]. Combining these findings and considering that PEG–albumin, a virtually identical molecule to PEG-Hb, also causes supraprefusion in extreme hemodilution [91], suggests that the properties of PEG–Alb are primarily due to increased shear stress, bioavailability of NO, and other endothelial-derived mediators of vasodilatation.

PEG-Hb (bovine) stored in the carboxy state has also been used with success in treating cerebral focal ischemia [48].

79.5 Large Hemoglobin Constructs

Although the vascular wall/shear stress association in eliminating vasoactivity from molecular hemoglobin solutions is to date not fully developed, the molecular dimension/vasoactivity relationship is well established. This led to the development of hemoglobin polymers and the conjugation of hemoglobin with large colloids, an approach that was initially devised to eliminate filtration through the kidneys and vasoactivity, given the finding of a strong correlation between hemoglobin extravasation and hypertension [86,87].

Large hemoglobin polymers were developed by the group of Bucci et al. [8] on the basis of “zero-linked” hemoglobin, made by direct polymerization of hemoglobin surface amino acids instead of using cross-linking agents. This material has molecular weight in the range of 33 mDa and high oxygen affinity [34,35] and is undergoing preclinical tests with the name of OxyVita, produced by OXYVITA Inc., New Windsor, NY.

Palmer et al. used the intrinsic relaxed (R) to tense (T) quaternary state transition of hemoglobin and chemical cross-linking reagents to freeze the quaternary structure of hemoglobin either in the R (relaxed/oxygenated) state or the T (tense/deoxygenated) state. This technique generates large-molecular-weight polymerized hemoglobins with low-to-high oxygen affinities with the ability to target oxygen delivery to tissues with distinct oxygenation requirements [58]. In a different approach, Palmer et al. polymerized human Hb using a dimaleimide poly(ethylene glycol) derivative (1,11-bis(maleimido)triethylene glycol). This resulted in PolyHb with a weight-averaged molecular weight of about 1.5 mDa and oxygen affinity of about 3 mm Hg [97].

Coupling hemoglobin to a large molecule such as dextran or starch increases its molecular dimensions. Furthermore, some of these molecules are already used as plasma expanders. This approach was reported by Wong [94] who conjugated hemoglobin and dextran. In a different formulation, hemoglobin was conjugated to benzene tetracarboxylate-substituted dextran producing a hemoglobin polymer (Dex-BTC-Hb) with a p50 of 28–29 mm Hg and reduced NO scavenging [43]. Blood substitutes were also formulated by conjugating starch and hemoglobin [19,21], but these studies have not been pursued to date.

Several studies have also been directed at coupling hemoglobin with enzymes that are naturally present in RBCs such as SOD and catalase that counter the formation of oxygen-free radicals. Another approach is conjugation with nitroxides that have enzyme-like antioxidant properties. This method is used by SynZyme Technologies LLC, Irvine, CA to produce polynitroxylated human Hb, a product labeled HemoZyme.

79.6 Naturally Occurring Large Hb Molecules

A molecular hemoglobin that complies with the dimensional requirements of Sakai et al. is the oxygen transporter of the marine invertebrate *Arenicola marina* [66,96]. This respiratory oxygen transporter is an extracellular respiratory pigment of high molecular weight (~3600 kDa) that does not require chemical additions or modification. This giant extracellular O₂ carrier consists of complexes of globin and nonglobin linker chains and has a large Hb oxygen-binding capacity, carrying up to 156 molecules of oxygen when saturated. This material, termed Hemarina-M101 (M101), is used to produce the HEMOXYcarrier® (Hemarina S.A., Morlaix, France) solution being developed as an oxygen-carrying plasma expander. This material is reported to have a comparatively high binding rate for carbon monoxide, and to dissociate into subunits of 290 kDa average molecular weight in the circulation.

Lumbricus terrestris, the ubiquitous earthworm, has a stable hemoglobin of approximately 4 mDa, which circulates extracellularly, and an oxygen affinity similar to human hemoglobin. Mice and rats models have been partially exchanged with this hemoglobin showing no behavioral or physical changes. Mice retransfused with this hemoglobin show no evidence of allergic response or death [38]. Although not explicitly stated, it is likely that the principal challenge of these very large molecules is their purification.

79.7 Fluorocarbons

A fundamentally different method of transporting oxygen is provided by PFCs, materials with high gas solubility. They have very low solubility in water, and water has a very low solubility in them (on the order of 10 ppm). PFCs are synthetic hydrophobic molecules that absorb oxygen (and most gases) in direct proportion to their partial pressure. They are gases at body temperature and therefore must be

emulsified before introduction into the circulation [64,77]. The emulsifying agent is taken up and slowly broken down by the reticuloendothelial system while the PFCs *per se* are removed by exhalation.

PFCs are currently being developed in the United States by Oxygen Biotherapeutics (formerly Synthetic Blood International, Costa Mesa, CA) under the trade name Oxycte. The most important difference between this and the former product Fluosol made by the Green Cross Corporation of Japan and Alpha Therapeutics (Grifols, Los Angeles, CA, USA) is the improvement of the solubilizing agent using egg yolk phospholipids, which allows for higher concentrations of material, increasing oxygen-carrying capacity over earlier Fluosol solutions by a factor of 3 [42]. Another PFC emulsion currently in use in Russia is Perftoran (PFT) (The Scientific-Productive Company "Perftoran," Pushchino, Institutskaya, Moscow Region, Russia). This material is also used in Mexico under the trade name Perftec.

A PFC emulsion with an oxygen-carrying capacity 4–5 times greater than Fluosol was developed by Alliance Pharmaceutical Corporation (San Diego, CA). This compound, called Oxygent, did not receive approval in phase III trials due to increased incidence of stroke in treated patients.

Fluorocarbons have a linear oxygen dissociation curve, therefore, oxygen delivery in the circulation requires that it must be saturated with high arterial pO_2 s. However, they carry comparatively little oxygen at the pO_2 where blood is half-saturated in the arteriolar microcirculation. This is due to the large oxygen gradients between blood and tissue in the central circulation that cause the early release of oxygen and the overoxygenation of the central blood vessels. Nonetheless, limited microcirculatory studies made in extreme hemodilution show that fluorocarbons maintain tissue oxygenation, provided that 100% oxygen inspiration is used [12]. It should be noted, however, that hyperoxic ventilation, *per se*, is successful as treatment at the critical Hct [45].

Fluorocarbon emulsions have many effects when introduced in the circulation that have neither been well characterized nor exploited for therapeutic purposes [11]. These effects are mostly due to their gas transport properties, particularly related to NO, which cause them to have beneficial anti-inflammatory and antithrombotic effects [36,61,62] unrelated to their ability to transport oxygen. Fluorocarbons are NO scavengers; however, they are different from hemoglobin since the NO scavenged remains partially available in the form of S-nitrosothiols; so, they are, in effect, also NO transporters.

Another example is the dynamics of volatile anesthetics in the presence of fluorocarbons in the circulation. Patients scheduled for cardiopulmonary bypass underwent normovolumic hemodilution prior to surgery to a 30% Hct, with crystalloid and colloid solutions and a study group received an infusion of PFT (5 mL/kg b.w.) after hemodilution [90]. Upon infusion, the fluorocrit was ~2%. Data for this nested analysis were available for 14 controls and 13 PFT-treated persons. The intravascular presence of PFC correlated with a difference in the time under anesthesia that was 5.0 ± 0.2 h for PFT and 4.0 ± 0.3 h for control, $P = 0.003$ nonparametric t-test. These findings show that in patients with identical anesthesia management, the effects of anesthesia were prolonged in time and exhibited a more uniform response in individuals treated with PFT. This result should be directly related to the increased gas solubility and plasma life of volatile anesthetics due to the presence of PFT in blood.

It is apparent that hemoglobin loads and delivers oxygen in a completely different way than do fluorocarbons. This difference could be exploited to carry more oxygen since hemoglobin saturates at a specific pO_2 , while fluorocarbon does not. The potential synergy between carriers was explored by Chen and Palmer in bioreactors for cellular maintenance and growth, finding that oxygen transport is significantly improved by the mixture of both carriers; thus, it would be of interest to perform similar experiments in the circulation [22].

79.8 Encapsulation of Hemoglobin

Hemoglobin encapsulation was first proposed by Chang in 1964 [20]. The concept was actively developed by the U.S. Army and Navy [67]. Currently, a major effort to encapsulate hemoglobin is underway in Japan. Encapsulation offers many advantages embodied in the RBC, where the most evident is the ability to introduce a very large amount of hemoglobin in the circulation without generating high

osmotic pressures. Furthermore, encapsulation removes the problem of dealing with the colligative properties, providing more flexibility on how to formulate the viscosity of the blood substitutes solution.

The composition of the encapsulating membrane is a combination of saturated phospholipids and cholesterol. The principal design feature of these constructs is the encapsulation ratio, that is, the ratio between the amount of hemoglobin contained versus the quantity of membrane used. One of the lowest ratios attained is 1.6 for the material developed by Tsuchida and coworkers [68] and similar results have been reported by Phillips and coworkers [5]. Another design parameter is particle size. As a general rule, the half-life of liposomes in the circulation is inversely proportional to particle size, and liposomes of diameter >200 nm are rapidly eliminated by the reticuloendothelial system. Complement activation was one of the early problems observed with the use of liposomes that was mostly solved by attaching PEG to the liposome surface [81]. This also prevented RBC aggregation and improved the dispersion state of the suspension and stabilization of the vesicles.

Encapsulation of hemoglobin also allows including allosteric effectors to regulate oxygen affinity. This was done by Sakai et al. [74] who used pyridoxal 5'-phosphate allowing it to vary p50 from 5 to 150 mm Hg. This flexibility in the design led to previously referred investigations to determine the optimal p50.

Hemoglobin vesicles are unique in having been extensively studied in preclinical investigations, including the microcirculation [73]. These studies documented the lack of vasoactivity of these suspensions when used in a concentration sufficient to sustain oxygen delivery. In addition, they confirmed the ability of delivering oxygen, and the lack of RBC aggregation effects. Extensive studies have also been made to understand the possible toxicities related to the clearing of materials from the circulation [71].

Hemoglobin vesicles appear to be safe and effective blood substitutes and circumvent many of the problems and limitations associated with using molecular hemoglobin solutions. They most closely approximate the functions of an RBC. A still unresolved problem, however, is their high cost of production and lingering concerns on the effect of introducing large amounts of phospholipids and cholesterol directly into the circulation.

Hemoglobin has also been encapsulated while introducing an actin matrix into the liposome aqueous core that is of interest because of its potential long-circulating half-life, similar to that of RBCs in the circulation [51]. Nanoscale hydrogel particle-encapsulated hemoglobin [59,60] is another innovative approach for preventing the direct contact of molecular hemoglobin with the endothelium.

79.9 Plasma Expanders

Resuscitation following blood losses is not solely determined by reestablishing oxygen supply: it also requires microvascular tissue perfusion. This is seldom satisfied by the currently available plasma expanders because they were not formulated to maintain microcirculatory conditions. Similarly, blood substitute development was focused on oxygen delivery, with plasma expansion being a by-product. However, plasma expansion that leads to microvascular recovery is fundamentally necessary for enabling blood substitutes to transport oxygen.

Treating blood losses offers, in principle, the option between the reintroduction of oxygen-carrying capacity, or to substitute this with an increase in oxygen delivery capacity. Furthermore, is oxygen transport capacity restoration needed during the initial phase of hemorrhagic shock treatment? Cabrales et al. [15] acutely resuscitated 50% hemorrhaged awake hamsters with normal blood, with non-oxygen-carrying blood equilibrated with carbon monoxide, and with blood in which the hemoglobin was converted into methemoglobin, finding that resuscitation was the same in all instances. In this scenario, blood provides resuscitation by reestablishing non-oxygen-related properties, namely volume and viscosity. These two parameters translate into improved blood pressure and capillary pressure and therefore FCD.

Non-oxygen-dependent mechanisms can further improve the efficiency of the microcirculation in oxygenation and in maintaining the tissue if capillary flow is substantially increased, an effect obtained

using “active” plasma expanders. This is a new conceptualization of the function of plasma expanders that restore microvascular flow to supranormal levels, maintaining oxygen delivery by trading lowered intrinsic oxygen-carrying capacity with increased blood flow. Furthermore, the increased flow increases shear stress promoting the production of NO, creating an anti-inflammatory environment that enhances microvascular function.

Active plasma expanders that cause supraperfusion were identified in experimental studies using high-viscosity fluids based on PEG–Alb [4,33,54,92], PEG–hemoglobin [17,93], PEG–dextran [39], high-viscosity alginates [13], high-viscosity hydroxyethyl starch, and high-viscosity dextran (Dex 500 kDa) [84]. The effectiveness of these molecules was studied in the microcirculation in the exchange transfusion procedure of extreme hemodilution.

Supraperfusion is a process directly driven by heart function, which must be able to provide the necessary flow. Plasma viscosity affects heart function depending on whether we consider the heart as a tissue or an organ. Viscous plasma perfusion should improve heart function since it improves tissue perfusion; however, viewing the heart as an organ, increasing plasma viscosity increases blood viscosity and energy requirements needed for pumping fluid with greater viscosity at a higher rate. These opposing effects can be titrated by optimizing the increase in viscosity and blood flow, a result obtained using PEG–albumin, which has moderate viscogenic properties. Microvascular studies of extreme hemodilution with PEG–albumin show increased oxygen delivery and extraction when compared to other plasma expanders [17]. A similar response should take place at the heart microvasculature, explaining the superior mechano-energetic responses produced by PEG–Alb compared to higher-viscosity plasma expanders.

Supraperfusion in resuscitation provides significant benefits and postpones the use of blood transfusion. It is a property that allows replacing blood in the initial phase of resuscitation; therefore, it would also be useful in decreasing the intrinsic oxygen-carrying capacity (hemoglobin or fluorocarbon concentration) of oxygen-carrying blood substitutes. Supra perfusion by plasma expander could also be an intermediate step to increasing endurance to the effects of blood loss [52].

79.10 Summary and Conclusions

Blood substitutes remain an unfulfilled need in medicine, the most compelling reason for this being that blood no longer presents a short- and long-term safety/benefits profile commensurate with the practice of medicine. Development of a blood substitute has been difficult because of the slow advances in the understanding of biological and physical properties of blood and how these interact with blood vessels and the tissue. Significant information has recently emerged on the effect of shear stress exerted by blood on the endothelium. It is remarkable that these experiments made in endothelial cell cultures are seldom performed with blood as the perfusing fluid.

Major efforts were directed at developing oxygen carriers that could be introduced in the circulation; however, it is questionable if oxygen deficit is what a blood transfusion treats in many interventions. Experimental studies show that a problem that arises early on with blood losses is the malfunction of the microcirculation due to defects in generating shear stress on the endothelium and its biological impairment, and seldom treated by increasing oxygen tension. There is evidence that a large portion of blood transfusions today can be avoided by improved surgical techniques, and the biophysical and pharmacological increase of the tolerance to anemia. However, the need for an oxygen-transporting fluid, such as blood, remains a necessity. Hemoglobin is the unsurpassed oxygen carrier; however, it is a source of many toxicities of which the scope is not well understood. In effect, vasoactivity, *per se*, has been shown to be a function of dosage [14], and to provide beneficial effects in shock that is at times treated with vasopressors [75].

NO appears to be a major component of molecular hemoglobin performance as an oxygen deliverer in the circulation, a problem that could be dealt with by directly introducing NO in nanoparticles [9]. Furthermore, encapsulation of the oxygen carriers in a construct that mimics RBC conceptually

provides the greatest design flexibility if encapsulation ratios could be reduced and the encapsulating material rendered innocuous.

In conclusion, the design of a blood substitute is progressing as we understand and use a continuity of emerging counterintuitive concepts, such as oxygen affinity greater than blood, a shift of focus to include shear stress production, increasing plasma viscosity, accepting a moderate increase in vasoactivity, substituting increasing oxygen-carrying capacity with increased oxygen delivery, and shifting focus to include the restoration of microvascular function as a target for transfusion. Furthermore, blood substitutes should be, first and foremost, effective plasma expanders, since this can compensate for a significant portion of the oxygen gap that they are intended to correct.

Acknowledgments

This study was supported in part by the USPHS Bioengineering Research Partnership grant R24-HL 064395 (MI), R01-HL 062354 (MI), R01-HL 076182 (PC), and USAMRAA award W81XWH1120012 (AGT).

References

1. Abuchowski, A., van Es, T., Palczuk, N.C., and Davis, F.F. Alteration of immunological properties of bovine serum albumin by covalent attachment of polyethylene glycol. *J Biol Chem* 252: 3578–3581, 1977.
2. Alayash, A.I. Oxygen therapeutics: Can we tame haemoglobin? *Nat Rev Drug Discov* 3: 152–159, 2004.
3. Alayash, A.I. Setbacks in blood substitutes research and development: A biochemical perspective. *Clin Lab Med* 30(2): 381–389, 2010.
4. Assaly, R.A., Azizi, M., Kennedy, D., Amuro, C., Zaher, A., Houts, F.W., Habib, R.H., Shapiro, J.I., and Dignam, J.D. Plasma expansion by polyethylene-glycol-modified-albumin. *Clin Sci* 107: 263–272, 2004.
5. Awasthi, V.D., Garcia, D., Klipper, R., Goins, B.A., and Phillips, W.T. Neutral and anionic liposome-encapsulated hemoglobin: Effect of postinserted poly(ethylene glycol)-distearoylphosphatidylethanolamine on distribution and circulation kinetics, *J Pharmacol Exp Ther* 309: 241–248, 2004.
6. Baines, A.D., Adamson, G., Wojciechowski, P., Pliura, D., Ho, P., and Kluger, R. Effect of modifying O₂ diffusivity and delivery on glomerular and tubular function in hypoxic perfused kidney. *Am J Physiol* 274: F744–F752, 1998.
7. Benesch, R., Benesch, R., Raenthal, R., and Maeda, N. Affinity labeling of the polyphosphate binding site of hemoglobin. *Biochemistry* 11(19): 3576–3582, 1972.
8. Bucci, E., Kwansa, H., Koehler, R.C., and Matheson, B. Development of zero-link polymers of hemoglobin, which do not extravasate and do not induce pressure increases upon infusion. *Artif Cells Blood Substit Immobil Biotechnol* 35: 11–18, 2007.
9. Cabrales, P., Han, G., Roche, C., Nacharaju, P., Friedman, A.J., and Friedman, J.M. Sustained release nitric oxide from long-lived circulating nanoparticles. *Free Radic Biol Med* 49: 530–538, 2010.
10. Cabrales, P., Martini, J., Intaglietta, M., and Tsai, A.G. Blood viscosity maintains microvascular conditions during normovolumic anemia independent of blood oxygen-carrying capacity. *Am J Physiol Heart Circ Physiol* 291: H581–H590, 2006.
11. Cabrales, P., Salazar Vázquez, B.Y., Chávez Negrete, A., and Intaglietta, M. Perfluorocarbons as gas transporters for O₂, NO, CO and volatile anesthetics. *Transfusion Altern Transfusion Med* 9: 294–303, 2008.
12. Cabrales, P., Tsai, A.G., Frangos, J.A., Briceño, J.C., and Intaglietta, M. Oxygen delivery and consumption in the microcirculation after extreme hemodilution with perfluorocarbons. *Am J Physiol* 287: H320–H330, 2004.

13. Cabrales, P., Tsai, A.G., and Intaglietta, M. Alginate plasma expander maintains perfusion and plasma viscosity during extreme hemodilution. *Am J Physiol* 288: H1708–H1716, 2005.
14. Cabrales, P., Tsai, A.G., and Intaglietta, M. Balance between vasoconstriction and enhanced oxygen delivery. *Transfusion* 48: 2087–2095, 2008.
15. Cabrales, P., Tsai, A.G., and Intaglietta, M. Hemorrhagic shock resuscitation with carbon monoxide saturated blood. *Resuscitation* 72: 306–318, 2007.
16. Cabrales, P., Tsai, A.G., and Intaglietta, M. Microvascular pressure and functional capillary density in extreme hemodilution with low and high plasma viscosity expanders. *Am J Physiol* 287: H363–H373, 2004.
17. Cabrales, P., Tsai, A.G., Winslow, R.M., and Intaglietta, M. Extreme hemodilution with, P.E.G-hemoglobin vs., P.E.G-albumin. *Am J Physiol* 289: H2392–H2400, 2005.
18. Cannon, R.O., 3rd, Schechter, A.N., Panza, J.A., Ognibene, F.P., Pease-Fye, M.E., Waclawiw, M.A., Shelhamer, J.H., and Gladwin, M.T. Effects of inhaled nitric oxide on regional blood flow are consistent with intravascular nitric oxide delivery. *J Clin Invest* 108: 279–287, 2001.
19. Cerny, L.C., Cerny, E.L., Robach, J., Reath, M., and Pontero, L. A blood substitute from hydroxyethyl starch and hemoglobin. *Appl Biochem Biotechnol* 10: 151–153, 1984.
20. Chang, T.M. Semipermeable microcapsules. *Science* 146: 524–525, 1964.
21. Chávez-Negrete, A., Oropeza, M.V., Rojas, M.M., Villanueva, T., and Campos, M.G. Starch-hemoglobin induces contraction on isolated rat aortic rings. *Artif Cells Blood Substit Immobil Biotechnol* 32: 549–561, 2004.
22. Chen, G. and Palmer, A.F. Mixtures of hemoglobin-based oxygen carriers and perfluorocarbons exhibit a synergistic effect in oxygenating hepatic hollow fiber bioreactors. *Biotechnol Bioeng* 105: 534–542, 2010.
23. Chen, J.Y., Scerbo, M., and Kramer, G. A review of blood substitutes: Examining the history, clinical trial results and ethics of hemoglobin-based oxygen carriers. *Clinics (Sao Paulo)* 64: 803–813, 2009.
24. Chien, S. Molecular basis of rheological modulation of endothelial functions: Importance of stress direction. *Biorheology* 43: 95–116, 2006.
25. Cosby, K., Partovi, K.S., Crawford, J.H., Patel, R.P., Reiter, C.D., Martyr, S., Yang, B.K. et al. Nitrite reduction to nitric oxide by deoxyhemoglobin vasodilates the human circulation. *Nat Med* 9: 1498–1505, 2003.
26. Dimmeler, S., Assmus, B., Hermann, C., Haendeler, J., and Zeiher, A.M. Fluid shear stress stimulates phosphorylation of Akt in human endothelial cells: Involvement in suppression of apoptosis. *Circ Res* 83: 334–341, 1998.
27. Faivre-Fiorina, B., Caron, A., Fassot, C., Fries, I., Menu, P., Labrude, P., and Vigneron, C. Presence of hemoglobin inside aortic endothelial cells after cell free hemoglobin administration in guinea pig. *Am J Physiol* 276: H776–H770, 1999.
28. Frangos, J.A., Eskin, S.G., McIntire, L.V., and Ives, C.L. Flow effects on prostacyclin production in cultured human endothelial cells. *Science* 227: 1477–1479, 1985.
29. Friesenecker, B.E., Tsai, A.G., Martini, J., Ulmer, H., Wenzel, V., Hasibeder, W.R., Intaglietta, M., and Dunser, M.W. Arteriolar vasoconstrictive response: Comparing the effects of arginine vasopressin and norepinephrine. *Crit Care* 10: R75, 2006.
30. Gaucher-Di Stasio, C., Paternotte, E., Prin-Mathieu, C., Reeder, B.J., Poitevin, G., Labrude, P., Stoltz, J.F., Cooper, C.E., and Menu, P. The importance of the effect of shear stress on endothelial cells in determining the performance of hemoglobin based oxygen carriers. *Biomaterials* 30: 445–451, 2009.
31. Gaucher, C. and Menu, P. How to evaluate blood substitutes for endothelial cell toxicity. *Antioxid Redox Signal* 10: 1153–1162, 2008.
32. Grabowski, E.F., Jaffe, E.A., and Weksler, B.B. Prostacyclin production by cultured endothelial cell monolayers exposed to step increases in shear stress., *J Lab Clin Med* 105: 36–43, 1985.

33. Hangai-Hoger, N., Nacharaju, P., Manjula, B.N., Cabrales, P., Tsai, A.G., Acharya, S.A., and Intaglietta, M. Microvascular effects following treatment with polyethylene glycol–albumin in lipopolysaccharide-induced endotoxemia. *Crit Care Med* 34: 108–117, 2006.
34. Harrington, J.P. and Wollocko, H. Pre-clinical studies using OxyVita hemoglobin, a zero-linked polymeric hemoglobin: A review., *J Artif Organs* 13: 183–188, 2010.
35. Harrington, J.P., Wollocko, J., Kostecki, E., and Wollocko, H. Physicochemical characteristics of OxyVita hemoglobin, a zero-linked polymer: Liquid and powder preparations. *Artif Cells Blood Substit Immobil Biotechnol* 39: 12–18, 2011.
36. Heard, S.O. and Puyana, J.C. The anti-inflammatory effects of perfluorocarbons: Let's get physical. *Crit Care Med* 28: 1241–1242, 2000.
37. Hermann, C., Zeiher, A.M., and Dimmeler, S. Shear stress inhibits H₂O-induced apoptosis of human endothelial cells by modulation of the glutathione redox cycle and nitric oxide synthase. *Arterioscler Thromb Vasc Bio* 17: 3588–3592, 1997.
38. Hirsch, R.E., Jelicks, L.A., Wittenberg, B.A., Kaul, D.K., Shear, H.L., and Harrington, J.P. A first evaluation of the natural high molecular weight polymeric *Lumbricus terrestris* hemoglobin as an oxygen carrier. *Artif Cells Blood Substit Immobil Biotechnol* 25: 429–444, 1997.
39. Intaglietta, M., Torchilin, V.P., Trubetskoy, V.S., and Tsai, A.G. Methods for increasing peripheral blood circulation., U.S. Patent 6,875,423. 2005.
40. Isbister, J.P., Shander, A., Spahn, D.R., Erhard, J., Farmer, S.L., and Hofmann, A. Adverse blood transfusion outcomes: Establishing causation. *Transfus Med Rev* 25: 89–101, 2011.
41. Iwashita, Y. Hemoglobin conjugated with polyoxyethylene. In: *Artificial Red Cells*, edited by Tsuchida, E. New York, NY.: John Wiley and Sons Ltd., 1995, pp. 151–176.
42. Jahr, J.S., Nesargi, S.B., Lewis, K., and Johnson, C. Blood substitutes and oxygen therapeutics: An overview and current status. *Am J Ther* 9: 437–443, 2002.
43. Jia, Y., Wood, F., Menu, P., Faivre, B., Caron, A., and Alayash, A.I. Oxygen binding and oxidation reactions of human hemoglobin conjugated to carboxylate dextran. *Biochim Biophys Acta* 1672: 164–173, 2004.
44. Johnson, P.C. Autoregulation of blood flow. *Circ Res* 59: 483–495, 1986.
45. Kemming, G.I., Meisner, F.G., Kleen, M., Meier, J.M., Tillmanns, J., Hutter, J.W., Wojtczyk, C.J., Packert, K.B., Bottino, D., and Habler, O.P. Hyperoxic ventilation at the critical haematocrit. *Resuscitation* 56: 289–297, 2003.
46. Kerger, H., Saltzman, D.J., Menger, M.D., Messmer, K., and Intaglietta, M. Systemic and subcutaneous microvascular pO₂ dissociation during 4-h hemorrhagic shock in conscious hamsters. *Am J Physiol* 270: H827–H836, 1996.
47. Kim, S., Ong, P.K., Yalcin, O., Intaglietta, M., and Johnson, P.C. The cell-free layer in microvascular blood flow. *Biorheology* 46: 181–189, 2009.
48. Klaus, J.A., Kibler, K.K., Abuchowski, A., and Koehler, R.C. Early treatment of transient focal cerebral ischemia with bovine, PE Gylated carboxy hemoglobin transfusion. *Artif Cells Blood Substit Immobil Biotechnol* 38: 223–229, 2010.
49. Kluger, R. Red cell substitutes from hemoglobin—Do we start all over again? *Curr Opin Chem Biol* 14: 538–543, 2010.
50. Lacroix, J., Hebert, P., Fergusson, D., Tinmouth, A., Blajchman, M.A., Callum, J., Cook, D., Marshall, J.C., McIntyre, L., and Turgeon, A.F. The age of blood evaluation (ABLE) randomized controlled trial: Study design. *Transfus Med Rev* 25: 197–205, 2011.
51. Li, S., Nickels, J., and Palmer, A.F. Liposome-encapsulated actin–hemoglobin (LEACHb) artificial blood substitutes. *Biomaterials* 26: 3759–3769, 2005.
52. Li, Y. and Alam, H.B. Modulation of acetylation: Creating a pro-survival and anti-inflammatory phenotype in lethal hemorrhagic and septic shock., *J Biomed Biotechnol* 2011: 523481, 2011.
53. Lui, F.E. and Kluger, R. Enhancing nitrite reductase activity of modified hemoglobin: Bis-tetramers and their PEGylated derivatives. *Biochemistry* 48: 11912–11919, 2009.

54. Martini, J., Cabrales, P., Ananda, K., Acharya, S.A., Intaglietta, M., and Tsai, A.G. Survival time in severe hemorrhagic shock after perioperative hemodilution is longer with PEG-conjugated human serum albumin than with HES 130/0.4: A microvascular perspective. *Crit Care* 12: R54, 2008.
55. Mazzoni, M.C., Borgstrom, P., Arfors, K.E., and Intaglietta, M. The efficacy of iso- and hyperosmotic fluids as volume expanders in fixed volume and uncontrolled hemorrhage. *Ann Emerg Med* 19: 350–358, 1990.
56. Nakai, K., Sakuma, I., Ohta, T., Ando, J., Kitabatake, A., Nakazato, Y., and Takahashi, T.A. Permeability characteristics of hemoglobin derivatives across cultured endothelial cell monolayers. *J Lab Clin Med* 132: 313–319, 1998.
57. Natanson, C., Kern, S.J., Lurie, P., Banks, S.M., and Wolfe, S.M. Cell-free hemoglobin-based blood substitutes and risk of myocardial infarction and death: A meta-analysis. *JAMA* 299: 2304–2312, 2008.
58. Palmer, A.F., Zhang, N., Zhou, Y., Harris, D.R., and Cabrales, P. Small-volume resuscitation from hemorrhagic shock using high-molecular-weight tense-state polymerized hemoglobins. *J Trauma* 71(4): 798–807, 2011.
59. Patton, J.N. and Palmer, A.F. Engineering temperature-sensitive hydrogel nanoparticles entrapping hemoglobin as a novel type of oxygen carrier. *Biomacromolecules* 6: 2204–2212, 2005.
60. Patton, J.N. and Palmer, A.F. Photopolymerization of bovine hemoglobin entrapped nanoscale hydrogel particles within liposomal reactors for use as an artificial blood substitute. *Biomacromolecules* 6: 414–424, 2005.
61. Paxian, M., Keller, S.A., Huynh, T.T., and Clemens, M.G. Perflubron emulsion improves hepatic microvascular integrity and mitochondrial redox state after hemorrhagic shock. *Shock* 20: 449–457, 2003.
62. Paxian, M., Rensing, H., Geckeis, K., Bauer, I., Kubulus, D., Spahn, D.R., and Bauer, M. Perflubron emulsion in prolonged hemorrhagic shock: Influence on hepatocellular energy metabolism and oxygen-dependent gene expression. *Anesthesiology* 98: 1391–1399, 2003.
63. Rabiner, S.F., Helbert, J.R., Lopas, H., and Friedman, L.H. Evaluation of a stroma-free hemoglobin solution for use as a plasma expander. *J Exp Med* 126: 1127–1142, 1967.
64. Riess, J.G. Understanding the fundamentals of perfluorocarbons and perfluorocarbon emulsions relevant to *in vivo* oxygen delivery. *Artif Cells Blood Substit Immobil Biotechnol* 33: 47–63, 2005.
65. Rohlf, R.J., Brunner, E., Chiu, A., Gonzales, A., Gonzales, M.L., Magde, D., Magde Jr., M.D., Vandegriff, K.D., and Winslow, R.M. Arterial blood pressure responses to cell-free hemoglobin solutions and the reaction with nitric oxide. *J Biol Chem* 273: 12128–12134, 1998.
66. Rousselot, M., Delpy, E., Drieu La Rochelle, C., Lagente, V., Pirow, R., Rees, J.F., Hagege, A., Le Guen, D., Hourdez S., and Zal, F. *Arenicola marina* extracellular hemoglobin: A new promising blood substitute. *Biotechnol J* 1(3): 333–345, 2006.
67. Rudolph, A.S. Encapsulated hemoglobin: Current issues and future goals. *Artif Cells Blood Substit Immobil Biotechnol* 22: 347–360, 1994.
68. Sakai, H., Hamada, K., Takeoka, S., Nishide, H., and Tsuchida, E. Physical properties of hemoglobin vesicles as red cell substitutes. *Biotechnol Prog* 12: 119–125, 1996.
69. Sakai, H., Hara, H., Yuasa, M., Tsai, A.G., Takeoka, S., Tsuchida, E., and Intaglietta, M. Molecular dimensions of Hb-based O₂ carriers determine constriction of resistance arteries and hypertension. *Am J Physiol* 279: H908–H915, 2000.
70. Sakai, H., Okuda, N., Takeoka, S., and Tsuchida, E. Increased viscosity of hemoglobin-based oxygen carriers retards, NO-binding when perfused through narrow gas-permeable tubes. *Microvasc Res* 81: 169–176, 2011.
71. Sakai, H., Sou, K., Horinouchi, H., Kobayashi, K., and Tsuchida, E. Hemoglobin-vesicle, a cellular artificial oxygen carrier that fulfills the physiological roles of the red blood cell structure. *Adv Exp Med Biol* 662: 433–438, 2010.

72. Sakai, H., Tsai, A.G., Rohlf, R.J., Hara, H., Takeoka, S., Tsuchida, E., and Intaglietta, M. Microvascular responses to hemodilution with Hb vesicles as RBC substitutes: Influence of O₂ affinity. *Am J Physiol* 276: H553–H562, 1999.
73. Sakai, H. and Tsuchida, E. Performances of PEG-modified hemoglobin-vesicles as artificial oxygen carriers in microcirculation. *Clin Hemorheol Microcirc* 34: 335–340, 2006.
74. Sakai, H., Yuasa, M., Onuma, H., Takeoka, S., and Tsuchida, E. Synthesis and physicochemical characterization of a series of hemoglobin-based oxygen carriers: Objective comparison between cellular and acellular types. *Bioconjug Chem* 11: 56–64, 2000.
75. Salazar Vázquez, B.Y., Hightower, C.M., Martini, J., Messmer, C., Friesenecker, B., Cabrales, P., Tsai, A.G., and Intaglietta, M. Vasoactive hemoglobin solution improves survival in hemodilution followed by hemorrhagic shock. *Crit Care Med* 39(6): 1451–1466, 2011.
76. Saltzman, D., DeLano, F.A., and Schmid-Schönbein, G.W. The microvasculature in skeletal muscle. VI. Adrenergic innervation of arterioles in normotensive and spontaneously hypertensive rats. *Microvasc Res* 44: 263–273, 1992.
77. Sloviter, H.A. and Kamimoto, T. Erythrocyte substitute for perfusion of brain. *Nature* 216: 458–460, 1967.
78. Smieško, V., Lang, D.J., and Johnson, P.C. Dilator response of rat mesenteric arcading arterioles to increased blood flow. *Am J Physiol* 257: H1958–H1965, 1989.
79. Steiner, M.E., Assmann, S.F., Levy, J.H., Marshall, J., Pulkrabek, S., Sloan, S.R., Triulzi, D., and Stowell, C.P. Addressing the question of the effect of RBC storage on clinical outcomes: The Red Cell Storage Duration Study (RECESS) (Section 7). *Transfus Apher Sci* 43: 107–116, 2010.
80. Suematsu, M., DiLano, F.A., Poole, D., Engler, R.L., Miyasaka, M., Zweifach, B.W., and Schmid-Schönbein, G.W. Spatial and temporal correlation between leukocyte behavior and cell injury in postischemic rat skeletal muscle microcirculation. *Lab Invest* 70: 684–695, 1994.
81. Torchilin, V.P. and Papisov, M.I. Why do polyethylene glycol-coated liposomes circulate so long? *J Liposome Res* 4: 725–739, 1994.
82. Tsai, A.G., Acero, C., Nance, P.R., Cabrales, P., Frangos, J.A., Buerk, D.G., and Intaglietta, M. Elevated plasma viscosity in extreme hemodilution increases perivascular nitric oxide concentration and microvascular perfusion. *Am J Physiol Heart Circ Physiol* 288: H1730–H1739, 2005.
83. Tsai, A.G., Cabrales, P., and Intaglietta, M. Microvascular perfusion upon exchange transfusion with stored RBCs in normovolumic anemic conditions. *Transfusion* 44: 1626–1634, 2004.
84. Tsai, A.G., Friesenecker, B., McCarthy, M., Sakai, H., and Intaglietta, M. Plasma viscosity regulates capillary perfusion during extreme hemodilution in hamster skin fold model. *Am J Physiol* 275: H2170–H2180, 1998.
85. Tsai, A.G., Hofmann, A., Cabrales, P., and Intaglietta, M. Perfusion vs. oxygen delivery in transfusion with “fresh” and “old” red blood cells: The experimental evidence. *Transfus Apher Sci* 43: 69–78, 2010.
86. Ulatowski, J.A., Bucci, E., Nishikawa, T., Razynska, A., Williams, M.A., Takeshima, R., Traystman, R.J., and Koehler, R.C. Cerebral O₂ transport with hematocrit reduced by cross-linked hemoglobin transfusion. *Am J Physiol* 270: H466–H475, 1996.
87. Ulatowski, J.A., Nishikawa, T., Matheson-Urbaitis, B., Bucci, E., Traystman, R.J., and Koehler, R.C. Regional blood flow alterations after bovine fumaryl beta beta-crosslinked hemoglobin transfusion and nitric oxide synthase inhibition. *Crit Care Med* 24: 558–565, 1996.
88. Vamvakas, E.C. and Taswell, H.F. Epidemiology of blood transfusion. *Transfusion* 34: 464–470, 1994.
89. van der Linden, P., Gazdzik, T.S., Jahoda, D., Heylen, R.J., Skowronski, J.C., Pellar, D., Kofranek, I. et al. A double-blind, randomized, multicenter study of MP4OX for treatment of perioperative hypotension in patients undergoing primary hip arthroplasty under spinal anesthesia. *Anesth Analg* 112: 759–773, 2011.

90. Verdín-Vásquez, R.C., Zepeda-Pérez, C., Ferra-Ferrer, R., Chávez-Negrete, A., Contreras, F., and Barroso-Aranda, J. Use of Perftoran emulsion to decrease allogeneic blood transfusion in cardiac surgery: Clinical trial. *Artif Cells Blood Substit Immobil Biotechnol* 34(4): 433–454, 2006.
91. Wettstein, R., Cabrales, P., Erni, D., Tsai, A.G., Winslow, R.M., and Intaglietta, M. Resuscitation from hemorrhagic shock with MalPEG–albumin: Comparison with MalPEG–hemoglobin. *Shock* 22: 351–357, 2004.
92. Wettstein, R., Tsai, A.G., Erni, D., Lukyanov, A.N., Torchilin, V.P., and Intaglietta, M. Improving microcirculation is more effective than substitution of red blood cells to correct metabolic disorder in experimental hemorrhagic shock. *Shock* 21: 235–240, 2004.
93. Winslow, R.M., Lohman, J., Malavalli, A., and Vandegriff, K.D. Comparison of PEG-modified albumin and hemoglobin in extreme hemodilution in the rat. *J Appl Physiol* 97: 1527–1534, 2004.
94. Wong, J.T. Rightshifted dextran–hemoglobin as blood substitute. *Biomater Artif Cells Artif Organs* 16: 237–245, 1988.
95. Yu, H., Zeng, Y., Hu, J., and Li, C. Fluid shear stress induces the secretion of monocyte chemoattractant protein-1 in cultured human umbilical vein endothelial cells. *Clin Hemorheol Microcirc* 26: 199–207, 2002.
96. Zal, F., Green, B.N., Lallier, F.H., Vinogradov, S.N., and Toulmond, A. Quaternary structure of the extracellular haemoglobin of the lugworm *Arenicola marina*: A multi-angle-laser-light-scattering and electrospray-ionisation–mass-spectrometry analysis. *Eur J Biochem/FEBS* 243(1–2): 85–92, 1997.
97. Zhang, N. and Palmer, A.F. Polymerization of human hemoglobin using the crosslinker 1,11-bis(maleimido)triethylene glycol for use as an oxygen carrier. *Biotechnol Prog* 26: 1481–1485, 2010.

Further Information

Blood Substitutes. R.M. Winslow, ed. Academic Press, London, 2006.

Chemistry and Biochemistry of Oxygen Therapeutics: From Transfusion to Artificial Blood. A. Mozzarelli and S. Bettati, eds. John Wiley & Sons Inc., West Sussex, UK.

82

Artificial Skin and Dermal Equivalents

Dennis P. Orgill

*Brigham and
Women's Hospital*

Raul Cortes

*Brigham and
Women's Hospital*

Ioannis V. Yannas

*Massachusetts Institute
of Technology*

82.1	The Vital Functions of Skin.....	82-1
82.2	Current Treatment of Massive Skin Loss.....	82-2
82.3	Two Conceptual Stages in the Treatment of Massive Skin Loss by Use of Artificial Skin.....	82-4
	The Effect of Skin Loss by Depth	
82.4	Design Principles for a Permanent Skin Replacement.....	82-4
	Stage 1 Design Parameters • Stage 2 Design Parameters	
82.5	Clinical Studies of a Permanent Skin Replacement (Artificial Skin)	82-8
	Clinical Studies • Clinical Parameters Used in the Evaluation • Short-Term Clinical Evaluation of Artificial Skin • Long-Term Clinical Evaluation of Artificial Skin • Clinical Use in Burn Patients • Reconstructive Surgery • Summary	
82.6	Alternative Approaches: CEA and SE	82-12
	Defining Terms	82-13
	References.....	82-14
	Further Information.....	82-15

82.1 The Vital Functions of Skin

Skin is a vital organ keeping fluid and electrolytes in the body and providing a barrier to microorganisms. In addition, it provides a number of other important features including mechanical protection, sensation, thermal regulation, immunological functions, protection from ultraviolet light, and aesthetic functions. As such, when pathophysiologic processes lead to skin loss, as in the case of thermal burns, various degrees of physiologic embarrassment ensue. With large enough loss, death is inevitable. Surgical and medical strategies have thus focused on skin restoration in addition to optimizing resuscitative efforts. One of the more successful surgical strategies, implemented in burn care since the 1970s, has focused on the process of early excision and grafting (Quinby et al. 1981). The resultant improvement in mortality rate since its implementation has created a new need for development of reliable methods of resurfacing large areas of skin.

One conventional approach to donor site maximization uses meshing to expand *split-thickness skin grafts*. Despite this, patients with extensive burns still lack enough donor sites and require repeated harvests of the same donor site. Any methods that diminish the need for donor sites while preserving the physiologic function of skin would, therefore, prove very useful. Additionally, limiting donor sites would minimize resultant disfigurement from harvesting scars and decrease the potential for development of hypertrophic scars. Engineering a structure that both resurfaces lost skin while minimizing donor site trauma would serve as an optimal modality in overcoming the challenges of skin loss.

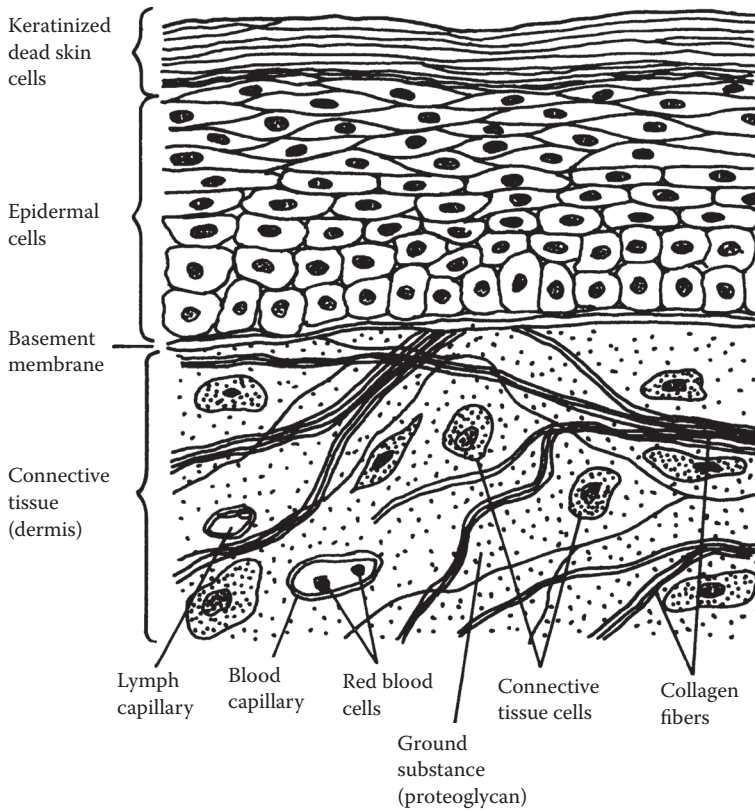


FIGURE 82.1 Schematic view of skin which highlights the epidermis, the basement membrane interleaved between the epidermis and the dermis, and the dermis underneath. Only a small fraction of the thickness of the dermis is shown. (Redrawn with permission from Darnell J.E., Lodish H.F., and Baltimore D. *Molecular Cell Biology*, 2nd Ed., Scientific American Books, New York, Chapter 23, Figure 23-2, p.905, 1990.)

Four important layers comprise normal skin. The *epidermis*, outside, is a 0.1-mm-thick sheet, comprising about 10 layers of keratinocytes at levels of maturation which increase from the inside out. The *dermis*, inside, is a 2–5-mm-thick layer of vascularized and innervated connective tissue with very few cells, mostly quiescent fibroblasts. Interleaved between the epidermis and the dermis is the *basement membrane*, an approximately 20-nm-thick multilayered membrane (Figure 82.1). A fourth layer, the *subcutis*, underneath the dermis and 0.4-mm in thickness, comprises primarily fat tissue. In addition to these basic structural elements, skin contains several appendages (*adnexa*) including hair follicles, sweat glands, and sebaceous glands. The latter are mostly embedded in the dermis, although they are derived from epidermal elements.

82.2 Current Treatment of Massive Skin Loss

The treatment of massive skin loss has traditionally required the use of agents to serve as temporary wound coverage. From as far back as 1500 BC, various temporary wound dressings have been described. Current solutions include the use of membranes or sheets fabricated from natural and synthetic polymers, skin grafts from human cadavers (homografts or *allografts*), and skin grafts from animals (heterografts or *xenografts*). Some of these modalities have been successful in allowing small or superficial injuries to heal; however, most do not provide satisfactory solutions for large, deep burns. Polymeric

membranes, which lack specific biologic activity, such as synthetic polymeric hydrogels, have to be removed after several days due to incidence of infection and lack of formation of physiologic structures. Although cadaver allografts are subject to epidermal rejection in the immunocompromised host, allograft skin can survive for longer periods (Pomahac et al. 2009). Xenografts do not integrate well into the underlying wound.

A more permanent wound solution, the split-thickness autograft, has become the standard to which other therapies are compared. When successful, the end result of the treatment of a third-degree burn with a *split-thickness autograft* is an almost fully functional skin which becomes incorporated into the patient's body and will remain alive and useful over a lifetime. Inherent to achieving success with *autografts* is a need for early excision of dead tissue and the provision of a viable wound bed to optimize the "take" of the autograft. In addition, despite a complete graft take, limitations still remain. Firstly, autografts lack hair follicles and previously present adnexae. Secondly, and perhaps more importantly, all autografts require the creation of an injury to a previously unaffected/uninjured area. Although remaining dermis eventually becomes epithelialized, it comes at the cost of synthesis of a *scar* over the *donor site*.

Meshing represents one method by which the amount of donor site needed for autografting can be minimized. In this technique, *sheet autografts* are passed through an apparatus, which cuts slits into the graft allowing expansion by several times and an immediate increase in graft coverage area. The inevitable long-term result is the scar synthesis in areas coinciding with the open slits and a resulting pattern of scar, which greatly reduces the value of the resulting new organ (Figure 82.2).

With these limitations in mind, current strategies to manage skin loss implement the use of bioengineered constructs that work by different regenerative pathways. The term "*artificial skin*" has been used to describe a cell-free membrane comprising a highly porous graft copolymer of type I collagen and chondroitin 6-sulfate, which degrades at a specific rate in the wound and regenerates the dermis in dermis-free wounds in animal models and patients (see below: *dermis regeneration template*, DRT). "*Skin equivalent*" (SE) refers to a collagen lattice which has been prepared by contraction of a collagen gel by heterologous fibroblasts ("*dermal equivalent*" or DE) and has subsequently been overlaid with a keratinocyte culture to induce formation of a mature, cornified epidermis *in vitro* prior to grafting of skin wounds. *Cultured epithelial autografts* (CEA) consist of a mature, cornified epidermis, which has been produced by culturing keratinocytes *in vitro* prior to grafting on skin wounds. The major goal of these treatments has been to replace definitively the use of the autograft in the treatment of patients with massive skin loss.



FIGURE 82.2 Comparison between treatment with the meshed autograft (R) and treatment with artificial skin (L). Autograft is usually meshed before grafting; scar forms in areas coinciding with the open slits of the autograft. Artificial skin treatment consists of grafting the excised wound bed with a skin regeneration template, followed by grafting on about day 14 with a very thin epidermal autograft. (Photo courtesy of J.F. Burke.)

82.3 Two Conceptual Stages in the Treatment of Massive Skin Loss by Use of Artificial Skin

82.3.1 The Effect of Skin Loss by Depth

The histologic depth of skin loss is a major determinant of reparative outcome. Both in reparative form and in physiologic outcome, the level of depth guides management approaches. Indeed, burn injuries are classified by the depth of skin loss. First-degree burns refer to the loss of epidermis alone; second-degree burns include loss of epidermis and a fraction of the thickness of the dermis. Lastly, third-degree burns are characterized by loss of the epidermis and the entire dermis down to muscle tissue. Each level of depth has characteristic healing patterns.

Loss of the epidermis alone often heals favorably. One clinical example is the epidermal loss that occurs after relatively mild burns such as a superficial scald burn. Experimentally, predictable epidermal loss can occur after repeated use of adhesive tape to peel off the keratinocyte layers in animal models. In either case, the long-term outcome is an apparently faithful regeneration of the epidermis by migration of epithelial cells from the wound edge, and from hair follicles roots over underlying basement membrane and dermis. Epidermal regeneration occurs spontaneously provided there is a dermal substrate over which epithelial migration and eventual anchoring to the underlying connective tissue can occur.

Loss at the level of the deep dermis has quite a different outcome. Once lost, the dermis does not regenerate spontaneously. Instead, the wound closes by contraction of the wound edges toward the center of the skin deficit and by synthesis of a scar—a distinctly different type of connective tissue.

The depth of skin loss is, therefore, a critical parameter in the design of treatment for a patient who has a skin deficit. In a human experimental scar model, Dunkin demonstrated levels of depth where the healing reaction varied experimentally. At less than 0.56 mm or 33% of the skin thickness, Dunkin showed that a scar did not form. In contrast, incisions deeper than this resulted in a permanent visible scar (Dunkin et al. 2007).

In addition to the healing patterns inherent to each level of depth, physiologic impacts are also determined by the depth and quantity of skin loss. In a massively injured patient, such as a patient with burns on 30% or greater body surface area, full-thickness injury presents an urgent problem to the clinician. Loss of skin integrity corresponds to, but is not limited to, deregulation of fluid and electrolytes homeostasis, and breakdown of the bacterial barrier. As stated above, scenarios with massive skin injury require use of temporary wound coverings designed to help the patient survive through the acute period while waiting for availability of autografts to provide permanent cover. If eventually allowed to heal without autografting, contraction and extensive scar synthesis will occur. Disfiguring scars and crippling contractures soon follow. Thus, even though a patient may have been able to survive a massive trauma, the formation of scars and contractures inhibit the resumption of an active, normal life.

82.4 Design Principles for a Permanent Skin Replacement

The analysis of the plight of the patient who has suffered extensive skin loss, presented above, leads logically to consideration of a wound cover that treats the problem in two stages. Stage 1 is the early phase of the clinical experience, in which protection against severe fluid loss and against massive infection are defined as the major design objectives. Stage 2 is the ensuing phase, in which the patient needs protection, principally against disfiguring scars and crippling contractures. Even though the conceptual part of the design is separated in two stages for purposes of clarity, the actual treatment is to be delivered concomitantly. The sequential utilization of features inherent in stages 1 and 2 in a single device can be ensured by designing the graft as a bilayer membrane (Figure 82.3). In this approach, the top layer incorporates the features of a stage 1 device, while the bottom layer delivers the performance expected from a stage 2 device. The top layer is subject to disposal after a period of about 10–15 days, during which

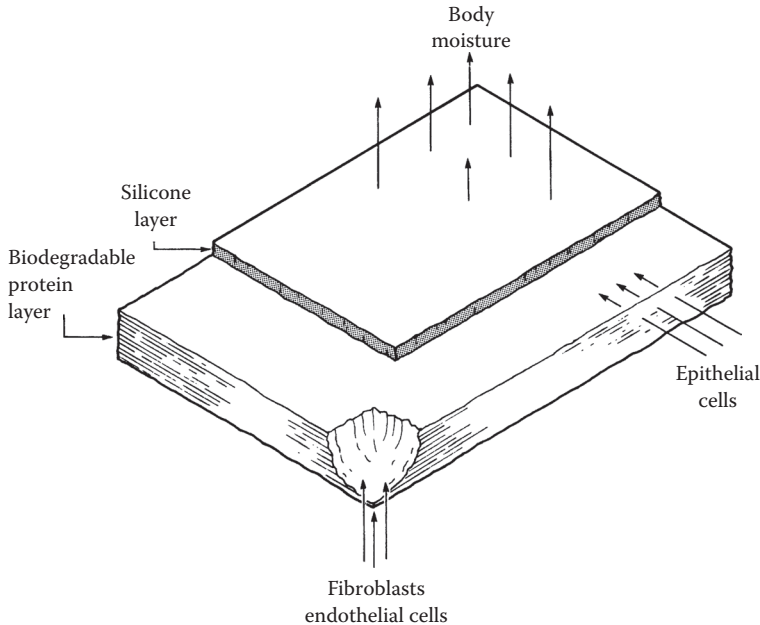


FIGURE 82.3 Schematic of the bilayer membrane which is known as artificial skin. The top layer is a silicone film which controls moisture flux through the wound bed to nearly physiologic levels, controls infection of the wound bed by airborne bacteria, and is strong enough to be sutured on the wound bed. The bottom layer is the skin regeneration template, which consists of a graft copolymer of type I collagen and chondroitin 6-sulfate, with critically controlled porosity and degradation rate. About 14 days after grafting, the silicone layer is removed and replaced with a thin epidermal autograft. The bottom layer induces synthesis of a nearly physiologic dermis and eventually is removed completely by biodegradation. (From Yannas I.V. et al. 1982. *Science* 215: 174–176.)

time the bottom layer has already induced substantial synthesis of new dermis. Following removal of the top layer, the epidermal cover is provided either by covering with a thin epidermal graft or by modifying the device (cell seeding) so that an epidermis forms spontaneously by about 2 weeks after grafting.

82.4.1 Stage 1 Design Parameters

As noted above, wound coverage devices designed to address stage 1 of skin replacement must prevent fluid loss and provide protection against infection. The overriding design approach is based on the observation that air pockets (“dead space”) at the graft–wound bed interface readily become sites of bacterial proliferation. Such sites can be prevented from forming by designing the skin replacement (i.e., graft) to displace air from the graft–wound interface by way of its inherent surface “wetness” properties (Figure 82.4). It follows that these physicochemical properties must be designed to ensure this occurs not only when the graft is placed on the wound bed but for several days thereafter. At this point, function of the graft would have moved clearly into stage 2, in which case the graft–wound bed interface has been synthesized *de novo* and the threat of dead space has been thereby eliminated indefinitely. Graft rigidity, surface characteristics, and water flux determine how well the substitute achieves the objectives of stage 1 repair.

Flexural rigidity of the graft, that is, the product of Young’s modulus and moment of inertia of a model elastic beam, must be sufficiently low to provide for a flexible graft which drapes intimately over a geometrically nonuniform wound bed surface and thus ensures that the two surfaces will be closely apposed. In practice, these requirements can be met simply by adjusting both the stiffness in tension

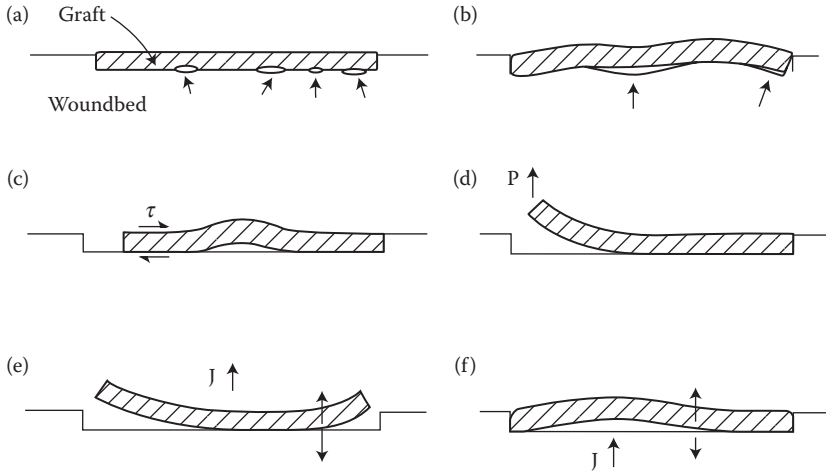


FIGURE 82.4 Certain physicochemical and mechanical requirements in the design of an effective closure for a wound bed with full-thickness skin loss. (a) The graft (cross hatched) does not displace air pockets (arrows) efficiently from the graft-wound bed interface. (b) Flexural rigidity of the graft is excessive. The graft does not deform sufficiently, under its own weight and the action of surface forces, to make good contact with depressions on the surface of the wound bed; as a result, air pockets form (arrows). (c) Shear stresses t (arrows) cause buckling of the graft, rupture of the graft-wound bed bond and formation of an air pocket. (d) Peeling force P lifts the graft away from the wound bed. (e) Excessively high-moisture flux rate J through the graft causes dehydration and development of shrinkage stresses at the edges (arrows), which cause lift-off away from the wound bed. (f) Very low-moisture flux J causes fluid accumulation (edema) at the graft-wound bed interface and peeling off (arrows). (From Yannas I.V. and Burke J.F. 1980. *J. Biomed. Mater. Res.* 14: 65-81.)

and the thickness of the graft to appropriately low values. Second, the graft will wet the wound bed if the surface energy of the graft-wound bed interface is lower than that of the air-wound bed surface, so that the graft can adequately displace air pockets from the air-wound bed surface. Although the measurement of a credible value of the surface energy is not a simple matter when the graft is based on certain natural polymers in the form of a hydrated gel, the requirement of adequate adhesion can be met empirically by chemical modification of the surface or by proper use of structural features such as porosity.

Third, the moisture flux through the graft must be maintained within bounds that are set by the following considerations. The upper bound to the moisture flux must be kept below the level where excessive dehydration of the graft occurs; without this, an alteration of the surface energy of the graft-wound bed interface would lead to loss of the adhesive bond between graft and wound bed. Further, when the graft is desiccated, shrinkage stresses develop which pull the graft away from the wound bed. If, by contrast, the moisture flux through the graft is lower than the desired low bound, water accumulates between the graft and the wound bed, and edema results with accompanying loss of the adhesive bond between the two surfaces.

An estimate of the maximum normal stress can be obtained by modeling the desiccating graft in one dimension as a shrinking elastic beam bonded to a rigid surface, is shown below

$$\sigma_m = 0.45\alpha(V_2 - V_1)E \quad (82.1)$$

In Equation 82.1, α is the coefficient of expansion of a graft which swells in water, V_1 and V_2 are initial and final values of the volume fraction of moisture in the graft, and E is Young's modulus of the graft averaged over the range $V_1 - V_2$, the latter range being presumed to be narrow.

82.4.2 Stage 2 Design Parameters

The leading design objectives in this stage are two: synthesis of new, physiologic skin and the eventual replacement of the graft with neoderms and epidermal autografts.

The lifetime of the graft, expressed as the time constant of biodegradation t_b , was modeled in relation to the time constant for normal healing of a skin incision t_h . The latter is about 25 days. In preliminary studies with animals, it was observed that when matrices were synthesized to degrade at a very rapid rate, amounting to $t_b < t_h$, the initially insoluble matrix was reduced early to a liquid-like state, which was incompatible with an effective wound closure. At the other extreme, matrices were synthesized and degraded with exceptional difficulty within 3–4 weeks, compatible with $t_b > t_h$. In these preliminary studies it was observed that a highly intractable matrix, corresponding to the latter condition, led to the formation of a dense fibrotic tissue underneath the graft, which eventually led to the loss of the bond between graft and wound bed. Accordingly, it was hypothesized that a rule of *isomorphous matrix replacement*, equivalent to assuming a graft degradation rate of order of magnitude similar to the synthesis rate for new tissue, and represented by the relation

$$\frac{t_b}{t_h} = 1 \quad (82.2)$$

would be optimal. Control of t_b is possible by adjustment of the crosslink density of the matrix. Equation 82.2 is the defining equation for a biodegradable scaffold that is coupled with, and therefore interacts with, the inflammatory process in a wound.

Migration of cells into the matrix is necessary for synthesis of new tissue. Such migration can proceed very slowly, defeating Equation 82.2, when fibroblasts and other cells recruited below the wound surface are required to wait until degradation of a potentially solid-like matrix has progressed sufficiently. An easier pathway for migration is provided by pore channels modified into the solid-like matrix. Average pore size must be at least as large as one cell diameter (about 10 μm) for ready access. Although this rationale is supported by experiment, results with animal studies have shown that not only is there a lower limit to the average pore diameter, but there is also an upper limit (see below).

Migration of cells into the porous graft can proceed only if nutrients are available to these cells. Two general mechanisms are available for transport of nutrients to the migrating cells, namely, diffusion from the wound bed and transport along capillaries that may have sprouted within the matrix (angiogenesis). Since capillaries would not be expected to form for at least a few days, it is necessary to consider whether a purely diffusional mode of transport of nutrients from the wound bed surface into the graft could immediately supply the metabolic needs of the invading cells adequately. To define this, the cell has been modeled as a reactor which consumes a critical nutrient with a rate r , in units of $\text{mol}/\text{cm}^3/\text{s}$; the nutrient is transported from the wound bed to the cell by diffusion over a distance l ; the nutrient concentration at or near the surface of the wound bed is c_0 , in units of mol/cm^3 ; and the diffusivity of the nutrient is D , in cm^2/s . The appropriate conditions were expressed in terms of a dimensionless number S , the *cell lifeline number*, which expresses the relative importance of the reaction rate for consumption of the nutrient by the cell to the rate of transport of the nutrient by diffusion alone:

$$S = \frac{rl^2}{Dc_0} \quad (82.3)$$

Equation 82.3 suggests that when $S = 1$, the critical value of the path length, l_c , corresponds to the maximum distance along which cells can migrate inside the graft without requiring angiogenesis (vascularization) for nutrient transport. The value of l_c defines the maximum thickness of graft that can be populated with cells within a few hours after grafting, before angiogenesis has had time to occur.

These conceptual objectives have been partially met by designing the graft as an analog of *extracellular matrix* (ECM) which possesses morphogenetic activity since it leads to partial regeneration of

dermis. The discovery of the specific ECM analog that possesses this activity has been based on the empirical observation that whereas the vast majority of ECM analogs apparently do not inhibit wound contraction, one of the analogs does. The activity of this analog, for which the term “regeneration template” has been coined, is conveniently detected as a significant delay in the onset of wound contraction. When seeded with (uncultured) autologous keratinocytes, an active regeneration template is capable of inducing simultaneous synthesis both of a dermis and an epidermis in the guinea pig and in the swine (Yorkshire pig). Although regeneration may seem complete, hair follicles and other skin adnexa are not formed. The resulting integument performs the two vital functions of skin, that is, control of infection and moisture loss, while also providing physiologic mechanical protection to the internal organs and, additionally, providing a cosmetic effect almost identical to that of intact skin.

The morphogenetic specificity of the DRT depends on certain structural characteristics. The overall structure is that of an insoluble, three-dimensional covalently cross-linked network. The primary structure can be described as that of a graft copolymer of type I collagen and a glycosaminoglycan (GAG) in the approximate ratio 98/2. The GAG can be either chondroitin 6-sulfate or dermatan sulfate; other GAGs appear capable of contributing approximately equal increments to morphogenetic specificity. The collagen fibers lack bonding almost completely although the integrity of the triple helical structure is retained through the network. The resistance of the network to collagenase degradation is such that approximately two-thirds of the mass of the network becomes solubilized *in vivo* within about 2 weeks. The structure of the network is highly porous. The pore volume fraction exceeds 95% while the average pore diameter is maintained in the range 20–125 μm . The regeneration template loses its activity rapidly when these structural features are flawed deliberately in control studies.

The DRT, a porous matrix unseeded with cells, induces synthesis of a new dermis and solves this old surgical problem. Simultaneous synthesis of a new, confluent epidermis occurs by migration of epithelial cell sheets from the wound edges, over the newly synthesized dermal bed. With wounds of relatively small characteristic dimension, for example, 1 cm, epithelial cells migrating at speeds of about 0.5 mm/day from each wound edge can provide a confluent epidermis within 10 days. In such cases, the unseeded template fulfills all the design specifications set above. However, the wounds incurred by a massively burned patient are typically of characteristic dimension of several centimeters, often more than 20–30 cm. These wounds are large enough to preclude formation of a new epidermis by cell migration alone within a clinically acceptable timeframe, say 2 weeks. Wounds of that magnitude can be treated by seeding the porous collagen–GAG template, before grafting, with at least 5×10^4 keratinocytes per square centimeter of wound area. These uncultured, autologous cells are extracted by applying a cell separation procedure, based on controlled trypsinization, to a small epidermal biopsy.

Mechanistic studies show that these dermal regeneration templates block contraction of wounds in a skin excision model and in peripheral nerves (complete trisection). These studies show there is extensive binding of myofibroblasts to integrin receptors within the template and that the orientation of contractile elements are dispersed in a multidirectional orientation rather than a linear orientation, as seen in scars (Yannas et al. 2011).

Details of the synthesis of the DRT, as well as those of other templates that regenerate peripheral nerves and the knee meniscus are presented elsewhere in this handbook. The DRT described in this section was first reported as a *synthetic skin* and as an artificial skin.

82.5 Clinical Studies of a Permanent Skin Replacement (Artificial Skin)

82.5.1 Clinical Studies

The skin regeneration template has been tested clinically on two occasions. In the first test, conducted during 1979–1980, one clinical center was involved and 10 severely burned patients were studied. In the second test, conducted during 1986–1987, 11 clinical centers were involved and 106 severely burned

patients were treated in a prospective, randomized manner. In each case, the results have been published in some detail. The second study led to a surgical report, a histologic report, and an immunologic report. There is now adequate information available to discuss the advantages and disadvantages of this prototype artificial skin in the treatment of the severely burned patient.

The artificial skin used in clinical studies so far, consists of the bilayer device illustrated in Figure 82.3. The outer layer is a silicone film, about 100 μm in thickness, which fulfills the requirements of stage 1 of the design (see above), and the inner layer is the skin regeneration template. In these clinical studies, this device has not been seeded with keratinocytes. Closure of the relatively large wounds by formation of an epidermis has been achieved instead by the use of a 100- μm -thin layer of the patient's epidermis (autoepidermal graft). The latter has been excised from an intact area of the patient's skin; the donor site can, however, be harvested repeatedly, since the excised epidermis regenerates spontaneously in a few days over the relatively intact dermal bed. Briefly, the entire procedure consists of preparation of the wound bed prior to grafting by excision of thermally injured tissue (*eschar*), followed by immediate grafting of the unseeded template on the freshly excised wound and ending, 3 weeks later, by replacing the outer, silicone layer of the device with a thin epidermal graft. The results of studies with a guinea pig model and a swine model have shown that seeding of the DRT with fresh, uncultured autologous keratinocytes prior to grafting leads to simultaneous synthesis of an epidermis as well as a dermis in about 2 weeks. However, definitive clinical studies of the keratinocyte-seeded template have yet to be performed.

The discussion below focuses on the advantages and disadvantages of (unseeded) artificial skin, and emerges from clinical observations during the treatment as well as from a limited number of follow-up observations extending over several years after the treatment. The controls used in the clinical studies included meshed autografts, allografts, and xenografts. Comparative analysis of the clinical data will focus on each of the two stages of treatment for the massively burned patient, that is, the early (acute) stage and the long-term stage, the conceptual basis for which has been discussed above.

82.5.2 Clinical Parameters Used in the Evaluation

The clinical parameters during the early stage of treatment (about 3 weeks) include quantification of the graft take, epidermal autograft donor thickness, epidermal autograft donor site healing time, and surgeon's qualitative assessment. Graft take is represented by the percentage of graft area, forming an adhesive bond of sufficient strength with the wound bed, that has become vascularized. In artificial skin wounds, two different measures of graft take are reported, namely, the take of the bilayer membrane onto the freshly excised wound bed, and the take of the epidermal graft applied on the neodermal bed about 3 weeks later. Donor dermis thickness is the required thickness of the epidermal autograft placed onto the neodermis. Donor site healing time represents the "cost" of the epidermal autograft. Lastly, the surgeon's overall qualitative evaluation of the treatment is compared relative to controls.

Long-term follow-up is now at least 1 year in approximately one-quarter of the patients. The long-term parameters include patients' reports of the relative incidence of nonphysiologic sensations, including itching, dryness, scaliness, lack of elasticity (lack of deformability), sweating, sensation, and erythema. The second parameter is based on the physicians' reports of the relative presence of hypertrophic scarring in the grafted area. A third parameter is the patients' evaluations of the physiologic feel and appearance of the donor sites. Finally, there is an overall evaluation of the preference of patients for a given grafted site as well as the physicians' evaluation of the same grafted site.

82.5.3 Short-Term Clinical Evaluation of Artificial Skin

The median percentage take of artificial skin was 80%, compared with the median take of 95% for all controls. Use of the Wilcoxin Rank Sum Test for the bimodally distributed data led to the conclusion that the take of artificial skin was lower than that of all controls with a p value of <0.0001 . The reported

difference reflected primarily the significantly lower take of artificial skin relative to the meshed autograft. There was no significant difference in take when artificial skin was compared with allograft (Wilcoxin Rank Sum $p > 0.10$). The take of the epidermal autograft was 86%.

Mean donor site thickness was 0.325 ± 0.045 mm for control sites and only 0.15 ± 0.0625 mm for epidermal grafts that were harvested for placement over the newly synthesized dermis; the difference was found to be significant by t test with a p value of <0.0001 . The thinner donor sites used in the artificial skin procedures healed, as expected, significantly faster, requiring 10.6 ± 5.8 days compared to 14.3 ± 6.9 days for control sites, with a p value of <0.001 by t test. It is worth noting that donor sites used in the artificial skin procedure were frequently reharvested sites from previous autografting. That is, despite the fact that artificial skin donor sites were reharvested sites (with expected slower healing times) artificial skin donor sites healed faster.

The subjective evaluation of the operating surgeons at the conclusion of the acute stage of treatment was a response to the question, "Was artificial dermis (artificial skin) advantageous in the management of this particular patient?" Sixty-three percent of the comments were affirmative, whereas in 36% of the responses, the acute (early) results were believed to be no better than by use of routine methods. The physicians who responded positively to the use of artificial skin commented on the ability to use thin donor sites that healed quickly, relative to the thicker donor sites which were harvested in preparation for an autograft. Positive comments also cited the handling characteristics of artificial skin relative to the allograft as well as the ability to close the wound without fear of rejection while awaiting healing of the donor site. Negative comments included a less-than-adequate drainage of serum and blood through the unperforated silicone sheet, the seemingly poor resistance of artificial skin to infection, and the need for a second operation.

82.5.4 Long-Term Clinical Evaluation of Artificial Skin

By 1 year after treatment, both experimental groups had undergone definitive coverage with an autograft. The experimental group differed in that the new integument was induced as a result of treatment with artificial skin; that is, the new skin represented partially regenerated dermis closed with an epidermal graft.

At 1 year, patients reported that itching was significantly less (Wilcoxin Rank Sum test $p < 0.02$) at the artificial skin site than at control sites. Dryness, scaliness, elasticity (deformability), sweating, sensation, and erythema were similar at both control and artificial skin sites. Hypertrophic scarring was reported to be less in artificial skin in 42% of sites and was reported to be equivalent between test and control sites 57% of the time. No patient reported that the artificial skin sites had more hypertrophic scar than the autografted sites. Even though donor sites that were used during treatment with the artificial skin were harvested repeatedly (recropping), 72% of patients reported that these artificial skin donor sites felt "more normal," 17% felt that there was no difference, and 11% felt that the control donor site was "more normal."

The results of the histologic study on this patient population showed that, in sites where artificial skin was used, an intact dermis was synthesized. Also, definitive closure by way of a complete epidermal layer occurred with minimal scarring. Immunologic evaluation showed that artificial skin patients had increased antibody activity to bovine skin collagen, bovine skin collagen with chondroitin sulfate, and human collagen; however, it was concluded that these increased levels of antibodies were not immunologically significant.

The overall evaluation by the patients showed that 26% preferred the new integument generated by use of artificial skin whereas 64% found that the sites were equivalent and 10% showed preference for the autografted site. Physician's overall evaluation showed that 39% preferred the artificial skin site, 45% found the sites to be equivalent, and 16% preferred the autografted site.

82.5.5 Clinical Use in Burn Patients

The take of the artificial skin was comparable to all other grafts and was inferior only to the meshed autograft. The latter showed superior take in part because meshing reduces drastically the flexural rigidity of the graft (see above), leading thereby to greater conformity with the wound bed (see Figure 82.4). The interstices in the meshed autograft also provided an outlet for drainage of serum and blood from the wound, thereby allowing removal of these fluids. By contrast, the continuity of the silicone sheet in the artificial skin accounted for increased flexural rigidity of the graft and prevented drainage of wound fluids resulting in increased incidence of fluid accumulation underneath the graft. Fluid accumulation was probably the cause of the reduced take of the artificial skin, since immediate formation of a physiochemical bond between the graft and the wound bed was thereby prevented (see Figure 82.4). The development of infection underneath artificial skin, noted by physicians in certain cases, can also be explained as originating in the layer of wound fluid, which presumptively collected underneath the artificial skin. This analysis suggests that meshing of the silicone layer of the artificial skin, without affecting the continuity of the collagen-GAG layer, could lead to improved take and probably to reduced incidence of infection.

The healing time for donor sites associated with use of artificial skin was shorter by about 4 days than that for conventionally obtained autografts. This can be explained by the reduced thickness of the epidermal graft required to close the neodermal bed. The average epidermal graft thickness reported in this study, 0.15 mm, was significantly thicker than that currently needed. Epidermal grafts, thinner by a range of 0.05–0.07 mm, that contain negligible amount of attached dermis, can be adequately obtained. Increasing familiarity of surgeons with the procedure for harvesting these thin epidermal grafts is expected to lead to harvesting of thinner grafts in future studies. The importance of harvesting a thin graft cannot be overestimated, since the healing time of the donor site decreases rapidly with decreasing thickness of harvested graft. It has been reported that the mean healing time for donor sites for artificial skin reported in the current study, about 11 days, is reduced to 4 days, provided that a pure epidermal graft, free of dermis, can be harvested.

Thicker grafts not only required increased healing time, but they also increase the risk of hypertrophic scarring at donor sites. This observation explains the higher incidence of hypertrophic scarring in donor sites associated with harvesting of autografts, since the latter were thicker by about 0.175 mm than the epidermal grafts used with the artificial skin. An additional advantage associated with use of a thin epidermal graft is the opportunity to reharvest (recropping) within a few days; this reflects the ability of epithelial tissues to regenerate spontaneously, provided there is an underlying dermal bed. When frequent recropping of donor graft is possible, the surface area of a patient that can be grafted within a clinically acceptable period increases rapidly. In the clinical study described here, a patient with deep burns, over as much as 85% body surface area, was covered with artificial skin grafts for 75 days while the few remaining donor sites were being harvested several times each.

In the long term, rarely did a patient or a physician in this clinical study prefer the new skin provided by the autograft to that provided by artificial skin treatment. This result is clearly related to the use of meshed autografts, a standard procedure in the treatment of massively burned patients. Meshing increases the wound area which can be autografted between 1.5 and 6 times, thereby alleviating a serious resource problem. However, meshing destroys the dermis as well as the epidermis; although the epidermis regenerates spontaneously and fills in the defects, the dermis does not. The long-term result is a skin site with the meshed pattern permanently embossed on it; artificial skin is a device that, in principle, is available in unlimited quantity; accordingly, it does not suffer from this problem (Figure 82.2). The result is a smooth skin surface, which was clearly preferred on average by patients and physicians alike.

It has been established that artificial skin regenerates the dermis effectively and therefore its use leads to complete inhibition of scar formation in full-thickness skin wounds. The regeneration is partial; however, skin adnexa (hair follicles, sweat glands) are not recovered.

82.5.6 Reconstructive Surgery

Use of the DRT in burns showed impressive long-term results for the softness and pliability of skin. Many surgeons have utilized these templates in a number of reconstructive cases. Iorio et al. (2011) showed that a large number of patients with diabetic foot wounds could be salvaged with the use of DRT onto freshly debrided wounds. Many case reports and retrospective case series in the literature have also used DRT successfully on small areas of exposed bone or tendon, after radiation, and following tumor resection. For large calvarial defects, the cranium can be burred down to the diploic space. Over a period of 6–8 weeks, the template is revascularized and can be subsequently closed with a skin graft. The encouraging results in the area of reconstructive surgery suggest that DRTs will have a significant role in the future in treating many complex problems involving skin loss (Janis et al. 2011).

82.5.7 Summary

Artificial skin leads to a new skin which appears similar to the patient's intact skin than does the meshed autograft. The take of artificial skin is as good as all comparative materials except for the unmeshed autograft, which is superior in this respect. Donor sites associated with artificial skin treatment heal faster, can be recropped much more frequently, and eventually heal to produce sites that look closer to the patient's intact skin than do donor sites harvested for the purpose of autografting. In comparison to the allograft, artificial skin is easier to use, has the same take, does not get rejected, and is free of the risk of viral infection associated with use of allograft.

82.6 Alternative Approaches: CEA and SE

The use of CEA has been studied clinically. In this approach, autologous epidermal cells are removed by biopsy and then cultured *in vitro* for about 3 weeks until a mature keratinizing epidermis has formed; the epidermis is then grafted onto the patient. The epithelial cells spread and cover the dermal substrate, eventually covering the entire wound. Early reports on two pediatric patients were very encouraging, describing the life-saving coverage of one-half of body surface with CEA, and the technique was eventually used in a large number of clinical centers in several countries. Later studies showed that the take of CEA was very good on partial thickness wounds but was questionable in full-thickness wounds. In particular, blisters formed within 2 weeks in areas grafted by CEA, a problem that has recurred persistently in clinical studies. The mechanical fragility of the resulting integument resulting from the use of CEA has been traced to lack three structural features that are required for formation of a physiological dermal–epidermal junction at the grafted site, namely, the 7-S domain of type IV collagen, anchoring fibrils, and rete ridges. Early studies of the connective tissue underlying the CEA grafts have shown lack of convincing dermal architecture as well as lack of elastin fibers. Currently, CEAs are frequently used in conjunction with skin allografts where the dermis is allowed to take and the epidermis (which rejects) is removed and replaced with the CEAs (Cuono et al. 1986). In another development, a SE has been prepared by populating a collagen lattice with heterologous fibroblasts, observing the contraction of the lattice by the cells and finally seeding the surface of the lattice with a suspension of epidermal cells from an autologous source or from cell banks. The latter attach, proliferate, and differentiate to form a multilayered epidermis in 7–10 days of exposure to the atmosphere, and the resulting SE is then grafted on wounds. In an early study (1988), the SE was used to partially cover full-thickness burn wounds covering over 15% of body surface area on eight patients. In every patient grafted with SE, an extensive lysis of the SE grafts was observed at the first dressing (48 h). Only in one patient, a significant percentage of take (40%) was observed 14 days after grafting. It was concluded that the SE was not completely appropriate to serve routinely as a substitute for the autograft. In a later study (1995), the wounds treated were acute, mostly the result of excision of skin cancers. Twelve patients had clinical takes at the time of

grafting and there was no evidence of rejection or toxicity following grafting with the SE. The wounds grafted with SE contracted by 10–15%, an extent larger than that observed following grafting with full-thickness skin. Biopsies of the grafted sites showed formation of scar tissue. The authors hypothesized that the SE was eventually replaced by host tissue. Recent studies of the SE have shown positive results in chronic wounds. It appears that these constructs provide an excellent coverage of the wounds and that the growth factors that are released facilitate wound closure.

Defining Terms

Adnexa: Accessory parts or appendages of an organ. Adnexa of skin include hair follicles and sweat glands.

Allograft: Human cadaver skin, usually maintained frozen in a skin bank and used to provide a temporary cover for deep wounds. About 2 weeks after grafting, the allograft is removed and replaced with autograft, which has become available by that time. Previously referred to as homograft.

Artificial skin: A bilayer membrane consisting of an upper layer of silicone and a lower layer of DRT. The template is a cell free, highly porous analog of ECM.

Autograft: The patient's own skin harvested from an intact area in the form of a membrane and used to graft an area of severe skin loss.

Basement membrane: An approximately 20-nm-thick multilayered membrane interleaved between the epidermis and the dermis.

Cell lifeline number: A dimensionless number that compares the relative magnitudes of chemical reaction and diffusion. This number, defined as S in Equation 82.3 above, can be used to compute the maximum path length, l_c , over which a cell can migrate in a scaffold while depending on diffusion alone for transport of critical nutrients that it consumes. When the critical length is exceeded, the cell requires transport of nutrients by angiogenesis in order to survive.

Cultured epithelial autografts: A mature, keratinizing epidermis synthesized *in vitro* by culturing epithelial cells removed from the patient by biopsy. A relatively small skin biopsy (1 cm²) can be treated to yield an area larger by about 10,000 in 2–3 weeks and then grafted on patients with burns.

Dermal equivalent: A term that has been loosely used to describe a device that replaces, usually temporarily, the functions of the dermis following injury.

Dermis: A 2–5-mm-thick layer of connective tissue populated with quiescent fibroblasts which lies underneath the epidermis. It is separated from the former by a very thin basement membrane. The dermis of adult mammals does not regenerate spontaneously following injury.

Dermis regeneration template: A graft copolymer of type I collagen and chondroitin 6-sulfate, average pore diameter 20–125 μm, degrading *in vivo* to an extent of about 50% in 2 weeks, which induces partial regeneration of the dermis in wounds from which the dermis has been fully excised. When seeded with keratinocytes prior to grafting, this analog of ECM has induced simultaneous synthesis both of a dermis and of an epidermis.

Donor site: The skin site from which an autograft has been removed with a dermatome.

Epidermis: The cellular outer layer of skin, about 0.1 mm thick, which protects against moisture loss and infection. An epidermal graft, for example, cultured epithelium or a thin graft removed surgically, requires a dermal substrate for adherence onto the wound bed. The epidermis regenerates spontaneously following injury, provided there is a dermal substrate underneath.

Eschar: Dead tissue, typically the result of a thermal injury, which covers the underlying, potentially viable tissue.

Extracellular matrix: A largely insoluble, nondiffusible macromolecular network, consisting mostly of glycoproteins and proteoglycans.

- Isomorphous matrix replacement:** A term used to describe the synthesis of new, physiologic tissue within a skin regeneration template at a rate that is of the same order as the degradation of the template. This relation, Equation 82.2 above, is the defining equation for a biodegradable scaffold that biologically interacts with the inflammatory process of the wound bed.
- Living dermal replacement:** A synthetic biodegradable polymeric mesh, previously cultured with fibroblasts, which is placed underneath a conventional meshed autograft.
- Meshed autograft:** A sheet autograft, which has been meshed and then expanded by a factor of 1.5–6 to produce grafts with a characteristic pattern.
- Regeneration template:** A biodegradable scaffold that, when attached to a missing organ, induces its regeneration.
- Scar:** The result of a repair process in skin and other organs. A scar is morphologically different from skin, in addition to being mechanically less extensible and weaker. The skin regeneration template induces synthesis of nearly physiologic skin rather than scar.
- Sheet autograft:** A layer of the patient's skin, comprising the epidermis and about one-third of the dermal thickness, that has not been meshed prior to grafting areas of severe skin loss.
- Skin:** A vital organ that indispensably protects the organism from infection and dehydration while also providing other functions essential to physiologic life, such as assisting in thermoregulation and providing a tactile sensor for the organism.
- Skin equivalent:** A collagen gel that has been contracted by fibroblasts cultured therein. Following culturing with keratinocyte until a cornified epidermis is formed over the contracted collagen lattice, it is grafted on skin wounds.
- Split-thickness autograft:** An autograft that is about one-half or one-third as thick as the full thickness of skin.
- Subcutis:** A layer of fat tissue underneath the dermis.
- Synthetic skin:** A term used to describe artificial skin in the early literature.
- Take:** The adhesion of a graft on the wound bed. Without adequate take, there is no physicochemical or biologic interaction between graft and wound bed.
- Xenograft:** Skin graft obtained from a different species: for example, pig skin grafted on human. Synthetic polymeric membranes are often referred to as xenografts. Previously referred to as heterograft.

References

- Boykin J.V., Jr. and Molnar J.A. 1992. Burn scar and skin equivalents. In I.K. Cohen, R.F. Diegelmann and W.J. Lindblad (Eds.) *Wound Healing*, Philadelphia, W.B. Saunders, p. 523–540.
- Burke J.F., Yannas I.V., Quinby W.C., Jr., Bondoc C.C., and Jung W.K. 1981. Successful use of a physiologically acceptable artificial skin in the treatment of extensive burn injury. *Ann. Surg.* 194: 413–428.
- Compton C.C. 1992. Current concepts in pediatric burn care: The biology of cultured epithelial autografts: An eight-year study in pediatric burn patients. *Eur. J. Pediatr. Surg.* 2: 216–222.
- Compton C.C., Gill J.M., Bradford D.A., Regauer S., Gallico G.G., and O'Connor N.E. 1989. Skin regenerated from cultured epithelial autografts on full-thickness burn wounds from 6 days to 5 years after grafting. *Lab. Invest.* 60: 600–612.
- Cuono C., Langdon R., and McGuire J. 1986. Use of cultured autografts and dermal allografts as skin replacement after burn injury. *Lancet* 1(8490): 1123–1124.
- Darnell J.E., Lodish H.F., and Baltimore D. 1990. *Molecular Cell Biology*, 2nd Ed., Scientific American Books, New York.
- Dunkin C.S., Pleat J.M., Gillespie P.H., Tyler M.P., Roberts A.H., and McGrouther D.A. 2007. Scarring occurs at a critical depth of skin injury: Precise measurement in a graduated dermal scratch in human volunteers. *Plast. Reconstr. Surg.* 119(6): 1722–1732; discussion 1733–1734.
- Eaglstain W.H., Iriondo M., and Laszlo K. 1995. A composite skin substitute (Graftskin) for surgical wounds. *Dermatol. Surg.* 21: 839–843.

- Gallico G.G., O'Connor N.E., Compton C.C., Kehinde O., and Green H. 1984. Permanent coverage of large burn wounds with autologous cultured human epithelium. *N. Engl. J. Med.* 311: 448–451.
- Hansbrough J.F., Dore C., and Hansbrough W.B. 1992b. Clinical trials of a living dermal tissue replacement placed beneath meshed, split-thickness skin grafts on excised burn wounds. *J. Burn Care Rehabil.* 13: 519–529.
- Heimbach D., Luterman A., Burke J., Cram A., Herndon D., Hunt J., Jordan M., McManus W., Solem L., Warden G., and Zawacki B. 1988. Artificial dermis for major burns. *Ann. Surg.* 208: 313–320.
- IORIO M.L., Goldstein J., Adams M., Steinberg J., and Attinger C. 2011. Functional limb salvage in the diabetic patient: The use of a collagen bilayer matrix and risk factors for amputation. *Plast. Reconstr. Surg.* 127(1): 260–7.
- Janis J.E., Kwon R.K., and Attinger C.E. 2011. The new reconstructive ladder: modifications to the traditional model. *Plast. Reconstr. Surg.*; 127(Suppl 1): 2055S–2212S.
- Michaeli D. and McPherson M. 1990. Immunologic study of artificial skin used in the treatment of thermal injuries. *J. Burn Care Rehabil.* 11: 21–26.
- Pomahac B., Garcia J.A., Lazar A.J., Tilney N., and Orgill D.P. 2009. The skin allograft revisited: A potentially permanent wound coverage option in the critically ill patient. *Plast. Reconstr. Surg.* 123(6): 1755–1758.
- Purdue G.F., Hunt J.L., Still J.M. Jr, Law E.J., Herndon D.N., Goldfarb I.W., Schiller W.R. et al. 1997. A multicenter clinical trial of a biosynthetic skin replacement, Dermagraft-TC, compared with cryopreserved human cadaver skin for temporary coverage of excised burn wounds. *J. Burn Care Rehabil.* 18: 52–57.
- Quinby W.C., Burke J.F., and Bondoc C.C. 1981. Primary excision and immediate wound closure. *Intensive Care Med.* 7(2): 71–76.
- Sabolinski M.L., Alvarez O., Auletta M., Mulder G., and Parenteau N.L. 1996. Cultured skin as a 'smart material' for healing wounds: experience in venous ulcers. *Biomaterials* 17: 311–320.
- Stern R., McPherson M., and Longaker M.T. 1990. Histologic study of artificial skin used in the treatment of full-thickness thermal injury. *J. Burn Care Rehabil.* 11: 7–13.
- Tompkins R.G. and Burke J.F. 1992. Artificial Skin. *Surg. Rounds* October: 881–890.
- Waserman D., Scotterer M., Toulon A., Cazalet C., Marien M., Cherruau B., and Jaffray P. 1988. Preliminary clinical studies of a biological skin equivalent in burned patients. *Burns* 14: 326–330.
- Yannas I.V. and Burke J.F. 1980. Design of an artificial skin I. Basic design principles. *J. Biomed. Mater. Res.* 14: 65–81.
- Yannas I.V., Burke J.F., Warpehoski M., Stasikelis P., Skrabut E.M., Orgill D., and Giard D.J. 1981. Prompt, long-term functional replacement of skin. *Trans. Am. Soc. Artif. Intern. Organs* 27: 19–22.
- Yannas I.V., Orgill D.P., and Burke J.F. 2011. Template for skin regeneration. *Plast. Reconstr. Surg.* 127(Suppl 1): 60S–70S.

Further Information

- Bell E., Erlich H.P., Buttle D.J., and Nakatsuji T. 1981. Living skin formed *in vitro* and accepted as skin-equivalent tissue of full thickness. *Science* 211: 1052–1054.
- Bell E., Ivarsson B., and Merrill C. 1979. Production of a tissue-like structure by contraction of collagen lattices by human fibroblasts of different proliferative potential *in vitro*. *Proc. Natl Acad. Sci. USA* 76: 1274–1278.
- Boyce S.T. and Hansbrough J.F. 1988. Biologic attachment, growth, and differentiation of cultured human keratinocytes on a graftable collagen and chondroitin 6-sulfate substrate. *Surgery* 103: 421–431.
- Eldad A., Burt A., and Clarke J.A. 1987. Cultured epithelium as a skin substitute. *Burns* 13: 173–180.
- Green H., Kehinde O., and Thomas J. 1979. Growth of cultured human epidermal cells into multiple epithelia suitable for grafting. *Proc. Natl Acad. Sci. USA* 76: 5665–5668.
- Langer R. and Vacanti J.P. 1993. Tissue engineering. *Science* 260: 920–926.

- O'Connor N.E., Mulliken J.B., Banks-Schlegel S., Kehinde O., and Green H. 1981. Grafting of burns with cultured epithelium prepared from autologous epidermal cells. *Lancet* 1: 75–78.
- Woodley D.T., Briggaman R.A., Herzog S.R., Meyers A.A., Peterson H.D., and O'Keefe E.J. 1990. Characterization of 'neo-dermis' formation beneath cultured human epidermal autografts transplanted on muscle fascia. *J. Invest. Dermatol.* 95: 20–26.
- Woodley D.T., Peterson H.D., Herzog S.R., Stricklin G.P., Bergeson R.E., Briggaman R.A., Cronce D.J., and O'Keefe E.J. 1988. Burn wounds resurfaced by cultured epidermal autografts show abnormal reconstitution of anchoring fibtils. *J. Am. Med. Assoc.* 259: 2566–2571.
- Yannas I.V. et al. 1982. Wound tissue can utilize a polymeric template to synthesize a functional extension of the skin. *Science* 215: 174–176.
- Yannas I.V., Burke J.F., Gordon P.L., and Huang C. 1977. Multilayer membrane useful as synthetic skin, US Patent no. 4,060,081, November 29.
- Yannas I.V., Lee E., Orgill D.P., Skrabut E.M., and Murphy G.F. 1989. Synthesis and characterization of a model extracellular matrix that induces partial regeneration of adult mammalian skin. *Proc. Natl Acad. Sci. USA* 86: 933–937.

VII

Drug Design, Delivery Systems, and Devices

Yong Wang

University of Connecticut

- 83 Physiological Barriers to Drug Transport** *Fan Yuan* 83-1
Introduction • Drug Transport within Tissues • Summary • References
- 84 Nucleic Acid Aptamers in Drug Delivery** *Mark R. Battig, Jing Zhou, and Yong Wang*..... 84-1
Introduction • Aptamer Discovery • Applications of Aptamers in Drug Delivery • Summary • References
- 85 Dendrimers for Drug Delivery** *Giridhar Thiagarajan and Hamidreza Ghandehari*..... 85-1
Introduction • Types of Dendrimers • Synthesis • Drug Delivery with Dendrimers • Targeting of Dendritic Drug Carriers • Routes of Administration • Nucleic Acid Delivery • Challenges and Future Directions • Acknowledgments • References
- 86 Noninvasive Targeted Protein and Peptide Drug Delivery** *Pradeep K. Karla, Durga K. Paturi, Nanda K. Mandava, Animikh Ray, Sulabh Patel, Ranjana Mitra, and Ashim K. Mitra*..... 86-1
Introduction • Oral Delivery of Proteins and Peptides • Buccal Delivery • Vaginal Delivery of Insulin • Transdermal Delivery • Rectal Delivery of Protein Drugs • Conclusion • References
- 87 Environment-Responsive Hydrogels for Drug Delivery** *Byung Kook Lee, Jong-Ryoul Kim, Kinam Park, and Yong Woo Cho* 87-1
Introduction • Thermoresponsive Hydrogels • pH-Responsive Hydrogels • Light-Responsive Hydrogels • Electroresponsive Hydrogels • Glucose-Responsive Hydrogels • Enzyme-Responsive Hydrogels • Inflammation-Responsive Hydrogels • Antigen-Responsive Hydrogels • Magneto-responsive Hydrogels • Ultrasound-Responsive Hydrogels • Redox/Thiol-Responsive Hydrogels • Concluding Comments • Abbreviation • References

88 Biodegradable PLGA Scaffolds for Growth Factor Delivery *Yusef Khan and Cato Laurencin*..... **88-1**
Introduction • Elements of Drug Delivery Related to Tissue Engineering • Tissue Engineering Scaffolds as Drug Delivery Vehicles • Musculoskeletal Tissue Engineering • Conclusion • References

Physiological Barriers to Drug Transport

83.1	Introduction	83-1
83.2	Drug Transport within Tissues	83-3
	Microcirculation • Transvascular Transport • Interstitial Transport	
83.3	Summary.....	83-12
	References.....	83-12

Fan Yuan

Duke University

83.1 Introduction

A drug that works *in vitro* may not be effective in treating the same disease *in vivo* if it cannot reach its targets in tissues or its concentration in target tissue is inadequate. An increase in dose is a simple way to raise the drug concentration and improve the biodistribution in the body, but it is often limited by normal tissue tolerance of the drug. Therefore, a better approach is to enhance the specificity of drug delivery. In the past few decades, scientists and engineers have made significant progresses in the development of novel drug and gene delivery vehicles.¹⁻⁶ These vehicles have been used to improve drug solubility and stability and alter the biodistribution in the body. The release of drugs and genes can be controlled through design and fabrication of novel materials that are biodegradable and responsive to external stimuli or local environmental factors (e.g., pH, temperature, and specific enzymes). Advances in molecular and cell biology research have also provided unique opportunities for targeted delivery, which is achieved through coating vehicles or conjugation of drugs with ligands that can bind to specific molecules in cells and tissues.^{7,8}

For both drugs and their delivery vehicles, transport in tissues is an important concern for improving drug delivery.⁹⁻¹² The rate of transport depends on physical and chemical properties of drugs, design of delivery vehicles, as well as molecular and cellular structures in tissues. Therefore, significant progresses have been made in the identification of physiological barriers that can hinder the transport, and in the development of strategies that can overcome or circumvent the barriers. The significance of each barrier to transport is drug-dependent. For example, oxygen has been observed to improve radiation therapy of cancer. The main barrier to oxygen delivery to tumors is the chaotic vascular network, which exhibits a high resistance to convection of oxygen in the blood.¹³ Physiological barriers in the extravascular space are negligible since oxygen can diffuse freely through cells and extracellular matrix (ECM) and the diffusion distance is less than a few hundred micrometers. As a result, oxygen delivery is limited only to regions with high blood supply, causing a fraction of tumor tissues to be hypoxic.¹⁴ However, drug delivery with pegylated liposomes is less dependent on tumor microcirculation since the liposomes have a long circulation half-life.¹⁵ Liposome transport to tumor cells is hindered mainly by cells and ECM in the extravascular space.¹⁶ These examples illustrate that delivery of different therapeutic agents may encounter different physiological barriers.

The barriers to drug transport also depend on whether the drug is administered systemically or locally. In local delivery, drugs are either injected/infused directly into target tissues or released from genetically engineered cells or synthetic devices implanted in the vicinity of targets.¹⁻⁵ Local delivery bypasses blood circulation and avoids transvascular transport, thereby significantly reducing systemic clearance and toxicity of drugs. The drawback of local delivery is, of course, the low efficiency for treating systemic diseases, for example, micrometastases, which are small tumors resulting from cells disseminated from primary tumors. Treatment of micrometastases requires drugs to circulate systemically through oral administration, intravenous injection, or injection into other tissues in the body, such as muscle and peritoneal cavity, where drug molecules can enter the systemic circulation after they are absorbed by microvessels. In the blood, drugs may bind to plasma proteins and be delivered to the liver, in which they may be metabolized. In some cases, the metabolites are active forms of drugs. Drug carriers in the liver can be internalized by Kupffer cells, a specialized macrophage lining the wall of sinusoids. Drugs in the systemic circulation are mainly cleared by the liver and kidney, and the mechanisms of clearance depend on physical and chemical properties of drugs or drug delivery vehicles. The plasma half-life of drugs (i.e., the time required for plasma concentration to be reduced to one half of its initial value) varies from a few seconds to a few days. Therapeutic agents remaining in the blood will move into target tissues. Most tissues can be divided into three compartments: vascular space for blood and lymph flow, interstitium, and cellular space. Exceptions include cartilage and cornea that are avascular under normal conditions. It is also interesting to know that there are no functional lymph microvessels in tumor tissues.^{17,18} The fractional volume of each compartment is tissue-dependent. The typical values in some normal organs are listed in Table 83.1. In solid tumors, the size of interstitial compartment is tumor-dependent.¹⁹ It is low (<15%) in human meningiomas and high (>50%) in rat fibrosarcomas.^{19,20} The average volume fraction of vascular space is less than 10% in most solid tumors,^{13,21-23} except some very bloody ones (e.g., hemangiomas). It may decrease with the growth of tumors.

Extensive research has been performed on drug and gene transport in solid tumors. Therefore, tumor tissues are frequently used in this chapter as examples to illustrate the general principles involved in drug and gene delivery. It should be pointed out that some unique transport phenomena are not covered in this chapter. They include transport across the barriers formed by the stratum corneum in transdermal drug delivery,^{28,29} the corneal epithelium in ocular drug delivery,³⁰ and the intestinal epithelium in oral drug delivery.^{31,32} These transport processes are tissue specific and have been reviewed extensively elsewhere. To simplify the discussion, the word “drug” used in this chapter may refer to a cytotoxic molecule, a therapeutic gene, a drug or gene carrier, or any pharmaceutical product unless it is specified in the text since the distinction among them is unimportant in terms of transport.

TABLE 83.1 Volume Fractions of Interstitial Fluid (IFV) and Blood (BV) in Rat Tissues

Tissue	IFV	BV	References
Lung	0.188	0.300	24
Heart	0.100	0.200	24
Skeletal muscle	0.120	0.026	24
Skin	0.302	0.019	24
Bone	0.115	0.042	25
Gut	0.094	0.188	24
Liver	0.163	0.125	24
Kidney	0.200	0.240	24
Brain	0.200	0.033	26,27

83.2 Drug Transport within Tissues

Drug delivery from the systemic circulation system to molecular targets in the nucleus of cells requires convective transport in blood vessels, transvascular transport, interstitial transport, transport across the plasma membrane, intracellular transport, and transport across the nuclear envelope (Figure 83.1). These transport processes will inevitably be hindered by various physiological barriers. The hindrance will reduce the efficiency of drug delivery but may also provide opportunities for improving the specificity of drug delivery to a target tissue (e.g., tumor tissues). The focus of this chapter is to discuss steps in each of the transport processes in the extracellular space as well as the barriers associated with them.

83.2.1 Microcirculation

Blood microcirculation in normal tissues is regulated by various mechanisms.³³ The rate of blood flow determines the rate of convective transport of a systemically administered drug to specific regions in tissues. For drugs with a plasma half-life shorter than the time scales for transvascular and interstitial transport, the blood flow is the rate-limiting factor.^{34,35} These drugs are often small molecules that do not bind to plasma proteins or at least within a short period after the intravenous injection when the molar concentration of the drugs is much higher than the total concentration of plasma proteins.

Nanoparticles that can be recognized by the reticuloendothelial system (RES), consisting of macrophages mainly in the liver and the spleen, also have a short half-life in the systemic circulation but their delivery to target tissues is nearly independent of the rate of blood flow. This is because transvascular and interstitial transport of nanoparticles is slow. A common approach to improving the delivery is to prolong their plasma half-life through coating the surface with polyethylene glycol (PEG)^{15,36,37} or other hydrophilic polymers.³⁸ The coated polymers create a steric barrier that blocks the absorption of plasma proteins, or the opsonins, on the surface of nanoparticles. Therefore, it is possible to increase the half-life from a few minutes to a few days.

Tumor microcirculation is unique in several aspects. It is much less regulated compared with normal microcirculation. Its vasculature is chaotic and heterogeneous in terms of microvessel length, diameter, and spatial distribution.¹³ It contains loops, shunts, and trifurcation of microvessels. In addition, there exist bifurcation of small vessels into larger ones and tiny vessels that do not allow red blood cells (RBCs) to pass through. The chaotic vasculature causes a heterogeneous blood supply. The vascular network also varies with time due to angiogenesis and vascular remodeling.^{39–41} Microscopically, RBC

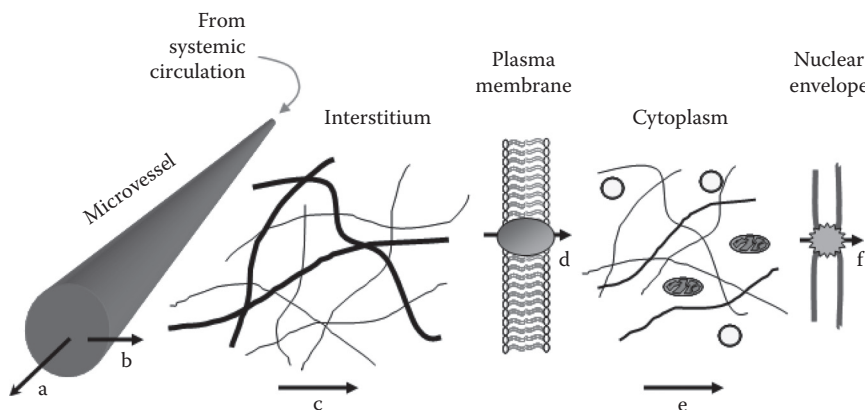


FIGURE 83.1 Schematic of transport processes and associated physiological barriers to systemic drug delivery. (a) Microcirculation, (b) transvascular transport, (c) interstitial transport, (d) transmembrane transport, (e) cytoplasmic transport, (f) transport through nuclear pores.

velocity varies both spatially and temporally in a random manner.^{13,14,42} There is no correlation between microvessel diameter and RBC velocity.^{13,43,44} In some microvessels, even the direction of blood flow changes with time, a phenomenon rarely observed in normal vessels.⁴² Because of these unique features, tumor microcirculation can be a rate-limiting factor even for drugs or drug carriers with long plasma half-lives.¹⁶ Therefore, improving blood flow is necessary for enhancing drug delivery to solid tumors, especially to poorly perfused regions.

83.2.2 Transvascular Transport

Transvascular transport is a necessary step in systemic drug delivery. The transport is limited by structures of microvessel wall, such as glycocalyx, endothelium, and basement membrane. Transvascular transport is not a rate-limiting step for delivery of small drugs (<1000 in molecule weight) in most tissues except in the brain and retina where endothelial cells are connected with tight junctions that block passive diffusion of drug molecules. Transport across the blood–brain barrier (BBB) and the blood–retina barrier (BRB) requires transmembrane carriers.^{45–47}

Macromolecules and nanoparticles with a size comparable to or larger than albumin cannot diffuse easily across the wall of continuous capillaries in normal tissues because the cutoff size of pores in the vessel wall is close to 10 nm.⁴⁸ However, the barrier to diffusion is compromised when the endothelium is treated with growth factors or vasoactive agents (e.g., histamine and vascular endothelial growth factors (VEGFs)),^{49–51} or damaged through exposure to ultrasound and circulating microbubbles.^{52,53} The wall of discontinuous capillaries, observed in the liver, granulation tissues, and solid tumors, contains large pores that allow macromolecules and some nanoparticles to pass through the wall. The pore size is on the order of 100 nm in liver sinusoids,⁵⁴ but is heterogeneous and tissue-dependent in solid tumors. It is less than 1 nm in some primary brain tumors⁴⁴ but >100 nm in other tumors.^{43,55–57} The maximum cutoff size of pores reported in the literature is ~2 μm, observed in a mouse mammary carcinoma.⁵⁶ Pores in isolated regions can be larger than RBCs since hemorrhage is often observed in tumors. These large pores provide pathways for extravasation of macromolecules and nanoparticles.

The difference between tumor and normal microvessels discussed above provides a unique opportunity to specifically deliver macromolecules and nanoparticles to solid tumors.^{10,11,43,58} For example, pegylated liposomes with a diameter of 100 nm accumulate preferentially in perivascular regions in solid tumors (see Figure 83.2a), but no extravasation is observed in normal subcutaneous tissues (see Figure 83.2d).¹⁶ Liposome uptake is only observed in a few endothelial cells in postcapillary and collecting venules in the subcutaneous tissues. These observations demonstrate that liposomes can be used to reduce drug accumulation in normal tissues and increase drug delivery to solid tumors. A case in point is the cancer chemotherapy with doxorubicin, a potent small-molecule drug for treating various tumors. When the free drug is injected systemically, it causes cardiomyopathy in a dose-dependent manner, presumably due to doxorubicin-induced apoptosis and senescence of myocytes.^{59,60} The toxicity problem can be radically reduced if doxorubicin is encapsulated in liposomes before it is injected into patients because liposomes are too large to cross the microvessel wall in the heart.⁶¹

Transvascular transport involves both convection and diffusion. Under normal physiological conditions, diffusion is the dominant mode of transport for small molecules and convection is more important for transport of macromolecules and nanoparticles.¹⁹ However, interstitial fluid pressure (IFP) at the center of solid tumors is elevated uniformly, and is approximately equal to the microvascular pressure.⁶² In addition, the osmotic pressure difference across the microvessel wall is minimal because of the vascular leakiness. Therefore, the driving force for convection is negligible in the middle of solid tumors. At the periphery, convection can be the dominant mode of transvascular transport of macromolecules due to the rapid decrease in the IFP.⁶³ The convection can make systemically administered macromolecules preferentially accumulate at the edge of tumors (see also the discussion on interstitial transport).^{58,64}

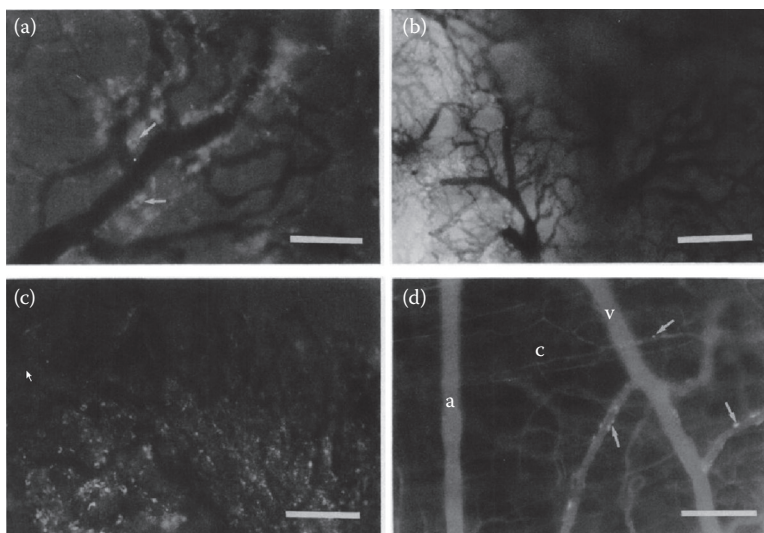


FIGURE 83.2 Extravasation of liposomes in normal and tumor tissues. The fluorescently labeled liposomes are shown as bright pixels and some of them are indicated by the arrows. Panel (a) shows that liposomes accumulate only in perivascular regions in solid tumors. Bar, 100 μm . Panel (b) shows that two vascular networks on the surface of a tumor have different patterns of liposome accumulation, indicating that microvascular permeability is heterogeneous in solid tumors. Bar, 400 μm . Panel (c) shows that extravasated liposomes are mostly located near the roots of capillary sprouts (bottom), while the capillary sprouts per se (top) are nearly impermeable to liposomes. Bar, 200 μm . Panel (d) shows that liposome accumulation in normal subcutaneous tissues occurs only in endothelial cells in postcapillary and collecting venules (6–25 μm in diameter). The letters “a,” “c,” and “v” represent arteriole, capillary, and venule, respectively. Bar, 100 μm . (Reprinted from Yuan F et al. *Cancer Res* 1994; 54: 3352–3356. With permission.)

Diffusion flux across the microvessel wall is proportional to the concentration difference and the proportionality constant is called microvascular permeability coefficient. The value of the permeability has been quantified in both normal and tumor tissues.^{43,65} It depends upon physical and chemical properties of drugs and structures of the microvessel wall. It decreases with increasing size of drugs, and is high for positively charged drugs and low for negatively charged ones if the sizes of these drugs are approximately the same.^{66,67}

Similar to the blood supply discussed above, microvascular permeability in tumors is heterogeneous. On average, the permeability in tumors is higher than that in normal tissues,^{9,43,58} which is part of the enhanced permeability and retention (EPR) effect proposed by Maeda in 1986.⁵⁸ However, there exist tumor regions where the microvessel wall is impermeable to macromolecules and nanoparticles. For example, the fluorescently labeled liposomes accumulate only in certain perivascular regions in solid tumors after intravenous injection (see Figure 83.2a).¹⁶ Even along the same vessel, the distribution of liposomes is nonuniform. Mechanisms of the heterogeneity are multifactorial and not well understood.⁴³

83.2.3 Interstitial Transport

Interstitial transport of small molecules is rapid and encounters little resistance from tissues, which is similar to transvascular transport discussed above. However, interstitial transport of small molecules over a distance that is significantly longer than the space between two adjacent microvessels ($\sim 200 \mu\text{m}$) is prohibited because of the absorption by microvessels.^{68,69} The absorption problem is critical for local

drug delivery as drug molecules have to diffuse from the site of administration to other regions in target tissues. Previous studies have shown that the maximum distance of diffusion in brain tissues is a few millimeters from the surface of controlled-release devices implanted.^{68,70} To increase the diffusion distance, investigators have proposed to conjugate small-molecule drugs with macromolecular carriers which are less likely to be absorbed by microvessels.⁶⁸ The trade-off of this approach to blocking drug absorption is reduced rate of interstitial diffusion.

The issue of interstitial barriers is important for delivery of macromolecules and nanoparticles, such as antibodies, liposomes, and gene delivery vectors,^{7,8,71,72} regardless of administration routes and techniques. The barriers block the transport to targets that are a few cell layers away from the microvessel wall at the site of administration. For example, the antibody-mediated drug delivery has shown promising results in treating leukemia and lymphoma,^{73,74} but is less effective in treating solid tumors, partly because of the limited interstitial penetration of antibodies.⁹ In a recent study, Kirpotin et al. showed that the amount of drugs delivered into solid tumors using immunoliposomes, which could bind specifically to breast tumor cells overexpressing HER2 receptor, was approximately the same as that with nontargeted liposomes,⁷⁵ indicating that the ligands on immunoliposomes could not reach the targets on tumor cells. This is not surprising since liposomes accumulate only in perivascular regions in solid tumors after intravenous injection (see Figure 83.2a). The maximum depth of interstitial penetration from the microvessel wall is $\sim 30 \mu\text{m}$ over a 2-day period.^{16,43} Even for macromolecules that are smaller than liposomes, the interstitial penetration is limited. Dreher et al. have shown that dextran molecules spread uniformly in tumor tissues if the molecular weight is 3300 (see Figure 83.3).⁷⁶ The uniformity decreases with increasing the size of dextran molecules. For dextran with a molecular

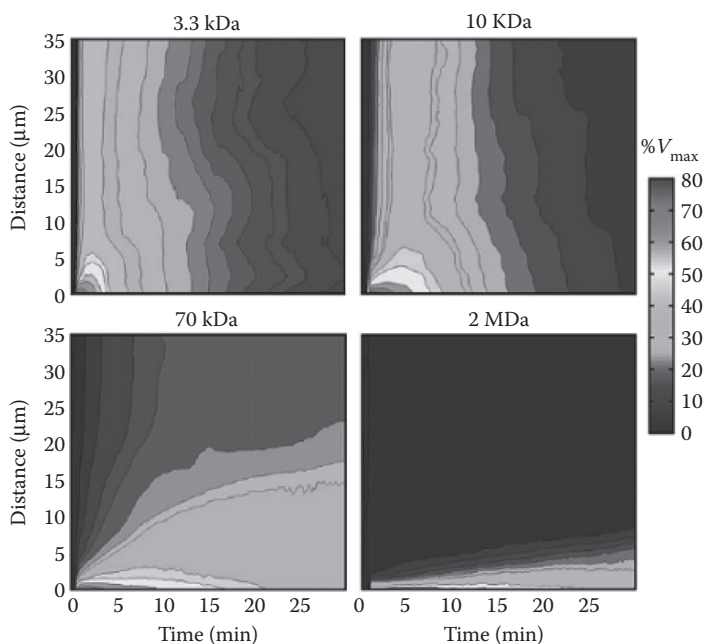


FIGURE 83.3 Average interstitial penetration of fluorescently labeled dextran in tumor tissues. The molecular weight of dextran is 3.3 kDa, 10 kDa, 70 kDa, or 2 MDa. At various time points after intravenous injection, the interstitial concentration of dextran, relative to the maximum intravascular concentration ($\%V_{\text{max}}$), is measured at each location in three-dimensional tissues using confocal microscopy. Meanwhile, the distance of that location to the nearest microvessel wall is quantified. The concentration data with the same distance and time are averaged and displayed in the pseudocolor maps. (Reprinted from Dreher MR et al. *J Natl Cancer Inst* 2006; **98**: 335–344. With permission.)

weight of 2,000,000, the average penetration depth in the extravascular space is less than the diameter of a tumor cell.

The physiological barriers make interstitial diffusion impractical for macromolecules and nanoparticles. Therefore, novel strategies have to be developed to overcome the barriers. In general, the strategies can be divided into two different categories. One is to alter tissue structures for reducing resistance to interstitial transport; another is to increase driving force for transport. Applications of the strategies will depend on mechanisms of transport and drug interactions with tissues in the interstitial space.

83.2.3.1 Convection

Convection is a mechanism of transport. It depends on interstitial fluid velocity that is tissue-dependent and may vary with location within a tissue. Few velocity data have been reported in the literature, but the average velocity in a given tissue is likely to be less than 1 $\mu\text{m/s}$ under normal, physiological conditions because the interstitial fluid is drained by lymphatic system and the estimated lymph velocity in microvessels is between 0.1 and 2 $\mu\text{m/s}$.⁷⁷ Chary and Jain⁷⁸ have examined interstitial fluid velocity in granulation tissues and VX2 mammary carcinoma grown in rabbit ear chambers,⁷⁸ which are thin tissue preparations ($\sim 40 \mu\text{m}$) allowing the use of the fluorescence recovery after photobleaching (FRAP) technique. The authors observed that the average velocities in both tissues were $\sim 0.6 \mu\text{m/s}$. In three-dimensional (3-D) solid tumor models, the IFP is elevated uniformly throughout the tissues except within a thin layer ($< 0.5 \text{ mm}$) near the surface of tumors.⁹ The pressure elevation abolishes the driving force for fluid flow at the center of tumors.^{62,63,79} At the periphery, the IFP decreases to zero within the thin tissue layer, which induces fluid flow from tumor to surrounding tissues. Based on a tissue-isolated tumor model, Butler et al. showed that the rate of fluid oozing out of a tumor is 0.14–0.22 mL/h-g tissue.⁸⁰ The outward flow carries drugs that have already been delivered into the interstitial space, thereby reducing the drug concentration in the tumor. The decrease in IFP at the tumor periphery also enhances the convection of drugs across the microvessel wall as discussed in Section 83.2.2. The combined effects of convection in microvessel wall and interstitial space cause macromolecules to accumulate preferentially at the tumor periphery,^{58,64} especially within a short period after intravenous injection. This pattern of drug distribution may not be beneficial for tumor treatment but can be exploited for tumor diagnosis when contrast agents for imaging are delivered systemically.

Convection in the center of tumors can be enhanced through intratumoral infusion. The technology is also called convection-enhanced delivery (CED) in the literature.^{81–83} Most studies on convective transport in solid tumors are related to intratumoral infusion.^{20,84–86} In addition, the CED has been used for improving the treatment of brain-related diseases^{81,83,87–90} because systemic drug delivery to brain tissues is blocked by the BBB. The infusion establishes a pressure gradient that drives fluid flow from the infusion needle tip to surrounding tissues. The ratio of the absolute velocities between drug and interstitial fluid is defined as the retardation coefficient.^{91,92} It is always smaller than unity since drug molecules are more likely to be hindered by tissue structures than water molecule. The retardation coefficients under specific experimental conditions have been measured.^{85,91,93} The data depend on flow rate as well as solute/tissue interactions.

The distribution volume of infused therapeutic agents is a function of time, infusion pressure, and flow rate.^{81,82,85,94} The ratio of distribution volume versus infused volume may decrease with increasing the infusion pressure, presumably due to infusion-induced tissue deformation that makes interstitial space more resistant to fluid flow.⁸⁵ Bobo et al. infused solutes into cat brain with a constant flow rate.⁸¹ They observed an inverse relationship between the distribution volume and molecular weight of the compound, implying that larger molecules are impeded by tissue structures more readily than smaller molecules. However, Lieberman et al. found no size dependence for molecule distribution in the rat brain because other parameters, such as concentration and infusion rate, may also affect the distribution volume.⁸³ Kroll et al. studied the effects of concentration and infusion rate on delivery of monocrystalline iron oxide nanocompounds (MIONs) in the brain.⁹⁴ The authors demonstrated that high concentration and low flow rate might produce a greater distribution volume. They also noted that

the infusion rate dependence of the distribution volume was more noticeable at higher concentrations. These relationships, nonetheless, were not corroborated by a later study by Chen et al.,⁸² who found that the distribution volume of ¹⁴C-albumin was independent of the concentration or the flow rate when the drug solution was diluted up to 4 times and the infusion rate was increased from 0.1 to 5 $\mu\text{L}/\text{min}$. The conflicting results discussed above suggest that drug infusion is a complex process, in which the infusion conditions are nonlinearly and dynamically coupled with physiological parameters, such as hydraulic conductivity, interstitial pressure, and retardation coefficient. Therefore, it is important for future studies to investigate how the physiological parameters change with infusion conditions.

83.2.3.1.1 Hydraulic Conductivity

Hydraulic conductivity, K , is a measure of fluid permeability of tissues. It is defined in Darcy's law as a ratio of fluid flow rate versus pressure gradient. The value of K depends upon the viscosity of the fluid and structures of tissues. During intratumoral infusion, the viscosity can be experimentally controlled, but tissue structures may change with time and infusion conditions due to tissue deformation.^{20,86,95,96}

The hydraulic conductivity has been investigated in different normal and tumor tissues.^{20,84,95-101} The investigation involves interstitial perfusion that will inevitably alter tissue structures through dehydration or edema,^{92,99} volume compression or expansion,^{95,98,99} and opening or closing of fluid channels in the tissue.⁹⁹ Thus, only the apparent hydraulic conductivity (K_{app}) can be measured experimentally.

The value of K_{app} is tissue-dependent. It varies from $3.1 \times 10^{-8} \text{ cm}^2/\text{cmH}_2\text{O}/\text{s}$ in Morris hepatoma 5123¹⁰⁰ to $1.8 \times 10^{-6} \text{ cm}^2/\text{cmH}_2\text{O}/\text{s}$ in a murine mammary carcinoma (MCAIV).¹⁰¹ The variation is likely to be due to the difference in tissue structures rather than experimental methods because the same methods have also been used to quantify K_{app} in a human colon adenocarcinoma (LS174T) in three different studies and the data from these studies are nearly identical.^{84,101} In addition to tissue structures, K_{app} depends on perfusion conditions. Guyton et al. demonstrated that K_{app} in the subcutaneous tissue of abdominal wall was extremely sensitive to the perfusion pressure.⁹⁹ A small pressure change from negative to positive values, relative to the atmosphere, could lead to five orders of magnitude increase in K_{app} . The increase in K_{app} was likely to be due to tissue deformation-induced opening of water channels within the tissue. Zakaria et al. demonstrated that the value of K_{app} in an unconstrained muscle in the abdominal wall could be increased from 0.9×10^{-5} to $4.7 \times 10^{-5} \text{ cm}^2/\text{min}/\text{mmHg}$ when the hydrostatic pressure in the peritoneal cavity was increased from 1.5 to 8 mmHg, which caused stretching of muscle tissues.⁹⁶ However, K_{app} in the same muscle but mounted to a plexiglass was decreased by one order of magnitude over the same range of pressure change, because the muscle tissues were compressed in the experiment. The study indicated again that tissue deformation had a significant effect on K_{app} . Effects of tissue deformation on K_{app} have also been observed in the articular cartilage,⁹⁵ although it is much less deformable than abdominal tissues. The dependence of K_{app} on tissue deformation has a direct impact on intratumoral infusion of drugs and genes. The infusion establishes an interstitial pressure gradient that may cause either compression or expansion of tumor tissues. Zhang et al. compared K_{app} in tumors under two *ex vivo* experimental conditions.²⁰ In the first experiment, tumor slices were perfused in the direction normal to the surface, that is, one-dimensional (1-D) perfusion. In the second experiment, tumor chunks were perfused radially through a needle inserted into the center of tumors. In both experiments, there existed a threshold pressure below which the perfusion of tissues could not be achieved, suggesting that the interstitial space was not well connected prior to the perfusion. To establish the connection, adequate tissue deformation induced by the perfusion is required. However, further deformation of tissues may either increase or decrease K_{app} . During the 1-D perfusion, tumor tissues were compressed by the pressure difference across the slice and K_{app} decreased with the perfusion pressure. During the radial perfusion, the perfusion caused tumor tissues to be compressed radially but stretched circumferentially. When the values of K_{app} in the same tissues but from different experiments were compared at the perfusion pressure of 163 cmH_2O , the difference was 80,260-fold.²⁰ The large discrepancy was caused by the difference in tissue deformation. Similar experiments had been performed *in vivo* in three different tumor models.⁸⁶ In this study, it was observed that the dependence

of K_{app} on the perfusion pressure was also influenced by the collagen concentration in tissues. K_{app} was a bell-shaped function of the pressure in tumors with high collagen content but increased monotonically with increasing the pressure in other tumors. These observations were consistent with the results from numerical simulations based on a poroelastic model, suggesting that the nonlinear relationships between K_{app} and the pressure were determined by the ways of tissue deformation.

83.2.3.1.2 Challenges in Intratumoral Infusion of Drugs

The discussions above demonstrate that direct infusion or CED can significantly enhance transport of macromolecules and nanoparticles in tissues. However, there are two challenges in applications of this technology for cancer treatment. One is that the insertion of the infusion needle may cause damage of blood vessels, which allows the infused drugs to leak out during the infusion.^{85,102} For example, >70% of adenoviral vectors infused into solid tumors for gene therapy were observed to be in the liver within 10 min after intratumoral infusion of these vectors.¹⁰³ The mechanisms of virus dissemination is infusion-induced convective transport of viral vectors into leaky tumor microvessels. One strategy to block the dissemination is to mix the viral vectors with polymeric solutions with high viscosity or with the solutions of temperature-sensitive polymers that are liquid at low temperature and gel at the body temperature.^{104,105} These polymeric solutions will enter the leaky vessels during the infusion and thus block the convection of viral vectors in tumor microvessels. Results from the previous studies showed that the polymeric solutions could reduce the virus concentration in the liver by two to three orders of magnitude.^{104,105} The second challenge in the CED is the leak-out of drugs through infusion-induced cracks in tumor tissues. It happens in most infusion experiments when the pressure is higher than a threshold level (e.g., 50 cmH₂O).⁸⁵ The cracks are more likely to form in locations with weak structures, which are necrotic regions and blood pockets at the macroscopic level,⁸⁵ and abnormal ECM at the microscopic level.^{101,106} The cracks create low resistance pathways for the flow of infused fluid, which will carry molecules or nanoparticles to leak out of the tumors.^{84,85,102} At present, there are no good solutions to solve this problem.

83.2.3.2 Diffusion

Diffusion is driven by a concentration gradient. As mentioned above, diffusion is the dominant mode of transport for small molecules and convection is more efficient for large molecule transport in normal tissues. In solid tumors, both small and macromolecules rely on diffusion because of the uniformly elevated IFP. For a given concentration gradient, the rate of diffusion is determined by the diffusion coefficient (D).^{9,77,107,108} It depends on a number of factors: molecular properties of solutes, structures of tissues, and temperature. The temperature dependence is less critical for drug delivery, since tissue temperature is stable and close to 37°C. The value of D is sensitive to tissue structures,^{101,108} such as the size and the volume fraction of available pores, the tortuosity of diffusion pathways, and the connectedness of pores. Diffusion of macromolecules is relatively faster in tissues with low collagen content¹⁰⁸ or tissues treated with collagenase.⁹⁷ However, there is no correlation between D and the concentration of total or sulfated glycosaminoglycans.⁹⁷ The dependence of D on molecular properties of solutes is complicated and often influenced by tissue structures. Empirically, effects of molecular weight (M_r) on D can be approximated by a power function, $D = a(M_r)^{-b}$, where a and b are functions of charge and configuration of solutes as well as structures of tissues.¹⁹ Effects of tissue structures on D increase with the size of solutes. For example, the ratio of diffusion coefficients in tissue versus water (D/D_0) is close to unity for oxygen,¹⁰⁹ but is reduced to 0.1–0.3 for albumin and IgG in tumor tissues.^{107,108} For larger molecules and nanoparticles, this ratio is expected to approach zero because their sizes are close to or larger than the cutoff size of pores in tissues.^{55,56,76,110} This phenomenon has significant ramifications for nanoparticle delivery (see [Figures 83.2](#) and [83.3](#)). As discussed above, liposomes have been used as vehicles for systemic delivery of drugs and genes.^{16,111,112} Liposomes may improve delivery, reduce toxicity, and provide selectivity of these agents, because they preferentially extravasate in solid tumors through leaky vasculature.^{16,56,113} However, once the liposomes extravasate in tumors, they can only diffuse a short distance (<30 μm) in the interstitial space and then are trapped in perivascular regions.^{16,43} The limited

penetration may cause a large fraction of drugs released from nanoparticles to be carried away by the blood circulation, which may reduce the efficacy of anticancer treatment although the perivascular accumulation of liposomal drugs can be exploited for antivascular therapy of cancer.^{114,115} The penetration problem is also an important concern in gene therapy since gene delivery vectors are nanoparticles as well, which cannot diffuse to cells that are not adjacent to the microvessel wall. As a result, only a tiny fraction of cells in target tissues can be transfected or infected by the vectors.

83.2.3.3 Available Volume Fraction

The rates of diffusion and convection in the interstitial space are closely related to the available space for fluid and solute transport. The available space is a fraction of the interstitial fluid space, and its size determines the maximum distribution volume of drugs in tissues. The value of available volume fraction (K_{AV}) depends on the size of drugs and the connectedness of the available pores in tissues.¹¹⁶ K_{AV} of different solutes have been quantified in different tissues (see Table 83.2). When drug concentrations in the body reach a steady state, K_{AV} can be determined by the concentration ratio between tissues and the plasma in *in vivo* studies or surrounding solution in *ex vivo* studies.¹¹⁷

83.2.3.4 Effects of Binding on Interstitial Transport

Targeted drug delivery often relies on binding of drugs or drug carriers to specific receptors or structures in tissues. The binding may improve the specificity of drug delivery but hinder the interstitial transport. For example, antibodies developed for targeting tumor-associated antigens have limited interstitial penetration in solid tumors after intravenous injection.⁹ The binding-induced resistance to interstitial transport has been coined the phrase “binding-site barrier.”¹³¹ The barrier can be lowered through saturation of available binding sites by increasing the dose of antibodies,¹³¹ or reduction in binding avidity.^{107,132} Therefore, there is a trade-off between interstitial penetration and delivery specificity.

Binding to extravascular structures can also be nonspecific, such as charge–charge interactions. The binding avidity depends on the number of bonds formed between the molecule of interest and fixed charges in tissues. Although the binding affinity between each pair of charges may be several orders of magnitude lower than antibody–antigen binding, the binding avidity between polyelectrolyte (e.g., DNA) and ECM can be higher. The high avidity may significantly reduce polyelectrolyte transport in tissues. Henshaw et al. have shown that diffusion of plasmid DNA (pDNA) is extremely slow in 0.1% (w/v) collagen gel compared to that in 0.1% agarose gel,¹³³ presumably due to the binding of pDNA to the free lysine groups on the collagen.¹³⁴ To improve pDNA transport, pulsed electric field has been applied to tumor tissues for breaking the chemical bonds between pDNA and ECM.^{12,133,135,136} As a result, the rate of pDNA transport is increased by several orders of magnitude, compared to the pure diffusion rate.

83.2.3.5 Tissue Dependence of Interstitial Transport

Tissue structures can significantly influence the interstitial transport of drugs and genes through different mechanisms. They can be generally classified into four different categories: structural, physical, chemical, and cellular, which may function alone or couple together to affect interstitial transport. Structural factors include the size and connectedness of pores available for interstitial transport as discussed above. The pore structures can change with time due to ECM remodeling and cell turnover.

Physical factors include mechanical stresses and temperature. In normal tissues, convection is driven by the pressure difference between blood and lymph vessels. In muscles, convection can also occur due to tissue contraction/relaxation. In solid tumors, there are no functional lymphatics and the IFP is elevated uniformly in the center. Thus, interstitial convection is negligible. In addition to the fluid pressure, drug transport may depend on solid stresses that can be elevated in regions with rapidly proliferating tumor cells,^{137–139} causing collapse of tumor microvessels and an increase in vascular resistance to convection in the blood. Temperature change can directly affect the diffusion coefficient and the hydraulic conductivity since both parameters are inversely proportional to the viscosity of interstitial fluid that decreases with increasing temperature. The temperature in tissues is stable and close to 37°C under normal conditions

TABLE 83.2 Available Volume Fraction (K_{AV}) of Macromolecules in Normal and Tumor Tissues

Tissue	Molecule	r^a	K_{AV}	References
Annulus fibrosus	PEG	3.2	0.14	118
Aorta	Albumin	3.6	0.11–0.20	119
	PEG	3.2	0.20	118
Cartilage	IGF-I	1.7	0.57	120
	Myoglobin	2.0	0.1	121
	Chymotrypsinogen	2.8	0.1	121
	Hemoglobin	2.8	0.01–0.03	122
	Ovalbumin	2.8	0.03	121
	Albumin	3.6	0.001–0.01	121
	Transferrin	3.7	0.001–0.01	121
	IgG	5.6	0.001–0.01	121
	PEG	3.2	0.02–0.09	118
	Dextran	2.6	0.1–0.2	122
	Dextran	5.2	0.03–0.07	122
Cecum	Albumin	3.6	0.15	123
Colon	Albumin	3.6	0.12	123
Cornea	PEG	3.2	0.00	118
Ileum	Albumin	3.6	0.10	123
Jejunum	Albumin	3.6	0.11	123
Nucleus pulposus	PEG	3.2	0.00	118
Muscle	Albumin	3.6	0.20	124
	Albumin	3.6	0.04	123
Paw	Albumin	3.6	0.10	123
Skin	Albumin	3.6	0.14–0.22	125
	PEG	3.2	0.6	118
Subcutis	Albumin	3.6	0.16	126
Tendon	Albumin	3.6	0.14	123
	PEG	3.2	0.46	118
	Albumin	3.6	0.22	127
Umbilical cord	Myoglobin	2.0	0.68	128
	Albumin	3.6	0.41	128
	Thyroglobulin	3.8	0.44	128
	Catalase	5.2	0.28	128
	Transferrin	8.2	0.0	128
	Dextran	8.0	0.62	129
	Dextran	11.7	0.55	129
	Dextran	16.0	0.42	129
Vitreous body	PEG	3.2	0.00	118
Fibrosarcoma	Albumin	3.6	0.13	117
	Dextran	2.6	0.25	117
	Dextran	3.7	0.33	117
	Dextran	5.2	0.33	117
	Dextran	6.9	0.14	117
	Dextran	36.8	0.04	117

Source: McGuire S, Zaharoff D, Yuan F. *Pharmaceutical Perspectives of Nucleic Acid-Based Therapeutics*. Taylor & Francis Books: London, 2002, pp 434–454.

^a r (nm) is the hydrodynamic radius of the molecules; it is either obtained from the literature or calculated based on the molecular weight of dextran.¹²⁹

but it can be manipulated through either hypo- or hyperthermia treatment, which can be exploited for targeted delivery of drugs and genes.

Chemical environment may affect interstitial transport through various mechanisms. The local pH affects the net charge of drugs, which in turn will influence the diffusion coefficient. The pH is approximately neutral in most normal tissues but acidic in solid tumors. The acidic environment has been exploited for targeted drug delivery across the plasma membrane of tumor cells or controlled release of drugs from polymeric devices and nanoparticles.¹⁴⁰⁻¹⁴³ The chemical environment also determines the half-life of drugs in the interstitial space through degradation, chemical modification, and binding to other molecules. Furthermore, several families of matrix-degrading enzymes and their inhibitors regulate ECM remodeling in tissues. The remodeling will change structures of interstitial space and thus affect interstitial transport.

Populations of cells in a given tissue may change with time due to cell proliferation or death as well as invasion of cells (e.g., macrophages) from other tissues. The change can have a significant impact on interstitial transport. In solid tumors, cell death can cause a decrease in IFP and solid stresses and an increase in interstitial fluid space, which may improve drug delivery. In previous studies, apoptotic agents (e.g., paclitaxel) have been used to pretreat tumors before the injection of macromolecular drugs or nanomedicines. The treatment, called tumor priming,¹⁴⁴ only kills a tiny fraction of tumor cells but significantly reduces the IFP¹³⁹ and improves interstitial transport of macromolecules and nanoparticles in solid tumors.^{144,145} In contrast, rapid proliferation of tumor cells can lead to an increase in solid stresses in tissues, which may decrease drug delivery locally when microvessels are squeezed by surrounding tumor cells.¹³⁷ In addition to the cell density change, molecules internalized or secreted by cells may alter the chemical environment that will in turn affect the interstitial transport of drugs as discussed above. Furthermore, cellular uptake of drugs will accelerate drug clearance in the interstitial space and affect concentration gradient of drugs, which is a driving force for diffusion.

83.3 Summary

Extracellular transport is an important issue in drug delivery. Especially, it is critical for drugs, such as most anticancer drugs, that have small therapeutic windows. This is because resistance to drug transport in target tissues can lead to either low efficacy in treatment or severe toxicity in normal tissues, depending on the dose of administration. The rate-limiting factor for transport of small-molecule drugs is blood supply in target tissues whereas the challenge to delivery of macromolecules and nanoparticles is the depth of interstitial penetration. The mechanisms of transport include convection and diffusion, which are dependent on administration methods, drug properties, and tissue environments. For charged molecules, the mechanisms of transport may also include electrophoresis and iontophoresis when tissues are exposed to external electric fields. Quantitative analyses of these mechanisms have led to the development of novel strategies for overcoming physiological barriers to drug transport. Further advances in drug transport research will rely on the development of new imaging technologies and contrast agents that can be used for more accurate measurement of transport parameters in tissues, and for monitoring drug delivery in individual patients.¹⁴⁶⁻¹⁴⁹ The new technologies can also be combined with sophisticated mathematical models for optimization of drug delivery.

References

1. Byrne ME, Park K, Peppas NA. Molecular imprinting within hydrogels. *Adv Drug Deliv Rev* 2002; **54**: 149–161.
2. Goldberg M, Langer R, Jia X. Nanostructured materials for applications in drug delivery and tissue engineering. *J Biomater Sci Polym Ed* 2007; **18**: 241–268.
3. Saltzman WM, Olbricht WL. Building drug delivery into tissue engineering. *Nat Rev Drug Discov* 2002; **1**: 177–186.

4. Yasuhara T, Date I. Intracerebral transplantation of genetically engineered cells for Parkinson's disease: Toward clinical application. *Cell Transplant* 2007; **16**: 125–132.
5. Young S, Wong M, Tabata Y, Mikos AG. Gelatin as a delivery vehicle for the controlled release of bioactive molecules. *J Control Release* 2005; **109**: 256–274.
6. Peer D, Karp JM, Hong S, Farokhzad OC, Margalit R, Langer R. Nanocarriers as an emerging platform for cancer therapy. *Nat Nanotechnol* 2007; **2**: 751–760.
7. Dang JM, Leong KW. Natural polymers for gene delivery and tissue engineering. *Adv Drug Deliv Rev* 2006; **58**: 487–499.
8. Platt VM, Szoka FC, Jr. Anticancer therapeutics: Targeting macromolecules and nanocarriers to hyaluronan or CD44, a hyaluronan receptor. *Mol Pharm* 2008; **5**: 474–486.
9. Jain RK. Delivery of molecular and cellular medicine to solid tumors. *Adv Drug Deliv Rev* 1997; **26**: 71–90.
10. Jain RK. Delivery of molecular medicine to solid tumors: Lessons from *in vivo* imaging of gene expression and function. *J Control Release* 2001; **74**: 7–25.
11. Wang Y, Yuan F. Delivery of viral vectors to tumor cells: Extracellular transport, systemic distribution, and strategies for improvement. *Ann Biomed Eng* 2006; **34**: 114–127.
12. Henshaw JW, Yuan F. Field distribution and DNA transport in solid tumors during electric field-mediated gene delivery. *J Pharm Sci* 2008; **97**: 691–711.
13. Jain RK. Determinants of tumor blood flow: A review. *Cancer Res* 1988; **48**: 2641–2658.
14. Dewhirst MW, Cao Y, Moeller B. Cycling hypoxia and free radicals regulate angiogenesis and radiotherapy response. *Nat Rev Cancer* 2008; **8**: 425–437.
15. Papahadjopoulos D, Allen TM, Gabizon A, Mayhew E, Matthay K, Huang SK et al. Sterically stabilized liposomes: Improvements in pharmacokinetics and antitumor therapeutic efficacy. *Proc Natl Acad Sci U S A* 1991; **88**: 11460–11464.
16. Yuan F, Leunig M, Huang SK, Berk DA, Papahadjopoulos D, Jain RK. Microvascular permeability and interstitial penetration of sterically stabilized (stealth) liposomes in a human tumor xenograft. *Cancer Res* 1994; **54**: 3352–3356.
17. Fukumura D, Jain RK. Tumor microvasculature and microenvironment: Targets for anti-angiogenesis and normalization. *Microvasc Res* 2007; **74**: 72–84.
18. Padera TP, Kadambi A, di Tomaso E, Carreira CM, Brown EB, Boucher Y et al. Lymphatic metastasis in the absence of functional intratumor lymphatics. *Science* 2002; **296**: 1883–1886.
19. Jain RK. Transport of molecules in the tumor interstitium: A review. *Cancer Res* 1987; **47**: 3039–3051.
20. Zhang XY, Luck J, Dewhirst MW, Yuan F. Interstitial hydraulic conductivity in a fibrosarcoma. *Am J Physiol Heart Circ Physiol* 2000; **279**: H2726–H2734.
21. Yuan F, Leunig M, Berk DA, Jain RK. Microvascular permeability of albumin, vascular surface area, and vascular volume measured in human adenocarcinoma LS174T using dorsal chamber in SCID mice. *Microvasc Res* 1993; **45**: 269–289.
22. Willett CG, Boucher Y, di Tomaso E, Duda DG, Munn LL, Tong RT et al. Direct evidence that the VEGF-specific antibody bevacizumab has antivascular effects in human rectal cancer. *Nat Med* 2004; **10**: 145–147.
23. Bremer C, Mustafa M, Bogdanov A, Jr., Ntziachristos V, Petrovsky A, Weissleder R. Steady-state blood volume measurements in experimental tumors with different angiogenic burdens a study in mice. *Radiology* 2003; **226**: 214–220.
24. Khor SP, Mayersohn M. Potential error in the measurement of tissue to blood distribution coefficients in physiological pharmacokinetic modeling. Residual tissue blood. I. Theoretical considerations. *Drug Metab Dispos* 1991; **19**: 478–485.
25. Tsuji A, Yoshikawa T, Nishide K, Minami H, Kimura M, Nakashima E et al. Physiologically based pharmacokinetic model for beta-lactam antibiotics I: Tissue distribution and elimination in rats. *J Pharm Sci* 1983; **72**: 1239–1252.

26. Perles-Barbacaru AT, Lahrech H. A new Magnetic Resonance Imaging method for mapping the cerebral blood volume fraction: The rapid steady-state T1 method. *J Cereb Blood Flow Metab* 2007; **27**: 618–631.
27. Sykova E, Nicholson C. Diffusion in brain extracellular space. *Physiol Rev* 2008; **88**: 1277–1340.
28. Mitragotri S, Edwards DA, Blankschtein D, Langer R. A mechanistic study of ultrasonically-enhanced transdermal drug delivery. *J Pharm Sci* 1995; **84**: 697–706.
29. Williams AC, Barry BW. Penetration enhancers. *Adv Drug Deliv Rev* 2004; **56**: 603–618.
30. Ghate D, Edelhauser HF. Barriers to glaucoma drug delivery. *J Glaucoma* 2008; **17**: 147–156.
31. Blanchette J, Kavimandan N, Peppas NA. Principles of transmucosal delivery of therapeutic agents. *Biomed Pharmacother* 2004; **58**: 142–151.
32. Goldberg M, Gomez-Orellana I. Challenges for the oral delivery of macromolecules. *Nat Rev Drug Discov* 2003; **2**: 289–295.
33. Segal SS. Regulation of blood flow in the microcirculation. *Microcirculation* 2005; **12**: 33–45.
34. Bischoff KB, Dedrick RL, Zaharko DS, Longstreth JA. Methotrexate pharmacokinetics. *J Pharm Sci* 1971; **60**: 1128–1133.
35. Jain RK. Delivery of novel therapeutic agents in tumors: Physiological barriers and strategies. *J Natl Cancer Inst* 1989; **81**: 570–576.
36. Lasic DD, Martin FJ, Gabizon A, Huang SK, Papahadjopoulos D. Sterically stabilized liposomes: A hypothesis on the molecular origin of the extended circulation times. *Biochim Biophys Acta* 1991; **1070**: 187–192.
37. Croyle MA, Chirmule N, Zhang Y, Wilson JM. PEGylation of E1-deleted adenovirus vectors allows significant gene expression on readministration to liver. *Hum Gene Ther* 2002; **13**: 1887–1900.
38. Putnam D. Polymers for gene delivery across length scales. *Nat Mater* 2006; **5**: 439–451.
39. Risau W. Mechanisms of angiogenesis. *Nature* 1997; **386**: 671–674.
40. Jain RK, Schlenger K, Höckel M, Yuan F. Quantitative angiogenesis assays: Progress and problems. *Nat Med* 1997; **3**: 1203–1208.
41. Jain RK. Molecular regulation of vessel maturation. *Nature Med* 2003; **9**: 685–693.
42. Kimura H, Braun RD, Ong ET, Hsu R, Secomb TW, Papahadjopoulos D et al. Fluctuations in red cell flux in tumor microvessels can lead to transient hypoxia and reoxygenation in tumor parenchyma. *Cancer Res* 1996; **56**: 5522–5528.
43. Yuan F. Transvascular drug delivery in solid tumors. *Semin Radiat Oncol* 1998; **8**: 164–175.
44. Yuan F, Salehi HA, Boucher Y, Vasthare US, Tuma RF, Jain RK. Vascular permeability and microcirculation of gliomas and mammary carcinomas transplanted in rat and mouse cranial windows. *Cancer Res* 1994; **54**: 4564–4568.
45. Mannermaa E, Vellonen KS, Urtti A. Drug transport in corneal epithelium and blood–retina barrier: Emerging role of transporters in ocular pharmacokinetics. *Adv Drug Deliv Rev* 2006; **58**: 1136–1163.
46. Tuma PL, Hubbard AL. Transcytosis: Crossing cellular barriers. *Physiol Rev* 2003; **83**: 871–932.
47. Pardridge WM. Drug and gene targeting to the brain with molecular Trojan horses. *Nat Rev Drug Discov* 2002; **1**: 131–139.
48. Renkin EM. Cellular and intercellular transport pathways in exchange vessels. *Am Rev Respir Dis* 1992; **146**: S28–S31.
49. Baluk P, Hirata A, Thurston G, Fujiwara T, Neal CR, Michel CC et al. Endothelial gaps: Time course of formation and closure in inflamed venules of rats. *Am J Physiol* 1997; **272**: L155–L170.
50. Roberts WG, Palade GE. Increased microvascular permeability and endothelial fenestration induced by vascular endothelial growth factor. *J Cell Sci* 1995; **108**: 2369–2379.
51. Feng D, Nagy JA, Hipp J, Dvorak HF, Dvorak AM. Vesiculo-vacuolar organelles and the regulation of venule permeability to macromolecules by vascular permeability factor, histamine, and serotonin. *J Exp Med* 1996; **183**: 1981–1986.

52. Price RJ, Skyba DM, Kaul S, Skalak TC. Delivery of colloidal particles and red blood cells to tissue through microvessel ruptures created by targeted microbubble destruction with ultrasound. *Circulation* 1998; **98**: 1264–1267.
53. Qin S, Ferrara KW. Acoustic response of compliant microvessels containing ultrasound contrast agents. *Phys Med Biol* 2006; **51**: 5065–5088.
54. Wisse E, Jacobs F, Topal B, Frederik P, De Geest B. The size of endothelial fenestrae in human liver sinusoids: Implications for hepatocyte-directed gene transfer. *Gene Ther* 2008; **15**: 1193–1199.
55. Yuan F, Dellian M, Fukumura D, Leunig M, Berk DA, Torchilin VP et al. Vascular permeability in a human tumor xenograft: Molecular size dependence and cutoff size. *Cancer Res* 1995; **55**: 3752–3756.
56. Hobbs SK, Monsky W, Yuan F, Roberts WG, Griffith L, Torchilin VP et al. Regulation of transport pathways in tumor vessels: Role of tumor type and microenvironment. *Proc Nat Acad Sci USA* 1998; **95**: 4607–4612.
57. Kong G, Braun RD, Dewhirst MW. Hyperthermia enables tumor-specific nanoparticle delivery: Effect of particle size. *Cancer Res* 2000; **60**: 4440–4445.
58. Maeda H. Tumor-selective delivery of macromolecular drugs via the EPR effect: Background and future prospects. *Bioconjug Chem* 2010; **19**: 797–802.
59. Frias MA, Lang U, Gerber-Wicht C, James RW. Native and reconstituted HDL protect cardiomyocytes from doxorubicin-induced apoptosis. *Cardiovasc Res*; **85**: 118–126.
60. Spallarossa P, Altieri P, Aloï C, Garibaldi S, Barisione C, Ghigliotti G et al. Doxorubicin induces senescence or apoptosis in rat neonatal cardiomyocytes by regulating the expression levels of the telomere binding factors 1 and 2. *Am J Physiol Heart Circ Physiol* 2009; **297**: H2169–H2181.
61. O'Brien ME, Wigler N, Inbar M, Rosso R, Grischke E, Santoro A et al. Reduced cardiotoxicity and comparable efficacy in a phase III trial of pegylated liposomal doxorubicin HCl (CAELYX/Doxil) versus conventional doxorubicin for first-line treatment of metastatic breast cancer. *Ann Oncol* 2004; **15**: 440–449.
62. Boucher Y, Jain RK. Microvascular pressure is the principal driving force for interstitial hypertension in solid tumors: Implications for vascular collapse. *Cancer Res* 1992; **52**: 5110–5114.
63. Boucher Y, Baxter LT, Jain RK. Interstitial pressure gradients in tissue-isolated and subcutaneous tumors: Implications for therapy. *Cancer Res* 1990; **50**: 4478–4484.
64. Graff BA, Kvinnsland Y, Skretting A, Rofstad EK. Intratumour heterogeneity in the uptake of macromolecular therapeutic agents in human melanoma xenografts. *Br J Cancer* 2003; **88**: 291–297.
65. Curry FR. The Eugene M. Landis Award Lecture. 1993. Regulation of water and solute exchange in microvessel endothelium; studies in single perfused capillaries. *Microcirculation* 1994; **1**: 11–26.
66. Adamson RH, Huxley VH, Curry FE. Single capillary permeability to proteins having similar size but different charge. *Am J Physiol* 1988; **254**: H304–H312.
67. Dellian M, Yuan F, Trubetskov VS, Torchilin VP, Jain RK. Vascular permeability in a human tumour xenograft: Molecular charge dependence. *Br J Cancer* 2000; **82**: 1513–1518.
68. Dang W, Colvin OM, Brem H, Saltzman WM. Covalent coupling of methotrexate to dextran enhances the penetration of cytotoxicity into a tissue-like matrix. *Cancer Res* 1994; **54**: 1729–1735.
69. Fung LK, Saltzman WM. Polymeric implants for cancer chemotherapy. *Adv Drug Deliv Rev* 1997; **26**: 209–230.
70. Fleming AB, Saltzman WM. Pharmacokinetics of the carmustine implant. *Clin Pharmacokinet* 2002; **41**: 403–419.
71. Beduneau A, Saulnier P, Benoit JP. Active targeting of brain tumors using nanocarriers. *Biomaterials* 2007; **28**: 4947–4967.
72. Reiter Y, Pastan I. Antibody engineering of recombinant Fv immunotoxins for improved targeting of cancer: Disulfide-stabilized Fv immunotoxins. *Clin Cancer Res* 1996; **2**: 245–252.

73. Kreitman RJ, Wilson WH, White JD, Stetler-Stevenson M, Jaffe ES, Giardina S et al. Phase I trial of recombinant immunotoxin anti-Tac(Fv)-PE38 (LMB-2) in patients with hematologic malignancies. *J Clin Oncol* 2000; **18**: 1622–1636.
74. Foon KA. Monoclonal antibody therapies for lymphomas. *Cancer J* 2000; **6**: 273–278.
75. Kirpotin DB, Drummond DC, Shao Y, Shalaby MR, Hong K, Nielsen UB et al. Antibody targeting of long-circulating lipidic nanoparticles does not increase tumor localization but does increase inter-nalization in animal models. *Cancer Res* 2006; **66**: 6732–6740.
76. Dreher MR, Liu W, Michelich CR, Dewhirst MW, Yuan F, Chilkoti A. Tumor vascular permeability, accumulation, and penetration of macromolecular drug carriers. *J Natl Cancer Inst* 2006; **98**: 335–344.
77. Swartz MA, Fleury ME. Interstitial flow and its effects in soft tissues. *Annu Rev Biomed Eng* 2007; **9**: 229–256.
78. Chary SR, Jain RK. Direct measurement of interstitial convection and diffusion of albumin in normal and neoplastic tissues by fluorescence photobleaching. *Proc Natl Acad Sci U S A* 1989; **86**: 5385–5389.
79. Baxter LT, Jain RK. Transport of fluid and macromolecules in tumors. I. Role of interstitial pressure and convection. *Microvasc Res* 1989; **37**: 77–104.
80. Butler TP, Grantham FH, Gullino PM. Bulk transfer of fluid in the interstitial compartment of mam-mary tumors. *Cancer Res* 1975; **35**: 3084–3088.
81. Bobo RH, Laske DW, Akbasak A, Morrison PF, Dedrick RL, Oldfield EH. Convection-enhanced delivery of macromolecules in the brain. *Proc Natl Acad Sci U S A* 1994; **91**: 2076–2080.
82. Chen MY, Lonser RR, Morrison PF, Governale LS, Oldfield EH. Variables affecting convection-enhanced delivery to the striatum: A systematic examination of rate of infusion, cannula size, infusate concentration, and tissue-cannula sealing time. *J Neurosurg* 1999; **90**: 315–320.
83. Lieberman DM, Laske DW, Morrison PF, Bankiewicz KS, Oldfield EH. Convection-enhanced dis-tribution of large molecules in gray matter during interstitial drug infusion. *J Neurosurg* 1995; **82**: 1021–1029.
84. Boucher Y, Brekken C, Netti PA, Baxter LT, Jain RK. Intratumoral infusion of fluid: Estimation of hydraulic conductivity and implications for the delivery of therapeutic agents. *Br J Cancer* 1998; **78**: 1442–1448.
85. McGuire S, Yuan F. Quantitative analysis of intratumoral infusion of color molecules. *Am J Physiol Heart Circ Physiol* 2001; **281**: H715–H721.
86. McGuire S, Zaharoff D, Yuan F. Nonlinear dependence of hydraulic conductivity on tissue deforma-tion during intratumoral infusion. *Ann Biomed Eng* 2006; **34**: 1173–1181.
87. Laske DW, Youle RJ, Oldfield EH. Tumor regression with regional distribution of the targeted toxin TF-CRM107 in patients with malignant brain tumors. *Nat Med* 1997; **3**: 1362–1368.
88. Morrison PF, Laske DW, Bobo H, Oldfield EH, Dedrick RL. High-flow microinfusion: Tissue pen-etration and pharmacodynamics. *Am J Physiol* 1994; **266**: R292–R305.
89. Carpentier A, Metellus P, Ursu R, Zohar S, Lafitte F, Barrie M et al. Intracerebral administration of CpG oligonucleotide for patients with recurrent glioblastoma: A phase II study. *Neuro Oncol* 2010; **12**: 401–408.
90. Sampson JH, Akabani G, Archer GE, Bigner DD, Berger MS, Friedman AH et al. Progress report of a Phase I study of the intracerebral microinfusion of a recombinant chimeric protein composed of transforming growth factor (TGF)-alpha and a mutated form of the Pseudomonas exotoxin termed PE-38 (TP-38) for the treatment of malignant brain tumors. *J Neurooncol* 2003; **65**: 27–35.
91. Levick JR. An analysis of the interaction between interstitial plasma protein, interstitial flow, and fenestral filtration and its application to synovium. *Microvasc Res* 1994; **47**: 90–125.
92. Fry DL, Cornhill JF, Sharma H, Pap JM, Mitschelen J. Uptake of low density lipoprotein, albumin, and water by deendothelialized *in vitro* minipig aorta. *Arteriosclerosis* 1986; **6**: 475–490.
93. Parameswaran S, Brown LV, Ibbott GS, Lai-Fook SJ. Hydraulic conductivity, albumin reflection and diffusion coefficients of pig mediastinal pleura. *Microvasc Res* 1999; **58**: 114–127.

94. Kroll RA, Pagel MA, Muldoon LL, Roman-Goldstein S, Neuwelt EA. Increasing volume of distribution to the brain with interstitial infusion: Dose, rather than convection, might be the most important factor. *Neurosurgery* 1996; **38**: 746–752.
95. Lai WM, Mow VC. Drag-induced compression of articular cartilage during a permeation experiment. *Biorheology* 1980; **17**: 111–123.
96. Zakaria ER, Lofthouse J, Flessner MF. *In vivo* hydraulic conductivity of muscle: Effects of hydrostatic pressure. *Am J Physiol* 1997; **273**: H2774–H2782.
97. Baldwin AL, Wilson LM. Endothelium increases medial hydraulic conductance of aorta, possibly by release of EDRF. *Am J Physiol* 1993; **264**: H26–H32.
98. Daniels BS, Hauser EB, Deen WM, Hostetter TH. Glomerular basement membrane: *In vitro* studies of water and protein permeability. *Am J Physiol* 1992; **262**: F919–F926.
99. Guyton AC, Scheel K, Murphree D. Interstitial fluid pressure. 3. Its effect on resistance to tissue fluid mobility. *Circ Res* 1966; **19**: 412–419.
100. Swabb EA, Wei J, Gullino PM. Diffusion and convection in normal and neoplastic tissues. *Cancer Res* 1974; **34**: 2814–2822.
101. Netti PA, Berk DA, Swartz MA, Grodzinsky AJ, Jain RK. Role of extracellular matrix assembly in interstitial transport in solid tumors. *Cancer Res* 2000; **60**: 2497–2503.
102. Wang Y, Wang H, Li CY, Yuan F. Effects of rate, volume, and dose of intratumoral infusion on virus dissemination in local gene delivery. *Mol Cancer Ther* 2006; **5**: 362–366.
103. Wang Y, Yang Z, Liu S, Kon T, Krol A, Li CY et al. Characterisation of systemic dissemination of nonreplicating adenoviral vectors from tumours in local gene delivery. *Br J Cancer* 2005; **92**: 1414–1420.
104. Wang Y, Hu JK, Krol A, Li YP, Li CY, Yuan F. Systemic dissemination of viral vectors during intratumoral injection. *Mol Cancer Ther* 2003; **2**: 1233–1242.
105. Wang Y, Liu S, Li CY, Yuan F. A novel method for viral gene delivery in solid tumors. *Cancer Res* 2005; **65**: 7541–7545.
106. Pucci-Minafra I, Andriolo M, Basirico L, Alessandro R, Luparello C, Buccellato C et al. Absence of regular alpha2(I) collagen chains in colon carcinoma biopsy fragments. *Carcinogenesis* 1998; **19**: 575–584.
107. Berk DA, Yuan F, Leunig M, Jain RK. Direct *in vivo* measurement of targeted binding in a human tumor xenograft. *Proc Natl Acad Sci U S A* 1997; **94**: 1785–1790.
108. Pluen A, Boucher Y, Ramanujan S, McKee TD, Gohongi T, di Tomaso E et al. Role of tumor-host interactions in interstitial diffusion of macromolecules: Cranial vs. subcutaneous tumors. *Proc Natl Acad Sci U S A* 2001; **98**: 4628–4633.
109. Bentley TB, Pittman RN. Influence of temperature on oxygen diffusion in hamster retractor muscle. *Am J Physiol* 1997; **272**: H1106–H1112.
110. Jain RK. The next frontier of molecular medicine—Delivery of therapeutics. *Nat Med* 1998; **4**: 655–657.
111. Torchilin V. Antibody-modified liposomes for cancer chemotherapy. *Expert Opin Drug Deliv* 2008; **5**: 1003–1025.
112. Zhi D, Zhang S, Wang B, Zhao Y, Yang B, Yu S. Transfection efficiency of cationic lipids with different hydrophobic domains in gene delivery. *Bioconjug Chem* 2010; **21**: 563–577.
113. Kong G, Dewhirst MW. Hyperthermia and liposomes. *Int J Hyperthermia* 1999; **15**: 345–370.
114. Chen Q, Krol A, Wright A, Needham D, Dewhirst MW, Yuan F. Tumor microvascular permeability is a key determinant for antivascular effects of doxorubicin encapsulated in a temperature sensitive liposome. *Int J Hyperthermia* 2008; **24**: 475–482.
115. Chen Q, Tong S, Dewhirst MW, Yuan F. Targeting tumor microvessels using doxorubicin encapsulated in a novel thermosensitive liposome. *Mol Cancer Ther* 2004; **3**: 1311–1317.
116. Yuan F, Krol A, Tong S. Available space and extracellular transport of macromolecules: Effects of pore size and connectedness. *Ann Biomed Eng* 2001; **29**: 1150–1158.

117. Krol A, Maresca J, Dewhirst MW, Yuan F. Available volume fraction of macromolecules in the extravascular space of a fibrosarcoma: Implications for drug delivery. *Cancer Res* 1999; **59**: 4136–4141.
118. Comper WD, Laurent TC. Physiological function of connective tissue polysaccharides. *Physiol Rev* 1978; **58**: 255–315.
119. Fry DL. Effect of pressure and stirring on *in vitro* aortic transmural ¹²⁵I-albumin transport. *Am J Physiol* 1983; **245**: H977–H991.
120. Schneiderman R, Snir E, Popper O, Hiss J, Stein H, Maroudas A. Insulin-like growth factor-I and its complexes in normal human articular cartilage: Studies of partition and diffusion. *Arch Biochem Biophys* 1995; **324**: 159–172.
121. Maroudas A. Transport of solutes through cartilage: Permeability to large molecules. *J Anat* 1976; **122**: 335–347.
122. Maroudas A. Distribution and diffusion of solutes in articular cartilage. *Biophys J* 1970; **10**: 365–379.
123. Wiig H, DeCarlo M, Sibley L, Renkin EM. Interstitial exclusion of albumin in rat tissues measured by a continuous infusion method. *Am J Physiol* 1992; **263**: H1222–H1233.
124. Barr L, Malvin RL. Estimation of extracellular spaces of smooth muscle using different-sized molecules. *Am J Physiol* 1965; **208**: 1042–1045.
125. Bert JL, Pearce RH, Mathieson JM. Concentration of plasma albumin in its accessible space in post-mortem human dermis. *Microvasc Res* 1986; **32**: 211–223.
126. Reed RK, Lepsøe S. Interstitial exclusion of albumin in rat dermis and subcutis in over- and dehydration. *Am J Physiol* 1989; **257**: H1819–H1827.
127. Aukland K. Distribution volumes and macromolecular mobility in rat tail tendon interstitium. *Am J Physiol* 1991; **260**: H409–H419.
128. Meyer FA. Macromolecular basis of globular protein exclusion and of swelling pressure in loose connective tissue (umbilical cord). *Biochim Biophys Acta* 1983; **755**: 388–399.
129. Meyer FA, Koblentz M, Silberberg A. Structural investigation of loose connective tissue by using a series of dextran fractions as non-interacting macromolecular probes. *Biochem J* 1977; **161**: 285–291.
130. McGuire S, Zaharoff D, Yuan F. Interstitial transport of macromolecules: Implication for nucleic acid delivery in solid tumors. In: Mahato RI, Kim SW (eds). *Pharmaceutical Perspectives of Nucleic Acid-Based Therapeutics*. Taylor & Francis Books: London, 2002, pp 434–454.
131. Juweid M, Neumann R, Paik C, Perez-Bacete MJ, Sato J, van Osdol W et al. Micropharmacology of monoclonal antibodies in solid tumors: Direct experimental evidence for a binding site barrier. *Cancer Res* 1992; **52**: 5144–5153.
132. Kaufman EN, Jain RK. Effect of bivalent interaction upon apparent antibody affinity: Experimental confirmation of theory using fluorescence photobleaching and implications for antibody binding assays. *Cancer Res* 1992; **52**: 4157–4167.
133. Henshaw J, Mossop B, Yuan F. Relaxin treatment of solid tumors: Effects on electric field-mediated gene delivery. *Mol Cancer Ther* 2008; **7**: 2566–2573.
134. Cohen-Sacks H, Elazar V, Gao J, Golomb A, Adwan H, Korchoy N et al. Delivery and expression of pDNA embedded in collagen matrices. *J Control Release* 2004; **95**: 309–320.
135. Henshaw JW, Zaharoff DA, Mossop BJ, Yuan F. Electric field-mediated transport of plasmid DNA in tumor interstitium *in vivo*. *Bioelectrochemistry* 2007; **71**: 233–242.
136. Zaharoff DA, Barr RC, Li CY, Yuan F. Electromobility of plasmid DNA in tumor tissues during electric field-mediated gene delivery. *Gene Ther* 2002; **9**: 1286–1290.
137. Yuan F. Stress is good and bad for tumors. *Nat Biotech* 1997; **15**: 722–723.
138. Helmlinger G, Netti PA, Lichtenbeld HC, Melder RJ, Jain RK. Solid stress inhibits the growth of multicellular tumor spheroids. *Nat Biotech* 1997; **15**: 778–783.
139. Griffon-Etienne G, Boucher Y, Brekken C, Suit HD, Jain RK. Taxane-induced apoptosis decompresses blood vessels and lowers interstitial fluid pressure in solid tumors: Clinical implications. *Cancer Res* 1999; **59**: 3776–3782.

140. Kratz F, Beyer U, Schutte MT. Drug-polymer conjugates containing acid-cleavable bonds. *Crit Rev Therap Drug Carrier Syst* 1999; **16**: 245–288.
141. Kozin SV, Shkarin P, Gerweck LE. The cell transmembrane pH gradient in tumors enhances cytotoxicity of specific weak acid chemotherapeutics. *Cancer Res* 2001; **61**: 4740–4743.
142. Ganta S, Devalapally H, Shahiwala A, Amiji M. A review of stimuli-responsive nanocarriers for drug and gene delivery. *J Control Release* 2008; **126**: 187–204.
143. Torchilin VP. Targeted pharmaceutical nanocarriers for cancer therapy and imaging. *AAPS J* 2007; **9**: E128–E147.
144. Lu D, Wientjes MG, Lu Z, Au JL. Tumor priming enhances delivery and efficacy of nanomedicines. *J Pharmacol Exp Ther* 2007; **322**: 80–88.
145. Nagano S, Perentes JY, Jain RK, Boucher Y. Cancer cell death enhances the penetration and efficacy of oncolytic herpes simplex virus in tumors. *Cancer Res* 2008; **68**: 3795–3802.
146. Guthi JS, Yang SG, Huang G, Li S, Khemtong C, Kessinger CW et al. MRI-visible micellar nanomedicine for targeted drug delivery to lung cancer cells. *Mol Pharm* 2010; **7**: 32–40.
147. Heiss JD, Walbridge S, Asthagiri AR, Lonser RR. Image-guided convection-enhanced delivery of muscimol to the primate brain. *J Neurosurg* 2010; **112**: 790–795.
148. Lammers T, Subr V, Peschke P, Kuhnlein R, Hennink WE, Ulbrich K et al. Image-guided and passively tumour-targeted polymeric nanomedicines for radiochemotherapy. *Br J Cancer* 2008; **99**: 900–910.
149. Paoli EE, Kruse DE, Seo JW, Zhang H, Kheiriloomoom A, Watson KD et al. An optical and microPET assessment of thermally-sensitive liposome biodistribution in the Met-1 tumor model: Importance of formulation. *J Control Release* 2010; **143**: 13–22.

Pradeep K. Karla
Howard University

Durga K. Paturi
*University of Missouri,
Kansas City*

Nanda K. Mandava
*University of Missouri,
Kansas City*

Animikh Ray
*University of Missouri,
Kansas City*

Sulabh Patel
*University of Missouri,
Kansas City*

Ranjana Mitra
*University of Missouri,
Kansas City*

Ashim K. Mitra
*University of Missouri,
Kansas City*

Noninvasive Targeted Protein and Peptide Drug Delivery

86.1	Introduction	86-1
86.2	Oral Delivery of Proteins and Peptides.....	86-2
	Nasal Route • Pulmonary Route	
86.3	Buccal Delivery	86-8
86.4	Vaginal Delivery of Insulin.....	86-10
86.5	Transdermal Delivery	86-10
	Ocular Route of Administration	
86.6	Rectal Delivery of Protein Drugs	86-12
86.7	Conclusion	86-13
	References.....	86-13

86.1 Introduction

Protein and peptide drug delivery remains a major area of interest to pharmaceutical scientists. Blood transfusions in 1665 by Dr. Richard Lower marked the first successful attempt of protein delivery to humans. Later, Edward Jenner in 1796 employed the protein vaccine of cow pox to prevent small pox. In 1922, the first pure therapeutic protein (insulin) was extracted and it marked the beginning of research aiming toward developing delivery strategies for various proteins [1]. Advances in biotechnology enabled the production of therapeutic proteins and peptides on a commercial scale, which can be employed to treat various hormones, growth factors, wound healing, and metabolic diseases. Recombinant proteins derived by incorporating a human gene into a different species marked a new era in protein drug development. FDA approval of genetically engineered human insulin is regarded as a milestone leading to extensive research in recombinant proteins targeting various diseases [1]. Currently, the FDA database indicates more than 120 protein and peptide drugs among various classes of pharmaceuticals of biological origin such as vaccines, peptides, blood products, and recombinant proteins. The global sales of 10 major classes of protein pharmaceuticals amounted to >\$30 billion as of 2002 [1]. Various classes of protein pharmaceuticals currently on the market along with a few examples are listed in [Table 86.1](#). Many promising protein and peptide molecules are in clinical trials. [Table 86.2](#) represents various protein pharmaceuticals in clinical trials as of May 2010.

However, developing drug delivery systems to maintain safety, efficacy, and stability still remains a challenge. Research in protein and peptide drug delivery is primarily focused on either employing non-invasive pathways or increasing the biological half life of drugs administered invasively. The size of the protein and its susceptibility to degradation form the basis for selecting a drug delivery route [1]. A schematic representation of invasive and noninvasive pathways with various protein-delivery techniques along with advantages and disadvantages is represented in [Figure 86.1](#). Delivery of proteins and peptides

TABLE 86.1 Examples of Various Classes of FDA-Approved Peptide and Protein Drugs

Drug (Protein/Peptide)	Use	Brand Name	Manufacturer
Peptides:			
1. Oxytocin	Labor induction	Pitocin [®]	Monarch Pharmaceuticals Inc.
2. Cyclosporine	Immunosuppressant	Sandimmune [®] , Neoral [®]	Novartis Pharmaceuticals
3. Leuprolide	Treatment of prostate/ breast cancers	Eligard [®]	Sanofi-Aventis
Proteins:			
1. Albumin	Shock/burns	Buminate [®]	Baxter Healthcare
2. Calcitonin	Paget's disease of bone/ postmenopausal osteoporosis	Miacalcin [®]	Novartis
3. Antivenom	Poisonous bites	Antivenin (based on species)	Various
Recombinant Protein Drugs:			
1. Antithrombin	Anticoagulant	ATryn [®]	GTC Biotherapeutics
2. Insulin	Diabetes	Humulin R [®]	Eli Lilly and Company
3. Interferon ALPHA-2B	Viral infections	Rebetron [®]	Schering-Plough Corporation
4. Tissue plasminogen activator	Stroke	ACTIVASE [®] rt-PA [®]	Roche
5. Recombinant human coagulation factor VIIa (rFVIIa)	Hemophilia A	NovoSeven [®]	Novo Nordisk Health Care AG
6. Pegademase bovine	Severe combined immunodeficiency disease (SCID)	Adagen [®]	Enzon Pharmaceuticals Inc
7. Trastuzumab	Breast cancer	Herceptin [®]	Genentech
8. Bevasizumab	Metastatic colorectal cancer	Avastin [®]	Genentech
9. Ranibizumab	Age-related macular degeneration	Lucentis [®]	Genentech
10. Rituximab	Rheumatoid arthritis	Rituxan [®]	Genentech

Source: Table drawn based on literature review in Brown LR. *Expert Opin Drug Deliv.* 2005;2(1):29–42 and online databases.

to the target organs is challenging due to barriers such as mucous membranes, size, and solubility. Noninvasive oral delivery is highly advantageous but even more challenging due to hepatic and intestinal metabolism and poor cellular permeability. Hence, the parenteral route is commonly employed for the delivery of proteins and peptides. Polymeric encapsulation via biodegradable polymers is also preferred to increase biological half-life and stability of protein molecules, providing a sustained release effect [1]. Although the noninvasive oral route is preferable, other routes such as nasal, pulmonary, and buccal have also been studied. The current review article provides detailed information on noninvasive routes for delivery of protein pharmaceuticals.

86.2 Oral Delivery of Proteins and Peptides

Oral administration of drugs is the most acceptable route of administration. However, the oral route for delivering protein and peptides continues to pose significant challenges. The main reasons for low oral bioavailability of proteins and peptides are presystemic enzymatic degradation and proteolysis in the stomach. However, several reports suggest that nutritional proteins are absorbed through intestinal mucosa and small amounts of peptides can be absorbed by specific transporters expressed on intestinal epithelium [2]. Over the past few years, extensive research has been carried out to delineate

TABLE 86.2 Ongoing Clinical Trials on Various Proteins and Peptides as of May 2010

Drug (Protein/Peptide)	Disease State	Pharmaceutical Industry
1. Drotrecogin Alfa (activated)	Severe sepsis	Eli Lilly and Company
2. Recombinant factor VIII Fc fusion protein	Severe hemophilia A	Biogen Idec
3. Bone morphogenetic protein 7	Osteoarthritis of the knee	Stryker Biotech
4. Recombinant protein-free factor VIII (rAHF-PFM)	Hemophilia-A subjects undergoing unilateral hip replacement	Baxter Health Corporation
5. Recombinant-human activated protein C	Severe sepsis	Academisch Medisch Centrum–Universiteit van Amsterdam (AMC–UvA)
6. Whey protein	Femur head necrosis	NIAMS/University of Arkansas
7. Activated protein C	Stroke	NHLBI
8. Parathyroid hormone-related protein ^a	Osteoporosis	University of Pittsburg/NIH/NIDDK
9. Milk protein extract immunotherapy	Cow’s milk allergy in children	Johns Hopkins University
10. Soy protein isolate	Hot flashes during prostate cancer therapy	Wake Forest University/NCI
11. Botulinum Neurotoxin (NT 201)	Sleep-disordered breathing	Merz Pharmaceuticals
12. Wilm’s tumor 1 protein vaccine	Cancers of blood	NCI
13. CD4-IgG	HIV infections	NIAID
14. Herceptin/Lapatinib	Advanced breast cancer	Baylor Breast Care Center
15. Recombinant factor IX Fc fusion protein	Severe hemophilia B	Biogen Idec
16. Drotrecogin alfa (activated)	Septic shock	Eli Lilly and Company
17. Golimumab	Arthritis, rheumatoid	Centocor, Inc./Schering-Plough

^a Data collected from U.S. National Institutes of Health public database on clinical trials.

absorption of protein and peptide drugs from the gastrointestinal (GI) tract and to identify the barriers that restrict absorption. We opine that further understanding of absorption mechanisms, overcoming obstacles such as proteolysis and enzymatic degradation, and designing of new delivery systems may present the oral route as a viable route of administration of protein and peptide therapeutics.

Most therapeutic proteins and peptides are hydrophilic in nature. Thus, passive diffusion across intestinal epithelium is negligible [3]. The molecular size of these drugs is too large for paracellular transport

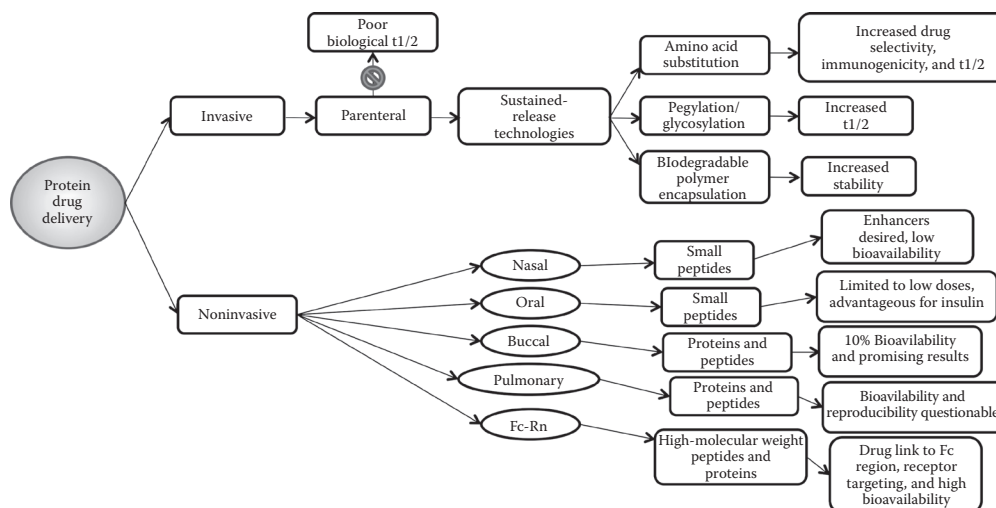


FIGURE 86.1 Schematic representation of various modes of protein drug delivery and advantages/limitations of invasive and major noninvasive modes of delivery. (Figure drawn based on Table 6 in Brown L.R. *Expert Opin Drug Deliv.* 2005;2(1):29–42.)

Downloaded by [JCR JCR] at 10:44 01 August 2015

[4]. For example, widely used protein therapeutic insulin is not transported by paracellular diffusion. It is demonstrated that insulin is transported by a process of endocytosis [5]. Some other proteins have been shown to be transported by binding to cell surface receptors and binding proteins [6]. However, only a small fraction is released at basolateral membrane and secreted into interstitial spaces in active intact form. Some reports demonstrated that therapeutic concentrations of proteins and peptides can be achieved if these compounds can withstand proteolytic enzymes in the GI tract [7].

Several strategies have been attempted to improve oral delivery of protein and peptide therapeutics. Utilization of permeation enhancers and/or protease inhibitors could be effective. However, this strategy is only successful in a laboratory setting; clinical testing poses a challenge to clinicians and regulatory bodies. Coadministering enzyme inhibitors in order to minimize enzymatic degradation of proteins and peptides may lead to adverse events such as absorption of unwanted proteins and degradation of nutrient proteins [8]. Another strategy attempted was modulating tight junction permeability to improve paracellular transport. This approach may enhance passive diffusion of not only proteins, but also potentially toxic molecules present in the GI tract. Since several therapeutic proteins are used in treating chronic conditions, long-term implication of toxins and xenobiotics absorption should be considered [9]. It is imperative that in order to deliver proteins efficiently by the oral route, the above-mentioned obstacles should be overcome. In order to achieve high oral bioavailability, several approaches have been investigated, such as modification physicochemical properties, use of a carrier system, or addition of functionality. It is imperative that these systems do not irreversibly alter tight junctions while maintaining the biological activity of the compounds. As discussed earlier, strategies such as increasing cell membrane permeability and opening tight junctions on intestinal epithelium are limited by the fact that toxins and other xenobiotics may be transported once cell membranes are permeabilized or tight junctions are opened. Notwithstanding this concern, various approaches have been attempted. Intestinal absorption has been improved by formulation therapeutics with safe excipients such as fatty acids, EDTA, surfactants, and glycerides. This strategy is successfully demonstrated in delivering insulin and calcitonin in animal models. Another approach is to deliver protein to the lower GI tract where absorption of proteins is known to be facilitated. To achieve this, standard delivery techniques such as enteric coating may be employed [10]. Modification of physicochemical property is another strategy. Drugs cannot be too lipophilic or hydrophilic. There should always be a compromise in the balance of hydrophilic and lipophilic characteristics. This strategy can be applied to improve enzymatic stability. For example, by synthesizing prodrugs and analogs, these compounds may have better enzymatic degradation [11]. Covalent conjugation of lipid moiety to protein may impart some lipophilicity. Several reports suggest that by conjugating polyethylene glycol (PEG), both solubility and stability of proteins can be achieved [12]. However, due to these modifications, biological activity of proteins should not be altered. To overcome this issue, a reversible lipidization technique has been employed to ensure the bioreversion to active protein molecule following oral administration. Nobex Corporation has modified recombinant human insulin at lysine -29 on β -chain by covalently conjugating PEG and an alkyl chain. Clinical trials demonstrated improved initial efficacy, but not much enhancement in bioavailability [13]. Emisphere's Eligen™ Technology makes use of small hydrophilic organic compounds that interact noncovalently with macromolecules [14]. Using this technology, several macromolecules have been delivered orally in a safe and effective manner. However, low bioavailability and large dose requirement still remain as significant problems. In the recent past, a class of small peptides known as cell penetrating peptides (CPPs) was investigated as carriers to deliver proteins efficiently. Several CPPs such as TAT have been identified, which allow a fused protein to transport across cell membranes. Some reports demonstrated that a TAT peptide derived from HIV TAT protein has the ability to transduce proteins and peptides into various cells [15]. These CPP compounds deliver proteins (cargo) into cytoplasm directly, perturbing the lipid bilayer, or by endocytosis. However, some CPPs cause damage to cell membrane. Overall, no significant toxicity or adverse events have been observed among *in vivo* applications. Even though very little information is available with regard to the use of CPPs in delivering peptides, it has been reported that transport of insulin improved across

Caco2 cells following conjugation with TAT [16]. One major drawback of this strategy is a nonspecific delivery mechanism. More safety and efficacy studies need to be conducted to employ this approach in delivering proteins and peptides orally [17]. Another important approach is utilizing particulate carrier systems. So far, polymeric drug delivery systems based on hydrogels, nanoparticles, microspheres, and lipid-based drug delivery systems such as microemulsions, liposomes, and solid lipid particles have been investigated for oral macromolecular drug delivery. Since proteins and peptides are hydrophilic in nature, lipid-based particles may not entrap proteins efficiently. In addition, these systems display low stability in the GI tract. Conventional liposomes and microemulsions have not met with success in oral delivery of hydrophilic macromolecules. Fusogenic liposomes that have glycoprotein envelop of sendai virus or liposomes and are coated with a mucoadhesive polymer exhibited significant improvement in intestinal absorption. Solid particles appear to be better than lipid-based particles for oral protein delivery. Desai et al. demonstrated that 100 nm poly (lactide-co-glycolic acid)(PLGA) particles diffuse throughout submucosal layers whereas 10 mm particles are localized on the epithelial lining [18]. So, nanoscale carriers made from biocompatible polymers appear to be promising for oral delivery of proteins and macromolecules.

Several reports suggest the use of chitosan nanoparticles for oral delivery of proteins. Insulin-loaded chitosan nanoparticles administered orally to diabetic rats reduced and maintained glucose levels in a normal range for 6–8 h [19]. Nanoparticles surface modified with lectins have shown to be translocated into cells by receptor mediated endocytosis. In recent years, utilization of polymeric nanomicelles is gaining attention as carriers for macromolecule delivery. Low drug-loading efficiency of proteins and particle aggregation are some problems which need to be solved [20]. Overall, for efficient delivery of oral proteins and peptides, stability of proteins and maximizing intestinal uptake are necessary. To improve and develop current oral protein delivery systems, development of superior biomaterials and carriers need to be focused.

86.2.1 Nasal Route

Intranasal administration is a potential noninvasive alternative for the delivery of protein and peptide therapeutics. Over the last 20 years, there has been increased interest in nasal delivery of proteins for the treatment of a variety of ailments. Owing to poor oral absorption, rapid enzymatic degradation, and hepatic first pass elimination, parenteral administration of proteins was favored to oral administration (14,21,22). Parenteral formulations must be sterile, highly purified, nonimmunogenic, and they require repeated administration due to the short half life of the proteins. Easy accessibility, high permeability for lipophilic and low molecular weight drugs, circumvention of hepatic first pass metabolism, rapid absorption, and rich vasculature are some of the numerous advantages associated with the nasal route of administration (23,24). In addition, this route has been explored to deliver proteins directly to the central nervous system via the olfactory neural pathway. The respiratory region of the nose has ciliated columnar epithelial cells covered by microvilli, providing a large surface area for absorption. Beneath this epithelium, a large dense network of capillaries can enhance the permeability of proteins. Mucus is the first barrier for the absorption of macromolecules. The rate of mucus flow is approximately 5–6 mm/min and the mucin present in the secretion can bind with permeant molecules preventing diffusion [25]. After passage through the mucus, molecules can be absorbed either by the paracellular route or transcellular route, or by tranicytosis. Cilia, which are finger-like projections (0.2–0.3 μm wide and 5 μm in length), are present on the apical surface of the cell. These tissues move at a frequency of 10 Hz in symmetrical wavy beats that clear the deposited particles. Cilia along with mucus form a mucociliary clearance process that protects the respiratory track from harmful inhaled substances [26]. Nasal absorption of peptides depends upon several factors such as molecular weight, lipophilicity, size, conformation, pH and pKa of the molecule, pathophysiological conditions, mucociliary clearance, formulation variables, and volume of delivery. Small molecular weight lipophilic compounds such as propranolol, progesterone, and estradiol exhibit rapid and efficient absorption upon intranasal administration. Large molecular weight peptides such as insulin, calcitonin, leuprolide, and glucagon are poorly absorbed (<1%).

Inefficient transport across the nasal mucosa and rapid clearance from the site of absorption are the two major factors responsible for lower bioavailability [27,28].

To overcome these barriers, formulations that reduce drug clearance and improve the rate of absorption have been developed. Also, nasal epithelium and secretions contain several peptidases such as exo- and endopeptidases that might cause rapid degradation at the mucosal site [29]. Peptide transport across nasal mucosa can be enhanced by improving the physicochemical properties of the permeant and/or the formulation. Proteins can be derivatized to their bioreversible prodrug forms and such derivatization can improve stability and solubility properties while pharmacological properties remain intact. Absorption enhancers are administered along with proteins to facilitate nasal absorption. These adjuvants induce reversible transient modifications on the lipid and protein assembly in the epithelial barrier and open the intercellular junctions, thereby improving paracellular transport. Anionic and cationic surfactants, chelators, bile salts, fatty acids, bile salt–fatty acid mixed micelles, fusidic acid derivatives, and phospholipids are some of the absorption-enhancing compounds studied to enhance nasal absorption [30,31]. Shao et al. studied the effect of methyl derivatives of cyclodextrins on the nasal absorption of insulin and observed that dimethyl- β -cyclodextrin was more effective than other compounds, such as α -cyclodextrin, β -cyclodextrin, hydroxypropyl- β -cyclodextrin, and γ -cyclodextrin [32]. Schipper et al. obtained an absolute bioavailability of $13 \pm 4\%$ with the intranasal administration of insulin/dimethyl- β -cyclodextrin powder relative to insulin/lactose powder formulation in rabbits [33]. Other enhancers such as bile salts, surfactants, and phospholipids improve transcellular transport of proteins by modifying permeability of the phospholipid bilayer. Incorporation of 4% w/v sodium glycocholate with human insulin 100 U/ml in a nasal spray solution resulted in an increase in serum insulin levels and lowered blood glucose levels over the control solution [34]. Furthermore, addition of mucoadhesive agents such as chitosan, alginate, and cellulose prolong nasal retention time and extend the contact time between the peptide and nasal mucosa. These agents absorb water, swell, and interpenetrate the mucus layer, thereby causing localization. Bioadhesive chitosan gels containing 2% median molecular weight of chitosan with ethylenediamine tetra-acetic acid caused an elevation in insulin absorption by 46% relative to intravenous administration [35]. Efficacy of the peptides administered by intranasal delivery depends upon the method of delivery of the drug to the nasal mucosa. Several nasal formulations containing liposomes, microspheres, and gels have been developed to improve nasal absorption of proteins. Sustained release formulations such as liposomes, microspheres, and nanoparticles stabilize protein formulations as well as maintain protein integrity. These formulations may contain adjuvants such as enzymatic inhibitors, absorption enhancers, and mucoadhesive gels to promote nasal absorption [36,37]. However, these adjuvants were tested for nasal irritation and damage to nasal mucosa. Jain et al. evaluated chitosan-coated multivesicular liposomes containing insulin for sustained noninvasive release of insulin. This study reported that chitosan-coated multivesicular liposomes released insulin for a period of 7–9 days in comparison to 24 h release for conventional liposomes [38]. Chitosan-*N*-acetyl-L-cysteine, lectin conjugated PEG-PLA, *N*-trimethyl chitosan, and starch nanoparticles have been utilized to increase intranasal bioavailability of proteins [39–42]. Absolute bioavailability of insulin-loaded microspheres containing chitosan and ascorbyl palmitate was found to be 44% and blood glucose levels were reduced by 67% in comparison to the intravenous route [43]. Because of their short half life and large oral dose requirements, luteinizing hormones and their analogs, desmopressin, oxytocin, and salmon calcitonin were investigated for alternate modes of delivery, other than the oral route. These analogs are already marketed for intranasal administration and were proven to be safe and effective in a larger number of patients. Dimethyl-beta-cyclodextrin has been added to enhance nasal absorption of buserelin, a potent nonapeptide LHRH agonist in rats [44]. Also, nasal absorption of nafarelin acetate was found to be 2% relative to subcutaneous administration [45]. Harris et al. reported that nasal spray of desmopressin has been proven to be more effective than nasal drops, describing the effects of mucociliary clearance and mode of administration on nasal absorption [46]. Intranasal administration of the human leucocyte interferon has been extensively investigated for local prophylaxis against rhinovirus and para-influenza viral infections.

TABLE 86.3 List of Current Peptide Drugs in the Market, Doses, and Bioavailability along with a Comparative Bioavailability Profile

Drug	No. of Amino Acids	M. wt (Da)	Daily Oral Dose (mg)	Bioavailability (%)
ORAL Peptide Drugs—Properties				
DDAVP	9	1183	0.050–0.80	0.16
Cyclosporine	11	1203	1500	30.0
Insulin (Experimental)	51	5808	35	1–5
NASAL Peptide Drugs—Properties				
DDAVP	9	1183	10–40	3.2
Synarel®	9	1322	400	2.8
Miacalcin®	32	3432	0.2	3.0

Source: Brown LR. *Expert Opin Drug Deliv.* 2005;2(1):29–42. With permission.

DDAVP: desmopressin acetate.

Commercially available peptide hormones delivered as nasal spray solutions include Synarel® (nafarelin), Stimat® NS (desmopressin), Suprefact® (buserelin acetate), and Miacalcin® (salmon calcitonin). A list of current drugs in the market, doses, and bioavailability along with a comparative bioavailability profile for oral desmopressin is presented in Table 86.3.

86.2.2 Pulmonary Route

The pulmonary route has been successfully utilized as an alternative for the systemic delivery of proteins. In particular, inhaled insulin has been explored extensively for the treatment of diabetes. Lungs offer a comparatively larger surface area (70 m²) than other mucosal tissue routes such as nasal, buccal, rectal, and vaginal. In addition, smaller thickness of the alveolar epithelium (0.1–0.5 μm), rich vascularization, rapid absorption followed by rapid onset of action, lower enzymatic degradation, and escape of first-pass liver metabolism renders the pulmonary route an attractive alternative for the delivery of proteins [47–49]. About 90% of the absorptive surface area is due to the alveolar sac region. Alveolar epithelial cells with tight intercellular junctions form a major barrier to the absorption of high-molecular weight substances [50]. Small molecular weight peptides (less than 40 kDa) are absorbed primarily by paracellular transport whereas larger proteins are absorbed mainly by transcytosis. Previous studies have shown that proteins with a molecular weight up to approximately 30 kDa generate systemic bioavailability between 20 and 50% [51,52]. Lower bioavailability is due to the degradation of proteins by proteolytic enzymes in the lungs. Penetration enhancers such as chelators, surfactants, bile salts, and fatty acids are often used to enhance the pulmonary absorption of proteins. These penetration enhancers might alter the integrity of the mucosal membrane, inhibit the proteolytic activity, and affect the membrane lipids and proteins [53,54]. Inhaled particles are filtered and subsequently deposited on the airways due to progressive branching of the tracheobronchial tree. These particles are then cleared primarily by two mechanisms: mucociliary clearance and alveolar macrophages. The mucociliary escalator results from the upward movement of mucus secretions (produced by the goblet cells and mucus-secreting glands) by the cilia that vibrate at about 1000–1500 beats per minute. Mucus is cleared at a rate of 0.5–20 mm/min toward the trachea and then passed into the gastrointestinal track [55,56]. Inhaled toxic particles are phagocytosized by alveolar macrophages present in the alveoli. Also, these macrophages secrete several inflammatory mediators such as interleukins, leukotrienes, granulocyte colony-stimulating factors, and proteases that degrade the proteins. However, to elicit proper systemic effect, the major challenge is to develop formulations that can deliver the aerosol particles to the deep lung. Particle size and velocity are the two main factors that govern the deposition of particles to the deep lung. For efficient deposition, the particles should have a mass median aerodynamic diameter between 1 and 3 μm. For targeted deposition to the alveolar region, the mass median aerodynamic diameter should not be more

than 3 μm [57–59]. Aerosol particles with a diameter greater than 6 μm are predominantly deposited in the oropharynx. Three major types of devices have been used to deliver aerosol particles to the lungs: metered dose inhalers, nebulizers, and dry powder inhalers. To achieve a reproducible dose, the delivery device should be properly used and there should be coordination between breathing and dispensing of the aerosol. With the use of metered dose inhalers and nebulizers, only 30–40% of the dose can reach the alveolar region. Dry powder inhalers are less efficient than metered dose inhalers or nebulizers [60,61]. To control the release of drug, proteins are encapsulated in particulate delivery systems such as liposomes, microparticles, nanoparticles, and dendrimers. PEG, PLGA, PLA, and chitosan are most commonly selected for encapsulating the proteins. These polymers improve physical as well as chemical stability and offer protection against enzymatic degradation [62,63]. Exubera was the first approved inhaled formulation of insulin developed by Pfizer for the treatment of hyperglycemia in type 1 and 2 diabetic patients. However, this product was discontinued due to its potential side effects and its inability to deliver precise insulin doses. Also, this product was not approved for patients with lung disorders such as asthma, emphysema, chronic obstructive pulmonary disease, or for smokers. AIR Insulin System (Eli Lilly), AER_x Insulin Diabetes Management System (Novo Nordisk), and Technosphere Insulin System (Mannkind) are some delivery devices currently in phase-III clinical trials for the delivery of inhaled insulin [61].

Intratracheal administration of insulin-loaded liposomes prepared by spray freeze drying has shown a 38.38% pharmacological bioavailability with prolonged hypoglycemic effect in diabetic rats. These liposomes consist of lung surfactants and synthetic lipids. These vesicles have been used for delivering peptide hormones for systemic effects as well as local conditions such as lung cancer, cystic fibrosis, and pulmonary distress [64]. Proteins such as parathyroid hormone, glucagon, amylin, erythropoietin, granulocyte colony stimulating factor, interleukins [2,6,11,12], interferons (γ , β , α), and growth hormones have been delivered through the lungs [65]. Shorter duration of action, chemical stability, immunogenicity, cost of manufacture, and lack of reproducible dosing are some of the challenges that need to be addressed for successful delivery of proteins via the pulmonary route.

86.3 Buccal Delivery

Buccal delivery of macromolecules through buccal mucosa represents an alternative route for noninvasive delivery of insulin. The buccal route gained attention due to its advantages, such as easy accessibility and high vascularity of mucosal membrane [53]. Noninvasiveness, avoidance of presystemic metabolism, and high systemic absorption of macromolecules are important therapeutic benefits. Painless administration, ease of drug withdrawal, mild and reversible damage or irritation to the mucosa by excipients, and low enzymatic activity are other advantages. Penetration enhancers and/or enzyme inhibitors can also be included in the formulation to facilitate macromolecular drug absorption. Limited absorption area, barrier properties such as washing effect of saliva and presence of digestive enzymes are major obstacles to the delivery of macromolecules such as insulin [66,67].

Various approaches have been employed to improve bioavailability of insulin and other polypeptides through the buccal mucosa by incorporating absorption enhancers/permeability enhancers (to improve the membrane permeability) and/or enzyme inhibitors (to increase the peptide stability). Common buccal penetration enhancers include bile salts and surfactants which primarily act by formation of reverse micelles and aqueous channels, perturb membrane proteins and/or extract such proteins and cause membrane fluidization. Fatty acid causes disruption of intercellular lipid packing. Azone evades region of fluidity in intercellular lipids and alcohols interact with lipid domain and change protein conformation [68–71]. However, permeation enhancers cause various side effects, such as irritation to buccal mucosa and loss of taste. Coadministration of peptide drugs with enzyme inhibitors such as aprotinin, bestatin, puromycin, and bile salts is another strategy to improve buccal absorption of peptides. These enzyme inhibitors act either by modulating enzyme activities or by changing conformation of peptides or proteins and/or rendering the drug less prone to enzymatic degradation [68,72]. Mucoadhesive agents also

play a key role in buccal delivery by prolonging retention time of formulations, thereby providing higher exposure of insulin at the site of absorption. Several mucoadhesive agents such as polyacrylic acid (PAA), polyvinyl alcohol (PVA), sodium carboxymethylcellulose (NaCMC), hydroxypropylmethyl cellulose (HPMC), hydroxyethyl cellulose (HEC), hydroxypropyl cellulose (HPC), sodium alginate, hyaluronic acid, gelatin, and carrageenan have been investigated for buccal delivery of insulin [73–79]. Various copolymers of acrylic acid, such as acrylic acid-polyethylene glycol monomethyl ether copolymer (P(AA-co-PEG)) and acrylic acid-2 ethylhexyl acrylate copolymer (P(AA-co-EHA)) are also being developed as mucoadhesive agents [80]. In recent years, lamellar and cubic liquid crystalline phases of glycerol monooleate (GMO), and lectins have been studied as specific mucoadhesives for buccal delivery [81,82].

Deformable vesicles of phospholipids, known as transfersomes, have recently been investigated for buccal delivery of insulin [83]. Transfersomes are morphologically identical to liposomes, but these vesicles can respond to external stresses by rapid shape transformations requiring low energy. This high deformability allows them to deliver therapeutics across buccal barriers. Sodium cholate or sodium deoxycholate is incorporated into the vascular membrane to prepare transfersomes. Pharmacological bioavailability of insulin after administration of deformable vesicles is higher relative to subcutaneous insulin and buccal conventional insulin vesicles.

Pluronic F-127 (PF-127) gel containing unsaturated fatty acids such as oleic acid, eicosapentaenoic acid (EPA), or docosahexaenoic acid (DHA) have been investigated for the insulin release profile and hypoglycemic effect after buccal administration gel in rats [84]. PF-127 gel containing oleic acid has shown rapid insulin release, high pharmacological availability ($15.9\% \pm 7.9\%$), and most relative hypoglycemic effect comparable to subcutaneous administration and PF-127 buccal gel containing other unsaturated fatty acids. However, gels containing EPA and DHA have shown a significant decrease in blood glucose levels relative to the gel containing insulin without fatty acids. These results clearly suggest that gel containing fatty acid could be a potential buccal formulation for noninvasive delivery of insulin.

Furthermore, insulin buccal spray (IBS) containing absorption enhancers such as soybean, lecithin, and propanediol in combination has released significantly higher amounts of insulin in the blood and improved the hypoglycemic effect in diabetic rabbits and rats [85]. Hypoglycemia lasted over 4 and 5 h in rats and rabbits, respectively. Moreover, blood glucose levels observed in controls were much higher in IBS-treated animals. Pharmacokinetic and pharmacodynamic observations showed that an IBS formulation could be a promising buccal delivery system. Venugopalan et al. have attempted to prepare pelleted mucoadhesive nanoparticles of insulin as an alternative buccal delivery system of insulin [86]. In another study, mucoadhesive buccal tablets of insulin were formulated with Carbopol 934, HPC, HPMC, and different absorption promoters; and the hypoglycemic effects of each formulation were studied in a beagle dog [87].

Novel liquid aerosol formulation (Oralin™, Genex Biotechnology, Canada) for buccal delivery of insulin is developed and currently in phase II clinical trials [88]. This system allows accurate insulin dose deposition via a metered dose inhaler in the form of fine aerosolized droplets through the mouth. A single-dose, randomized, crossover study was conducted with an oral insulin spray in 21 patients with type 2 diabetes mellitus. Oralin™ and placebo puffs with antidiabetic drug (OAD) such as metformin and glyburide were evaluated for lowering postprandial glucose levels. A regimen including combinations of OAD such as metformin and glyburide with an oral spray of insulin significantly lowered 2 h postprandial glucose rise and raised serum insulin levels more than in combination of metformin and glyburide plus the placebo puffs. This novel pain-free insulin formulation has a number of advantages, such as simple administration technique, precise dosing control, bolus delivery, and rapid absorption.

The major obstacles for transmucosal delivery of insulin are the barrier properties of mucosa, rapid degradation, and limited absorption area [89,90]. Hence, strategies studied to overcome these obstacles include the use of materials that combine mucoadhesive, enzyme inhibitory and penetration-enhancing properties, which can improve patient compliance and prolong the contact time of drugs to mucosal membrane. However, further efforts are needed to design standardized *in vitro* and *ex vivo* biological

models which can mimic *in vivo* physiological conditions and can allow one to characterize and compare different materials and formulations in terms of their ability to prolong drug absorption via the buccal route.

86.4 Vaginal Delivery of Insulin

Several noninvasive alternative routes have been explored for the delivery of insulin in the treatment of diabetes type I and type II. Among these alternative routes, the vaginal route appears to be a potential for the administration of insulin due to large surface area, rich blood supply, and high permeability to a wide range of peptides and proteins. However, lower bioavailability of the insulin may be due to poor absorption across the vaginal epithelium and degradation by enzymes in vaginal lumen [91,92]. Besides being gender specific, estrogen concentration strongly alters the permeability of the vagina, which can influence systemic drug absorption [91,93]. Absorption of insulin through the vaginal epithelium can be improved by inclusion of absorption enhancers and polyacrylic acid aqueous gel [94,95]. In addition, enzymatic degradation can be minimized by encapsulating insulin in various delivery systems such as liposomes, microspheres, and niosomes [96–98].

In a recent study, Ning and coworkers selected sorbitan monoester (Span 40 and Span 60) to prepare insulin encapsulated niosomes for vaginal administration. Hypoglycemic effects and systemic bioavailability of insulin in rats were determined after vaginal application of insulin vesicles and the results were compared with subcutaneous administration of insulin in solution [99]. This study reported that bioavailability of insulin after vaginal administration was comparable to its bioavailability after subcutaneous administration. In another study, vaginal delivery of insulin–chitosan formulation was evaluated in rabbits [100]. Simultaneously, this study demonstrated the effects of absorption enhancers such as dimethyl- β -cyclodextrin (DM- β CD) and sodium taurocholate. Pharmacokinetic profiles of three insulin-loaded formulations, that is, chitosan-gel, DM- β CD-chitosan-gel, and Tau-chitosan-gel were compared with IV administration. DM- β CD-chitosan-gel formulation showed promising results with higher C_{max} ($71.6 \pm 15.2 \mu\text{g/mL}$) and t_{max} (60 min) relative to C_{max} ($65.8 \pm 11.0 \mu\text{g/mL}$) and t_{max} (45 min) observed after IV administration of insulin. Thus, chitosan gels can control the release of insulin while DM- β CD can enhance the penetration of insulin through the vaginal mucosa.

Richardson et al. evaluated the effects of penetration enhancers on insulin uptake across the vaginal epithelium of ovariectomized rats [101]. The study revealed that coadministration of sodium taurodi-hydrofusidate, polyoxyethylene-9-lauryl ether, lysophosphatidylcholine, palmitoylcarnitine chloride, and lysophosphatidylglycerol significantly enhanced the hypoglycemic activity of insulin. Moreover, histological studies further revealed low to severe toxicity of the penetration enhancers on the vaginal epithelium.

Combinations of penetration enhancers have given limited success in the delivery of insulin through the vagina. However, the subject of insulin delivery across the vaginal membrane is still a challenge for future researchers and scientists in the field of vaginal delivery.

86.5 Transdermal Delivery

Transdermal delivery of proteins offers an attractive option for noninvasive delivery of therapeutic proteins and peptides. It shares advantages such as avoiding first pass degradation in the GI tract or liver and less enzymatic degradation compared to other routes [102]. In addition, most proteins and peptides are intended for systemic action; many peptides have potential therapeutic advantage if they can be delivered locally at the target site [103]. Even though transdermal delivery of proteins and peptides is an exciting opportunity, several challenges exist. One challenge is that bioavailability tends to be low in some penetration enhancement technologies. Most therapeutic proteins and peptides are large and hydrophilic, and do not cross the stratum corneum efficiently. Before reaching systemic circulation,

topically applied proteins and peptides should permeate through the stratum corneum and epidermis. Because proteins and peptides are large in size, and hydrophilic, transdermal permeation is limited. Hence, to deliver them efficiently several enhancement technologies are being investigated, such as formulation optimization, and energy driven and minimally invasive approaches [104]. Formulation optimization includes chemical modification of a drug, encapsulation technologies, and usage of penetration enhancers. Extensive research has been conducted to improve the intestinal absorption of peptides by chemical modification. Foldvori et al. reported that palmitoyl derivative of interferon alpha (P-IFN α) exhibited 5–6 times higher cutaneous absorption than IFN α . The total amount of P-IFN α and IFN α in the whole skin after 24 h treatment was $2.106 \pm 1.216 \mu\text{g}/\text{cm}^2$ and $0.407 \pm 0.108 \mu\text{g}/\text{cm}^2$ respectively. These results indicate that this strategy can be employed to deliver proteins and peptides across skin. However, following chemical modification, extensive efficacy and toxicological evaluations need to be conducted [105]. Extensive research has been performed on penetration enhancers and their mechanism, side effects and effect on transdermal permeation of molecules [106,107]. Most of the studies concluded that proteins and peptides may not be stable in the presence of penetration enhancers. Another important aspect is adverse events such as irritation rendered by permeation enhancers makes this approach less attractive. Another strategy which is extensively investigated is encapsulation technologies such as microspheres, nanoparticles, liposomes, and niosomes. They are effective in forming drug depot in the upper layers of skin and aid in controlled delivery of proteins. This strategy offers advantages such as minimizing degradation of protein drugs [108,109].

Energy-driven methods to improve transdermal delivery of proteins include iontophoresis, electroporation, phonophoresis, and sonophoresis. Iontophoresis is an old technology developed to deliver charged molecules through skin. This technique has some limitations. For example, there is a size limit of the molecule and the technology requires a high isoelectric point so that protein does not precipitate within skin [104,110]. Transdermal delivery of numerous peptides including thyrotropin-releasing hormone, sandostatin, calcitonin, angiotensin, and insulin has been reported [111–115]. Owing to advanced transdermal iontophoretic research and development, these delivery systems are well characterized. For example, LidositeTM and IonosysTM (Alza Corporation) offer a good platform which can be potentially adapted and customized for transdermal delivery of proteins and peptides [116,117]. Electroporation involves exposure of skin to relatively high voltages for short periods of time, unlike iontophoresis, which involves small currents for longer periods of time. Sen et al. demonstrated 20-fold enhancement in insulin delivery utilizing electroporation and absorption enhancers simultaneously [118].

Skin microporation is investigated for transdermal delivery of water-soluble small drugs and macromolecules such as proteins. It involves the creation of micron dimension transport pathways in the skin using a minimally invasive technique, such as microneedles, thermal microporation, or radiofrequency ablation. An applicator can be used to apply the microneedles on the skin to create the micropores followed by patch application. Alternatively, the drug can be coated directly on the microneedles. The latter approach has been used for vaccine delivery since the amount of protein antigen needed to generate immune response is very small and the dose can be accommodated by coating the microneedles [110].

Thermal microporation involves thermal ablation of the stratum corneum to create microchannels in the skin. It is accomplished by the application of a short pulse of electrical current to an array of metallic filaments, which convert electricity to thermal energy. The rapid creation and conduction of thermal energy into the surface of the skin, in an area about the width of a human hair, painlessly ablates the stratum corneum under each filament to create an array of aqueous microchannels. After the microchannels are formed, the protein patch is applied using a simple fold-over design that aligns it with the newly formed microchannels. This technology is being developed by Altea Therapeutics (Atlanta, GA) [110].

Phonophoresis or sonophoresis is another transdermal enhancement technology utilized to deliver macromolecules across the skin. A coupling medium is needed and several mechanisms have been proposed for delivery, including cavitation, acoustic microstreaming, heating, or radiation pressure. Recently, it has been suggested that phonophoresis also creates micropores in the skin. Miniaturization

of these ultrasound applicators has not advanced to the point of enabling wearable devices, as is now possible with iontophoretic patches [110].

Several other enhancement technologies, such as laser-assisted thermal ablation, RF-microchannels, controlled heat-assisted delivery, particle-mediated immunization, or the possible use of dermabrasion, chemical enhancers, or carrier molecules, such as liposomes or cyclodextrins, can also be utilized.

86.5.1 Ocular Route of Administration

Systemic noninvasive delivery of drugs through the ocular route has been reported by several research groups. An efficient systemic absorption comparable to injection with the added advantage of easier administration makes ocular administration an attractive route for drug delivery. Ocular tissues are less prone to immune responses than any other tissues [119]. First-pass gastrointestinal and liver metabolisms which are the major reasons for low bioavailability of peptide and other drugs can be avoided to a large extent. Despite these advantages, delivery of protein and peptide drugs through the ophthalmic route suffers from some inherent weaknesses. The most important of them is the dynamics of the lachrymal drainage system. This system is responsible for introduction and rapid drainage of tear fluid. From any instilled formulation, solution is drained rapidly from the precorneal area into the nasal cavity and throat from where it traverses into the gastrointestinal tract. This high rate of drug elimination results in short duration of contact with the absorptive layers in the cornea and conjunctiva, which results in lower bioavailability. Other drawbacks include local irritation and inflammation. Several delivery systems have been devised to overcome these disadvantages.

Numerous absorption enhancers have been evaluated for delivery of insulin via the ocular route. Most commonly used among them were polyoxyethylene-9-lauryl-ether (POELE), sodium glycocholate, sodium taurocholate, sodium deoxycholate, saponin, sorbic acid, and Brij-99. In-vivo data in cats suggest that saponin is a strong absorption enhancer, though unfortunately it is irritating to the eye. Other commonly used absorption enhancers such as POELE, and Brij-99, which are nonionic surfactants, are less irritating [120]. Nomura et al. attempted to enhance systemic absorption in diabetic dogs by increasing viscosity of insulin eye drops by the addition of hyaluronic acid. However, this approach did not lead to substantial bioavailability increase. Yamamoto et al. also attempted to increase bioavailability by suspending the peptide in a variety of vehicles such as peanut oil, artificial tears, liquid parafilm, and sesame oil, but the bioavailability produced by the suspension method has not been clinically successful. Encapsulating insulin into a liposome for systemic delivery via the ocular route has been investigated by various research groups including Soni et al (1998). Positively charged insulin containing liposomal formulation has been effective in reducing blood sugar levels of rabbits by 30–35% for 5 h. This shows that liposomal formulation might be effective as a noninvasive delivery system for protein and peptide therapeutics [121]. Yamamoto also suggested that ocular inserts might be another promising delivery system for insulin as the insert remains in contact with the conjunctival sac for a prolonged period of time, unlike suspensions and emulsions. This can allow sustained release of insulin. Simamora et al. (1996) introduced an insert in which Gelfoam® (absorbable gelatin sponge, USP, size 100) was the drug carrier and Brij-78 was an absorption enhancer. The Gelfoam device is potentially ideal for insulin delivery as diffusion occurs in the aqueous phase between the gelatin fibers rather than through a membrane. Therapeutic efficacy of insulin substantially improves with the use of an ophthalmic device [122,123].

86.6 Rectal Delivery of Protein Drugs

In the recent past, rectal delivery of protein drugs has generated significant interest among researchers. Insulin delivery via the rectal route offers some advantages. (a) The rectal route is independent of intestinal motility, gastric-emptying time, and diet. (b) It helps in avoiding hepatic first-pass metabolism. Hosny et al. observed that a suppository containing insulin incorporated in deoxycholic acid, sodium

taurocholate, or both, when placed in the rectum of hyperglycemic rabbits, caused a significant lowering in plasma glucose. Concentrations compared with those observed for insulin injected subcutaneously [124]. The most pronounced effect was observed when polycarbophil was added to a suppository formulation having a combination of deoxycholic acid and sodium taurocholate. This formulation produced 56% relative hypoglycemia compared with that achieved with a subcutaneous injection. These suppository formulations are promising alternatives to currently prevalent insulin injections, since these systems generate almost 50% glucose lowering response relative to subcutaneous injections. Studies have recently shown that the formation of an adhesive interaction between delivery system and the rectal mucosa can be harnessed as an absorption modifier since it enhances the contact time of the coadministered drug and most probably acts as a sustained-release polymer. A thermoreversible liquid insulin suppository that underwent a phase transition to a bioadhesive gel at body temperature elevated insulin bioavailability [125]. However, despite the promises, the bioavailability of rectally delivered peptides remains low. Other disadvantages include patient compliance and discomfort associated with rectal administration. Its irreproducible bioavailability and special storage conditions required are other hindrances that need to be overcome.

86.7 Conclusion

Research advances in biotechnology have evolved protein pharmaceuticals into a commercially viable field. Effective targeting of various disease states employing specific proteins and peptides as molecular targets resulted in positive clinical outcome. However, the majority of the proteins are administered parenterally; few are administered via oral/nasal routes. Table 86.3 represents various commercially available peptide drugs administered via oral and nasal routes. The bioavailability of large molecular weight proteins such as insulin is low via oral and nasal routes. Delivery of insulin via the pulmonary route showed promise in clinical studies and is the current area garnering the attention of researchers and pharmaceutical industries [1]. Exubera® is the first inhalation insulin product to be FDA approved and is marketed by Pfizer pharmaceuticals. Various improved inhalation devices developed by Eli Lilly Corp., and Novo Nordisk are in phase III clinical trials for improved delivery of proteins (insulin) via the noninvasive pulmonary route. Incidence of diseases, such as type 1 diabetes, which require invasive protein (insulin) drug delivery, is increasing statistically across the globe. A noninvasive mode of protein drug delivery should provide an efficient, patient-compatible option with increased safety profile. Though moderate success was achieved, noninvasive delivery of proteins remains a formidable challenge. A majority of the compounds in the pipeline for drug development are monoclonal antibodies with molecular weights of ~150 kDa [1]. Also, the antibodies currently in the market (Table 86.1) are administered at high doses. High molecular weight and high dosing requirement pose a formidable challenge to developing efficient strategies for noninvasive protein delivery. Also, significant effort is required to develop cost-effective techniques for isolation and purification of proteins. It can be concluded that the majority of noninvasive delivery of proteins and peptides is limited to small molecular weight peptides and extensive research is being performed to evaluate promising noninvasive routes, such as pulmonary and oral, for delivery of large molecular weight proteins.

References

1. Brown LR. Commercial challenges of protein drug delivery. *Expert Opin Drug Deliv.* 2005;2(1):29–42.
2. Lee YH, Sinko PJ. Oral delivery of salmon calcitonin. *Adv Drug Deliv Rev.* 2000;42(3):225–38.
3. Camenisch G, Alsenz J, van de Waterbeemd H, Folkers G. Estimation of permeability by passive diffusion through Caco-2 cell monolayers using the drugs' lipophilicity and molecular weight. *Eur J Pharm Sci.* 1998;6(4):317–24.

4. Rubas W, Cromwell ME, Shahrokh Z, Villagran J, Nguyen TN, Wellton M, Nguyen TH, Mrsny RJ. Flux measurements across Caco-2 monolayers may predict transport in human large intestinal tissue. *J Pharm Sci*. 1996;85(2):165–9.
5. Gordon Still J. Development of oral insulin: Progress and current status. *Diabetes Metab Res Rev*. 2002;18 Suppl 1:S29–37.
6. Bastian SE, Walton PE, Belford DA. Transport of circulating IGF-I and LR3IGF-I from blood to extracellular wound fluid sites in rats. *J Endocrinol*. 2000;164(1):77–86.
7. Tozaki H, Odoriba T, Iseki T, Taniguchi T, Fujita T, Murakami M, Muranishi S, Yamamoto A. Use of protease inhibitors to improve calcitonin absorption from the small and large intestine in rats. *J Pharm Pharmacol*. 1998 Aug;50(8):913–20.
8. Shah RB, Ahsan F, Khan MA. Oral delivery of proteins: Progress and prognostication. *Crit Rev Ther Drug Carrier Syst*. 2002;19(2):135–69.
9. Salamat-Miller N, Johnston TP. Current strategies used to enhance the paracellular transport of therapeutic polypeptides across the intestinal epithelium. *Int J Pharm*. 2005;294(1–2):201–16.
10. Soltero R, Ekwuribe N. The oral delivery of protein and peptide drugs. Innovations in pharmaceutical technology (Online Journal). 106–110.
11. Hichens M. A comparison of thyrotropin-releasing hormone with analogs: Influence of disposition upon pharmacology. *Drug Metab Rev*. 1983;14(1):77–98.
12. Basu A, Yang K, Wang M, Liu S, Chintala R, Palm T, Zhao H et al. Structure-function engineering of interferon-beta-1b for improving stability, solubility, potency, immunogenicity, and pharmacokinetic properties by site-selective mono-PEGylation. *Bioconj Chem*. 2006;17(3):618–30.
13. Kipnes M, Dandona P, Tripathy D, Still JG, Kosutic G. Control of postprandial plasma glucose by an oral insulin product (HIM2) in patients with type 2 diabetes. *Diabetes Care*. 2003;26(2):421–6.
14. Goldberg M, Gomez-Orellana I. Challenges for the oral delivery of macromolecules. *Nat Rev Drug Discov* 2003;2(4):289–95.
15. Zorko M, Langel U. Cell-penetrating peptides: Mechanism and kinetics of cargo delivery. *Adv Drug Deliv Rev*. 2005;57(4):529–45.
16. Liang JF, Yang VC. Insulin-cell penetrating peptide hybrids with improved intestinal absorption efficiency. *Biochem Biophys Res Commun* 2005;335(3):734–8.
17. Vives E. Present and future of cell-penetrating peptide mediated delivery systems: Is the Trojan horse too wild to go only to Troy? *J Control Release* 2005;109(1–3):77–85.
18. Desai MP, Labhasetwar V, Walter E, Levy RJ, Amidon GL. The mechanism of uptake of biodegradable microparticles in Caco-2 cells is size dependent. *Pharm Res* 1997;14(11):1568–73.
19. Ma Z, Lim TM, Lim LY. Pharmacological activity of peroral chitosan-insulin nanoparticles in diabetic rats. *Int J Pharm*. 2005;293(1–2):271–80.
20. Morishita M, Peppas NA. Is the oral route possible for peptide and protein drug delivery? *Drug Discov Today* 2006;11(19–20):905–10.
21. Johnson-Léger C, Power CA, Shomade G, Shaw JP, Proudfoot AE. Protein therapeutics—Lessons learned and a view of the future. *Expert Opin Biol Ther* 2006;6(1):1–7.
22. Fasano A. Novel approaches for oral delivery of macromolecules. *J Pharm Sci*. 1998;87(11):1351–6.
23. Illum L. Nasal drug delivery—possibilities, problems and solutions. *J Control Release* 2003;87(1–3):187–98.
24. Pires A, Fortuna A, Alves G, Falcão A. Intranasal drug delivery: How, why and what for? *J Pharm Pharm Sci*. 2009;12(3):288–311.
25. Wang J, Bu G. Influence of the nasal mucociliary system on intranasal drug administration. *Chin Med J (Engl)*. 2000;113(7):647–9.
26. Merkus FW, Verhoef JC, Schipper NG, Martin E. Nasal mucociliary clearance as a factor in nasal drug delivery. *Adv Drug Deliv Rev* 1998;29(1–2):13–38.

27. Huang CH, Kimura R, Nassar RB, Hussain A. Mechanism of nasal absorption of drugs I: Physicochemical parameters influencing the rate of *in situ* nasal absorption of drugs in rats. *J Pharm Sci.* 1985;74(6):608–11.
28. Costantino HR, Illum L, Brandt G, Johnson PH, Quay SC. Intranasal delivery: Physicochemical and therapeutic aspects. *Int J Pharm.* 2007;337(1–2):1–24.
29. Irwin WJ, Dwivedi AK, Holbrook PA, Dey MJ. The effect of cyclodextrins on the stability of peptides in nasal enzymic systems. *Pharm Res.* 1994;11(12):1698–703.
30. Davis SS, Illum L. Absorption enhancers for nasal drug delivery. *Clin Pharmacokinet.* 2003;42(13):1107–28.
31. Sharma S, Kulkarni J, Pawar AP. Permeation enhancers in the transmucosal delivery of macromolecules. *Pharmazie* 2006;61(6):495–504.
32. Shao Z, Krishnamoorthy R, Mitra AK. Cyclodextrins as nasal absorption promoters of insulin: Mechanistic evaluations. *Pharm Res.* 1992;9(9):1157–63.
33. Schipper NG, Romeijn SG, Verhoef JC, Merkus FW. Nasal insulin delivery with dimethyl-beta-cyclodextrin as an absorption enhancer in rabbits: Powder more effective than liquid formulations. *Pharm Res.* 1993;10(5):682–6.
34. Pontiroli AE, Alberetto M, Pajetta E, Calderara A, Pozza G. Human insulin plus sodium glycocholate in a nasal spray formulation: Improved bioavailability and effectiveness in normal subjects. *Diabete Metab.* 1987;13(4):441–3.
35. Varshosaz J, Sadrai H, Heidari A. Nasal delivery of insulin using bioadhesive chitosan gels. *Drug Deliv.* 2006;13(1):31–8.
36. Illum L. Nanoparticulate systems for nasal delivery of drugs: A real improvement over simple systems? *J Pharm Sci.* 2007;96(3):473–83.
37. Illum L. Nasal drug delivery: New developments and strategies. *Drug Discov Today.* 2002;7(23):1184–9.
38. Jain AK, Chalasani KB, Khar RK, Ahmed FJ, Diwan PV. Muco-adhesive multivesicular liposomes as an effective carrier for transmucosal insulin delivery. *J Drug Target.* 2007;15(6):417–27.
39. Wang X, Zheng C, Wu Z, Teng D, Zhang X, Wang Z, Li C. Chitosan-NAC nanoparticles as a vehicle for nasal absorption enhancement of insulin. *J Biomed Mater Res B Appl Biomater.* 2009;88(1):150–61.
40. Gao X, Tao W, Lu W, Zhang Q, Zhang Y, Jiang X, Fu S. Lectin-conjugated PEG-PLA nanoparticles: Preparation and brain delivery after intranasal administration. *Biomaterials* 2006;27(18):3482–90.
41. Amidi M, Romeijn SG, Borchard G, Junginger HE, Hennink WE, Jiskoot W. Preparation and characterization of protein-loaded N-trimethyl chitosan nanoparticles as nasal delivery system. *J Control Release.* 2006;111(1–2):107–16.
42. Jain AK, Khar RK, Ahmed FJ, Diwan PV. Effective insulin delivery using starch nanoparticles as a potential trans-nasal mucoadhesive carrier. *Eur J Pharm Biopharm.* 2008;69(2):426–35.
43. Varshosaz J, Sadrai H, Alinagari R. Nasal delivery of insulin using chitosan microspheres. *J Microencapsul* 2004;21(7):761–74.
44. Matsubara K, Abe K, Irie T, Uekama K. Improvement of nasal bioavailability of luteinizing hormone-releasing hormone agonist, buserelin, by cyclodextrin derivatives in rats. *J Pharm Sci.* 1995;84(11):1295–300.
45. Chaplin MD. Bioavailability of nafarelin in healthy volunteers. *Am J Obstet Gynecol.* 1992;166(2):762–5.
46. Harris AS, Svensson E, Wagner ZG, Lethagen S, Nilsson IM. Effect of viscosity on particle size, deposition, and clearance of nasal delivery systems containing desmopressin. *J Pharm Sci.* 1988;77(5):405–8.
47. Agu RU, Ugwoke MI, Armand M, Kinget R, Verbeke N. The lung as a route for systemic delivery of therapeutic proteins and peptides. *Respir Res.* 2001;2(4):198–209.
48. Rau JL. The inhalation of drugs: Advantages and problems. *Respir Care.* 2005;50(3):367–82.
49. Corkery K. Inhalable drugs for systemic therapy. *Respir Care.* 2000;45(7):831–5.

50. Crandall ED, Matthay MA. Alveolar epithelial transport. Basic science to clinical medicine. *Am J Respir Crit Care Med*. 2001;163(4):1021–9.
51. Patton JS. Mechanisms of macromolecule absorption by the lungs. 1996;16(1):3–36.
52. Wall DA. Pulmonary absorption of peptides and proteins. 1995;2(1):1–20.
53. Labiris NR, Dolovich MB. Pulmonary drug delivery. Part I: Physiological factors affecting therapeutic effectiveness of aerosolized medications. *Br J Clin Pharmacol*. 2003;56(6):588–99.
54. Labiris NR, Dolovich MB. Pulmonary drug delivery. Part II: The role of inhalant delivery devices and drug formulations in therapeutic effectiveness of aerosolized medications. *Br J Clin Pharmacol*. 2003;56(6):600–12.
55. Hastings RH, Folkesson HG, Matthay MA. Mechanisms of alveolar protein clearance in the intact lung. *Am J Physiol Lung Cell Mol Physiol*. 2004;286(4):L679–89.
56. Toews GB. Pulmonary defense mechanisms. *Semin Respir Infect*. 1993 Sep;8(3):160–7.
57. Edwards DA, Ben-Jebria A, Langer R. Recent advances in pulmonary drug delivery using large, porous inhaled particles. *J Appl Physiol*. 1998;85(2):379–85.
58. Weers JG, Tarara TE, Clark AR. Design of fine particles for pulmonary drug delivery. *Expert Opin Drug Deliv*. 2007;4(3):297–313.
59. Vanbever R, Mintzes JD, Wang J, Nice J, Chen D, Batycky R, Langer R, Edwards DA. Formulation and physical characterization of large porous particles for inhalation. *Pharm Res*. 1999;16(11):1735–42.
60. Chougule MB, Padhi BK, Jinturkar KA, Misra A. Development of dry powder inhalers. *Recent Pat Drug Deliv Formul*. 2007;1(1):11–21.
61. Siekmeier R, Scheuch G. Systemic treatment by inhalation of macromolecules—Principles, problems, and examples. *J Physiol Pharmacol*. 2008;59 Suppl 6:53–79.
62. Smola M, Vandamme T, Sokolowski A. Nanocarriers as pulmonary drug delivery systems to treat and to diagnose respiratory and non respiratory diseases. *Int J Nanomed*. 2008;3(1):1–19.
63. Bailey MM, Berkland CJ. Nanoparticle formulations in pulmonary drug delivery. *Med Res Rev*. 2009;29(1):196–212.
64. Bi R, Shao W, Wang Q, Zhang N. Spray-freeze-dried dry powder inhalation of insulin-loaded liposomes for enhanced pulmonary delivery. *J Drug Target*. 2008;16(9):639–48.
65. Scheuch G, Kohlhaeufel MJ, Brand P, Siekmeier R. Clinical perspectives on pulmonary systemic and macromolecular delivery. *Adv Drug Deliv Rev*. 2006;58(9–10):996–1008.
66. Bernstein G. Delivery of insulin to the buccal mucosa utilizing the RapidMist system. *Expert Opin Drug Deliv*. 2008;5(9):1047–55.
67. Merrill JR. The “gift” of delirium. *Hosp Pract (Off Ed)*. 1990;25(10A):16.
68. Hao J, Heng PW. Buccal delivery systems. *Drug Dev Ind Pharm*. 2003;29(8):821–32.
69. Dodane V, Amin Khan M, Merwin JR. Effect of chitosan on epithelial permeability and structure. *Int J Pharm*. 1999;182(1):21–32.
70. Bernkop-Schnürch A. Chitosan and its derivatives: Potential excipients for peroral peptide delivery systems. *Int J Pharm*. 2000;194(1):1–13.
71. Tengamnuay P, Sahamethapat A, Sailasuta A, Mitra AK. Chitosans as nasal absorption enhancers of peptides: Comparison between free amine chitosans and soluble salts. *Int J Pharm*. 2000;197(1–2):53–67.
72. Veuilleux F, Kalia YN, Jacques Y, Deshusses J, Buri P. Factors and strategies for improving buccal absorption of peptides. *Eur J Pharm Biopharm*. 2001 Mar;51(2):93–109.
73. Rossi S, Sandri G, Ferrari F, Bonferoni MC, Caramella C. Buccal delivery of acyclovir from films based on chitosan and polyacrylic acid. *Pharm Dev Technol*. 2003;8(2):199–208.
74. Nafee NA, Boraie MA, Ismail FA, Mortada LM. Design and characterization of mucoadhesive buccal patches containing cetylpyridinium chloride. *Acta Pharm*. 2003;53(3):199–212.
75. Perioli L, Ambrogi V, Rubini D, Giovagnoli S, Ricci M, Blasi P, Rossi C. Novel mucoadhesive buccal formulation containing metronidazole for the treatment of periodontal disease. *J Control Release*. 2004;95(3):521–33.

- 76 Sandri G, Rossi S, Ferrari F, Bonferoni MC, Muzzarelli C, Caramella C. Assessment of chitosan derivatives as buccal and vaginal penetration enhancers. *Eur J Pharm Sci.* 2004;21(2-3):351-9.
77. Han RY, Fang JY, Sung KC, Hu OY. Mucoadhesive buccal disks for novel nalbuphine prodrug controlled delivery: Effect of formulation variables on drug release and mucoadhesive performance. *Int J Pharm.* 1999;177(2):201-9.
78. Senel S, Kremer MJ, Kaş S, Wertz PW, Hincal AA, Squier CA. Enhancing effect of chitosan on peptide drug delivery across buccal mucosa. *Biomaterials.* 2000;21(20):2067-71.
79. Patel D, Smith AW, Grist N, Barnett P, Smart JD. An *in vitro* mucosal model predictive of bioadhesive agents in the oral cavity. *J Control Release.* 1999;61(1-2):175-83.
80. Shojaei AH, Paulson J, Honary S. Evaluation of poly(acrylic acid-co-ethylhexyl acrylate) films for mucoadhesive transbuccal drug delivery: Factors affecting the force of mucoadhesion. *J Control Release.* 2000;67(2-3):223-32.
81. Lee J, Kellaway IW. Peptide washout and permeability from glyceryl monooleate buccal delivery systems. *Drug Dev Ind Pharm.* 2002;28(9):1155-62.
82. Smart JD. Lectin-mediated drug delivery in the oral cavity. *Adv Drug Deliv Rev.* 2004;56(4):481-9.
83. Yang TZ, Wang XT, Yan XY, Zhang Q. Phospholipid deformable vesicles for buccal delivery of insulin. *Chem Pharm Bull (Tokyo).* 2002;50(6):749-53.
84. Morishita M, Barichello JM, Takayama K, Chiba Y, Tokiwa S, Nagai T. Pluronic F-127 gels incorporating highly purified unsaturated fatty acids for buccal delivery of insulin. *Int J Pharm.* 2001;212(2):289-93.
85. Xu HB, Huang KX, Zhu YS, Gao QH, Wu QZ, Tian WQ, Sheng XQ, Chen ZX, Gao ZH. Hypoglycaemic effect of a novel insulin buccal formulation on rabbits. *Pharmacol Res.* 2002;46(5):459-67.
86. Venugopalan P, Sapre A, Venkatesan N, Vyas SP. Pelleted bioadhesive polymeric nanoparticles for buccal delivery of insulin: Preparation and characterization. *Pharmazie.* 2001;56(3):217-9.
87. Hosny EA, Elkhesheh SA, Saleh SI. Bucco-adhesive tablets for insulin delivery: In-vitro and in-vivo studies. *Boll Chim Farm.* 2002;141(3):210.
88. Modi P, Mihic M, Lewin A. The evolving role of oral insulin in the treatment of diabetes using a novel Rapid Mist System. *Diabetes Metab Res Rev.* 2002;18 Suppl 1:S38-42.
89. Khafagyel-S, Morishita M, Onuki Y, Takayama K. Current challenges in non-invasive insulin delivery systems: A comparative review. *Adv Drug Deliv Rev.* 2007;59(15):1521-46.
90. Owens DR. New horizons—Alternative routes for insulin therapy. *Nat Rev Drug Discov.* 2002;1(7):529-40.
91. Hussain A, Ahsan F. The vagina as a route for systemic drug delivery. *J Control Release.* 2005;103(2):301-13.
92. Valenta C. The use of mucoadhesive polymers in vaginal delivery. *Adv Drug Deliv Rev.* 2005;57(11):1692-712.
93. Vermani K, Garg S. The scope and potential of vaginal drug delivery. *Pharm Sci Technol Today.* 2000;3(10):359-364.
94. Richardson JL, Illum L, Thomas NW. Vaginal absorption of insulin in the rat: Effect of penetration enhancers on insulin uptake and mucosal histology. *Pharm Res.* 1992;9(7):878-83.
95. Morimoto K, Takeeda T, Nakamoto Y, Morisaka K. Effective vaginal absorption of insulin in diabetic rats and rabbits using polyacrylic acid aqueous gel bases. *Int. J. Pharm.* 1982;12:107-11.
96. Kisel MA, Kulik LN, Tsybovsky IS, Vlasov AP, Vorob'yov MS, Kholodova EA, Zabarovskaya ZV. Liposomes with phosphatidylethanol as a carrier for oral delivery of insulin: Studies in the rat. *Int J Pharm.* 2001;216(1-2):105-14.
97. Jerry N, Anitha Y, Sharma CP, Sony P. *In vivo* absorption studies of insulin from an oral delivery system. *Drug Deliv.* 2001;8(1):19-23.
98. Chattaraj SC, Das SK. Physicochemical characterization of influenza viral vaccine loaded surfactant vesicles. *Drug Deliv.* 2003;10(2):73-7.
99. Ning M, Guo Y, Pan H, Yu H, Gu Z. Niosomes with sorbitan monoester as a carrier for vaginal delivery of insulin: Studies in rats. *Drug Deliv.* 2005;12(6):399-407.

100. Değim Z, Değim T, Acartürk F, Erdoğan D, Ozoğul C, Köksal M. Rectal and vaginal administration of insulin-chitosan formulations: An experimental study in rabbits. *J Drug Target*. 2005;13(10):563–72.
101. Richardson JL, Illum L, Thomas NW. Vaginal absorption of insulin in the rat: Effect of penetration enhancers on insulin uptake and mucosal histology. *Pharm Res*. 1992;9(7):878–83.
102. Benson HA, Namjoshi S. Proteins and peptides: Strategies for delivery to and across the skin. *J Pharm Sci*. 2008;97(9):3591–610.
103. Shah PK, Borchardt RT. A comparison of peptidase activities and peptide metabolism in cultured mouse keratinocytes and neonatal mouse epidermis. *Pharm Res*. 1991;8(1):70–5.
104. Schuetz YB, Naik A, Guy RH, Kalia YN. Emerging strategies for the transdermal delivery of peptide and protein drugs. *Expert Opin Drug Deliv*. 2005;2(3):533–48.
105. Foldvari M, Attah-Poku S, Hu J, Li Q, Hughes H, Babiuk LA, Kruger. Palmitoyl derivatives of interferon alpha: Potential for cutaneous delivery. *S J Pharm Sci*. 1998;87(10):1203–8.
106. Ahad A, Aqil M, Kohli K, Chaudhary H, Sultana Y, Mujeeb M, Talegaonkar S. Chemical penetration enhancers: A patent review. *Expert Opin Ther Pat*. 2009;19(7):969–88.
107. Thong HY, Zhai H, Maibach HI. Percutaneous penetration enhancers: An overview. *Skin Pharmacol Physiol*. 2007;20(6):272–82.
108. Foldvari M, Badea I, Wettig S, Baboolal D, Kumar P, Creagh AL, Haynes CA. Topical delivery of interferon alpha by biphasic vesicles: Evidence for a novel nanopathway across the stratum corneum. *Mol Pharm*. 2010 Jun 7;7(3):751–62.
109. Foldvari M, Baca-Estrada ME, He Z, Hu J, Attah-Poku S, King M. Dermal and transdermal delivery of protein pharmaceuticals: Lipid-based delivery systems for interferon alpha. *Biotechnol Appl Biochem*. 1999 Oct;30 (Pt 2):129–37.
110. Banga AK. Theme section: Transdermal delivery of proteins. *Pharm Res*. 2007;24(7):1357–9.
111. Clemessy M, Couarraze G, Bevan B, Puisieux F. Mechanisms involved in iontophoretic transport of angiotensin. *Pharm Res*. 1995;12(7):998–1002.
112. Lau DT, Sharkey JW, Petryk L, Mancuso FA, Yu Z, Tse FL. Effect of current magnitude and drug concentration on iontophoretic delivery of octreotide acetate (Sandostatin) in the rabbit. *Pharm Res*. 1994;11(12):1742–6.
113. Craane-van Hinsberg WH, Bax L, Flinterman NH, Verhoef J, Junginger HE, Boddé HE. Iontophoresis of a model peptide across human skin in vitro: Effects of iontophoresis protocol, pH, and ionic strength on peptide flux and skin impedance. *Pharm Res*. 1994;11(9):1296–300.
114. Thysman S, Hanchard C, Pr at V. Human calcitonin delivery in rats by iontophoresis. *J Pharm Pharmacol*. 1994 Sep;46(9):725–30.
115. Lvovich VF, Matthews E. AC electrokinetic platform for iontophoretic transdermal drug delivery. *J Control Release*. 2010 Apr 24. [Epub ahead of print]
116. Kalia YN, Naik A, Garrison J, Guy RH. Iontophoretic drug delivery. *Adv Drug Deliv Rev*. 2004;56(5):619–58.
117. Gonz alez Meli B, D az G omez LA, Hern andez Ramos A, G omez Balboa P. [Congenital short urethra: Surgical treatment] *Actas Urol Esp*. 1992;16(5):409–12.
118. Sen A, Daly ME, Hui SW. Transdermal insulin delivery using lipid enhanced electroporation. *Biochim Biophys Acta*. 2002;1564(1):5–8.
119. Al-Tabakha MM, Arida AI. Recent challenges in insulin delivery systems: A review. *Indian J Pharm Sci*. 2008;70(3):278–86.
120. Yamamoto A, Luo AM, Dodda-Kashi S, Lee VH. The ocular route for systemic insulin delivery in the albinorabbit. *J Pharmacol Exp Ther*. 1989 Apr;249(1):249–55.
121. Soni V, Singh R, Srinivasan R, Jain SK. Pulsatile insulin delivery through the ocular route. *Drug Deliv*. 1998;5(1):47–51.
122. Simamora P, Lee YC, Yalkowsky SH. Ocular device for the controlled systemic delivery of insulin. *J Pharm Sci*. 1996;85(10):1128–30.

123. Lee YC, Yalkowsky SH. Ocular devices for the controlled systemic delivery of insulin: *In vitro* and *in vivo* dissolution. *Int J Pharm.* 1999;181(1):71-7.
124. Hosny EA. Relative hypoglycemia of rectal insulin suppositories containing deoxycholic acid, sodium taurocholate, polycarbophil, and their combinations in diabetic rabbits. *Drug Dev Ind Pharm.* 1999;25(6):745-52.
125. Yun MO, Choi HG, Jung JH, Kim CK. Development of a thermoreversible insulin liquid suppository with bioavailability enhancement. *Int. J. Pharm.* 1999;189:137-45.

Environment-Responsive Hydrogels for Drug Delivery

87.1	Introduction	87-1
87.2	Thermoresponsive Hydrogels	87-2
	Structure and Property • Application to Drug Delivery	
87.3	pH-Responsive Hydrogels	87-7
	Structure and Property • Application to Drug Delivery	
87.4	Light-Responsive Hydrogels	87-10
87.5	Electroresponsive Hydrogels.....	87-11
87.6	Glucose-Responsive Hydrogels.....	87-12
87.7	Enzyme-Responsive Hydrogels	87-14
87.8	Inflammation-Responsive Hydrogels.....	87-15
87.9	Antigen-Responsive Hydrogels	87-15
87.10	Magneto-responsive Hydrogels	87-16
87.11	Ultrasound-Responsive Hydrogels	87-16
87.12	Redox/Thiol-Responsive Hydrogels.....	87-17
87.13	Concluding Comments.....	87-17
	Abbreviations	87-18
	References.....	87-18

Byung Kook Lee
Hanyang University

Jong-Ryoul Kim
Hanyang University

Kinam Park
Purdue University

Yong Woo Cho
Hanyang University

87.1 Introduction

Diverse activities of biomolecules, cells, tissues, organs, and organisms are regulated through rapid, reversible, and repeated responses to a wide variety of environmental stimuli. For example, the mechanism of vision in human eyes is based on photoresponsive cis-trans isomerization of the retinal in rhodopsin. Influenza virus for infection and replication gains access to cytosol by pH-responsive conformational change of hemagglutinin protein (HA). A Venus flytrap closes its trap rapidly in response to the environmental stimulus of an insect landing on it. All living organisms, at their most basic levels, have macromolecules that vary physicochemical properties in response to environment stimuli.

Drug-delivery systems are intended to deliver drugs at proper times at proper sites. During the past two decades, a lot of work has been dedicated to the development of smart drug-delivery systems that can control drug release in response to environmental stimuli. Indeed, conventional drug formulations have moved forward to the smart drug-delivery systems that can sense disease signals, alter their physicochemical properties, and release the right amount of drug at the target sites at the right time. A variety of types of stimuli-responsive drug-delivery systems have been reported, which can respond to the external changes in environmental conditions, such as temperature, pH, light, glucose,

enzymes, antigens, inflammation, redox/thiol, ultrasound, magnetic, and electric field (Li and Keller 2009; Kojima 2010; Stuart et al. 2010). The term “environment-responsive” can be described in various ways. Typically, environment-responsive polymers in aqueous media vary their individual chain dimensions, secondary structures, ionization, solubility, intermolecular association, and supramolecular architecture. In most cases, the physical or chemical stimuli induce formation or destruction of secondary forces (hydrogen bonding, hydrophobic interaction, van der Waals forces, electrostatic interactions, etc.), chemical reactions of moieties pendant to the polymer backbone, or osmotic pressure differentials. Incorporating multiple environment-responsive groups along a polymer backbone can result in synergistic amplification for dramatic changes in macroscopic polymer properties. This approach is a form of biomimicry, since many biological macromolecules dramatically alter their conformation and three-dimensional (3D) structures in response to specific chemical species in their surroundings (Roy et al. 2010).

Water-soluble polymers can be physically or chemically cross-linked to form hydrogels, which are water-swollen polymeric materials with a 3D network structure (Kim et al. 1992). Owing to their high water content, the hydrogels exhibit excellent biocompatibility and have been widely used in the development of smart drug-delivery systems (Hamidi et al. 2008; Meng et al. 2009b; Oh et al. 2009). The 3D network can be formed by cross-linking polymer chains through covalent bonds, hydrogen bonding, hydrophobic interactions, or physical entanglements. Although individual polymer chains remain soluble in water, the cross-linking prevents individual molecules from dissolving in aqueous media. Instead, the polymer network swells as water diffuses into the interstices of the network while maintaining the physical integrity of the network itself. In this manner, the extent of cross-linking determines the extent of swelling and, also, the distance between chains within the cross-linked network. When entrapped molecules within the network are diffusing out, the rate of diffusion is dependent on the interchain separation and the size of the diffusing molecules.

Intelligent hydrogels have been extensively applied to the development of new drug-delivery matrices responding to several physiological stimuli arising from disease states or metabolic events in the human body (Onaca et al. 2009). One key strategy for drug-delivery systems was the spatiotemporal control of drug release responding to any changes in body physiology at specific sites (Kwon 2005). Stimuli-responsive hydrogels change their swelling degree or undergo phase transition in response to minimal changes in environmental conditions. Numerous monomers and cross-linking agents have been used for the synthesis of hydrogels with a wide range of chemical compositions. In this chapter, several types of stimuli-responsive hydrogels are introduced, and their applications to drug-delivery systems are discussed.

87.2 Thermo-responsive Hydrogels

87.2.1 Structure and Property

Temperature-responsive hydrogels are probably the most commonly studied class of environment-responsive systems in a drug-delivery field. Most natural polymers such as gelatin, agarose, and carrageenan show a thermo-responsive sol–gel phase transition with an upper critical solution temperature (UCST). That is, their aqueous solutions form a gel when the temperature is lowered. The sol phase is defined as a flowing fluid, whereas the gel phase is a nonflowing fluid, maintaining its integrity. These polymers undergo temperature-sensitive conformational change. Above UCST, they adopt a random coil conformation in the solution. Upon cooling, a continuous network is formed by partial helix conformation (Figure 87.1). However, the most extensively studied thermo-responsive hydrogels in smart drug-delivery systems are based on an inverse thermo-responsive sol–gel transition exhibiting a lower critical solution temperature (LCST). These polymers are readily soluble in water below LCST and form a gel above LCST. Figure 87.2 represents typical thermo-responsive polymers such as copolymers of *N*-isopropylacrylamide (NiPAAM), methylcellulose (MC), hydroxypropyl methylcellulose (HPMC), polyorganophosphazenes, and poly(*N,N*-diethylacrylamide) (PDEAAm). All these polymers share in

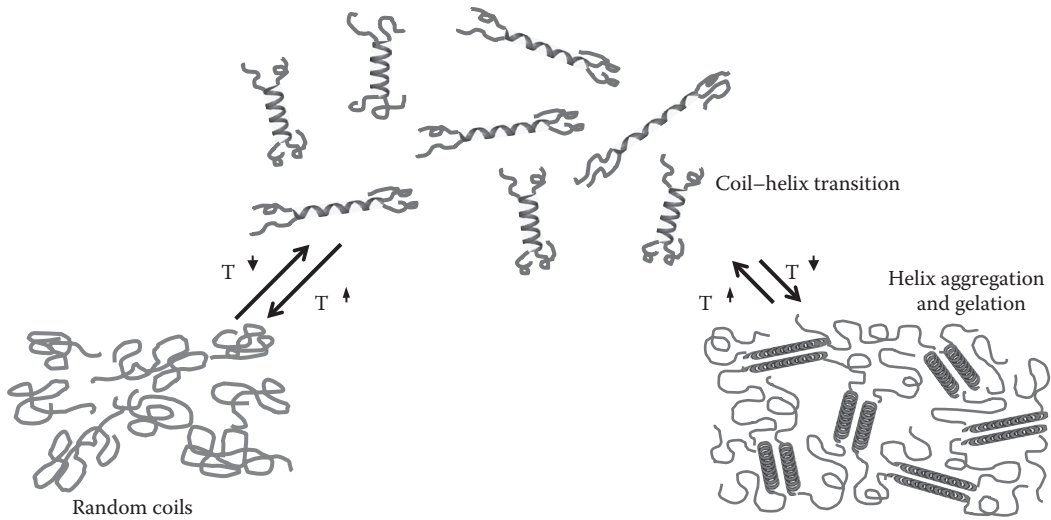


FIGURE 87.1 Schematic representation of thermoresponsive sol-gel phase transition of polymers with UCST.

common a unique hydration chemical structure in aqueous milieu that is metastable and can be altered by increasing thermal energy in the system. They are amphiphilic copolymers, having both hydrophilic and hydrophobic moieties, and their phase transitions are governed by the balance of hydrophilic and hydrophobic moieties on polymer chains. The main driving force for the thermoresponsive gelation is the temperature-triggered intermolecular association between hydrophobic groups. At lower temperatures, the polymers are fully hydrated in an aqueous medium, producing a clear solution. There are only simple entanglements of polymer chains that occur via weak polymer-polymer interactions. As the temperature rises, hydrogen bonds between water molecules and polymers gradually weaken, and hydrophobic association becomes more pronounced, thereby resulting in the formation of a hydrogel

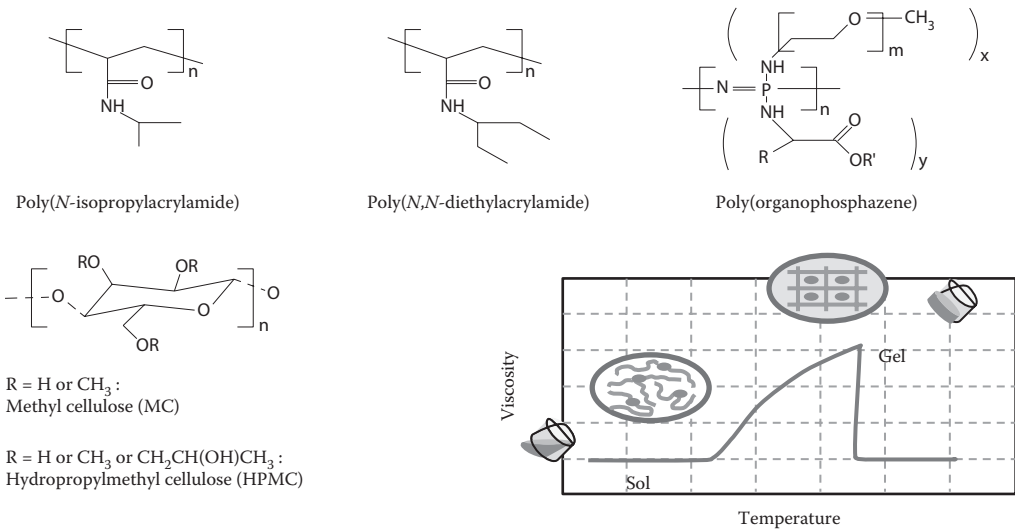


FIGURE 87.2 Structural formula of representative thermoresponsive polymers with LCST and schematic illustration of the sol-gel transition behavior.

Downloaded by [JCR JCR] at 10:44 01 August 2015

structure. This phase transition is reversible, with some characteristic hysteresis, upon reversal of the temperature change.

As described above, the LCST of thermoresponsive polymers is governed by the balance between hydrophilicity and hydrophobicity. For example, the LCST of NiPAAM copolymers can be controlled by copolymerizing with other monomers with different hydrophobicity. The more hydrophobic comonomers, the lower the LCST. The presence of salts as a third component in aqueous solutions of thermosensitive polymers influences their thermogelling behaviors. The effect of salt is of importance, because salts are ubiquitous in biological systems. Salting-out solutes, such as NaCl, KF, $(\text{NH}_4)_2\text{SO}_4$, and Na_2CO_3 decrease the gelation temperature via their water-structure-making property, whereas salting-in solutes, such as KI, tend to result in increases in gelation temperature due to their water-structure-breaking properties.

Certain types of block copolymers including triblock copolymers of poly(ethylene oxide) and poly(propylene oxide) (PEO-PPO-PEO), and triblock copolymers of poly(ethylene glycol) and poly([D,L-lactide-co-(glycolide)]) (PEG-PLGA-PEG) also exhibit an inverse temperature-responsive sol-gel phase transition (Zhao and Xu 2010) (Figure 87.3). A variety of PEO-PPO-PEO block copolymers are commercially available under the trade names of Pluronic[®] (or Poloxamer[®]) and Tetronics[®], with varying compositions of PEO and PPO blocks (Wang et al. 2009b). The triblock copolymers form micelles above the critical micelle concentration (CMC). As the temperature increases, the equilibrium shifts from unimers to micelles, reducing the number of unassociated unimers in solution, leading to an increase in the micelle volume fraction (ϕ_m). The micelle volume fraction increases abruptly in a certain temperature range, which is dependent on the concentration. When the micelle volume fraction exceeds a critical value, the micellar solution becomes a gel by micelle packing.

Block copolymers composed of PEG and PLGA have received significant attention in a drug-delivery field, especially in an injectable *in situ* depot-forming system. PEG-PLGA-PEG triblock copolymers also show an inverse thermoresponsive gelation. Proper combinations of molecular weight and polymer architecture resulted in different LCSTs. Monomethoxy-PEG was used as a macroinitiator, to initialize the ring-opening polymerization of lactide and glycolide. Then two diblock copolymers (PEG-PLGA)

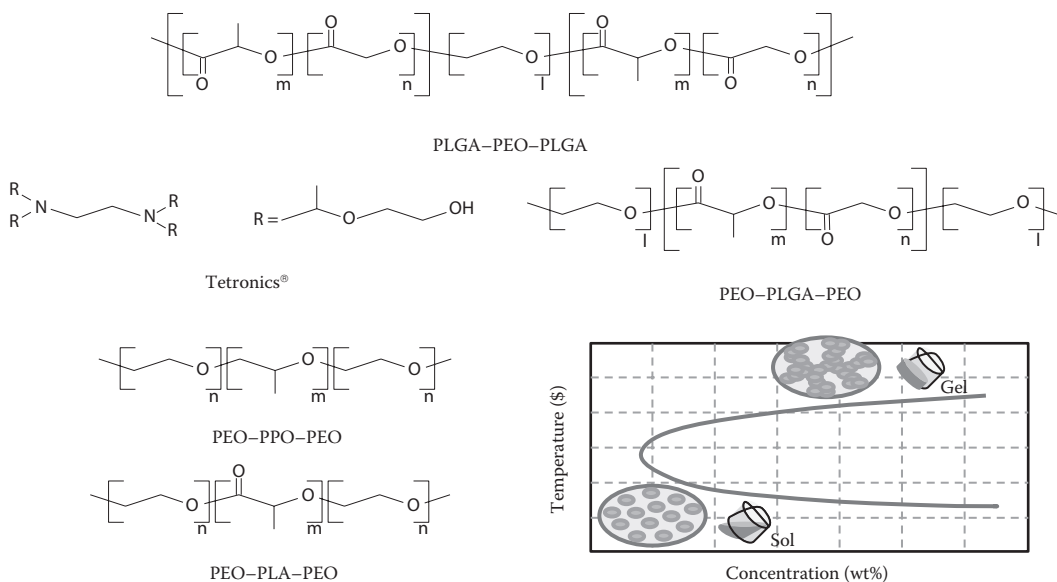


FIGURE 87.3 Structural formula of representative block copolymers with LCST and schematic illustration of the sol-gel transition behaviors.

were coupled using hexamethylene diisocyanate to form PEG–PLGA–PEG triblock copolymers that exhibited a relatively narrow molecular weight distribution ($M_w/M_n \sim 1.2$). The LCSTs were 30–36°C at polymer concentrations of 17–40 g/dL. A further increase in temperature affected gel appearance, from transparent to turbid, translucent, turbid, and then finally dissolving back to an opaque solution at a critical temperature ranging from 44°C to 70°C (Jeong et al. 1999b, 2002a).

PLGA–PEG–PLGA triblock copolymers can be synthesized via the bulk polymerization of PEG with lactide and glycolide in the presence of stannous 2-ethylhexanoate. These triblock copolymers had an analogous but inverted structure, compared to PEG–PLGA–PEG (Jeong et al. 1999a,b, 2000, 2002a). They showed three phases: solution, gel, and precipitate, depending on temperature. During the sol-to-gel transition, the aqueous solution of 23 g/dL showed large viscosity changes (approximately four orders of magnitude) from 0.4 P in the sol state to 5700 P at the onset of gelation at 13.6°C. Such a viscoelastic behavior was reproducible with repeated temperature changes. The *in vitro* degradation showed more rapid degradation at higher temperatures. Complete degradation occurred after 6–8 weeks at 37°C, whereas, at low temperatures, polymers were stable for 20–30 weeks at 5°C and more than 2 years at –10°C. The *in vivo* degradation after subcutaneous injection indicated that the hydrogel appearance dramatically changed between 2 and 4 weeks: initially, the polymer hydrogels decreased in size during the first 2 weeks; then, they became a mixture of gel and a viscous liquid, and then a completely viscous liquid with no gel; finally, the matrices were completely absorbed into the body, and followed a simple hydrolysis mechanism (Jeong et al. 1999a).

87.2.2 Application to Drug Delivery

Biodegradable, inverse thermoresponsive polymers with LCST are highly attractive as drug-delivery carriers because (1) their formulation requires no organic solvent; (2) the triblock copolymer matrices can be stored as dry, solid forms before administration; (3) highly hydrophobic, and thus practically insoluble drugs can be dissolved dramatically by simple mixing at ambient temperatures; and (4) drugs with a delivery vehicle can be injected directly by a syringe so that no surgical operation is necessary (Figure 87.4).

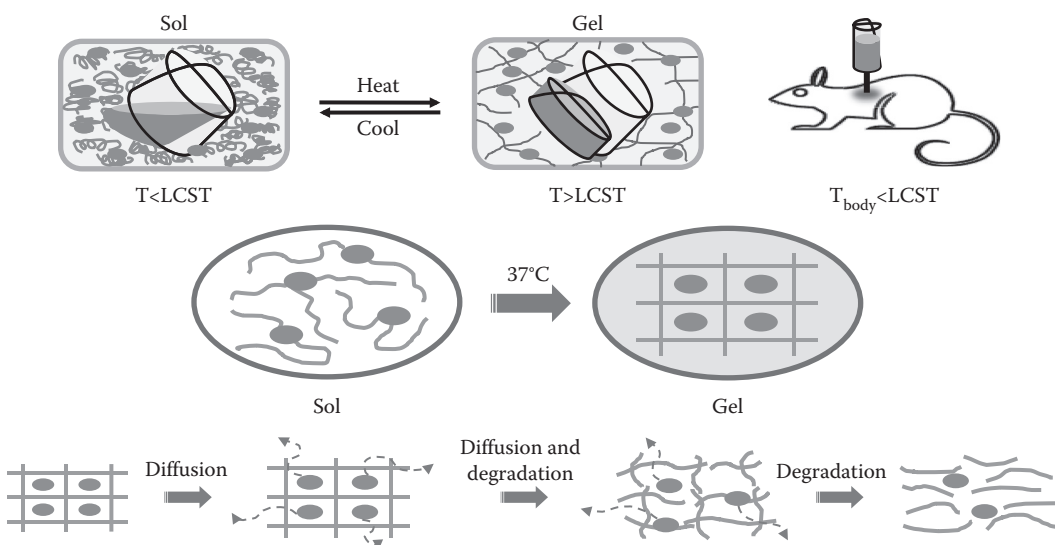


FIGURE 87.4 Schematic illustration of an injectable *in situ* depot-forming system using thermoresponsive sol-gel transition polymers.

Highly hydrophobic drugs such as paclitaxel ($\sim 1 \mu\text{g/mL}$) and cyclosporine A ($\sim 4 \mu\text{g/mL}$) can be dissolved by simply mixing these drugs with PLGA-PEG-PLGA triblock copolymer, a dramatic solubility increase over 2000-fold. These drugs were stable in the triblock copolymer formulations, with more than 85% stability. Paclitaxel release profiles showed a two-phase release pattern: a diffusion-governed mechanism for the initial 14 days, and the combined mechanism of diffusion and polymer degradation for the next 50 days. Direct injection of paclitaxel-containing triblock copolymer solutions to solid tumor in mice resulted in the gelation of polymers at injection sites, that is, within the tumor tissue. The drug remained at the tumor site for 42 days after injection, by which time it had gradually decreased to 20% (Zentner et al. 2001). PLGA-PEG-PLGA triblock copolymers were utilized for the delivery of peptide drugs including insulin (Kim et al. 2001), growth hormones (GHs), and granulocyte colony-stimulating factor (G-CSF). The *in vitro* protein drug release was monotonous and lasted for approximately 2 weeks after injection. The *in situ* forming hydrogels were applied to injectable cell delivery, so that cells stayed at desired sites. Such an approach has recently received a great deal of attention. Recent studies demonstrated that injected cells responded to external signals and produced bioactive compounds (Wang et al. 2009a).

Most polymers increase their water solubility as the temperature increases. Polymers with LCST, however, decrease their water solubility as the temperature increases. Hydrogels composed of LCST polymers shrink as the temperature increases above LCST. As described previously, the LCST can be changed by adjusting the ratio of the hydrophilic and hydrophobic segment. Such a strategy can be exploited so that a hydrogel's transition temperature can be controlled and then the drug release behavior can be regulated (Bromberg and Ron 1998). Below the LCST, drugs show diffusion-dependent release from a swollen gel (Figure 87.5a). The drug release profile can be altered when the temperature-triggered collapse of the gel occurs (Figure 87.5b). The entrapped drugs can be released by "squeezing-out effect" from the collapsed gel above the LCST. Figure 87.5c shows the "on-off" control of drug passage through

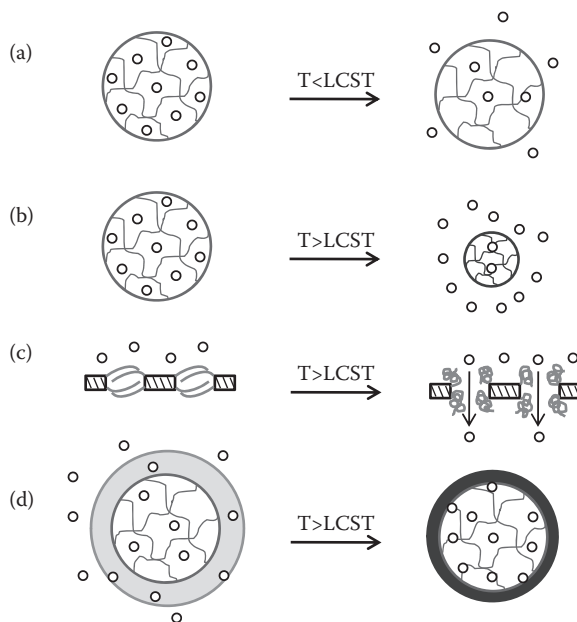


FIGURE 87.5 Smart drug-delivery systems using thermoresponsive polymers. (a) Diffusion-controlled drug release below LCST. (b) "Squeezing out" effect above LCST. (c) "On-off" control of drug release. (d) Heterogeneous microgels with a thermo-responsive shell. (Adapted from Bromberg, L. E., and Ron, E. S. 1998. Temperature-responsive gels and thermogelling polymer matrices for protein and peptide delivery. *Adv. Drug Deliv. Rev.*, 31: 197–221.)

the membranes that contain thermoresponsive hydrogel segments. Swollen gel blocks drug passage through the pores, and allows permeation when collapsed. Figure 87.5d describes another pulsatile drug release system. When a shell layer is made of thermoresponsive hydrogels with LCST, it may form a dense shell layer of the collapsed component while the core remains swollen.

The drug release behavior from PEG-PLGA-PEG *in situ* forming hydrogels has been extensively studied. For example, two low-molecular-weight compounds, ketoprofen and spironolactone, were used as model drug molecules having different hydrophobicities. The relatively hydrophilic ketoprofen was released monotonously through diffusion mechanisms, with approximately 90% of the drug released within 5 days. In contrast, the more hydrophobic spironolactone showed a sigmoid curve, with the release extending over 50 days. Given that the polymeric micellar structure was maintained within the triblock copolymer gels, the spironolactone molecules in PEG shell layers were released mainly by a diffusion process, while drugs preferentially existing in the hydrophobic micelle core were released via diffusion and bulk micelle matrix degradation. Thus, the longer-term sustained release of drugs was achieved using PEG-PLGA-PEG triblock copolymer hydrogels (Jeong et al. 2000, 2002b).

87.3 pH-Responsive Hydrogels

87.3.1 Structure and Property

The pH sensitivity has been one of the important parameters in designing a smart drug-delivery system because the pH change frequently occurs at pathological sites. For ionic hydrogels, the degree of swelling and drug release significantly depend on the environmental pH. The pH-responsive polymers can be classified as acidic weak polyelectrolytes containing pendant acidic groups (e.g., carboxylic and sulfonic acids) and basic weak polyelectrolytes with pendant basic (e.g., amine) groups (Figure 87.6). They accept or release protons in response to changes in environmental pH. Typical acidic pH-sensitive polymers containing carboxylic groups include poly(acrylic acid) (PAA), poly(methacrylic acid) (PMA), poly(L-glutamic acid), and alginate (Figure 87.7). Typical examples of the basic polyelectrolytes containing amine groups include poly(tertiary amine methacrylate), poly(2-vinylpyridine), poly(L-lysine), poly(L-histidine), poly(β -amino ester), and chitosan (Figure 87.7).

The presence of ionizable groups on polymer chains results in swelling of the hydrogels; far beyond that, it can be achievable by nonelectrolyte polymer hydrogels. Since the swelling of polyelectrolyte hydrogels is mainly due to the electrostatic repulsion among charges present on polymer chains, the extent of swelling is influenced by any changes that reduce or enhance electrostatic repulsion, such as pH, ionic strength, and type of counterions (Qiu and Park 2001). Swelling of ionic hydrogels sharply

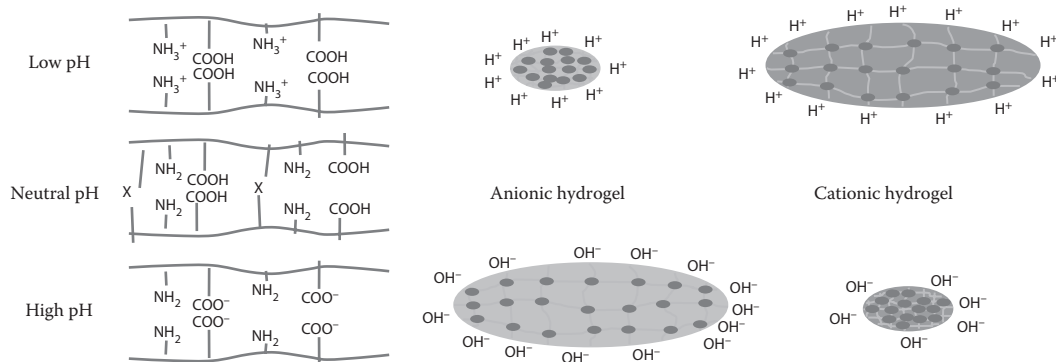


FIGURE 87.6 Schematic illustration of swelling/deswelling behaviors of different types of pH-responsive hydrogels.

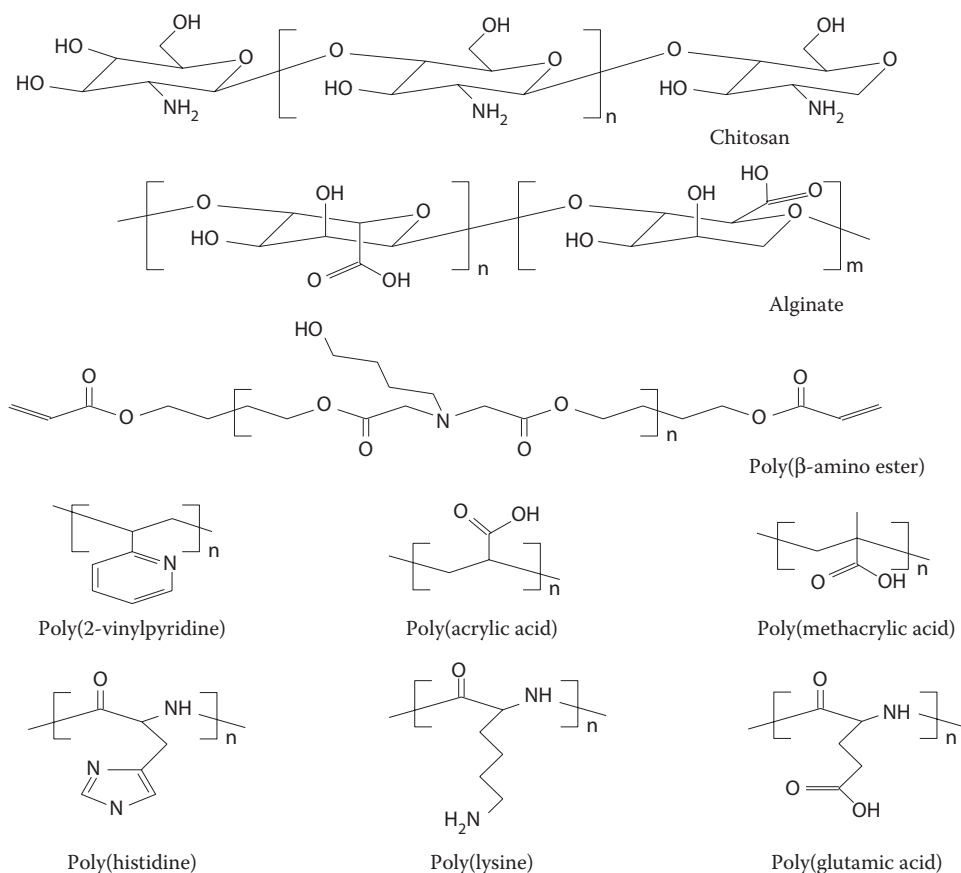


FIGURE 87.7 Structural formula of various pH-responsive polymers.

changes in the vicinity of their pK_a or pK_b values. Anionic hydrogels deprotonate and swell more when external pH is higher than pK_a of the ionizable groups bonded on polymer chains, while cationic hydrogels protonate and swell more when external pH is lower than the pK_b of the ionizable groups. By using two or more ionic monomers, the pH-dependent swelling curves can exhibit two or more inflection points near the pK_a/pK_b of the ionizable groups. As described above, the pendant acidic or basic groups on polymers undergo ionization such as acidic or basic groups of monomers. However, it should be noted that the ionization on the polymer is more difficult due to electrostatic effects exerted by other adjacent ionized groups. This tends to make the apparent dissociation constant (K_a) different from that of the corresponding monoacid or monobase.

The pH-responsive swelling/deswelling of polyelectrolyte hydrogels can be further manipulated by adding nonionic comonomers, such as 2-hydroxyethyl methacrylate (HEMA), methyl methacrylate (MMA), and maleic anhydride (MA) (Zentner et al. 2001). Different comonomers provide different hydrophobicity to the polymer chain, leading to different pH-responsive behaviors (Kim et al. 2001). At low pH, the acidic protons of the carboxyl groups of PMA interact with the ether oxygen of PEG through hydrogen bonding, and such complexation results in shrinkage of the hydrogels. As the carboxyl groups of PMA become ionized at high pH, the resulting decomplexation leads to the swelling of the hydrogels. Cross-linked copolymer hydrogels of poly(L-glutamic acid) and PEO showed rapid swelling and deswelling behavior. The swelling of this hydrogel varied with pH and increased at higher ionization of the poly(L-glutamic acid), which resulted from not only the electrostatic effects but also the secondary

structural change associated with the polypeptide backbone. By modifying the hydrophobicity of polypeptide and the degree of ionization, the overall extent of pH-responsive swelling could be controlled.

Just like temperature-responsive sol-gel transition polymers, block copolymers composed of pH-responsive polymers and neutral polymers exhibit pH-sensitive sol-gel transition. Some triblock copolymers, such as poly(diphenylamine)-poly(2-methacryloyloxyethyl phosphorylcholine)-poly(diphenylamine) (PDPA-PMPC-PDPA), form physical hydrogels at 37°C. At pH of 8 or less, the amino group is protonated and the block copolymers remain in solution, while under alkaline pH conditions, PDPA is sufficiently hydrophobic to form physical hydrogels. Triblock and three-arm star diblock copolymers can be synthesized with atom transfer radical polymerization (ATRP) initiated by bifunctional and trifunctional initiators, respectively, with the central block, poly(glycerol methacrylate) (PGMA), and the outer pH-responsive PDEA or PDPA blocks. The hydrogel from these block copolymers showed reversible, pH-responsive sol-gel transition; the free-standing gel formation was observed at neutral or higher pH, but dissolved in acidic solution. Armes and coworkers synthesized pH-responsive microgels with a diameter of approximately 250 nm by the emulsion polymerization of 2-(diethylamino)ethyl methacrylate (DEAEMA) with a bifunctional oligo(propylene oxide)-based diacrylate cross-linker and a PEO-based macromonomer. The microgels showed reversible swelling properties in response to pH. At low pH, microgels swelled due to the protonation of the tertiary amine units. On the contrary, compact latex particles due to the deswelling occurred when pH was >7.

87.3.2 Application to Drug Delivery

pH-responsive hydrogels have been frequently used to develop controlled-release formulations for oral administration. The gastrointestinal tract is known to possess a wide pH range, from a gastric pH of 1–2 to an intestinal tract pH of 7–8. Such significant changes can be utilized for the design of pH-responsive drug-delivery devices. Tumor sites and some sites of infection are known to have local acidic pH values amenable to pH-responsive release systems (Ghandehari et al. 1997). For polycationic hydrogels, the swelling is minimal at neutral pH, thus minimizing drug release from the hydrogels.

Hydrogels made of polyanions (e.g., PAA) cross-linked with azoaromatic cross-linkers were developed for colon-specific drug delivery. Swelling of such hydrogels in the stomach is minimal and thus, the drug release is also minimal. The extent of swelling increases as the hydrogel passes down the intestinal tract due to increase in pH leading to ionization of the carboxylic groups. But, only in the colon, can the azoaromatic cross-links of the hydrogels be degraded by azoreductase produced by the microbial flora of the colon (Ghandehari et al. 1997; Akala et al. 1998). The degradation kinetics and pattern can be controlled by the cross-linking density. The kinetics of hydrogel swelling can also be controlled by changing the polymer composition (Akala et al. 1998).

pH-responsive hydrogels can be placed inside capsules (Gutowska et al. 1997) or silicone matrices (Ghandehari et al. 1997; Akala et al. 1998) to modulate drug release. The release patterns of several model drugs having different aqueous solubilities and partitioning properties (including salicylamide, nicotinamide, clonidine HCl, and prednisolone) were correlated with the pH-dependent swelling pattern. At pH 1.2, the hydrogel swelling was low and the release was limited to an initial burst. At pH 6.8, the network became ionized and higher swelling resulted in increased release (Qu et al. 2006).

ABA-type triblock copolymers showing pH-responsive micelle formation and gelation were prepared through an ATRP. The A block consisted of either poly(2-(diisopropylamino) ethyl methacrylate) (PDPEA) or poly(2-(diethylamino) ethyl methacrylate) (PDEMA), and the B block contained poly(2-methacryloyloxyethyl phosphorylcholine) (PMPC). At low pH regions, the amino groups in the A blocks were protonated and highly soluble in water, whereas they were deprotonated at neutral or higher pH ranges. At neutral pHs, the triblock copolymers became micelles in which the A blocks formed hydrophobic aggregated cores and the neutral hydrophilic B blocks formed the outer shell. At higher polymer concentrations in the basic pH solution, physical gels were formed. Thus, at physiological pH, drugs

could be incorporated into the micelle cores, and a slow release of the drugs was achieved. At pH 2, the polymer gels immediately dissolved and released drugs rapidly (Ma et al. 2003).

87.4 Light-Responsive Hydrogels

Photoresponsive polymers are macromolecules that change their physicochemical properties by irradiation with an appropriate wavelength (Kumar and Neckers 1989; Dai et al. 2009). Potential applications of the photoresponsive polymers include reversible optical storage, polymer viscosity control, photomechanical transduction and actuation, bioactivity switching of proteins, tissue engineering, and pulsatile drug-delivery devices (Shimoboji et al. 2002a,b). It is an important aspect of photoresponsive hydrogel systems that irradiation as a stimulus is a relatively straightforward and noninvasive method of inducing responsive behaviors. These types of polymers have been investigated for many years, but there has been a recent expansion in research to create complex macromolecular architectures.

Typically, the photoresponsive polymer is constructed by incorporating chromophores that can transfer light energy into a change in conformation. The chromophore should show a property change during isomerization large enough to cause a conformational change in the polymer. The chromophore is transformed under photoirradiation into isomers that return to the initial state either thermally or photochemically. This isomerization is called “photochromism.” During the photochromism, some physicochemical properties of the chromophores are changed including geometrical structures, dipole moment, and charge generation. Figure 87.8 shows the typical chromophores that are often incorporated into the photoresponsive polymers (Irie 1990; He et al. 2009) into the backbone or side chains.

Azobenzene is the most frequently used chromophore. It undergoes isomerization from the trans- to the cis-form under ultraviolet (UV) irradiation (300–400 nm). The cis-form can return thermally or photochemically to the trans-form. The trans-to-cis isomerization causes three important physical property changes: (1) a change in the absorption spectrum—a decrease in the intense absorption at 320 nm and an increase in absorption at 440 nm, (2) a change in geometry—a shortening of the distance between the 4- and 4'-carbon from 0.9 nm (trans) to 0.55 nm (cis), and (3) a change in dipole moment from 0.5 D (trans) to 3.1 D (cis). The photomechanical effect of photoresponsive hydrogels that show a reversible contraction and expansion is based on the geometrical change of azobenzene embedded in the polymer hydrogel network. When the polymer hydrogel network containing azobenzene chromophores as a cross-linker is stretched, the azobenzene chromophores are preferentially oriented parallel to the stretching axis. With irradiation of such an oriented sample with UV light, the conformational change of azochromophores is expected to cause a macroscopic change in the overall hydrogel shape.

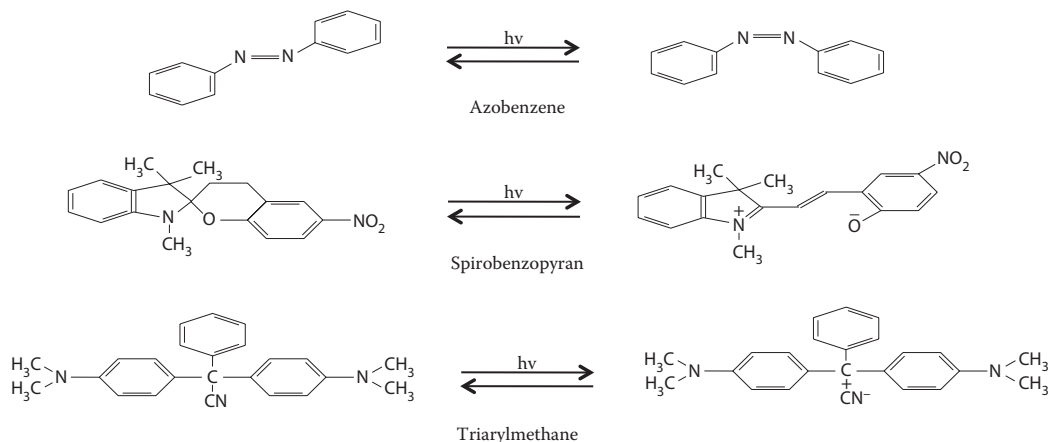


FIGURE 87.8 Structural formula of representative chromophores.

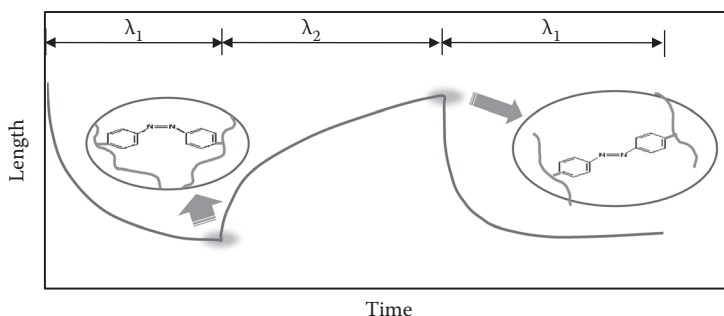


FIGURE 87.9 Schematic illustration of the photomechanical behavior of azobenzene-containing hydrogels on irradiation.

A typical photomechanical behavior of the polymer hydrogel network is described in Figure 87.9. By changing the irradiation wavelength to the visible region, the *cis*-form changes to the *trans*-form, and the dimension recovery is observed. This contraction recovery can be repeated many times.

Spirobenzopyran undergoes ring opening on UV irradiation, with the production of intensely colored merocyanine. The merocyanine can return thermally or photochemically to colorless spiropyran. Physical property changes associated with this isomerization are as follows: (1) a change in absorption spectrum, (2) a change in dipole moment, and (3) a geometric structural change. Spirobenzopyran can be incorporated into backbone or pendant groups to polymer hydrogel networks. A change in dipole moment caused by spiropyran–merocyanine isomerization would be expected to alter intramolecular interaction of polymer chains. The change of intramolecular interaction induces a conformational change in the polymer and thus causes swelling or shrinking polymer hydrogels. A change in dipole moment on irradiation could affect the adsorption–desorption behavior of drugs, particularly proteins on the polymer. This feature may be useful for the design of “on–off” control of drug release in a pulsatile delivery system. The photoresponsive hydrogels can also be synthesized by introducing triarylmethane into the polymer network (Mamada et al. 1990). The triarylmethane can be ionized upon UV irradiation. The hydrogels discontinuously swell in response to UV irradiation but shrink when the UV light is removed. The UV light-induced swelling is attributed to an increase in osmotic pressure within the gel due to the appearance of cyanide ions formed by UV irradiation.

A typical function of photoresponsive hydrogels is to change their volume reversibly on irradiation of UV or visible lights. Photoresponsive hydrogels respond to “on–off” stimulus of lights, which induces the gel swelling–shrinking that contributes to the release of drug molecules (Qiu and Park 2001). The molecular weight of the polymer may affect the photoresponsive property; in polymers with smaller molecular weight, the photoresponsive macroscopic change is induced more effectively. While the action of stimulus (light) is instantaneous, the reaction of hydrogels in response to such action is still relatively slow.

87.5 Electroresponsive Hydrogels

Electroresponsive hydrogels transform electrical energy directly into mechanical energy. Basically, electroresponsive hydrogels are made of polyelectrolytes, swellable polymer networks that carry cations or anions. The electroresponsive hydrogels change a macroscopic shape in response to an electric field (Figure 87.10) (Filipcsei et al. 2000). When a hydrogel is negatively charged, it swells near the anode and contracts near the cathode. Generally, the response rate is proportional to the external electric current. The commonly used electroresponsive polymers include conducting polymers, polyelectrolyte gels, and ionic polymer–metal composites. Electroresponsive polymers are an increasingly important class of smart materials (Kim et al. 1998; Ramanathan and Block 2001; Bajpai et al. 2008). They have promising

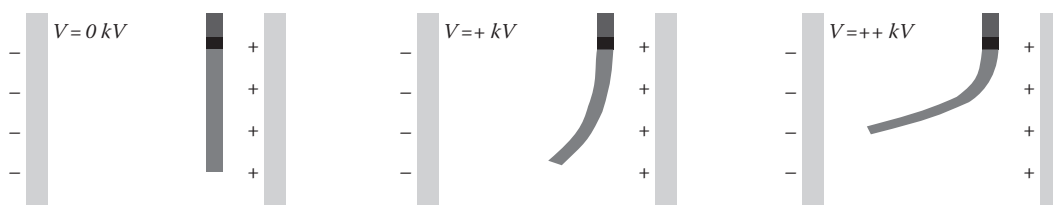


FIGURE 87.10 Schematic illustration of the bending phenomena of an electroresponsive polymer hydrogel.

applications in biomechanics, artificial muscle actuation, sensing, energy transduction, sound dampening, chemical separations, and controlled drug delivery. Gel deformation in an electric field is influenced by a number of factors, including variable osmotic pressure based on the voltage-induced motion of ions in the solution, pH or salt concentration of the surrounding medium, position of the gel relative to the electrodes, thickness or shape of the gel, and the applied voltage (Gao et al. 2008). Transforming the application of an electric field into a physical response by a polymer generally relies on collapse of a gel in an electric field, electrochemical reactions, electrically activated complex formation, ionic polymer–metal interactions, electrorheological effects, or changes in electrophoretic mobility (Filipcsei et al. 2000; Kim et al. 1998, 2004).

A typical function of electroresponsive hydrogels is to change their volume reversibly under the influence of an electric field. The volume change can be utilized for solute permeation control through hydrogels in controlled drug delivery. Electroresponsive hydrogels respond to “on–off” stimulus of electrical currents, which induces the gel swelling–shrinking that contributes to the release of drug molecules. The control of “on–off” drug release can be achieved by varying the intensity of electric stimulation. Hydrogels made of poly(2-acrylamido-2-methylpropane sulfonic acid-co-n-butylmethacrylate) were able to release edrophonium chloride and hydrocortisone in a pulsatile manner in response to electric current (Gong et al. 1994). Poly(sodium acrylate) microparticle gels containing pilocarpine showed a current-dependent pilocarpine release. However, a complete “on–off” drug release regulation is still challenging since it is difficult to completely stop drug release upon termination of the electrical stimulus (Kulkarni et al. 2010). Kwon et al. prepared cross-linked poly(2-acrylamide-2-methylpropanesulfonic acid-co-butyl methacrylate) [P(AMPS-co-BMA)] hydrogels and evaluated the feasibility of these hydrogels for electroresponsive drug-delivery devices (Kwon et al. 1991). They used a cationic drug molecule, edrophonium chloride, within the negatively charged hydrogel. Rapid drug release from the hydrogels resulted from an application of electric fields through the ion exchanges between positively charged drug molecules and protons at the cathode. The squeezing effects arising from the electric field application induced rapid drug release from the gels, which increased as the voltages increased in a dose-dependent manner. Using the P(AMPS-co-BMA) hydrogels, an “on–off” drug release regulation was achieved under an “on–off” application of electric current. The group further investigated the electric current-induced release of anionic heparin from a positively charged polyallylamine polyion complex. Rapid structural changes and an apparent dissociation of the polyion complex occurred upon application of an electric current. During the electric current application, the positively charged polyallylamine was neutralized at the cathode owing to the microenvironmental pH changes, and apparent dissociation of the polyion complex occurred. Although bioactive heparin was released by electric current application, polyallylamine was also released.

87.6 Glucose-Responsive Hydrogels

Insulin-dependent diabetes mellitus patients lack the pancreatic function that releases insulin in response to blood glucose levels. These patients require daily self-injections of an appropriate amount of insulin that helps them to avoid hyperglycemia. Diabetic patients suffer from a gradual decline in the efficiency of various organs, leading to vision loss and long-term diseases. Severe conditions may even

lead to patient death. Thus, injection of properly dosed insulin at proper times is required for insulin-dependent diabetes mellitus therapy. Self-injection of insulin, however, results in patient discomfort, varied bioavailability, and sometimes a hypoglycemic coma due to an overdose of insulin. Alternatively, insufficient insulin induces hyperglycemia and related complications. Therefore, the precise control of blood glucose levels with an effective, stimuli-responsive insulin release would be of great utility. A large number of formulations incorporating hydrogels for glucose concentration-dependent insulin release have been reported.

Glucose-responsive hydrogel systems are based on: (1) enzymatic oxidation of glucose by glucose oxidase (GOx), (2) binding of glucose to concanavalin A (Con A), and (3) reversible sol–gel phase transition hydrogels. In the glucose-responsive systems using GOx, the glucose sensitivity is not caused by direct interaction of glucose with the responsive polymer, but rather by the response of the polymer to the by-products that result from the enzymatic oxidation of glucose. The substrate glucose reacts with GOx, which produces gluconic acid and H₂O₂. Typically, a pH-responsive moiety is incorporated into glucose-responsive hydrogel networks, and the gluconic acid induces a pH-responsive swelling or collapse of the hydrogel matrix that contains insulin. Several insulin-release systems utilize the glucose-responsive hydrogels based on glucose–GOx. For example, Chu et al. reported the covalent modification of a cellulose film with GOx-conjugated PAA (Chu et al. 2004). At neutral and high pH levels, the carboxylate units of the PAA chains were negatively charged and extended due to electrostatic repulsion, which resulted in occlusion of the pores in the cellulose membrane. The gluconic acid that resulted from the addition of glucose led to a local pH reduction, protonation of the PAA carboxylate moieties, and concomitant collapse of the chains obscuring the membrane pores, with the latter event facilitating the release of entrapped insulin.

Con A has also been frequently used in modulated insulin delivery. In this type of the system, insulin molecules are attached to a support or carrier through specific interactions that can be interrupted by glucose itself. Kim and coworkers reported the synthesis of monosubstituted conjugates of glucosyl-terminal PEG (G-PEG) and insulin (Liu et al. 1997). The G-PEG–insulin conjugates were bound to Con A that was grafted along a PEG–poly(vinylpyrrolidone-co-acrylic acid) backbone. When the concentration of glucose in the surrounding aqueous media increased, competitive binding of glucose with Con A led to displacement and release of the G-PEG–insulin conjugates.

Obaidat and Park reported glucose-responsive systems that underwent sol–gel phase transition depending on the glucose concentration in the environment (Obaidat and Park 1996). The reversible sol–gel phase transition required glucose-responsive cross-linking. Since diffusion of insulin through the sol phase was an order of magnitude faster than that through the gel phase, the insulin release could be controlled by the glucose concentration in the environment. Another type of sol–gel transition polymers responsive to glucose was prepared using a water-soluble copolymer of acrylamide and allyl glucose. The resulting polymers were cross-linked in the presence of lectin and Con A. Since binding constants of native glucose molecules are higher than those of glucose moieties on the copolymer side chains, an exchange reaction occurred between added glucose and copolymer glucose moieties, inducing a gel-to-sol phase transition. Such changes can be utilized for the permeation control of insulin.

All the above-mentioned examples used proteins such as GOx and Con A. The exposure of these proteins and peptides to the body may cause an undesirable immune response upon contact. Therefore, these naturally derived proteins and peptides, and their whole systems, should be separated from the body using semipermeable membranes. Matsumoto et al. prepared synthetic polymers with glucose-responsive functions (Matsumoto et al. 2003). They focused on the unique characteristics of phenylboronic acid as a glucose-responsive moiety. Boronate is known to form reversible bonding with polyols such as *cis* diol sugar compounds such as glucose. They prepared water-soluble copolymers containing phenylboronic acid side chains using *m*-acrylamidophenylboronic acid (AAPBA) and various water-soluble monomers, including *N*-vinylpyrrolidone, acrylamide, and (*N,N*-dimethylacrylamide) DMAAm. The resulting copolymers formed reversible complexes with polyol compounds such as poly(vinyl alcohol) (PVA). These complexes dissociated with the addition of glucose in a concentration-dependent

manner. Such complex formation and dissociation could be attributed to the different dissociation constants of phenylboronate anions with PVA or glucose.

87.7 Enzyme-Responsive Hydrogels

Enzymes play a critical role in most biological pathways. Enzymes are highly selective and work under mild conditions present *in vivo* (aqueous, pH 5 – 8, 37°C). Generally, enzyme-responsive hydrogels consist of two components: (i) an enzyme-responsive substrate and (ii) a component that directs or controls interactions that cause macroscopic transitions (Figure 87.11) (Thornton et al. 2005; Ulijn 2006). The molecular interactions include hydrogen bonding, electrostatic interactions, van der Waals forces, hydrophobic interactions, π - π interactions, and their combinations. Catalytic action of the enzyme on the substrate can lead to changes in surface properties, self-assembly, supramolecular architectures, and swelling/collapse of gels (Ulijn 2006).

In situ depot-forming enzyme-responsive hydrogels were synthesized by using enzymatic dephosphorylation to induce a sol-gel transition (Yang et al. 2004; Yang and Xu 2004; Thornton et al. 2007). When fluorenylmethoxycarbonyl (Fmoc)-tyrosine phosphate was exposed to a phosphatase, the phosphate groups were removed, which resulted in reduction in electrostatic repulsions, supramolecular assembly by π -stacking of the fluorenyl groups, and eventually gelation. The incorporation of functional moieties that can react with enzymes is another typical approach to produce enzyme-responsive hydrogels. Exposure of the functional groups to a specific enzyme can lead to the creation of new covalent linkages that cause a change in macroscopic properties. For example, transglutaminase, a blood-clotting enzyme, had the ability to cross-link the side chains of lysine (Lys) residues with glutamine (Gln) residues.

Various approaches have been studied to prepare protease-responsive hydrogels. When the hydrogels are exposed to a protease, hydrolysis of protein or peptide leads to gel degradation and subsequent release of encapsulated drugs. Moore and coworkers prepared chymotrypsin-responsive hydrogels by incorporating a degradable (cysteine-tyrosine-lysine-cysteine) CYKC tetrapeptide sequence as a cross-linker within polyacrylamide hydrogels (Plunkett et al. 2005). The CYKC sequence contains a terminal cysteine conjugation site, a tyrosine residue that can be cleaved at the carboxyl side by chymotrypsin, and a Lys residue. When subjected to α -chymotrypsin, the micron-sized gels dissolved due to the degradation of CYKC by α -chymotrypsin. Ulijn reported protease-responsive hydrogels that were applicable to the removal of toxins or entrapment of drug molecules (Ulijn 2006). In this case, the response was caused by a change in osmotic pressure instead of cross-link degradation. Copolymer beads composed of acrylamide and PEG-macromonomers were modified via an enzyme-cleavable tripeptide comprising combinations of glycine, phenylalanine, and positively charged arginine residues that imparted swelling due to electrostatic repulsions. Upon the addition of proteases, the tripeptide was cleaved, and the resulting loss of arginine groups led to a reduction in electrostatic repulsions and subsequent collapse of the hydrogel.

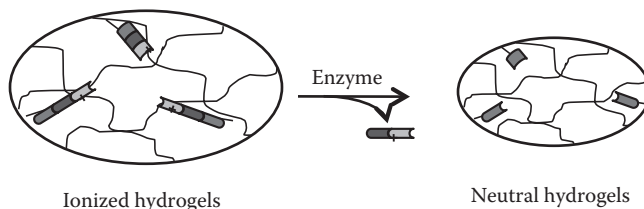


FIGURE 87.11 Enzymatic cleavage and drug release from enzyme-responsive hydrogels. (Adapted from Thornton, P. D., McConnell, G., and Ulijn, R. V. 2005. Enzyme responsive polymer hydrogel beads. *Chem. Commun.*, (47): 5913–5.)

87.8 Inflammation-Responsive Hydrogels

Inflammatory reactions are commonly observed at injury sites. Inflammation-responsive cells such as macrophages and polymorphonuclear leukocytes (PMNs) play a key role in normal healing processes after injury. The oxygen metabolites such as hydroxyl radicals ($\bullet\text{OH}$) are produced from the inflammation-responsive cells at the injured tissues. Yui et al. designed a hydroxyl radical-responsive drug-delivery system (Yui et al. 1992,1993). They used hyaluronic acid (HA), a linear mucopolysaccharide consisting of repeating units of *N*-acetyl-D-glucosamine and D-glucuronic acid, for preparing inflammation-responsive hydrogels because the hydroxyl radicals produced at injured sites can effectively degrade HA. HA was cross-linked with ethylene glycol diglycidylether or polyglycerol polyglycidylether. HA degradation in response to hydroxyl radicals was observed only at the surface of the gel, indicating surface erosion degradation. Further utilization of these hydrogels involved the introduction of microspheres as model drug carriers in the hydrogels. The release of microsphere-encapsulating drugs followed the surface erosion of the gels. These HA gels could be useful *in vivo* for inflammation-induced drug-delivery systems, specifically for chronic inflammatory problems including rheumatoid arthritis.

87.9 Antigen-Responsive Hydrogels

Antigen-antibody interactions are highly specific and are associated with complex immune responses that help recognize and neutralize foreign infection-causing objects in the body. The high affinity and specificity of their interactions have been extensively used to yield a variety of antigen-responsive polymer systems. In most cases, antigen-responsive hydrogels have been prepared by physically entrapping antibodies or antigens in networks, chemical conjugation of the antibody or antigen to the network, or using antigen-antibody complexes as reversible cross-linkers within networks (Lu et al. 2003).

A typical antigen-responsive polymer can be synthesized by copolymerization of vinyl-functionalized antigen or antibody with acrylamide or *N,N'*-methylenebisacrylamide (MBA). The copolymerization results in a hydrogel cross-linked both covalently and by antigen-antibody interactions. When free antigen molecules are added to the solution with immersed antigen-immobilized hydrogels, the antibodies in the hydrogel network change partners with free antigen, owing to the difference in the binding constants. This antigen-competitive exchange results in a decreased number of cross-linking points in the hydrogels, and thus promotes the swelling of hydrogels. This antigen-responsive swelling behavior of an antigen-immobilized hydrogel is irreversible (Figure 87.12a), but, when both antigen and antibody are immobilized on polymer hydrogel networks, reversible swelling and deswelling occur (Figure 87.12b). Such changes are very antigen specific, so that the addition of other antigens does not alter hydrogel swelling.

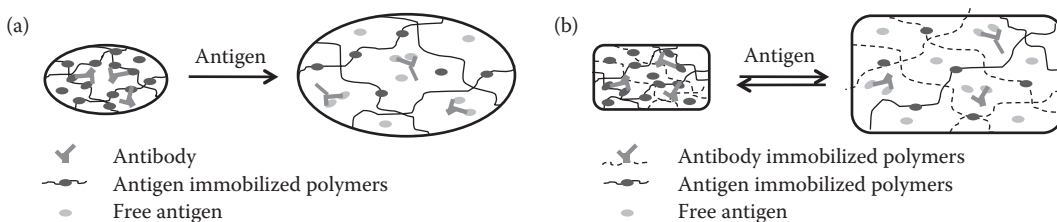


FIGURE 87.12 Irreversible (a) and reversible (b) antigen-responsive hydrogels. (Adapted from Miyata, T., Asami, N., and Uragami, T. 1999. *Nature*, 399: 766–9.)

87.10 Magnetoresponse Hydrogels

For designing a magnetoresponse hydrogel delivery system, several factors should be considered, including the magnetic properties of the delivery systems, field strength, field geometry, drug/gene-binding capacity, and physiological parameters such as the depth to target, the rate of blood flow, vascular supply, and body weight. Generally, inorganic magnetic particles are physically entrapped within or covalently immobilized to a 3D cross-linked network. In principle, in the presence of a magnetic field gradient, a translational force is exerted on the drug-delivery hydrogel complexes. This effectively traps the complex in the field at the target site and pulls it toward the magnet (Pankhurst et al. 2003).

A major challenge of chemotherapeutic approaches to cancer treatment is that they are nonspecific. Magnetoresponse hydrogels have been explored extensively as possible drug carriers for site-specific drug delivery and controlled release. Although theoretically very effective, magneto drug-delivery systems still have numerous obstacles. Magnetoresponse hydrogel systems generally require a relatively strong gradient in an external field. There is also the potential for embolization as the fraction of magnetoresponse hydrogels may accumulate and block flow or they may also concentrate in the liver (Dobson 2006). There are other limitations such as the depth that the magnet may function, as is encountered when scaling up from small animals with near-surface targets to larger animals and humans.

Another type of magnetoresponse hydrogels exhibit the shape and size distortions that occur reversibly and instantaneously in the presence of a nonuniform magnetic field (Zrinyi et al. 1997; Starodoubtsev et al. 2003; Wang et al. 2006). Such hydrogels have received significant attention for use as soft biomimetic actuators, sensors, cancer therapy agents, artificial muscles, switches, separation media, membranes, and drug-delivery systems (Zrinyi et al. 1997; Szabo et al. 1998, 2000; Zrinyi 2000; Babinocova et al. 2001; Starodoubtsev et al. 2003; Wang et al. 2006; Pyun 2007).

87.11 Ultrasound-Responsive Hydrogels

The application of stimuli-responsive polymers to drug delivery needs the target-specific delivery and the controlled release of therapeutic compounds at a specified rate. The drug-delivery systems are generally guided to the target site—which has an environment that stimulates release—by passive or active transport mechanisms. The change in environmental conditions spontaneously induces drug release at the target site. However, in most cases, to locally apply the stimulus at the targeted site is not simple. For instance, a change in temperature could lead to release in thermoresponsive hydrogels *in vitro*, but localized heating and cooling *in vivo* are not always trivial at sites deep within the body.

Ultrasound is a particularly effective stimulus that can be applied externally on demand and has proven to be effective at triggering drug release within the body. One of the pioneering approaches of exploiting ultrasound in drug delivery involves directing the ultrasound directly at the hydrogel matrix (Serksen and West 2002). This approach of ultrasound-responsive drug delivery achieved a 27 times increase in the release of 5-fluorouracil from a poly(ethylene-co-vinyl acetate) (PEVAc) matrix (Miyazaki et al. 1985). Ultrasound regulated drug delivery in which the release rates were repeatedly responsive (Kost and Langer 1988). Biodegradable polymers that have been used for ultrasound-responsive systems include poly(D,L-lactide) (PGA), poly(D,L-glycolide) (PLA), poly(bis(p-carboxyphenoxy))alkane-anhydrides (PCPX), and their copolymers with sebacic acid. When induced to ultrasound, these bioerodible polymer hydrogels responded rapidly and reversibly. It is believed that the ultrasound causes an increase in temperature in the delivery system, which facilitates diffusion (Mathiowitz and Cohen 1989). The concept of using ultrasound-responsive hydrogels for controlled drug delivery is attractive because the method is essentially noninvasive and has been successfully used in other areas of medical treatment and diagnostics (Noriis et al. 2005).

The success of ultrasonic mediation of drug delivery is generally ascribed to cavitation, which is the alternating growth and shrinkage of gas-filled microbubbles that results from high- and low-pressure

waves generated by ultrasound energy (Lentacker et al. 2006). Eventually, these cavitating microbubbles implode, generating local shock waves that can disrupt polymer assemblies in their vicinity.

87.12 Redox/Thiol-Responsive Hydrogels

Redox/thiol-responsive hydrogel materials are another class of responsive hydrogels that have recently received increased attention, especially in various fields of controlled drug delivery (Meng et al. 2009a). The interconversion of thiols and disulfides is a key step in many biological processes, plays an important role in the stability and rigidity of native proteins in living cells (Castellani et al. 1999), and has been commonly used for various bioconjugation protocols (Saito et al. 2003). Since disulfide bonds can be reversibly converted into thiols by exposure to various reducing agents (e.g., mercaptoethanol, dithiothreitol (DTT), and glutathione (GSH)) and/or undergo disulfide exchange in the presence of other thiols, polymers containing disulfide linkages can be considered both redox and thiol responsive (Oh et al. 2007). GSH, the most abundant reducing agent in most cells (Bulmus et al. 2003), has a typical intracellular concentration of about 10 mM, whereas its concentration is only about 0.002 mM in the cellular exterior (Jones et al. 1998). This significant variation in concentration has been utilized to design thiol/redox-responsive drug-delivery systems that specifically release therapeutics upon entry into cells (Ghosh et al. 2009).

87.13 Concluding Comments

Development of smart hydrogels as effective drug-delivery systems has been limited, mainly due to a few reasons. First, the chemical structures of most smart hydrogels contain functional groups that have not been used in clinical applications. This makes it rather difficult to use them in humans, as their safety has not been unequivocally demonstrated. Until the safety is proven, the pharmaceutical, as well as biomedical, industries are not willing to develop clinical products. Second, the smart hydrogels are obviously smarter than ordinary hydrogels by being able to sense the environmental changes and react to them, but they cannot overcome the inherent limitations of hydrogels in terms of drug loading and release. Unless a hydrogel can deliver a drug at a therapeutically significant level for a sufficiently long period of time, any control on drug release has no clinical meaning. Third, most of the smart hydrogels are not biodegradable, although they may be biocompatible. Thus, it is not practical using the smart hydrogels as implantable drug-delivery systems. Without biodegradation in the body, the utilization of smart hydrogels will be limited. Biodegradability can be achieved by employing synthetic polymers with biodegradable backbones or natural polymers.

Synthesizing new polymers to make environment-responsive hydrogels will continue. Synthetic polymers possess attractive potential because experts in the field can easily alter their design to achieve the desired characteristics of hydrogels that respond to different stimuli (Kwon 2005). The single environmental-responsive property of intelligent hydrogels would limit their practical applications. It would be favorable if the intelligent hydrogels could respond to more than one stimulus simultaneously. For example, more effective drug therapies for complicated diseases may require polymeric materials, the functions of which are variable or switchable in response to several kinds of stimuli. Indeed, the diagnosis of patients suffering from some diseases is generally achieved by monitoring several physiological changes. Therefore, multi-responsive hydrogels have attracted more and more attentions (Ji et al. 2007; Ju et al. 2009). The combination of two or more responses is particularly useful to optimize the control of drug release.

Recent advances in nanofabrication have allowed utilization of smart hydrogels in the nano-/micro-systems. Application of smart hydrogels to microfluidic systems, bioseparation, and biosensors is a good example. Their application has been extended to high-throughput screening, such as peptide, protein, and deoxyribonucleic acid (DNA) array. Micropatterned hydrogels can be employed as a template for preparing nano-/microparticles of predefined size and shape. Nanofabricated smart hydrogels can be used in various aspects in tissue engineering, including cell sheet technique, artificial extracellular matrix materials, and 3D scaffolds with chemical patterning or microchannels.

Abbreviations

- DEA 2-(diethylamine)
 DPA 2-(diisopropylamine)
 MPC 2-methacryloyloxyethyl phosphorylcholine

References

- Akala, E. O., Kopeckova, P., and Kopecek, J. 1998. Novel pH-sensitive hydrogels with adjustable swelling kinetics. *Biomaterials*, 19: 1037–47.
- Babinocova, M., Leszczynska, D., Sourivong, P., Cicmanec, P., and Babinec, P. 2001. Superparamagnetic gel as a novel material for electromagnetically induced hyperthermia. *J. Magn. Magn. Mater.*, 225: 109–12.
- Bajpai, A. K., Bajpai, J., and Soni, S. N. 2008. Preparation and characterization of electrically conductive composites of poly(vinyl alcohol)-g-poly(acrylic acid) hydrogels impregnated with polyaniline (PANI). *Express Polym. Lett.*, 2: 26–39.
- Bromberg, L. E., and Ron, E. S. 1998. Temperature-responsive gels and thermogelling polymer matrices for protein and peptide delivery. *Adv. Drug Deliv. Rev.*, 31: 197–221.
- Bulmus, V., Woodward, M., Lin, L., Murthy, N., Stayton, P., and Hoffman, A. 2003. A new pH-responsive and glutathione-reactive, endosomal membrane-disruptive polymeric carrier for intracellular delivery of biomolecular drugs. *J. Control. Release*, 93: 105–20.
- Castellani, O. F., Martinez, E. N., and Anon, M. C. 1999. Role of disulfide bonds upon the structural stability of an amaranth globulin. *J. Agric. Food Chem.*, 47: 3001–8.
- Chu, L.-Y., Li, Y., Zhu, J.-H., Wang, H.-D., and Liang, Y.-J. 2004. Control of pore size and permeability of a glucose-responsive gating membrane for insulin delivery. *J. Control. Release*, 97: 43–53.
- Dai, S., Ravi, P., and Tam, K. C. 2009. Thermo- and photo-responsive polymeric systems. *Soft Matter*, 5: 2513–33.
- Dobson, J. 2006. Magnetic nanoparticles for drug delivery. *Drug Develop. Res.*, 67: 55–60.
- Filipcsei, G., Feher, J., and Zrinyi, M. 2000. Electric field sensitive neutral polymer gels. *J. Mol. Struct.*, 554: 109–17.
- Gao, Y., Xu, S., Wu, R., Wang, J., and Wei, J. 2008. Preparation and characteristics of electric stimuli responsive hydrogel composed of polyvinyl alcohol/poly(sodium maleate-co-sodium acrylate). *J. Appl. Polym. Sci.*, 107: 391–5.
- Ghandehari, H., Kopeckova, P., and Kopecek, J. 1997. *In vitro* degradation of pH-sensitive hydrogels containing aromatic azo bonds. *Biomaterials*, 18: 861–72.
- Ghosh, S., Yesilyurt, V., Savariar, E. N., Irvin, K., and Thayumanavan, S. 2009. Redox, ionic strength, and pH sensitive supramolecular polymer assemblies. *J. Polym. Sci. A Polym. Chem.*, 47: 1052–60.
- Gong, J. P., Nitta, T., and Osada, Y. 1994. Electrokinetic modeling of the contractile phenomena of polyelectrolyte gels. One-dimensional capillary model. *J. Phys. Chem.*, 98: 9583–7.
- Gutowska, A., Bark, J. S., Kwon, I. C., Bae, Y. H., Cha, Y., and Kim, S. W. 1997. Squeezing hydrogels for controlled oral drug delivery. *J. Control. Release*, 48: 141–8.
- Hamidi, M., Azadi, A., and Rafiei, P. 2008. Hydrogel nanoparticles in drug delivery. *Adv. Drug Deliv. Rev.*, 60: 1638–49.
- He, J., Tong, X., and Zhao, Y. 2009. Photoresponsive nanogels based on photocontrollable cross-links. *Macromolecules*, 42: 4845–52.
- Irie, M. 1990. Properties and applications of photoresponsive polymers. *Pure Appl. Chem.*, 62(8): 1495–502.
- Jeong, B., Bae, Y. H., and Kim, S. W. 1999a. Biodegradable thermosensitive micelles of PEG–PLGA–PEG triblock copolymers. *Colloids Surf. B*, 16: 185–93.
- Jeong, B., Kim, S. W., and Bae, Y. H. 2002a. Thermosensitive sol–gel reversible hydrogels. *Adv. Drug Deliv. Rev.*, 54: 37–51.

- Jeong, B., Lee, K. M., Gutowska, A., and An, Y. H. 2002b. Thermogelling biodegradable copolymer aqueous solutions for injectable protein delivery and tissue engineering. *Biomacromolecules*, 3: 865–8.
- Jeong, B. M., Bae, Y. H., and Kim, S. W. 1999b. Thermoreversible gelation of PEG–PLGA–PEG triblock copolymer aqueous solutions. *Macromolecules*, 32: 7064–9.
- Jeong, B. M., Bae, Y. H., and Kim, S. W. 2000. Drug release from biodegradable injectable thermosensitive hydrogel of PEG–PLGA–PEG triblock copolymers. *J. Control. Release*, 63: 155–63.
- Ji, S. C., Kwon, I. K., and Park, K. 2007. Smart polymeric gels: Redefining the limits of biomedical devices. *Prog. Polym. Sci.*, 32: 1083–122.
- Jones, D. P., Carlson, J. L., Samiec, P. S., Jr., Mody, V. C., Jr., Reed, R. L., and Brown, L. A. S. 1998. Glutathione measurement in human plasma evaluation of sample collection, storage and derivatization conditions for analysis of dansyl derivatives by HPLC. *Clin. Chem.*, 275: 175–84.
- Ju, X.-J., Xie, R., Yang, L., and Chu, L.-Y. 2009. Biodegradable intelligent materials in response to chemical stimuli for biomedical applications. *Expert Opin. Ther. Pat.*, 19(5): 683–96.
- Kim, S. J., Kim, H. I., Shin, S. R., and Kim, S. I. 2004. Electrical behavior of chitosan and poly(hydroxyethyl methacrylate) hydrogel in the contact system. *J. Appl. Polym. Sci.*, 92: 915–19.
- Kim, S. W., Bae, Y. H., and Okano, T. 1992. Hydrogels: Swelling, drug loading, and release. *Pharm. Res.*, 9(3): 283–90.
- Kim, S. Y., Shin, H. S., Lee, Y. M., and Jeong, C. N. 1998. Properties of electroresponsive poly(vinyl alcohol)/poly(acrylic acid) IPN hydrogels under an electric stimulus. *J. Appl. Polym. Sci.*, 73: 1675–83.
- Kim, Y. J., Choi, S., Koh, J. J., Lee, M., Ko, K. S., and Kim, S. W. 2001. Controlled release of insulin from injectable biodegradable triblock copolymer. *Pharm. Res.*, 18(4): 548–50.
- Kojima, C. 2010. Design of stimuli-responsive dendrimers. *Expert Opin. Drug Deliv.*, 7(3): 307–19.
- Kost, K., and Langer, R. 1988. Ultrasonically controlled polymeric drug. *Macromol. Chem. Macromol. Symp.*, 19: 275–85.
- Kulkarni, R. V., Setty, C. M., and Sa, B. 2010. Polyacrylamide-g-alginate-based electrically responsive hydrogel for drug delivery application: Synthesis, characterization, and formulation development. *J. Appl. Polym. Sci.*, 115: 1180–8.
- Kumar, G. S., and Neckers, D. C. 1989. Photochemistry of azobenzene-containing polymers. *Chem. Rev.*, 89: 1915–25.
- Kwon, G. S. 2005. *Polymeric Drug Delivery Systems*. Taylor & Francis Group, Boca Raton, FL, 680 pp.
- Kwon, I. C., Bae, Y. H., and Kim, S. W. 1991. Electrically erodible polymer gel for controlled release of drugs. *Nature*, 354(28): 291–3.
- Lentacker, I., Geest, B. G. D., Vandenbroucke, R. E., Peeters, L., Demeester, J., Smedt, S. C. D., and Sanders, N. N. 2006. Ultrasound-responsive polymer-coated microbubbles that bind and protect DNA. *Langmuir*, 22: 7273–8.
- Li, M. H., and Keller, P. 2009. Stimuli-responsive polymer vesicles. *Soft Matter*, 5: 927–37.
- Liu, F., Song, S. C., Mix, D., Baudys, M., and Kim, S. W. 1997. Glucose-induced release of glycosylpoly(ethylene glycol) insulin bound to a soluble conjugate of concanavalin A. *Bioconjug. Chem.*, 8: 664–72.
- Lu, Z.-R., Kopeckova, P., and Kopecek, J. 2003. Antigen responsive hydrogels based on polymerizable antibody Fab' fragment. *Macromol. Biosci.*, 3(6): 296–300.
- Ma, Y., Tang, Y., Billingham, N. C., and Armes, S. P. 2003. Synthesis of biocompatible, stimuli-responsive, physical gels based on ABA triblock copolymers. *Biomacromolecules*, 4: 864–8.
- Mamada, A., Tanaka, T., Kungwachakun, D., and Irie, M. 1990. Photoinduced phase transition of gels. *Macromolecules*, 23: 1517–9.
- Mathiowitz, E., and Cohen, M. D. 1989. Polyamide microcapsules for controlled release: I characterization of the membranes. *J. Membr. Sci.*, 40: 1–26.
- Mathiowitz, E., and Cohen, M. D. 1989. Polyamide microcapsules for controlled release: II release characteristics of the microcapsules. *J. Membr. Sci.*, 40: 27–41.

- Matsumoto, A., Ikeda, S., Harada, A., and Kataoka, K. 2003. Glucose-responsive polymer bearing a novel phenylborate derivative as a glucose-sensing moiety operating at physiological pH conditions. *Biomacromolecules*, 4: 1410–6.
- Meng, F., Hennink, W. E., and Zhong, Z. 2009a. Reduction-sensitive polymers and bioconjugates for biomedical applications. *Biomaterials*, 30: 2180–98.
- Meng, F., Zhong, Z., and Feijen, J. 2009b. Stimuli-responsive polymersomes for programmed drug delivery. *Biomacromolecules*, 10(2): 197–209.
- Miyata, T., Asami, N., and Urugami, T. 1999. A reversibly antigen-responsive hydrogel. *Nature*, 399: 766–9.
- Miyazaki, S., Hou, W. M., and Takada, M. 1985. Controlled drug release by ultrasound irradiation. *Chem. Pharm. Bull.*, 33: 428–31.
- Noriis, P., Noble, M., Francolini, I., Vinogradov, A. M., Stewart, P. S., Ratner, B. D., Costerton, J. W., and Stoodley, P. 2005. Ultrasonically controlled release of ciprofloxacin from self-assembled coatings on poly(2-hydroxyethyl methacrylate) hydrogels for *Pseudomonas aeruginosa* biofilm prevention. *Antimicrob. Agents Chemother.*, 49: 4272–9.
- Obaidat, A. A., and Park, K. 1996. Characterization of glucose dependent gel–sol phase transition of the polymeric glucose-concanavalin A hydrogel system. *Pharm. Res.*, 13: 989–95.
- Oh, J. K., Lee, D. I., and Park, J. M. 2009. Biopolymer-based microgels/nanogels for drug delivery applications. *Prog. Polym. Sci.*, 34: 1261–82.
- Oh, J. K., Siegwart, D. J., Lee, H.-i., Sherwood, G., Peteanu, L., Hollinger, J. O., Kataoka, K., and Matyjaszewski, K. 2007. Biodegradable nanogels prepared by atom transfer radical polymerization as potential drug delivery carriers: Synthesis, biodegradation, *in vitro* release, and bioconjugation. *J. Am. Chem. Soc.*, 129: 5939–45.
- Onaca, O., Enea, R., Hughes, D. W., and Meier, W. 2009. Stimuli-responsive polymersomes as nanocarriers for drug and gene delivery. *Macromol. Biosci.*, 9: 129–39.
- Pankhurst, Q. A., Connolly, J., Jones, S. K., and Dobson, J. 2003. Applications of magnetic nanoparticles in biomedicine. *J. Phys. D: Appl. Phys.*, 36: 167–81.
- Plunkett, K. N., Berkowski, K. L., and Moore, J. S. 2005. Chymotrypsin responsive hydrogel: Application of a disulfide exchange protocol for the preparation of methacrylamide containing peptide. *Biomacromolecules*, 6: 632–7.
- Pyun, J. 2007. Nanocomposite materials from functional polymers and magnetic colloids. *Polym. Rev.*, 47: 231–63.
- Qiu, Y., and Park, K. 2001. Environment-sensitive hydrogels for drug delivery. *Adv. Drug Deliv. Rev.*, 53: 321–39.
- Qu, J. B., Chu, L.-Y., Yang, M., Xie, R., Hu, L., and Chen, W.-M. 2006. A pH-responsive gating membrane system with pumping effects for improved controlled release. *Adv. Funct. Mater.*, 16: 1865–72.
- Ramanathan, S., and Block, L. H. 2001. The use of chitosan gels as matrices for electrically-modulated drug delivery. *J. Control. Release*, 70: 109–23.
- Roy, D., Cambre, J. N., and Sumerlin, B. S. 2010. Future perspectives and recent advances in stimuli-responsive materials. *Prog. Polym. Sci.*, 35: 278–301.
- Saito, G., Swanson, J. A., and Lee, K.-D. 2003. Drug delivery strategy utilizing conjugation via reversible disulfide linkages: Role and site of cellular reducing activities. *Adv. Drug Deliv. Rev.*, 55: 199–215.
- Sershen, S., and West, J. 2002. Implantable, polymeric systems for modulated drug delivery. *Adv. Drug Deliv. Rev.*, 54: 1225–35.
- Shimoboji, T., Ding, Z. L., Stayton, P. S., and Hoffman, A. S. 2002a. Photoswitching of ligand association with a photoresponsive polymer–protein conjugate. *Bioconjug. Chem.*, 13: 915–9.
- Shimoboji, T., Larenas, E., Fowler, T., Kulkarni, S., Hoffman, A. S., and Stayton, P. S. 2002b. Photoresponsive polymer enzyme switches. *Prog. Natl. Acad. Sci. USA*, 99(26): 16592–6.
- Starodoubtsev, S. G., Saenko, E. V., Khokhlov, A. R., Volkov, V. V., Dembo, K. A., Klechkovskaya, V. V., Shtykova, E. V., and Zanaevskina, I. S. 2003. Poly(acrylamide) gels with embedded magnetite nanoparticles. *Microelec. Eng.*, 69: 324–9.

- Stuart, M. A. C., Huck, W. T. S., Genzer, J., Muller, M., Ober, C., Stamm, M., Sukhorukov, G. B. et al. 2010. Emerging applications of stimuli-responsive polymer materials. *Nature Mater.*, 9: 101–13.
- Szabo, D., Czako-Nagy, I., Zrinyi, M., and Vertes, A. 2000. Magnetic and Mossbauer studies of magnetite-loaded polyvinyl alcohol hydrogels. *J. Colloid. Interface. Sci.*, 221: 166–72.
- Szabo, D., Szeghy, G., and Zrinyi, M. 1998. Shape transition of magnetic field sensitive polymer gels. *Macromolecules*, 31: 6541–8.
- Thornton, P. D., Mart, R. J., and Ulijn, R. V. 2007. Enzyme-responsive polymer hydrogel particles for controlled release. *Adv. Mater.*, 19: 1252–6.
- Thornton, P. D., McConnell, G., and Ulijn, R. V. 2005. Enzyme responsive polymer hydrogel beads. *Chem. Commun.*, (47): 5913–5.
- Ulijn, R. V. 2006. Enzyme-responsive materials: A new class of smart biomaterials. *J. Mater. Chem.*, 16: 2217–25.
- Wang, C., Adrianus, G. N., Sheng, N., Toh, S., Gong, Y., and Wang, D.-A. 2009a. *In vitro* performance of an injectable hydrogel/microsphere based immunocyte delivery system for localized anti-tumor activity. *Biomaterials*, 30: 6986–95.
- Wang, G., Tian, W. J., and Huang, J. P. 2006. Response of ferrogels subjected to an AC magnetic field. *J. Phys. Chem. B.*, 110: 10738–45.
- Wang, Y.-C., Xia, H., Yang, X.-Z., and Wang, J. 2009b. Synthesis and thermoresponsive behaviors of biodegradable pluronic analogs. *J. Polym. Sci. A. Polym. Chem.*, 47: 6168–79.
- Yang, Z., Gu, H., Fu, D., Gao, P., Lam, J. K., and Xu, B. 2004. Enzymatic formation of supramolecular hydrogels. *Adv. Mater.*, 16: 1440–4.
- Yang, Z., and Xu, B. 2004. A simple visual assay based on small molecule hydrogels for detecting inhibitors of enzymes. *Chem. Commun.*, 2424–5.
- Yui, N., Okano, T., and Sakurai, Y. 1992. Inflammation responsive degradation of crosslinked hyaluronic acid gels. *J. Control. Release*, 22: 105–16.
- Yui, N., Okano, T., and Sakurai, Y. 1993. Regulated release of drug microspheres from inflammation responsive degradable matrices of crosslinked hyaluronic acid. *J. Control. Release*, 25: 133–43.
- Zentner, G. M., Rathi, R., Shih, C., McRea, C. J., Seo, M.-H., Oh, H., Rhee, B. G., Mestecky, J., Moldoveanu, Z., Morgan, M., and Weitman, S. 2001. Biodegradable block copolymers for delivery of proteins and water-insoluble drugs. *J. Control. Release*, 72: 203–15.
- Zhao, S. P. and Xu, W. L. 2010. Thermo-sensitive hydrogels formed from the photocrosslinkable polypseudorotaxanes consisting of β -cyclodextrin and pluronic F68/PCL macromer. *J. Polym. Res.*, 17: 503–510.
- Zrinyi, M. 2000. Intelligent polymer gels controlled by magnetic fields. *Colloid. Polym. Sci.*, 278: 98–103.
- Zrinyi, M., Barsi, L., and Szabo, D. 1997. Direct observation of abrupt shape transition in ferrogels induced by nonuniform magnetic field. *J. Chem. Phys.*, 106: 5685–92.

VIII

Personalized Medicine

Gualberto Rúaño

Genomas, Inc.

Genetics Research Center

Hartford Hospital

- 89 Physiogenomic Contours: The Application of Systems Biology for Engineering Personalized Healthcare** *Andreas Windemuth, Richard L. Seip, and Gualberto Rúaño* 89-1
Physiogenomics and Systems Biology • PG Marker Discovery • Example: Diabetes Treatment • Additional Applications and Prospects • References
- 90 The Evolution of Massively Parallel Sequencing Technologies: Facilitating Advances in Personalized Medicine** *Ian Toma, Georges St. Laurent III, Samuel Darko, and Timothy A. McCaffrey*..... 90-1
Genomics and Personalized Medicine • A Short History of Sequence Detection • Technology of Massively Parallel Sequencing • Short Read Alignment and Cluster Computing • The Limitations of Genomics and NGS • Proteomic Strategies • Future Directions • References
- 91 Computational Methods and Molecular Diagnostics in Personalized Medicine** *Roland Valdes, Jr. and Mark W. Linder*91-1
Introduction • The Problem • Fundamentals (PGx and Pharmacology) • Modeling and Clinical Applications • Future Extensions of Genotype–Phenotype Modeling • Summary • References
- 92 Need for Point-of-Care Testing Devices for Cardiac Troponin in Patients with Acute Coronary Syndromes** *Alan H.B. Wu and Amy E. Herr* 92-1
Role of Troponin in Cardiovascular Diseases • Current Cardiac Troponin Assays • Novel Technologies for POCT for Cardiac Troponin • Summary • References

Physiogenomic Contours: The Application of Systems Biology for Engineering Personalized Healthcare

Andreas
Windemuth

Genomas, Inc.

*Genetics Research Center
Hartford Hospital*

Richard L. Seip

Genomas, Inc.

Gualberto Ruaño

Genomas, Inc.

*Genetics Research Center
Hartford Hospital*

89.1	Physiogenomics and Systems Biology	89-1
	Introduction • Fundamentals of PG • PG Contours	
89.2	PG Marker Discovery.....	89-4
89.3	Example: Diabetes Treatment.....	89-5
	Thiazolidinedione (TZD) Drugs • Log Scores • Response and Stimulus Profiles • PG Contours • Clusters	
89.4	Additional Applications and Prospects.....	89-9
	References.....	89-10

89.1 Physiogenomics and Systems Biology

89.1.1 Introduction

Ten years after the groundbreaking sequencing of the first complete human genome, we are looking back on a decade of unprecedented technological progress in the life sciences. While the first sequencing of a human genome took 15 years to complete at a cost of \$2.7 billion, the street price for a complete human genome sequence at the time of this writing is \$10,000, and rapidly approaching the “magic” benchmark of \$1000. This pace amounts to a slashing of costs by half every 6 months, far faster than the widely admired Moore’s law, which governs the exponential increase in the capacity of integrated circuits. Similar advances have been made in other areas of biotechnology such as genotyping, expression analysis, proteomics, metabolomics, and other methods of system-wide data acquisition, putting a veritable menagerie of “-omics” at the disposal of life science researchers.

Yet, this technological progress has not been matched by similarly rapid advances in healthcare, causing some to express disappointment about the impact that the human genome project has had.^{1,2} It has become apparent that the limiting factor for progress in healthcare is not our ability to acquire and accumulate biological information, but our ability to interpret this information and distill it into a fundamental understanding of its clinical significance.

Translating system-wide information into fundamental understanding is the domain of systems biology. Physiogenomics (PG) is a powerful systems biological method that utilizes genetic variation, the differences between individual genomes, to link genes and physiological characteristics into pathways,

and to study the detailed interactions between them. Genetic variation has been used for biological investigation at least since the days of Mendel, and has led to the discovery of the causes of many Mendelian diseases, so named in his honor. Each of these diseases has shined a spotlight onto particular genes, allowing the detailed investigation of individual cause and effect relationships and greatly advancing our understanding of biology and the etiology of disease. What is new today is the ability to gather and process information system wide, to illuminate an entire organism, and to map its mechanistic pathways from a global point of view. This approach did not exist prior to the last decade.

In its simplest application, PG analysis effectively identifies genotype(s) related to a singular phenotype. Here, in a hypothesis-free context made more complex by inclusion of multiple phenotypes, we describe the expansion of PG analysis to incorporate multiple phenotypes and then generate PG contours which depict the most significant relationships among genetic markers and phenotypes.

89.1.2 Fundamentals of PG

In the most general sense, a biological organism can be understood as a system that receives external stimuli (lifestyle, pathogens, drugs) and produces responses (medical outcomes, physiological responses) (Figure 89.1). The function that connects input to output is complex, and contains a large number of fixed parameters (genes) which determine the innate characteristics of the organism. Conventional medical research is concerned mostly with the relation between stimulus and response. PG is a new paradigm that integrates response to stimulus with the response to genomic variation, as naturally present in a population.

As such, PG is a medical application of sensitivity analysis, the study of the dependence of a system on changes in its components.³ In PG, single nucleotide polymorphisms (SNPs) provide the variable components of genes, and analysis of the relationship between that variation and the physiological response to external stimuli provides information about which genes play important roles in the physiological process.^{4,5} This approach has been advanced in human clinical studies of the responses to exercise,^{6,7} diet^{8,9} and drug response,¹⁰⁻¹⁴ and in animal models.⁵ The associated gene markers are combined into SNP ensembles harnessing their combined predictive power to estimate functional variability among individuals similarly treated.^{4,15}

The use of genetic markers rather than continuous biomarkers such as gene expression and/or protein activity offers a number of advantages. Foremost among them is the stability of genetic markers, which do not change over the lifetime of an individual. In most fields relying on statistical analysis, there is a fundamental problem of assigning causality based on observed associations. Is increased body mass a consequence of diabetes, or is diabetes caused by increased body mass? Association analysis cannot distinguish causality. Genetic markers, on the other hand, never change, meaning that causality can be assigned unambiguously: it is the genotype that causes the phenotype, never the other way around.

The stability of genetic information also eliminates concern about noise from fluctuations, and its digital and inherently precise nature eliminates concern about measurement error. Finally, the complete system-wide genotype can be determined from a small sample of peripheral blood or saliva, without the invasive biopsy often required for other biomarkers. That said, however, PG is not restricted to genetic

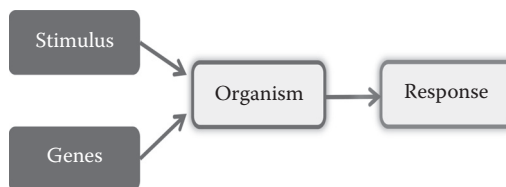


FIGURE 89.1 Illustration of a biological organism as viewed by PG.

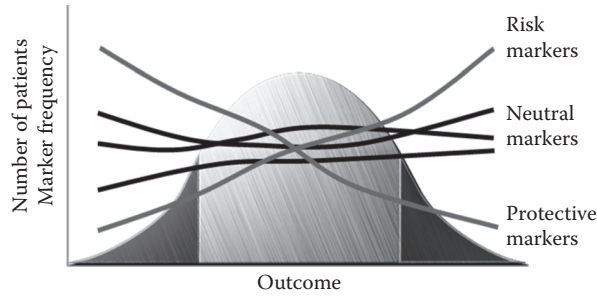


FIGURE 89.2 PG analysis of gene marker frequency as a function of phenotype variability.

information. PG can be used to investigate relationships among intermediate phenotypes, but this is outside of the scope of this chapter.

The environmental stimuli studied in PG span the gamut from exercise and diet to drugs and toxins and from extremes of temperature, pressure, and altitude to radiation. The phenotypes can range from gene expression, physiological measurements such as blood pressure, serum lipids, and neurological activity, to the diagnosis of specific diseases. In the case of complex diseases, we are likely to find both baseline characteristics and response phenotypes to as yet undetermined environmental triggers. Variability in a genomic marker among individuals that tracks with the variability in physiological characteristics establishes associations and mechanistic links with specific genes (Figure 89.2).

89.1.3 PG Contours

PG marks the entry of genomics into systems biology by enabling a comprehensive approach to the study of complex biological systems.⁴ With the recent availability of genome-wide genotyping and next generation sequencing technologies, we can study variation across the full complement of genes, providing a detailed and system-wide view into the internal processes that determine an organism's state and response to environmental triggers. By studying the effect of every gene in the genome on a phenotype of interest, those that are involved in the pathways leading to the phenotype are revealed, a technique that has recently been exploited through genome-wide association analysis (GWAS).

With PG contours, we carry this approach one step further into a multidimensional analysis of multiple related phenotypes, not only associating individual genes with phenotypes, but also determining the relationships among the genes and among the phenotypes. The PG contour is a map placing individual genetic loci into a space whose farthest reaches are defined by point locations assigned to different phenotypes. The map location of any individual genetic locus is defined by that locus' degree of association to each of the phenotypes. Individual loci migrate toward a phenotype's point location by virtue of the strength of the correlation between locus and phenotype. The penultimate location of a genetic locus is a function of the independent associations to phenotypes. The premise is that loci of like function will cluster together and a detailed picture of the mechanisms within the black box that is the organism will emerge.

PG contours can also be generated in a space defined by different treatments, rather than phenotypes, which is why they are particularly well suited for the investigation of pharmacogenetics. In standard pharmacogenetics, genetic markers are sought that enhance or inhibit response to a particular drug. With PG contours, we can instead seek genetic markers that are involved differentially between drugs and hone in on their mechanistic differences.

PG contours also can greatly enhance the sensitivity of genetic analysis. In GWAS, generally we set a stringent significance threshold and look only at those markers that satisfy the criteria, ignoring any information that remains within the large number of markers that may be involved, but the effect of which is

not large enough to lift them above the statistical noise. PG contours are generated with the data for all loci, taking into account even small hints of association, allowing them to become significant in combination with other factors. Because of the consideration of multiple independent responses or stimuli, the statistical noise is averaged down and the signal stands out more clearly than in a typical GWAS.¹⁶⁻¹⁸

Creating PG contours requires several steps of marker discovery and multidimensional analysis. We will describe each of these interrelated components in the remainder of this chapter.

89.2 PG Marker Discovery

The purpose in marker discovery is to identify any of a large set of genetic markers that have an influence on any of the phenotypes being observed. Individual markers are tested for association according to accepted multivariate methods in epidemiology,¹⁹ mainly multivariate linear and logistic regression techniques.

A major issue to be addressed in marker discovery is multiple comparison adjustment. With millions of SNPs and tens of phenotypes, there are potentially tens of millions of spurious genotype-phenotype associations that appear in the data analysis as statistical noise. The required sample size to overcome this limitation can become prohibitively costly and operationally impractical. PG profiles help by permitting the use of information from all associations, whether statistically significant or not. In addition, we also employ a successive information reduction strategy to further reduce the effect of statistical noise. Figure 89.3 illustrates the different data reduction steps employed in constructing the PG contours within the PG Platform when screening for genetic associations using SNP arrays. This process constitutes a data reduction pipeline resulting in a handful of markers that are found to be associated with the phenotype. In the following paragraphs, each data reduction step will be discussed separately.

The raw data analysis and genotype calling is the first step and handled by the instrumentation software to yield genotype calls for each SNP and subject. The PG SNP Screen software links the sample identifiers back to the clinical database and performs extensive quality control analysis. Quality control includes comparison of genotypes from replicates of the same sample and from control samples to known genotypes. Verification of Hardy Weinberg equilibrium and analysis of quality scores supplied by the instrumentation software assists in establishing quality thresholds on SNPs and DNA samples.

Whole genome SNP arrays are so dense that they exhibit a significant amount of linkage disequilibrium among SNPs that are neighbors in the genome sequence. SNP genotypes are therefore not independent, and the amount of data can be reduced substantially by inferring haplotype alleles from individual SNP data.²⁰ It has been shown that haplotype inference is quite accurate,²¹ so that no important information is removed through this reduction process. The International HapMap project²² has compiled haplotype data on a reference population that is very useful for this step.

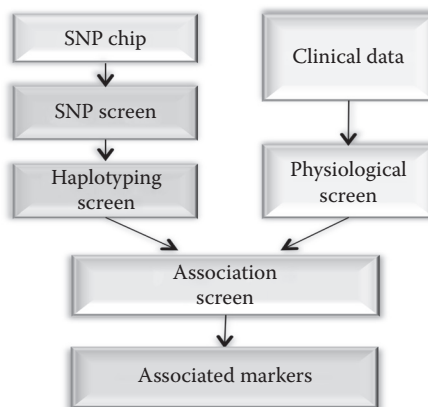


FIGURE 89.3 Illustration of the marker discovery process.

Information reduction can also be performed on the phenotype data. There are likely to be some groups of phenotypes that are jointly determined by more fundamental, underlying variables that cannot be measured directly. The Physiological Screen module can detect and define such underlying variables using principal component analysis (PCA) or factor analysis, and determine their values from their observed correlates. This has multiple advantages. With fewer underlying variables, multiple testing for associations can be reduced, with corresponding increase in sensitivity. In addition, the values of the underlying variables are determined from multiple measurements of correlates, reducing the impact of random measurement errors. Finally, the underlying variables will be more closely linked to their genetic determinants, increasing the chance of detecting the association.

The genetic information from the Haplotyping Screen and the physiological variables from the Physiological Screen are then combined by the Association Screen. Here, every combination of genetic and physiological variables is tested for association, and an accurate measure of the likelihood of association for each association is found. Top associations that are statistically significant are identified using the False Discovery Rate (FDR) procedure.²³ Data reduction consists of the assignment of a significance score, which allows the selection of the most statistically significant associations from the large number of possible pairings, and is used as the input data for PG profiles and PG contours.

89.3 Example: Diabetes Treatment

89.3.1 Thiazolidinedione (TZD) Drugs

As an example of the application of PG profiles we will describe a study of the safety and efficacy of thiazolidinedione (TZD) therapy in type 2 diabetes mellitus.¹³ Drawing from a clinical registry and DNA sample repository of 187 patients treated with TZD and incretin drugs at an outpatient diabetes clinic, we genotyped 180 patients using the PG Array, a SNP genotyping panel designed to investigate a broad array of 222 genes known to be associated with various aspects of metabolism. Our initial published work investigated the safety phenotypes of body mass index (BMI) and edema, both side effects of the TZD drug class.¹³ Subsequently, we investigated HbA1c level as an efficacy phenotype.

The analysis utilized a clinical practice protocol and was designed to discover PG associations to edema and BMI in patients receiving rosiglitazone or pioglitazone. We hypothesized that genetic variability in pathophysiologic pathways underlies TZD-associated weight gain due to adiposity and/or edema. We analyzed the 384 SNPs of the PG Array in a subset of 87 outpatients (57 men, 30 women) with type 2 diabetes receiving TZD therapy. PG analysis was used to discover associations with BMI and edema.

The phenotypes were analyzed for covariate dependence on age, gender, ethnicity, and treatment. Using linear regression and ANOVA, we found that none of the covariates had a significant effect on the phenotypes, except a marginally significant contribution of 5% to the BMI variation by age ($p = 0.035$), with BMI decreasing by 0.15 points for each year of age. PG marker discovery was performed as described above in section 89.2. A total of 346 SNPs were tested for association of minor allele copy number (0, 1, or 2) with the covariate adjusted endpoints using linear regression. The SNPs were ranked by the F-statistic p -value of the genotype coefficient, and false discovery rates (FDR)¹¹⁻¹³ were calculated.

Previous physiological studies of TZDs have mostly used animal models. To our knowledge, this analysis is the first to examine clinical response in humans as a source of mechanistic discovery. Our results suggest that polymorphism in genes relevant to interlocking physiological pathways may affect the symptomatology of TZD side effects. We reported an association of BMI during TZD therapy with polymorphisms in genes affecting adenosine, an adiponectin receptor, pyruvate kinase (muscle), and uncoupling protein 2. In contrast, edema induced by TZD therapy is associated with polymorphisms in genes controlling vascular permeability. Consequently, it is possible that TZD safety may require monitoring a constellation of independent syndromes with varying innate predispositions in the population and diverse physiological mechanisms encompassing various gene pathways.

89.3.2 Log Scores

Out of the marker discovery by Association screening we obtain for each marker studied a coefficient estimating the magnitude of the marker effect, and a statistic describing the extent to which the data shows deviation from the null hypothesis of no involvement. For PG contours, we focus on the statistic. This is in part because we are interested more in whether or not a marker has an effect on the phenotypes of interest rather than how much effect. The statistic is also universal, that is, scale-free and comparable across different phenotypes and different population subgroups. This latter property is what makes PG profiles a powerful and general tool in the investigation of complex biological systems.

To better exploit this universality, we first convert the associations statistic to a uniformly distributed p-statistic, as is commonly done to yield the measure of statistical significance known as the p-value. The p-value is then transformed using the decadic logarithm, yielding a score that increases with increasing significance. Because the logarithm is decadic, it is easy to convert between p-values and scores ($p = 10^{-5}$ yields $s = 5$, $p = 10^{-12}$ yields $s = 12$, etc.). The commonly used threshold for statistical significance of $p < 0.05$ translates to $s > 1.3$.

In order to distinguish between effects that are equally significant, but opposite in direction, we assign negative scores to markers where the effect of the variant allele is beneficial, and positive scores to associations where the variant allele puts the patient at risk.

89.3.3 Response and Stimulus Profiles

Each phenotype or physiological response can be associated with an array of scores, one for each marker in the association analysis with that response. This array is termed the *physiogenomic profile* of the response. A profile can consist of several hundred scores, as in the example, or of a million or more in the context of genome-wide analysis. Often we will only look at a subset of markers that are associated above a certain significance level with at least one of the responses under investigation, since there is little or no information contained in nonsignificant scores.

The response profiles are generated by associating markers for different phenotypes in a single population. Similarly, we can create profiles for the same response, but in different subgroups of the patient population that differ in the type of environmental stimulus they receive, such as drug treatment. Stimulus profiles require larger patient samples; because each subgroup must be provided sufficient power for an association analysis. In the example, we did not investigate stimulus profiles, but they have proven powerful tools in investigating pharmacogenetic mechanisms in other projects.

The PG response profiles for multiple stimuli will be described symbolically as a score matrix S_{sm} , where s is the index enumerating stimuli, and m is the index enumerating all genetic markers.

89.3.4 PG Contours

The profiles provide information about which genes are involved in the pathways regulating the response or stimulus in question. A PG contour map is a planar diagram depicting the locations of all significant genotype markers relative to phenotypes, where the phenotypes are positioned as distant points on the plane, and where marker proximity to a phenotype is determined by the strength of its association to that phenotype. Each marker has a profile, which describes its positions relative to each of the phenotypes under consideration. A critical element of PG contours is the triangulation of each gene as found in multiple profiles. When looking at two responses or stimuli, as in the example, we can represent the combination of both profiles by plotting each marker on a scatter plot with each axis representing one of the responses.

Figure 89.4 shows this for our example, plotting the profiles of two important responses to the TZDs. The responses are presence or absence of edema, and body mass quantified by the BMI. The marker set used is that of the PG array, which includes 384 SNPs distributed across 222 genes. Genes in the dark shaded squares have high scores in the edema profile, showing evidence of belonging to pathways

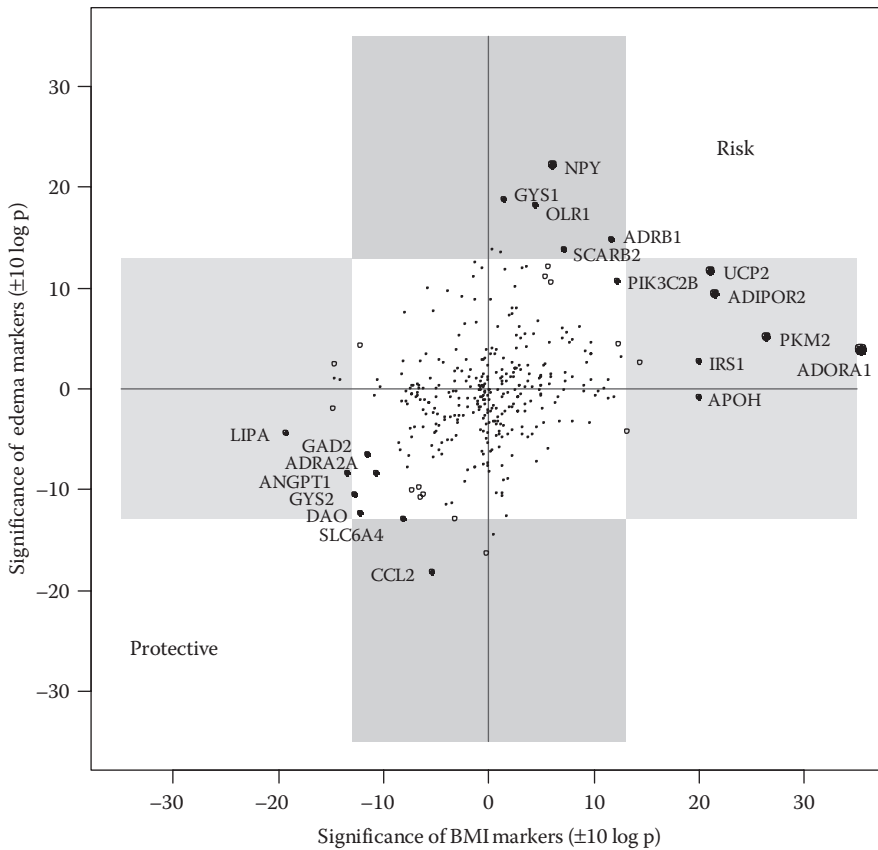


FIGURE 89.4 PG contours of the associations for BMI and edema, showing risk markers on the upper right quadrant and protective markers on the lower left quadrant. Each axis represents a scale with scores that are 10 times the absolute value of the log of the p value for the SNP association. The score was assigned a positive or negative value to correspond with the sign of the regression coefficient derived from the regression of allele score (0,1,2) against phenotype score (edema presence: not present, 0; present, 1; or BMI value). Sizes of data points are proportional to sum of the scores corresponding to both axes. Vertical and horizontal borders between shaded and unshaded sectors represent the unadjusted significance threshold $p < 0.05$, or ± 13 at $(\pm 10 \times |\log(0.05)|)$. Reprinted from Ruaño G, et al., *Clinica Chimica Acta*, 400(1-2):48-55, 2009, with permission statement from Elsevier, Ltd.)

involved in that physiological response. Genes in the light shaded squares have high scores in the BMI profile, showing evidence of belonging to pathways involved in body mass regulation. Importantly, as can be gleaned from the sector around the origin, most SNPs tested are not associated to either outcome, effectively serving as controls for the predictive markers.

Given the contours, we can now place each gene in one of four possible categories: Those not related to either response, those in pathways for one of them, and those that are part of a common pathway. Interestingly, there are no genes that have significant scores in both, which is evidence that none of the genes in the array are involved in both responses, suggesting that the two responses are produced by distinct mechanisms. This is a new insight that would not have been apparent by looking at the two profiles in isolation.

Finally, for each associated SNP there is a biologically plausible connection to the phenotypes based on existing biochemical and physiological knowledge. As the SNPs represent genes in different but interlocking pathways, their combined predictive power can be harnessed by multigene predictive models of

drug response. With a larger cohort, the combined predictive power of SNP ensembles can be quantified and formalized mathematically as algorithms for DNA-guided clinical management of TZDs.

We can extend the treatment to more than two dimensions, although it becomes more difficult to visualize the data. To address this, we have developed a polar system of coordinates that allows the representation of the multidimensional data in a two-dimensional plot, termed the *pole graph*, such that the relations between genes and responses become clear, as well as the similarities and differences of genes with respect to their mechanistic contributions to the responses. Figure 89.5 depicts a pole graph representing a three-dimensional PG contour for the same dataset as Figure 89.4, but now including, in addition to their side effects, the drugs' efficacy as measured via the glycosylation of hemoglobin A1c. The coordinates of each marker are calculated as

$$x_m = \sum_{r=1}^R S_{rm} \sin \frac{2\pi}{R}(r - 1)$$

$$y_m = \sum_{r=1}^R S_{rm} \cos \frac{2\pi}{R}(r - 1),$$

where R is the number of responses and S_{rm} are the R response profiles. A marker with no associations will have scores close to zero and appear in the center of the plot, as will a marker that is equally

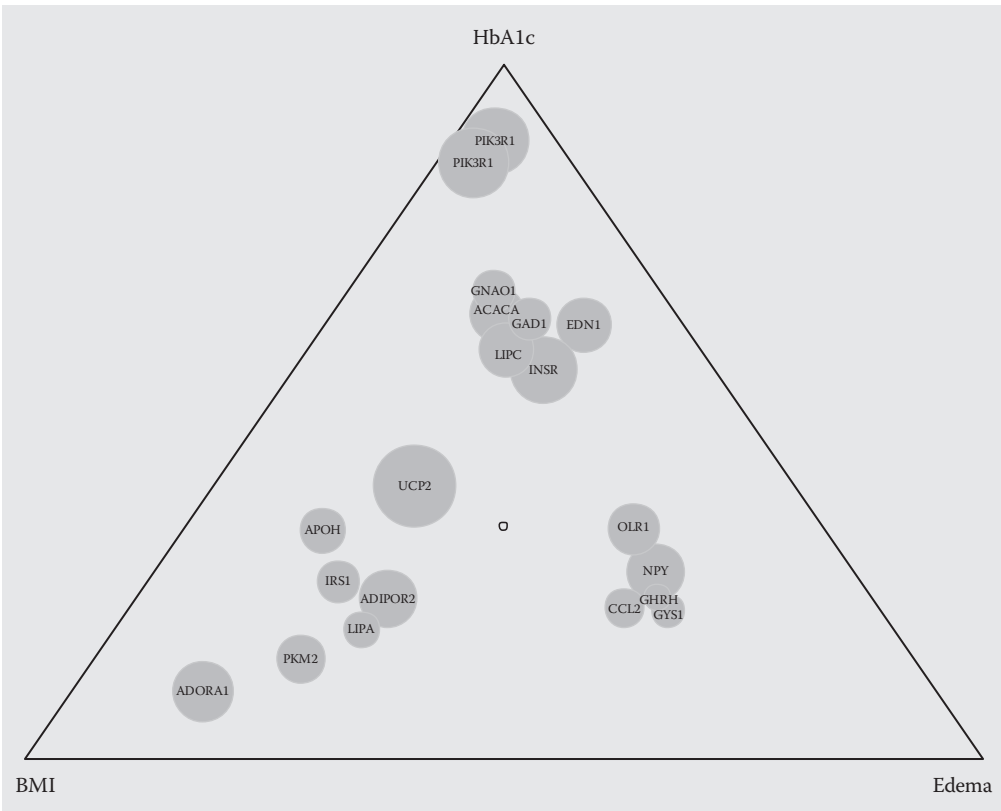


FIGURE 89.5 Pole graph showing the PG contour for TZDs with respect to three responses. The overall degree of association (circle size) and relative degree of association between responses (circle position) are both visible.

Downloaded by [JCR JCR] at 10:46 01 August 2015

associated with all responses. Markers associated with only one response will be found in the corresponding corner, and markers associated with two responses will be in the middle between the two corresponding corners. In addition to the coordinates, we also calculate a combined score

$$z_m = \sum_{r=1}^R S_{rm}$$

which is used as the radius of the circle to be drawn for the marker, with larger circles indicating stronger association.

89.3.5 Clusters

PG contours provide useful information on the function of and relationships between genes. It is also possible to summarize across all genes and investigate similarity relationships between phenotypes and stimuli. For this we define the PG distance as a distance relationship between phenotypes

$$d_{ij} = \sqrt{\sum_{m=1}^M (S_{im} - S_{jm})^2}$$

where the sum extends over all M markers, and the S are the PG profiles as defined above. This expression defines a Euclidean metric on the profiles, and because of the nature of the log-scores, significant associations will dominate the measure. Given this distance metric, we can then use standard cluster analysis to group phenotypes with similar mechanistic basis together. The same procedure can be used for stimulus profiles to group together and/or set apart treatments according to their biological mechanism of action.

89.4 Additional Applications and Prospects

PG contours should be very useful when applied to medical outcomes, adverse events and important intermediary phenotypes (endophenotypes), particularly when participant genes and candidate pathways are numerous. For example, consider the complex interplay of exercise and cardiovascular pathology. Exercise integrates responses of cardiopulmonary, peripheral vascular, skeletal muscular microvascular, neural, and metabolic pathways. Exercise capacity predicts prognosis in patients with suspected²⁴ or documented cardiovascular disease²⁵ and diabetic²⁶ patients. In persons in whom metabolic or cardiovascular disease is not documented, chronic exercise alters known risk factors for disease such as blood pressure, lipoprotein lipid concentrations, body fat, and body mass. Regular exercisers therefore develop many protective metabolic, cardiopulmonary, and vascular adaptations that are complex phenotypes.^{27,28} Using PG contour analysis, we may be able to better understand genetic components of selected endophenotypes, and identify genetic markers that characterize those endophenotypes related to disease endpoints.

Another application of PG contours could be comparison of drugs in the same class. PG contours can contrast the genomic basis of class-wide versus drug-specific effects, as suggested by second-generation antipsychotic drugs (SGAs). These drugs are indicated in the treatment for schizophrenia, bipolar disorder, and psychotic depression and frequently used in other psychiatric disorders. Their main drawback is metabolic derangements including weight gain, hyperlipidemia, and increased risk of diabetes. These psychotropic-induced metabolic side effects are serious adverse reactions which vary widely in extent between drugs and from patient to patient.²⁹

PG contours of the major SGAs were characterized and consisted of multiple genetic markers that increased or decreased metabolic susceptibility and together explained a substantial part of the variation of side effects within the patient population. Furthermore, the contours differed among the SGA drugs. We used PG analysis to identify significant genetic associations to three metabolic phenotypes: triglyceride levels (TRIG), total cholesterol (TC), and BMI. We found that the PG contours differ substantially between the three drugs for each of the phenotypes. Consistently for the three phenotypes, the contours of olanzapine and quetiapine are more similar to each other than they are to that of risperidone. We identified a number of candidate genes that may be responsible for these differences and similarities among the drugs.

Differences in the PG contours point to mechanistic differences between physiological responses to treatments or to the environment. The genes represented by their respective associated DNA markers can provide valuable insight into underlying mechanisms. The differences can be exploited through the use of DNA-guided rules for treatment decisions on a patient individualized basis, thus enabling personalized healthcare.

References

1. Collins F. The bridge between lab and clinic. *Nature* 2010;468(7326):877.
2. Hamburg MA, Collins FS. The path to personalized medicine. *N Engl J Med* 2010;363(4):301–4.
3. Saltelli A, Chan K, Scott EM. *Sensitivity Analysis*. Chichester: John Wiley and Sons; 2000.
4. Rúaño G, Windemuth A, Holford T. Physiogenomics: Integrating Systems Engineering and Nanotechnology for Personalized Medicine. In: Bronzino JD, ed. *The Biomedical Engineering Handbook*. 3rd edition ed. CRC Press; 2005. p. 28-1–28-9.
5. Twigger SN, Pasko D, Nie J, Shimoyama M, Bromberg S, Campbell D, Chen J et al. Tools and strategies for physiological genomics: the Rat Genome Database. *Physiol Genomics* 2005;23(2):246–56.
6. Rúaño G, Seip RL, Windemuth A, Zollner S, Tsongalis GJ, Ordovas J, Otvos J et al. Apolipoprotein A1 genotype affects the change in high density lipoprotein cholesterol subfractions with exercise training. *Atherosclerosis* 2006;185(1):65–9.
7. Windemuth A, Calhoun VD, Pearlson GD, Kocherla M, Jagannathan K, Ruano G. Physiogenomic analysis of localized fMRI brain activity in schizophrenia. *Ann Biomed Eng* 2008;36(6):877–88.
8. Rúaño G, Windemuth A, Kocherla M, Holford T, Fernandez ML, Forsythe CE, Wood RJ, Kraemer WJ, Volek JS. Physiogenomic analysis of weight loss induced by dietary carbohydrate restriction. *Nutr Metab (Lond)* 2006;3:20.
9. Seip RL, Volek JS, Windemuth A, Kocherla M, Fernandez ML, Kraemer WJ, Ruano G. Physiogenomic comparison of human fat loss in response to diets restrictive of carbohydrate or fat. *Nutr Metab (Lond)* 2008;5:4.
10. Rúaño G, Thompson PD, Windemuth A, Smith A, Kocherla M, Holford TR, Seip R, Wu AH. Physiogenomic analysis links serum creatine kinase activities during statin therapy to vascular smooth muscle homeostasis. *Pharmacogenomics* 2005;6(8):865–72.
11. Rúaño G, Goethe JW, Caley C, Woolley S, Holford TR, Kocherla M, Windemuth A, Leon JD. Physiogenomic comparison of weight profiles of olanzapine- and risperidone-treated patients. *Mol Psychiatry* 2007;12:474–82.
12. Rúaño G, Thompson PD, Windemuth A, Seip RL, Dande A, Sorokin A, Kocherla M, Smith A, Holford TR, Wu AH. Physiogenomic association of statin-related myalgia to serotonin receptors. *Muscle Nerve* 2007;36(3):329–35.
13. Rúaño G, Bernene J, Windemuth A, Bower B, Wencker D, Seip RL, Kocherla M, Holford TR, Petit WA, Hanks S. Physiogenomic comparison of edema and BMI in patients receiving rosiglitazone or pioglitazone. *Clin Chim Acta* 2009;400(1–2):48–55.

14. Ruaño G, Thompson PD, Kane JP, Pullinger CR, Windemuth A, Seip RL, Kocherla M, Holford TR, Wu AHB. Physiogenomic Analysis of Statin-Treated Patients: Domain Specific Counter Effects within the *ACACB* Gene on LDL Cholesterol? *Pharmacogenomics* 2010;11:959–71.
15. Holford TR, Windemuth A, Ruano G. Designing physiogenomic studies. *Pharmacogenomics* 2006;7(2):157–8.
16. Cardon LR, Bell JI. Association study designs for complex diseases. *Nat Rev Genet* 2001;2(2):91–9.
17. Wilke RA, Mareedu RK, Moore JH. The pathway less traveled: Moving from candidate genes to candidate pathways in the analysis of genome-wide data from large scale pharmacogenetic association studies. *Curr Pharmacogenomics Person Med* 2008;6(3):150–9.
18. Watanabe RM. Statistical issues in gene association studies. *Methods Mol Biol* 2011;700:17–36.
19. Holford TR. *Multivariate Methods in Epidemiology*. New York: Oxford Press; 2002.
20. Judson R, Stephens JC, Windemuth A. The predictive power of haplotypes in clinical response. *Pharmacogenomics* 2000;1(1):15–26.
21. Adkins RM. Comparison of the accuracy of methods of computational haplotype inference using a large empirical dataset. *BMC Genet* 2004;5:22.
22. The International HapMap Consortium. A haplotype map of the human genome. *Nature* 2005;437(7063):1299–320.
23. Benjamini Y, Hochberg Y. Controlling the false discovery rate: a practical and powerful approach to multiple testing. *J Roy Stat Soc Series B* 1995;57:289–300.
24. Gulati M, Shaw LJ, Thisted RA, Black HR, Bairey Merz CN, Arnsdorf ME. Heart rate response to exercise stress testing in asymptomatic women: The st. James women take heart project. *CIRC* 2010;122(2):130–7.
25. Balady GJ, Arena R, Sietsema K, Myers J, Coke L, Fletcher GF, Forman D et al. Clinician's guide to cardiopulmonary exercise testing in adults: A scientific statement from the American Heart Association. *Circulation* 2010;122(2):191–225.
26. Nylen ES, Kokkinos P, Myers J, Faselis C. Prognostic effect of exercise capacity on mortality in older adults with diabetes mellitus. *J Am Geriatr Soc* 2010;58(10):1850–4.
27. Erbs S, Hollriegel R, Linke A, Beck EB, Adams V, Gielen S, Mobius-Winkler S, Sandri M, Krankel N, Hambrecht R, Schuler G. Exercise training in patients with advanced chronic heart failure (NYHA IIIb) promotes restoration of peripheral vasomotor function, induction of endogenous regeneration, and improvement of left ventricular function. *Circ Heart Fail* 2010;3(4):486–94.
28. Mandic S, Myers JN, Oliveira RB, Abella JP, Froelicher VF. Characterizing differences in mortality at the low end of the fitness spectrum. *Med Sci Sports Exerc* 2009;41(8):1573–9.
29. Ruaño G, Zöllner S, Goethe JW. Drug-induced metabolic syndrome (DiMS) in Psychiatry: a diagnostic need uniquely suited to pharmacogenomics. In: Wong SHY, Linder MW, Valdes R, Jr., eds. *Pharmacogenomics and Proteomics: Enabling the Practice of Personalized Medicine*. Washington, D.C.: AACC Press; 2006. p. 277–82.

90

The Evolution of Massively Parallel Sequencing Technologies: Facilitating Advances in Personalized Medicine

Ian Toma
*George Washington
University Medical Center*

Georges St.
Laurent III
University of Antioquia

Samuel Darko
*National Institutes
of Health*

Timothy A.
McCaffrey
*George Washington
University Medical Center*

90.1	Genomics and Personalized Medicine	90-1
	Improved Diagnostic Classification • Improved Prognostic Information to Guide Therapy • Identification of New Therapeutic Targets	
90.2	A Short History of Sequence Detection	90-3
	Hybridization-Based Detection • Microarrays: Hybridization-Based Detection on a Genomic Scale • Massively Parallel Sequencing	
90.3	Technology of Massively Parallel Sequencing.....	90-5
	Amplification-Dependent Massively Parallel Sequencing • Amplification-Independent Massively Parallel Sequencing • SMS Technology	
90.4	Short Read Alignment and Cluster Computing	90-10
90.5	The Limitations of Genomics and NGS	90-11
	The “Curse” of Dimensionality • The Human Genome Contains Repeated Sequence • Identifying True Phenotypes	
90.6	Proteomic Strategies.....	90-12
90.7	Future Directions.....	90-13
	References.....	90-13

90.1 Genomics and Personalized Medicine

Genomics is a vast field that is growing more diverse by the day. All living animals, fungi, bacteria, viruses, and plants use nucleotide-coded information to direct chemical “work” such as energy metabolism, growth, locomotion, communication, and reproduction. Genomics is most easily defined as **genetic anatomy**: *the examination of the sequence and function of all the DNA- and RNA-based information in a cell*. While the historical field of genetics examined the relationship between single traits, such as eye color and their inheritance pattern, only later found to be transmitted by DNA, genomics can examine *all* DNA and RNA information simultaneously and relate it to complex traits and phenotypes. The goals of genomics in biomedical research are to identify new therapeutic targets for the treatment of complex diseases and to inform the physician about optimization of treatment strategies based on an

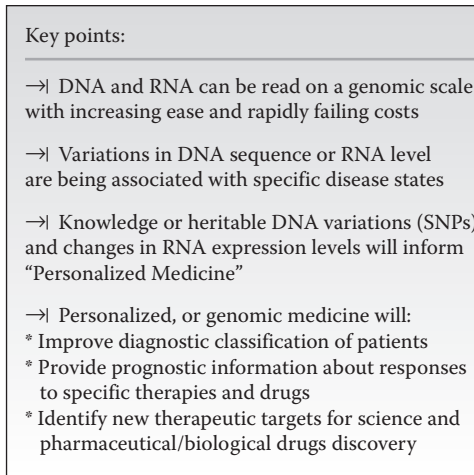


FIGURE 90.1 Summary of key points.

individual’s genome. The strategy of personalized medicine will be achieved, in part, by the following threefold approach, summarized in Figure 90.1.

90.1.1 Improved Diagnostic Classification

By examining the heritable DNA sequences that a person brings to every medical situation, it is hoped that high-risk individuals can be identified. More frequent monitoring of high-risk individuals and more aggressive prevention of risk factors might prevent certain illnesses and needless deaths. Examination of the genes that are actively transcribed into RNA may lead to more accurate diagnosis of various diseases without increasing the cost and complexity of testing. Combinations of DNA and RNA profiling will potentially be able to identify high-risk individuals for heart attack, stroke, cancer, and a variety of other diseases. DNA-based tests are already available to identify patients with a genetic risk of heart attack (1), aortic aneurysm (2), atrial fibrillation (3), and long Q/T syndrome (4), and to predict the likelihood of recurrence of various types of cancer (5–7). Online commercial services such as deCodeMe, 23andMe, and Navigenics can now scan a person’s genome and identify variations that increase their risk of more than 40 diseases.

90.1.2 Improved Prognostic Information to Guide Therapy

After a patient is properly diagnosed, genomic testing provides key additional information to choose the optimal therapies for a patient based on their ability to respond to drugs or devices. For instance, after a heart attack, it would be useful to know the likelihood that a particular patient will progress to heart failure, so as to direct early prevention strategies. As mentioned, currently available genetically based tests of a tumor’s gene expression assists in informing whether the patient has an aggressive tumor that requires chemotherapy, or a milder type of tumor that is unlikely to recur (7). Probably the most immediate application of genomics is in the area of “pharmacogenomics,” which uses natural genetic variations between people (single-nucleotide polymorphisms, SNPs) in certain common metabolic genes that process drugs in order to predict the response to specific medications. SNP-based tests for VKORC1 and cytochrome P450 genes are available to predict the metabolism of coumadin (8), and studies are underway to determine whether that information can help to improve the management of patients receiving this important anticoagulant for conditions including hip replacement, mitral valve replacement, and atrial fibrillation. In the area of infectious disease, new DNA-based tests can more

accurately diagnose patients infected with tuberculosis (TB) and simultaneously predict whether the TB will respond to the major antibiotics in routine use (9).

90.1.3 Identification of New Therapeutic Targets

The long-term goal of genomic approaches is to fully understand the molecular pathophysiology of complex diseases such as cancer and cardiovascular pathologies so that rational therapies can be implemented. Prior to genomics, researchers could only examine a few genes at a time in any given disease, essentially guessing whether it might have a role or not. Genomic approaches have allowed researchers to measure essentially all genes simultaneously and thereby efficiently identify unexpected genetic changes that may have a role in the disease process. A limitation to this approach is the fact that many genetic changes will *correlate* with a disease without actually being a *cause* of the disease. Separating *causation* from *correlation* is a more difficult process involving the selective expression or deletion of the gene/gene product to determine whether the disease is affected. Despite these difficulties, genomic strategies are beginning to inform the pharmaceutical companies and regulatory authorities on effectiveness and potential complications of drugs that come to market and are helping to design new drugs targeted to specific molecules or pathways. Regardless of the causation/correlation distinction, many of the genomic changes can serve as valuable biomarkers of the disease, which can then speed the development of therapeutics.

90.2 A Short History of Sequence Detection

90.2.1 Hybridization-Based Detection

The simplest methods of DNA detection make use of the fact that nucleic acid strands, composed of the nucleotides adenosine, guanosine, cytosine, and thymidine (uracil in RNA), have a four-base code. The code is written in a complementary double strand with noncovalent bonds between the two strands and obligate pairing of bases A to T (or U) and C to G. This provides the opportunity, extensively capitalized upon, to use one strand to recognize the other so-called “base pairing,” “annealing,” or most commonly “hybridization.” By immobilizing one strand, typically by covalent bonding to a surface, the complementary strand can be captured from a solution containing all possible DNAs or RNAs. Then, under appropriate conditions, only the complementary strand will hybridize. Labeling one strand with a radioactive or fluorescent molecule allows scientists to use one strand to identify the other. Agarose gel electrophoresis separates RNA or fragments of DNA by their size prior to immobilization, thus providing further information about the length of the strand. The major impediment to this strategy is that only 10–20 samples per gel can be quantified for the presence of a single gene. In a *Southern blot* technique, named after its inventor Edward Southern, genomic DNA is fragmented by enzymes, shear force, or ultrasonic cavitation; the fragments are separated by size through an agarose gel, transferred to a nitrocellulose or nylon membrane, and a radioactive probe is annealed to identify the size and copy number of the complementary strands. In a *Northern blot* technique, RNA molecules are separated by gel electrophoresis and are identified with DNA probes. RNA molecules naturally exist in 1000–10,000 bp (=10 kilobases, kb) single-stranded oligomers that do not require fragmentation prior to sizing on a gel. While DNA typically has two copies of a gene (one maternal, one paternal, known as alleles) per cell, those alleles can produce hundreds or thousands of RNA molecules per cell.

90.2.2 Microarrays: Hybridization-Based Detection on a Genomic Scale

In many cases, the most efficient means of determining which gene is affected in a disease is to observe the levels of the mRNA transcript. For decades, this has been performed by the Northern blot technique, one gene at a time, on about a dozen samples and taking several days. Using genomic microarrays, it is

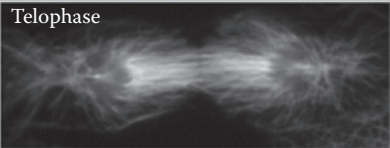
now routine to measure 54,000 different transcript levels in multiple samples with only hours of processing time. In this method, the mRNA is reverse transcribed to DNA, fluorescently labeled and then hybridized to a microarray containing immobilized probes to each transcript. As the transcripts sort themselves to the complementary probe, the fluorescent label accumulates at that probe position. After washing away the nonhybridized transcripts, the fluorescence is read by a confocal microscope, and the levels of each transcript are computed by virtue of knowing the sequence of the probe at each position in the array (spatially addressed). Transcript profiling provides valuable insights into the regulation of gene expression during inflammation (10), wound healing, cancer, cardiovascular diseases (11, 12), diabetes, neurological diseases (13), aging (14), and interferon responses (15). Similarly, hybridization-based methods can be used to read DNA by immobilizing both a normal DNA sequence and a variant of one or more base pairs and then hybridizing a patient's DNA to each of the possible variations. Because millions of DNA sequences are easily immobilized, it is possible to interrogate millions of DNA variations (SNPs) on a single array using photolithographic synthesis.

90.2.3 Massively Parallel Sequencing

Almost all sequencing strategies take advantage of the fact that while the human genome is a very large book, it is broken into 23 chapters (chromosomes), and each chapter is further divided into paragraphs (recombination units), and sentences (genes). The human genome is about 3×10^9 bp, or roughly equivalent to 1000 King James Bibles. If it were unwound, the DNA from a single cell would be about 6 ft long (Figure 90.2). The human genome was first sequenced by shattering the genomic DNA into smaller pieces, sequencing the pieces about 800 bp at a time, and then using supercomputers to reassemble the pieces into the optimal "fit" or "assembly" (Figure 90.3). The complete reference human genome and a wealth of known variations are readily accessible through NCBI Entrez, the UCSC genome browser, and many other sites that provide intuitive maps to the entire human genome, allowing anyone to zoom into any particular area and read it. Historically, DNA sequences have been read essentially 1 bp at a time by Sanger sequencing at the rate of up to 600 bp/h. Using modified fluorescent Sanger sequencing methods, on sequencers with 96 channels per machine, and hundreds of machines, it took years to sequence a single person because the most accurate "reads" and assembly occur when any given region is sequenced 30 times or more (30× oversequencing). However, newer *massively parallel methods* have the potential to sequence a person's DNA, read all of the relevant polymorphisms genome wide, or sequence the RNA transcripts within a matter of hours to days.

The problem of reading DNA

- *The genome is 3 billion letters long, that is, 1000 Bibles long*



Telophase

- *Unwinding DNA from 1 cell would be a thread 6 ft long*
- *The DNA from your whole body is 520,000 times larger than the distance from the Earth to the Moon!*
- *Every cell in the body has the same DNA unless an error occurs, called a mutation.*
- *Any 2 people differ in about 3 million letters, called SNPs, which are really just different spellings of the same word.*

FIGURE 90.2 The size of the human genome.

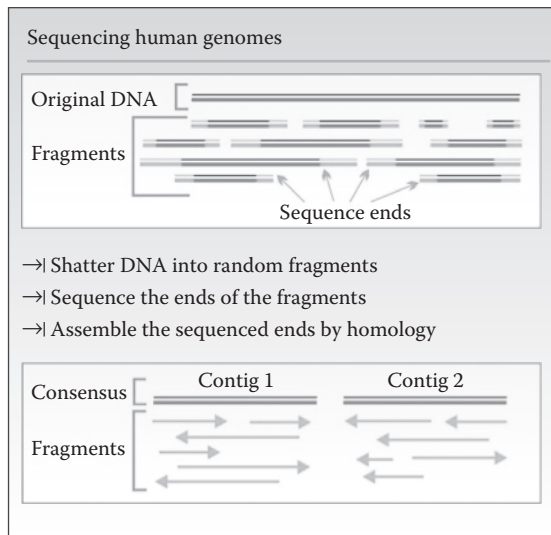


FIGURE 90.3 Cleaving, sequencing, and reassembling genomes.

The complete sequencing of just a small number of people provided the first complete image of a genome, and consequently a reference to use in mapping and comparing to all other individuals. It is therefore possible to compare the reference draft of the genomic “book” to other versions of the genome by shattering the individual genome into phrase-size pieces and comparing the phrases to the reference draft to look for deviations. Simple and predictable methods such as radiation, physical shearing through a small orifice, or restriction enzymes are used to break the genome into readable pieces. By way of an analogy, enter “to be or not to be” into any search engine and observe how easily the remainder of the quote is retrieved. Consequently, instead of reading 23 strands that are each about 130 million letters long, the strands are cleaved into millions of pieces that are each only a few hundred bases long. Because every cell has two copies of a gene, and 1 cc of tissue can have millions of cells, fragmenting the DNA from even a small sample of blood, saliva, or tissue produces millions of random and overlapping fragments. *The key to this strategy is that the overlapping ends of the fragments allow the sequence to be reassembled by complementary sequences from other fragments which span gaps created by other pieces.* If these fragments had to be sequenced in order, on one device, there would be no performance gain in this strategy. However, an enormous performance gain is achieved because these fragments can be read simultaneously using massively parallel processing by “next generation” sequencing (NGS) strategies, sometimes called “deep sequencing.”

90.3 Technology of Massively Parallel Sequencing

Massively parallel sequencing has two general approaches: *pyrosequencing* and *hybrid-based sequencing*. Both make use of the simultaneous performance of tens of millions of chemical reactions. The basic Sanger sequencing reaction depends on the fact that to reconstruct a sequence, one only needs to know the length of a random strand and what the last base is, with the last nucleotide being identified by a “e terminator reaction.” Pyrosequencing uses a different chemistry to cause light to be emitted when a particular base is added to one strand extending along a template. The main difference between Sanger sequencing and pyrosequencing is that Sanger’s technique detects the nucleotide by chain termination with dideoxynucleotides, while pyrosequencing detects the signal from the pyrophosphate released when a nucleotide is incorporated. Hybrid-based sequencing makes use of the fact that DNA is double stranded and hybridizes to its complement with elegant specificity. Even a single base pair mismatch

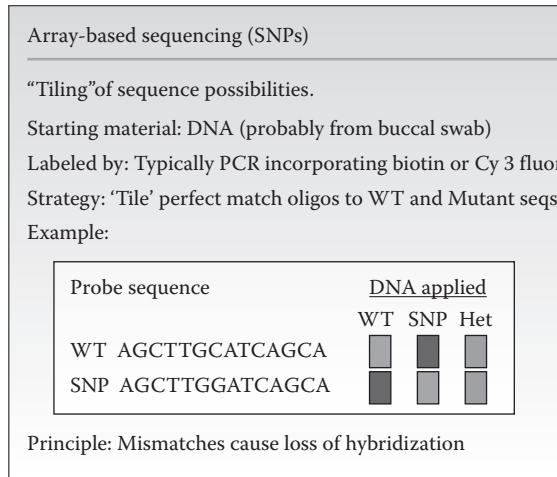


FIGURE 90.4 Principles of sequencing by hybridization. Blue is a positive hybridization, red is no hybridization.

over a stretch of 20 identical bases will significantly disrupt the hybrid. This specificity is used to read DNA by immobilizing known sequences called *probes* on a glass surface applying unknown sequences in solution, and determining whether they anneal or not. The anneal reaction is detected by fluorescent labels attached to the unknown DNA in the solution. After washing, the presence of fluorescence on the immobilized probes is indicative of a successful hybridization reaction.

In initial implementations of hybrid-based sequencing, only a few DNA probes were immobilized on a surface and each of the probes would interrogate a particular nucleotide option at a given position, as shown in Figure 90.4. By reading the level of fluorescence of the probe positions, it is possible to infer whether the sample applied is homozygous or heterozygous for a particular SNP. The power of this method was rapidly expanded by using robotic microarray printers to make thousands of probe spots on a glass slide. Further advances in photolithographic methods of chemical synthesis have produced microarrays capable of carrying more than 4 million probe spots, with each spot being only 10 μm^2 in size. The resulting arrays are capable of determining as many as 950,000 SNPs with >99% accuracy.

Pyrosequencing, in particular, can be adapted to a similar massively parallel solid-state format. By fragmenting DNA into short, single-stranded templates and then immobilizing them onto a solid substrate, pyrosequencing can be performed simultaneously on millions of templates. Each added base is detected by the transient production of light when the correct base is extended. Using time-lapse scanning of the surface, it is possible to directly read the synthesis of the strand. Variations on this basic concept currently allow tens of millions of sequences of about 50–150 bp to be read over a period of days, putting the technology within reach of overnight genome sequencing.

90.3.1 Amplification-Dependent Massively Parallel Sequencing

An important technical difference between NGS techniques is whether the input DNA or RNA must be amplified in quantity before sequencing. This matters because the methods of amplifying DNA/RNA can introduce errors in the sequence and also introduce biases in the sequences that are amplified. Typical thermostable polymerases, used for amplifying DNA/RNA in polymerase chain reactions (PCR), introduce mutations at a rate of 1 in 9000 nucleotides. This rate sounds rare, but the multiple amplification cycles necessarily (up to 40) can yield a number of sequence errors. Furthermore, particular types of sequences called microsatellites, such as long stretches of adenine nucleotides, may cause an even higher error rate. Likewise, polymerases often amplify GC-rich sequences at lower efficiency

because these sequences have unfavorable secondary structures. Such amplification bias creates problems for quantification in downstream analysis of sequence reads generated by these approaches. Nonetheless, there are powerful NGS techniques which utilize small amounts of input DNA/RNA and then amplify each strand to create small clonal “clusters” of the sequence and then sequence the “cluster” or bead by some variation of pyrosequencing. Examples of amplification-dependent technologies are the 454 Life Sciences/Roche, Illumina/Solexa Genome Analyzers, which employ clusters on plates, and the ABI SOLID line of bead-based sequencers.

90.3.2 Amplification-Independent Massively Parallel Sequencing

A major advance in sequencing capacity and efficiency came about with the development of amplification-independent techniques, also called *single-molecule sequencing (SMS) by synthesis*. SMS technology can minimize the biases introduced by the DNA amplification procedures present in other massively parallel sequencing methods. The main principle of SMS is the recording of synthesis events as they occur in each molecule attached or hybridized to a solid surface on a flow cell or microchip. Incorporation of new nucleotides is reported and recorded in the form of fluorescence (Helicos Biosciences, Pacific Biosciences) or as a voltage fluctuation caused by a change in pH of the solution upon nucleotide incorporation and the release of a hydrogen ion (Ion Torrent Systems).

90.3.3 SMS Technology

90.3.3.1 Helicos Biosciences: “HeliScope” Sequencer

Currently, the HeliScope Sequencer is the only commercially available SMS, but other implementations are near to market. The target sample (DNA or RNA) is polyadenylated on the 3′ end and hybridized to oligo-dT molecules covalently attached to the surface of the flow cell. Up to 50 samples may be loaded in one run and the run typically lasts for 8 days, depending on the user’s preset parameters (16). In an innovative variant of this approach, covalent attachment of sequence-specific oligomers to the flowcell surface can function to capture targeted sequence from any chromosomal locus. Algorithms similar to those for creating siRNAs can effectively target almost any genomic loci for sequencing, allowing in-depth analysis of disease-specific alleles.

Chemical reactions consist of repeated cycles in which fluorescently labeled nucleotides are added, the reaction is terminated by a virtual terminator nucleotide, the excess unincorporated nucleotides are washed out, the fluorescent signals on the template are recorded, and the fluorescent label is cleaved from the recorded strand (Figure 90.5). Each reaction adds one of the four nucleotides (A, C, G, and T) and the template position is mapped to the signal detected on the flow cell. In this way, the exact sequence of the template strand is recorded after each cycle, including the total length in nucleotides per synthesized molecule. The overall technical performance of the HeliScope is presented in Table 90.1.

90.3.3.2 Pacific Biosciences

Pacific Biosciences Inc. is another technology leader with the potential to revolutionize the deep sequencing field. Their proprietary technology monitors and records the DNA synthesis by an immobilized DNA polymerase as synthesis occurs. Their methodology has a high signal-to-noise ratio during sequencing because it fluorescently detects, in real time, the incorporation of individual fluorophore-linked nucleotides. The major advantages are the high speed of the real-time reads, 3–4 bp/s, and the very long read lengths, potentially 1–10 kb under ideal conditions, which translates to run times of hours instead of days.

The active DNA polymerase is attached to the bottom of a zero-mode waveguide (ZMW), which is a tiny cylindrical hole in a 100 nm metal film, creating a visualization chamber capable of focusing light into the lower region of a very small volume (20 zeptoliters = 10^{-21} L). A single DNA polymerase

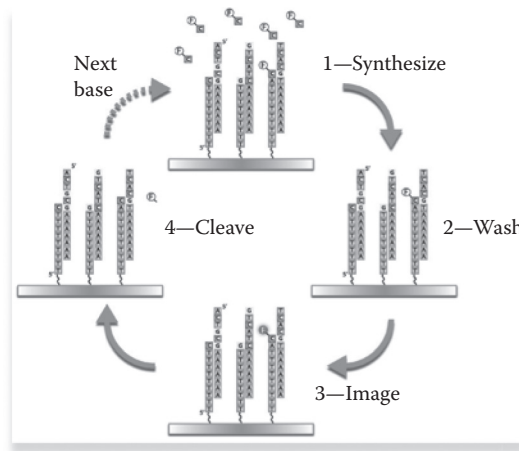


FIGURE 90.5 Basic Helicos method.

TABLE 90.1 Output Capabilities and Technical Performance of the Helicos NGS Technology

Strand output	12–16 M usable strands per channel 600–800 M usable strands per run
Total output	420–560 Megabases per channel 21–28 Gigabases per run
Throughput	105–140 Megabases per hour
Read length	25–55 bases in length 30–35 average length
Accuracy	>99.995% consensus accuracy at >20× coverage
Raw error rate	≤5% (~0.5% for substitutions) Consistent from 20 through 80% GC content of target DNA Independent of read length and template Size
Template size	25–5000 bases

molecule is present at the bottom of the ZMW and a high concentration of four nucleotides (A, C, G, and T), each linked to a different colored fluorophore at the phosphate group, is added to the ZMW. As each nucleotide is incorporated in the DNA strand, the nucleotide fluorophore is briefly brought to the bottom of the ZMW, where the excitation is stimulated and emission is read by a photometer. As incorporation is completed, the fluorescent group is cleaved and quickly diffuses out of a tiny detection volume. The presence of the incorporated fluorophore-linked nucleotide in the detection volume for tens of milliseconds produces a bright flash of light which is terminated once the natural cleavage of phosphate takes place. The light emitted by each fluorophore passes through a prism dispersive element, where it is separated by its color-specific wavelength and is detected on a single-photon CCD array (Figure 90.6). The process is repeated thousands of times over the area of the CCD array. Each sequencing chip contains more than 100 K ZMW, allowing for simultaneous and continuous detection across all ZMW in real time. Currently, the technology only populates 30–40% of the theoretically available ZMWs during a run, limiting the number of sequence reads to 30–40 K.

90.3.3.3 Ion Torrent Systems Inc.: Personal Genome Machine

Ion Torrent Systems Inc. is a major developer of third-generation SMS technology. As its proprietary name, “Personal Genome Machine” (PGM™), suggests, the main target of Ion Torrent is an individual’s genome, which could be sequenced in a very short time at the point of care during a visit to a healthcare

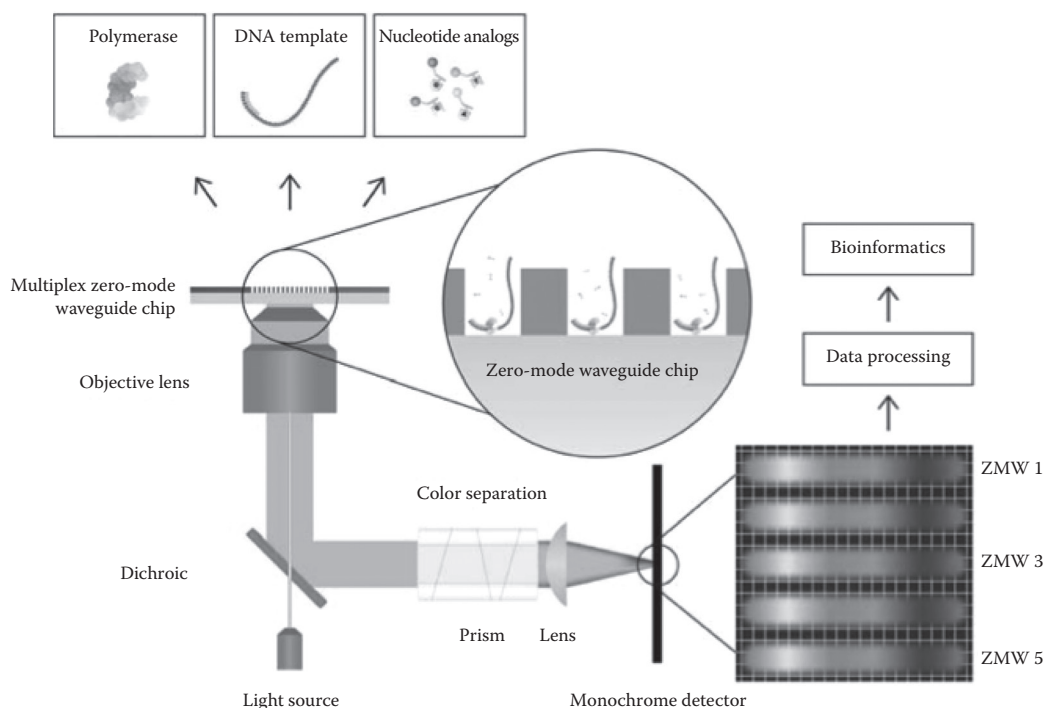


FIGURE 90.6 PacBio ZMW single molecule sequencing.

provider. The initially announced price of PGM is in the range of \$50 K USD, which, along with its compact size and light weight of about 50 lbs, makes the machine affordable for private medical practices, hospitals, diagnostic labs, and small research labs. PGM technology is based on a high-density array of wells containing different DNA templates, beneath which is placed an ion-sensitive layer, followed by a proprietary ion sensor. The principle of sequencing (Figure 90.7) is based on the release of H^+ ions that occurs during nucleotide incorporation into the synthesized molecule and detection of the subsequent pH changes by an ion-sensitive layer and sensor. The sensor converts the chemical reaction into digital information, which is deconvolved into sequence.

90.3.3.4 Nanopore-Based Technologies

Nanopore-based SMS, a novel technology in development, is believed to be capable of sequencing the whole human genome for under \$1 K USD within 24 h. The main principle of existing variations is modulation of current changes by nucleotide of DNA/RNA molecules driven by electrophoresis through a nanopore while the technology measures the ionic current through the pore. The nanopore-based ion-current modulating sequencing approaches presently in development (17) include

- Detection of ionic current fluctuation through an α -hemolysin pore created by a blockage of a pore by a strand of synthesized DNA
- Blockage delay of current caused by exonuclease cleavage of dNMP off the DNA strand driven into an adaptor lodged within the nanopore
- Sequencing using synthetic DNA stripped off as it passes through a nanopore, detected as a short-lived photon bursts
- Detection of tunneling currents that traverse through the nucleotides of DNA electrophoretically driven through the nanopore

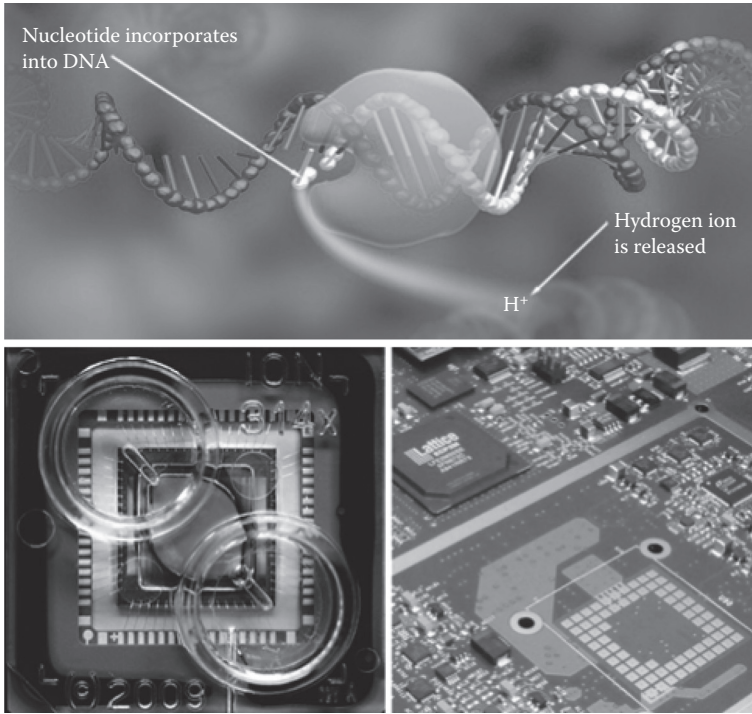


FIGURE 90.7 Ion Torrent personal genome machine.

90.4 Short Read Alignment and Cluster Computing

The vast technical improvements in DNA/RNA sequencing are necessitating equally transformative improvements in the computational aspects of genomics. For the foreseeable future, long DNA strands like chromosomes will be broken into smaller pieces, sequenced, and then reassembled. The first assembly of the human genome in 1998 required more than 700 CPUs and 70 TB of storage. By comparison, in 2010 the alignment of 40 million short reads of RNA to the known genome can be accomplished on a fast desktop computer in hours with only 4 GB of RAM. Nonetheless, the computational success of alignment is a critical element of success in NGS, and nearly inherent problems of alignment and statistical analysis will limit this strategy for years to come.

Vladimir Levenshtein's 1965 manuscript detailed a method to measure the amount of distance between two strings of characters (18). Later improved in 1970 by Needleman and Wunsch and in 1981 by Smith and Waterman (19), sequence alignment has been a daily operation in almost every biomedical research laboratory. In 1990, the algorithm "basic local alignment search tool" (BLAST) demonstrated notable speed enhancements over prior algorithms, while maintaining nearly the same level of accuracy. BLAST quickly became the most widely used bioinformatics program in history (20). BLAST "seeds" the alignment by finding small segments from the query and target sequences that are highly similar and then attempting to increase the alignment from there. Segments that are highly similar are called "maximal segment pairs" (MSP) or "high-scoring segment pairs" (HSP). In this way, local maximums are found and returned as probable alignments.

The previously discussed alignment algorithms were more than sufficient for the individual DNA and RNA sequences of up to 800 bp obtained using Sanger sequencing. However, with the advent of NGS, the alignment problems became significant. To align millions of short reads by traditional means would require intensive time and computational resources. Thus, new heuristic alignment algorithms, such as

those used by the software package Bowtie, have been developed (21). Bowtie can align 35-bp reads at a rate of greater than 25 million reads per CPU-hour. To allow Bowtie to run at such speeds on a PC, it employs a Burrows–Wheeler index on the full-text minute-space (FM) index, requiring a memory footprint of only about 1.3 GB for the entire human genome.

Once next-generation sequence reads are aligned, they serve as input for many other bioinformatic approaches to understanding the biological implications of these genome-wide measurements. Some of the major algorithms evaluate: sequence conservation between organisms, expression patterns within a single study or between studies (22), secondary structure predictions for RNAs, biological annotation such as splice sites protein coding regions, gene ontology, pathway enrichment (23), and network analysis (24). The vast information content of the NGS dataset is critical for the outcome of these bioinformatic algorithms.

Computationally, these more sophisticated algorithms are being implemented on increasingly powerful computer architectures. The NGS platforms typically include multiblade cluster computers, which divide the alignment problems into parallel problems, with each problem assigned to separate compute “nodes.” Compute nodes are typically blades with quad processors, 4–8 GB RAM and an on-board hard drive. These nodes perform alignment and then return the results to a master node for a “meta assembly.” Increasingly, these physical compute nodes are being replaced by virtual machines residing on:

“cloud” computers like Amazon’s Elastic Compute Cloud (EC2), which harness the aggregate computing power of interconnected servers around the world. Cloud computing has the advantages of essentially no investment in physical infrastructure or personnel, on-demand scalability, and nearly complete software flexibility, but is somewhat hindered by concerns over the security of the highly sensitive personal data which reside within the cloud.

90.5 The Limitations of Genomics and NGS

90.5.1 The “Curse” of Dimensionality

While these massively parallel methods provide impressive power to generate new hypotheses and potentially understand and cure diseases, there are limitations that require consideration. A major limitation to the NGS methods is a direct function of their major strength. By measuring millions of independent genetic events, one has excellent coverage, but each measurement has low, but significant random noise. When the random noise of millions of events is accumulated, it essentially insures that false-positive and false-negative results will occur. For instance, in a conventional statistical analysis involving measurements of blood pressure in two groups of people, one accepts a 5% risk of a given difference occurring by random chance. However, if one measures 54,000 transcript levels, and accepts the same 5% risk for each measure, then by chance alone, 2700 transcripts will be observed to change randomly between any two groups. The problem is further enhanced at the genomic level, where it might be necessary to measure 1–3 million SNPs or more to even roughly cover the genome at sufficient resolution. Known as the false discovery rate (FDR), this intrinsic limitation of highly dimensional data can only partially be overcome by using large numbers of subjects so that the random noise is averaged out, leaving the true signal to emerge. For example, several large genome-wide association studies have employed 10–15,000 patients per study in order to have sufficient power to detect SNPs associated with CAD (25, (26), diabetes, Crohns, and bipolar disorder (27). The agreement between studies on some of these markers strongly suggest that sufficient power was reached in each of the studies.

Fortunately, NGS technologies offer a level of measurement precision unattainable with microarrays, reducing the FDR and increasing the statistical significance of genome-wide experiments. Especially at lower levels of transcript expression, microarray platforms suffer from a background level of hybridization that reduces the signal-to-noise characteristics. In contrast, because each individual aligned sequence reads in an NGS study depends on multiple independent experimental observations (as many

as the length of the sequence read itself), the net information content provided by the experiment increases 10–50-fold over microarrays. This additional information content permits higher resolution at low expression levels, better overall quantitation, lower p -values, and a lower FDR.

90.5.2 The Human Genome Contains Repeated Sequence

Unlike a large novel, in which any 35 sequential letters might occur in only a single position within the book, as much as 70% of the human genome is composed of nearly identical sequences called “repeats” and otherwise low complexity sequences such as GCGCGCGC. By analogy, the letters “and the” occur more than 20 times in this short chapter. While repeated sequences may be necessary for chromatin structure and function, repeated sequence is problematic for alignment because they can be aligned to thousands of positions in the genome, and thus, are typically discarded by “filtering.” For this reason, longer reads are easier to align because they are more likely to contain unique sequence that “seeds” the alignment to a unique location. Currently, as much as 70% of RNA reads are discarded because they do not align uniquely to the genome.

90.5.3 Identifying True Phenotypes

A major impediment to fully discovering the genotype–phenotype relationship lies in the definition of clear and singular phenotypes. While genotypes can now be completely characterized by NGS, phenotypes, in the form of traits or diseases, are often far less clear. Take one of the simplest traits: Is there only one type of blue eyes? Evidence to date indicates that potentially hundreds of genes may define precise eye color, a trait once thought to have a single gene or a few at best. Diseases such as cancer and cardiovascular or autoimmune diseases may be many times more complicated. For instance, breast cancer is defined clinically as a mass in the breast, which then can be separated into several finer phenotypes, such as estrogen receptor positive or negative, benign or metastatic, and so on. Genetically, however, there may be hundreds of “disease genotypes” that are associated with particular functional phenotypes. It will be essential to track the behavior of precise genetic subtypes of a disease.

Another challenge for using NGS to characterize phenotypes pertains to multiple cell types. Even relatively simple physiological functions rely on a number of different cell types functioning within a specific anatomical microregion in a coordinated, goal-oriented fashion. More complex functions such as inflammation can recruit dozens of cell types from peripheral blood flow and drive the context-specific differentiation of many other cell types from recruited cells. The genomic characterization of disease phenotypes requires a simultaneous understanding of gene expression in these many cell types that participate in the physiological functions relevant to disease etiology. Many current experimental frontiers focus on the enrichment of specific cell types for genomic analysis within a disease context.

90.6 Proteomic Strategies

When DNA transcribes RNA, the complexity of the signal is actually significantly reduced because the mRNA is simpler than the DNA which produced it. However, as mRNA is translated into protein, the protein is typically modified by cleavage, dimerization, phosphorylation, glycosylation, lipid modification, and protein–protein interactions, which all drastically increase the complexity of the proteome. Current methods of protein identification and quantitation, such as mass spectrometry, are extremely sophisticated but are still far short of determining all of these potential protein variations in a complex protein mixture such as serum. Nonetheless, there are increasingly useful strategies for fractionating complex biological samples, cleaving the proteins into peptide fragments, and then analyzing the peptides by one of several mass spectrometry methods.

90.7 Future Directions

Genomics, proteomics, and bioinformatics are by far the most explosive areas of biomedical research, and they are quickly making inroads into clinical practice. By 2011, it is likely that complete sequencing of individual human genomes will be affordable to the average American, probably for less than the cost of a laptop computer. However, fully interpreting the massive amounts of information, especially the gene-gene interactions that modify diseases, will be a sizeable task. Further, not all diseases can be diagnosed by DNA sequence alone, and so RNA profiling and improved proteomic methods will be crucial to advancing biomedical research. In addition, recent discoveries have demonstrated that the human transcriptome contains far more transcripts than originally predicted from the approximately 25,000 protein coding genes (28, 29). While most of these transcripts do not code for proteins, some have important functionality in cellular physiology, such as micro-RNAs (miRNAs) (30), piwi associated RNAs (piRNAs) (31), long intergenic noncoding RNAs (lincRNAs) (32), and natural antisense transcripts (NATs) (33).

As a result of such emerging complexity, large-scale, well-controlled prospective studies will be required to determine whether genomic information is actually useful in informing the diagnosis and treatment of patients. In some cases, it is quite possible that clinical “titration” (to test and adjust the levels) of coumarin doses, for instance, may be advantageous. Once the empirical value of genetic information is established in specific indications, it should be easier to engage physicians and patients in its routine use (34). There is little doubt, however, that a genomic era of medicine is beginning in which the physician will have intricate knowledge of the genetic anatomy of the patient. As with any tool, it is the task of the physicians and scientists to apply that knowledge for the greatest good of the patient.

References

1. Helgadóttir, A., Thorleifsson, G., Manolescu, A., Gretarsdóttir, S., Blondal, T., Jonasdóttir, A., Sigurdsson, A., Baker, A., Palsson, A., Masson, G. et al. 2007. A common variant on chromosome 9p21 affects the risk of myocardial infarction. *Science* 316:1491–1493.
2. Helgadóttir, A., Thorleifsson, G., Magnusson, K.P., Gretarsdóttir, S., Steinthorsdóttir, V., Manolescu, A., Jones, G.T., Rinkel, G.J., Blankensteijn, J.D., Ronkainen, A. et al. 2008. The same sequence variant on 9p21 associates with myocardial infarction, abdominal aortic aneurysm and intracranial aneurysm. *Nat Genet* 40:217–224.
3. Gudbjartsson, D.F., Arnar, D.O., Helgadóttir, A., Gretarsdóttir, S., Holm, H., Sigurdsson, A., Jonasdóttir, A., Baker, A., Thorleifsson, G., Kristjansson, K. et al. 2007. Variants conferring risk of atrial fibrillation on chromosome 4q25. *Nature* 448:353–357.
4. Ackerman, M.J. 2004. Cardiac channelopathies: It's in the genes. *Nat Med* 10:463–464.
5. Glas, A.M., Floore, A., Delahaye, L.J., Witteveen, A.T., Pover, R.C., Bakx, N., Lahti-Domenici, J.S., Bruinsma, T.J., Warmoes, M.O., Bernards, R. et al. 2006. Converting a breast cancer microarray signature into a high-throughput diagnostic test. *BMC Genomics* 7:278.
6. Knauer, M., Mook, S., Rutgers, E.J., Bender, R.A., Hauptmann, M., van de Vijver, M.J., Koornstra, R.H., Bueno-de-Mesquita, J.M., Linn, S.C., and van't Veer, L.J. 2010. The predictive value of the 70-gene signature for adjuvant chemotherapy in early breast cancer. *Breast Cancer Res Treat* 120:655–661.
7. Kim, C. and Paik, S. 2010. Gene-expression-based prognostic assays for breast cancer. *Nat Rev Clin Oncol* 7:340–347.
8. Oldenburg, J., Bevans, C.G., Fregin, A., Geisen, C., Muller-Reible, C., and Watzka, M. 2007. Current pharmacogenetic developments in oral anticoagulation therapy: The influence of variant VKORC1 and CYP2C9 alleles. *Thromb Haemost* 98:570–578.
9. Helb, D., Jones, M., Story, E., Boehme, C., Wallace, E., Ho, K., Kop, J., Owens, M.R., Rodgers, R., Banada, P. et al. Rapid detection of *Mycobacterium tuberculosis* and rifampin resistance by use of on-demand, near-patient technology. *J Clin Microbiol* 48:229–237.

10. Calvano, S.E., Xiao, W., Richards, D.R., Felciano, R.M., Baker, H.V., Cho, R.J., Chen, R.O., Brownstein, B.H., Cobb, J.P., Tschoeke, S.K. et al. 2005. A network-based analysis of systemic inflammation in humans. *Nature* 437:1032–1037.
11. Zohlhofer, D., Richter, T., Neumann, F., Nuhrenberg, T., Wessely, R., Brandl, R., Murr, A., Klein, C., and Baeuerle, P. 2001. Transcriptome analysis reveals a role of interferon- γ in human neointima formation. *Mol Cell* 7:1059–1069.
12. McCaffrey, T.A., Fu, C., Du, B., Eksinar, S., Kent, K.C., Bush, H., Jr., Kreiger, K., Rosengart, T., Cybulsky, M.I., Silverman, E.S. et al. 2000. High-level expression of Egr-1 and Egr-1-inducible genes in mouse and human atherosclerosis. *J Clin Invest* 105:653–662.
13. Avramopoulos, D., Szymanski, M., Wang, R., and Bassett, S. 2011. Gene expression reveals overlap between normal aging and Alzheimer's disease genes. *Neurobiology of Aging* 32(12):2319.e27–2319.e34.
14. Wennmalm, K., Wahlestedt, C., and Larsson, O. 2005. The expression signature of *in vitro* senescence resembles mouse but not human aging. *Genome Biol.* 6:R109.
15. Gagarin, D., Yang, Z., Butler, J., Wimmer, M., Du, B., Cahan, P., and McCaffrey, T.A. 2005. Genomic profiling of acquired resistance to apoptosis in cells derived from human atherosclerotic lesions: Potential role of STATs, cyclinD1, BAD, and Bcl-XL. *J Mol Cell Cardiol* 39:453–465.
16. Ozsolak, F., Ting, D.T., Wittner, B.S., Brannigan, B.W., Paul, S., Bardeesy, N., Ramaswamy, S., Milos, P.M., and Haber, D.A. 2010. Amplification-free digital gene expression profiling from minute cell quantities. *Nat Methods* 7:619–621.
17. Branton, D., Deamer, D.W., Marziali, A., Bayley, H., Benner, S.A., Butler, T., Di Ventra, M., Garaj, S., Hibbs, A., Huang, X. et al. 2008. The potential and challenges of nanopore sequencing. *Nat Biotechnol* 26:1146–1153.
18. Levenshtein, V.I. 1966. Binary codes capable of correcting deletions, insertions, and reversals. *Sov Phys Dokl* 10:707–710.
19. Smith, T.F., and Waterman, M.S. 1981. Identification of common molecular subsequences. *J Mol Biol* 147:195–197.
20. Altschul, S.F., Gish, W., Miller, W., Myers, E.W., and Lipman, D.J. 1990. Basic local alignment search tool. *J Mol Biol* 215:403–410.
21. Langmead, B., Trapnell, C., Pop, M., and Salzberg, S.L. 2009. Ultrafast and memory-efficient alignment of short DNA sequences to the human genome. *Genome Biol* 10:R25.
22. Cahan, P., Ahmad, A.M., Burke, H., Fu, S., Lai, Y., Florea, L., Dharker, N., Kobrinski, T., Kale, P., and McCaffrey, T.A. 2005. List of lists-annotated (LOLA): A database for annotation and comparison of published microarray gene lists. *Gene* 360:78–82.
23. Salomonis, N., Hanspers, K., Zambon, A.C., Vranizan, K., Lawlor, S.C., Dahlquist, K.D., Doniger, S.W., Stuart, J., Conklin, B.R., and Pico, A.R. 2007. GenMAPP 2: New features and resources for pathway analysis. *BMC Bioinformatics* 8:217.
24. Bogner, V., Leidel, B.A., Kanz, K-G., Mutschler, W., Neugebauer, E.A.M., and Biberthaler, P. 2011. Pathway analysis in microarray data: A comparison of two different pathway analysis devices in the same dataset. *Shock* 35(3):245–251.
25. Samani, N.J., Erdmann, J., Hall, A.S., Hengstenberg, C., Mangino, M., Mayer, B., Dixon, R.J., Meitinger, T., Braund, P., Wichmann, H.E. et al. 2007. Genomewide association analysis of coronary artery disease. *N Engl J Med* 357:443–453.
26. McPherson, R., Pertsemlidis, A., Kavaslar, N., Stewart, A., Roberts, R., Cox, D.R., Hinds, D.A., Pennacchio, L.A., Tybjaerg-Hansen, A., Folsom, A.R. et al. 2007. A common allele on chromosome 9 associated with coronary heart disease. *Science* 316:1488–1491.
27. Burton, P., Ahmad, T., Attwood, A., Ball, S., Balmforth, A., Ban, M., Barbour, J., Barrett, J., Barton, A. et al. 2007. Genome-wide association study of 14,000 cases of seven common diseases and 3000 shared controls. *Nature* 447(7145):661–678.

28. Katayama, S., Tomaru, Y., Kasukawa, T., Waki, K., Nakanishi, M., Nakamura, M., Nishida, H., Yap, C.C., Suzuki, M., Kawai, J. et al. 2005. Antisense transcription in the mammalian transcriptome. *Science* 309:1564–1566.
29. Kapranov, P., Cheng, J., Dike, S., Nix, D.A., Dutttagupta, R., Willingham, A.T., Stadler, P.F., Hertel, J., Hackermuller, J., Hofacker, I.L. et al. 2007. RNA maps reveal new RNA classes and a possible function for pervasive transcription. *Science* 316:1484–1488.
30. Krol, J., Loedige, I., and Filipowicz, W. 2010. The widespread regulation of microRNA biogenesis, function and decay. *Nat Rev Genet* 11:597–610.
31. Thomson, T. and Lin, H. 2009. The biogenesis and function of PIWI proteins and piRNAs: Progress and prospect. *Annu Rev Cell Dev Biol* 25:355–376.
32. Huarte, M., Guttman, M., Feldser, D., Garber, M., Koziol, M.J., Kenzelmann-Broz, D., Khalil, A.M., Zuk, O., Amit, I., Rabani, M. et al. 2010. A large intergenic noncoding RNA induced by p53 mediates global gene repression in the p53 response. *Cell* 142:409–419.
33. Faghihi, M.A., Modarresi, F., Khalil, A.M., Wood, D.E., Sahagan, B.G., Morgan, T.E., Finch, C.E., St Laurent, G., 3rd, Kenny, P.J., and Wahlestedt, C. 2008. Expression of a noncoding RNA is elevated in Alzheimer's disease and drives rapid feed-forward regulation of beta-secretase. *Nat Med* 14:723–730.
34. Scheuner, M.T., Sieverding, P., and Shekelle, P.G. 2008. Delivery of genomic medicine for common chronic adult diseases: A systematic review. *JAMA* 299:1320–1334.

91

Computational Methods and Molecular Diagnostics in Personalized Medicine

Contents

91.1	Introduction	91-1
91.2	The Problem.....	91-2
91.3	Fundamentals (PGx and Pharmacology).....	91-3
	<i>CYP2C9</i> PGx • <i>VKORC1</i> PGx	
91.4	Modeling and Clinical Applications.....	91-6
	Interpretive Guidance of PerMIT:Warfarin • Estimation of Maintenance Dose • Practical Support for Dosage Adjustment	
91.5	Future Extensions of Genotype–Phenotype Modeling	91-8
91.6	Summary.....	91-9
	References.....	91-10

Roland Valdes, Jr.
University of Louisville
School of Medicine
PGXL Laboratories

Mark W. Linder
University of Louisville
School of Medicine
PGXL Laboratories

91.1 Introduction

The future of linking molecular information to clinical outcomes requires a substantial change in present paradigm, where practice is based on intuitive knowledge, toward a more targeted practice now referred to as “precision medicine.” One example of this concept is in the implementation of pharmacogenetics (PGx) as a basis for providing individualized therapy. A major challenge in this application is in providing clinically actionable information to practitioners. In the area of drug therapeutics, one solution involves optimizing the dosing of medications which requires establishing quantifiable relationships between the genotype of an individual and their anticipated response to a particular drug. Combining both metabolism and receptor genotypic information is advantageous; however, it is not sufficient unless kinetic and dynamic parameters are both integrated into quantifiable decision-making approaches. In this chapter, we review the development of a decision-support tool based on combining PGx genotyping with both pharmacokinetic and -dynamic parameters to optimize dosing decisions in real time (Figure 91.1). This model is applied to relationships designed to predict optimum dosing for warfarin, the most commonly prescribed oral anticoagulant for the treatment and prevention of thromboembolic events. The correct maintenance dose of warfarin for a given patient is difficult to predict; the drug carries a high risk of toxicity, and variability among patients means that the safe dose-range differs widely between individuals. Recent PGx studies indicate that the routine incorporation of genetic testing into warfarin therapy protocols could substantially ease both the financial and health risks currently associated with this treatment. In particular, the variability in warfarin dose requirement is now recognized to be due in large part to polymorphisms in two genes: cytochrome P4502C9 (*CYP2C9*)

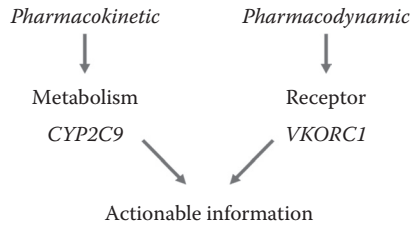


FIGURE 91.1 Combined insight into inherited contributions to variability in pharmacokinetic and pharmacodynamic properties of medications provides the foundation for comprehensive clinical decision support systems.

- *CYP2C9* sets the rate: accumulation and elimination
 - Influences warfarin *clearance* and is also associated with need for decreased maintenance dosages
- *VKORC1* sets the amount: effective concentration
 - Influences warfarin *pharmacodynamic response* and is also associated with specific warfarin maintenance dose

FIGURE 91.2 Conceptual summary of the inherited sources of variance in S-warfarin pharmacology.

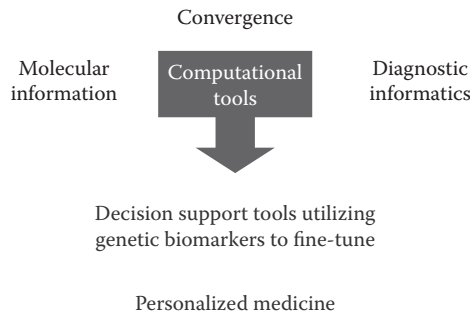


FIGURE 91.3 Computational tools to assist with the integration of diagnostic information are increasingly utilized in clinical decisions.

and the vitamin K epoxide reductase complex subunit 1 (*VKORC1*) (Figure 91.2). The development of computational decision support tools, which integrate all the relevant genetic and physical factors into comprehensive, individualized predictive models for warfarin dose selection, may be used to translate the results of PGx testing into actionable clinical application, Figure 91.3. Of substantial interest is that similar computational models have application in other therapeutic settings.

91.2 The Problem

Warfarin is the most commonly prescribed oral anticoagulant, with four million U.S. patients taking the drug for treatment and prevention of atrial fibrillation, stroke, deep vein thrombosis, or pulmonary embolism, and for those who have had heart valve replacement surgery. Adverse reactions to warfarin

precipitated 43,000 emergency room visits in 2004–2005, a number second only to that of adverse reactions to insulin (<http://biotech.seekingalpha.com/article/10378>).

Current warfarin dosing practices involve initiating dosing at a daily dose of 5–10 mg for 3–4 days, followed by dosing adjustments based on the results of international normalized ratio (INR) testing to measure the degree of anticoagulation. This process is fundamentally flawed and commonly results in suboptimal care for up to 70% of patients who have an inherited deficiency in warfarin metabolism or increased sensitivity for warfarin response [1]. Inherited differences in the cytochrome P450 2C9 (*CYP2C9*), and vitamin K epoxide reductase complex protein 1 (*VKORC1*) genes can produce delayed metabolic clearance of S-warfarin, and a lower concentration threshold for response, respectively [2]. These inherited characteristics have a profound effect on the clinical pharmacology of warfarin and defeat the utility of standard dosing and monitoring practices [3]. The ideal induction and maintenance dosage rate of medications is dictated by the rate of drug metabolism (clearance, half-life) and target therapeutic concentration. Knowledge of these variables establishes the basis for calculation of tailored induction and maintenance dosing regimens. It is also important to ensure that therapeutic monitoring is done when drug concentrations remain constant over the dosing interval, otherwise known as steady state (see figure in section below). Steady-state blood concentrations of warfarin develop over a period of time equal to seven elimination half-lives of the medication. Approximately 40% of patients have diminished *CYP2C9* capacity and have not yet achieved steady state when standard therapeutic monitoring is performed during therapy initiation and following dosage changes. Standard warfarin dosing and monitoring practices are fundamentally inappropriate for application to patients who possess these genetic variants.

91.3 Fundamentals (PGx and Pharmacology)

To begin, a brief introduction to the field of PGx is warranted. PGx links inherited gene structure variants with drug metabolism and response. PGx can be utilized to provide phenotype prediction based on genotype as a means to decrease the incidence of adverse drug reactions (ADRs). Ideally, a patient's PGx information would be known prior to initiation of a new therapeutic regimen so that the physician could base decisions of medication selection and dosing on the patient-specific genotype. The utilization of PGx *a priori* would allow for identification of patients with an increased risk of ADRs before they experience an event. Genotyping as a retrospective diagnostic analysis, on the other hand, can also provide useful information as to the potential cause and mechanistic basis of an ADR.

91.3.1 *CYP2C9* PGx

Inherited genetic polymorphisms in hepatic drug-metabolizing enzymes have been linked to increased risk of ADRs associated with a multitude of common medications [4,5]. The polymorphic cytochrome P450 2C9 enzyme metabolizes 6–10% of commonly prescribed medications including S-warfarin, phenytoin, several of the NSAIDs, and sulfonylurea [5,6,7]. Approximately 20% of the wide interindividual variability in warfarin dosage is due to the metabolic capacity of *CYP2C9* [8,9]. The *CYP2C9* gene contains many single nucleotide polymorphisms (SNPs) represented by over 30 alleles, many of which result in altered enzymatic activity. A complete and up-to-date list of all known *CYP2C9* alleles can be found on the Human Cytochrome P450 Allele Nomenclature Committee website (<http://www.cypalleles.ki.se/cyp2c9.htm>). The most common allele is *CYP2C9**1 and represents the reference “normal” active allele. The frequency of variant alleles differs depending on the ethnic diversity of a population. Among Caucasian populations, approximately 82% of all alleles are *CYP2C9**1, while the remaining alleles are comprised primarily of the *CYP2C9**2 and *CYP2C9**3 variants [5,10]. In contrast, greater than 95% of alleles in African-American and Asian populations are *CYP2C9**1. In these ethnic groups, the *CYP2C9**2 and *3 alleles are less common, comprising only 1–2% of the alleles. Several other variant SNPs are rare and will not be described here [6,10,11].

The functional consequences of the *CYP2C9**2 and *3 alleles on enzyme activity have been well characterized. *CYP2C9**2 has been shown to have as little as 12% of the metabolic capacity of *CYP2C9**1, and as much as 70% capacity, with most studies demonstrating ~70% [12–14]. The *CYP2C9**3 allele, however, has consistently been shown to have roughly 5% of the enzymatic activity of *CYP2C9**1 [2,5,13]. Patients with these variants are intrinsically hypersensitive to *CYP2C9* substrates, including warfarin, in an apparent gene-dose manner. The primary pharmacokinetic change associated with *CYP2C9* metabolic deficiency is a decreased S-warfarin clearance rate [2,6,13]. Decreased clearance subsequently leads to an increased elimination half-life, increased time to reach steady-state plasma concentrations, and ultimately lower dose requirement. The different pharmacokinetic responses to a given dose of warfarin associated with the *CYP2C9**2 and *CYP2C9**3 variants are illustrated in Figure 91.4. In a patient without a *CYP2C9* deficiency (*CYP2C9**1/*1), the S-warfarin plasma concentration would be expected to reach both the therapeutic range, corresponding to an INR between 2.0 and 3.0, and steady state within 3–5 days following dose initiation or adjustment. However, the decreased S-warfarin clearance and increased half-life associated with *CYP2C9* deficiency lead to significantly higher plasma concentrations and a prolongation of the time required to reach steady-state concentrations of the medication following dose initialization or adjustment, the magnitude of each being dependent on which variant is present. For a patient with the *CYP2C9**1/*2 genotype, the expected plasma concentration and time required to reach steady state would be approximately twice that of a *CYP2C9**1/*1 patient on the same dose (Figure 91.4). Even more severe is the case of a patient with at least one *CYP2C9**3 allele, in which the plasma concentration and time to steady state are at least threefold greater than that of a wild-type patient for a given dose (Figure 91.4).

Because *a priori* genotyping is not yet standard of care, a lower dose requirement typically is not identified until after the lengthy trial and error dosing strategies have been utilized, wherein resides the highest risk of adverse events described earlier in this review. Indeed, warfarin ADRs and low dose requirement are significantly associated with the presence of at least one *CYP2C9* variant [15,16]. Several studies have demonstrated that patients with either the *CYP2C9**2 or *3 variants were 2–4 times as likely to experience a bleeding event as those with the *CYP2C9**1 allele [14,15,17]. Presence of the *CYP2C9**2

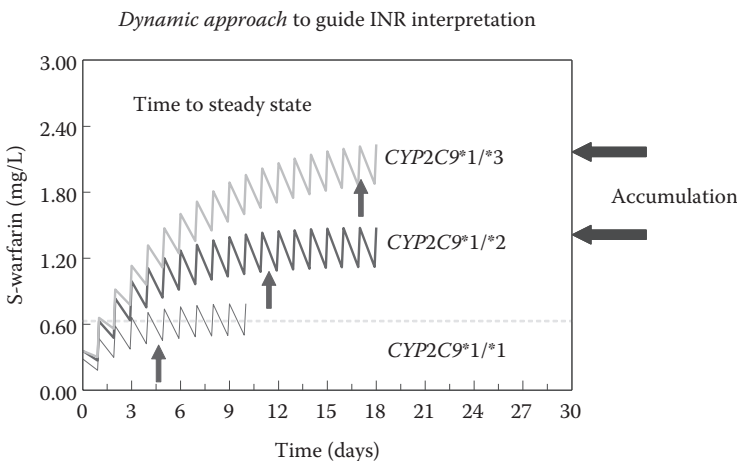


FIGURE 91.4 Impact of *CYP2C9* genotype-dependent changes in S-warfarin clearance on plasma concentration of S-warfarin resulting from a fixed dosage and on the rate of achieving steady state. Scenarios are presented for a 65 y/o female subject, weighing 150 lbs who is administered 4 mg daily dosages. Note the effects of this individual of having a single *CYP2C9**2 allele or *CYP2C9**3 allele. Plasma concentrations accumulate to supra-therapeutic levels and do not achieve steady state until 12–18 days following initiation of dosing. (Adapted from Linder MW et al. *J Thromb Thrombolysis* 14(3), 227–232, 2002.)

and/or *CYP2C9**3 variants also conferred up to a sixfold increased risk of supra-therapeutic INR during the induction phase of warfarin therapy over that of the *1 genotype [15,18,19].

Although *CYP2C9* genetic variation has been established as an independent risk factor for warfarin low dose requirement and adverse events, *CYP2C9* genotype only accounts for 5–20% of the variability in warfarin dose depending on the ethnic population in question [9,20–24]. Approximately 80% of variability in dose cannot be predicted by *CYP2C9* genotype alone. Other factors that affect dose include age (17%), gender (13%), body surface area (15–25%), and the pharmacodynamic changes associated with genetic variation in the gene that encodes VKOR [22,25,26].

91.3.2 *VKORC1* PG_x

The target enzyme of warfarin inhibition, VKOR, is encoded by the recently identified vitamin K epoxide reductase complex subunit 1 gene (*VKORC1*) [27,28]. Numerous recent studies have identified several noncoding region polymorphisms that have been associated with warfarin sensitivity and low dose requirements [25,29,30]. In 2005 Rieder et al. determined that by haplotyping warfarin patients using 10 different *VKORC1* SNPs, they could stratify patients into low, intermediate, or high dose groups, and could explain 25% of dose variability [29]. Concurrent studies found that the *VKORC1* 1173 C > T SNP of intron 1, significantly affected warfarin dose requirement [22,25]. This SNP was included in the low dose haplotype described by Rieder at position 6484 [29]. However, additional analysis has demonstrated that this SNP is in tight linkage disequilibrium with the promoter variant –1639 G > A, which has the strongest association with low-dose warfarin requirement [9,25,26,30]. Patients with the homozygous –1639 GG genotype have been reported to require on average 4.5 mg/day of warfarin, significantly greater than that of the heterozygous GA genotype group, who required 3.8 mg/day, and the homozygous AA genotype group who required 2.2 mg/day [9,30,31]. Other studies have reported similar differences in warfarin dose according to the *VKORC1* –1639 genotype. Figure 91.5 summarizes the distribution of warfarin daily dose requirements across *VKORC1* –1639 G > A genotypes in Caucasians [9,22,24,29], and illustrates that presence of the –1639 A allele is associated with a lower warfarin dose than the –1639 G allele. The pharmacodynamic variability is attributed to the fact that the variant lies within the promoter of *VKORC1*, potentially resulting in decreased transcription of the gene product. Decreased expression of the VKOR enzyme results in decreased warfarin demand to maintain adequate

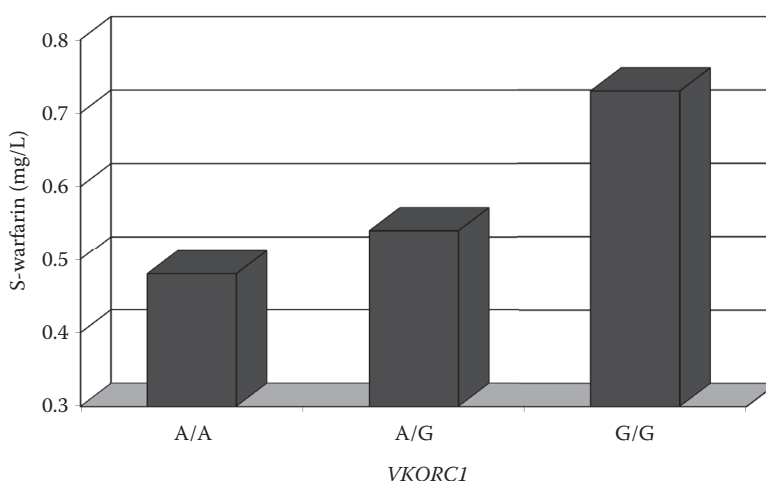


FIGURE 91.5 Association between *VKORC1* –1639 genotype, warfarin maintenance dose, and plasma concentration of S-warfarin required to maintain therapeutic anticoagulation. (Adapted from Zhu, Y. et al. *Clin Chem* 53:1199–1205, 2007.)

anticoagulation. In other words, the effective warfarin concentration is lower in the presence of the –1639 A allele. In Caucasians, the *VKORC1* –1639 G and A allele frequencies are approximately 58% and 42%, respectively [32]. This corresponds to genotype frequencies of approximately 39% for GG, 47% for GA, and 14% for AA in the general Caucasian population [26,32].

91.4 Modeling and Clinical Applications

91.4.1 Interpretive Guidance of PerMIT:Warfarin

The application of PGx diagnostics to warfarin therapy is hindered by the absence of clear guidance on whether and how genotyping may be used to improve patient therapy. The Personalized Medicine Interface (PerMIT:Warfarin) applies PGx modeling as a method for the interventional application of *CYP2C9* and *VKORC1* genetic diagnostics to individually tailored warfarin dosing and evaluation of therapeutic response. PerMIT:Warfarin calculates a warfarin maintenance dose estimate based on a multivariate equation that accounts for the effects of *CYP2C9* and *VKORC1* genotypes [33]. Then, based on the relationship between *CYP2C9* and warfarin elimination half-life, PerMIT models the influence of repeated dosing on plasma drug concentration. This model provides guidance during the transition from induction to maintenance therapy and limits the potential for misinterpretation of INR measurements by clearly displaying the relationship between a patient's dosing regimen and their progress toward steady state.

91.4.2 Estimation of Maintenance Dose

The PGx panel of *CYP2C9* and *VKORC1* (–1639 G > A) accounts for both the pharmacokinetic and pharmacodynamic aspects of warfarin therapy. While *CYP2C9* sets the rate of drug accumulation and elimination, *VKORC1* sets the amount, or effective concentration required to achieve therapeutic success. As indicated above, together, the two genes account for approximately 35–40% of the variability in warfarin dose requirement. Even with this improvement, the majority of variability is unaccounted for with genotyping alone.

Several recent multivariate analyses, like the one presented in [Table 91.1](#), have shown that the addition of patient characteristics such as age, gender, height, weight, and other medications to *CYP2C9*, *VKORC1*, and/or other genomic information accounts for approximately 50–60% of warfarin dose variability [9,21,22,34,35]. However, the study by Sconce et al. was the first to promote the use of a published regression equation that included both *CYP2C9* and *VKORC1* as “a new dosing regimen” [9]. These types of mathematical algorithms may be used currently to estimate an individual patient's maintenance dose requirement, typically to within 1 mg/day of the actual optimal dose [36]. It is important to note that the maintenance dose estimates that can be achieved with an algorithm approach are not expected to replace standard loading induction therapy practices at this time. Application of a genotype-guided maintenance dose at the onset of therapy could result in a long lag before the plasma concentration accumulates to the therapeutic level (dictated by *VKORC1*) and reaches steady state (dictated by *CYP2C9*) [Figure 91.6](#). This would result in a significant risk that the onset of anticoagulation would be delayed, particularly in patients requiring acute therapy. Delayed anticoagulation could lead to thrombosis and/or a misinterpretation by the physician to prematurely increase the dose, leading to a possible overshoot of the target INR. Support for standard initial doses was demonstrated by a study in 2004 which confirmed that significant differences in dose requirements based on *CYP2C9* genotype do not diverge until day four [19]. Therefore, a physician who needs to start a patient on warfarin in the emergent setting can do so regardless of the patient's genotype.

When results of genetic testing are not immediately available, our recommended scenario is that patients begin therapy based on standard induction protocols (e.g., 5 mg/day) with careful INR monitoring for the first 3–4 days. Samples for genotyping should be collected and sent to laboratory on the first

TABLE 91.1 Calculated Estimation of Warfarin Maintenance Dose Based on Clinical and Genetic Attributes of Individual Patients

Predictor(s)	Regression Equation	Model P-value	R ²
Age	$\log(D) = 2.870 - 0.020 (\text{Age})$	0.0003	0.18
Sex	$\log(D) = 1.276 + 0.415 (\text{Sex})$	0.0024	0.13
Weight	$\log(D) = 0.298 + 0.006 (\text{Weight})$	<0.0001	0.28
VK3673	$\log(D) = 1.349 - 0.426 (\text{VK3673-M}) + 0.426 (\text{VK3673-W})$	0.0001	0.27
2C9*	$\log(D) = 1.659 - 0.248(2C9^*2) - 0.625 (2C9^*3)$	0.0003	0.22
Full model (all variables)	$\log(D) = 1.35 - 0.008 (\text{Age}) + 0.116 (\text{Sex}) + 0.004 (\text{Weight}) - 0.376 (\text{VK3673-M}) + 0.271 (\text{VK3673-W}) - 0.307 (2C9^*2) - 0.318 (2C9^*3)$	<0.0001	0.61

Source: Zhu, Y. et al. *Clin Chem* 53, 1199–1205, 2007.

Note: Combined variables included in the full model account for 61% of the interindividual variability in warfarin maintenance dose requirement.

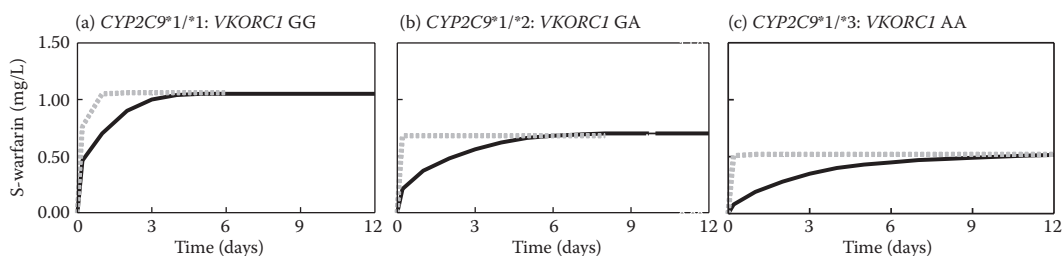


FIGURE 91.6 Each of the three panels depicts a 55 y/o female patient of 5'7" and 145 lbs with a target INR of 2.5. (a) Patient genotype is *CYP2C9**1*1:*VKORC1* GG, estimated maintenance dose is 5.8 mg/day (solid line) and a custom loading strategy of 10 mg; day 1, 8 mg; day 2 (dotted gray line); (b) patient genotype is *CYP2C9**1*2:*VKORC1* GA, estimated maintenance dose of 3.3 mg/day (solid line) and a custom loading dosage of 9 mg (dotted gray line); (c) patient genotype is *CYP2C9**1*3:*VKORC1* AA, estimated maintenance dose of 2.2 mg/day (solid line) versus tailored loading dose of 7 mg (dotted gray line).

day of therapy. Genotype results and maintenance dose estimate modeling would be available by day four for analysis by the clinician in context of the overall patient management strategy. This approach is expected to account for ~50–60% of the variability that influences warfarin dose requirement and result in improved safety and efficacy. For patients already in the maintenance phase of therapy, PGx information nevertheless can provide insight into the individual's pharmacodynamic sensitivity or S-warfarin clearance rate, which significantly influences future dose adjustments, INR monitoring, and interpretation.

The significance of the algorithm-based approach should not be underestimated. In our experience, prior to the advent of the genotype-guided dose calculation, the most common reason cited by physicians for not genotyping patients is that they do not know how to use the information; that there is no perceived actionable information gleaned from a genotyping result is the barrier to implementation. The addition of an estimated maintenance dose with the genotype result provides the physician with information that can directly guide dose selection.

91.4.3 Practical Support for Dosage Adjustment

Once the genotype and patient demographic-based optimal dose is achieved, what remains is management of chronic stable therapy. Although the maintenance dose estimate is itself an important advancement in warfarin therapy, understanding the mechanistic basis for how it is determined, as well as what can alter it, have significant implications for dose adjustments, INR monitoring, and

long-term management. Ultimately, the characteristics identified by genotyping and an algorithm-based approach are not absolute doses, but how a given dose would be expected to behave in an individual. These behaviors include the magnitude of the plasma concentration following each dose and the rate of change in concentration between doses. These are defined by known pharmacokinetic parameters associated with *CYP2C9* genotype, which can be applied to provide clinicians with personalized management tools.

In patients with a *CYP2C9* variant, the rate of change between doses is slower than in a wild-type patient. The slower rate requires an alternate approach to monitoring. Although the majority of patients will reach steady state within 5 days following dose initiation or adjustment, those with *CYP2C9* variants will not; they will require more time. Without understanding the effect of the *CYP2C9* variant, the physician could misinterpret an INR measurement after 5 days as representative of steady state, potentially resulting in a premature dose adjustment. These differences have several implications for monitoring and dose adjustment practices. Consider the following example: an INR measured 3–5 days after a patient's dose adjustment in the maintenance phase is in the therapeutic range (e.g., 2.5), prompting the physician to maintain the current dose. In a patient who has the *CYP2C9**3 variant, the plasma concentration has not yet reached peak, steady-state concentrations by day five; thus, the INR of 2.5 is ultimately low in comparison to where it will be approximately 10 days later when the plasma concentration has reached steady state. Upon a follow-up visit, which may be a week to two weeks later, the patient now has an INR > 3.0 on the same dose. The INR of 2.5 was essentially a transitional measurement that was misinterpreted as one at steady state. Had the delay in reaching the peak concentration been appreciated at the visit on day five, the physician might have considered alternate dosages or monitoring intervals. Additionally, once the dose is again adjusted due to the high INR, another 12–15 days will be needed for S-warfarin in the plasma to again reach steady-state concentrations and the INR to transition into the context of an interpretable measurement. Although the timing of INR measurements illustrated in this example does not represent the optimal follow-up scenario, it is intended to represent not only how long it takes to for the INR to transition to steady state in patients with the variants, but also to depict real-world scenarios in which follow-up diligence remains a problem and is dependent on the out-patient setting. The genotype-guided maintenance dose estimate may reduce the likelihood that a patient is prescribed an inappropriately high dose, however, adjustments may periodically be necessary based on changing health or nutritional status. Insight into the time required to transition into a new steady state will allow clinicians to synchronize monitoring within each adjustment phase to maintain stable therapy.

91.5 Future Extensions of Genotype–Phenotype Modeling

PGx testing has the potential to revolutionize the practice of medicine; however, the direct application of clinical PGx to the creation of individualized dosing strategies has not yet been achieved to an appreciable extent. The development of algorithm-based approaches such as the one described here integrating the relevant *CYP2C9* and *VKORC1* genetic factors and physical attributes into a comprehensive, individualized predictive model for warfarin dose can be used to translate the results of PGx testing into actionable clinical application. As shown in [Figure 91.6](#) maintenance dose estimate models allow the physician to determine what optimal dose would be required in each of three genotypically divergent patients who otherwise have identical physical characteristics. These are patients who, without knowledge of the genotype differences, the physician would treat identically, with potentially severe consequences. The result of such an algorithm-based strategy is that all three patients would receive the individually optimized doses required to reach the target INR within their respective effective concentration ranges ([Figure 91.6](#), panels a–c). Genotype-based maintenance dose estimates facilitate optimized therapy, with the goal of every patient safely reaching the therapeutic range with the optimal effective dose to achieve stable anticoagulation.

Conventional dosing of any medication is fundamentally associated with drug clearance and effective body burden of the drug, typically indicated by the steady-state drug concentration in plasma associated

with the desired pharmacodynamic effect. These parameters establish what dose (unit/time) is required to off-set clearance (unit/time) while maintaining the required therapeutic concentration. It is not a coincidence that the most common warfarin dose is ~5 mg/day. In fact, this is the dosage rate that is required to counter typical warfarin clearance and maintain safe and effective S-warfarin concentrations in the majority of patients, that is, those with *CYP2C9**1/*1 and *VKORC1* -1639 AG genotypes. Differences in S-warfarin clearance and the effective concentration are well-defined by *CYP2C9* and *VKORC1* genotyping, respectively; therefore, it makes sense to adjust dosage *a priori* to accommodate differences in S-warfarin clearance or required concentrations estimated from the PGx testing results. As an example, when differences in aminoglycoside clearance are anticipated due to hepatic or renal impairment it is common practice to make dosage adjustments that compensate for these differences.

Perhaps, the apparent lack of appreciation for the current capabilities of PGx testing is due to the way in which the majority of studies have addressed the issues. There is a perceived “leap to conclusion” that genotyping can predict differences in dose requirement. This is because many studies report differences in dose requirement between genotype categories, without emphasizing that the mechanistic basis for this relationship is the direct result of decreased clearance or requirement for lower effective concentrations (Figure 91.6, panel c). It is the inadequate description and understanding of this intermediate, mechanistic step that promotes the misconception of a “leap” when in fact, the logical middle step for warfarin is clearly defined. Studies have indeed elucidated the relationships between genotype, decreased clearance, and differences in dose requirement, as described in detail in this review. It is because this intermediate step is well-defined that warfarin genotyping can be implemented now to estimate individual maintenance dose requirements, and calculate tailored loading strategies to accommodate the individuals pharmacologic needs (Figure 91.6, panels a–c). This illustrates the need for future studies in the area of PGx in general to better define this intermediate step—the mechanistic basis between observed genotype effects and dose requirement—so that this fundamental knowledge can be applied to the development of rational, quantitative modifications to treatment practices.

The inclusion of genotyping information now can provide significant insight into how to prescribe warfarin more safely and effectively. In support of this, an FDA clinical pharmacology advisory committee concluded in November 2005 that “sufficient mechanistic and clinical evidence exists to support the recommendation to use lower doses of warfarin for patients with genetic variations in *CYP2C9* and *VKORC1* that lead to reduced activities” (<http://www.fda.gov/ohrms/dockets/ac/05/transcripts/2005-4194T1.pdf>), and has since included a table of genotype associated maintenance dose estimations. What now remains is the quantitative assessment of how precisely genotyping can predict both an individual’s, loading or transitions dosages, maintenance dose, and the timing of INR measurements for optimal outcomes.

91.6 Summary

The authors believe there are several key factors that will be essential for the integration of PGx information into warfarin management strategies as a standard of care. The first is FDA recognition of the improvements in dose stratification based on PGx information. As mentioned above, an FDA clinical pharmacology advisory committee recently concluded that the warfarin monograph should be updated to include *CYP2C9* and *VKORC1* genomic and test information, and a potential recommendation to use lower doses of warfarin for patients with genetic variations in *CYP2C9* and/or *VKORC1*. It is unclear when the label update will occur. In more general terms, the rapid strides that not only PGx but also proteomics as disciplines are making in laboratory medicine are evident in the recent interest the FDA has expressed in regulating the use of patterns of analytes as well as use of computational algorithms for interpretation of combined data. In addition to the concern expressed by the FDA, the suggestion of FDA oversight of molecular diagnostic testing has also recently surfaced. It is too early to know how these ideas will turn out; however, they all point to a rapid expansion in the application of novel technologies

that are quickly changing the face of laboratory medicine and its role in healthcare. "Prediction, prediction, prediction" is the new dogma, and the application of PGx to warfarin therapy is but one of the available new approaches for achieving that end.

The second key factor for integration is test availability and standardization. The application of PGx testing to direct medical practice will require building consensus by several groups of healthcare practitioners. These groups span the collective of physicians, clinical laboratorians, IVD manufacturers, third-party payers, as well as government regulatory agencies. Building initial practice guidelines is currently the focus of new Laboratory Medicine Practice Guidelines being developed by the National Academy of Clinical Biochemistry (NACB, www.nacb.org). Other organizations, such as the American College of Molecular Genetics (ACMG), are putting forth efforts to provide similar guidelines. The key recognition by many is that the clinical laboratory plays a central role in catalyzing the transition of these novel test modalities into clinical practice. For this to be practical, a strong partnership is required between the immediate healthcare practitioner and the laboratory, and new guidelines in the area of PGx are setting the stage for establishing this partnership in the application of this new discipline.

The third important component necessary for integration of PGx information into warfarin management strategies is cost, from the perspectives of reimbursement and cost savings to the healthcare system. An important element in the practical equation of bringing PGx testing to patient care is defining who will bear the cost of testing and whether it will be deemed medically necessary, for reimbursement purposes. Several estimates indicate that the end result should be a considerable financial savings to the healthcare system, which may drive payers toward approving reimbursement. The recent AEI-Brookings Joint Center for Regulatory Studies publication titled "Health Care Savings from Personalized Medicine Using Genetic Testing: The Case of Warfarin" determined that formally integrating genetic testing into routine warfarin therapy could avoid 85,000 serious bleeding events and 17,000 strokes annually, and could save the healthcare system an average of \$1.1 billion (range of \$100 million to \$2 billion) annually [37]. Interestingly, the evaluation only included the impact of *CYP2C9* genetic variation; the addition of *VKORC1* polymorphisms in practice is likely to provide additional significant impact on the avoidable adverse events and overall cost savings.

The fourth crucial element is the use of evidence-based medicine to demonstrate efficacy and educate physicians. Central to the application of any new diagnostic test is educating the healthcare practitioner as to its utility. Medical and pharmacy schools are now beginning to introduce the topic of PGx as part of their courses in clinical pharmacology. However, the speed with which PGx is moving will also require more immediate education of practicing physicians. This shifts the burden of providing education and demonstration of utility to the profession of clinical PGx and to the design of rigorous, prospective, evidence-based clinical trials. The importance of this must be realized by organizations that are willing to share or shoulder the costs of making this possible through professional organizations, supported by regulatory agencies, pharmaceutical companies, IVD manufacturers, and even hospital and third-party payer groups, all of whom stand to benefit from the results.

We believe that prospective studies are required in this area, not as justification for the current applicability of the information, but rather, to better establish and refine quantifiable strategies for dosing and monitoring that best leverage this testing. For now, the anticipated effects of *CYP2C9* and *VKORC1* genetic variants on the pharmacokinetics and pharmacodynamics of warfarin can be applied to clinical decisions regarding selection and titration of dosage, and interpretation of INR response to dosage changes. How precisely this can be accomplished and the magnitude of the improvement in quality of care remains to be determined.

References

1. Higashi MK, Veenstra DL, Kondo LM, Wittkowsky AK, Srinouanprachanh SL, Farin FM et al.: Association between *CYP2C9* genetic variants and anticoagulation-related outcomes during warfarin therapy. *JAMA* 287(13), 1690–1698, 2002.

2. Linder MW, Looney S, Adams JE, 3rd, Johnson N, Antonino-Green D, Lacefield N et al.: Warfarin dose adjustments based on CYP2C9 genetic polymorphisms. *J Thromb Thrombolysis* 14(3), 227–232, 2002.
3. Bon Homme, M., Reynolds, K.K., Valdes, R. Jr., and Linder, M.W: Dynamic pharmacogenetic models in anticoagulation therapy. *Clin Lab Med* 28, 539–552, 2008.
4. Ingelman-Sundberg M: Pharmacogenetics of cytochrome P450 and its applications in drug therapy: The past, present and future. *Trends Pharmacol Sci* 25(4), 193–200, 2004.
5. Linder MW, Evans WE, and McLeod HL: Application of pharmacogenetic principles to clinical pharmacology. In: *Applied Pharmacokinetics & Pharmacodynamics: Principles of Therapeutic Drug Monitoring*. Burton M.E. et al. (Eds.). Lippincott Williams & Wilkins, Baltimore, MD, 165–185, 2005.
6. Takahashi H and Echizen H: Pharmacogenetics of warfarin elimination and its clinical implications. *Clin Pharmacokinet* 40(8), 587–603, 2001.
7. Kirchheiner J and Brockmoller J: Clinical consequences of cytochrome P450 2C9 polymorphisms. *Clin Pharmacol Ther* 77(1), 1–16, 2005.
8. Hillman MA, Wilke RA, Caldwell MD, Berg RL, Glurich I, and Burmester JK: Relative impact of covariates in prescribing warfarin according to CYP2C9 genotype. *Pharmacogenetics* 14(8), 539–547, 2004.
9. Sconce EA, Khan TI, Wynne HA, Avery P, Monkhouse L, King BP et al.: The impact of CYP2C9 and VKORC1 genetic polymorphism and patient characteristics upon warfarin dose requirements: Proposal for a new dosing regimen. *Blood* 106(7), 2329–2333, 2005.
10. Gage BF and Eby CS: Pharmacogenetics and anticoagulant therapy. *J Thromb Thrombolysis* 16(1–2), 73–78, 2003.
11. Imai J, Ieiri I, Mamiya K, Miyahara S, Furuumi H, Nanba E et al.: Polymorphism of the cytochrome P450 (CYP) 2C9 gene in Japanese epileptic patients: Genetic analysis of the CYP2C9 locus. *Pharmacogenetics* 10(1), 85–89, 2000.
12. Rettie AE, Wienkers LC, Gonzalez FJ, Trager WF, and Korzekwa KR: Impaired (S)-warfarin metabolism catalysed by the R144C allelic variant of CYP2C9. *Pharmacogenetics* 4(1), 39–42, 1994.
13. Scordo MG, Pengo V, Spina E, Dahl ML, Gusella M, and Padriani R: Influence of CYP2C9 and CYP2C19 genetic polymorphisms on warfarin maintenance dose and metabolic clearance. *Clin Pharmacol Ther* 72(6), 702–710, 2002.
14. Voora D, Eby C, Linder MW, Milligan PE, Bukaveckas BL, McLeod HL et al.: Prospective dosing of warfarin based on cytochrome P-450 2C9 genotype. *Thromb Haemost* 93(4), 700–705, 2005.
15. Aithal GP, Day CP, Kesteven PJ, and Daly AK: Association of polymorphisms in the cytochrome P450 CYP2C9 with warfarin dose requirement and risk of bleeding complications. *Lancet* 353(9154), 717–719, 1999.
16. Taube J, Halsall D, and Baglin T: Influence of cytochrome P-450 CYP2C9 polymorphisms on warfarin sensitivity and risk of over-anticoagulation in patients on long-term treatment. *Blood* 96(5), 1816–1819, 2000.
17. Margaglione M, Colaizzo D, D'Andrea G, Brancaccio V, Ciampa A, Grandone E et al.: Genetic modulation of oral anticoagulation with warfarin. *Thromb Haemost* 84(5), 775–778, 2000.
18. Voora D, McLeod HL, Eby C, and Gage BF: The pharmacogenetics of coumarin therapy. *Pharmacogenomics* 6(5), 503–513, 2005.
19. Peyvandi F, Spreafico M, Siboni SM, Moia M, and Mannucci PM: CYP2C9 genotypes and dose requirements during the induction phase of oral anticoagulant therapy. *Clin Pharmacol Ther* 75(3), 198–203, 2004.
20. Gage BF, Eby C, Milligan PE, Banet GA, Duncan JR, and McLeod HL: Use of pharmacogenetics and clinical factors to predict the maintenance dose of warfarin. *Thromb Haemost* 91(1), 87–94, 2004.
21. Tham LS, Goh BC, Nafziger A, Guo JY, Wang LZ, Soong R et al.: A warfarin-dosing model in Asians that uses single-nucleotide polymorphisms in vitamin K epoxide reductase complex and cytochrome P450 2C9. *Clin Pharmacol Ther* 80(4), 346–355, 2006.

22. Wadelius M, Chen LY, Downes K, Ghori J, Hunt S, Eriksson N et al.: Common VKORC1 and GGCX polymorphisms associated with warfarin dose. *Pharmacogenomics J* 5(4), 262–270, 2005.
23. Obayashi K, Nakamura K, Kawana J, Ogata H, Hanada K, Kurabayashi M et al.: VKORC1 gene variations are the major contributors of variation in warfarin dose in Japanese patients. *Clin Pharmacol Ther* 80(2), 169–178, 2006.
24. Veenstra DL, You JH, Rieder MJ, Farin FM, Wilkerson HW, Blough DK et al.: Association of Vitamin K epoxide reductase complex 1 (VKORC1) variants with warfarin dose in a Hong Kong Chinese patient population. *Pharmacogenet Genomics* 15(10), 687–691, 2005.
25. D'Andrea G, D'Ambrosio RL, Di Perna P, Chetta M, Santacroce R, Brancaccio V et al.: A polymorphism in the VKORC1 gene is associated with an interindividual variability in the dose-anticoagulant effect of warfarin. *Blood* 105(2), 645–649, 2005.
26. Yuan HY, Chen JJ, Lee MT, Wung JC, Chen YF, Charng MJ et al.: A novel functional VKORC1 promoter polymorphism is associated with inter-individual and inter-ethnic differences in warfarin sensitivity. *Hum Mol Genet* 14(13), 1745–1751, 2005.
27. Li T, Chang CY, Jin DY, Lin PJ, Khvorova A, and Stafford DW: Identification of the gene for vitamin K epoxide reductase. *Nature* 427(6974), 541–544, 2004.
28. Rost S, Fregin A, Ivaskovicus V, Conzelmann E, Hortnagel K, Pelz HJ et al.: Mutations in VKORC1 cause warfarin resistance and multiple coagulation factor deficiency type 2. *Nature* 427(6974), 537–541, 2004.
29. Rieder MJ, Reiner AP, Gage BF, Nickerson DA, Eby CS, McLeod HL et al.: Effect of VKORC1 haplotypes on transcriptional regulation and warfarin dose. *N Engl J Med* 352(22), 2285–2293, 2005.
30. Bodin L, Verstuyft C, Tregouet DA, Robert A, Dubert L, Funck-Brentano C et al.: Cytochrome P450 2C9 (CYP2C9) and vitamin K epoxide reductase (VKORC1) genotypes as determinants of acenocoumarol sensitivity. *Blood* 106(1), 135–140, 2005.
31. Reynolds, K.K., Valdes, R. Jr., Hartung, B., and Linder, M.W.: Individualizing Warfarin Therapy. *Personalized Medicine* 4(1):33–53, 2007.
32. Geisen C, Watzka M, Sittlinger K, Steffens M, Daugela L, Seifried E et al.: VKORC1 haplotypes and their impact on the inter-individual and inter-ethnic variability of oral anticoagulation. *Thromb Haemost* 94(4), 773–779, 2005.
33. Zhu, Y., Reynolds, K.K., Johnson, N., Herrnberger, M., Valdes, R. Jr., and Linder, M.W.: Estimation of warfarin maintenance dose requirements based on VKORC1 and CYP 2C9 gene polymorphisms and rationale for application in clinical practice. *Clin Chem* 53, 1199–1205, 2007.
34. Kimura R, Miyashita K, Kokubo Y, Akaiwa Y, Otsubo R, Nagatsuka K et al.: Genotypes of vitamin K epoxide reductase, gamma-glutamyl carboxylase, and cytochrome P450 2C9 as determinants of daily warfarin dose in Japanese patients. *Thromb Res* 120(2), 181–186, 2007.
35. Vecsler M, Loebstein R, Almog S, Kurnik D, Goldman B, Halkin H et al.: Combined genetic profiles of components and regulators of the vitamin K-dependent gamma-carboxylation system affect individual sensitivity to warfarin. *Thromb Haemost* 95(2), 205–211, 2006.
36. Schelleman H, Chen J, Chen Z, Christie J, Newcomb CW, Bresinger CM, Price M, Whitehead AS, Kealy CF, Thorn CF, Samaha FF, and Kemmel SE. Dosing algorithms to predict warfarin maintenance dose in Caucasians and African Americans. *Clin Pharm Ther* 84(3), 332–339, 2008.
37. McWilliam A, Lutter R, and Nardinelli C, *Health Care Savings from Personalizing Medicine using Genetic Testing: The Case of Warfarin*. AEI-Brooking Joint Center for Regulatory Studies Working Paper 06-23, November 2006.

Need for Point-of-Care Testing Devices for Cardiac Troponin in Patients with Acute Coronary Syndromes

92.1	Role of Troponin in Cardiovascular Diseases.....	92-1
	From Atherosclerosis to Acute Coronary Syndromes • Biochemical Changes Following ACS • Cardiac Troponin in ACS • Need for Rapid Reporting of Results for Cardiac Troponin	
92.2	Current Cardiac Troponin Assays.....	92-4
	Central Laboratory-Based Troponin Assays • Point-of-Care Troponin Assays	
92.3	Novel Technologies for POCT for Cardiac Troponin.....	92-5
	Microfluidic Technologies for Next-Generation POCT • Microfluidic Integration of Multiple Functions in a Self-Contained POCT • Quantitative and Multianalyte Measurements in POCT • Signal Transduction in Microfluidic POCT • Emergency POCT Advances Dovetail with Global Health Diagnostic Innovations	
92.4	Summary.....	92-9
	References.....	92-9

Alan H.B. Wu
*University of California,
 San Francisco*

Amy E. Herr
*University of
 California, Berkeley*

92.1 Role of Troponin in Cardiovascular Diseases

92.1.1 From Atherosclerosis to Acute Coronary Syndromes

Cardiovascular disease begins with atherosclerosis, the gradual deposition of lipid-filled plaque within the coronary arteries that takes place over years and decades. During the initial years, most subjects are free from symptoms. Clinical laboratory tests such as total cholesterol, low-density lipoprotein cholesterol, high-sensitivity C-reactive protein, and others are used to assess the risks of atherosclerosis towards the development of acute coronary disease. Stable angina is defined as chest pain upon exercise, and is one of the first indicators of atherosclerosis disease progression, that is, the narrowing of the coronary arteries by plaque. The pain is caused when an increased demand for oxygenated blood exceeds the delivery in these subjects, and is a signal for the individual to reduce physical activity. Treatment with nitroglycerin and other vasodilators can increase blood flow to peripheral tissues. Stable angina can be diagnosed by stress testing. Subjects are instructed to exercise on a treadmill or are given pharmacologic

stress agents (e.g., dobutamine), and are monitored by changes in the electrocardiogram (ECG) and nuclear imaging modalities for the presence of ischemia. For patient safety, the test is terminated once ischemia is noted.

Acute coronary syndromes (ACS) are the culmination of long-standing atherosclerosis and stable angina. ACS is caused by the rupture of a coronary artery plaque. The exposure of the contents of plaque to circulating blood stimulates the aggregation of platelets and the formation of a blood clot, part of the natural repair process to damaged blood vessels. Thrombus formation causes a reduction of blood flow to the coronary artery that was already narrowed by atherosclerosis. There are two degrees of severity associated with ACS. Patients with unstable angina have chest pain at rest due to plaque rupture and reduced blood flow. These patients have a partial block of their coronary artery and the amount of myocardial damage downstream to the point of occlusion is minimal. Multiple episodes of unstable angina can eventually lead to acute myocardial infarction (MI), characterized by a complete blockage of the coronary artery and extensive myocardial injury. The ECG is an important test for diagnosis and classification of ACS. In the context of chest pain, MI patients either have an ST elevation of the ST lead (STEMI) or show no elevation (NSTEMI). These designations have an impact on the severity of MI and the therapeutic approach taken to manage these patients.

92.1.2 Biochemical Changes Following ACS

The reduced or absent blood flow caused by a partial or total occlusion of the coronary artery, respectively, causes damage to myocardial cells that are distal to the point of occlusion. As needed for the efficient production of ATP, the lack of blood flow causes a deficit. Myocytes can initially survive for a few hours during reversible ischemia by transition to anaerobic metabolism and suspending the ATP-dependent sodium/potassium pump. If coronary artery blood flow is not restored to the affected vessel as seen in permanent occlusion, irreversible damage occurs. This is characterized by the release of macromolecules such as enzymes and proteins through damaged membranes. The time between reversible and irreversible injury provides a window for therapeutic intervention that can have a significant effect on the clinical outcome of patients with ACS. For example, patients treated with clot dissolving enzymes such as streptokinase and tissue plasminogen activator can reduce the extent of myocardial injury if given within the first few hours after the onset of ACS. Alternately, patients can be treated with balloon angioplasty via cardiac catheterization to reperfuse occluded coronary arteries and to restore blood flow.

92.1.3 Cardiac Troponin in ACS

Serum biomarkers of acute coronary syndrome play a critical role in the diagnosis and risk stratification of patients with ACS. Myocardial necrosis observed in patients with ACS releases a variety of proteins into blood that can be used as biomarkers. Antiquated markers include aspartate aminotransferase, lactate dehydrogenase (LD) and its isoenzyme (LD1), myoglobin, and creatine kinase (CK) and its isoenzyme (CK-MB). While some of these markers are still in routine use, there is consensus among experts in the field of cardiology, emergency medicine, and laboratory medicine that cardiac troponin is the gold standard marker for ACS.

Troponin is the regulatory complex of three proteins of the thin filament of myocytes. Troponin “T” binds to tropomyosin, troponin “I” is an inhibitory protein, and troponin “C” binds to calcium needed for muscle contraction. Following irreversible myocyte damage, unbound troponin subunits are initially released into blood from the cytosolic pools. This is followed by a sustained release of the tri-troponin complex due to the breakdown of the myocyte itself. Once in blood, the complex is further degraded into the binary troponin I–C complex, and frees troponin T. [Figure 92.1](#) shows the kinetics of troponin subunit release. Troponin is superior to the other biomarkers for cardiac injury for two

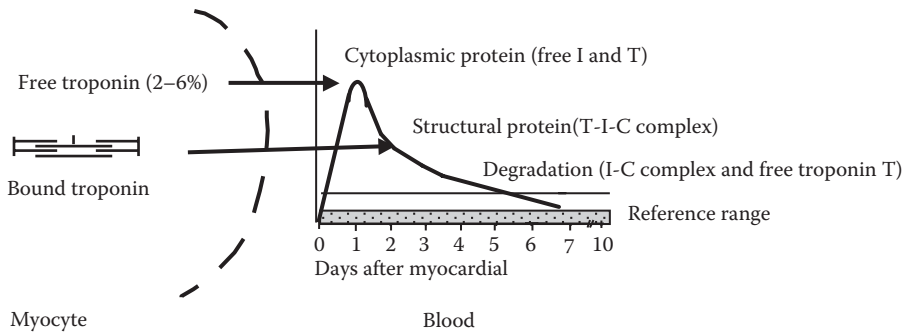


FIGURE 92.1 Release of cardiac troponin from damaged myocytes.

principal reasons: (1) the tissue content is higher than that for other proteins and enzymes, making the marker highly sensitive for myocardial injury, and (2) cardiac troponins T and I are structurally distinct from the corresponding skeletal muscle forms making this marker highly specific for myocardial injury. In 2000, and updated in 2007, a Joint Task Force of experts in cardiology and laboratory medicine redefined acute myocardial infarction (AMI) to be predicated on an increase in troponin with clinical and other laboratory evidence of myocardial ischemia (Antman et al., 2000; Thygesen et al., 2007). Therefore, by definition, the clinical sensitivity of troponin for the diagnosis of MI is now 100%. The cutoff concentration for detection of MI is designated at the 99th percentile of a healthy reference population. Troponin tests should have an intrassay imprecision of 10% or less at the cutoff concentration.

Results of cardiac troponin are also used to stratify risk for future short-term cardiovascular events for patients who have been ruled out for MI. It has been known for many decades that patients with large MIs have a high incidence of cardiac death and reinfarction. More recent studies have shown patients with minor myocardial injury have the same risk for adverse events. These clinical studies have stimulated the development of higher sensitivity troponin assays in order to stratify the risk of as many cases as possible. More aggressive clinical therapeutics and intervention are warranted for patients deemed to be at high risk.

92.1.4 Need for Rapid Reporting of Results for Cardiac Troponin

The closure of emergency departments (ED), especially in the United States but also elsewhere in the world, has forced ED physicians to be more efficient in the triaging of patients with chest pain. This pressure has led to the development of “chest pain centers,” where there is an accelerated protocol to rule out AMI for patients who present with suggestive symptoms. Given the importance of troponin in the diagnosis of AMI, a rapid turnaround time for test results is desirable. As such, the National Academy of Clinical Biochemistry (NACB), has recommended that test results be reported within 60 min, measured from the time of blood collection (Apple et al., 2007). This is a challenge for the central laboratory as there are many steps involved in reporting a result. These include specimen transport to the laboratory, labeling and accessioning, centrifuging to obtain serum or plasma, aliquoting (if necessary), loading onto an immunochemistry analyzer, actual testing itself (typically 20 min), and reporting to a hospital information system. Given these time constraints, many hospitals have adopted point-of-care testing (POCT) platforms for cardiac troponin. POCT can eliminate transport time, centrifugation (the whole is tested), and aliquoting. The analytical analysis time is also reduced in many cases. Several studies have shown that the use of POCT within an ED substantially reduces reporting turnaround times, and enables compliance with NACB guidelines. The worldwide POCT market was estimated, in 2008, at US\$490 million, growing at a rate of 12% per year (Labmedica, 2008).

92.2 Current Cardiac Troponin Assays

92.2.1 Central Laboratory-Based Troponin Assays

All cardiac troponin assays are based on immunoassays using two or more antibodies specific to the target analyte. At least one is used as the capture antibody and is bound to an inert surface, usually a paramagnetic particle. The other is the signal antibody that is labeled with a reporter molecule such as a fluorescent or chemiluminescent tag (Figure 92.2). The selection of antibodies and their epitope recognitions are important elements for cardiac troponin T (cTnT) and I (cTnI) assays. Antibodies directed towards the N- or C-terminus of troponin are degraded in blood and these amino acid sequences are rapidly removed from the circulation. Clinical laboratory guidelines have suggested that antibodies directed toward the central part of the molecule should be used (Panteghini et al., 2001).

A central laboratory-based cTnT assay is commercially available through a manufacturer (Roche Diagnostics) due to patent rights. There are no patent restrictions to the development and commercialization of cTnI assays and thus there are many automated commercial assays available. The current generation troponin T and I assays have a limit of detection (LOD) of about 10 pg/mL, diagnostic MI cutoff (99th percentile) of 40 pg/mL, and a total assay imprecision of 10% at this cutoff (Wu, 2008). At this level of analytic sensitivity, these assays can reliably detect troponin in blood of only a fraction of healthy subjects. Prototype research troponin assays have been developed with an LOD under 1 pg/mL and the 99th percentile cutoff of 10 pg/mL. Using these assays, troponin is detectable in all or most subjects in a reference population. As such, further improvements in assay sensitivity will be unnecessary.

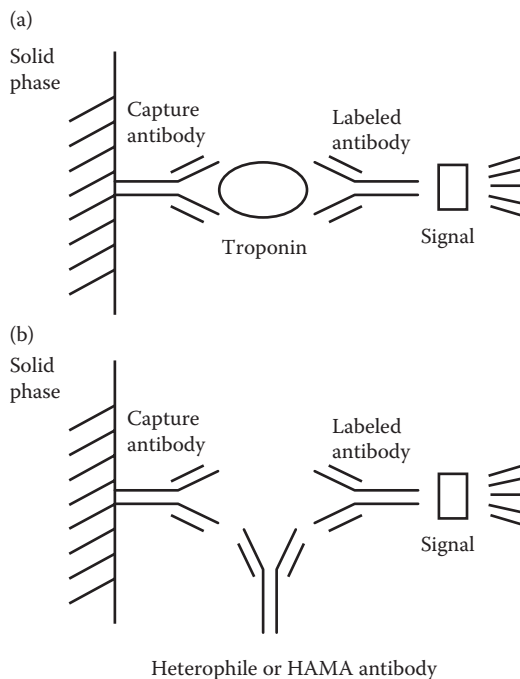


FIGURE 92.2 Schematic diagram of a sandwich immunoassay for cardiac troponin. (a) True positive result in the presence of the antigen. (b) False-positive result in the presence of an interfering antibody. HAMA = human antimouse antibody.

92.2.2 Point-of-Care Troponin Assays

Qualitative and quantitative POCT assays are commercially available for troponin T and I. These assays are relatively easy to perform, require minimal equipment, and are designed for testing at the bedside or ED by nonlaboratory personnel, that is, caregivers. Most of these assays are based on lateral flow technology and visual or fluorescence detection. Point-of-care troponin assays have not sufficiently improved, widening the analytical and clinical performance gap between them and the central laboratory-based assays. Currently, the analytical sensitivity of these assays is approximately 10-fold lower than the current central laboratory assays, and 100-fold lower than the research prototype assays.

There have been several clinical studies demonstrating POCT assays to be lower in performance. Singh et al. (2009) showed that the point-of-care device failed to identify 13% of 206 samples that were positive on a high-sensitivity central laboratory troponin platform. In many of these patients, there was clinical evidence of myocardial necrosis that was missed by POCT. James et al. (2004) compared a central laboratory cTnT assay against a POCT cTnI assay for their ability to risk stratify cardiac patients. The rapid assay detected fewer cases of patients who went on to suffer death or MI. These observations prompt the need for higher precision for sampling low volumes and high-sensitivity detection schemes, while maintaining a rapid assay turnaround time, whole blood usage, and simplicity for technical operation.

92.3 Novel Technologies for POCT for Cardiac Troponin

In essence, next-generation diagnostic technology aims to “decentralize” the diagnostic test—moving the measurement away from the laboratory and to the patient. Christensen et al. (2009) stated: “technologically advanced solutions go to where the problems are.” Decentralized diagnostic solutions are especially relevant to AMI diagnosis and assessment. Assuming that rapid turnaround for troponin test reporting will impact patient outcomes, next-generation approaches to diagnosis of AMI in near-patient environments are needed and are under active development.

One POCT approach does not satisfy all user or clinical needs. Before inventing or adopting diagnostic solutions to address clinical challenges, assay and technology developers first start by identifying the end user(s) and application space. For early diagnosis of AMI, several near-patient environments stand out as likely candidates including the ED (including “chest pain centers”), ambulance or emergency transport, work place, clinics, and offsite locations (e.g., a cruise ship). Consideration of the use environment and POCT user inform the design of, most importantly, the user interface: *How is the diagnostic fluid sample collected and introduced to the POCT diagnostic? Should the troponin report be qualitative or quantitative?*

While application space considerations are critically important and must be addressed with a singular focus during all stages of POCT design and development, some POCT specifications do not vary significantly regardless of usage space. In light of these crucial commonalities among near-patient diagnostics, we focus here on troponin diagnostics for use in EDs. It is worthwhile to emphasize that the assay principles of both point-of-care instruments and laboratory medicine instruments are the same. Warsinke (2009) provided an overview of the current and future directions in protein-based POCT. The target end user and application space of the POCT are, however, different from that of laboratory instruments. Consequently, POCT instruments are designed and engineered to be compact, easy to use and interpret, and to complete measurements quickly. Much innovation has focused on meeting these critical near-patient operating specifications.

92.3.1 Microfluidic Technologies for Next-Generation POCT

To supplant current laboratory assays, troponin POCT technology must have analytical sensitivity and specificity parameters that are equal to or better than those currently obtained in clinical labs.

Consequently, there has been significant effort in rigorous technology validation (against gold standard laboratory results). Attaining the required POCT performance requires well-controlled handling and preparation of the diagnostic sample, assays for multiple markers of AMI, and robust quantitation, even at low protein levels. A rapid troponin result drives development of POCT for AMI—performance that is not possible with current centralized laboratory testing approaches. To meet these rigorous performance demands new diagnostic technologies are being invented, explored, and developed. Among the most promising new diagnostic paradigms is microfluidic technology; which is uniquely suited to address rapid next-generation troponin POCT challenges.

92.3.2 Microfluidic Integration of Multiple Functions in a Self-Contained POCT

Troponin measurement at the patient bedside is a systems integration design goal that is commonly known as a “bleed-to-read” paradigm. Maturing microfluidic technology has shown promise in underpinning the streamlined integration of sophisticated sample handling and measurement modalities needed for clinical assays. Evolving from design and fabrication approaches common in the semiconductor and microelectromechanical systems (MEMS) fields, microfluidic devices can be relatively small (credit card size or smaller), inexpensive, and disposable. Currently, the technology is in a nascent form as regards both clinical and point-of-care diagnostics. An important hallmark of microfluidic technology is integration of multiple functions, including sample preparation and high-performance protein measurements (Figure 92.3).

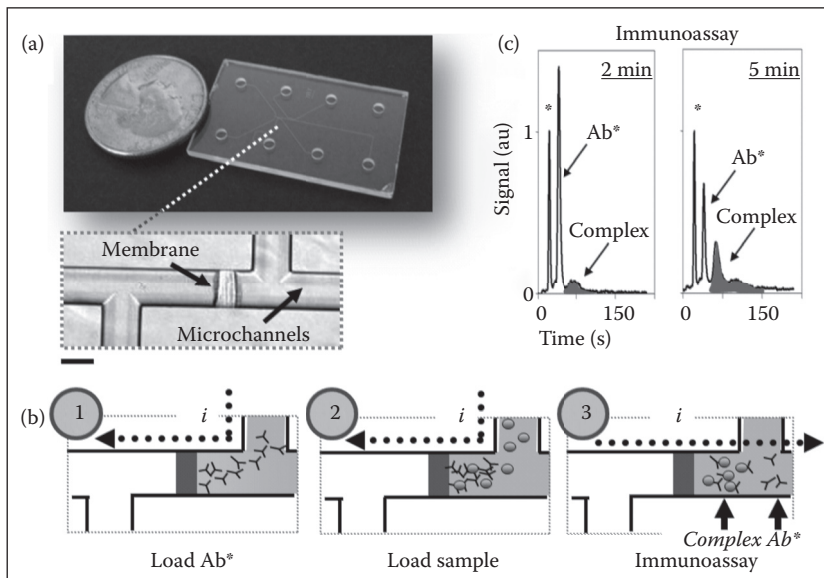


FIGURE 92.3 Microfluidic technology allows streamlined integration of preparatory and analytical functions, here protein enrichment and homogeneous electrophoretic immunoassays. (a) Image of representative glass microfluidic device with US quarter. (inset) Bright-field image of microchannels housing photopatterned polyacrylamide gel (molecular weight cutoff filter). Scale bar is 100 microns. (b) Integrated enrichment of sample and fluorescently labeled antibody probe (1), diffusive mixing in confined geometry (2), and contiguous homogeneous electrophoretic immunoassay which resolve Ab* from immunocomplex (3). Electrophoresis driven by an applied current (i) is used to meter and mix samples. (c) Duration of enrichment dictates assay sensitivity with the immunocomplex detection enhanced here by extending the enrichment step duration (2 vs. 5 min of enrichment). “*” is an internal standard, Ab* is the fluorescently labeled antibody probe.

Seamless integration of complementary serial processes and/or parallel assay stages is especially desirable for high fidelity diagnostics in an ED. The ability to assess troponin in a whole blood sample, perhaps from a finger prick, would expedite the sample collection and analysis workflow. Nevertheless, a major limitation of common POCT technologies is the precision by which samples are delivered to the test areas. Lateral flow technology depends on capillary action for the movement of samples to the region where the heterogeneous immunoassay takes place (test zones). The rate of material and fluid transfer is variable and dependent on environmental conditions (temperature, humidity, etc.), sample viscosity, specimen type (serum, urine, plasma, etc.), preservatives used (EDTA, heparin, citrate), and other factors. The variability in transfer can affect the precision of the assay. If the reading occurs too soon, or if samples are slow to react in the reaction zones, falsely low results may be produced. If there is a delay in reading results, there may be an overestimate of the true analyte concentrations. These factors can have a major impact on the precision of the assay and limit the clinical utility of the marker. Further, lateral flow assays are rarely quantitative or multiplexed (Weigl et al., 2008).

Metered sample handling and integrated sample preparation have been demonstrated in clinically relevant studies using microfluidic technology (Herr et al., 2007). Repeatable, controlled handling of diminishingly small sample volumes (<1 μL) is common with these formats. Preparatory stages include, but are not limited to, removal of high abundance potentially confounding matrix constituents, enrichment of target analytes, buffer exchange, dilution, and on-chip mixing. A clinically relevant example of streamlined protein assays from minimally pretreated biological fluids is the integration of sample enrichment with protein measurement for matrix metalloproteinase (MMP) concentrations for use in MMP inhibitor therapy monitoring (Herr et al., 2007). Integrated sample preparation must address minimization of interference from endogenous components found in the sample matrix.

92.3.3 Quantitative and Multianalyte Measurements in POCT

Measurement of multiple troponin forms in a single diagnostic workflow would aid rapid diagnosis of AMI, potentially yielding the stringent clinical specificity and sensitivity required of a screening diagnostic. Microfluidic technology, utilizing either homogeneous or heterogeneous immunoassays, is particularly well suited to multiplexed measurement with numerous examples reported for each format (Hou and Herr, 2008). Analysis of multiple analytes informs diagnosis, but it can also expedite assay readout when the measurements are made from a single sample at the bedside. While not in a POC device, Phillips and Wellner (2006) demonstrated multiplexed analysis of inflammatory markers as a means to assess the severity of skin lesions. Solubilized dissected human tissue biopsies were analyzed. The microfluidic system integrated micellar electrokinetic electrophoresis measurement with automated on-chip immunoaffinity extraction and fluorescence labeling as sample preparation. Building on this technology, the same group measured inflammatory neuro-peptides and postinflammatory cytokines in interstitial tissue fluids to assess severity of muscle pain and effectiveness of anti-inflammatory treatment (Phillips and Wellner, 2007).

While microfluidic solutions are promising, it is worthwhile to note that assay concerns are common with conventional measurement technology and also of concern with microfluidic technology, namely analytical specificity (and cross reactivity), analytical sensitivity, and dynamic detection range (Dupuy et al., 2005). Common POCT analytical capabilities include agglutination, immunofiltration, and lateral flow assays, with growing introduction of homogeneous immunoassays (no washing steps needed), and both direct and indirect biosensors (Warsinke, 2009).

Current immunoassays make use of polyclonal or monoclonal antibodies to capture test analytes from serum or plasma samples. A limitation for all sandwich-type immunoassays occurs when the patient sample contains heterophile or human anti-animal antibodies. These antibodies occur in patients with autoimmune diseases and exposure to animal antigens, respectively. When present, these antibodies bind to both the capture and signal antitroponin antibodies, thereby producing a falsely positive signal in the absence of the analyte (Figure 92.2b). Commercial assays for cardiac troponin are not immune

to these effects. In order to avoid these interferences, a novel approach would be the use of aptamers in lieu of antibodies. Aptamers are oligonucleic or peptide molecules that can be targeted towards specific target molecules. Large-scale screening procedures are commercially available for aptamer production. Next-generation troponin assays using aptamers for the capture, detection, or both, may be free from these interferences.

Further, quantitation (not simply binary outputs) is a desired but challenging goal. Quantitative assays are needed to monitor the rise and fall of cardiac markers and to enable risk stratification. Quantitation of multiple analytes in a single assay sometimes requires a wide dynamic range for each target to be optimized. In the microfluidic example given previously, online enrichment of sample analytes at a tiny molecular weight cutoff filter embedded in the device allows dynamic tuning of the dynamic detection range. Extended enrichment periods allow measurement of low-concentration species, while short enrichment periods allow detection of high abundance species. Further, quantitation requires inclusion of appropriate controls and calibration standards, as well as a data processing infrastructure that can provide the user with either a concentration or qualitative assessment based on threshold comparisons. Inclusion of the said controls can build off of approaches used for multiplexed analysis of protein targets and conventional multianalyte assays.

92.3.4 Signal Transduction in Microfluidic POCT

Detection limits or analytical sensitivity of the troponin assay will ultimately need to match or exceed that of laboratory medicine instrumentation. Promising advances are being made for gaining high-sensitivity detection benefits, from technology spanning high-performance instrumentation to ultra-efficient molecular probes. Nonoptical detection schemes, such as electrochemical, are under development and in use for POCT (Warsinke, 2008). Myers and Lee (2008) prepared a comprehensive review of microfluidic systems that rely on low-cost integration and quantitative results from optical sensor approaches. Several common optical readout modes have been integrated with microfluidic systems (absorbance, fluorescence, chemiluminescence, interferometry, and surface plasmon resonance), yet often the methods suffer in performance in microscale devices or require costly or large “reader” instrumentation. While powerful, researchers are actively inventing and adopting new detection approaches using nanoparticles and nanoengineered materials. Nanoparticle-based signal generation approaches include quantum dots and up-converting phosphors. These promising probes are tunable and yield an intensity and longevity that is sometimes even better than commonly employed organic dyes. New nanomaterial-based detection approaches rely on localized surface plasmon resonance and detection modalities that do not depend on sample volume (which is diminished in microfluidic technologies, as compared to some conventional approaches) but instead depend on near-field surface interactions. While these new technologies will surely open new avenues for sensing and measurement, it is worthwhile to note that commonly available sensing technologies, such as diode lasers and charge coupled device (CCD) sensors are dramatically decreasing in cost and will continue to play a role in portable sensing including POCT.

92.3.5 Emergency POCT Advances Dovetail with Global Health Diagnostic Innovations

Substantial recent focus has centered on use of microfluidic design approaches for development of instrumented and noninstrumented diagnostic technologies for global health (Weigl et al., 2008). In fact, recent advances in global health diagnostics are leading approaches to design facile, high-performance near-patient measurements (Yager et al., 2008). Viable microfluidic, or any POCT technologies, must have fixed and operational costs that are either competitive on the open market or suitable for health insurance reimbursement and approval (Soper et al., 2006). If large numbers of patients will be screened, the reagent and other consumable costs must be included in the financial considerations.

Utilization of plastics as a basis for forming the disposable, small microfluidic POCT technologies has been demonstrated and is under active development (Yager et al., 2006). Exciting possibilities for rapid sharing of data and improved organization if comprehensive patient test results arise with the advent of decentralized POCT technologies with the capabilities of wireless, digital communication, and recording of results. Realization of a “bleed-to-read” level of integration could ultimately translate into a diagnostic that is easy to use, fast, and quantitative for early AMI diagnoses.

92.4 Summary

Troponin has emerged as the biomarker of choice for diagnosis and risk stratification of patients with ACS. Optimum use of this biomarker requires improvements in the performance of analytical measurements made from the central laboratory, especially from POCT platforms. To meet the current and future clinical needs, troponin assays must be faster, more analytically sensitive, and more convenient from a standpoint of information transfer. This requires development of novel delivery and detection schemes, and approaches towards data connectivity. This “real-world” problem illustrates the need for cooperation between clinical laboratory science, biomedical engineering, and informational science.

References

- Antman, E., Bassand, J.P., Klein, W., Ohman, M., Lopez Sendon, J.L., Rydén, L., Simoons, M., Tendera, M. Myocardial infarction redefined—a consensus document of the Joint European Society of Cardiology/American College of Cardiology committee for the redefinition of myocardial infarction. *J. Am. Coll. Cardiol.* 2000;313:959–969.
- Apple, F.S., Jesse, R.L., Newby, L.K., Wu, A.H.B., Christenson RH. National Academy of Clinical Biochemistry and IFCC Committee for Standardization of Markers of Cardiac Damage Laboratory Medicine Practice Guidelines: Analytical issues for biomarkers of acute coronary syndromes. *Clin. Chem.* 2007;53:547–551.
- Christensen, C.M., Grossman, J.H., Hwang, J. *The Innovator's Prescription: A Disruptive Solution for Health Care*. New York: McGraw-Hill, 2009.
- Dupuy, A., Lehmann, S., Cristol, J. Protein biochip systems for the clinical laboratory. *Clin. Chem. Lab. Med.* 2005;43:1291–1302.
- Herr, A.E., Hatch, A.V., Throckmorton, D.J., Tran, H.M., Brennan, J.S., Giannobile, W.V., Singh, A.K. Microfluidic immunoassays as rapid saliva-based clinical diagnostics. *Proc. Natl. Acad. Sci. USA* 2007;104:5268–5273.
- Hou, C., Herr, A.E. Clinically relevant advances in on-chip affinity-based electrophoresis and electrochromatography. *Electrophoresis* 2008;29:3306–3319.
- James, S.K., Lindahl, B., Armstrong, P., Califf, R., Simoons, M.L., Venge, P., Wallentin, L. The GUSTO-IV ACS Investigators. A rapid troponin I assay is not optimal for determination of troponin status and prediction of subsequent cardiac events at suspicion of unstable coronary syndromes. *Int. J. Cardiol.* 2004;93:113–120.
- Labmedica. Cardiac marker POC tests now widely used in hospitals 2008. http://labmedica.com/?option=com_article&Itemid=294727244.
- Myers, F.B., Lee, L.P. Innovations in optical microfluidic technologies for point-of-care diagnostics. *Lab. Chip.* 2008;8:2015–2031.
- Panteghini, M., Gerhardt, W., Apple, F.S., Dati, F., Ravkilde, J., Wu, A.H. Quality specifications for cardiac troponin assays. *Clin. Chem. Lab. Med.* 2001;38:175–179.
- Phillips, T.M., Wellner, E.F. Analysis of inflammatory biomarkers from tissue biopsies by chip-based immunoaffinity CE. *Electrophoresis* 2007;28:3041–3048.
- Phillips, T.M., Wellner, E.F. Measurement of naproxen in human plasma by chip-based immunoaffinity capillary electrophoresis. *Biomed. Chromatogr.* 2006;20:662–667.

- Singh, J., Akbar, M.S., Adabag, S. Discordance of cardiac troponin I assays on the point-of-care i-STAT and architect assays from Abbott Diagnostics. *Clin. Chim. Acta* 2009;403:259–260.
- Soper, S.A., Brown, K., Ellington, A., Frazier, B., Garcia-Manero, G., Gau, V., Gutman, S.I. et al. Point-of-care biosensor systems for cancer diagnostics/prognostics. *Biosens. Bioelectron.* 2006;21:1932–1942.
- Thygesen, K., Alpert, J.S., White, D., on behalf of the Joint ESC/ACCF/AHA/WHF Task Force for the Redefinition of Myocardial Infarction. Universal definition of myocardial infarction. *J. Am. Coll. Cardiol.* 2007;350:2173–2195.
- Warsinke, A. Electrochemical biochips for protein analysis. *Adv. Biochem. Eng. Biotechnol.* 2008;109:155–193.
- Warsinke, A. Point-of-care testing of proteins. *Anal. Bioanal. Chem.* 2009;393:1393–1405.
- Weigl, B., Domingo, G., Labarre, P., Gerlach, J. Towards non- and minimally instrumented, microfluidics-based diagnostic devices. *Lab. Chip.* 2008;8:1999–2014.
- Wu, A.H.B., Fukushima, F., Puskas, R., Todd, J., Goix, P. Development and preliminary clinical validation of a high sensitivity assay for cardiac troponin using a capillary flow (single molecule) fluorescence detector. *Clin. Chem.* 2006;52:2157–2159.
- Yager P, Domingo GJ, Gerdes J. Point-of-care diagnostics for global health. *Ann. Rev. Biomed. Eng.* 2008;10:107–144.
- Yager P, Edwards T, Fu E, Helton K, Nelson K, Tam MR, Weigl BH. Microfluidic diagnostic technologies for global public health. *Nature* 2006;442:412–418.

An Introduction to Bioethics and Ethical Theory for Biomedical Engineers*

93.1	Introduction	93-1
93.2	Hippocratic Origins	93-2
93.3	Nazi Germany and the Origins of Formal Bioethics	93-3
93.4	Philosophical Foundations.....	93-5
93.5	Ethical Theory.....	93-5
93.6	Principlism.....	93-5
93.7	Consequentialism	93-6
93.8	Utilitarianism.....	93-6
93.9	Virtue Ethics.....	93-7
93.10	Consent.....	93-7
93.11	Doctrine of Double Effect.....	93-8
93.12	Resolving Ethical Conflicts.....	93-8
93.13	Ethical Issues Specific to Biomedical Engineering.....	93-9
93.14	Example 1: The Therac-25 Cancer Treatment System.....	93-9
93.15	Example 2: The Case of the Abbott Pain Control Machine.....	93-9
93.16	Example 3: The Case of the Bjork–Shiley Heart Valve.....	93-10
93.17	Discussion of Practical Ethical Issues	93-10
93.18	Summary and Conclusions	93-11
	References.....	93-11
	Further Reading.....	93-12

D. John Doyle
Cleveland Clinic
Case Western Reserve
University

93.1 Introduction

The last few decades have seen an enormous growth in ethical issues that have arisen in medicine in general and in biomedical engineering in particular. Many of these issues are a direct consequence of technological innovations in which biomedical engineers have played a key role (Saha and Saha, 1997). The purpose of this chapter is to present an overview of these issues.

* Sections of this chapter are based on the author's publications in the *Journal of Long Term Effects of Medical Implants* and in *Ethics in Biology Engineering and Medicine: An International Journal*. In addition, aspects were previously presented at *The Third International Conference on Ethical Issues in Biomedical Engineering*, Rochester, New York, June 5, 2005.

Ethics is that branch of philosophy which seeks to address questions about proper conduct, rightness and wrongness, goodness and evil, virtue, honor, integrity, justice, and related notions. It is often divided into a number of overlapping branches. *Applied ethics* is concerned with the problem of how ethical outcomes might be achieved in real-world situations. This field includes subfields such as business ethics, military ethics, and bioethics. *Descriptive ethics* is concerned with documenting and interpreting what moral principles people actually abide by. Descriptive ethics stands in contrast with *normative ethics*, which is concerned with ethical theories that *prescribe* how people *ought* to act (as opposed to merely describing how people actually act.) Normative ethical theories include deontological (duty-based) approaches (e.g., Kant's Categorical Imperative), consequentialist approaches, (e.g., utilitarian ethics), virtue ethics, and other theories.

A number of overlapping subdivisions of bioethics can be envisioned. *Clinical bioethics* is concerned with the day-to-day ethical decisions clinicians encounter in caring for patients. Clinical bioethics may be subdivided into a number of subfields, such as pain management bioethics, anesthesiology bioethics, biomedical engineering ethics, and so on. Some examples may be helpful here.

An example of a pain management bioethical issue concerns the appropriateness of being "generous" in the administration of potentially addictive opiates such as morphine in patients with severe nonmalignant pain syndromes. An example of an anesthesiology bioethical issue concerns the appropriateness of aggressively resuscitating terminally ill "Do Not Resuscitate" (DNR) patients who are doing poorly while undergoing palliative care surgery. An example of a biomedical engineering ethical issue concerns the safety testing requirements for a new medical product awaiting clinical deployment; for example, a new drug infusion pump.

A second major division of bioethics, *theoretical bioethics*, is concerned with the philosophical foundations of bioethics. This field is concerned with issues such as the merits of the deontological approach versus the utilitarian approach versus other approaches in handling ethical issues, or the problem of handling an ethical issue when a conflict in principles arises.

A third division of bioethics, *cultural bioethics*, is concerned with ethical questions in relation to cultural and social settings. Ideological, religious, and historical dimensions often influence the discourse here. For instance, some feminists advocate an approach to bioethics emphasizing an ethic of caring where human relationships, feelings, and emotions are more pertinent to making ethical decisions than traditional rationalistic approaches based on abstract philosophical principles (most of which have been developed by male philosophers).

Finally, *regulatory and policy bioethics* is concerned with ethical issues such as clinical trial design, drug approval ethics, use of embryonic tissue in research and clinical treatment, human cloning, organ procurement for transplantation, xenotransplantation, assisted suicide, euthanasia, formulation of brain death policy, allocation of scarce healthcare resources, and so on.

93.2 Hippocratic Origins

In antiquity, Hippocrates, a profoundly influential Greek physician, developed a professional oath for his students. The original Hippocratic Oath forbids a number of activities, such as abortions, bladder stone surgery, euthanasia, disclosure of confidential information without permission, and sex with patients. Some of these rules have changed over time and are no longer appropriate to contemporary medical practice (e.g., the rule against bladder stone surgery would upset many urologists), which explains why medical students today usually take a modified Hippocratic Oath (or an entirely different oath) rather than the original one.

The World Medical Association has published their version of the Hippocratic Oath in October 1949. Known variously as the *Declaration of Geneva* or the *WMA International Code of Medical Ethics*, the most recent revision, published in 2006, can be viewed online at <http://www.wma.net/en/30publications/10policies/c8/index.html>. It is notably different from the original Hippocratic Oath in that no mention is made of prohibitions to conducting abortions, bladder stone surgery, or (surprisingly) euthanasia. The World Medical Association has also issued a companion policy document widely known as the

Declaration of Helsinki. It is a set of ethical principles regarding human experimentation, and is widely regarded as the ethical foundation for human research. The most recent revision, issued in 2008, may be viewed online at <http://www.wma.net/en/30publications/10policies/b3/index.html>.

As a consequence of these and other developments, in 1979 the USA issued its own policy document on the ethical conduct of research involving human subjects. Known as the Belmont Report, it is the basis for the complex regulatory framework that governs human subject research in the United States. The report may be viewed online at <http://ohsr.od.nih.gov/guidelines/belmont.html>.

93.3 Nazi Germany and the Origins of Formal Bioethics

During World War II, a sizable number of Nazi physician-scientists performed medical experiments using concentration camp prisoners (Barondess, 1996). While many of these experiments were of no value, reflecting a lack of planning and discipline, some of the experiments were comparatively well executed (from a strictly amoral perspective) and resulted in potentially useful scientific information. Regardless, all these experiments were highly unethical, because nearly all the experimental subjects endured tremendous unnecessary suffering and distress, because the experimental protocols were usually designed with a fatal outcome as the end point (to allow for postmortem examination), and since the participants were all enrolled against their will.

Following the war, 20 Nazi doctors were charged with War Crimes and Crimes Against Humanity before the International Military Tribunal at Nuremberg. At the tribunal one of the more pragmatic experimental programs reviewed concerned developing various means to mitigate the clinical response to hypothermia, an important issue for Luftwaffe pilots, who were known to occasionally crash into the cold North Sea. In response to this need, and with the explicit support of Reichsführer Heinrich Himmler, Dr. Sigmund Rascher, a physician as well as a Luftwaffe officer, initiated a research program at Dachau in which prisoners were immersed in ice water baths. While immersed, rectal temperature, heart rate, the level of consciousness, and the degree of shivering were meticulously recorded. In all, 300 individuals were sacrificed. Perhaps the most important thing learned was that victims of hypothermia will usually die (from ventricular fibrillation, it turns out) when the rectal temperature drops below 25°C (77°F) (Berger, 1990).

Not all the test subjects died, at least not immediately, since some of the rewarming methods studied were quite effective. While immersion in warm water proved to be one highly effective method (and remains in use to this day), the experimenters—allegedly at the suggestion of Himmler himself—even placed some male test subjects in a warm bed with a naked woman (also a camp prisoner), to explore the rewarming potential of sexual intercourse.

One ethical issue that arose decades later with the Nazi hypothermic data concerned the ethics of incorporating this information, previously unpublished, into a scientific review of the topic. This issue faced the editor of the *New England Journal of Medicine* in the late 1980s when the editor, at that time Arnold Relman, ultimately refused permission to publish parts of the Nazi hypothermia data as a component of a potentially life-saving research report from the Hypothermia Laboratory at the University of Minnesota (Angell, 1990). Naturally, such a position has the unfortunate consequence that potentially important information that may help patients may end up being denied to these individuals and, furthermore, the process of repeating the experiments so that they are in full compliance with regulations may expose new experimental subjects to new risks so as to obtain information that was already available. As a result, some ethicists favor a policy for such cases where the paper in question is accepted, but is published with an accompanying editorial in which the ethical aspects of the manuscript are critically discussed.

One very important consequence of the horrible Nazi medical experiments was the recognition that there existed a pressing need for a formal code of ethics to guide medical research involving human subjects. In fact, during the Nuremberg trials, some of the accused had argued that there was no law or code that differentiated between legal/ethical and illegal/unethical medical experiments. The result was the development of a 10 point policy statement that constituted the “Nuremberg code” (Figure 93.1).

1. The voluntary consent of the human subject is absolutely essential. This means that the person involved should have legal capacity to give consent; should be so situated as to be able to exercise free power of choice, without the intervention of any element of force, fraud, deceit, duress, overreaching, or other ulterior form of constraint or coercion; and should have sufficient knowledge and comprehension of the elements of the subject matter involved as to enable him to make an understanding and enlightened decision. This latter element requires that before the acceptance of an affirmative decision by the experimental subject there should be made known to him the nature, duration, and purpose of the experiment; the method and means by which it is to be conducted; all inconveniences and hazards reasonable to be expected; and the effects upon his health or person which may possibly come from his participation in the experiment.

The duty and responsibility for ascertaining the quality of the consent rests upon each individual who initiates, directs, or engages in the experiment. It is a personal duty and responsibility which may not be delegated to another with impunity.

2. The experiment should be such as to yield fruitful results for the good of society, unprocurable by other methods or means of study, and not random and unnecessary in nature.
3. The experiment should be so designed and based on the results of animal experimentation and knowledge of the natural history of the disease or other problem under study that the anticipated results will justify the performance of the experiment.
4. The experiment should be so conducted as to avoid all unnecessary physical and mental suffering and injury.
5. No experiment should be conducted where there is an a priori reason to believe that death or disabling injury will occur; except, perhaps, in those experiments where the experimental physicians also serve as subjects.
6. The degree of risk to be taken should never exceed that determined by the humanitarian importance of the problem to be solved by the experiment.
7. Proper preparations should be made and adequate facilities provided to protect the experimental subject against even remote possibilities of injury, disability, or death.
8. The experiment should be conducted only by scientifically qualified persons. The highest degree of skill and care should be required through all stages of the experiment of those who conduct or engage in the experiment.
9. During the course of the experiment the human subject should be at liberty to bring the experiment to an end if he has reached the physical or mental state where continuation of the experiment seems to him to be impossible.
10. During the course of the experiment the scientist in charge must be prepared to terminate the experiment at any stage, if he has probable cause to believe, in the exercise of the good faith, superior skill and careful judgment required of him that a continuation of the experiment is likely to result in injury, disability, or death to the experimental subject.

FIGURE 93.1 The Nuremberg code. (Reprinted from *Trials of War Criminals before the Nuremberg Military Tribunals under Control Council Law No. 10*, Vol. 2, pp. 181–182. Washington, DC: U.S. Government Printing Office, 1949. See also <http://ohsr.od.nih.gov/guidelines/nuremberg.html>.)

93.4 Philosophical Foundations

One of the first philosophers to systematically explore the philosophical foundations of ethics was Aristotle, famous for his *Nicomachean Ethics* and many other works. Other philosophers who have contributed greatly to the philosophical foundations of ethics include Thomas Aquinas, Immanuel Kant, Baruch Spinoza, Jeremy Bentham, John Stuart Mill, and countless more.

Immanuel Kant was a profoundly influential German philosopher of the Enlightenment. Kant said that we must treat people as ends in themselves, and never as a means to an end, by which he intended that we should always treat people with humanity and dignity, and never use individuals as “mere instruments” as a means to our own happiness (Beauchamp and Childress, 2001). Another way of expressing *Kant’s Categorical Imperative* is: “Always act in such a way that the maxim of your action can be willed as a universal law.” In other words, one should act only in such a way that one would want all men to act, and not treat individuals as mere “means to an end.” Kantian ethics are an example of a deontological approach to ethics (*vide infra*).

Utilitarianism is a school of moral philosophy frequently identified with the writings of Jeremy Bentham and John Stuart Mill. Classical Utilitarianism advocates the principle of providing “the greatest happiness to the greatest number” as the basis for assessing the morality of various actions (Gillon, 1985). Utilitarian ethics are an example of a consequentialist approach to ethics (*vide infra*).

93.5 Ethical Theory

The Kantian and utilitarian approaches to ethics just mentioned are two examples of ethical theories. Moral or ethical theory can be approached from a number of viewpoints. The *deontological approach* to morality (from the Greek word *deon*, or duty) is based on specific obligations or duties. These can be either positive (such as to care for our family) or negative (such as not to steal). This approach is also sometimes called *nonconsequentialist* since these principles are held to be obligatory regardless of any good or bad consequences of that might result. For example, it is wrong to kill even if it results in great overall benefit.

Other deontological approaches include “duty theory” popularized by David Ross and “rights theory” (concerned with rights that all people have, and which the rest of us must respect). Ross’s duty theory defines duties of beneficence, nonmaleficence, justice, self-improvement, reparation, gratitude, and promise keeping. He calls these *prima facie* duties. This approach was developed as an alternative to utilitarianism because of perceived failures of utilitarianism as a satisfactory moral theory.

Rights theory is concerned with rights that all humans have, and which other humans must respect. A right is a benefit (e.g., a liberty, a power, a prerogative, an immunity) that someone gains by virtue of his or her particular status as a citizen, a human being, a woman, a man, a child, a minority, a sentient animal, and so on. Rights can be positive, such as rights to food, clothing, and shelter, or negative, such as the right to be left alone. Rights theory thus offers an approach to moral action in that actions that violate the rights of others are said to be immoral.

93.6 Principlism

One commonly used approach to tackling bioethical problems is to invoke the guiding principles of the “Georgetown School” of bioethics, a profoundly influential philosophical school so named because of its origins in the University of Georgetown. The Georgetown School calls upon four ethical principles (Beauchamp and Childress, 2001). These are (1) *autonomy* (the right to actively participate in medical decisions concerning oneself without being dictated to or controlled by other parties); (2) *beneficence* (the requirement that caregivers, all else being equal, should do what they can to improve the patient’s situation); (3) *justice* (requiring the fair and impartial treatment of all persons, especially in the context of resource allocation); and (4) *nonmaleficence* (the requirement to avoid bringing harm to the patient).

These principles, as discussed in the Belmont Report, are also the foundation for U.S. federal regulations that govern clinical research.

Of these four bioethical principles, the principle of autonomy is one that is central to a good deal of contemporary bioethical discourse, and appears as an important issue in a number of present-day bioethical debates, such as medical research on human subjects, and the right of patients to refuse clinically necessary medical treatments.

93.7 Consequentialism

In contrast to the various deontological approaches to morality, the *consequentialist* approach determines moral responsibility by weighing the consequences of one's actions. According to the consequentialist view, correct moral actions are determined by a cost-benefit analysis concerning the consequences of an action. Several subtypes of consequentialism have been proposed: (1) the view that an action is morally correct if its consequences are more positive or favorable than negative to the person performing the action (*ethical egoism*); (2) the view that an action is morally correct if the consequences of that action are more positive than negative to everyone except the person doing the action (*ethical altruism*); and (3) the view that an action is morally correct if the action's consequences are more positive than negative to everyone (*utilitarianism*).

93.8 Utilitarianism

Classical utilitarianism advocates the principle of providing "the greatest happiness to the greatest number" as the basis for assessing the morality of various actions (Gillon, 1985). Over the years utilitarianism has undergone a number of refinements, such as "act utilitarianism," "rule utilitarianism," "negative utilitarianism," and "preference utilitarianism." *Act utilitarianism* takes the position that, when facing a moral choice, one must consider the expected consequences of various potential actions and, based on this analysis, choose to do what we believe will generate most happiness or pleasure for the most people. *Rule utilitarianism*, by contrast, analyses a moral dilemma by looking at potential rules of action that may be applicable, and adheres to the rule that would be expected to produce the most happiness or pleasure. *Negative utilitarianism* requires us to act so as to produce the least amount of evil or harm for the greatest number of people. *Preference utilitarianism*, advocated by controversial philosopher Peter Singer, seeks to meet the preferences of the greatest number of people.

It should be noted that utilitarianism sometimes falters badly when it is applied to questions of social or individual justice. Because classical utilitarianism seeks to maximize the total amount of a particular "utility" (like happiness or preferences) over an entire social group, it seeks whichever arrangement achieves maximum utility. But such an arrangement may end up distributing benefits and burdens in a way that violates common-sense notions of justice.

Perhaps the most quoted example of how classical utilitarianism sometimes violates common sense is the scenario where killing one innocent individual would save the lives of many; under the act utilitarian ethical model such action would be appropriate. Such a situation arose in the 1968 movie "The Magus," where the mayor of a small Greek village under WW II German occupation is ordered by the Nazi Commandant to personally kill three Greek freedom fighters responsible for the deaths of German soldiers. If the mayor refused, the Germans would kill the freedom fighters as well as all the villagers.

Another serious criticism of utilitarianism is that under the goal of maximizing happiness or some other utility, the wishes and desires of sadists and perverts are lumped in with the wishes and desires of everyone else when an overall determination of utility is made. By espousing a system in which the satisfaction of *all* desires is to be maximized, utilitarianism can end up violating our intuitive precepts of natural justice.

Such paradoxes led the philosopher John Rawls and others to take the position that we must reject most forms of utilitarianism and instead develop a genuine understanding of what is right and wrong

as a basis for making ethical decisions. What is needed, Rawls argues, is moral theory with justice at its core. Although a detailed explanation of Rawls's philosophy as set forth in his book, *A Theory of Justice*, is well beyond the scope of this chapter, in essence he argues that a fair and rational person operating behind a "veil of ignorance" would choose two general principles as the basis for social justice. The first principle would be the *Principle of Equal Liberty*, where each person in a society would have an equal right to the most extensive liberties compatible with similar liberties for all. The second principle, called the *Difference Principle*, would require that any social and economic inequalities in a society should be the result of an arrangement that provides the greatest benefit to the least advantaged persons, and is associated with positions or offices open to all.

93.9 Virtue Ethics

Virtue ethics is yet another approach to handling ethical issues. This approach focuses on the character of the person (moral agent) handling the moral issue, not on any specific ethical rules (as the deontological approach emphasizes) or on the consequences of any ethical decision (as the utilitarian approach requires). Consider the question as to whether it is ever moral for a physician to lie to a patient "for their own good." For instance, an anesthesiologist might be asked by a patient about to undergo emergency surgery whether the surgeon about to do the case is highly qualified. Suppose that, in fact, the anesthesiologist does not hold the surgeon in high regard, since he seems to lose far more blood than other surgeons. However, he is concerned that the patient might refuse to undergo clinically necessary surgery should his reply not be favorable. What, then, should his reply be?

In this situation a deontologist would be expected to argue that lying to a patient is always wrong, regardless of any future "good" that would be expected to result, that the rightness or wrongness stems from the character of the act itself rather than the outcome of the act. A consequentialist would argue, however, that the morality of the act would depend on the expected outcome, and that lying to a patient might be appropriate if the result is that the patient's life is saved. Finally, a virtue ethicist would focus on what a virtuous person would do in such a setting.

93.10 Consent

As noted earlier, the historical origins for the principle of autonomy stem in part from a need to develop a philosophical framework for ethically managing randomized controlled trials (where patients are administered one of a number of forms of medical treatment on the basis of chance alone), as well as a response to clear ethical abuses that have occurred in the past. In addition, a number of legal decisions have reinforced the notion of patient autonomy.

Informed consent arises in two principal contexts; clinical and experimental. In the clinical context, patients are provided with information pertaining to the risks, benefits, and the alternatives to proposed medical interventions such as surgical procedures. Usually, but not always, the process includes the use of a paper consent form that is signed, dated, and witnessed.

In the experimental context, research subjects (who in medical research studies are often also patients) agree to participate in an approved experimental protocol that may not have the benefit of the experimental subject as a primary or even as a likely outcome (e.g., testing the safety of a new drug on healthy human volunteers).

In either case, establishing informed consent from the individual is the central ethical concern, and both require that the individual is capable of understanding the issues involved and (in the case of research studies) additionally require that special safeguards be employed if the individual is a member of a "vulnerable" population, such as children, prison inmates, or pregnant women.

Consent can be implied or explicit, the latter involving a more or less formal process carried out verbally with or without explicit documentation in writing. Implied consent exists (for instance) when one

unhesitatingly rolls up one's shirt sleeve in preparation for a blood test or when an unconscious patient is taken to hospital for emergency treatment of life-threatening injuries.

Explicit consent is usually sought prior to clinical interventions that entail some risk of harm or have the potential to cause a substantial degree of pain or discomfort. Some institutions have a policy that a consent form must be signed by the patient prior to surgical procedures but may not have a similar requirement for other risky interventions such as blood transfusion, central line insertion, or lumbar puncture. If a signed and witnessed consent form is not required, and the intervention involves a non-trivial risk, clinicians are usually advised to write a detailed note in the patient's medical record to establish that the consent process has taken place, with specific mention of risks, benefits, and alternatives.

As emphasized earlier, central to informed consent is an explanation of the risks, benefits, and alternatives associated with any proposed clinical or experimental intervention. However, in some cases, such data may not be fully available, while, in some other cases, the amount of information available may be so large that it has the potential to overwhelm even well-informed and experienced patients. In addition, special problems may occur in providing risk information to patients. For instance, the only risk information available for an intervention may be that for the medical community at large and may not be specific to a particular institution or a particular clinician.

In some situations, such as complex cancer treatments, the issues involved may be so multifaceted that, at times, only highly trained individuals can fully understand them. This is particularly true in controversial areas of medicine where competing viewpoints may arise as a result of methodological and even cultural differences. As a result, providing full information may potentially require special methods of patient education or may be so complex that it is beyond the cognitive capabilities of some patients.

A final issue concerns how much information to provide to patients. Some clinicians and bioethicists suggest that patients should be told of common risks with low morbidity as well as rare risks with a high associated morbidity, but need not necessarily be provided with an exhaustive list of all possible risks regardless of their likelihood or their severity. Of interest, this is precisely the position taken by some legal authorities.

93.11 Doctrine of Double Effect

The doctrine of double effect makes a moral distinction between acting with the intention to harm someone or bring about their death versus performing an act where harm or death is foreseeable but is an unintended consequence. Thus, performing an act such as the administration of a clinically appropriate dose of morphine to reduce suffering is morally right because of its good consequences, even though the good consequences may sometimes only be achievable by putting the patient at significant risk of a harmful side effect like respiratory depression.

93.12 Resolving Ethical Conflicts

It is sometimes possible that some of the principles in a medical theory come into conflict with each other in some particular settings. For example, in the setting of principlism, ethical difficulties may arise when a competent adult patient's desires conflict with a caregiver's beneficent duty to work for the best clinical interests of the patient. The best known example of this is the Jehovah's Witness patient who refuses a clinically necessary blood transfusion or a patient with peripheral vascular disease who refuses to quit smoking. In Western culture, it is held that as long as the patient is a competent adult and understands the consequences of the decision, then the physician should respect the patient's decision, despite the fact that the decision is unwise and imprudent. However, not everyone is comfortable with such a position. For example, in countries like China, where personal autonomy is often taken to be less important than the needs of the state, one could imagine bioethicists offering a different position.

93.13 Ethical Issues Specific to Biomedical Engineering

While there is considerable overlap in the ethical issues in the fields of biomedical engineering and medicine, biomedical engineers also sometimes face ethical dilemmas that are unique to their profession. Issues such as safety, intellectual property ownership, risk disclosure, whistle blowing, and engineering professional codes of ethics are all examples. The Center for the Study of Ethics in the Professions at the Illinois Institute of Technology is a valuable resource in this regard, and may be accessed online at <http://ethics.iit.edu>. In the following sections some brief case studies are offered for review and discussion.

93.14 Example 1: The Therac-25 Cancer Treatment System

Computers are now increasingly being introduced into safety-critical systems like nuclear power plants and aircraft and, as a consequence, have been involved in a number of deadly mishaps. A particularly noteworthy medical example concerns a computerized radiation therapy machine called the Therac-25 used to treat cancer patients. In 1986, two cancer patients died when they received lethal doses of radiation from the Therac-25 system utilizing a computer-based controller. An investigation revealed that one contributor to this catastrophe was failure of the design team to recognize a “race condition,” a miscoordination between concurrent tasks.

Although the technical details of the failure remain secret as a result of a legal settlement, experts have come up with the following account as the most likely accident scenario. A modern radiation therapy machine is based on a linear accelerator that produces a high-energy electron beam. One may direct the electrons directly into the patient, or, to produce x-rays, one places a heavy metal target in the electron beam, so that when the electron beam hits the target, x-rays come out from the other end. The target is moved in and out of the beam automatically under software control, depending on whether an electron beam or an x-ray beam is selected to treat the patient. Also, the current in the electron beam is programmed to be much greater in x-ray mode because of energy losses that result when the target is used in making x-rays.

However, in the overdose cases, because of a software design error, the computer “thought” it was in x-ray mode rather than in electron mode, resulting in excessive radiation. The problem was a subtle error that no one had detected during the extensive testing the machine had undergone before being introduced into clinical use. In fact, the error surfaced only when an operator happened to use a specific, unusual combination of keystrokes to instruct the machine about the radiation parameters to be used. Specifically, if an extremely fast-typing operator inadvertently selected the x-ray mode instead of the electron beam mode, and then used an editing key to correct the command to select the electron beam mode instead, it was possible for the computer to lag behind the orders. The result was that the device appeared to have made the correction but, in fact, still had incorrect settings.

How could this happen? Experts speculate that the software developer might not have considered it necessary to guard against this failure mode or might not have even imagined it, since radiation therapy designers have traditionally used electromechanical interlocks to ensure safety in this setting. Also, systems analysts reviewing the case noted that the unit should have been programmed to discard “unreasonable” readings—as the injurious setting presumably would have been. Finally, there should have been no way for the computer’s verifications on the video screen to become unsynchronized from the keyboard commands.

93.15 Example 2: The Case of the Abbott Pain Control Machine

In the case of the Therac-25 system, the unit did not operate as the designers intended. However, poor ergonomic (human factors) design of complex medical equipment can lead to patient morbidity and mortality even while still operating “correctly.” The following case study illustrates this situation.

Patient-controlled analgesia (PCA) is a computer-based medical technology now used extensively to treat postoperative pain via the self-administration of analgesic agents such as morphine. Potential

benefits include superior pain control, automatic electronic documentation, and improved utilization of nursing resources. Unfortunately, however, analgesics are also a frequent cause of adverse drug events, usually related to respiratory depression. A typical PCA machine contains an embedded computer programmed to give, for instance, 1 mg of morphine intravenously every time the patient pushes a button on the end of a cable. To help prevent excessive drug administration, the onboard computer ignores further patient demands until a lockout period (usually set for 5–10 min) has passed. In addition, 1 h or 4 h cumulative limits also are available in some models.

Despite such safety features, numerous reports of respiratory depression and death associated with PCA pumps have appeared. One particularly notorious unit was the Abbott Lifecare 4100 PCA Plus II machine. This machine was easily misprogrammed by caregivers, who must manually enter the PCA parameters. Consequently, a number of patients received drug overdoses when using this product. However, an important consideration in the case of the Abbott PCA machine is that the device operated exactly as specified in the technical and operations manuals—the problem was primarily one of unwise selection of user defaults. This makes that situation different from design flaws such as those in the Therac-25 where the flawed unit operates in a manner differently than the design specifications require. While some individuals might argue that there is no design flaw present in the Abbott PCA unit in the sense that it operated exactly as intended, it should be clear that where an alternative design exists that is safer and no more costly or difficult to implement, the original design must be considered to be flawed.

93.16 Example 3: The Case of the Bjork–Shiley Heart Valve

Another example offered for consideration is the Bjork–Shiley Convexo–Concave heart valve, an early generation artificial heart valve that would occasionally fail catastrophically due to fracture of a strut. As many as 480 deaths have been estimated to have occurred as a result. Since only a relatively small fraction of the approximately 80,000 implanted convexo–concave valves actually failed, not all valves were removed and replaced, given that the comparatively small risk of valve fracture must be balanced against the not insubstantial risk and cost of the surgery needed to replace the valve.

Complicating this matter is the fact that according to a US government lawsuit, the maker of the valve, Shiley Inc., issued false reports to the FDA both to obtain initial approval of the device, as well as to keep the valve on the market. For instance, Shiley did not inform the FDA that in some cases they polished, rather than rewelded, cracked valve struts in order to make them look normal in appearance. In 1986 the FDA stopped sales of the valve. By 1990 there were 100 lawsuits pending against the manufacturer.

93.17 Discussion of Practical Ethical Issues

The above examples indirectly raise the concept of “permissible deaths,” a thorny ethical issue that regulators and policy makers must deal with in a great many settings. Just as generals conducting military campaigns must decide how many combatant deaths on either side are tolerable, as well as decide how many unavoidable innocent civilian deaths are acceptable, safety engineers must strike a balance between the cost of a safety feature and the number of lives saved, since, for instance, relatively few people would be willing to buy a car costing \$400,000 no matter how safe. Likewise, adding numerous extra safety features to medical equipment could conceivably make these products too expensive to be affordable.

Finally, consider the case of the pain killer Tylenol, the popular nonprescription analgesic known by the scientific name of acetaminophen. Although the use of acetaminophen is advocated for a number of mild-to-moderate pain conditions such as headaches and arthritis, it is less well-known that in large doses acetaminophen can be lethal. In fact, acetaminophen liver toxicity, often from an intentional overdose, causes more than 450 deaths annually in the United States. While there is little doubt that this number could be substantially reduced by restricting access to the drug, such as removing its nonprescription status, or even removing the drug from the market entirely (as happened with the painkiller Vioxx), the fact is that regulatory authorities like the FDA must view this number of deaths as being

acceptable in light of the enormous overall clinical benefits the drug provides. (After all, if they didn't feel this way, they presumably would do something about it). By contrast, in the case of the defective Bjork-Shiley Convexo-Concave heart valve the FDA removed the product from the market. Whether or not this happens will depend on the specific circumstances involved. Failure to mandate a recall of medical devices that harm patients may occur for several reasons. First, the remedy may be so expensive as to be impractical. Second, the medical device may involve an old design that is approaching the end of its life cycle anyway. Third, regulatory agencies with limited resources must prioritize their goals, with the result that medical devices that injure or kill only a small handful of people may not get the regulatory attention that victims and their families would otherwise like. In such cases, legal remedies may be the only option available.

In addition to safety issues, other factors sometimes play a role in medical equipment design. Manufacturers of medical equipment operate in a highly competitive environment that requires that careful attention be paid to market forces. In particular, early market penetration can be very helpful to ensure that a large market share is ultimately obtained. On the other hand, delays in introducing a product to market may be necessary in order to add improvements to the design early in the project design or to carry out ergonomic testing prior to release of the product. In some such cases, the costs of delaying a product launch may be considerable, since the costs of additional testing and refinement can be sizeable, and because valuable market share may be lost. Consequently, manufacturers are sometimes caught in a conflict between their responsibilities to their shareholders and their responsibilities to the public.

While a variety of ethical principles might be considered as the basis for ethical decision making in such a setting, the ethical principle of nonmaleficence would obviously figure prominently in any discussions. This principle is usually expressed in terms of health or safety issues. For instance, the first requirement of the IEEE code of ethics is "to accept responsibility in making engineering decisions consistent with the safety, health, and welfare of the public, and to disclose promptly factors that might endanger the public or the environment," while the NSPE code of ethics requires that engineers "hold paramount the safety, health, and welfare of the public." Unfortunately, some corporate executives take a completely amoral approach to business decision making, focusing entirely on what is legal and expedient rather than being driven by any moral or ethical compass.

93.18 Summary and Conclusions

This chapter presented an overview of the field of bioethics and its theoretical foundations, focusing on a number of issues likely to be of interest to the biomedical engineering community. The origins of medical ethics were discussed starting with reference to the Hippocratic oath, while the need for formal ethical codes for the conduct of human research was shown to have been motivated, at least in part, by some of the Nazi medical experiments. The chapter then presented a brief synopsis of the Kantian and utilitarian approaches to ethics, and their generalization into deontological and consequentialist approaches. The four principles behind principlism (respect for autonomy, beneficence, nonmaleficence, and justice) were then discussed. Also discussed were some of the issues in informed consent, and the doctrine of double effect. Finally, three real-life biomedical engineering ethical case studies were presented and discussed.

References

- Angell, M. The Nazi hypothermia experiments and unethical research today. *N Engl J Med.* 1990;322(20):1462-4.
- Barondess, JA. Medicine against society. Lessons from the Third Reich. *JAMA* 1996 Nov 27;276(20):1657-61. Pub Med PMID: 8922452.
- Beauchamp, T.L. and Childress, J.F. 2001. *Principles of Biomedical Ethics*. Oxford, UK: Oxford University Press.

- Berger, R.L. Nazi science—The Dachau hypothermia experiments. *N Engl J Med*. 1990 May 17;322(20):1435–40. Pub Med PMID: 2184357.
- Gillon, R. Utilitarianism. *Br Med J*. (Clin Res Ed). 1985 May 11;290(6479):1411–3. Pub Med PMID: 3922515; Pub Med Central PMCID: PMC1415603.
- Saha, S. and Saha, P.S. Biomedical ethics and the biomedical engineer: A review. *Crit Rev Biomed Eng*. 1997;25(2):163–201. Pub Med PMID: 9315431.
- Trials of War Criminals before the Nuremberg Military Tribunals under Control Council Law No. 10*, Vol. 2, pp. 181–182. Washington, DC: U.S. Government Printing Office, 1949. See also <http://ohsr.od.nih.gov/guidelines/nuremberg.html>

Further Reading

- Beauchamp, T. The legacy and the future. 30 years after the Belmont Report, Beauchamp sets the record straight. *Prot Hum Subj*. 2004 Summer;(10):1–3. Pub Med PMID: 15835026.
- Beauchamp, T.L. and Childress, J.F. 2001. *Principles of Biomedical Ethics*. Oxford, UK: Oxford University Press.
- Davey, L.M. The oath of hippocrates: An historical review. *Neurosurgery* 2001Sep; 49(3):554–66. Pub Med PMID: 11523662.
- Dolan, P. Utilitarianism and the measurement and aggregation of quality—Adjusted life years. *Health Care Anal*. 2001; 9(1):65–76. Pub Med PMID: 11372576.
- Doyle, D.J. Biomedical engineers and participation in judicial executions: Capital punishment as a technical problem. *J Long-Term Eff Med Implants*. 2007; 17(4): 297–302.
- Doyle, D.J. Ergonomics, patient safety, and engineering ethics: A case study and cautionary tale. *J Long-Term Effects Med Implants*. 2007; 17(1):27–33.
- Doyle, D.J. An Introduction to bioethics and ethical theory. *Ethics Biol, Eng Med*. 2010 1(1):19–41.
- Friedlander, W.J. The evolution of informed consent in American medicine. *Perspect Biol Med*. 1995 Spring;38(3):498–510. Pub Med PMID: 11644691.
- Gandjour, A. and Lauterbach, K.W. Utilitarian theories reconsidered: Common misconceptions, more recent developments, and health policy implications. *Health Care Anal*. 2003 Sep;11(3):229–44. Pub Med PMID: 14708935.
- Gardiner, P. A virtue ethics approach to moral dilemmas in medicine. *J Med Ethics*. 2003 Oct;29(5):297–302. Pub Med PMID: 14519840; Pub Med Central PMCID: PMC1733793.
- Heubel, F. and Biller-Andorno, N. The contribution of Kantian moral theory to contemporary medical ethics: A critical analysis. *Med Health Care Philos*. 2005;8(1):5–18. Pub Med PMID: 15906935.
- Katz, J. The Nuremberg code and the Nuremberg trial. A reappraisal. *JAMA* 1996 Nov 27;276(20):1662–6. Pub Med PMID: 8922453
- Lifton, R.J. 1986. *The Nazi Doctors, Medical Killing & the Psychology of Genocide*. New York: Basic Books.
- Saha, S. and Saha, P.S. Biomedical ethics and the biomedical engineer: A review. *Crit Rev Biomed Eng*. 1997;25(2):163–201. Pub Med PMID: 9315431.